

AD 740547

COMPUTER ORIENTED ANALYSIS OF SHELL STRUCTURES

JUNE 1971

*PROCEEDINGS OF A CONFERENCE HELD AT
PALO ALTO, CALIFORNIA
AUGUST 10-14, 1971*

*SPONSORED BY
LOCKHEED MISSILES AND SPACE COMPANY
AND
AIR FORCE FLIGHT DYNAMICS LABORATORY*

This document has been approved for public release;
its distribution is unlimited.

AIR FORCE FLIGHT DYNAMICS LABORATORY
AIR FORCE SYSTEMS COMMAND
WRIGHT-PATTERSON AIR FORCE BASE, OHIO 45433

Reproduced by
NATIONAL TECHNICAL
INFORMATION SERVICE
Springfield, Va 22151

1301

NOTICE

When Government drawings, specifications, or other data are used for any purpose other than in connection with a definitely related Government procurement operation, the United States Government thereby incurs no responsibility nor any obligation whatsoever; and the fact that the government may have formulated, furnished, or in any way supplied the said drawings, specifications, or other data, is not to be regarded by implication or otherwise as in any manner licensing the holder or any other person or corporation, or conveying any rights or permission to manufacture, use, or sell any patented invention that may in any way be related thereto.

Copies of this report should not be returned unless return is required by security considerations, contractual obligations, or notice on a specific document.

UNCLASSIFIED

Security Classification

DOCUMENT CONTROL DATA - R & D

(Security classification of title, body of abstract and indexing annotation must be entered when the overall report is classified)

1. ORIGINATING ACTIVITY (Corporate author)		2a. REPORT SECURITY CLASSIFICATION	
Lockheed Palo Alto Research Laboratory 3251 Hanover Street Palo Alto, California 94304		Unclassified	
2. REPORT TITLE		2b. GROUP	
Computer Oriented Analysis of Shell Structures - Proceedings of a Conference Held at Palo Alto, California August 10-14, 1976		N/A	
3. DESCRIPTIVE NOTES (Type of report and inclusive dates)			
Proceedings of a Conference Held August 10-14, 1976			
4. AUTHOR(S) (First name, middle initial, last name)			
Richard F. Hartung, Editor			
5. REPORT DATE		7a. TOTAL NO. OF PAGES	7b. NO. OF REFS
June 1971		1284	N/A
6a. CONTRACT OR GRANT NO. F33615-69-C-1523		6b. ORIGINATOR'S REPORT NUMBER(S)	
b. PROJECT NO. 1467		AFFDL-TR-71-70	
c. Task No. 146703		6d. OTHER REPORT NO(S) (Any other numbers that may be assigned this report)	
d.		N/A	
10. DISTRIBUTION STATEMENT			
This document has been approved for public release; its distribution is unlimited.			
11. SUPPLEMENTARY NOTES		12. SPONSORING MILITARY ACTIVITY	
None		Air Force Flight Dynamics Laboratory Air Force Systems Command Wright-Patterson Air Force Base, Ohio 45433	
13. ABSTRACT			
<p>The Conference on Computer Oriented Analysis of Shell Structures, sponsored jointly by Lockheed Missiles & Space Company and Air Force Flight Dynamics Laboratory, was held at the Lockheed Palo Alto Research Laboratory in Palo Alto, California, on 10-14 August 1976. The primary objective of the conference was to bring together specialists in the field of computer analysis of shells and shell-like structures for an exchange of information through the presentation of papers, panel discussions and informal discussions. Particular emphasis was placed on recent developments in discrete methods for analyzing the static and dynamic response of shell structures and on the related problems of computer technology, numerical analysis and applications to engineering problems.</p>			

DD FORM 1473

FORM 1 NOV 68

Security Classification

Security Classification

14. KEY WORDS	LINK A		LINK B		LINK C	
	ROLE	WT	ROLE	WT	ROLE	WT
1. Shell Analysis						
2. Computer Analysis of Shells						
3. Structural Analysis Computer Program						
4. Static						
5. Finite Element Methods						
6. Finite Difference Methods						
7. State of the Art of Shell Analysis						
8. Dynamic						
9. Stability						
10. Vibration						
11. Shell Analysis Conference Proceedings						

COMPUTER ORIENTED ANALYSIS OF SHELL STRUCTURES

EDITED BY

*RICHARD F. HARTUNG
LOCKHEED PALO ALTO RESEARCH LABORATORY*

*PROCEEDINGS OF A CONFERENCE HELD AT
PALO ALTO, CALIFORNIA
AUGUST 10-14, 1971*

SPONSORED BY

*LOCKHEED MISSILES AND SPACE COMPANY
AND
AIR FORCE FLIGHT DYNAMICS LABORATORY*

**This document has been approved for public release;
its distribution is unlimited.**

FOREWORD

The Conference on Computer Oriented Analysis of Shell Structures, sponsored jointly by Lockheed Missiles & Space Company and Air Force Flight Dynamics Laboratory, was held at the Lockheed Palo Alto Research Laboratory in Palo Alto, California, on 10-14 August 1970. The primary objective of the conference was to bring together specialists in the field of computer analysis of shells and shell-like structures for an exchange of information through the presentation of papers, panel discussions and informal discussions. Particular emphasis was placed on recent developments in discrete methods for analyzing the static and dynamic response of shell structures and on the related problems of computer technology, numerical analysis and applications to engineering problems.

The conference was attended by 161 persons: 85 from industrial organizations, 45 from universities and 31 from government agencies.

Twenty-seven invited papers were presented at the conference in 13 sessions as indicated on page viii. In addition there were three panel discussions: Meeting the Demands of Advancing Aerospace Technology, Finite Element Versus Finite Differences, and the Large General Purpose Computer Code. Extensive discussions followed each paper and these were tape recorded. The tapes were later transcribed and edited and are included in these proceedings following the appropriate paper. The panel discussions were also tape recorded, transcribed and edited and are also included. Considerable liberties were taken by the editor in order to condense the discussion, and for that reason most comments and questions are printed anonymously. Where names are mentioned, these people were given the opportunity to examine and approve the edited version.

This report contains the proceedings of the conference. These proceedings were prepared by the Lockheed Palo Alto Research Laboratory,

Palo Alto, California, under Air Force Contract No. F33615-69-C-1523. It was administered under the Structures Division, Air Force Flight Dynamics Laboratory with Mr. T. N. Bernstein (FDTR) acting as Project Engineer. The proceedings were edited by Dr. Richard F. Hartung, Manager, Structural Mechanics Laboratory, LMSC.

This report has been reviewed and is approved.

A handwritten signature in dark ink, appearing to read "Francis L. Land, Jr.", is positioned above the printed name.

FRANCIS L. LAND, JR.
Chief, Solid Mechanics Branch
Air Force Flight Dynamics Laboratory

HAROLD C. MARTIN MEMORIAL

It seems especially appropriate that the present volume, in consideration of its content, should contain some words of appreciation in memory of Dr. Harold C. Martin. Because of his professional involvement over the past thirty year period in the field of structural engineering - as practicing engineer, educator, research worker, author and consultant - it was inevitable that a symposium devoted to numerical shell analysis should include a large number of his friends, former students, and co-workers among its participants.

Harold was born in Brooklyn, New York on March 30, 1913. He attended the public schools in that area through high school and continued his education at New York University, where, in 1934 and 1937 respectively, he received a B.S. degree in Mechanical Engineering and a M.S. degree in Aeronautical Engineering. The next two years were spent at Boeing in Seattle, followed by two years as a stress analyst at Republic Aviation in Farmingdale. He returned to New York University as Instructor in Aeronautics in 1941, and thereafter his primary occupation was in engineering education and research. In 1942 he moved to Princeton as Instructor in Aeronautics. During the period 1944 to 1948 he served as Instructor and Research Assistant in Aeronautics at the California Institute of Technology, while completing most of the requirements for the PhD degree. In 1948 he began his career at the University of Washington as Associate Professor in Aeronautical Engineering, and he retained his affiliation with the University until the time of his death on August 23, 1970. After completing his thesis, "Elastic Instability of Deep Cantilever Struts Under Combined Axial and Shear Loads at the Free End," he was awarded the PhD from the California Institute of Technology in 1950. In 1952 he was promoted to the rank of Professor at Washington, and from 1957 through 1960 he served as Department Head in Aeronautical Engineering. While at Washington, he also served at various times as Visiting Professor at the University of Hawaii and at Stanford University. Starting in 1952, he was a technical consultant in structural analysis at The Boeing Company.

Throughout his professional career Harold's interests were concentrated in the area of structural analysis. These interests did not take the form of a dedication to exact analysis as an end in itself, but clearly originated from a sincere belief in the inherent worth of analytical effort. Harold was convinced that analytical methods constitute an important tool for solving practical problems and that the social value of engineering accomplishments resulting from such endeavor provides a valid motivation for the work. During the years of World War II and those immediately following, his research and teaching were mainly concerned with stability analysis and applications of the theory of elasticity. It was a natural outgrowth of his practical motivation that Harold became greatly intrigued by the potentialities of matrix methods in conjunction with high speed digital computers for the analysis of complex structures. Subsequent to 1953, his research concentrated principally in this area.

Within the available space it is impossible to give a complete account of Harold's technical accomplishments and publications. Therefore, we shall only mention three important works. In 1953 Harold and several colleagues began work on the formulation and implementation of the finite element displacement method. This work led to the paper, "Stiffness and Deflection Analysis of Complex Structures," published in 1956 in the Journal of The Aeronautical Sciences, and pioneered the application of the finite element structural analysis approach which has had world-wide application in recent years. Another paper, "On the Derivation of Stiffness Matrices for the Analysis of Large Deflection and Stability Problems" (Proceedings of the Conference on Matrix Methods in Structural Mechanics, Wright-Patterson Air Force Base, 26-28 October, 1965) deals with large deflection and geometrically nonlinear problems in finite element analysis; it contains a clear exposition of the fundamental principles of this subject and a historical review of its development prior to 1965. The third work is the excellent textbook Introduction to Matrix Methods of Structural Analysis, McGraw-Hill, 1966. The dedication of this book is a clear statement of the professional philosophy of its author; the statement is: "This book is dedicated to the structural engineer who, by using his talents and knowledge, benefits mankind."

Although he did not often volunteer his opinions on religious matters, it was apparent to all who knew him well that Harold had sincere Christian convictions

and that these convictions were the primary foundation of his philosophy of life. He expressed genuine love for human life, and concern over the problems facing people today, resulting from the pressure of increasing world population and from the moral and spiritual degeneration of society. He felt that most of the problems of man could be solved if men would have true consideration for others, and if they would approach problems with the conviction that a reasoned attitude would lead to a reasonable solution. He was disturbed and disappointed to find that others often did not share these views.

Among the reminiscences of those who knew him well there is the common message that Harold was a valued friend, one whose passing is felt as a definite loss. Harold was a stimulating colleague, and it was always a pleasure to be with him. He was sincerely interested in people, and he took time to listen to what they had to say. He was loyal to friend and acquaintance alike. Harold's friends were many; they came from diverse walks of life; and they all valued his friendship. Harold deeply appreciated his friendships and associations; they were an essential part of his life.

This memorial is closed with a quotation from the Bible. It was one of Harold's favorites, and it describes him and his philosophy more clearly than the many words written above.

Micah 6:8

He has showed you, O man, what is good;
and what does the Lord require of you
but to do justice, and to love kindness,
and to walk humbly with your God?

CONTENTS

OPENING REMARKS:	Dr. W. C. Griffith Col. R. J. Myers	4
SESSION I: GENERAL OVERVIEW - I		
Session Chairman: W. Walton		
THE IMPACT OF THE COMPUTER ON SHELL ANALYSIS		5
M. Stein		
THE NUMERICAL METHODS OF DISCRETE SHELL ANALYSIS		
G. A. Greenbaum and A. P. Capelli		34
SESSION II: GENERAL OVERVIEW - II		
Session Chairman: W. Crichlow		
A SURVEY OF SPARSE MATRIX TECHNOLOGY		
R. A. Willoughby		65
THE DEVELOPMENT OF LARGE SCALE DIGITAL COMPUTER CODES FOR PRODUCTION STRUCTURAL ANALYSIS		172
D. N. Yates, T. J. Vinson and W. W. Sable		
PANEL DISCUSSION A - MEETING THE DEMANDS OF ADVANCING AEROSPACE TECHNOLOGY		223
Chairman: P. E. Grafton L. A. Riedinger, R. B. Baird, C. K. Grimes and R. W. Leonard		

SESSION III: FINITE ELEMENT METHODS
- I

Session Chairman: J. A. Stricklin

DYNAMIC FINITE ELEMENT ANALYSIS OF
ARBITRARY THIN SHELLS 244

R. Clough and E. L. Wilson

MIXED FORMULATIONS FOR FINITE ELEMENT
SHELL ANALYSIS 290

L. Herrmann and W. E. Mason

SESSION IV: FINITE DIFFERENCE METHODS
- I

Session Chairman: W. Hubka

FINITE-DIFFERENCE ENERGY METHOD FOR
NONLINEAR SHELL ANALYSIS 337

D. Bushnell and B. O. Almroth

A LARGE DEFLECTION TRANSIENT ANALYSIS OF
ARBITRARY SHELLS USING FINITE DIFFERENCES 395

R. D. Krieg and H. C. Monteith

SESSION V: FINITE ELEMENT METHODS
- II

Session Chairman: J. T. Oden

FESTRAN: SCOPE AND LIMITATIONS 457

L. Schmit and W. Gibson

NONLINEAR MATERIAL AND GEOMETRIC BEHAVIOR
OF SHELL STRUCTURES 485

G. A. Dupuis, H. D. Hibbitt,
S. F. McNamara, and P. V. Marcal

SESSION V. (CONT'D)

THE ANALYSIS OF THIN SHELLS WITH A DOUBLE
CURVED ARBITRARY QUADRILATERAL FINITE ELEMENT

517

S. W. Key

SESSION VI: FINITE DIFFERENCE METHODS
- II

Session Chairman: P. Radkowski

A PROGRAM FOR THE NONLINEAR STATIC AND
DYNAMIC ANALYSIS OF ARBITRARILY LOADED
SHELLS OF REVOLUTION

590

R. E. Ball

FINITE DIFFERENCE TECHNIQUES FOR
VARIABLE GRIDS

618

P. S. Jensen

SESSION VII: OTHER METHODS

Session Chairman: A. Liesa

NUMERICAL METHOD FOR MIXED BOUNDARY VALUE
PROBLEMS OF SHELLS OF REVOLUTION

646

A. Kalnins

THE INTERACTION OF ASYMPTOTIC AND COMPUTER
METHODS OF SHELL ANALYSIS

690

C. R. Steele

SESSION VIII: ADDITIONAL CONSIDERATIONS
IN ANALYSIS OF SHELLS

Session Chairman: S. Jordan

SOME ASPECTS OF THE POST BUCKLING BEHAVIOR OF
IMPERFECTION-SENSITIVE SHELL STRUCTURES IN THE
PLASTIC RANGE

720

J. Hutchinson

SESSION VIII (CONT'D)

SOLUTION OF STRUCTURAL EIGENVALUE
PROBLEMS USING SPARSELY POPULATED MATRICES 746

H. A. Kamel and R. L. Lambert

PANEL DISCUSSION B - FINITE ELEMENTS VERSUS FINITE
DIFFERENCES -- their strengths and
weaknesses (or is there really a
future for finite. . . ?) 798

Chairman: R. M. Jones
D. Bushnell, S. W. Key, R. D. Krieg,
E. L. Stanton

SESSION IX: NUMERICAL METHODS

Session Chairman: R. E. Jones

SHELL ANALYSIS WITH LARGE GENERAL PURPOSE
PROGRAMS 825

C. McCormick

THE IMPACT OF FUTURE DEVELOPMENTS IN
COMPUTER TECHNOLOGY 843

W. R. Graham

SESSION X: OPTIMIZATION

Session Chairman: S. McIntosh

THE OPTIMUM APPROACH TO ANALYSIS
OF ELASTIC CONTINUA 862

R. J. Melosh

DESIGN OF OPTIMUM STRUCTURES 899

V. B. Venkayya

SESSION XI: DYNAMIC PROBLEMS

Session Chairman: G. Morosow

INTEGRATION OPERATORS FOR TRANSIENT
STRUCTURAL RESPONSE 993

R. S. Dunham, R. E. Nickell,
and D. C. Stickler

SESSION XI. (CONT'D)

THE ROLE OF COMPONENT MODAL TECHNIQUES IN
DYNAMIC ANALYSIS OF ENGINEERING STRUCTURES 1022

C. W. Coale and W. A. Loden

PANEL DISCUSSION C - THE LARGE GENERAL PURPOSE COLE 1063

Chairman: D. Warren
C. W. McCormick, Y. Rashid, R. Melosh,
S. Jordan

SESSION XII: STABILITY OF SHELL STRUCTURES

Session Chairman: Z. Zudans

IMPERFECTION SENSITIVITY OF ELASTIC STRUCTURES:
THE SECOND APPROXIMATION FOR UNIQUE MODE BUCKLING 1107

G. Cohen

THE APPLICATION OF GRADIENT MINIMIZATION METHODS
AND HIGHER ORDER DISCRETE ELEMENTS TO SHELL
BUCKLING AND VIBRATION EIGEN-PROBLEMS 1138

E. L. Stanton and D. J. McGovern

SESSION XIII: STATE OF THE ART EVALUATION

Session Chairman: F. J. Janik

STRESS, BUCKLING AND VIBRATION ANALYSIS OF
SHELLS OF REVOLUTION 1173

M. S. Anderson, R. E. Tulton,
W. L. Heard and J. E. Walz

GENERAL SUMMARY 1250

K. J. Forsberg

OPENING REMARKS

DR. GRIFFITH: Good morning, ladies and gentlemen.

On behalf of the management and staff of the Lockheed Missiles and Space Company, it is my privilege to bid you welcome for the five days of this conference. We're honored to be your hosts for these meetings at our Palo Alto Research Laboratory. Particular note needs to be made of the instrumental role of the Air Force Flight Dynamics Laboratory in making this conference possible. Without their foresight and wisdom, it would have been impossible to hold this conference and we're very grateful to the Flight Dynamics Laboratory for what they have done and what they will do during the course of our meetings. We must also recognize the additional role of the Flight Dynamics Laboratory within their own laboratories and the support that they have given to studies in other parts of the services, in industry and in our universities for development of the subject. Without that we would have a far less rich topic to cover this week.

In these acrimonious times we hear a good deal about the "military-industrial complex," and I think it is important to note that the weeks' program will shed some light on this whole subject in terms of what is right and what is wrong with the charges. Certainly to oversimplify is wrong and I would claim that in using the term military-industrial, the matter has been oversimplified. Clearly it should be expanded. As one sees both from the program and the roster of registrants, the correct descriptor is "military-

industry-university complex"; and I urge you academic representatives to insist upon your full share of the action. In another regard, however, I think the designation is indeed correct. Certainly our relationships as institutions with one another and even amongst ourselves and the problems that we work on are certainly complex and we do have a very valid assertion.

In shell analysis there are two fundamental questions which one addresses himself to. Both of these will be recurring themes through the papers and the panel discussions and summary remarks that you will have during the week. The first question would appear to be: What is the correct mathematical description of a real structure and the properties of the materials from which that structure is made? And the second underlying question is: How accurately can these mathematical representations be analyzed at reasonable cost and in reasonable time to predict and understand the behavior of the structures which the mathematics describes? I believe that you will find the material to be presented this week will add a great deal of information and understanding on an approach to answering these two questions.

COL. J. R. MYERS: The primary objective of this conference is to present and promote, if you will, the most recent developments in structural shell analysis. As I understand it, emphasis will be placed on numerical methods and the associated computer technology required to apply these analyses to practical engineering problems and, gentlemen, let me repeat that last phrase--required to apply these analyses to practical engineering problems. Within the last several months we have seen a

number of new starts within the Air Force. The F15, the B1 advanced bomber, AWAC, AX, and so on. Now these aircraft as such will be in environments that are really going to press us and we haven't solved some of the current problems as yet.

As most of you know, Lockheed has been working under Air Force contract during the past year in order to assess current shell analysis capability throughout the United States. Many of the organizations represented here this morning have been interviewed and this conference is being held so that you may share the wealth of general information, valuable experience, unpublished ideas that have been uncovered during this study.

Most of us here today are concerned with research and development needs and are keenly aware of the current R&D climate which confronts us. In this regard, I would like to quote from remarks made by Gen. Ferguson at the recent Fatigue and Fracture Conference held at Miami Beach last December (1969).

"The causes for the present anti-military climate are numerous, divergent and sometimes only marginally related. Nonetheless, military and military-related activities present such a large and obvious target that all sorts of diverse dissatisfactions converge upon the man in uniform, and all those in any way associated with it--universities as well. If nothing succeeds like success, success in the case of the military R and D would appear to have succeeded a little too well. Certainly a strong case could be made that the so-called military-industrial complex has helped the United States to survive, to grow and prosper in a hostile world, but the very essence of art, it is said, is to hid the labor that went into its creation. And

so having succeeded so well in countering every threat to our national security, we have perhaps made it seem that there is no threat. Or that we are internally immune from any external threats. At a time when the Soviets are expanding in every area of research, development and production of weapon systems and Red China is testing missiles to deliver its nuclear warheads, many elements in the United States are turning against defense research and development. "

We in research and development face some lean years in spite of increased responsibility. We've got to achieve our technological goals for advanced systems with fewer resources. This will be the real challenge to our creativeness, ingenuity and resourcefulness. Gentlemen, during the past several years, I have fostered this business of computer techniques as applied to shells because, in my own mind as Chief of the Lab, I think that this is an opportunity for high payoffs to this country. I think you've got kind of an exciting week ahead of you. Thank you very much for coming.

DESIGN PROBLEMS OF SHELL STRUCTURES AND THE IMPACT OF THE COMPUTER ON SHELL ANALYSIS

By Manuel Stein

NASA Langley Research Center
Hampton, Virginia

SUMMARY

A brief description of the essential nature of shell theory and the shell equations is followed by a survey, with examples, of the types of shell problems that are of important concern to the structural designer and, therefore, of interest to the shell analyst. The principal approaches to the shell problem solution are outlined and some of the important effects that the computer has had on shell analysis and the analyst are discussed. Deficiencies in shell technology, requiring additional research, are indicated.

INTRODUCTION

Solutions of problems in shell structures were attempted as early as 1744 by Euler (see ref. 1). Such problems were among those which motivated the formulation of the general equations of elasticity by Navier in 1821. In 1850 Kirchhoff developed the theory of plates, and this theory was used by Aron in 1874 to develop the first theory of shells. Some inaccuracies in Aron's theory were found and corrected by Love in 1888 (see ref. 2). The theory of shells based on the hypotheses of Kirchhoff and the development by Love is not unique, and many other formulations have been developed. In 1960, Koiter (ref. 3) defined a criterion for judging the accuracy of linear shell theories, and showed that most other theories differ from Love's by insignificant terms only.

For the benefit of those people who are not shell experts, this paper gives the engineering definition of a shell, describes the basic ideas which lead to the theory of shells, and discusses some important problems facing the designer of shell structures. A number of examples will be given to illustrate the kinds of problems involved in the analysis of shells. A second objective is to characterize the two principal approaches to obtaining solutions to the shell equations.

Because of the extreme complexity of shell theory, only the simplest cases could be solved before the advent of the digital computer. However, the analysis of shell structures has expanded in quantity and scope as the capabilities of the computer have grown. A study of the journals indicates that initially the application of the computer to shell analysis was gradual. In the early 1960's computers were used for some problems, but it was not until the middle 1960's that the words "computer solution" appeared in titles and that the operations involved were tailored for calculations carried out by

computers rather than those carried out by hand. The third objective of this paper is to review the tremendous expansion of shell analysis and the corresponding growing pains associated with computer solutions and to suggest what, in the author's opinion, is needed for the immediate future.

FUNDAMENTALS OF SHELL ANALYSIS

Shell structures appear in a great variety of applications including aircraft fuselages, launch vehicle tanks and intertank structures, pressure vessels, rocket motor cases and nozzles, gas turbine engine cases, submersible vessels, and ground based storage tanks. Detailed shell wall configurations may take a wide variety of forms including, for example, isotropic, stiffened in one or more directions, laminated, and filamentary composite (see Fig. 1).

A shell is defined as a body having one dimension - the thickness - small compared with the other two dimensions. The general shape of the shell wall can be represented by a curved surface in space usually termed the reference surface (see Fig. 2). Thus the shell geometry may be determined from the shape of the reference surface, the shell wall thickness, and the shape of the boundary. The analysis of shells is based on the fundamental laws of solid continuum mechanics. The assumptions listed below (which are called Kirchhoff assumptions) are generally admissible because of the thinness of the shell wall:

(a) Straight lines normal to the shell reference surface before deformation remain straight and normal after deformation, and these lines do not change in length during deformation of the shell.

(b) Stresses normal to the shell reference surface are negligible in comparison with the other stresses in the shell wall.

Integration through the thickness permits a two-dimensional formulation of the theory of shells in terms of the coordinates of the reference surface. This formulation transfers attention from stresses to forces and moments which are fundamental quantities in shell analysis.

The quantities which the analyst must determine in order to describe the behavior of the shell are shown in Figure 2. These quantities are the moments, rotations, forces, and displacements associated with the reference surface. In Figure 2, the sketch on the lower right shows the so-called membrane forces and the shears and the sketch on the upper right shows the moments and torques applied to an element of the shell wall. The equations required to determine the behavior of the shell include equations which define the equilibrium of forces (that is, membrane forces and shears, moments and torques) on elements of the shell wall, equations representing the relations between these forces and quantities associated with the deformation of the shell wall called strains, relations between these strains and the displacements of the shell reference surface, and the proper boundary, continuity and initial conditions. Equilibrium equations may be obtained directly from considerations of the forces on an element or may be derived from a variational principle. The variational

principles which are commonly used in shell theory include the Principles of Minimum Potential Energy, Minimum Complementary Energy, and Virtual Work, and Hamilton's Principle. All of these principles stem from fundamental laws of solid mechanics. Advantages of these variational principles in the derivation of the equilibrium equations are that they permit certain freedom in selection of candidate solution functions and that with their use the correct boundary conditions to physical problems are generated automatically.

One indication of the relative difficulty of solution of shell problems, perhaps, is represented by the order of the differential equations involved in the theory. Many difficult problems in mathematical physics deal with equations of second order in the space variables. The equations of plate theory are fourth order. The equations of shell theory, however, are of eighth order. Another consideration which may complicate the solution of shell problems is the fact that nonlinearities are often important. Usually, the elastic deformation of solid bodies leads to small displacements and linear differential equations. In shell problems, however, the shell wall may displace several times its thickness under load, and in this circumstance, even though the strains may remain small, as is usual in solid bodies, they may depend nonlinearly on displacements.

TYPES OF SHELL ANALYSIS

Various types of problems must be faced by the shell structure designer and analyst. In general, the strength of the shell structure is of foremost importance. Assessment of strength requires analysis of the forces or stresses in the shell wall under all pertinent loading conditions and comparison of these values with appropriate allowable values. Shells are often subject to bending and compression and are, therefore, prone to structural instability (buckling). Where oscillating load inputs are present, knowledge of the vibration behavior of a shell structure is of vital importance to prevent resonances which might damage the structure. If the structure is subject to very suddenly applied (or dynamic) loadings, the transient response might be of importance. Finally, interaction between aerodynamic forces and structural deformations may cause flutter problems, or so-called aeroelastic problems, which play a significant role in the structural design of aerospace vehicles. In this section, examples of these various types of shell problems are presented to characterize them and to indicate the kinds of mathematical problems involved in their analysis.

Stress and Deflection Analysis

The efficient use of space available in launch vehicles sometimes leads designers to toroidal shell configurations for the purpose of containing high pressure fluids. Such shells present especially interesting stress analysis problems. Results of stress and deflection analysis of a toroidal shell under internal pressure are shown in Figure 3 (from ref. 4). The crown of this shell (identified in Fig. 3) is a special location, marking the boundary between the

outer region of the shell, where the principal curvatures of the reference surface are both positive, from the inner region where one curvature is negative. While many pressure vessels are designed on the basis of the simplest form of shell theory - linear membrane theory - application of this theory to the torus leads to a discontinuity of displacements at the crown, an obviously unacceptable result. The use of bending shell theory, on the other hand, yields physically reasonable results. The comparison is shown at the right in Figure 3, where the linear membrane result has been taken from reference 5. On the left in Figure 3 is plotted an outer fiber stress distribution, that is a direct stress at the shell wall thickness surface, as a function of the angular coordinate as calculated by both linear membrane theory and linear bending theory. Note that the simple membrane theory yields stresses which differ from the bending results by only 20 percent. It should be pointed out that the geometric parameters of this relatively simple example have been chosen so that linear bending theory indeed gives accurate results. It is important to further note that, for thinner toroidal shells, even linear bending theory is not sufficiently accurate and nonlinearity must be introduced.

Buckling

Because the shell wall thickness is small relative to the other dimensions, shell structures are susceptible to a mode of failure termed structural instability or buckling. Buckling occurs in shell structures in two forms. In one form a gradual increase in normal or lateral deflections may occur with increase in external loading until a maximum load level is reached. In the other form (bifurcation), there occurs an abrupt change in configuration at a load level where the initial equilibrium configuration becomes unstable. These two forms of buckling are illustrated in Figure 4 in which a characteristic load parameter is plotted as a function of the corresponding displacement measure. The maximum load type buckling problem is illustrated in Figure 4(a); the analysis required involves increasing the loading in a stress and deflection calculation until a situation is reached in which additional displacement occurs accompanied by no increase in load. A nonlinear shell theory is required for such calculations. The bifurcation type buckling is illustrated in Figure 4(b); in this case a stress and deflection analysis provides a solution which must be examined for stability by studying small excursions from it. The origins of alternate paths (the bifurcation points) occur at the eigenvalues of a system of homogeneous linear differential equations derived from the general equilibrium equations, and, of course, the eigenvalues are the buckling loads and they depend on the prebuckling solution. In bifurcation buckling problems, the prebuckling solution may be obtained from either a linear or nonlinear stress and deflection analysis.

Both types of buckling behavior are exhibited by a shallow spherical cap under uniform lateral pressure. The shallow spherical cap might represent the nose of a planetary entry vehicle or heat shield of a manned space capsule. Results for this problem are shown in Figure 5. The buckling pressure is plotted as a function of a geometric parameter which measures the ratio of the rise of the shell to its wall thickness. For very shallow shells, maximum-load type buckling occurs with the deformation pattern symmetric about the axis of the cap. For values of rise-thickness parameter greater than 5, bifurcation buckling occurs; the

symmetric prebuckling configuration becomes unstable and an asymmetric buckle pattern appears. The number of waves in the asymmetric buckle pattern which is appropriate to each value of the rise-thickness parameter is indicated on the curves.

Vibration

Shell structures for launch vehicles and spacecraft, for example, may be subjected to high frequency oscillating loads from rocket engines. To avoid resonant conditions which might cause structural damage, it is important to know the natural vibration behavior of such shells. The equations required to determine vibration behavior of shell structures are linear and homogeneous and, in fact, are quite similar to the equations required for bifurcation buckling calculations. The eigenvalues of the system are now the natural frequencies of vibration; one key difference between the vibration and the bifurcation buckling problem lies in the fact that several natural frequencies are of importance to the designer whereas, generally, only the lowest buckling load is of interest.

Some illustrative results for vibration of a shell structure are shown in Figure 6 (from r.f. 6) where natural frequencies for a simply supported cylindrical shell are plotted as a function of the number of axial half waves, m . Each value of m , the numbers of axial half waves, and n , the number of circumferential waves, determine a natural frequency for the cylinder. For this simple problem elementary functions satisfy the differential equations and the boundary conditions and exact results are easy to obtain.

For particular values of the axial wave number parameter, the natural frequencies tend to cluster together; in this case they cluster near the lowest frequency. For more complex shells where numerical methods are required, the closeness of the eigenvalues can lead to numerical difficulties such as slow convergence or failure to determine all frequencies in the range of interest. Another consideration which may increase computational difficulties in shell vibration problems is also illustrated in Figure 6. Note that the lowest frequencies do not necessarily correspond to the lowest wave numbers in contrast to the behavior of simpler structures such as beams and plates where the lowest frequencies almost always are associated with the simplest wave forms.

Transient Response

Shell structures are sometimes subjected to very suddenly applied or dynamic loads. In such cases the inertia of the shell may be important, and calculation of the transient response of the structure may be necessary to determine whether or not stresses or deflections remain within acceptable limits. In transient response problems an additional independent variable, time, is introduced. The shallow spherical shell cap, hinged at the boundary, under a distributed lateral pressure loading provides an illustrative example for these problems. Solutions were obtained in reference 7 for a lateral

pressure with a step variation in time and having a linear variation across the chord diameter starting from zero at one point on the boundary. Transient response results based on nonlinear shell theory are shown in Figure 7 where the change in volume under the shell (a measure of the average lateral displacement) is plotted as a function of time. The various curves in Figure 7(a) are for different values of the magnitude of the average step pressure loading. The maximum volume changes from the response curves in Figure 7(a) are plotted in Figure 7(b) as a function of the magnitude of the average step pressure. With increasing magnitude of the pressure, the curve in Figure 7(b) changes abruptly at a value of the average pressure parameter equal to about 0.27. The loads at which such behavior is exhibited in shell structures have been termed "dynamic buckling" loads in a rough analogy to the maximum load type of static buckling discussed previously. From the computational standpoint, a significant feature of transient response problems in shells is that, effectively, a complete static stress and deflection analysis must be performed at each time increment, and often many time increments must be taken to establish meaningful results. Computation times for transient response problems are, therefore, substantially longer than for corresponding problems in static stress analysis, buckling, or vibrations.

Flutter

Fluid flow along the surface of a shell structure may cause a self-induced oscillation termed "flutter." The flutter phenomenon involves an interaction between the deformations of the shell structure and time-dependent or unsteady aerodynamic forces, and the resulting physical system turns out to be nonconservative. Flutter is essentially an instability in the nonconservative system, and its calculation involves the determination of complex eigenvalues of complex matrix equations. The usual requirement is to determine a stability or flutter boundary by finding under what conditions the real part of a complex eigenvalue changes from negative to positive. In order to accomplish this task, a whole spectrum of complex eigenvalue problems must be solved on the computer.

The form which one of these solutions takes is illustrated by results for a circular conical shell in supersonic flow shown in Figure 8. Given in the figure is an equation for the deflection w of the shell defining its dependence on the complex eigenvalue λ . Real and imaginary parts of the eigenvalue are plotted as a function of the velocity, and the flutter velocity is indicated at the point where $\text{Re}(\lambda)$ becomes positive and, hence, w increases exponentially with time. At velocities less than the flutter velocity, oscillations with frequencies associated with the imaginary part of λ decay, due to aerodynamic damping.

METHODS OF SHELL ANALYSIS

In problems as complicated as those dealing with shells, almost all methods of analysis will involve numerical calculations. For the purposes of this

paper, shell analysis methods will be classified either as (1) analytical methods if the differential equations are attacked classically and reduced to algebraic equations which are then solved numerically or (2) numerical methods where the differential equations are first replaced by their numerical counterpart and then solved directly.

Analytical Methods

Analytical methods in shell analysis usually result in closed-form solutions or series solutions. Closed-form solutions are sometimes exact solutions of the differential equations, but they may also be identified with so-called boundary-layer techniques. In boundary-layer techniques, the equations are broken into a set of simple equations for the interior of a shell structure and a more complicated set for a zone near the boundary. Such techniques can be tailored to study the behavior of shells for loadings and boundary conditions in which all important deformations occur in a narrow zone near the shell boundary. Series solutions, on the other hand, are identified usually with approximation techniques such as the Galerkin or Ritz methods or Fourier expansions of the differential equations. Such methods, if carried far enough, lead to an accurate solution at any point within a shell contour.

The advantages of analytical methods stem from having available explicit equations to examine which, in themselves, may give the analyst important information on shell behavior as design changes are made. The equations may be manipulated so that limiting cases may be determined precisely in order to check the solution. Parameters natural to the problem may be identified and they may be varied conveniently to determine rapidly the essential behavior of the shell over a wide range of values.

Analytical methods have two distinct disadvantages. First, they require a knowledge of a variety of sophisticated solution techniques of ordinary or partial differential equations. Second, a given form of analytical solution is invariably limited to shells of simple geometric shape such as cylindrical, conical, or spherical, and subject to simple loadings.

Numerical Methods

There are three important approaches in numerical methods of shell analysis: the finite element method, the finite difference method, and the forward integration method. In the finite element approach, the structure is broken up into a finite number of relatively simple physical elements and the set of equations for each element is solved approximately except for a group of constants. These constants are determined to satisfy conditions of continuity and/or equilibrium among the elements. Use of a variational procedure automatically provides a best choice of the finite element equations governing a structure within the limits assumed for element models. In the finite difference approach, derivatives in the equations are simply replaced by difference expressions and integrals by sums. In the forward integration method, the problem is converted into an initial value problem and the solution is projected

forward in space by a technique such as the standard Runge-Kutta method. A comparison of the characteristics of the forward integration and the finite difference methods along with their advantages and disadvantages is presented in reference 8 for shells of revolution. All three approaches give solutions approaching the exact solution if enough properly defined elements or enough difference or integration stations are used.

Numerical methods have the advantage of very general application; that is, a formulation may be applied to wide varieties of problems with minor modifications. Practical shell problems invariably have complications such as variable thickness, wall stiffening, a variety of loading conditions or combinations of loads, a variety of boundary conditions or complicated shapes not easily specified by equations. Such complications are almost impossible to handle by analytical methods, but can be handled in almost routine fashion by numerical methods.

There are some disadvantages to numerical methods. Obviously, there must be a computer of adequate capacity available to the analyst. The output of a computer using numerical methods is often a vast array of numbers, and this situation sometimes obscures trends that might be obvious from an algebraic formula. Finally, numerical methods are sometimes difficult to check, and limiting cases may not be as easily obtained as with the use of analytical methods.

THE IMPACT OF THE COMPUTER

Numerical methods could not be used extensively until computer capability had been increased to present-day levels. Only now are we able to use general purpose computer programs that will handle wide classes of shell configurations. Of course, the computer has also expanded our analytical capability. In the sections that follow, some of the consequences of the use of the computer will be examined.

The Effect of the Computer on Solution Techniques

The use of the computer requires all analyses to be reduced to a set of algebraic equations. Solution techniques as used here are those sequences of operations required to solve these algebraic equations.

Analytic solution techniques.- The impact of the digital computer on analytic techniques has been modest. Primarily, it has allowed more terms to be taken in series solutions so that solutions with slowly converging series are now feasible. The computer has also permitted accepted standards for the accuracy of such solutions to improve. The computer does not appear to have stimulated the development of new analytic solution techniques.

Numerical solution techniques.- By contrast, the availability of high-speed digital computers has spurred a number of advances in numerical solution procedures. For example, for nonlinear problems involving many equations, the powerful Newton-Raphson solution technique has been developed for numerical use. Hybrid combinations of Newton-Raphson and other nonlinear solution techniques have also been developed with great success. Because of their great capability for repetitive application of simple operations, and because of their great speed, computers also admit numerical methods that were too cumbersome previously, such as the method of forward integration. Similarly, the computer has given finite difference and finite element methods great significance by admitting problems of great scope involving large numbers of simultaneous equations.

Shell Analysis and Design

This section will present a discussion of the recent expansion of shell studies, the effect of this expansion on the analyst and designer, new communication problems of the analyst and designer, and, finally, some missing links which are limiting the potential for computer analysis of shell structures.

Expansion of shell analysis and design capability.- Numerical methods have led to the general purpose shell computer program so that almost any problem can be solved with minimum idealization of the shell's structural detail. For example, the effects of discrete stiffening attached to one side of a shell can be included in the analysis instead of considering the overall, smeared out, effect of stiffening. This point is illustrated further by the fact that a "complicated" problem solved 10 years ago was the nonlinear axisymmetric buckling of a spherical cap of uniform thickness (refs. 9 and 10), whereas a "complicated" problem solved just recently is illustrated in Figure 9 taken from reference 11. In the older problem, numerical methods were used with even station spacing, together with an iteration technique. In the newer problem, the axisymmetric shell structure of Figure 9 was symmetrically and nonsymmetrically loaded and is a layered orthotropic, longitudinally stiffened shell reinforced by rings which were treated as discrete structures. A general purpose computer program was used which was formulated from the energy with the method of finite differences. Different station spacing was used in different segments. Maximum stresses and buckling loads and configurations were determined. This general program can work the 10-year-old problem routinely and with ease. This is a fairly dramatic extension of analysis capability.

With on-the-shelf general purpose programs available, the designer can quickly check out a wide variety of design systems or design changes in order to investigate the impact on weight. In fact, such programs will be an integral part of direct synthesis programs for minimum weight shells. Developments of this type have already begun. A program for the automated design of integrally stiffened cylinders under combined loads is already operational and a program for the automated design of stiffened cones is essentially complete. Results from the latter program are shown in Figure 10* where it has been

*The author is indebted to Dr. W. A. Thornton, Clarkson College, for this example.

applied to the design of a minimum weight conical shell subject to a given external pressure. The shell is clamped at its small end and assumed to have an essentially inextensible ring at its large end. Four design variables, the shell thickness, and the thickness, diameter, and spacing of tubular rings, have been determined for minimum weight subject to a number of constraints. These include sheet minimum gages, skin and ring yielding, panel buckling, ring buckling, and general shell instability. Design results are shown on the lower left. The margins of safety at the lower right reveal that skin yielding, gross buckling, and panel buckling were the important considerations.

The most difficult aspect of this analysis is the accurate calculation of general shell instability. In many previous synthesis programs such as for cylinders, simple analytic expressions were used that could not be extended with accuracy to more complicated geometries that might result in the least weight. This program makes use of a general shell of revolution computer program indicating that extension of synthesis problems to more general shapes yet retaining necessary accuracy is feasible.

With the present expansion of shell analysis, it is logical to assume that interdisciplinary analysis will increase in importance. Aeroelastic analysis and coupled hydroelastic or thermoelastic analysis are examples of types of analysis which will become more prominent. Figure 11 presents a sample of some results in a coupled hydroelastic analysis (ref. 12). These results were obtained by the numerical solution of the rather complicated combined hydrodynamic and shell equations. The pressure results for axisymmetric impact of shells on water are compared with the pressure obtained if the shell were a rigid body. Such an impact loading may be a critical design condition and obviously serious errors (not necessarily conservative) in stress and buckling results would occur if the interaction were not included.

Influence on the analyst and designer. - One clear impact of the computer has been the growth of perspective of the shell analyst. The day of the specialist who devotes a lifetime of research to a narrow class of shell problems and solution techniques is gone. The power to examine a broad spectrum of shell structures and problems, which the computer has provided, forces the analyst to a broader outlook and probably brings his outlook and that of the designer closer together. Of course, the shell synthesis program represents a unity of these two viewpoints.

But computerized shell analysis can have a powerful hypnotic effect, too. The lazy analyst is tempted to rely too heavily on the machine and to accept inefficient solution techniques, and there is the danger of total reliance on numerical computer results to the neglect of the analyst's intuitive judgment of the physical nature of the problem. Another danger for the unwary analyst is inherent in the nature of the usual computer output - a blizzard of numbers. Errors in the solution are thus often difficult to detect. Automated plotting and other visual displays of results tend to remedy this problem; however, these devices are often neglected in computer program development and there is a need to implement methods in new programs for the most effective display of results so that the physical meaning is understood and errors are easily detected.

Communication.- Program documents usually contain a writeup of basic theory and a user's manual including a listing of the program. The process of assimilating this information is usually difficult and laborious. Often, the analyst would rather set up his own less general program than try to fathom an available program which was devised to do essentially his problem. This duplication and wasted effort can only be avoided if the program is easy to use with relatively simple input and the documentation accompanying the program is complete, clear, and concise so it offers the user an advantage in investing his time in learning the new program.

It is worthwhile for the developer, as well as the receiver, that the documentation and the computer program itself be frequently updated. For example, errors may be found in parts of the program that were not used previously. Algorithms in weak parts of the program may be improved. New limitations of the program may be determined. Moreover, use of a program helps debug it and improve it; thus, use increases the value of the program. Proprietary programs which lie unused may thus stagnate and become obsolete. The author believes that shared programs, with their greater potential for frequent use, will grow in their solution power and pay bigger dividends to the developer and, through sharing, the quality of the analysis of shells will rise to the level of the best engineering talent.

In a similar vein, the value of a computer program to a designer is proportional to its use. The designer will be able to apply intuitive judgment for problems involving geometry and loads within his previous experience, but would probably have difficulty for problems beyond his previous experience. A wider scope of experience can be provided if development of each new computer program is immediately followed by a limited parameter study leading to published charts. Each study should explore a new parameter regime made accessible by the development of the program. This would automatically lead to extension of the shell designer's knowledge of shell behavior and contribute to safer, more efficient designs. Therefore, the author strongly recommends that every new general purpose program be accompanied by such parameter studies.

Influence on shell theory and experiment.- The computer analysis of shells will be no more accurate than the theory on which the analysis is based. Therefore, a few major weaknesses of theory should be mentioned. A criterion for establishing relative merits of various versions of linear theory exists (ref. 3), but a corresponding criterion for establishing the relative merits of the various versions of nonlinear shell theory has not been derived to the author's knowledge. With the number of such theories growing and their extreme complexity undiminished, the analyst needs some convenient basis for a rational choice.

The buckling load of thin shells is often considerably lowered by the presence of small imperfections in shape. The present method of studying imperfection sensitivity is by analysis of the initial postbuckling behavior of perfect shells. This approach has been partly successful, but needs much more development before it is ready for practical application by the analyst in support of shell design. The capacity for brute force account of known imperfections in shape by nonlinear, general-shell computer programs is emerging, but is likely to be very costly for the foreseeable future. Especially difficult will

be development of methods to account (perhaps statistically) for probable imperfections in shells before their manufacture.

Experimental research has not kept up with our ability to solve theoretical shell problems of great complexity. For example, the computer has made possible the analysis of end ring stiffness requirements for shells of revolution. This is significant advancement in design capability, but there is, as yet, no experimental verification of these methods. Therefore, their application by the practical designer will be inhibited by his natural reluctance to use unproven methods. There is an obvious deficiency here, and the author strongly recommends that experimental programs be accelerated to study the limitations of computerized methods.

CONCLUDING REMARKS

For the benefit of those who are not shell experts, this paper has reviewed the complexity of thin-walled shell structures, described the basic ideas leading to shell theories, and surveyed the important kinds of shell behavior and shell problems of interest to the designer.

The availability of the electronic, digital computer has greatly affected the capacity of the analyst to deal with shell problems. It has stimulated the development of numerical solution techniques and greatly increased the analyst's solution power. A principal impact is the new capacity to obtain solutions for very general shell configurations incorporating structural details that occur in practical design. The computer has forced the analyst to learn a new language to prepare for its effective use and has greatly increased his perspective, bringing it closer to that of the designer. The great complexity of computer programs makes them difficult to communicate and their output difficult to interpret.

The consideration of these factors has led to a number of recommendations. Program documentation should be precise, complete, and frequently updated; programs should be freely shared because of their tendency to improve with use to the benefit of all. New programs should be applied to parametric analyses for generation of design charts to help extend the shell designer's knowledge. Certain missing links in shell theory should be developed, criteria for a proper choice of nonlinear shell theories should be established, and methods for account of imperfections in buckling analysis need further development. Finally, experimental programs must be accelerated to verify computerized shell analysis methods so that they merit the designer's confidence.

REFERENCES

1. Love, A. E. H.: A Treatise on the Mathematical Theory of Elasticity. Fourth Ed., Dover, 1927.
2. Novoshilov, V. V.: Thin Shell Theory. Second Ed., English Translation, P. Noordhoff, Ltd., 1964.
3. Koiter, W. T.: A Consistent First Approximation to the General Theory of Thin Elastic Shells. Proceedings of the Symposium on the Theory of Thin Shells, North Holland Publishing Co., Amsterdam, 1960.
4. Kalnins, A.: Analysis of Shells of Revolution Subjected to Symmetrical and Nonsymmetrical Loads. Journal of Applied Mechanics, Trans. of the ASME, vol. 31, ser. E, no. 3, 1964.
5. Jordan, Peter F.: Stresses and Deformation of the Thin-Walled Pressurized Torus. Jour. of the Aerospace Sci., vol. 29, no. 2, 1962.
6. Arnold, R. N.; and Warburton, G. B.: Flexural Vibrations of the Walls of Thin Cylindrical Shells Having Freely Supported Ends. Proc. Royal Soc., vol. 197, ser. A, no. 1048, 1949.
7. Liepins, Atis A.: Asymmetric Nonlinear Dynamic Response and Buckling of Shallow Spherical Shells. NASA CR-1376, 1969.
8. Anderson, M. S.; Fulton, R. E.; Heard, W. L., Jr.; and Walz, J. E.: Stress, Buckling, and Vibration Analysis of Shells of Revolution. Conference on Computer Oriented Analysis of Shell Structures. Palo Alto, Calif., Aug. 10-14, 1970.
9. Keller, Herbert E.; and Reiss, Edward L.: Spherical Cap Snapping. Jour. of the Aerospace Sci., vol. 26, no. 10, 1959.
10. Budiansky, B.: Buckling of Clamped Shallow Spherical Shells. Proceedings of the Symposium on the Theory of Thin Shells, North Holland Publishing Co., Amsterdam, 1960.
11. Bushnell, David: Computer Analysis of Complex Shell Structures. AIAA Paper No. 70-138. AIAA Eighth Aerospace Sciences Meeting, New York, N.Y., Jan. 19-21, 1970.
12. Wilkinson, J. P. D.; Capelli, A. P.; and Salzman, R. N.: Study of Apollo Water Impact. North American Aviation, Inc., Space Division Report SID 67-498, vol. 3, May 1967.
13. Stein, Manuel: Some Recent Advances in the Investigation of Shell Buckling. AIAA Journal, vol. 6, no. 12, 1968.

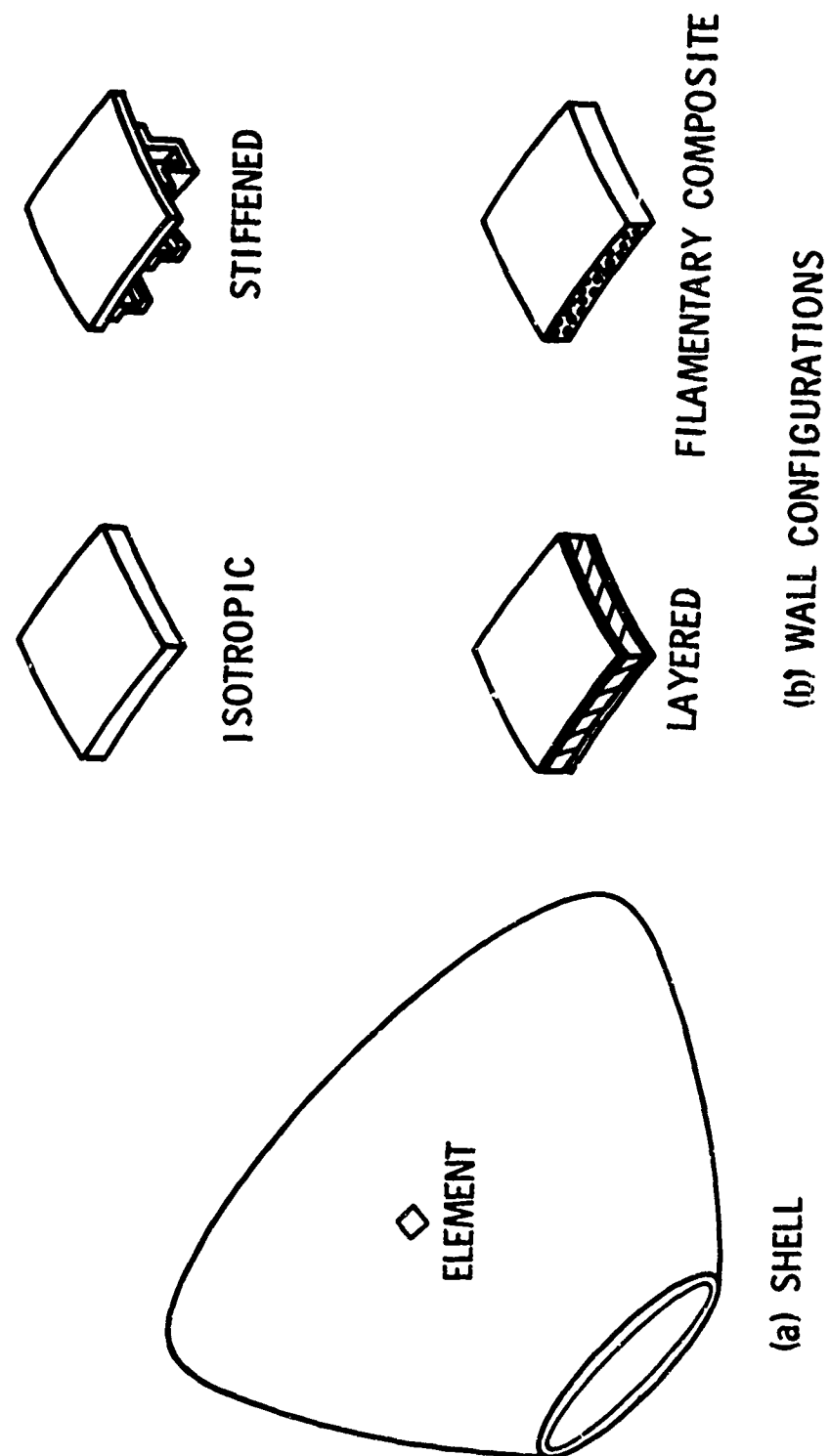
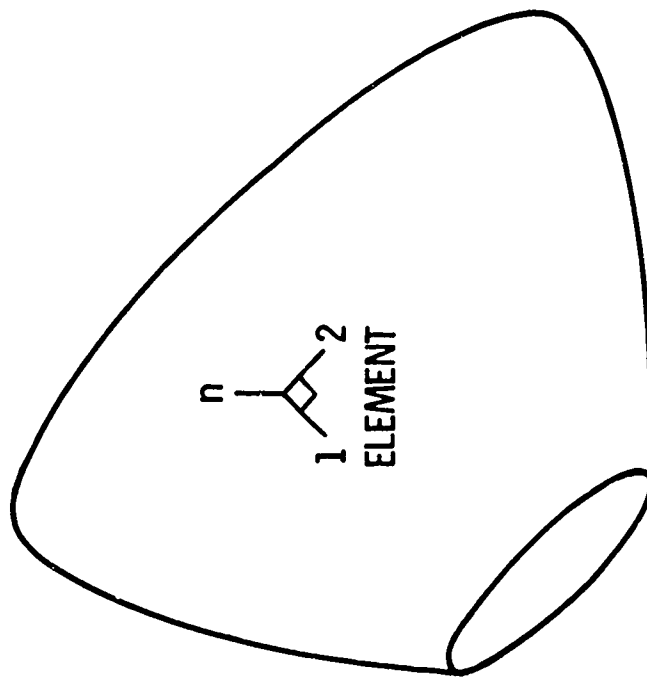


Figure 1.- Sketches illustrating various shell wall configurations.



SHELL REFERENCE SURFACE

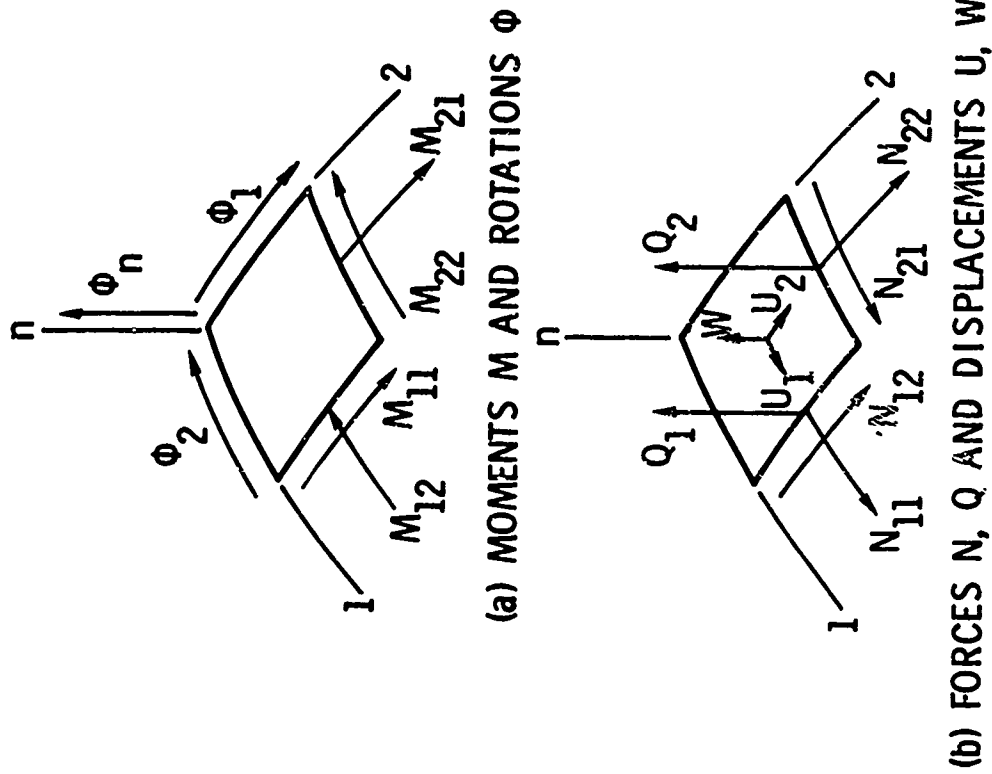


Figure 2.- Sketches showing the moments, rotation, forces, and displacements associated with the shell reference surface.

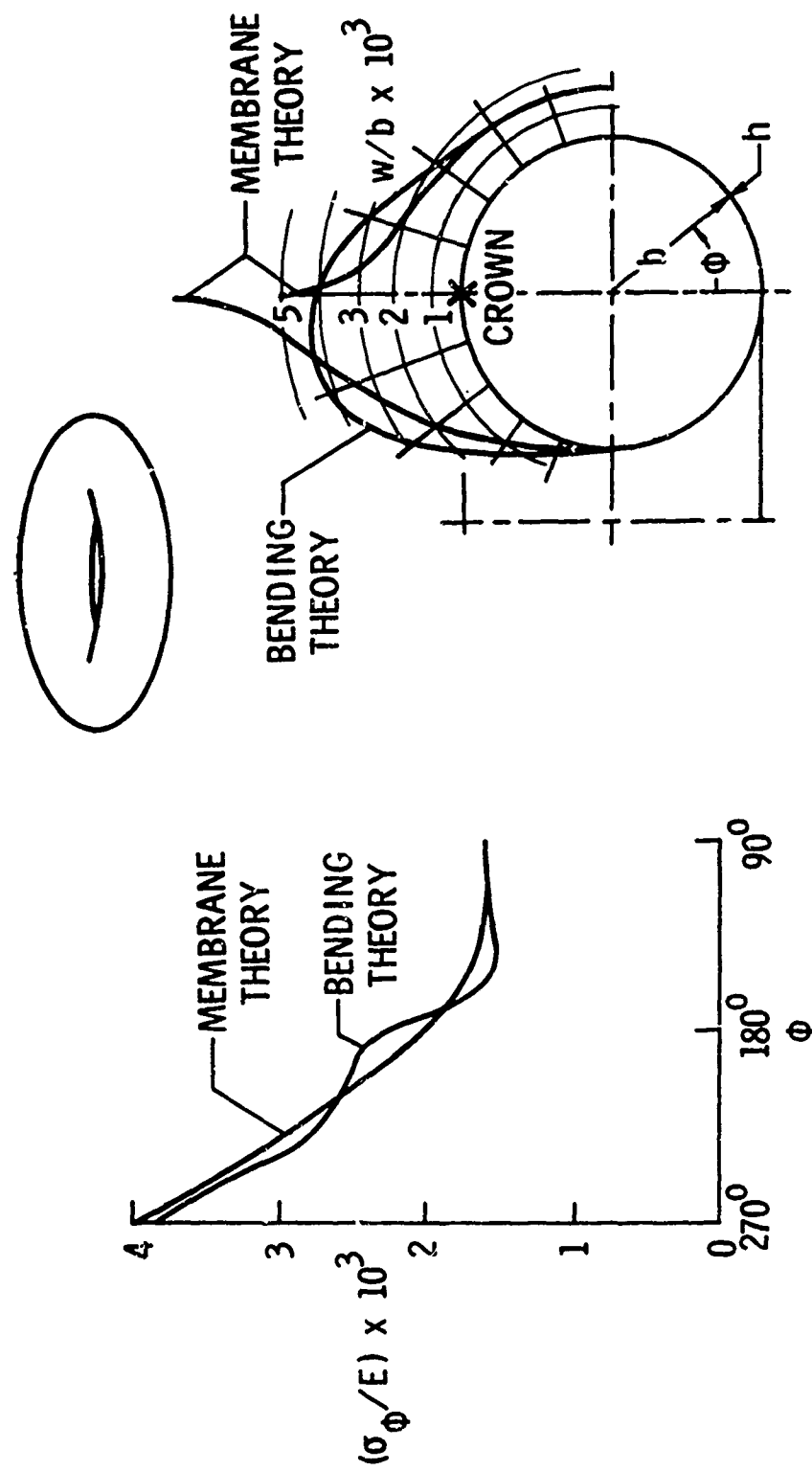
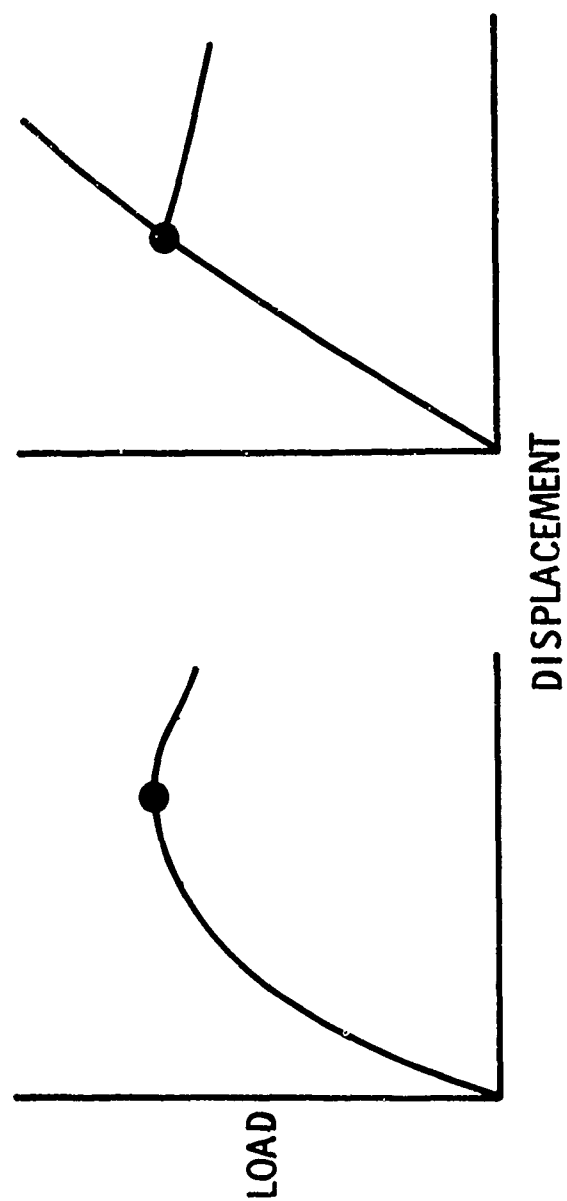


Figure 3.- Meridional outer fiber stress σ_ϕ and normal displacement w of a pressurized torus (ref. 4). Pressure parameter $p b / E h = 0.002$. Thickness-radius ratio $h / b = 0.05$.



(a) MAXIMUM LOAD (b) BIFURCATION BUCKLING

Figure 4.- Sketches illustrating the characteristic load-displacement curves for bifurcation and nonbifurcation buckling.

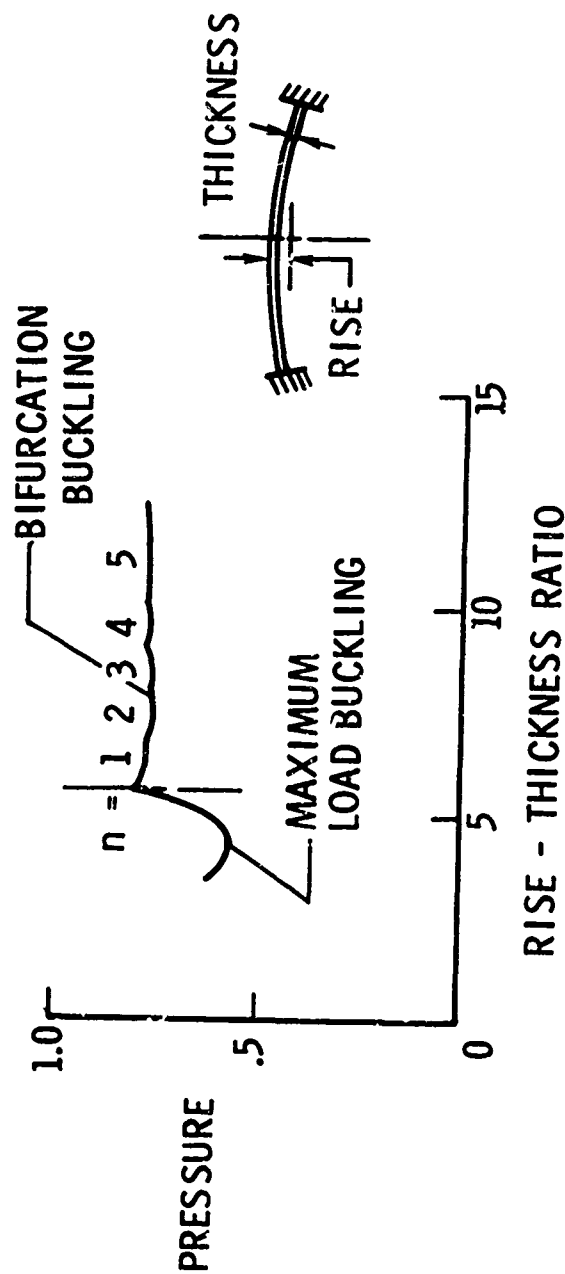


Figure 5.- Buckling pressure for shallow spherical shells under external pressure (see ref. 13);
 n = number of circumferential waves.

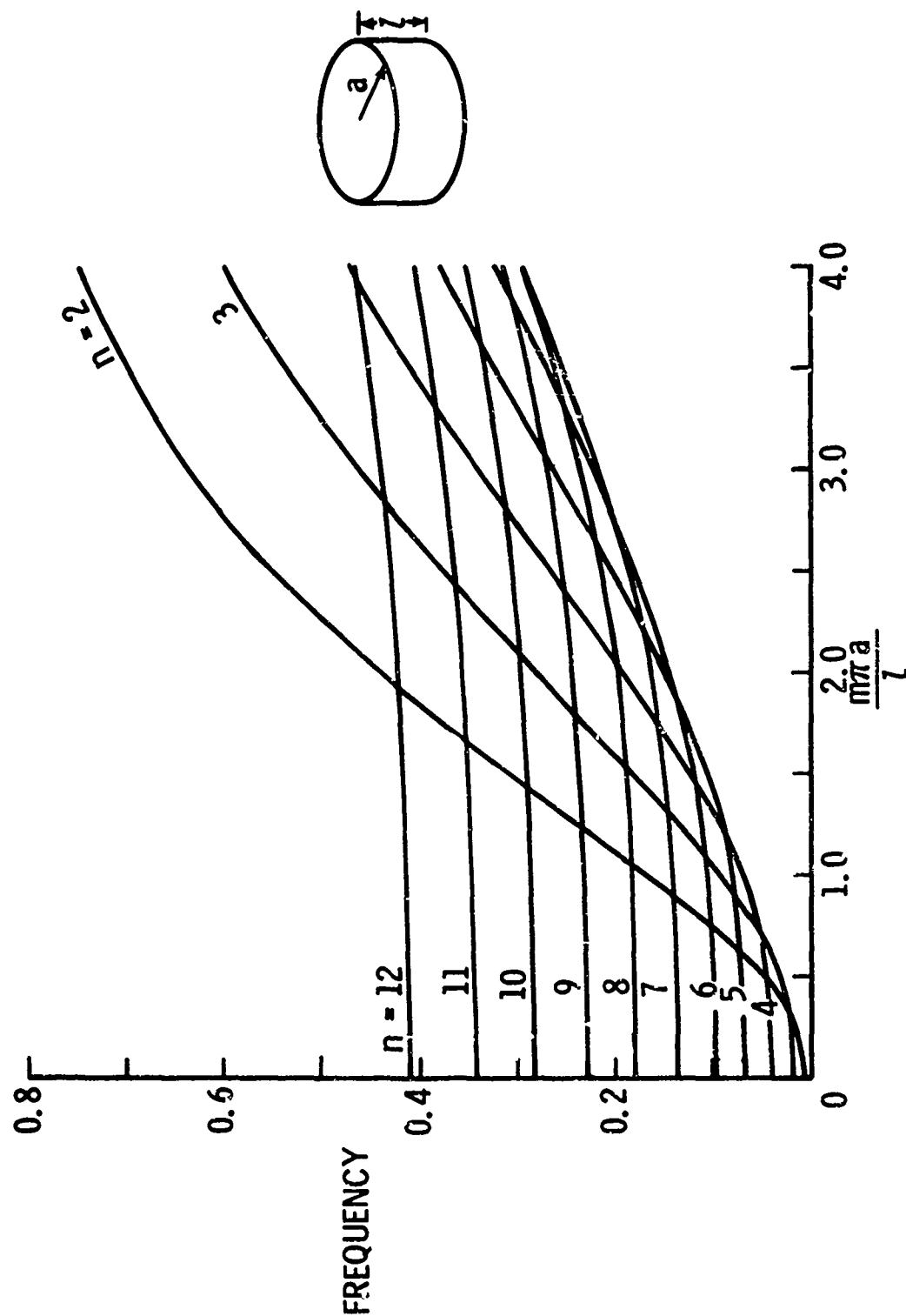


Figure 6.- Nondimensional natural frequencies for simply supported cylinders (ref. 6). Thickness-radius ratio = 0.01; m is the number of axial half waves; n is the number of circumferential waves.

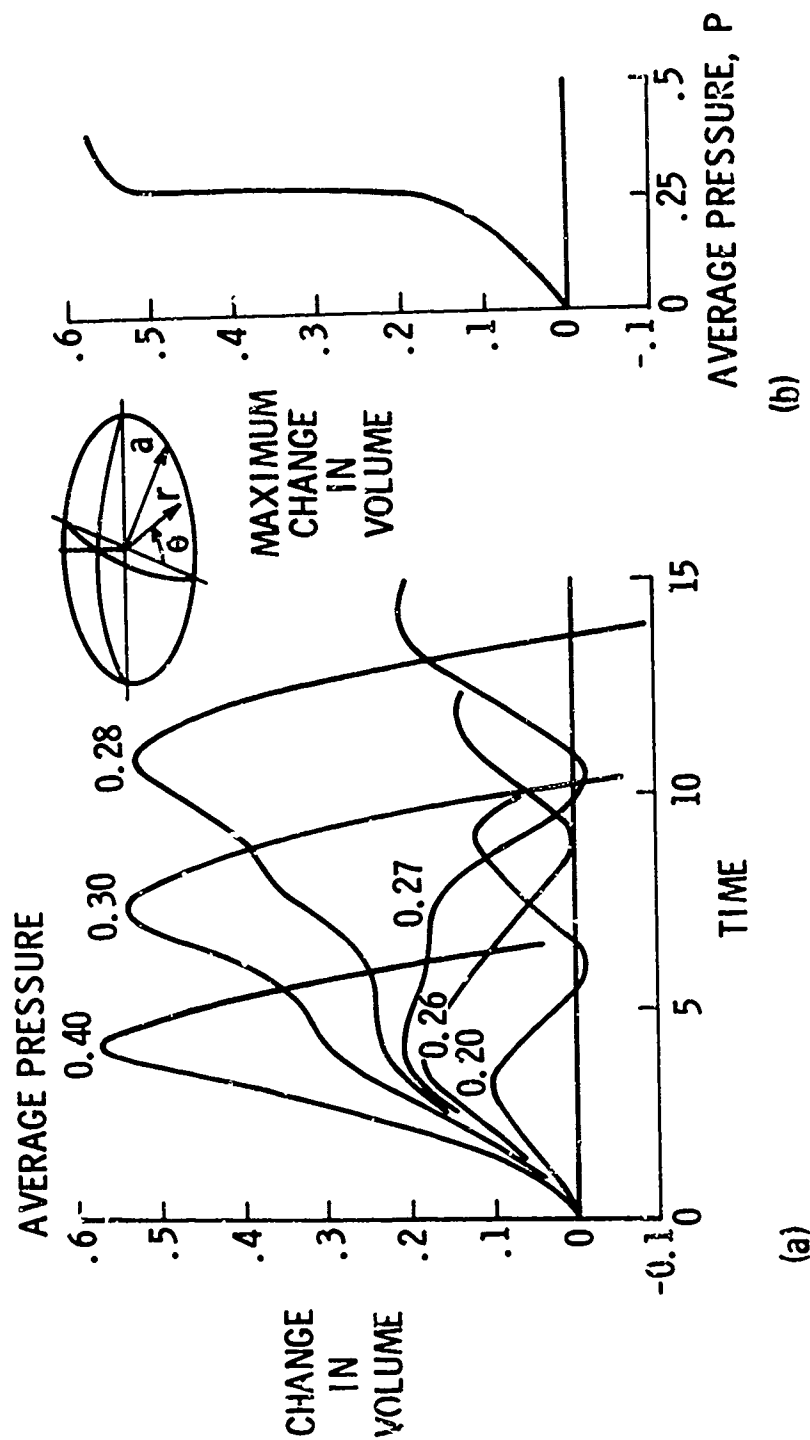


Figure 7.- Transient loading of a simply supported shallow spherical shell with a (step, linear-across-a-diameter) pressure distribution, zero for time less than zero, $P(1 - \frac{r}{a} \cos \theta)$ for time greater than or equal to zero (ref. 7).

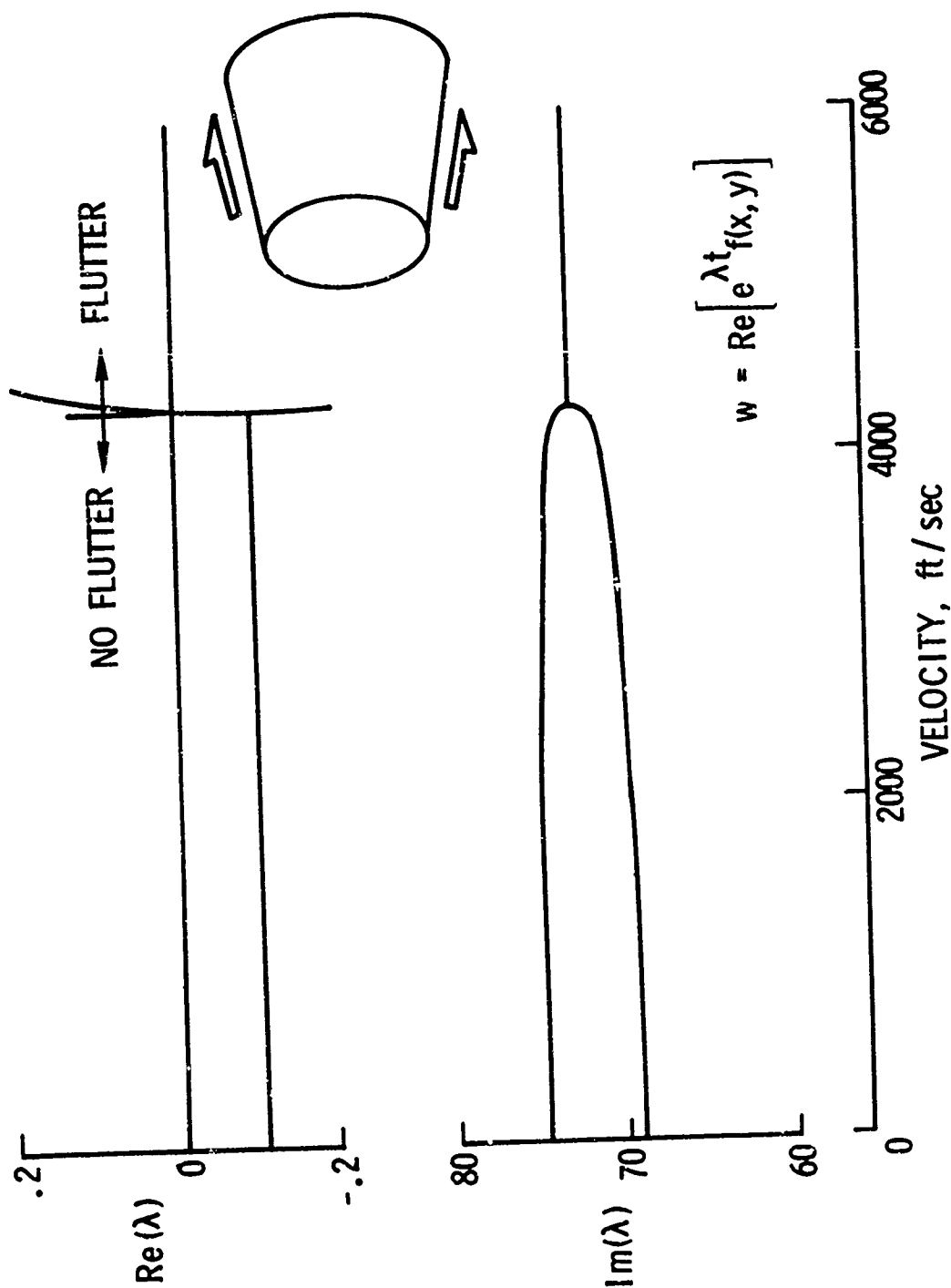


Figure 8.- Form of the real and imaginary parts of the complex eigenvalue λ appearing in the equation for the deflection w for the flutter of a circular conical shell in supersonic flow.

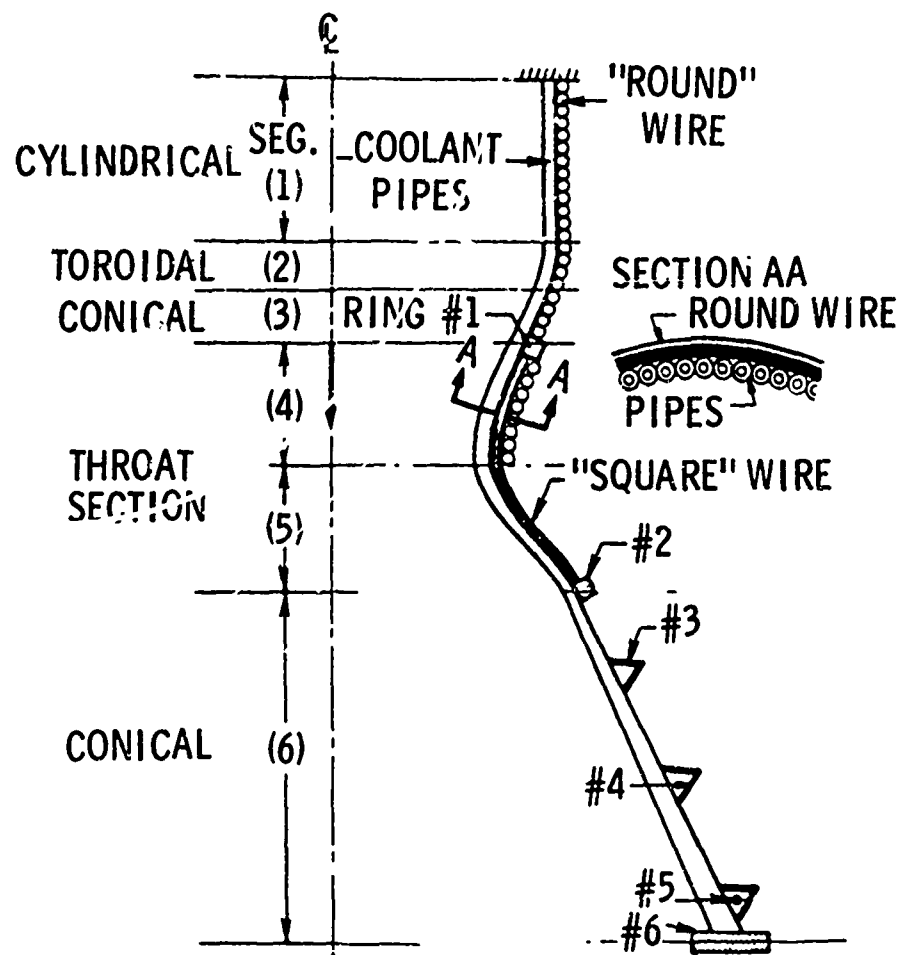
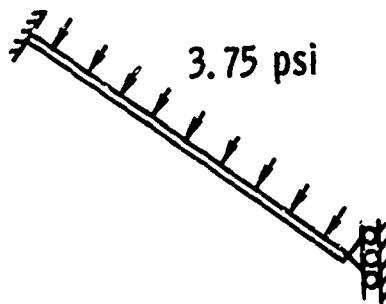
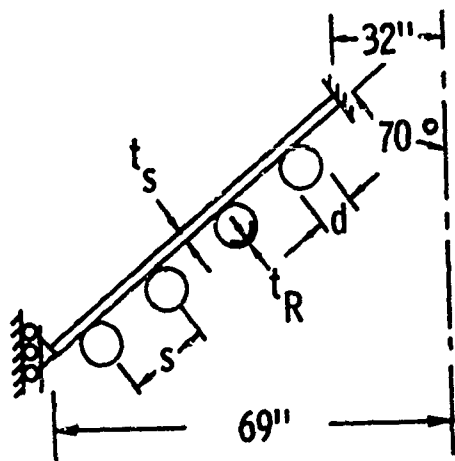


Figure 9.- Wall construction of complex nozzle structure (ref. 11).



(a) CHOSEN VALUES AND UNSPECIFIED PARAMETERS

MAGNESIUM

$$t_s = .048''$$

$$t_R = .010'' \text{ (Min. Ga.)}$$

$$d = 1.02''$$

$$s = 1.83''$$

$$\text{WEIGHT} = 52.7 \text{ lb}$$

MARGINS OF SAFETY

$$\text{SKIN YIELDING} \quad .004 \leftarrow$$

$$\text{RING YIELDING} \quad .276$$

$$\text{RING BUCKLING} \quad .497$$

$$\text{GROSS BUCKLING} \quad .027 \leftarrow$$

$$\text{PANEL BUCKLING} \quad .057 \leftarrow$$

(b) FINAL DESIGN

Figure 10.- Automated design of a stiffened conical shell.

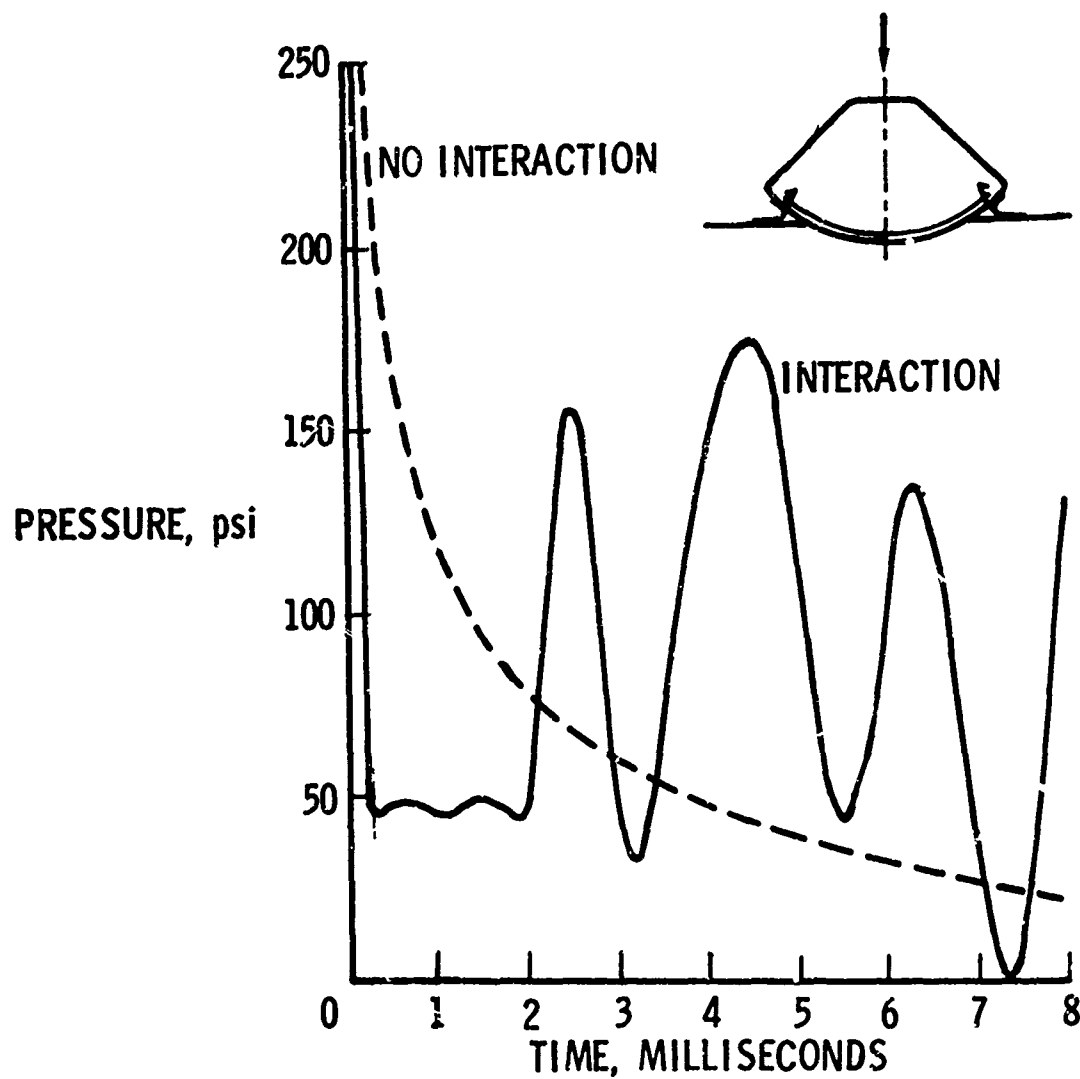


Figure 11.- Time history of pressure at the shell apex for axisymmetric impact of shells on water (ref. 12).

QUESTIONS AND COMMENTS FOLLOWING STEIN'S PAPER

QUESTION: Would you care to comment on how we might avoid the generation of excessive output from the computer? If we don't put the results on the printed page, where do we put it and in what form?

STEIN: One of the recommendations in my paper was that plotting techniques should be used. Computer programs should be planned so that those quantities which are important to the analyst or other program user can be plotted.

QUESTION: We are all aware of the difficulties encountered in getting a program which was developed on one piece of hardware to work on another piece of hardware. If we go one step further and incorporate plot routines in the program, do you anticipate greater problems; or should each user organization have their own plotting routines and then put those into the program?

STEIN: One of the principal uses for plotting is in the development stage where it is great for debugging and checkout. When it comes time to share the program with users having different equipment, there will, of course, be problems. However, these are by no means insurmountable.

COMMENT: It has been my experience that it requires considerably more effort to make a computer program user oriented than it does to develop the program. A tremendous amount of effort is associated with

documentation, checkout, parameter studies and preparation of user's manuals. Historically, funding agencies have not provided the funds necessary to do much more than develop the code. As a result, many such codes have never realized their full potential. I think we are going to have to face up to the fact that it costs money to make new technology user oriented.

COMMENT: You touched on the reluctance of analysts to accept for use programs with which they are not familiar. Because it takes so much time to learn a new program, he may not use the most efficient program for his problem, or he may derive a special program for his particular problem. In cases where a number of people in an organization are occupied with shell analysis, it might be a good idea to have a specialist on computer programs who learns the new programs as they come out, and if he thinks they are worthwhile, he can implement them and act as a consultant to others who may use them.

COMMENT: Two comments: first, I liked your remark on generating design charts with any new program of general nature, but it's practically impossible to find anybody who is willing to put up with the bulk of computer time that is required for such studies. Second, we find that it's possible to eliminate much unnecessary computer printout by simply not even generating printed output the first shot. Instead, we look at the plotted output. It's very much easier to plot stress isobars on any shape you have, look at them and then select and print out only the areas of interest for your highest stress and so forth. We do that routinely.

COMMENT: First, I want to say that at Ford we are using computer graphics quite extensively for structural analysis on a production basis. Basically, the engineer picks out what he wants from a graphical display and has hard copy plots made. This includes input and output data, checking, and so forth and so on. I also have a question with regard to the automatic design example you consider in Figure 10. Did you use a special purpose algorithm for optimization for this specific problem or was a general purpose optimization routine used to find the minimum weight?

STEIN: The computer program that was used in this work was for an axisymmetric shell. I believe the parameters were chosen and computer algorithms were then used to find minimum weight.

QUESTION: Were these general purpose algorithms, or were they for this specific problem? In other words, do you use a general purpose optimization technique coupled with a general purpose structural program?

STEIN: The example was based on a problem solved by Bill Thornton who is at Clarkson University. I believe he used a Fletcher Powell algorithm or something of that sort. That's all the information I have on the problem.

COMMENT: I believe that some of the excessive computer output which has been discussed here today is caused by dumps requested by the user "just in case." In order to minimize this, I can conceive of employing an auxiliary storage facility connected to the computer on which a dump would be made automatically in the event of an error. The dump

could then be requested by the user for a period of up to 24 hours after the run if he felt it was necessary. After that time the dump would be scratched without ever having been printed.

COMMENT: I've heard several comments here today to the effect that more money should be spent to generate design charts and perform parameter studies. It seems to me that no matter how many charts we generate, you never seem to be able to find the particular problem you have amongst those included in the charts. This is especially true for multiparameter problems. Thus, you end up having to generate the answer to your problem anyway. In my opinion, it's much better to forego the parametric studies and design charts and develop a well documented computer code which can be given to others so that they can generate the answers to their own specific problems.

COMMENT: I think we're missing the boat a little bit on the parameter study. The principal value is not the charts that come out; certainly they're helpful but I think it's the exercise that the code goes through in generating the charts that is valuable. It helps us find the bugs and make the code more reliable. So I really don't think the previous comment is valid.

One further remark and that is that plots are not always the answer. I've gotten rolls of plots that are just as bad as stacks of output. It seems that invariably the plot I want is in the middle of the roll or at the end. I would like to see the rolls done away with and have the plots produced in flatfold form in the same way the output is so that you can thumb through and go to the middle or the back and not have to roll it all out on your desk.

COMMENT: We sponsor quite a few parameter studies at Oakridge National Laboratories and have found the results to be very useful. People in the pressure vessel field, for example, save a lot of money using design charts and more could be saved if parameter studies were available for the analysis of many off-the-shelf items.

COMMENT: I refer again to this question of parameter studies. I think that one important aspect that really hasn't been brought forward here is that when you have a general purpose code developed and operational many people tend to think that all of the problems in engineering have been solved and that when a new problem comes up all you do is run to that code and get the answer. In fact, we have found that even when using our general purpose codes which are debugged and are reliable, it takes often many months or as much as a year to solve complex problems. Having parametric studies performed by the engineers who will use the code gives a great deal more insight so that the next time around you could use the code much more efficiently, avoid many of the pitfalls in modeling and many other pitfalls which lead to poor results. I think that parameter studies are also very useful when you consider trying to solve a new class of problems. So I think these parametric studies have a lot of value that is really being overlooked here.

THE NUMERICAL METHODS
OF
DISCRETE SHELL ANALYSIS

By

Gilbert A. Greenbaum, Manager, Applied Mechanics
Universal Analytics, Inc.

Anthony P. Cappelli, President
Universal Analytics, Inc.

ABSTRACT

This paper reviews the numerical methods used to analyze shell structures. For presentation purposes, shell configurations are classified according to the number of directions in which the shell must be discretized in order to determine a solution. One-, two-, and three-dimensional shell configurations are then discussed for each numerical method presented. The paper limits detail discussion to the finite difference, numerical integration, and finite element methods. Major advantages and disadvantages of each method are given, and areas which need further study are outlined. The paper concludes with a discussion of the types of problems solved by all three methods. It is pointed out that all three methods have been successfully used to solve many shell problems and each has a definite place in shell analysis.

1. INTRODUCTION

During the past decade great strides have been made in the design and analysis of shell structures. These advances have been made possible by application of discrete numerical analysis methods using high speed digital computers. By using these numerical methods it is possible to obtain solutions to shell problems involving such complexities as irregular surfaces, variable thicknesses, anisotropic material properties, and nonlinear behavior.

This paper is being presented at this shell conference to define and compare the most widely used numerical discrete shell analysis methods. In particular the paper will solely be concerned with the finite difference [1-7]*; numerical integration [8-12], and finite element displacement methods [13-43]. It is recognized that other numerical methods (e.g., collocation [44]) have been successfully used in shell analyses. However, in most cases these applications have been limited to specialized shell problems and for this reason will not be presented here.

It should be pointed out at the beginning that the paper will not present any new technique nor seek to ascertain or establish the "best" numerical method. However, an attempt will be made to present the fundamental basis for each method and review the application of each method in solving shell problems. Advantages and disadvantages of each method will be pointed out for specific shell classifications. Although many improvements have been made in the three numerical methods discussed, there are still areas which require further refinement. Therefore the paper will also attempt to cite these areas.

The various shell computer programs which employ the reviewed numerical methods will not be discussed in this paper. They will be presented by other shell conference papers, and a comprehensive assessment of these programs is given by Hartung [45].

2. SHELL CLASSIFICATIONS

Prior to discussion of numerical methods, it is convenient for this presentation to classify various shell configurations. Adopting a procedure similar to Hartung [45], shell configurations will be classified according to the number of directions in which the shell must be discretized in order to obtain a solution.

Based on this classification, the simplest problems involve thin shells of revolution subjected to axisymmetric loading. This problem need only be discretized in the meridional direction, since the shell solution does not vary in the circumferential direction. At the other end of the spectrum is the three-dimensional (3-D) class, which includes thick shell problems. In

*Numbers in brackets refer to references at the end of the text.

general the 3-D class requires that the shell be discretized through the thickness as well as over its surface. A partial list of shell configurations classified according to the above standard is given below.

One-Dimensional (1-D) Problems

- Thin Shells of Revolution - Axisymmetric Loads
- Thin Shells of Revolution - Nonsymmetric Loads (uncoupled Fourier harmonics)
- Thin Shells of Revolution - Nonsymmetric Properties (coupled Fourier harmonics)
- Thin Shells of Revolution - Nonlinear Behavior (coupled Fourier harmonics)
- .
- .
- .

Two-Dimensional (2-D) Problems

- Thin "Shells of Revolution" with cutouts or nonhomogeneous boundaries
- Arbitrary Thin Shells
- Intersecting Thin Shells
- Thick Shells of Revolution - Axisymmetric Loads
- Thick Shells of Revolution - Nonsymmetric Loads (uncoupled or coupled Fourier harmonics)
- .
- .
- .

Three-Dimensional (3-D) Problems

- Thick "Shells of Revolution" with cutouts or nonhomogeneous boundaries
- Arbitrary Thick Shells
- .
- .
- .

Generally, the classification is dictated by the number of independent variables required to describe the problem. However, as noted above, advantage can be taken of shells of revolution configurations to reduce an apparent two-dimensional problem to a one-dimensional discretization. For example, in treating thin shells of revolution under nonsymmetric loading, the loading and shell response variables can be expanded in a Fourier series in the circumferential direction [1-3]. For linear problems this results in a set of uncoupled problems, one for each Fourier harmonic considered. Each of these uncoupled harmonic problems is solved using a one-dimensional meridional discretization, and the solution to the original problem is obtained by superposing harmonic solutions.

For nonlinear problems [6,10] or shells having variable circumferential stiffness properties [3], the Fourier decomposition technique results in a set of equations in which the harmonics are coupled. Although this problem is much

more complicated than the uncoupled problem, the resulting equations still only require a one-dimensional discretization. Unlike Hartung [45], the present authors feel that this type of problem should still be generally classified as one-dimensional. It should be mentioned that sometimes these types of problems are better solved using a two-dimensional discretization. An example of this would be a shell having a discontinuous or highly localized circumferential stiffness or loading variation. For these cases, if a two-dimensional discretization is used, then according to the above standard the problem is classified as 2-D.

Several one- and two-dimensional problems are shown in Figure 1. One-dimensional configurations for simple, stacked and branched shells of revolution are illustrated in Figures 1a, b, and c respectively. Figures 1d, e, and f show typical two-dimensional configurations. Shaded regions indicate areas where a three-dimensional analysis may be required.

3. FINITE DIFFERENCE METHOD

The finite difference method is a widely used technique for the numerical solution of the shell differential equations. The fundamental basis of the method is the approximate evaluation of continuous derivatives using discrete point formulas. The method can be applied directly to the governing differential shell field equations (e.g., [1-6]) or to the potential energy expression [7]. In the latter case the final algebraic equations are obtained by minimizing the potential energy.

The specific finite difference expressions used are dependent on the form of the differential equations. As an example, let us consider the eight-order system of field equations (e.g., see [46]) frequently used in the linear analysis of shells. This system can be represented in the form of two partial differential equations, each of fourth order, or four second order differential equations, etc. A fourth order formulation would, of course, require finite difference formula for approximating fourth derivatives, and similarly for other derivatives.

To illustrate the application of the finite difference method, let us consider the eight-order shell of revolution system represented, after Fourier harmonic expansion, by four second order ordinary differential equations [1]. The matrix form of this set of field equations is given by

$$\left[A(x) \right] \left[\frac{d^2 y}{dx^2} \right] + \left[B(x) \right] \left[\frac{dy}{dx} \right] + \left[C(x) \right] [y] = [Q(x)] \quad (1)$$

where A, B and C are (4, 4) matrices representing the shell stiffness and geometry properties. The dependent variable y is a (4, 1) vector considered in [1] as three displacements and the meridional bending moment.

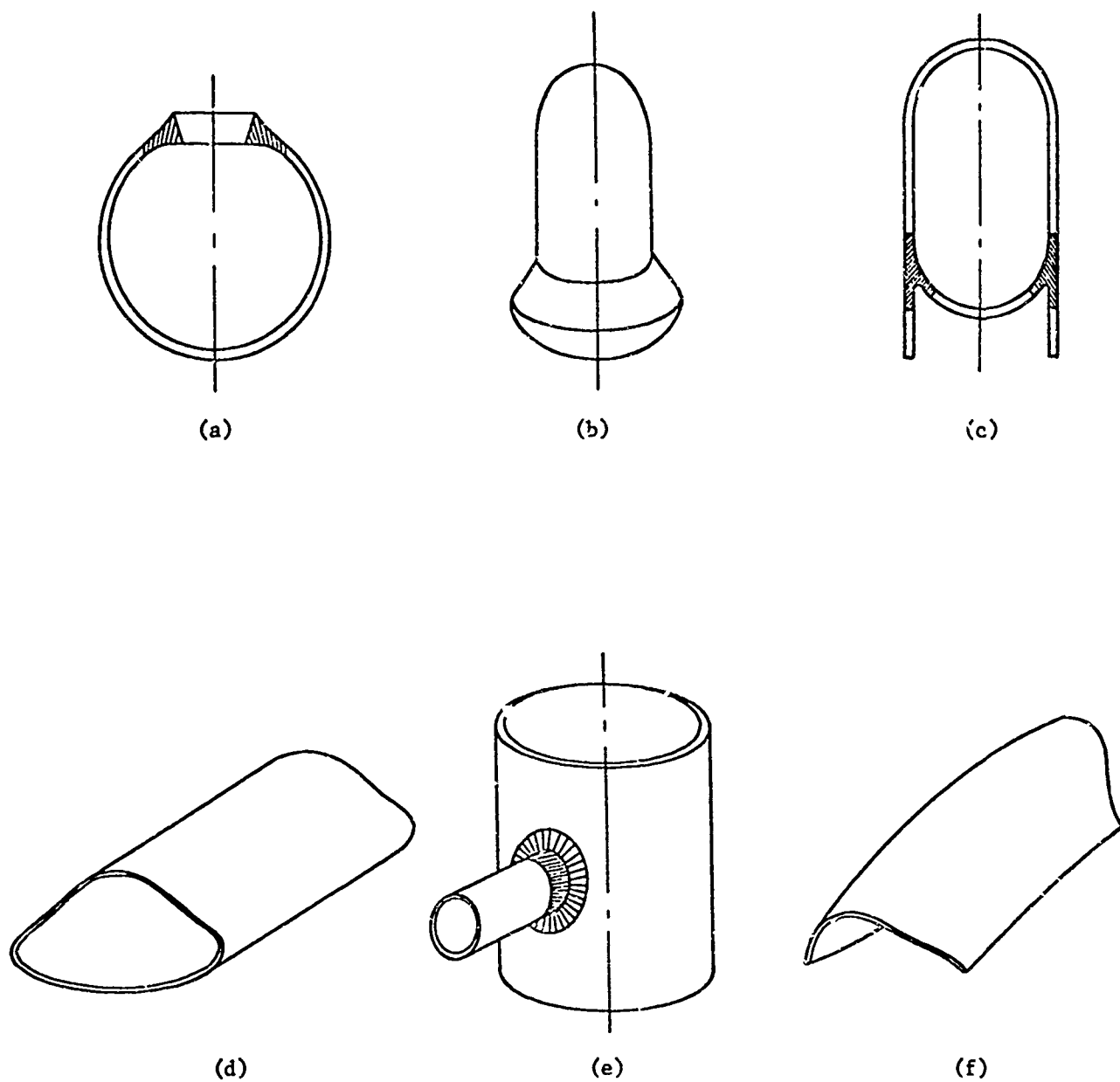


Figure 1. Typical Shell Configurations

In its simplest form the application of the finite difference method is initiated by dividing the shell into equally spaced intervals as shown in Figure 2, for a one-dimensional shell of revolution.

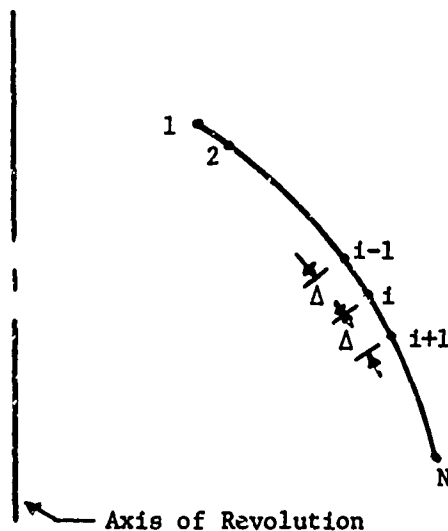


Figure 2. Finite Difference Mesh

The central difference expressions for approximating derivatives in Eq. (1) are given by

$$\left. \begin{aligned} \frac{d^2y}{dx^2} &= \frac{y_{i+1} - 2y_i + y_{i-1}}{\Delta^2} \\ \frac{dy}{dx} &= \frac{y_{i+1} - y_{i-1}}{2\Delta} \end{aligned} \right\} \quad (i = 2, 3, 4, \dots, N-1) \quad (2)$$

where i refers to a particular station or control point associated with the finite difference interval Δ . The above expressions were obtained by curve fitting a parabola through three successive points. The error associated with the above expressions is order (Δ^2) . Thus the smaller the increment $(\Delta \rightarrow 0)$, the better the approximation of the derivative. Formulas using higher order curves to approximate derivative expressions are available and will give smaller errors of order (Δ^n) . However, as would be expected, additional control points

are required for these representations, and thus they increase the bandwidth of the algebraic equations. The bandwidth is defined as the maximum number of terms to the left and right of the main diagonal. Since the time for solving the set of algebraic equations is proportional to the bandwidth squared, higher order formulas are usually avoided.

Continuing with the example, Eqs. (2) are only valid at interior points in the shell discretization. At boundaries, forward or backward differences or expressions requiring the addition of a fictitious point [2] may be used. For example, in [1] the following forward and backward difference of error order (Δ) was used

$$\left. \begin{aligned} \frac{dy}{dx} &= \frac{y_2 - y_1}{\Delta} & \text{at } i = 1 \\ \frac{dy}{dx} &= \frac{y_N - y_{N-1}}{\Delta} & \text{at } i = N \end{aligned} \right\} \quad (3)$$

Application of the finite difference formulas (2) and (3) to the shell differential equations (1) results in a set of algebraic equations which can be expressed in matrix form

$$[K][y] = [Q] \quad (4)$$

where K is a (MN, MN) matrix, M being the number of dependent variables at each control point and N the number of control points. For this example K is a $(4N, 4N)$ matrix. Since, in general, K is a highly banded matrix, it may be very efficiently solved on a digital computer. In reference [1] a special Gaussian elimination method (Potter's Method) was used to solve Eqs. (4). The procedure involved only the inversion of $(4, 4)$ matrices.

In general, application of finite differences to any consistent form of linear shell equations will result in a matrix equation of the form given by Eq. (4). Although the example given was for a one-dimensional discretization, the method is equally applicable to two- and three-dimensional shell problems. The finite difference method can also be conveniently used to solve nonlinear problems. In this case the resulting algebraic equations are nonlinear and are solved by an iteration or step-by-step technique.

Application of the Finite Difference Method to Shell Configurations

The finite difference method has been applied to one-, two-, and three-dimensional shell configuration problems. The convenience of application and accuracy depends on the specific problem and type of shell configuration considered.

Although variable interval finite difference formulas are available, the method is most conveniently applied to a uniform mesh. One of the difficulties encountered in the application of the finite difference method is the selection a priori of a mesh size to obtain economical solutions within accuracy requirements. This is particularly true at boundaries or in regions where rapid changes of loading or stiffness properties occurs. Finer mesh or higher order difference expressions are desirable in these areas. For example, it was found for one-dimensional shell of revolution problems [2] that use of the three point forward and backward expression (error (Δ^2)) in place of the two point expression in Reference [1] greatly increased the solution accuracy in the boundary region. The use of fictitious points and central differences also increased accuracy [2].

Theoretically, finite difference cannot be used at locations where derivatives are discontinuous. However, for shells of revolution this problem can be eliminated by application of transition or compatibility and equilibrium expressions at discontinuities as suggested in Reference [1]. The shell configuration may be divided into multiple regions or segments to handle discontinuous configurations with each region tied together by appropriate transition equations. This procedure may also be used to allow changes in mesh size between regions. Care must be taken that the mesh size is not too different between regions, since numerical round-off errors could occur when using a digital computer.

There are various other permutations of the basic finite difference approach that improve accuracy. Perhaps the best formulation to use with the finite difference method is a formulation which minimizes the highest order derivative. In References [5, 6] a six-order and eight-order set of six and eight first order equations, respectively, were solved. The dependent variables were stress resultants, displacements, and rotations. In both of these formulations the interior differences were of order (Δ^2) and it was not necessary to use derivatives at boundaries. Furthermore, a higher order derivative formulation such as given in [1] requires that finite differences be used in the calculation of stress resultants. This can result in added inaccuracies which the first order system formulation does not have.

The application of the finite difference method has characteristically been restricted to orthogonal coordinate systems (mesh). Therefore, difficulties occur in treating complex shell structures (arbitrary stiffened shell) or shells with irregular boundaries or cutouts. Boundary conditions at irregularities are especially awkward to treat. A part of this complexity is removed when using the finite difference method in conjunction with minimization of the potential energy [7].

In summary, the finite difference method yields excellent results in treating one-dimensional problems. For two- or three-dimensional problems finite difference is very useful for treating problems only requiring an orthogonal mesh of equal spaced intervals. It becomes difficult to apply to general complex shell configurations with irregular boundaries.

4. NUMERICAL INTEGRATION METHOD

The numerical integration method is applicable to solving any system of m first order ordinary differential equations which can be written in the form

$$\left[\frac{dy(x)}{dx} \right] = [A(x,y)] [y(x)] + [B(x)] \quad a \leq x \leq b \quad (5)$$

where $y(x)$ is an $(m, 1)$ column vector which contains the m unknown dependent variables; $A(x,y)$ is an (m, m) matrix which for nonlinear problems contains functions of the dependent variable y ; $B(x)$ is an $(m, 1)$ column vector which contains the nonhomogeneous load terms; and x is the independent variable. The boundary conditions for Eqs. (5) may be stated in the form

$$[F_a] [y(a)] + [F_b] [y(b)] = [G] \quad (6)$$

where F_a and F_b are (m, m) matrices and G is an $(m, 1)$ column vector, which prescribes the boundary conditions at $x = a$ and $x = b$.

The numerical integration method of solving Eqs. (5) and (6) for linear problems is straightforward and is described below. The solution of nonlinear or eigenvalue problems is similar, but also requires an iteration technique to arrive at the correct solution [8-11]. For linear problems $A(x,y) = A(x)$ and the complete solution of Eqs. (5) may be written in the form

$$[y(x)] = [Y(x)] [y(a)] + [Z(x)] \quad (7)$$

where $Y(x)$ is an (m, m) matrix whose columns are m independent solutions to the homogeneous part of Eqs. (5). $[Y(x)]$ may be obtained by using a numerical forward integration method subject to the initial conditions that $[Y(a)]$ equals the identity matrix. The $(m, 1)$ column vector $Z(x)$ is the particular solution of Eqs. (5) and may also be obtained by forward integration subject to the initial condition that $Z(a)$ equals zero. It should be noted that when carrying out the forward integration use could be made of a predictor-corrector integration technique which automatically selects the step size [8].

By evaluating Eq. (7) at $x = b$, the dependent variable $y(b)$ may be related to $y(a)$ by the equation

$$[y(b)] = [Y(b)] [y(a)] + [Z(b)] \quad (8)$$

Thus one may see that Eqs. (8), together with the boundary conditions (6) constitute a system of $2m$ equations from which the $2m$ unknowns $y(a)$ and $y(b)$ are determined. Once $y(a)$ is known, the solution $y(x)$ at any value of x is obtained from Eq. (7), provided that the homogeneous and particular solution, $Y(x)$ and $Z(x)$ respectively, have been retained.

Application of the Numerical Integration Method to Shell Configurations

The application of numerical integration to shell problems is limited to solving problems which only require a one-dimensional discretization, normally in the meridional direction. Furthermore, while the method described above is theoretically correct and sound in principle, in practice it cannot be used to solve shell problems whose meridional length L is greater than approximately

$$L > (3/\lambda) \quad (9)$$

where λ is of the order of magnitude

$$\lambda = O\left(\frac{1}{\sqrt{Rh}}\right) \quad (10)$$

where R is the minimum radii of curvature of the shell and h is the shells thickness [8]. The reason for this limitation is that the homogeneous solution for the shell equations has a term of the form $e^{\lambda x}$. Hence in solving Eqs. (7) for $Y(b)$, very large magnitudes are obtained when $L > 3\lambda$. Then in attempting to determine $y(a)$ and $y(b)$ by solving Eqs. (6) and (8), it is found that a complete loss of accuracy results because of the subtraction of large numbers of almost equal magnitude. Therefore, some other procedure must be used to solve shell problems of arbitrary meridional length.

The method used to solve shell of revolution problems of any arbitrary meridional length is called the multi-segment method, [8-11]. In using this method the shell is divided into M contiguous segments denoted by S_i , where $i = 1, 2, \dots, M$. Each segment is chosen so that its length is smaller than $(3/\lambda)$. Consider the shell segments shown in Figure 3. For descriptive reasons the left edge of each shell is numbered starting at 1 for segment 1 and ending with $M+1$ at the right edge of segment M .

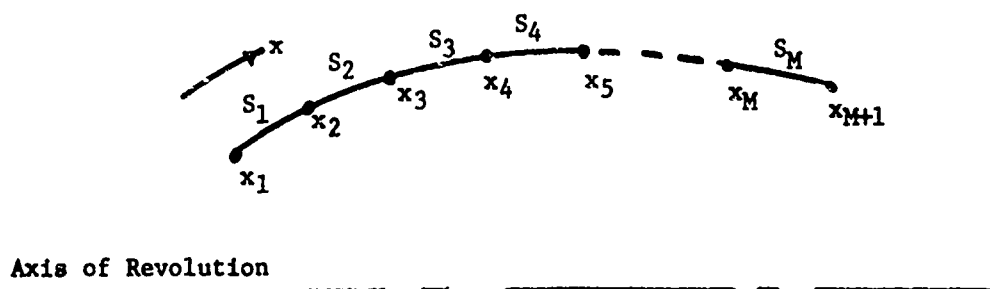


Figure 3. Shell Segments

The governing shell equations are reduced to a system of eight ordinary first order differential equations in terms of eight dependent variables (consisting of stress resultants, displacement, and rotations) and the independent variable x , the meridional coordinate. In analogy to Eqs. (7), the solution to the governing equations within any segment is given by

$$\left[y(x) \right]_i = \left[Y(x) \right]_i \left[y(x_1) \right]_i + \left[Z(x) \right]_i \quad (i = 1, 2, \dots, M) \quad (11)$$

where the subscript i on the matrices denotes that they correspond to segment i . The solution at the end of each segment is therefore

$$\left[y(x_{i+1}) \right]_i = \left[Y(x) \right]_i \left[y(x_1) \right]_i + \left[Z(x) \right]_i \quad (i = 1, 2, \dots, M) \quad (12)$$

To complete the governing shell equations, the boundary conditions at x_1 and x_{M+1} may be written as

$$\left[F_a \right] \left[y(x_1) \right] + \left[F_b \right] \left[y(x_{M+1}) \right] = \left[G \right] \quad (13)$$

and the continuity equations which hold for contiguous segments are given by

$$\left[T_a \right]_i \left[y(x_{i+1}) \right]_i + \left[T_b \right]_{i+1} \left[y(x_{i+1}) \right]_{i+1} = \left[F \right] \quad (i = 1, 2, \dots, M-1) \quad (14)$$

where T_a and T_b are (m, m) matrices which relate the dependent variables at the right edge of i , $\{y(x_{i+1})\}_i$, to the dependent variables at the left edge of segment $i+1$, $\{y(x_{i+1})\}_{i+1}$. Eqs. (12), (13), and (14) form a complete system of equations from which the $2mM$ unknown variables at the edge of each segment may be determined. Once these variables are found, the solution at any value of x is obtained by Eq. (11).

As mentioned previously, numerical integration is limited to solving problems which only require one-dimensional discretization. Thus the method requires that the shell equations which represent the shell configuration be reducible to a system of ordinary differential equations with one independent variable. Hence in applying this method to the shell of revolution subject

to asymmetric loads, the governing partial differential equations must first be reduced to a system of ordinary differential equations with one independent variable. As described earlier, this is done by expanding all the dependent variables in a Fourier series in the circumferential direction. The resulting ordinary differential may then be solved by the numerical integration method.

Problems which cannot be reduced to a system of ordinary differential equations may sometimes be solved by combining the numerical integration and finite difference methods. For example, Kalnins [12] has solved the problem of a curved thin walled shell of revolution by using a finite difference representation in the circumferential direction and numerical integration in the meridional direction. Other mixed methods of this type are also possible.

5. FINITE ELEMENT METHOD

The representation of a continuum by an assemblage of a finite number of structural elements, each of which may be characterized by independent deformation modes, is called the "finite element" method [13, 14]. The major distinction between the finite element method and the finite difference method is that the finite difference method discretizes the differential equations which describe the structure's behavior, while the finite element method discretizes the structure, and then constructs the governing equations for the discretized model of the structure.

There are two forms of the finite element method called 1) the "force" method and 2) the "displacement" or "stiffness" method [13-15]. The force method treats the internal forces or stresses as the basic unknown variables and is usually associated with the Principle of Minimum Complementary Energy. The displacement or stiffness method considers the displacements as the basic unknowns and is usually associated with the Principle of Minimum Potential Energy. Of the two methods, the displacement method is usually preferred because its formulation and computation automation is relatively simple, and yet it is still general. Since most finite element shell analyses use the displacement method, the remainder of this section will only discuss this method.

The application of the finite element displacement method is best described by the following steps:

1. Idealize the structure. Choose the types of elements which will represent the structure and construct a discretized finite element model of the structure.
2. Calculate the stiffness matrix for each of the elements which make up the structure.

3. Assemble the element stiffness matrices to form the structural stiffness matrix for the entire structure. These equations are the equilibrium equations applied at each nodal point of the structure.
4. Obtain the unknown displacements at each nodal point of the structure by solving the equilibrium equations subject to the imposed boundary restraints.
5. Determine the internal strains, stresses, and forces in the structure.

All of the above steps are standard for solving problems using the displacement F.E. method. The only differences which may exist between formulations is the method by which the element stiffness matrix is obtained (Step 2). Two basic techniques have been used to derive element stiffness matrices [15, 16]. They are 1) the "equivalent force" and 2) the "energy" methods.

The equivalent force method is based on assuming stress functions to represent the behavior of the element. The element strains and displacement modes are obtained by integrating the stresses. In addition, "equivalent" forces are calculated by integrating the stresses along the element boundary, and lumping the forces at the nodes. Finally, by evaluating the displacements at the nodal points and comparing these relations with the equivalent force relations, the element stiffness matrix is obtained.

The energy method has been the predominate method used to derive element stiffness matrices, since it is based on variational principles that provide a sound theoretical basis for the finite element method [17-19]. Although numerous variational principles have been used to derive element stiffness relation [20-22], the displacement method is normally associated with the Theorem of Minimum Potential Energy. A general formulation of the displacement method based on the Theorem of Minimum Potential Energy was presented by Melosh [17]. A discussion of the criteria for insuring the monotonic convergence of the F.E. energy method solution is given in References [17-19].

It was pointed out by these investigators that the convergence of the finite element solution to the exact solution as the shell element sizes are decreased is dependent on a number of conditions. The two primary conditions for convergence are that the deformation of each element maintain compatibility along interelement boundaries, and be capable of representing a state of constant inplane strain and bending curvature. In addition, although not necessary from a convergence viewpoint, the deformation of each element should include a complete set of rigid body modes which yield zero strains for the shell theory used.

It should be noted that many finite element stiffness matrices have been derived which do not satisfy the above conditions but still yield good solutions [23, 24, 43]. Nevertheless, finite element stiffness matrices which satisfy the above conditions are the objective of most finite element investigators.

The general method for determining the element stiffness matrix by application of the Principle of Minimum Potential Energy is given below. In applying the finite element method, the body is first divided into a large number of discrete elements as shown in Figure 4.

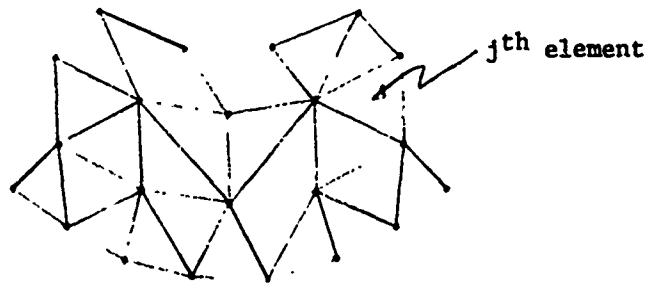


Figure 4. The Element Model

The strain energy of the element, U_j , and work done by surface or boundary tractions acting on the element, W_j may be written as

$$U_j = \frac{1}{2} \int_V ([D]\{u\})^T [E] ([D]\{u\}) dV \quad (15)$$

$$W_j = \int_S \{P\}^T \{u\} dS \quad (16)$$

where $[E]$ is a function of the material properties, the matrix $[D]$ is a differential operator, and the vector $\{u\}$ is the displacement or rotation of any point within or on the boundary of the element. The deformations $\{u\}$ of the element are now assumed to be representable by a series of functions ϕ whose coefficients are the displacements or rotations, δ , at the "nodal points" of the element, i.e.

$$\{u\} = [\phi] \{\delta\} \quad (17)$$

The functions ϕ are chosen to satisfy the convergence criteria conditions discussed earlier.

The Principle of Minimum Potential Energy states that of all displacement functions which satisfy the displacement boundary conditions, the one which satisfies equilibrium makes the potential energy an absolute minimum. This principle may be written as

$$\delta \left[\sum_{j=1}^M (U_j - W_j) \right] = 0 \quad (18)$$

Substitution of Eqs. (15), (16), and (17) into (18) then yields the final equilibrium equation for the body

$$\sum_{j=1}^M ([k]_j \{\delta\} - \{F\}_j) = 0 \quad \text{or} \quad [K] \{\delta\} = \{F\} \quad (19)$$

where the summation means that Eqs. (19) must be summed for all elements of the body subject to continuity constraints. The matrix $[k]$ is the element stiffness matrix and the force vector $\{F\}$ is the generalized external forces acting on each element.

$$\left. \begin{aligned} [k] &= \int_V ([D][\phi])^T [E] ([D][\phi]) dv \\ [F] &= \int_S [P]^T [\phi] dS \end{aligned} \right\} \quad (20)$$

It should be noted that Eq. (19) is of similar form as Eq. (4) of the finite difference method. It is conceivable that for specific problems, application of the finite element and finite difference methods can result in an identical set of algebraic equations.

As in the finite difference method, the final matrix K is very sparse and by judicious choice of a nodal point numbering scheme can be put in a highly banded format. Automatic matrix re-ordering schemes have been employed in the finite element method to minimize the matrix bandwidth.

Application of the Finite Element Method to Shell Configurations

The major advantage of the finite element method is its complete generality and ease of application to complex problems. The finite element method has been used to analyze all types of shell configurations. These analyses

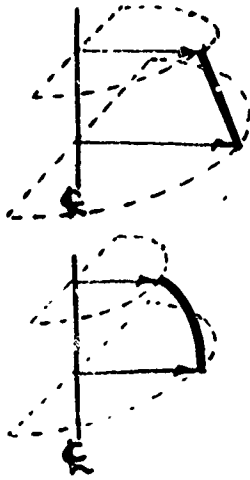
make use of four basic element types (Figure 5): 1) conical and meridionally curved axisymmetric shell elements [25-30]; 2) triangular or quadrilateral flat and curved elements [21-23, 31-37]; 3) axisymmetric solid of revolution elements [38-40]; and 4) three-dimensional solid elements [41]. In addition, stiffened shell structures use straight and curved beam elements to represent stringers and frames.

The first type of element used to analyze axisymmetric shells of revolution were the conical elements [25-29]. As in the finite difference and numerical integration methods, the Fourier series expansion technique was used to treat nonsymmetric loads. However, as pointed out by Jones and Strome [42], the use of conical shell elements to represent curved shells sometimes gave inaccurate results. These inaccuracies were predominate in problems where distributed loads induced large membrane stress resultants. Development of meridionally curved shell element [28-30] permitted a more accurate idealization which yielded improved accuracy.

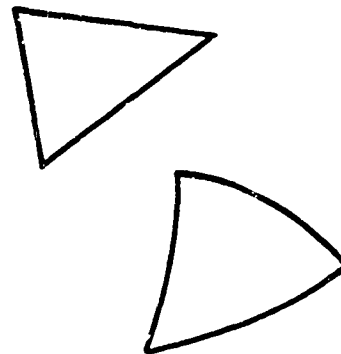
Similarly, the first elements used to represent general curved shell structures were flat triangle elements [31]. The flat element stiffness matrix was improved by many investigators [21-23, 32]; however, it still has the same inadequacies as those encountered with the conical element, and may not always give accurate results for curved shell structures [33-37]. To overcome this deficiency, many investigators have been working on developing an adequate curved shell element [33-37] which satisfies the proper convergence and rigid body conditions. This work has included using more degrees of freedom per node to represent the shell deformation as well as using more nodes to represent an element. In both cases the complexity of the element stiffness matrix is increased as well as the computer computational time. Even so, there does not appear to be any general curved triangular or quadrilateral element which completely satisfies all convergence and rigid body conditions.

Two- and three-dimensional solids are treated using either the axisymmetric triangular ring element or the general solid element (e.g., a tetrahedron) [38-41]. The first axisymmetric element used a linear displacement field to represent its behavior. It was found, however, that for some problems, the stresses in contiguous elements would be greatly different if the mesh was not exceptionally fine. This problem was reduced by combining triangular elements to form a quadrilateral element, and then calculating stresses for the quadrilateral element or by averaging stresses of elements attached to the same node. Improvements in the solution were also obtained by using a quadratic displacement to represent the element, and adding nodes to the sides of the elements [41].

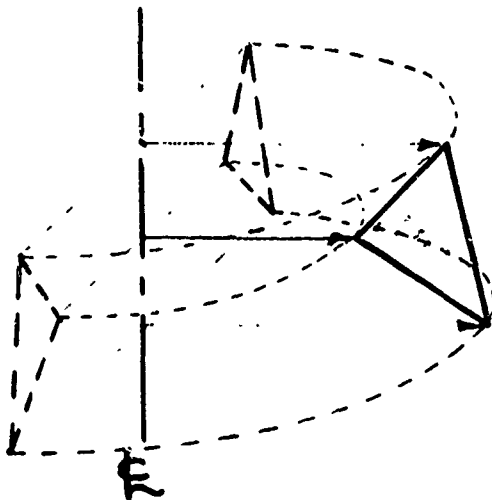
Other techniques to improve the accuracy of solution have been studied and include mixed hybrid formulations [21] and mixed displacement and force methods [15].



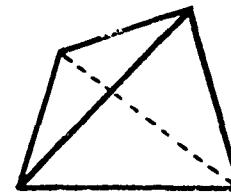
(a) Axisymmetric Thin Shell Element



(b) Triangular Flat and Curved Shell Elements



(c) Axisymmetric Thick Shell Element



(d) Three-Dimensional Solid Element

Figure 5. Shell Finite Elements

6. PROBLEMS SOLVED USING THE THREE NUMERICAL METHODS

Hartung [45] recently completed an extensive survey and assessment of current capability for computer analysis of shell structures. This assessment includes descriptions of major types of problems solved to date by the finite difference, numerical integration and finite element methods. Table 1 is based on this information, and shows the types of problems which have been solved by the three numerical methods.

The table shows that one-dimensional discretization problems have been extensively studied using all three numerical methods. The finite difference and finite element methods are more extensively used than numerical integration. The finite element method has not been applied as yet to buckling imperfection sensitivity studies.

Two- and three-dimensional applications have not been as extensive as one-dimensional applications. Furthermore, many of the problems studied in this classification were done for special geometries and are not generally available for solving arbitrary shell problems.

7. SUMMARY AND CONCLUSIONS

This review has presented the major features and limitations of the finite difference, numerical integration, and finite element methods. Each discrete method was shown to be based on well founded principles, which guarantees that the solution error approaches zero as the mesh or step size is decreased. The finite difference and numerical integration methods have one source of error (not including computational round-off error inherent in all computerized methods). This error is due to discretizing the governing differential equations, and approaches zero as the mesh or step size is decreased. The finite element method has two sources of error: 1) geometric idealization errors, and 2) structural idealization errors. The first source is due to representing the actual shell geometry with an approximate finite element idealization. The second source is due to representing the deformation behavior of each element with only a finite number of degrees of freedom. The error due to geometric idealization does, of course, vanish when the actual geometry is used. However, when curved shell surfaces are represented with flat plate elements, the error may not vanish [42, 43]. Errors due to structural idealization can be proved to vanish in the limit, provided that the deformation modes of the element satisfy the proper convergence criteria.

All three numerical methods have been extensively used to solve one-dimensional problems, and if used with the refinements mentioned, gave very good results. In addition, for one-dimensional problems, all three methods are about equal in ease of application.

APPLICATION OF FINITE DIFFERENCE, NUMERICAL INTEGRATION,
AND FINITE ELEMENT METHOD COMPUTER PROGRAMS TO SHELL PROBLEMS

Problem Type	One-Dimensional			Two- and Three-Dimensional		
	F.D.	N.I.	F.F.	F.D.	N.I.*	F.E.
Static Analysis						
Linear Elastic	X	X	X	X	X	X
Geometric Nonlinearity	X	X	X	X		X
Material Nonlinearity	X		X	X		X
Buckling Analysis						
Linear Elastic	X	X	X	X		X
Geometric Nonlinearity	X	X	X	X		X
Material Nonlinearity	X		X			
Imperfection Sensitivity	X	X				
Dynamic Analysis						
Linear Elastic						
Free Vibration	X	X	X	X		X
Direct Integration	X		X	X		X
Geometric Nonlinearity	X		X	X		X
Material Nonlinearity	X		X	X		X

*To solve two- or three-dimensional problems, numerical integration must be combined with another method.

Table 1

Two-dimensional discretization problems can only be solved by the finite difference or finite element methods. Numerical integration is not applicable for this classification unless it is combined with another discrete method. The finite element method is the easiest method to apply to two- and three-dimensional arbitrary shell structures. It can easily handle surface irregularities, variable material properties, and different types of structural elements. Application of the finite difference method to two- and three-dimensional problems has been limited, so far, to using orthogonal meshes which are usually equally spaced.

Further work in the three reviewed numerical methods should include the following:

1. Investigation of advantageous methods of combining numerical integration with other discrete numerical methods
2. Development of techniques for treating arbitrary nonorthogonal finite difference meshes
3. Development of an arbitrary curved triangular finite element which meets all convergence and rigid body criteria

If a conclusion can be made from this review, it would be that each of the discrete numerical methods presented exhibits some unique features that make it a valuable shell analysis method.

REFERENCES

1. Budiansky, B. and Radkowski, P.P., "Numerical Analysis of Unsymmetrical Bending of Shells of Revolution," AIAA J., Vol. 1, p. 1833, 1963.
2. Cappelli, A.P., "Study of Apollo Water Impact," Vol. 7, Modification of Shell of Revolution Analysis, North American Aviation, Inc. Report SID 67-498, (Contract NAS9-4552, G.O. 5264) May 1967.
3. Cappelli, A.P., Nishimoto, T.S., and Radkowski, P.P., "Analysis of Shells of Revolution Having Arbitrary Stiffness Distributions," AIAA J., Vol. 7, No. 10, p. 1909, October 1969.
4. Famili, J. and Archer, R., "Finite Asymmetric Deformation of Shallow Spherical Shells," AIAA J., Vol. 3, p. 506, 1965.
5. Stephens, W.B. and Fulton, R.E., "Axisymmetric Static and Dynamic Buckling of Spherical Caps Due to Centrally Distributed Pressures," AIAA 7th Aerospace Sciences Meeting, N.Y., January 1969.
6. Greenbaum, G.A. and Conroy, D.C., "Post-Wrinkling Behavior of a Conical Shell of Revolution Subjected to Bending Loads," AIAA J., Vol. 8, No. 4, 1970.
7. Brogran, F. and Almoth, B.O., "Buckling of Cylinders with Cutouts," AIAA J., Vol. 8, No. 2, p. 236, February 1970.
8. Kalnins, A., "Analysis of Shells of Revolution Subjected to Symmetrical and Nonsymmetrical Loads," J. of Applied Mechanics, ASME Series E, Vol. 31, p. 467, 1964.
9. Cohen, G.A., "Computer Analysis of Asymmetric Deformation of Orthotropic Shells of Revolution," AIAA J., Vol. 2, No. 5, p. 932, May 1964.
10. Mason, P., Rung, R., Rosenbaum, and Ebrus, R., "Non-Linear Numerical Analysis of Axisymmetrically Loaded Arbitrary Shells of Revolution," AIAA J., Vol. 3, No. 7, p. 1307, July 1965.
11. Svaldonas, V., and Angrisano, N., "Numerical Analysis of Shells - Volume 1 - Unsymmetric Analysis of Orthotropic Reinforced Shells of Revolution," NASA CR-61299, September 1966.
12. Kalnins, A., "Analysis of Curved Thin-Walled Shells of Revolution," AIAA J., Vol. 6, No. 4, p. 584, April 1968.
13. Turner, M.J., Clough, R.J., Martin, H.C., and Topp, L.J., "Stiffness and Deflection Analysis of Complex Structures," J. Aeronaut. Sci., Vol. 23, No. 9, p. 805, 1956.

14. Argyris, J.H., Energy Theorems and Structural Analysis, Butterworth's Scientific Publications, London, 1960.
15. Gallagher, R.H., A Correlation Study of Methods of Matrix Structural Analysis, Macmillan Co., New York, 1964.
16. Gallagher, R.H., "Techniques for the Derivation of Element Stiffness Matrices," AIAA J., p. 1431, June 1963.
17. Melosh, R.J., "Bases for Derivation of Matrices for the Direct Stiffness Method," AIAA J., p. 1631, July 1963.
18. Pian, T.H.H. and Tong, P., "Basis of Finite Element Methods for Solid Continua," International Journal for Numerical Methods in Engineering, Vol. 1, p. 3, 1969.
19. Tong, P. and Pian, T.H.H., "The Convergence of Finite Element Method in Solving Linear Elastic Problems," Intl. J. Solids and Structures, Vol. 3, p. 865, 1967.
20. Greene, B.E., Jones, R.E., McLay, R.W., and Strome, D.R., "On the Application of Generalized Variational Principles in the Finite Element Method," AIAA/ASME 9th Structures, Structural Dynamics and Materials Conference, Palm Springs, California, April 1-3, 1968.
21. Pian, T.H.H., "Element Stiffness Matrices for Boundary Compatibility and for Prescribed Boundary Stresses," Conf. on Matrix Methods in Structural Mechanics, October 1965.
22. Fraeijis de Veubeke, B., Upper and Lower Bounds in Matrix Structural Analysis, AGARD ograph 72, Pergamon Press, Oxford, 1964.
23. Clough, R.W. and Toucher, J.L., "Finite Element Stiffness Matrices for Analysis of Plate Bending," Conf. on Matrix Methods in Structural Mech., Wright-Patterson AFB, Dayton, Ohio, October 1965.
24. Bazeley, G.P., et al., "Triangular Elements in Plate Bending - Conforming and Non-Conforming Solutions," Conf. on Matrix Methods in Structural Mechanics, Wright-Patterson AFB, Dayton, Ohio, October 1965.
25. Grafton, P.E. and Strome, D.R., "Analysis of Axisymmetric Shells by the Direct Stiffness Method," AIAA J., Vol. 1, No. 10, p. 2342, October 1963.
26. Popov, E.P., Penzien, J., and Lu, Z.A., "Finite Element Solution for Axisymmetric Shells," J. of Engr. Mech. Div., ASCE, p. 119, October 1969.
27. Percy, J.H., Pian, T.H.H., Navaratna, and Klein, S., "Application of the Matrix Displacement Method to the Linear Elastic Analysis of Shells of Revolution," AIAA J., Vol. 3, No. 11, p. 2138, November 1965.

28. Jones, R.E. and Strome, D.R., "Direct Stiffness Method Analysis of Shells of Revolution Utilizing Curved Elements," AIAA J., Vol. 4, No. 9, p. 1519, September 1966.
29. Strickland, Navaratna, D.R., and Pian, T.H.H., "Improvements on the Analysis of Shells of Revolution by the Matrix Displacement Method," AIAA J., Vol. 4, No. 11, p. 2059, November 1966.
30. Witmer, E.A., Pian, T.H.H., Mack, E.W., and Berg, B.A., "An Improved Discrete Element Analysis and Program for the Linear Elastic Analysis of Meridionally-Curved, Variable-Thickness, Branched Thin Shells of Revolution Subjected to General External Mechanical and Thermal Loads. Part 1 - Analysis and Evaluation," SAMSO TR 68-310, Part 1 (also MIT ASRL TR 146-4, Part 1), March 1966.
31. Wiekell, R.C., Greene, B., and Strome, D.R., "Application of the Stiffness Method to the Analysis of Shell Structures," ASME Paper 61-AV-58, March 1961.
32. Clough, R.W. and Felippa, C.A., "A Refined Quadrilateral Element for Analysis of Plate Bending," Second Conf. on Matrix Methods in Structural Mechanics, October 1968.
33. Key, S.W. and Bersengu, Z.E., "The Analysis of Thin Shells with Transverse Shear Strains by the Finite Element Method," Second Conf. on Matrix Methods in Structural Mechanics, Wright-Patterson AFB, Dayton, Ohio, October 1968.
34. Cantin, G. and Clough, R.W., "A Curved Cylindrical Shell Finite Element," AIAA J., Vol. 6, No. 6, June 1968.
35. Atluri, S., "Static Analysis of Shells of Revolution Using Doubly Curved Quadrilateral Elements Derived from Alternate Variational Models," SAMSO TR 69-354, June 1969.
36. Bogner, F.F., Fox, R.L., and Schmidt, L.A., "A Cylindrical Shell Discrete Element," AIAA J., Vol. 5, No. 4, April 1967.
37. Olson, M.D. and Lindberg, G.M., "Vibrational Analysis of Cantilever Curved Plates Using a New Cylindrical Shell Finite Element," Second Conf. on Matrix Methods in Structural Mechanics, Wright-Patterson AFB, Dayton, Ohio, October 1968.
38. Clough, R.W. and Rashid, Y., "Finite Element Analysis of Axi-Symmetric Solids," J. of Eng. Mech. Div., ASCE, Vol. 91, p. 71, February 1965.
39. Wilson, E.L., "Structural Analysis of Axisymmetric Solids," AIAA J., Vol. 3, No. 12, p. 2269, October 1965.
40. Hofmeister, L.D. and Greenbaum, G.A., "Large Strain Axisymmetric Finite Element Analysis," (to be published).

41. Argyris, J.H., "Matrix Analysis of Three-Dimensional Elastic Media Small and Large Displacements," AIAA J., Vol. 3, No. 1, p. 45, January 1965.
42. Jones, R.E. and Strome, L.R., "A Survey of the Analysis of Shells by the Displacement Method," Conf. on Matrix Methods in Structural Mechanics, Dayton, Ohio, October 1965.
43. Walz, J.E., Fulton R.E., and Cyrus, N.J., "Accuracy and Convergence of Finite Element Approximations," Second Conf. on Matrix Methods in Structural Mechanics, October 1968.
44. Leissa, A.W., "Investigation of the Utilization of the Point Matching Method for the Solution of Various Boundary Value Problems," AFFDL-TR-66-186, 1966.
45. Hartung, R.F., "An Assessment of Current Capability for Computer Analysis of Shell Structures," AFFDL Technical Report (Prelim. Draft), Feb. 1970.
46. Sanders, J. Lyell, Jr., "Nonlinear Theories for Thin Shells," Quart. Appl. Math., Vol. 21, p. 21, 1963.

QUESTIONS AND COMMENTS FOLLOWING GREENBAUM'S TALK

COMMENT: When you listed the errors involved in the finite difference method, I think that you omitted geometric idealization errors. This is the same kind of error that you listed for finite element methods. For example, in a one dimensional shell of revolution problem, if I take large intervals between node points along the meridian, then I'm going to get poor answers by either method because of geometric idealization error.

GREENBAUM: Let me restate what I said. In the finite difference method we discretize the governing equations. However, in those governing equations we actually do treat, for example, the curvature of the shell and we do express the curvature at each nodal point. Now in the finite element technique, however, when we represent the same structure with a flat element we do not include the curvature of the element. This is what I really referred to by the phrase geometric errors.

COMMENT: On the same question I'd like to comment that there is a close connection between the type of errors in the finite and the finite difference methods. I think you use finite differences in the finite element method in as much as you base it on the variational equation. You approximate the derivatives in the energy integral by their finite difference approximations and then you perform a numerical integration. As you mentioned, you can derive equations based on finite differences which coincide with equations based on finite elements. If you can come up with the same equations, the errors must be closely related in both methods.

I'd like to comment further that you didn't mention mixed methods in your list of methods. While they are less well known, I know of one mixed where a curved triangular element was devised and excellent practical results were obtained with it. However, no theoretical convergence proof was provided for the method.

QUESTION: In equation 4, you included only linear terms. If you have nonlinear terms, would you comment on the way in which this affects the finite difference formulation, the solution procedures used and / advantage which might accrue to finite difference or finite element .ods? Is the bandwidth of the matrices affected?

GREENBAUM: Normally, in a nonlinear problem, you wind up with a series of nonlinear algebraic equations. You can use several techniques to obtain a solution to this set of equations. The most common technique used today and perhaps the best one from a convergence standpoint is Newton's method, in which you essentially assume a solution plus a correction for that solution and then iterate until the solution converges. However, the nonlinearity itself does not really increase the bandwidth of the equations. It just complicates the solution of the final nonlinear equations.

As far as a difference between finite element techniques and finite difference in treating nonlinear problems, this depends upon the background of the analyst. I have heard it said by finite difference experts that finite difference techniques are easier to use and, of course, similar statements have been made by finite element experts. So I really would leave the question as to which method is better, from the linear or nonlinear standpoint, to the individual investigators. I really could not distinguish a difference

there myself between finite difference and finite element.

COMMENT: I believe that Dr. Dupuis of Brown has developed a curved triangular element which is compatible and convergent. Some of the results are shown in his paper to be presented tomorrow.

QUESTION: I guess my question stems from ignorance about the finite element method. I don't really understand whether we are discretizing the structure in the finite element method. Suppose we take a general curved shell and divide it into small regions without discretizing the structure at all. Now within each region we assume the displacement to have a certain polynomial form with undetermined coefficients. We then form the energy expression and minimize it with respect to these coefficients in the presence of constraint conditions between the regions which have to do with displacement compatibility. Now if we set up the problem in the way that I've just outlined, what are the differences, say, in that method and the finite element method? And if there are none, then I don't see where the structural idealization comes in.

GREENBAUM: That type of technique could be used to essentially derive an element stiffness matrix; that is, you could use the actual shell geometry. You also could use some numerical technique to integrate the actual geometry over the proper thickness and the proper surface. Strictly speaking, if you did this, it would be called the finite element method. However, I would like to point out that that is not normally how the finite element method is used in practice. In practice we normally discretize the structure with an assemblage of elements which do not actually represent the real geometry. They approximate it but they are not exact.

COMMENT: I was wondering if you had given some thought to representing the undeformed geometry using things like Coon surface patches which people at General Motors and other places use to model surfaces. I think it might be appropriate in finite differences in locating points on the surface and in finite elements in defining the geometry for making your integrations. Maybe some of the surface representation work that's been done around the country by people not normally in structural analysis might be interesting to investigate.

COMMENT: I've heard some vague comments concerning various other methods of solving large shell problems. One of them is a spline fit method and the other would be a direct search method. Can you make any comments on the appropriateness of these techniques for very large problems?

GREENBAUM: I would say that the energy search technique is a procedure that we use to solve the final equations; it is not, in my estimation, the method itself. For example, the finite element method can employ direct energy search techniques. So I would label this as a mathematical tool to solve the final algebraic equations but not to be a new numerical method. I'm not familiar with the spline technique you mentioned.

QUESTION: You really didn't deal with the force method of structural analysis and did not refer to the force method of getting the stiffness element. Would you explain why? Paul Denke has warned us that the stiffness method can fail due to loss of numerical significance when element stiffnesses vary greatly. Experience at rather crucial times in development programs has indicated that this

does happen and the force method, again according to him, is not subject to this sort of failure. I think this is a fact we should at least continue to recognize.

GREENBAUM: I'm afraid that my experience with the force method is rather limited. However, many people believe that the force method is extremely hard to use. The displacement method, on the other hand, is a lot easier to use and yet is more general, and hence they tend to use it. If there is a force method exponent in the audience, I'd prefer to leave it to him to answer that.

COMMENT: Perhaps the following remarks will help. We set up equilibrium conditions and continuity conditions within the total structure at a finite number of node points, using a finite number of force variables and a finite number of displacement variables. We can set up the governing equations for this system consisting of equilibrium conditions and displacement continuity conditions at all the nodes of the structure. If we then attempt to solve the equilibrium conditions among the forces first and thereafter the continuity conditions, we arrive at the force method. And this method requires that we designate in one way or the other the so-called redundant forces which Denke and others have accomplished by the so-called structural cutter or automatic selection of the redundants. In the displacement method, the continuity condition is first resolved by the assumption of a unit displacement and then the equilibrium conditions at the nodes are set up in terms of the displacements. The elements which are used in these two methods could be the same type. They do not have to be in any way subject to the restriction that a force element has to be used in

the force method or displacement method developed element in the displacement method. Once the selection of the redundants, which is the most difficult part of the force method, has been made, from that moment on the force method is as easy to use as the displacement method. You can always make a badly behaving structure or a well behaving structural model in the two methods.

WALTON: Each chairman has been asked to close his session with a summary of at least what he considers the important points raised. From my own personal point of view the most important thing said was Dr. Stein's statement in favor of shared computer programs. I concur. I too believe that the test of use by many different people in different institutions is the best way to hone a program to excellence. I would add that mere distribution of computer programs, however, is not sharing in this sense. It is essential to share the experience with them as well. A point in this connection which Dr. Stein did not raise but which I think is important concerns the matter of confidence in a program. Too often we find the situation where a program will actually have the capability to provide us with information on which to base a better engineering decision but engineering management will fall back on older and more conservative methods of judgment simply because there is not a broad enough basis of confidence in a new program. If a program is good and many people use it, then many people know it is good and it becomes much easier to induce management to actually cut metal on the basis of the program results.

It is noteworthy, I think, that both authors agreed on the existence of basically three significant approaches to numerical analysis of shells.

Finite elements, finite differences, and forward integration. I was interested in Dr. Greenbaum's assessment that all three methods worked for the essentially one dimensional problems, and that for this class of problems all three are about equal in ease of application. I would like to note what I consider an important exception to Dr. Stein's statement where he said that the computer has not had much of an impact on analytical solutions, that is, exact solutions. It was only through the advent of the digital computer that it became possible to compute exact exponential solutions of the eighth order equations for cylindrical shells as first proposed, I think by Flugge, and implemented by Dr. Forsberg of Lockheed.

Finally, I think we should all take note of Dr. Greenbaum's evident feeling and I did not hear it challenged that a truly adequate finite element does not yet exist. I think we should before this week is out try to bring to the surface the reasons why such an element is so long in forthcoming.

A SURVEY OF SPARSE MATRIX TECHNOLOGY *

Ralph A. Willoughby
IBM Thomas J. Watson Research Center
Yorktown Heights, New York

ABSTRACT

Efficient techniques for handling sparse matrix calculations are an important aspect of problem solving in a wide spectrum of applications. There is a long history of mathematical development of iterative techniques for the numerical solution of partial differential equations which will not be systematically surveyed here. Instead the emphasis will be on direct methods for solving $Ax=b$ for x where most of the elements of A are zero. These latter techniques have arisen independently in such application areas as computational circuit design, linear programming, power systems, and structural mechanics. Each application area involves a certain set of special features relative to sparse matrix problem classes. These features are exploited in program packages to achieve a high degree of efficiency for the application. There is an inner core of common mathematical and computational features, and an important aim of this paper is to survey these "common features."

The comments in the paper concerning the interaction of sparse matrix technology with the architecture of the hardware and systems software of evolving information processing systems are those of the author himself. They reflect his point of view as a long-time numerical analyst and computer user in various large problem areas. Details concerning existing and planned hardware and software systems are beyond the scope of this survey.

* Extended version of invited lecture at the Conference on Computer Oriented Analysis of Shell Structures, Lockheed, Palo Alto Research Laboratory (August 1970) co-sponsored by Lockheed Missiles and Space Company, Palo Alto, California and Air Force Flight Dynamics Laboratory, Wright-Patterson Air Force Base, Ohio.

I. INTRODUCTION

The emphasis in this survey is on recent developments in direct methods for solving sparse matrix problems. There are a large number of computer programs for sparse matrix calculations but only a relatively small number of basic mathematical ideas underlying these programs. A primary objective of this paper is to provide an understanding of these concepts.

The concepts^{*} underlying sparse matrix calculations fall into four classes: (a) combinatorial analysis of the ordering of rows and columns, (b) floating point operations on scalars, vectors and matrices, (c) data management, and (d) programming. Programming is a critical aspect of the efficiency of the sparse matrix calculations, but it is beyond the scope of this paper to discuss programming details.

Frequent use is made throughout the paper of three letter mnemonics for important concepts. A mnemonics dictionary is provided in section 14, and this also serves as an index for where these concepts are discussed. An extensive bibliography and author list is also given in section 14. Three parts of the bibliography are organized chronologically by subject. They are: E. Eigenvalues and Eigenvectors, Sparse Matrices; F. Computer Architecture, Parallelism, Memory Hierarchy, Data Management; and G. Preserving Sparseness. There are 119 more references and these are listed in alphabetical order of the first author.

The primary motivation for a number of people working in sparse matrix research has been the computational design of large scale integrated circuits. This work will be discussed briefly in section 2.

^{*} Problem modeling is an important related concept, but will only be mentioned in passing in this paper.

Success with this part of sparse matrix technology led to an investigation of other application areas. Literature search and personal contact focused the author's attention on linear programming [73], power systems [91], and structural mechanics [103]. It became clear that cross fertilization in the field of sparse matrix computations would be very useful. Thus, a Symposium on Sparse Matrices and Their Applications was held at the IBM Research Center on September 9-10, 1968. The table of contents for the proceedings [112] is given in section 3, along with the table of contents for a similar conference [78] organized by the Institute of Mathematics and Its Applications and held at Oxford University, England, April 6-8, 1969. When reference is made to papers in these proceedings, it is via the mnemonics SMO (Sparse Matrix Oxford conference, p. 3.2) and SMY (Sparse Matrix Yorktown conference, p. 3.3).

Algorithm preliminaries are presented in section 4. In section 5, the following algorithms are discussed: Crout Triangular Factorization, Row Gaussian Elimination, Product Form of the Inverse, and Elimination Form of the Inverse.

Symmetric matrices are the subject of section 6, and band matrices together with band-like domains are discussed in section 7. Some comments are also made in section 7 about certain iterative methods. Those aspects of graph theory which directly relate to the ordering problem for sparse matrix calculations are discussed in section 8. Partitioning techniques are considered in section 9.

If Pivoting For Size (PFS) is involved in a disorderly sparse matrix, then the traditional strategies for pivot choice are often replaced by threshold

pivoting. This is especially true in the linear programming area. There is as yet no adequate treatment for the error analysis associated with this strategy.* However, a sketch of the general error analysis situation in numerical linear algebra is given in section 10. Also, a detailed discussion of matrix reducibility is included here, since it is related to some aspects of error analysis.

Sections 11-13 concern various aspects of the relationship between sparse matrix technology and the architecture of the hardware and systems software for information processing systems.

* At least, as far as the author is aware of in the existing literature.

2. SPARSE MATRICES IN NETWORK DESIGN

A novel approach [41] to the numerical treatment of sparse matrix problems has been motivated by computational design of large scale integrated circuits. This section is devoted to a discussion of the sparse matrix technology associated with a special class of computational design problems; namely, the optimal design of transistor switching circuits [41; G-46].*

The technology is aimed at achieving efficiency in the numerical solution of time dependent ordinary differential equations. One does not necessarily have the property of diagonal dominance nor of symmetry. Moreover, the coefficient matrix can have a highly irregular sparseness pattern. This level of generality in the coefficient matrix is also present in the sparse matrix problems for linear programming.

The computational circuit design problems have a special feature; namely, the sparseness structure of the coefficient matrix is fixed over a large number of cases. The systematic exploitation of this feature has resulted in a high level of efficiency for the computational design programs which use this sparse matrix technology.

In the subsequent paragraphs, a brief description is given of the mathematical aspects of the computational design of transistor switching circuits. One is concerned in these problems with determining how the transient switching behavior depends on a vector of design parameters, p , and modifying p so that the behavior is "optimal." This behavior is characterized by the solution.

* G-46 means reference 46 in the Preserving Sparseness part, G, of the bibliography at the end of this paper.

$w = w(t)$, to the initial value problem,

$$\dot{w} = f(t, w, p) \quad (2.1)$$

on the time interval, $t_0 \leq t \leq t_F$. Associated with (2.1) is a criterion function $C = C(p) > 0$, and the aim of the analysis is to determine the vector p which minimizes C . In order for optimization studies of this type to be feasible for realistic circuit models (e.g., 100-1000 equations in (2.1)), highly efficient numerical integration techniques are required.

The system (2.1) was usually stiff (i.e., there were widely different time constants in the system), and, as a result, predictor-corrector and explicit Runge-Kutta methods were not suitable. Liniger and the author proposed [56], along with others (see [56] for references) the use of an "essentially" unconditionally stable integration formula for (2.1) of the implicit form,

$$w_{n+1} - ah\dot{w}_{n+1} = R, \quad (2.2)$$

where R involves w, \dot{w} for $t \leq t_n$, and $t_{n+1} = t_n + h$. The nonlinear system (2.2) must be solved by a strongly convergent method, and Newton's method^{*} was proposed.

$$(I - ahJ^{(k)}) \Delta w = R + ah\dot{w}_{n+1}^{(k)} - w_{n+1}^{(k)}, \quad (2.3)$$

^{*} In order to control the growth of roundoff error, it is important to solve first for Δw in (2.3) and then find the new w from (2.5). The form (2.3) is closely related to the method of Iterative Refinement [64, 66] for linear algebraic equations, and this will be discussed later in sections 4 and 10.

$$w_{n+1}^{(0)} = w_n, \quad (2.4)$$

$$w_{n+1}^{(k+1)} = w_{n+1}^{(k)} + \Delta w, \quad (2.5)$$

where $J = \partial f / \partial w$ = Jacobian Matrix. In [G-46], a similar approach was adapted to a modified form of Gear's method.*

It has been repeatedly shown that this strongly implicit approach greatly relaxes the conditions controlling the choice of $\Delta t = h$. Efficiency of the method depends critically on the ability to solve (2.3) fast, reliably, and automatically.

System (2.3) is of the form

$$Ax = b, \quad (2.6)$$

and, fortunately, the coefficient matrix, A , is usually sparse.** Moreover, (2.6) will be solved a large number of times, but $SSI(A)$ *** (Sparseness Structure Information of A) is fixed, and this has been an important aspect of the sparse matrix technology developed in this area.

* C. W. Gear, Proc. IFIP Congress, Edinburgh, Scotland (1968) pp.A81-A85, [128].

** That is, the number $N(A)$ of nonzero elements of A is $< n^2$, where A is an $n \times n$ matrix.

*** For notational convenience, $SSI(A)$ is often represented by the Boolean Sparseness Matrix (BSM) associated with A , where 1 means nonzero. In sparse matrix programs, however, a Threaded index List with Pointers (TLP) is more appropriate [72]. See also Zollenkopf's paper SMO-6 [78].

The matrix A is not positive definite symmetric nor is it diagonally dominant. Moreover, $SSI(A)$ is arbitrary. However, if one fixes, a priori, the order in which the equations and unknowns are processed in Gaussian elimination or in triangular factorization, then the entire sequence of machine operations needed to solve (2.6) is also determined, a priori, simply from $SSI(A)$. The sparseness in b could also be utilized, but usually b is considered full.

Let $A = LU$ where $L = (l_{ij})$, $l_{ij} = 0$ for $j > i$ (lower triangular), $U = (u_{ij})$, $u_{ii} = 1$, $u_{ij} = 0$ for $j < i$ (unit upper triangular). It is convenient to introduce a composite $L \setminus U$ matrix as $C = (c_{ij})$ where $c_{ij} = l_{ij}$ for $j \leq i$ and $c_{ij} = u_{ij}$ for $j > i$. Each element of C is generated by a single formula*

$$c_{ij} = (c_{ij} - \sum_{k=1}^{m-1} c_{ik} c_{kj})d \quad (2.7)$$

where $m = \min(i, j)$, $d = 1$ for $i \geq j$, and $d = c_{ii}^{-1}$ if $i < j$. If $a_{ij} = 0$ and, for $1 \leq k \leq m-1$, $c_{ik} c_{kj} = 0$, then c_{ij} is "logically zero." Otherwise, a reduced formula defines c_{ij} . In this formula only nonzero numbers occur.

Gustavson created a highly efficient Symbolic Factorization Program (SFP), GNSO (GeNerate SOLve) [40]. GNSO uses $SSI(A)$ to generate a linear (loop-free) code SOLVE, which is specifically tailored to the zero-nonzero structure of A . Only nonzero quantities are stored and processed. $SSI(C)$ and operation counts in SOLVE are biproducts of GNSO. GNSOIN is similar to GNSO, but uses TLP's to represent SSI 's. A FORTRAN listing for GNSOIN is available upon request to

* $\sum_{k=\alpha}^{\beta} s_k = 0$ by definition if $\beta < \alpha$.

Gustavson. These ideas have been refined and extended in [G-46].

The program SOLVE can be very long, and as a result, Chang [112, pp. 113-122] created a program SFACT,* which uses SSI(A) to generate SSI(C) in the context of the Row Gaussian Elimination (RGE) programs developed by Tinney and his colleagues [71, 72, 83, 98].

Developments of this type and others have resulted in vastly improved network analysis programs and work is still continuing in this area. However, much of the work done is of a general nature not particular to network design and can be utilized in other application areas. In particular, computational design in engineering is, itself, a vast area which can greatly benefit by advances in sparse matrix technology. It is expected that these advances will continue for many more years.

* Presented at the Sparse Matrix Yorktown (SMY) conference. The table of contents for the proceedings [112] are given here in section 3 along with the contents for the proceedings of the Sparse Matrix Oxford (SMO) conference [78].

3. SPARSE MATRIX SYMPOSIA

Sparse matrix problems play an important role in a number of application areas; e.g., (a) Partial Differential Equations (PDE's) [28, 101, 102], (b) electronic circuits [16], (c) linear programming [73], (d) power systems [91], and (e) structural mechanics [103]. Sparse Matrix Algorithms (SMA's) have been extensively developed in each application area, and special features have been exploited in program packages to achieve a high degree of efficiency. There is, however, an inner core of common features, and two recent sparse matrix symposia [78, 112] were organized to help identify some of these features and to survey the field of sparse matrix methods.

Certain important topics were basically not covered in either symposium; e.g., (a) SMA's for PDE's,* (b) eigenvalue, eigenvector calculations [E-R1], and (c) error analysis [109]. However, many important topics relating to sparse matrix problems were covered, and certain of these topics will be discussed in other sections of this paper. As an aid to the reader and for referencing purposes, the tables of contents are given on the succeeding pages for the two conferences.

* Weinstein [112, pp.139-148] presented a paper on Stone's method [22,23,93,104] for solving certain classes of PDE's.

SMO - SPARSE MATRIX OXFORD CONFERENCE PROCEEDINGS [78]

Large Sparse Sets of Linear Equations

J. K. Reid (Ed.), Academic Press, London (1971), organized by the Institute of Mathematics and Its Applications, and held at Oxford University, England (April 1970).

TABLE OF CONTENTS

1. Beale, L., Sparseness in Linear Programming.
2. Allwood, R., Matrix Methods of Structural Analysis.
3. Larcombe, M., A List Processing Approach to the Solution of Large Sparse Sets of Matrix Equations and the Factorization of the Overall Matrix.
4. Walsh, J., Direct and Indirect Methods.
5. Ashkenazi, V., Geodetic Normal Equations.
6. Zollenkopf, K., Bi-factorization - Basic Computational Algorithm and Programming Techniques.
7. Jennings, A., Tuff, A., A Direct Method for the Solution of Large Sparse Symmetric Simultaneous Equations.
8. Baumann, R., Sparseness in Power System Equations.
9. Churchill, M., A Sparse Matrix Procedure for Power Systems Analysis Programs.
10. Harary, F., Sparse Matrices and Graph Theory.
11. Tewarson, R., Sorting and Ordering Sparse Linear Systems.
12. Baty, J., Stewart, K., Organization of Network Equations Using Dissection Theory.
13. Carre, B., An Elimination Method for Minimal-cost Network Flow Problems.
14. de Buchet, J., How to Take into Account the Low Density of Matrices to Design a Mathematical Programming Package. Relevant Effects on Optimization and Inversion Algorithms.
15. Ogbuobiri, E., Sparsity Techniques in Power-System Grid-Expansion Planning.
16. Reid, J., On the Method of Conjugate Gradients for the Solution of Large Sparse Systems of Linear Equations.
17. Willoughby R., Sparse Matrix Algorithms and Their Relation to Problem Classes and Computer Architecture.

SMY - SPARSE MATRIX YORKTOWN CONFERENCE PROCEEDINGS [112]

Organized and sponsored by the Mathematical Sciences Department, and held at the IBM Thomas J. Watson Research Center, Yorktown Heights, N. Y. (Sept. 1968).

TABLE OF CONTENTS

1. R. A. Willoughby, Introduction	xi - xxi
2. F. G. Gustavson, * W. M. Liniger, R. A. Willoughby, Symbolic Generation of an Optimal Crout Algorithm for Sparse Systems of Linear Equations.	1 - 10
3. R. L. Weil, Jr., P. C. Kettler, * An Algorithm to Provide Structure for Decomposition.	11 - 24
4. W. F. Tinney, Comments on Using Sparsity Techniques for Power System Problems.	25 - 34
5. R. P. Tewarson, The Gaussian Elimination and Sparse Systems.	35 - 42
6. R. K. Brayton, * F. G. Gustavson, R. A. Willoughby, Some Results on Sparse Matrices.	43 - 58
7. W. Orchard-Hays, MP Systems Technology for Large Sparse Matrices.	59 - 64
8. D. V. Steward, Tearing Analysis of the Structure of Disorderly Sparse Matrices.	65 - 74
9. H. Lee, An Implementation of Gaussian Elimination for Sparse Systems of Linear Equations.	75 - 84
10. G. B. Dantzig, R. P. Harvey, * R. D. McKnight, S. T. Smith, Sparse Matrix Techniques in Two Mathematical Programming Codes.	85 - 100
11. E. L. Palacol, The Finite Element Method of Structural Analysis.	101 - 106
12. P. Wolfe, Trends in Linear Programming Computation.	107 - 112
13. A. Chang, Application of Sparse Matrix Methods in Electric Power System Analysis.	113 - 122
14. W. M. Liniger, * R. A. Willoughby, Efficient Numerical Integration of Stiff Systems of Ordinary Differential Equations.	123 - 126
15. D. M. Smith, Data Logistics for Matrix Inversion.	127 - 138
16. H. G. Weinstein, Iteration Procedure for Solving Systems of Elliptic Partial Differential Equations.	139 - 148
17. F. Canin, Jr., Computer Methods of Network Analysis.	149 - 154
18. C. McCormick, Application of Partially Banded Matrix Methods to Structural Analysis.	155 - 158
19. P. Wolfe (Chairman), W. Givens, C. W. McCormick, C. B. Moler, W. Orchard-Hays, W. F. Tinney, Panel Discussion on New or Needed Work and Open Questions.	159 - 184

* Presented talk.

4. ALGORITHM PRELIMINARIES

A. General Remarks

There are a large number of methods which take advantage of special properties of the coefficient matrix, but if A is simply a general $n \times n$ sparse matrix, then there are three main types of direct sparse matrix algorithms for solving $Ax=b$ for x . These are based respectively on Gaussian elimination, triangular factorization, and Gauss-Jordan complete elimination. There are methods based on orthogonal transformations, such as the QR method [E-1,-2] which are very important for eigenvalue-eigenvector calculations, but they are not, in general, economical when applied to unsystematically sparse matrices.

Each direct algorithm has two stages: FIN (Form of the INverse) stage, that is, the factorization or transformation of A into a form appropriate for repeated application of the second stage; (2) SUB (SUBstitution) stage, that is, the applying of the $FIN(A)$ to the vector b .

Even if there is a single right hand vector, b , the SUB stage is often applied repeatedly because of the method of ITERative Refinement (ITR) [64,66] which will be described later in this section.

If it were true that A^{-1} is sparse, and many SUB stages are to be performed, then it would be an easy matter to code a sparse matrix-vector multiplication and then form $x = A^{-1}b$. However, A^{-1} is logically full unless A is reducible; that is, unless $B = P_1 A P_2$ is Block Lower Triangular (BLT) for some pair of permutation matrices P_1, P_2 [25,113; G-6,-10,-11,-20,-29].

Sparse Matrix Algorithms (SMA's) are designed to preserve sparseness in $FIN(A)$ in the context of numerically stable pivoting.* Matrices which are

* That is, a few applications of ITR are sufficient to achieve desired accuracy in the solution vector.

DID (Diagonally Dominant) or SYP (SYmmetric and Positive definite) have the desirable feature of allowing diagonal pivoting in any order. Here the ordering to preserve sparseness (see part G in the bibliography at the end of the paper for references) strategies can be applied a priori to SSI(A). This is followed by PDX (Pivoting down the Diagonal in Natural order). If, also, SSI(A) is fixed over a large number of cases, then SFP's are important.

For some classes of problems PFS (Pivoting For Size) is required,^{*} and many SMA's have a PFS version. Of course, for PFS to be effective, the matrix must not be poorly scaled.

A SMA designed to solve $Ax=b$ for x can be extended to solve $A^T z=c$ for z , where A^T is the transpose of A . The system $A^T z=c$ is the same as $z^T A = c^T$, so in the second stage, one replaces column SUB by row SUB.

B. Goals of SMA's

- (1) Avoid operating with and storing zero floating point numbers.^{**}
- (2) Order equations and unknowns to achieve efficiency in operations count and/or access to information (data and code).
- (3) Achieve sequential memory referencing^{***} both at the element and at the vector level.
- (4) Have efficient methods for handling the data management aspects of SMA's.

^{*} This is especially true for SYI (SYmmetric Indefinite) matrices [13,14; E-8, -25] and for the calculation of eigenvalues and eigenvectors by the method of INI (INverse Iteration) [E-R1, -18].

^{**}

Thus the usual $A(I,J)$ notation is replaced by $A(K)$, say, where $A(K) \neq 0$.

^{***}

The simplest schemes store and process the nonzero a_{ij} 's row by row or column by column, but other schemes, such as rows on one side of the diagonal and columns on the other side, are also used.

- (5) Incorporate automatic segmentation for efficient use of serial backup store on large problems (see section 12, and part F of the bibliography).
- (6) Exploit special properties of the matrix and/or the problem class.

C. Basic Macro-Operations (MOP's)*

$$\alpha \leftarrow \alpha - \beta\gamma/\delta, \quad (4.1)$$

$$\alpha \leftarrow (\alpha - v^T w)\rho, \quad (4.2)$$

$$v \leftarrow v - \sigma w, \quad (4.3)$$

$$v^T \leftarrow v^T - \sigma w^T; \quad (4.4)$$

where $\alpha, \beta, \gamma, \delta, \sigma$ are scalars; $\rho=1$ or $\rho=\delta^{-1}$ ($\delta=\text{pivot}$); v, w are column vectors; and $v^T w = \sum_i v_i w_i = \text{inner product}$.

MOP (4.1) is the classic element transformation which is used in each pivot step for Gaussian elimination, whereas (4.2)-(4.4) are vector oriented MOP's. MOP (4.2) has the advantage of requiring only one temporary extended register (or storage location(s)) to hold the accumulation of extra precision products $v_i w_i$. On the other hand (4.3) and (4.4) are inherently parallel. MOP (4.2) is basic in the FIN stage for triangular factorization, whereas it is (4.3) or (4.4) in the FIN stage of Gaussian or Gauss-Jordan elimination. Which of the MOP's are involved in the SUB stage depends on the type of substitution (row or column) and on how the matrices involved in the FIN(A) are stored.

* " \leftarrow " means "is the result of evaluating" as in the programming language APL [47]. This language has many features which make it desirable for representing SMA's and other algorithms which deal with arrays as well as a variety of numbers such as integers, Boolean 0 and 1, and floating point. APL/360 Primer Student Text is available through IBM branch offices. Note that expressions (4.1)-(4.3) are not "pure" APL expressions as they stand, since it is not assumed that the reader knows the powerful operation set and conventions associated with APL.

If v is being processed repeatedly via (4.2)-(4.4), then it is a common technique to store v as a full vector, zeros and all. In this way one can execute (4.2)-(4.4) by merely indexing over the nonzero components of the sparse vector w .

D. Method of Iterative Refinement (ITR) [64,66]

Assume one is solving $Ax=b$ for x and an adequate^{*} $FIN(A)$ has been formed, then ITR proceeds as follows:

- (1) Given an approximate solution $x^{(k)}$ (e.g., take $x^{(0)} = 0$), form^{**}

$$r^{(k)} = b - Ax^{(k)} \quad (4.5)$$

and exit if $r^{(k)}$ and/or $x^{(k)}$ is satisfactory, otherwise go to (2).

- (2) Apply SUB stage to $FIN(A)$ to solve for Δx in
$$A\Delta x = r^{(k)} \quad (4.6)$$

- (3) Set $x^{(k+1)} = x^{(k)} + \Delta x$, then go to (1).

E. Elementary Matrices [46, p.3].

The rank one^{***} matrix wv^T , whose (i,j) element is $w_i v_j$, plays a number of important roles in numerical linear algebra, and is especially important when used in the form of an elementary matrix, $I + wv^T$, where I is the identity matrix. Note that, if $E = I + wv^T$, then $\delta(E)$ = determinant of $E = 1 + v^T w$. Moreover, if $\delta(E) \neq 0$, then $E^{-1} = I - \rho wv^T$ where $\rho = (1 + v^T w)^{-1}$.

One class of applications for elementary matrices are the Methods of Modified Matrices (MMM's) [4,8,116-119; 45, pp. 79,83,84]^{****}. There is a special

* One purpose of ITR is to obtain an assurance that $FIN(A)$ is adequate, and the other is to repeat ITR until a satisfactory x is obtained.

** It is important to form $b - Ax^{(k)}$ in extended precision because of numerical cancellation.

*** That is, every 2×2 submatrix is singular but at least one element is $\neq 0$.

This is an aspect of Kron's method of tearing [52: G-1,-2,-3,-4,-5,-7,-19,-20; SMO-12; SNY-8].

sparse matrix version of a MM which assumes that $\Gamma IN(A)$ has been formed and that

$$M = A + wv^T. \quad (4.7)$$

The algorithm for solving $Mz = c$ for z then proceeds as follows:

- (1) Solve $Ax=c$ and $Au=w$ for x and u respectively. Comment. Note that, $M=A+wv^T = A(I+uv^T)$, and, if $(I+uv^T)z = x$, then $Mz=c$.
- (2) Form $\alpha = v^T x$ and $\beta = v^T u$. If $1+\beta=0$, then exit with message, "M is singular," otherwise go to (3).
- (3) Form $\sigma = (1+\beta)^{-1}\alpha$.
- (4) Form $z = x - \sigma u$ and exit normally. Comment. $z = (I+uv^T)^{-1}x = (I - (1+\beta)^{-1}uv^T)x = x - \sigma u$.

An important special class of elementary matrices are those which involve only one nontrivial column or one non-trivial row; that is, when v^T is a row of I or w is a column of I , respectively. As is customary, one lets e_k represent the k^{th} column of I

One has in particular the class of Elementary Column Matrices (ECM's)* whose properties are described below.

- (1) Let $t_k^T = (t_{1k}, \dots, t_{kk}, \dots, t_{nk})$, and

$$T_k = \begin{array}{|c|c|c|c|c|c|c|} \hline 1 & & & & t_{1k} & & \\ \hline & \cdot & & & \cdot & & \\ \hline & & \cdot & & \cdot & & \\ \hline & & & 1 & \cdot & & \\ \hline & & & & t_{kk} & & \\ \hline & & & & \cdot & 1 & \\ \hline & & & & \cdot & & \cdot \\ \hline & & & & t_{nk} & & 1 \\ \hline \end{array}$$

* One also has ECM's, but only ECM's are described since they have been the backbone of linear programming algorithms [62,73; 75, vol.2, pp.271-284; G-31].

Comment. $T_k = I + (t_k - e_k)e_k^T$, $T_k e_j = e_j$ for $j \neq k$, and $T_k e_k = t_k$.

- (2) Assume $t_{kk} \neq 0$ and let $\rho_k = t_{kk}^{-1}$, then T_k is nonsingular, and T_k^{-1} is trivial to form. In fact,

$$T_k^{-1} = I - \rho_k (t_k - e_k)e_k^T$$

$$= (I - t_k' e_k^T) D_k,$$

where $t_k' = t_k - t_{kk}e_k$, and $D_k = \text{diag. } (1, \dots, 1, \rho_k, 1, \dots, 1)$. That is,

$$T_k^{-1} = \begin{array}{|c|c|c|c|c|c|c|c|} \hline 1 & & & & -t_{1k} & & & \\ \hline & \ddots & & & \vdots & & & \\ \hline & & \ddots & & \vdots & & & \\ \hline & & & \ddots & \vdots & & & \\ \hline & & & & 1 & & & \\ \hline & & & & \vdots & \ddots & & \\ \hline & & & & -t_{nk} & & & 1 \\ \hline \end{array} \times \begin{array}{|c|c|c|c|c|c|c|c|} \hline 1 & & & & & & & \\ \hline & \ddots & & & & & & \\ \hline & & \ddots & & & & & \\ \hline & & & \ddots & & & & \\ \hline & & & & \rho_k & & & \\ \hline & & & & & \ddots & & \\ \hline & & & & & & 1 & \\ \hline & & & & & & & 1 \\ \hline \end{array}$$

- (3) Column SUB. If $c = T_k^{-1}b$ then c is calculated as follows.

(a) Let $\sigma = \rho_k b_k = c_k$. If $\sigma = 0$, then $c=b$, so assume $\sigma \neq 0$.

(b) For $j \neq k$, $c_j = b_j - \sigma t_{jk}$.

Comment. MOP(4.3) is involved here.

- (4) Row SUB. If $c^T = b^T T_k^{-1}$, then c^T is calculated as follows.

(a) If $j \neq k$ then $c_j = b_j$.

(b) $c_k = (b_k - b^T t_k') \rho_k$.

Comment. MOP (4.2) is involved here.

- (5) Column MM. Let $A'e_j = Ae_j$ for $j \neq k$ while $A'e_k = a'_k$ and

$Ae_k = a_k \neq a'_k$; that is, the k^{th} column of A' is a'_k , otherwise A' is A .

Algorithm for solving $A'z = c$ for z proceeds as follows:

(a) Solve $Ax=c$ and $At_k = a'_k$ for x and t_k respectively. Comment.

Define T_k as in (1).

(b) If $t_{kk} = 0$ then A' is singular so exit with message, otherwise go to (c).

(c) Form $z = T_k^{-1}x$. Comment. T_k^{-1} is formed as in (2) and z is formed according to (3), then $z = T_k^{-1}x = T_k^{-1}(A^{-1}c) = (A')^{-1}c$.

5. SPARSE MATRIX ALGORITHMS (SMA's). GENERAL CASE

A. General Remarks

In the FIN stage of SMA's there are two pivoting situations, namely (1) PDN (Pivoting down the Diagonal in Natural order) and (2) PFS (Pivoting For Size). Wilkinson [E-R1, pp. 225-227] has a TRIangular Factorization (TRF) method with interchanges, which Forsythe [29] published as an algorithm for the full matrix case.* The disorderly sparse matrix is not well adapted to PFS versions of triangular factorization, but, by keeping row and/or column permutation lists the other SMA's can be adapted to certain PFS strategies.

B. Notation

$$A = (a_{ij}) \quad 1 \leq i, j \leq n$$

$$L = (l_{ij}), \quad l_{ij} = 0 \text{ for } j > i \text{ (lower triangular)}$$

$$U = (u_{ij}), \quad u_{ii} = 1, \quad u_{ij} = 0 \text{ for } j < i \text{ (unit upper triangular)}$$

$$C = \text{composite } L \setminus U \text{ matrix} = (c_{ij})$$

$$c_{ij} = \begin{cases} l_{ij} & \text{for } j < i \\ u_{ij} & \text{for } j > i \end{cases}$$

$$D = \text{diag. } (l_{11}, l_{22}, \dots, l_{nn}) = \text{diagonal matrix of pivots.}$$

$$W = LD^{-1} = \text{unit lower triangular matrix}$$

$$R = DU = \text{upper triangular matrix}$$

$$A = LU = WR = WDU.$$

C. Crout Triangular Factorization **

(1) FIN Stage. $1 \leq m \leq n$, $m \leq i \leq n$, $m+1 \leq j \leq n$ ($m \neq n$),

* Band matrices (see section 7) are another case which has been considered [E-8].

** As before $\sum_{k=\alpha}^{\beta} S_k = 0$ by definition if $\beta < \alpha$.

$$\ell_{im} = a_{im} - \sum_{k=1}^{m-1} \ell_{ik} u_{km},$$

$$\rho_m = \ell_{mm}^{-1} (\ell_{mm} \neq 0)$$

$$u_{mj} = (a_{mj} - \sum_{k=1}^{m-1} \ell_{mk} u_{kj}) \rho_m$$

(2) Forward SUB. Ly = b, $1 \leq m \leq n$,

$$y_m = (b_m - \sum_{k=1}^{m-1} \ell_{mk} y_k) \rho_m.$$

(3) Backward SUB. Ux = y, $n \geq m \geq 1$,

$$x_m = y_m - \sum_{k=m+1}^n u_{mk} x_k.$$

D. Row Gaussian Elimination (RGE). *

Remarks. Here, $A = WR$, and all storage and processing for A, W, and R is by rows. W is formed element by element, and MOP (4.4) is used repeatedly in the FIN stage (this is commonly called the elimination stage in RGE). Column SUB is the most common situation, and since W and R are stored by rows, forward and backward SUB has (4.2) as the basic MOP. Only the FIN stage is outlined below.

$$(1) \quad r_1^T + a_1^T$$

$$(2) \quad \text{For } 2 \leq k \leq n, \quad v^T + a_k^T;$$

(a) For $1 \leq j \leq k-1$,

$$w_{kj} = v_j / r_{jj},$$

$$v^T + v^T - w_{kj} r_j^T;$$

(b) $w_{kk} = 1$, $w_{kj} = 0$ for $j > k$;

$$(c) \quad r_k^T + v^T.$$

*

Let $a_k^T = e_k^T A = k^{\text{th}}$ row of A, etc.

E. Product Form of the Inverse (PFI)*

(1) FIN stage. $T_n^{-1} \dots T_2^{-1} T_1^{-1} A = I;$

(a) $t_1 = a_1 = Ae_1,$

(b) For $2 \leq k \leq n,$

$$t_k = T_{k-1}^{-1} \dots T_1^{-1} a_k \text{ where } a_k = Ae_k.$$

(2) SUB stage (column case)

$$x = A^{-1}b = T_n^{-1} \dots T_1^{-1} b.$$

F. Elimination Form of the Inverse (EFI)

(1) FIN stage: $L_n^{-1} \dots L_1^{-1} A = U;$

(a) $L_1 = T_1$ as in PFI;

(b) For $2 \leq k \leq n$ let $v_k = L_{k-1}^{-1} \dots L_1^{-1} a_k$ where $a_k = Ae_k$, then

$$v_{jk} = \begin{cases} u_{jk} & \text{for } j < k \\ l_{jk} & \text{for } j \geq k; \end{cases}$$

$$L_k =$$

1						
	.					
		1				
			l_{kk}			
	.		.	1		
			.		.	
	.		l_{nk}			1

(c) By a trivial factorization

$$U = U_n \dots U_2$$

where

*Elementary column matrices (see section 4, part E) are the basic tools in the PFI algorithm.

$U_k =$

1			u_{jk}			
	.		.			
		1	$u_{k-1,k}$			
			1			
				1		
					.	
						1

(2) SUB stage (column case)

$$x = A^{-1}b = U_2^{-1} \dots U_n^{-1} L_n^{-1} \dots L_1^{-1} b.$$

Remarks. The EFI algorithm as presented is column-oriented. However, if one applies the transpose operation to each formula in the factorization stage of algorithm F above, the result is a row EFI algorithm, which is an alternate way of handling RGE. Elementary row matrices which are either upper triangular or unit lower triangular are the basic operational tool in row EFI.

The PFI algorithm has an elegant simplicity in its formulation, but it has the sparseness structure of $L \setminus U^{-1}$ rather than the preferred $L \setminus U$ of the other algorithms discussed here [G-43].

G. Pivoting For Size (PFS)

Remarks. PFS has been a critical aspect of algorithms for matrices which are neither positive definite symmetric nor diagonally dominant. The computational price one pays for this in dealing with full or band matrices is reasonable, but where the sparseness structure is arbitrary, this is not necessarily the case.

Care must be exercised in choosing pivots to also preserve sparseness. Clearly, zeros and near-zeros cannot be used as pivots, so some threshold criterion at least is necessary. This threshold approach has been standard in LP calculations.

In full matrix and band matrix algorithms, one has two options. The first is to interchange rows and/or columns to bring the m^{th} pivot element into the (m,m) position. This option has the advantage of simplifying subsequent indexing operations. The second option leaves the elements in their natural location and builds instead a row permutation $(\mu_1, \mu_2, \dots, \mu_n)$ and/or a column permutation $(\nu_1, \nu_2, \dots, \nu_n)$ where (μ_m, ν_m) is the position of the m^{th} pivot. This requires more involved indexing, but has the advantage of not requiring the interchange of compacted vectors of different length.

For simplicity PFS will be discussed only for the PFI algorithm, but a similar extension can easily be made for the RGE and EFI algorithms. The Crout algorithm is less suitable for this purpose when sparse matrices are involved.

The PFI algorithm with PFS is essentially the same as for the one given, except that at the k^{th} step, one deals with column ν_k of A and with the μ_k^{th} component of this vector as the pivot. The nontrivial column of T_k^{-1} is the μ_k^{th} . After n steps, the A matrix has been transformed into a permutation, P , of the identity matrix, that is

$$A^{-1} = P^T T_n^{-1} \dots T_1^{-1}$$

where for $1 \leq k \leq n$, $i = \mu_k$, $j = \nu_k$,

$$P e_j = e_i$$

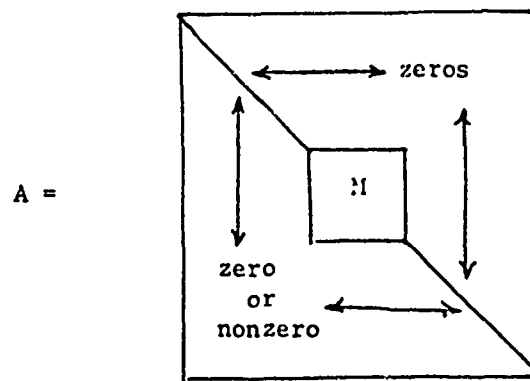
and

$$P^T e_1 = \dots$$

since

$$P^{-1} = P^T.$$

The v permutation is introduced to partially preserve sparseness in the form of the L matrix. For example, one could process the columns in order of increasing number of nonzeros in each column. Because of the $L \setminus U^{-1}$ sparseness structure of the form of the inverse in the PFI algorithm, a standard practice in L has been to reorder rows and columns relative to singletons* to reduce the matrix to the special block lower triangular form shown below.



A^{-1} also has this same form, but, in fact, only the kernel matrix M has to be factored if the PFI algorithm is suitably modified. The set of SMA's presented here certainly do not represent a complete list, but they provide insight into the character of SMA's for the general case.

* A singleton row (column) has exactly one nonzero component. As in Gaussian pivot reduction, one strikes out the row and column of the pivot element and continues to search for singletons.

6. SYMMETRIC MATRICES

A. General Remarks

If $A = A^T$ (i.e., $a_{ij} = a_{ji}$) and diagonal pivoting is feasible, as in the case of positive definite or diagonally dominant matrices,^{*} then considerable saving can be achieved in both storage and operations count. However, in the case of sparse matrices, this requires more intricate indexing because both row and column access to elements is required in the factorization stage.

It is interesting to note that, if A is even symmetrical in sparseness pattern and diagonal pivoting is feasible, then advantage can be made of this in the design of a factorization algorithm. This is the motivation for Zollenkopf's Bi-Factorization (BIF) Algorithm [78; SMO-6] in which he operates on the left of A by a sequence of elementary column matrices,^{**} and at the same time, on the right by a sequence of elementary row matrices.^{***} At the end, A has been transformed into the identity matrix, and one thereby has created a Form of the INverse (FIN). This is similar in character to Markowitz's Elimination Form of the Inverse (EFI)[62] and is an extension of techniques pioneered by Tinney and his colleagues [G-14,-34;71,72]. Zollenkopf's article is very detailed, with flow charts, diagrams of the various matrices and examples of handling SST's via Threaded index Lists with Pointers (TLP's).

As before, let $A = LU = WR = WDU$. Since $A = A^T$, then $W = U^T$, and thus $u_{ji} = w_{ij} = l_{ij}/l_{jj} = l_{ij}\rho_j$. If $\rho_j > 0$ for $1 \leq j \leq n$, then one also has the Cholesky factorization, $A = GG^T$, where $G = WD^{1/2}$. The main point of using

^{*}In Power System Analysis [91] A is often complex symmetric with diagonal dominance.

^{**}Which are also lower triangular.

^{***}Which are also unit upper triangular.

the Cholesky factorization over $A = U^T D U$ is that $\sqrt{\rho(1+\epsilon)} \approx \sqrt{\rho}(1 + \frac{1}{2}\epsilon)$ so that one achieves an extra bit of significance in the pivots. This has to be balanced against the extra cost of calculating $\ell_{jj}^{-1/2}$ instead of ℓ_{jj}^{-1} . If $\ell_{jj} < 0$ or is complex, then the square root approach is not considered.

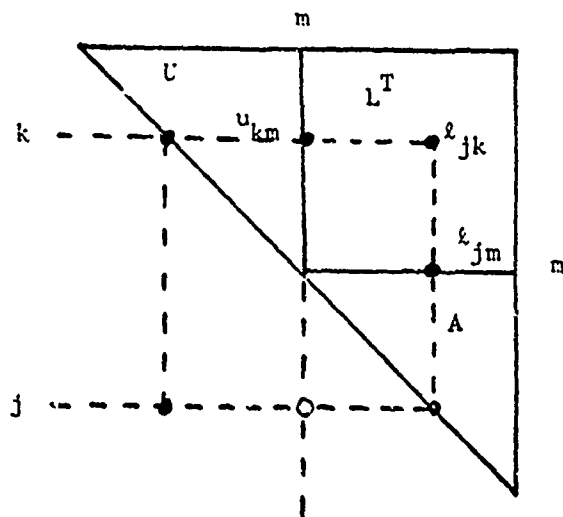
B. $A = U^T D U$ Factorization*

- (1) Remarks. The upper triangular portion of A will be stored and processed row by row. As the processing proceeds, the diagonal element a_{mm} is replaced by $\rho_m = \ell_{mm}^{-1}$ and a_{mj} is replaced by ℓ_{jm} for $m+1 \leq j \leq n$. Recall that

$$\ell_{jm} = a_{jm} - \sum_{k=1}^{m-1} \ell_{jk} u_{km}$$

and that $u_{km} = \ell_{mk} \rho_k$. The element u_{km} will be formed when it is first needed, and it will then replace ℓ_{mk} , which is no longer needed.

The diagram below illustrates this storage situation.



* Only a full matrix version is presented since the sparse matrix algorithm requires more detail than is suitable for a survey such as this.

(2) Details of Algorithm.

- a. $\rho_1 = a_{11}^{-1}$.
- b. $\ell_{k1} = a_{1k}$ for $2 \leq k \leq n$.
- c. DO for $2 \leq m \leq n$:*
 - 1 DO for $m \leq k \leq n$, $c_k = a_{mk}$.
 - 2) DO for $1 \leq k \leq m-1$;
 - a) $d = \ell_{mk} \rho_k$,
 - b) DO for $m \leq j \leq n$,

$$c_j = c_j - \ell_{jk} d,$$
 - c) $u_{km} = d$ (stored in (k,m) location in place of ℓ_{rk}).
 - 3) $\rho_m = c_m^{-1}$ (stored in (m,m) location in place of a_{mm}).
 - 4) DO for $m+1 \leq k \leq n$.

$$\ell_{km} = c_k$$
 (stored in (m,k) location in place of a_{mk}).

Comments. The quantities, c_k , $m \leq k \leq n$, are the partial accumulated inner products. For accuracy purposes it is desirable to use extended precision in the formation and storage of the c_k 's.

C. Conjugate Gradients Method (CGM)

Reid [78; SMO-16] wrote the following in the introduction to his paper on CGM.

"The method of conjugate gradients has been known for some time, having been developed independently by E. Stiefel and by M. R. Hestenes with the cooperation of J. B. Rosser, G. Forsythe and L. Paige, but it has received little attention recently. It is difficult to see why this has been so since the method has several very pleasant features when regarded not as a direct method for the solution of full systems of equations but as an iterative method for the solution of large and sparse systems. It is our purpose here to explain these features and to report on some numerical experiments which compare the various versions of the algorithm that are available."

* Comment. $\rho_k, \ell_{jk}, u_{ki}$ have been formed for $1 \leq k \leq m-1$, $k+1 \leq j \leq n$, $k+1 \leq i \leq m-1$, but ℓ_{jk} is needed now only for $m \leq j \leq n$.

Livesley [57, p.37] found difficulties in using CGM in structural problems. Others seem to have found difficulties which caused them to abandon CGM as a basic sparse matrix algorithm for SYP (SYmmetric and Positive definite) matrices. Stanton and his colleagues, on the other hand, are systematically developing these methods for structural mechanics problems [33, 92]. They report that preconditioning via scaling of the coefficient matrix is an important practical consideration.

Assuming that CGM can be made numerically insensitive to accumulated round-off error, and can achieve sufficiently accurate results in a reasonable number of steps, then CGM has an attractive feature of effectively utilizing the sparseness of the A matrix, no matter how irregular the sparseness structure is. There are only three basic macro-operations involved in the calculation, namely, $v \leftarrow Av$, $\alpha \leftarrow w^T v$, and $v \leftarrow v + \beta w$. Here again, one would treat v in each case as a full vector but store A compactly row by row.

Further discussion of CGM is contained in [7, 19, 20, 34, 35, 43].

D. SYmmetric Indefinite (SYI) Matrices

If $M = M^T$ but M is neither positive definite nor diagonally dominant, then the problem of solving $Mx = b$ is more complicated. Of course, one can ignore the symmetry property of A and proceed to PFS [E-R1]. However, more storage and operations are required by this approach. A different approach has been taken in [13, 14]. Here, one applies a mixture of scalar and 2×2 block diagonal pivoting so that symmetry is preserved in the reduction process. This approach has been shown to be stable when the proper care is exercised in the choice of the 2×2 blocks.

An interesting PFS strategy is discussed in [E-25] for the case in which the coefficient matrix is of the form $M = A - \lambda B$ where λ is real, A and B are real band symmetric, and B is positive definite. The pivoting is stable but, also, the product of the first k pivots is the determinant of the first k rows and columns of M . The Sturm sequence property is then used to determine the number of eigenvalues which are greater than λ [E-R1, p.300].

7. BAND MATRICES AND BAND-LIKE DOMAINS (BLD's)

A matrix $A = (a_{ij})$ is said to have bandwidth $2k+1$ if k is the smallest index such that $a_{ij} = 0$ for $|i-j| > k$. A bandwidth of 5 for an 8×8 matrix is shown below.

A =

a_{11}	a_{12}	a_{13}					
a_{21}	a_{22}	a_{23}	a_{24}				
a_{31}	a_{32}	a_{33}	a_{34}	a_{35}			
	a_{42}	a_{43}	a_{44}	a_{45}	a_{46}		
		a_{53}	a_{54}	a_{55}	a_{56}	a_{57}	
			a_{64}	a_{65}	a_{66}	a_{67}	a_{68}
				a_{75}	a_{76}	a_{77}	a_{78}
					a_{86}	a_{87}	a_{88}

Band matrices are an important special class of sparse matrices, and many efficient algorithms have been developed [36, 63, 82, 95, 97; E-R1, -8]. If A allows PDN then the algorithms are especially easy, and if $a_{ij} \neq 0$ if and only if $|i-j| \leq k$ (full bands), then $SSI(C) = SSI(A)$.

Assume PFS is involved, but that the m^{th} pivot position is chosen from among the positions (i,m) where $m \leq i \leq m+k$, then in the worst case, the semiband width above the diagonal in U is doubled [E-8, -25].

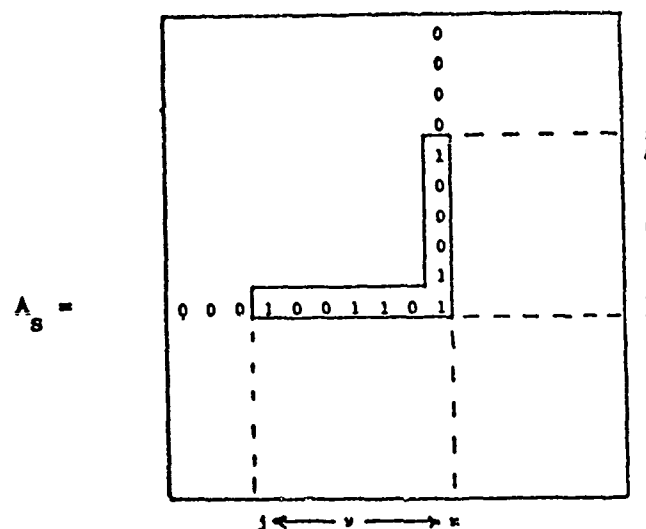
* Of course, one ignores the generation of zeros by exact numerical cancellation in dealing with SSI's.

If a high level of storage and operational efficiency is desired, then band matrices are too restrictive a class for many sparse matrix applications. Again, assume A allows PDN, then the following Band-Like Domain (BLD) for A is a useful sparse matrix generalization of band matrices.

Definition. Assume $1 \leq m \leq n$ then

- (1) $(m, m) \in \text{BLD}(A)$.
- (2) For $1 \leq \mu < m$, $(\mu, m) \in \text{BLD}(A)$ if and only if $a_{i\mu} \neq 0$ for some i such that $1 \leq i \leq \mu$.
- (3) For $1 \leq \nu < m$, $(m, \nu) \in \text{BLD}(A)$ if and only if $a_{m j} \neq 0$ for some j such that $1 \leq j \leq \nu$.

This domain is indicated, for a typical m , in the diagram below.* A_s denotes the BSM associated with A , where $(A_s)_{ij} = 1$ means $a_{ij} \neq 0$.



A and C both have only zeros outside $\text{BLD}(A)$ but C may fill some of the zero positions inside the BLD. In fact, for "tridiagonal plus" matrices,** the entire BLD for C is full. The 8x8 example shown below illustrates this

* Only the pertinent zeros and nonzeros are shown.

** A tridiagonal matrix is a band matrix with $k=1$; the "plus" means that not only is $a_{ij} \neq 0$ for $|i-j| \leq 1$ but also for certain other positions.

band-like character and tridiagonal plus fill-in.*

$$A_s = \begin{bmatrix} 1 & 1 & 0 & 0 & 0 & 0 & 0 & 1 \\ 1 & 1 & 1 & 0 & 1 & 1 & 0 & \emptyset \\ 0 & 1 & 1 & 1 & \emptyset & \emptyset & 0 & \emptyset \\ 1 & \emptyset & 1 & 1 & 1 & \emptyset & 0 & \emptyset \\ 0 & 0 & 0 & 1 & 1 & 1 & 1 & \emptyset \\ 0 & 1 & \emptyset & \emptyset & 1 & 1 & 1 & \emptyset \\ 1 & \emptyset & \checkmark & \emptyset & \emptyset & 1 & 1 & 1 \\ 0 & 0 & 0 & 1 & \emptyset & \emptyset & 1 & 1 \end{bmatrix}$$

Note that the tridiagonal plus sparseness structure is not necessarily preserved under reorderings of the matrix A .

Jennings [48, 49, 78; SMO-7] has exploited BLD's in his algorithms for SYP matrices. Melosh and Bamford [65] use a related idea in their wavefront approach to data handling, and NASTRAN [58,59,60,112;SMY-18,pp.155-158] has an active column feature for those columns where the nonzeros extend above the band.

Tri-Diagonal Matrices (TDM's) are, in many ways, an ideal type of sparse matrix. A great many numerical analysis papers have been devoted to TDM's [see E-R1,-R2 for references]. TDM's are basic in many areas of numerical

*The symbol \emptyset means $a_{ij} = 0$, $c_{ij} \neq 0$.

analysis, such as eigenvalue-eigenvector calculations and differential equations. These matrices, together with the more general class of Tri-Diagonal Like (TDL) matrices are the cornerstone of the iterative methods referred to as Alternating Direction Implicit, Splitting, and Fractional Step.

Definition. A is a TDL matrix means

- (1) $a_{ij} \neq 0$ if and only if $a_{ji} \neq 0$.
- (2) For $1 \leq m \leq n-1$ there is exactly one i such that $m+1 \leq i \leq n$ and $a_{im} \cdot a_{mi} \neq 0$.
- (3) A allows PDN.

Note that $SSI(C) = SSI(A)$. See section 8 and [G-9, -21] for a graph theoretic discussion of TDL matrices.

One solves multidimensional partial differential equations by cycling through a sequence of TDL problems. See [10,21,28,39,61,101,102] for surveys and some of the earlier references. This is a very active subject, and many articles continue to appear in standard numerical analysis journals. The mathematical analysis is largely limited to the case of commuting operators [106].

These methods^{*} are a part of a broad spectrum of iterative methods [101]. The tradeoffs between using sparse direct methods and various types of iterative methods is rather poorly understood except for certain model problems [24]. For a completely regular model problem, one can precisely estimate the computational complexity as $n \rightarrow \infty$ where n is the order of the coefficient matrix. However, this type of analysis can be misleading. If the model problem is the practical problem to be solved, then there are special techniques such as the use of Fourier transforms which can be used to achieve very high efficiency. On the other hand, if the problem is irregular, then the computational complexity as

^{*}That is, those which are based on the computational efficiency associated with solving TDL systems.

$n \rightarrow \infty$ can be vastly different than that predicted by the model problem.

Stone's method [22,23,93,104; SMY-16,pp.139-148] holds considerable promise for certain classes of problems. The idea here is to let $M = A + N$ where N is chosen to kill the propagation of nonzeros inside the BLD. Let $M = LU$, and C be the composite $L \setminus U$ matrix, then M is fuller than A but $SSI(C) = SSI(A)$. This has been shown to be an effective procedure for sparse matrix problems arising in the petroleum industry even for certain types of coupled systems of partial differential equations.

The Finite Element Methods (FEM's) provide a whole new spectrum of sparse matrix problems which have a quite different computational complexity than the finite difference methods. For one thing, the size of the matrix is much smaller. However, the generation of the matrix elements is quite involved for the more sophisticated classes of finite elements. In comparing computational complexity of finite difference versus finite element methods, it is important to define the problem class, and to determine the extent to which one time symbolic preprocessing can be utilized in a parameter variation study. There is a vast literature associated with FEM's but is not referenced here. However, a recent report by Segethova [84] deals with direct sparse matrix methods for matrices arising in FEM's.

8. GRAPHS. UNDIRECTED, DIRECTED, AND BIPARTITE.

There are a number of ways in which Sparseness Structure Information (SSI) can be represented and manipulated. The use of Threaded index Lists with Pointers (TLP's) is a powerful approach in the automatic machine computation, but other representations are more suitable from a conceptual point of view.

The Boolean Sparseness Matrix (BSM) associated with a given sparse matrix A is one tool.* However, graphs of the sparseness structure have the advantage of being invariant under certain classes of reorderings of the matrix A .

Graph theory is a vast field in its own right. References [42,77] provide an introduction to certain applications of graph theory, and contain a large number of references. However, only a small part of graph theory impacts the field of direct sparse matrix algorithms.

Three types of graphs will be described briefly; namely, undirected, directed and bipartite graphs. A number of authors** have used graph theory techniques to develop pivot strategies.

Rose [79,80] has made a systematic study of the fill problem for matrices with symmetric sparseness structure*** where diagonal pivoting in any order is allowed. An undirected graph G is associated with A_s . The vertices i and j , where $i \neq j$, are connected by an undirected edge if and only if $a_{ij} \neq 0$. The labeling of the nodes is not intended to imply the order in which the nodes are eliminated. When a pivot sequence has been specified, there is associated with

* This matrix will be denoted by A_s ; $(A_s)_{ij} = 1$ if and only if $a_{ij} \neq 0$.

** See part G (Preserving Sparseness) in the bibliography for some of the references.

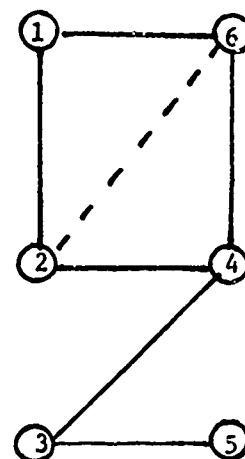
*** That is, $A_s^T = A_s$.

G , a graph G' which represents the sparseness structure for the C matrix (i.e., the composite $L \cup$ matrix).

The diagram below illustrates a 6x6 example.

$A_s =$

1	1	0	0	0	1
1	1	0	1	0	0
0	0	1	1	1	0
0	1	1	1	0	1
0	0	1	0	1	0
1	0	0	1	0	1



After "eliminating" vertex j , the vertices adjacent^{*} to j form a clique, that is, the principal submatrix associated with the set of these vertices forms a full matrix. From the graph it is clear that 5,3,4,2,1,6 is an optimal pivot sequence, and only one new edge^{**} is introduced in creating G' . On the other hand, the pivot sequence, 4,3,2,1,6,5 introduces 6 new edges and hence is undesirable as a pivot strategy.

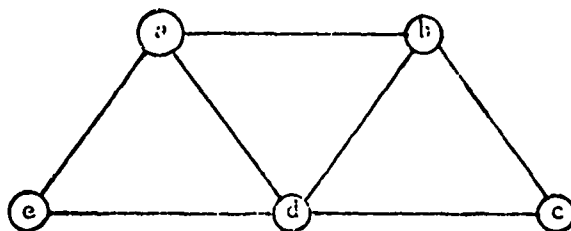
The vertex 5 has a special significance because only one vertex is adjacent to it. Such terminal vertices create no fill when they are eliminated. In terms of the matrix A_s , terminal vertices are associated with rows which have

* If $i \neq j$ then vertex i is adjacent to vertex j provided $a_{ij} \neq 0$.

** Joining vertex 2 and vertex 6.

exactly two non-zero elements. If the graph is a tree (i.e., has no cycles) then one can always choose a terminal node at each pivot step [G-9]. A TDL matrix is an optimally ordered^{*} tree, and Carré [G-21] has exploited this idea in an ordering scheme for block iteration.

The class of graphs G' have been characterized by Rose as being triangulated.^{**} The minimum fill problem, then, is that of determining a triangulation of a given graph G which introduces the least number of new edges. An example of a triangulated graph with 5 vertices and 7 edges is shown below.



If a graph G is triangulated then there exist pivot sequences such that no fill occurs in the elimination process.

Ordering to achieve minimum bandwidth or compact BLD is motivated by a desire to create systematic sparseness structure and/or reasonable sized moving Template of Active Storage (TAS). Which of the many approaches to ordering is more fruitful depends upon the problem class and the nature of the computing system on which the problem is to be run. Clearly, if memory access is not a

^{*} Relative to a pivot sequence.

^{**} Every cycle with more than three edges has a chord.

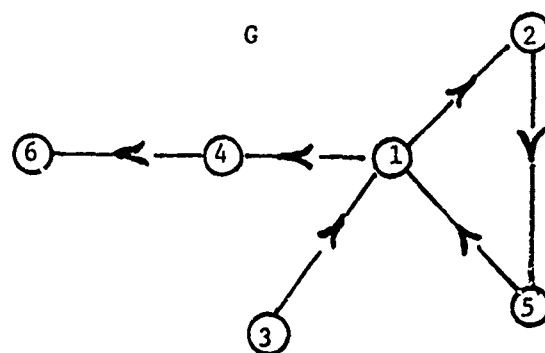
limiting factor and a large number of cases are to be run where the sparseness structure is fixed, then Rose's triangulated graph approach is a desirable strategy.

Now, assume $A_S^T \neq A_S$, but diagonal pivoting in any order is allowed. This means, in particular, that $a_{ii} \neq 0$ for $1 \leq i \leq n$. Associated with the given sparseness structure, in this case, is a directed graph G where, for $i \neq j$, there is a directed edge from vertex j to vertex i if $a_{ij} \neq 0$. This assignment of direction for the edge associated with a_{ij} is best motivated by considering the method of substitution, as in Signal Flow Graphs (SFG's) [124-126]. In a SFG each equation is explicitly solved for the diagonal unknown and solution proceeds by substitution of the right hand side expression into the other equations.

A 6x6 nonsymmetric BSM with its associated directed graph is shown below.

$A_S =$

1	0	1	0	1	0
1	1	0	0	0	0
0	0	1	0	0	0
1	0	0	1	0	0
0	1	0	0	1	0
0	0	0	1	0	1



This matrix is reducible and one fill is the optimal situation. A pivot sequence which achieves this is 3,1,2,5,4,6. The reordered matrix is shown

below:

$C_8 =$

1	0	0	0	0	0
1	1	0	1	0	0
0	1	1	0	0	0
0	0	1	1	0	0
0	1	0	0	1	0
0	0	0	0	1	1

There are a number of matrix reducibility algorithms [25,113; G-6,-11,-11, -20,-29] which determine if a given matrix is reducible, and, if it is, to specify the permutation P such that $B = P^T A P = (B_{ij})$ is Block Lower Triangular (BLT) with each B_{ii} irreducible. In terms of the directed graph, this means finding the strong components of the directed graph [G-6].

There are a number of other uses of the directed graph, such as finding all subgraphs with some desirable feature, determining clustering [71], or finding almost BLT orderings [52; G-20].

So far as this author knows, there is no characterization of the class of G' graphs which is independent of a preassigned diagonal pivot sequence. Rose has indicated in discussions with the author and his colleagues that the directed graph case is much more difficult to systematize than the corresponding undirected case. Some general considerations of operations on directed graphs is contained in [25].

The most general case is a sparse matrix in which the diagonal plays no particular or special role^{*} and where the matrix can even be of order $m \times n$ with $m \neq n$. Then there is associated with A_s a bipartite graph with r row vertices and n column vertices. There is an edge connecting row vertex i with column vertex j provided $a_{ij} \neq 0$ [6-29]. This graph has no restriction on ordering of rows and columns, and can be used to study the fill in the case of arbitrary pivot order.

Graph theory has important conceptual advantages, but it has a number of shortcomings relative to automatic digital computation. Only humans "see" a graph as a whole and as parts, and can identify patterns^{**} when the structure of the graph is below some threshold of complexity. Speculation as to what further algorithmic breakthroughs can be attained from graph theory insights is beyond the scope of this paper.

^{*} That is, there has not been an assignment of unknowns to equations, where equation i is associated with unknown i and $a_{ii} \neq 0$.

^{**} At least for the "unintelligent" information processing systems which are available at present.

9. PARTITIONING

There are a variety of reasons why matrices are partitioned.* One of the early reasons had to do with segmenting problems so that the subproblems could be successively solved within the limitations of the existing memories. This had the advantage of keeping the analysis in the form of matrix equations and was an aid to the problem poser. With the advent of modern automatic memory hierarchies and excellent vector-oriented sparse matrix algorithms, other methods of segmenting are available in an automatic form which do not require clever insight on the part of the problem poser.

The Successive Over Relaxation (SOR) method was shown to be valid for certain classes of sparse block matrices [1]. Block iterative methods have been extensively developed [e.g., 18,26,101]. Carre [G-21] discusses computational techniques for partitioning an undirected graph associated with SYP matrices into a small number of trees. The diagonal blocks will be TDL matrices, and a Block SOR iteration is applied to the partitioned system of equations.

In some cases there is a natural partitioning imposed by the physical nature of the problem. Here the partitioning may be completely regular, and the elements of A are, say, 6×6 matrices. If the matrix is SYP or DID, then the algorithms given earlier can be generalized to include block diagonal pivoting. In fact, one could write highly efficient 6×6 matrix algebra subroutines.**

* That is, the elements of the matrix are, themselves, matrices.

** It defeats the purpose of this approach if one has to deal with nontrivial sparseness for the 6×6 's themselves.

Partitioning also plays a role in the analysis of the fill associated with several stages of Gaussian elimination. Let A be the following 2×2 partitioned matrix where A_{11} is a $k \times k$ nonsingular matrix [46, p.130]

$$A = \begin{array}{cc} & \begin{array}{c} k \qquad n-k \end{array} \\ \begin{array}{c} k \\ n-k \end{array} & \left[\begin{array}{c|c} A_{11} & A_{12} \\ \hline A_{21} & A_{22} \end{array} \right] \end{array}$$

Then, $Ax=b$ can be written in the form

$$A_{11}x_1 + A_{12}x_2 = b_1,$$

$$A_{21}x_1 + A_{22}x_2 = b_2.$$

Solving for x_1 in the first equation yields $x_1 = A_{11}^{-1} b_1 - A_{11}^{-1} A_{12} x_2$. This result is substituted into the second equation, and one obtains the reduced equation $A'_{22} x_2 = b'_2$ where

$$A'_{22} = A_{22} - A_{21} A_{11}^{-1} A_{12} \quad (9.1)$$

and

$$b'_2 = b_2 - A_{21} A_{11}^{-1} b_1 \quad (9.2)$$

Let S_1 and S_2 be two $k \times k$ nonsingular matrices and let

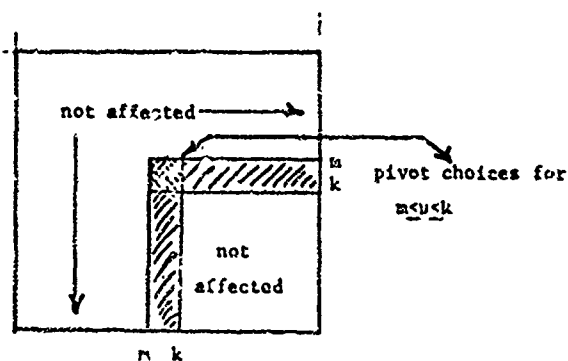
$$B = \begin{bmatrix} S_1 & 0 \\ 0 & I \end{bmatrix} \begin{bmatrix} A_{11} & A_{12} \\ A_{21} & A_{22} \end{bmatrix} \begin{bmatrix} S_2 & 0 \\ 0 & I \end{bmatrix}$$

$$= \begin{bmatrix} R_{11} & R_{12} \\ R_{21} & R_{22} \end{bmatrix}.$$

Then $B_{11} = S_1 A_{11} S_2$, $B_{12} = S_1 A_{12}$, $B_{21} = A_{21} S_2$, and $B_{22} = A_{22}$. Moreover,

$$\begin{aligned} B'_{22} &= B_{22} - B_{21} B_{11}^{-1} B_{12} \\ &= A_{22} - A_{21} S_2 (S_1 A_{11} S_2)^{-1} S_1 A_{12} \\ &= A_{22} - A_{21} A_{11}^{-1} A_{12} = A'_{22}. \end{aligned}$$

The invariance of the Block Gaussian Reduction (BGR) formula under linear transformations of the first k rows and columns of A has a number of important consequences. For one thing, it shows that the resulting reduced matrix A'_{22} does not depend* on the details of how $\text{FIN}(A_{11})$ is obtained. Thus, for example, one can apply Gaussian elimination to A , but restrict the choice of the first k pivots to the first k rows and columns. This also shows that there is a kind of local "continuity" of orderings of rows and columns which lead to a sparse C (i.e., the composite LU matrix). If at the m^{th} reduction stage, $a_{mm}^{(m-1)}$ is not suitable as a pivot, then it is necessary to disturb the natural sequence of pivot positions. Assume that this disturbance can be limited to a few reduction stages, say $m, m+1, \dots, k$, and that the pivots $a_{ij}^{(p)}$, $m \leq p \leq k$, satisfy $m \leq i, j \leq k$. The only portion of the matrix C , which is affected by the PFS strategy for $m \leq p \leq k$, is shown as the shaded region in the figure below.



*To within roundoff error, of course.

There are other reasons why the 2x2 block matrix approach is useful. For one thing, the successive (lower right hand corner) reduced matrices tend to be progressively more dense. Jennings [49] has an interesting discussion of the overhead associated with nonband sparse versus full algorithms. If this overhead must be paid for each solution vector, then there is a threshold of density where it no longer pays to use a sparse matrix method. Thus for each sparse matrix A there is a $k < n$ such that the $(n-k) \times (n-k)$ matrix A'_{22} should be considered full. This applies also to a priori ordering to preserve sparseness algorithms.*

The matrices A_{11}, A_{12}, A_{21} may have special properties which make it desirable to have the first k pivots confined to A_{11} . If only the elements of A_{22} , in the lower right hand corner of A , vary from case to case then the matrix $A_{21}A_{11}^{-1}A_{12}$ is constant, and it can be precomputed and saved. If $A_{11}^T = A_{11}$ and $A_{12} = \pm A_{12}^T$ then $(A'_{22})^T = (A_{22} - A_{21}A_{11}^{-1}A_{12})^T = A_{22}^T \mp A_{12}^T A_{11}^{-1}A_{12} = A'_{22}$ provided $A_{22}^T = A_{22}$. When real and complex matrix elements are both involved in the matrix A , then it is desirable, if possible, to limit the complex elements to the matrix A_{22} . Of course, here A is assumed to be irreducible.

Suppose $A = B - sI$ where, either B is real and s is a complex scalar or B is a constant matrix and s varies from case to case. Then every row and every column of A contains an s -dependent element. Half of the factorization can be made independent of s by ordering either the rows or the columns (but not both) of A backward (i.e., $n, n-1, \dots, 1$). This places the s -dependence on the antidiagonal. This fact is more a curiosity than the basis of a practical method, since stable pivoting** is a necessary aspect of any practical method.

* Gustavson observed this in working with his ordering program OPTORD [G-46].

** By stable pivoting is meant the ability to achieve desired accuracy in the solution with a reasonable floating point precision together with a small number of Iterative Refinement (ITR) steps [64,66].

10. ERROR ANALYSIS

A sketch of general error analysis relative to computational linear algebra is presented below as a prelude to some aspects of error analysis which are peculiar to sparse matrix problems. The case of direct methods for disorderly sparse matrices which are neither diagonally dominant nor positive definite symmetric is of especial importance. It is beyond the scope of this survey to present any quantitative results, and the reader should consult the references presented in survey papers [30,50,67,110,111], the books [31,45,46,76,105,109; E-R1], and the matrix bibliography by Householder [E-R2]. Two conferences on errors in digital computation were sponsored by the Mathematics Research Center, University of Wisconsin, Madison, Wisconsin in October 1964 and April 1965 [75].

The extensive and careful evolution of valid algorithms and computer programs in the field of computational linear algebra should serve as a guide^{*} for similar developments in the nonlinear areas [74, 120; E-R3]. The Special Interest Group in NUMerical Mathematics (SIGNUM) of the Association for Computing Machinery (ACM) has fostered interest in validation and testing of algorithms and periodically reports results in its newsletter, which is edited by Professor Cleve Moler, University of Michigan.

The modern evolution of matrix error analysis begins with the appearance in the late 1940's of the classic papers of von Neumann and Goldstine [69] and Turing [99]. At first, error analysis was limited to a study of fixed point arithmetic algorithms.^{**} Fixed point arithmetic has a distinct advantage

^{*} The Handbook Series Linear Algebra in Numerische Mathematik are a notable series of this type.

^{**} All numbers and operations on numbers are scaled such that they lie in the range $-1 \leq x \leq 1$.

over normalized floating point arithmetic in regard to signed addition and subtraction. Severe numerical cancellation shows up in the form of leading zeros. However, significance can be lost in fixed point multiplication of two small numbers unless the product is scaled in an appropriate manner.

There has been a strong migration to algorithms based on floating point arithmetic. These relieve the user, to some extent,^{*} of the task of analyzing the size of all intermediate calculations. With the advent of automatic floating point hardware in the mid-fifties, one no longer paid a factor of up to ten in time over fixed point arithmetic.

In the late 1950's, Wilkinson^{**} [107-111; E-R1] laid the foundations for "backward" floating point error analysis. Wilkinson [109, p.33] credits the origin of backward error analysis to the papers [69,99] and more explicitly to Givens [37]. In backward error analysis one establishes that, in the computational procedure for solving $Ax=b$ for x given the matrix A and the vector b , one is actually calculating the exact solution to a slightly perturbed problem. That is, if x_c is the calculated solution, then x_c satisfies

$$(A + \delta A)x_c = b + \delta b$$

where bounds are specified on the norms [46, p.37] of δA and δb .

Volume 7, number 4 (December 1970) of the SIAM Journal on Numerical Analysis is a special issue honoring Professor Alston S. Householder on his sixty-fifth birthday. In the preface to this issue, Varga states that Householder's early systematic use of norms in numerical analysis profoundly affected later

* Certainly not of the problem of severe numerical cancellation.

** See E-R2 for a more complete set of references.

developments in the field, and his periodic Gatlinburg (Tenn.) Conferences provided enormous stimulation. It was a lecture by Householder in the spring of 1953 at Georgia Institute of Technology that convinced the author of the present survey paper that numerical analysis is an important and challenging field of specialization.

In the case where A is a matrix of a special form, e.g., symmetric or sparse, then the perturbation δA should preserve this form. In fact, in the field of ill-posed problems [55],^{*} deliberate perturbations are sometimes imposed so that the solution will be unique and satisfy auxiliary conditions.

With the perturbation approach to error analysis, this analysis is separated into two aspects: EAB (Error Analysis, Backward) and EAS (Error Analysis, Sensitivity). The latter concerns how much the "exact" solution is altered by perturbations in the input numbers. Babuska has introduced the concept of "maximally stable" algorithms [2,3] where one tries to minimize^{**} the uncertainty in the answer which is due to the algorithm and to the finite precision of the arithmetic. Of course, the uncertainty in the answer which is due to the physical uncertainty in the input data is another matter, and cannot be resolved by the algorithm. This point is made by Lanczos [53, p.149].

The mathematical cornerstone of sensitivity estimates is the condition number of a matrix [31, p.20; 105, p.88; 110],

$$\text{cond}(A) = \|A\| \cdot \|A^{-1}\| \geq 1.$$

^{*} A better terminology would be "incompletely posed" problems. These arise in certain modeling questions where one knows answers and seeks the model.

^{**} Within the context of a reasonable degree of floating point precision and computational complexity.

If one uses the Euclidean norm,

$$||A||^2 = \sum_{i,j} |a_{ij}|^2,$$

then $\text{cond}(A) = \mu_1/\mu_n$ where μ_1, μ_n are the largest and smallest singular values of A , respectively [4; 31, p.5; 38].

The condition number of a matrix is effected by scaling, and Bauer [5,6] has pointed out that a major aspect of scaling has to do with the effectiveness of PFS strategies. Unfortunately optimal scaling is rarely achievable in practical problem solving [15], and may, in some cases, conflict with physically meaningful scaling.* A recent series of papers by van der Sluis [88-90] represent a major contribution to this field.

When experienced numerical analysts are faced with an unacceptable degree of sensitivity to input perturbations in a practical problem solving context, the standard practice is to check with the problem modeler to see if the ill-conditioning is due to poor problem formulation. In many cases this is the cause, and a reformulation removes the difficulty.

In some cases, the ill-conditioning is unavoidable and then the method of Iterative Refinement (ITR) [64,66] is the main tool. Of course, sufficient accuracy must be achieved in the factorization stage to enable ITR to converge. Wilkinson recommends ITR in any case as a means of providing a degree of assurance of the accuracy of the solution.

The INverse Iteration (INI) method [100; E-R1, pp.319-333] requires PFS strategies and this normally means not preserving symmetry in the factorization [E-8,-25].

*See Givens' remarks [112,p.166 (SMY-19)].

The mixing of scalar diagonal pivoting with 2x2 block diagonal pivoting can be used to preserve symmetry and, at the same time, provides a stable pivoting strategy for symmetric indefinite matrices [13,14].

At times it is possible to take advantage of the symbolic form of the matrix elements to avoid numerical cancellation in the factorization stage. The Nodal Admittance Matrix (NAM) [11], which arises in the analysis of electrical networks, has this character. NAM's are a special case of a more general class of M-matrices [101, p.85] which satisfy the following conditions: (1) A is a real $n \times n$ matrix, (2) $a_{ij} \leq 0$ for $i \neq j$, (3) A is nonsingular, and (4) $A^{-1} \geq 0$ (i.e., all elements are non-negative). In a number of applications including NAM's and Cost Model Matrices (CMM's) [70] the diagonal elements are expressed as a sum which includes the sum of the absolute values of the off-diagonal elements in the same column (or row),

$$a_{mm} = \sum_{i \neq m} |a_{im}| + |a_{n+1,m}|$$

where $a_{n+1,m} \leq 0$. This summation property guarantees that the matrix A is diagonally dominant. If, in addition, A is irreducible* and $a_{n+1,m} < 0$ for at least one m such that $1 \leq m \leq n$, then A is nonsingular and $A^{-1} > 0$.

It is interesting to note that, while diagonal pivoting is considered stable for the case of diagonally dominant matrices, the calculation of the pivot elements l_{mm} , in this case, by the usual formula

$$l_{mm} = a_{mm} - \sum_{j=1}^{m-1} l_{mj} u_{jm} \quad (10.1)$$

* That is, cannot be reordered to be Block Lower Triangular (BLT). The question of reducibility will be discussed later in this section.

involves exact symbolic cancellation as shown by the following 2x2 example.

$$A = \begin{bmatrix} a+\epsilon & -b \\ -a & b \end{bmatrix} \quad a, b > 0, |\epsilon| \ll a.$$

If $A = LU$ then $\ell_{11} = a+\epsilon$, $\ell_{21} = -a$, $u_{12} = -\frac{b}{a+\epsilon}$, $\ell_{22} = b - (-\frac{b}{a+\epsilon})(-a) = b - \frac{ab}{a+\epsilon} = \frac{b(a+\epsilon) - ab}{a+\epsilon} = \frac{b\epsilon}{a+\epsilon}$. The inherent accuracy in the small number ϵ can be lost in forming the sum $a+\epsilon$ so that ℓ_{22} can have a high relative error. This type of cancellation was brought to the author's attention by Calahan [16, pp.30-32;17].

Many engineers have developed circuit motivated techniques for avoiding cancellation based, for example, on the use of the "star-mesh" transformation [81] or of the indefinite admittance matrix [86,87]. A method based on a zero sum augmented matrix* was presented by the author at the Oxford Sparse Matrix Conference [SMO-17]. This method which is presented below is merely a slight variation of a technique reported earlier by Bingham [9]. Let $A' = \begin{bmatrix} A \\ -e^T A \end{bmatrix}$ where $e^T = (1, 1, \dots, 1)$. A' has zero column sums and this property remains invariant under Gaussian reduction.** If $A = LU$ then

$$A' = \begin{bmatrix} A \\ -e^T A \end{bmatrix} = \begin{bmatrix} L \\ -e^T L \end{bmatrix} U.$$

The zero column sum property of the augmented L matrix provides the following cancellation free formula for ℓ_{nm} as an alternate to (10.1),

$$\ell_{nm} = \sum_{k=m+1}^{n+1} |\ell_{km}|. \quad (10.2)$$

*This is the indefinite admittance matrix in nodal analysis.

**Row and/or column sums are used in desk calculations as error and/or blunder checks.

In the formula for ℓ_{nm} , use is made of the properties $\ell_{ij}, u_{ji} \leq 0$ for $j \neq i$. If the alternate formula is used for calculating ℓ_{nm} then there is no numerical cancellation in forming all of L and U for this class of M -matrices. This also applies to the SUB stage if $b \geq 0$. The m^{th} component of $-e^T A$ is $a_{n+1,m}$, which is an input number, and the diagonal elements of L are formed rather than the diagonal elements of A .

The following theorem for the class of matrices which are strictly diagonally dominant M -matrices (that is, $a_{n+1,m} < 0$ for $1 \leq m \leq n$) forms the motivation for a Matrix Reducibility Algorithm (MRA) [113].

Theorem. $A^{-1} > 0$ if and only if L and U^T (U transpose) each have their last column as their unique singleton column (i.e., a column with exactly one nonzero element).

For this class of matrices, $A^{-1} > 0$ if and only if A is irreducible. Thus by forming $SSI(C)$, where C is the composite $L \cup U$ matrix, one has a test for reducibility. Suppose A is reducible, then there exists a permutation matrix, P , such that $B = P^T A P$ is BLT. The square diagonal blocks, B_{kk} , will be irreducible. Moreover, B^{-1} is also BLT, and has $B_{kk}^{-1} > 0$ as its diagonal blocks. The following condition characterizes the indices i, j such that a_{ii} and a_{jj} belong in the same irreducible diagonal block of B ,

$$a_{ij}^I \cdot a_{ji}^I \neq 0, \quad A^{-1} = (a_{ij}^I). \quad (10.3)$$

Reducibility of a matrix is a purely logical question which depends only on whether elements are zero or not zero. The proposed MRA, though motivated by ideas relating to strictly diagonally dominant M -matrices, requires only

the condition, $a_{mm} \neq 0$ for $1 \leq m \leq n$. In many applications, this condition is already satisfied. If it is not, then one first applies to A an Assignment Algorithm [G-27] which is a special part of the general field of network flows [27].

The various Symbolic Factorizations Programs (SFP's) which generate SSI(C) from SSI(A) can be extended to include both row and column symbolic forward and backward SUB. In this way, SSI can be obtained for row i and column i of A^{-1} , and this information determines the set of indices which belong in the same irreducible diagonal block of B . The following properties are numerically true for strictly diagonally dominant M-matrices and "logically true"* for matrices A such that $a_{mm} \neq 0$ for $1 \leq m \leq n$.

$$\left. \begin{array}{l} a_{ij} \neq 0 \Rightarrow c_{ij} \neq 0 \Rightarrow a_{ij}^I \neq 0 \\ b_m \neq 0 \Rightarrow y_m \neq 0 \Rightarrow x_m \neq 0 \end{array} \right\} \quad (10.4)$$

where $Ly = b$ and $Ux = y$ (i.e., $A = LU$ and $Ax = b$).

Since C is at least as full as A , the first 8x8 matrix on the following page is irreducible by inspection since there is a nonzero in row m to the right of the diagonal and a nonzero in column m below the diagonal for $1 \leq m \leq 7$. The second 8x8 is also irreducible by inspection of SSI(C). **

* That is, in the Boolean sense and ignoring creation of zero by exact numerical cancellation for a particular matrix A .

** The symbol \emptyset is used to represent $a_{ij} = 0$, $c_{ij} \neq 0$.

IRREDUCIBLE MATRICES

$A_1 =$

1	0	0	1	0	0	0	0
0	1	0	1	0	0	0	0
1	1	1	1	0	0	0	0
0	0	0	1	0	0	1	0
0	0	1	1	1	0	1	0
0	0	0	0	0	1	1	0
0	0	0	0	1	1	1	1
0	0	0	0	0	0	1	1

$A_2 =$

1	0	0	0	0	0	0	1
1	1	0	0	0	0	0	0
0	1	1	0	0	0	0	0
0	0	1	1	0	0	0	0
0	0	0	1	1	0	0	0
0	0	0	0	1	1	0	0
0	0	0	0	0	1	1	0
0	0	0	0	0	0	1	1

$C_2 =$

1	0	0	0	0	0	0	1
1	1	0	0	0	0	0	0
0	1	1	0	0	0	0	0
0	0	1	1	0	0	0	0
0	0	0	1	1	0	0	0
0	0	0	0	1	1	0	0
0	0	0	0	0	1	1	0
0	0	0	0	0	0	1	1

Trivial reducibility can be removed from A as a preliminary operation. For example, all rows and columns of A associated with singletons can be a priori struck out of A and ordered directly into the BLT matrix B . Also, the sparseness structure of certain elements of the various matrices and vectors are either known a priori or are irrelevant to subsequent calculations. For example, (10.4) provides a priori information, and, if an irreducible block has been found, the sparseness structure information associated with the indices in the block is irrelevant to the determination of subsequent irreducible blocks. Thus index skip lists can be generated during the algorithm and utilized to bypass unnecessary operations.

The 8x8 reducible matrix, A , shown on the next page, illustrates a number of aspects of the proposed MRA. A permutation, σ , of $(1,2,3,4,5,6,7,8)$ is determined such that B is BLT and row (column) i of B is row (column) σ_i of A . Search for singletons provides $\sigma_1 = 5$, $\sigma_8 = 4$, and $\sigma_7 = 1$. These provide 1x1 diagonal blocks in B , and now the indices 5,4,1 are irrelevant. The matrix C is formed,* and A is found to be still reducible because $c_{87} = 0$. The relevant part of row and column 2 of A^{-1} is determined, and $a_{2j}^I \cdot a_{j2}^I \neq 0$ if and only if $j \in \{2,6,8\}$. The indices $\{3,7\}$ form a 2x2 block which must follow $\{2,6,8\}$. Thus $\sigma_2 = 2$, $\sigma_3 = 6$, $\sigma_4 = 8$, $\sigma_5 = 3$, $\sigma_6 = 7$; that is, $\sigma = (5;2,6,8;3,7;1;4)$.

*The symbol $\$$ in C means value is irrelevant.

REDUCIBLE MATRIX

A =

1	1	0	0	1	0	0	0
0	1	0	0	0	0	0	1
0	0	1	0	1	0	1	0
1	1	0	1	1	0	1	0
0	0	0	0	1	0	0	0
0	1	0	0	0	1	0	0
0	1	1	0	0	0	1	1
0	0	0	0	1	1	0	1

C =

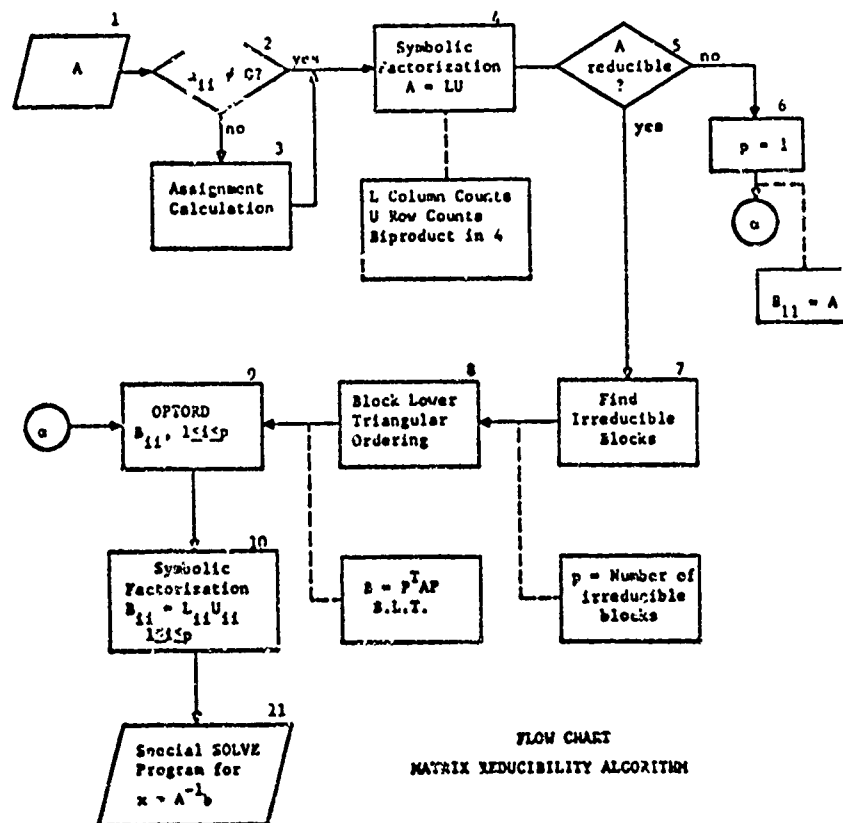
5	5	5	5	5	5	5	5
5	1	0	5	5	0	0	1
5	0	1	5	5	0	1	0
5	5	5	5	5	5	5	5
5	5	5	5	5	5	5	5
5	1	0	5	5	1	0	0
5	1	1	5	5	0	1	1
5	0	0	5	5	1	0	1

B =

1	0	0	0	0	0	0	0
0	1	0	1	0	0	0	0
0	1	1	0	0	0	0	0
1	0	1	1	0	0	0	0
1	0	0	0	1	1	0	0
0	1	0	1	1	1	0	0
1	1	0	0	0	0	1	0
1	1	0	0	0	1	1	1

MATRIX REDUCIBILITY ALGORITHM (MRA)

1. Given SSI(A) generate SSI(C) via a SFP.
2. Check column counts in L and row counts in U for reducibility (theorem p. 10.7).
3. If A is reducible, find irreducible blocks of B via repeated use of (10.3). The set $S = \{1, 2, \dots, n\}$ is partitioned into equivalence classes $R = \{R_1, R_2, \dots, R_p\}$ of indices belonging to the same irreducible diagonal block of P_B .
4. Define $p \times p$ Boolean matrix $M = (m_{ij})$, where $m_{ij} = 1$ if and only if for some $i \in R_j$ and some $j \in R_i$, $a_{ij} \neq 0$. M is reordered to achieve a lower triangular form by successive symbolic Gaussian reduction, using at each step as pivot the unique nonzero element in a singleton row.
5. The reordering permutation for M, together with the partition R, determine a permutation matrix P such that $B = P^T A P$ is BLT and the square diagonal blocks B_{kk} are irreducible for $1 \leq k \leq p$.
6. Instead of solving $Ax=b$, one solves $Bz=g$ where $z = P^T x$ and $g = P^T b$. Only the diagonal blocks are factored, and z is determined via block forward SUB.



FLOW CHART
MATRIX REDUCIBILITY ALGORITHM

The following 3x3 example shows why it can be dangerous, from an accuracy point of view, to pivot outside the irreducible blocks. Let $f = 2a+1$ where $a \geq 1$.

$$A = \begin{bmatrix} -f & -a & a \\ -a & 1 & 0 \\ a & 0 & 0 \end{bmatrix} \quad A^{-1} = \begin{bmatrix} 0 & 0 & a^{-1} \\ 0 & 1 & 1 \\ a^{-1} & 1 & h^{-1} \end{bmatrix}.$$

Note that $\lambda_{22} = 1+g$, where $g = a(a/f)$, and $\lambda_{33} = g - g[g/(1+g)] = [a/(a+1)]^2 = h$. Maximum pivoting was used in each step, but λ_{33} is of the form $\infty - \infty$ as $a \rightarrow +\infty$. Let $c(A)$ = condition number of $A = \|A\| \cdot \|A^{-1}\|$, then $c(A) \geq 2a$, since $\|A\| \geq$ spectral radius of $A \geq 2a$, and $\|A^{-1}\| \geq 1$. However, if the matrix A is scaled by dividing the first row and first column by a , then the resulting condition number is less than 9 for all $a \geq 1$. The (1,1) element is now $-(2a+1)/a^2$, which is clearly a poor pivot choice for $a \gg 1$.

Consider now a BLT matrix, $B = (B_{ij})$, where the diagonal blocks, B_{ii} , are irreducible and nonsingular. One can independently scale the diagonal blocks B_{ii} to achieve an optimum condition number for that block. In addition, let D = block diagonal matrix = $\text{diag. } (\epsilon I_1, \epsilon^2 I_2, \dots, \epsilon^n I_n)$ where $0 < \epsilon < 1$ and I_i is the identity matrix having the same order as B_{ii} . If $T = DBD^{-1} = (T_{ij})$ then $T^{-1} = DB^{-1}D^{-1} = (T_{ij}^I)$ and $T_{ii} = B_{ii}$, $T_{ii}^I = T_{ii}^{-1}$, $T_{ij} = \epsilon^{i-j} B_{ij}$, and $T_{ij}^I = \epsilon^{i-j} B_{ij}^I$ for $1 \leq j < i \leq n$. Thus optimal scaling demands that pivoting be restricted to the irreducible diagonal blocks.

It is important to realize that the number zero in matrix calculations is qualitatively different from a number which may, in a given context, be

negligibly small, ϵ , say. The number zero is invariant under scaling of rows and columns, whereas ϵ certainly is not, e.g., $\epsilon \cdot \epsilon^{-1} = 1$.

Numerical analysts create pathological examples^{*} as a caution to the unwary. A well-known example of a qualitative difference between ϵ and 0 is exhibited in the eigenvalue-eigenvector analysis of the following $n \times n$ matrix.

$$A_\alpha = \begin{bmatrix} 0 & 1 & & & & & & \\ & 0 & 1 & & & & & \\ & & \cdot & \cdot & & & & \\ & & & \cdot & \cdot & & & \\ & & & & \cdot & \cdot & & \\ & & & & & \cdot & \cdot & \\ & & & & & & \cdot & \\ & & & & & & & 1 \\ \alpha & & & & & & & 0 \end{bmatrix}$$

If $\alpha = 0$ then A_α is in Jordan canonical form [45, pp.34-37], $\lambda = 0$ is the only eigenvalue, and $x = e_1$ (= first column of the identity matrix) is the normalized eigenvector (otherwise there are only principal vectors [45, p.32]). On the other hand, if, for example, $\alpha = 10^{-n}$, then there are n distinct eigenvalues $\lambda_i = w^{i-1} \cdot 10^{-1}$, $1 \leq i \leq n$, where $w = e^{\theta i} =$ primitive n^{th} root of unity, and $\theta = 2\pi/n$. All these eigenvalues have modulus 10^{-1} . If $n=20$, for example, then $\alpha = 10^{-20}$.

In sparse matrix problems, $a_{ij} = 0$ typically means " x_j does not occur in equation i " rather than "the effect of x_j in equation i is negligibly small." Casting out insignificant terms in problem modeling has been the domain of the

^{*} Kahan [50] and Wilkinson [107, 108] are experts in this area.

applied mathematician. However, in the realm of nonlinear evolutionary problem modeling, this "casting out" is being replaced^{*} by "putting in and see what happens."

There has not, in general, been any particular emphasis on error analysis in the various specialized sparse matrix applications areas. Rosanoff^{**} and Shaw [85] have analyzed the question of conditioning in Structural Mechanics, and Fox and Stanton [33] stress the importance of scaling to minimize the eigenvalue spread in applying a CGM in cases where A is SYP. Finally, Wolfe [75, Vol. 2, pp.271-281] discusses the question of error analysis in the linear programming field. Linear programming represents an area requiring the most general approach to sparse matrix calculations.

PFS has been a critical aspect of algorithms for matrices which are neither SYP nor DID. The computational price one pays for this in dealing with full or band matrices is reasonable, but where the sparseness structure is arbitrary this is not necessarily the case. Care must also be exercised in choosing pivots which preserve sparseness. Clearly, zeros cannot and near-zeros should not be used as pivots, ^{***} least some threshold criterion is necessary.

As far as the author is aware, there does not yet exist in the literature a systematic analysis of the accuracy achievable^{****} in the factorization stage using some form of threshold pivoting. Of course, it is always desirable to use extended precision inner product accumulation, and this may be crucial in the case of threshold pivoting.

* This marks a move towards large scale scientific calculations.

** Structural Mechanics Conference, Flight Dynamics Laboratory, Wright-Patterson Air Force Base, Ohio (October 1968).

*** That is, $|L_{\text{min}}| \geq \alpha$ where α is some absolute or relative threshold.

**** In the context of a priori specified precision in the floating point arithmetic.

11. COMPUTATIONAL COMPLEXITY AND EFFICIENCY

The whole question of computational complexity and of efficiency of numerical methods is just beginning to receive the attention it deserves in the field of practical problem solving. The maximum size of matrix problems attempted has always been at the limit of the capacity of information processing systems. In order to enhance the evolution towards solving larger problems, there needs to be developed a detailed understanding of how the computational feasibility and efficiency depends on the problem formulation, the algorithm, and the architecture of the computer hardware and system software.

Efficiency is measured in terms of Cost/Performance (C/P). Both cost and performance are hard qualities to quantize. In its broadest sense, efficiency is the measurement of the human and computer factors involved from the time a problem is first conceived until results are available in a form suitable for the user's ultimate need. Here the chargeable CPU^{*} time may be completely negligible, especially if no production code is available for the calculation. In the narrowest sense, one is measuring the throughput in the CPU for important inner loop calculations. Even this is poorly specified if one is operating in a time-sharing or multiprocessing mode.

Consider the question of efficiency in solving $Ax=b$ for x given the vector b and the sparse $n \times n$ matrix A . There are undoubtedly critical cross-over points and elbows on efficiency versus n plots, but meaningful plots of this type are hard to obtain for nontrivial situations, and these plots have to be viewed in the larger C/P environment of the total problem being considered. Moreover, the efficiency should be averaged over some spectrum of computer runs

* Central Processing Unit, that is, the arithmetic and program control registers as distinct from memory.

in a realistic operating environment.

Wolfe [112, pp.107-112; SMY-12] has given an excellent indication of the evolution of computing power in the field of linear programming. The first graph shows the size of the largest problem users reported solving at various periods in time. It is interesting to note that, at the time^{*} of the symposium, 10,000 equations seemed to be the production frontier in both linear programming and in structural mechanics. The character of the sparse matrix problems and the algorithms are vastly different in the two fields. The second graph shows an equally important type of evolution; namely, the decrease in running time for a model problem as both the computer system and the algorithm evolved.

We need more graphs of both types for a spectrum of applications, and also detailed timing charts for certain large-scale calculations which are at the frontier of capability of current systems.

A measure of computational complexity in linear algebra has typically been the number of multiplications involved. This has been reasonable with regard to floating point operations since multiply-add is the basic operation except for the calculation of n reciprocals $\rho_i = 1/\ell_{ii}$ for $1 \leq i \leq n$. Recent work [12,32,44,51,94,114,115] has addressed the question of minimizing the number of multiplications in numerical calculations. These, of course, do not necessarily cover the question of computational complexity in disorderly sparse matrix problems. For sparse matrix calculations, there is, in addition to the complexity of the floating point processing, the logical manipulation of sparseness structure information as well as the questions concerning access to information in a memory hierarchy and under a variety of operating conditions.

* September 1968.

The whole question of computational complexity is becoming increasingly fuzzy because of the advent of sophisticated operating systems, virtual memories [F-44]^{*} and parallel [123], pipeline [F-47] and array processors [F-25]. Multiprocessing, especially in a time-sharing environment [F-35] also increases the difficulty of accessing computational complexity and efficiency. The relationships between sparse matrix calculations and computer systems will be discussed further in sections 12 and 13.

^{*} That is, automatic data management in a memory hierarchy environment.

12. MEMORY HIERARCHIES AND DATA MANAGEMENT

Access to information, both data and code, is an important aspect of computational complexity and efficiency. Some problems are CPU bound, but others are memory bound. The latter seems to be a critical bottleneck in certain large scale direct sparse matrix calculations, and has been a strong argument favoring iterative methods. However, as problems become more irregular, many iterative methods become ineffective because of a degraded rate of convergence [104; 112, pp.139-148; SMY-16]. There needs to be a continual assessment of the relative tradeoffs between direct and iterative techniques as the problem classes, the algorithms, and the computing systems evolve.

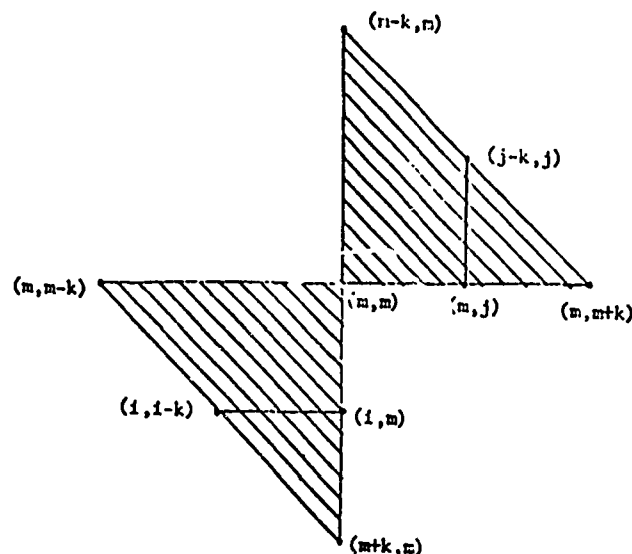
Highly sophisticated memory hierarchy systems are appearing, and the aim of these systems is to make the functioning of the hierarchy transparent (i.e., be of no concern) to the user by means of automatic memory management [F-44,-45]. Some reasonable rules relative to ordering must be followed [68; F-39] if efficiency is to be achieved in matrix computations. Basically, the main ideas are: (1) When blocks of information are moved up in the hierarchy they should have a utilization which is directly related to the size of the block; (2) Where information resides in the hierarchy should be related to the effect of its access on the overall efficiency of the processing.

Efficient I/O and memory management are two of the most critical problems in the design of large scale production codes. The resolution of these problems often dictates the level of generality which can be tolerated in the code without seriously degrading the computational efficiency in the typical production runs.*

* Having too many special purpose codes, on the other hand, tends to create a high level of human inefficiency.

Sparse matrix problems have a number of special characteristics. For one thing, there are long chains of streaming and merging in these calculations which are well suited to multiple memory pipelining. Some information is used repeatedly such as the rows of the U matrix in the FIN stage of Gaussian elimination, whereas, in each pass through the SUB stage, the rows of L and of U are used exactly once.

Let A be a band matrix such that $a_{ij} \neq 0$ for $|i-j| \leq k$ where $k \ll n$, but otherwise $a_{ij} = 0$. Also assume that pivoting can proceed down the diagonal in the natural order (PDN). This class of matrices are ideal from a sparse matrix point of view. In the factorization stage there is a Template of Active Storage (TAS) required to form the m^{th} column of L and the m^{th} row of U. This TAS is the shaded area in the diagram below.



Of course, all ^{*}indices are also greater than or equal to one and less than equal to n . There are at most $k^2 + 3k + 1$ locations involved in this TAS. This is a moving template which progresses as m increases from one to n .

* There are schemes which augment the diagonals with zeros at the beginning and/or the end to avoid special cases for the terminal indices.

This local active store also applies to the x and y vectors in the SUB stage, and again is a desirable feature in memory situations which are not random access. It is partly for these reasons that a number of authors have developed bandwidth minimization algorithms [G-15,-35,-38,-42].*

For the general sparse matrix and the RGE algorithm, the active storage requirements can be very chaotic, both with and without PFS. In the first place, the storage needed for the nonzero elements in A is, in general, not adequate for the storage of the nonzero elements of C because of the fill occurring in C . If only diagonal pivoting in the natural order is involved, then an upper bound for the number of nonzeros in C is obtained from the BLD approach to fill. If PFS is involved, the estimations of active and total storage requirements for C are much more difficult to obtain.** Of course, one can deal with upper and/or lower semi-bandwidths in this estimation, but this approach may be too gross.

One approach to Gaussian reduction is to process all remaining rows with the pivot row and thereby obtain a reduced matrix which has an order of one less than the matrix being reduced. In fact, this approach was used in the early Gauss-Jordan complete elimination algorithms [F-1]. Here, the active storage remains at somewhat more than n^2 , since the entire matrix is updated at each stage. After n stages, one has either A^{-1} or a permutation of A^{-1} in place of A . One has the widest choice of pivot strategies if this approach to Gaussian reductions is used.

A quite different approach can be taken in processing the rows of A in the RGE algorithm. The rows of A are first stored compactly in serial backup

* See also Tewarson's survey article on sparse matrix methods [96].

** The author acknowledges informative discussions with colleagues, A. Blaser and H. Pretsch, at IBM Germany who are investigating memory estimation techniques for general sparse matrices where PFS is involved.

store. At the m^{th} reduction stage, one processes the m^{th} row of A against rows $1, 2, \dots, m-1$ of U , and obtains then the m^{th} row of U . Some subset of the first m rows of U are needed in compact form in active storage for processing row $m+1$ of A .

If PFS is not involved and one is going to solve a number of cases where $SSI(A)$ is fixed, then $SSI(C)$ can be obtained a priori, and the moving TAS can be constructed. Moreover, reordering schemes can be applied which are aimed at making the maximum size of the template reasonable. This can be especially important in large-scale calculations which are memory bound.

There are, of course, a number of other tradeoffs in a priori ordering strategies such as achieving: (1) minimum operation count in forming C ; (2) sparsest C ; and (3) systematic sparseness structures (e.g., band, triangular, block triangular, or structures which are "near" these in some sense).^{*} The effectiveness of these strategies is sensitive to the problem class, the computing system, the dynamic operating conditions when a problem is being run, and, of course, the excellence of the programming.

Repeated restarts of slow serial backup stores, such as magnetic tapes, can be a limiting factor for the size sparse matrix problems which are feasible in a production computation environment. Large core store, high speed discs and drums help extend the size of feasible problems. On the other hand, operating systems, problem oriented supervisors, and dynamic storage programs may eat up in overhead a large portion of the added memory power. If substantial overlays of code and/or data are required in the inner loops of a large-scale calculation, the effective rate of computation can be considerably degraded.

^{*}See Part G in the bibliography and [96] for detailed references.

13. COMPUTER ARCHITECTURE AND PROGRAMMING

There is no question that many classes of sparse matrix calculations could be enhanced by special purpose hardware such as parallel, pipeline, and array processors. Also important algorithms could be microcoded* to improve the throughput. However, the C/P figures for these special aids to a small class of users may cause them to be unfeasible, except for critical real time applications where cost is not a primary criterion.

Parallelism has many forms. For example, one can either have a single instruction stream with vector processing in parallel, or several instruction streams with a number of arithmetic registers. In pipeline processing, one segments the operation "multiply-add," say, into a number of successive but separate steps. As soon as one step is completed in the sequence, new operands can be processed in a pipeline mode. If the pipeline is long, data-dependent branches which drastically interrupt the flow are to be avoided whenever possible. Memory pipelining has already been mentioned in the previous section.

It is very difficult to predict the evolution of information processing systems, but some general remarks seem appropriate. First of all, multiprocessing has become a standard approach in large-scale systems. Moreover, there will be a continuing evolution towards more powerful general purpose computers which satisfy the needs of information and data processing, as well as the small market for large scale scientific calculations. As indicated in the last section, one of the important developments will be automatic memory management which will be coupled with simple user rules for structuring and segmenting code and data.

* Wilkes, M. V., "The growth of interest in microprogramming: a literature survey," Comput. Surveys 1 (1969) 139-145.

Terminal oriented computation with an interactive graphic facility,^{*} will have steadily improved C/P characteristics. However, in order to be feasible at the individual user level, there must be a drastic reduction in the current C/P figure for interactive graphics. The terminals may have stand-alone memory and computer capability, but they will also largely be a part of a communication net of terminals and large-scale central computer systems.

There are two underlying criteria involved in the evolution of computer systems; namely, (1) compatibility and (2) improved C/P.^{**} The first is important since then costly production codes are not made obsolete. Without (2) no new general purpose system has any reason for being. Moreover, the enhanced C/P should be achieved in the context of high level languages such as FORTRAN, APL and PL/1, and should not require extensive user tuning of existing programs.

The preceding remarks could be interpreted as referring mainly to hardware evolution, but what is hardware and what is software can be a very vague distinction. Software engineering is a rapidly developing discipline in the systems programming area, and will continue to be the pioneer for hardware innovations when C/P characteristics dictate a shift from sophisticated software to efficient hardware.

In sparse matrix problems, there are a small number of important underlying mathematical ideas which must be understood and exploited, but it is in the applications programming, itself, that the efficiency is achieved. The programmer should be aware of the computer architecture considerations in planning his programs, but extensive "fine tuning" may make the program subject

^{*} As well as hard copy option at the graphics terminal.

^{**} Reliability and serviceability are a part of C/P.

to continual modification because of changes in hardware and/or systems software. Clever programming is a fascinating game, but it must be played by reasonable rules if the resulting program is to be useful to a large class of problem solvers. Basically, programming has two aspects: (1) flow charting, and (2) coding. Aspect (2) should be an implementation of prior development of aspect (1) and not vice versa. Fine tuning may be a necessity, in some cases, of important inner loops, but these should be clearly identified in the program for easy updating.

In summary then, while it would be desirable to have computing systems which are tailored to the specific needs of users, C/P characteristics dictate that users adapt to the structure of the evolving systems. Sophisticated scientific users should take the effort to clearly identify their needs and, where necessary, show that these needs are not being effectively satisfied by current systems. In this way, C/P studies can be made relative to these needs so that unnecessary bottlenecks can be removed from future systems. The users might start their interaction with computer architects by reading the story of the planning of a large high performance computer [F-7].

It is the contention of the author and his colleagues that, if a computing system is effective in a C/P sense for sparse matrix calculations, then this system will also be effective for a broad spectrum of other uses.

14. MNEMONICS DICTIONARY AND BIBLIOGRAPHY

A. General Remarks

In writing this survey, the author found that he was often referring to certain concepts such as triangular factorization. It became convenient to refer to these concepts by means of mnemonics. Thus, TRIangular Factorization is assigned the mnemonic TRF.

In part B of this section, a mnemonics dictionary is presented which serves also as a subject guide for the references and an index for the survey itself.

The references are by no means complete, especially in the applications area. Certain references are cited in each application. These either represent a text which can serve as survey of the application or papers which concern a particular aspect of sparse matrix technology. The use of Band Like Domains in structural mechanics problems is one example of this type.

As Householder has pointed out many times in his Mathematical Reviews contributions, there is repeated discovery of known results in practical numerical analysis. One reason for this is the very recent acceptance of algorithms as publishable in their own right, and the rather meager set of adequate surveys and annotated bibliographies for various practical aspects of numerical analysis.

Cross discipline symposia are an important remedy for this defect. These symposia should be addressed to the understanding of the underlying mathematical modeling techniques and the current state of feasible and/or efficient computational methods.

One purpose of this survey has been to provide an extensive bibliography for sparse matrix technology. Parts E, F and G are organized chronologically by subject matter as follows: E. Eigenvalues and Eigenvectors, Sparse Matrices; F. Computer Architecture, Parallelism, Memory Hierarchy, and Data Management; and G. Preserving Sparseness. Part C is an author list, and part D is a set of general references, which are alphabetical by first author.

Two references E-R2, -R3 refer to the two volumes of Householder's extensive bibliography of numerical linear algebra E-R2, Vol. 1 (First) Authors A-J, Vol. 2 Authors K-Z), and one volume on references for numerical treatment of nonlinear equations. Where known, the reference includes a citation concerning where the article is reviewed in MR (Mathematical Reviews), CR (Computing Reviews), RZ (Referativnyi Zhurnal. Matematika),* and ZBL (Zentralblatt für Mathematik und ihre Grenzgebiete).** The abbreviations for the journals are those listed in the index issues of MR. There is also an author index and a KWIC (Key Word in Context) index. Also, each reference has a four-digit identification which starts at 0001 for each volume. All told there are approximately 3500 references in the three volumes.

In most cases, if a reference in the present survey occurs in Householder's bibliography, the Householder number is given together with his CR and/or MR citation. For example, the Daniel [20] reference ends with H0563, CR9 13,478, MR36 2315. This means Householder [E-R2, Vol. 1]*** 0563; Computing Reviews, volume 9, review number 13,478; Mathematical Reviews, volume 36, review number 2315.****

*Published in Moscow.

** Published in Berlin.

*** If E-R3 is intended, this will be denoted by H(NL)xxxx.

**** Starting with volume 20 (1959), MR numbers the reviews starting from one each year. Before that reviews were referred to by volume and page. CR numbers each review consecutively without starting at one each year.

Both in the references in this survey and in Householder's bibliography, the title of the article or book is translated into English when the article is in another language. The language of the article is indicated in parentheses. In most cases, CR and MR reviews indicate if there are summaries of the article in other languages.

B. Mnemonics Dictionary

- ACM Association for Computing Machinery; see also SIGNUM; p. 10.1.
- APL A Programming Language; [47]; pp. 4.3, 13.2.
- BGR Block Gaussian Reduction; see also RGE, SYI; [13, 14, 45, 46; F-41]; pp. 6.4, 9.1-9.4, 10.5.
- BIF BI-factorization; see also ECM, EFL, ERM, SYP; [78(SMO-6)]; pp. 2.3, 3.2, 6.1.
- BIM Block Iteration Method; see also DID, PDE, SOR, SYP, TDL; [e.g., 1, 18, 26; G-21]; pp. 8.3, 9.1.
- BLD Band-Like Domain; see also BMM, SSI, TDL; [48, 49, 58-60, 65, 78 (SMO-7), 84]; pp. 3.2, 7.2-7.3, 7.5, 8.3, 12.3, 14.1.
- BLT Block Lower Triangular; see also MRA; [25, 113; G-6, -10, -11, -20, -29]; pp. 4.1, 5.6, 8.5, 10.5, 10.7-10.13.
- BMM Band Matrix Method; see also BLD, TDL, TDM; [e.g., 36, 63, 82, 95, 97; E-R1, -8, -25; G-15, -35, -38, -42]; pp. 7.1, 12.2-12.4.
- BSM Boolean Sparseness Matrix; see also SFP, SSI, TLP; [e.g., 40]; pp. 2.3, 7.2-7.3, 8.1-8.5.
- C/P Cost Performance ratio; see part F of references; pp. 11.1, 13.1-13.3.
- CAP Computer Application; see also CCD, LP, NLE, PDE, PSA, SDE, SPP, STM; [4, 10, 11, 16, 17, 21, 24, 27, 28, 32-35, 41, 42, 48, 49, 52-62, 65, 70-75, 78-87, 91-93, 98, 101-104, 112, 113]; pp. 3.1-3.3; also see particular applications.
- CAR Computer ARchitecture, see also MEH, MOP, TAS; [e.g., 123; F-7, -25, -47]; pp. 4.2-4.4, 8.3-8.4, 9.1, 11.1-11.3, 12.1-12.4, 13.1-13.3.
- CCD Computational Circuit Design; see also CAP, NAM, NLE, PSA, SDE; [9, 11, 16, 17, 41, 42, 52, 71, 72, 78 (SMO-17), 81, 83, 86, 87, 98, 112 (SMY-17), 113; G-1 through -5, -7, -23, -26, -28, -46]; pp. 1.1, 2.1-2.4, 3.1-3.3, 10.5-10.7; see Cornell Conference reference p. 2.1.
- CGM Conjugate Gradients Method, see also SYP; [7, 19, 20, 24, 33-35, 43, 46, 57, 76, 78 (SMC-16), 92, 105]; pp. 3.2, 6.3-6.4.
- CMM Cost Model Matrices; see also CAP, DID, M-MAT, NAM; [70]; p. 10.5.
- CPU Central Processing Unit; see part F of references; pp. 11.1, 12.1, 13.1.
- DID Diagonally Dominant; see also BGR, BIM, PDN, SYP; [9, 17, 26, 54, 70, 78, 81, 83, 91, 96, 101, 112, 113; E-R2]; pp. 4.2, 6.1, 9.1, 10.5-10.7.
- EAB Error Analysis, Backward; see also EAN, EAS, PFS, SCA; [e.g., 109]; pp. 10.2-10.3.

- EAN Error Analysis; see also EAB, EAS, SCA, SUR; [2-6, 9, 13-17, 30, 31, 33, 37, 38, 45, 46, 50, 67, 69, 75, 76, 85, 88-90, 99, 105, 107-111, 113; E-R1, -R2]; pp. 1.3, 2.2, 3.1, 4.1, 4.4, 6.4-6.5, 9.4, 10.1-10.15; see especially [109].
- EAS Error Analysis, Sensitivity; see also EAB, EAN, PFS, SCA; for references, see EAN; pp. 10.3-10.4.
- ECM Elementary Column Matrix; see also BIF, EFI, ERM, FIN, MMM, PFI; [4, 62, 73, 78, 96, 112, 121; G-31, -43]; pp. 3.2, 3.3, 4.5-4.7, 5.3-5.6, 6.1.
- EFI Elimination Form of the Inverse; see also BIF, ECM, ERM, PFI, RGE, SMA, TRF; [4, 62, 73, 78, 96, 112; G-43]; pp. 3.2, 3.3, 5.3-5.5, 6.1; see in particular, SMY-10.
- ERM Elementary Row Matrix; see also BIF, EFI, FIN, MMM, PFI, RGE; [4, 62, 71-73, 78, 83, 96, 98, 112, 116-119; G-43]; pp. 3.2, 3.3, 4.5, 5.2, 5.4, 6.1.
- EVV Eigen-Values and -Vectors; see also CGM, INI, PDE, SYI, TDL, TDM; [e.g., E-R1]; pp. 3.1, 6.4-6.5, 7.4, 9.4, 10.13-10.14.
- FEM Finite Element Method; see also BLD, BMM, CGM, DID, PDE, SOR, SYP; [33-35, 84, 112 (SMY-11)]; p. 7.5.
- FIN Form of the Inverse; see also BGR, BIF, EFI, MMM, PFI, RGE, SUB, TRF; see particular type of FIN for references; pp. 3.1-3.3, 4.1-4.7, 5.1-5.6, 6.1-6.3, 9.3, 10.15, 12.2-12.4.
- I/O Input and Output; see part F of references; pp. 12.1, 13.2.
- INI INverse Iteration; see also EVV, PFS, SYI; [E-R1, -R2, -18]; pp. 4.2, 10.4.
- IPP Improperly Posed Problem; see also EAN; [e.g., 55]; p. 10.3.
- ITR Iterative Refinement; see also EAN, FIN, SUB; [e.g., 64, 66]; pp. 2.2, 4.1, 4.4, 9.4, 10.4.
- LP Linear Programming; see also CAP, ECM, EFI, MMM, PFI, THP; [4, 32, 62, 73, 75, 78 (SMO-1, -14, -17), 96, 112 (SMY-1, -3, -6, -7, -10, -12, -15), 121, 127; G-31, -43]; pp. 1.2, 3.1-3.3, 4.5, 5.3-5.6, 10.14-10.15.
- M-MAT M-MATrix; see also CAP, CMM, DID, NAM, PDE, SYP; [e.g., 101, p. 85; 113]; pp. 10.5-10.8.
- MEH MEMory Hierarchy; see also CAR, MOP, TAS; [e.g., 122; F-44, -45]; pp. 4.2-4.4, 8.3-8.4, 9.1, 11.1-11.3, 12.1-12.4, 13.1-13.3.
- MMM Method of Modified Matrices; see also ECM, EFI, ERM, FIN, PFI; [4, 8, 45 (pp. 79, 84) 52, 78 (SMO-12), 96, 112 (SMY-8), 116-119, 121; G-1 through -5, -19, -20, -31]; pp. 4.4-4.7.

Reproduced from
best available copy.

MOP Macro-Operation; see also FIN, SMA, SUB; pp. 4.3, 4.6, 5.2, 6.4.

MRA Matrix Reducibility Algorithm; see also BLT; [25, 113; G-6,-10,-11,-20,-29]; pp. 1.3, 8.5, 10.7-10.12.

NAM Nodal Admittance Matrix; see also CAP, CCD, CMM, DID, M-MAT, MMM, SYP; [e.g., 9, 11, 16, 17]; pp. 10.5-10.8.

NLE Nonlinear Equation; see also CAP, PDE, SDE; [19, 74, 120; E-R3]; pp. 2.1-2.4, 10.1.

PDA Pivoting on the Diagonal in Arbitrary order; see also DID, SYP; [e.g., 71, 79, 80, 96; part G]; pp. 4.2, 6.1-6.4, 8.1-8.5, 9.1.

PDE Partial Differential Equation; see also BLD, BIM, BMM, CAP, CGM, DID, FEM, SOR, SYP, TDL; [1, 10, 18, 21-24, 26, 28, 39, 61, 74, 79, 80, 82, 93, 101, 102, 104, 106, 112 (SMY-16); G-21]; pp. 3.1, 3.3, 7.4-7.5, 12.1.

PDN Pivoting down the Diagonal in Natural order; see also DID, FIN, FDA, PFS, SFP, SYP, THP, TRN; pp. 2.3-2.4, 4.2, 5.1-5.4, 6.1-6.3, 7.1-7.5, 12.2-12.4.

PFI Product Form of the Inverse; see also BIF, ECM, EFI, FIN, MMM, SMA; [e.g., 73, 121; G-31,-43]; pp. 3.2, 3.3, 4.5-4.7, 5.3-5.6.

PFS Pivoting For Size; see also INI, ITR, SYI, THP; [e.g., E-R1, -R2]; pp. 1.3, 4.2, 5.1, 5.4-5.6, 6.4-6.5, 7.1, 9.3, 10.4-10.5, 12.3-12.4.

PRO PROGRAMming; see also CAP, CAR, MEH, SFP, SMA, SPP; [e.g., 40, 78, 112; F-28,-40]; pp. 1.1, 2.3-2.4, 3.1-3.3, 6.2, 9.4, 10.12, 13.2-13.3.

PSA Power System Analysis; see also CAP, CCD, DID; [54, 71, 72, 78(SMO-6, -8,-9,-15), 79, 80, 83, 91, 98, 112 (SMY-4, -13); G-13,-17,-22,-36]; pp. 1.2, 3.1-3.3, 6.1.

RGE Row Gaussian Elimination; see also EFI, FIN, SMA, TRF; [e.g., 51, 83, 96, 98]; pp. 2.4, 4.1, 4.3, 5.2, 5.4-5.5, 12.3-12.4.

SCA SCALing; see also EAN, SUR; [e.g., 5, 6, 15, 33, 88-90, 112(SMY-19); 113]; pp. 4.2, 6.4, 10.1-10.2, 10.4, 10.13-10.15.

SDE Stiff Differential Equations; see also CCD, NLE, PDE; [40, 41, 56, 78 (SMO-17), 112 (SMY-1,-2,-14), 128, 129; G-46]; pp. 2.1-2.4.

SFG Signal Flow Graph; see also SPP; [124-126]; p. 8.4.

SFP Symbolic Factorization Program; see also BSM, SFG, SPP, SSI, TLP; [40, 78 (SMO-17), 112 (SMY-2,-9,-13)]; pp. 2.4, 4.2, 10.7-10.12.

SIAM Society for Industrial and Applied Mathematics; pp. 10.2-10.3.

SIGNUM Special Interest Group in NUMerical Mathematics; see also ACM; [67]; p. 10.1.

- SMA Sparse Matrix Algorithm; see also BIF, BIM, BMM, BGR, CGM, EFI, INI, ITR, MPM, PFI, PFS, RGE, SFP, SOR, TDL, THP, TRF; [e.g., 78, 112]; pp. 2.4, 3.1-3.3, 4.1-4.7, 5.1-5.6, 6.2-6.5, 7.1-7.5, 10.5-10.12.
- SMO Sparse Matrix Oxford conference; [78]; pp. 1.2, 2.3, 3.1-3.2, 4.4, 6.1, 6.3, 7.3, 10.6-10.7.
- SMY Sparse Matrix Yorktown conference; [112]; pp. 1.2, 2.4, 3.1, 3.3, 4.4, 7.5, 11.2, 12.1.
- SIM Strongly Implicit Method; see also BIM, BLD, BMM, PDE, SOR, TDL, TRF; [22, 23, 93, 104, 112 (SMY-6)]; pp. 3.1, 3.3, 7.5, 12.1.
- SOR Successive Over Relaxation; see also BIM, PDE, SIM, TDL; [e.g., 101; E-R2; F-34,-37,-42]; p. 9.1.
- SPP Symbolic Processing Programs; see also SFG, SFP; [125, 126]; pp. 7.5, 8.4.
- SSI Sparseness Structure Information; see also BSM, SFP, TLP; [e.g., 72, 78 (SMO-6)]; pp. 2.3-2.4, 3.2, 4.2, 6.1, 6.4, 7.1-7.5, 8.1-8.6, 9.3-9.4, 12.2-12.4.
- STM Structural Mechanics; see also BGR, BLD, CAP, CGM, DID, FEM, PDE, SYP; [33-35, 48, 49, 57-60, 65; 78 (SMO-2,-7), 84, 85, 92, 102, 112 (SMY-11,-18); G-24]; pp. 1.2, 3.1-3.3, 6.4, 7.3, 7.5, 9.4, 10.14.
- SUB SUBstitution; see also FIN, ITR, SMA; pp. 4.1-4.7, 5.2-5.4, 12.2-12.4.
- SUR SURvey; see also CAP, EAN, EVV, PDE, SMA; [10, 11, 16, 21, 24, 28, 30, 31, 42, 45, 46, 50, 52-56, 61, 67, 74-78, 82, 91, 96, 98, 101-103, 105, 109-112, 119-130; E-R1,-R2,-R3,-3,-9,-17,-29; F-2,-7,-9,-17,-26,-28,-32,-35, -40,-44 through -47; G-23,-26,-28,-29].
- SYI SYmmetric INdefinite; see also BGR, FIN, INI, ITR, PFS; [13, 14; E-R1, -R2, -8, -25]; pp. 4.2, 6.4-6.5, 10.4-10.5.
- SYP SYmmetric and Positive definite; see also BIF, CGM, DID, PDE; [e.g., 78 (SMO-6), 79, 80]; pp. 4.2, 6.1-6.4, 7.1-7.5, 8.1-8.4, 9.1.
- TAS Template of Active Storage; see also BLD, BMM, FEM, PDE, SOR, SFP, SSI; pp. 8.3, 12.2-12.4.
- TDL Tri-Diagonal Like; see also PDE, SYP, TDM; [10, 21, 28, 39, 79, 82, 101, 102, 106; G-9,-21]; pp. 7.4, 8.3, 9.1.
- TDM Tri-Diagonal Matrix; see also BMM, EVV, PDE, TDL; [e.g., E-R1, -R2]; p. 7.2.
- THP Threshold Pivoting, see also EAN, LP, PFS, SCA, SMA; [4, 13, 14, 73, 75, 78, 96, 112, 127]; pp. 1.3, 2.3, 5.5, 6.4, 9.3, 10.14-10.15.
- TLP Threaded index List with Pointers; see also BSM, SFP, SSI; e.g., 72, 78 (SMO-3,-6), 112(SMY-7,-9,-10,-13,-15)]; pp. 2.3, 2.4, 3.2, 3.3, 6.1, 8.1.
- TRF TRIangular Factorization; see also BGR, BIF, EFI, FIN, PFI, RGE, SFP; [e.g., 40; E-R1,-R2]; pp. 2.3-2.4, 3.2, 3.3, 4.1, 4.3, 5.1-5.2, 10.5-10.13.

C. Author List

- Akyuz, F. A.; [G-35]; p.12.3.
- Allwood, R.; [78(SMO-2)]; p.3.2.
- Alway, G. G.; [G-15]; p.12.3.
- Anderson, J. P.; [F-14].
- Arms, L. J.; [1]; p.9.1.
- Ashkenazi, V.; [78(SMO-5)]; p.3.2.
- Babushka, I.; [2,3]; p.10.3.
- Bamford, R. M.; [65]; p.7.3.
- Barnes, G. H.; [F-25]; p. 11.3.
- Barron, D. W.; [F-3,-26].
- Bartels, R. H.; [4]; pp. 4.4, 10.4.
- Berth, W.; [F-7].
- Baty, J.; [78 (SMO-12)]; p. 3.2.
- Bauer, F. L.; [5, 6; E-15]; p. 10.4.
- Baumann, R.; [78 (SMO-8)]; p. 3.2.
- Beale, L.; [78 (SMO-1)]; p. 3.2.
- Beckman, F. S.; [7]; p. 6.4.
- Belady, L. A.; [122].
- Bennett, J. M.; [8]; p. 4.4.
- Bibb, J.; [F-11].
- Bingham, J. A.; [9]; p. 10.6.
- Birkhoff, G.; [10]; p. 7.4.
- Blaser, A.; p. 12.3.
- Branin, F. H., Jr.; [11, 112 (SMY-17); G-4, -5, -23; F-15]; pp. 3.3, 4.4, 10.5.
- Brayton, R. K.; [112 (SMY-6); G-43, -46]; pp. 2.1-2.4, 3.3, 5.4, 9.4.
- Brent, R. P.; [12]; p. 11.2.
- Brooks, F. P., Jr.; [F-36].
- Brown, R. H.; [F-25]; p. 11.3.
- Bryant, P. M.; [G-28].
- Buchet, J. de; [78 (SMO-14)]; p. 3.2.
- Buchholz, W.; [F-7]; p. 13.3.
- Bunch, J. R.; [13, 14]; p. 4.2, 6.4, 10.5.
- Businger, P. A.; [15; E-22]; p. 10.4.
- Bussell, B.; [F-11].
- Calahan, D. A.; [16, 17]; pp. 2.1, 3.1, 10.6.
- Carlitz, R. M.; [F-15].
- Carpentier, J.; [G-13].
- Carre, B. A.; [78 (SMO-13); G-21]; pp. 3.2, 7.4, 8.3, 9.1.
- Chang, A.; [112 (SMY-13)]; pp. 2.4, 3.3.
- Chartres, B. A.; [F-8].
- Chazan, D.; [F-37].
- Chen, T. C.; [F-15, -47]; p. 11.3.
- Churchill, M.; [78 (SMO-9)]; p. 3.2.
- Coffman, E. G.; [F-39]; p. 12.1.
- Cuthill, E. H.; [18; G-42]; pp. 9.1, 12.3.
- Daniel, J. W.; [19, 20]; p. 6.4.
- Dantzig, G. B.; [112 (SMY-10)]; p. 3.3.
- de Buchet, J.; see Buchet, J. de
- Denning, P. J.; [F-44]; pp. 11.3, 12.1.
- Dickson, J. C.; [G-16].
- Douglas, J., Jr.; [21]; p. 7.4.
- Driscoll, G. C.; [F-34].
- Dulmage, A. L.; [G-10, -29]; pp. 4.1, 8.5, 8.6.
- Dupont, T.; [22, 23]; pp. 3.1, 7.5.
- Eberlein, P. J.; [E-28].
- Edelmann, H.; [G-17, -22, -36].
- El-Abiad, A. H.; [91]; pp. 1.2, 3.1, 6.1.
- Elmaghraby, S. E.; [F-13].
- Engeli, M.; [24]; p. 7.4.
- Estrin, G.; [F-11, -12, -20].
- Eufinger, J.; [25; G-37]; pp. 4.1, 8.5.
- Even, R. K.; [G-30].
- Falkoff, A. D.; [F-9].
- Faulkner, R. A.; [E-29].
- Feingold, D. G.; [26]; p. 9.1.
- Ford, L. R., Jr.; [27]; p. 10.8.
- Fulkerson, D. R.; [27]; p. 10.8.
- Forsythe, G. E.; [26, 29, 30, 31]; pp. 3.1, 5.1, 7.4, 10.1, 10.3, 10.4.
- Fox, R. L.; [32]; p. 11.2.
- Fox, R. L.; [33]; pp. 6.4, 10.14.

- Francis, J. G. F.; [E-1]; p. 4.1.
- Fried, I.; [34, 35]; p. 6.4.
- Gargantini, I.; [E-23].
- Garwick, J.; [36]; p. 7.1.
- Gates, L. D.; [1]; p. 9.1.
- Gear, C. W.; [128, 129]; p. 2.2.
- Gecsei, J.; [F-45]; p. 12.1.
- Gill, S.; [F-2].
- Gilmore, P. A.; [F-27].
- Ginsberg, Th.; [24]; p. 7.4.
- Givens, W.; [37, 112 (SMY-19)]; pp. 3.3, 10.4.
- Goldstine, H. H.; [69]; pp. 10.1, 10.2.
- Colub, G. H.; [4, 38]; pp. 4.4, 10.4.
- Gourlay, A. R.; [39]; p. 7.4.
- Grapes, T. E.; [17]; pp. 2.1, 10.6.
- Gunn, J. E.; [21]; p. 7.4.
- Gustavson, F. C.; [40, 112 (SMY-2, -6); G-43, -46]; pp. 2.1-2.4, 3.3, 5.4, 9.4.
- Nachtel, G. D.; [41; G-46]; pp. 2.1-.
- Hall, L. V.; [F-15].
- Harary, F.; [42, 78 (SMO-10); G-6, -11]; pp. 3.2, 4.1, 8.1, 8.5.
- Harvey, R. P.; [112 (SMY-10)]; p. 3.3.
- Heller, J.; [F-4].
- Hershdorfer, A. M.; [G-24].
- Hestenes, M. R.; [43]; p. 6.4.
- Hickerson, N.; [G-39].
- Hobbs, L.C.; [123]; p. 11.3.
- Hopcroft, J. E.; [44]; p. 11.2.
- Housholder, A. S.; [45, 46; E-R2, -R3]; pp. 4.4, 7.3, 9.2, 10.1, 10.2, 10.3, 10.14.
- Mumphrey Davies, M. W.; [54].
- Iliffe, J. K.; [F-10].
- Iverson, K. W.; [47]; pp. 4.1, 13.2.
- Jaeger, A.; [G-37].
- Jennings, A.; [46, 49, 78 (SMO-7)]; pp. 3.2, 7.3, 9.4.
- Jodelt, J. G.; [F-10].
- Kahan, W.; [38, 50; E-4, -5, -6]; pp. 10.1, 10.4, 10.13.
- Karp, R. M.; [F-6, -18, -19, -38].
- Kato, M.; [F-25]; p. 11.3.
- Kendall, R. P.; [22]; pp. 3.1, 7.5.
- Kerr, L. R.; [44]; p. 11.2.
- Kettler, P. C.; [112 (SMY-3)]; p. 3.3.
- Klyuyev, V. V.; [51]; p. 11.2.
- Kokovkin-Shcherbak, N. I.; [51]; p. 11.2.
- Knuth, D. E.; [F-28].
- Kotov, V. E.; [F-29].
- Kron, G.; [52; G-1, -2, -3]; pp. 4.4, 8.5; see also E-17; G-4, -5, -7, -17, -20, -23; SMO-12; SMY-8.
- Kublanovskaya, V. N.; [E-2]; p. 4.1.
- Kuck, D. J.; [F-25, -30]; p. 11.3.
- Kuchner, J.; [F-32].
- Kwan, T. V.; [104]; pp. 3.1, 7.5, 12.1.
- Lanczos, C.; [53]; p. 10.3.
- Larcombe, R.; [78 (SMO-3)]; p. 3.2.
- Laski, J. G.; [F-31].
- Laughton, M. A.; [54].
- Lavrentev, M. M.; [55]; p. 10.3.
- Lee, H.; [112 (SMY-9)]; p. 3.3.
- Lehman, M. M.; [F-23].
- Liebl, P.; [G-25].
- Liniger, W.; [40, 56, 112 (SMY-2, -14)]; pp. 2.-2.4, 3.3.
- Lipson, J. D.; [125]; p. 8.4.
- Livesley, R. K.; [57]; p. 6.4.
- McCormick, C. W.; [58, 60, 112 (SMY-18, -19)]; pp. 3.3, 7.3.
- McKee, J.; [G-42]; p. 12.3.
- McKellar, A. C.; [F-39]; p. 12.1.
- McKnight, R.D.; [112 (SMY-10)]; p. 3.3.
- MacNeal, R. H.; [59, 60]; p. 7.3.
- Mack, T. E.; [92]; p. 6.4.
- Marchuk, G. I.; [61]; p. 7.4.
- Maringani, A. S.; [F-29].
- Markowitz, H. M.; [62]; pp. 4.5, 6.1.
- Martin, D.; [F-20].

- Martin, D. W.; [G-15]; p. 12.3.
- Martin, R. S.; [63, 64; F-7, -8, -10 through -13, -30]; pp. 2.2, 4.1, 4.2, 4.4, 5.1, 7.1, 9.5, 10.4.
- Mason, S. J.; [124]; p. 8.4.
- Mattson, R. L.; [F-45]; p. 12.1.
- Mayoh, B. H.; [G-18].
- Melosh, R. J.; [65]; p. 7.3.
- Mendelsohn, N. S.; [G-10, -29]; pp. 4.1, 8.5, 8.6.
- Miller, R. E.; [F-16, -19, -38].
- Minty, G. J.; [G-26].
- Miranker, W. L.; [F-37, -46].
- Mitchell, A. R.; [39]; p. 7.4.
- Moler, C. B.; [31, 66, 67, 68, 112 (SMY-19)]; pp. 2.2, 3.3, 4.1, 4.4, 9.5, 10.1, 10.3, 10.4, 12.1.
- Morrell, A. J. H.; [70, 128, 129]; pp. 2.2, 10.5.
- Nathan, A.; [G-30].
- Naur, P.; [F-40].
- Neumann, J. von; [65]; pp. 10.1, 10.2.
- Noble, A. S.; [70, 128]; p. 10.5.
- Ogbunbiri, E. C.; [71, 72, 78 (SMO-15)]; pp. 2.3, 2.4, 3.2, 6.1, 8.5.
- Orchard-Hays, W.; [73, 112 (SMY-7, -19)]; pp. 1.2, 3.1, 3.3, 4.5.
- Ortega, J. M.; [74, 120]; p. 10.1.
- Palacol, E. L.; [112 (SMY-11)]; p. 3.3.
- Parlett, B. N.; [13; E-3, -14, -24]; pp. 4.2, 6.4, 10.5.
- Parter, S.; [G-8, -9]; pp. 7.4, 8.3.
- Pease, H. C. III; [F-21, -41].
- Peters, G.; [64; E-25, -30]; pp. 2.2, 4.1, 4.2, 4.4, 6.5, 7.1, 9.5, 10.4.
- Petrie, G. W. III; [F-1]; p. 12.3.
- Pottle, C.; p. 2.1.
- Pretsch, H.; p. 12.3.
- Raab, A. R.; [G-24].
- Rachford, H. H., Jr.; [22]; pp. 3.1, 7.5.
- Rall, L. B.; [75]; pp. 4.5, 10.1, 10.14.
- Ralston, A.; [76]; p. 10.1; see also [7, 110].
- Randell, B.; [F-32, -40].
- Reed, R.; [77]; p. 8.1; see also [79].
- Reid, J. K.; [78 (Ed., SMO-16)]; pp. 1.2, 2.3, 2.4, 3.1, 3.2, 6.1, 6.3, 7.3, 10.6.
- Reinsch, C.; [E-10, -15, -24].
- Reiter, R.; [F-33].
- Rheinboldt, W. C.; [74, 120]; p. 10.1.
- Rohrer, R. A.; [41]; p. 2.1.
- Kollett, J. S.; [F-5].
- Rosanoff, R. A.; 10.14 (reference).
- Rose, D. J.; [79, 80; G-44, G-45]; pp. 2.1, 8.1-9.5; see also [77].
- Rosen, A.; [81]; p. 10.6.
- Rosen, R.; [G-38]; p. 12.3.
- Rosenberg, D. V. von; [82]; p. 7.1.
- Rosenfeld, J. L.; [F-34, -42].
- Roth, J. P.; [G-7]; p. 4.4.
- Rutishauser, H.; [24; E-26]; p. 7.4.
- Sato, N.; [83; G-14]; pp. 2.4, 6.1.
- Saunders, M. A.; [4]; pp. 4.4, 10.4.
- Schwartz, E. S.; [F-6].
- Schwartz, J. T.; [F-17].
- Schwarz, H. R.; [E-16].
- Sedlacek, J.; [G-25].
- Segethova, J.; [84]; p. 7.5.
- Shaw, J. M.; [85]; p. 10.14.
- Shedler, G. S.; [F-22, -23].
- Shkel, J.; [85, 87]; p. 10.6.
- Simpson, A.; [E-17].
- Slotnick, D. L.; [F-25]; p. 11.3.
- Sluis, A. van der; [88, 89, 90]; p. 10.4.
- Slutz, D. R.; [F-45]; p. 12.1.
- Smith, D. M.; [112 (SMY-15); F-43]; p. 3.3.
- Smith, S. T.; [112 (SMY-10)]; p. 3.3.
- Spillers, W. R.; [G-19, -39]; p. 4.4.
- Stagg, G. W.; [91]; pp. 1.2, 3.1, 6.1.
- Stanton, E. L.; [33, 92]; pp. 6.4, 10.14.
- Steward, D. V.; [112 (SMY-8); G-12, -20]; pp. 3.3, 4.1, 4.4, 8.5.
- Stewart, K.; [78 (SMO-12)]; pp. 3.2, 4.4.
- Stiefel, E.; [24, 43]; pp. 6.4, 7.4.

- Stokes, K. A.; [F-25]; p. 11.3.
- Stone, H. L.; [93, 104]; pp. 3.1, 7.5, 12.1; see also Weinstein.
- Strassen, V.; [94]; p. 11.2.
- Sturman, G. M.; [G-24].
- Suez, J.; [F-15].
- Swinerton-Dyer, H. P. F.; [F-3].
- Tabarook, B.; [E-17].
- Tewarson, R. P.; [78 (SMN-11), 95, 96, 112 (SMN-5), 121; E-31; G-31, -32, -33, -40, -41]; pp. 3.2, 3.3, 7.1, 12.3, 12.4.
- Thurnau, D.; [97]; p. 7.1.
- Tinney, W. F.; [71, 83, 98, 112 (SMN-4, -19); G-14, -34]; pp. 2.4, 3.3, 6.1, 8.5.
- Tobey, R. C.; [124]; p. 8.4.
- Traiger, I. L.; [F-45]; p. 12.1.
- Tuff, A.; [78 (SMO-7)]; pp. 3.2, 7.3.
- Turing, A. M.; [99]; pp. 10.1, 10.2.
- Turn, R.; [F-11, -12].
- Utku, S.; [G-35]; p. 12.3.
- van der Sluis, A.; see Sluis, A. van der.
- Varah, J. M.; [100; E-6, -18, -27]; pp. 4.2, 4.4.
- Varga, R. S.; [10, 18, 26, 101]; pp. 3.1, 7.4, 9.1, 10.5.
- von Neumann, J.; see Neumann, J. von.
- von Rosenberg, D. V.; see Rosenverg, D. V. von.
- Wachspress, E. L.; [102]; pp. 3.1, 7.4.
- Waite, W. M.; [F-24].
- Walker, J. W.; [71, 98; G-34]; pp. 2.4, 6.1, 8.5.
- Walsh, J.; [78 (SMO-4); E-9]; p. 3.2.
- Wasow, W. R.; [28]; pp. 3.1, 7.4.
- Weaver, W. Jr.; [103]; pp. 1.2, 3.1.
- Weil, R. L., Jr.; [112 (SMY-3)]; p. 3.3.
- Weinstein, H. G.; [104, 112 (SMY-16)]; pp. 3.1, 3.3, 7.5, 12.1; see also Stone.
- Wenke, K.; [G-37].
- Westlake, J. R.; [105]; pp. 10.1, 10.3.
- Widlund, O. B.; [106]; p. 7.4.
- Wilf, H. S.; [76]; p. 10.1; see also [7, 110].
- Wilkes, M. V.; [130; F-35]; pp. 11.3, 13.1.
- Wilkinson, J. H.; [63, 64, 107-111; E-R1, -7 through -13, -19, -20, -21, -25, -30; F-5]; pp. 2.2, 3.1, 4.1, 4.2, 5.1, 6.4, 6.5, 7.1, 7.3, 9.5, 10.1-10.4, 10.13.
- Willoughby, R. A.; [40, 56, 78 (SMO-17), 112 (Ed., SMN-1, -2, -6, -14), 113; G-43]; pp. 1.2, 2.1-2.4, 3.1-3.3, 4.1, 5.4, 8.5, 10.6-10.13.
- Winograd, S.; [114, 115; F-19]; p. 11.2.
- Wolfe, P. S.; [75, 112 (SMN-12, -19), 127]; pp. 3.3, 4.5, 10.1, 10.14, 11.2.
- Yaspan, A.; [G-27]; p. 10.8.
- Young, D. M.; [10]; p. 7.4.
- Zielke, G.; [116-119]; p. 4.4.
- Zollenkopf, K.; [78 (SMO-6)]; pp. 2.3, 3.2, 6.1.
- Zondek, B.; [1]; p. 9.1.

D. General References

1. Arms, L. J., Gates, L. D., Zondek, B., "A method of block iteration," SIAM J. Appl. Math. 4 (1956) pp.220-229, H0112.
2. Babuska, I., "Numerical stability in mathematical analysis," Proc. IFIP Congress; Edinburgh (1968).
3. _____, "Numerical stability in problems in linear algebra," SIAM National Meeting, Denver, Colorado (June 1970).
4. Bartels, R. H., Golub, G. H., Saunders, M. A., "Numerical techniques in mathematical programming," Stanford CS-70-162 (1970).
5. Bauer, F. L., "Optimally scaled matrices," Numer. Math. 5 (1963) pp.73-87, H0200, MR 28 2629.
6. _____, "Remarks on optimally scaled matrices," Numer. Math. 13 (1969) pp.1-3.
7. Beckman, F. S., "The solution of linear equations by the conjugate gradient method," Mathematical Methods for Digital Computers, Vol. 1, (A. Ralston and H. S. Wilf, Eds.) Wiley, New York (1960) pp.62-72, H0222.
8. Bennett, J. M., "Triangular factors of modified matrices," Numer. Math. 7 (1965) pp.217-222, H0260, MR 31 1766.
9. Bingham, J. A., "A method of avoiding loss of accuracy in nodal analysis," Proc. IEEE 55 (1967) pp.409-410.
10. Birkhoff, G., Varga, R. S., Young, D. M., "Alternating direction implicit method," Advances in Computers 3, Academic Press, New York (1962) pp.189-273, H0297, MR 29 5395.
11. Branin, F. H., Jr., "Computer methods of network analysis," Proc. IEEE 5 (1967) pp.1787-1801.
12. Brent, R. P., "Algorithms for matrix multiplication," Stanford CS-70-157 (1970).
13. Bunch, J. R., Parlett, B. N., "Direct methods for solving symmetric indefinite systems of linear equations," SIAM J. Numer. Anal. to appear.
14. Bunch, J. R., "Analysis of the diagonal pivoting method," SIAM J. Numer. Anal., to appear.
15. Businger, P. A., "Matrices which can be optimally scaled," Numer. Math. 12 (1968) pp.346-348, MR 39 1096.

16. Calahan, D. A., Computer Aided Network Design, McGraw-Hill, New York (1968).
17. Calahan, D. A., Grapes, T. E., "Cancellation avoidance in matrix based network analysis," Intern. Symp. on Circuit Theory, Atlanta, Georgia (Dec. 1970).
18. Cuthill, E. H., Varga, R.S., "A method of normalized block iteration," J. Assoc. Comput. Mach. 6 (1959) pp.236-244, H0558.
19. Daniel, J. W., "The conjugate gradient method for linear and nonlinear operator equations," SIAM J. Numer. Anal. 4 (1967) pp.10-26.
20. _____, "Convergence of the conjugate method with computationally convenient modifications," Numer. Math. 10 (1967) pp.125-131, H0563, CR9 13,478. MR36 2315.
21. Douglas, J., Jr., Gunn, J. E., "A general formulation of alternating direction methods, I. Parabolic and hyperbolic problems," Numer. Math. 6 (1964) pp. 428-453, H0632, CR6 8619.
22. Dupont, T., Kendall, R. P., Rachford, H. H., Jr., "An approximate factorization procedure for solving self-adjoint elliptic difference equations," SIAM J. Numer. Anal. 5 (1968) pp.559-573.
23. Dupont, T., "A factorization procedure for the solution of elliptic difference equations," SIAM J. Numer. Anal. 5 (1968) pp.753-782.
24. Engeli, M., Ginsberg, Th., Kutishauser, H., Stiefel, E., "Refined iterative methods for computation of the solution and the eigenvalues of self-adjoint boundary value problems," Birkhauser, Basel (1959) H0704, MR26 3218.
25. Eufinger, J., "Operations on directed graphs," J. Reine Angew. Math., to appear (part of Ph.D. thesis, U. of Mainz, Germany).
26. Feingold, D. G., Varga, R. S., "Block diagonally dominant matrices and generalizations of the Gerschgorin circle theorem," Pacific J. Math. 12 (1963) pp.1241-1250, H0768, MR27 1458.
27. Ford, L. R., Jr., Fulkerson, D. R., Flows in Networks, Princeton University Press (1962).
28. Forsythe, G. E., Wasow, W. R., Finite-Difference Methods for Partial Differential Equations, J. Wiley, New York (1960), H0843.
29. Forsythe, G. E., "Algorithm 16. Crout with pivoting," Comm. ACM 3 (1960) pp. 507-508.
30. _____, "Today's computational methods of linear algebra," SIAM Rev. 9 (1967) pp. 489-515, H0830, CR9 14, 751, MR36 1089.

31. Forsythe, G. E., Moler, C. B., Computer Solution of Linear Algebraic Equations, Prentice-Hall, Englewood Cliffs, N. J. (1967), H0836, CR9 13,468, MR36 2306.
32. Forst, B. L., "Accelerating LP algorithms," Comm. ACM 12 (1969) pp. 384-385.
33. Fox, R. L., Stanton, E. L., "Developments in structural analysis by direct energy minimization," AIAA J. 6 (1968) pp. 1036-1042.
34. Fried, I., "More on gradient iterative methods in finite element analysis," AIAA J. 7 (1969) pp. 565-567.
35. ———, "Gradient methods of finite element eigenproblems," AIEE J. 7 (1969) pp. 739-741.
36. Garwick, J., "ALGOL programming (section): Contribution 7. Solution of a linear system with a band coefficient matrix," BIT 3 (1963) pp. 207-208.
37. Givens, W., "Numerical computation of the characteristic values of a real symmetric matrix," Oak Ridge National Laboratory, ORNL-1574 (1954) H0925.
38. Golub, G. H., Kahan, W., "Calculating the singular values and pseudo inverse of a matrix," SIAM J. Numer. Anal. 2 (1965) pp. 205-224, H0965, MR32 587.
39. Gourlay, A. R., Mitchell, A. R., "The equivalence of certain alternating direction and locally one-dimensional difference methods," SIAM J. Numer. Anal. 6 (1969) pp. 37-46.
40. Gustavson, F., Liniger W., Willoughby, R., "Symbolic generation of an optimal Crout algorithm for sparse systems of linear equations," J. Assoc. Comput. Mach. 17 (1970) pp. 87-109.
41. Hachtel, G. D., Rohrer, P. A., "Techniques for the optimal design and synthesis of switching circuits," IEEE Proc. 55 (1967) pp. 1864-1877.
42. Harary, F. (Ed.) Graph Theory and Theoretical Physics, Academic Press, New York (1967).
43. Hestenes, M. R., Stiefel, E., "Methods of conjugate gradients for solving linear systems," J. Res. Nat. Bur. Standards, Sect. B. 49 (1952) pp. 409-436, H1099.
44. Hopcroft, J. E., Kerr, L. R., "On minimizing the number of multiplications necessary for matrix multiplication," SIAM J. Appl. Math. 20 (1971) pp. 30-36.
45. Householder, A. S., Principles of Numerical Analysis, McGraw-Hill, New York (1953).

See also special issue in honor of A. S. Householder, SIAM J. Numer. Anal. 7, 4 (Dec. 1970).

46. Householder, A. S., The Theory of Matrices in Numerical Analysis, Blaisdell, New York (1962).
47. Iverson, K. W., A Programming Language, Wiley, New York (1962).
48. Jennings, A., "A compact storage scheme for the solution of symmetric linear simultaneous equations," Comput. J. 9 (1966) pp. 281-285.
49. _____, "A sparse matrix scheme for the computer analysis of structures," Internat. J. Comput. Math. 2 (1968) pp. 1-21.
50. Kahan, W., "Numerical linear algebra," Canadian Math. Bull. 9 (1966) pp. 757-801, H0008.
51. Klyuyev, V. V., Kokovkin-Shcherbak, N. I., "On the minimization of the number of arithmetic operations for the solution of linear algebraic systems of equations," Stanford CS24, transl. by G. I. Tee, (1965).
52. Kron, G., Special issue on G. Kron's work in J. Franklin Inst. 286 (December 1968). See also [G-1,-2,-3].
53. Lanczos, C., Applied Analysis, Prentice-Hall, Englewood Cliffs, New Jersey (1956)H0138.
54. Laughton, M. A., Humphrey Davies, M. W., "Numerical techniques in solution of power-system load-flow problems," Proc. IEE (London) 111 (1964) pp. 1575-1588.
55. Lavrentev, M. M., Some Improperly Posed Problems of Mathematical Physics, Transl. of 1962 Russian Edition revised by R. J. Sacker, Springer-Verlag, New York (1967).
56. Liniger, W., Willoughby, R., "Efficient integration of stiff systems of ordinary differential equations," SIAM J. Numer. Anal. 7 (1970) pp. 47-66.
57. Liveslev, R. K., "The analysis of large structural systems," Comput. J. 3 (1960) pp. 34-39.
58. McCormick, C. W., "Application of partially banded matrix methods to structural analysis," [112; SMY-18, pp. 155-158].
59. MacNeal, R. H., NASTRAN theoretical manual, NASA Report, Contract No. NAS5-10049, Sect. 11.3 (1970).
60. MacNeal, R. H., McCormick, C. W., The NASTRAN computer program for structural analysis, Society Automotive Engineers Trans., to appear.
61. Marchuk, G. I., "Some applications of splitting-up methods to the solution of mathematical physics problems," Apl. Mat. 13 (1968) pp. 103-132.

62. Markowitz, H. M., "The elimination form of the inverse and its application to linear programming," Management Sci. 3 (1957) pp. 255-269.
63. Martin, R. S., Wilkinson, J. H., "Handbook Series Linear Algebra. Symmetric decomposition of positive definite band matrices," Numer. Math. 7 (1965) pp. 355-361, H0354, CR7 10,509.
64. Martin, R. S., Peters, G., Wilkinson, J. H., "Handbook Series Linear Algebra. Iterative refinement of the solution of a positive definite system of equations," Numer. Math. 8 (1966) pp. 203-216, H0352, CR8 12,007.
65. Melosh, R. J., Bamford, R. M., "Efficient solution of load deflection equations," J. Struct. Div. ASCE, Proc. Paper #6510 (April 1969) pp. 661+
66. Moler, C. B., "Iterative refinement in floating point," J. Assoc. Comput. Mach. 14 (1967) pp. 316-321, H0447.
67. _____, "State of the art in matrix computations," SIGNUM Newsletter 4, 1 (January 1969) pp. 22-28.
68. _____, "Matrix computations with FORTRAN and paging," Comm. ACM, to appear.
69. Neumann, J. von, Goldstine, H. H., "Numerical inverting of matrices of high order," Bull. Amer. Math. Soc. 53, (1947) pp. 1021-1099, H0511.
70. Noble, A. S., "Input-output cost models and their uses for financial planning and control," Proc. IFIP Congress, Edinburgh (1968), see [128].
71. Ogbuehiri, E. C., Tinney, W. F., Walker, J. W., "Sparsity-directed decomposition for Gaussian elimination on matrices," IEEE Trans. PAS-89 (1970) pp. 141-150.
72. _____, "Dynamic storage and retrieval in sparsity programming," IEEE Trans. PAS-89 (1970b) pp. 150-155.
73. Orchard-Hays, W., Advanced Linear Programming Computing Techniques, McGraw-Hill, New York (1968).
74. Ortega, J. M., Rheinboldt, W. C. (Eds.), Numerical Solutions of Nonlinear Problems: Studies in Numerical Analysis 2, Proc. Symp. sponsored by Office of Naval Research at the Fall SIAM meeting (October 1968), SIAM, Philadelphia, Penna. (1970).
75. Rall, L. B. (Ed.), Error in Digital Computation, Volumes 1 and 2, Wiley, New York (1965). Proc. Symp. Mathematics Research Center, University of Wisconsin, Madison, Wisconsin (October 1964 and April 1965).
76. Ralston, A., Wilf, H. S. (Eds.) Mathematical Methods for Digital Computers, Vol. 1 (1960), Vol. 2 (1967), Wiley, New York.
77. Reed, R. (Ed.) Formal Theory and Computing, Academic Press, New York (1971).

78. Reid, J. K. (Ed.) Large Sparse Sets of Linear Equations, Academic Press, London (1970). Proc. of Conference organized by the Institute of Mathematics and Its Applications, and held at Oxford University, England (April 1970).
79. Rose, D. J., "Symmetric elimination on sparse positive definite systems and the potential flow network problem," Ph.D. Thesis, Mathematics, Harvard University (1970). To appear in part and in revised form in [77].
80. _____, "Triangulated graphs and the elimination process," J. Math. Anal. Appl. 32 (1970) pp. 597-609.
81. Rosen, A., "A new network theorem," J. IEE (London) 62, (1924) pp. 916-918.
82. Rosenberg, D. V. von, Methods for the Numerical Solution of Partial Differential Equations, American Elsevier, New York (1969).
83. Sato, N., Tinney, W. F., "Techniques for exploiting the sparseness of the network admittance matrix," IEEE Trans. PAS-82 (1963) pp. 944-950.
84. Segethova, J., "Elimination procedures for sparse symmetric linear systems of a special structure," U. of Maryland, Computer Science Center, College Park, Md. Tech. Rep. 70-121 (NGL-21-002-008) (July 1970).
85. Shaw, J. M., "Ill-conditioned stiffness matrices," J. Struct. Div. ASCE 92, ST6(1966)pp. 443-457.
86. Shekel, J., "Matrix representation of transistor circuits," Proc. IRE 40 (1952) pp. 1493-1497.
87. _____, "Analysis of linear networks," Sc.D. Thesis, MIT. (1957)
88. Siu, A. van der, "Condition numbers and equilibration of matrices," Numer. Math. 14 (1969) pp. 14-23.
89. _____, "Stability of solutions of linear algebraic systems," Numer. Math. 14 (1970) pp. 246-251, CR11 20,353.
90. _____, "Condition, equilibration and pivoting in linear algebraic systems," Numer. Math. 15 (1970) pp. 74-86, CR11 20,354.
91. Stagg, G. W., El-Abiad, A. H., Computer Methods in Power System Analysis, McGraw-Hill, New York (1968).
92. Stanton, E. L., Mack, T. E., "MINI-FORMAT: A gradient solution procedure for the displacement methods," MDC G039, McDonnell Douglas Astronautics Company (1970).
93. Stone, H. L., "Iterative solution of implicit approximations of multi-dimensional partial differential equations," SIAM J. Numer. Anal. 5 (1968) pp. 530-558.

94. Strassen, V., "Gaussian elimination is not optimal," Numer. Math. 13 (1969) pp. 354-356.
95. Tewarson, R. P., "Solution of linear equations with coefficient matrix in band form," BIT 8 (1968) pp. 53-58, H1132, CR9 15,431, MR37 2425.
96. _____, "Computations with sparse matrices," SIAM Rev. 12 (1970) pp. 527-543. (Survey with 65 references.)
97. Thurnau, D., "Algorithm 195. Bandsolve," Comm. ACM 6 (1963) p. 441.
98. Tinney, W. F., Walker, J. W., "Direct solutions of sparse network equations by optimally ordered triangular factorization," Proc. IEEE 55 (1967) pp. 1801-1809.
99. Turing, A. M., "Rounding-off errors in matrix processes," Quart. J. Mech. Appl. Math. 1 (1948) pp. 287-308, H1194.
van der Sluis, A. (See reference 64, this paper)
100. Varah, J. M., "The calculation of the eigenvectors of a general complex matrix by inverse iteration," Math. Comp. 22 (1968) pp. 785-792, H1214.
101. Varga, R. S., Matrix Iterative Analysis, Prentice-Hall, Englewood Cliffs, N. J. (1962), H1226, CR4 4236, MR28 1725.
von Neumann, J. (See reference 69, this paper.)
von Rosenberg, D. V. (See reference 82, this paper.)
102. Wachspress, E. L., Iterative Solution of Elliptic Systems and Applications to the Neutron Diffusion Equations of Reactor Physics, Prentice-Hall, Englewood Cliffs, N. J. (1966).
103. Weaver, W. Jr., Computer Programs for Structural Analysis, Van Nostrand, Princeton, N. J. (1967).
104. Weinstein, H. G., Stone, H. L., Kwan, T. V., "An iterative procedure for the solution of systems of parabolic and elliptic equations in three dimensions," I&EC Fundamentals 8 (1969) pp. 281-287.
105. Westlake, J. R., A Handbook of Numerical Matrix Inversion and Solution of Linear Equations, Wiley, New York (1968), H1296, CR9 14,753, MR36 4794.
106. Widlund, O. B., "On the rate of convergence of an alternating direction implicit method in a non-commutative case," Math. Comp. 20 (1966) pp. 500-515.
107. Wilkinson, J. H., "The evaluation of ill-conditioned polynomials, I, II," Numer. Math. 1 (1959) pp. 150-180, H(NL)1133, MR22 321.

108. Wilkinson, J. H., "Instability of the elimination method of reducing a matrix to tri-diagonal form," Comput. J. 5 (1962) pp. 61-70. H1347, CR3 3337, MR25 747.
109. _____, "Rounding Errors in Algebraic Processes, Prentice-Hall, Englewood Cliffs, N. J. (1963), H1350, CR5 6341, MR28 4661.
110. _____, "The solution of ill-conditioned linear equations," pp. 65-93 in Mathematical Methods for Digital Computers, Volume II, A. Ralston and H. S. Wilf (Eds.) Wiley, New York (1967), H1357, CPA 12,400.
111. _____, "A survey of error analysis of matrix algorithms," Apl. Mat. 13 (1968) pp. 93-102. H1358, MR37 3797.
112. Willoughby, R.A., Sparse Matrix Proceedings, RA-1 IBM Research Center, Yorktown Heights, New York (March 1969). Proc. Symp. on Sparse Matrices and Their Applications, organized and sponsored by the Mathematical Sciences Department (Sept. 1968) MR39 1106.
113. _____, "Some pivot considerations in direct methods for sparse matrices," Proc. Mexico 1971 International IEEE Conf. on Systems, Networks and Computers, Oaxtepec, Mex., Mexico (Jan. 1971).
114. Winograd, S., "A new algorithm for inner-product," IEEE Trans. CT-17 (1968) pp. 693-694.
115. _____, "On the number of multiplications necessary to compute certain functions," Comm. Pure Appl. Math. 23 (1970) pp. 165-179.
116. Zielke, G., "Adjustment of the inverse of a symmetric matrix when two symmetric elements are changed," Comm. ACM 11, (1968) p. 118.
117. _____, "Inversion of modified symmetric matrices," J. Assoc. Comput. Mach. 15 (1968) pp. 402-408, H1421, CR9 15,596.
118. _____, "Variation of the inverse of a symmetric matrix under symmetric variation of rows and columns," Computing 3 (1968) pp. 76-77 (German), H1422.
119. _____, Numerical Computation of Modified Inverse Matrices and Linear Systems of Equations, (German) Friedr. Vieweg and Sohn GmbH, Verlag, Braunschweig, Germany (1970).

Added in proofreading:

120. Ortega, J. M., Rheinboldt, W. C., Iterative Solutions of Nonlinear Equations in Several Variables, Academic Press, New York (1970).
121. Tewarson, R. P., "On the product form of inverse of sparse matrices," SIAM Rev. 8 (1966) pp. 336-342, H1126, CR9 14,306, MR34 8631.

122. Belady, L. A., "A study of replacement algorithms for a virtual storage computer," IBM Systems J. 5 (1966) pp.78-101.
123. Hobbs, L. C. et al. (Eds.), Parallel Processor Systems, Technologies, and Applications, Proceedings of Symposium sponsored by the Office of Naval Research, the Naval Postgraduate School, the Naval Weapons Center, and Hobbs Associates, Inc.; held at the Naval Postgraduate School in Monterey, California, June 25-27, 1969, Spartan Books, New York (1970).
124. Mason, S. J., "Feedback theory - some properties of signal flow graphs," Proc. IRE 41 (1953) pp. 1144-1156.
125. Lipson, J. D., "Symbolic methods for the computer solution of linear equations with applications to flowgraphs," (44 references), pp. 233-300 in [126].
126. Tobey, R. G. (Ed.), Proceedings of the 1968 Summer Institute on Symbolic Mathematical Computation, IBM Boston Programming Center, 545 Technology Square, Cambridge, Massachusetts 02139.
127. Wolfe, P. S., "Error in the solution of linear programming problems," pp. 271-284 in [75, vol.2].
128. Morrell, A. J. H. (Ed.), Information Processing 68, Proceedings IFIP Conference, North-Holland Publishing Company, Amsterdam (1968).
129. Gear, C. W., "The automatic integration of stiff ordinary differential equations," pp. 187-193 in [128].
130. Wilkes, M. V., "The growth of interest in microprogramming: a literature survey," Comput. Surveys 1 (1969) pp. 139-145.
131. Young, D. M., Iterative Solution of Large Linear Systems, Academic Press, New York (1971).

E. EIGENVALUES AND EIGENVECTORS, SPARSE MATRICES

Basic Reference Book:

- R1. Wilkinson, J. H., The Algebraic Eigenvalue Problem, Clarendon Press, Oxford, England (1965), H1355, MR32, 1894.

Basic Bibliographic Sources:*

- R2. Householder, A. S. KWIC Index for Matrices in Numerical Analysis, Vol. 1. Primary Authors A-J; Vol. 2. Primary Authors K-Z, ORNL-4418.
- R3. Householder, A. S., KWIC Index for the Numerical Treatment of Nonlinear Equations. ORNL-4595.

* Available from National Technical Information Service, U. S. Department of Commerce, Springfield, Virginia 22151, Price: \$3.00 per volume, Microfiche \$0.65.

1961

1. Francis, J. G. F., "The QR transformation--a unitary analogue to the LR transformation," I, Comput. J. 4, 265-271, H0250, CR3 2250, MR23 B3143; II, Ibid., 332-345, H0860, CR3 2253, MR25 744.
2. Kublanovskaya, V. K., "On some algorithms for the solution of the complete eigenvalue problem," Z. Vychisl. Mat. i Mat. Fiz. 1, 555-570, translation in U.S.S.R. Comput. Math. and Math. Phys. 1, 637-357, MR24 B2097.

1964

3. Parlett, B. N., "The development and use of methods of LR type," SIAM Rev. 6, 275-294, H0629, CR6 6981, MR30 2669 (Survey)

1966

4. Kahan, W., "Accurate eigenvalues of a symmetric tridiagonal matrix," computer Science Dept., Stanford University, Tech. Report CS41, H0004.
5. Kahan, W., "Then to neglect off-diagonal elements of symmetric tri-diagonal matrices," Ibid, CS42, H0005.
6. Kahan, W., Varah, J. M., "Two working algorithms for the eigenvalues of a symmetric tridiagonal matrix," Ibid. CS43, H0010.

1967

7. Barth, W., Martin, R. S., Wilkinson, J. H., "Handbook Series Linear Algebra. Calculation of the eigenvalues of a symmetric tridiagonal matrix by the method of bisection," Numer. Math. 9, 387-393, 4170, CR9 13 471.
8. Martin, R.S. Wilkinson, J. H., "Handbook Series Linear Algebra. Solution of symmetric and unsymmetric band equations and the calculation of eigenvectors of band matrices," Numer. Math. 9, 273-301, H0355, CR9 12,837.

E. EIGENVALUES AND EIGENVECTORS, SPARSE MATRICES

1967 (continued)

9. Wilkinson, J. H., "Calculation of eigensystems of matrices," pp. 27-62 in Numerical Analysis, an Introduction, J. Walsh, Ed., Thompson Book Co., Washington, D. C., H1356, CR8 12,391 (Survey).

1968

10. Martin, R. S., Reinsch, C., Wilkinson, J. H., "Handbook Series Linear Algebra. Householder's Tridagonalization of a Symmetric Matrix," Numer. Math., 11, 181-195, H0353, CR10 16,601.
11. Martin, R.S., Wilkinson, J. H., "Handbook Series Linear Algebra. Similarity reduction of a general matrix to Hessenberg form," Numer. Math. 12, 349-368, H0357.
12. Martin, R. S. Wilkinson, J. H., "Handbook Series Linear Algebra. The Modified LR Algorithm for Complex Hessenberg Matrices," Numer. Math. 12, 369-376, H0358.
13. Martin, R. S., Wilkinson, J. H., "Handbook Series Linear Algebra. The Implicit QL Algorithm," Numer. Math. 12 377-382, H0359.
14. Parlett, B. N., "Global convergence of the basic QR algorithm on Hessenberg matrices," Math. Comp. 22, 803-818, H0636.
15. Reinsch, C., Bauer, F. L., "Handbook Series Linear Algebra. Rational QR transformation with Newton shift for symmetric tridiagonal matrices," Numer. Math. 11, 264-272, H0779.
16. Schwarz, H. R., "Handbook Series Linear Algebra. Tridiagonalization of a symmetric band matrix," Numer. Math. 12, 231-241, H0927, CR10 17,519.
17. Simpson, A., Tabarook, B., "On Kron's eigenvalue procedure and related methods of frequency analysis," Quart. J. Mech. Appl. Math. 21, 1-39, H0983.
18. Varah, J. M., "The calculation of the eigenvectors of a general complex matrix by inverse iteration," Math. Comp. 22, 785-792. H1214.
19. Wilkinson, J. H., "Almost diagonal matrices with multiple or close eigenvalues," Linear Algebra and Appl. 1, 1-12, H1360, MR37 1386.
20. Wilkinson, J. H., "Global convergence of tridagonal QR algorithm with origin shifts," Linear Algebra and Appl. 1, 409-420, H1361, MR38 2938.
21. Wilkinson, J. H., "Global convergence of QR algorithm," IFIP Congress, Edinburgh, submitted papers, Mathematics, North Holland Publ. Co., Amsterdam, A22-24, H1362.

E. EIGENVALUES AND EIGENVECTORS, SPARSE MATRICES

1969

22. Businger, P. A., "Extremal properties of balanced tridiagonal matrices," Math. Comp. 23, 193-200.
23. Gargantini, I., "On the computation of the eigenvalues of a tridiagonal matrix," Math. Comp. 23, 403-405.
24. Parlett, B. N., Reinsch, C., "Handbook Series Linear Algebra. Balancing a matrix for calculation of eigenvalues and eigenvectors," Numer. Math. 13, 293-304, H0638.
25. Peters, G., Wilkinson, J. H., "Eigenvalues of $Ax = \lambda Bx$ with band symmetric A and B," Comput. J. 12, 398-404, CR11 19,108.
26. Rutishauser, H., "Computational aspects of F. L. Bauer's simultaneous iteration method," Numer. Math. 13, 4-13, H0868.
27. Varah, J. H., "Computing invariant subspaces of a general matrix when the eigenspace is poorly conditioned," University of Wisconsin, Mathematics Research Center, MRC-962, H1216. Also, Math. Comp 24, (1970) 137-150.

1970

28. Eberlein, P. J., "Solution to the complex eigenproblem by a norm reducing Jacobi type method," Numer. Math. 14, 232-245.
29. Faulkner, R. A., "Diagonalization of Hermitian matrices; maximization of speed and accuracy," in Computational Methods in Band Theory, P. M. Marcus, J. F. Janak, A. R. Williams, Eds., Plenum Press, New York.
30. Martin, R. S., Peters, G., Wilkinson, J. H., "Handbook Series Linear Algebra. The QR Algorithm for Real Hessenberg Matrices," Numer. Math. 14, 219-231.
31. Tewarson, R. P., "On the transformation of symmetric sparse matrices to the triple diagonal form," Inter. J. Comput. Math., to appear.

F. COMPUTER ARCHITECTURE, PARALLELISM,
MEMORY HIERARCHY, AND DATA MANAGEMENT

1953

1. Petrie, G. W., III, "Matrix inversion and solution of simultaneous linear algebraic equations with the IBM 604 electronic calculating punch," Nat. Bur. Standards Appl. Math. Ser. 29, 105-110, H0686.

1958

2. Gill, S., "Parallel programming," Comput. J. 1, 2-10.

1960

3. Barron, D. W., Swinnerton-Dyer, H. P. F., "Solution of simultaneous linear equations using a magnetic tape store," Comput. J. 3, 28-33.

1961

4. Heller, J., "Sequencing aspects of multiprogramming," J. Assoc. Comput. Mach. 8, 426-439.
5. Rollett, J. S., Wilkinson, J. H., "An efficient scheme for the codiagonalization of a symmetric matrix with a two-level store," Comput. J. 4, 177-180, H0323, MR23 B2163.
6. Schwartz, E. S., "An automatic sequencing procedure with application to parallel processing," J. Assoc. Comput. Mach. 8, 513-537.

1962

7. Buchholz, W. (Ed.), Planning a Computer System, McGraw-Hill, New York.

F. Computer Architecture, Parallelism,
Memory Hierarchy, and Data Management

1962 (cont'd)

8. Chartres, B. A., "Adaptation of the Jacobi method for a computer with magnetic-tape backing store," Comput. J. 5, 51-60, H0499, CR3 3340, MR25 750.
9. Falkoff, A. D., "Algorithms for parallel search memories," J. Assoc. Comput. Mach. 9, 488-501.
10. Illiffe, J. K., Jodeit, J. G., "A dynamic memory allocation scheme," Comput. J. 5, 200-209.

1963

11. Estrin, G., Bussell, B., Turn, R., Bibb, J., "Parallel processing on a restructurable computer system," IEEE Trans. EC-12, 747-754.
12. Estrin, G., Turn, R., "Automatic assignment of computations in a variable structure computer system," IEEE Trans. EC-12, 755-773.

1964

13. Elmaghraby, S. E., "An algebra for the analysis of generalized activity networks," Management Sci. 10, 494-514.

1965

14. Anderson, J. P., "Program structures for parallel processing," Comm. ACM 8, 786-788.
15. Branin, F. H., Jr., Hall, L. V., Suez, J., Carlitz, R. M., Chen, T. C., "An interpretative program for matrix arithmetic," IBM Systems J. 4, 2-24.

F. Computer Architecture, Parallelism,
Memory Hierarchy, and Data Management

1966

16. Karp, R. M., Miller, R. E., "Properties of a model for parallel computations: Determinacy, termination, queueing," SIAM J. Appl. Math. 14, 1390-1411.
17. Schwartz, J. T., "Large parallel computers," J. Assoc. Comput. Mach. 13, 25-32.

1967

18. Karp, R. M., "Some bounds on the storage requirements of sequential machines and Turing machines," J. Assoc. Comput. Mach. 14, 478-489.
19. Karp, R. M., Miller, R. E., Winograd, S., "The organization of computations for uniform recurrence equations," J. Assoc. Comput. Mach. 14, 563-590.
20. Martin, D., Estrin, G., "Models of computations and systems evaluation of vertex probabilities in graph models of computations," J. Assoc. Comput. Mach. 14, 281-299.
21. Pease, M. C., III, "Matrix inversion using parallel processing," J. Assoc. Comput. Mach. 14, 757-764.
22. Shedler, G. S., "Parallel numerical methods for solution of equations," Comm. ACM 10, 286-290.
23. Shedler, G. S., Lehman, M. M., "Evaluation of redundancy in a parallel algorithm," IBM Systems J. 6, 142-149.
24. Waite, W. M., "Path detection in multidimensional iterative arrays," J. Assoc. Comput. Mach. 14, 300-310.

F. Computer Architecture, Parallelism,
Memory Hierarchy, and Data Management

1968

25. Barnes, G. H., Brown, R. M., Kato, M., Kuck, D. J., Slotnick, D. L., Stokes, R. A., "The ILLIAC IV computer," IEEE Trans. C-17, 746-757.
26. Barron, D. W., Recursive Techniques in Programming, American Elsevier, New York.
27. Gilmore, P. A., "Structuring of parallel algorithms," J. Assoc. Comput. Mach. 15, 176-192.
28. Knuth, D. E., The Art of Programming, Vol. 1, Addison-Wesley, Reading, Mass.
29. Kotov, V. E., Maringani, A. S., "On transformations of sequential programs into asynchronous parallel programs," IFIP Congress, Edinburgh, 437-45.
30. Kuch, D. J., "ILLIAC IV software and application programming," IEEE Trans. C-17, 758-770.
31. Laski, J. G., "Segmentation and virtual address topology--an essay in virtual research," Comput. J. 11, 35-40.
32. Randell, B., Kuehner, J., "Dynamic storage allocation systems," Comm. ACM 11, 297-306.
33. Reiter, R., "Scheduling parallel computations," J. Assoc. Comput. Mach. 15, 590-599.
34. Rosenfeld, J. L., Driscoll, G. C., "Solution of the Dirichlet problem on a simulated parallel processing system," IFIP Congress, Edinburgh, 499-507.
35. Wilkes, M. V., Time-Sharing Computing Systems, Elsevier, New York.

F. Computer Architecture, Parallelism,
Memory Hierarchy, and Data Management

1969

36. Brooks, F. P., Jr., "Mass memory in computer systems," IEEE Trans. MAG-5, 635-639.
37. Chazan, D., Miranker, W. L., "Chaotic relaxation," Linear Algebra and Appl. 2, 199-222.
38. Karp, R. M., Miller, R. E., "Parallel program schemata," J. Comput. System Sci. 3, 147-195.
39. McKellar, A. C., Coffman, E. G., "Organizing matrices and matrix operations for a paged memory system," Comm. ACM 12, 153-165.
40. Naur, P., Randell, B. (Eds.), Software Engineering, Proc. Conf. Garmish, Germany, Scientific Affairs Division, NATO, Brussels 39, Belgium.
41. Pease, M. C., III, "Inversion of matrices by partitioning," J. Assoc. Comput. Mach. 16, 302-314.
42. Rosenfeld, J. L., "A case study in programming for parallel processors," Comm. ACM 12, 645-655.
43. Smith, D. M., "Data logistics for matrix inversion," [112; SMY-15, pp.127-138].

1970

44. Denning, P. J., "Virtual Memory," Comput. Surveys 2 (1970) 155-189 (84 references.)
45. Mattson, R. L. Gecsei, J., Slutz, D. R., Traiger, I. L., "Evaluation techniques for storage hierarchies," IBM Systems J. 9, 78-117.
46. Miranker, W. L., "A survey of parallelism in numerical analysis," SIAM Rev. 12, to appear.

1971

47. Chen, T. C., "Parallelism, pipelining and computer efficiency," Computer Design (Jan. 1971) 69-74.

G. PRESERVING SPARSENESS

1953

1. Kron, G., 'A set of principles to interconnect the solutions of physical systems," J. Appl. Phys. 24, 965-980, H0105.

1955

2. Kron, G., "Solving highly complex elastic structures in easy stages," J. Appl. Mech. 22, 235-244.
3. Kron, G., "Tearing and interconnecting as a form of transformation," Quart. Appl. Math. 13, 147-159.

1956

4. Branin, F. H., Jr., "Kron's method of tearing and its applications," Proc. Second Midwest Symp. Circuit Theory, Michigan State Univ.

1959

5. Branin, F. H., Jr., "The relation between Kron's method and the classical methods of network analysis," IRE WESCON Convention Record, Part 2, 1-29.
6. Harary, F., "A graph theoretic method for the complete reduction of a matrix with a view towards finding its eigenvalues," J. Math. and Phys. 38, 104-111.
7. Roth, J. P., "An application of algebraic topology: Kron's method of tearing," Quart. Appl. Math. 17, 1-24, H0840.

1960

8. Parter, S., "On the eigenvalues and eigenvectors of a class of matrices," SIAM J. Appl. Math. 8, 376-388, H0640.

1961

9. Parter, S., "The use of linear graphs in Gauss elimination," SIAM Rev. 3, 119-130, H0642, CR3 1792, MR26 908.

1962

10. Dulmage, A. L., Mendelsohn, N. S., "On the inversion of sparse matrices," Math. Comp. 16, 494-496, H0655, CR5 5718, MR27 6375.

G. PRESERVING SPARSENESS

1962 (continued)

11. Harary, F., "A graph theoretic approach to matrix inversion by partitioning," Numer. Math. 4, 128-135, H1036, CR4 4436.
12. Steward, D. V., "On an approach to techniques for the analysis of the structure of large systems of equations," SIAM Rev. 4, 321-342, H1047, CR4 4253, MR26 3121

1963

13. Carpentier, J., "Ordered elimination: a procedure reducing the number of operations in the solution of linear equations," Proc. Congress of Computing and Information Processing, Toulouse, France, pp. 63-71.
14. Sato, N., Tinney, W. F., "Techniques for exploiting the sparsity of the network admittance matrix," IEEE Trans. PAS-82, 944-950.

1965

15. Alway, G. G., Martin, D. W., "An algorithm for reducing the bandwidth of a matrix of symmetric configuration," Comput. J. 8, 264-272, CR7 10,098.
16. Dickson, J. C., "Finding permutation operations to produce a large triangular submatrix," National Meeting, Operations Research Society of America, Houston, Texas.
17. Edelmann, H., "Optimal strategies for the direct solution of systems of linear equations with sparse coefficient matrices," Z. Angew. Math. Mech. 45, T13-T18, (German), MR34 3766.
18. Mayoh, B. H., "A graph technique for inverting certain matrices," Math. Comp. 19, 644-646, H0373, CR7 9366, MR33 5108.
19. Spillers, W. R., "On diakoptics: Tearing an arbitrary system," Quart. Appl. Math. 23, 188-190, H1027, MR38 1818.
20. Steward, D. V., "Partitioning and tearing systems of equations," J. Soc. Indust. Appl. Math. Ser. B Numer. Anal. 2, 345-365, H1048, CR7 10,120, MR36 2307.

1966

21. Carre, B. A., "The partitioning of network equations for block iteration," Comput. J. 9, 84-96, H0479, CR7 10,910, MR33 3445.
22. Edelmann, H., "Ordered triangular factorization of matrices," Proc. Power System Computation Conf., Stockholm, Sweden.

G. PRESERVING SPARSENESS

1966 (continued)

23. Branin, F. H., Jr., "The algebraic-topological basis for network analogies and the vector calculus," Generalized Networks, 453-491, Microwave Research Institute Symposium Series, Brooklyn Polytechnic Press 16.
24. Bershdorfer, A. M., Paab, A. R., Sturman, G. M., "On the efficient inversion of large structured matrices," Proc. Engineering Mechanics Division ASCE Specialty Conference, Washington D. C.
25. Liebl, P., Sedlacek, J., "Transformation of square matrices into quasi triangular form by means of graph theory," Apl. Mat. 11, 1-9, (German)
26. Minty, G. J., "On the axiomatic foundations of the theories of directed linear graphs, electrical networks and network-programming," J. Math. Mech. 15, 485-520.
27. Yaspan, A., "On finding a maximal assignment," Operations Res. 14, 646-651.

1967

28. Bryant, P. R., "Graph theory applied to electrical networks," Graph Theory and Theoretical Physics (F. Harary, Ed.), Academic Press, New York, 111-138.
29. Dulmage, Al. L., Mendelsohn, N. S., "Graphs and matrices," Graph Theory and Theoretical Physics (F. Harary, Ed.), Academic Press, New York, 167-227.
30. Nathan, A., Even, R. K., "The inversion of sparse matrices by a strategy derived from their graphs," Comput. J. 10, 190-194, H0498, CR9 13,474, MR35 5128.
31. Tewarson, R. P., "On the product form of inverses of sparse matrices and graph theory," SIAM Rev. 9, 91-99, H1127, MR36 1092.
32. Tewarson, R. P., "Row column permutation of sparse matrices," Comput. J. 10, 300-305, H1130, CR9 14,307, MR36 1091.
33. Tewarson, R. P., "Solution of a system of simultaneous linear equations with a sparse coefficient matrix by elimination methods," BIT 7, 226-239, H1129, CR9 13,863, MR36 2308.
34. Tinney, W. F., Walker, J. W., "Direct solutions of sparse network equations by optimally ordered triangular factorization," Proc. IEEE 55, 1801-1809, H1158.

G. PRESERVING SPARSENESS

1968

35. Akyuz, F. A., Utku, S., "An automatic relabeling scheme for bandwidth minimization of stiffness matrices," AIAA J. 6, 728-730.
36. Edelmann, H., "Measures to reduce the amount of computation in analyzing large electrical networks," Electronic Rechenanlagen 10, 118-123 (German).
37. Eufinger, J., Jaeger, A., Wenke, K., "An algorithm for the partitioning of a large system of sparse linear equations using graph theoretical methods," I, Operations Research-Verfahren 6, 118-123.
38. Rosen, R., "Matrix bandwidth minimization," ACM National Conf., Las Vegas, Nevada.
39. Spillers, W. R., Hickerson, N., "Optimal elimination for sparse symmetric systems as a graph problem," Quart. Appl. Math. 26, 425-432, H1028.
40. Tewarson, R. P., "On the orthonormalization of sparse vectors," Computing 3, 268-279, H1133, CR10 17,521.
41. Tewarson, R. P., "The Crout reduction for sparse matrices," Comput. J. 12, 158-159, H1135.

1969

42. Cuthill, E., McKee, J., "Reducing the bandwidth of sparse symmetric matrices," ACM National Meeting, 157-172.

1970

43. Brayton, R., Gustavson, F., Willoughby, R., "Some results on sparse matrices," Math. Comp., 24, 937-954.
44. Rose, D. J., "Symmetric elimination on sparse positive definite systems and the potential flow network problem," Ph.D. Thesis, Mathematics Department, Harvard.
45. Rose, D. J., "Triangulated graphs and the elimination process," J. Math. Anal. Appl., 32, 597-609.

1971

46. Hachtel, G. D., Brayton, R. K., Gustavson, F. G., "The sparse tableau approach to network analysis and design," IEEE Trans. CT-18, 101-113 (Special Issue on Computer Aided Circuit Design).

QUESTIONS AND COMMENTS FOLLOWING WILLOUGHBY'S PAPER

QUESTION: How big a problem can GMSO handle?

WILLOUGHBY: The biggest problem we've handled so far was 1,024 by 1,024. After clever generation, not of the long code but of the sparseness structure for the triangular factors (re: Albert Chang), the solution for the 1,024 by 1,024 for the factorization and back substitutions on the IBM model 9J required .75 seconds. However, it took four minutes to get the program to do it in .75 second, so if you're only going to do it once you have to say four plus minutes. That time can be greatly reduced by clever ordering. Typically we're used to working with several hundred very sophisticated equations and not masses of very simple equations. You could go up to about 1000 or beyond if you used Chang's approach because then all you do is generate the code as you go.

QUESTION: With regard to the future of hardware in handling structural problems, I notice that you did not mention any of the possibilities of micro-programming where the programmer might be able to construct a computer image to handle his kind of problem. Are you envisioning anything like this?

WILLOUGHBY: It is certainly feasible to do that but whether or not it is accepted to do that is something I cannot comment on. It's certainly feasible--technologically. Economically and legally I don't know the answer to that and I cannot comment further.

QUESTION: Is IBM interested in going to parallelism in arithmetic units such as Iliac has or is that a question I shouldn't ask?

WILLOUGHBY: Parallelism is a poor word to use; I prefer to use multi-processing. The word parallelism, unfortunately, means one thing being split up into many things; but it should also include many things being split up into many things as, for example, when you are solving a great big problem, a little dinky problem, and everything else in between. The word parallelism is a very dangerous word. We want to understand, in structural engineering, for example, what are the avoidable bottlenecks in present speed of computation, i. e., getting things in and out. The trouble with parallelism is that you've got a thousand adders all working but where are you going to get all the stuff to keep all those adders busy all the time.

QUESTION: Have you dealt with the problems of band reduction or packing of data and unpacking of data, eliminate zeroes and so forth?

WILLOUGHBY: No, but I believe that McCormack is going to comment on that when he gives his paper later this week.

QUESTION: You mentioned the work of Kron. I wanted to ask your opinion on his work and do you think it's worth further pursuit?

WILLOUGHBY: This (the use of electrical engineering techniques for structural problems) is something which has been thoroughly explored (by G. Kron and later by Fenves and F. Banin).

QUESTION: Through representation of matrices in the sparsely populated form, there are two main advantages to be gained. Number one is the storage. You can compress very large sparse matrices in to little space. The other advantage is the speed. Since you are eliminating all the zeroes from the computation, your iteration time or cycle time decreases con-

siderably. Could you give us a comment on the relative importance of the two factors. If you are using, for example, a purely iterative scheme like Gauss-Siedel, maybe it takes longer, but then you never fill up your matrix. Whereas if you are using any of the techniques you mentioned, you start filling it up and you never know really how much it is going to fill until it's too late.

WILLOUGHBY: You made a very good comment and I'll try to answer the statement about the tradeoff. You know with certainty how much work you have to do per iteration step. In Gauss-Siedel, for example, you don't fill anything in. There is a whole spectrum of iterative methods. First, we have what is called the point relaxation where you just solve each individual equation for the diagonal element and then update the solution either as you go along or all at the end. This approach has been then elevated to methods called alternating direction in which each basic step is something that looks like a triadiagonal matrix which you can solve very fast. This is a little closer to solving the equation, but again you know exactly how much work is involved. There is also work from partial differential equations which is called multi-line iteration where you simultaneously solve information on several lines which again is closer to direct methods. So, there is a whole transition here and the tradeoff is very simple. As you get closer to direct methods, the number of iterations that you have to make through the process to get the answer decreases, but you get uncertainty as to how much storage is required and how many operations per iteration you'd have to do. At the other end of the spectrum is simple relaxation for which the number of times you have to iterate kills you. To estimate how many iterations are required, you have to have ways

of analytically estimating the rate at which the error vector is decreased. This is called the eigenvalue estimation problem. In a recent work by Stone, the author goes kind of whole hog on a new approach which he's used in petroleum problems including coupled nonlinear systems. It works but the eigenvalue analysis is very difficult. The results of studies on model problems were that it was competitive with the very best routines. It didn't degrade with nonuniformity, irregular boundaries and all the things that practical problems are prone to. The iterative approach is definitely a possibility and if you could guarantee that the rate of iteration is good enough, then I'll take it every time; but you'd have to guarantee it to me.

QUESTION: I'd like to make just a brief comment on the business of looking at these problem solutions and their economic effects. We find in engineering application, especially in large scale problems, that the time required to generate the inputs, the time required to form the equations, to form the matrix, has now become a very considerable part of both the engineering man labor and the machine time in setting up equations to be solved. Have there been studies in the combination of preprocessor and simultaneous solution during the process?

WILLOUGHBY: Yes, that has been studied and is being studied very heavily at the present time.

QUESTION: I'd like to understand how you make decisions in the way of setting this (GNSO) up as to which elements are zero and which are not. I found, for example, that if I have to make that decision I might as well multiply. It takes about the same time.

WILLOUGHBY: Where the zeros and nonzeros occur doesn't depend on what the numerical values are for the nonzeros. The SOLVE code is generated by GNSO for a whole class of matrices with the same sparseness structure and can be used repeatedly.

COMMENT: The reason I am asking this question is because I have in mind a dynamics problem in structural analysis. Now if this procedure of eliminating multiplication by zero is a general one which could be applied to such things, we could realize big savings. It would probably require a very significant effort, however, to generate something like that for a general structural problem.

WILLOUGHBY: I know what you're saying, but I don't know the answer since I do not know in detail what computations are involved in structural analysis. You have many degrees of freedom at each node and in each branch and the mechanization of all that in this context is not obvious. I think there will be a lot of work involved. If someone was willing to do it and did have this context of solving the same problem repeatedly with the same structure, there may be a very nice payoff. This is especially true if J , the Jacobian, is known to have this positive definiteness, diagonal dominance or something where you know ahead of time that you don't have to pivot for size. I don't know that you're going to realize much saving because some of your structural engineering problems are two and three dimensional and no matter how clever you order things, the matrices do fill in. Extensions of band matrix techniques by Bamford, Jennings, McCormick and others are probably more suitable than the GNSO approach for many multi-dimensional structural problems.

THE DEVELOPMENT OF LARGE SCALE DIGITAL COMPUTER CODES FOR PRODUCTION STRUCTURAL ANALYSIS

D. N. Yates*
T. J. Vinson**
W. W. Sable***

Missile Systems Division, Lockheed Missile and Space Company

All too often computer codes, particularly in the finite element domain, are constructed by the researcher and professional programmer without sufficient cognizance being taken of the requirements of those individuals who would use the code as a production analysis tool. In addition to the fundamental requirement of accuracy of results, there are certain features that must be embodied in every computer code that is to be effectively and efficiently used for daily analysis problems.

This paper discusses input, output, and engineering details that should be incorporated into each code as it is written and the work performed within the Missile Systems Division of Lockheed to develop such capabilities. A range of data input techniques, including automatic mesh generation, data card, and FORTRAN statement should be provided as standard features; while a variety of output features such as pictorial and graphical playback of the model, deflected shapes, and stresses, along with a number of output formats are considered mandatory in order that a given program's potential be fully exploited and engineering errors minimized. The program should be constructed in a modular fashion to enable the user to quickly adjust and update the program functions and capabilities to suit the needs of particular analysis problems. Engineering realities such as large displacement and elastic-plastic options should be incorporated wherever possible to extend the problem solving range of a given code.

Finally, the development of a number of highly automated programs demonstrating the above features is presented, and research being currently pursued summarized.

* Group Engineer, Vehicle Shell Systems/Loads, Structures & Dynamics

** Stress Engineer, Vehicle Shell Systems/ Loads, Structures & Dynamics

*** Structures Engineer, Vehicle Shell Systems/Loads, Structures & Dynamics

SECTION I INTRODUCTION

The interest of the writers in the development of large scale advanced digital computer codes stems from the nature of our duties at Lockheed. Our department is responsible for the structural integrity of all products of the Missile Systems Division of the company; a range of products that encompasses the Polaris and Poseidon FBM systems in addition to advanced concepts such as ULMS, SCAD, and various other classified programs. Our interests include: ballistic missile structures, reentry systems, motors, ground support equipment, and flight control systems. As an adjunct to such activities, we are also called upon to perform special studies for other Lockheed companies and to analyze various other components of weapons systems such as launcher concepts, submarine structures, and propulsion systems. Finally, we have of late found our field of interest being radically widened by the application of our programs to the analysis of structures outside of Lockheed's traditional aerospace market by means of technology contracts with other companies.

The nature of our work, together with its demands that we be fully responsive in terms of rapid results to complex problems, led us, in 1965, to start development of a series of highly user-oriented computer codes with primary emphasis being placed on accuracy of results, speed of input/output, program flexibility and modularity, ease of program extension and update, and adequate program size to cope with all potential problem demands. This commitment to advanced techniques - a commitment which is being continually expanded and accelerated - initially led to an investigation of available programs and their applicability to our problems. We were fortunate in that Lockheed's Solid Mechanics Laboratory at Palo Alto had developed a strong capability in the area of finite difference techniques for shell structures and this led to our obtaining codes such as BOSOR 1 developed by Bushnell⁽¹⁾. Subsequent cooperation with the Solid Mechanics group led to the development and acquisition of more advanced codes such as BOSOR 2⁽²⁾ and 3⁽³⁾ generated by Bushnell for shells of revolution, STAGS developed by Almroth and Brogan⁽⁴⁾ for collapse analysis of shell structures subjected to generalized loadings, and the STAR code developed by Sobel, Silsby and Wrenn⁽⁵⁾ for transient response analysis of shells of revolution. This range of programs has given us excellent capability in the area of finite difference analyses of shell structures, and these programs have proven their worth during the course of the past six years when applied to a series of engineering problems.

In the domain of finite element analysis - an area where our interest is very high - we gained our initial capability, as have so many people in the aerospace industry, by obtaining the program written by Wilson⁽⁶⁾ for the analysis of axisymmetric solids. We were fortunate in having Prof. Wilson located close by at Berkeley and in developing an active association with him which still continues. Other programs initially obtained included the SABOR shell series developed at M.I.T.^(7,8), the Rohm and Haas axisymmetric code⁽⁹⁾, the FRAN⁽¹⁰⁾ and STRESS⁽¹¹⁾ frame codes, and a frame program written by

Whetstone⁽¹²⁾. Our requirements in the area of mixed structures, by which nomenclature we define an assemblage of links, beams, membranes, plates, and solids, next demanded that we obtain and develop a range of programs designed for this class of problems. This need led, in 1966, to a contract with Prof. Kamel of the University of Arizona to develop the MINI-ASKA code⁽¹³⁾. This association has proved of great value and is, happily, still active today. Other advanced mixed structures codes subsequently obtained were the REXBAT series developed by Loden⁽¹⁴⁾ and the SNAP series developed by Whetstone⁽¹⁵⁾. These codes have also been successfully used in the course of our projects. Finally, a series of codes were developed or obtained to perform the analysis of such specialized problems as creep buckling, nose tip analyses, and orthotropic properties determination.

In essence, therefore, we have found it most advantageous to mainly obtain our basic codes from university and research sources based on active association and cooperation with such sources, and direct our own major research and development activity to the extension of such programs to a highly automated production status. It is to the discussion of these extensions, and the techniques employed therein, that this paper primarily addresses itself.

We note that during the course of our research and development we encountered a large number of programs which were found to possess little utility and potential. Our reasons for such conclusions are fully discussed later in this paper when we outline our requirements which any of our codes must fulfill in order to qualify as a production tool. Assuming that such programs had to be discarded, we concentrated our research efforts on the remaining range of basic programs and attempted to bring these to a highly automated, reliable, and usable form. This particular area of computerized structural analysis has all too often been neglected, but it is here that we have found that the large scale program has the greatest benefit and impact. Our basic equipment to achieve this end has been three Univac 1108 computers, a range of smaller computers such as the SDS 910, and - as a major factor - a Stromberg-Carlson 4020 electronic plotter.

With this basic, and expensive, equipment came a set of responsibilities which our group had to develop in order to efficiently exploit its full potential. These may be summarized as:

- o A strong background in the theory and application of finite element and other numerical techniques.
- o Wide experience with a program, its limitations, and its advantages.
- o A high degree of knowledge and skill regarding the computer system in use and its limitations.
- o An excellent level of programming and modeling ability and experience.
- o An ability to rapidly generate or incorporate new elements, techniques, or program modifications.
- o An expertise in computer graphics and plotter programming techniques.

- o An ability to equate mathematical techniques to engineering realities.
- o The capability and duty to always generate hand or approximate solutions to check complex mathematical models.

Such responsibilities as these are as often neglected by the program user as are the later set of responsibilities cited with respect to the basic program writer. All too often engineers use an advanced program with no knowledge of its limitations, accepting its answers on faith rather than fact, and probably having had it solve the wrong problem in the first place. With respect to this final point, we believe that it is imperative that a pictorial playback of the computer model input be provided to eliminate such errors and, additionally, that as much output as possible be provided in a visual format with a minimum of data reduction. Computer run times rapidly fade into insignificance if three weeks are required each side of the run for input data preparation and output reduction and assimilation, even making the tenuous assumption that errors can be rapidly detected and corrected without pictorial displays of the model.

The impact of the highly automated computer codes on the engineering organization and operation of a company are substantial. At Lockheed the traditional concept of designers and structural analysts as separate entities, each functioning in a narrow field of interest, has largely disappeared. If the computer and its high speed plotter can rapidly and accurately both draw and analyze a structure there is little point to the designer drawing the structure and then transmitting it to the structural engineer for analysis. In this regard, it is noted that the SCH020 plot speed is approximately 0.3 seconds/plot with good resolution. In similar fashion, by coupling programs, thermo-structural analyses can be performed as a single step rather than as individual thermal and structural analyses. Similar changes have occurred in the area of coupling dynamic response and structural analysis.

Finally, a major change has occurred in the manner in which a proposal or preliminary design is generated and analyzed. Now a wide range of structural concepts can be rapidly drawn, analyzed, and documented within the narrow time constraints imposed by a customer, rather than only analyzing perhaps two, or at best several, design concepts. Without the ability to input and pictorially playback a model in a matter of hours, analyze that structure within minutes, providing pictorial and graphical output shortly thereafter, and at the same time yielding accurate answers, a program cannot claim to be a production tool for structural engineers. Of course, many structures are far too complex to ever achieve this goal but, all too often, programmers or engineers are at fault for not striving to attain such a nirvana. Our group at Lockheed has set itself such a goal since 1965 and we will present results to date after first discussing overall program requirements as we view them, a short study of analysis costs and output demands, the need for modularity, and our present program capabilities within the Missile Systems Division of Lockheed. Finally, we conclude with a summary of our present research in the area of advanced computer programs.

SECTION II

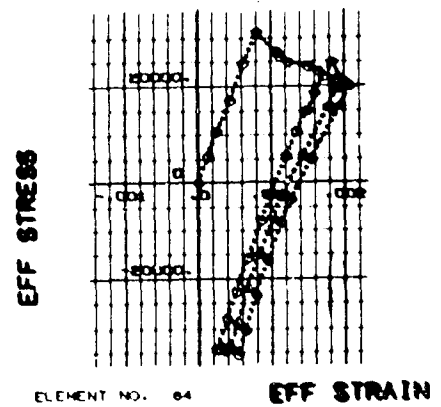
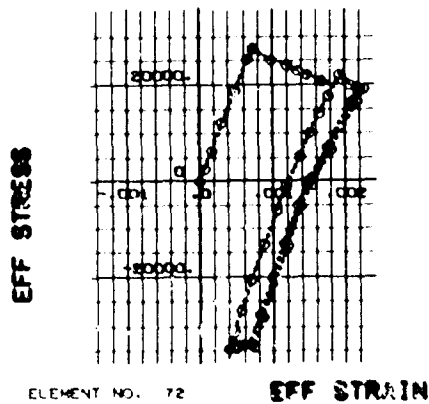
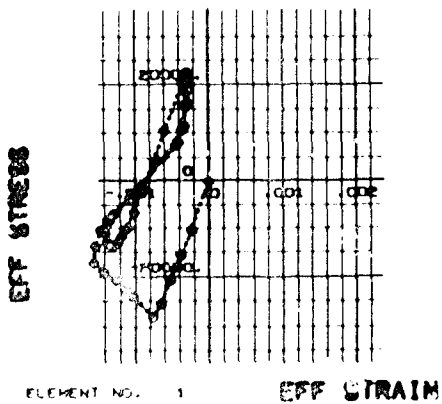
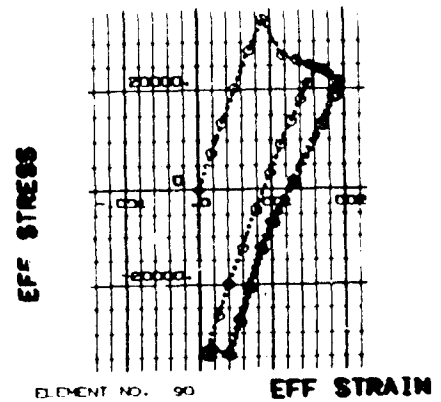
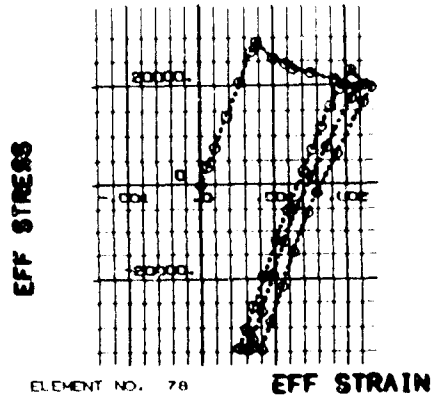
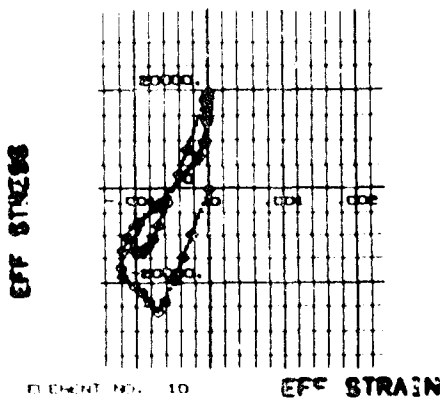
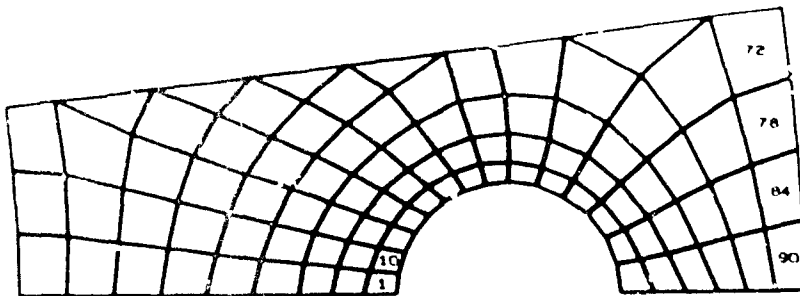
OVERALL PROGRAM REQUIREMENTS

Aerospace structural analysis places heavy demands on large scale digital computer programs. We are faced with complicated structures subjected to unusual and severe environments with the added constraint that weight must be minimized. To verify the structural integrity of a missile component, and the degree to which it approaches an optimum, proper account must be taken of plastic deformation, geometric nonlinearities, stability, thermal loadings, fatigue, and, quite frequently, rather strange material properties. Historically, designers do not produce concepts on the basis of our stress analysis capability; rather, a designer must utilize the most advanced materials and techniques available to him, consistent with cost and manufacturing constraints. It is therefore the responsibility of structural engineers to develop analysis tools of the level of sophistication required to provide adequate support and guidance to the design organizations in this operational context.

Our philosophy toward incorporating a new method of analysis is quite simple; if it affords an improvement over current methods, we must use it. However, we cannot always afford to wait for such improvements, but must employ existing analytical tools. Hence, a bilinear elastic solution is perfectly acceptable in the absence of a sophisticated non-linear Prandtl-Reuss technique. And we will, in general, prefer a highly reliable approximation to an unstable "exact" solution. A lack of theoretical nicety cannot cause us to refuse to undertake an analysis. We must find a legitimate approach to a given problem and employ it, for design schedules cannot wait on long-term research.

Spacecraft and missile structures are often designed on the basis of ultimate strength, that is; the ability to sustain load past some permanent deformation criteria to actual failure of part. Since few materials exhibit linear stress-strain curves to failure, an adequate analysis of a yielding structure should include some approximation for changing stiffness and load distribution. Iterative and incremental approaches are used currently in the Wilson and MINI-ASKA codes, respectively. Incipient or existing yield conditions are detected according to some criterion, such as Von Mises, Maximum Shear Stress, or Maximum Strain, and areas designated as critical cause alteration or reformulation of the stiffness matrix. A recent contract for the analysis of thermal fatigue led to the development of a step solution accounting for element yielding, thermal degradation of material properties, and shifting of the yield surface. The results of this approach have been extremely encouraging and the program is to be described in detail in a forthcoming paper. This problem, illustrated in Figure 1 makes obvious the necessity of graphical output when one considers that a complete strain history of every element must be maintained throughout several thermal loading cycles for each of 1200 elements. We are not aware of the existence of a working truly nonlinear analysis providing improved accuracy over this technique without great cost in capacity and reliability.

FIGURE 1: STRESS-STRAIN HISTORY OF SIX FINITE
ELEMENTS OF AN AIRCRAFT DISC BRAKE COMPONENT.
1/22 SYMMETRICAL SLICE SHOWN, LOADING WAS
THERMAL TIME HISTORY FOR ONE BRAKING CYCLE



An incremental solution is a basic adjunct of any finite element program. Structures exhibiting geometric, as well as material, nonlinearities are not uncommon in missile components; for example: glass motors, pressure vessels, and movable nozzles. A single pass linear solution based on small deflection theory is simply unsatisfactory in the analysis of a geodesic or tori-spherical head, since some deflections actually reverse as the load increases. The C3 Poseidon motor dome model, for example, yielded a stable solution only when initial load steps were cut to one-sixteenth of operating pressure. Another example is threaded or flanged joints in which contact surfaces and bearing points change during load application. Sophisticated finite difference programs have come to us for shell-type analysis; but nozzles, bolted joints, threaded joints, etc., require the geometric generality afforded as yet only by finite element programs. To meet this requirement we have, therefore, developed a special one-layer element which is introduced between such flanged joints. This element is totally incapable of resisting tension or compression until this strain reaches 1.0, at which point its compressive motion is stopped and flange faces, now bearing, accept load.

Stability analysis is still very much the province of finite difference methods, although we are currently pushing research in the finite element domain also. We feel that capability for shell stability analysis here at Lockheed is very high. Extensive use of programs by Bushnell (1,2,3) and Almroth and Brogan (4) of the Palo Alto group during the Poseidon program has shown that large-scale finite difference programs are now beyond the research tool stage and that they can be of great benefit in practical production analyses. Examples of results of such programs compared with actual test results are presented in Table 1. The STAGS program has provided us, for the first time, with a viable method for stability analysis of a geometry reproducing an actual production item, i.e., an assemblage of rings, stiffeners, doors, and cutouts held together by pieces of tin, whereas in the past, such structures have received the misnomer of 'Shells' and the misfortune of being analyzed as such. Both BOSOR 3 and STAGS are relatively new and are now undergoing the only reliable checkout procedure -- extensive use. It is anticipated that these codes will be widely employed, with associated production-oriented development, during subsequent Lockheed contracts, although present usage is inestimably aided by close working association with the authors.

Exotic materials abound in aerospace work. Glass-wound motors, carbon fiber wrapped pressure vessels, plywood nose-fairings, honeycomb support structure, nearly incompressible propellants, and high anisotropic reentry vehicle nose tips continually challenge the analyst to provide constitutive relations having a reasonable relationship with reality. Flexibility in this area is extremely valuable. Shell programs normally contain a set of subroutines for several standard wall constructions, while our three-dimensional solids programs (13)(16) have been upgraded since their acquisition to include orthotropic materials for standard applications such as reentry vehicles and pressure vessel or heat exchanger tubesheets.

Perhaps it would seem at this point that we expect each computer program we receive to be quite broad in scope. Certainly, a tool capable of solving all our structural problems would be appreciated, but we are not so naive as to expect a structural researcher to examine all aspects of all possible applications

of his program prior to its release. Still we labor under the somewhat tenuous assumption that structural research has structural application as its end, and this calls for certain concessions on the part of the programmer, usually at very small cost. A useful production program must be flexible and a requirement for continual dependence on the author for slight changes ensures that a given code will rapidly fall into disuse.

The experience of our group has been that many programs have to be discarded because they have been generated without a sufficient degree of awareness of user requirements and, in too many cases, possessing so many limitations in terms of accuracy, usability, and applicability as to render them virtually useless for a practical range of engineering problems. Examples of such limitations are:

- c Programs which sacrifice usability for speed of solution by, for example, imposing narrow allowable band widths.
We have to solve general structures, not tall slender towers, and such narrow banding techniques are anachronistic at best and unacceptable at worst.
- o Programs with incorrect or outdated elements.
Too often we find that many finite element analyses are useless because of this.
- o Programs which prove impossible to understand, modify, or update.
Such techniques may provide job security in the short term, but ensure a rapidly obsolete program in the longer term.
- o Programs which do not completely solve the problem.
For a stress analysis program to give forces and moments for 2000 elements rather than stresses is not acceptable.
- o Programs with very inefficient storage and assembly and solution techniques.
Our problems are large and must be solved rapidly and efficiently.
- o Programs requiring a large and inflexible data input scheme.
If structures are mathematically describable then FORTRAN should be used as input.
- o Programs where the user has no warning of any numerical problems being encountered in solution.
There is no point in inverting an ill-conditioned or singular stiffness matrix.
- o Programs which cannot be highly automated.
We cannot afford the time or errors inherent in hand checking the large quantities of printed output inherent in most finite element analysis programs.

- o Programs which give incorrect answers.

This happens all too often, and perhaps derives from pressures to publish or, to take an unkind view, lack of care.

Attention to such details will increasingly determine the appreciation and, still more important, the amount of support that research groups receive from industry sources.

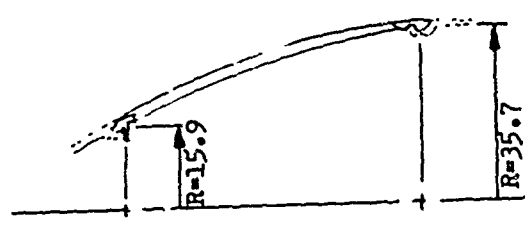
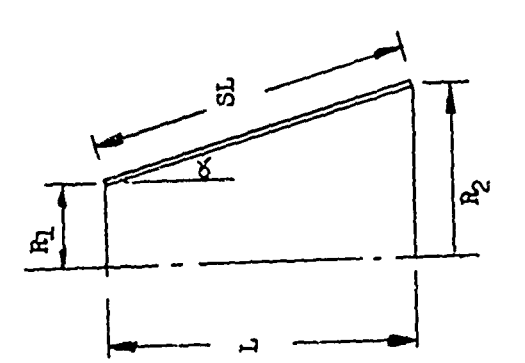
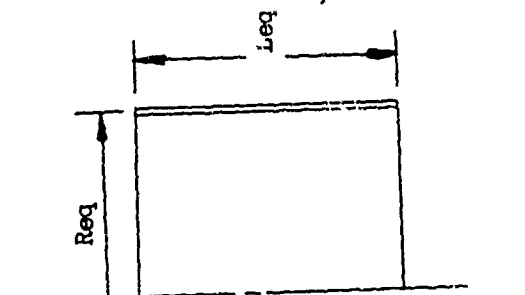
All these topics, of course, ultimately bear directly on user confidence. The time always arrives, in any industry that produces a real product, when someone must put a signature on a drawing certifying the product's adequacy. Three alternatives are available to a person in such a position of responsibility concerning the use of advanced programs: he can refuse such tools, he can use (or misuse) them in ignorance, or he can use them with a reasonable amount of confidence and knowledge. All three positions are currently taken by practicing structural analysis, but, in our opinion, only the third is acceptable.

The ultimate condition, intimate knowledge of a given computer code, is seldom if ever, achieved. Hence, the importance of user confidence and understanding cannot be over emphasized. Ideally, the following items should accompany a digital code intended for use by someone other than the author:

- o A reasonable set of non-trivial test cases -- preferably compared with test results.
- o A thorough user's manual explaining, in at least a rudimentary fashion, the manner in which data input is used, and output interpreted.
- o Documentation of sufficient depth to allow the user to conveniently increase his knowledge of basic program functions.
- o Checks included in the code to indicate the occurrence of numerical errors.
- o Some kind of accuracy check, for example: equilibrium, energy, or iterative techniques.

These few features largely relieve the danger of misapplication of large scale digital computer codes.

TABLE 1 ACCURACY OF COMPUTERIZED ANALYSIS AND TEST COMPARISONS FOR A NOSE FAIRING

	OGIVE FAIRING		CONE APPROXIMATION		"EQUIVALENT" CYLINDER		ANALYSIS ERROR
							
FAIRING FORWARD JOINT FOR HOIST CAPABILITY							
FAIRING SHELL BURST PRESSURE CAPABILITY							
FAIRING SHELL EXTERNAL CRUSHING PRESSURE CAPABILITY							
A) COMPUTER							
B) EQUIVALENT CYLINDER							

Materials are orthotropic and moisture content dependent being a plywood and aluminum laminate composite structure.

SECTION III

A DISCUSSION OF THE SINGLE LARGE PROGRAM APPROACH

In common with many other groups performing computerized structural analysis on a wide scale, we are often concerned with assessing the merits of employing a single ultra-large scale program to solve all varieties of structural problems. Generally, we are wary of such an approach for its cumbersome and inflexible nature, at least with respect to the responsibilities of our group. Specifically, we are concerned because experience has shown that we are forced to constantly modify, update, and expand our own general purpose programs to meet the demands of a particular analysis problem, to enhance a program's capabilities and to incorporate numerous improvements made possible by revised computer software routines. Without this in-house capability, we would not be able to undertake many of the advanced analyses that we do, because on so many occasions a program has to be radically modified or extended to meet the demands of a new class of problem. For example, although we started with a single MINI-ASKA general purpose program, we now have a range of special purpose MINI-ASKA's in addition to our standardized program. Such special programs include: an orthotropic solids version, a large displacement and plasticity version, and a completely double precision version. These versions were able to be rapidly created due to two reasons; the first being the modular fashion in which the program was written, and the second being that our engineers are intimately familiar with every subroutine and its function.

This second reason raises another philosophical point regarding the use of large scale computer programs which has been much debated in structural analysis and other engineering circles. Obviously, we oppose the contention that the engineers employing a program are not required to know the structure, theory, and programming techniques used in that program. We do not believe that a person's engineering responsibilities cease, or are, in some mysterious metaphysical fashion, transferred to a computer program when he inputs the data cards as instructed. Already, too many companies are hiring excellent young engineers, giving them a set of data instructions without those engineers having any comprehension of what they are doing or why. Sadly, it is often the case that the program being used in such a fashion is either outmoded or inefficient and the very people who could contribute to its updating, expansion, or replacement are sitting like automatons with their brains turning to concrete.

Hence, we have concluded general purpose codes are excellent if they are designed for comprehension, modification, and updating by the user, but will become rapidly obsolete or mistrusted otherwise. We believe that in any group performing advanced analyses a library of special purpose and general purpose programs is required, that rivalry between competing programs will drive advanced development faster, and that the inefficient or inaccurate code will be rapidly discarded. The spectre of "duplication of effort" is often raised in this regard, but managers, engineers, and researchers do not generally tolerate true

duplication for long, nor does much that is labeled 'duplication' actually prove to be so under closer examination. Thus, we welcome advanced research, advanced techniques, and advanced programs and will seek to use them if they prove of benefit, and drop them if they do not.

SECTION IV

ANALYSIS COST SUMMARY

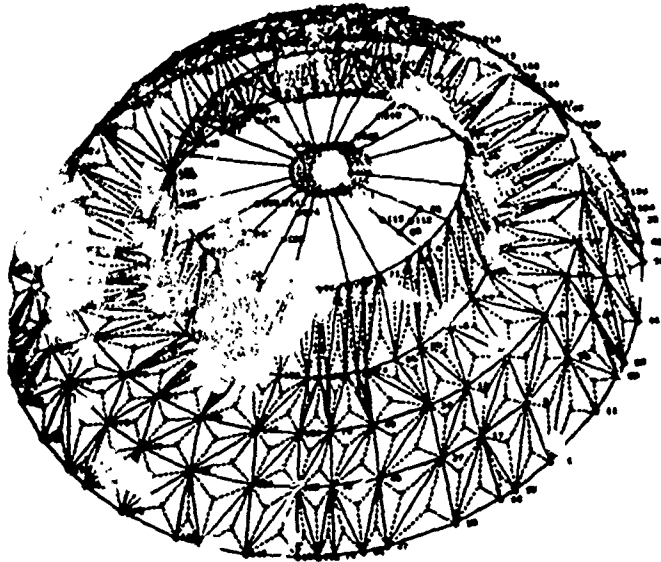
In order to establish areas where development effort should be placed, it is first necessary to determine where potentially the greatest savings can accrue.

Too often a great deal of time and money is expended to reduce the program run time to its theoretical minimum; admittedly a challenging aesthetic exercise, however, in practice, often resulting in loss of program generality or flexibility. This is not to say that we are disinterested in speed or that our programs are slow, but merely that speed of computation is only one factor in building up a successful computer capability, and that the primary goals must always be accuracy of results and rapid input-output. Studies have shown that computation accounts for only 10-15% of the total analysis time and costs. On a recent technology contract, for example, computer costs were only \$1200 of a total cost of \$17,000. Unless the computer program is quite highly inefficient initially, small savings in run time come only after large development expenditures and, given a limited development budget, alternative approaches to raising overall efficiency generally yield a more substantial return.

Data input and checkout requires the greatest expenditure of time and money on most jobs. Although slightly dependent on the program complexity, typically 50% or more of the total analysis time and dollars is spent generating and checking the input data and performing necessary programming modifications. Data reduction, evaluation, and presentation requires a further 35 to 40% of the total analysis time and costs. Hence, automatic mesh generation features, enhanced graphical I/O, and other options should obviously be developed; however it appears that little research work is presently being done to reduce these two cost areas which account for 80-90% of the total expenditures for most tasks. Our own efforts in these areas are described in the following sections.

SECTION V

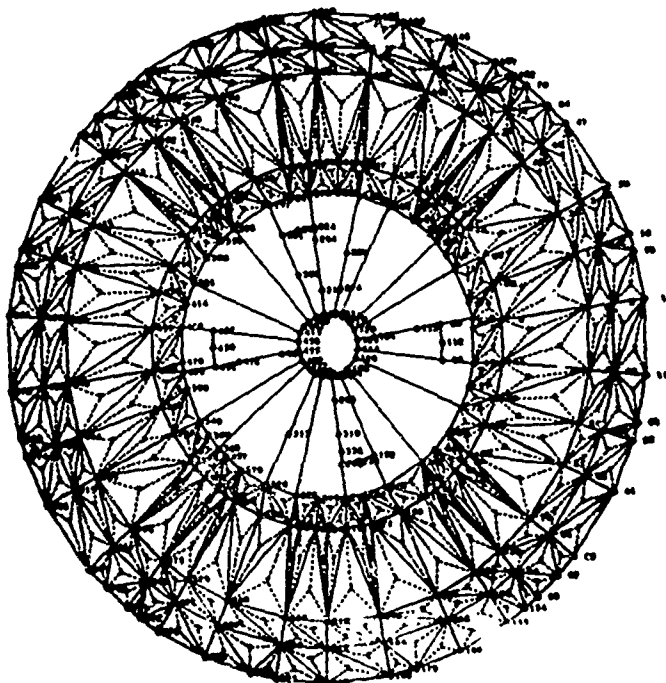
PROGRAM INPUT REQUIREMENTS



As stated above, preparation of the required input data along with initial necessary program modifications account for approximately 50% of the total analysis time and cost. Figures 2 and 3 are computer plots of actual analysis problems that are offered to illustrate the structure complexities often encountered.

The optimum method data generation is yet to be discovered which will allow efficient modeling of the most general structures. Until this method is developed, we believe that every computer program should make available a range of data input options. Options presently incorporated into our large scale programs are as follows:

- o Data card input
- o FORTRAN statement
- o I-J mesh generation
- o Combinations of the above



Data card input is used when the structure is irregular and must be described point by point and element by element. Input using data cards is quite time consuming in that each parameter must be calculated by the analyst, written on a coding form, and then keypunched. Errors are, of course, possible using this method, while the computer operator has been known to drop a box of cards at the crucial point in the analysis. However, on highly complex and irregular structures, it is the only reliable input method currently available. Figure 2 shows an example of a structure that was analyzed using data card input. Input consisted of five boxes (1800 cards/box) of data cards. This structure also illustrates why we contend that banded solutions are often unacceptable, for this model has an average semi-bandwidth of 540 D.O.F. with a maximum of 1000 D.O.F.

FIGURE 2: COMPLEX TORI-CONICAL STRUCTURE
COMPOSED OF BEAMS, PLATES, AND MEMBRANES

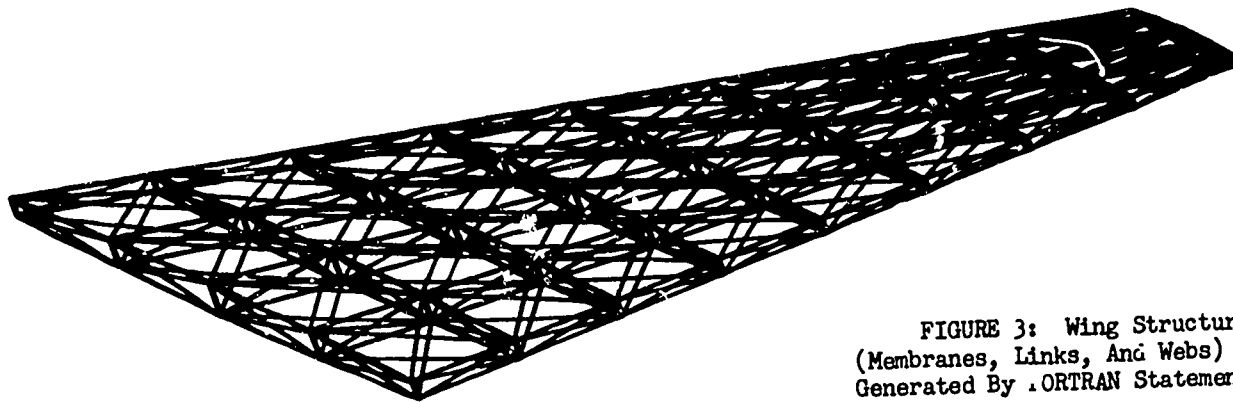


FIGURE 3: Wing Structure
(Membranes, Links, And Webs)
Generated By FORTRAN Statements

FORTTRAN statement input is a method highly favored by our group, whereby the analyst constructs a FORTRAN driving routine to generate the input data and to direct the analysis. Figure 3 is an example of a wing structure modeled using a FORTRAN driving routine constructed by the analyst and requiring no data cards at all. Coordinate calculations, meshing, and loading were totally performed by the computer; hence little room for error exists. The disadvantage of this method is that the analyst must know basic FORTRAN (a handicap seldom encountered any longer) and it is only applicable to structures that are mathematically formulatable or regular. We note that to change aspect ratio, sweepback, or dihedral of this wing structure requires the substitution of a single card. The driving routine required 40 cards whereas a data card deck would require approximately 700.

I-J mesh generation is a technique whereby element connectivity is simplified to a rectangular grid work which is then conformally mapped into the actual shape of the structure with all internal nodal points being automatically computed and assigned. Figure 4 shows an example of such a model that was generated with only 10 data cards and no additional FORTRAN statements, while Figure 5 demonstrates the application of this technique to a solid motor case analysis.

In contrast, the motor nozzle shown in Figure 11 was one of our first finite element analyses problems in which all nodal points were calculated and input by data cards, a process which took three weeks and many heartaches. Today such a problem is input in approximately 4-6 hours with far less chance of error.

Any useful production finite element program should have all of the above features as input options. Additional subroutines should be included for recurring shapes and meshes and much work remains to be done to further simplify data input. For example, the I-J mesh generation feature is presently only applied to two dimensional problems and such conformal mapping technique applied to three dimensional shapes would appear to have merit in simplifying the data input required for 3-D mixed structures.

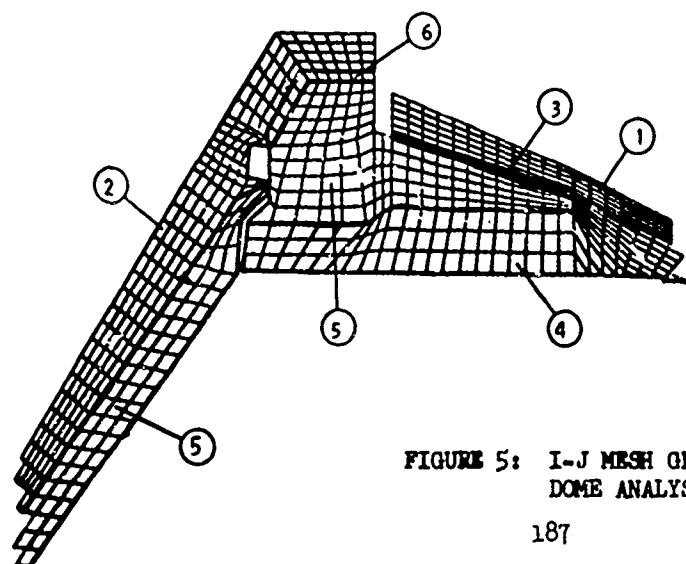
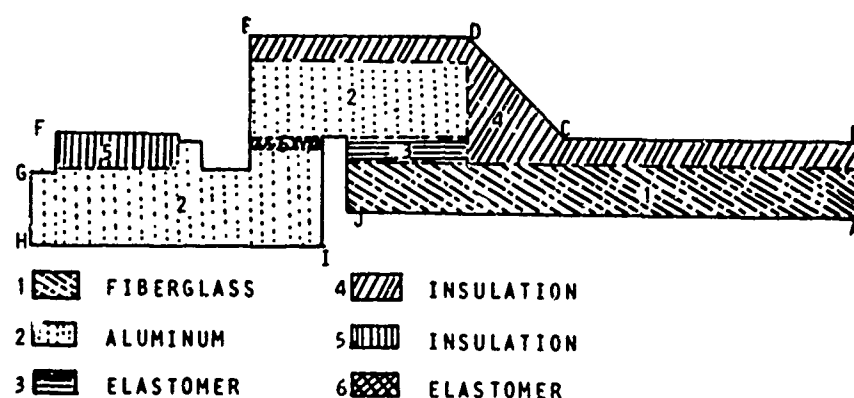
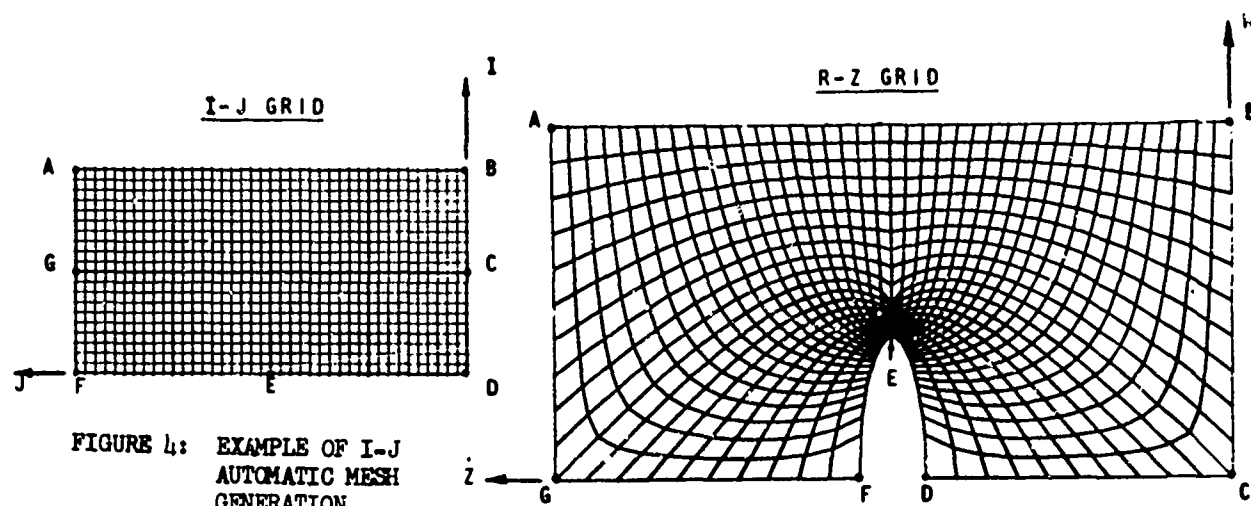


FIGURE 5: I-J MESH GENERATION FOR MOTOR CHAMBER DOME ANALYSIS

SECTION VI

PROGRAM OUTPUT REQUIREMENTS

Information from a finite element analysis can be expanded or compressed to build as high a stack of printed output as desired. Reduction, evaluation, and presentation of the typical output stack typically requires 35 to 40% of the total analysis time and budget. In this area there are basically three requirements that must be met before the program can be considered useful. The program must rapidly playback in both printed and, more importantly, pictorial format the model as input by the analyst. Output must include print-out and graphical displays of stress and deflection quantities in the format and reference system chosen by the analyst. Finally, it is necessary that accuracy checks and diagnostics be printed out as the solution process proceeds to warn the analyst of possible impending numerical disaster.

Figure 6 shows an example of an error in input geometry that could easily go undetected if only a cursory check of input geometry were to be made, while Figure 7 repeats the model with the error removed. Such errors would be well hidden if only a coordinate table were to be printed out. Even if the error was detected by examining the output list the time required could well run into days. Worse yet, the error could go undetected and incorrect conclusions made regarding the validity of results.

The time required for reduction and evaluation of output quantities such as deflections, stresses, and strains has been greatly reduced in the Lockheed MSD organization through extensive use of the SC4020 electronic plotter. Deflected figures of the loaded model, such as that shown in Figure 8, provide a rapid check on the validity of the analysis and identify potential problem areas. Figure 9 represents use of the plotter for displaying the stresses along any line within the structure. Not only does this provide the analyst with useful stress information, but additionally is quite helpful for reporting and presentation purposes. Contours of stresses, strains, or any other quantity, as demonstrated in Figure 10, significantly aid rapid data reduction of all quantities of interest to a degree where little additional hand effort is required. Hence, output data reduction requirements, which are normally quite time consuming and error prone, can be minimized by the extensive application of advanced graphical and pictorial output techniques.

Finally, to be useful and reliable as a analysis tool, a program must also provide, as a fundamental part of its output, accuracy checks and diagnostics at the critical steps of the solution process. We have encountered cases where the stiffness matrix became singular during decomposition due to accumulation of roundoff and truncation errors, but where the program continued through the complete solution process without printing a single diagnostic or warning message. Such errors are not always detected through examination of the stress and deflection output, but naturally the solution is invalid. There are numerous other checks that should be included; however, on the basis of the aforementioned examples, the necessity for this form of output over what is classically provided appears obvious.

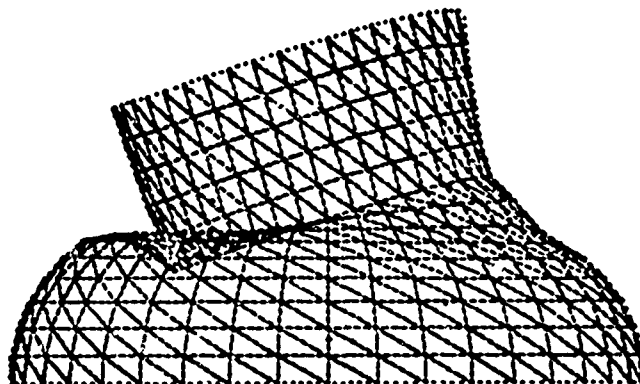


FIGURE 8: DEFLECTED SHAPE OF
COMPUTER MODEL OF PRESSURE
VESSEL DOME

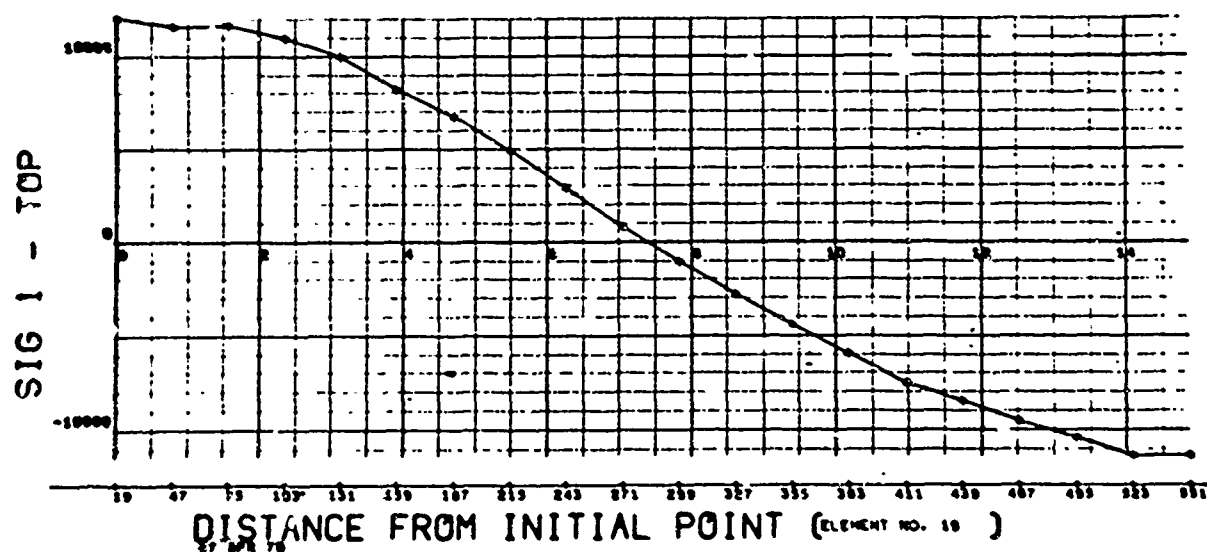
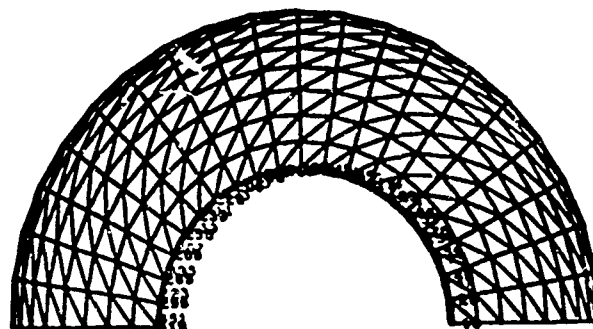


FIGURE 9: STRESSES IN ELEMENTS
ADJACENT TO INTERSECTION REGION
OF PRESSURE VESSEL DOME

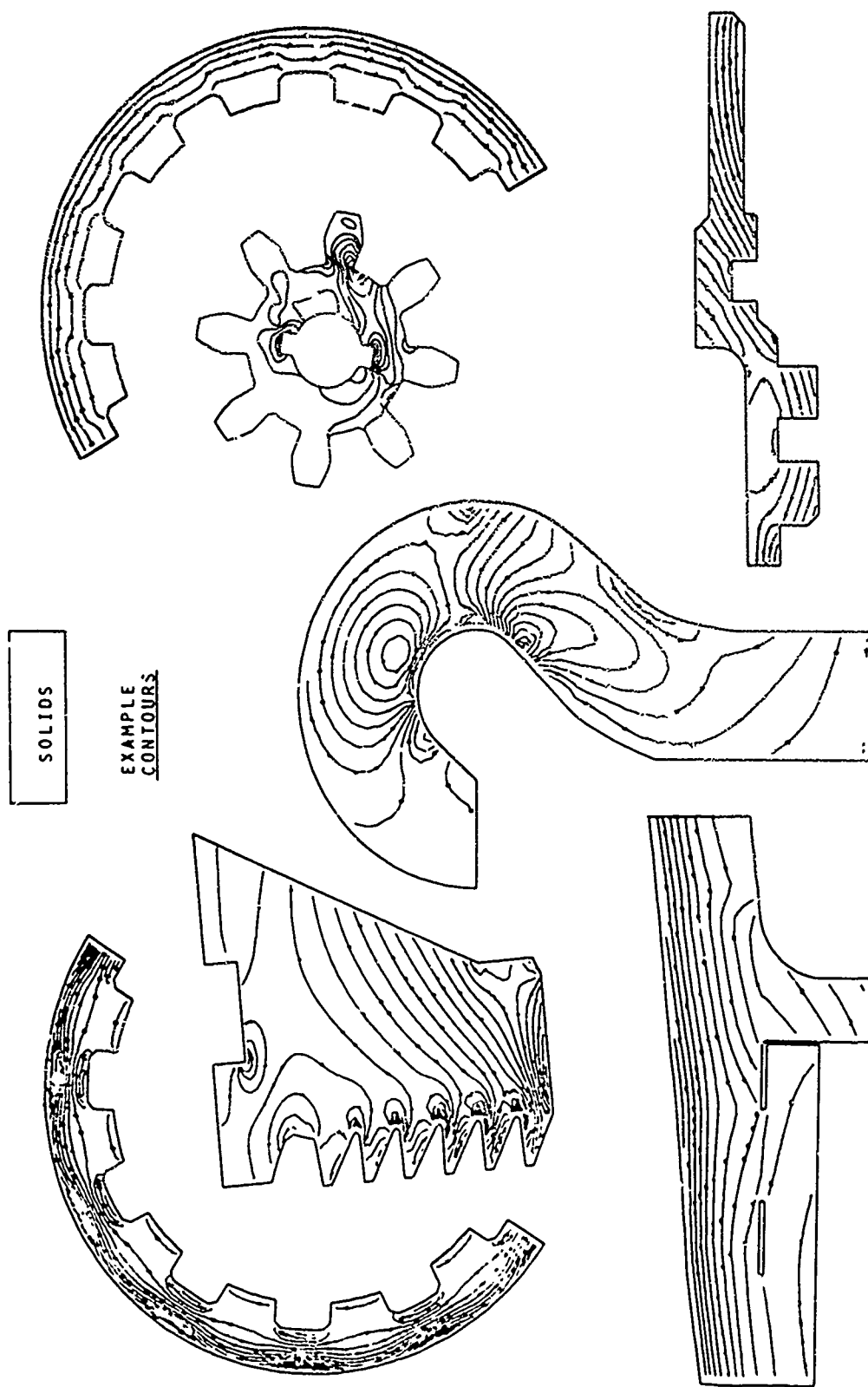


FIGURE 10: EXAMPLES OF CONTOUR STRESS GRAPHICAL OUTPUT

SECTION VII

MODULARITY REQUIREMENTS

Rapid response to unusual design situations is required for a stress analysis group to efficiently perform its function of ensuring that only reliable designs go into production or into a proposal. The alternative of waiting an indefinite period for proper analytical methods to be developed is simply not available; current resources in the form of existing analytical techniques and personnel background must therefore be employed immediately. Preliminary design and proposal efforts, increasingly important in aerospace companies, are governed by a general rule: if it can't be done in a very short time, it can't be done at all (at least on a computer).

Digital computer codes must, then, be of very broad capability, or in a form conducive to rapid alteration by the analyst. We emphasize that the analyst should be in a position to alter in a reasonable time any facet of the program within his knowledge, since program authors or programmers with intimate knowledge of the subject code are not generally available on short notice, if at all, for extensive effort devoted to the solution of a specific analysis problem. The high frequency with which projects are encountered requiring program modification has led us to place an extremely high premium on program modularity.

Three very recent examples of short-notice alterations to program functions serve to illustrate typical analysis problems requiring maximum program flexibility and modularity together with an intimate user knowledge of program content and structure.

- o Analysis of a geodesic fiberglass motor dome, modeled on a linear two-dimensional program, showed very poor results, deflections in some areas showing the wrong sign. Coding was introduced to allow a step solution, thereby accounting for the geometrically nonlinear behavior of the dome.
- o Supplementary equations of equilibrium were included in the analysis of an oil tanker web frame to prevent the buildup of reactions at displacement boundary condition points.
- o An alternate method of specifying constitutive relations for fiberglass motors was supplied to prevent numerical problems caused by theoretically predicted high Poisson's ratios.

Schedules demanded that each of these new facilities function correctly within two days. The first and third of the previous examples were completed properly because the program employed⁽⁶⁾ has been at Lockheed for several years, and many members of our group are extremely familiar with its organization. The second example was accomplished in the required time only because of the modular organizational scheme of Dr. Kamel's program, MINI-ASIA⁽¹³⁾.

Modularity, in the Missile Systems Division of Lockheed Missiles & Space Company, means that any specific function performed with some degree of repetition is separated into a distinct subroutine with conscious effort on the part of the programmer to make the routine's function obvious. A user may then impose a new program procedure without fear of generating coding problems in other areas. Separation of mass secondary storage access routines, for example, allows simple adoption of new software routines. Of still greater importance, however, is the fact that someone other than the author may keep a program from becoming obsolete by incorporating new elements, solution methods, and facilities as they become available.

SECTION VIII

PROGRAM CAPABILITY REQUIRED FOR PRODUCTION ANALYSIS

Presented here is a brief summary of our general capabilities to indicate what we feel to be the breadth required for large scale production structural analysis. The following four paragraphs outline our present capabilities in each of four main areas: solids and plane stress structures, mixed structures, stability critical structures, and specialized general structures.

Solids and Plane Stress Structures

Programs are available with up to 15,000 unknowns and 5,000 elements for the rapid solution of both axisymmetric and arbitrary solids.

Element types available:

- CS & LS Triangles
- CS & LS Quadrilaterals
- Tetrahedrons
- Higher Order Solids

Special Features:

- Low Cycle Thermal Fatigue
- Incremental Loading
- Non-Linear Analysis
- Displacement Restraints
- Thermal Gradients
- Orthotropic and Layered Structures
- Non-Symmetric Loadings
- Stress Outputs
- Extensive Graphical and Pictorial Output Display Options
- Linear and Rotational Acceleration Loads
- Mixed Materials
- Plane Stress and Strain Options
- Highly Automated Mesh Generation

Mixed Structures

Programs employing rapid solution techniques while permitting up to 18,000 degrees of freedom are available for the solution of general structures.

Element types available:

- Links
- Beams
- Triangular CS & LS Membranes
- Triangular Plates (including Thermal Gradients)
- Quadrilateral Membranes
- Quadrilateral Plates
- Tetrahedrons
- Higher Order Solids

Specialized General Structures

The following programs were developed to solve unique forms of structures:

- | | |
|--------|---|
| Bencyl | - Stability of orthotropic core and cushion supported shells |
| Alan | - Creep buckling of cones and cylinders (thick shells) under longitudinal loads |
| Creep | - Cylindrical shells with non-symmetrical temperature and axial load |
| Fancap | - Fully automatic nose cap analysis program |
| Star | - Elastic-plastic dynamic response and dynamic collapse of cylinders subjected to time-varying non-symmetric pressure and axial loads |

Shell Buckling

Several programs are operational permitting the rapid solution of virtually any axisymmetric shells.

Permitted shell properties:

Orthotropic & Isotropic
Cutouts & Holes
Discrete Rings
Discrete Stringers
Multi-Layered
Core Supported
Non-Uniform Thickness

Special Features:

Solution by finite difference and numerical integration
Dynamic and thermal buckling
Thermal effects and gradients
Large deflection effects
Plasticity effects
Extensive plot and graphical output options
Arbitrary meridional or circumferential loadings

SECTION IX

DEVELOPMENT OF LARGE SCALE HIGHLY-AUTOMATED PRODUCTION PROGRAMS

When received from an independent programmer, computer programs are seldom ready for the production analysis tasks that daily occur. We have described earlier the general requirements that every production code should fulfill and our interest in the development of some highly automated extensions to such basic codes. To illustrate this process, historical development sketches of two programs, one for analysis of axisymmetric solids and one for the analysis of general mixed structures, are now summarized.

Axisymmetric Solids Program

This section devotes itself to a brief historical account of our development of Dr. Wilson's axisymmetric solid of revolution program⁽⁶⁾ since 1965 when we received it. This was the first finite element program that we received and was rapidly brought to a production status. It is a tribute to the utility and flexibility of this program, however, that it is still undergoing very active development here at Lockheed today, although in vastly different form to the original version.

Figure 11 shows the first analysis project attempted using the Wilson program. A 5:1 scale layout was made and the nodal points and mesh were superimposed by hand since no mesh generation features were available. Program input consisted of over 2000 data cards and output consisted of its usual listed tables of element stresses and strains and nodal deflections. The program utilized a constant stress quadrilateral element, and had capability for thermal and mechanical loads. Solution was linear elastic with provision for an iterative plasticity solution using a bilinear stress strain relationship. The time required for modeling and input was three weeks and this span emphasized clearly that, as received, the program could not be used for production jobs requiring a speedy analytical response. The utility and power of the program and its finite element techniques, however, was obvious in that it gave us a greatly extended analytical capability.

A number of test cases were next constructed and run to determine program element pitfalls and limitations. The results of cantilever beam test cases (a standard test case employed) were extremely poor due to solution roundoff and truncation errors. A version which assembled and solved in double precision corrected the errors and excellent results were then obtained. Additional test cases were run substantiating the decision that, for certain classes of problems, it is necessary that the program use double precision variables. A series of investigations were also made concerning element aspect ratios which resulted in allowable limits being set. This point is often neglected and can lead to disastrous results which may be believed by the user.

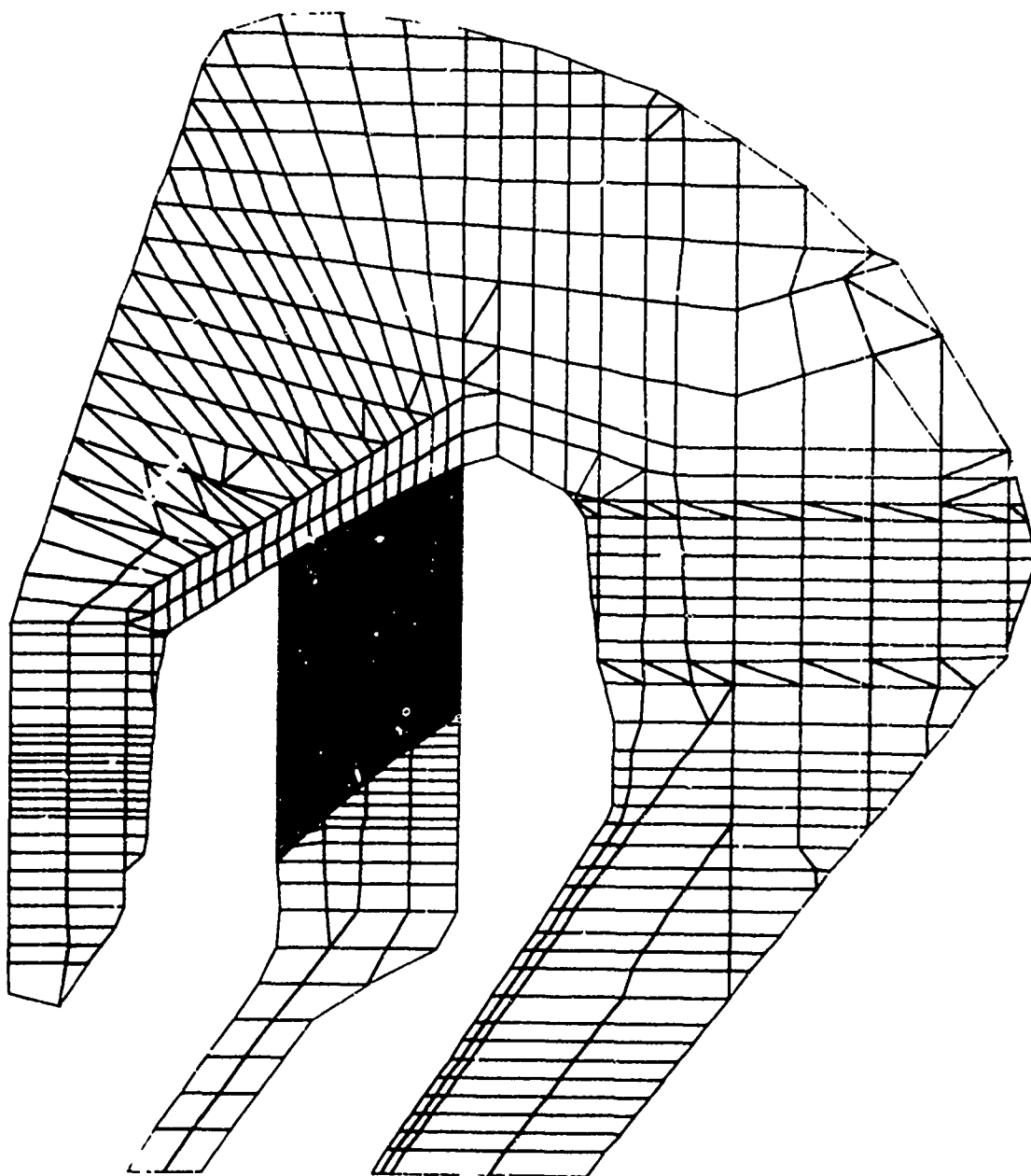


FIGURE 11: FINITE ELEMENT MESH CONSTRUCTED ENTIRELY BY PROGRAMMER AND REQUIRING OVER 2,000 DATA CARDS TO INPUT MESH AND GEOMETRY

Next the I-J mesh generation feature was added, resulting in an order of magnitude decrease in input time and costs. For example, the model shown in Figure 11 could now be input in 4 - 6 hours rather than the original 3 weeks. Figure 4 demonstrates this approach where, in this example, the coordinates of 862 nodal points and the connectivity of 800 elements was generated using an input of 7 data cards. At the same time an early graphics package was developed and added so that the nodal geometry and element meshes were automatically plotted, using the SCH020 electronic plotter. The results of these first extensions were that data input error was greatly reduced and the required time and cost of input was cut to less than 10% of previous needs.

Additional pictorial output features were then added so that the deflected geometry of the model, as well as contour lines of constant stress, strains, and other quantities were available to the analyst as optional program output. Examples of such output techniques are shown in Figure 12. Data reduction time was substantially decreased at the expense of only a second of computer run time by the use of these options.

A new version of his basic program which allowed full orthotropic material properties was then received from Dr. Wilson and incorporated into our program library after all of the above modifications had been made. This new version became our basic axisymmetric solids program.

To minimize still further the effort involved in reporting analysis results the pictorial format shown on the following page in Figure 13 was developed and incorporated. The SCH020 output is thereby entered directly to a report, and a large amount of data quickly and neatly presented.

An advanced Zienkiewicz-Irons type numerically integrated isoparametric linear strain quadrilateral membrane element was subsequently incorporated into all program versions. Figure 14 demonstrates the increase in accuracy over the previous constant strain quadrilateral elements while a further bonus was realized in the form of a reduction in run-time of 20%. In addition to these basic changes and the incorporation of advanced input/output techniques, a continual development program was optimizing the codes for the 1108 system and ensuring that full advantage was being taken of software changes.

Next, a new code was required to analyze an aircraft brake disc subjected to extreme thermal loading cycles that could result in low cycle thermal fatigue cracks. The Prandtl-Reuss equations for incremental plastic flow were incorporated and an incremental solution for each cycle using the tangent modulus approach obtained. In this code material properties are input as a function of temperature and calculations are made considering the strain history and element temperature for each increment of loading. Present programming requires that the material be isotropic and linear strain hardening. This program version was developed to accomplish a specific task; however, it has greatly enhanced our analytical capabilities in the general field of low cycle thermal fatigue. Figure 1 which was discussed earlier, demonstrates the application of this code. Figure 15 demonstrates the finite element model, the thermal input, and the isostress contours for an analysis step within the cycle summarized in Figure 1.

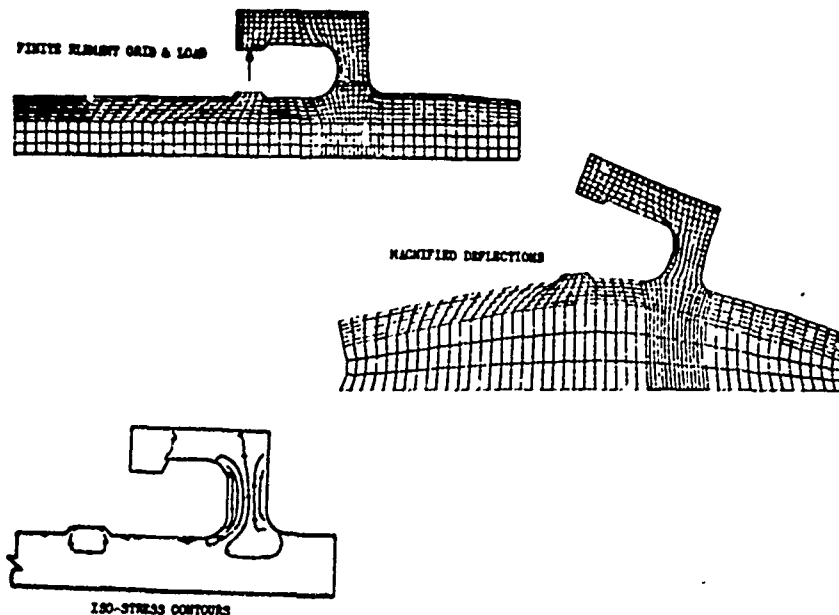


FIGURE 12: FINITE ELEMENT MODEL, DEFLECTED SHAPE, AND ISO-STRESS CONTOURS FOR A MISSILE COMPONENT

A number of examples follow of problems where this basic program and its derivatives has been successfully applied. Figure 16 represents the forward motor dome of a solid propellant motor. Analysis was made to determine propellant to insulation stresses when the motor was subjected to ignition pressures and loads. The model consists of 1302 elements and 1160 nodal points and is constructed of 17 different materials, ranging from highly orthotropic to nearly incompressible, and possessing a series of widely disparate stiffnesses. Initial runs were made using a single precision version of the program. During decomposition, truncation and roundoff errors occurred to such a degree that negative numbers appeared on the main diagonal of the stiffness matrix, producing the interesting, though disconcerting, result that a load on a nodal point was reacted by a deflection in the opposite direction. By using a double precision version of the program, we were able to obtain reasonable results; however, output reduction to check equilibrium of the external forces and internal reactions disclosed the solution still in error. Printout of the stress-strain transformation matrices of the orthotropic case material disclosed the error in the basic code. The program was rerun, and a force balance now indicated equilibrium to be within 0.25%. The solution was stable and the results considered successful.

Another analysis problem recently solved using this program is the motor skirt to case bond region. The two different loading conditions run were internal pressure and axial loading of the skirt. It was found that the pressure analysis could not be solved by linear theory (the motor shape changes having a large influence on the final stress distribution) and the final solution involved, in addition to many minor problems, modifying the program to apply the loads incrementally with the model geometry being updated at each step. This technique permitted the formulation of a valid monotonically convergent solution to the

PREPARED	UNIVAC 1130	DATE	05 NOV 69	LOCKHEED MISSILES & SPACE COMPANY AERONAUTICAL DIVISION OF LOCKHEED AIRCRAFT CORPORATION	PAGE
CHECKED	T. CHINN	TITLE TAP 01700 50 BETA LIMIT LOADS			MODEL
APPROVED	R. D. TETER				REPORT NO.

CASE NO. 3 MATERIAL SET 1

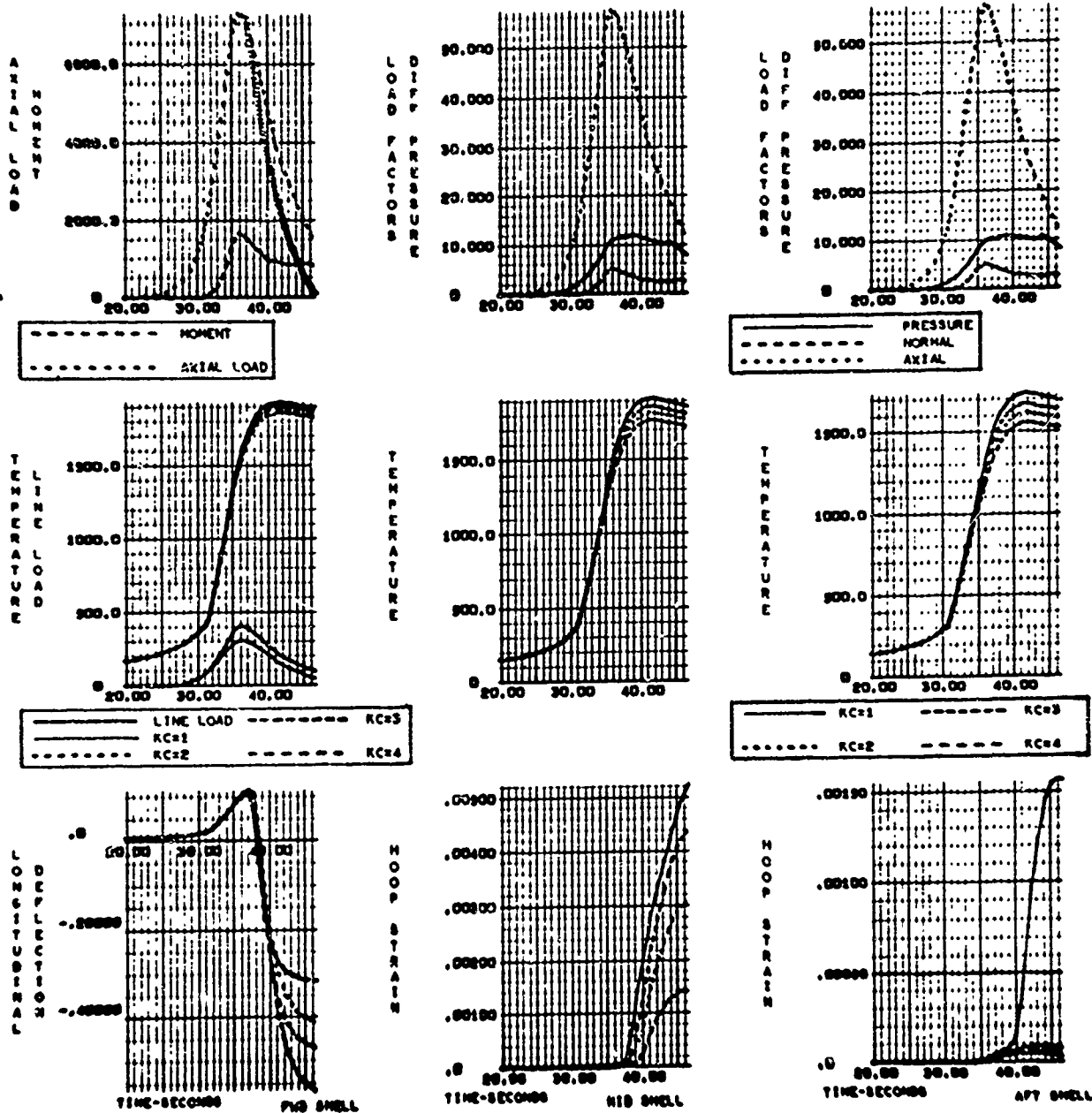
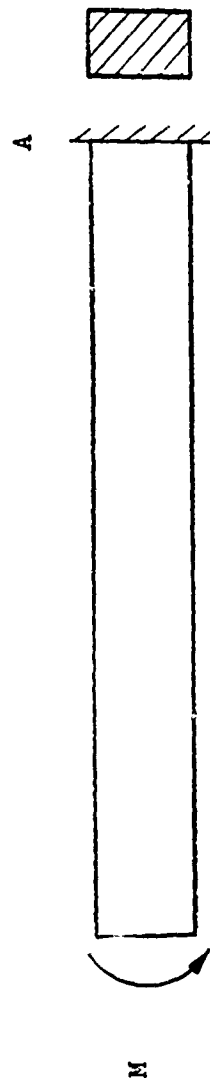


FIGURE 13: COMPUTER GENERATED GRAPHICAL OUTPUT IN REPORT FORMAT

FIGURE 14: COMPARISON OF LINEAR STRESS WITH CONSTANT STRESS QUADRILATERAL MEMBRANE ELEMENTS



TEST CASE	THEO. MC I	MC/I AND ERROR AT POINT 'A'									
		LSQ		LSQ		CSQ		CSQ		M.	
		SINGLE	PREC.	DBL.	PREC.	SINGLE	PREC.	DBL.	PREC.	DBL.	PREC.
		MC/I	ERROR	MC/I	ERROR	MC/I	ERROR	MC/I	ERROR	MC/I	ERROR
5 ELEM. THRU THICKNESS 22" LONG - 1:2 ASPECT RATIO	3200	2200	31%	3200	0%	1750	46%	3140	2%		
5 ELEM. THRU THICKNESS 89" LONG - 2:1 ASPECT RATIO	3200	0	100%	3200	0%	0	100%	2920	9%		
3 ELEM. THRU THICKNESS 22" LONG - 1:2 ASPECT RATIO	2666	2440	8.5%	2666	0%	2170	19%	2600	2.5%		
2 ELEM. THRU THICKNESS 22" LONG - 2:2 ASPECT RATIO	2000	1950	2.5%	2000	0%	1680	16%	1780	11%		
2 ELEM. THRU THICKNESS 22" LONG - 2:1 ASPECT RATIO	2000	1960	1.9%	2000	0%	1680	16%	1800	10%		

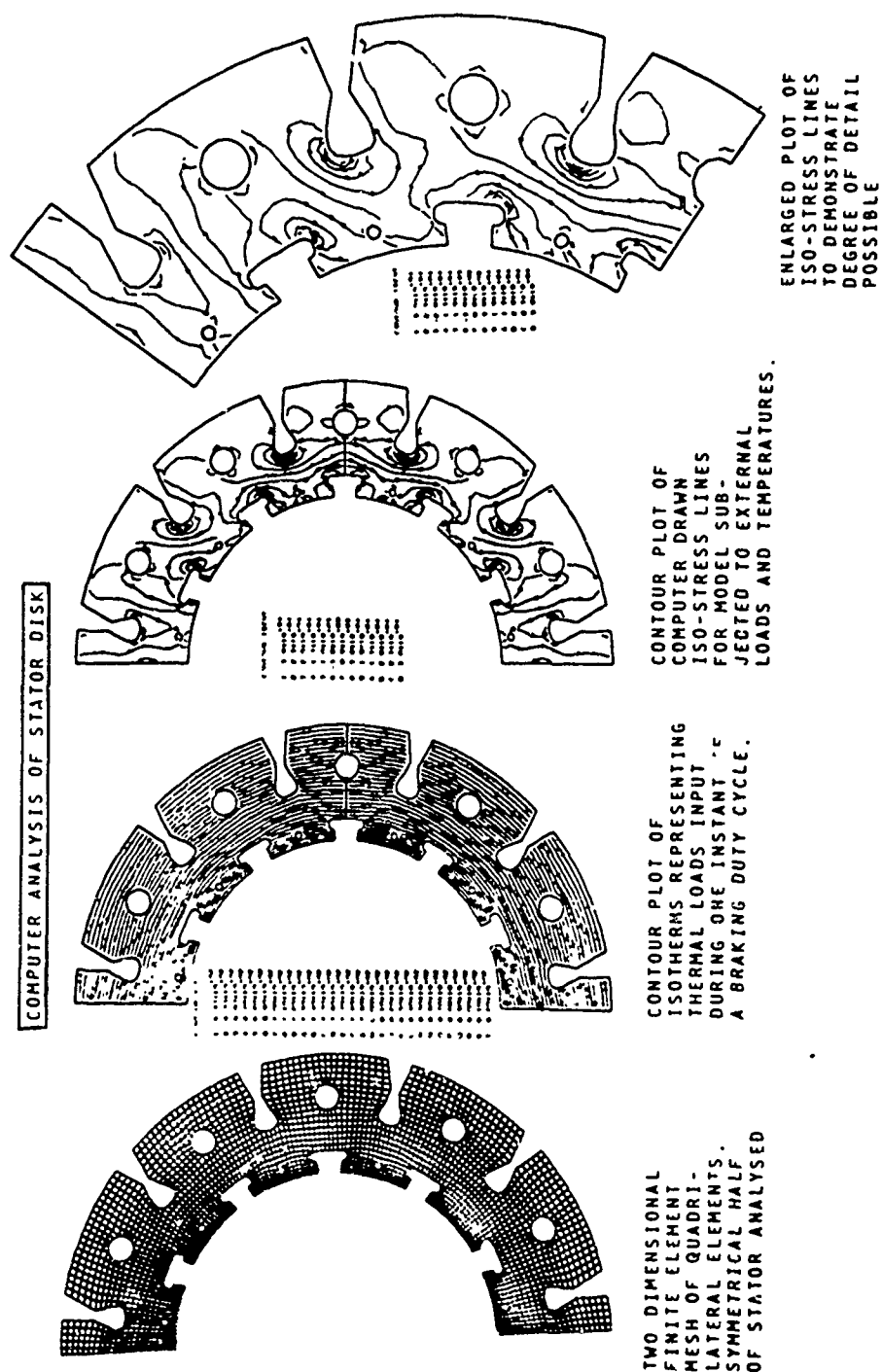


FIGURE 15: FINITE ELEMENT MODEL, THERMAL LOADS, AND ISO-STRESS CONTOURS OF A BRAKE STATOR COMPONENT

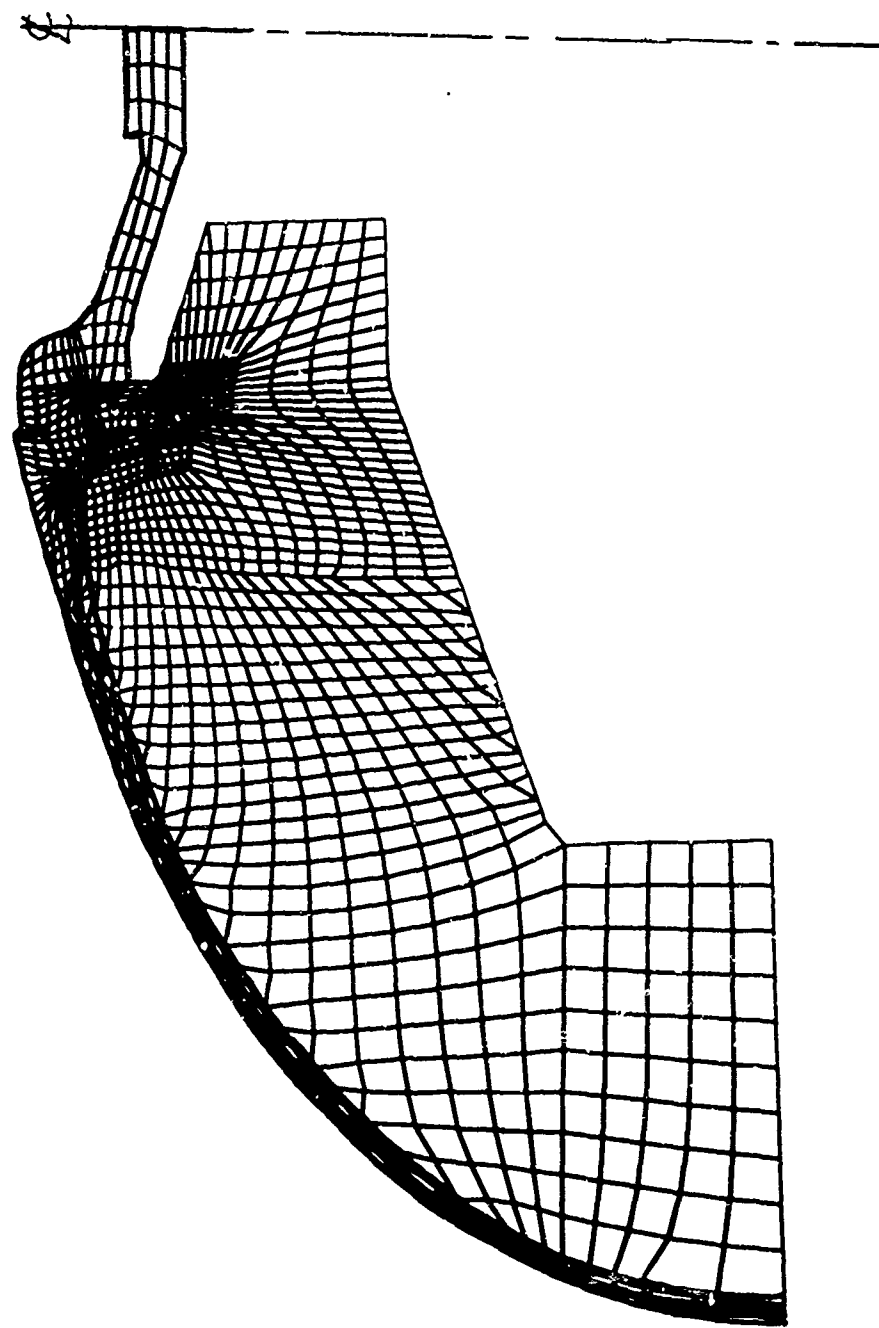


FIGURE 16: FINITE ELEMENT MODEL OF THE FORWARD DOME OF A SOLID PROPELLANT
ROCKET MOTOR

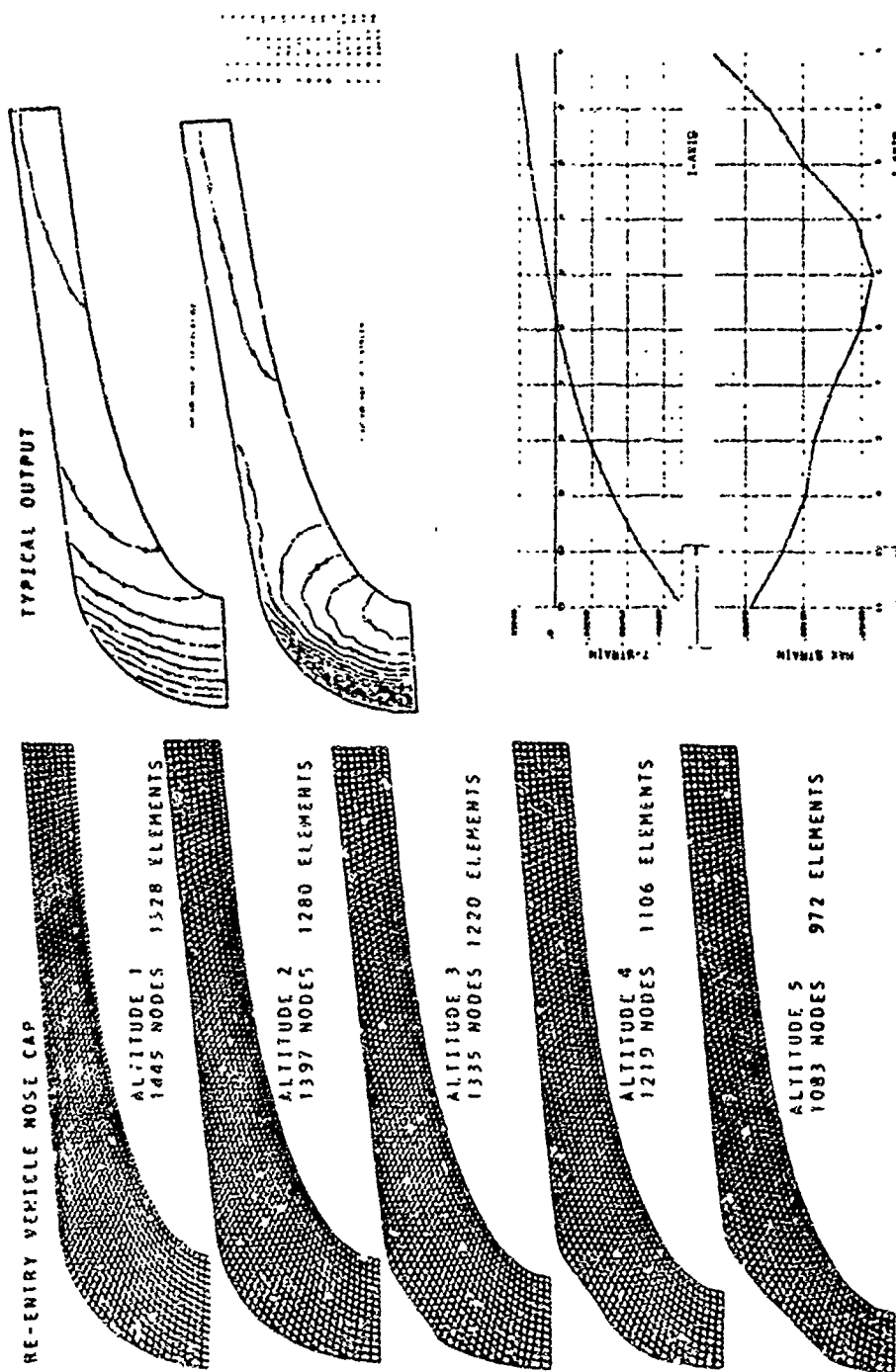
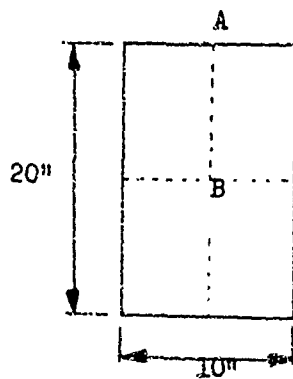


FIGURE 17: FINITE ELEMENT MODEL OF AN AXISYMMETRIC RE-ENTRY VEHICLE, DEMONSTRATING AUTOMATIC MODELLING VARIATION AS A FUNCTION OF ALTITUDE. TYPICAL OUTPUT QUANTITIES ARE ALSO SHOWN.

FIGURE 18



Simply-Supported Rectangular Plate
With Linear Thermal Gradient

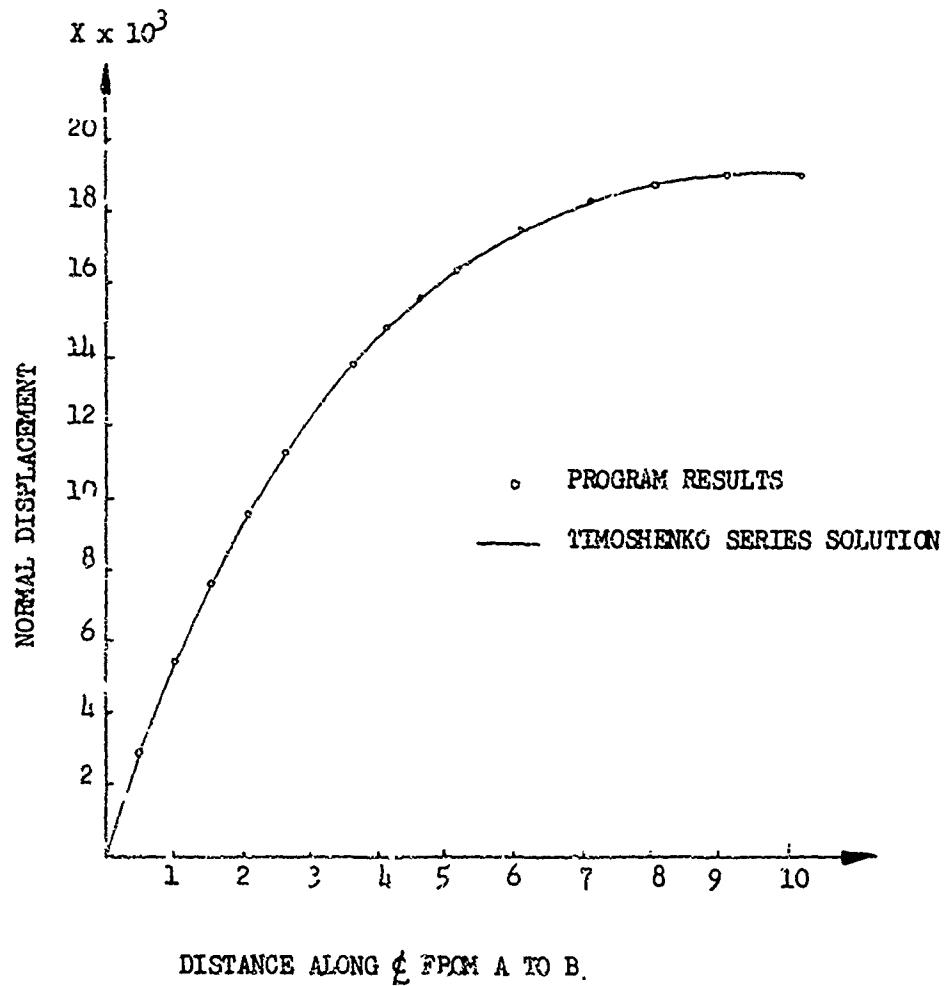
$$E = 10.6 \times 10^6$$

$$\nu = 0.33$$

$$t = 1.0$$

$$\alpha = .128 \times 10^{-4}$$

$$\Delta T = \pm 100^\circ F$$



large deflection problem. The analysis considered the skirt to case bond in various configurations, one of which was where the bond had initially separated for a short length. This requirement imposed an additional complication to the pressure analysis in that the cracked portion of the bond, while unable to carry shear and tension, can and does carry compression loads from the pressurized motor case into the skirt. These bond elements were, therefore, given the regular value of elastic modulus but a low modulus in shear. Although the final output showed a few elements carrying a small tension, it was not considered significant. A rigorous solution where the bond elements could carry compression, but not tension, would raise the run times from high to astronomical.

A second example of the program usage is in the area of reentry nose cap analysis. Figure 17 shows the automatic model geometric changes as the nose cap ablates and demonstrates the variation in the structure with altitude that is used as thermal load input. Input to the program is almost entirely taken from the thermodynamics output tape. Contained as output on the tape are temperatures at a number of locations within the confines of the structure as well as coordinates of a number of points on the inside and outside surfaces. The stress routines calculate the coordinates of the intermediate points on the surface and then using the I-J grid generation routine constructs the model. The temperatures of each element are calculated using a weighted interpolation scheme, and then the element material properties are automatically calculated through a linear interpolation from a table of properties vs. temperature. The entire analysis is automatic and a complete stress analysis is accomplished in 24 hours including stress, strain, temperatures, and geometric histories -- automatically prepared and pictorially summarized in report format.

Many other examples could be given here since this program and its derivatives are some of workhorse programs in daily use. That this program is still undergoing active development some five years after its original version was received is a high compliment to Dr. Wilson's basic program format.

Mixed Structures

This section concerns the development of automated and advanced versions of Dr. Kamel's three-dimensional mixed structures finite element program⁽¹³⁾ which came initially to us in 1966. It was our first exposure to a computer program where the author assumed some programming knowledge on the part of the user, and provided extensive documentation to ensure that the code could be used with maximum efficiency. Furthermore, the extreme modularity and organizational clarity of the code makes reading the listing more educational than most textbooks for beginning practical analysis. The rapid development and heavy usage of the program since 1966 attests to its favor with members of our group who must perform day-to-day analyses for design purposes. The input for this program is generally by the FORTRAN method discussed earlier, but input by data cards is an available, if not a widely employed, alternative.

Transmitted to us as a 32K core version capable of handling 240 unknowns for 100 nodes and 200 elements with five element types available, the program was immediately expanded to over 3000 unknowns for 1000 nodes and 2000 elements by

making use of the full capacity of our computer system. Program sizes are now considerably higher than these figures while use of 1108 systems routines and buffering technique have greatly reduced run times. All dimensions are contained in one PDP (Procedural Data Processing) block, and all accessing of mass secondary storage is separated into routines for each type of quantity accessed. Thus program dimensions may be altered, and efficient use made of a given software capability, without great familiarity with the program or fear of generating severe coding problems. Because of its structure, our major developments since the program was received have, therefore, been accomplished with minimal consultation with the author.

In our work the need often arises for an incremental solution. Whenever a structural problem exhibits nonlinear behavior due to geometry changes or material property changes, some means must be found to approximate the deviation from linear behavior. In finite element programs iterative or incremental methods are usually employed. MINI-ASKA's incremental mode was quickly debugged and tested, thereby enabling the user to update the state of the structure at each step for large deflection or plasticity analyses. This incremental mode has been since successfully used on glass motors, a wing, and an undersea oil pipeline. Additionally, an elastic/plastic version of the program has been developed and successfully used in our analysis activities.

When trying to perform an analysis of a small wing, we were made aware of the shortcomings of constant strain elements. Figure 2, presented earlier, (a plot of a wing configuration), has dimensions that are not unusual, but the solution yielded deflections of about one-fourth of the correct answer. Refining the grid of the vertical web members improved the ability of constant stress elements to model flexure, but also increased the bandwidth and total number of unknowns, and produced a very bad aspect ratio resulting in significant errors. Incorporating the iso-parametric linear strain quadrilateral element⁽²²⁾ for this problem seemed the obvious step, and in two days the stiffness and stress matrices were placed in MINI-ASKA and checked out successfully. Deflections for the wing immediately matched the hand-calculated value using only one membrane element for vertical webs. Another occasion required, for reasons of core storage limitations, a beam with six degrees of freedom in the local coordinate system to eliminate the need for using three elements to model each flexural member (one beam for each plane of bending and a torsion member). The new beam was installed in one day allowing us to proceed with the solution.

Reentry vehicles are sometimes arbitrary three-dimensional non-axisymmetric orthotropic continua. Until recently, modeling these bodies with some axisymmetric approximation was the best an analyst hoped to achieve, there being no arbitrary solids analysis programs available. Using the basic organization of MINI-ASKA and its constant stress tetrahedron, a separate 6000 element version was established and a routine written to provide orthotropic constitutive relations. Again, the organization and high segmentation capability of the program allowed the user to put together the routines necessary to perform a job rapidly and without disturbing the rest of the program's organization.

Thermal loading analysis capability has been extended to include gradients through the thickness of plates. The standard approach to thermal loadings in the finite element method is to calculate free thermal deflections of an element, multiply the stiffness by these deflections, and apply the 'fictitious forces' so obtained as loads. A subroutine INICD (INITial Corner Deflections) calculates non-rotational free in-plane thermal deflections and a subroutine INICF (INITial Corner Forces) multiplies the stiffness by the deflections and enters the resulting forces into the load vector. All that was required to include thermal gradients through the thickness for flexural elements was to provide a subroutine INICR (INITial Corner Rotations). The analysis then proceeds normally. Figure 18 indicates results obtained by this method.

Displacement and skew boundary conditions are a very useful adjunct to any program, allowing the user to take advantage of symmetry planes not in coordinate planes and also to apply deflections as edge conditions. Figure 19 a plot of a recently analyzed oil tanker web frame, illustrates the use of displacement boundary conditions. Use of symmetry conditions for a current analysis of a nuclear pressure vessel jet pump analysis allows us to model only 1/32 of the geometry instead of one-fourth, thereby cutting analysis cost in half, and probably increasing the accuracy of results.

Systems of equations involving 4500 unknowns are often subject to serious accuracy loss due to numerical error during solution. Validity of results may be checked in several standard methods such as idealization of a structure allowing theoretical solution or equilibrium checks, but the problem remains as to what should be done when numerical errors occur. A good production program will have built-in checks and output to indicate serious numerical trouble. Such problems, when encountered, are then combated through resorting to double precision arithmetic, remeshing the model, or executing some accuracy improvement scheme. Double precision versions of all of our finite element programs are operational but, unfortunately, doubling word size tends to cut modeling capacity in half. An alternate approach is to find some method of improving a given solution. Iterative schemes are readily available in numerical analysis texts, and a Newton's matrix iteration⁽¹⁷⁾ method was therefore programmed for use with large scale equations sets having a tendency toward accuracy loss and incorporated into MINI-ASKA. The modular nature of the code allowed the programmer to use matrix manipulation routines and secondary storage routines without great familiarity with the solution process. We have found accuracy improvement to be generally more reliable than our double precision, which is subject to some system peculiarities.

A comprehensive plot package based on the SCL020 has been developed and incorporated including: full and partial geometry playback, deflected shapes, selected stresses along cuts through the structure, and isostress contours for projections or mappings of three dimensional geometries. We must repeatedly emphasize that these graphical routines are not merely niceties but necessities for intensive large scale production analysis. Figure 20, a plot of the submarine-launch tube intersection, illustrates the physical impossibility of computing all the coordinates by hand and checking the configuration as understood by the computer. The element description alone requires thirty pages of printed output. The parabolic antenna of Figure 21 shows the use of geometry plots for only certain types of

REFLECTED SHAPE AND APPLIED LOADS - RUN NO. 2

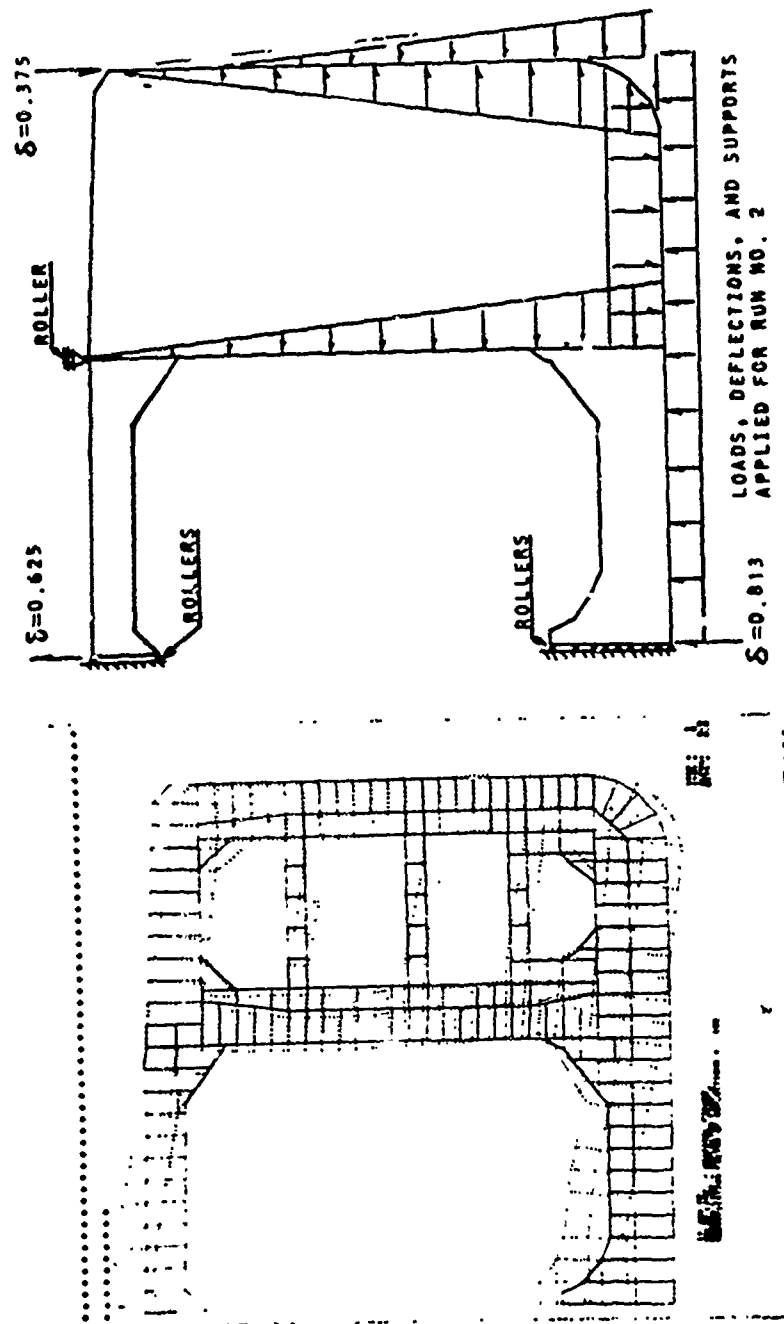


FIGURE 19: FINITE ELEMENT ANALYSIS OF A TANKER WEB FRAME

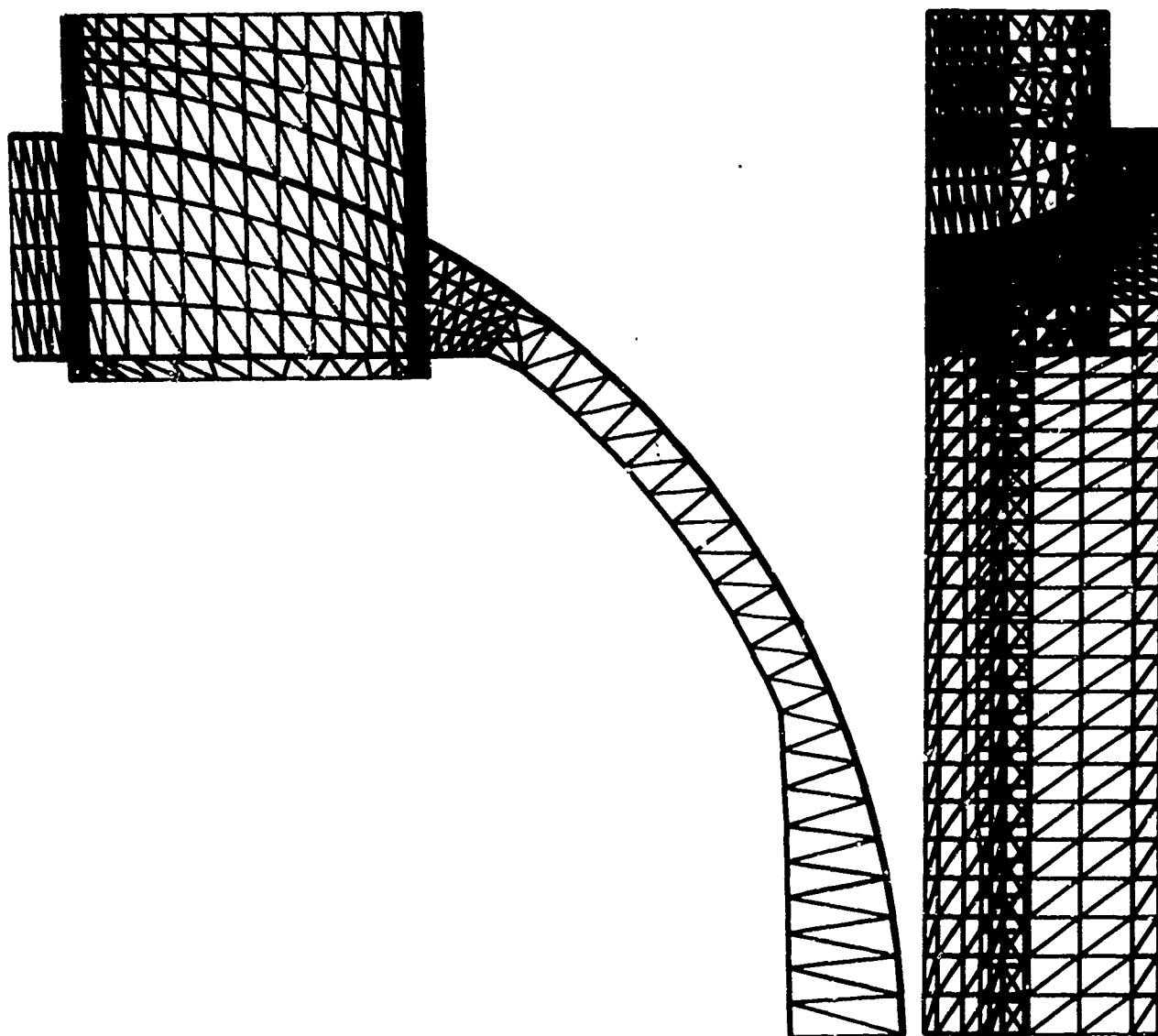


FIGURE 20: FINITE ELEMENT MODEL OF A SYMMETRIC SECTION OF THE INTERSECTION REGION BETWEEN A SUBMARINE PRESSURE HULL AND MISSILE LAUNCH TUBE

FIGURE 21: EXAMPLE OF USE OF GEOMETRIC PLOTS TO DETECT INPUT ERRORS

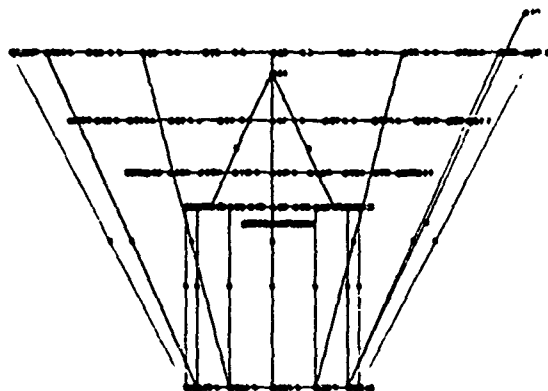


FIGURE A

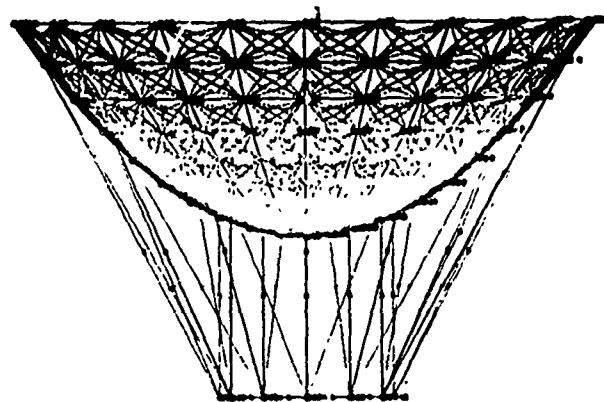


FIGURE B

DETECTING ERRORS.

- PLOTS OF THE GEOMETRY ENABLE THE PROGRAMMER TO DISCOVER ERRORS IN HIS INPUT WHICH MAY HAVE OTHERWISE GONE UNDETECTED, AND PINPOINT PROBLEM AREAS ALMOST IMMEDIATELY.
- PARTIAL PLOTS OF A SINGLE ELEMENT TYPE SHOW UP ERRORS IN THE STRUCTURE WHICH MAY HAVE BEEN COVERED BY THE PRESENCE OF ANOTHER ELEMENT TYPE.
- IN FIGURE A, 'NODE 230' CLEARLY STANDS OUT AS BEING INCORRECT, WHILE IN FIGURE B IT IS OBSCURED BY THE PRESENCE OF OTHER ELEMENT TYPES.

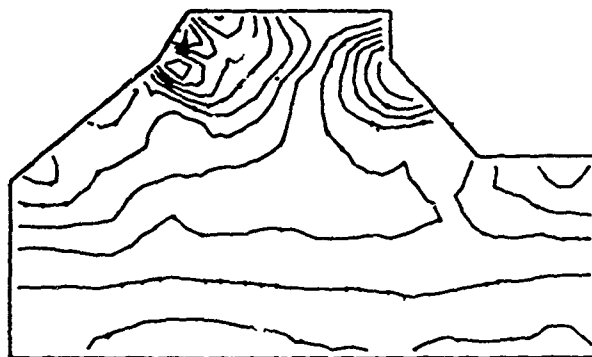


FIGURE 22: LINES OF CONSTANT STRESS IN THE LOWER CENTER OF THE TANKER WEB FRAME SHOWN IN FIGURE 23

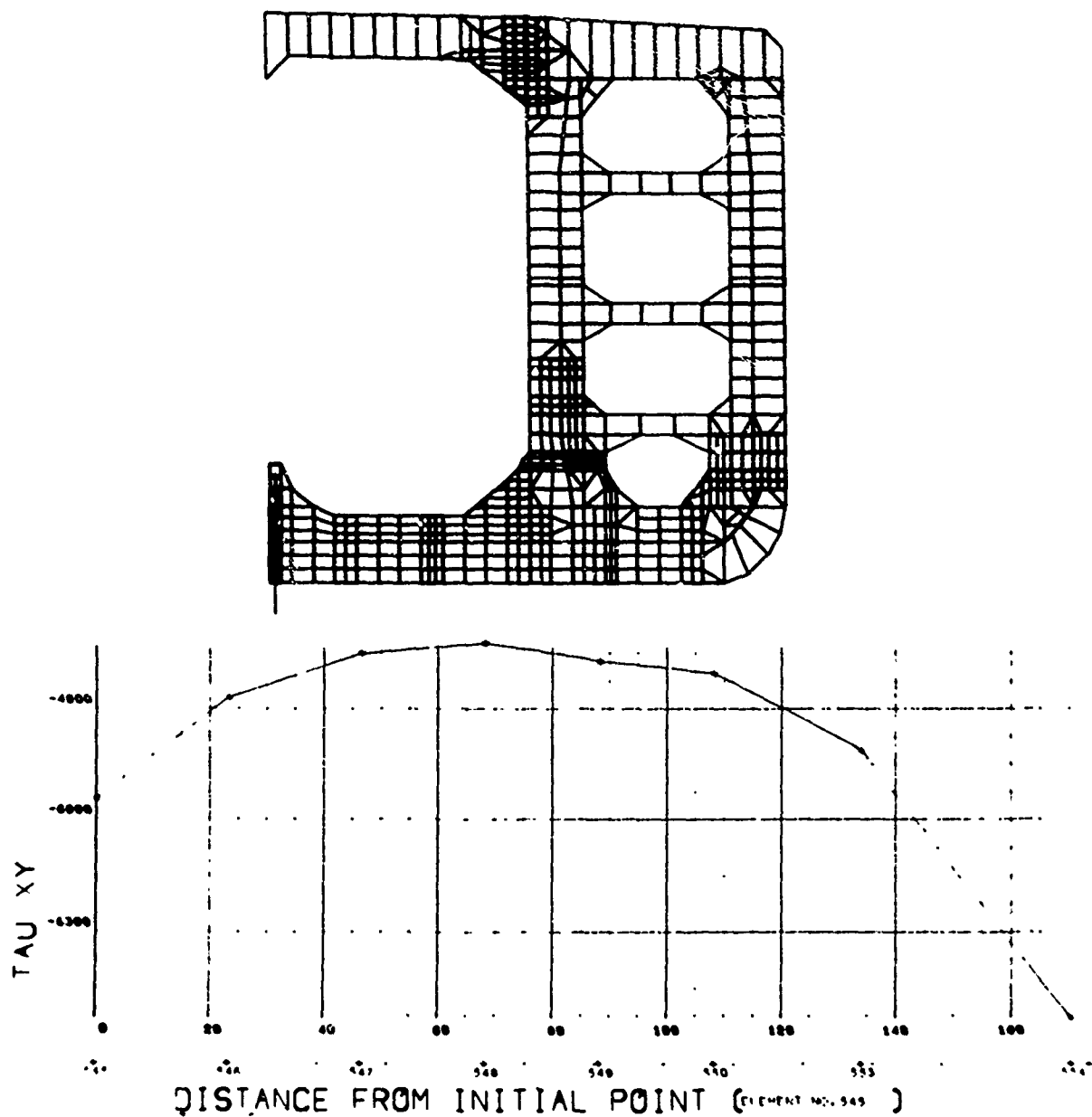


FIGURE 23: GRAPH OF SHEAR STRESS IN THE TANKER WEB FRAME ALONG A ROW OF ELEMENTS ADJACENT TO THE KEEL STRUCTURE

elements; the misplaced node (230) is completely hidden in the full geometry plot. Figure 19 of the oil tanker web frame mentioned earlier shows the use of deflected plots to confirm the analysts physical intuition of how the structure should behave under load. Deflections of the wrong sign, or showing a lack of smoothness are immediately evident in the picture, but may be well hidden in printed output. Another example of the use of deflected shape plots is Figure 8 where a pressure vessel manifold is subjected to a bending moment. The smooth anti-symmetric behavior is precisely what it should be. Even for this relatively small, 560 element model, the printed stress output covers 150 pages, ensuring that the analyst would soon be myopic, if not slightly insane, without the availability of pictorial and graphical output. The use of stress contours and stress cuts is illustrated in Figures 22/23, the highly visible form making abundantly clear areas of stress concentration.

In summation, the MINI-ASKA program has proved a great value in its capacity to grow with the needs of the user, while at small sacrifice in run-time great generality has been achieved. The development and incorporation of advanced elements, automated input and a wide range of pictorial and graphical display options has enabled this program achieve its current status as a code well suited to our needs for a production analysis tool where speed of response, flexibility and accuracy of results are paramount considerations.

SECTION X

PRESENT RESEARCH

Our present range of research interests encompasses a number of areas. In the field of graphics we are pursuing techniques of plotting stress contours for mixed structures including various projection and development schemes in addition to improving our orthographic projections, particularly with respect to the well researched hidden line problem. Our graphical presentations and automated report formats are being constantly improved and extended. Lockheed is studying our requirements for advanced electronic plotters which will improve both resolution and speed over our present SC4020 equipment. We are naturally interested in real time computer graphics and expect to be highly active in this field when equipment facilities expand to the size required for large scale production problems, which would represent problems in the 4000 D.O.F. range. In this regard we note that we have already successfully generated movies using finite element models coupled with the microfilm option on the SC4020, a technique which is of interest for studying the response of complex structures to arbitrary loadings.

To extend our finite element capabilities, we are active in the area of stability and dynamic versions of mixed structure codes and are working towards more advanced mesh generation schemes with particular emphasis on general structures and arbitrary solids. Advanced versions of mixed structures problems are being checked out for use in elastic-plastic analyses while advanced plate and beam elements are being tested. Receiving particular emphasis, however, is the iso-parametric numerically integrated hexahedron solid originated by Zienkiewicz and Irons⁽¹⁸⁾⁽¹⁹⁾ (20) and currently being developed by Wilson and Clough⁽²¹⁾ at the University of California. This element appears to possess wide applicability to the analysis of such structures as; tubesheets, thick walled vessels, and pipe tee intersections. Our test cases have yielded excellent results and we have successfully developed an orthotropic version of this element. We are currently developing suitable mesh generation and plotting routines in order to bring this program to full production status.

We are continuing work in the areas of applying programs to preliminary design and proposal activities, particularly in the realm of minimizing input and allowing full visual playback of input and output. Solution procedures and improved schemes for detection of numerical instability continue to receive attention, while run times are being reduced where program generality and usability are not compromised. Improved programs for buckling and transient response of arbitrary structures are being checked out and have yielded highly encouraging results to date. Finally, our capabilities in the area of low cycle thermal fatigue analysis is being rapidly extended and is finding an increasingly wide field of interest and application.

SECTION XI

CONCLUSIONS

The urgent need for the development of highly automated input/output techniques to enable the use of large scale computer programs on a daily production basis is clear. Our work in this area has shown the dramatic reduction in analysis effort and time made possible by the development of a wide range of advanced pictorial and graphical schemes as standard options. Similarly the necessity of intimate user familiarity with all internal functions is obvious, if full advantage is to be taken of a given program's basic potential. Finally, our requirements for more advanced programs improved accuracy of results, and extended automated input/output schemes ensures that such areas will continue to receive our attention.

SECTION XII

REFERENCES

1. Bushnell, David, "Symmetric and Non-Symmetric Buckling of Finitely Deformed Eccentrically Stiffened Shells Of Revolution," Solid Mechanics Report 6-67-66-15, Lockheed Missiles and Space Co., Sunnyvale, Calif., Aug. 1966
2. Bushnell, David, "Buckling and Vibration of Segmented, Ring-Stiffened Shells of Revolution, Users Manual for BOSOR-2," Lockheed Missiles & Space Company Report IMSC 6-78-68-40, Sept. 1968
3. Bushnell, David, "Stress, Stability, and Vibration of Complex Shells of Revolution: Analysis and Users Manual for BOSOR 3," SAMSO TR-69-375
4. Almroth, B. O., Brogan, F. A., and Marlowe, M. G., "Collapse Analysis for Elliptical Cones," to be presented at 6th U.S. National Congress of Applied Mechanics, Harvard University, June 1970
5. Sobel, L. H., Silsby, W., and Wrenn, E. G., "Computer Users Manual - Nonsymmetric and Nonlinear Transient Response of Thin Shells, Computer Program STAR," Lockheed Missiles & Space Co. Report IMSC-DOC6673, April 1970
6. Wilson, Edward L. and Jones, Robert M., "Finite Element Stress Analysis of Axisymmetric Solids with Orthotropic, Temperature Dependent Material Properties," Air Force Report No. BSD-TR-67-228, Sept. 1967
7. Percy, J. H., Navaratha, D. R., and Klein, D., "SABOR III: A Fortran Program for the Linear Elastic Analysis of Thin Shells of Revolution by Using the Matrix Displacement Method," ASRL TR 121-6 MIT Aeroelastic and Structures Research Laboratory, May 1965
8. Mack, E. W., Berg, B. A., and Witmer, E. A., "An Improved Discrete Element Analysis and Program for the Linear Elastic Static Analysis of Meridionally-Curved, Variable-Thickness, Branched Thin Shells of Revolution Subjected to General External and Mechanical Loads
9. Becker, B., and Brispance, J. J., "Application of the Finite Element Method to Stress Analysis of Solid Propellant Rocket Grains" Rohm and Haas Co., Huntsville, Ala., Nov. 1965
10. FRAN Post Processing Programs, The Rust Engineering Co., July, 1964
11. Fencs, S. J., Logcher, R. D., and Mauch, S. P., "STRESS Reference Manual," The M.I.T. Press, Cambridge, Mass., 1964
12. Whetstone, W. D., "Computer Analysis of Large Linear Frames," J. Struct. Div., HSCE, Nov. 1969

13. Kamel, H. A. "MINI-ASKA User's Manual and Documentation," Research performed for Lockheed Missiles & Space Co. under Research Contract No. POAPZ8J9280A, May 1968
14. Loden, W. "Rexbat 5 Users Manual" Unpublished Report, Lockheed Missiles & Space Co., Sunnyvale, Calif., July, 1970
15. Whetstone, W. D., "SNAP Users Manual, U-1108 Version," Lockheed Missiles & Space Co. Report LMSC/HREC D 162293, Huntsville, Ala., June 1970
16. "Three-Dimensional Solids Program: 8 Nodal Brick" Programmed by H. H. Dovey, Department of Civil Engineering, University of California, Berkeley, Dec. 1969
17. Forsythe, G. and Moler, C. B., "Computer Solution of Linear Algebraic Systems," Prentiss Hall, Inc., 1967
18. Irons, B. M., "Engineering Applications of Numerical Integration in Stiffness Method" A.I.A.A. Journal, Vol. 4, p. 2035-2037, 1966
19. Ergatroudis, J., Irons, B. M., Zienkiewicz, O. C., "Curved Isoparametric, Quadrilateral Elements for Finite Element Analysis," Int. Journal of Solids and Structures, Vol. 4, p 31-42, 1968
20. Irons, B. M. and Zienkiewicz, O. C., "The Isoparametric Finite Element System - A New Concept in Finite Element Analysis," Conference on Recent Advances in Stress Analysis, Joint British Committee on Stress Analysis, London, March 1968
21. Clough, R. W., "Comparison of Three Dimensional Finite Elements," Symposium on Applications of Finite Element Methods in Civil Engineering, Vanderbilt University, Nov. 1969
22. Doherty, W. P., Wilson, E. L. and Taylor, R. L., "Stress Analysis of Axisymmetric Solids Utilizing Higher-Order Quadrilateral Finite Elements" Dept. of Civil Engineering, University of California at Berkeley
23. Przemieniecki, J. S., Theory of Matrix Structural Analysis, McGraw-Hill Book Co., 1968
24. Zienkiewicz, O., The Finite Element Method in Structural and Continuum Mechanics, McGraw-Hill Book Publishing Co., Ltd., England 1967
25. Pestel, E. C. and Lecke, F. A., Matrix Methods in Elastomechanics, McGraw-Hill Book Co., 1963
26. "Proceedings of 2nd Conference on Matrix Methods in Structural Mechanics," Report AFFDL-TR-68-150, Air Force Flight Dynamics Laboratory, December 1969

QUESTIONS AND COMMENTS FOLLOWING VINSON'S PAPER

QUESTION: I was interested in your low cycle fatigue study. What size of structure were you interested in and what type of constitutive equations were you using?

VINSON: I'm not sure, but if I remember correctly they involved something on the order of 700 elements and a Prandtl-Reuss material law was used.

QUESTION: Are you ever blocked in production by loss of numerical significance in the solution of the simultaneous equations with the stiffness matrix approach?

VINSON: We haven't run into one yet where we haven't eventually come to a satisfactory solution through some kind of accuracy improvement or going to an iterative technique or to a double precision version. It will happen though, I'm sure.

QUESTION: I'm not familiar with your graphics facility. To what extent can you interact and specify, for example, what views you want to see and can you make corrections from a graphics unit?

VINSON: I think you're referring to some kind of interaction idea where you change things as the analysis goes on or as you look at pictures. We don't generally do that. Our structures are large and have to go on the 1108 and on the 1108 you don't use real time.

QUESTION: Apparently most of the analysis using the techniques you described is done by a small group in the division rather than the design

engineers themselves? Is that correct?

VINSON: That's correct.

QUESTION: We have about 200 design engineers using these techniques and I'm curious to see what your reaction to this type of operation is.

VINSON: I don't generally like the approach because a large group tends to deal with computer programs that are the be-all and end-all and they don't even know when they're in trouble. You know, there are people who believe anything a computer puts out. They need somebody around with considerable engineering experience to keep them straight.

QUESTION: So, in other words, you're in favor of your type of operation rather than having the design engineers themselves do the analysis with the systems.

VINSON: I would hope that the difference would disappear. I would hope that people who do design also understand the fundamentals of structural analysis and analysis methods. Now that may be naive but I'd like to see that.

QUESTION: Typically, in your experience, how many times after you have constructed one of these splendid and elaborate models, do you cycle it in the sense that you modify the design and repeat the analysis. I have had the experience of talking with other organizations who have capabilities similar to yours and they've indicated that for a typical application they recycle, as far as reanalysis goes, relatively few times. I wonder if that has also been your experience. Do you recycle typically

three times, change the design and recycle three times, ten or twenty?
What kind of number could you give us?

VINSON: Do you mean changing the models to get the right answers or altering the actual design?

COMMENT: Let's assume for the sake of discussion that the modeling has been successful and you have confidence in the analysis but it shows excessive deflection or excessive stress or some undesirable behavior characteristics and you wish to modify the design.

VINSON: Preliminary designs are changed, I would say, quite often, more and more often--but the fact is that you don't arrive at a refined design early. You talk about things, you try a lot of concepts and when you get to the point where you have a pretty good idea of what's going on, then you do a refined drawing. What we're really pushing for is a higher interaction where the designer doesn't sit in his cubicle until he's got an idea, do a beautiful production drawing for three weeks and then come to you. We don't think that's the way to go. The analyst should interact throughout the entire design process.

QUESTION: If I understand you correctly, you say that the number of re-analyses is small. Let me ask this one further question. Is it more likely that you would conduct the analysis over again as a consequence of a discovery in the change of the loads rather than a major modification of the design?

VINSON: I couldn't say--usually it's awfully late in the program when loads begin to go down and all this really does is give you more flexi-

bility, in my experience.

COMMENT: I might add on that point that it's perhaps equally likely you'll be modifying the model for loads as for structure problems. It's very seldom you'll repeat an analysis without having something modified--either in flexibilities or loads or member configuration or something. So we're forever developing modifications and re-running with differences.

QUESTION: In your paper, you mention a computer program MINIASKA. Is this in any way related to the ASKA program?

VINSON: Perhaps Prof. Kamel who developed MINIASKA would like to comment on that.

KAMEL: The name intended for the program was DAISY. The name MINIASKA was given to the program as a joke stemming from my early association with Argyris' group in Europe. MINIASKA resembles ASKA, but it has been completely rewritten. For one thing, ASKA was all in machine language and MINIASKA is all in FORTRAN IV.

QUESTIC: I noted in your stress contours you've shown here that you invariably plotted some particular component of stress. We often find it useful to plot some failure criteria because it's indeed that information that the designer would most like to have. Also we have found it useful to try and anticipate design changes and use a substructuring scheme to advantage so that under changes in load or changes in geometry we do not have to repeat the entire analysis. Have you found substructuring

advantageous in examples like you showed today?

VINSON: Substructuring has been used at Lockheed on various programs. Most of the problems I've run in to have been associated with missiles. The problems are segmented well enough that we can easily do a complete model of the area we're interested in. As far as plotting some kind of a failure criteria, I think there were some graphs there showing effective stress and maximum shear strain criteria. These are all available. If information is available for printout, it can be plotted.

QUESTION: You implied that you've used a lot of general purpose programs and I'm wondering what kind of programming staff it takes to maintain and update these programs.

VINSON: Our group engineer has 14 working for him and a parallel group has about the same number. Together, we do it all. We don't have a closed computer shop and if an engineer feels that he can program something faster than he can explain it to a programmer, he programs it. Most of our programs are highly modular. If there's a particular part of that program that you understand, you can go in there and make it do what you wish it to do in a week without messing up all kinds of coding in the rest of the problem. This is why we stress flexibility. We can't support a large programming staff.

CRICHLLOW: In this session we have had a very excellent overview in three major segments of the business. The mathematicians are quite often satisfied with a solution that may be a long equation which no one can do anything with until some programmers take over and produce a

computer program which still is of no particular use until an engineer takes it up and applies it to an actual structure. Now the end point of the whole scheme from the initial mathematics through the programming and ultimately to engineering application is really to produce an article for sale. I think this point was well made by Mr. Vinson's very extensive demonstration of different types, sizes, styles of structures and problems. I would like to add a point of my own. What the designer is really interested in are the dimensions of his structure. I think our analysis system is upside down in this respect. While we treat the analyses very completely and determine stresses and relate these to strengths, the designer doesn't care what the stresses are so long as he can be assured that they are less than some strength constraint. The dimensions are really the dependent variables of the problem.

PANEL DISCUSSION A

MEETING THE DEMANDS OF ADVANCING AEROSPACE TECHNOLOGY

Chairman: P. E. Grafton, The Boeing Company,
Seattle, Washington
L. A. Riedinger, Lockheed-California
Company, Burbank, California
R. B. Baird, USAF Headquarters,
Washington, D. C.
R. Bader, AFFDL, Wright-Patterson
Air Force Base, Ohio
R. W. Leonard, NASA Langley Research
Center, Virginia

GRAFTON: We are going to conduct an open forum panel discussion this afternoon on the topic of "Meeting the Demands of Advancing Aerospace Technology." In particular, we will discuss how these demands will influence the development of analysis capability for complex structure--especially shell structures. From my own personal point of view, I suspect that some of what we have to say here today some of you may not want to hear. That is, in many cases, challenges which confront the structural analyst are not the development of new methodology but rather are characterized by the needs of producing operational structural analysis tools.

We will begin the panel discussion with opening remarks from the panelists. Discussion amongst the panelists will follow after which I will open the discussion to questions from the audience.

I have been associated for some years with the development of structural analysis techniques. Now I am out of that business and I tend to view it as somewhat of an outsider looking in at it. However, one thing strikes me on reflecting back and that is the time that is involved between the development of new methodology in an area like this and the final application of

this methodology to the design and analysis of new hardware. I suspect that any new developments in structural analysis that come about in the next year will probably not significantly effect the design of systems that become operational much before 1980. So we are going to have to look pretty far downstream if the developments on which we are working today are to have a significant impact. Without trying to look at specifics of systems or operational requirements, one thing seems very clear to me; that is the increasing utilization of what I like to categorize as multi-function aerospace structures. In the past we used to think of structures as having a very simple fundamental role to play. They were designed primarily to provide aerodynamic configuration for an airplane and to carry the loads involved during flight. We've already long departed from that concept in many fields. I'm sure some of you have heard of the airborne warning and control system (AWACS). As part of this system, a rotodome which is about a thirty-foot diameter disc, is mounted on top of an airplane. As you might guess, it becomes a fairly significant part of the aerodynamic configuration of such a system and as such provides an excellent example of a multi-function aerospace structure. The design of the rotodome was governed not only by strength considerations, but also by some very exacting aerodynamic requirements to minimize the drag of the combined airplane rotodome system and some electromagnetic requirements to prevent distortion of the radar beams coming through the radome shell wall. This type of interdisciplinary design is commonplace today and is going to be the rule. Any time you have a single function structure ten years from now, I think that's going to be the extreme exception and we must bear in mind the impact of interdisciplinary design requirements in developing analysis capability. One very simple example may illustrate what I mean by this. In areas where we are concerned with the interaction of structure and aerodynamic loads, we find that the aerodynamics people, whether it be for steady state or unsteady state aerodynamics, are usually working with finite and discrete types of analysis techniques today. Supersonic air loads are a classic case in point where we deal with discrete modal networks. However, an aerodynamicist likes to work with a modal network that suits his problems best, while the structures man wants to work with a modal network that makes sense from a structural

standpoint. But ultimately they have to be tied together and if there's one place where you can get significant gross inefficiencies in the actual conduct of analysis, it's working at these interfaces. I think most of us have seen many long and drudging manhours with potential for mistakes and errors, spent to convert the output from one analysis form suitable for the input to another analysis.

Like most practical structures this roto dome presents a large number of potentially critical design load conditions. If you consider the various combinations of rotated positions and various flight conditions of the airplane, you can rapidly get a couple of dozen potentially critical flight conditions. Add to that the electromagnetic heat from the radar propagation, the potential for blast loading from weapons effects, and the potential for gust loading effects, in addition to the normal steady state aerodynamic maneuvers of the airplane, and it becomes quickly apparent that the selection of an appropriate set of critical design load conditions becomes very difficult to determine.

I'd like to make just a couple of other points, one of which has already been touched on this afternoon, and that is the problem of analysis versus design. The main reason that we run analyses are to verify designs and to assist in the creation of a design. But somewhere along the line we've got to capitalize more fully on the tools that are available and develop new tools where they are needed in order to permit the design process to be conducted in a rational integrated fashion rather than the current iterative procedure of conceptual design, analysis, modified conceptual design, more analysis and so forth. It's a fertile field I think for anyone to consider if they're looking for a challenge. We've got to move forward in this area.

There is another problem that frequently arises whenever a large number of people make use of computer tools for analysis and I characterize it by configuration control on computer analysis programs. It is highly desirable to provide the engineer with a capability to modify programs when the problem demands it, but it is also absolutely mandatory that when computer codes are used for production purposes and from multiple locations

that the configuration of the program be known to the analyst. In years past we've had our share of sad experiences in this regard. It has occurred, for example, when some engineer with his own particular problem has tinkered with some of the internal logic in a computer program and the next user to come along didn't know about it. Disaster is the usual result. Here it turns out that the computer itself is a very useful tool for helping to enforce configuration control and in our commercial airplane operations we've been looking at the possibility of using a file check stored in the data on the computer as a means of checking the configuration of the program. If the checks indicate that something has been changed, it will refuse to run the program. Now this sounds like it's being very brutal to people who want to use the computer for their own programs, but is a way to enforce the discipline of knowing what is on those programs and to maintain control over them.

RIEDINGER: Since the early 1950's we've seen great strides in computers, improved methods as to speeds and capacity. I think the structures people led the industry as far as the other disciplines are concerned and I think they've done a very good job of it. They had to change their intellectual process, however, and their sense of values. They had to rethink their models, to their advantage, of course, in order to take advantage of this new computing tool and the rapidity of it. We've seen the force method back in the early 50's and that was primarily due to thicker air foil sections. We had space to install spar caps in the wing. We had large discrete type components in the structural model of the design. Simultaneously, the manufacturing people began to improve their methods as to milling, processing, etc., and we were able to employ thicker skins. Using this capability in such a way, we were able to design optimum structures, so to speak. In other words, the wing bending load, as an example, must be distributed across a relatively thick skin-stringer chordwise section designed by "optimum design" structural analysis. This was required due to higher and higher speeds where thin airfoils are employed and where thin skins and spar caps per se are out of the question for many reasons. So that requirement led to the so-called displacement method with appropriate finite elements; and that's about where we are today. I do have some recom-

mendations here but keep in mind that we seem to overestimate the near future and underestimate the far future. Computers, remember, are only tools. However, better structural methods are possible knowing what the computer can do. We're going to have to look into a crystal ball as to what they are going to be within the next fifteen to twenty years. Also there are many things which must happen simultaneously and this is where I guess the structures man, the analyst himself, comes into play, and management. Efficient coordination of research and development--also please minimize the input-output phases. I think there's just too much time spent. I believe we can obtain shorter methods and not kill a moth with a cannon like somebody mentioned a little while ago. Get in the computer and move out and have some meaningful output like realistic stress distributions. Let's try to get the allowables in there also and coordinate everything so that when we insert in the external loads, we obtain the stresses, interject the allowables, calculate our margins of safety on the spot, know how to read the data and let the designers know how to read it and then if it isn't optimum, iterate. But it's got to go faster than it is now. I could cite example after example but time is short. In other words, model a little bit better, faster. Some designer may change the design but be ready for it. If the loads change, be ready for them. Be versatile. Design synthesis--Dr. Schmidt's favorite subject I believe. Let's get up on the step on that and don't be afraid that the designers are going to use computer graphics. I think it will evolve that a better design will be obtained and schedules met faster. Composites--I guess I could talk all afternoon on that -- but we do have a splice problem. We've got allowable determination problems. For instance in the macrosense, if the shear modulus is in error by 20%, that could mean the modulus of elasticity in compression is off 20%. Of the three popular formulae for shear modulus, they vary about 15%. In general, increasing computer capability, more accuracy is obtained. However, don't overelaborate just because it's available. Zero plus 10% conservatism is most acceptable--at least to me. As the previous speaker mentioned, creep is a very important consideration. Fatigue considerations, life assurance of a transport that's supposed to last 30-40,000 hours. Crack propagation is another emerging science, shall we say, and I've seen examples of finite element analysis taking care of that and predicting the

growth. Again, maybe new methods can be formulated in knowing what the computer can do.

Now a word about the future -- I guess anything said about the next fifteen to twenty years -- it would probably evolve that it would be very conservative.

The memories of computers will keep increasing while the sizes will decrease. I look to the future when remote stations will be maybe as small as a cigar box and you'll probably be able to talk into it. The CDC 7900-- that type of computer will probably be only one tenth the size it is now.

I'd now like to characterize briefly three new types of aircraft which may be produced in the future. These are the large transonic transport, the intra-urban aircraft and the STOL with vertical lift engines. The transonic transport (see Figure 1) would be designed to operate at about Mach 1.15 and would introduce buffeting problems. This aircraft would not be designed as are the current wide bellied air buses. In order to minimize drag rise, it would be thin with the fuselage designed according to Whitcomb's area rule. Thus, the designer would have to deal with bending of a fuselage with variable cross section. The plane would be over 400 feet long and carry 600 passengers 6000 miles. It would be powered by a radio-isotope engine. With no fuel load in the wing to decrease the relative wing load factor, the bending loads will be greater. Furthermore, the wing will be thin with a supercritical design which means that the upper surface won't have that nice curvature that now aids us by increasing the buckling allowable. We think that such a plane would offer the structural analyst many new problems.

The intra-urban airplane (see Figure 2) would be used in metropolitan areas in combination with ground transportation. Problems will arise from the fact that it will make a relatively large number of landings per mile and will have perhaps six large double doors to allow for rapid entry and exit. Very low fuel capacity will mean high wind loading in a positive sense.

Then you have the STOL aircraft (see Figure 3) with vertical lift engines



Figure 1. Proposed Transonic Transport

Reproduced from
best available copy.

IENT
T - 2 AISLES

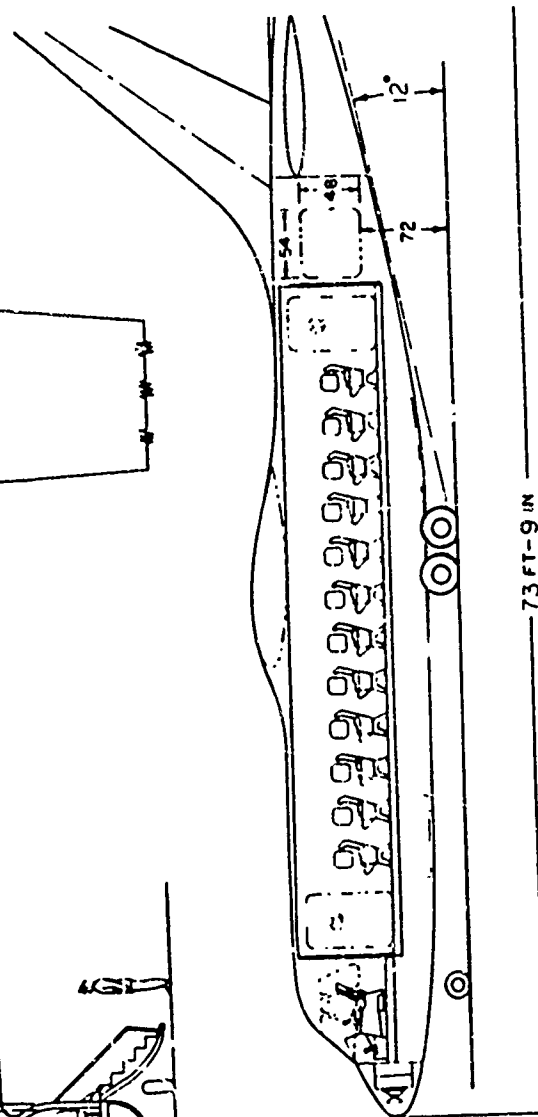
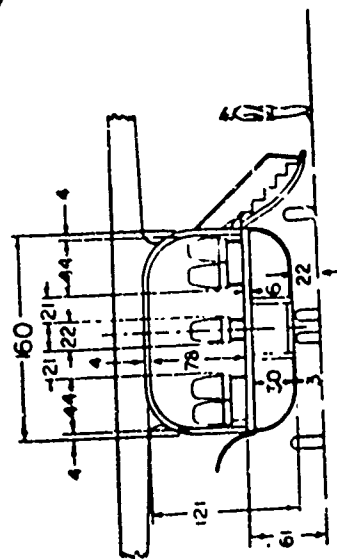


Fig. 2. Inter-Urban Airplane

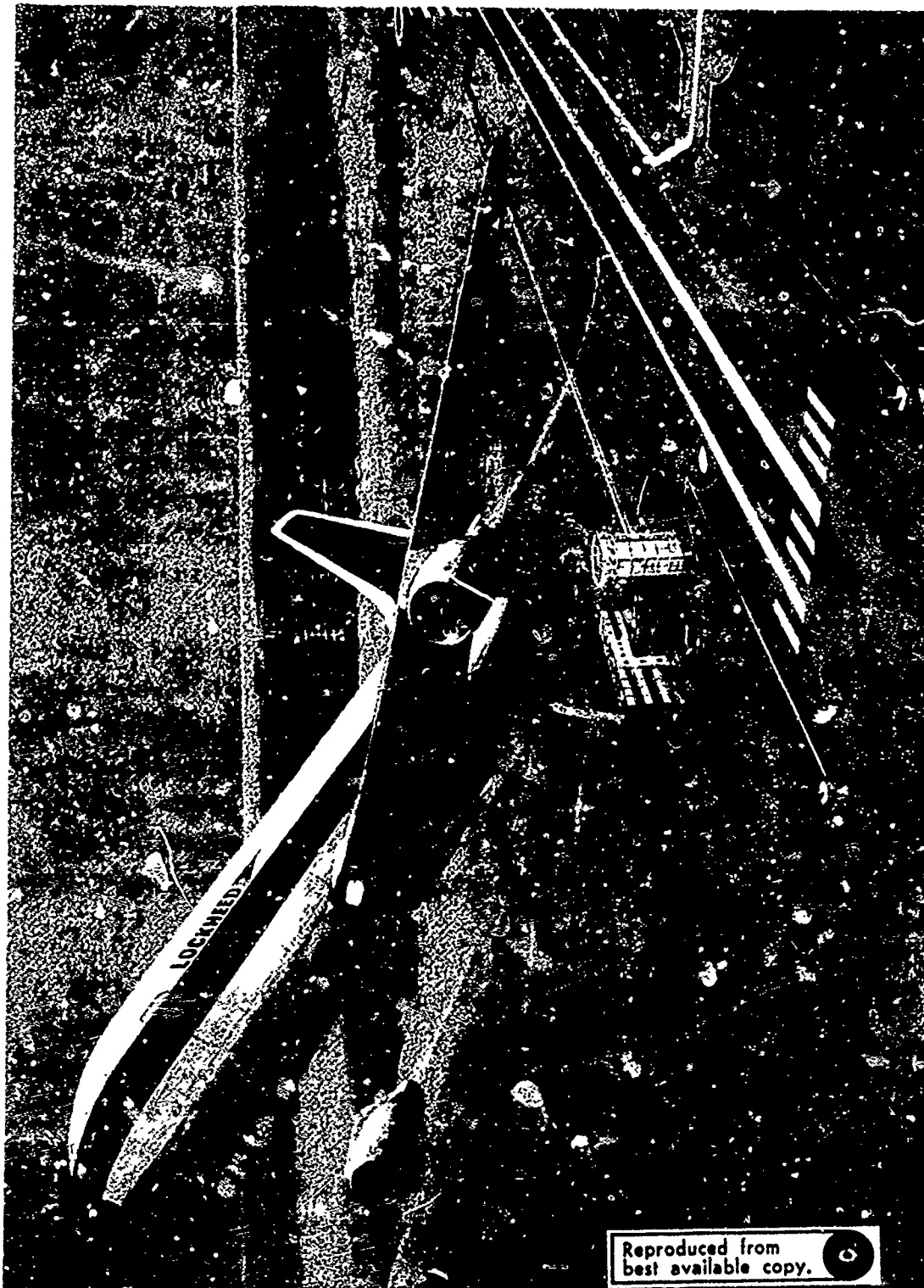


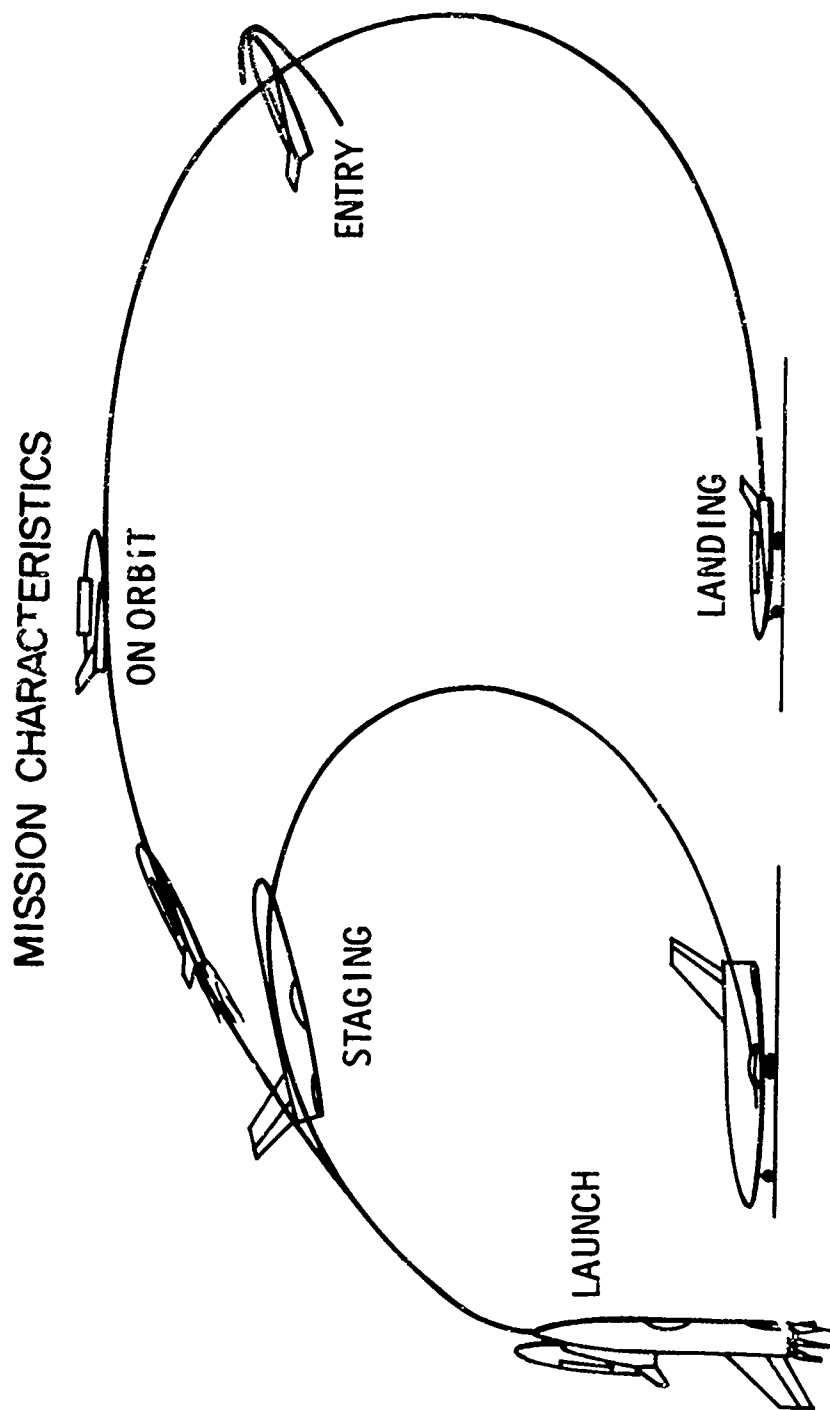
Figure 3. Inter-city STOL Aircraft with Vertical Lift Engine in the Fuselage

right through the fuselage or out on the wings. A number of new vibration problems will result in either case and these will require extensive study. I think that these and other new airframe concepts will leave the shell analyst of the future with an ample supply of new problems.

BADER: I'd like to bring up two points for possible further discussion during the afternoon. One is a reiteration of many things that were said earlier today and that is the importance of data management in computer programs. I believe that in the structural design process there are two other finites that we have to keep in mind in addition to finite elements and finite differences. These are finite productive time and finite dollars which are available to do the structural analysis work. The use of such things as automatic grid generation and coordinate calculation, plotting of output and interactive computer graphics are excellent example of what can be done to streamline the data management process and I think that it is the development of these kinds of things that demand our attention.

My other point concerns the new DOD fly before you buy concept of procurement. In the B1 and AWACS programs the Air Force is buying limited numbers of airframes and I wonder what effect this will have on the economics and philosophy of structural analysis. Will the airframe manufacturers try to use a more refined analysis in order to try and come up with a more saleable product or will they be satisfied with a cruder preliminary design approach in the interest of minimizing costs if the plane sees only limited production?

LEONARD: My assignment as a panelist was rather specific. I was to characterize for you the space shuttle and some of its possible requirements with respect to shell analysis. There are a number of competing concepts but the primary one, which is shown in Figure 4, consists of a two stage transportation system to orbit with both stages being completely recoverable and reusable for about 100 times. Both stages involve large aircraft type vehicles subject to loads from launch reentry and landing environments.



- LARGE AIRCRAFT-TYPE VEHICLES
- SEVERE LOADS AND HEATING
- REUSE FOR 100 FLIGHTS

Figure 4. Mission Characteristics of a Two-Stage Space Shuttle System

Probably the most popular concept today for the booster portion of this dual system is shown in Figure 5. It looks like a large airplane but actually it's a launch vehicle composed almost entirely of cryogenic tankage. The cryogenic tankage will probably look much like our conventional launch vehicle tankage today. To start with, it will be circular in cross section and carry the launch and bending loads as well as the internal propellant pressure loads. It will have a new wrinkle, however--the attachment of probably hot aerodynamic surfaces which lead to concentrated load inputs. There will probably be a second shell structure associated with the booster. This will be an external fairing which will serve as a heat shield. It will have some concentrated loads at a few attachment points which are widely separated to accommodate thermal expansion. It will be unsymmetrical as indicated in Figure 5 and it will have large thermal gradients from the underside (which is the stagnation area) to the back surface.

The orbiter concept is not quite as well defined today. Figure 6 shows one of several competing orbiter concepts which would satisfy both Air Force and NASA requirements. The orbiter is dominated by a huge payload bay. This particular class of orbiter would have an external primary structure to carry the launch thrust loads and the bending loads which would approximate closely the mold line of the vehicle. As indicated in Figure 6, it is a very unsymmetrical structure and has a number of bulkheads as well as frames and longerons. The tankage would be suspended within the structure at a few points to accommodate thermal contraction. While it's shown here in circular cross section, I'd like to emphasize that the need to utilize the volume of this vehicle efficiently may drive the designer to rather unsymmetrical cross sections. The thermal environment of the orbiter is considerably more severe than the booster and therefore there will be heat shields at least on the underneath surface and insulation to protect the vehicle during entry.

There have been a number of studies of the space shuttle to date and there has been one message which has come through in each of these: the shuttle shows a rather severe weight sensitivity problem. This means that the shuttle will require a degree of structural analysis sophistication which

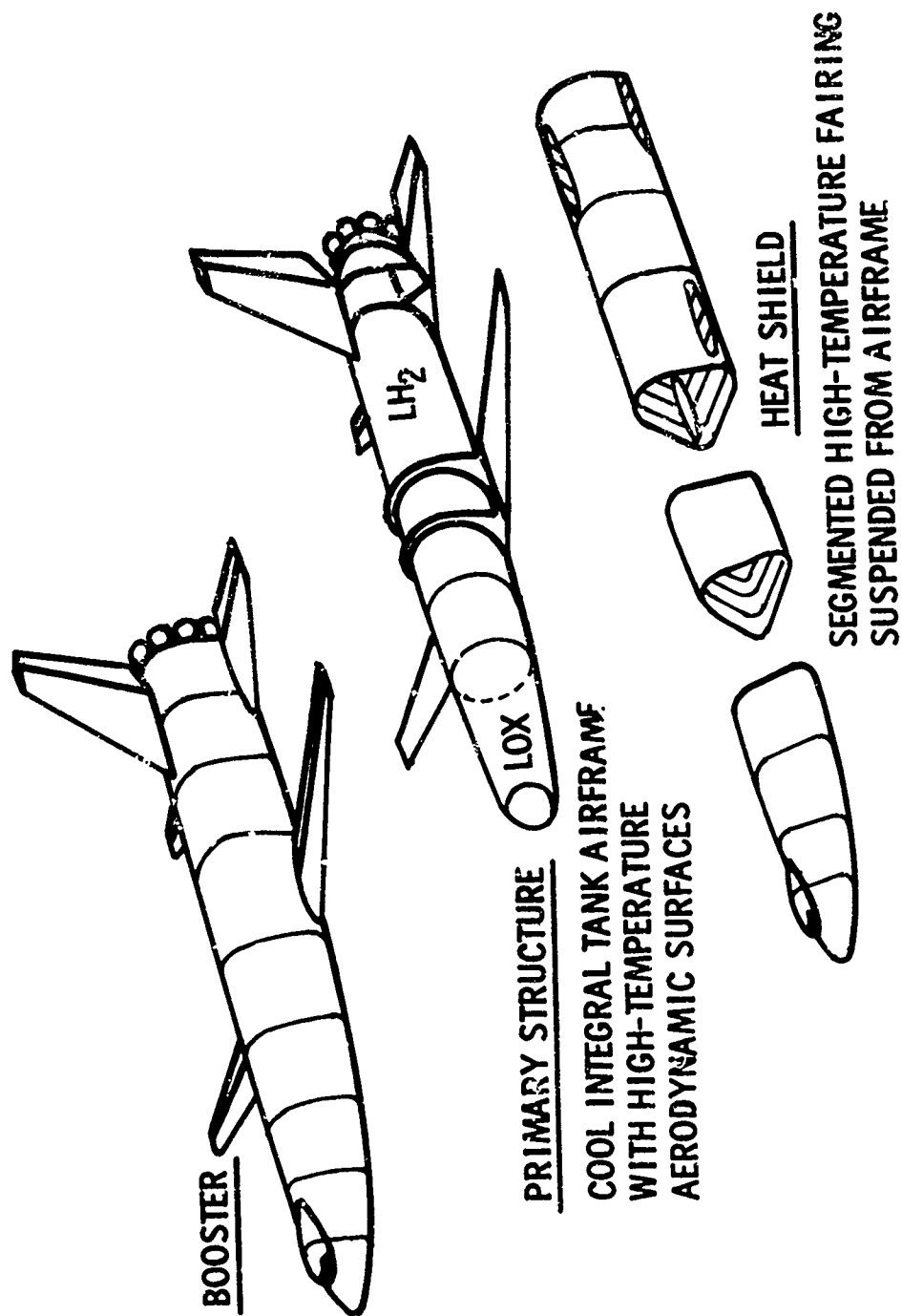


Figure 5. Proposed Booster Portion of the Space Shuttle

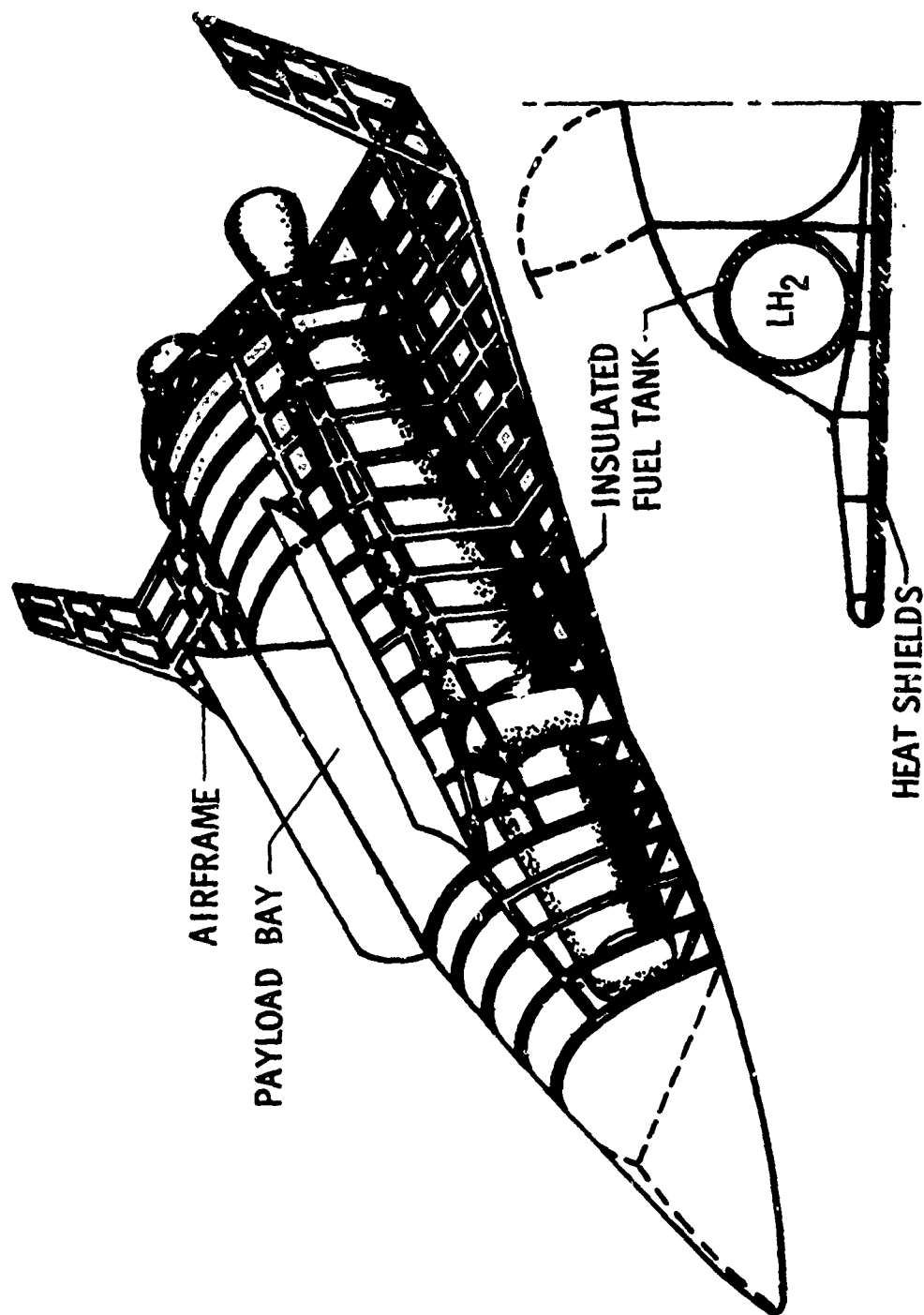


Figure 6. Proposed Space Shuttle Orbiter Design

simply has no precedent in the major vehicle systems of the past. Several of these are indicated below.

NEED FOR UNPRECEDENTED DESIGN ACCURACY AND EFFICIENCY

UNSYMMETRICAL, COMPLEX SHELL STRUCTURES

**ADVANCED MATERIALS, INCLUDING COMPOSITES
(ORTHOTROPY, NONLINEARITY)**

**ELEVATED AND VARYING TEMPERATURES
(VARIABLE STIFFNESSES, CREEP, THERMAL STRESSES)**

**CYCLIC LOADS AND TEMPERATURES
(RESIDUAL DEFORMATIONS, DESIGN FOR FRACTURE
CONTROL)**

The first problem is that many of the shell structures that are currently conceived for the shuttle are very unsymmetrical. The need for extreme efficiency in the shuttle will undoubtedly force the reliance on advance materials and this may very well include the first real application of composites to genuine primary structure. This, of course, will bring with it the attendant characteristics of orthotropy and possibly nonlinearity which will have to be dealt with by the analysts. The shuttle will be subjected to elevated and varying temperatures and again the need to achieve great efficiency in the structural design may force the analysts to take into account the dependence of material properties on temperature, for example. Creep may very well become an important factor in shuttle design and, of course, thermal stresses will be there. It should be pointed out, too, that with 100 reuses proposed, cyclic loads and temperatures are a major problem for the shuttle. This will lead to worry about residual deformations. It will certainly force the designer to consider design for fracture control and this will require rather detailed knowledge of the stresses around stress raisers, etc.

Referring now to Figure 7, I think that with respect to the need for advanced

methods in computer programs the shuttle obviously will require at least moderate extensions of our on-the-shelf analysis capability. I'm not prepared to say that it absolutely demands automated shell design programs for direct synthesis but it certainly provides a ready market for procedures for rapid design that lead to minimum weight.

ADVANCED METHODS AND COMPUTER PROGRAMS

MODERATE EXTENSIONS FOR ANALYSIS

RAPID DESIGN FOR MINIMUM WEIGHT

DESIGNER ACCEPTANCE

FOCUS ON USER CONVENIENCE AND RELIABILITY

METHODS VALIDATION THROUGH TEST

Figure 7. Messages for the Shell Analyst

I've been scooped several times already today with respect to the next point--designer acceptance. I was prepared to say that I think the most important problem of all is getting the designer to use not just the new capability that we might develop for the shuttle but the best of the capability that we already have on the shelves. And, of course, this means that the analyst needs to focus more than he does even now on user convenience and on simplicity in order to achieve the kind of reliability that enables the relatively uninitiated to make use of these programs in a design sequence with a certain amount of safety. We have to remember too, of course, the designers' inherent distrust of unproven methods. This means that we must take every opportunity to compare new methods with existing data and we ought to take every opportunity to promote the generation of additional data.

I hate to end on a negative note but while I've pointed to the need for considerable extension of analytical methodology for the shuttle, I have to admit that the schedule for the shuttle doesn't really admit the development of much of this and its application to the shuttle itself. I would think, therefore, that new methods for the shuttle would be developed rather selectively.

BAIRD: I want to mention two developments that have come out of our Air Force flight vehicle technology programs that may significantly influence the airplane of the future and have some effects on the shell analyst's job. These are the fly-by-wire flight control system and composite materials for structural components. In the fly-by-wire control system, when the pilot moves his control stick, it produces an electronic signal which is transmitted to the control surfaces over electrical wires. Hence the term fly-by-wire. It replaces the conventional system in which motion of the control stick is transmitted to the control surfaces through a system of linkages and hydraulic components. Advantages of the fly-by-wire system include low initial cost, low maintenance cost, short control surface response times and light weight. I don't have to tell anyone in the audience the importance of light weight in an aircraft structure. Currently, the weight of an aircraft is minimized by the designer through analysis, tests, choice of materials and configuration. I believe that fly-by-wire control systems coupled with the use of composite materials for aircraft components can provide the capability for further weight reductions via aerodynamic tailoring or a form of variable geometry structures. What I mean by this is you can add aerodynamic devices to the wing or the tail structures and control those devices when you maneuver. These devices will change the air load distribution and therefore can be made to decrease such things as the bending moment on the wing structure. This is what we call maneuver load control. You can also use the fly-by-wire flight control system to control flutter and this we call active flutter control. If you couple these two devices with the composite structure, which is anisotropic and allows us to make this structure twist and deform in a given manner, then when you maneuver you can then unload the tips, decreased bending moment, and you can also effectively change aspect ratio of the wing which essentially increases performance.

One other area that was touched on earlier is that of transonic maneuvering. What this allows you to do is raise the buffet limits and coupled with the fly-by-wire flight control system it now makes feasible remotely controlled vehicles that can fly at high g levels much higher than a pilot could stand.

GRAFTON: I'd like to select just a couple of topics to get a discussion around the table here going. One of them is something that I've always been concerned with and that is this question of validation. The need for validation of analysis techniques has been long recognized. Let me just pose a pragmatic question. When do you have sufficient confidence in analyses that you're willing to talk about eliminating tests? I raise this question because it does have a severe economic impact in many cases on what it's going to cost in the course of development of the system.

BAIRD: I don't think we're ever going to have that and I'll tell you why. If we continued to design structures the way we do it today then maybe eventually we could do away with part of the tests. But when you keep using new concepts such as changing configurations with fly-by-wire control systems--which I firmly believe we're going to see 10 to 15 years from now--then I don't think we'll ever be able to replace a significant number of the tests which we have to perform to guarantee structural integrity.

RIEDINGER: Static testing requirements may change. However, with the fatigue spectrum we are stuck with I think that fatigue tests are mandatory forever.

GRAFTON: Let me just point out one factor in this regard. As you get more sophisticated and more complex in the analysis that you undertake, if the cost of accomplishing that analysis keeps increasing, the first question that program management is going to ask, whether it's internal or whether it's a customer, is: What does that buy me if I still have to test? I think that's something that has to be borne in mind. But I personally feel that we will eventually back off in terms of the amount of the development testing that we may feel we need in the course of evolving a new design. However,

we are always going to want the confirmation testing in the course of developing new aeronautical systems. There's no question about that either in my mind. I think one of the challenges here is whether you can reach a point of confidence in analyses that will permit you to forego a major portion of the development test activity to show a net savings of the cost of development.

BAIRD: I think the only way you can do that is to get enough experience with the analysis techniques that we're using today and see how well we predict structural failures before you can make a conclusion like that. Study the amount of structural failures that we've had. For example, since World War II out of 33 static test programs run on Air Force aircraft, there have only been seven that went through the test program without a major failure, and of those seven there was only one that was a first model. The others were B and C models of an original model. That isn't a very good record of major failures, so I don't really see how we are ready to reduce testing at this point in time.

GRAFTON: We must also remember that as we get into structures with new functions and different applications we're going to be right back insisting on development tests for the understanding that's required. I think, Bob, you people are recognizing this in the shuttle as you're getting into the details of what may be required.

LEONARD: Well, the shuttle of course is a good example of this situation where the need for ultra efficiency and accuracy on the design makes it even more imperative to get plenty of development test results. In this discussion so far we seem to have mixed up qualification testing and development testing. I certainly can agree that, for structures of the future, analysis is never going to replace qualification testing which basically is there to uncover the stupid mistake rather than to uncover deficiencies in analysis. I would think, however, that we ought to be able to minimize the required need for development testing by improving our analysis. Improving our confidence in analysis. I agree with Dick, we can never eliminate tests.

GRAFTON: I think at this time I will open the discussion to comments and questions from the audience.

COMMENT: With regard to the matter of test versus analysis, I'd like to offer the following comment. I think that if you have the proper communication between the analytical people and the experimental people, use of analytical results in advance of the test often provides a much better test and can also save a lot of retesting. It has been my experience that a test is often run with very little thought ahead of time and things go wrong which would have been avoided if even limited analytical work had preceded the test. Even if the analysis isn't absolutely correct, it points you in the right direction.

QUESTION: Would the panel care to comment on what they see as the future of design based on reliability concepts directly rather than indirectly? In other words, the quest for reliability is always present, but now we tend to build it in through deterministic framework. We operate deterministically in attempting to reflect the realities of a statistical situation. Philosophically, it appears ideal to handle the reliability problem directly but technically it appears to be a very difficult almost insurmountable challenge. How far in the future do you see such capability being developed?

BAIRD: Well, Flight Dynamics Lab has sponsored work to make these kinds of changes--such as getting rid of the factor of safety, limit load and ultimate load ideas and going reliability criteria in this area. Your question is when do you think you will see it. I don't think we'll see it in the next ten years.

GRAFTON: I guess I'd like to make one comment in that area having moved out of the structures field and into an area deeply involved in operations research and manipulation of statistical problems. I guess I could think of no worse nightmare perhaps than trying to run a Monte Carlo simulation of a statistical shell structural response problem including nonlinearities.

COMMENT: I would like to say that at this point we do not have even a deterministic large scale design capability suitable for handling something

like an aircraft fuselage with all of its cutouts, rings and longerons. We have an analysis capability, but not a design or optimization capability for structures of this complexity. So before we begin to think about incorporating statistics into the design process, we need to first learn how to handle the deterministic case and perhaps automate the entire design process.

LEONARD: One more comment relative to deterministic versus statistical design for reliability. It is obvious that a major barrier to our achieving the latter in the near future is the lack of the kind of statistical data base that permits the definition of allowables on a reliability basis and I might add the cost of getting this kind of data base will always be a tremendous barrier. So I'm not sure that we'll ever really achieve this.

GRAFTON: I will try to summarize very briefly a few of what I consider to be the key points we've tried to touch on this afternoon. Some of the real challenges in the field of computerized analysis of shell structures--I suspect are not really technical challenges. They are what I would categorize as economic challenges and they have to do with how we conduct ourselves in the course of an analysis. This isn't new to the engineering profession--it's been with us for many years and I think we're in an environment today that sees an increased emphasis on it. I do not want to unduly discourage new development; however, I think we have to recognize one of the prime challenges of today's environment is to truly use effectively the technology capability that we essentially have in hand or near in hand today. I have an associate that made the comment to me that part of the problem here is the fact that it is much more fun to conceive children than it is to raise children. I think that is a point we might all bear in mind in the course of truly getting the capability and the utility out of computerized analysis techniques that we have been building over the past year and will want to continue to build into the future.

DYNAMIC FINITE ELEMENT ANALYSIS OF ARBITRARY THIN SHELLS

by

Ray W. Clough⁽¹⁾ and Edward L. Wilson⁽²⁾

ABSTRACT

A brief review of the development of finite element procedures for the analysis of thin shells is presented, together with a discussion of the four types of approximations involved in the application of the method. Then two factors which influence the efficiency of the finite element solution are considered: the properties of the individual elements (including curvature, deformation refinement, etc.) and the nodal degree of freedom representing rotation about the shell surface normal. Comparative analyses are presented to illustrate the influence of these factors in practical cases.

Finally, the formulation of the finite element system equations of motion is discussed and techniques of solution are outlined, taking account of both linear and non-linear classes of problems. A series of examples (both linear and non-linear) are presented which demonstrate the effectiveness and generality of this dynamic analysis technique.

-
1. Professor of Civil Engineering, University of California, Berkeley.
 2. Associate Professor of Civil Engineering, University of California, Berkeley.

DYNAMIC FINITE ELEMENT ANALYSIS OF ARBITRARY THIN SHELLS

by

Ray W. Clough and Edward L. Wilson⁽¹⁾

INTRODUCTION

Since the earliest phases of its development, the finite element method has appeared to be ideally suited to the analysis of general shell structures because of its flexibility in accounting for arbitrary geometries, loadings and material property variations. Indeed, it was evident that a general shell analysis program could be developed as soon as effective plate bending and plane stress elements were available; and early efforts with the pioneering elements of these types clearly demonstrated the feasibility of the finite element approach to shell analysis [1,2].

In these original developments, only flat plate elements were considered, thus their membrane and bending responses were uncoupled at the element level and the element stiffness matrices were formed as simple combinations of the previously developed plane stress and plate bending stiffnesses. Rectangular elements were used for the analysis of cylindrical shells, while triangular elements were employed in the idealization of general shell shapes.

After these preliminary studies, further progress with the finite element analysis of general shells was delayed by the inadequacies of the available triangular plate bending elements. However, with the development of an efficient general plate bending element [3], the study of the shell analysis problem was continued, and three different shell programs based on flat triangular elements were soon developed at Berkeley [4,5,6]. These all use the plate bending element of Reference 3, and differ only in the refinement with which the membrane behavior is represented.

(1) Department of Civil Engineering, University of California, Berkeley.

Although the flat plate element is appealing in its simplicity, it imposes a seemingly undesirable geometric approximation in the idealization of general shells and considerable efforts have been directed toward the development of curved shell elements which might lead to improved efficiencies. Some success has been obtained with both cylindrical [7] and general shallow shell elements [8,9,10] based on thin shell theory. However, recent work on the derivation of general curved three-dimensional solid elements appears even more promising [11,12]. These new elements automatically account for varying curvatures and thickness within the element region, and also include a shear distortion mechanism which becomes significant in thick shells.

The purpose of this paper is to describe briefly some of the more effective shell elements which have been developed to date and to compare results which have been obtained with them. Both static and dynamic analyses will be discussed; non-linear geometric effects will be included in some analyses for comparison. Specific factors which will be dealt with are the relative efficiencies of curved and flat plate elements, the number of degrees of freedom to be considered at the element nodes and the relative merits of consistent and lumped mass formulations of dynamic problems. Also a brief summary of the approximations involved in the finite element idealization of a general shell problem will be presented.

FINITE ELEMENT APPROXIMATIONS

A finite element analysis of a general shell structure introduces several different types of approximations in the formulation. First is the geometric approximation involved in replacing the actual continuous shell surface by an assemblage of discrete structural elements. In order to simplify the evaluation of the shell stiffness, each of the elements usually is prescribed to be of a single limited form which may range from a flat

triangle in the simplest case to a surface of linearly varying curvature. It is evident that the assemblage of these specially shaped elements can provide only a limited approximation of an arbitrary shell surface.

The second basic assumption is that the strains (and displacements) in each element may be only of a limited form, as specified by a prescribed set of nodal interpolation functions. Depending on the complexity of the strain variations that are to be represented in the actual shell, these prescribed strain patterns may provide a fair to good approximation. Clearly the refined elements which include linear or quadratic strain variations, will provide more realistic approximations than the basic constant strain elements for any given degree of mesh refinement.

The errors due to both the geometric and the displacement function approximations tend to vanish as the element mesh is refined. For any given mesh size, however, the refinement which is imposed by the chosen interpolation functions should be made consistent with the level of geometric approximation. Thus, it would not be reasonable to assume highly refined displacement interpolations in a flat plate idealization of a doubly curved shell. Similarly, it is inappropriate to employ a curved shell geometry in an element in which the strains are assumed to be constant. Inasmuch as any desired degree of accuracy can be achieved by mesh refinement with either simple or refined finite elements, the only meaningful criterion for selection of the optimum degree of element refinement (with regard both to geometry and to displacement interpolations) is computational efficiency, i.e., the amount of computer time required to achieve a given level of accuracy in any prescribed problem situation.

A third approximation which may be present in some finite element shell analyses is that the assumed displacement patterns may not maintain

inter-element compatibility as the shell is loaded and deformed. Usually the finite element interpolation functions are such as to maintain continuity in a flat plate assemblage; however, incompatibility will develop if the elements meet at a finite angle and if the membrane and bending interpolations are of different forms. Some types of curved elements provide improved performances in this regard; in any case this discretization error also tends to vanish with reduction of mesh size.

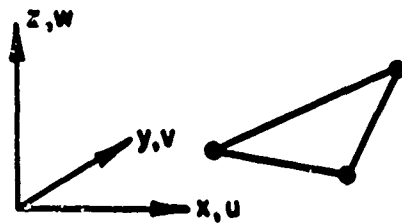
The fourth approximation is basic to all shell theory, regardless of whether the analysis is to be performed by the finite element method or not. This is the assumption that the shell may be treated as a two-dimensional surface and involves simplifying constraints on the variations of displacements through the shell thickness. A finite element formulation may employ any standard assumptions of shell theory for this purpose, such as the Kirchhoff hypothesis. However, it is interesting to note that somewhat less restrictive assumptions can be made in forming a shell element by degeneration of a general three-dimensional element, with the result that shear distortions may be accounted for without difficulty by this approach.

FACTORS AFFECTING SOLUTION EFFICIENCY

Element Properties

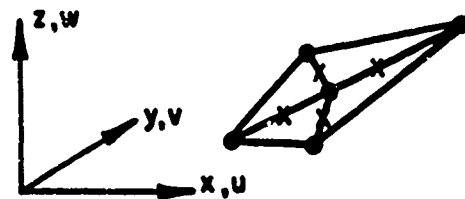
From the preceding discussion, it is apparent that the types of elements employed in a finite element analysis may have a major effect on the efficiency of the analytical procedure. To illustrate this effect in a specific example, seven different elements were employed in the analysis of a simple cylindrical shell roof structure. These elements are divided into three categories: (1) flat plates, (2) curved triangles based on shell theory, (3) degenerate three-dimensional hexahedrons of quadratic form. They are portrayed in Fig. 1, and their principal features are listed below.

FLAT TRIANGLES



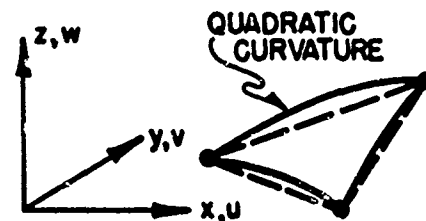
- A. u, v - linear
 w - cubic
5 DOF per node
- B. u, v, w - cubic
9 DOF per node

QUADRILATERAL ASSEMBLAGE



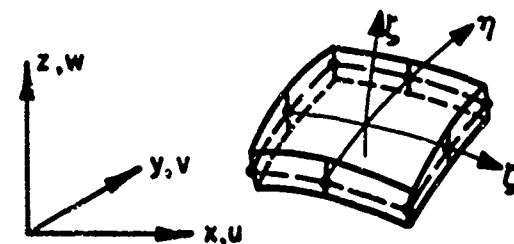
- C. u, v - partially
constr. quadratic
 w - cubic
5 DOF per external node
Corners generally not in
same plane.

CURVED TRIANGLES



- D. u, v - linear
 w - cubic
5 DOF per node
- E. u, v, w - cubic
9 DOF per node

DEGENERATE 3-D



- F. x, y, z } quadratic
 u, v, w }
No deformation on lines
in z direction
5 DOF per node
- G. Similar to F, but with
selective integration
of strain energy.

FIG. 1 TYPES OF ELEMENTS CONSIDERED

(1) Flat Plate Elements:

A. Simple Triangle [4]. The membrane stiffness of this element is represented by the well-known constant strain triangle [13] while its plate bending property is given by the fully compatible HCT element [3] based on cubic displacement patterns. It has five degrees of freedom (DOF) per node.

B. Refined Triangle [5]. This element also has the HCT bending stiffness, but provides a refined membrane behavior by employing the same cubic interpolation for the in-plane displacements. Interelement compatibility is thereby maintained, but a total of 9 DOF are defined at each node, including membrane strains.

C. Quadrilateral [14]. This element has the same HCT bending stiffness, but employs a partially restrained linear strain triangle to improve the membrane behavior. For reasons of computational efficiency, four triangle elements are assembled into a general quadrilateral, the central node being located at the average of the coordinates of the four corner nodes. The interior degrees of freedom are eliminated at the element level prior to assembling, thus the quadrilateral effectively has only 20 DOF, 5 per node.

A slightly improved version of this element is employed in two shell programs currently in use at Berkeley. It uses the LCCT-11 plate bending element [15], so a rotational DOF is added at each interior mid-side node. These 4 extra DOF are also eliminated at the element level, thus the final quadrilateral retains only 20 DOF.

(2) Curved Triangles:

D. Basic Element [16]. This is essentially a curved equivalent of the simple flat triangle (A) above, with linear membrane displacements and cubic bending displacements. It is based on shallow shell theory, and the surface is curved quadrilaterally relative to the base triangle.

E. Refined Element [17]. This is the curved equivalent of the flat refined element (B) above, with exactly the same types of membrane and

bending displacements. It has the same quadratically curved surface as (D), and also is based on shallow shell theory.

(3) Degenerate 3-Dimensional Elements:

F. Basic Quadratic Element [18]. This shell element is derived from a standard 20 node isoparametric element, by introducing the constraint that any line through the element thickness (z direction) displaces in translation or rotation without distortion. This is equivalent to part of the Kirchhoff shell theory assumption, but retains a simple shear distortion capability. The mid-surface geometry is quadratically curved, and the thickness may vary quadratically as well. The element derivation is based on general three-dimensional elasticity; the displacement interpolations are of a bi-quadratic form.

G. Improved Quadratic Element [19]. This element is based on Element (F), but its stiffness results from a modified evaluation of the strain energy. The essential difference is that the number and location of the Gauss integration points used in the evaluation of the shear strain energy are selected differently. The details of the procedure used are too complicated to be discussed here, but the essential concept of the improvement can be explained easily with reference to a rectangular plane stress model (Fig. 2).

This simple rectangular element is notoriously poor in its representation of simple bending, such as would be induced by the end moments of Fig. 2B. The assumed displacement functions require that the element edges remain straight, thus the deformation produced by the pure moment loading is as shown by the solid lines rather than the correct curved shape shown by the dashed lines. The difference between these is represented by the shear strain energy developed in the solid line deformed shape in Fig. 2b; if this shear strain energy were omitted the stiffness representation of the element would be greatly improved. Of course, it would not be effective to omit the

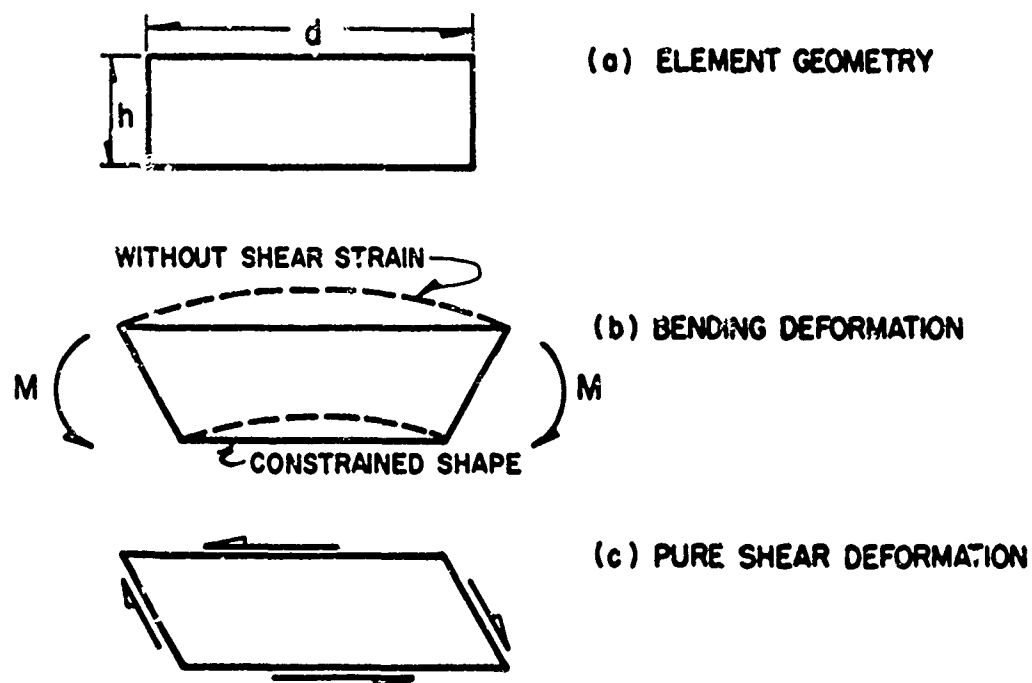


FIG.2 DISTORTION BEHAVIOR OF PLANE STRESS
ELEMENT

shear strain energy under all conditions of deformation; for example, the strain due to the pure shear loading of Fig. 2c should be retained. The practical procedure to obtain a suitable representation of the shear strain energy for this element is to use its centroid as the only shear strain integration point; this neglects the shear strain of Fig. 2b, and includes that of Fig. 2c.

This simple example illustrates the idea of utilizing modified integration points selected so as to suppress undesirable element behavior. It is important to note that this modification becomes more significant as the element becomes more elongated (as h/d gets smaller). It is because of this fact that the modified integration procedure is so important in improving three-dimensional elements which are to be used as thin or moderately thick shell elements. The problem is somewhat less acute when dealing with a quadratic element such as (F) rather than the simple linear element of this discussion, but the resulting improvement in performance is still noteworthy.

The structure considered in this element comparison is shown in Fig. 3, a cylindrical shell supported by rigid diaphragms at each end. The vertical deflections computed at the mid-span section of the shell are shown in Fig. 4, the results from a coarse mesh (4×5) in the upper graph and the fine mesh results (8×12) below. Comparing the results obtained for the flat plate elements A, B and C, it is evident that the membrane interpolation functions have a major effect on the analysis -- a constant strain element does not have enough flexibility. Comparing elements A and D it appears that the curvature in element D is beneficial, however, the curvature is less important than the membrane interpolation functions, as is apparent in comparing B and D. The worst performance of all elements is given by F -- it is clear

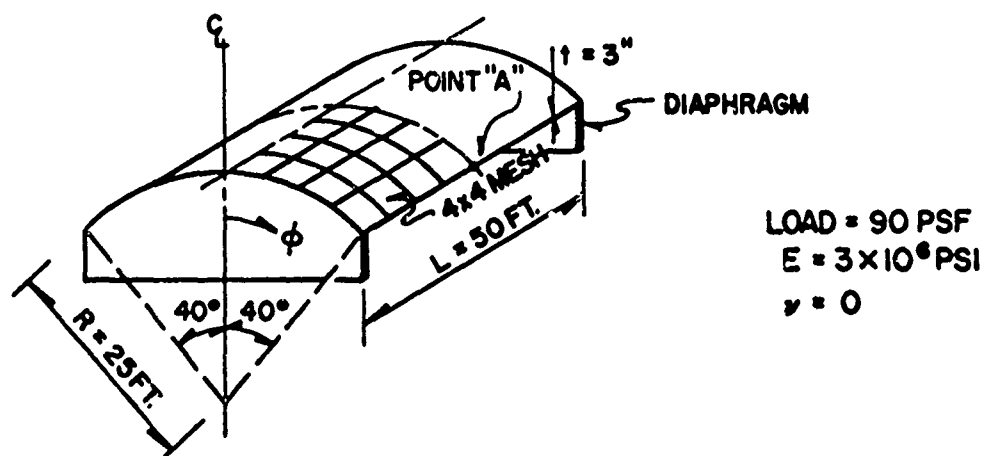


FIG. 3 CYLINDRICAL SHELL - STATIC ANALYSIS

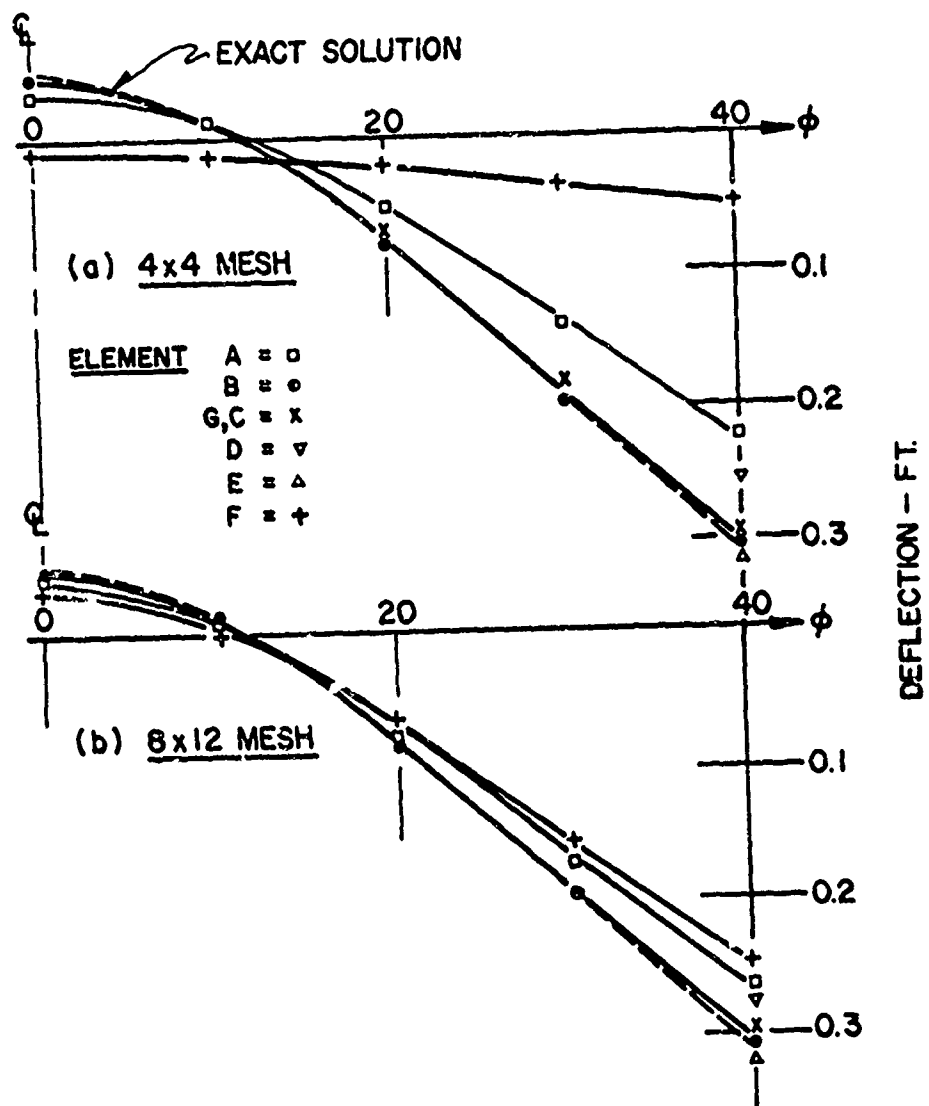


FIG. 4 VERTICAL DEFLECTION AT MID-SPAN

that this degenerate three-dimensional element cannot deform like a thin shell element. However, by merely introducing selective integration as in element G the results are competitive with the best of the thin shell elements. Similar conclusions can be drawn from the stress distribution results of Fig. 5. Although only the longitudinal membrane forces are shown here, the same relative element efficiency was observed with regard to all components of shell stress.

Although this single example can hardly be considered as conclusive evidence, it appears from this analysis that curvature is not essential in a finite element, and that the form of displacement assumption is as important as the geometric assumption. The degenerate three-dimensional element with selective strain integration appears to offer great promise as a general analytical tool.

Nodal "Sixth" Degree of Freedom

It will be noted in the element descriptions of Fig. 1 that most of the elements have 5 DOF per node, when defined in the local element coordinate system. However, when the element properties are transformed to the global coordinates for assembly, a sixth degree of freedom must be considered. The manner of treating this sixth DOF has a major effect on the analysis efficiency as will be explained in this section. For convenience, this discussion will consider a flat plate system in which membrane and bending stiffnesses are uncoupled; similar observations apply to curved elements, however.

With reference to a local (x, y, z) Cartesian coordinate system, the stiffness of an element may be expressed

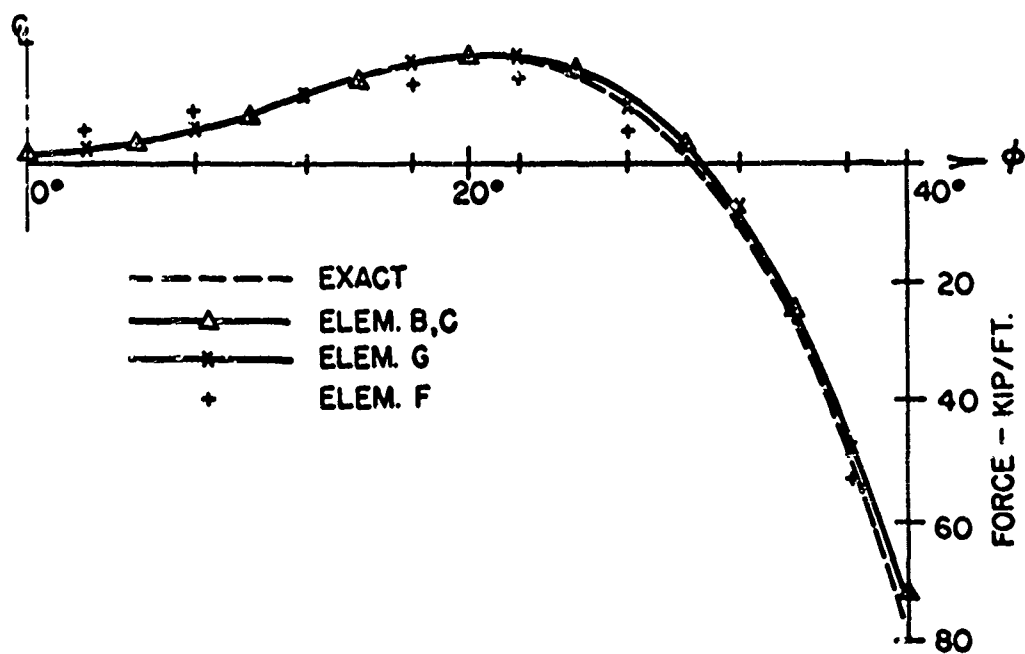


FIG. 5 LONGITUDINAL FORCE @ MID-SPAN

$$\begin{Bmatrix} N_x \\ N_y \\ Q \\ M_x \\ M_y \\ T \end{Bmatrix} = \begin{bmatrix} k_{11} & k_{12} & 0 & 0 & 0 & 0 \\ k_{21} & k_{22} & 0 & 0 & 0 & 0 \\ 0 & 0 & k_{33} & k_{34} & k_{35} & 0 \\ 0 & 0 & k_{43} & k_{44} & k_{45} & 0 \\ 0 & 0 & k_{53} & k_{54} & k_{55} & 0 \\ 0 & 0 & 0 & 0 & 0 & 0 \end{bmatrix} \begin{Bmatrix} u \\ v \\ w \\ \theta_x \\ \theta_y \\ \theta_z \end{Bmatrix} \quad (1)$$

or, in abbreviated form

$$\underline{S} = \underline{k} \underline{r} \quad (2)$$

In Eq. 1, each term in the force and displacement vector represents a subvector of dimensions corresponding to the number of element nodes, and the stiffness matrix terms are square matrices of the same dimensions. The 2 x 2 set of stiffness submatrices represents the membrane stiffness while the 3 x 3 set is the bending stiffness. The sixth row and column of \underline{k} are associated with the "sixth" degree of freedom, the rotation about the normal to the element surface. In ordinary shell theory, this type of displacement is not involved in describing the structural displacements; nor is it needed to represent the element stiffness in the local coordinates, as will be noted from the fact that the terms in the sixth row and column are zero. It is included to facilitate the transformation to the global coordinate system.

The relationship between translational displacements expressed in the local coordinates and in a global Cartesian coordinate system (\hat{x} , \hat{y} , \hat{z}) may be expressed

$$\begin{Bmatrix} u \\ v \\ w \end{Bmatrix} = \hat{\underline{\Phi}} \begin{Bmatrix} \hat{u} \\ \hat{v} \\ \hat{w} \end{Bmatrix} \quad (3)$$

where $\hat{\underline{\Phi}}$ is an appropriate arrangement of the direction cosines. The rotational displacement relationship is expressed similarly

$$\begin{Bmatrix} \theta_x \\ \theta_y \\ \theta_z \end{Bmatrix} = \hat{\Phi} \begin{Bmatrix} \hat{\theta}_x \\ \hat{\theta}_y \\ \hat{\theta}_z \end{Bmatrix} \quad (4)$$

Thus, the complete transformation becomes

$$\underline{r} = \begin{bmatrix} \hat{\Phi} & 0 \\ 0 & \hat{\Phi} \end{bmatrix} \underline{\hat{r}} = \underline{\Phi} \underline{\hat{r}} \quad (5)$$

and the transformed element stiffness matrix is given by

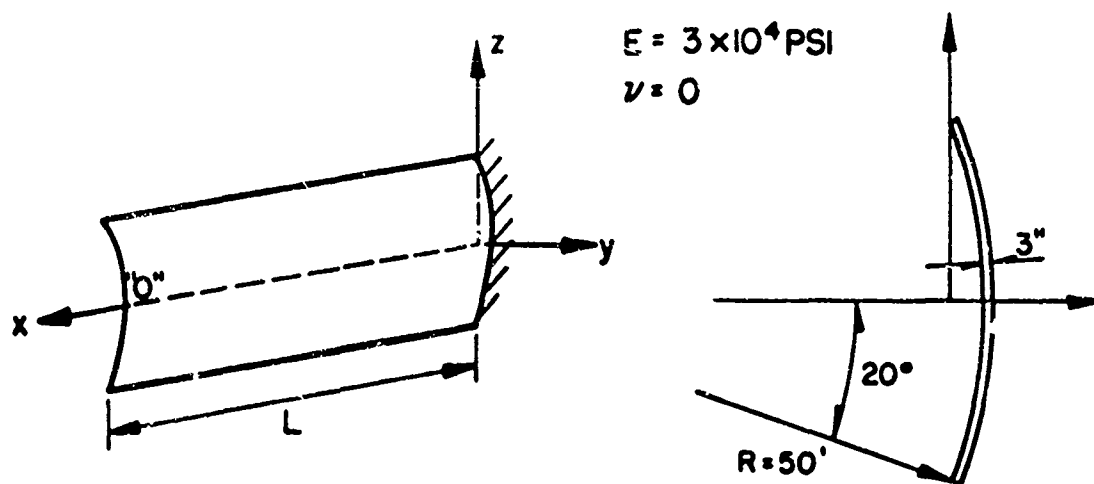
$$\underline{\hat{k}} = \underline{\Phi}^T \underline{k} \underline{\Phi} \quad (6)$$

In general, the element stiffness matrix expressed in global coordinates, $\underline{\hat{k}}$, will be fully populated even though the local coordinate matrix is very sparse. Thus the sixth degree of freedom becomes a factor in the analysis after the global transformation and a variety of procedures have been employed to account for its effect.

In principle, the 6th DOF need cause no complication in the analytical procedure. It is possible merely to carry out the transformation as indicated and to consider the full set of 6 DOF at each node of the assembled structure in the displacement solution. A problem will arise in this procedure if all the elements associated with any one node lie in the same plane because the resultant stiffness in the 6th DOF at this node will be zero. This singularity of the stiffness matrix can be eliminated easily, however, by merely replacing the zero diagonal term by any arbitrary number. The major disadvantage of this direct analytical approach is the loss of computational efficiency. Only 5 DOF per node are needed to represent the deformations of the shell. The 6th DOF is an unnecessary quantity and to include it increases the equation solution time by a factor of approximately $(6/5)^3 = 1.728$ which is a significant cost.

In order to eliminate the sixth DOF, it obviously is necessary that the global coordinate system be associated with the tangent plane at each node of the assemblage. A practical expedient is to take as the normal the average of the normal directions associated with each of the elements connected at the node. When the structural stiffness has been transformed to this coordinate system, the sixth DOF may be eliminated by merely eliminating the corresponding row and column from the stiffness matrix. (In actual practice, this degree of freedom would be omitted in the assembly process [4].) Eliminating this DOF is equivalent to introducing a constraint in the structure corresponding with the normal rotation at each node.

In most circumstances, this constraint has a negligible effect on the structural behavior because the structural configuration would permit only small rotations of this type in any case, and the coupling stiffness coefficients are small when the angle between elements is small. Comparative studies made with the same finite element system, merely including or excluding the sixth DOF have shown that the results are essentially the same for any practical structure. An example of such studies is shown in Fig. 6 [20] -- a circular cylindrical shell is clamped at one end, and allowed to deflect under its own weight. Five different lengths were considered, ranging from 25 to 200 feet; the plane quadrilateral element "C" was used with a mesh having 4 elements in the circumferential direction and from 5 to 10 in the longitudinal direction, depending on this length. The vertical deflections computed at the mid-point of the free end for the five cases are listed in Table I. These results show that even in the very flexible cantilever cases the sixth DOF constraint causes only a negligible reduction of deflection -- much less than one percent.



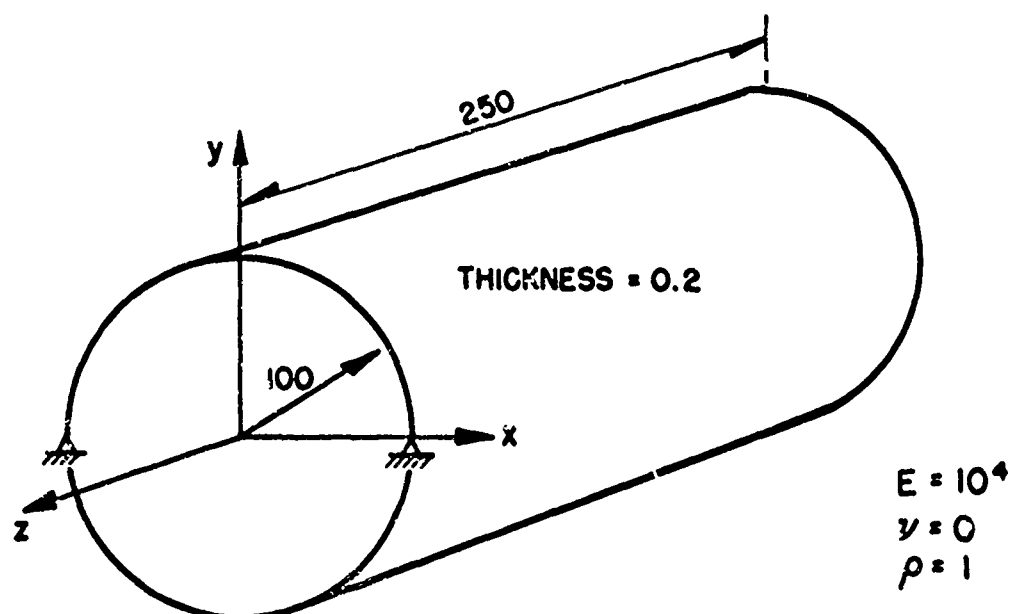
**FIG.6 INFLUENCE OF SIXTH DEGREE OF FREEDOM -
CANTILEVER SHELL**

Table 1: Deflection of Cylindrical Shell

Length	Deflection of Point "0" (ft)		
	5 DOF	6 DOF	Difference
25	0.03695	0.3696	0.03
50	0.2374	0.2375	0.04
100	1.303	1.307	0.31
160	4.501	4.509	0.18
200	8.064	8.075	0.14

In any case where the actual structure is free to rotate without constraint, it is evident that the nodal constraints in the 5 DOF system will have a more significant effect. In order to investigate this condition, the vibration frequencies were evaluated for a very flexible circular cylinder supported by hinges at one end and free at the other. The dimensions and physical properties of the shell are shown in Fig. 7. Taking account of double symmetry, only one quarter of the shell was considered in the analysis, using 5 elements in the circumferential direction and 7 longitudinally. The first three modes of vibration computed for the 5 and 6 DOF systems are listed in Table II. The influence of the nodal constraint is clearly evident in the first mode frequency. In this structure, the rotation about the support hinges should be unconstrained and the frequency of this mode should be zero. The constraint completely invalidates the result for the first mode -- however, it is evident that the effect on the frequencies of the higher modes is negligible, a fraction of a percent.

On the basis of these studies, it may be concluded that the constraint of the sixth DOF is a practical expedient for increasing computational efficiency in ordinary shell analysis. The sixth DOF can be retained if it is desired for any reason, as in the analysis of structures which may undergo rigid body rotations. In such analyses, there is no physical justification for the inclusion of an artificial membrane stiffness associated with the normal rotation; however, it has been found expedient in some programs to avoid singularities and solution sensitivity by introducing a small external spring in this DOF.



**FIG.7 INFLUENCE OF SIXTH DEGREE OF FREEDOM -
HINGED SHELL**

Table II: Frequency of Hinged Cylinder (rad/sec)

Mode	5 DOF	6 DOF
1	0.000274	0.000001311
2	0.004221	0.004211
3	0.004863	0.004841

LINEAR DYNAMIC ANALYSIS

Equation of Motion

The dynamic analysis of shell structures idealized by an assemblage of finite elements is not significantly different from the analysis of other types of structural systems. The equations of motion for an elastic structural system may be written as

$$\underline{M} \ddot{\underline{r}} + \underline{c} \dot{\underline{r}} + \underline{k} \underline{r} = \underline{P}(t) \quad (7)$$

in which

- \underline{M} = the mass matrix
- \underline{c} = the viscous damping matrix
- \underline{k} = the elastic stiffness matrix
- \underline{r} = the nodal displacement vector
- $\underline{P}(t)$ = the corresponding nodal force vector

and where the dots denote differentiation with respect to time.

The stiffness, damping and mass matrices are formed by a direct assembly process of the corresponding element matrices which are formed in a local coordinate system and transformed to the global system.

The approximations introduced in the development of the stiffness idealization were discussed in the previous section. The errors associated with the damping matrix are difficult to define, since the internal energy absorption mechanism in the structure is seldom known well enough to permit a formal development of the damping matrix. Instead it is customary to establish the damping ratio for each mode of vibration of the structure on the basis of experience with similar structures. These modal damping ratios may then be used directly in a mode superposition analysis, or they may be transformed to an equivalent damping matrix if an explicit relationship is required. The development of the mass matrix may be based on a physical mass lumping approach or the consistent mass method; the advantages and disadvantages of both of these methods will be discussed later.

After all matrices are defined in equation (7) it is possible to solve for the dynamic response of the system "exactly"; however, in order to reduce the number of numerical operations additional approximations are often necessary. In the mode superposition method all the frequencies of the system may not be required. In the direct step-by-step integration of the equations of motion it may be possible to use a larger time step.

Mass Approximation

For all shell elements it is possible to develop a consistent mass matrix based on the same displacement field assumptions as used in the development of the element stiffness matrix. For some structures this approach leads to improved accuracy; however, there is a significant increase in computational effort which must be evaluated in comparison with the physical mass lumping procedure. For other structures, however, the consistent mass approach yields less accurate results [21]. For example, in wave propagation problems the consistent mass formulation causes undesirable oscillations near the wave front. If the consistent mass formulation is used with a displacement compatible element one can prove that the resulting frequencies are larger than the true frequencies; since most shell elements have some form of incompatibility this bounding advantage of the consistent mass formulation is lost. With a lumped mass system the frequencies may be above or below the true frequencies; this, of course is one reason why more accurate results can be obtained with the lumped mass model for many structures.

The most important disadvantage of the consistent mass formulation is the increase in computational effort. The consistent mass matrix for an element may be expressed by the following integral equation

$$\underline{m} = \int_{vol} \rho \underline{\phi}^T \underline{\phi} dv , \quad (8)$$

where ρ is the mass density and $\underline{\phi}$ is the basic displacement field approximation within the element. For a simple shell element the displacements are of cubic

order; therefore, the terms in the consistent mass matrix involve the integration of terms of sixth or higher order. This may cause problems in numerical sensitivity; or, if numerical integration is used a large number of integration points within the element may be required in order to accurately evaluate these higher order functions. In fact, the numerical effort involved in evaluating the consistent mass matrix may be greater than required for the development of the element stiffness matrix.

For shells the mass associated with the normal rotational degree of freedom is not defined. As in the formation of the stiffness matrix, the transformation of the local element mass matrices to global coordinates produces mass terms for all six degrees of freedom. For flat plates or shallow shells a singularity in the mass matrix may exist. It is apparent that the frequencies associated with the normal rotations may be in great error and have little physical significance. It appears that the reduction of the nodal mass matrix to five degrees of freedom by the same technique used to reduce the stiffness matrix is a reasonable approach.

Mode Shapes and Frequencies

For most systems, the most significant numerical difficulty associated with the use of the consistent mass matrix is in the solution of the eigenvalue problem

$$\underline{k} \underline{X} = \omega^2 \underline{M} \underline{X} . \quad (9)$$

For large systems, where both the stiffness and mass matrices are symmetric, positive definite and banded, a direct solution is complex. If the inverse iteration technique is used, the banded characteristics of the system are recognized and a single eigenvalue can be determined with a reasonable amount of numerical effort. However, if large numbers of eigenvalues are required the approach can require a large amount of computer time. The use of a diagonal lumped mass matrix reduces the required computer storage and time by approximately a factor of two.

For many systems where only the lower frequencies are required the Rayleigh-Ritz method can be employed in order to reduce the computational requirements. A family of approximate displacements can be generated by the application of different load patterns to the system. These displacements are then used to generate an eigenvalue problem of reduced size. Except in the evaluation of the consistent mass matrix at the element level very little additional computations are required to use the consistent mass approach with the Rayleigh-Ritz method, since both the lumped and consistent mass representations yield an eigenvalue problem of reduced size with a full mass matrix. If a rational approach is developed which automatically selects the required load patterns this approach provides a very efficient technique for the evaluation of the eigenvalues of large shell structures.

Mode Superposition Analysis

In general, the mode superposition method is advantageous when a limited number of modes can be used to describe the response of the structure. If a large number of modes are required the computational effort in the evaluation of the frequencies and mode shapes and in the superposition of the modal effects can be large. Structures for which the Rayleigh-Ritz method is applicable are ideal for analysis by the mode superposition method. This approach has been used for large structural systems subjected to long duration earthquake loads and the required numerical effort was not significantly larger than for a static analysis with the same number of load conditions.

Step-by-Step Analysis

The direct step-by-step integration of the equations of motion is an approach which does not require the solution of the eigenvalue problem. It is particularly advantageous for large systems subjected to short duration loads where a large number of modes are excited. Therefore, this approach is generally

used for blast or impact problems. For structures where nonlinear materials or large deformations are important it is the only feasible method.

There are many different techniques available for the direct numerical integration of the dynamic equilibrium equations. They can be classified into two groups -- implicit and explicit.

The implicit method requires a solution of equations at each time step. However, for linear systems with a constant time interval the equations need be triangularized only once. Only a forward reduction and a back substitution are required at each time step.

The principal disadvantage of all explicit, or extrapolation, methods is that they are unstable if the time interval is not selected sufficiently small; therefore, those methods are not practical for many types of applications. It is of interest to point out, however, that the well known 'method of characteristics' is equivalent to a lumped mass idealization and a simple extrapolation procedure. This approach essentially selects a time integration procedure with errors that conceal the errors in the stiffness and mass approximations. Since this is only possible on simple systems it has little practical value in the solution of complex shell structures.

Many implicit methods are also unstable. The addition of artificial damping may increase the stability limit. If the largest frequency of the system is known it is possible to select a time step to insure stability. For most shell structures, however, the frequencies associated with the membrane component are very large; therefore it is not practical to select the time step sufficiently small to insure stability. In general one can say "the finer the mesh the larger the frequencies". Just one small stiff element may cause the system to have a very high frequency component.

The step-by-step method which has been found to be very effective in the solution of both shell and solid finite element systems is an implicit approach which is unconditionally stable for all time steps [22]. The operations required by this method are summarized in Table III. The errors associated with this technique have the effect of producing damping of the high frequency components and are a function of the ratio of the time step to the period. Therefore, a time step can be selected which produces an acceptable level of damping in these higher modes. If the frequency components of the applied loads are examined, this may serve as a guideline for the selection of the time step. This error has the effect of truncating the number of frequencies which participate in the response.

The use of a full consistent mass matrix in the step-by-step approach requires approximately twice as many numerical operations as the lumped mass idealization. Also, additional computer storage is required for the full mass matrix; since it is desirable to retain all necessary data in core storage during the step-by-step procedure the additional storage requirements can be important.

NONLINEAR DYNAMIC ANALYSIS

Equation of Motion

The force equilibrium equation of motion at time t for a structural system with nonlinear stiffness properties may be written as

$$M \ddot{r}_t + c \dot{r}_t + (\underline{E}_{t-\Delta t} + \underline{K}_t \underline{\Delta r}) = \underline{P}_t \quad (10)$$

where $(\underline{E}_{t-\Delta t} + \underline{K}_t \underline{\Delta r})$ represents the internal nodal forces carried by the system of structural elements in which

$\underline{E}_{t-\Delta t}$ = the nodal forces at the previous time step

$\underline{K}_t \underline{\Delta r}$ = the change in nodal forces during time step

$\underline{\Delta r} = \underline{r}_t - \underline{r}_{t-\Delta t}$ = the change in nodal displacements during time step

Table III: Step-by-Step Dynamic Analysis (Linear Systems)

A. Initial Calculation

1. Form stiffness matrix \underline{K} and mass matrix \underline{M} .

2. Calculate the following constants. Assume $\underline{C} = \alpha \underline{M} + \beta \underline{K}$.

$$\begin{aligned} \tau &= 1.5 \Delta t & a_5 &= 3 \beta a_4 / \tau - 4 / \tau^2 \\ a_0 &= (6 + 3\alpha\tau) / (\tau^2 + 3\beta\tau) & a_6 &= 2 \beta a_4 - 4 / \tau \\ a_1 &= 6 / \tau^2 + 3(\alpha - \beta a_0) / \tau & a_7 &= (\beta \tau a_4 - 2) / 2 \\ a_2 &= 6 / \tau + 2(\alpha - \beta a_0) & a_8 &= \Delta t / 2 \\ a_3 &= 2 + (\alpha - \beta a_0) / 2 & a_9 &= \Delta t^2 / 3 \\ a_4 &= 4 / (3\beta\tau + \tau^2) & a_{10} &= \tau^2 / 6 \end{aligned}$$

3. Form effective stiffness matrix $\underline{K}^* = \underline{K} + a_0 \underline{M}$.

4. Triangularize \underline{K}^* .

B. For Each Time Increment

1. Form effective load vector \underline{P}^*

$$\underline{P}^* = \underline{P}_t + \underline{M} [a_1 \underline{r}_{t-\Delta t} + a_2 \dot{\underline{r}}_{t-\Delta t} + a_3 \ddot{\underline{r}}_{t-\Delta t}] .$$

2. Solve for effective displacement vector \underline{r}^*

$$\underline{K}^* \underline{r}^* = \underline{P}^* .$$

3. Calculate new acceleration, velocity and displacement vectors

$$\begin{aligned} \ddot{\underline{r}}_t &= a_4 \underline{r}^* + a_5 \underline{r}_{t-\Delta t} + a_6 \dot{\underline{r}}_{t-\Delta t} + a_7 \ddot{\underline{r}}_{t-\Delta t} \\ \dot{\underline{r}}_t &= \dot{\underline{r}}_{t-\Delta t} + a_8 (\ddot{\underline{r}}_t + \ddot{\underline{r}}_{t-\Delta t}) \\ \underline{r}_t &= \underline{r}_{t-\Delta t} + \Delta t \dot{\underline{r}}_{t-\Delta t} + a_9 \ddot{\underline{r}}_{t-\Delta t} + a_{10} \ddot{\underline{r}}_t . \end{aligned}$$

4. Calculate element stresses if desired.

5. Repeat for next time increment.

\underline{K}_t = the tangent stiffness matrix.

Since $\underline{E}_{t-\Delta t}$ can be calculated and the damping is normally neglected in nonlinear analysis, equation (10) can be rewritten

$$\underline{M} \ddot{\underline{r}}_t + \underline{K}_t \underline{\Delta r} = \underline{P}_t - \underline{E}_{t-\Delta t} \quad (11)$$

This equation can be solved by the same stable step-by-step method used for linear dynamic analysis. The sequence of operations for a nonlinear dynamic analysis is given in Table IV.

Evaluation of Tangent Stiffness

The tangent stiffness matrix at a particular time is the sum of the incremental elastic stiffness matrix, \underline{K}_i , and the geometric stiffness matrix, \underline{K}_g ,

$$\underline{K}_t = \underline{K}_i + \underline{K}_g$$

The incremental elastic stiffness matrix is formed in the deformed position by the standard approach. For nonlinear materials the appropriate incremental stress-strain relationship associated with the stresses at that time must be used. The geometric stiffness matrix is a function of the stresses within the element. As in the evaluation of the consistent mass matrix, a formal procedure can be used which is a function of all displacements and all stresses within the element. It has been found that for both plate and shell structures an approximate equation for the geometric stiffness yields satisfactory results. It involves only the membrane components of stress and the displacements normal to the shell surface.

In the element coordinate system it is given by

$$\underline{k}_g = \int_{vol} \begin{bmatrix} \underline{\phi}_{,1} & \underline{\phi}_{,2} \end{bmatrix}^T \begin{bmatrix} \tau_{11} & \tau_{12} \\ \tau_{21} & \tau_{22} \end{bmatrix} \begin{bmatrix} \theta_{,1} \\ \phi_{,2} \end{bmatrix} dv \quad (12)$$

where 1 and 2 are the coordinate axes associated with the membrane stresses and $\underline{\phi}$ is the interpolating function for the displacement normal to the shell.

In Equation (12), τ_{ij} are the membrane components of stress.

Table IV: Step-by-Step Nonlinear Dynamic Analysis

A. Initial Calculations

1. Form stiffness matrix \underline{K} and mass matrix \underline{M} .
2. Solve for initial displacements, strains, stresses and internal forces due to static loads.
3. Calculate the following constants:

$$\begin{array}{lll}
 \theta = 1.5 & a_2 = a_0/\theta & a_6 = \tau/2 \\
 \tau = \theta \Delta t & a_3 = a_1/\theta & a_7 = \tau^2/6 \\
 a_0 = 6/\tau^2 & a_4 = a_1/a_0 & a_8 = 2a_7 \\
 a_1 = 6/\tau & a_5 = 2/a_0 &
 \end{array}$$

B. For Each Time Increment

1. Calculate tangent stiffness matrix \underline{K}_t
2. Form effective stiffness matrix $\underline{K}^* = \underline{K}_t + a_0 \underline{M}$.
3. Triangularize \underline{K}^* .
4. Form effective load vector \underline{P}^* .

$$\underline{P}^* = \underline{P}_t - \underline{E}_{t-\Delta t} + a_0 \underline{M} [a_4 \dot{\underline{r}}_{t-\Delta t} + a_5 \ddot{\underline{r}}_{t-\Delta t}] .$$

5. Solve for change in displacements \underline{r}^*

$$\underline{K}^* \underline{r}^* = \underline{P}^* .$$

6. Calculate new acceleration, velocity and displacement vectors

$$\ddot{\underline{r}}_t = a_2 \underline{r}^* - a_3 \dot{\underline{r}}_{t-\Delta t} - \ddot{\underline{r}}_{t-\Delta t}$$

$$\dot{\underline{r}}_t = \dot{\underline{r}}_{t-\Delta t} + a_6 [\ddot{\underline{r}}_t + \ddot{\underline{r}}_{t-\Delta t}]$$

$$\underline{r}_t = \underline{r}_{t-\Delta t} + \Delta t \dot{\underline{r}}_{t-\Delta t} + a_7 (\ddot{\underline{r}}_{t-\Delta t} + 2\ddot{\underline{r}}_{t-\Delta t}) .$$

7. Calculate strains, stresses and internal force vector.
8. For next time step return to 1 or 4.

Also, it has been found that an approximate normal displacement function which does not involve joint rotations can be used; therefore, ϕ_1 and ϕ_2 represent an average surface rotation of the shell element. Also, if numerical integration is used a very low order method may be employed.

Evaluation of Element Forces

The evaluation of the element forces, E , at a given time is the most important step in the nonlinear analysis. If they are calculated by summing incremental changes in forces it is possible to accumulate errors. However, if they are evaluated directly from the total displacements of the system, errors will not accumulate and the need for a very accurate tangent stiffness is eliminated. It is of interest to note that for static nonlinear analysis equation (11) reduces to a check of the equilibrium of the system in the deformed position.

A formal approach for the evaluation of the force vector E is as follows:

1. Within each element calculate the strain distribution from the total displacements by the direct application of the nonlinear strain displacement equations.
2. From the appropriate stress-strain relationship calculate the corresponding stresses (force per unit area in the deformed position).
3. From virtual work the nodal forces at the element level can be calculated from the stress distribution.
4. The element forces are transformed to the global system and combined to form the total force vector E .

However, for most structures with linear materials and small strains, this formal method is not required. It is possible to calculate nodal element forces by multiplying the incremental elastic stiffness by the total displacement in the deformed position of the element.

EXAMPLES OF FINITE ELEMENT ANALYSES

Vibration Frequencies of Cylindrical Shell [20]

The lowest vibration mode shapes and frequencies of the cylindrical roof structure shown in Figure 8 were computed by inverse iteration, using successively refined mesh arrangements to determine the convergence behavior of the finite element method for this class of structure. The type of finite element used was a quadrilateral assemblage of flat plate triangles (element type C as described above). The results of the analysis, showing the first six symmetric vibration frequencies for meshes 2, 4, 6 and 8 elements along each side of one quarter of the shell, are presented in Table V. From these results it is clear that the 4 x 4 mesh gives quite good behavior, and even the very crude 2 x 2 mesh gives meaningful values for the first two modes.

Dynamic Response of Cylindrical Shell [20]

The structure of Figure 8 was next subjected to a uniformly distributed half sine wave impulsive loading, with a peak intensity of 90 psf as shown in Figure 9a. The first two analyses were carried out without consideration of the inertia forces, thus they were effectively "static" analyses even though the displacements changed with time. One of these analyses was linear, i.e., it was assumed that the geometry was unchanged during the analysis and the geometric stiffness was neglected. The second analysis included both of these nonlinear effects. The vertical deflection of the mid point of the free edge computed in these analyses is shown in Figure 9b; the deflection is reduced by about 25 percent in the nonlinear case. Figure 9c shows the corresponding solutions for the two dynamic cases in which inertial forces are considered. The dynamic deflections are larger than the static, as would be expected. Also the nonlinear vibratory response is somewhat faster than the linear.

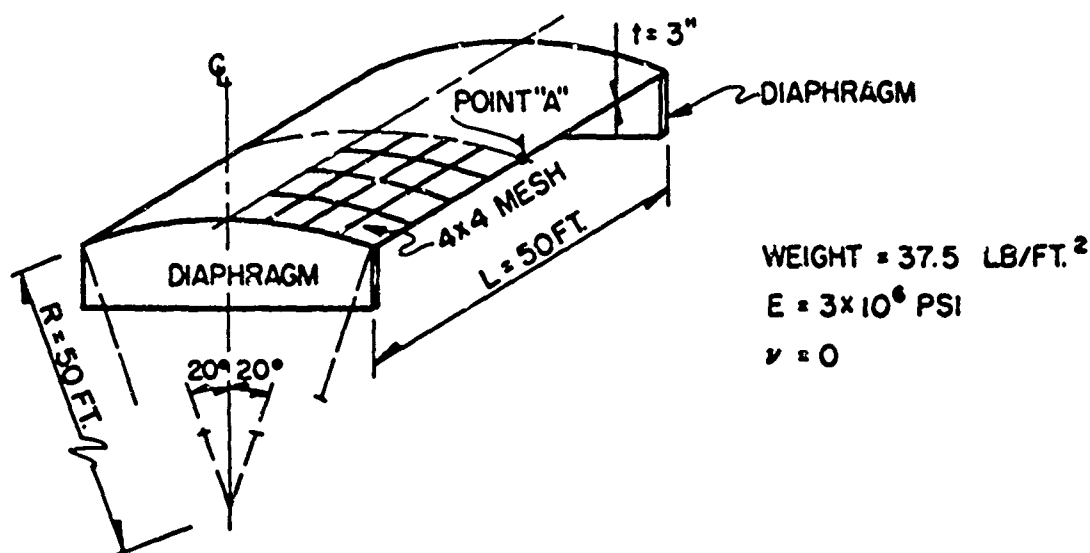


FIG. 8 CYLINDRICAL SHELL — DYNAMIC ANALYSIS

Table V: Symmetrical Vibration Frequencies

Mode Mesh	1	2	3	4	5	6
2 x 2	8.614	22.52	-----	-----	-----	-----
4 x 4	9.643	24.49	33.88	42.81	64.20	68.95
6 x 6	9.765	24.24	34.17	44.99	68.99	70.31
8 x 8	9.777	24.09	34.08	45.95	69.73	70.93

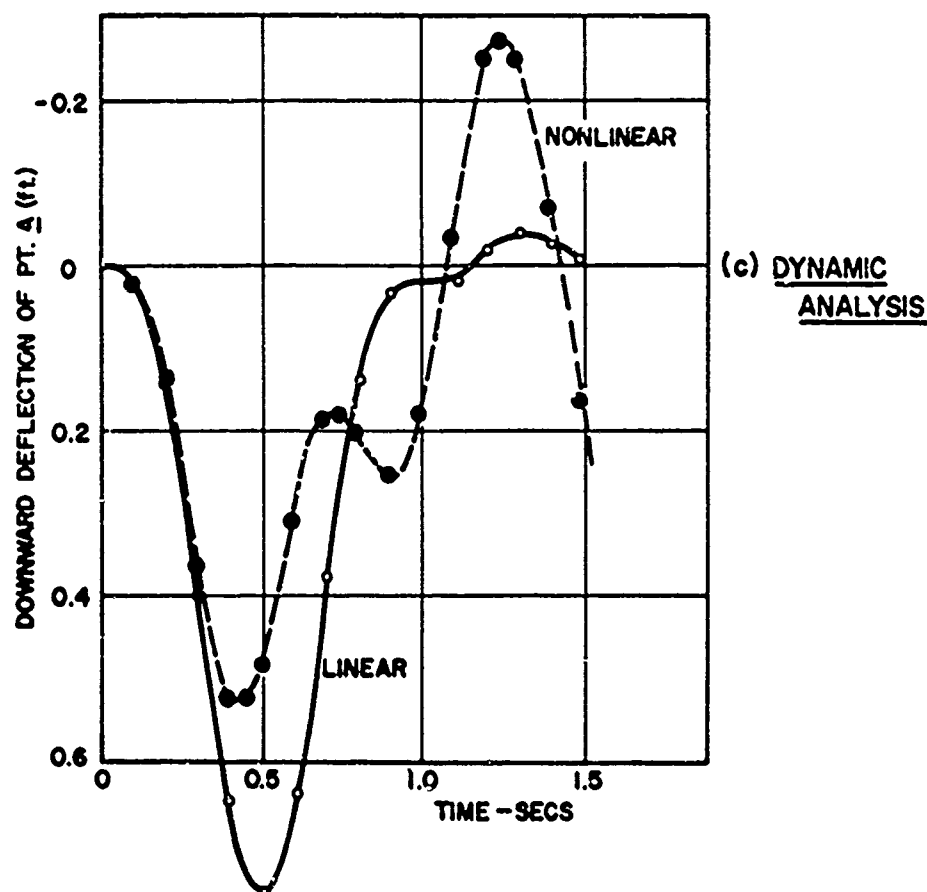
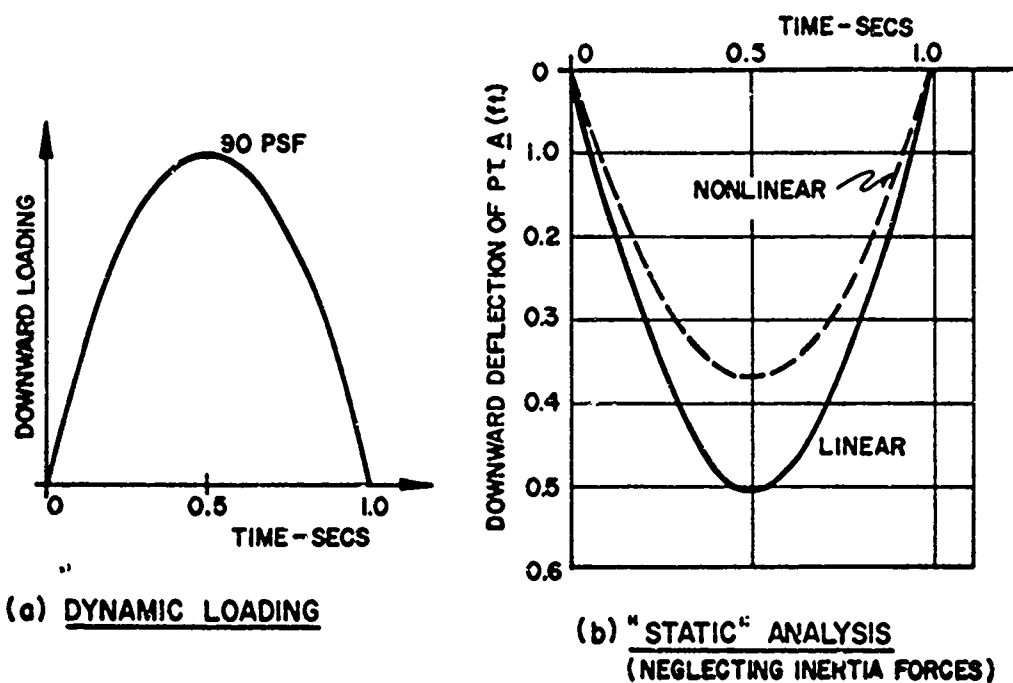


FIG. 9 DYNAMIC RESPONSE OF CYLINDRICAL SHELL

Snap-Through of Spherical Shell [20]

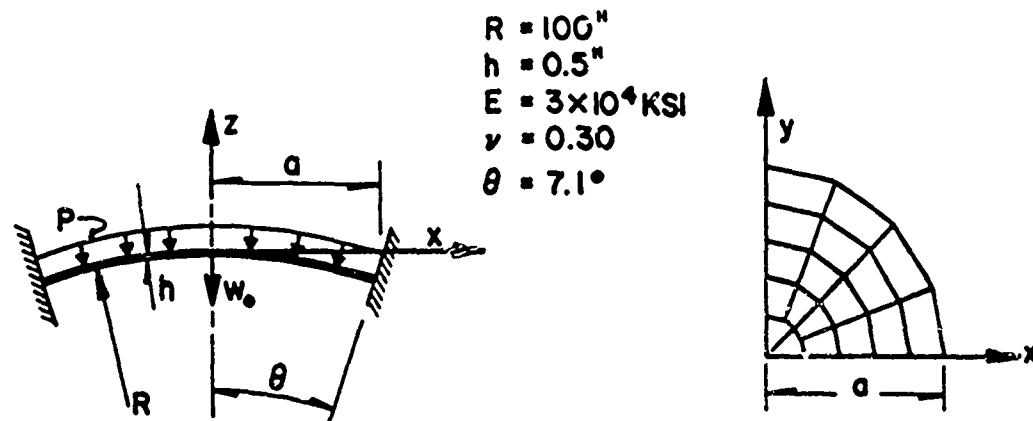
An example of the snap-through buckling of a spherical shell is shown in Figure 10. This example demonstrates the effectiveness of the simple incremental, load-balancing nonlinear analysis procedure described above. The geometry of the shell is shown in Figure 10a, the finite element mesh in Figure 10b. The vertical deflection of the middle of the shell produced by increasing load is shown in Figure 10c. It will be noted that the analytical process is somewhat erratic as the deflection behavior nearly develops a negative slope, but the inherent stability of the procedure is demonstrated by the return to the correct behavior in the later stages of loading.

Wind Loading of a Cooling Tower [20]

A practical application of the nonlinear dynamic analysis procedure is presented in Figures 11-13. The basic dimensions of a typical cooling tower are shown in Figure 11a, together with the finite element mesh for one-quarter of the structure (actually, half of the shell was included in the analysis). The distribution of radial wind pressure about the shell is shown in Figure 11b, and the assumed time variation of loading is shown in Figure 11c. It will be noted that the peak pressure is 0.2 psi, or 28.8 psf.

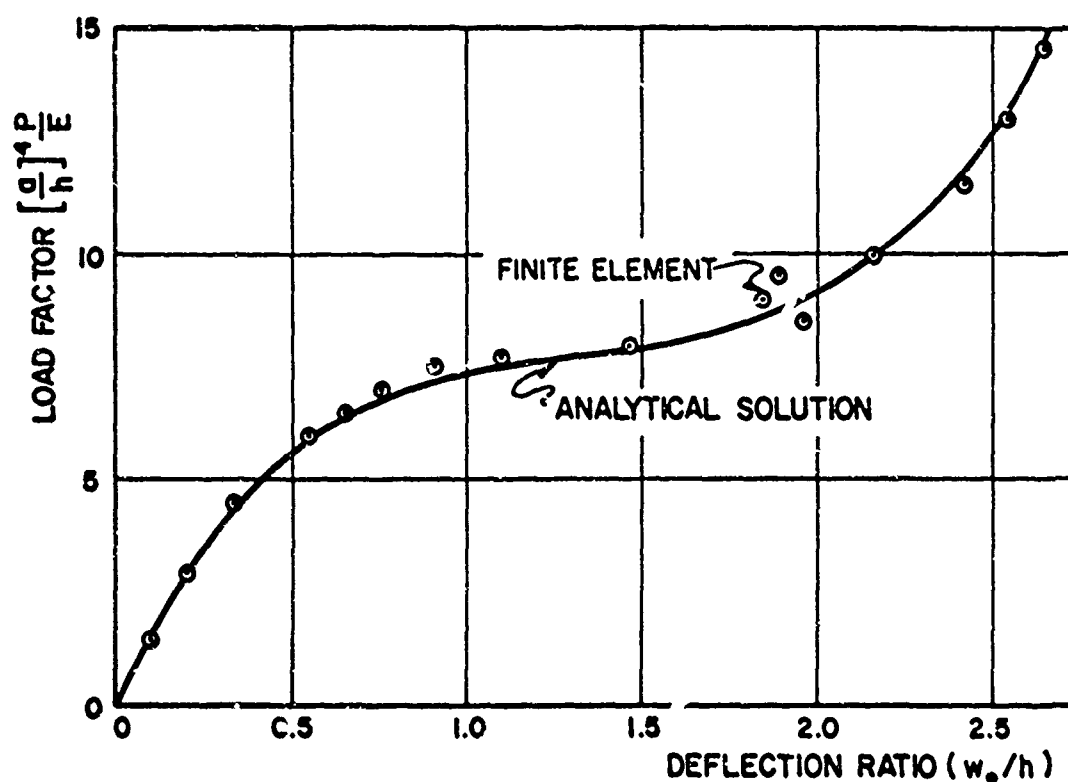
The wind is applied in the negative x direction, i.e., it acts directly against nodes 1 through 8 on the x axis. The dynamic radial (inward) deflection of nodes 1, 3, 5, 7 is shown in Figure 12, in the solid lines. Also shown in this figure (with the dashed lines) are the deflections computed in a second analysis using a peak pressure of 1.0 psi. These deflections have been divided by 5 to permit their comparison with the previous analysis. The deviation of the dashed curves from the solid lines demonstrates the influence of nonlinearity in the response.

With the increased loading, the analysis showed that the deflections became very large after about $t = 0.55$ seconds, i.e., a dynamic buckling occurred.



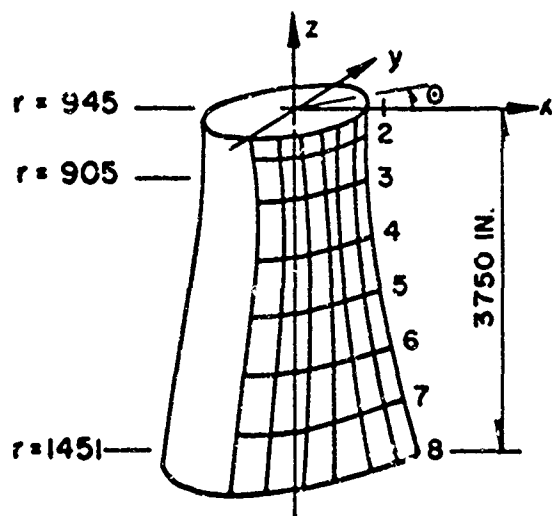
(a) GEOMETRY AND LOADING

(b) FINITE ELEMENT MESH

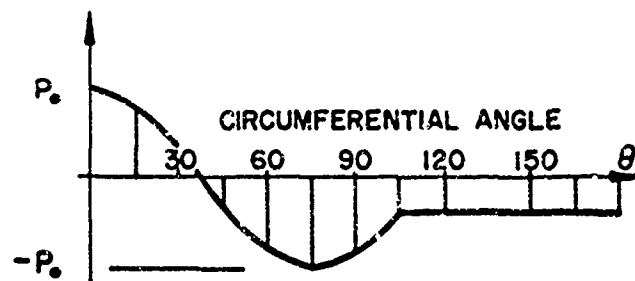


(c) COMPUTED DEFLECTIONS

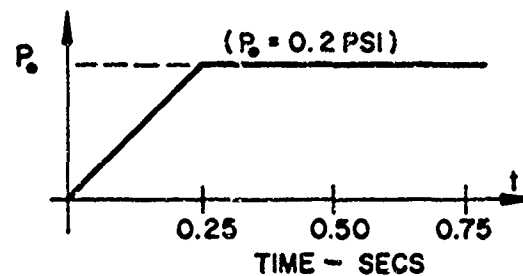
FIG. 10 SNAP-THROUGH OF SPHERICAL SHELL



a. GEOMETRY & MESH LAYOUT



b. LOAD DISTRIBUTION



c. TIME VARIATION OF LOAD

FIG. II DYNAMIC ANALYSIS OF COOLING TOWER

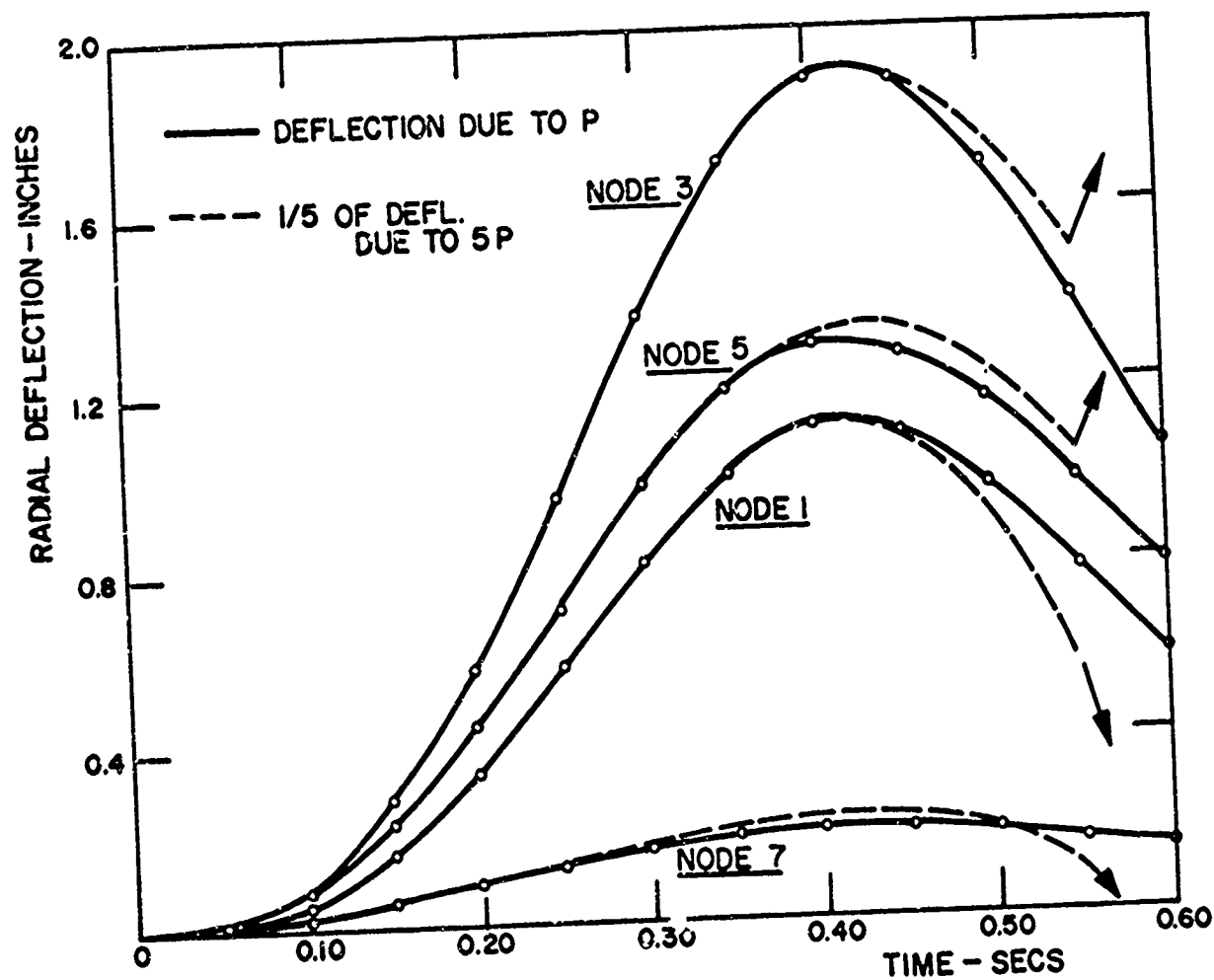


FIG. 12 DYNAMIC RESPONSE OF COOLING TOWER

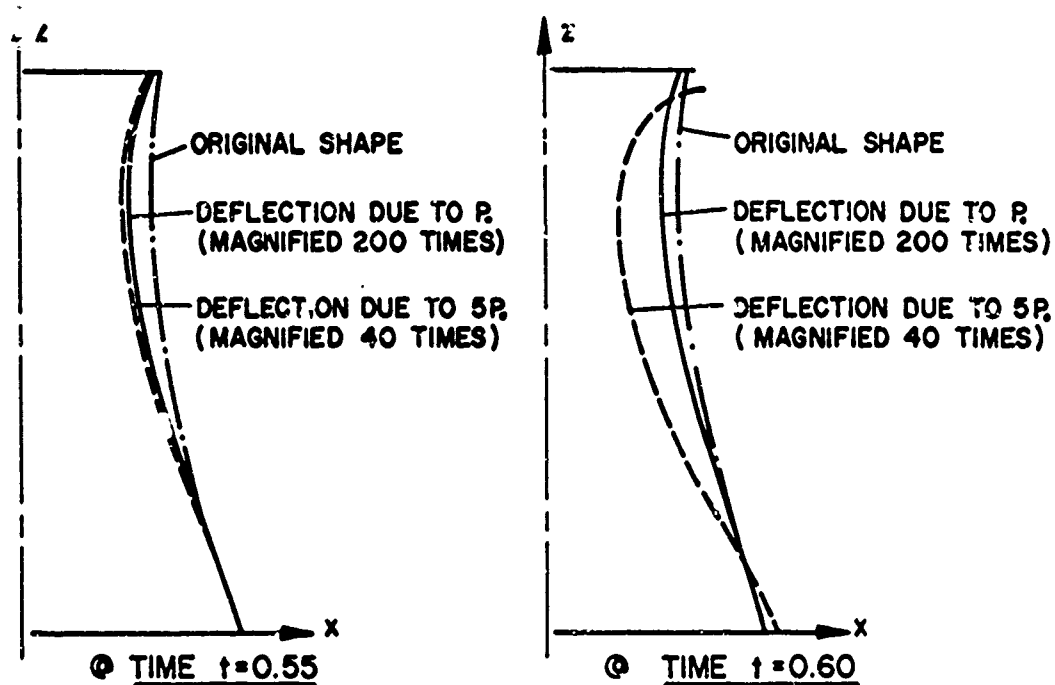


FIG. 13 DEFLECTIONS PRECEDING COLLAPSE

Figure 13 shows the deflections building up immediately prior to collapse. The deflections are multiplied many times to make it possible to see the collapse behavior. The drastic change of the dashed line shape between $t = 0.55$ and $t = 0.60$ shows that collapse has already started.

CONCLUSIONS

1. The finite element method provides an effective means for the analysis of arbitrary shell structures. The linear response to dynamic loadings which excite only a few modes of vibration may be computed conveniently by mode-superposition. The linear response to high rate, localized loads, and analyses accounting for material or geometric non-linearities may be obtained by simple step-by-step procedures.
2. Shell analysis programs based on many different types of finite elements have been found to give satisfactory results. Valid comparisons between them can be made only on the basis of computational efficiency, and the quadrilateral formed of flat triangles has been found to be among the most efficient.
3. In developing a general shell element, the approximation made with regard to element geometry should be consistent with the displacement interpolation approximation. Preliminary results indicate that shell elements which are degenerated from quadratic isoparametric three dimensional elements (and therefore have a consistent geometric and deformation assumption) may prove to be more efficient than present types.
4. Constraint of the sixth DOF (rotation about the shell normal) is desirable for computational efficiency, and has no significant effect on the shell behavior except in cases where the shell is free to rotate as a rigid body. In this type of system, a complete 6 DOF formulation should be used.

5. The consistent mass formulation leads to a higher order approximation of inertia forces than of the forces associated with elastic deformations, whereas in most systems the inertia forces are of lesser importance. For this reason, and also because other approximations (such as interelement incompatibilities and numerical integrations) invalidate the energy bound principle, the use of consistent masses is seldom justified in the analysis of shell structures. A lumped mass approximation is recommended for use with elements employing low order displacement interpolations. For higher order elements, a low order (possibly linear) displacement interpolation will provide a satisfactory mass approximation. It should be noted that a diagonal (lumped) mass matrix leads to a significant simplification of a direct eigenvalue solution; however, a banded mass matrix imposes essentially no penalty in a Raleigh-Ritz vibration analysis.

REFERENCES

1. Adini, A., "Analysis of Shell Structures by the Finite Element Method", Ph.D. Thesis, University of California, Berkeley, 1961.
2. Clough, R. W. and Tocher, J. L., "Analysis of Thin Arch Dams by the Finite Element Method", Proc. Symp. on Theory of Thin Arch Dams, University of Southampton, Pergamon Press, 1965.
3. Clough, R. W. and Tocher, J. L., "Finite Element Stiffness Matrices for the Analysis of Plate Bending", Proc. (First) Conf. on Matrix Methods in Structural Mechanics, Wright-Patterson AFB, Ohio, 1965.
4. Clough, R. W. and Johnson, C. P., "A Finite Element Approximation for the Analysis of Thin Shells", International Journal of Solids & Structures, Vol. 4, Pergamon Press, Great Britain, 1968.
5. Carr, A. J., "A Refined Finite Element Analysis of Thin Shell Structures Including Dynamic Loadings", Structural Engineering Laboratory Report No. 67-9, University of California, Berkeley, California, 1967.
6. Johnson, C. P., "The Analysis of Thin Shells by a Finite Element Procedure", Structural Engineering Laboratory Report No. 67-22, University of California, Berkeley, California, 1967.
7. Cantin, R. and Clough, R., "A Curved Cylindrical Shell Discrete Element", AIAA Journal, Vol. 6, No. 5, May 1968.

8. Utku, S., "Stiffness Matrices for Thin Triangular Elements of Non-Zero Gaussian Curvature", AIAA Journal, Vol. 5, No. 9, September 1967.
9. Dhatt, G., "Numerical Analysis of Thin Shells by Curved Triangular Elements Based on Discrete-Kirchhoff Hypothesis", Proc. of Symposium on Application of Finite Element Methods in Civil Engineering, Vanderbilt University, 1969.
10. Key, S. W. and Beisinger, Z., "The Analysis of Thin Shells with Transverse Shear Strains by the Finite Element Method", Proc. (Second) Conf. on Matrix Methods in Structural Mechanics, Wright-Patterson AFB, Ohio, 1968.
11. Ahmad, S., Irons, B. and Zienkiewicz, O., "Analysis of Thick and Thin Shell Structures by Curved Finite Elements", International Journal for Numerical Methods in Engineering, Vol. 2, No. 3, July 1970, pp. 419-451.
12. Pawsey, S., "Analysis of Moderately Thick to Thin Shells by Finite Elements", Ph.D. Thesis, University of California, Berkeley, September 1970.
13. Turner, M. J., et al., "Stiffness and Deflection Analysis of Complex Structures", Journal of Aeronautical Science, Vol. 23, No. 9, 1956.
14. Clough, R. W. and Johnson, C. P., "Finite Element Analysis of Arbitrary Thin Shells", ACI Symposium on Concrete Thin Shells, April 1970, New York.
15. Clough, R. W. and Felippa, C. A., "A Refined Quadrilateral Element for Analysis of Plate Bending", Proc. (Second) Conf. on Matrix Methods in Structural Mechanics, Wright-Patterson AFB, Ohio, 1968.
16. Strickland, G. and Loden, W., "A Doubly-Curved Triangular Shell Element", Proc. (Second) Conf. on Matrix Methods in Structural Mechanics, Wright-Patterson AFB, Ohio, 1968.
17. Dhatt, G., "Numerical Analysis of Thin Shells by Curved Triangular Elements Based on Discrete-Kirchhoff Hypothesis", Proc. of Symposium on Application of Finite Element Methods in Civil Engineering, Vanderbilt University, 1969.
18. Ahmad, S., Irons, B. and Zienkiewicz, O., "Analysis of Thick and Thin Shell Structures by Curved Finite Elements", International Journal for Numerical Methods in Engineering, Vol. 2, No. 3, July 1970, pp. 419-451.
19. Pawsey, S., "Analysis of Moderately Thick to Thin Shells by Finite Elements", Ph.D. Thesis, University of California, Berkeley, September 1970.
20. Yeh, C. H., "Dynamic Non-Linear Analysis of Thin Shells", Ph.D. Thesis, University of California, Berkeley, to be completed December 1970.
21. Clough, R. W., "Structural Vibrations and Dynamic Response", Proceedings, Japan-U.S. Seminar on Matrix Methods of Structural Analysis and Design, August 1969, Tokyo, Japan.
22. Farhoomand, I., "Nonlinear Dynamic Stress Analysis of Two-Dimensional Solids", Ph.D. Thesis, University of California, Berkeley, June 1970.

FIGURE TITLES

- Figure 1. Types of Elements Considered
- Figure 2. Distortion Behavior of Plane Stress Element
- Figure 3. Cylindrical Shell - Static Analysis
- Figure 4. Vertical Deflection at Mid-Span
- Figure 5. Longitudinal Force at Mid-Span
- Figure 6. Influence of Sixth Degree of Freedom - Cantilever Shell
- Figure 7. Influence of Sixth Degree of Freedom - Hinged Shell
- Figure 8. Cylindrical Shell - Dynamic Analysis
- Figure 9. Dynamic Response of Cylindrical Shell
- Figure 10. Snap-Through of Spherical Shell
- Figure 11. Dynamic Analysis of Cooling Tower
- Figure 12. Dynamic Response of Cooling Tower
- Figure 13. Deflections Preceding Collapse

LIST OF TABLES

	<u>Page</u>
Table I. Deflection of Cylindrical Shell	11a
Table II. Frequency of Hinged Cylinder	12a
Table III. Step-By-Step Dynamic Analysis (Linear Systems)	18a
Table IV. Step-By-Step Nonlinear Dynamic Analysis	19a
Table V. Symmetrical Vibration Frequencies	21a

QUESTIONS AND COMMENTS FOLLOWING CLOUGH'S PAPER

QUESTION: I have a comment and a question. The comment concerns the sixth degree of freedom. As you realize, the sixth degree of freedom may be degenerate. A similar degeneracy may also arise due to any mathematical formulation which results in a stiffness matrix that has fewer elastic degrees of freedom than the difference between the total and rigid body degrees of freedom. Thus, the analyst can have a structure that is kinematically unstable and a degeneracy can arise; the question is what do you do about it? Well, if you are an analyst, you understand the sixth degree of freedom is degenerative and you can strike it out. That's perfectly proper if you have a flat plate and you analyze it in rotated coordinates. However, the computer should be able to understand this problem. There's no need to delete the sixth degree of freedom and it is dangerous to do so, I feel. I think the computer should recognize the inconsistency in the equations that is introduced if you introduce a load in the sixth degree of freedom and it should automatically delete any extra equations in the solution process. In other words, you can perform the decomposition independent of the degeneracies. You can decompose a singular stiffness matrix. However, when we proceed to the backward solution process, you will then reach a point where you must divide by a zero diagonal. If the right-hand sides are also zero, the equations are consistent and you can proceed. If they are not, you have an inconsistency in the formulation; then the analyst should be thrown off the computer.

My question is concerned with the collapse of the structure in your transient response analysis. It's been our experience that this collapse may be a

pseudo-collapse due to the time interval being too large compared with the high frequencies of the system and my question is, is this a real collapse of the structure or are we talking about an analysis collapse?

CLOUGH: I agree that you can get a pseudo-collapse from numerical effects. In this particular instance, however, I'm sure it is a collapse associated with the development of instabilities in local parts of the structure as evidenced by the geometric stiffness terms that are generated. In addition, the collapse clearly is associated with a time scale related to the dynamic response of the complete structure.

As far as your comments on the sixth degree of freedom are concerned, I agree with what you say in general. However, in a flat plate assemblage approximation of a shell structure, the sixth degree of freedom is not a degenerative degree of freedom, of course. What you're talking about is throwing out this degree of freedom as a part of the numerical analysis procedure. I'm talking about eliminating it as a result of structural intuition, I would say. I'm throwing it out and recognizing that in doing so I'm constraining the structure relative to that degree of freedom. This is an actual physical constraint and it shows up in that one example of the rigid body rotation capability.

COMMENT: We've had some experience with the sixth degree of freedom also. As Prof. Clough has pointed out, if six degrees of freedom are used at every node, then it is possible in modeling shell structures to end up with uncoupled degrees of freedom or an implied uncoupling in the final stiffness matrix. Under these circumstances, numerical difficulties can cause the run to be aborted or large errors to occur in the rotational

displacements (but not in the translational displacements). On the other hand, it is possible in modeling a shell to eliminate the rotation about the normal to the shell surface and use only five degrees of freedom at a node. Because of the finite angles between the plate elements, however, this leads to unwanted constraints which may or may not cause significant errors in the solution.

We have used both of these approaches on occasion, utilizing engineering judgment to decide which way to go. When we use six degrees of freedom, we insert very soft beams or torsional springs into the structure where necessary to prevent uncoupling of the rotation. In using only five degrees of freedom, we rely on rigid body checks of the unconstrained stiffness matrix to indicate the magnitude of error to expect in solving problems with the model.

CLOUGH: I think it's very appropriate to do what you do which is to use your judgment on whether those sixth degrees of freedom are important to your problem or not. For civil engineering classes of structures, I'm convinced that we don't permit flexibilities in the structure sufficient that this kind of artificial constraint will ever be meaningful, but in aeronautical structures and mechanisms in general I'm sure that this conclusion is not always going to be true.

MIXED FORMULATIONS FOR FINITE ELEMENT SHELL ANALYSES

by

Leonard R. Herrmann
Professor of Civil Engineering
University of California
Davis Campus

and

William E. Mason, Graduate Student
University of California
Davis Campus

ABSTRACT

The paper briefly discusses: (1) the basic concepts underlying a mixed formulation finite element shell analysis, (2) a general shell analysis program based upon a low order mixed formulation flat element, (3) proposed higher order mixed formulation flat elements, and (4) mixed formulation curved shell elements.

A general discussion of the advantages and disadvantages of displacement and mixed finite element procedures is given. The relative accuracy of mixed formulation and displacement predictions is discussed. The basic theory underlying the authors' development of a mixed finite element shell analysis is presented. Particular attention is given to the problem of maintaining compatibility at shell intersections and at the interfaces of flat elements used to approximate curved surfaces.

A description is given of the particular low order mixed formulation element utilized in the development of a static linear program for arbitrary

shells. Results for analyses of both simple and complicated shell configurations are given. The significance of the artificial discontinuity moments which may be generated due to the representation of a curved surface by flat elements is discussed and illustrated.

Possible advantages and disadvantages of higher order mixed formulation flat and curved shell elements are discussed.

INTRODUCTION

One approach used for the development of finite element analyses utilizes the Ritz procedure in conjunction with a variational equation expression of the physical problem [1, 2, 3, 4]. Probably the most fundamental variational descriptions of structural problems are given by the principles of virtual displacements and virtual variations of the state of stress [5]; for this discussion descriptions which are special cases of these principles are employed. The behavior of structural shells can alternatively be expressed by variational equations derived from the theorem of minimum potential energy or the theorem of minimum complementary energy, or by mixed variational equations [6,7].

A finite element analysis based upon the theorem of minimum potential energy yields approximate solutions which (a) exactly satisfy internal compatibility (assuming that the approximate displacement field satisfies the admissibility conditions of the theorem of minimum potential energy), displacement boundary conditions, and the stress strain law, and (b) approximately satisfies the equilibrium equations and the traction boundary conditions. A finite element analysis based upon the theorem of minimum complementary energy yields approximate solutions which (a) exactly satisfy the equilibrium equations, the stress boundary conditions, and the stress strain law and (b) approximately satisfy compatibility and the displacement boundary conditions. Finite element procedures based upon mixed variational equations yield approximate solutions that exactly and approximately satisfy the governing field and boundary equations in some other combination than those described above.

With so many possibilities existing for the development of competing forms of finite element procedures, the question of which procedure should be utilized for a given class of structural problems needs to be considered.

It appears that most investigators have adopted the displacement approach

without thoroughly investigating the alternative possibilities. Their a priori adoption of a displacement approach would appear to be a consequence of their experiences with frame analyses for which displacement procedures appear to have inherent advantages over force approaches. It would appear, however, that the question should be re-examined for each class of structural problems. Such considerations have revealed certain applications for which mixed formulations are definitely preferable [4] and have indicated others for which stress approaches may be preferable [8].

The objective of the present paper is to stimulate interest in the question of the desirability of developing and utilizing mixed formulation finite element analyses for structural shells. The consideration of mixed formulation finite element procedures is motivated by the fact that they would appear to overcome several difficulties which are associated with traditional displacement approaches.

Because of the high order displacement expansions that must be used in order to permit the satisfaction of the compatibility requirements, displacement plate and shell bending elements are inherently quite complex. These algebraic complexities result in significant "element form times" (rather large "element form times" are particularly significant for those incremental analyses for which it is necessary to reform the element matrices for each increment). The mixed formulation shell elements utilized to date are significantly less complicated and hence considerably fewer operations are involved in the formulation of the element matrices. Because of this relative simplicity the development of a mixed curved shell element may be more straightforward than the analogous displacement formulation development.

Many of the displacement analyses that have been developed to date utilize different order membrane, transverse deflection and rotation expansions, hence, although they satisfy compatibility for plate applications, they violate compatibility (i.e., they do not completely satisfy the admissibility conditions of the theorem of minimum potential energy) for those applications for which adjacent elements do not lie in a common plane. Adjacent elements do not, in general, lie in a common plane when a shell surface is approximated by plate elements and/or at folded plate or shell intersections. The question, of the importance of these incompatibilities, has not been completely resolved. The mixed formulation elements employed to date satisfy the admissibility conditions of the underlying variational equation even though adjacent elements do not lie in a common plane.

There is considerable controversy regarding the inability of displacement approaches to account for normal (to the shell surface) rotational degrees of freedom. Because mixed formulation procedures do not employ rotational degrees of freedom, this question does not arise.

Lastly, displacement shell analyses may be criticized for the fact that the moments, which are usually the quantities of primary interest, are calculated by taking derivatives of the approximate displacement field, an operation which leads to a considerable loss of accuracy. In the mixed approach, however, the moments are calculated directly and thus should be more accurate.

The main criticism, to date, of mixed formulations concerns the computational effort required to solve the simultaneous equations. Because mixed elements usually have unknowns associated with side points, even

though the number of elements and the number of degrees of freedom per element should be the same, the number of equations and band width would be considerably greater for a mixed approach than for a displacement approach. Additionally, at common intersections of three or more shells it is necessary, due to the non-uniqueness of the normal moment quantity, to introduce still additional unknowns. Questions concerning possible undesirable characteristics of the simultaneous equations caused by the mixing of displacement and stress unknowns and the resulting appearance of zeroes (these zeroes, of course, disappear during the solution of the equations) on the diagonal have been raised. The authors, however, have experienced little difficulty in solving the equations with conventional elimination codes (care has been taken to normalize the unknowns so that numerically they are of the same order of magnitude).

The actual significance of the several suggested advantages and disadvantages of mixed and displacement formulations has not really been evaluated, hence, at this point no definitive statement of the relative merits of the two approaches can be made. Ultimately the relative merits of the two procedures can only be judged by comparing the cost of the computational effort necessary to achieve comparable results for a wide class of shell problems. Such a comparison must be deferred until decisions concerning the best types of displacement and mixed elements have been reached and until a single investigator has at his disposal programs specifically tailored for each of the two procedures. The programs used for such a comparison must each take advantage of the special characteristics of the appropriate formulation.

MIXED FORMULATION

Mixed variational equations may be obtained by specializing the general variational equations given in references [6,7] or may be constructed as alternative statements of a particular partial differential equation expression of the physical problem. The latter procedure was employed in the development of the formulation to be discussed herein [9,10]. Other possibilities for expressing the plate equations by a mixed variational equation of course exist.

The plane stress and bending behavior of a plate may be described by the following variational equation:

$$\delta(F + \Pi_m) = 0 \quad (1)$$

where

$$\begin{aligned} F = & \iint_B \left\{ -qw - Sm_T (M_x + M_y) + M_{x,x} w_{,x} \right. \\ & + M_{y,y} w_{,y} + M_{xy,y} w_{,x} + M_{xy,x} w_{,y} \\ & \left. - S \left[(1 + \nu) M_{xy}^2 + \frac{1}{2} M_x^2 + \frac{1}{2} M_y^2 - w_{,x} M_{,y} \right] \right\} dx dy \\ & - \oint_{S_1} w_{,s} M_{ns} ds - \int_{S_2} V_n^a w ds \\ & - \int_{S_3} R_n^a M_n ds \end{aligned} \quad (2)$$

$$S = \frac{12}{Eh^3} \quad (3)$$

$$m_T = E \int_{-h/2}^{h/2} \alpha_T \Delta T z dz \quad (4)$$

The potential energy for a state of plane stress expressed as a function of the in-plane displacements (u, v) is denoted as Π . The symbols $q, w, (M_x, M_y, M_{xy}), (E, \nu), h, \alpha_T$ and ΔT , respectively, denote the transverse load, the transverse deflection, the bending moments, the elastic constants, the plate thickness, the linear coefficient of thermal expansion, and the temperature change.

The surface integral is evaluated over the entire plate B . The first line integral is evaluated counterclockwise around each element representing the plate. The second and third line integrals are evaluated (in a counterclockwise direction) along those portions of the plate boundaries where V_n and R_n are respectively specified. The symbols V_n^a and R_n^a , respectively, denote specified values of effective shear and normal rotation.

The values of the resultants along a boundary whose outward normal is denoted by n , are (β denotes the angle between x and n)

$$M_n = M_x (\cos \beta)^2 + M_y (\sin \beta)^2 + M_{xy} \sin 2\beta \quad (5)$$

$$M_{ns} = \frac{1}{2}(M_y - M_x) \sin 2\beta + M_{xy} \cos 2\beta \quad (6)$$

$$Q_n = Q_x \cos \beta + Q_y \sin \beta \quad (7)$$

The primary dependent variables are the reference surface displacement components (u, v, w) and the moment components (M_x, M_y, M_{xy}) . An admissible state for the primary variables is one in which (a) the prescribed moment and reference surface displacement boundary conditions are satisfied, (b) there are continuous second derivatives within each element, and (c) the expressions for u, v, w and M_n are continuous across all element interfaces.

The Euler equations for the above variational equation are (a) the in-plane equilibrium equations expressed in terms of the displacements u and v , (b) the moment curvature relationships, and (c) the transverse equilibrium equation expressed in terms of the moments. The essential boundary conditions are the prescription of the reference surface displacements and the normal moment on the plate boundaries and their continuity across all element interfaces. The natural boundary conditions are the prescription of the in-plane forces, effective shear and normal rotation on the boundaries and their continuity across all element interfaces. Thus, a finite element analysis which utilizes Equ. (1) (a) exactly satisfy reference surface displacement continuity and boundary conditions, and moment equilibrium across element and actual boundaries, and (b) will approximate slope continuity, slope boundary conditions, force boundary conditions, the equilibrium equations and the moment curvature relationships. It needs to be emphasized that this approximation of slope continuity is not at all the same as the violation of compatibility by a non-conforming displacement element. In the latter case certain of the admissibility conditions of the governing variational equation are violated (this violation may vanish in the limit as the element size shrinks to

zero) whereas in the former case they are not.

The displacement approach for plates admissibility requirement of continuity of slopes is a consequence of the fact that the minimization of the potential energy is equivalent to a fourth order partial differential equation expression of the problem. The slope continuity admissibility condition is not a requirement of Equ. (1) because this variational equation is equivalent to a second order partial differential equation description of the plate problem.

It is of interest to examine the specialization of Equ. (1) for beam bending (in the absence of thermal effects):

$$\delta F = 0 \quad (8)$$

where

$$F = \int_0^L \left[-qw + M_{,x} w_{,x} + \frac{1}{2EI} (M)^2 \right] dx - \sum V^a w - \sum R^a M \quad (9)$$

The symbols V^a and R^a denote specified shears and rotations. The admissibility conditions for the primary dependent variables w and M are continuity and satisfaction of the displacement and moment boundary conditions.

Equ. (8) is equivalent to the following differential equation expression of the beam bending problem.

$$M = EI \frac{d^2 w}{dx^2} \quad (10)$$

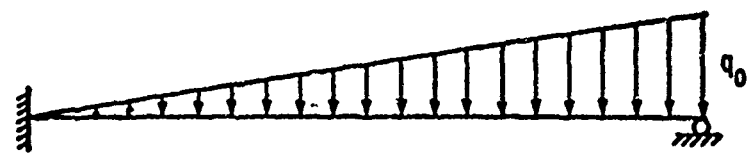
and

$$\frac{d^2 M}{dx^2} = q \quad (11)$$

A finite element analysis for beams can be simply developed by approximating M and w as linear functions within each element and relating these expansions to node point values of M and w . The resulting mixed formulation beam element has four degrees of freedom. Alternatively defining a cubic expansion for w in terms of the node values of w and $w_{,x}$ and utilizing the theorem of minimum potential energy. A displacement finite element analysis may be developed. The resulting displacement beam element also has four degrees of freedom.

It is of interest to compare results obtained from these two analyses. A comparison was made by utilizing the same number of elements for each of the two procedures. Employing the same element representations resulted in identically sized system matrices and hence the same computational effort for solving the simultaneous equations. It should be noted, however, that the formation of the mixed formulation element matrix takes considerably fewer operations than the analogous step in the displacement analysis. Consequently, a more meaningful comparison would have resulted had the number of mixed elements been increased until the total computational efforts of the two procedures were identical. It was unfortunately not possible to obtain a sufficiently accurate measure of computational effort to permit this refinement.

Results for a simple beam problem (Figure 1) are presented in Figures 1, 2 and 3. The convergence of the mixed formulation analysis is clearly illustrated (the question of convergence of analyses based upon stationary principles such as Equ. (1) is apparently not easily answered from a



Beam Configuration

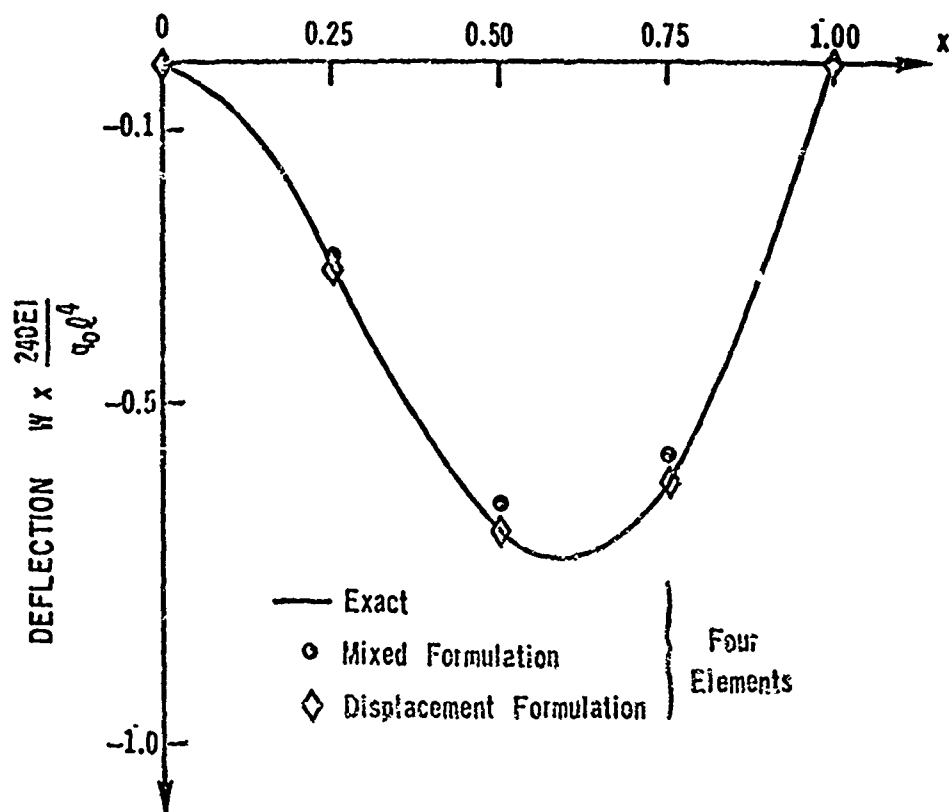


Figure 1. Deflection Results for Beam Problem

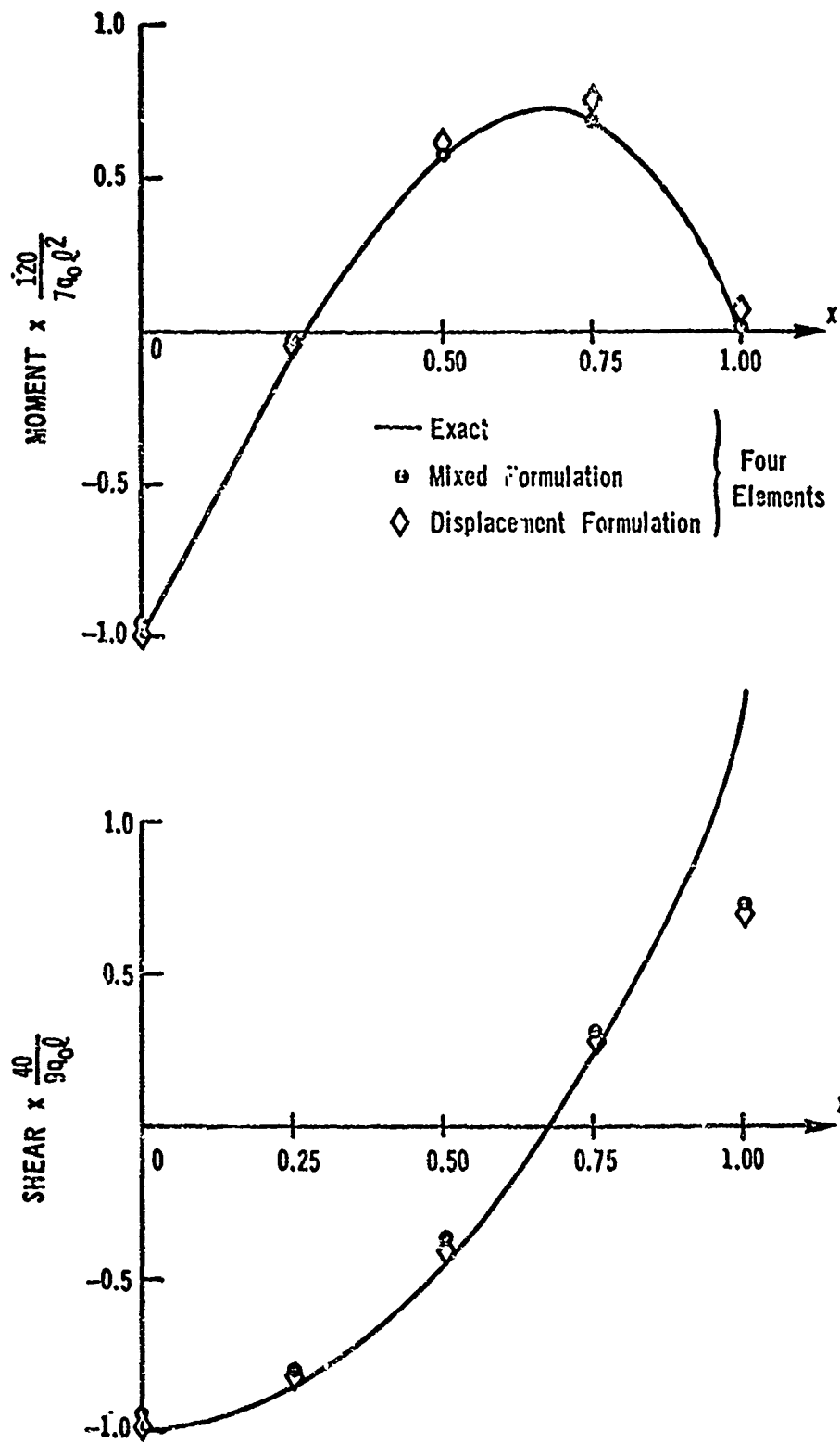


Figure 2. Shear and Moment Results for Beam Problem

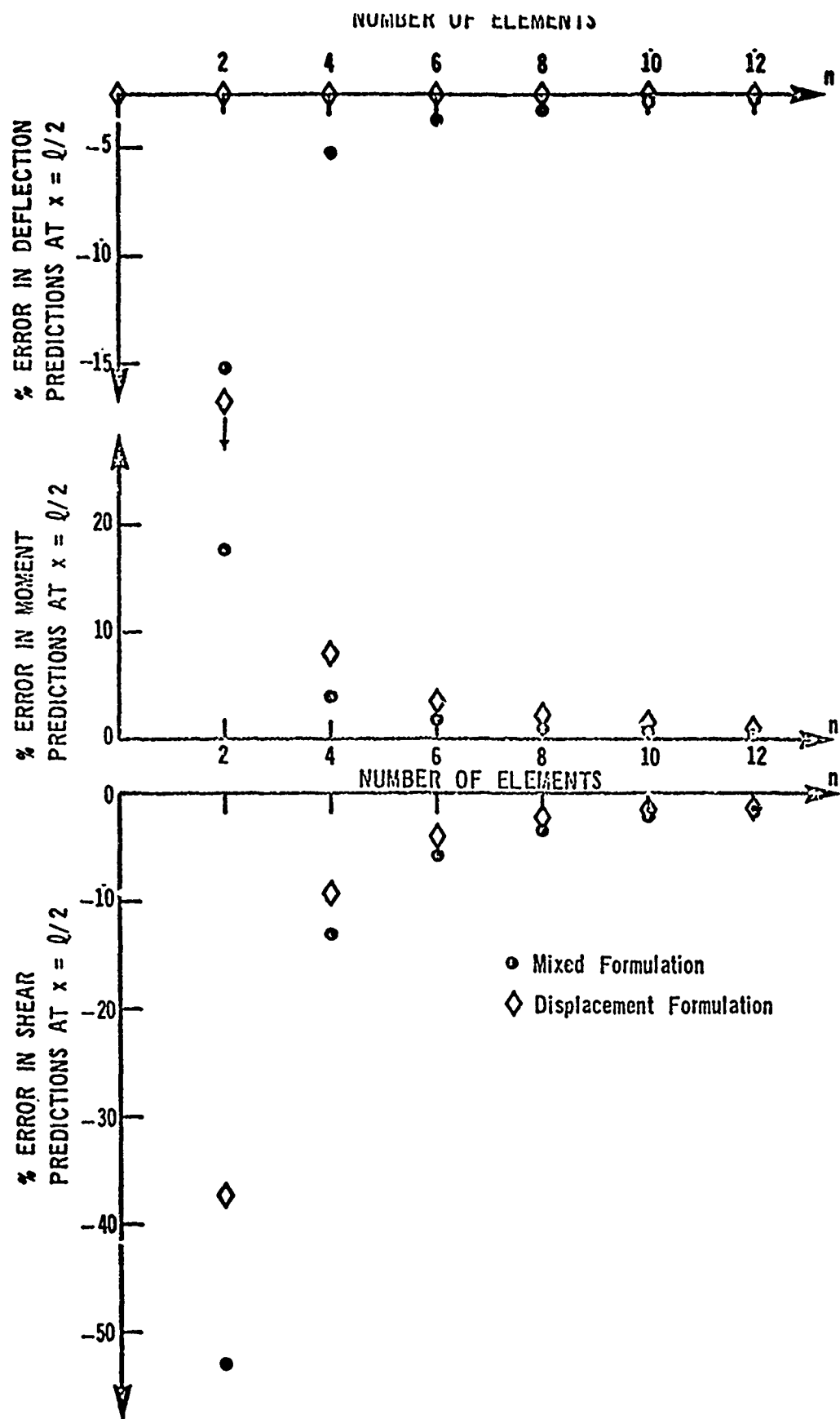


Figure 3. Error in Finite Element Predictions ($x = Q/2$) for Beam Problem

theoretical consideration). The use of the mixed formulation achieves an increased accuracy for the moment predictions at the expense of displacement and shear accuracy.

MIXED FORMULATION FINITE ELEMENT SHELL ANALYSES

Mixed formulation finite element analyses for thin plates have been reported in references [10, 11, 12] (an analysis for thick plates is reported in [9]; difficulties with this analysis for irregular grid representations have been experienced). The flat bending elements reported in [10, 11], in combination with displacement membrane elements, have been used to approximate the behavior of general shells [12, 13]. Mixed formulation elements have also been used in the solution of eigenvalue problems [14].

The bending element reported in [12] is of much higher order than the one reported in reference [13] and discussed herein, and for a given number of elements leads to much more accurate results. A comparison, however, needs to be made of the computational effort necessary to achieve a given accuracy; it is the author's opinion that the higher order element will prove to be the more economical. An added advantage of the higher order element is that it should lead directly to rather accurate predictions for transverse shears, whereas, the lower order element does not directly lead to such predictions.

It is stated in reference [12] that the utilization of the twelve degree of freedom mixed formulation bending element results in about the same accuracy as does the utilization of the twelve degree of freedom displacement element [15]. It is also noted that the computational effort for forming the mixed formulation element matrix is less than that required for the displacement element matrix. However, it is not noted that the resulting number of equations and band width are considerably increased and, hence, if standard solution procedures are used, an increased computational effort will be required to solve the mixed formulation equations.

The equations obtained from the mixed formulation analysis have many more zeroes within the band than their displacement formulation counterpart and, thus, it may be possible to develop an "equation solver" which utilize this characteristic to reduce the computational effort. The authors, to date, have had some success in such a development.

The low order flat triangular element, used by the authors, employs the approximations of linear expansions for the reference surface displacements (defined by "corner node" values, see Figure 4) and constant values for M_x , M_y and M_{xy} (defined by "side node" values of the normal moments). Four of these twelve (six bending and six membrane) degree of freedom triangular elements are combined to form a quadrilateral element (the four triangular sub-elements do not, in general, lie in the same plane) which has after the elimination of the unknowns associated with the five internal points, sixteen degrees of freedom. The element matrix is given in [13]. The element matrix formation time can be reduced by noting that the matrix $[H]$ may be written in the form (the notation is described in [13]):

$$[H] = \begin{bmatrix} \beta_1 - \beta_2 & \beta_2 & -\beta_1 \\ -\frac{(a_2)^2}{2\lambda} & -(\beta_2 + \beta_3) & \beta_1 - \beta_2 \\ -(\beta_2 + \beta_3) & \beta_3 & \beta_2 \end{bmatrix}$$

where

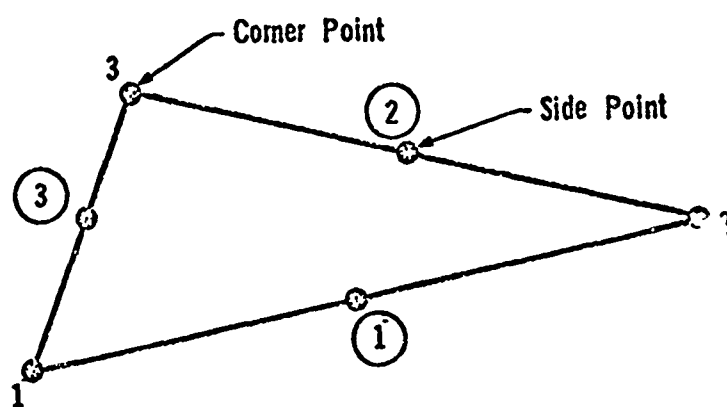


Figure 4. Plate Element

$$\beta_1 = \frac{x_2}{y_3}$$

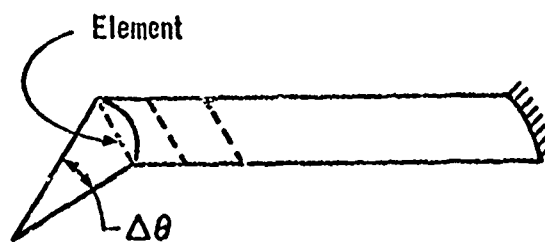
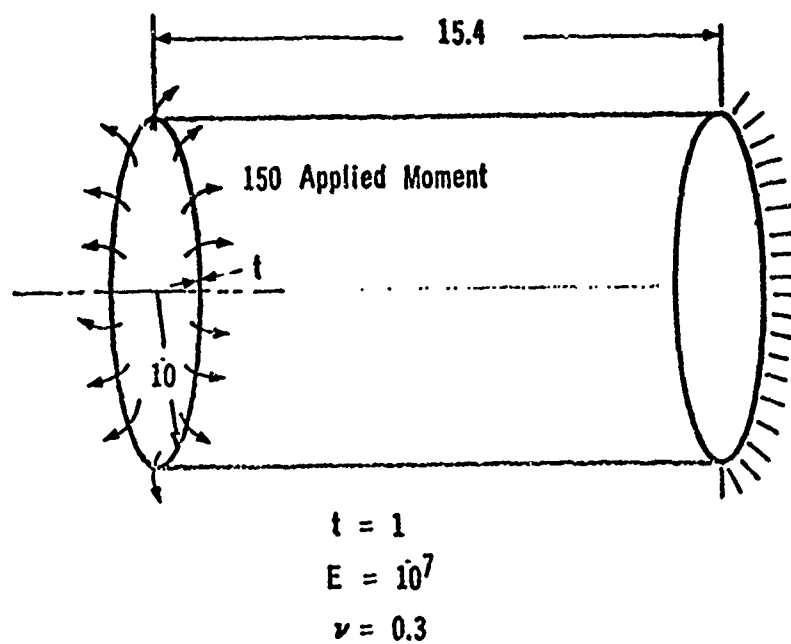
$$\beta_2 = \frac{x_3}{y_3}$$

$$\beta_3 = -\frac{(a_3)^2}{2\lambda}$$

In addition to the several examples presented in [13] three example analyses will be considered herein.

The first two examples demonstrate the applicability of the analysis to singly and doubly curved shells. The first example considers the axisymmetric bending of a cylindrical shell, see Figure 5. Some indication of the consequences of approximating a curved surface by flat elements is obtained by comparing the results for 5° and 15° element spans, see Figures 6 and 7. For this example, where there is very little membrane action, it will be noted that the prediction for moments is more accurate than for transverse deflection. The second example (see Figures 8, 9 and 10) considers the pressurization of a toroidal shell and illustrates applicability to doubly curved shells.

The third example illustrates the potential of finite element shell analyses for applications to extremely complicated shell structures. The finite element results presented in Figures 11, 12 and 13 were obtained by State of California, Department of Water Resources personnel utilizing the program described in reference [13]. The model test results are taken from reference [18]; additional experimental results are available in reference [19]. The structure consists of a 60° Y-junction with three



Element Representation

Figure 5. Example of Axisymmetric Bending of a Cylindrical Shell

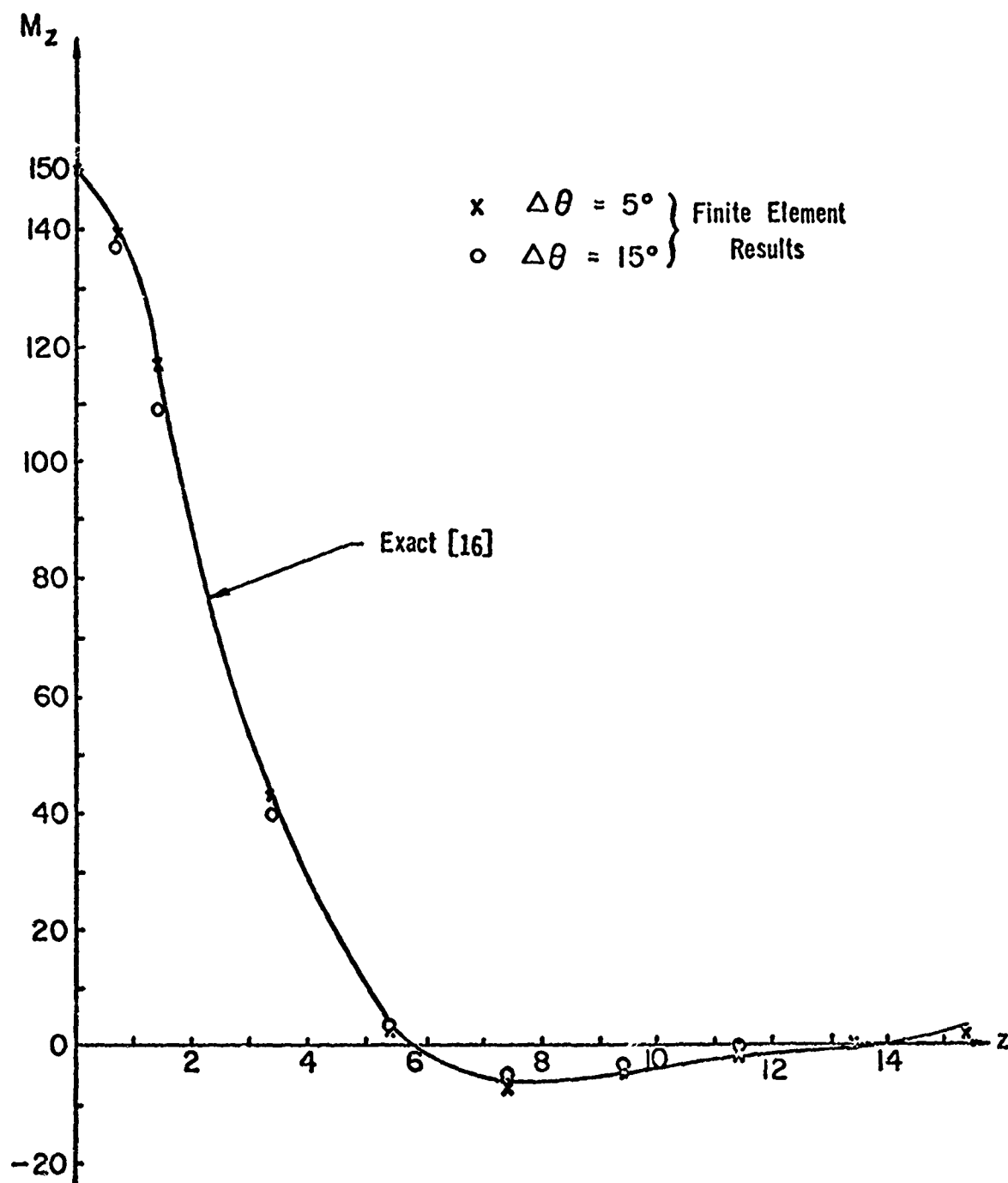


Figure 6. Comparison of Approximate and Exact Moment Distributions for the Axisymmetric Cylindrical Shell Example

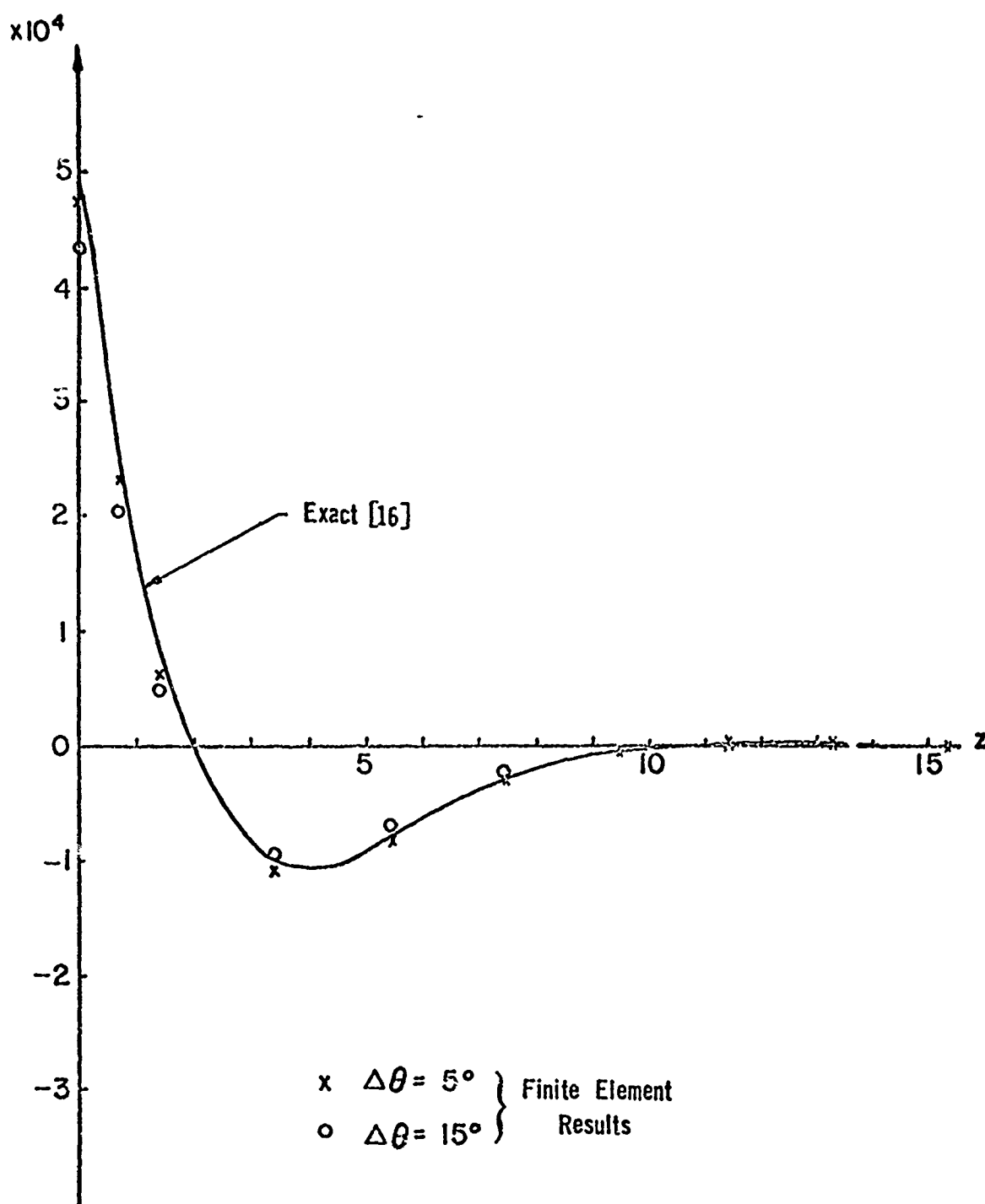


Figure 7. Comparison of Approximate and Exact Transverse Deflection Distributions for the Axisymmetric Cylindrical Shell Example

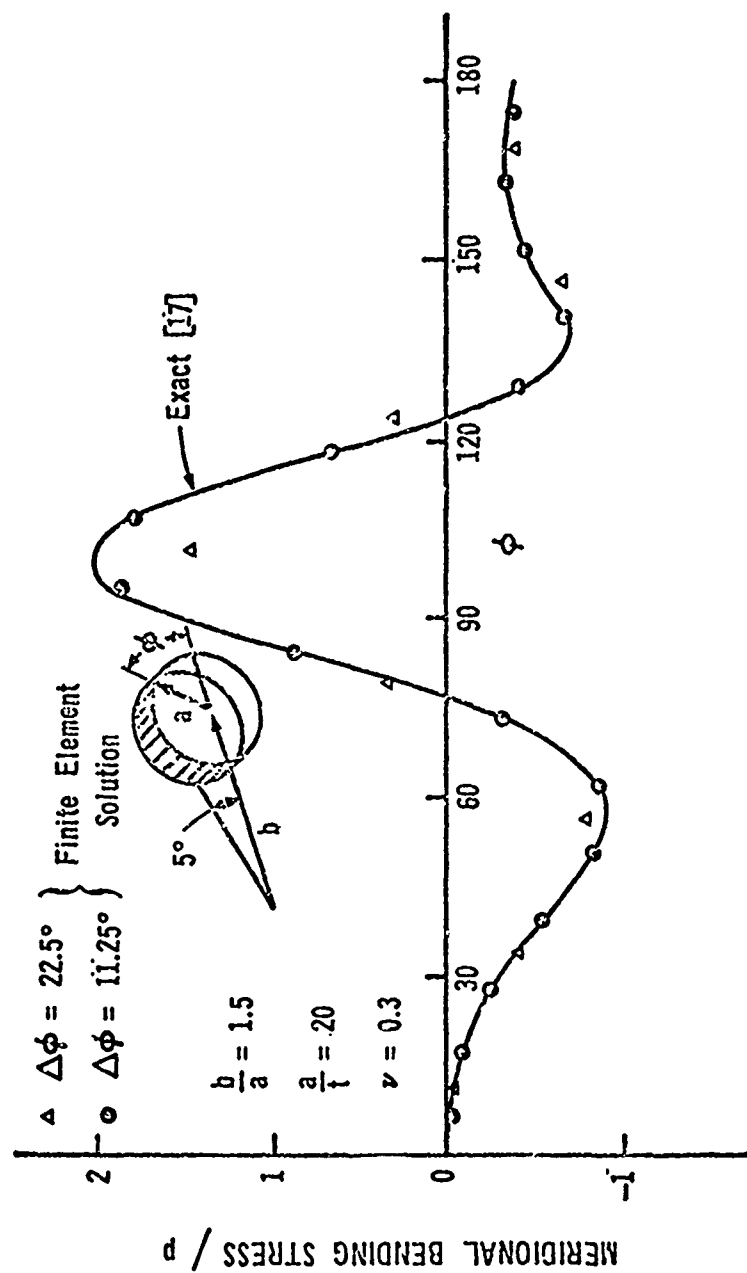


Figure 8. Meridional Bending Stress - Complete Torus Under Internal Pressure

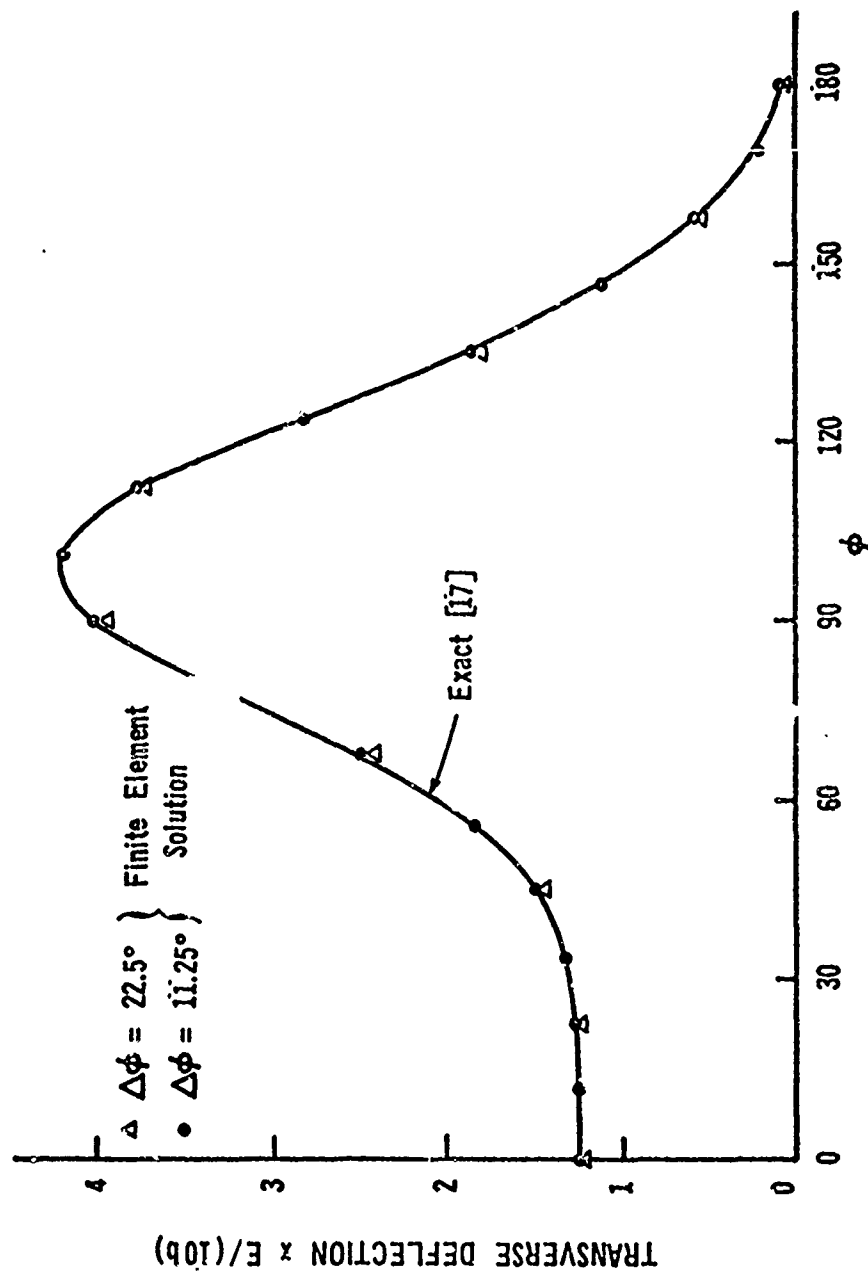


Figure 9. Deformation of a Complete Torus Under Internal Pressure

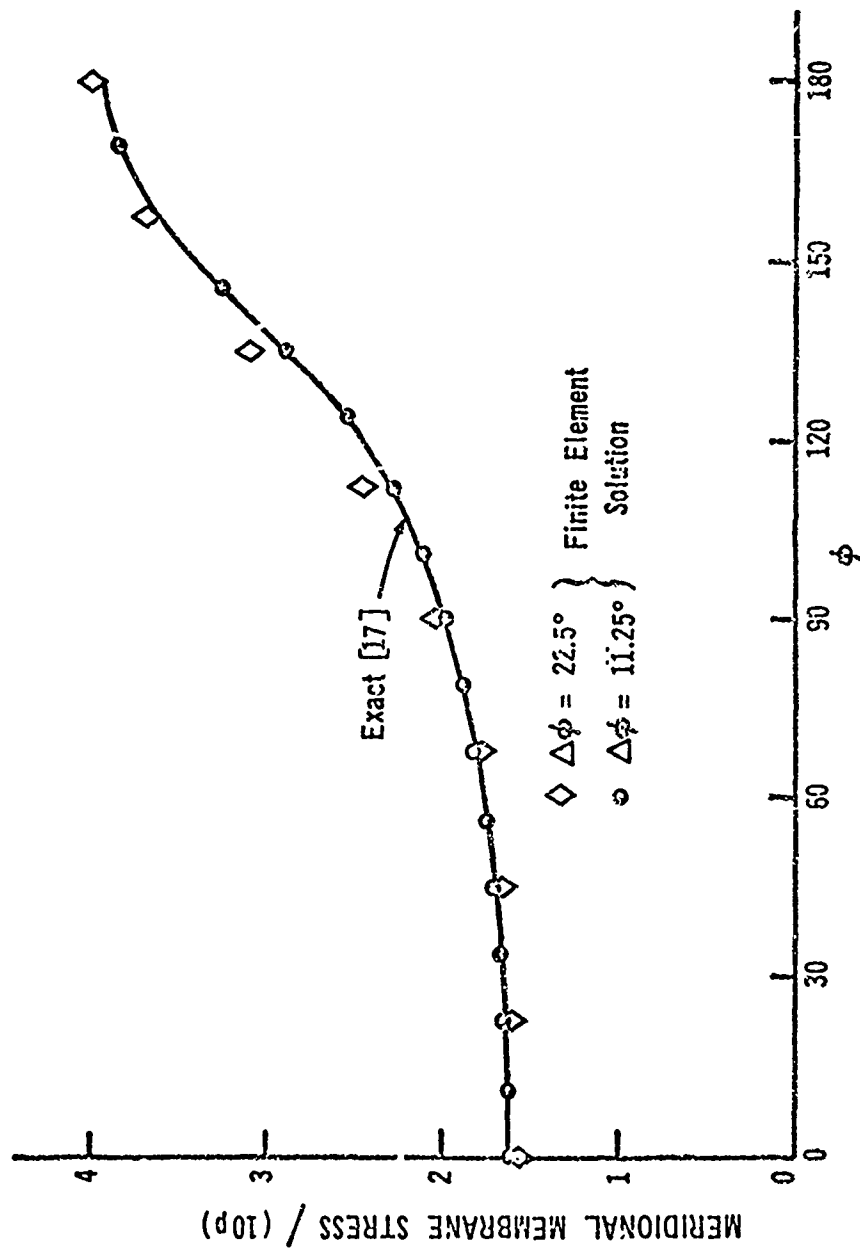
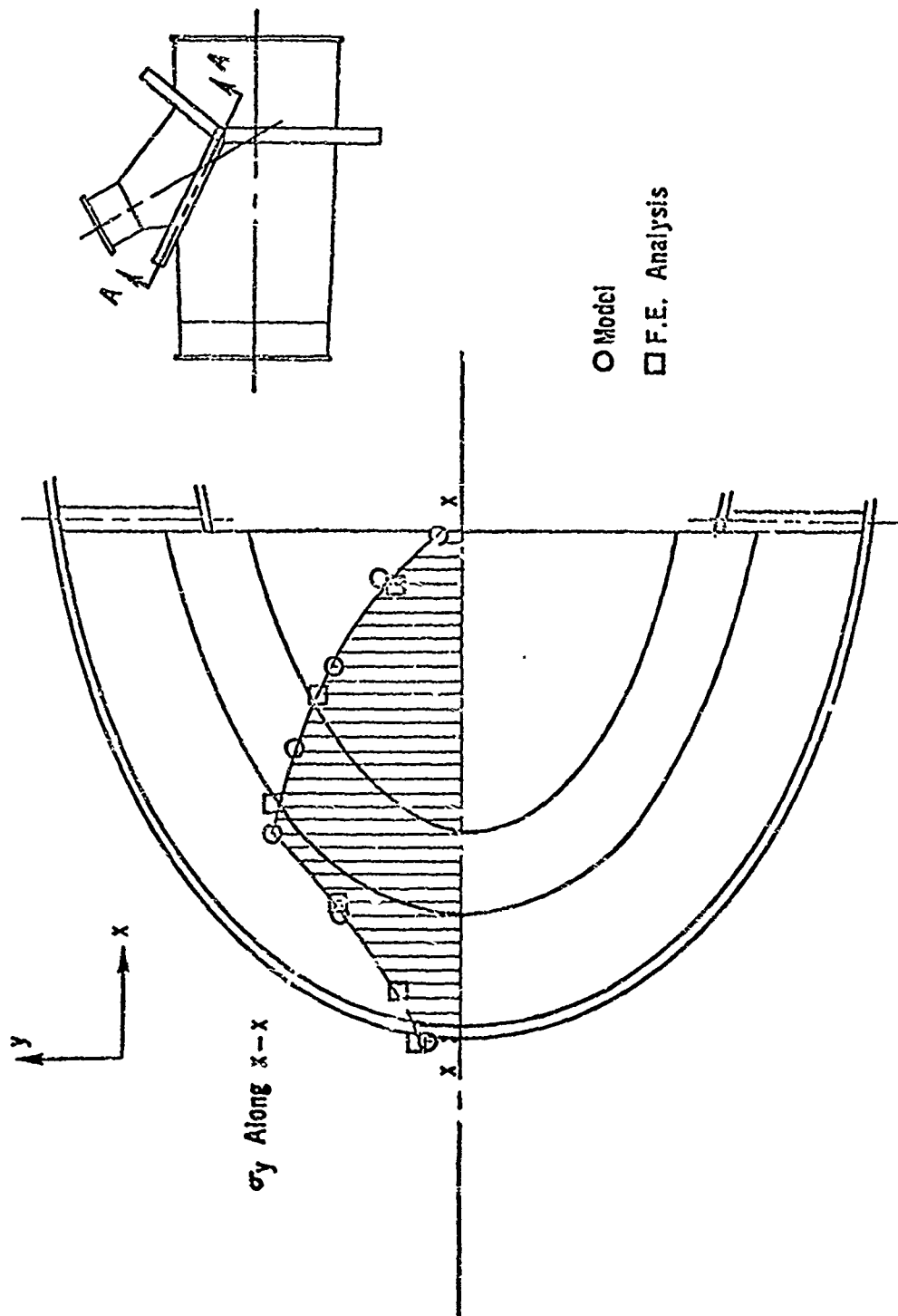


Figure 10. Meridional Membrane Stress – Complete Torus Under Internal Pressure



SECTION A - A

Figure 11. 60° Y-Junction with Full Splitter Plate

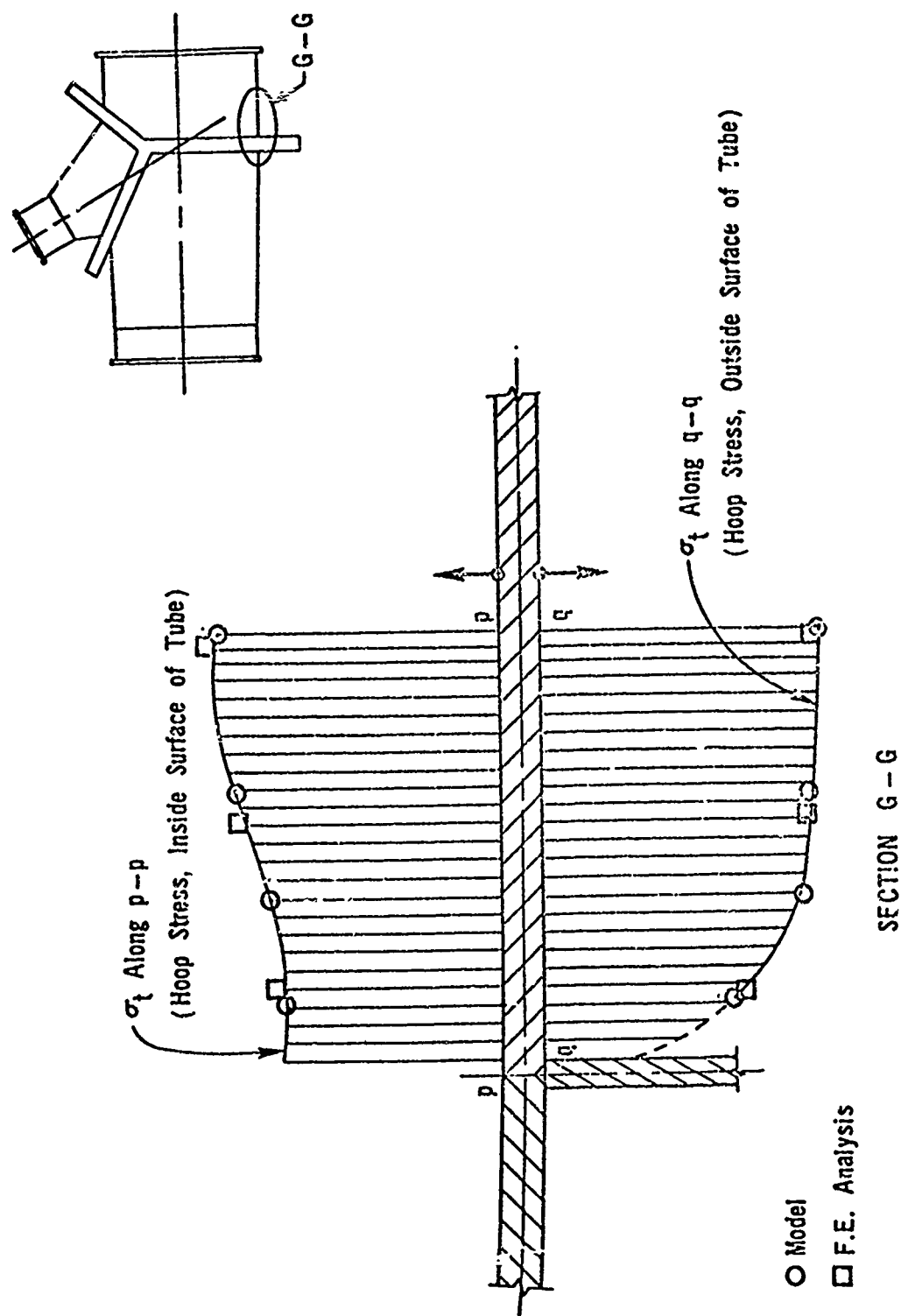


Figure 12. 60° Y-Junction with Partial Splitter Plate

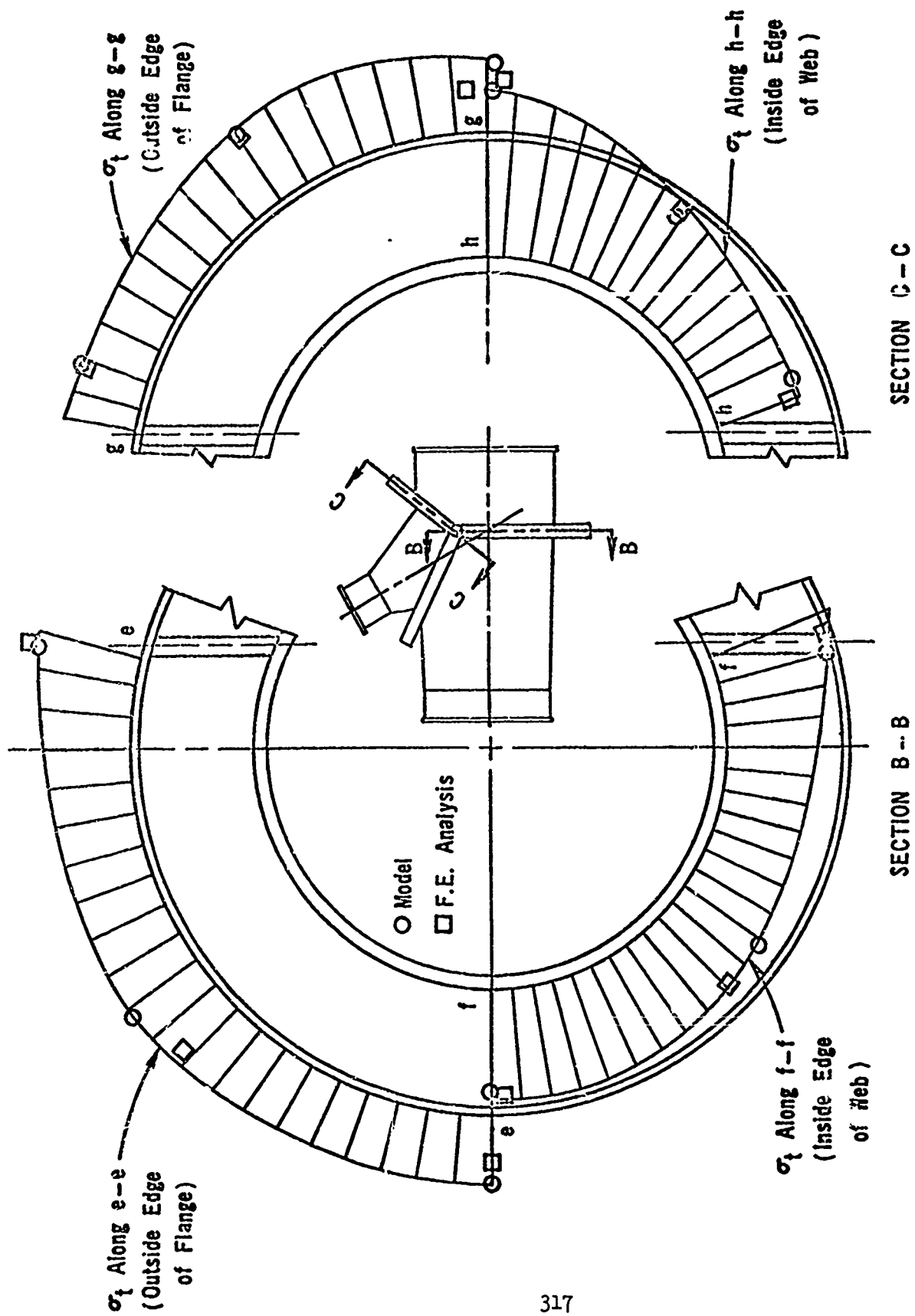


Figure 13. 60° Y-Junction with Partial Splitter Plate

external stiffener plates (with external flanges) and one internal splitter plate, see Figure 11. Results [18] of measurements taken from an instrumented plexiglas model subjected to internal pressure are shown on the figures as circles (the stress curves were drawn thru these points). Superimposed upon these curves are finite element results obtained by representing (approximately 2400 degrees of freedom) the complete structure by a rather coarse grid of flat elements, see Figure 14 (Figure 14 is taken from a computer plot of the grid).

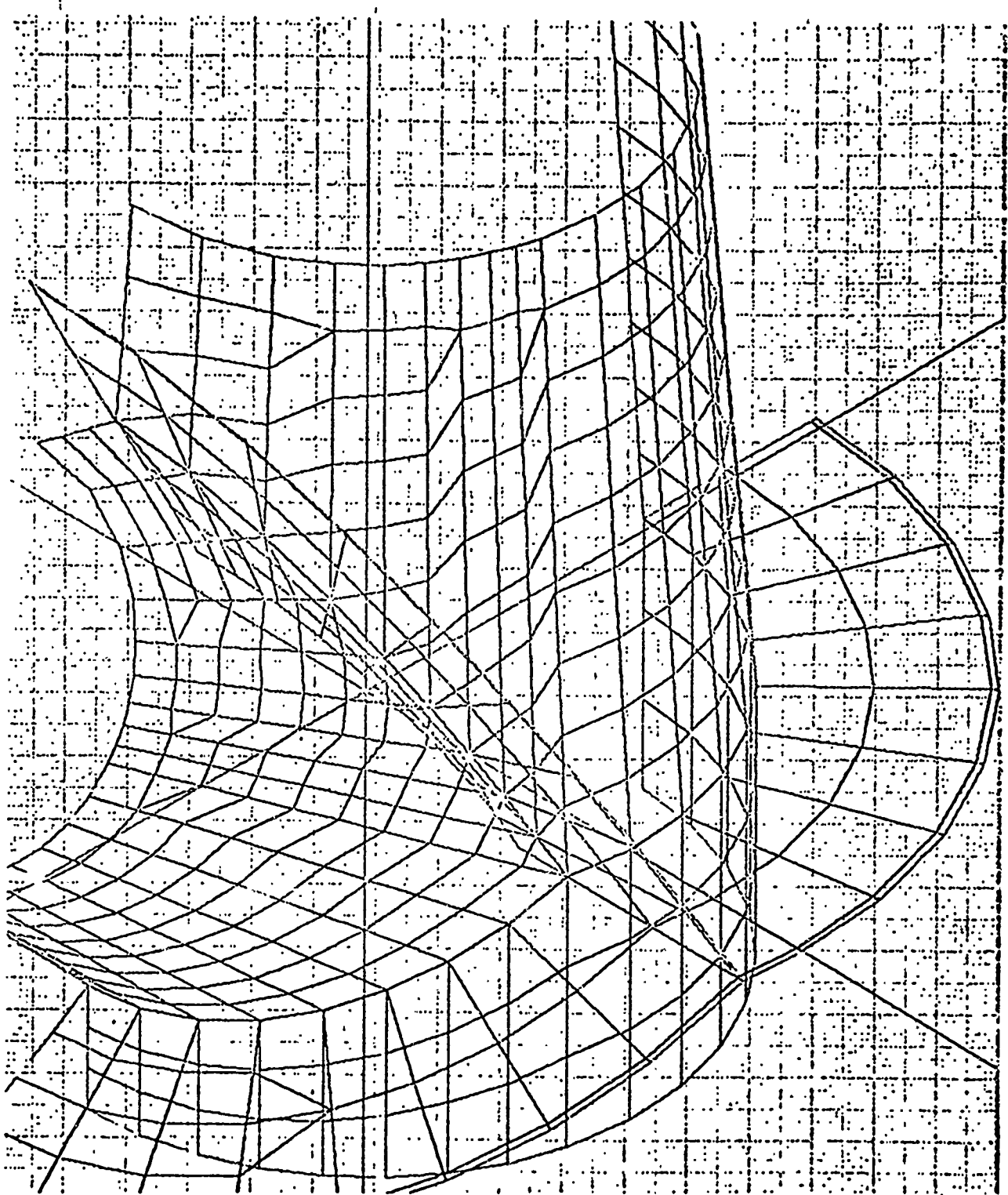


Figure 14. Finite Element Grid for 60° Y-Junction.

CURVED SHELL ELEMENTS

Concern has been expressed that analyses which represent a curved shell surface by flat elements (see Figure 15) might be rather inaccurate due to artificial discontinuity moments generated at the intersections of the flat elements.

For the purpose of this discussion a structure made up of a series of triangular plate panels, which is identical in shape to a flat element idealization of a shell, will be called the AFPS (associated folded plate structure). The point of concern is that the finite element solution might represent the behavior of the AFPS rather than that of the shell (a very serious concern as the two behaviors may be grossly different). If a low order plate element is utilized then one would not expect the finite element solution to be a good approximation of the behavior of the AFPS as it would require a rather fine subdivision of each plate panel (rather than one element per panel) to accurately capture their complicated behavior. However, even if the finite element solution should only grossly approximate the behavior of the AFPS this could be very undesirable. The above discussion suggests that low order flat elements, because they are less capable of representing the behavior of the AFPS, may at times be more accurate than higher order ones for shell analysis purposes.

Experience gained from the application of the shell program discussed in [13] has led the authors to the following general conclusions: (1) The values of the normal moments calculated at the element side points reflect the influence of the artificial discontinuity moments to a greater degree than the element moments (reported for the centers of the quadrilateral elements). (2) The three factors which tend to greatly magnify the

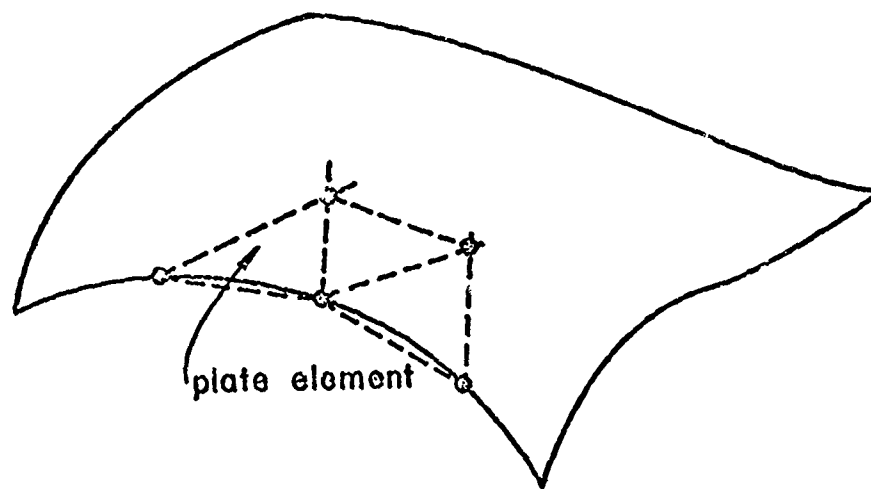
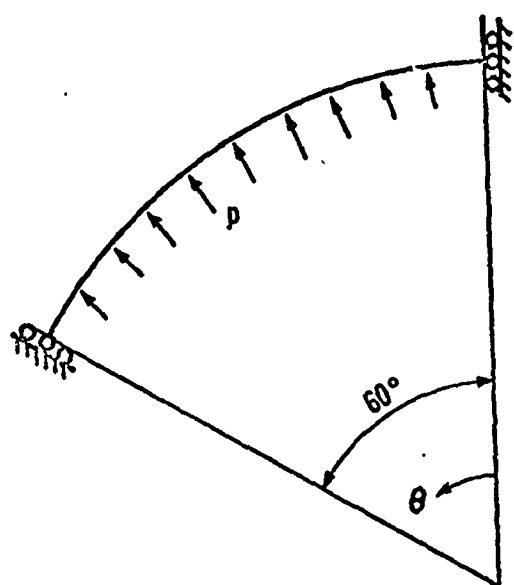


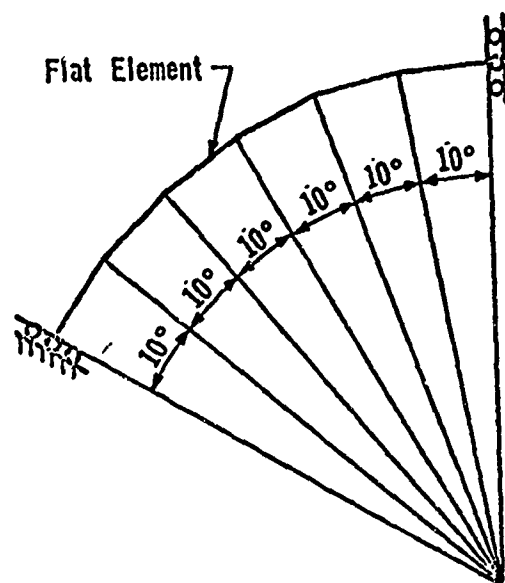
Figure 15. Representation of Arbitrary Shell with Plate Elements.

difficulties are non-positive Gaussian curvature, large R/t ratios, and variable element sizes.

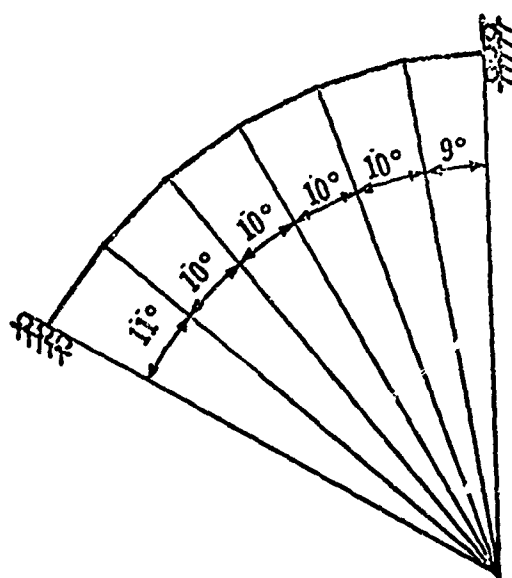
In an attempt to illustrate the above observations the authors performed a study of the simple example of the pressurization of a thin cylindrical shell. Utilizing symmetry a 60° segment of the shell was analyzed. The shell configuration is shown in Figure 16 along with three different flat element representations; the node points lie on the middle surface of the cylinder. The results presented in Figures 17, 18 and 19 are for $R/t = 100$. The values of the hoop moments (M_θ) have been multiplied by a factor such that a magnitude of 1.0 indicates that the extreme fiber bending stress is equal to the membrane stress (the membrane stress predictions were identical for all cases). The "folded plate solution" is an exact analysis of the AFPS; the "finite element solution" was obtained using the analysis described in [13]. The results presented in Figure 17 illustrate that the side point moments reflect the artificial discontinuity moments to a greater degree than do the element moments; in fact for equally sized elements the element moments are exact. (Because of these recognized inaccuracies, the side point moments are not shown in subsequent figures.) It is to be noted, for this example, that when the AFPS has panels of equal lengths that the average hoop moment and the displacements of the nodes are identical to those of the shell. Inspecting Figures 19 and 20, it is apparent that any small deviation of the ratios of panel lengths from 1.0 results in a drastic change in the behavior of the AFPS. Thus, except for the case of equally sized panels, the response of the AFPS is considerably different from that of the shell. Unfortunately the finite element solutions are highly influenced by the basic trends of the AFPS



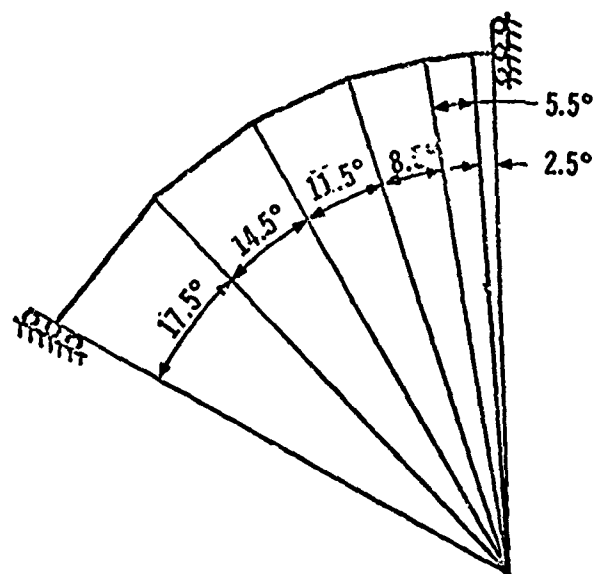
STRUCTURAL CONFIGURATION



ELEMENT IDEALIZATION #1



ELEMENT IDEALIZATION #2



ELEMENT IDEALIZATION #3

Figure 16. Element Configurations for Artificial Discontinuity Study

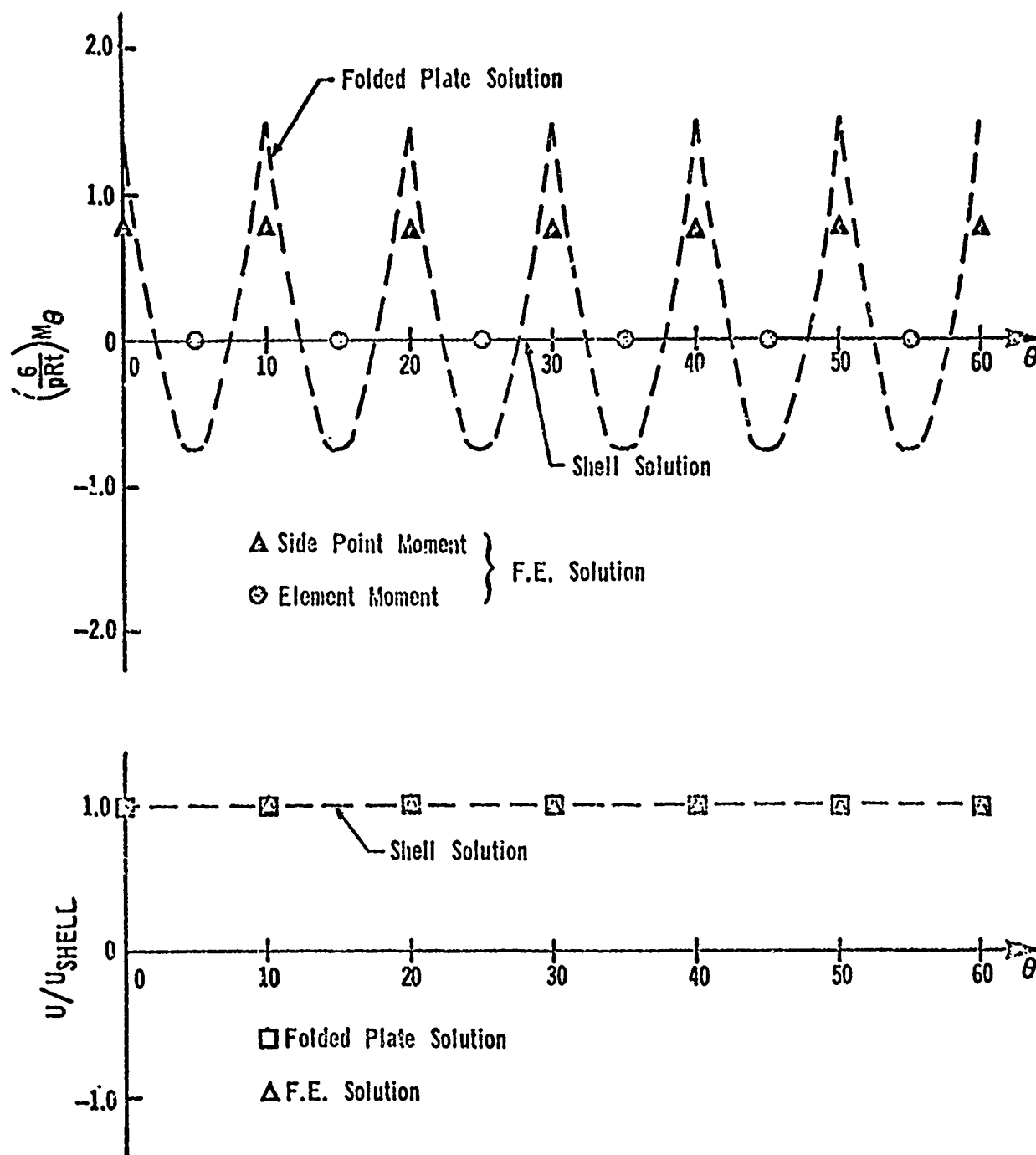


Figure 17. Hoop Moment and Radial Displacement for Idealization #1

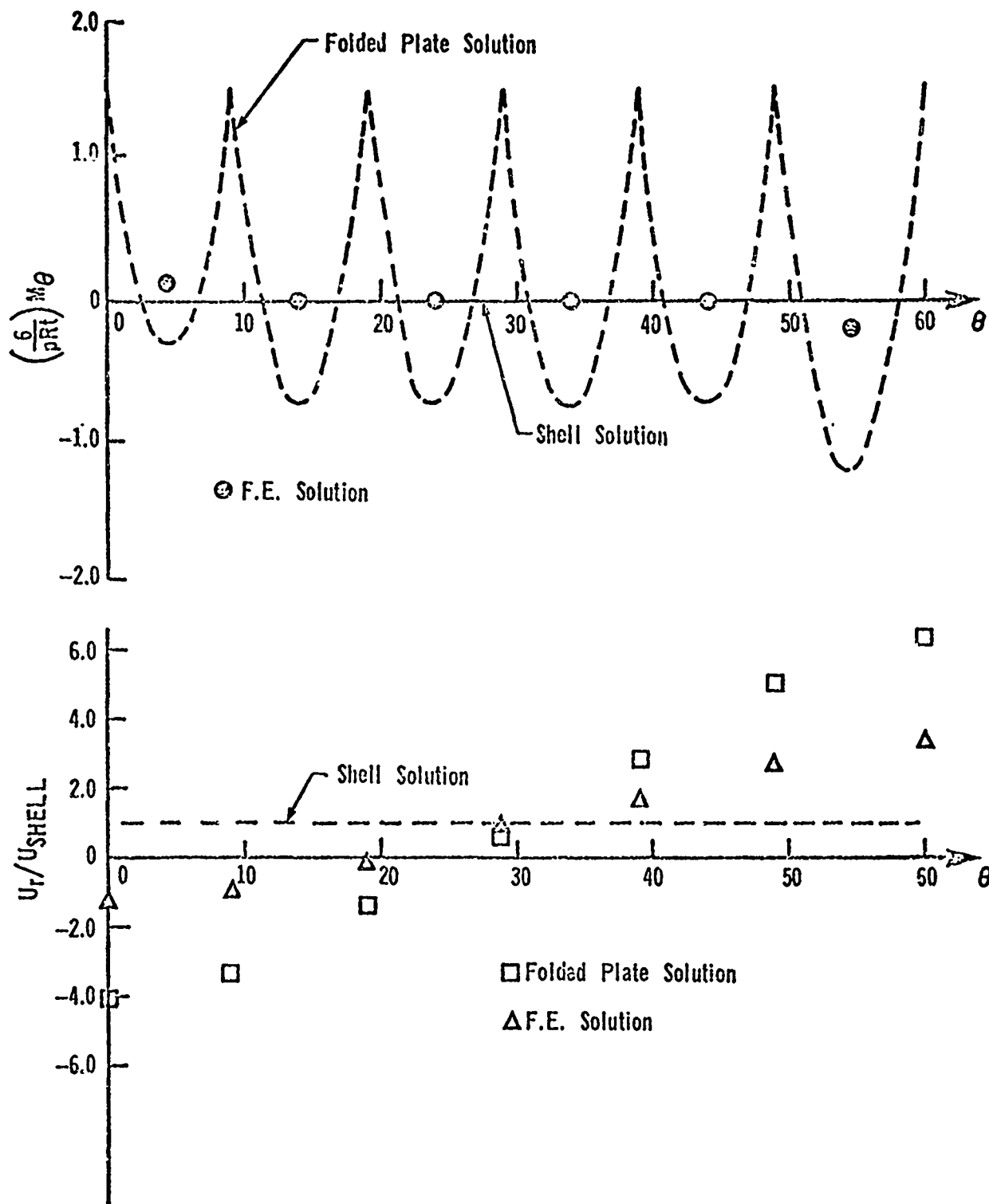


Figure 18. Hoop Moment and Radial Displacement for Idealization #2

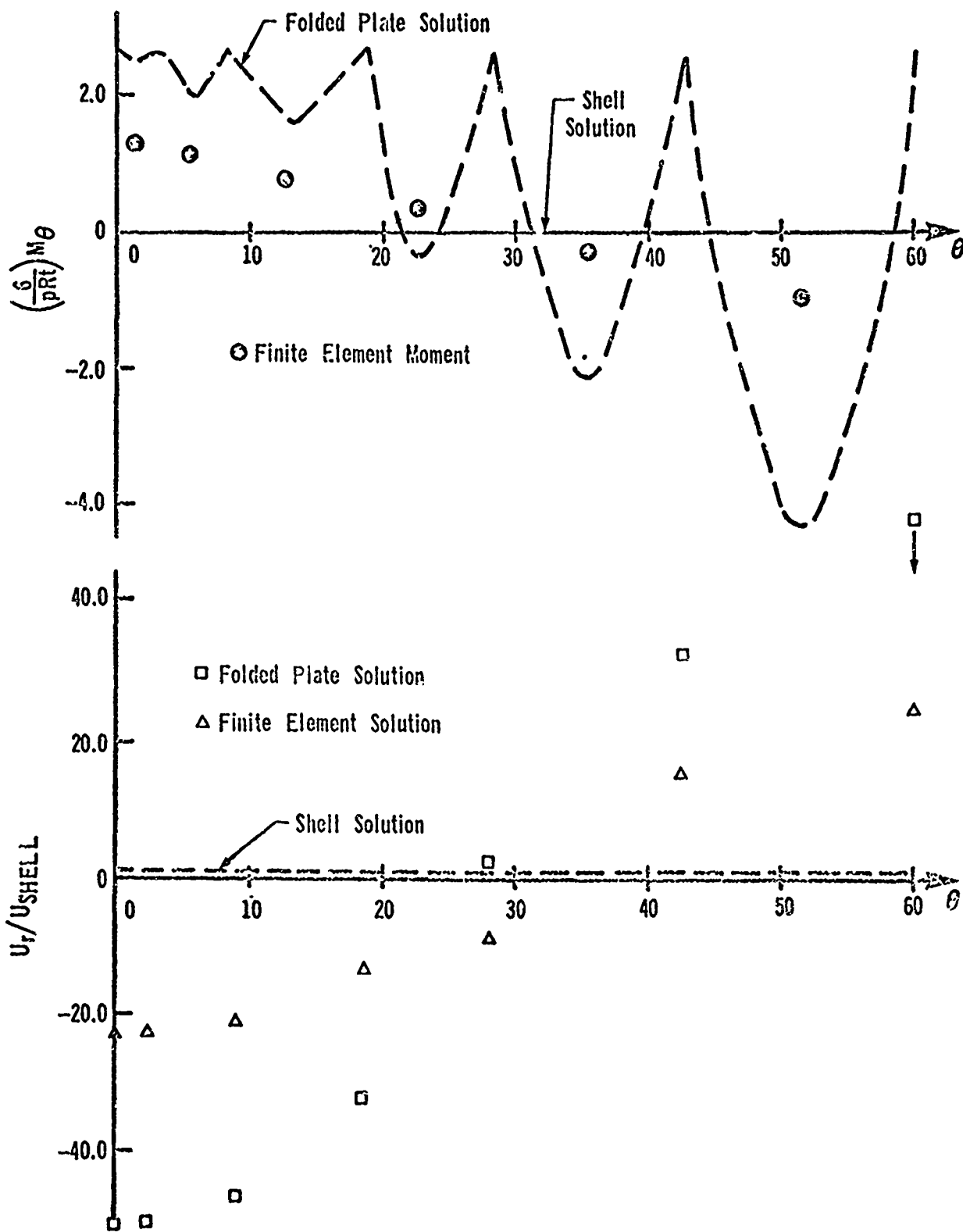


Figure 19. Hoop Moment and Radial Displacement for Idealization #3

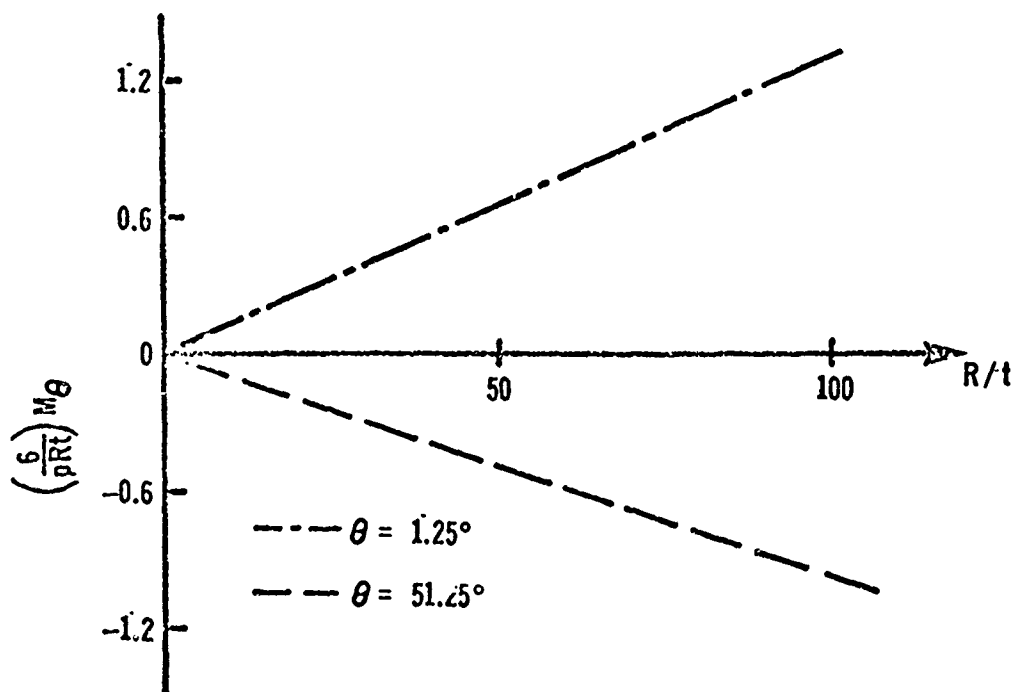
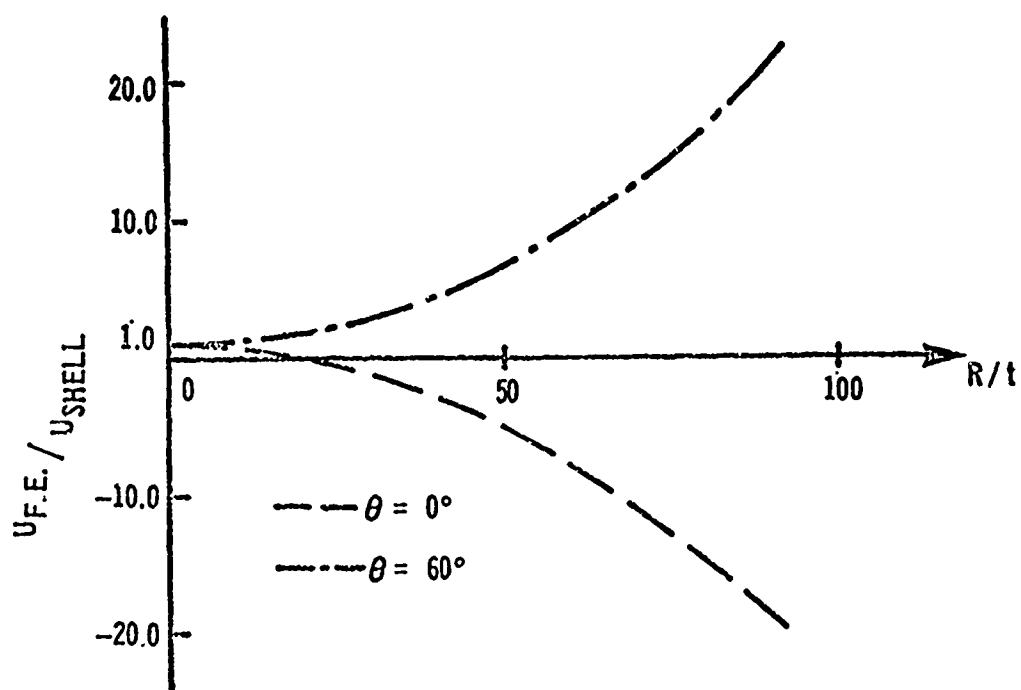


Figure 20. Artificial Discontinuity Effects (Configuration #3) - R/t

behavior (the displacement predictions are particularly inaccurate). The increased significance of these inaccuracies for large R/t ratios is illustrated by Figure 20 where the dependence of the finite element predictions upon the R/t ratio is given for this example. It is the authors' opinion that these inaccuracies are not nearly so significant for shells of positive Gaussian curvature.

One obvious remedy for this difficulty is to use curved elements for those shell configurations where a flat element representation may lead to problems. The development of a general curved shell element has been impeded by the difficulty of including the rigid body motion terms in the displacement expansions. Two possible approaches suggest themselves: (a) use of polynomial expansions which contain the rigid body motion terms in the limit as the element size shrinks to zero, and (b) use of Fourier terms in the displacement expansions to exactly account for rigid body motion. The former approach has the advantage of relative simplicity and the disadvantage of limiting the maximum element size that may be employed. The latter approach has the advantage of permitting the utilization of very large elements and the disadvantage of extreme algebraic complexity due to the difficulty of satisfying the element interface admissibility conditions and evaluating the necessary surface integrals.

Recently a mixed formulation doubly curved triangular shell element which utilizes polynomial displacement expansions has been reported [20].

The authors have undertaken the development of curved mixed formulation elements which completely describe rigid body motion. Only a few brief comments concerning the development will be given at this time as a detailed report will be given in a later publication. The authors have

found it necessary, in order to easily satisfy the admissibility conditions, to restrict their attention to coordinate line elements and to particular type shells, e.g., cylindrical, spherical, conical, etc. It might appear that such restrictions would seriously detract from the usefulness of the development, however, it is felt that when such elements are used in combination and in combination with general elements, such as those given in [13] and [20], and when provisions are made for permitting boundary elements to have non-coordinate line boundaries, and for grids to have "hanging nodes," that it will prove to be quite practical and useful. "Hanging nodes" are the termination of grid lines which bound small elements in the sides of adjacent larger elements. One possible way of considering non-coordinate line shell intersections would be by using a fine grid of general flat [13] or curved [20] triangular elements adjacent to the intersection and relatively large coordinate line elements for the remainder of the shell.

An analysis which utilizes coordinate line curved cylindrical shell elements has given, for the example presented in Figure 16, essentially exact results for all element idealizations.

CONCLUSIONS

The feasibility and practicality of developing and utilizing mixed formulation finite element shell analyses has been conclusively demonstrated. Relative advantages and disadvantages of displacement and mixed formulation finite element solutions have been suggested but not firmly established. Finally the importance of using curved elements for the representation of thin shells of non-positive Gaussian curvature has been illustrated.

REFERENCES

- [1] Courant, R. and Hilbert, D., Methods of Mathematical Physics, Interscience, Vol. 1, p. 177 (1953).
- [2] Melosh, R., "Basis for Derivation of Matrices for the Direct Stiffness Method," AIAAJ, Vol. 1, pp. 1631-1637 (1963).
- [3] Jones, R. E., "A Generalization of the Direct-Stiffness Method of Structural Analysis," AIAA J. Vol. 2, pp. 821-826 (1964).
- [4] Herrmann, L. R., "Elasticity Equations for Incompressible and Nearly Incompressible Materials by a Variational Theorem," AIAA J. Vol. 3, No. 10, pp. 1896-1901 (1965).
- [5] Novozhilov, V. V., Theory of Elasticity, The Israel Program for Scientific Translations, pp. 99-127 (1961).
- [6] Reissner, E., "On a Variational Theorem in Elasticity," J. Math. Phys. 29, pp. 90-95 (1950).
- [7] Prager, W., "Variational Principles of Linear Elastostatics for Discontinuous Displacements, Strains and Stresses," Recent Progress in Applied Mec., John Wiley & Sons, pp. 463-474 (1967).
- [8] Chan, S.T.K., "Investigation of Finite Element Procedures Based on the Theorem of Minimum Complementary Energy," M.S. Thesis, Univ. of Calif., Davis, Calif. (1965).
- [9] Herrmann, L. R., "A Bending Analysis for Plates," AFFDL-TR-66-80, Proceedings, Conference on Matrix Methods in Structural Mechanics, Wright-Patterson Air Force Base, Ohio, pp. 577-604 (1965).
- [10] Herrmann, L. R., "Finite Element Bending Analysis for Plates," J. of the Eng. Mec. Div., Proc. of the ASCE, Vol. 93, No. EM5, pp. 13-26 (1967).

- [11] Cook, D. R., Discussion of "Finite-Element Bending Analysis for Plates," J. of the Eng. Mec. Div., Proc. of ASCE, Vol. 94, No. EM3, pp. 895-898 (1968).
- [12] Visser, V., "A Refined Mixed-Type Plate Bending Element," AIAA J. Vol. 7, No. 9, pp. 1801-1803 (1969).
- [13] Herrmann, L. R. and Campbell, D. M., "A Finite-Element Analysis for Thin Shells," AIAA J., Vol. 6, No. 10, pp. 1842-1847 (1968).
- [14] Cook, R. D., "Eigenvalue Problems with a Mixed Plate Element," AIAA J., Vol. 7, No. 5, p. 982 (1969).
- [15] Clough, R. W. and Felippa, C. A., "A Refined Quadrilateral Element for Analysis of Plate Bending," Proceedings of the USAF Second Conference on Matrix Methods in Structural Mechanics, Dayton, Ohio (1968).
- [16] Timoshenko, S., Theory of Plates and Shells, McGraw-Hill Book Co., Inc., New York, N. Y. (1940).
- [17] Kalnins, A., "Analysis of Shells of Revolution Subjected to Symmetrical and Nonsymmetrical Loads," J. of Appl. Mec., ASME, Vol. 31 (1964).
- [18] Godden, T. G. and Griffith, A. R., "Model Analysis of the A. D. Edmonston Pumping Plant Discharge Line Manifolds," Structures and Materials Research Report No. 69-25, Dept. of Civil Engineering, Univ. of Calif., Berkeley (1969).
- [19] Kiesling, E. W., "Final Report-Test on Wye Branch of Discharge Manifold," Kaiser Steel Corp. Fabrication Div., Fontana, Calif. (1968).
- [20] Visser, W., "The Application of a Curved, Mixed-Type Shell Element," Harvard Univ. Report SM-38 (1970).

QUESTIONS AND COMMENTS FOLLOWING HERRMANN'S PAPER

QUESTION: In this last example of your curved beam, how was your load vector computed when you took the distributed load? Was it a consistent load vector? Did it include the moments in addition to radial forces?

HERRMANN: Yes, it was a consistent vector.

QUESTION: If you had eliminated the moments, would that have yielded better results here?

HERRMANN: We didn't try that.

QUESTION: A philosophical point. You said that you were getting excellent agreement with the evenly spaced grid, even when the stress distributions within your elements departed radically from the true stress distributions of the structure at points. This excellent agreement that you were obtaining was simply based on an empirical procedure by which you picked the point at which you evaluated the stress. Is that a correct assumption of the situation?

HERRMANN: That's true. After running some of these simple examples, we gained enough experience to know how to interpret our results in that way. Yes, it's true that certain parts of the element could have very fictitious results.

QUESTION: Could another interpretation of your experience be that we cannot really rely on that sort of experience? That is, must we have an element in which the stresses everywhere agree with the true stress

distribution of the structure?

HERRMANN: I think the engineering experience is valuable and I think we can rely upon it, but I do agree that for certain types of shells--very thin shells--it is important that we develop curved elements.

COMMENT: I'd like to report on an application of a mixed method using a curved triangular element. For example, a program for shell analysis was done at MIT two years ago by Carlos Brato. I was involved in this and I can report that excellent results were obtained for practically all cases he studied; and he really tested just about all kinds of shell surfaces. He used shallow shell theory for the element, linear functions of the coordinates for the displacements and linear functions for the stress couples as well. He didn't use any side points and with this the results of the stress couples at the nodes were always good. He made some comparisons with the displacement method and always his results were at least as good as those with the displacement method. Also I'd like to mention that there are other kinds of mixed formulations in which you can take the rotations to represent the bending behavior and stress functions to represent the membrane behavior. Also in this shell theory one would assume if you take the stress couples you're making M_{xy} equal M_{yx} or M_{12} equal M_{21} , and if you want to include the general shell theory where this is not so, you would have four stress couple unknowns instead of three.

HERRMANN: I might add that we've looked at curved shells and we've repeated these same examples with a curved mixed formulation element and obtained excellent results for all gradation of element sizes. Another comment is that there are many different combinations that you

can use and there's one thing that we would like to look at, which is including the membrane behavior by a force or a complimentary energy approach. We have such a membrane element and I would like to see what would happen when we combined it with the mixed formulation bending element. We have not done this to date.

QUESTION: It appears that the example where the curved element gives trouble is also one which physically is very unstable in that it's ideally suited for the symmetrical loading and with any other type of loading you get a tremendous side sway. When you have something with very little bending properties, almost like a balloon type structure, probably this is a physical indication to watch out for. In this type of structure also you probably should be using large deformation theory so maybe an elastic analysis like this is sort of meaningless anyway. The specific question I had for you is, what is the potential for extending the mixed model to dynamic analysis?

HERRMANN: There is a reference to this in my paper. I've spoken with two different investigators, one said he had no problem at all-- it extended beautifully. The other person said he had difficulties. I don't really want to pass along their difficulties or their successes. I'll leave it to them to report it. I'd like to add a comment related to Prof. Clough's statements concerning the order of expansions versus the geometric approximations. At least on the surface of things, it looks like a higher order element at times will give you poorer results when you're having curvature difficulties because the higher order element can more closely capture the complicated folded beam or folded plate behavior and you really don't want this. You want to avoid capturing it. So it appears that, at

least at times, a low order approximation is consistent with neglecting curvature. If you want to use a higher order element, it's probably desirable to include curvature effects.

COMMENT: I'd like to make just one observation on a possible problem that may occur in dynamic analysis using your mixed model. You have emphasized that your mixed model is excellent for representing stresses. If this is your primary purpose, fine, but in the dynamic analysis deflections completely control your inertial forces. Consequently if you are not representing deflections with adequate accuracy your dynamic analysis will tend to break down.

HERRMANN: It's possible. Some of the references I've given in the paper use higher order approximations for the displacements and I personally think that higher order elements are far superior to what I've presented here. If the mixed formulation has any future, it will be with these higher order approximations.

COMMENT: I completely agree with this author in his observations about flat versus curved elements. Some of this information has been in the literature before and he's added an additional element to it showing that there's a trend in the displacements and the stresses which extends from one end of the arc to the other. He did this for a beam element. It was previously done for shell elements. For the shell element, this trend does not exist. However, the shell element is not semi-unstable, as was suggested in an earlier comment. The point I'm trying to make here is that you can have very definite trouble with shell elements for shells which do not tend toward instability in any way.

STRICKLAND: We have been asked to give a summary of the important points made in this particular session. I'd like to summarize by noting two points which have been made. First, if you have two triangular elements coming together at some angle, we need equal order displacement functions in all variables. Prof. Clough has shown that if we use equal order displacement functions, we may obtain good results using flat elements. The other point concerns the mixed formulation. In the mixed formulation the potential depends only on the variables and their first derivatives. Consequently, as pointed out by Prof. Herrmann, it is only necessary to satisfy continuity of the parameters and not continuity of the slopes between elements. This may be done in the displacement method by using that equivalent Kirchhoff hypothesis or in fact it may be accomplished by degenerating the three-dimensional element to a corresponding two-dimensional element.

FINITE-DIFFERENCE ENERGY METHOD FOR NONLINEAR SHELL ANALYSIS

David Bushnell*

Bo O. Almroth**

Lockheed Palo Alto Research Laboratory
Palo Alto, California

Abstract

Two computer programs, BOSOR3 and STAGS, have been developed for the nonlinear analysis of shells. BOSOR3 performs stress, stability, and vibration analyses of ring-stiffened, segmented shells of revolution with various wall constructions. STAGS performs similar analyses for shells of general shape. The analysis method for both programs is similar to the finite-element method in that extensive use is made of matrix algebra in the development of the governing equations. These equations are derived by the digital computer in terms of mesh point displacement variables. Several example cases from BOSOR3 and STAGS are given, showing effects of various finite-difference schemes, comparison with finite-element results, and complex nonlinear behavior involving large-deflections and redistribution of stress during loading.

*Staff Scientist

**Staff Scientist, Senior

FINITE-DIFFERENCE ENERGY METHOD FOR NONLINEAR SHELL ANALYSIS

David Bushnell
Bo O. Almroth
Lockheed Palo Alto Research Laboratory
Palo Alto, California

INTRODUCTION

Application of energy principles in computerized structural analysis has been limited for the most part to the finite element method. During the past few years the authors have developed general computer programs for the analysis of shells in which the principle of minimum potential energy is used in conjunction with the finite difference method. Two programs have been developed: BOSOR3 (Ref. 1) is a program for calculation of stress, stability, and vibration of segmented, ring-stiffened shells of revolution with various wall constructions; STAGS (Ref. 2) is a program for the calculation of stress, stability, and vibration of general shells. Both programs are based on the usual thin shell approximations. In STAGS and BOSOR3 the expression for the total energy, originally an integro-differential form, is converted to an algebraic form by substitution of appropriate finite difference formulas for displacement derivatives in the kinematic relations and by numerical integration over the shell surface. This algebraic form is "minimized" with respect to the mesh point displacement components u_i , v_i , and w_i .

The algebraic forms for the total potential and kinetic energy of the system are derived through extensive use of matrix algebra. The developments are similar to that used in the finite element method, and are ideally suited for programming on the digital computer. Other investigators (Refs. 3,4) have also based their analyses on energy minimization in which the displacement derivatives appearing in the kinematic relations are replaced by appropriate finite difference forms.

BOSOR3 SUMMARY

The BOSOR3 program represents the codification of three distinct analyses:

1. A nonlinear stress analysis for axisymmetric behavior of axisymmetric shell systems (large-deflections, elastic)
2. A linear stress analysis for axisymmetric and nonsymmetric behavior of axisymmetric shell systems submitted to axisymmetric and nonsymmetric loads
3. An eigenvalue analysis in which the eigenvalues represent buckling loads or vibration frequencies of axisymmetric shell systems submitted to axisymmetric loads (eigenvectors may correspond to axisymmetric or nonsymmetric modes).

The independent variables of the BOSOR3 analysis are the arc length, s , measured along the shell reference surface and the circumferential coordinate, θ . The dependent variables are the displacement components, u , v , and w of the shell wall reference surface. For the three analyses listed above, it is possible to eliminate the circumferential coordinate, θ , by separation of variables: in the nonlinear stress analysis θ is not present; in the linear stress analysis the nonsymmetric load system is expressed as a sum of harmonically varying quantities, the shell response to each harmonic being calculated separately; and in the eigenvalue analysis the eigenvectors vary harmonically around the circumference. Thus, the θ -dependence (where applicable) is eliminated by the assumption that $u(s, \theta)$, $v(s, \theta)$, $w(s, \theta)$ are given by $u_n(s) \sin n\theta$, $v_n(s) \cos n\theta$, $w_n(s) \sin n\theta$ or by $u_n(s) \cos n\theta$, $v_n(s) \sin n\theta$, $w_n(s) \cos n\theta$. In the BOSOR3 analysis the first three harmonically varying displacement components correspond to values $n > 0$; the last three to $n \leq 0$.

The advantages of being able to eliminate one of the independent variables cannot be overemphasized. The number of calculations performed by the computer for a given mesh point spacing along the arc length s is greatly reduced, leading to significant reductions in computer time. Because the numerical analysis is "one-dimensional" a rather elaborate composite shell structure can be analyzed in a single "pass" through the computer. The disadvantage is, of course, the restriction to axisymmetric structures.

STAGS SUMMARY

The STAGS computer program represents the codification of two distinct analyses:

1. Nonlinear stress and stability analysis for general shells (large deflections, elastic-plastic)
2. An eigenvalue analysis in which the eigenvalues represent vibration frequencies of arbitrarily loaded shells.

The independent variables of the STAGS analysis are the arc length measures along reference surface coordinate lines which need not be orthogonal. The dependent variables, as in BOSOR3, are the mesh point displacement components u_i , v_i , and w_i . In this analysis the independent variables cannot be separated, so that a "two-dimensional" numerical analysis is required. The advantage of the STAGS computer program is its very broad range of applicability. It has been used, for example, for calculation of collapse loads of axially compressed cylinders with cutouts and elliptical cones (Ref. 5,6). Vibration frequencies of cylinders with reinforced cutouts have been calculated (Ref. 7). STAGS can be used to determine the buckling loads and post-buckling behavior of thin shells with arbitrary initial imperfections. A two-dimensional nonlinear analysis gives a more complete description of the shell behavior but is much more expensive in terms of computer time.

In this paper the analyses on which BOSOR3 and STAGS are based will be described, numerical results will be given, various problems encountered during the development will be mentioned, and future proposed work will be outlined.

BOSOR3 ANALYSIS

References 8 and 9 give details of the analysis on which the BOSOR3 code is based. Only highlights from the bifurcation buckling and vibration analyses will be repeated here.

The results from the nonlinear axisymmetric stress analysis are used in the eigenvalue analyses for buckling and vibration. The "prebuckling" or "prestress" meridional and circumferential stress resultants N_{10} and N_{20} and the meridional rotation χ_0 appear as known variable coefficients in the energy expression which governs buckling and vibration. This expression is a homogeneous quadratic form. The values of a parameter (load or frequency) which render the quadratic form stationary with respect to infinitesimal variations of the dependent variables represent buckling loads or natural frequencies. These "eigenvalues" are calculated from a set of linear, homogeneous equations.

The same linear "stability" equations, with a "right-hand-side" vector added, are used for the linear stress analysis of axisymmetrically and non-symmetrically loaded shells. The "right-hand-side" vector represents load terms and terms due to thermal stress. The variable coefficients, N_{10} , N_{20} , and χ_0 , mentioned above are zero of course since there is no non-linear "prestress" analysis in this case.

The energy method used in the eigenvalue analysis is based on the definition of the Hamiltonian corresponding to an n-wave deformation pattern:

$$H_n = U_s + \sum_{k=1}^M U_r^k - \left(T_s + \sum_{k=1}^M T_r^k \right) + \sum_{i=1}^{K+1} U_c^i \quad (1)$$

where

- U_s = shell strain energy
- U_r^k = strain energy of kth ring stiffener
- T_s = shell kinetic energy
- T_r^k = kinetic energy of kth ring stiffener
- U_c^i = ith set of constraint conditions.

The functional H_n is given in terms of the shell wall displacements and their derivatives. Integration along the shell meridian is performed numerically. The derivatives with respect to the meridional coordinate "s" are simulated by two and three point finite-difference formulas.

The derivatives with respect to the circumferential coordinate θ are eliminated because $U = u_n \sin n\theta$, $V = v_n \cos n\theta$, $W = w_n \sin n\theta$. In this way H_n , which is originally an integro-differential quadratic form, becomes an algebraic quadratic form. The constraint conditions are equations of displacement and rotation compatibility at junctures between shell segments and at the shell boundaries.

The algebraic quadratic form H_n is expressed as:

$$H_n = [q]([K_1] + [K_2] + \Omega^2[M]), \quad (2)$$

The vector $[q]$ represents the dependent variables. These include the displacements at the meridional stations in the finite difference mesh and Lagrange multipliers corresponding to the constraint conditions. The matrix $[K_1]$ represents the stiffness matrix (including constraints) of the undeformed and unstressed structure; $[K_2]$ represents the contribution of the known prestress terms N_{10} , N_{20} , N_{or} , and χ_0 to the stiffness matrix; and $[M]$ represents the mass matrix. These matrices are symmetric.

The problem is to find the values (eigenvalues) of a parameter which cause H_n to be an extremum. In vibration problems the eigenvalue parameter is the square of the frequency Ω^2 . In buckling problems the eigenvalue parameter may be the pressure or temperature amplitude or any line load or moment applied to any ring. If some applied load is regarded as the eigenvalue parameter, the kinetic energy terms T_s and T_r^k are zero. The lowest eigenvalue then represents the bifurcation load and the eigenvector represents the mode shape. If, however, the applied load is fixed and Ω^2 is regarded as the eigenvalue parameter, the terms T_s and T_r^k are non-zero. The eigenvalues and eigenvectors then represent frequencies and mode shapes for prestressed shells of revolution. Minimization of H_n with respect to all of the q -components generates a set of simultaneous linear homogeneous algebraic equations, the coefficient matrix of which is symmetric. Non-trivial solutions are obtained for these equations on the digital computer.

Derivation of $[K_1]$, $[K_2]$, and $[M]$

In the following derivation variables are used which are defined in Figs. 1(a) and 1(b). These figures show a segmented, ring-stiffened shell supported at the end A by a ring and clamped at B. There are two intermediate rings, one in segment #1 and one between segments 1 and 2. Fig. 1(a) shows the structure and Fig. 1(b) shows the corresponding finite-difference model.

It is necessary first to define the various components of strain energy and kinetic energy. The shell strain energy U_s can be written as:

$$U_s = \frac{\pi}{2} \int_A^B \{ [S]\{\epsilon\} + [\omega][N_0]\{\omega\} + [d][P]\{d\} \} r \, ds \quad (3)$$

where

$$\begin{aligned} [S] &\equiv [N_1, N_2, N_{12}, M_1, M_2, M_t] \\ [\epsilon] &\equiv \{\epsilon\}^T \equiv [\epsilon_1, \epsilon_2, \epsilon_{12}, \kappa_1, \kappa_2, 2\kappa_{12}] \\ [\omega] &\equiv [\chi, \psi, \gamma] \\ [N_0] &= \begin{bmatrix} N_{10} & 0 & 0 \\ 0 & N_{20} & 0 \\ 0 & 0 & (N_{10} + N_{20}) \end{bmatrix} \\ [d] &\equiv [u, v, w] \\ [P] &= \begin{bmatrix} -p/R_1 & 0 & -p' \\ 0 & -p/R_2 & 0 \\ -p' & 0 & p(1/R_1 + 1/R_2) \end{bmatrix} \end{aligned} \quad (4)$$

and

$$\begin{Bmatrix} N_1 \\ N_2 \\ N_{12} \\ M_1 \\ M_2 \\ M_t \end{Bmatrix} = [C] \{ \epsilon \} = \begin{bmatrix} C_{11} & C_{12} & 0 & C_{14} & C_{15} & 0 \\ C_{12} & C_{22} & 0 & C_{24} & C_{25} & 0 \\ 0 & 0 & C_{33} & 0 & 0 & C_{36} \\ C_{14} & C_{24} & 0 & C_{44} & C_{45} & 0 \\ C_{15} & C_{25} & 0 & C_{45} & C_{55} & 0 \\ 0 & 0 & C_{36} & 0 & 0 & C_{66} \end{bmatrix} \begin{Bmatrix} \epsilon_1 \\ \epsilon_2 \\ \epsilon_{12} \\ \kappa_1 \\ \kappa_2 \\ 2\kappa_{12} \end{Bmatrix} \quad (5)$$

$$\epsilon_1 = u' + w/R_1 + \chi_0 \chi$$

$$\epsilon_2 = -nv/r + r'u/r + w/R_2 \quad (6)$$

$$\epsilon_{12} = v' - r'v/r + nu/r + \chi_0 \psi$$

$$\kappa_1 = \chi'$$

$$\kappa_2 = -n\psi/r + r'\chi/r \quad (7)$$

$$2\kappa_{12} = 2(-n\chi/r + r'\psi/r + v'/R_2)$$

$$\chi = w' - u/R_1$$

$$\psi = nw/r - v/R_2 \quad (8)$$

$$\gamma = \frac{1}{2}(nu/r - rv'/r - r'v/r).$$

The first term in the integrand of equation (3) is contained in equation (3) of Ref. 10; the second term appears in equation (2) of Ref. 11; and the third term appears in equation (9) of Ref. 12. The coefficients C_{ij} of the constitutive equations (5) are given for various types of shell walls (eccentrically stiffened, layered orthotropic, fiber-wound, corrugated) in Ref. 13. The kinematic relations (6)-(8) which relate infinitesimal buckling strains, changes in curvature, and rotations to infinitesimal buckling displacements are given in equations (4.23) and equations (3.16) of Ref. 14 and equations (7) and (12) of Ref. 10.

Figure 1(b) shows the shell meridian with stations 1,2,3,4,...,13 identified. The Hamiltonian H_n is expressed at these stations in terms of the displacement components u_i , v_i , and w_i , and the integration in equation (3) is replaced by summation over all stations. The tangential displacement components u_i and v_i occur at stations midway between the stations for w_i and w_{i+1} . A similar arrangement of mesh points was used by Stein in Ref. 3. At the ends of each segment there are "fictitious"

points, shown as circles, which correspond to w -values. The effects of these fictitious points are discussed in the section on numerical results. The arrangement of mesh points and displacements shown in Fig. 1(b) has been determined to be superior to an arrangement in which u_i , v_i and w_i correspond to displacement components at a single point. More will be said about this in the section on numerical results. The station spacing in each segment is constant, but different spacings are used in different segments ($h_1 \neq h_2$ in Fig. 1(b)). The displacements and their derivatives at the i th station are:

$$\begin{aligned} u &= (u_i + u_{i-1})/2 & v &= (v_i + v_{i-1})/2 & w &= w_i, \\ u' &= (u_i - u_{i-1})/h & v' &= (v_i - v_{i-1})/h & w' &= (w_{i+1} - w_{i-1})/2h, \\ w'' &= (w_{i+1} - 2w_i + w_{i-1})/h^2. \end{aligned} \quad (9)$$

It is convenient to define the vector $[q_i]$ by

$$[q_i] \equiv \{q_i\}^T = [w_{i-1}, u_{i-1}, v_{i-1}, w_i, u_i, v_i, w_{i+1}]. \quad (10)$$

From equations (6)-(10) it follows that

$$\{e_i\} = [[B_{11}] + \chi_{e1}[B_{12}]]\{q_i\} \quad (11)$$

$$\{\omega_i\} = [R_i]\{q_i\} \quad (12)$$

$$\{d_i\} = [D_i]\{q_i\} \quad (13)$$

in which $[B_{11}]$, $[B_{12}]$, $[R_i]$, and $[D_i]$ are given in Ref. 9.

Insertion of equations (5) and (11)-(13) into equation (3), and replacement of the integral with summation over the number of stations in the finite-difference mesh leads to

$$\begin{aligned} U_s = \frac{\pi}{2} \sum_{i=1}^N r_i \Delta s_i [q_i] & \{ [[B_{11}]^T + \chi_{e1}[B_{12}]^T][C_i] \{ [[B_{11}] + \chi_{e1}[B_{12}]] \\ & + [R_i]^T[N_{e1}][R_i] + [D_i]^T[P_i][D_i] \} \{q_i\}. \end{aligned} \quad (14)$$

The integration weights Δs_1 are equal to h for all stations except the end stations of each segment, at which $\Delta s_1 = h/2$.

The strain energy of the k th ring stiffener can be written in the form

$$U_s^k = \frac{\pi}{2} r_c^k \{u_s^*, v_s^*, w_s^*, \chi\}^T [G_1^k + G_2^k] \begin{Bmatrix} u_s^* \\ v_s^* \\ w_s^* \\ \chi \end{Bmatrix} \quad (15)$$

in which r_c^k is the radius to the centroid of the k th ring and u_s^* , v_s^* , and w_s^* are the axial, circumferential, and radial displacements of the ring shear center. The G_1^k and G_2^k are the ring stiffness matrices given in Ref. 9. Displacements u_s^* , v_s^* , and w_s^* are related to the displacement vector q_j by matrices $[E_1^k]$, $[E_2^k]$, and $[T]$ given in Ref. 9. Subscript j is the meridional station number corresponding to the discrete ring attachment point. The final expression for the strain energy of the k th discrete ring is

$$U_s^k = \frac{\pi}{2} r_c^k \{q_j\}^T [T]^T [E_1^k + \chi_s E_2^k]^T [G_1^k + G_2^k] [E_1^k + \chi_s E_2^k] [T] \{q_j\}. \quad (16)$$

The kinetic energy of the shell is given by

$$T_s = \frac{\pi}{2} \Omega^2 \int_A m(u^2 + v^2 + w^2) r ds \quad (17)$$

which, by use of equations (4e) and (13), and with numerical integration can be written in the form

$$T_s = \frac{\pi}{2} \Omega^2 \sum_{i=1}^N m r_i \Delta s_i \{q_i\}^T [D]^T [I] [D] \{q_i\}. \quad (18)$$

The quantity m_i represents the mass/area at the i th station and $[I]$ is the identity matrix. The kinetic energy of the k th ring is given by

$$T_k^k = \frac{\pi}{2} \Omega^2 \rho_r^k r_c^k [A^k (u_{c,j}^{*2} + v_{c,j}^{*2} + w_{c,j}^{*2}) + I_p^k \chi_j^2 + I_s^k \psi_j^2 + I_n^k \gamma_j^2 - 2I_{sn}^k \psi_j \gamma_j]. \quad (19)$$

The quantities ρ_r^k , A^k , I_p^k , I_s^k , I_n^k , and I_{sn}^k , are the ring material mass density, cross-section area, and area moments of inertia with respect to axes normal and tangential to the shell reference surface at the ring attachment point j . Subscript c denotes ring centroid and j denotes meridional station corresponding to the ring attachment point. In this work the centroid is assumed to coincide with the shell reference surface. Hence, the ring kinetic energy can be written in the form

$$T_k^k = \frac{\pi}{2} \Omega^2 \rho_r^k r_c^k [q_j] \{ A^k [T]^T [E_1^k + \chi_0 E_2^k] [T_A^k] [E_1^k + \chi_0 E_2^k] [T] + [R]^T [T_B^k] [R] \} \{ q_j \} \quad (20)$$

where $[T_A^k]$ and $[T_B^k]$ are given in Ref. 9.

The m th constraint condition U_c^m can be written in the form

$$U_c^m = [\lambda_1^m, \lambda_2^m, \lambda_3^m, \lambda_4^m] \left[[L] \begin{Bmatrix} u^{*+} \\ v^{*+} \\ w^{*+} \\ \chi^+ \end{Bmatrix} + [Q] + \chi_0 [Q_2] \begin{Bmatrix} v^{*-} \\ w^{*-} \\ \chi^- \end{Bmatrix} \right] \quad (21)$$

in which subscript l refers to the meridional station corresponding to the m th juncture between segments, and $[Q_1^m]$ and $[Q_2^m]$, given in Ref. 9, contain terms involving the meridional discontinuities d_1 and d_2 (Fig. 1a) and the circumferential wavenumber n . The λ_1^m , λ_2^m , λ_3^m , and λ_4^m are the m th set of Lagrange multipliers associated with the l th station at which constraints are imposed on the quantities u^* , v^* , w^* and χ . For example, the constraint conditions between Segments #1 and #2 in Fig. 1 ($m = 2, l = 7$) arise from the requirement that the motion during buckling or vibration of point D relative to point C involves no deformation of the ring cross-section. The quantity λ_1^m corresponds to

compatibility of axial displacements u^{*-} and u^{*+} ; λ_2^m corresponds to compatibility of circumferential displacements v^{*-} and v^{*+} ; λ_3^m to compatibility of radial displacements w^{*-} and w^{*+} ; λ_4^m to compatibility of meridional rotations χ^- and χ^+ .

Displacement boundary conditions applied at the A and B ends of the meridian (see Fig. 1) take the form

$$U_c^m = [\lambda_1^m, \lambda_2^m, \lambda_3^m, \lambda_4^m][K^m][Q_1^T + \chi, Q_2^T] \begin{Bmatrix} u^* \\ v^* \\ w^* \\ \chi \end{Bmatrix} \quad (22)$$

in which at the end A of the meridian $m = 1$ with

$$[K^m] = \begin{bmatrix} K_{A1} & 0 & 0 & 0 \\ 0 & K_{A2} & 0 & 0 \\ 0 & 0 & K_{A3} & 0 \\ 0 & 0 & 0 & K_{A4} \end{bmatrix} \quad (23)$$

and at the end B of the meridian $m = K + 1$ ($K = \text{number of shell segments}$) with

$$[K^m] = \begin{bmatrix} K_{B1} & 0 & 0 & 0 \\ 0 & K_{B2} & 0 & 0 \\ 0 & 0 & K_{B3} & 0 \\ 0 & 0 & 0 & K_{B4} \end{bmatrix} \quad (24)$$

The quantities $K_{A1}, K_{A2}, \text{etc.}$ and $K_{B1}, K_{B2}, \text{etc.}$ are assigned values, either unity if the corresponding displacement is zero or zero if the corresponding force component is zero. The displacement conditions correspond to a shell which is supported at distances d_1^m and d_2^m from the reference surface. For the shell in Fig. 1(a) the $K_{A1}, K_{A2}, \text{etc.}$ would all be zero and the $K_{B1}, K_{B2}, \text{etc.}$ would all be unity. In Ref. 9 the constraint conditions (21) and (22) are written in terms of the vectors $\{q^+\}$ and $\{q^-\}$ as symmetric quadratic forms:

$$U_c^m = [q^-, \lambda, q^+][F] \begin{Bmatrix} q^- \\ \lambda \\ q^+ \end{Bmatrix} \quad (25)$$

with

$$\lambda \equiv [\lambda_1^m, \lambda_2^m, \lambda_3^m, \lambda_4^m] \quad (26)$$

$$[F] = \begin{bmatrix} 7 \times 7 & 7 \times 4 & 7 \times 7 \\ [0] & [QT]^T & [0] \\ 4 \times 7 & 4 \times 4 & 4 \times 7 \\ [QT] & [0] & [T] \\ 7 \times 7 & 7 \times 4 & 7 \times 7 \\ [0] & [T]^T & [0] \end{bmatrix} \quad (27)$$

$$Q \equiv [QT + x_0, Q\bar{T}] \quad (28)$$

The boundary conditions (22) take a similar form:

$$U_c^m = [q^-, \lambda, q^+] \begin{bmatrix} [0] & [KQT]^T & [0] \\ [KQT] & [0] & [0] \\ [0] & [0] & [0] \end{bmatrix} \begin{Bmatrix} q^- \\ \lambda \\ q^+ \end{Bmatrix} \quad (29)$$

The three coefficient matrices $[K_1]$, $[K_2]$ and $[M]$ in equation (2) can now be written through use of equations (14), (16), (18), (20), (21) and (25). The following expressions are obtained:

$$[q][K_1]\{q\} = \frac{\pi}{2} \sum_{i=1}^N \left\{ [q_i][r_i \Delta s_i [B_{i1}]^T [C_i] [B_{i1}] + \delta_i [T]^T [E_i]^T [G_i] [E_i] [T]] \{q_i\} \right. \\ \left. + \delta_i [q^-, \lambda, q^+] [F_1] \begin{Bmatrix} q^- \\ \lambda \\ q^+ \end{Bmatrix} \right\} \quad (30)$$

$$[q][K_2]\{q\} = \frac{\pi}{2} \sum_{i=1}^N \left\{ [q_i][r_i \Delta s_i (\chi_{oi} [B_{i1}]^T [C_i] [B_{i2}] + \chi_{oi} [B_{i2}]^T [C_i] [B_{i1}] \right. \\ + \chi_{oi}^2 [B_{i2}]^T [C_i] [B_{i2}] + [R_i]^T [N_{oi}] [R_i] + [D_i]^T [P_i] [D_i]) \\ + \delta_i \{ [T]^T (\chi_{oi} [E_i]^T [G_1 + G_2] [E_2] + \chi_{oi} [E_2]^T [G_1 + G_2] [E_1] \\ + \chi_{oi}^2 [E_2]^T [G_1 + G_2] [E_2] + [E_i]^T [G_2] [E_i] [T]) \} \{q_i\} \\ \left. + \delta_i [q^-, \lambda, q^+] [F_2] \begin{Bmatrix} q^- \\ \lambda \\ q^+ \end{Bmatrix} \right\} \quad (31)$$

$$[q][M]\{q\} = \frac{\pi}{2} \sum_{i=1}^N [q_i][m_i r_i \Delta s_i [D]^T [I] [D] \\ + \delta_i \rho_i r_i (A [T]^T [E_1 + \chi_{oi} E_2]^T [T_A] [E_1 + \chi_{oi} E_2] [T] + [R]^T [T_B] [R])] \{q_i\}. \quad (32)$$

The δ_1^j and δ_1^l are Kronecker deltas, and $[F_1]$ and $[F_2]$ refer to equation (27) with the first and second parts of the matrix Q , respectively [equation (28)].

The coefficient matrices $[K_1]$, $[K_2]$ and $[M]$ have the form shown in Fig. 2. This matrix corresponds to the shell modeled as shown in Fig. 1(b). The boundary conditions at A contribute the elements $[KQT]_1$ and $[KQT]_1^T$; the compatibility conditions for conformity of displacements and rotation at the juncture between Segment #1 and Segment #2 contribute the elements $[QT]_2$, $[QT]_2^T$, $[T]$, and $[T]^T$; and the boundary conditions at B contribute the elements $[KQT]_3$ and $[KQT]_3^T$. Expression of H_n at each of the stations 1 through 13 leads to the sub-arrays of elements so labeled in Fig. 2.

It can be shown that the equations generated by minimization of H_n [equation (33)] with respect to the displacement components u_i , v_i and w_i [indicated in Fig. 1(b)] are the Euler equations of the variational problem in finite difference form. The equations corresponding to $\partial H_n / \partial u_i = 0$ and $\partial H_n / \partial v_i = 0$ represent equilibrium of in-plane forces at the stations where the u_i and v_i are specified; those corresponding to $\partial H_n / \partial w_i = 0$ represent equilibrium of normal forces at the stations where the w_i are specified.

Solution of the eigenvalue problem

The buckling loads or vibration frequencies are calculated from the set of linear, homogeneous, algebraic equations

$$[[K_1] + [K_2] + \Omega^2[M]]\{q\} = 0 \quad (33)$$

for which non-trivial solutions exist if

$$|[K_1] + [K_2] + \Omega^2[M]| = 0. \quad (34)$$

The matrices $[K_1]$, $[K_2]$ and $[M]$ are strongly banded. In vibration problems for prestressed shells a "classical" eigenvalue problem

$$[K_1 + K_2]q + \Omega^2[M]q = 0 \quad (35)$$

is formulated, and the power method (Refs. 15,16) is used for calculation of the lowest few eigenvalues Ω^2 for a particular wave number n . The number of eigenvalues which can be determined accurately depends on the number of mesh points in the finite difference analysis and the complexity ("waviness" in the meridional direction) of the mode shapes. Successive eigenvalues are determined accurately by means of orthogonalization and spectral shifting.

In buckling problems the eigenvalues of $[K_1 + K_2]$ for given n can be found by "plotting" $[K_1 + K_2]$ versus the eigenvalue parameter λ ($\lambda \equiv p, N_{10}$, or other load) to obtain the load for which $[K_1 + K_2]$ first vanishes. This technique was used in Ref. 17 for calculation of bifurcation loads of shells of revolution. On the other hand, a technique of successive approximation for buckling problems can be used. This technique involves the definition of a sequence of "classical" eigenvalue problems which yields a sequence of loads that converges to the load for which $[K_1 + K_2] = 0$. A typical "classical" eigenvalue problem in the sequence is

$$[K_1 + K_2]q + \lambda_1[K_2]q = 0. \quad (36)$$

Suppose the original load is p_1 . The prestress terms N_{10} , N_{20} , $N_{\theta r}$ and χ_0 which appear in $[K_2]$ are calculated for this load by means of the nonlinear analysis described in Ref. 8. Then from equation (36) a value λ_1 is obtained. The new load is $p_2 = p_1(1 + \lambda_1)$. New values of N_{10} , N_{20} , etc. corresponding to p_2 are now calculated from the nonlinear analysis of Ref. 8 and a new matrix $[K_2]$ is obtained. Then λ_2 is calculated from equation (36). The next value of the load is $p_3 = p_2(1 + \lambda_2)$. The iteration process continues until λ_k , the k th correction, is smaller than some preassigned number. Convergence in some typical cases is discussed in the section on numerical results.

BOSOR3 NUMERICAL RESULTS

The computer program based on the nonlinear stress analysis of Ref. 8 and the linear stability and vibration analysis presented above has been checked through cases for which solutions are known. A rather extensive investigation has been performed of the convergence properties of the eigenvalues with respect to number of points in the finite difference mesh and with respect to number of iterations required for the solution of nonlinear problems. Additional numerical results, including comparisons between test and theory, are given in Ref. 18.

Convergence properties

Table 1 gives six examples of the convergence of the sequence of eigenvalue problems as defined by equation (36). The first two examples are for an externally pressurized shallow spherical cap with an edge ring and a constant applied edge moment, M_0 (see Fig. 3(a) for geometry). The zeroth iteration represents the program user's initial guess of the critical load. In Example 1 the convergence criterion for the pressure (0.1%) is satisfied after four iterations. Example 2 represents a problem in which nonlinear effects are dominant because of the large edge moment $M_0 = 0.8$ in-lb/in., applied to the spherical cap. Convergence of the pressure is rather slow, and calculations are terminated before the solution has converged to the required accuracy of 0.1%. With a better initial guess for p_{cr} or if iterations are allowed to continue, a solution of $p_{cr} = 0.582$ psi is obtained. Examples 3-6 all apply to the same axially compressed cylindrical shell for which various numbers of mesh points are used (see Fig. 3(b) for geometry). The first three examples give results from single-precision calculations and the last example gives results from double-precision calculations. The accuracy required for computer "approval" of the solution is 0.01%. It is seen that roundoff errors cause some difficulty in Example 4 and prevent completely convergence in Example 5. It is also clear from Example 5 that a convergence criterion could be chosen (such as 1%) which would lead to "approval" of the solution 8135.2 lb-in. This load is not within 1% of the correct load (7788.1 lb/in.). It is evident from

the double-precision calculations of Example 6, that round-off errors cause the discrepancy. Figure 4 shows how round-off errors can lead to erroneous results when calculations are performed in single precision. The loads corresponding to 41 and 51 mesh points are "converged" solutions in the sense of Table 1, but they do not have the required accuracy when compared with the solutions labeled "Double Precision". Further increase in the number of mesh points with single-precision calculations leads to further deterioration in the accuracy of the results.

Table 2 gives buckling loads for a spherical shell with an edge angle $\alpha = 160^\circ$ and a free edge. The geometry and loading is shown in Fig. 3(c). The wave number $n = 2$. Loads are tabulated as a function of the number and the distribution of mesh points. Run times for the Univac 1108 digital computer are also given. These are the times in seconds required for calculation of the buckling load for a single value of the wave number n . Nonlinear prebuckling effects are included. It is seen that much accuracy is gained in this case by division of the shell into two segments. Mesh points are concentrated in the edge region where the modal displacements vary rapidly. For two cases double-precision calculations were made as a check on the single-precision results.

Figure 3(d) shows a cylindrical shell stiffened by small and large rings. It is desired to find the buckling pressure of this shell. In the analysis the small rings are "smeared out" (see Ref. 13) and the intermittent large rings are treated as discrete elastic structures. The large rings cause significant local disturbances in the prebuckling and buckling modal behavior, as seen in Fig. 5. It is therefore advantageous to analyze the single shell in segments, concentrating mesh points near the large rings where prebuckling and buckling modal displacements vary rapidly.

Comparison of two finite difference schemes

Figures 6 and 7 show comparisons between a finite-difference scheme in which all the displacement components u_1 , v_1 and w_1 are specified at the same point (Scheme #1) and the scheme indicated in Fig. 1(b) and equations (9)(Scheme #2). In the Scheme #1 central differences are used everywhere

except at the ends "A" and "B" of the shell, where forward and backward differences are used, respectively. With Scheme #1 the coupling between adjacent u_i and v_i values is weak, since no second derivatives of these variables appear in the energy expression. This situation often leads to the "jumpy" behavior of the eigenvector and affects the accuracy of the eigenvalue. Figure 6 shows the fundamental vibration mode of a ring-stiffened cylinder as calculated by the two schemes. The cylinder and ring geometry are shown in Figure 3(e). Figure 7 shows the buckling modal displacement u of the axially compressed cylinder depicted in Fig. 3(b). Convergence of the critical load with number of mesh points is far more rapid with the finite-difference Scheme #2 than with Scheme #1.

Comparison of Numerical Behavior With and Without W-Fictitious Points

Note that at segment ends in the finite-difference model shown in Fig. 1(b) there exist "extra" mesh points for the normal displacement component w . In a straightforward central difference formulation these so-called "fictitious" points are required for expression of the first and second w -derivatives with respect to arc length s . Figures 8 and 9 show comparisons of finite-difference formulations in which the w -fictitious points are included and not included. In the latter case forward differences are used at beginnings of segments and backward differences at segment ends.

Figure 8 shows convergence of critical axial load for a free-clamped cylinder with diameter 20 inches, length 40 inches, and thickness 0.1 inch. Both finite-difference formulations converge to the exact solution for a free-edge cylinder, which is 0.37 of the classical buckling load. It is interesting to note that convergence with fictitious points is not monotonic but, as would be expected, the buckling loads so calculated are always lower than those calculated without fictitious points.

The presence of w -fictitious points can sometimes lead to erroneous solutions in the case of eigenvalue problems. Figure 9 shows buckling loads and mode shapes for an axially compressed clamped cylindrical shell with radius = 10 inches, length = 2000 inches, thickness = 1 inch, modulus $E = 10^7$ psi and Poisson's ratio $\nu = 0.3$. One-half the cylinder is analyzed,

symmetry conditions being imposed at one end. The buckling loads are given in a table included as part of Fig. 9. Linear prebuckling analysis is used, and the circumferential wavenumber is fixed at 15. The lowest two eigenvalues are calculated for the finite-difference model in which w-fictitious points are included, and the lowest eigenvalue is calculated for the case labeled "without fictitious points". The table shows convergence with increasing numbers of mesh points. Notice that the lowest eigenvalue for the case "with fictitious points" changes drastically with increasing number of mesh points and that the second eigenvalue for this case is always slightly lower than the first eigenvalue for the case without fictitious points. The lowest eigenvalue in the first case represents an extraneous solution, and in fact tends to approach the buckling load for a shell with a free edge at the juncture between the two segments when the mesh spacing becomes large. Figure 9 shows the buckling mode shapes for the first and second eigenvalues of the case with fictitious points. The eigenvectors corresponding to the lowest eigenvalue of the case without fictitious points are identical to those on the right-hand-side of Figure 9.

STAGS ANALYSIS

The BOSOR3 computer program applies to problems in which the independent variables can be separated: analysis of shells of revolution with respect to nonlinear axisymmetric and linear nonsymmetric behavior. This separation of variables leads to a "one-dimensional" numerical problem -- a formulation in which the coefficient matrices of the governing equations in finite-difference form have very narrow bandwidths, of the order of 10 variables. Such problems can thus be solved on the digital computer in seconds to minutes. Very "dense" meshes can be used because of the small amount of core storage space required. However, the class of problems which can be solved is necessarily rather limited.

The STAGS code has been developed for the linear and nonlinear analysis of shells of general shape under general loading. It is not possible to separate the independent variables for such problems, and one must thus live with a "two-dimensional" numerical analysis. Such analyses lead to coefficient

matrices with bandwidths of order 100, and computer solutions require from several minutes to more than an hour per case. Finite-difference mesh density is limited both by computer time and core storage available. The advantage of such an analysis is of course its generality.

In the analysis of shells of revolution it is frequently very useful to predict stability limits by means of an analysis in which one searches for load values which correspond to non-uniqueness of equilibrium. These loads or eigenvalues frequently correspond to failure of the shell. Such bifurcation buckling analyses are less meaningful in the case of nonsymmetric shells, since these shells almost always fail by large-deflection collapse, analogous to the behavior of a very shallow spherical shell or arch clamped at the edges and subjected to external pressure. Bifurcation buckling can occur only into buckling modes which are orthogonal to the prebuckling displacements. In the case of general shells, deformations on the fundamental load-displacement branch (through the origin) generally contain components of all possible buckling modes. These modes grow rapidly as the load limit point is reached. It is therefore necessary in the case of general shells to perform a complete nonlinear analysis and to find the collapse load as a maximum or "limit point" in the load-displacement curve. The STAGS program is intended for the nonlinear analysis of general shells. The scope of the program and of extensions which are now in progress is shown in Table 3.

For a problem of this type one faces the choice between finite-difference and finite-element methods for discretization of the basic equations or of the shell geometry. Finite-element methods have a somewhat wider range of applicability as presently it is necessary in the finite-difference approach to define mathematically the reference surface of the shell and a suitable set of gridlines. However, the range within which the finite-difference method is applicable is still very wide, and the method appears to be quite superior in terms of computer economy, particularly for application to nonlinear problems. Thus a two-dimensional finite-difference analysis was selected as a basis for the STAGS program.

In order that the STAGS program not be unduly restrictive the finite-difference model is general enough to allow the use of nonorthogonal surface coordinates or gridlines. This choice extends the finite difference analysis

into an area which previously has been one of exclusive dominion by finite-element methods.

In the following paragraphs the shell strain energy density function for an isotropic material is developed. The contribution to the total energy of symmetrically placed discrete stiffeners is discussed in Ref. 5, and this capability has been extended so that stiffener eccentricity effects are included in the latest working version of STAGS. The discrete stiffener energy will not be included here in order to save space. Treatment of discrete stiffeners is analogous to that described in connection with BOSOR3.

The expressions for strain and curvature change used in STAGS are [Ref. 19]

$$\epsilon_{\alpha\beta} = \frac{1}{2} (\gamma_{\alpha\beta} + \gamma_{\beta\alpha}) + \frac{1}{2} \beta_{\alpha} \beta_{\beta} + \frac{1}{2} \gamma_{\rho\alpha} \gamma_{\rho\beta} \quad (37)$$

$$\kappa_{\alpha\beta} = \beta_{\beta|\alpha} + b_{\alpha}^{\rho} \gamma_{\rho\beta} - b_{\alpha\beta} \gamma_{\rho}^{\rho}$$

where $b_{\alpha\beta}$ is the curvature tensor and $\gamma_{\alpha\beta}$ and β_{α} are the displacement gradients defined by

$$\gamma_{\alpha\beta} = u_{\alpha|\beta} - b_{\alpha\beta} w \quad (38)$$

$$\beta_{\alpha} = w_{,\alpha} + b_{\alpha}^{\beta} u_{\beta}$$

While the strain tensor used is a standard expression, the curvature change tensor is not well known. This tensor differs from Sander's (Ref. 20) curvature change tensor in that it is valid for much larger out of plane rotations. A complete and rigorous derivation is given in Ref. 19.

The strain energy density expression in tensor form is

$$U = \frac{1}{2} \frac{E}{1-\nu} \left[(1-\nu) a^{\alpha\beta} a^{\beta\lambda} + \nu a^{\alpha\rho} a^{\beta\lambda} \right] \left[t \epsilon_{\alpha\rho} \epsilon_{\beta\lambda} + \frac{t^3}{12} \kappa_{\alpha\rho} \kappa_{\beta\lambda} \right] \quad (39)$$

After the metric tensor $a^{\alpha\beta}$ has been expressed in terms of the Lamé coefficients of the shell surface and implied summations have been carried out, U becomes

$$\begin{aligned}
 U = \frac{D}{2} & \left\{ (A \sin \theta)^{-4} \epsilon_x^2 - \frac{4A \cos \theta}{B} (A \sin \theta)^{-4} \epsilon_x \epsilon_{xy} \right. \\
 & + 2[1-(1-\nu) \sin^2 \theta] (AB \sin^2 \theta)^{-2} \epsilon_x \epsilon_y + 2(AB \sin^2 \theta)^{-2} [(1-\nu) + (1+\nu) \cos^2 \theta] \epsilon_{xy}^2 \\
 & - \frac{4B \cos \theta}{A} (B \sin \theta)^{-4} \epsilon_{xy} \epsilon_y + (B \sin \theta)^{-4} \epsilon_y^2 \Big\} \\
 & + \frac{K}{2} \left\{ (A \sin \theta)^{-4} \kappa_x^2 - \frac{4A \cos \theta}{B} (A \sin \theta)^{-4} \kappa_x \kappa_{xy} \right. \\
 & + 2[1-(1-\nu) \sin^2 \theta] (AB \sin^2 \theta)^{-2} \kappa_x \kappa_y + 2(AB \sin^2 \theta)^{-2} [(1-\nu) \cos^2 \theta] \kappa_{xy}^2 \\
 & - \frac{4B \cos \theta}{A} (B \sin \theta)^{-4} \kappa_{xy} \kappa_y + (B \sin \theta)^{-4} \kappa_y^2 \Big\} \quad (40)
 \end{aligned}$$

Here A and B are the coefficients of the first fundamental form

$$ds^2 = A^2 dx^2 + 2 AB (\cos \theta) dx dy + B^2 dy^2 \quad (41)$$

and θ represents the angle between the surface coordinate lines x and y . The strain energy expression (40) can be used for practical analysis after the strains and changes of curvatures have been expressed in terms of the physical components of displacement. Such equations are long and complicated. They are not shown here, but are available in Ref. 6.

Plasticity Theory used in STAGS

The plasticity theory used in the STAGS computer program has been proposed by Besseling (Ref. 21) and is based on a principle which originally was suggested by White (Ref. 22). This theory is very promising because it is rather simple in its application yet retains such features as strain hardening and the Bauschinger effect. The White-Besseling theory as applied in STAGS assumes that the material consists of several components which all have identical elastic properties and exhibit ideal plasticity (no strain hardening) but have different yield strengths. As the strain is the same in all components the stress-strain curve will experience a decrease in slope as the stress reaches the yield limit for any of the components which then ceases to take additional load. The composite thus exhibits strain hardening with a piecewise linear stress-strain relation. Use of only one component will, of course, result in application of ideal plasticity theory. As the stress is reversed after loading beyond the yield limit for one or more components, yield will occur in the reversed direction at an average stress in the composite which is lower than the stress for original yield. To introduce the Bauschinger effect this way is appealing because it reflects the microstress theory which is now generally accepted as the explanation of the Bauschinger effect.

STAGS Numerical Method

The numerical solution is based upon a two-dimensional finite-difference approximation. The shell surface is covered with mesh lines parallel to the coordinate lines, and the unknowns of the system are the normal displacements, w , at the grid points and the tangential displacements, u and v , at the same points or at points between adjacent grid points. The mesh spacing is variable over the surface.

The finite-difference formulation with u , v , w all located at grid points is called "whole-station" spacing. The formulation with u and v points located between w points is called "half-station" spacing. Three alternative finite-difference schemes have been explored:

1. "whole-station" spacing with membrane and bending energies integrated over the same shell element area
2. "whole-station" spacing with membrane and bending energies integrated over different shell element areas
3. "half-station" spacing with membrane and bending energies integrated over the same shell element area

The first scheme has been discarded because it leads to "jumpy" solutions as encountered in the "whole-station" scheme in BOSOR3 (see Figs. 6 and 7) and because it fails completely in cases where the mesh spacing varies. Schemes 2 and 3 are illustrated in Fig. 10. For the "whole-station" scheme 2, u, v , and w are located at the stations represented by small circles. In the "half-station" scheme 3, u and v are located at the dots labeled 1, 2, 3, and 4. For Scheme 2 the membrane energy is integrated over the area elements bounded by (x_{i-1}, y_{j-1}) , (x_{i-1}, y_j) , (x_i, y_j) , and (x_i, y_{j-1}) , for example. The bending energy is integrated over the shaded area R_{ij} . For Scheme 3 both membrane and bending energies are integrated over the shaded area, R_{ij} , and the functional values and derivatives of the displacements are evaluated at the large dark point located at the centroid of R_{ij} . The second scheme seems to give the best numerical behavior in the case of shells of such a wall construction that no coupling exists between membrane and bending energy. The third scheme shows promise for more complex wall constructions, since it is not necessary to integrate over different elements of area for membrane and bending shell energies. Some comparison of results with Schemes 2 and 3 will be given in the section on numerical results.

After replacement of the displacements and their derivatives in Eq. (40) by finite-difference approximations, the strain energy density at mesh station i can be written in the form

$$\Delta U^i = \frac{1}{2} Z^{i*} D^i Z^i \quad (42)$$

where D^i is a 6×6 positive definite matrix of constants and Z^i is the vector of strain and curvature changes at station i . D^i and Z^i are functions of the geometric parameters of the shell; in addition, D^i is dependent on the material properties. The vector of stress

resultants at station i is given by

$$S^i = D^i Z^i \quad (43)$$

ΔU^i is a 4th order polynomial in the displacement components since the components of Z^i are either linear or quadratic expressions in the displacement components.

The total potential energy, V , of the shell is obtained by combination of the strain energy and the work done by the external forces,

$$V = U - W$$

where
$$U = \sum_i^m \Delta U^i \cdot a^i$$

and
$$W = X \cdot F + X \cdot QX$$

Here X denotes the vector of displacement components, F is the vector of external forces, a^i is the area (R_{ij} in Fig. 10, for example) of the i^{th} subregion, and Q represents the pressure-rotation effect. A necessary condition for static equilibrium is that the total potential energy be stationary.

"Minimization" leads to a nonlinear equation system where the right-hand side is composed of terms corresponding to applied loads or displacements, temperatures or initial geometric imperfections. Through solution of the nonlinear system for increasing values of the load parameter the displacement configurations are found as functions of the load and collapse predicted as a limit point in the load-displacement curve.

Modified Newton-Raphson Method

For solution of the nonlinear system a modified Newton-Raphson iteration scheme is used. This is illustrated in Fig. 11 for the one-dimensional case. In the regular Newton-Raphson approach the value of the unknown X

is estimated and the function as well as its derivative is determined for this value. The correction of the estimate is the function value divided by the slope. Convergence is very rapid, as seen schematically in Fig. 11(a). In the modified method the slope is retained at its value for the first estimate and only the function value is recomputed for each iteration. Obviously convergence is now much slower, as seen in Fig. 11(b). However, in a two-dimensional numerical analysis the computation of a new slope corresponds to factoring a very large matrix. The computer time required for one iteration with the regular Newton-Raphson method is often more than ten times that required for one iteration with the modified method. Therefore it is advantageous to retain the slope even after the load has been changed. After a few load steps the rate of convergence deteriorates, and the matrix must be refactored to obtain a better estimate of the slope at the current load. One refactoring of the matrix gives the "exact" slope at the previous load step.

Various Strategies Used for Nonlinear Analysis

To use a computer program for nonlinear shell analysis requires considerable experience. The computer time depends on the strategy chosen. When convergence is difficult the step size may be decreased or the coefficient matrix refactored. The case can also be expedited through choice of a less severe convergence criterion. In addition, over- or under-relaxation can be used depending on whether convergence is uniform or oscillating. The strategy adopted varies with each case and with the load level of a particular case. It is necessary for economic analysis that intermediate data be saved on tape for subsequent restart of the case after the strategy has been reconsidered.

The use of initial imperfections may also be considered as a part of the strategy. In a buckling analysis for a circular cone, for example, it is necessary to include a small imperfection which is not orthogonal to the critical buckling mode. For an elliptical cone or cylinder with sufficient eccentricity all symmetric modes are present. These will grow rapidly as the critical load is approached. If the eccentricity is very

small the growth of the "buckling pattern" at each iteration is small in comparison to round-off errors in the total displacements. Hence, it is difficult to set a suitable convergence criterion. For marginal cases initial imperfections can be used to expedite the analysis. If there are planes of symmetry in load as well as in geometry, bifurcation is possible into modes which are antisymmetric with respect to these planes. Such buckling modes can be found only through inclusion of antisymmetric initial imperfections.

STAGS EXAMPLE CASES

The scope of the STAGS computer program may best be illustrated through presentation of some of the results which have been obtained in its application.

Axially Compressed Elliptic Cylinder

Numerical results were obtained with STAGS for an elliptic cylinder with a length of 1.0 in., a thickness of 0.0144 in., and semiaxes of 1.75 in. and 1.0 in. Young's modulus was 10^7 psi and Poisson's ratio was 0.3. The cylinder was subjected to a uniform end shortening with the edges free to rotate but restrained from moving in the radial and circumferential directions. The objective was to calculate collapse loads for the cylinder.

Since the "buckling patterns" were expected to be confined to the areas of least curvature, it appeared that antisymmetric behavior with respect to the normal plane through $S = 0$ (Fig. 12) could be excluded. Hence, the analysis was restricted to a 180° arc ($0 \leq S \leq 4.4$ inches) with symmetry conditions enforced at $S = 0, 4.4$. A uniform finite-difference grid was chosen with 11 points in the axial and 29 points in the circumferential directions. Results obtained with finer grids indicate that use of the chosen grid leads to accurate computations of the collapse load.

Due to the symmetry of the prebuckling deformation about the plane at midlength and about the normal plane through $S = 2.2$, it is necessary to excite nonsymmetric deformations by the use of small antisymmetric imperfections.

Despite the presence of these imperfections a deformation pattern develops at collapse which is symmetric about both of these planes. Therefore, further analysis was restricted to arc lengths covering half the cylinder length and one quarter of the circumference.

For the particular cylinder considered (aspect ratio of 1.75) it is possible to determine the critical load without the use of symmetric imperfections. As the load is increased, a very sharp maximum is found in the load-displacement curve (point A in Fig. 12). Beyond point A convergence cannot be obtained; hence the postbuckling curve cannot be directly determined for the perfect shell.

The displacement mode which develops at collapse for a perfect shell is used as a guide in the choice of a suitable initial imperfection mode:

$$\bar{w}_{\text{imp}}/t = -\xi \sin\left(\frac{\pi x}{L}\right) \cos(6\theta)$$

Load-displacement curves were computed for several different values of the imperfection amplitude ξ . The results are shown in Fig. 12, in which the total axial load in pounds is plotted versus the end shortening divided by shell thickness. The normal displacement at $S = 2.2$, $x = L/2$ is shown as a function of the axial load and ξ in Fig. 13. From Fig. 12 it can be seen that for a sufficiently large imperfection amplitude, the first sharp maximum does not exist - the curve is smooth and it is possible to find equilibrium configurations in the postbuckling range. After such configurations have been found they can be used as starting values for an analysis in which the imperfection amplitude is gradually changed until a point is found on the postbuckling curve for perfect shells. After such a point is found it is easy to establish the postbuckling load-displacement curve for a perfect shell (curve ABC in Fig. 12).

After the first sharp maximum A the postbuckling curve exhibits two additional limit points B and C which correspond to secondary buckling. The curve was not pursued beyond the third maximum because the deformations are then so large that the applicability of the basic equations is questionable. Also the buckle pattern is close to the point of maximum curvature and bifurcation into an antisymmetric mode is likely.

In a test on this shell, sudden changes in the deflection pattern (buckling) would be noticed at A, B, and C. Notice that the shell may carry more load than the initial peak A indicates. While the primary buckling load A is rather sensitive to imperfections it appears that the second maximum B is relatively insensitive to imperfections. Hence, it may be suitable as a design limit. Results similar to these have been presented by Kempner, et al., for oval shells (Refs. 23, 24). However, Kempner's shells are not elliptic and a direct comparison is not possible.

The curves Δw versus S at the bottom of Fig. 12 are "buckling modes" calculated by subtracting displacement vectors obtained in two sequential steps in end shortening and normalizing the result. Such a subtraction yields the shape of the fastest growing displacement component, which might be interpreted as a buckling mode. As one traces one's way along the load-deflection curve OABC, the axial stress in the shell is constantly being redistributed by the local growth of normal displacement. For example, early in the "load" history the most rapid growth of normal displacement occurs at the point labeled S = 2.2, the area of minimum curvature. This growth relieves the axial stress there and permits loading above the initial peak A. At point B the most rapid growth of normal displacement is about halfway between the ends of the minor and major axes. This growth relieves the axial stress in the corresponding area and thus permits loading to an even higher peak, C, where the rapid growth of normal displacement occurs near the end of the major axis in an area of relatively large curvature.

Collapse of Axially Compressed "Pear-Shaped" Cylinder

The "pear-shaped" cylinder shown in Fig. 14(a) is typical of the fuselage cross-section of a proposed space shuttle vehicle configuration. The behavior of this shell subjected to uniform end shortening was investigated with the STAGS code. The theoretical results given in Figs. 14(b-d) are based on a finite-difference model with 45 circumferential nodes and 9 axial nodes covering $1/2^\circ$ of the circumference and $1/2$ of the length. Approximately 75 minutes of UNIVAC 1108 computer time were required for generation of the complete load-deflection curve with single-precision calculations.

As seen from Fig. 14(b) the linear range in this case represents less than 1/30 of the total load history of the shell. The rapid change in slope of the load-deflection curves at about $P = 100$ lbs. corresponds to rapid growth in normal deflection (buckling) of the flat portions of the shell. Associated with this rapid growth in w is a redistribution of the axial stress so that the curved portions begin to take up a larger percentage of the total axial load P . As more and more of the axial load is born by the curved portions, the slope of the load-end-shortening curve increases until just before collapse, at which load the entire structure fails. Figures 14(c) and 14(d) show the circumferential distributions of normal outward displacement w and axial compression/length N_x at the shell midlength for $P = 1164$ lbs. At this load both w and N_x are growing very rapidly with P in the curved portions $0 \leq \theta \leq 45^\circ$ and $90^\circ \leq \theta \leq 157\frac{1}{2}^\circ$.

The rather complex behavior in this case indicates the need for a flexible strategy for calculation of collapse loads of shells. Small load steps and frequent refactoring of the equation system matrix are required in the load region between 100 and 200 lbs. even though the displacements are relatively small in this range. Farther out on the load-end-shortening curve, where the displacements are larger, rather large load steps can be used and few refactorings are necessary. Efficient use of the STAGS code, or any code for predicting nonlinear behavior of shells, requires a sophisticated iteration strategy built into it and a well-trained user to take advantage of this strategy.

Comparison with Finite-Element Method

Results from a linear version of the STAGS program were compared with those from the REXBAT program, a general-purpose finite element code (Ref. 25). The axially compressed "pear-shaped" cylinder was used as a test case. Figure 15(a) shows the normal displacement as a function of circumferential coordinate θ calculated with both programs. With STAGS the "whole-station" scheme was used with 9 axial and 97 circumferential mesh points. With REXBAT 4 axial and 150 circumferential elements were used. These seemed to be the optimum distributions of mesh points for the two programs. Many fewer stations are required in the axial direction since $w(x)$ for given θ resembles a half-sine wave.

Figure 15(b) shows rates of convergence of normal displacement w with increasing number of circumferential stations for STAGS and REXBAT. Six axial stations were used in STAGS and 5 axial elements were used in REXBAT (same number of mesh spaces in both programs). In STAGS the "whole-station" scheme was found in this case to be much superior to the "half-station" scheme. Further comparisons of finite element and finite difference codes should be made to obtain an unbiased picture of the relative advantages of each method in various cases.

Nonlinear Analysis of Clamped and Simply-Supported Cylindrical Panels under Concentrated Load

The STAGS code was applied to shallow cylindrical panels with geometry and material properties given in Fig. 16. One-quarter of the panel was investigated, symmetry conditions being used at the midlength and midcircumference. Two cases were treated: a panel clamped at the two curved edges and a panel simply-supported at the two curved edges. The straight edges were free in both cases. Ten axial and nine circumferential mesh points were used in the "half-station" finite-difference analysis. In the clamped case there was no collapse because of development of axial membrane tension. Collapse in the case of simple support is indicated by a maximum in the load-deflection curve and by an abrupt decrease in value of the coefficient matrix determinant as the limit load is approached.

Axially Compressed Cylinder with Cutout

The benefit derived from the use of a variable mesh spacing has been evaluated by re-examining the axially compressed cylinder with cutouts for which test results are reported in Ref. 5. The cylinder geometry and material properties are given in Fig. 17. The cylinder has two diametrically opposite cutouts and a radius-to-thickness ratio of 400. It is reported in Ref. 5 that a reasonably accurate analysis for such cylinders would require excessive computer time. Numerical results for a finite-difference net with 9 axial x 20 circumferential points presented in Ref. 5 are shown

here in Figure 17 (curve A). Due to improvements in the efficiency of the computer program, it is now possible to obtain much better results even with constant grid spacing. Curve B is obtained with such a net (16 x 20). A finite-difference mesh was designed also in which the minimum grid spacing is identical to that used for Curve B, but which gradually increases away from the cutout until it is approximately doubled. The displacements corresponding to this analysis are practically identical to those obtained by use of grid with constant spacing, but the computer time is reduced by about 40%.

Curve C was determined by use of a minimum grid spacing of 0.2 in. at the edge of the cutout. The spacing increases with distance from the cutout by a factor of 1.2 from one mesh point to the next until the maximum grid size of 0.6 in. is obtained. For Curve D the minimum spacing is 0.12 in., the factor is 1.5, and the maximum size is again 0.6 in. It appears that the results obtained by use of the latter mesh are in very good agreement with the experimental results.

The computer time corresponding to the determination of one of these curves is approximately 0.5 hours (UNIVAC 1108, single precision). For analyses with even finer mesh sizes, therefore, the analysis was restricted to loads below 845 lbs. The results in Table 4 show that additional refinement of the mesh would not substantially change the results shown in Curve D.

Conclusions and Further Work Needed

The energy method with finite-differences is attractive with respect to suitability as a basis of efficient computer programs and numerical stability. Matrix methods are used extensively to develop the governing equations. In fact the only "hand" analysis involves establishment of the Hamiltonian in terms of stresses and strains and the choice of appropriate kinematic relations. The digital computer derives the equations. This simplicity of approach permits great flexibility in the analysis. It is easy to incorporate thermal effects, smeared and discrete stiffeners, orthotropic layers, variable thickness, and segmented shells. Furthermore, large-deflection effects, plasticity, and non-orthogonal nets with variable

mesh spacing present no major obstacles. The method appears to be competitive with the finite-element method in terms of generality, and from preliminary comparisons more efficient on the computer, particularly for nonlinear problems.

The BOSOR3 program is a general computer shell of revolution analyzer. Ring-stiffened, segmented shells with various wall constructions are analyzed for stress, stability, and vibrations. Nonlinear large-deflection effects are included in the axisymmetric prestress analysis. Two finite-difference schemes, "whole" and "half" station, are explored, and the "half-station" scheme is found to be much superior in terms of rapidity of convergence and numerical stability. The advantage of dividing a simple shell into segments in order to achieve greater accuracy with less computer time is revealed. A method is described in which a "nonlinear eigenvalue problem" is solved by iterative solution of a sequence of "classical" eigenvalue problems. Finite-difference schemes in which w -fictitious points are included and neglected are compared, and it is found that solutions with the w -fictitious points tend to converge faster with increasing numbers of mesh points, but that extraneous eigenvalues sometimes appear when these "extra" degrees of freedom are present. Large complex shells of revolution can be analyzed with a reasonably dense mesh in very short computer times because of the narrow bandwidth of the coefficient matrix due to the one-dimensional character of the numerical analysis. However, the applicability of BOSOR3 is limited to shells of revolution.

The STAGS program is a general shell analyzer. Eccentrically stiffened isotropic shells with variable thickness are analyzed for stress, stability, and vibrations. Nonlinear large-deflection effects and plasticity are included. The program requires more computer time per case than BOSOR3 because of the two-dimensional character of the numerical analysis and hence much wider bandwidths of the coefficient matrices. The advantage of the code is its greater generality. Approximate bifurcation buckling models are not necessary because detailed pre and post buckling behavior is revealed in the general nonlinear analysis. Limited evaluation indicates that the two-dimensional energy method with finite differences appears to be faster on the computer than the finite-element method, particularly in

the case of nonlinear problems. The difference in time in the cases studied is attributable to faster convergence of the finite-difference solutions with number of degrees of freedom and shorter times required for formation of stiffness matrices, particularly after the first iteration for nonlinear solutions. Various finite-difference schemes, including "whole" and "half" station with constant and variable mesh spacing are explored. Preliminary results indicate that the variable spacing "whole" station scheme with different elemental areas of integration for bending and membrane energies gives the most rapidly convergent solution with the greatest degree of numerical stability. Applicability of this scheme to shells in which coupling exists between membrane and bending energy is an open question. The modified Newton-Raphson method in which the coefficient matrix is factored only when required for convergence seems to be the most efficient and reliable of those explored during the development of STAGS. The strategy chosen for solution of nonlinear problems is important for computer economy as well as accuracy of results. Variation of convergence criterion, relaxation parameters, imperfection amplitudes and shapes, load steps, and other numerical, physical, and geometrical parameters all play a part in the solution of nonlinear problems. The importance of strategy will increase as more and more sophisticated programs requiring ever larger investments of computer dollars are created. This is evident if one hopes to solve, for example, the large-deflection, elastic-plastic and creep problem for a general shell with temperature-dependent material properties. STAGS example cases reveal complex behavior of nonlinear systems. Redistribution of stress during loading is an example. This phenomenon leads to rapid variations in the slope of load-deflection curves and post-buckling strength which exceeds initial buckling loads.

Work is in progress to include branched shells in the BOSOR3 program capability. Inclusion of plasticity in the axisymmetric large-deflection prebuckling analysis is an effort warranted by the frequent occurrence of buckling of practical shells of revolution at loads above the proportional limit of the wall material but below loads corresponding to material failure. The STAGS capability is currently being extended to include thermal loading, orthotropic shell wall properties, bifurcation buckling, and cutouts of general shape. Further extensions needed for the solution of practical

problems include introduction of temperature effects on elastic-plastic material properties, temperature-dependent creep, and dynamic response and buckling. The need for further comparative evaluation of the finite-difference and finite-element methods for linear and nonlinear problems cannot be overemphasized. Investigations of various finite-difference schemes such as "whole" and "half" station should continue, and efforts should be made to place the finite-difference energy method on a firmer mathematical foundation. Various strategies for the solution of complex problems involving geometric as well as material property nonlinearity should be continuously investigated. Application of these methods to a large variety of problems will reveal on a broad basis their relative advantages and disadvantages, thus permitting the establishment of appropriate "confidence" or "usefulness" indices for computer programs based on them.

REFERENCES

1. Bushnell, D., "Stress, Stability, and Vibration of Complex Shells of Revolution: Analysis and User's Manual for BOSOR3", SAMSO TR 69-375, LMSC Report N-5J-69-1, Lockheed Missiles & Space Company, Sept. 1969
2. STAGS User's Manual
3. Stein, M., "The Effect on the Buckling of Perfect Cylinders of Prebuckling Deformations and Stresses Induced by Edge Support", NASA TN D-1510, Dec. 1962, p. 217.
4. Budiansky, E. and Anderson, D.G.M., "Numerical Shell Analysis - Nodes without Elements," 12th International Congress of Applied Mechanics, Stanford Univ., August 26-31, 1968.
5. Brogan, F. and Almroth, B., "Buckling of Cylinders with Cutouts," AIAA J., Vol. 8, No. 2, p. 236-241, Feb. 1970.
6. Almroth, B. O., Brogan, F. A., and Marlowe, M. B., "Collapse Analysis for Elliptic Cones," to be published in AIAA J., 1970.
7. Brogan, F. A., Forsberg, K., and Smith, S., "Experimental and Analytical Investigation of the Dynamic Behavior of a Cylinder with a Cutout," AIAA/ASME 9th Structures, Structural Dynamics and Materials Conference, AIAA Paper No. 68-318, April 1968.
8. Bushnell, D., "Analysis of Ring-Stiffened Shells of Revolution Under Combined Thermal and Mechanical Loading," presented at AIAA/ASME 11th Structures, Structural Dynamics and Materials Conference, Denver, April 1970.
9. Bushnell, D., "Analysis of Buckling and Vibration of Ring-Stiffened, Segmented Shells of Revolution," Int. Journal of Solids, Structures, Vol. 6, p. 157-181, 1970.
10. Cohen, G. A., "Computer Analysis of Asymmetric Buckling of Ring-Stiffened Orthotropic Shells of Revolution," AIAA J., Vol. 6, p. 141, 1968.
11. -----, "Buckling of Axially Compressed Cylindrical Shells with Ring-Stiffened Edges," AIAA J., Vol. 4, p. 1859, 1966.
12. -----, "Conservativeness of a Normal Pressure Field Acting on a Shell," AIAA J., Vol. 4, p. 1885, 1966.
13. Bushnell, D., B. O. Almroth and L. H. Sobel, "Buckling of Shells of Revolution with Various Wall Constructions, Vol. 2 - Basic Equations and Method of Solution," NASA CR-1050, May 1968.
14. Novoshilov, V. V., The Theory of Thin Shells, Chapter 1, pp. 18 and 24, Noordhoff, 1959

15. Bodewig, F., Matrix Calculus, North-Holland, 1959.
16. Tsui, E. Y., Brogan, F. A., and Stern, P., "Juncture Stress Fields in Multicellular Structures," Lockheed Missiles & Space Co. Report M-77-65-5, Vol. 1, 1965.
17. Almroth, B. O., and Bushnell, D., "Computer Analysis of Various Shells of Revolution," presented AIAA 6th Aerospace Sciences Meeting, New York, Jan. 1968, AIAA J , Vol. 6, p. 1848, 1968.
18. Bushnell, D., "Buckling and Vibration of Ring-Stiffened, Segmented Shells of Revolution, Part 2, Numerical Results," Proc. First International Piping and Pressure Vessel Technology Conference, Delft, 1969.
19. Marlowe, M. B. and Flugge, W., "Some New Developments in the Foundations of Shell Theory," Lockheed Missiles & Space Company Report IMSC-6-78-68-13, May 1968.
20. Sanders, J. L., Jr., "Nonlinear Theories for Thin Shells," Quarterly of Applied Mathematics, Vol. 21, No. 1, p. 21-36, 1963.
21. Besseling, J. F., "A Theory of Elastic, Plastic, and Creep Deformations of an Initially Isotropic Material," SUDAER No. 78, Dept. of Aero. Eng., Stanford University, April 1958
22. White, G. N., Jr., "Application of the Theory of Perfectly Plastic Solids to Stress Analysis of Strain Hardening Solids," TR 51, Dept. of Applied Math., Brown, Aug. 1950.
23. Kempner, J. and Chen, Y.-N., "Buckling and Postbuckling of an Axially Compressed Oval Cylindrical Shell," Proc. Symposium on the Theory of Shells to Honor Lloyd Hamilton Donnell, Univ. of Houston, McCutchan Publ. Corp., May 1967, p. 141-183; also PIBAL Rept. No. 917, Polytechnic Institute of Brooklyn.
24. -----, "Postbuckling of an Axially Compressed Oval Cylindrical Shell," Applied Mechanics, Proc. 12th Int. Congress of Applied Mechanics, Stanford Univ., Aug. 26-31, 1968, p. 246-268; also PIBAL Rept. No. 98-31, Polytechnic Institute of Brooklyn.
25. Loden, W. A., "User's Manual for REXBAT 5," in preparation at Lockheed Palo Alto Research Laboratory.

TABLE 1. CONVERGENCE OF SEQUENCE OF EIGENVALUE PROBLEMS $[K_1 + K_2]\{q\} + \lambda_2[K_2]\{q\} = 0$

Iteration number k	Ex. 1† Sph. cap $M_0 = 0.2$ p_{cr} (psi)	Ex. 2 Sph. cap $M_0 = 0.8$ p_{cr} (psi)	Ex. 3 Cyl. 11 points N_{cr} (lb/in.)	Ex. 4 Cyl. 41 points N_{cr} (lb/in.)	Ex. 5 Cyl. 91 points N_{cr} (lb/in.)	Ex. 6 Cyl. 91 pts. D.P. N_{cr} (lb/in.)
0	0.20000	0.1000	7750.0	7750.0	7750.0	7750.0
1	0.65002	0.1407	7960.0	7766.3	7917.8	7775.5
2	0.78577	0.1927	8021.9	7777.7	8098.0	7784.0
3	0.77928	0.2546	8039.6	7781.5	8247.0	7786.8
4	0.77965	0.3221	8044.6	7782.5	8103.4	7787.8
5		0.3883	8046.0	7778.4	8128.1	7768.1
6		0.4462	8046.4	7771.2	8135.2	
7		0.4917		7779.6	8216.1	
8		0.5245		7781.4	8260.4	
9		0.5466			8192.8	
10		0.5609			8009.8	
11		0.5699			8257.6	

†Ex. 1 and 2 are for externally pressurized spherical caps with edge rings (see Fig. 3(a)). Ex. 3-6 are for axially compressed, longitudinally stiffened cylinders (see Fig. 3(b)). Ex. 6 calculations in double precision.

TABLE 2. BUCKLING LOADS OF A SPHERICAL SHELL, $\alpha = 160^\circ$, $A = 0$, $E = 0.91$, $\nu = 0.3$ CONVERGENCE WITH NUMBER AND DISTRIBUTION OF MESH POINTS; COMPUTER TIME

Number of mesh points	How distributed	Buckling pressure $p_{cr} \times 10^7$ (lb/in ²) single precision	Buckling pressure $p_{cr} \times 10^7$ (lb/in ²) double precision	Univac 1108 computer time (seconds) single precision
30	1 Segment	19.345		8.511
40	1 Segment	26.978		10.235
50	1 Segment	30.730		10.186
60	1 Segment	32.650		11.794
70	1 Segment	33.761		10.411
80	1 Segment	34.417		11.847
90	1 Segment	34.866		9.614
97	1 Segment	35.056		10.069
10, 10	2 Segments			
	(0°-135°) (135°-160°)	33.594		4.574
15, 15	2 Segments			
	(0°-135°) (135°-160°)	35.405		5.626
20, 20	2 Segments			
	(0°-135°) (135°-160°)	35.872		6.946
25, 25	2 Segments			
	(0°-135°) (135°-160°)	36.039		8.595
30, 30	2 Segments			
	(0°-135°) (135°-160°)	36.090		9.434
35, 35	2 Segments			
	(0°-135°) (135°-160°)	36.160	36.175	10.670
40, 40	2 Segments			
	(0°-135°) (135°-160°)	36.157		11.981
45, 45	2 Segments			
	(0°-135°) (135°-160°)	36.206	36.223	13.223

TABLE 3
SCOPE OF THE STAGS PROGRAM

<u>Present Capability</u>	<u>Under Development</u>
General Geometry for Ref. Surface	Thermal Loading
Geometric Nonlinearity	Variable Elastic Properties
Cutout on Coordinate Lines	Bifurcation Buckling
Eccentric Discrete Stiffeners	General Form of Cutout
Initial Imperfections	Orthotropic Material
Variable Thickness	White-Besseling Plasticity Theory
General Boundary Conditions	
General Loading	
Displacement Loading	
Variable Grid	

TABLE 4
DISPLACEMENT w_1 AT P = 845 LBS.

	Finite-Difference Mesh		Min. Spacing	Factor	Max. Spacing	w_1
	No. Axial Points	No. Circum. Points				
D	13	21	.12	1.5	.60	.00877
E	18	25	.12	1.2	.60	.00850
F	21	35	.12	1.2	.30	.00858
G	21	38	.08	1.2	.60	.00873

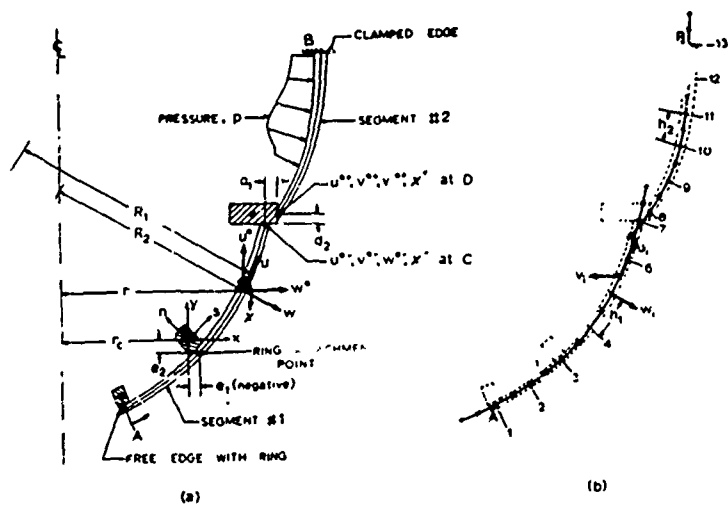


FIG. 1. Ring-stiffened shell with two segments

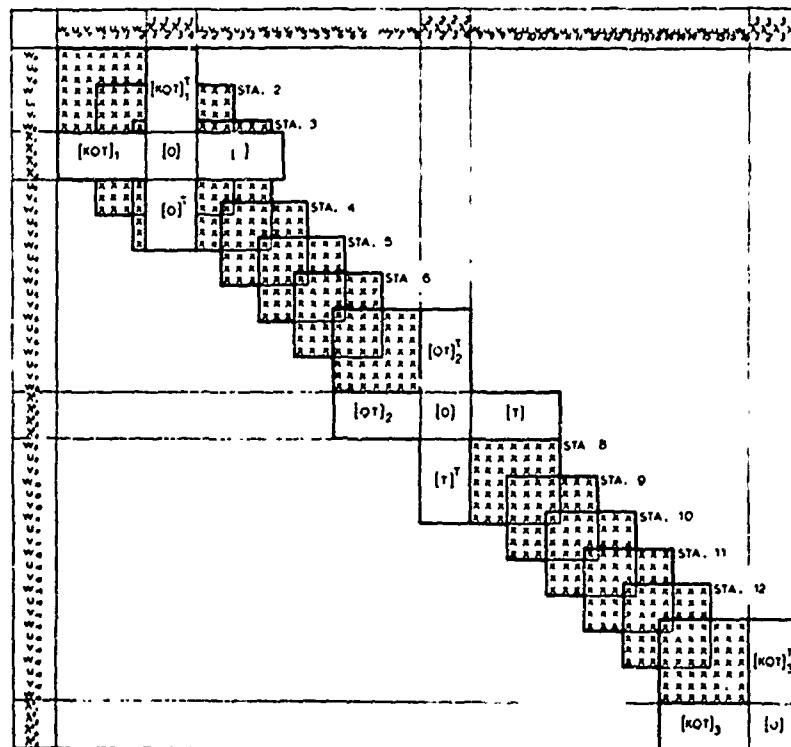
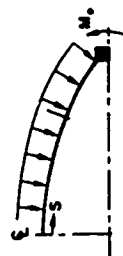
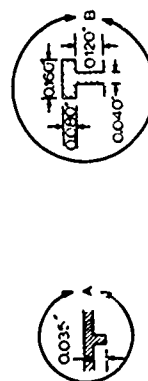


FIG. 2. Form of coefficient matrix with constraint conditions. This matrix corresponds to the model in Fig. 1(b)



(a) Geometry for Examples 1 and 2, Table 1



(d) Geometry of Ring-Stiffened Cylinder Subjected to External Hydrostatic Pressure Corresponding to Results in Fig. 5.

(c) Geometry for Results in Table 2

(b) Geometry for Examples 3 through 6, Table 1, Fig. 4 and Fig. 7

(c) Geometry of Vibrating Ring-Stiffened Cylinder Corresponding to Results in Fig. 6.

Figure 3 Configurations Corresponding to Results Given in Tables 1 and 2 and Figs. 4-7

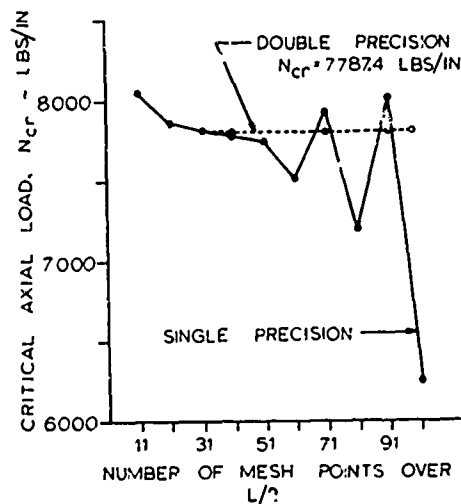


Figure 4 Convergence of Buckling Load with Increase in Number of Mesh Points

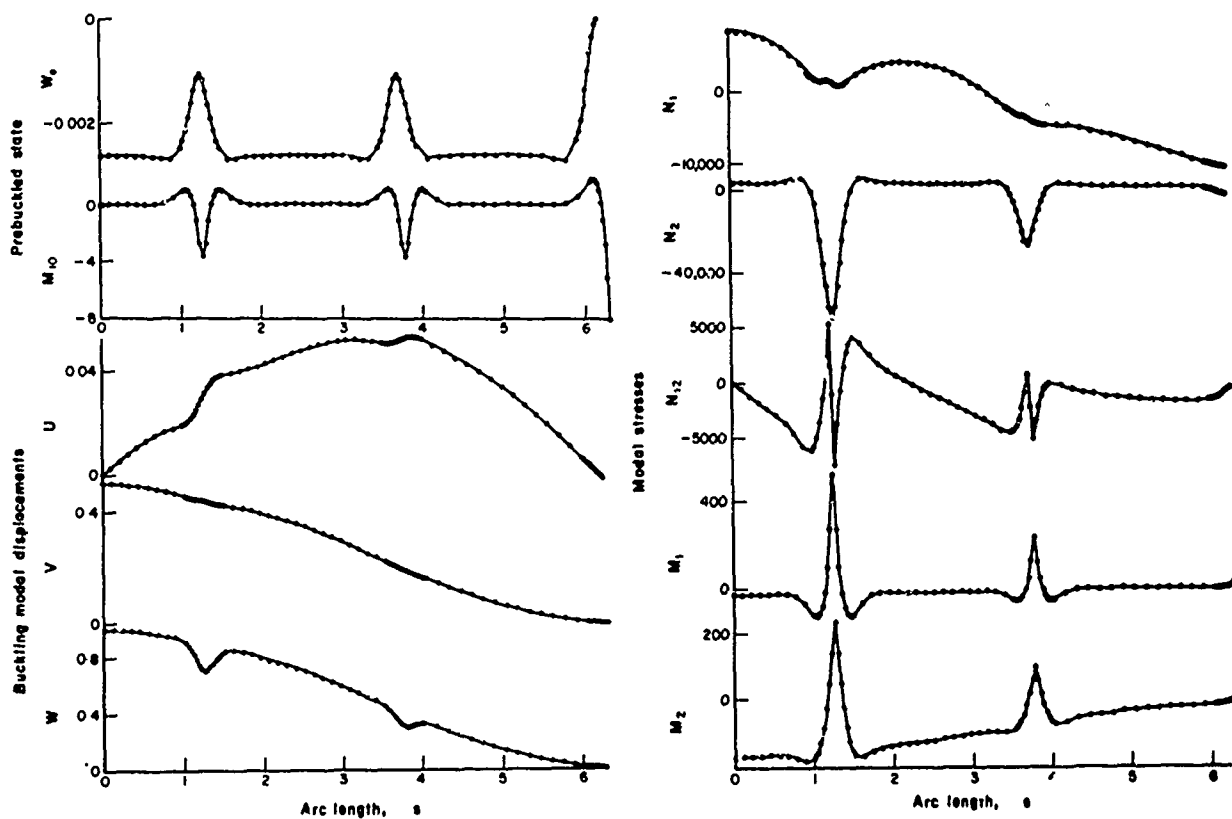
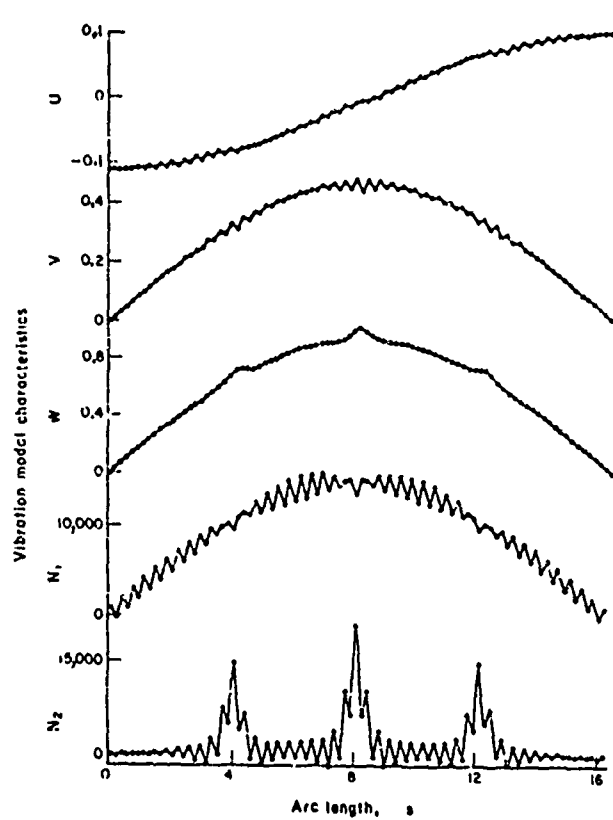
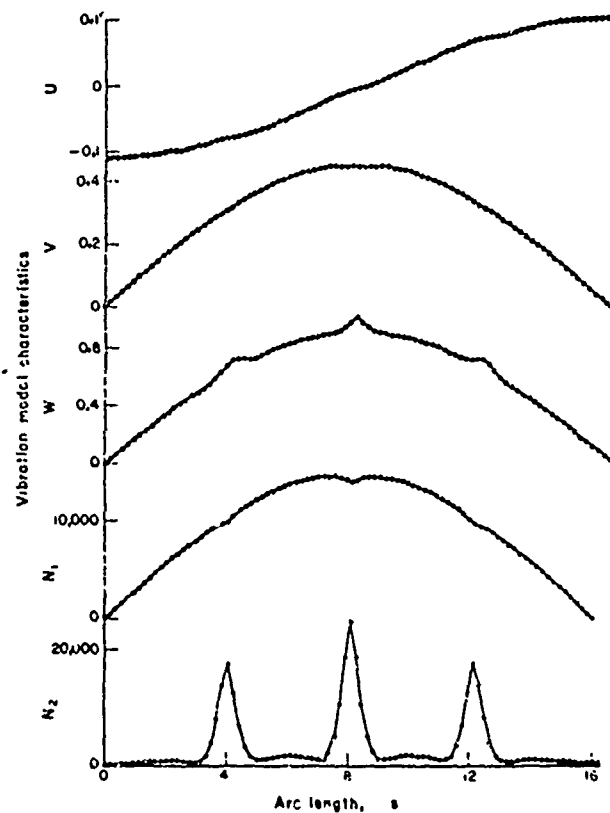


Figure 5 Prestress State and Buckling Modal Characteristics of the Externally Pressurized, Ring-Stiffened Cylinder Shown in Fig. 3(d). Single Shell Analyzed as Six Segments with Mesh Points Concentrated Around Large Rings.

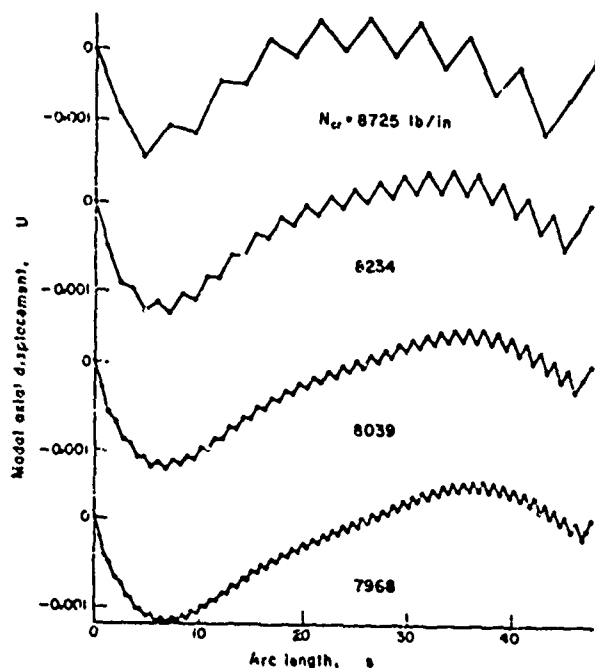


(a) Finite difference scheme #1

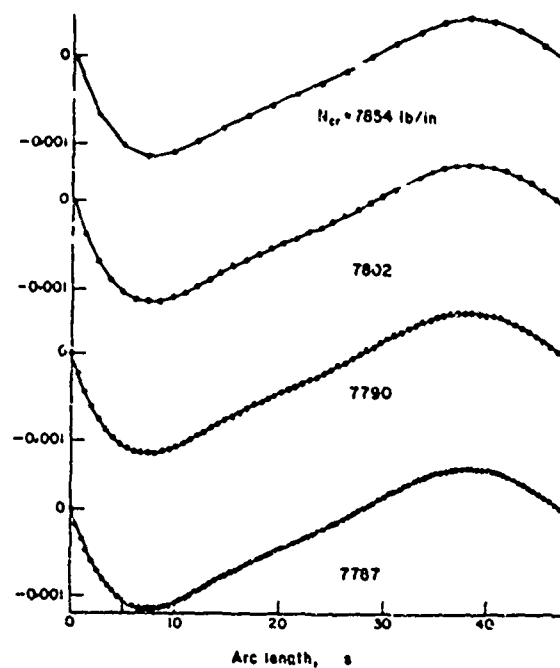


(b) Finite difference scheme #2

FIG. 6. Comparison of vibration modal characteristics with finite-difference schemes No. 1 and No. 2 for the ring-stiffened cylinder shown in Fig. 3a



(a) Finite difference scheme #1



(b) Finite difference scheme #2

FIG. 7. Comparison of buckling modal displacement u with finite-difference Schemes No. 1 and No. 2 for the axially compressed cylinder shown in Fig. 3a

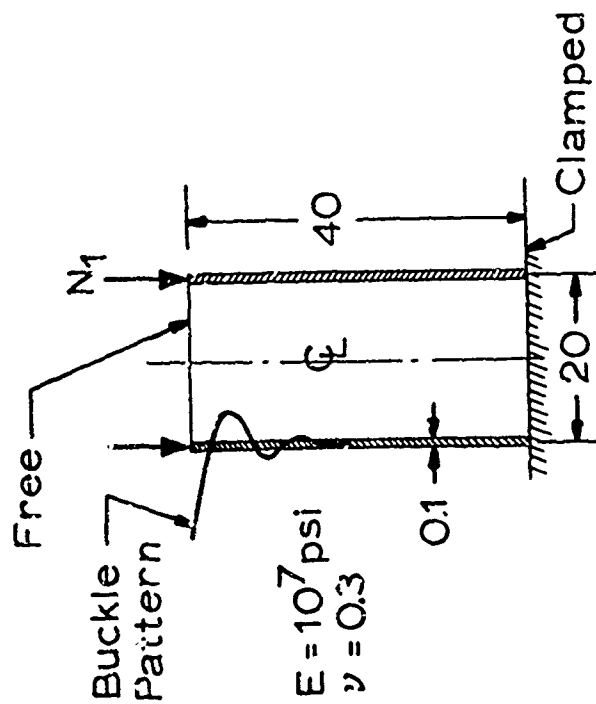
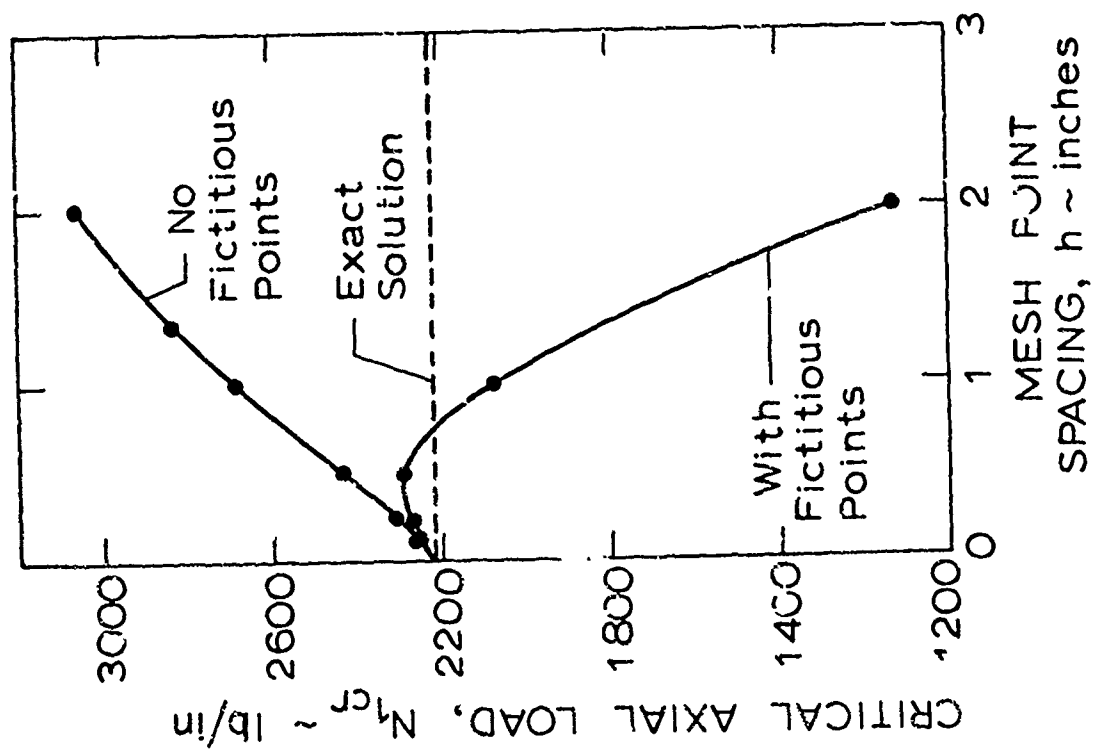


Figure 8 Buckling Load Convergence With and Without w-Fictitious Points. Axially Compressed Cylinder Free at One End, Clamped at the Other.

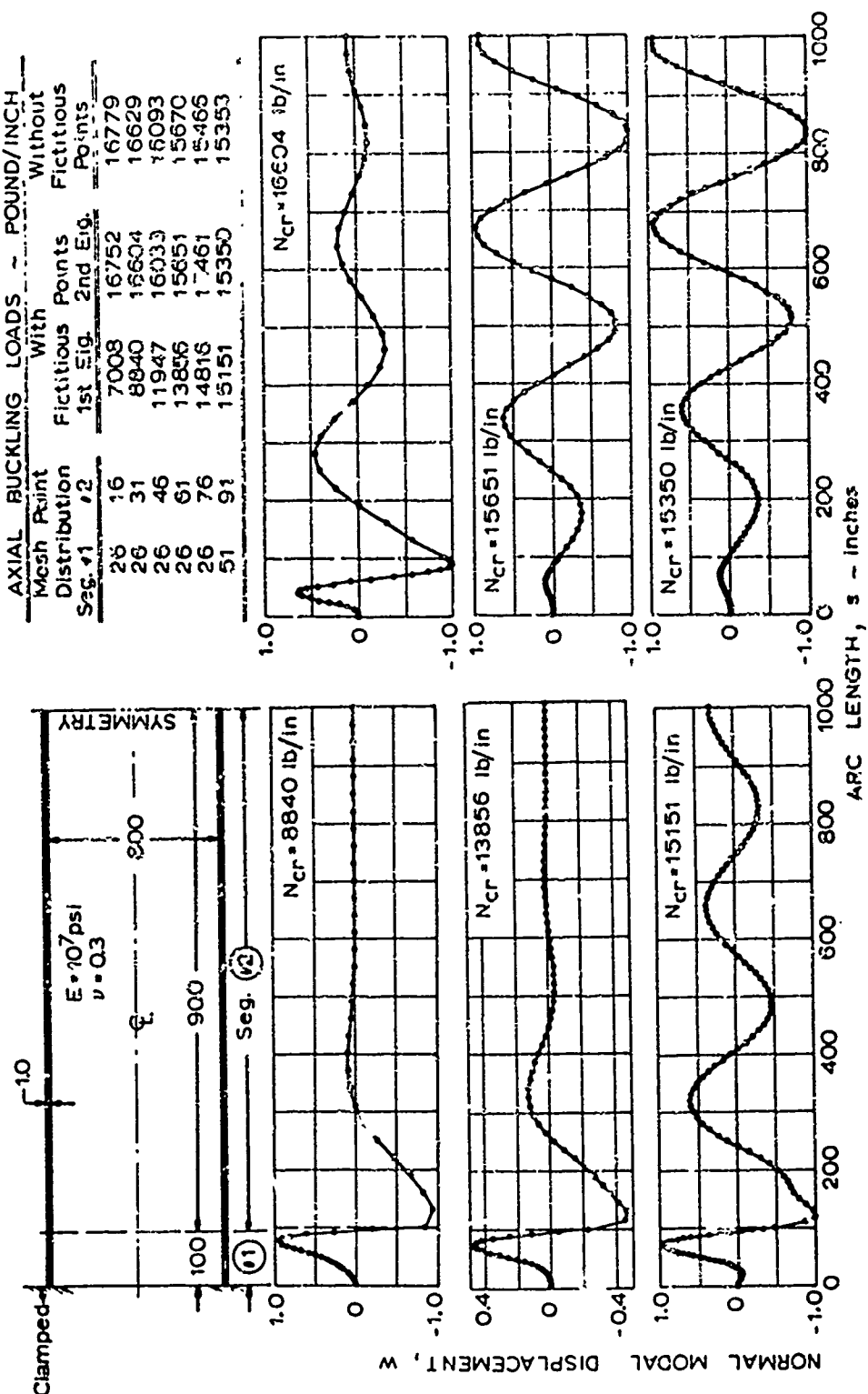


Figure 9 Effect of w-Fictitious Points in the Analysis of an Axially Compressed Cylinder Treated as a Shell of Two Segments

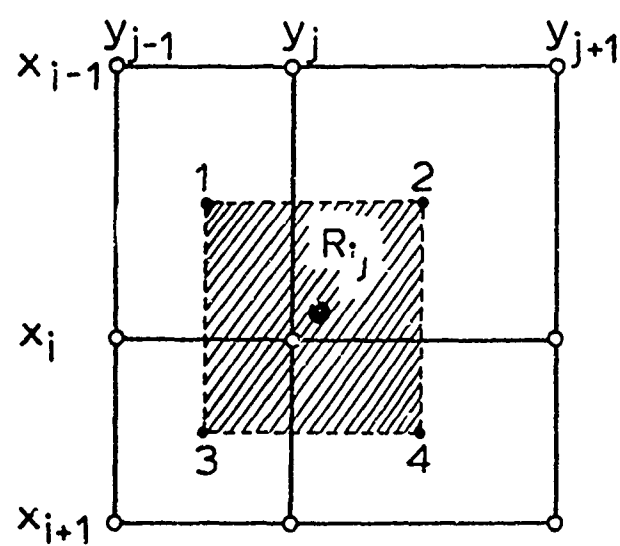


Figure 10 STAGS Finite-Difference Mesh Schemes Showing Location of Discrete Variables

$$FX = C_p$$

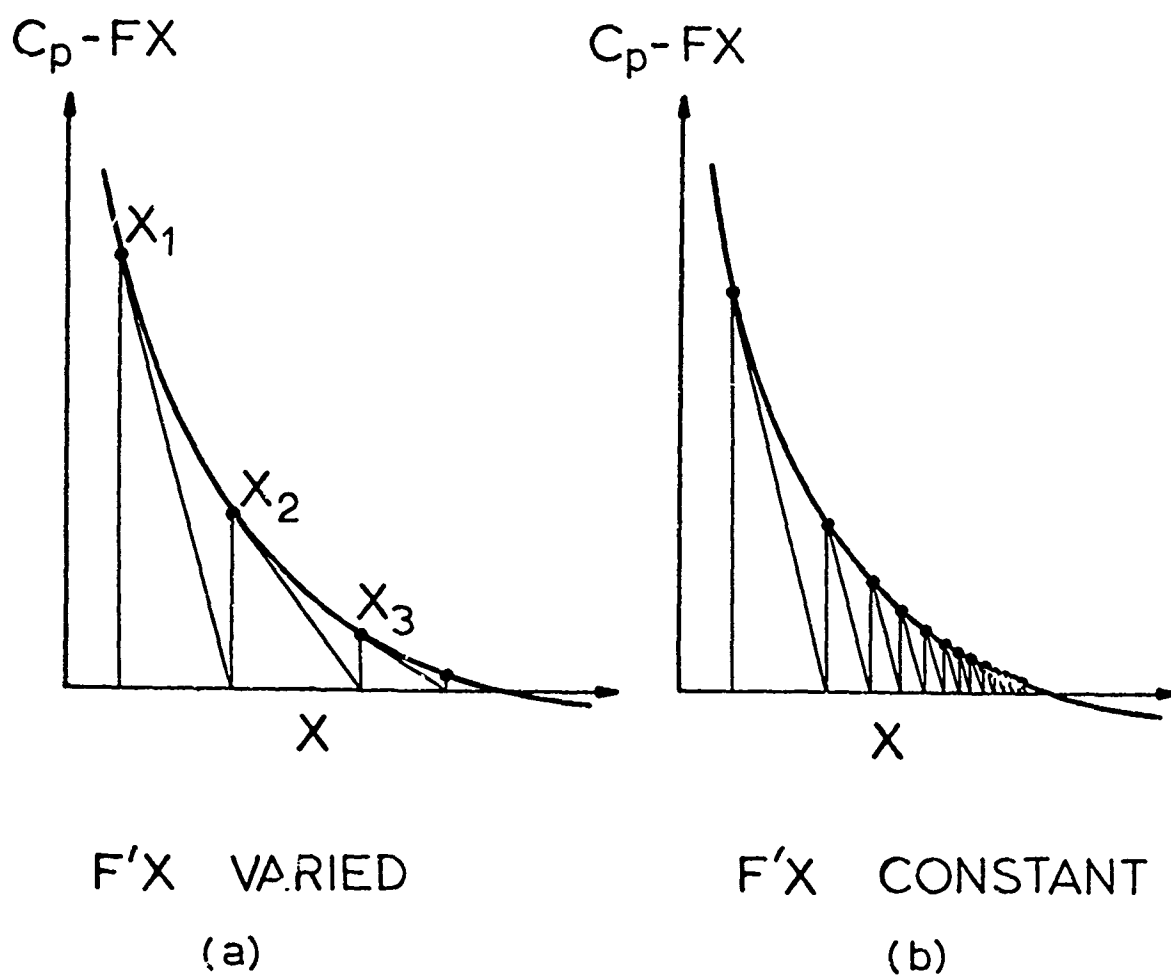


Figure 11(a) Newton Method; (b) Modified Newton Method to Solve $FX = C_p$

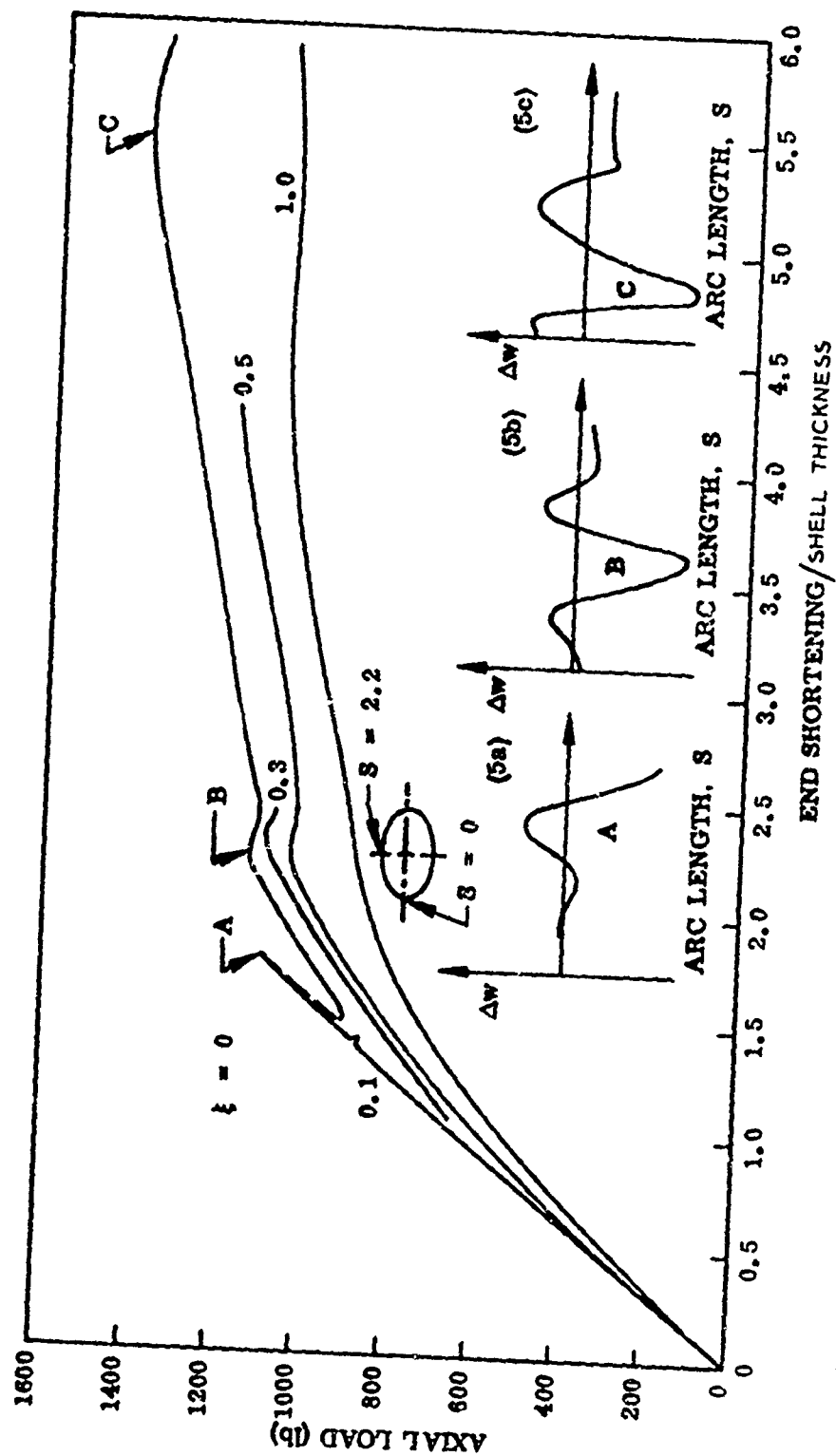


Figure 12 Load-Deflection Curves for Axially Compressed Perfect and Imperfect Elliptic Cylinders

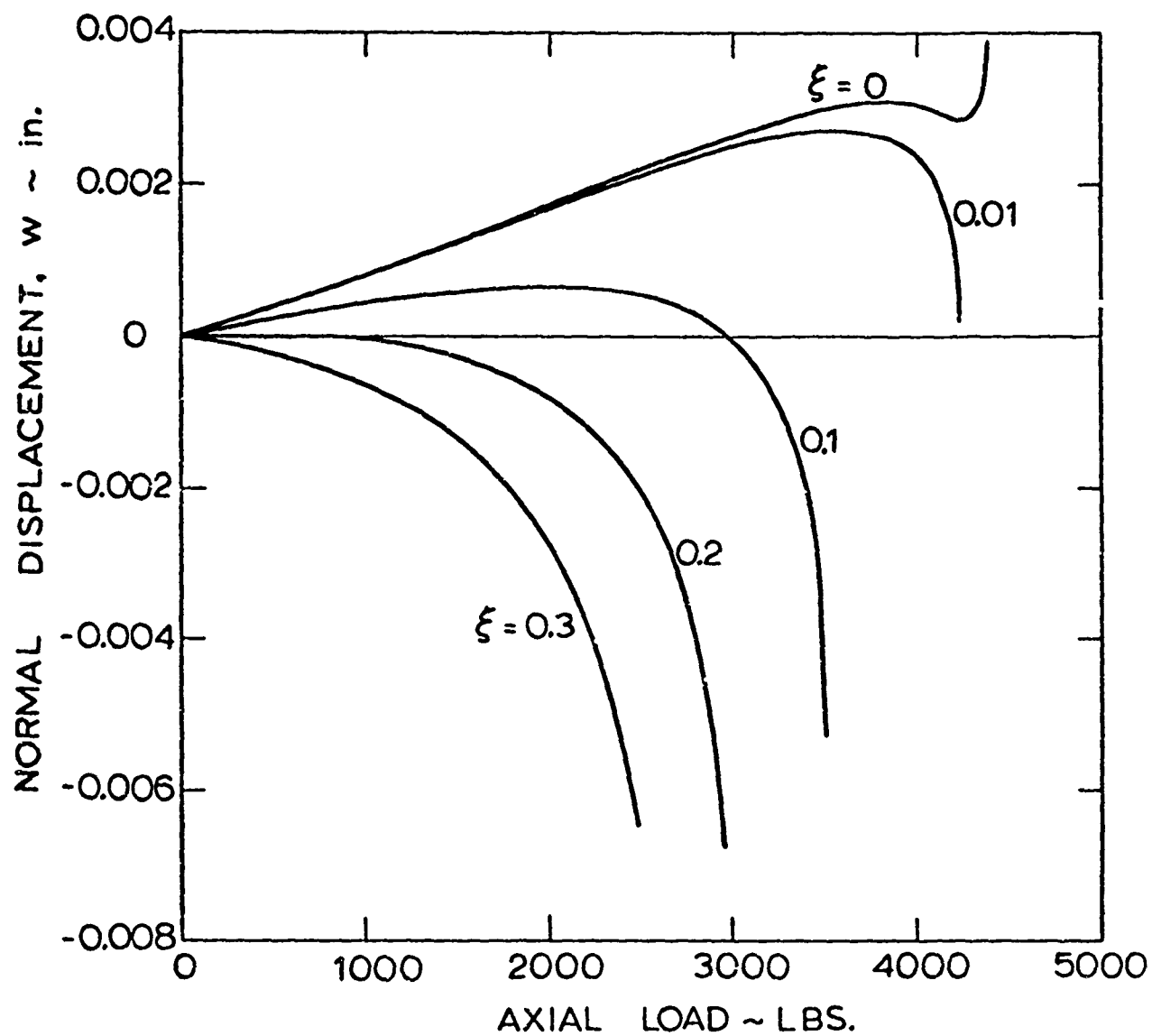


Figure 13 Normal Displacement Versus Axial Load for Various Imperfection Amplitudes ξ

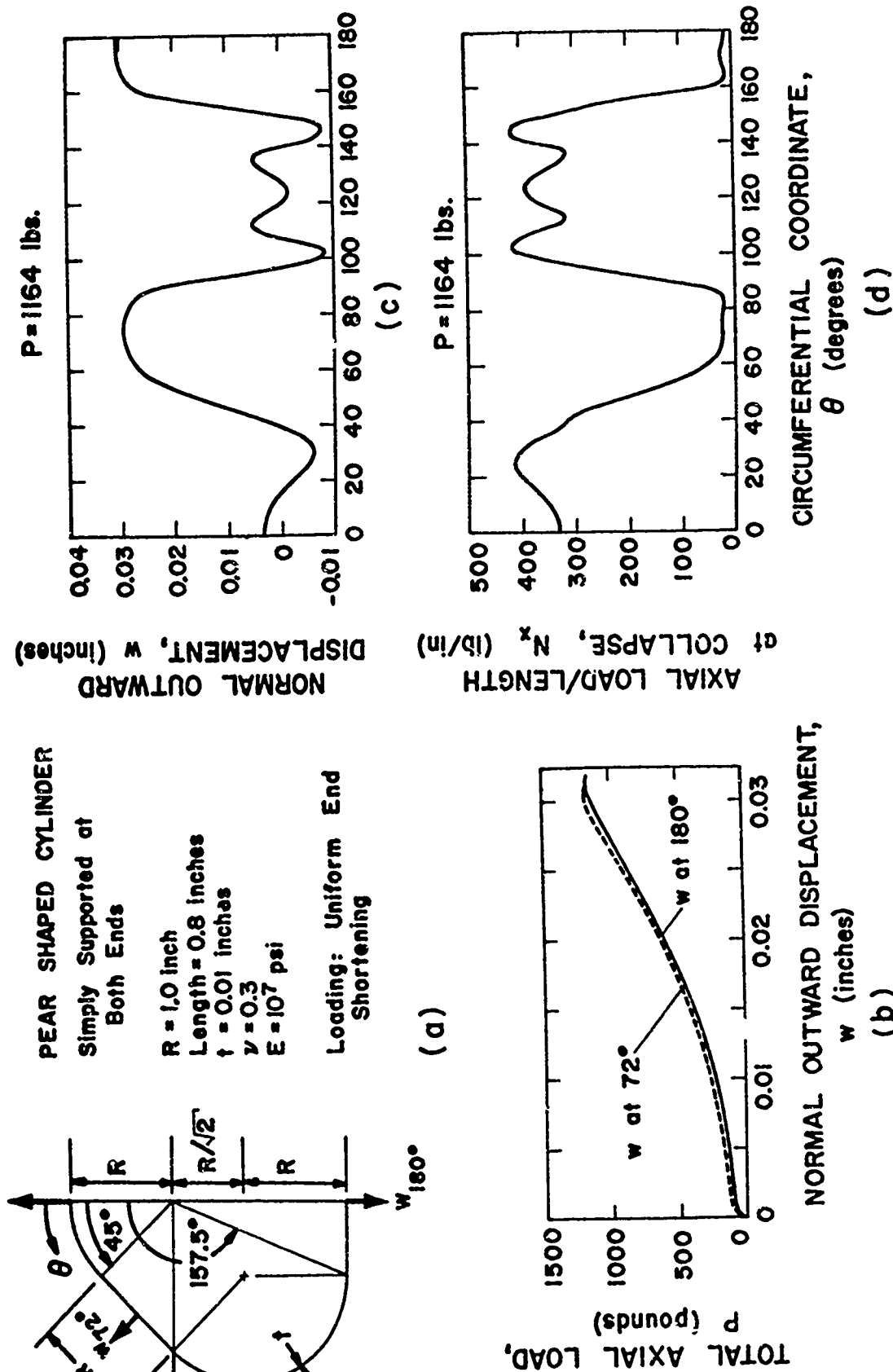


Figure 14 "Pear-Shaped" Cylinder Under Uniform End Shortening

- (a) Cylinder Geometry
- (b) Load-Deflection Curves
- (c) Normal Displacement at Midlength at Collapse
- (d) Axial Line Load at Midlength at Collapse

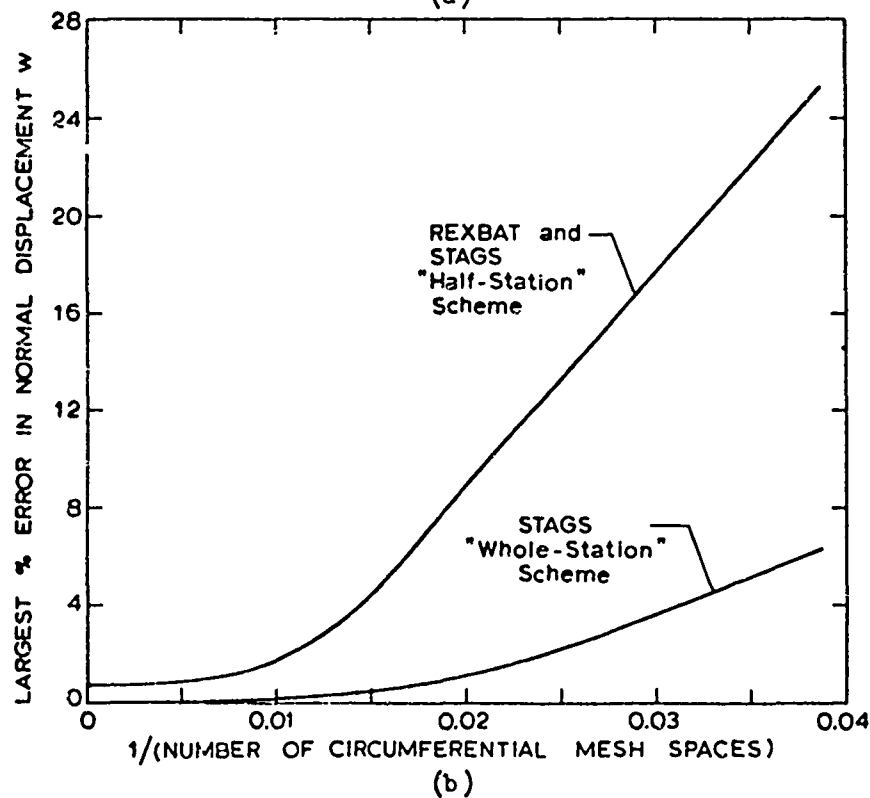
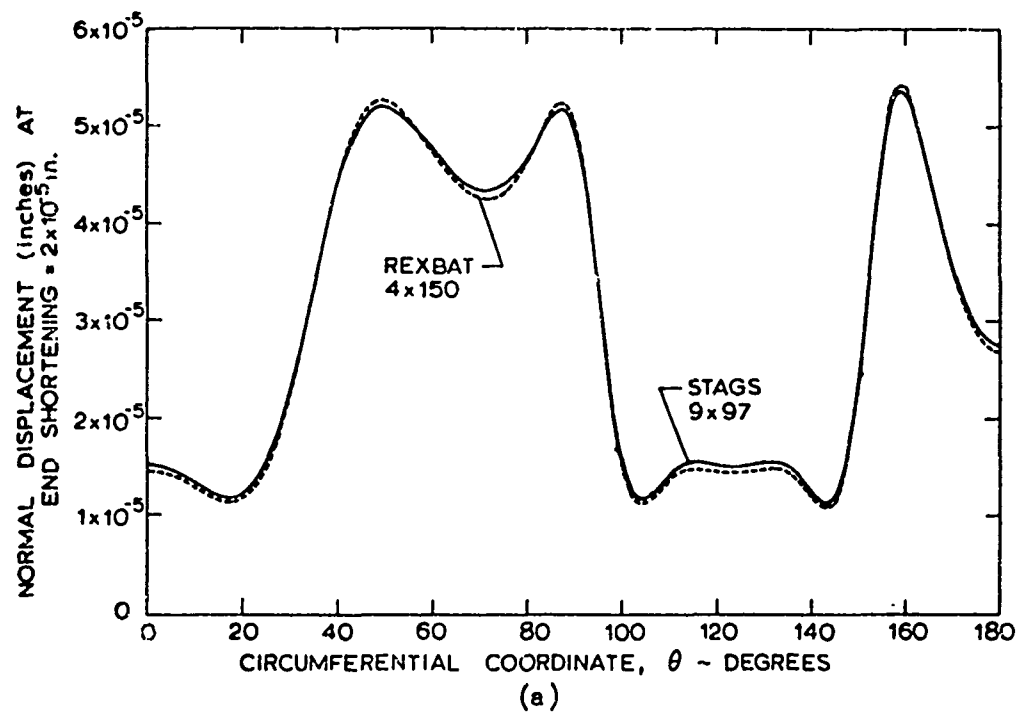


Figure 15 Comparison of Finite-Element and Finite-Difference Methods for Linear Analysis of "Pear-Shaped" Cylinder
 (a) Normal Outward Displacement at Midlength
 (b) Convergence with Increasing Degrees of Freedom

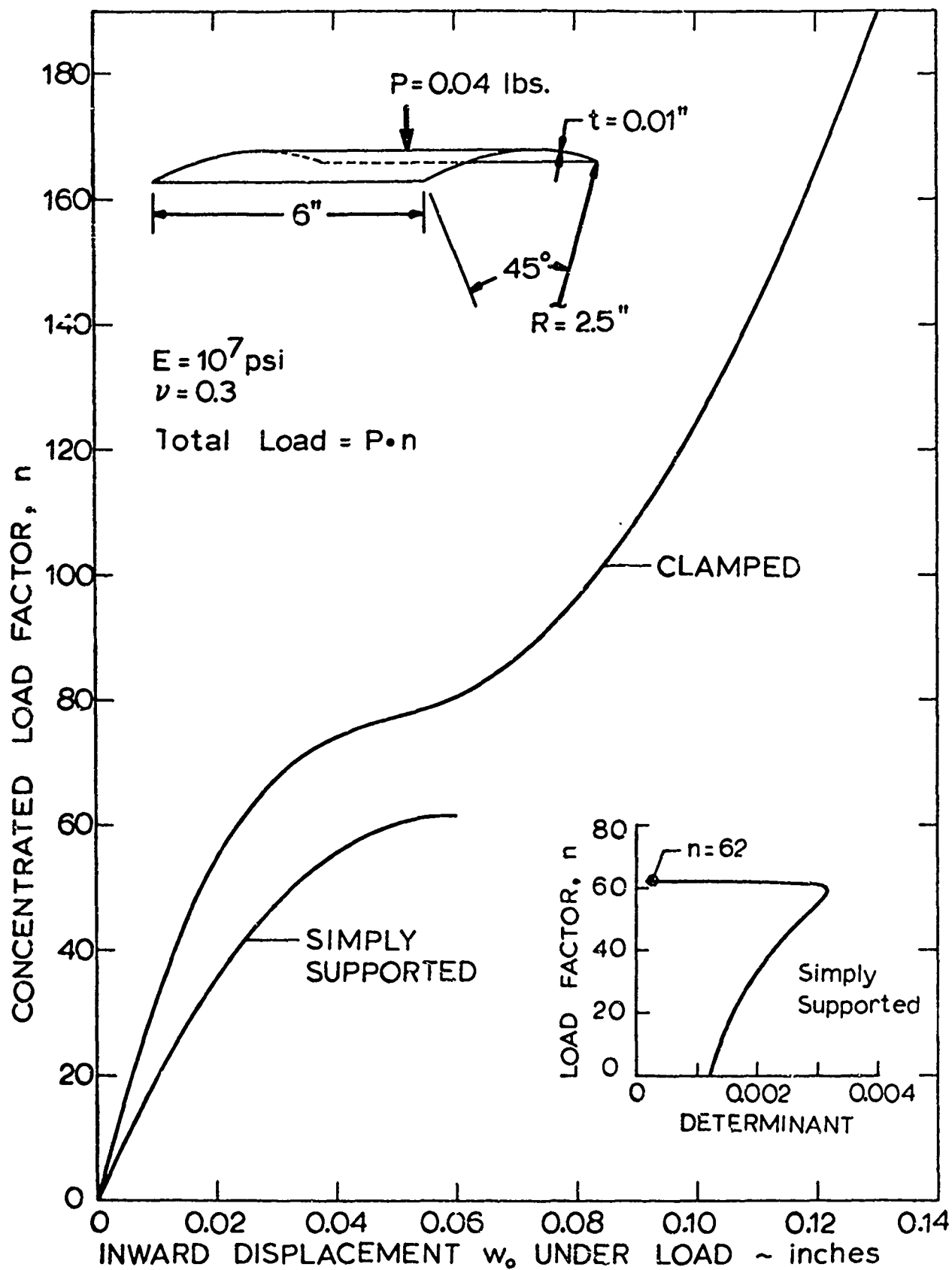


Figure 16 Load-Deflection Curves for Cylindrical Panels Clamped and Simply-Supported on the Curved Edges

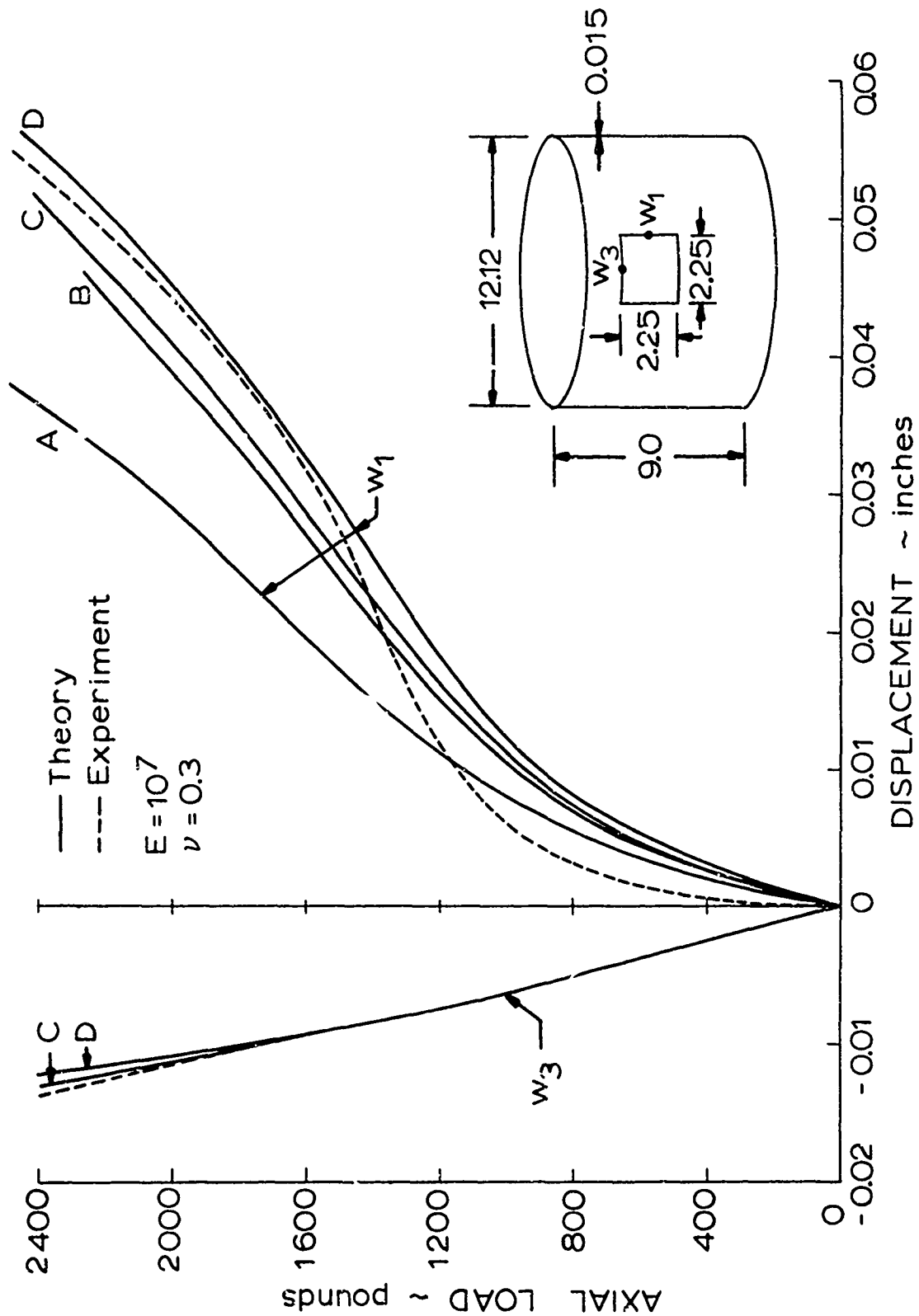


Figure 17 Load-Deflection Curves for Axially Compressed Cylinder With Two Diametrically Opposed Cutouts

QUESTIONS AND COMMENTS FOLLOWING BUSHNELL'S PAPER

QUESTION: You gave us the size and time for the one-dimensional calculation with the bandwidth of 7 and 100 unknowns and you talked about a semi-bandwidth of 100 for the two-dimensional problem. What size in terms of number of unknowns do you think would be feasible for a nonlinear study? And what would be a reasonable length of computer time on the UNIVAC 1108, for example, to get the results? I have no feeling but I think it's an interesting thing if we can get an insight so modelers can be a better feeling what they can afford to model. They'll obviously model in as much detail as they can afford in terms of computer costs and computer time.

BUSHNELL: To give some numbers--for the pear-shaped cylinder, for example--the load deflection curve became nonlinear very soon. It took 75 minutes of 1108 time in single precision. The semi-bandwidth was 63 and about 1200 degrees of freedom were used. Really what you want to know also is how many times for the entire case a linear equation was solved and how many factorings were required. You don't factor every load step. That's wasteful. It's really the amount of time per some kind of computation that is a little hard to identify. I think we'll be getting into some of this in the panel discussion tomorrow. In general, the time goes up as the square of a bandwidth and linearly with the number of degrees of freedom, so that's cubic with the number of degrees of freedom if you have a square plate with a regular array of nodal points. I presume the computer time starts increasing rapidly when you have to start using auxiliary storage; you have a lot of input-output. I don't think we've solved any problems with

the full capacity of the STAGS program, mainly because of expense.

QUESTION: Do you have any feeling of what would be a reasonable length of time to have such a problem as this run? In other words, is eight hours reasonable?

BUSHNELL: I don't think that eight hours is reasonable for two reasons. First, it's not possible for administrative reasons. Second, that's not really the way these problems are solved. They're solved in pieces; that is, you go a little ways up the load-deflection curve and then look at the deflections. Then you change your nonlinear strategy in order to make the next part more efficient. You never really let the case run eight hours and then look at the results and say, "my gawd, I forgot to put in the modulus." None of our runs have taken more than two hours of computer time or involved more than some seventy load steps. Typically, we make one factoring for every ten solves and a factoring takes about ten to twenty times as long as a solve.

QUESTION: With your STAGS program, have you ever solved the problem of a cylindrical segment cantilevered from one straight edge and, if so, which of your finite difference schemes did you use? I used a similar procedure to what you're speaking of here to try and solve that problem and had a great deal of difficulty.

BUSHNELL: No, we haven't solved that one. The venetian blind problem is as close as we came.

QUESTION: This half station scheme that you use was applied to cylindrical shells by Chang and Vilistos at the University of Illinois some-

where in the late 1950's or early 1960's. They showed that if you compute the governing equations using a minimum energy approach and compare that to the finite difference/equilibrium approach you get the same set of equations provided you use a staggered or half-station differencing scheme. If you do not use that staggered scheme, that is, if you use the whole station approach, you do not get the same set of equations. Have you taken a look at the problem from this point of view for the more general shell of revolution.

BUSHNELL: I think this point really should be looked at in more detail than I have given it. I found that if the mesh spacing is constant with that of the whole station spacing, the equations do look the same except at the boundaries. You can get almost anything at the boundaries depending on what you do with fictitious points, but in the interior they're the same. If somebody would have time to look at these various schemes, at the areas you integrate over, at how you make the finite difference model for various types of shell (not just isotropic but also shells in which you have coupling between membrane and bending), it would be a very worthwhile project.

COMMENT: In trying to determine the natural frequencies of cylinders, I had the same experience as you did. That is, if one uses the whole station scheme, the natural frequencies for the very low order modes ($N = 2$ and 3) are significantly in error.

QUESTION: Have you found a critical band size as related to core size beyond which computer times go way up?

BUSHNELL: We haven't run any systems for which this is true. We block, factor and solve in and out, on and off the drum all the time.

QUESTION: How about when you run out of core and start to use auxiliary tape storage?

BUSHNELL: We don't use auxiliary tapes, except to store the final data. Every so often data are stored on tape so that they will be available for restarting the same case at some later time. During a run data are stored on drum and everything is buffered. It's not as bad as having to stick with tapes or sequential input-output. There's random access capability on the 1108 so you don't have to count through a whole lot of stuff to get to the data you need.

A LARGE DEFLECTION TRANSIENT ANALYSIS OF
ARBITRARY SHELLS USING FINITE DIFFERENCES

Raymond D. Krieg, Staff Member
and
Henry C. Monteith, Staff Member
at Sandia Corporation, Albuquerque, N. M.

A computer program for the transient large displacement response of shells is described. Finite differencing is used in time and space to solve the equations. The paper is written in two parts. The first part is a derivation of equations and the second part is a discussion of several aspects of the numerical methods used to solve the equations. Advantages of rotary inertia and transverse shear in the differencing are illustrated and their disturbing behavior in the solution is explained. Roundoff and stability of time integration methods are discussed and illustrated.

ABBREVIATIONS AND SYMBOLS

- \underline{a}_α - Base vectors in Euclidian three space of coordinates on the reference surface.
- $a_{\alpha i} = \underline{a}_\alpha \cdot \underline{e}_i$ - Cartesian component of the base vector, \underline{a}_α .
- $a = \det \begin{bmatrix} a_{\alpha\beta} \end{bmatrix}$ - Metric of the reference surface.
- da_r - Differential reference surface area in deformed configuration.
- \underline{d} - Unit vector along deformed fiber. This vector coincides in the initial configuration with the unit normal to the reference surface.
- \dot{E}_{ij} - Components of the strain-rate tensor.
- $\underline{\Delta}$ - Body force load vector.
- \underline{F} - Net load vector.
- \underline{g}_i - Base vectors of the shell coordinate system which coincide with \underline{a}_i on the reference surface.
- g - Metric of the shell coordinates.
- dm - Differential mass element.
- m_i - Mass ($i = 0$) and mass moments ($i = 1, 2$) of a finite section of the shell.
- $M^{\beta\alpha}$ - Moment.
- \underline{n} - Unit normal vector to the surface.
- $N^{\beta\alpha}$ - Membrane generalized stress.
- \underline{p} - Position vector of generic particle in the shell.
- \underline{p}_r - Position vector of a generic particle on the reference surface.
- q^α - Shear generalized stress.
- R_j^i - Relator

- $\underline{t}(\underline{v})$ - Stress vector which acts on the surface with unit normal, \underline{v} .
- T^{ij} - Cauchy stress tensor components.
- x^i - Shell coordinates. The x^3 coordinate is along the vector \underline{g} .
- η - Unknown function in the vector equation of motion. This function does not appear in the component form of the equation.
- \underline{v}^α - Unit normal to the boundary of the deformed reference surface element. Note that $\underline{v} \cdot \underline{n} = 0$.
- ρ_0 - Initial material density.
- $(\)_\alpha, (\)^\alpha$ - Components with respect to reference surface base vectors ($\alpha = 1, 2$).
- $(\)_{\underline{i}}$ - Cartesian components in Euclidian three space ($\underline{i} = 1, 2, 3$).
- $(\underline{\ })$ - Denotes a vector.

INTRODUCTION

Computer programs to analyze the large deflection transient motion of shells have been available for roughly a decade. Peech, Pian, Witmer and Herrmann[1] wrote the computer program DEPROSS to solve the problem for symmetric beams and rings which included a quite accurate plasticity model. This program used finite differencing in space and time. Other programs such as GIRLS[3] and UNIVALVE[4,5] have been written for shells with one dimensional reference surfaces using the same basic ideas. These ideas are now being extended to the two-dimensional reference surface. Leech, Morino, and Witmer[6] are developing PETROS; Silsby, Sobel and Wrenn[7] are developing STAR, and the present paper concerns GRIVET.

These programs are directed at the very nonlinear problem, particularly at material nonlinearities with unloading. Geometrical descriptions in these programs are also very general, however and are capable of handling problems such as the elastica, for example. These radical changes in material and geometry mean that the "stiffness matrix" must be extensively revised at frequent intervals of time. This reformulation of the stiffness matrix makes the finite difference approach attractive, since it basically reformulates the "stiffness matrix" at every sweep through the equations.

The shell formulation used in GRIVET is not a standard formulation. The equations of motion are expressed in a global sense and use both a general shell coordinate system and an inertial Cartesian coordinate system. For these reasons, the equation derivations are covered in more detail than usual.

Rotary inertia and transverse shear are included in the formulation. The purpose of inclusion is not primarily for accuracy in the basic formulation. Instead, it is to simplify the numerical techniques used to solve the equations. This is explained further in the third section along with an important disadvantage of rotary inertia and transverse shear.

Roundoff errors are always a consideration in numerical techniques. The computer program GRIVET uses a velocity formulation of time integration. Although it is identical in the real number system to the usual displacement formulation, it can produce quite different results when computer arithmetic is used. This is illustrated in the third section.

In that same section, time integration methods are discussed. The Newmark beta method[8] and Houbolt method[9] are quite popular at the present time in linear analyses, since they are both unconditionally stable. Unfortunately, they are also both implicit methods. For a non-linear problem, the explicit methods, or more precisely, those which do not require the inverse of the "stiffness matrix", are much more attractive. A study is made of explicit time integration methods to determine whether one exists which is unconditionally stable.

The differencing grid is illustrated in the third section. A method is chosen which is not particularly economical in storage space but does not have the deficiencies of at least one other commonly used method.

Results of the computer program are omitted here, but will be reported upon in the oral presentation.

DERIVATIONS AND DISCUSSION OF EQUATIONS

The geometrical concepts in shell theory are fairly complex and are usually complicated by coordinate systems and indices. This report is no exception.

A fixed rectangular Cartesian coordinate system with the set of base vectors $\{\underline{e}_1, \underline{e}_2, \underline{e}_3\}$ is used to describe all vectors. In particular, the accelerations and velocities of particles are expressed in Cartesian components. A shell coordinate system is also used. Two coordinates define the reference surface and the third coordinate is initially normal to this. The generalized stresses and the strains are expressed in terms of these coordinates. The base vectors of the reference surface $\{\underline{a}_1, \underline{a}_2, \underline{a}_3\}$ are expressed in terms of their rectangular Cartesian components. In this way, the Christoffel symbols and the curvature tensor are avoided. The gradients of the components of the reference surface base vectors take their place in the derivations. The coordinate systems are shown in Figure 1.

The shell coordinate system is taken as a convected coordinate system. The coordinates of any particle are then the same for all time, but the base vectors $\{\underline{a}_1, \underline{a}_2, \underline{a}_3\}$ change in both magnitude and direction.

A hybrid notation is used in this report. The method of mixing together components and vectors in a single equation is found to be a convenient method, since two coordinate systems are needed. All second-order tensors and some vectors are represented in shell coordinate component form. These

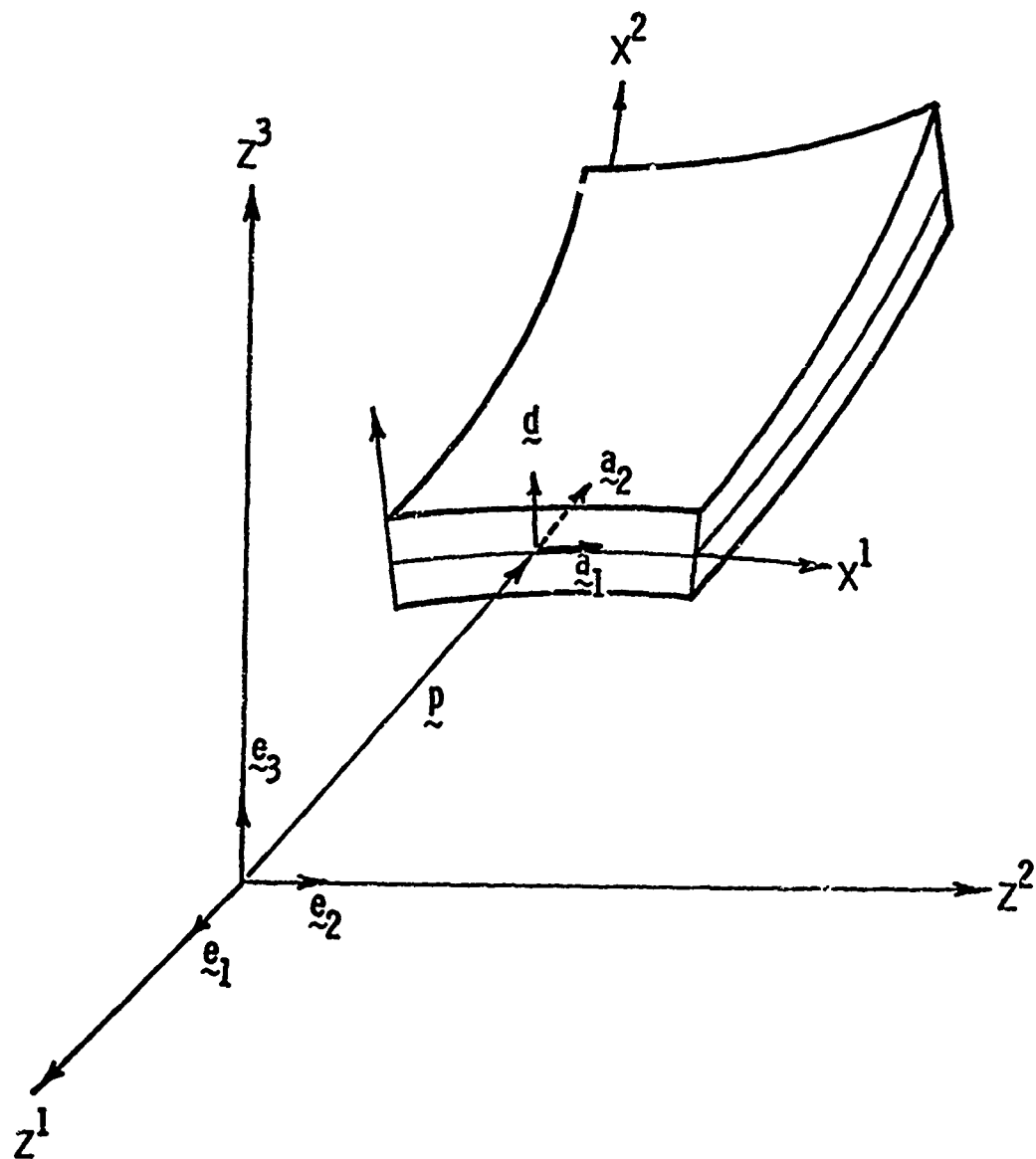


FIGURE 1. SHELL SEGMENT WITH SHELL COORDINATES AND AN INERTIAL RECTANGULAR CARTESIAN COORDINATE SYSTEM.

coordinates are considered to be curvilinear, and both contravariant and covariant components are used. The summation convention is used between repeated upper and lower indices. If the index is a Roman letter, the summation is over the values 1, 2, and 3. If the index is a Greek letter, the summation is only over the values 1 and 2.

The accelerations, velocities, positions, and base vectors are considered simply as vectors in the usual three-dimensional Euclidean point space. These vectors are denoted by a wavy underscore to distinguish them from scalars.

The Cartesian components of the above vectors, which arise later, are distinguishable from the shell components by italicized Roman letters. All Cartesian indices are placed as subscripts, since there is no distinction between contravariant and covariant components. The summation convention between repeated indices in a term is still used.

Equations of Motion

The principles of linear and angular momentum in a global sense are given by Eringen[10] as

$$\frac{d}{dt} \int_P \dot{\underline{p}} \, d\mathbf{a} = \int_{\partial P} \underline{t}_{(v)} \, d\mathbf{a} + \int_P \underline{f} \, d\mathbf{a} \quad (2.1)$$

$$\frac{d}{dt} \int_P \underline{p} \times \dot{\underline{p}} \, d\mathbf{a} = \int_{\partial P} \underline{p} \times \underline{t}_{(v)} \, d\mathbf{a} + \int_P \underline{p} \times \underline{f} \, d\mathbf{a} ,$$

where P is a part of the body with boundary, ∂P , which consists of

a fixed set of particles. The surface tractions on the part of the boundary with normal \underline{v} is denoted by $\underline{t}(\underline{v})$, the position vector is \underline{p} , the body force per unit mass is \underline{f} , and mass and boundary area elements are denoted as dm and da , respectively. The stress vector is represented as the Cauchy stress tensor $(T^{ij} \hat{v}_j \underline{g}_i)$, where \hat{v}_j denotes the components of the unit boundary normal, and \underline{g}_i denotes the base vectors in the body defined as:

$$\underline{g}_i = \frac{\partial \underline{p}}{\partial x^i}. \quad (2.2)$$

The particles in the body are located by means of the embedded coordinate system (x^1, x^2, x^3) . The reference surface of the body is defined by $(x^1, x^2, 0)$ and the coordinate, x^3 , is taken to be a physical coordinate which is normal to the reference surface at time zero. The base vectors on the reference surface are designated as $(\underline{a}_1, \underline{a}_2, \underline{a}_3)$.

The base vectors and dual base vectors on and off the reference surface are related as follows:

$$\underline{g}^i(x^1, x^2, x^3) = R^i_{\cdot j} \underline{a}^j(x^1, x^2, 0) \quad (2.3)$$

$$\underline{g}_i(x^1, x^2, x^3) = R^j_{\cdot i} \underline{a}_j(x^1, x^2, 0)$$

For ease of discussion, the function $R^i_{\cdot j}$ will be called the relator function. The relator, which is a function of position in the body and the selection of a reference surface is restricted such that the

relator and its inverse exist everywhere in the shell.

The metric off the reference surface can be shown to be

$$\sqrt{g} = R^{-1} \sqrt{a} \quad (2.4)$$

Integration over the body in Equation (2.4) can be expressed as a triple integral where dm is replaced as $\rho R^{-1} \sqrt{a} dx^1 dx^2 dx^3$ and the first and last terms of Equation (2.1) are:

$$\frac{d}{dt} \int_P \dot{\underline{p}} dm = \int_{x^1} \int_{x^2} \int_{x^3} \ddot{\underline{p}} \rho R^{-1} \sqrt{a} dx^1 dx^2 dx^3 \quad (2.5)$$

and

$$\int_P \underline{f} dm = \int_{x^1} \int_{x^2} \int_{x^3} \underline{f} \rho R^{-1} \sqrt{a} dx^1 dx^2 dx^3 .$$

A basic assumption is now invoked on the motion of particles, viz: the position vector of a generic particle is taken to be approximated by

$$\underline{p}(x^1, x^2, x^3) = \underline{p}_r(x^1, x^2, 0) + x^3 \underline{d}(x^1, x^2) \quad (2.6)$$

for all time.

The second time derivative of Equation (2.6) is substituted into Equation (2.5) and integration carried out on x^3 over the shell thickness. Equation (2.1) is now expressed as:

$$\int_{x^1} \int_{x^2} (\ddot{\underline{p}}_r \underline{m}_0 + \ddot{\underline{d}} \underline{m}_1) \sqrt{a} dx^1 dx^2 = \int_P \underline{t}(v) da + \int_{x^1} \int_{x^2} \underline{f} \sqrt{a} dx^1 dx^2 . \quad (2.7)$$

where

$$\begin{aligned}
 m_0 &= \int_{x^3} \rho R^{-1} dx^3, \\
 m_1 &= \int_{x^3} \rho R^{-1} x^3 dx^3 \\
 m_2 &= \int_{x^3} \rho R^{-1} (x^3)^2 dx^3.
 \end{aligned}
 \tag{2.8}$$

are the generalized shell masses and the generalized body force loading function is

$$\hat{f} = \int_{x^3} f \rho R^{-1} dx^3. \tag{2.9}$$

The boundary, ∂P , consists of two types. One type is assumed to be a surface of the form (x^1, x^2, c) , where c is some constant. The traction integral in Equation 2.1 for this type of surface (the lateral surfaces) is stated as

$$\int_{\partial P} t(v) da = \int_{x^1} \int_{x^2} \left[\left(T^{ij} v_j R^{-1} \ell_{.i} a_{\ell}^{R^{-1}} \right) \right]_{-x^3}^{+x^3} \sqrt{a} dx^1 dx^2, \tag{2.10}$$

where a and R^{-1} are defined at a generic point based on the base vectors, $\{a_1, a_2, \underline{n}\}$ and $\{g_1, g_2, \underline{n}^*\}$, where \underline{n} and \underline{n}^* are unit normals to the reference surface and x^3 -surface, respectively.

The second boundary type, called an edge, is defined as a boundary surface formed by the loci of fibers.¹ Edges are restricted to have continuous

¹A fiber is taken to be a line of constant x^1 and x^2 .

partial derivations with respect to x^1 and x^2 except at a finite number of places.

If \underline{dl}_z is an elemental length along a path of constant x^3 on the edge boundary, then

$$\underline{v} ds = \underline{dl}_z \times \underline{g}_3 dx^3 \quad (2.11)$$

If \underline{dl}_r is an elemental vector length along the reference surface, which can be written as

$$\underline{dl}_r = \underline{a}_1 dx^1 + \underline{a}_2 dx^2$$

where

$$\underline{dl}_z = \underline{g}_1 dx^1 + \underline{g}_2 dx^2$$

and dx^1 and dx^2 are the same for both cases, then the two elemental lengths are expressed using Equation 2.3 such that Equation 2.11 can be written in component form as

$$\begin{aligned} v_j da &= \left[\left(\underline{R}^{-1}_{\cdot k} \right)^r_{\cdot \alpha} (\underline{dl})^\alpha \underline{a}_k \right] \times \left(\underline{R}^{-1}_{\cdot 3} \underline{a}_l dx^3 \right) \cdot \underline{g}_j \\ &= \left[\left(\underline{a}_k \underline{R}^{-1}_{\cdot k} \right)^r_{\cdot \alpha} (\underline{dl})^\alpha \right] \times \left(\underline{a}_l \underline{R}^{-1}_{\cdot 3} dx^3 \right) \cdot \underline{R}^{-1}_{\cdot j} \underline{a}_m . \end{aligned}$$

From Bowen[11] this can be written in terms of the determinant and then rearranged and simplified as

$$v_j da = \underline{R}^{-1} \begin{matrix} r & r \\ \underline{v}_j & da \end{matrix} , \quad (2.12)$$

where \underline{v}_j^r denotes the components of the unit normal to the edge of the reference surface which is tangent to the reference surface.

Equation (2.12) is a very ambiguous expression in the use of indices. The components, v_j , are associated with the base vectors, g_j , and the components $\overset{r}{v}_j$, are associated with the base vectors, \underline{a}_j . The traction integral in Equation 2.1 for an edge boundary is then

$$\int_{\partial P} \underline{t}(v) d\mathbf{a} = \int_{L_r} \int_{x^3} T^{1j} \overset{-1}{R} \overset{-1}{k}_{.1} \overset{-1}{R} \overset{r}{v}_j \underline{a}_k dx^3 d\ell_r.$$

This expression is substituted into Equation (2.7) to obtain

$$\int_{x^1}^1 \int_{x^2}^2 (\ddot{\underline{p}}_1 m_0 + \ddot{\underline{q}}_1 m_1 - \overset{*}{\underline{f}}) \sqrt{a} dx^1 dx^2 = \int_{L_r} (N^{\beta\alpha} \underline{a}_\beta + q^\alpha \underline{a}) \overset{r}{v}_\alpha d\ell_r \quad (2.13)$$

where the generalized stresses are defined as

$$N^{\beta\alpha} = \int_{x^3}^3 \overset{-1}{R} \overset{-1}{\beta}_{.1} T^{1\alpha} \overset{-1}{R} dx^3 \quad \alpha, \beta = 1, 2 \quad (2.14)$$

$$\text{and} \quad q^\alpha = \int_{x^3}^3 \overset{-1}{R} \overset{-1}{3}_{.1} T^{1\alpha} \overset{-1}{R} dx^3 \quad \alpha = 1, 2. \quad (2.15)$$

and where $k v_3$ is taken as zero. The loading terms have all been combined into $\overset{*}{\underline{f}}$, a load vector per unit reference surface area and defined as

$$\overset{*}{\underline{f}} = \hat{\underline{f}} + \left[T^{1j} v_j \overset{-1}{R} \overset{-1}{l}_{.1} \overset{-1}{R} \right]_{-x^3}^{+x^3} \sqrt{\frac{\overset{*}{a}}{a}} \underline{a}_l. \quad (2.16)$$

Equation (2.13) is the form of the linear momentum principle which will be differenced. The form is identical to that of Ericksen[12] except that inertia terms are included here. Another difference is that the surface quantities are related to three-dimensional quantities here.

A weakness of the indicial tensor notation in shells is apparent in Equations (2.14) and (2.15). Two systems of base vectors are associated with the indices. The Cauchy stress components are in terms of g_1 , but

R^{α}_{β} , $H^{\beta\alpha}$, and q^{α} are in terms of a_1 . This ambiguous use of indices is inherent if components are used, but only appears to be a problem in the definition of generalized stresses.

The reduction of Equation (2.1b) to a usable form is complicated by the position vector, \underline{p} , which must be specified in an inertial frame or with respect to the center of mass of the section of the shell, P . If \underline{p}_c is the center of mass of P , with respect to an inertial frame, then \underline{p} can be decomposed as

$$\underline{p} = \underline{p}_c + \underline{p}_t + x^3 \underline{a}_3, \quad (2.17)$$

where \underline{p}_t is the position of $(x^1, x^2, 0)$ for a generic particle, with respect to the center of mass. Equation (2.1b) is expanded in terms of Equation 2.17, and the vector \underline{p}_c is noted to have zero as its coefficient if Equation 2.1a is satisfied identically. The result is then

$$\begin{aligned}
& \int_{x^1}^1 \int_{x^2}^2 \underline{p}_t \times (\ddot{\underline{p}}_r m_0 + \ddot{\underline{d}} m_1 - \frac{f}{\underline{z}}) \sqrt{a} dx^1 dx^2 - \oint_{\underline{l}_r} \underline{p}_t \times (N^{\beta\alpha} \underline{a}_\beta + q^{\alpha d}) \underline{v}_\alpha^r d\underline{l}_r \\
& = - \int_{x^1}^1 \int_{x^2}^2 \underline{d} \times (\ddot{\underline{p}}_r m_1 + \ddot{\underline{d}} m_2) \sqrt{a} dx^1 dx^2 + \oint_{\underline{l}_r} \underline{d} \times (M^{\beta\alpha} \underline{a}_\beta) \underline{v}_\alpha^r d\underline{l}_r, \quad (2.18)
\end{aligned}$$

$$M^{\beta\alpha} = \int_{x^3}^3 R^{\beta\alpha} T^{\alpha\beta} x^3 dx^3. \quad (2.19)$$

The last term in Equation 2.18 has a moment shear omitted since it is in the direction \underline{d} and its cross product with \underline{d} is zero.

The reduction of Equation 2.18 to a usable form requires the use of the divergence theorem in the forms derived in Appendix A. Equation A.3 is applied to the first term in the line integral on the left side of Equation 2.18, and the partial derivative of \underline{p} is recognized as a surface base vector to give the result:

$$\begin{aligned}
& \int_{\underline{l}_r} \underline{p}_t \times N^{\beta\alpha} \underline{a}_\beta \underline{v}_\alpha^r d\underline{l}_r = \int_{x^1}^1 \int_{x^2}^2 \left[\underline{a}_\alpha \times \underline{a}_\beta N^{\beta\alpha} \right. \\
& \quad \left. + \underline{p}_t \times (N^{\beta\alpha} |_\alpha \underline{a}_\beta + \underline{n} N^{\beta\alpha} B_{\alpha\beta}) \right] \sqrt{a} dx^1 dx^2. \quad (2.20)
\end{aligned}$$

The second term in the line integral of Equation 2.18 is converted with Equation A.2, where \underline{x} is replaced with $\underline{p}_t \times \underline{d}$. The result is:

$$\int_{\ell_r} \underline{p}_t \times \underline{d} q^\alpha \underline{v}_\alpha d\ell_r = \iint_{x^1 x^2} \left[\underline{p}_t \times \left(\frac{\partial \underline{d}}{\partial x^\alpha} q^\alpha + \underline{d} q^\alpha|_\alpha \right) - \underline{d} \times \underline{q} \right] \sqrt{a} dx^1 dx^2. \quad (2.21)$$

Equations 2.20 and 2.21 are substituted into Equation 2.18, and the terms are regrouped as follows:

$$\begin{aligned} & \int_1^2 \int_{x^2} \underline{p}_t \times \left[\underline{\ddot{p}}_r m_0 + \underline{\ddot{d}} m_1 - \underline{\ddot{q}} - \underline{a}_\beta N^{\beta\alpha}|_\alpha - \underline{n} N^{\beta\alpha}{}_\beta - \frac{\partial \underline{d}}{\partial x^\alpha} q^\alpha \right. \\ & \left. - \underline{d} q^\alpha|_\alpha \right] \sqrt{a} dx^1 dx^2 - \iint_{x^1 x^2} (N^{21} - N^{12}) \underline{a}^3 \sqrt{a} dx^1 dx^2 \\ & = - \int_1^2 \int_{x^2} \underline{d} \times (\underline{\ddot{p}}_r m_1 + \underline{\ddot{d}} m_2 + \underline{q}) \sqrt{a} dx^1 dx^2 + \oint_{\ell_r} \underline{d} \times (M^{\beta\alpha} \underline{a}_\beta) \underline{v}_\alpha d\ell_r. \quad (2.22) \end{aligned}$$

If the area elements in Equations 2.13 and 2.22 are very small, then the first integral in Equation 2.22 is zero. This is shown by converting Equation 2.13 to an area integral, using Equations A.2 and A.4, with the result:

$$\int_{x^1}^1 \int_{x^2}^2 \left(\ddot{\underline{p}}_r m_0 + \ddot{\underline{d}} m_1 - \frac{1}{2} \ddot{\underline{q}} - N^{\beta\alpha} \left|_{\alpha} \underline{a}_{\beta} - N^{\beta\alpha} B_{\alpha\beta} \underline{n} - g^{\alpha} \frac{\partial \underline{d}}{\partial x^{\alpha}} - \underline{d} g^{\alpha}_{\alpha} \right) \sqrt{a} dx^1 dx^2 = 0. \quad (2.23)$$

If Equation 2.23 is satisfied for every arbitrary area, then the integrand must be zero. This, in turn, implies that the integrand of the first integral in Equation 2.22 is zero. The condition on the area can be relaxed slightly, however. If the integrand of Equation 2.23 is non-zero, but constant over the area, the first integral in Equation 2.22 will still vanish, since the constant can be factored out, leaving

$$\left(\int_{x^1}^1 \int_{x^2}^2 \underline{p}_t \sqrt{a} dx^1 dx^2 \right) \times (\text{constant vector}).$$

The vector on the left is approximately zero, since \underline{p}_t is measured from the center of mass.

The second integral in Equation 2.22 is zero if $R^{\beta}_{\alpha 1} = \delta^{\beta}_{\alpha 1}$, since $N^{\beta\alpha}$ as defined by Equation 2.14 is then symmetric. This condition holds for a point on the shell where \underline{d} is constant in some neighborhood of the point. The term is, in fact, almost proportional to the local curvature. In any case, the term is a vector which is normal to the surface.

If a small reference surface area is used, then \underline{d} is approximately constant and can be factored out of the integrals on the right side of Equation 2.22. If \underline{a}^3 is approximately \underline{d} , then the result can be stated as

$$\int_{x^1}^1 \int_{x^2}^2 (\ddot{\underline{p}}_r m_1 + \ddot{\underline{d}} m_2 + \underline{q}) \sqrt{a} dx^1 dx^2 - \oint_{\ell_r} M^{\beta\alpha} \underline{a}_{\beta} \underline{v}_{\alpha}^r d\ell_r = \eta \underline{d}_0, \quad (2.24)$$

where η is some arbitrary scalar function and some averaged value of \underline{d} on the reference surface is denoted as \underline{d}_0 . Only the components of Equation 2.24 which are normal to \underline{d}_0 are useful since η is unknown. The Equations 2.13 and 2.24 then form a set of 5 scalar equations which is usual in this type of shell theory.

The integrals given as Equations 2.13 and 2.24 are the equations of motion which are used in the computer in component form. The shell is decomposed into segments and the integrals applied to each segment. The mean value theorem is applied to the acceleration integral, and the resulting acceleration is assigned to a particle inside the region. Segments adjoining the shell boundaries have portions of line integrals which are evaluated along the shell boundaries. In these segments the accelerations are assigned to a particle on the boundary of the shell (and segment) rather than to a particle in the interior of the segment.

The integral formulation includes the boundary conditions. Either enough information is known on the boundary to evaluate the integrals (stress boundary conditions) or the integrals do not need to be evaluated (displacement boundary conditions). Combinations of these are the mixed boundary conditions.

The density parameter m_1 defined by Equation 2.8 is made zero by proper choice of the reference surface in the program. This simplifies the application of various edge conditions. They can be summarized as follows:

$$\text{Either } \ddot{\underline{d}} = 0$$

$$\text{or } \oint_{l_r} N^{\beta\alpha} \underline{a}_\beta \underline{v}_\alpha^r d\underline{l}_r = \int \int_{x^1 x^2} \underline{q} \sqrt{a} dx^1 dx^2 = 0$$

and

$$\text{either } \ddot{\underline{p}}_r \cdot \underline{d} = 0 \text{ and } \oint_{l_r} q^{\underline{u}} \underline{\tilde{v}}_\alpha d\underline{l}_r = 0$$

$$\text{or } \ddot{\underline{p}}_r \times \underline{d} = 0 \text{ and } \underline{d} \times \oint_{l_r} N^{\beta\alpha} \underline{v}_\alpha^r \underline{a}_\beta d\underline{l}_r = 0$$

$$\text{or } \ddot{\underline{p}}_r = 0$$

$$\text{or } \oint_{l_r} (N^{\beta\alpha} \underline{a}_\beta + q^{\underline{u}} \underline{\tilde{a}}) \underline{v}_\alpha^r d\underline{l}_r = 0$$

Up to the present time, only three of the combinations have been put into the program. The remaining combinations will be installed in the future.

Strain Rate Velocity Relation

As stated in the introduction, the computer program GRIVET was written specifically for nonlinear materials. Many of these materials are strain rate sensitive. For this reason, the usual strain-displacement relation is replaced by a rate relation which may be integrated in time where necessary.

The Eulerian strain rate tensor components are defined[13] as

$$\dot{E}_{ij} = \frac{1}{2} \left(\underline{g}_i \cdot \frac{\partial \underline{\dot{p}}}{\partial x^j} + \underline{g}_j \cdot \frac{\partial \underline{\dot{p}}}{\partial x^i} \right). \quad (2.25)$$

The base vector can be expanded using Equations 2.2 and 2.6 as

$$\underline{g}_\alpha = \underline{\tilde{a}}_\alpha + x^3 \frac{\partial \underline{\tilde{d}}}{\partial x^\alpha} \text{ and } \underline{g}_3 = \underline{\tilde{d}}.$$

Partial derivatives of \underline{p} with respect to t and x^α can also be found using Equation 2.6.

The resulting forms of the strain rate components are:

$$\begin{aligned} \dot{E}_{\alpha\beta} = & \frac{1}{2} \left(\underline{\tilde{a}}_\alpha \cdot \frac{\partial \underline{\dot{p}}_r}{\partial x^\beta} + \underline{\tilde{a}}_\beta \cdot \frac{\partial \underline{\dot{p}}_r}{\partial x^\alpha} \right) + \frac{x^3}{2} \left(\frac{\partial \underline{\tilde{d}}}{\partial x^\alpha} \cdot \frac{\partial \underline{\dot{p}}_r}{\partial x^\beta} + \frac{\partial \underline{\tilde{d}}}{\partial x^\beta} \cdot \frac{\partial \underline{\dot{p}}_r}{\partial x^\alpha} + \underline{\tilde{a}}_\alpha \cdot \frac{\partial \underline{\dot{d}}}{\partial x^\beta} \right. \\ & \left. + \underline{\tilde{a}}_\beta \cdot \frac{\partial \underline{\dot{d}}}{\partial x^\alpha} \right) + \frac{(x^3)^2}{2} \left(\frac{\partial \underline{\tilde{d}}}{\partial x^\alpha} \cdot \frac{\partial \underline{\dot{d}}}{\partial x^\beta} + \frac{\partial \underline{\tilde{d}}}{\partial x^\beta} \cdot \frac{\partial \underline{\dot{d}}}{\partial x^\alpha} \right) \end{aligned} \quad (2.26)$$

and

$$\dot{E}_{\alpha 3} = \frac{1}{2} \left(\underline{\tilde{d}} \cdot \frac{\partial \underline{\dot{p}}_r}{\partial x^\alpha} + \underline{\tilde{a}}_\alpha \cdot \underline{\dot{d}} \right)$$

$$\text{and } \dot{E}_{33} = 0$$

The component \dot{E}_{33} is simply $\dot{\underline{d}} \cdot \underline{d}$ which is of course zero since \underline{d} has unit magnitude. A linear term in x^3 in the component $\dot{E}_{\alpha 3}$ also vanishes since the partial derivative of $(\dot{\underline{d}} \cdot \underline{d})$ with respect to x^α is also zero.

The quadratic term in x^3 in the expression for $\dot{E}_{\alpha\beta}$ is dropped in the computer program from an ordering consideration.

The resulting strain rate expressions give zero strain rate under all possible rigid body motions. This is demonstrated directly from the general expression for rigid body motion given by

$$\dot{\underline{p}} = \underline{v}_0 + \underline{\omega} \times (\underline{p} - \underline{p}_0)$$

where the body has an angular velocity $\underline{\omega}$ about the point \underline{p}_0 and a linear velocity \underline{v}_0 at this point. Equation 2.26 is used to expand \underline{p} and $\dot{\underline{p}}$, and coefficients of like powers of x^3 are equated to give:

$$\dot{\underline{p}}_r = \underline{v}_0 + \underline{\omega} \times \underline{p}_r$$

and $\dot{\underline{d}} = \underline{\omega} \times \underline{d}$

These expressions are substituted into Equations 2.26 which are further simplified using the substitutions:

$$\frac{\partial \dot{\underline{p}}_r}{\partial x^\alpha} = \frac{\partial}{\partial x^\alpha} \left(\underline{v}_0 + \underline{\omega} \times \underline{p}_r \right)$$

$$= \underline{\omega} \times \underline{a}_\alpha$$

$$\frac{\partial \dot{\underline{d}}}{\partial x^\alpha} = \underline{\omega} \times \frac{\partial \underline{d}}{\partial x^\beta}$$

The resulting expressions for strain rate components are

$$\begin{aligned} \dot{\underline{E}}_{\alpha\beta} = & \frac{1}{2} \left[\underline{a}_\alpha \cdot (\underline{\omega} \times \underline{a}_\beta) + \underline{a}_\beta \cdot (\underline{\omega} \times \underline{a}_\alpha) \right] + \\ & \frac{x^3}{2} \left[\frac{\partial \underline{d}}{\partial x^\alpha} \cdot (\underline{\omega} \times \underline{a}_\beta) + \frac{\partial \underline{d}}{\partial x^\beta} \cdot (\underline{\omega} \times \underline{a}_\alpha) + \underline{a}_\alpha \cdot \left(\underline{\omega} \times \frac{\partial \underline{d}}{\partial x^\beta} \right) \right. \\ & + \underline{a}_\beta \cdot \left(\underline{\omega} \times \frac{\partial \underline{d}}{\partial x^\alpha} \right) \left. \right] + \left(\frac{x^3}{2} \right)^2 \left[\frac{\partial \underline{d}}{\partial x^\alpha} \cdot \left(\underline{\omega} \times \frac{\partial \underline{d}}{\partial x^\beta} \right) + \right. \\ & \left. \left(\underline{\omega} \times \frac{\partial \underline{d}}{\partial x^\alpha} \right) \cdot \frac{\partial \underline{d}}{\partial x^\beta} \right] \end{aligned}$$

Permutation of a triple scalar product changes its sign so that all terms cancel in pairs. It may be noted that exclusion of the $(x^3)^2$ term will not affect rigid body strain. The analysis for $\dot{\underline{E}}_{\alpha 3}$ is similar to that for $\dot{\underline{E}}_{\alpha\beta}$.

Generalized Stresses

The generalized stresses defined in Equations 2.14, 2.15 and 2.19 required the stress components $T^{i\alpha}$. The strain rate components found were $\dot{\underline{E}}_{\alpha i}$.

Constitutive relations are usually stated in terms of mixed components of stress rate and strain rate. In effect, all of the difficulties of the tensor notation seem to be concentrated in the computation of generalized stresses.

The base vector \underline{g}_1 is expanded using the definition of \underline{g}_1 from Equation 2.2, the expansion of \underline{p} using Equation 2.6, and the definition of \underline{a}_α to produce

$$\underline{g}_1 = \delta_1^\alpha \left(\underline{a}_\alpha + x^3 \frac{\partial \underline{a}}{\partial x^\alpha} \right) + \delta_1^3 \underline{a} . \quad (2.27)$$

The inner product of this expression with \underline{a}^j is compared with Equation 2.3 to give the components of the inverse of the relator:

$$\left(R_{\cdot\beta}^j \right)^{-1} = \delta_{\cdot\beta}^j + x^3 D_{\cdot\beta}^j$$

$$\left(R_{\cdot 3}^\alpha \right)^{-1} = \underline{a} \cdot \underline{a}^\alpha$$

$$\left(R_{\cdot 3}^3 \right)^{-1} = 1 .$$

The quantities $D_{\cdot\beta}^j$ are defined as

$$D_{\cdot\beta}^j = \underline{a}^j \cdot \frac{\partial \underline{a}}{\partial x^\beta} . \quad (2.28)$$

For small transverse shear strains, \underline{a} is approximately normal to the deformed reference surface. The components $D_{\cdot\beta}^3$ and $\underline{a} \cdot \underline{a}^\beta$ are approximately zero so that the inverse relator and the relator are approximated as:

$$\begin{aligned}
(R_{\beta}^{\alpha})^{-1} &= \delta_{\beta}^{\alpha} + x^3 D_{\beta}^{\alpha} & R_{\beta}^{\alpha} &\approx \delta_{\beta}^{\alpha} - x^3 D_{\beta}^{\alpha} + (x^3)^2 D_{\gamma}^{\alpha} D_{\beta}^{\gamma} \\
(R_{\beta}^3)^{-1} &\approx (R_3^{\alpha})^{-1} \approx 0 & R_{\beta}^3 &\approx R_3^{\alpha} \approx 0 \\
(R_3^3)^{-1} &\approx 1. & R_3^3 &\approx 1.
\end{aligned} \tag{2.29}$$

The determinant follows immediately as

$$R^{-1} \approx 1 + x^3 \operatorname{tr}(D_{\beta}^{\alpha}) + (x^3)^2 \det(D_{\beta}^{\alpha}). \tag{2.30}$$

Equations 2.27 and 2.28 are used to obtain

$$\begin{aligned}
g^{\sigma\beta} &= (\delta_{\varphi}^{\sigma} - x^3 D_{\varphi}^{\sigma}) (\delta_{\psi}^{\beta} - x^3 D_{\psi}^{\beta}) a^{\varphi\psi} \\
&\approx a^{\sigma\beta} - x^3 (D_{\varphi}^{\beta} a^{\varphi\sigma} + D_{\psi}^{\sigma} a^{\beta\psi})
\end{aligned} \tag{2.31}$$

The two term approximation given by Equation (2.31) is used to shift the indices of \dot{E}_{α}^{β} . The mixed tensor \dot{E}_{α}^{β} is truncated to two terms which are:

$$\dot{E}_{\alpha}^{\beta} \approx \dot{E}_{\alpha\alpha}^{\beta} a^{\beta\sigma} + x^3 \left[\dot{E}_{\sigma\alpha}^{\beta} a^{\beta\sigma} - \dot{E}_{\sigma\alpha}^{\beta} (D_{\varphi}^{\beta} a^{\varphi\sigma} + D_{\psi}^{\sigma} a^{\beta\psi}) \right] \tag{2.32}$$

$$\dot{E}_{\alpha}^3 \approx \dot{E}_{3\alpha}$$

The isotropic, homogeneous, linear elastic constitutive equation is expressed in tensor components as

$$T_{\beta}^1 = \lambda \delta_{\beta}^1 \int_0^t \dot{E}_{\alpha}^1 dt + 2\mu \int_0^t \dot{E}_{\beta}^1 dt \quad (2.33)$$

The contravariant stress components are found using Equation 2.31. The generalized stresses are then approximated with two term approximations for $\bar{R}^{1\beta} \bar{R}^{-1}_{\beta 1}$ as:

$$N^{\alpha\beta} = \int_{x^3} T^{\sigma\alpha} \left[\delta_{\sigma}^{\beta} + x^3 \left(D_{\sigma}^{\beta} + \delta_{\sigma}^{\beta} \text{tr} (D_{\gamma}^{\alpha}) \right) \right] dx^3$$

$$q^{\alpha} = \int T^{3\alpha} \left(1 + x^3 \text{tr} (D_{\beta}^{\alpha}) \right) dx^3 \quad (2.34)$$

$$M^{\alpha\beta} = \int_{x^3} T^{\sigma\alpha} \left[\delta_{\sigma}^{\beta} + x^3 \left(D_{\sigma}^{\beta} + \delta_{\sigma}^{\beta} \text{tr} (D_{\gamma}^{\alpha}) \right) \right] dx^3$$

Complete Shell Theory

The three most important and most involved parts of the shell theory are derived in the previous sections. These equations are still in vector form and must be supplemented by other equations to form a complete shell theory. The necessary equations are presented here.

All vectors, whether they are base vectors, positions, velocities, or accelerations will be expressed in terms of the components of a fixed rectangular Cartesian coordinate system. Other coordinate systems could have been used, for example a normal shell coordinate system or cylindrical coordinate system.

The advantage of the Cartesian system is that the base vectors are constant over the space and can be used with equal ease on shells of any shape. Fig. 1 illustrates the two coordinate systems and associated base vectors.

All indices which refer to Cartesian components will be underlined. For example $a_{\alpha\underline{1}}$ denotes $\underline{a}_\alpha \cdot \underline{e}_1$.

The scalar equations of motion are:

$$M_o \ddot{p}_{\underline{1}} = \oint_{l_r} \left(M^{\beta\alpha} a_{\beta\underline{1}} + q^\alpha d_{\underline{1}} \right) v_\alpha d\ell + \int_{x^1}^1 \int_{x^2}^2 \frac{1}{r} \sqrt{a} dx^1 dx^2 \quad (2.35)$$

and

$$M_2 \ddot{d}^\beta = \oint_{l_r} \left(M^{\beta\alpha} v_\alpha d\ell - \int_{x^1}^1 \int_{x^2}^2 q^\beta \sqrt{a} dx^1 dx^2 \right) \quad (2.36)$$

where

$$\ddot{d}_{\underline{1}} = \ddot{d}^\beta a_{\beta\underline{1}}$$

$$M_o = \int_{x^1}^1 \int_{x^2}^2 m_o \sqrt{a} dx^1 dx^2 \quad (2.37)$$

$$M_2 = \int_{x^1}^1 \int_{x^2}^2 m_2 \sqrt{a} dx^1 dx^2$$

In order to obtain Equation 2.36 from Equation 2.24, the base vectors \underline{a}_α are taken to be approximately constant over the region of integration. The reference surface is chosen to make $m_1 = 0$ so that definition of an M_1 is unnecessary.

The strain rate components are:

$$\begin{aligned} \dot{E}_{\alpha\beta} = \frac{1}{2} \left(a_{\alpha 1} \frac{\partial u_1}{\partial x^\beta} + a_{\beta 1} \frac{\partial u_1}{\partial x^\alpha} \right) + \frac{x^3}{2} \left(\frac{\partial \dot{d}_1}{\partial x^\alpha} \frac{\partial u_1}{\partial x^\beta} + \frac{\partial \dot{d}_1}{\partial x^\beta} \frac{\partial u_1}{\partial x^\alpha} + a_{\alpha 1} \frac{\partial \dot{d}_1}{\partial x^\beta} \right. \\ \left. + a_{\beta 1} \frac{\partial \dot{d}_1}{\partial x^\alpha} \right) \end{aligned} \quad (2.38)$$

$$\dot{E}_{\alpha 3} = \frac{1}{2} \left(d_1 \frac{\partial u_1}{\partial x^\alpha} + a_{\alpha 1} \dot{d}_1 \right)$$

$$\dot{E}_{33} = 0$$

where the quadratic term in x^3 has been dropped from the expression for $\dot{E}_{\alpha\beta}$.

The required equations for obtaining generalized stresses for the isotropic elastic case are outlined in the previous section.

The base vector components $a_{\alpha 1}$ and d_1 are functions of time and are found by integration as follows:

$$a_{\alpha 1} = a_{\alpha 1}(t=0) + \int_0^t \left[\dot{a}_{\alpha 1}(t=0) + \int_0^t \frac{\partial \ddot{p}_1}{\partial x^\alpha} dt \right] dt$$

The expression for d_1 is evaluated in a similar manner.

All equations necessary to the theory have been presented with the exception of some trivial details. The method of solution of these equations is the topic of the next section.

NUMERICAL SOLUTION OF EQUATIONS

The numerical solution of the equations presented involve several important and interrelated topics. These topics are:

1. The advantages of rotary inertia and transverse shear in the formulation of the problem.
2. The general method of writing the time derivatives in the formulation to minimize roundoff errors in numerical integration.
3. The particular numerical method of time integration used in the formulation.
4. The method of stepping through a two dimensional grid-work to minimize storage.

The first three topics will be covered next in the order listed. These topics are not illustrated with the actual equations used in the computer program but rather with simplified equations. The fourth topic which is covered last incorporates the conclusions of the first three topics and incorporates the actual equations in the program.

Advantages of Rotary Inertia and Transverse Shear

The Bernoulli-Euler equations for a straight beam with small displacements are combined with the membrane equations to produce the following set:

$$\dot{v}_x = \frac{1}{\mu} \frac{\partial N}{\partial S}$$

$$\dot{v}_y = \frac{1}{\mu} \frac{\partial Q}{\partial S}$$

$$\dot{N} = EA \frac{\partial v_x}{\partial S} + f_1(N, M, Q) \quad (3.1)$$

$$\dot{M} = EI \frac{\partial^2 v_y}{\partial S^2} + f_2(N, M, Q)$$

$$Q = \frac{\partial M}{\partial S}$$

where v_x and v_y are the velocity components parallel and transverse to the beam axis; S is a coordinate along the beam axis; and M , N , and Q are the bending moment, membrane force, and shear force, respectively. The functions f_1 and f_2 are zero for the linear elastic case but may become dominant for the elastic-plastic case. The point in including the functions f_1 and f_2 is to show the reason for the restraint of requiring that all the stress components be evaluated at common points along the beam. Another restraint is that the velocity components be evaluated at common points along the beam. The velocity locations need not coincide with the stress locations.

The principal difficulties in differencing the equations are:

1. It is very difficult to include Q in the functions f_1 and f_2 . To evaluate \dot{N} and \dot{M} at time n based on N, M , and Q at time $n-1$ is very error prone. Time consuming iterative methods are required to evaluate \dot{N} and \dot{M} at time n based on N, M , and Q at time n .

2. Lowest order central differencing of all quantities is impossible.

There are several ways of compromising to carry out the differencing of Equations 3.1. One method which is followed in principle in UNIVALVE[4,5] is:

$$(\dot{v}_x)_j = \frac{1}{\mu} \frac{N_j - N_{j-1}}{\Delta S}$$

$$(\dot{v}_y)_j = \frac{1}{I_p} \frac{M_{j+1} - 2M_j + M_{j-1}}{\Delta S^2}$$

$$\dot{N}_j = EA \frac{(v_x)_{j+1} - (v_x)_j}{\Delta S} + f_1(N_j, M_j, 0)$$

$$\dot{M}_j = EI \frac{(v_y)_{j+1} - 2(v_y)_j + (v_y)_{j-1}}{\Delta S^2} + f_2(N_j, M_j, 0)$$

The plasticity functions f_1 and f_2 are taken to be independent of shear force, Q . The net effect of this has not been evaluated but could possibly be serious.

The membrane force rate, \dot{N} , and the acceleration component, \dot{v}_x , are not properly centered in the equations. However, if the material is linearly elastic then $f_1(M, N, 0) \equiv 0$ and the improper centering of the two quantities introduces errors which exactly cancel each other. Unfortunately, the plastic case is an important case.

The set of Timoshenko beam equations corresponding to Equations 3.1 are

$$\dot{v}_x = \frac{1}{\mu} \frac{\partial N}{\partial S}$$

$$\dot{v}_y = \frac{1}{\mu} \frac{\partial Q}{\partial S}$$

$$\dot{v}_\psi = \frac{1}{I_p} \left(\frac{\partial M}{\partial S} - Q \right)$$

$$\dot{N} = EA \frac{\partial v_x}{\partial S} + f_1(M, N, Q) \quad (3.2)$$

$$\dot{Q} = k \left(\frac{\partial v_y}{\partial S} + v_\psi \right) + f_3(M, N, Q)$$

$$\dot{M} = EI \frac{\partial v_\psi}{\partial S} + f_2(M, N, Q)$$

where f_1 , f_2 , and f_3 are again some plasticity functions. The consideration of locating the velocities at common points and generalized stresses at common points still holds. This set of equations is much easier to difference, however.

The generalized stress rate equations are all independent so that the shear stress can be accommodated in the plasticity functions. The first difficulty with the Bernoulli-Euler equations does not arise here.

The velocities are located at half mesh points and the generalized stresses at whole mesh points. All quantities are center differenced. The differenced equations are illustrated below.

$$(\dot{v}_x)_j = \frac{1}{\mu} \frac{N_{j+\frac{1}{2}} - N_{j-\frac{1}{2}}}{\Delta S}$$

$$(\dot{v}_y)_j = \frac{1}{\mu} \frac{Q_{j+\frac{1}{2}} - Q_{j-\frac{1}{2}}}{\Delta S}$$

$$(\dot{v}_\theta)_j = \frac{1}{I_\rho} \left(\frac{M_{j+\frac{1}{2}} - M_{j-\frac{1}{2}}}{\Delta S} - \frac{Q_{j+\frac{1}{2}} + Q_{j-\frac{1}{2}}}{2} \right)$$

$$\dot{N}_{j-\frac{1}{2}} = EA \left[\frac{(v_x)_j - (v_x)_{j-1}}{\Delta S} \right] + f_1(M_{j-\frac{1}{2}}, N_{j-\frac{1}{2}}, Q_{j-\frac{1}{2}})$$

$$\dot{Q}_{j-\frac{1}{2}} = k \left[\frac{(v_y)_j - (v_y)_{j-1}}{\Delta S} + \frac{(v_x)_j + (v_x)_{j-1}}{2} \right] +$$

$$f_3(M_{j-\frac{1}{2}}, N_{j-\frac{1}{2}}, Q_{j-\frac{1}{2}})$$

$$\dot{M}_{j-\frac{1}{2}} = EI \left[\frac{(v_\theta)_j - (v_\theta)_{j-1}}{\Delta S} \right] + f_2(M_{j-\frac{1}{2}}, N_{j-\frac{1}{2}}, Q_{j-\frac{1}{2}})$$

The shear in the third and v_θ in the fifth equations are averaged values of quantities a half mesh away. For the linear elastic case this introduces errors of order $(\Delta S)^2$ which is the same order as the derivative approximations in the differenced equations. Thus, the differencing of Equations 3.2 does not have the second difficulty outlined above for Equations 3.1.

A third advantage of Equations 3.2 over Equations 3.1 is that the boundary conditions are much easier to apply to Equations 3.2. If Equations 3.1 were written entirely in terms of displacements and their time derivatives, then the acceleration at a given position j would involve displacements at

positions $j \pm 1$ and $j \pm 2$. Thus, the boundary conditions enter the difference equations two meshes away from the boundary. Equations 3.1 when written entirely in terms of displacements and their time derivatives only involve second derivatives in space. The boundary conditions are only felt one mesh away.

The boundary conditions require that different difference algorithms must be used near the boundaries. Since the Bernoulli-Euler equations influence equations twice as far from the boundaries as the Timoshenko equations, the boundary logic becomes somewhat easier to handle in Timoshenko theory.

In summary then, inclusion of rotary inertia and transverse shear simplifies the handling of complex materials, simplifies and decreases errors in differencing, and simplifies the logic near boundaries. These same conclusions can be applied when the equations are generalized to include large deflections and expanded to two dimensional surfaces.

Roundoff Errors in Time Integration

Consider a simple spring mass system with mass m and spring constant k . The equation of motion with no external force is

$$m\ddot{u} = -ku \quad (3.3)$$

where u is the displacement of the mass. The second derivative on the left side is approximated with a central difference and the resulting equation is rearranged as:

$$u_{n+1} = (2 - \frac{k}{m} \Delta t^2) u_n - u_{n-1} \quad (3.4)$$

The constants m and k are known and a stable time step, $\Delta t < 2\sqrt{\frac{m}{k}}$ is chosen.

If u_n and u_{n-1} are known from previous steps, then the new value of u_{n+1} is

found directly. The approximate solution of Equation 3.3 is easily found in this manner. Note that computer storage is required for the displacements at two previous time steps.

Equation 3.3 can also be solved in another way by adding a new variable, the velocity, v . The equivalent equation pair is

$$\begin{aligned} m \dot{v} &= -ku \\ \dot{u} &= v \end{aligned} \tag{3.5}$$

The velocity is now centered at half time steps and the displacement at whole time steps. The resulting central differenced equations are:

$$\begin{aligned} v_{n+\frac{1}{2}} &= v_{n-\frac{1}{2}} - \left(\frac{k}{m} \Delta t\right) u_n \\ u_{n+1} &= u_n + v_{n+\frac{1}{2}} \Delta t \end{aligned} \tag{3.6}$$

For known values of $v_{n-\frac{1}{2}}$ and u_n and a stable time step $\Delta t < 2\sqrt{m/k}$, the equations are used to find values of $v_{n+\frac{1}{2}}$ and u_{n+1} .

In the real number system, Equation 3.6 is equivalent to Equation 3.4. This is seen by solving the second of Equation 3.6 for $v_{n+\frac{1}{2}}$ and then for $v_{n-\frac{1}{2}}$ and substituting into the first of the equation pair. The result is Equation 3.4 identically.

Unfortunately, computers do not use the real number system, but instead are plagued with roundoff. Equations 3.4 and 3.6 can behave quite differently when roundoff is introduced. This is best illustrated with an example.

Consider a spring mass system with $(k/m) = 1 \times 10^6 \text{ sec}^{-2}$. This system will have a natural frequency of $1 \times 10^3 \text{ rad/sec}$. If a time step of $1 \times 10^{-5} \text{ sec}$

is used, then either of the differenced equations should have a "natural frequency" of 1.000004×10^3 rad/sec.

This problem was run using six place arithmetic with both methods. Starting values were computed from the expected real value solution. The results at every eighth calculation are plotted in Figure 2 for the two methods. Agreement is excellent over the single oscillation. Figure 3 is a similar plot using five place arithmetic. The solution of Equations 3.6 is virtually the same as before, but the apparent frequency of the solution of Equation 3.4 is noticeably higher.

Figures 4 and 5 are similar plots using four and three place arithmetic respectively. In these last plots, the term $(k \Delta t^2/m)$ has been lost completely in the roundoff. The solution of Equations 3.6, however, is very good with four place arithmetic and only begins to show bad behavior with the three place arithmetic of Figure 5. A pronounced damping occurs, although the error in frequency is well under 2%.

The plots shown used truncated arithmetic, e.g., the product of 0.11 and .99 using two place truncated arithmetic is .10. The same problem was worked using numbers rounded to the nearest n places, and then rounding upward. The three methods of rounding gave virtually identical runs for the velocity formulation of Equations 3.6. The differences in the damped peak amplitude near 620 cycles using the two other methods of rounding was less than 2% from the value illustrated in Figure 5.

The purpose of this section is two fold. The primary purpose is to illustrate that the velocity formulation of the form of Equations 3.6 is much less prone to roundoff than the displacement formulation of the form of Equation 3.4.

× DISPLACEMENT FORMULATION
 + VELOCITY FORMULATION

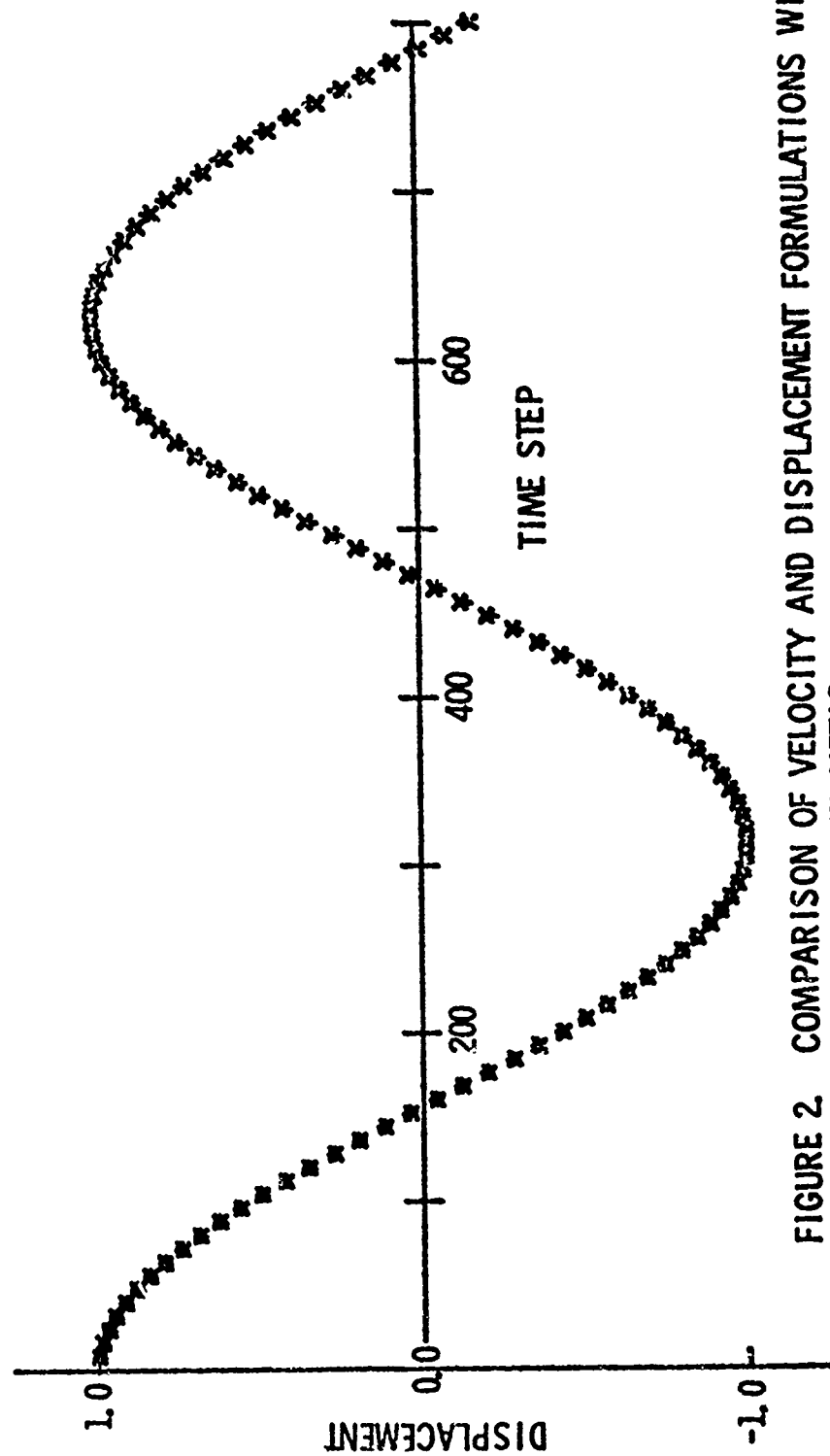


FIGURE 2. COMPARISON OF VELOCITY AND DISPLACEMENT FORMULATIONS WITH SIX PLACE ARITHMETIC.

× DISPLACEMENT FORMULATION
+ VELOCITY FORMULATION

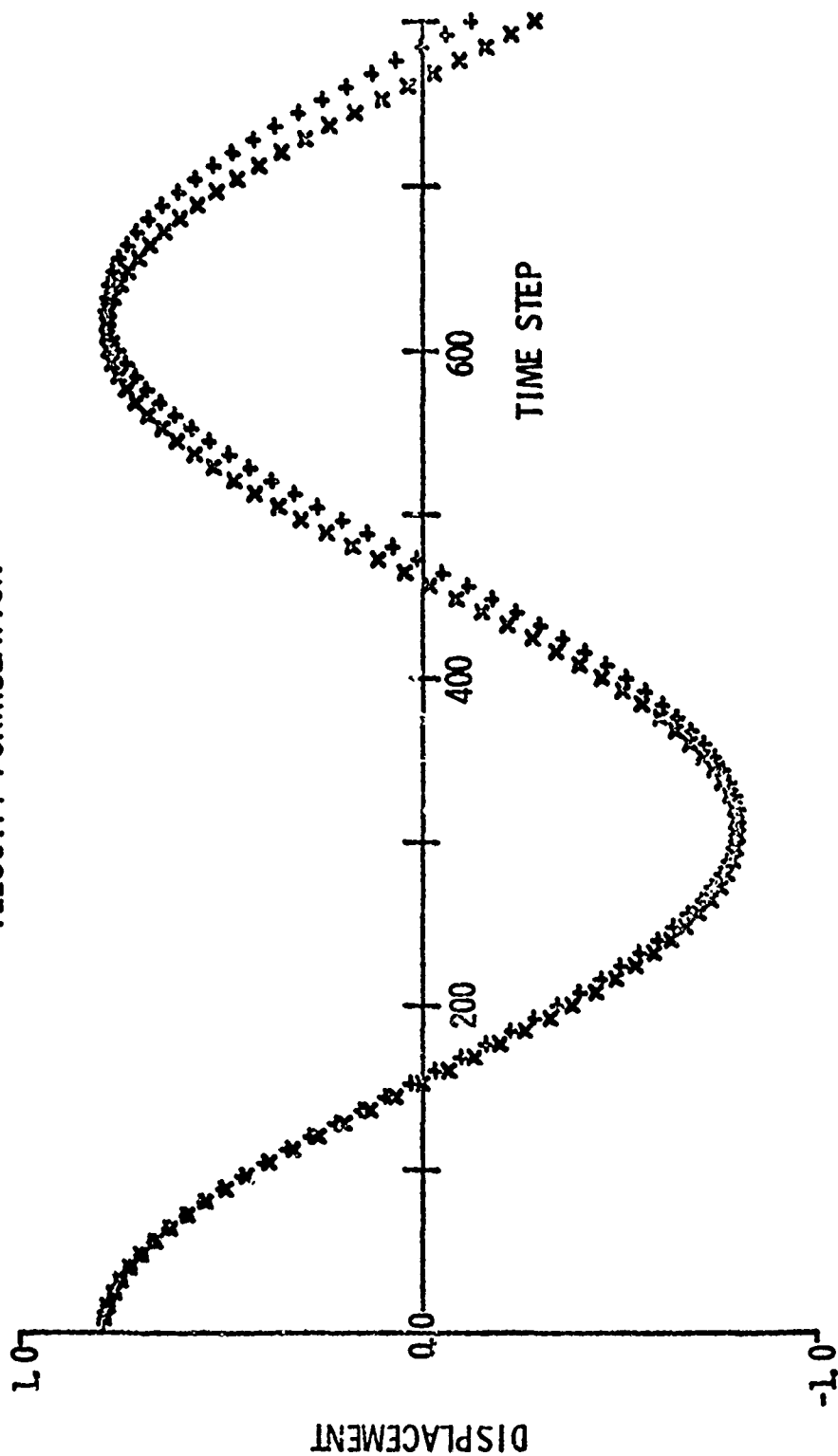


FIGURE 3. COMPARISON OF VELOCITY AND DISPLACEMENT FORMULATIONS WITH FIVE PLACE ARITHMETIC.

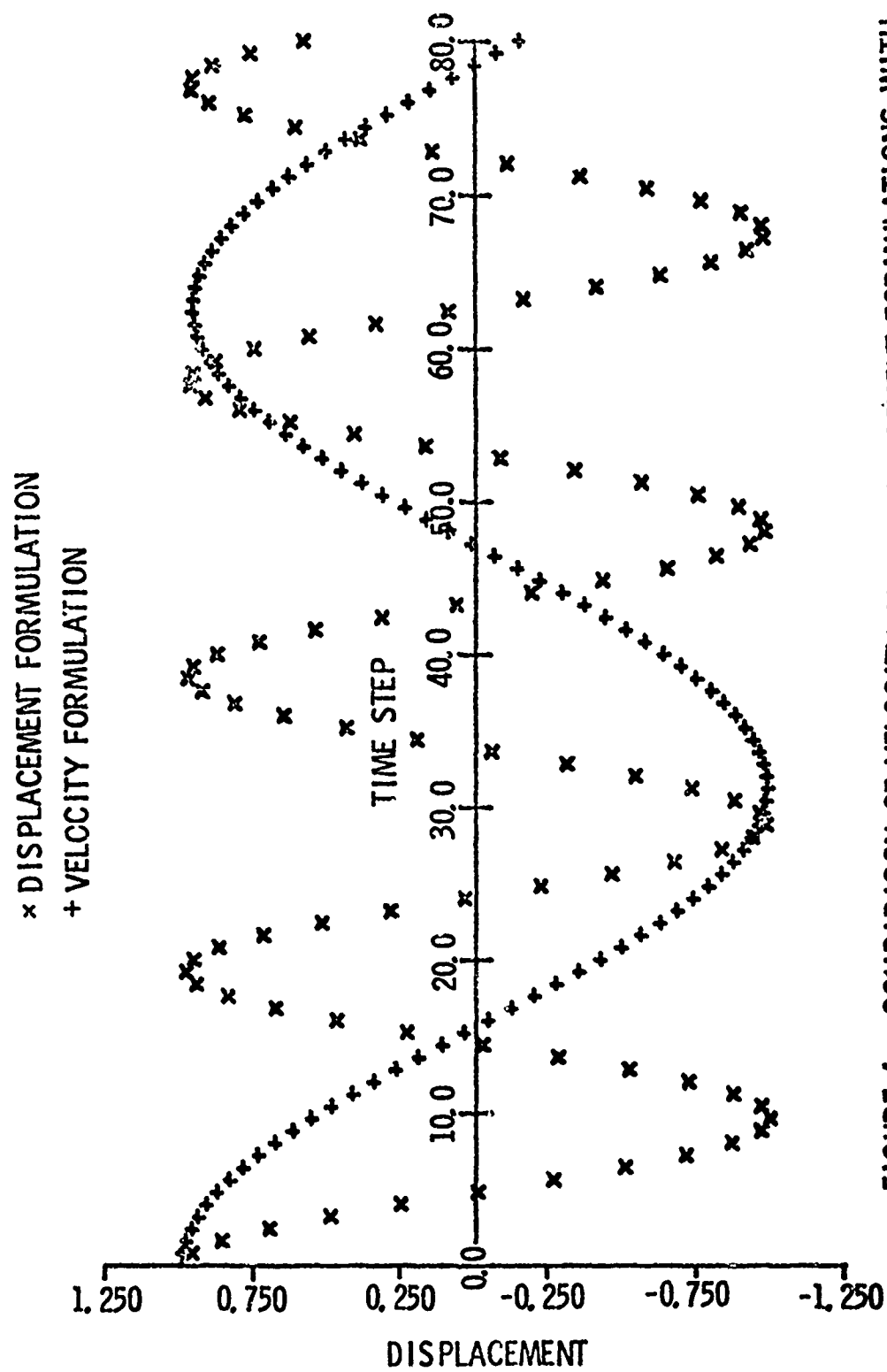


FIGURE 4. COMPARISON OF VELOCITY AND DISPLACEMENT FORMULATIONS WITH FOUR PLACE ARITHMETIC.

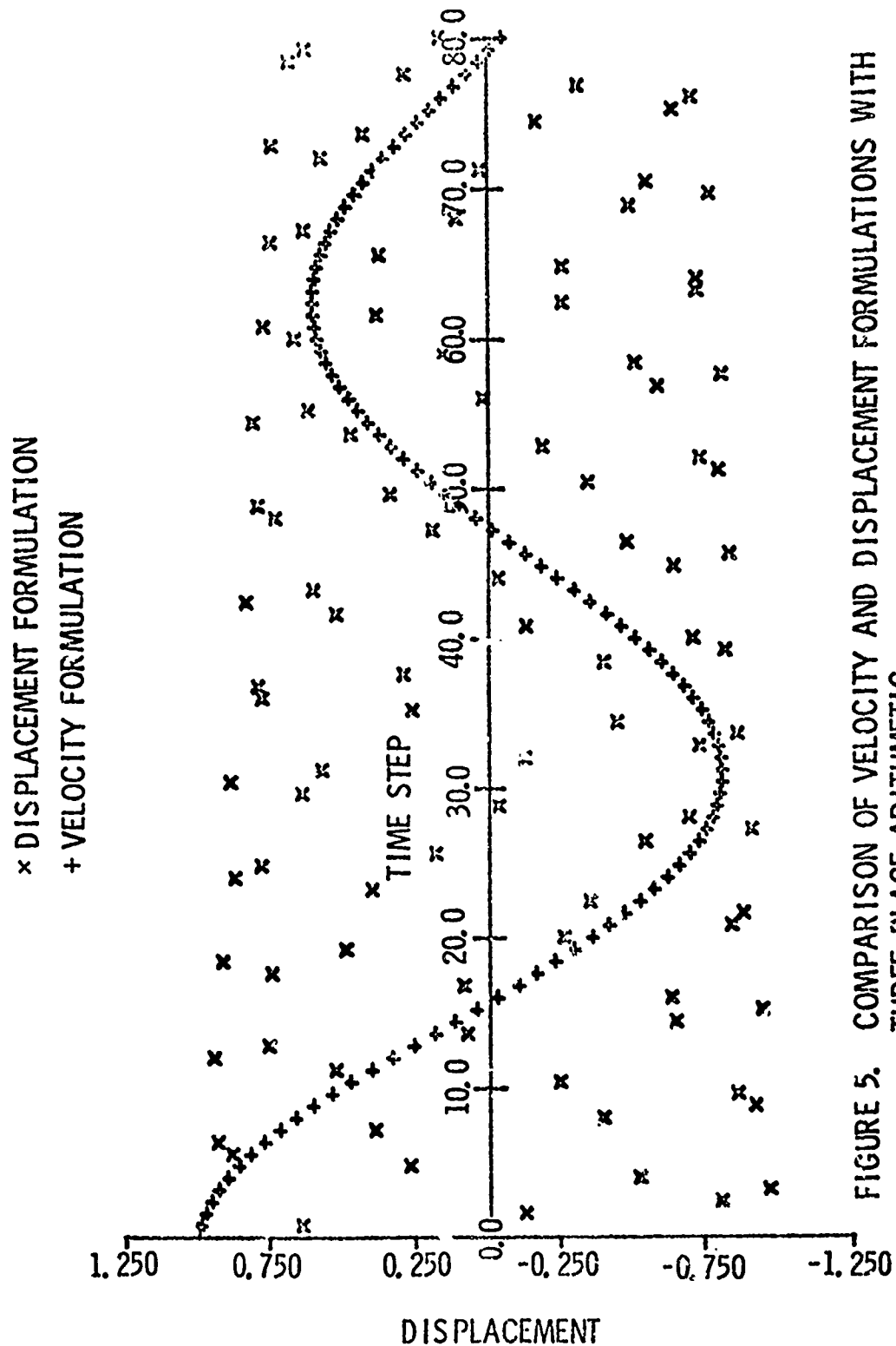


FIGURE 5. COMPARISON OF VELOCITY AND DISPLACEMENT FORMULATIONS WITH THREE PLACE ARITHMETIC.

The same storage space is required for the two methods, so there is no penalty in using the velocity formulation.

The second purpose of this section is to caution that computer arithmetic can negate many logical theorems and analyses. For example, if a given time step is stable, then a smaller step is usually better. This is not the case using the displacement formulation of Equation 3.4 where $k\Delta t^2/m$ may be lost in roundoff when subtracted from 2. Another consideration is that when roundoff does influence the results, then linearity no longer holds. Decomposition into normal coordinates, adding modal responses, and numerical stability analyses are all based on linearity.

Stability analyses in particular are suspect. If Equations 3.6 are evaluated on a computer with specific constants and time step size and if Figure 5 results, then one might incorrectly conclude that the time integration method exhibits damping. A stability analysis using the real number system separates the roundoff error into an independent consideration and eliminates this confusion. Alternately, the specific evaluation method might be carried out with different accuracy arithmetic to show that roundoff is not a consideration.

The velocity formulation is of course used in the computer program GRIVET. The central difference time integration method illustrated is also used in the program although the velocity formulation should be applicable to any explicit integration method.

Differencing in Two Dimensions

The sequence of solution of the equations is most easily explained using a picture of the gridwork. Figure 6 shows a portion of the reference surface

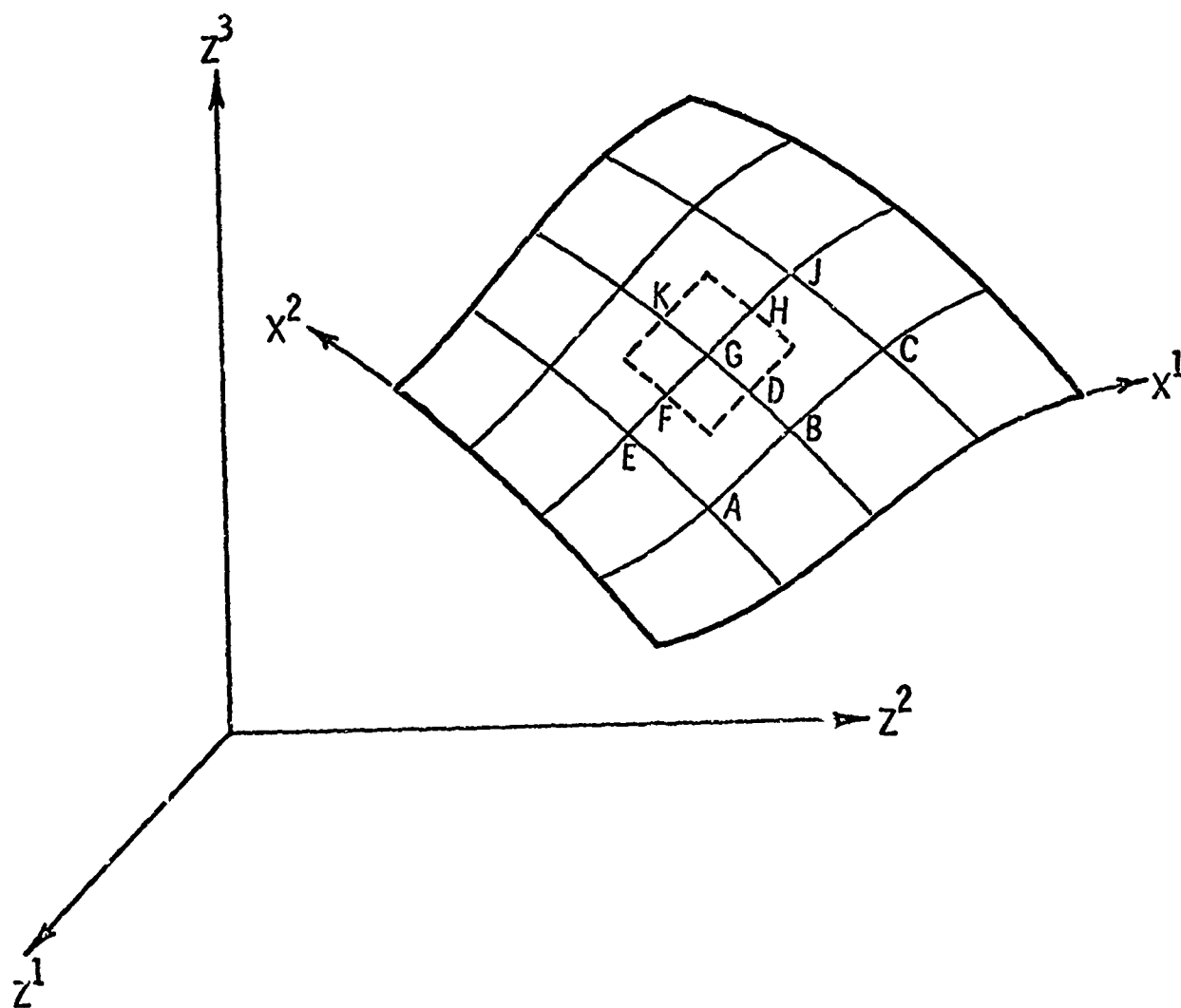


FIGURE 6. REFERENCE SURFACE WITH SHELL COORDINATES AND DIFFERENCING GRID WHICH IS USED IN GRIVET.

of a shell with (x^1, x^2) coordinates on the surface. Grid lines are drawn along lines of constant x^1 and x^2 .

The differencing in two dimensions is patterned after the differencing of Equations 3.2. The velocities and positions, $p_{\underline{1}}, \dot{p}_{\underline{1}}, d_{\underline{1}}, \dot{d}_{\underline{1}}$; the generalized masses, M_0, M_2 ; and the forcing function integral $\int_{x^1} \int_{x^2} f_{\underline{1}}^* \sqrt{a} \, dx^1 dx^2$

are located at the grid intersections such as points A, B, C in Figure 6. The stresses T_{α}^1 , and derivatives of positions and velocities such as $\partial \dot{p}_{\underline{1}} / \partial x^{\alpha}$, $\partial \dot{d}_{\underline{1}} / \partial x^{\alpha}$, and $a_{\alpha \underline{1}}$ are located between grid intersections such as points D, F, H and K.

The elemental region about which the equations of motion are written are "rectangular" regions such as the dashed region containing point G in Figure 6. The stress line integrals along a side are approximated with the value of the integrand at the midpoint of the line times the line length. For example, along one side, say side D in Figure 6, the integral is approximated as:

$$\int_D N^{\alpha \beta} v_{\beta} a_{\alpha \underline{1}} d\ell \approx (N^{\alpha \beta})_D (a_{\alpha \underline{1}})_D (v_{\beta} \Delta \ell)_D$$

where $(v_{\beta} \Delta \ell)_D$ is the product of the physical line length of side D and the v_{β} component of the unit outer normal on side D. Other contour integrals are approximated in a similar manner. The area integration of shear stress in Equation 2.46 is approximated as:

$$\left(\int_{x^1}^2 \int_G q^\beta \sqrt{a} \, dx^1 dx^2 \right) \approx \frac{1}{4} (q_D^\beta + q_H^\beta + q_K^\beta + q_F^\beta) A_G$$

where A_G is the physical area of the dashed segment containing point G.

This averaging is necessary since all components of the stress tensor must be calculated at the same place, particularly if a yield surface is involved.

The generalization of the differencing of Equations 3.2 to two dimensions can be carried out another way. The "between mesh" quantities such as stresses and derivatives could be located as shown by the points D, E, J or K in Figure 7. The elemental regions would then be the diamond shaped region which is dashed in Figure 7. The diamond shaped region has one important advantage, viz, that there are only half as many "between mesh" locations as for the rectangular regions of Figure 6. This advantage is offset by two advantages of the rectangular region. The first advantage is that the resulting equivalent differencing method has a smaller error bound for the rectangular than for the diamond region. The second advantage of the rectangular region is that it accounts for a very important mode shape, the keystone shape shown in Figure 8. This pattern which is observed in two dimensional continuum computer programs[14], should not be as troublesome in a shell program. Curvature along the x^1 axis in Figure 8 introduces coupling which produces some stress for the keystone mode. The keystone mode, however, could appear in plate or cylinder problems where the x^1 axis of Figure 8 would coincide with the cylinder axis.

The unknown effect of the keystone mode on the solution of a general problem prompted the adoption of the rectangular region of Figure 6. The increased storage requirements and computation time were accepted as known costs of the choice.

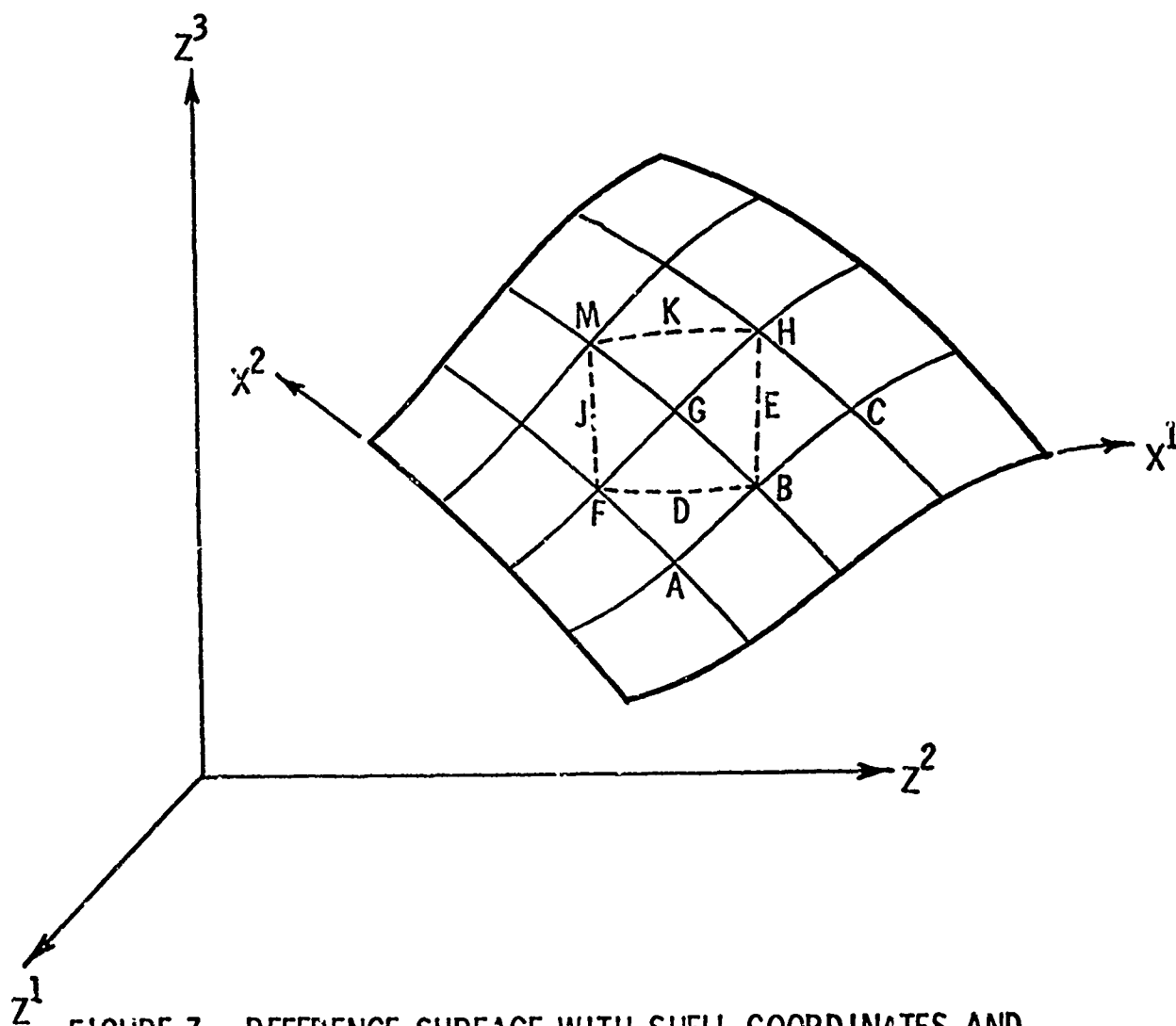


FIGURE 7. REFERENCE SURFACE WITH SHELL COORDINATES AND DIFFERENCING GRID WHICH IS KEYSTONE PRONE.

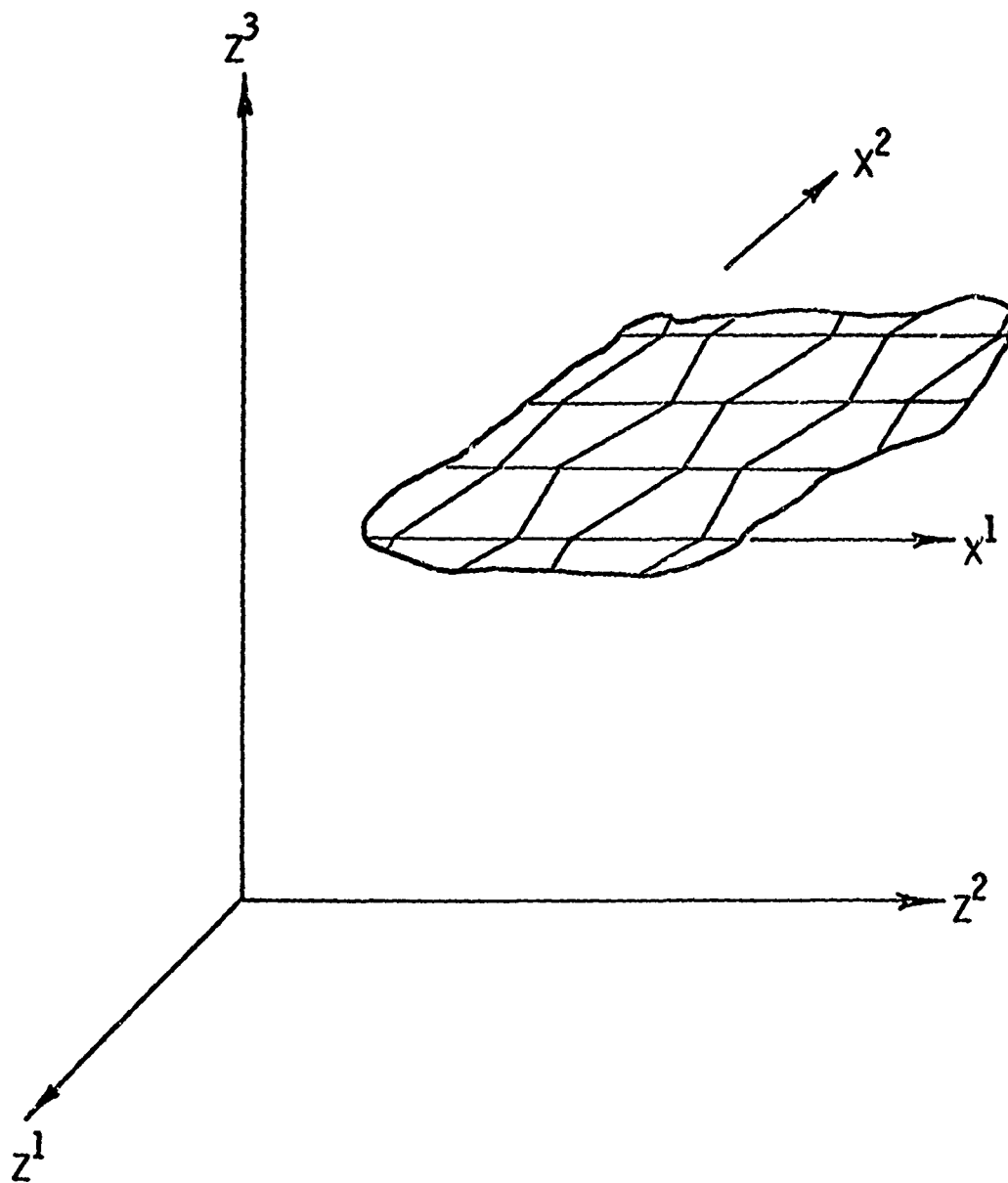


FIGURE 8. KEYSTONE PATTERN ON A PORTION OF A PLATE.

A Search for Simple Time Integration Methods

If the system of equations are differenced in space, then for a linearized set the equations could be stated in the form

$$\{\ddot{q}\} + [K]\{q\} = 0 \quad (3.7)$$

where no forcing function is used and the vector $\{q\}$ is a generalized displacement function. This equation is to be integrated numerically in time. The section on roundoff showed the definite advantage of the velocity formulation of this problem if computer arithmetic is to be used. In the analysis of this section, the real and complex number systems are used so roundoff is not a consideration. The displacement formulation is identical to the velocity formulation in this case.

Various numerical integration methods are available for integration of Equation 3.7. The simplest is derived by expressing the second time derivative with a central difference expression and solving for the forward displacement, viz,

$$\{q\}_{n+1} = (2 [I] - [K] \Delta t^2) \{q\}_n - \{q\}_{n-1}.$$

This integration method is very fast computationally but is limited to small time step sizes for stability.

There are also time integration methods which are stable for any time step size. The Houbolt[9] and Newmark[8] methods are the best known of these methods. Unfortunately, both of these methods are of the form:

$$(a[I] + b[K] \Delta t^2) \{q\}_{n+1} = \sum_{j=0}^N (a_j[I] + b_j \Delta t^2 [K]) \{q\}_{n-j}$$

The solution for $\{q\}_{n+1}$ then either requires the solution of a set of algebraic equations or the evaluation of $(a[I] + b[K] \Delta t^2)^{-1}$. Neither of these alternatives is particularly attractive, especially when the result is generalized to the non-linear problem of interest.

The place for this problem is a numerical integration method of the form

$$\{q\}_{n+1} = - \sum_{j=0}^N (a_j[I] + b_j[K]) \{q\}_{n-j} \quad (3.8)$$

(for some small integer N) which would be stable and convergent for all time step sizes. Such a method does not exist for $N \leq 2$. This is proved [5] as follows. The solutions of Equations 3.7 and 3.8 are compared for small values of Δt . Three consistency equations are derived by making these solutions coincide to order $(\Delta t)^2$. This leaves five arbitrary coefficients in Equation 3.8. A stability equation is derived by assuming an exponential solution for the difference equation. This equation is transformed into a polynomial of order $(N + 1)$ with the linear mapping $\exp \beta = (1 + z)/(1 - z)$. Numerical instability of the differencing method is associated with roots of the polynomial which lie in the right half plane. The Routh-Hurwitz criteria are applied to show that some value of Δt will give a root in the right half plane regardless of how cleverly the remaining five coefficients are chosen.

Although no unconditionally stable time integration method of the form of Equation 3.8 exists for $N \leq 2$, this does not rule out the existence of very

stable methods of that form. Until a more complete study is made, however, the simplicity and accuracy of the simple central difference method make it appear most attractive at the present time.

A Disadvantage of Rotary Inertia and Transverse Shear

Some advantages of rotary inertia and transverse shear have been listed but no disadvantages have been mentioned. An unexpected characteristic of the extra degrees of freedom from the transverse shear is an additional set of vibrational modes. Unfortunately, the frequencies associated with these modes are very high. These high frequencies usually dictate the critical time step size. Usually the critical time step size in a structural program can be increased simply by making the mesh or element size larger. In the transverse shear formulation, the critical time step size is essentially independent of mesh size.

The shape and characteristics of the high frequency shear modes can be studied by examining the Timoshenko beam equations.

The transverse shear mode phase velocity is shown by Fung[16] to be unbounded for long wavelengths. The frequency of course is bounded and can be approximated for finite length beams as follows.

Flügge[19], p. 61-15 gives the mode shapes as

$$w(x,t) = \varphi(x) \sin(\omega t + \epsilon)$$

$$\psi(x,t) = \psi(x) \sin(\omega t + \epsilon)$$

where $\psi(x)$ and $\varphi(x)$ are linear combinations of hyperbolic and circular sines and cosines of $\alpha x/\ell$ and $\beta x/\ell$ where x is a coordinate along the beam and ℓ is its length. For ordinary Bernoulli-Euler theory $\alpha = \beta = \lambda_n$ where λ_n depends

upon the boundary conditions and mode number and are listed in Table 61.1 of Ref. [17]. For Timoshenko theory, the values are given by

$$\frac{\alpha^2}{\beta^2} = \frac{p^2}{2} \left[1 + (1+B) + \left\{ (1-B)^2 + \frac{b}{p^2} \right\}^{\frac{1}{2}} \right]$$

where $p^2 = \omega^2 \ell^2 \rho / E$

$$b = 48 \ell^2 / h^2$$

$$B = \frac{3E}{2G}$$

The product $\alpha^2 \beta^2$ can be formed and the result solved for p^2 as

$$p^2 = \frac{b}{8B} \left[1 + \left(1 - \frac{64B\alpha^2\beta^2}{b^2} \right)^{\frac{1}{2}} \right]$$

For long wavelengths, α^2 and β^2 are very nearly the Bernoulli-Euler values and the second term under the square root is very small compared to one. A two term binomial expansion then gives the approximate values:

$$p_1^2 \approx 4 \lambda_n^4 / b$$

$$p_2^2 \approx b / 4B$$

In terms of frequencies then

$$\omega_1^2 \approx \left(\frac{\lambda_n}{\ell} \right)^4 \frac{h^2 E}{12 \rho}$$

$$\omega_2^2 \approx \frac{8}{h^2} \frac{G}{\rho}$$

The first frequency is the ordinary Bernoulli-Euler value, while the second corresponds to the transverse shear branch.

Note in particular that although the bending frequency is a strong function of wavelength, the shear wave frequency, to a first approximation, is independent of wavelength for long wavelengths. It is this characteristic which clarifies the time step problem.

For short wavelengths, finite differencing can sometimes distort solutions with beneficial results. This is true of the ordinary differencing of the Bernoulli-Euler equations where phase velocity versus wavelength can be beneficially tailored by proper selection of mesh and time step sizes[18]. Almost any consistent differencing will be adequate to describe long wavelengths. Furthermore, mesh size will have almost no effect. In essence, the high frequency shear mode will be present unless the basic mathematical model is changed.

The critical time step size for the ordinary central difference time integration method is given by

$$\tau_c \leq \frac{2}{\omega}$$

for all frequencies, ω . The rotary inertia then defines a critical time step:

$$\tau_{cRI} = \frac{h}{(2G/\rho)^{1/2}}$$

Unless a small mesh size is chosen so that membrane behavior becomes a consideration, the time step size will be dictated by the above transverse shear mode.

SUMMARY AND CONCLUSIONS

The equations are developed which govern the dynamic large deflection response of a general shaped shell including rotory inertia and transverse shear. The remainder of the paper lists several problem areas associated with the finite difference solution of the equations. The advantage in using rotory inertia and transverse shear is that the equations are essentially a system of second order differential equations rather than fourth order. The treatments of boundary conditions and complex materials are thereby simplified, and the differencing of equations is simplified and errors decreased. A disturbing factor is that an additional high frequency mode is introduced by the shear and rotory inertia which usually dictates the time step size for any conditionally stable time integration method.

The velocity formulation of time integration which is used is compared to the usual displacement formulation and is justified on its resistance to roundoff errors. The displacement formulation of time integration is shown to be roundoff error prone while the velocity formulation is very roundoff resistant. Time integration methods for an undamped linear structure which do not require the inverse of the stiffness matrix or solution of a set of algebraic equations are investigated. No such method exists which is unconditionally stable, even if displacements at up to four time steps are involved. The usual central difference method is used in the computer program because of its computational simplicity and accuracy.

LIST OF REFERENCES

1. Leech, J. W., T. H. H. Pian, E. A. Witmer, and W. Herrman, "Dynamic Response of Shells to Externally-Applied Dynamic Loads," M.I.T., ASD-TDR-62-612, Nov., 1962.
2. Ball, E. R., "A Geometrically Nonlinear Analysis of Arbitrarily Loaded Shells of Revolution," NASA CR-909, Jan., 1968.
3. Samuelson, L. A., "Nonlinear Analysis of a Circular Cylindrical Shell Under Nonuniform Creep," Report B-70-68-1, Lockheed Missiles and Space Co., Jan., 1968.
4. Krieg, R. D., and Key, S. W., "UNIVALVE, A Computer Code for Analyzing Dynamic Large Deflection Elastic-Plastic Response of Beams and Rings," SC-RR-66-2682, Sandia Laboratories, Jan., 1968.
5. Krieg, R. D., and Duffey, T. A., "UNIVALVE II, A Code to Calculate the Large Deflection Dynamic Response of Beams, Rings, Plates and Cylinders," SC-RR-68-303, Sandia Laboratories, Oct., 1968.
6. Leech, J. W., Morino, L., and Witmer, E. A., "PETROS 2: A New Finite-Difference Method and Program for the Calculation of Large Elastic-Plastic Dynamically-Induced Deformations of General Thin Shells," Aeroelastic and Structures Research Laboratory, M.I.T., ASRL TR-152-1.
7. Silsby, W., Sobel, L. H., and Wrenn, B. G., "Nonsymmetric and Nonlinear Dynamic Response of Thin Shells, Vol. 1, User's Manual for STAR (Shell Transient Asymmetric Response)," Report B-70-69-19, Lockheed Missiles and Space Co., Dec. 1968.

8. Newmark, N. M., "A Method of Computation for Structural Dynamics,"
Proc. of ASCE, E.M. 3, 67-94(July 1959).
9. Johnson, D. E., "A Proof of the Stability of the Houbolt Method,"
AIAA J. 4, pp 1450-1451 (Aug. 1966).
10. Eringen, A. C., "Nonlinear Theory of Continuous Media,"
McGraw-Hill, 1962, p 96.
11. Bowen, R. M., "Lectures on Continuum Mechanics," SC-M-67-326,
Sandia Corporation, May 1967, p 49.
12. Ericksen, J. L., and Truesdall, C., "Exact Theory of Stress and
Strain in Rods and Shells," Arch. Rational Mech. Anal., Vol. 1,
1959, p. 318.
13. Naghdi, P. M. and Wainwright, W. L., "On the Time Derivative of
Tensors in Mechanics of Continua," Quart. Appl. Math., 19, p. 101.
14. Petschek, A. G., and Hanson, M. E., "Difference Equations for Two
Dimensional Elastic Flow," J. of Comp. Phys., Vol. 3, No. 2,
Oct. 1968, p. 307.
15. Krieg, R. D., "Unconditional Stability in Numerical Time Integration
Methods," SC-DR-70-400, Sandia Corporation, 1970.
16. Fung, Y. C., "Foundations of Solid Mechanics," Prentice-Hall, 1965,
pp. 322-324.
17. Flügge, W., "Handbook of Engineering Mechanics," McGraw-Hill, 1962,
pp 61-15 to 61-17.
18. Krieg, R. D., "Phase Velocities of Elastic Waves in Structural Computer
Programs," Sandia Corp., Albuquerque, N. M., Report No. SC-TM-67-816,
Nov. 1967.

APPENDIX A FORMS OF THE DIVERGENCE THEOREM

The two-dimensional divergence theorem can be written[21] as

$$\oint_{\partial a} v^\alpha v_\alpha d\ell = \int_a v^\alpha|_\alpha da. \quad (A.1)$$

For the purposes of this report, a modified form of this equation is required. The desired form can be found from Equation A.1.

A vector, \underline{u} , which is constant over the field, is postulated. Then Equation A.1 is rewritten as:

$$\oint_{\partial a} \underline{u} \cdot \underline{v} q^\alpha v_\alpha d\ell = \int_a \left(\underline{u} \cdot \underline{v} q^\alpha \right)|_\alpha da = \int_a \left[q^\alpha \frac{\partial}{\partial x^\alpha} (\underline{u} \cdot \underline{v}) + (\underline{u} \cdot \underline{v}) q^\alpha|_\alpha \right] da.$$

The vector \underline{u} is constant and may be taken out of the integrals. This is written as:

$$\underline{u} \cdot \left[\oint_{\partial a} \underline{v} q^\alpha v_\alpha d\ell - \int_a \left(q^\alpha \frac{\partial \underline{v}}{\partial x^\alpha} + \underline{v} q^\alpha|_\alpha \right) da \right] = 0.$$

Inasmuch as the constant vector \underline{u} is arbitrary, the vector in brackets must be zero. The first modified form of the divergence theorem is then

$$\oint_{\partial a} \underline{v} q^\alpha v_\alpha d\ell = \int_a \left(q^\alpha \frac{\partial \underline{v}}{\partial x^\alpha} + \underline{v} q^\alpha|_\alpha \right) da. \quad (A.2)$$

The second form of the divergence theorem uses the vector $\underline{u} \cdot (\underline{p} \times N^{\beta\alpha} \underline{a}_\beta) \underline{a}_\alpha$, or, more correctly, the α^{th} component of this vector. Equation A.1 is written then as

$$\oint_{\partial a} \underline{u} \cdot (\underline{p} \times \underline{a}_\beta N^{\beta\alpha}) \underline{v}_\alpha d\ell = \int_a \left[\underline{u} \cdot (\underline{p} \times \underline{a}_\beta N^{\beta\alpha}) \right] \Big|_\alpha da$$

$$= \int_a \underline{u} \cdot \left[\frac{\partial}{\partial x^\alpha} (\underline{p} \times \underline{a}_\beta N^{\beta\alpha}) + \left\{ \frac{\alpha}{\alpha\gamma} \right\} (\underline{p} \times \underline{a}_\beta N^{\beta\gamma}) \right] da.$$

The vector \underline{u} is again noted to be constant so that it can be taken outside the integrals and noted to be arbitrary so that the intermediate statement is:

$$\oint_{\partial a} \underline{p} \times \underline{a}_\beta N^{\beta\alpha} \underline{v}_\alpha d\ell = \int_a \left[\frac{\partial \underline{p}}{\partial x^\alpha} \times \underline{a}_\beta N^{\beta\alpha} + \underline{p} \times \left\{ \frac{\gamma}{\alpha\beta} \right\} \underline{a}_\gamma N^{\beta\alpha} \right.$$

$$\left. + \underline{p} \times \left\{ \frac{3}{\alpha\beta} \right\} \underline{a}_\beta N^{\beta\alpha} + \underline{p} \times \underline{a}_\beta \frac{\partial N^{\beta\alpha}}{\partial x^\alpha} + \left\{ \frac{\alpha}{\alpha\gamma} \right\} (\underline{p} \times \underline{a}_\beta N^{\beta\gamma}) \right] da.$$

The Christoffel symbols are combined into the covariant partial derivative of $N^{\beta\alpha}$. The final result is then

$$\oint_{\partial a} \underline{p} \times \underline{a}_\beta N^{\beta\alpha} \underline{v}_\alpha d\ell = \int_a \left[\frac{\partial \underline{p}}{\partial x^\alpha} \times \underline{a}_\beta N^{\beta\alpha} + \underline{p} \times \underline{a}_\beta N^{\beta\alpha} \Big|_\alpha + \underline{p} \times \underline{a}_\beta N^{\beta\alpha} B_{\alpha\beta} \right] da, \quad (A.3)$$

where $B_{\alpha\beta}$ denotes the components of the deformed surface curvature tensor.

A simplified form of Equation A.3 is obtained in a similar manner. The derivation is omitted, since it follows the above method. The result is simply:

$$\int_{\partial a} N^{\beta\alpha} \tilde{a}_{\beta} v_{\alpha} d\ell = \int_a \left(N^{\beta\alpha}|_{\alpha} \tilde{a}_{\beta} + N^{\beta\alpha}{}_{\beta} \tilde{a}_{\alpha} \right) da. \quad (\text{A.4})$$

QUESTIONS AND COMMENTS FOLLOWING KRIEG'S PAPER

QUESTION: Would you give the number of time steps, the computer time, and the computer used in that last example involving the cone?

KRIEG: We had 289 meshes and we ran 750 time steps ($2 \mu s$) using a CDC 6600. The time for that was 412 central processor seconds. In addition to that, we required 30 seconds to initialize that tape and 146 peripheral processor seconds. So it's roughly a seven minute run.

MONTEITH: This plot routine is extremely fast and it automatically scales everything. You just give it the angle that you want to view from and you tell it how far away from it you want to be and that's the end of it. Actually, it is a three part routine consisting of input, calculation and the plot. These can be used independently. The plot routine package can also be taken and used for other programs which have similar inputs.

KRIEG: I might add that the CDC 6600 central processor time for the cone movie was about 400 seconds. The entire cost of the movie was about \$80.

QUESTION: I'd like to ask the author when his program is finished, will he be able to handle cutouts which do not lie along the coordinate axes?

KRIEG: Currently, it cannot. But we hope to provide a capability to locally distort the coordinate system to follow cutout boundaries in the area of a cutout in a shell of revolution. It certainly appears feasible to do this and my interior equations should do the job. But right now, I can't

initialize such a mesh, and have given the problem only a cursory examination.

QUESTION: I'm trying to determine where we now stand with the finite difference method and where we intend to go. Frank Brogan, could you tell me if STAGS can handle arbitrary cutouts?

BROGAN: The linear version of STAGS does handle cutouts that don't follow coordinate lines. We have not completed the work to add this feature to the nonlinear analysis but that should be completed by April 1971.

QUESTION: I'm still trying to recover from the short computer time you quoted in that cone example. Is your numerical integration scheme unconditionally stable? Let me put it another way: how does the time increment that you used compare to the period of the highest natural frequency of the system? Do you know?

KRIEG: The interaction scheme is conditionally stable with a critical time step of approximately $1/\pi$ times the highest frequency present. As I recall, for my meshwork, the critical time step was 3 or 4 microseconds. I was using 2 μ sec as suggested by Lockheed. I used a coarser meshwork than they suggested, however, because I didn't have room in my dimension statements.

QUESTION: You feel that you were carrying out a stable integration?

KRIEG: That's right. I might add that results obtained using a 1 μ sec time step were virtually identical with the 2 μ sec results.

QUESTION: Earlier you said that you distort the finite difference mesh to fit the boundaries of the cutout. Will you encounter serious difficulties then in defining the geometry of the shell subject to that mesh? What I mean by that is you may no longer have formulas that define the geometry of the shell in your coordinate system.

KRIEG: To be practical, the local distortion of the coordinate system would have to be internally generated. The important thing is that we have allowed for the use of such information. This coordinate system X_1 - X_2 is completely arbitrary. There's no limitations on it except continuity. And we calculate positions in the rectangular cartesian system Z_1 , Z_2 , Z_3 , so we always have the non-moving rectangular cartesian system to which quantities can be referred. And, if you'd like to convert the output to some other coordinate system, that would be done at print time.

QUESTION: Do you mean that the program contains a transformation which brings the known geometry into the distorted coordinate system that you use.

KRIEG: No, we simultaneously carry along two coordinate systems at every time step. We always know where every point is in the rectangular cartesian system and we actually find positions in the Z_1 , Z_2 , Z_3 coordinate system. In other words, we define geometry, curvatures, and all this sort of thing in the X_1 , X_2 surface coordinate system.

QUESTION: I'd like to get your opinion on two things. First of all, you use an explicit integration scheme and I would like to have your comments as to what you envision regarding the possibilities for some kind of an implicit scheme. Secondly, we've seen a finite difference approximation used by

Bushnell and Almroth with an energy formulation and then we've seen one like yours based on momentum formulation. Would you care to comment on the ultimate capability of both of these techniques for dynamic problems? By that I mean being able to handle realistic engineering structures, one with a number of discrete rings, reinforced cutouts and more or less arbitrary boundaries and shell wall construction.

KRIEG: With regard to your question on explicit and implicit time integration schemes, I spent some time looking for unconditionally stable time integrators. In particular, I wanted an explicit unconditionally stable time integrator. By explicit I mean only matrix multiplication and addition are required. I think I've proved that there isn't any if you use only positions at the present time step and up to three previous ones. That is why I stuck to the simplest explicit one. When you go to the higher order schemes, you begin to pick up strange modes which don't exist physically and which may or may not damp out. This occurs, for example, with some implicit schemes such as the Hubolt method. You have another mode so to speak and although it is very very highly damped you may be pouring energy into it; and I'm a little bit scared of energy absorbers in perfectly elastic problems. The solution technique for an implicit method would, of course, be much more involved than for an explicit method.

With regard to your second question, I think Bushnell's and Almroth's method is very good. I wasn't aware of it until now. It seems to be just a matter of development to get it to work dynamically. As far as the future of the thing, I think there are big advantages to having stiffness matrices which are symmetric and positive definite. My stiffness matrix

will not be symmetric. The numerical stability analyses that I have done assume a symmetric positive-definite matrix and I can only hope that my equations will behave accordingly. They have so far.

HUBKA: I have a few comments in summary. Bushnell and Almroth have described the BOSOR3 and STAGS computer codes. According to Yates, Vincent and Sable, yesterday, these codes are being used in the production and analysis of very complex shell structures. The correlation between theory and experiment in the limited cases that are presented is quite good. I don't think this says so much for the finite difference method, but I do think it says that the theory is formulated correctly and the applications are correct in an engineering sense. We've seen that the non-orthogonal variable finite difference mesh can be used. Up until this meeting, I think almost everyone thought that this was possibly an area where finite differences could not be used. That idea should be fairly well dissipated by now. One advantage of Bushnell's and Almroth's approach is that it uses matrix algebra extensively and this is well anchored in everyone's mind. I would say that these codes will be particularly useful in the study of post buckling behavior. Instead of having to go out in the post buckled region and find the solution by hit and miss procedures, one could take an approach which is similar to a modified Newton's approach or possibly the Koiter theory and expand the solution about those limit points and bifurcation points and get starting points on the post buckled solution right in the neighborhood of the critical point. This would, I believe, enhance the performance of these computer codes.

Krieg and Monteith have described the GRIVET computer code which can be

used for the transient response of shells of arbitrary shape. Their approach is significantly different than approaches that have been used in the past to do shell dynamics using finite differences. They've used the global equations of motion along with the convected Lagrangian coordinate system. Other codes that you might be familiar with such as PETROS, for example, used the convected Lagrangian incoordinate system but not the global type of integration approach. STAR which was developed here at Lockheed uses a Lagrangian approach without the convected coordinates and without the global integration as does SMERSH which is a code that I've been involved with. So, there are many different approaches right now to the calculation of dynamic response using finite differences and one of the research projects I believe should be performed in the future is to evaluate these different approaches. A more intensive study of mesh centering is also called for.

Roy Krieg showed that the velocity formulation tends to hold your solution accuracy for longer periods of time. This is also known as the incremental displacement approach which is used by other people and indeed that is an area where solutions can be improved over a long period of time. A final question I have, though, is whether the global or the convected coordinates approach to calculation tend to run up your computing time inordinately since in each time step you generally have to compute new Christoffel symbols and so forth for your equations of motion. In the Lagrangian finite deflection codes that do not use convected coordinates, this is not the case and I think you buy some time.

FESTRAN: SCOPE AND LIMITATIONS

by
Warren C. Gibson^{*}
and
Lucien A. Schmit, Jr.^{**}

presented at the
CONFERENCE ON
COMPUTER ORIENTED ANALYSIS OF SHELL STRUCTURES

at the
Lockheed Palo Alto Research Laboratory
Palo Alto, California
August 10-14, 1970

^{*}Graduate assistant, Case Western Reserve University, Cleveland, Ohio

^{**}Professor of Structures, Case Western Reserve University, Cleveland Ohio

ABSTRACT

A computer program, FESTRAN (for Finite Element STRuctural ANalysis) is described. The program predicts the static structural response of plate and shell type structures using the finite element displacement method. Geometrically nonlinear effects (due to finite displacements or instabilities) are incorporated directly into these elements. Rectangular or annular flat plate elements, cylindrical shell elements, and straight or curved stiffener elements are included. Either homogeneous or layered composite linearly elastic material is assumed. Problems are solved either by a matrix decomposition routine, or by direct minimization of the total potential energy.

Applications to test problems are discussed, including a pinched cylinder, an unbalanced layered composite strip under thermal load, and post-buckling behavior of a curved panel.

ACKNOWLEDGEMENT

The research reported in this paper was carried out at Case Western Reserve University under United States Air Force Contract Nos. AF 33(615)-3432 and F33615-69-C-1209, administered by the Air Force Flight Dynamics Laboratory, Wright-Patterson Air Force Base, Ohio. Dr. Laszlo Berke (FDTR) was the project engineer.

INTRODUCTION

This paper is concerned with the capabilities and limitations of a computer program, FESTRAN (for Finite Element STRuctural ANalysis). The program incorporates several kinds of four-sided plate and shell elements, representing linearly elastic structures, including both bending and stretching behavior, with some second-order terms retained in the strain-displacement relations. These nonlinear terms allow prediction of finite deflection and buckling behavior. A rectangular flat plate element, an annular sector flat plate element, a cylindrical shell element, and straight and curved stiffener elements are included, as shown in Figure 1. (More details on these elements can be found in References 1, 4, and 5.) Ordinary thin plate and shell theory with transverse shear deformations neglected, are used to form potential energy expressions for these elements in terms of independent coefficients (element degrees of freedom) which are values of the displacements and certain of their derivatives at the corners of the elements. Either homogeneous or layered composite materials may be represented. In the latter case equivalent homogeneous anisotropic stiffness coefficients are computed.

DISPLACEMENT FUNCTIONS

Products of cubic Hermite polynomials are used to form displacement functions. The transverse displacement w as a function of the co-ordinates x and y is

$$w(x,y) = \sum_{i=1}^2 \sum_{j=1}^2 \{ H_{01}(x) H_{01}(y) w_{ij} + H_{02}(x) H_{01}(y) w_{xij} + H_{01}(x) H_{02}(y) w_{yij} + H_{02}(x) H_{02}(y) w_{xyij} \} \quad (1)$$

There are sixteen element degrees of freedom representing w : w_{ij} , the values of w at corner (i,j) , the slopes w_{xij} and w_{yij} , and the twist curvatures w_{xyij} , all at corner (i,j) , where the corners are numbered $(1,1)$, $(1,2)$, $(2,2)$, and $(2,1)$, proceeding clockwise around the element from the origin of co-ordinates. The $H_{kl}(x$ or $y)$ are the osculatory Hermite polynomials

$$\begin{aligned} H_{01}(x) &= 1 - 3 \left(\frac{x}{a}\right)^2 + 2 \left(\frac{x}{a}\right)^3 \\ H_{02}(x) &= 3 \left(\frac{x}{a}\right)^2 - 2 \left(\frac{x}{a}\right)^3 \\ H_{11}(x) &= a \left\{ \left(\frac{x}{a}\right) - 2 \left(\frac{x}{a}\right)^2 + \left(\frac{x}{a}\right)^3 \right\} \\ H_{12}(x) &= a \left\{ -\left(\frac{x}{a}\right)^2 + \left(\frac{x}{a}\right)^3 \right\} \end{aligned} \quad (2)$$

where $0 \leq x \leq a =$ length of the $y=\text{constant}$ side (substitute b , the

length of the $x=\text{constant}$ side for $H_{kl}(y)$).

This type of function is complete in that it contains all products $x^i y^j$ for $i, j = 0$ to 4 , and in that all rigid-body and constant-strain displacement modes are included (except for the cylindrical shell and annular plate elements, in which some of these modes are closely approximated). Such functions make it easy to impose continuity of displacements and rotations across element boundaries (conditions necessary for convergence of the potential energy as the element grid is refined) by simply matching element degrees of freedom at corners bounding edges where elements meet. Also, after these necessary conditions have been imposed, enough degrees of freedom are left over to allow imposition of inter-element curvature continuity when appropriate. The same functions, with sixteen degrees of freedom, are used for both of the in-plane displacements u and v (making a total of 48 degrees of freedom per element). Continuity of u and v , and optional continuity of in-plane strains, are also achieved by matching degrees of freedom at corners. Bi-linear interpolation of u and v might seem more appropriate than bi-cubic interpolation since only first derivatives of u and v appear in the energy expression, while second derivatives of w appear. Bi-cubic interpolation is nevertheless used so that elements may be joined at right angles or at arbitrary acute angles, in which case w displacements in one element must be matched with u or v displacements in another, so that u , v , and w must all use the same interpolation functions.

POTENTIAL ENERGY FORMULATION

The potential energy formulation begins with Hooke's law relating stresses σ_i to strains ϵ_j and the temperature rise ΔT for a plane anisotropic material:

$$\sigma_i = \sum_{j=1}^3 E_{ij} \epsilon_j - Q_i \Delta T, \quad i = 1, 2, 3 \quad (3)$$

and the following nonlinear strain-displacement relations for a thin plate or cylinder:

$$\begin{aligned} \epsilon_1 = \epsilon_x &= \frac{\partial u}{\partial x} + \frac{1}{2} \left(\frac{\partial w}{\partial x} \right)^2 - z \frac{\partial^2 w}{\partial x^2} \\ \epsilon_2 = \epsilon_y &= \frac{\partial v}{\partial y} + \frac{w}{R} + \frac{1}{2} \left(\frac{\partial w}{\partial y} \right)^2 - z \left(\frac{\partial^2 w}{\partial y^2} - \frac{1}{R} \frac{\partial v}{\partial y} \right) \\ \epsilon_3 = \gamma_{xy} &= \frac{\partial u}{\partial y} + \frac{\partial v}{\partial x} + \frac{\partial w}{\partial x} \frac{\partial w}{\partial y} - 2z \left(\frac{\partial^2 w}{\partial x \partial y} - \frac{1}{R} \frac{\partial v}{\partial x} \right) \end{aligned} \quad (4)$$

to obtain the strain energy for an element in terms of displacements from

$$\pi_p = \int_{vol} \sum_{i=1}^3 \sigma_i d\epsilon_i \quad (5)$$

After the potential energy has been formed by substituting Equations (3) and (4) into (5) and carrying out the integration through the depth of the element, stiffness matrices are formed by substituting the assumed displacement modes (Equation 1) into this expression and integrating. This process is carried out automatically during the

setup phase of FESTRAN, using exact formulas for polynomial integration, rather than a numerical method. The results are packed into matrices $\tilde{K}^{(i)}$ in such a way as to minimize storage requirements. If the 48 degrees of freedom are denoted by a vector $\tilde{X}_j^{(i)}$, a concatenation of three vectors $\tilde{U}_j^{(i)}$, $\tilde{V}_j^{(i)}$, and $\tilde{W}_j^{(i)}$, each of length 16, containing the u, v, and w variables respectively, then the potential energy for element i is expressed as

$$\begin{aligned}
 \pi_p = & \sum_{j=1}^{48} \tilde{K}_j^{(1i)} \tilde{X}_j^{(i)} \\
 & + \sum_{j=1}^{48} \sum_{k=1}^j \tilde{K}_{jk}^{(2i)} \tilde{X}_j^{(i)} \tilde{X}_k^{(i)} \\
 & + \sum_{j=1}^{16} \sum_{k=1}^{16} \sum_{\ell=1}^k \tilde{K}_{jk\ell}^{(3ui)} \tilde{U}_j^{(i)} \tilde{W}_k^{(i)} \tilde{W}_\ell^{(i)} \\
 & + \sum_{j=1}^{16} \sum_{k=1}^{16} \sum_{\ell=1}^k \tilde{K}_{jk\ell}^{(3vi)} \tilde{V}_j^{(i)} \tilde{W}_k^{(i)} \tilde{W}_\ell^{(i)} \\
 & + \sum_{j=1}^{16} \sum_{k=1}^j \sum_{\ell=1}^k \tilde{K}_{jk\ell}^{(3wi)} \tilde{W}_j^{(i)} \tilde{W}_k^{(i)} \tilde{W}_\ell^{(i)} \\
 & + \sum_{j=1}^{16} \sum_{k=1}^j \sum_{\ell=1}^k \sum_{m=1}^\ell \tilde{K}_{jk\ell m}^{(4i)} \tilde{W}_j^{(i)} \tilde{W}_k^{(i)} \tilde{W}_\ell^{(i)} \tilde{W}_m^{(i)} \quad (6)
 \end{aligned}$$

Here $\tilde{K}_j^{(1i)}$ represents linear terms (due to thermal loads), $\tilde{K}_{jk}^{(2i)}$ represents ordinary quadratic stiffness terms, $\tilde{K}_{jk\ell}^{(3ui)}$ and

$\tilde{K}_{jkl}^{(3vi)}$ are cubic uw^2 and vw^2 terms, and $\tilde{K}_{jkl}^{(3wi)}$ and $\tilde{K}_{jklm}^{(4i)}$ represent w^3 and w^4 terms in the strain energy expression.

EQUALITY CONSTRAINTS

With most finite element methods, a set of independent degrees of freedom is constructed by matching corner variables wherever two elements meet. In the present method, linear constraint equations are generated in addition to one-to-one matchings among the corner variables. Such equations arise from four sources:

(1) Elements may be joined at arbitrary angles, so that, for example, the transverse displacements on one edge of one element must be expressed as a linear combination of the transverse and in-plane displacements of the other.

(2) Curvature continuity between elements is an optional additional condition (first pursued by Stanton, Reference 3) which results in linear equality constraints. Whenever curvatures are matched between two elements, four equations are generated which involve contributions from all four corners of each of the two elements. This option serves to reduce the number of independent degrees of freedom (and thus the running times), and to insure continuity of bending moments between elements in some cases. Overall results are generally not degraded, and they are sometimes improved by this procedure.

(3) Force boundary conditions are also an optional additional condition which serve to reduce the number of degrees of freedom, usually without any deterioration of results.

(4) Skew displacement boundary conditions, wherein an edge of a plate may be required to slide along an inclined surface, for example, are a fourth source of equality constraints which sometimes arise.

Equality constraints may contain constant terms which arise from non-zero prescribed boundary values (displacements or forces). These values may be prescribed as simple constants, or as user-defined symbols. Values are not assigned to these symbols until after the setup phase of FESTRAN is complete, so that solutions may be obtained for various values of these symbols without regeneration of stiffness matrices or load vectors (mechanical or thermal loads may also be prescribed in terms of user-defined symbols). User-defined symbols are concatenated onto the end of the solution vector X_m and are kept constant during the solution process.

Once the required equality constraints have been determined for a particular job, they are then processed in three stages:

First, the one-to-one constraints are resolved in the normal manner: by assigning the same degree-of-freedom number to each of the variables.

Second, the one-to-many constraints are handled by assigning to the variable on the left-hand side a pointer locating a "correlation packet" in a storage pool, in which the coefficients and degree-of-freedom numbers and/or symbol numbers are recorded. Thus, if $\tilde{x}_j^{(i)}$, the j^{th} of 43 element degrees of freedom for element i is related to m_{ij} of the master (independent) degrees of freedom and/or

user-defined symbols X_m by

$$\tilde{X}_j(i) = \sum_{\mu=1}^{m_{ij}} \alpha_{ij\mu} X_{l_{ij\mu}} \quad (7)$$

then the correlation packet for this element degree of freedom consists of two lists: the master degree-of-freedom numbers $l_{ij\mu}$ and the coefficients $\alpha_{ij\mu}$.

Third, the many-to-many coupled constraint equations are set up in matrix form and processed by Gauss elimination, using a pivotal selection scheme to choose the variables to be eliminated. Then the newly dependent variables are expressed in terms of the remaining independent variables and/or user-defined symbols, by means of the packet scheme described above. Finally, any previous packets containing references to the newly dependent variables are patched up so that they refer only to independent variables and user-defined symbols.

SOLUTION METHODS

Solutions are carried out by either of two means:

First, a matrix decomposition routine with forward and backward substitution (Reference 6) is available for linear solutions (second-order terms in Equations 4 dropped). This routine uses the "wavefront" method of packing the master stiffness matrix so as to eliminate needless storage and processing of zeroes. The master stiffness matrix is formed directly from the element stiffness matrices by examination of the correlation packets for each element

degree of freedom. The (j,k) element stiffness matrix entry for element i is distributed to the master stiffness matrix by getting row numbers and multipliers from the i,j^{th} correlation packet and master column numbers and multipliers from the i,k^{th} correlation packet. In symbols, each master stiffness matrix entry K_{mn} is formed by

$$K_{mn} = \sum \alpha_{ij\mu} \alpha_{ik\nu} \tilde{K}_{jk}^{(i)} \quad (8)$$

summed over all i,j,k, μ , ν for which $\alpha_{ij\mu} = m$ and $\alpha_{ik\nu} = n$.

Second, a function minimization routine comprising both the variable metric (Davidon-Fletcher-Powell, Reference 8) and conjugate gradient (Fletcher-Reeves, Reference 9) methods can be employed for direct minimization of the total potential energy for either linear or nonlinear problems. The total potential energy is formed by summing the element potentials, using element stiffness matrices, and adding a load potential term. Minimization is the only means provided for solving nonlinear problems. Linear problems may be solved by minimization, but decomposition always turns out to be more efficient.

EXAMPLE PROBLEMS

(1) A 1" by 8" strip, 0.08" thick composed of a layer of aluminum bonded to eight layers of boron composite material was modeled by FESTRAN elements so that warping due to cooling of the material from the bonding temperature down to room temperature might

be studied. The boron composite plies were each .0052" thick and had fibers oriented at 60° , 0° , -60° , 0° , 0° , -60° , 0° , and 60° from the long direction, and the aluminum layer was .04" thick. The results obtained are shown in Figure 2 and are compared with experimental results and with a bimetallic strip analysis given in Reference 10. Both the FESTRAN results and the simple bimetallic strip theory are seen to correlate well with the experimental results.

(2) A closed aluminum cylindrical shell 10.35" long, 0.094" thick, with a 4.953" radius, pinched by self-equilibrating loads (Figure 3) was analyzed, and the results compared with experiment (Reference 11) and with an inextensional shell theory analysis given by Timoshenko (Reference 7). Because of symmetry only one octant was modelled. Both eight-element and four-element models were run, using cylindrical shell elements (the eight-element modelling is shown in Figure 3). Additional runs were made with flat plate elements joined at angles of 22.5° (eight elements) and 45° (four elements) in an attempt to study the additional error incurred in this problem by using flat plate elements to model a curved structure. Figure 4 shows a comparison of the four-element displacement results, along the arc ABCDE (see Figure 3). Surprisingly, the flat model correlates better with Timoshenko's results than does the curved model (although it is no closer to the experimental data points). The error resulting from the use of flat elements in this case seems to be on the excess-flexibility side, thus cancelling out some of the artificial stiffness generally

inherent in finite elements formulated in terms of displacements. Both eight-element models correlated almost exactly with the inextensional solution.

Figure 5 shows circumferential bending moment results for the flat and curved eight-element models, again compared with the inextensional shell theory analysis. The results are somewhat cruder since the bending moments depend on second derivatives of the approximate displacement functions.

(3) A curved panel is shown in Figure 6, mounted in a rigid frame, with a force applied to one end through a rigid sliding block. The panel is steel, 24" square and 0.1" thick, with a camber of 0.48". Its edges are considered simply supported all around. One quarter of the panel was modelled by four elements, restricting this study to doubly symmetric buckling shapes. Again, both curved and flat elements were used. As the load versus end-shortening curve in Figure 7 shows, the responses of the two models were identical in the initial linear regime, but differed considerably after buckling.

It is not clear whether the use of flat elements in this case introduces excess stiffness or flexibility. The ridges formed where the elements are joined act like stiffeners, but between these ridges the coupling stiffness present in curved elements is lacking. While there is no experimental data to corroborate the results obtained, at least it is clear that the use of flat elements, even though they are joined at angles of only 2.26° , produces results which are quite different from those predicted by the curved-element

simulation.

CONCLUSIONS

The FESTRAN program contains elements with advantages not found in some other programs: conformity of displacements and rotations between elements is assured in all cases; rigid-body and constant-strain displacement modes are well represented; elements may be joined at arbitrary angles; curvature continuity, strain continuity, and force boundary conditions can be optionally imposed; laminated materials with full bending-stretching coupling can be handled; and geometrically nonlinear effects are treated in a straightforward manner. An efficient decomposition routine and a reliable minimizer are included. Application of the program to test problems has shown good correlation with experimental and analytical results in several cases.

There are serious limitations, though: all elements are four-sided whereas triangular elements are much more versatile. Forty-eight degrees of freedom per element are a lot, although the total for a structure can be cut down by equality constraints. Storage requirements and consequently running times for nonlinear problems can be quite high.

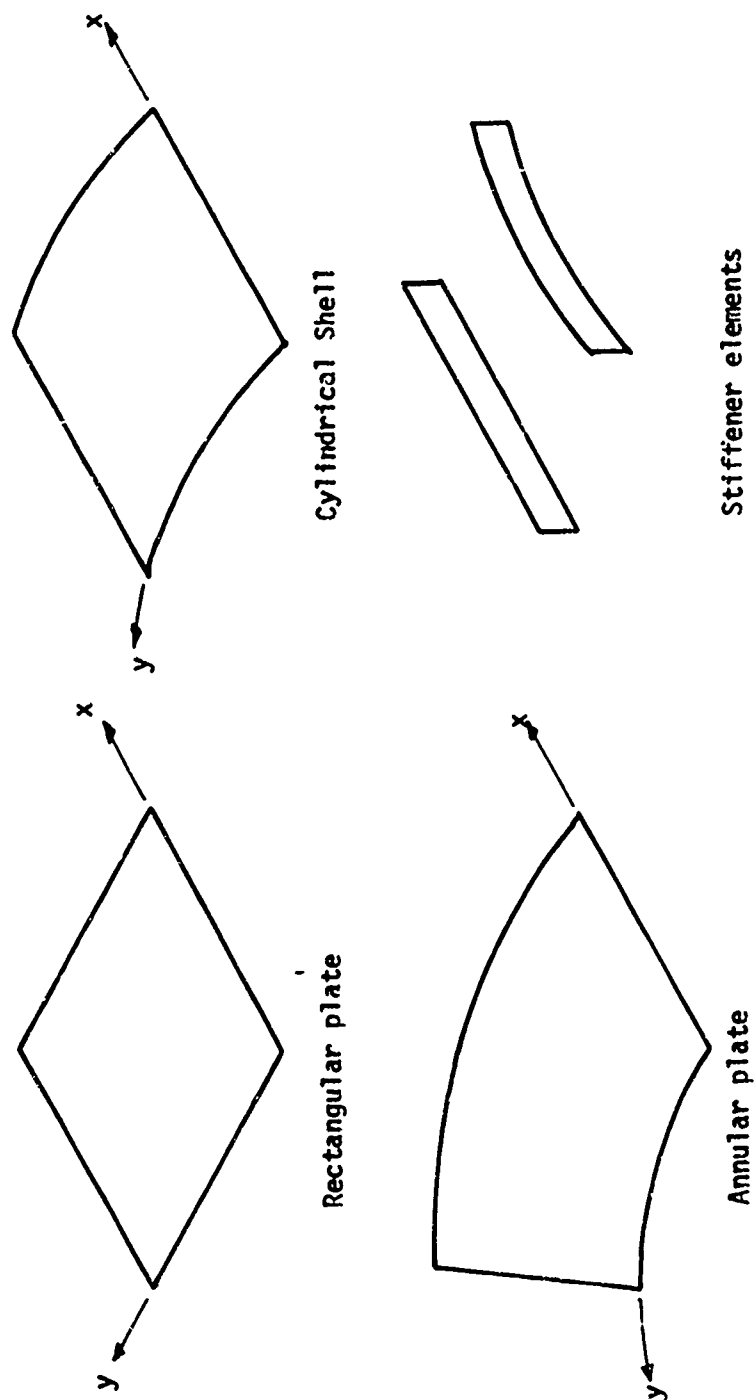


Figure 1. FEM Finite Elements

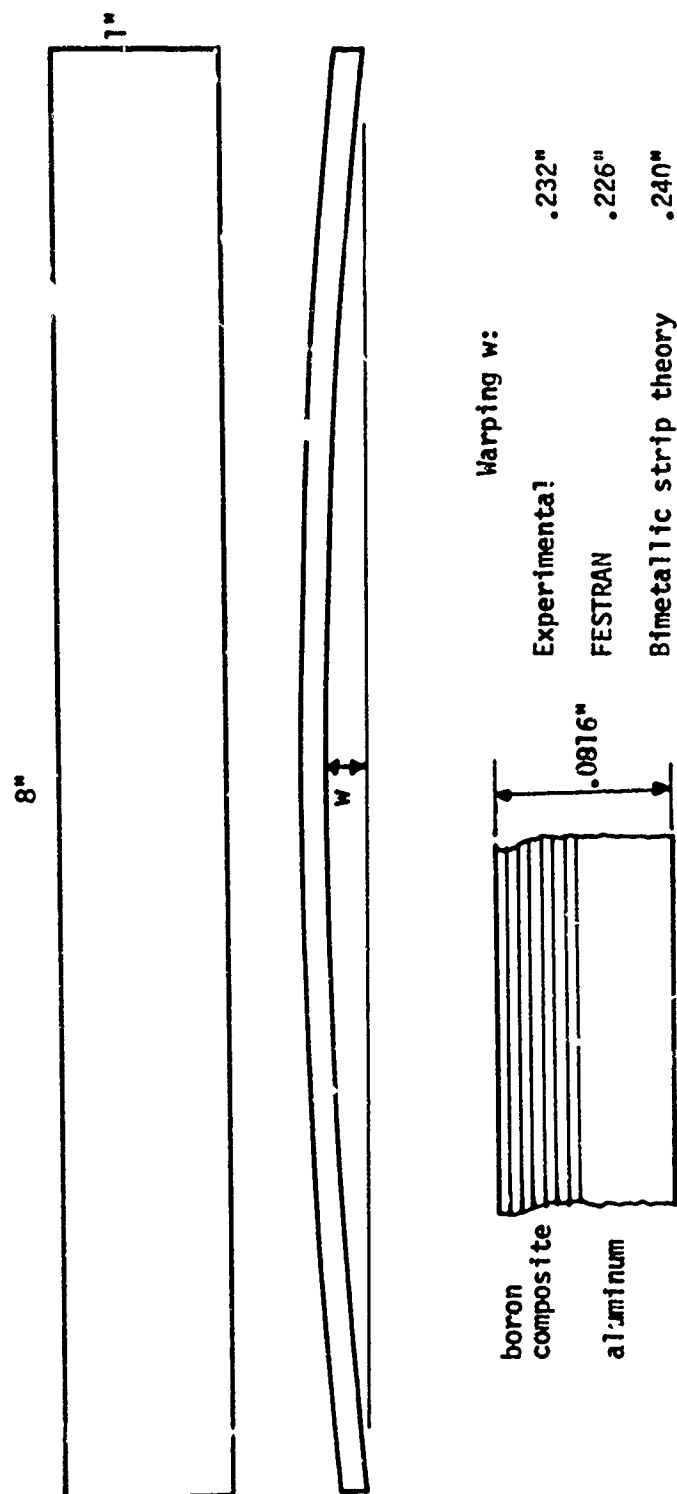


Figure 2. Thin strip under thermal load

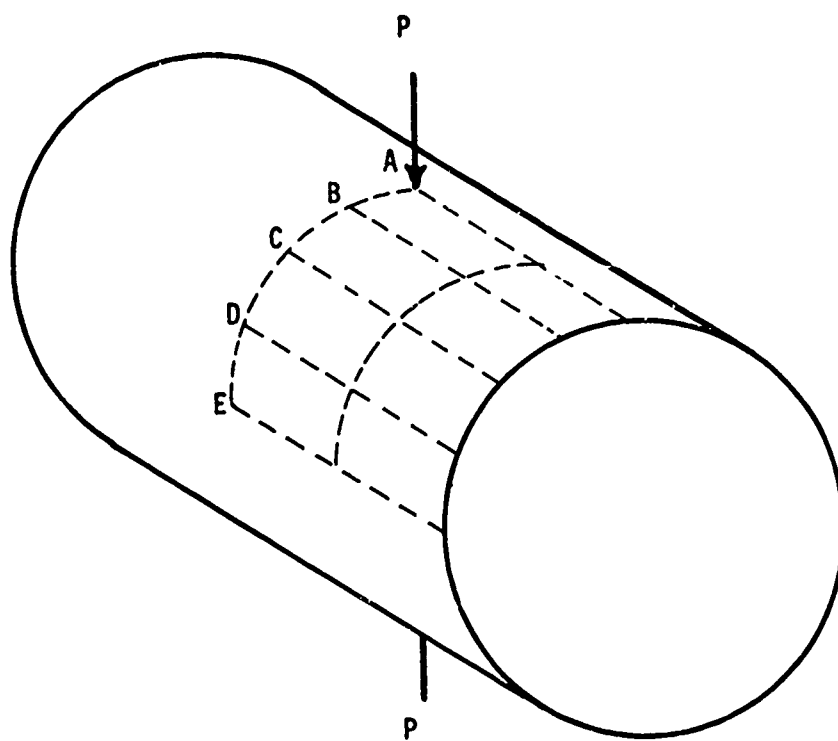


Figure 3. Pinched cylinder

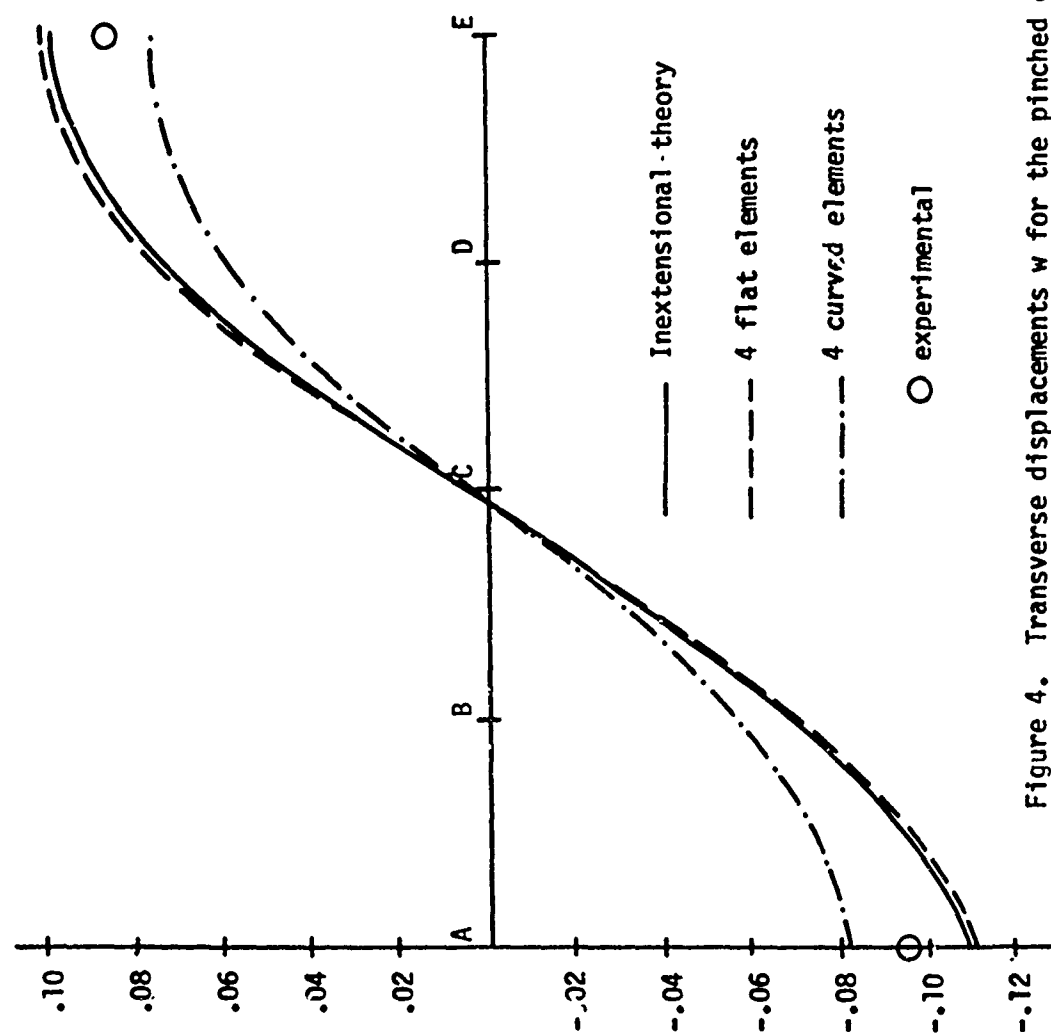


Figure 4. Transverse displacements w for the pinched cylinder

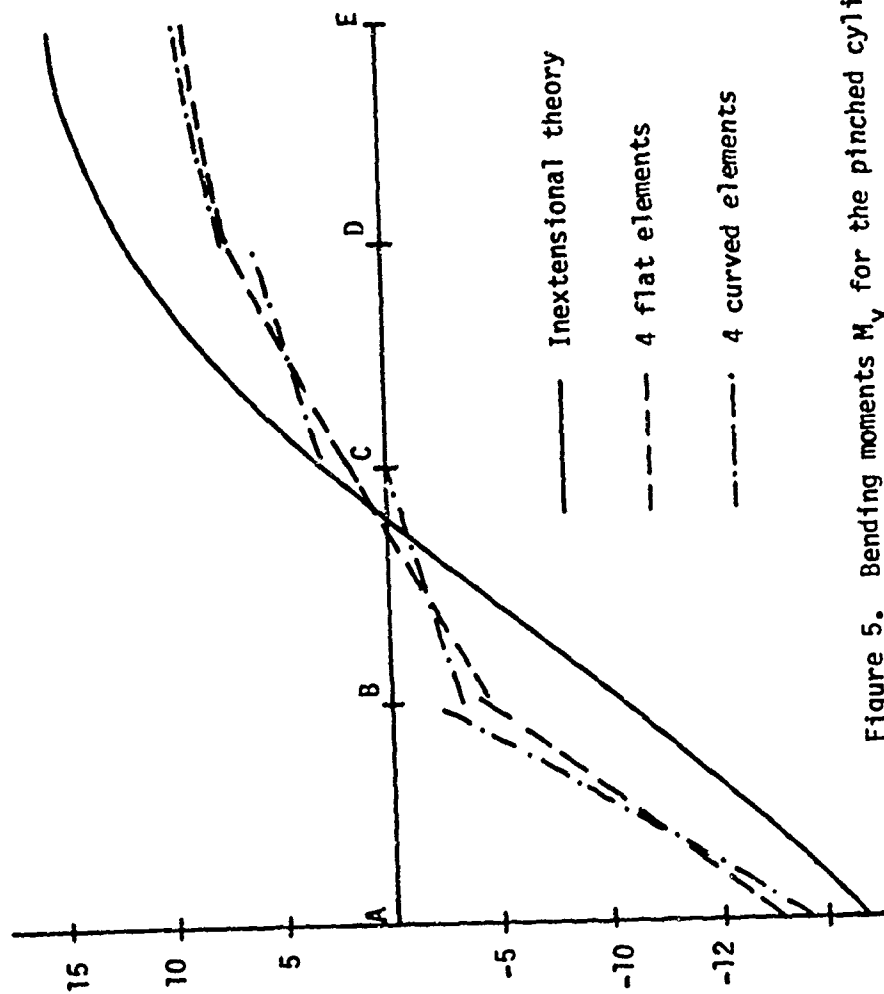


Figure 5. Bending moments M_y for the pinched cylinder

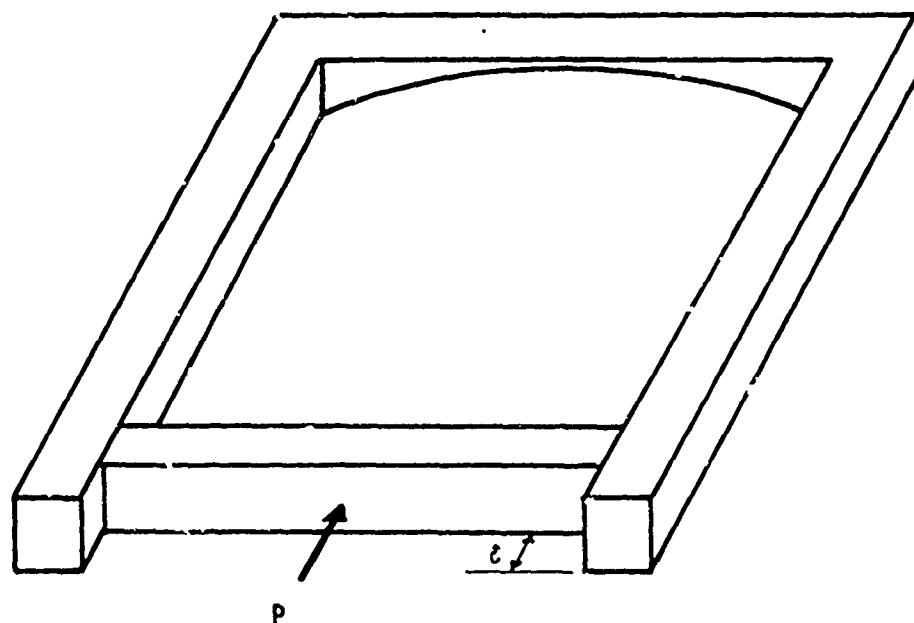


Figure 6. Curved panel

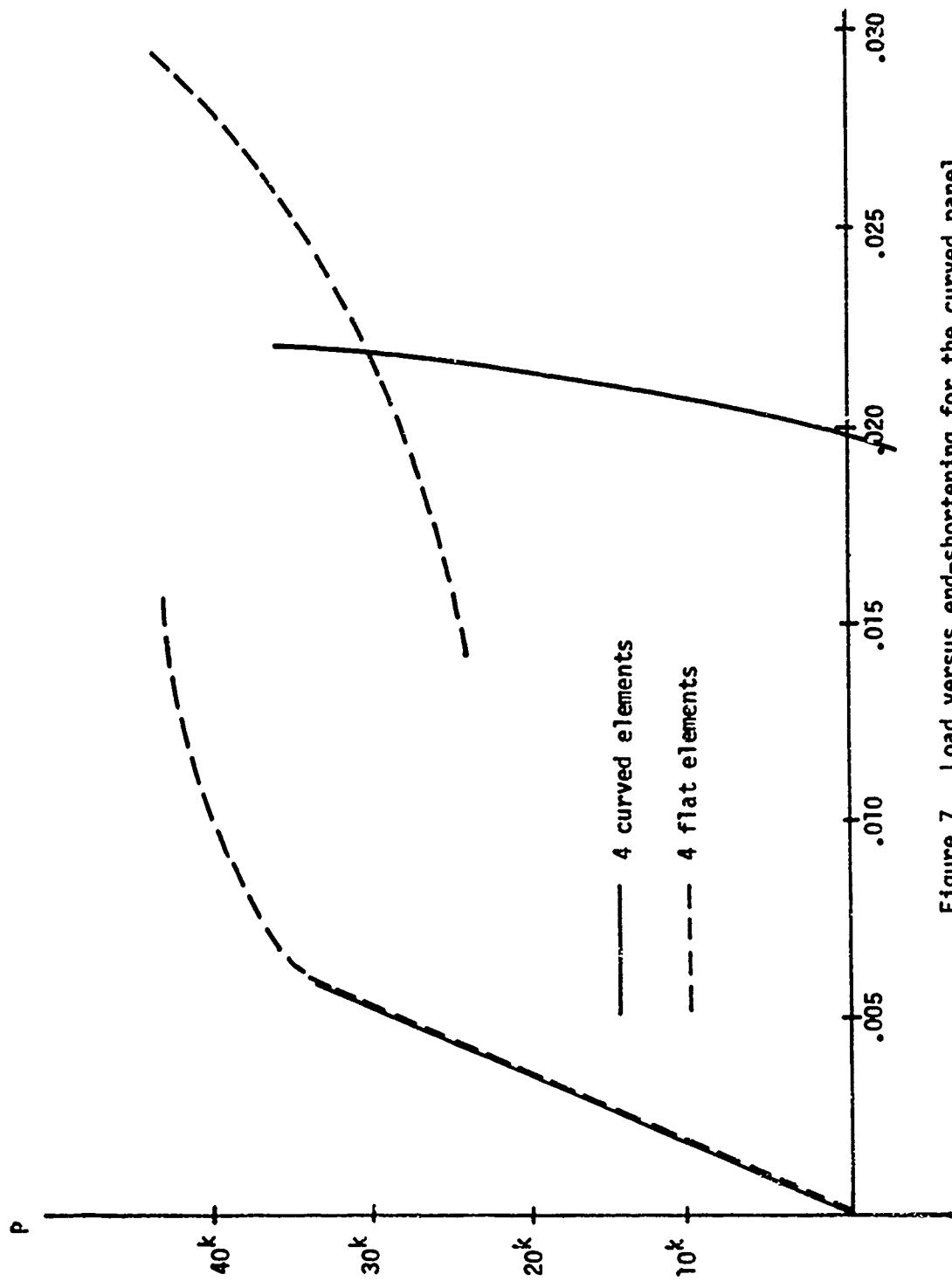


Figure 7. Load versus end-shortening for the curved panel

REFERENCES

1. Bogner, F. K., Finite Deflection Discrete Element Analysis of Shells, AFFDL TR-67-185, June 1968.
2. Case Western Reserve University, SMSMD Div., Developments in Discrete Element Finite Deflection Structural Analysis by Function Minimization, AFFDL TR-68-126, September 1968.
3. Stanton, E. L., A Discrete Element Analysis of Elastoplastic Plates by Energy Minimization, Report No. 27, SMSMD Div., Case Western Reserve University, October 1968.
4. Gibson, W. C., Finite Element Analysis of Flat Plates in Polar Co-ordinates, Report No. 34, SMSMD Div., Case Western Reserve University, June 1969.
5. Monforton, G. R., Discrete Element Finite Displacement Analysis of Anisotropic Sandwich Shells Report No. 39, SMSMD Div., Case Western Reserve University, January 1970.
6. Melosh, R. J. And R. M. Bamford, "Efficient Solution of Load-Deflection Equations", J. Struct. Div. Asce, 95(ST4): 661-676 (1969).
7. Timoshenko, S. P. And S. Woinowsky-Krieger, Theory of Plates and Shells, Second Edition, McGraw-Hill Book Co., New York, 1961.
8. Fletcher, R. and M. J. D. Powell, "A Rapidly Convergent Descent Method for Minimization", Computer Journal, 6: 163-168 (1963).
9. Fletcher, R. and C. M. Reeves, "Function Minimization by Conjugate Gradients", Computer Journal, 7: 163-168 (1964).

10. Petit, P. H., Lockheed-Georgia Co., private communication, 1969.
11. Guyan, R. J., A Study of the Effectiveness of the Stiffness Method of Structural Analysis in Selected Applications, Ph.D. Thesis, Case Institute of Technology, 1964.

QUESTIONS AND COMMENTS FOLLOWING GIBSON'S PAPER

COMMENT: I'm really surprised at the curved element results for the pinched cylinder. We've run the same problem with lower order curved elements and I think our results are much better than yours, compared to Timoshenko. It's a bit surprising.

GIBSON: That surprises me too.

COMMENT: I'd like to say something more about that pinched cylinder problem. The curved shell element does give you the Timoshenko solution as you add more elements to the grid. I think maybe you might have given the impression with that one grid solution that it might not come up to it, but it does come up to it very nicely and I think Fred Bogner has those results in a couple of his papers

QUESTION: I'd like to speak in support of the author's summary about the compatability or incompatibility of flat elements when you have non-coplanar intersections; specifically right angle intersections. It's been my experience in developing a cubic bending-cubic membrane element that unless you include the shear deformation you cannot prove compatability of these elements which have equal membrane and equal bending displacement fields along the edge. The influence of the membrane shear strain on the membrane displacement derivative leads to incompatibility with the Kirchhoff assumption of the plate bending on the perpendicular element and I was wondering if anybody else could comment.

GIBSON: Are you talking about transverse shear deformations?

COMMENT: Transverse shear deformations in the plate element. Unless you include that I don't think you can get compatability.

GIBSON: If you simply look at the expressions for u , v and w in our element and evaluate them along those edges you will find that you do get the same expressions for the two displacement fields provided the degrees of freedom in the corners are matched up.

QUESTION: You mentioned that you use Melosh's front solution technique. Do you have any experience in comparing it to other techniques? Can you quantify your statements comparing solution times, storage requirements and so forth?

GIBSON: All I can say is it's a lot better than just the standard full matrix procedure and it's better than any constant bandwidth method in problems where there's quite a bit of scattering of the sparseness in the stiffness matrix.

QUESTION: I have a brief question concerning extensions of these minimization procedures to dynamics problems. Have you given any consideration to such extensions or any problems where you don't have a positive definite operator?

GIBSON: Yes, as a thesis topic at Case, direct minimization of the Rayleigh quotient has been used as a means of obtaining eigenvectors and eigenvalues.

QUESTION: Well, I think in principle the procedure could be

applied to virtually any type of operator and I was wondering if you knew of any work that had attempted to do this.

GIBSON: I don't know of anything beyond that one example of the Rayleigh quotient.

COMMENT: I have one negative example, but it did not involve a positive definite system. A number of years ago we did some work on mixed formulation using a Reissner energy formulation of the problem in which we used stresses and displacements as the variables along the same lines as Professor Herrmann's work. We tried to use a minimization on this and found that since the Reissner energy is not positive definite, you can't do it by minimization. We then had recourse to formulating the problem using residual, that is, taking basically the equations governing the system, using the sum of the squares forming this and then attempting to minimize it. This didn't prove to be, as you might well imagine, a very efficient scheme. We did it without scaling the variables at that time and I think it would work somewhat better if you scaled the variables as is done routinely today in connection with mixed formulations. I still have my doubts about whether or not this scheme would be competitive, in terms of competitive efficiency. It certainly would be a viable scheme if you used scaling and a residual formulation. But a direct attack on the energy for a non-positive definite formulation is clearly not possible using minimization algorithms.

COMMENT: But you could use it as an extra problem rather than a minimization problem. I mean certainly the basic philosophy of the conjugate gradient has been extended to arbitrary operators, at least theoretic-

cally. So, in principle, it still may work even for non-positive definite operators.

COMMENT: I want to continue with the discussion of intersection of shells. The assumptions that you make in your shell theory probably already tell you that you cannot have any rotation that's normal to the shell; so when you join two cylinders you should be taking this condition into account. Due to some other experience I've had I would never advise anybody to analyze intersecting shells using shell theory. Especially if you are worried about the stresses at the intersection.

GIBSON: Well, we don't have a very wide variety of elements at present in this program, so there are not too many intersecting shell type problems that we could do. About the only one would be where a cylinder connects up with a flat plate. In that case as far as I can see there would be no problem.

COMMENT: I'm implying there are certain implied conditions in the shell theory that say you've got to take into account the fact that you have no normal rotation throughout the shell.

Nonlinear Material and Geometric Behavior of Shell Structures

by

G. A. Dupuis, H. D. Hibbitt, S. F. McHamara and P. V. Marcal
Division of Engineering, Brown University, Providence, R. I. 02912

Abstract

The nonlinear analysis of shell structures is studied by both the Eulerian and the Lagrangian approach. Current methods are discussed on the basis of both formulations. It is found that the widely used updated procedure is a combination of both approaches. From the current standpoint it makes use of a mixture of incremental stiffnesses derived by both approaches. The 'bowing' effect was found to be the main source of error in this updated procedure, and this effect was shown to be negligible when a large number of elements were used. Case studies investigate various aspects of the nonlinear behavior of arches, axisymmetric shells of revolution, flat plates, and arbitrary shells.

Paper presented at the
joint Lockheed Company and Air Force Flight Dynamics Laboratory
Conference on
"Computer Oriented Analysis of Shell Structures"
Palo Alto, California

Reproduction in whole or in part is permitted for any purpose
of the United States Government.

Introduction and Review of Literature

The development of nonlinear finite element analysis of shells has been a part of the general progress in the development of the finite element method for both linear and nonlinear problems. It has both benefited from and stimulated further developments in finite element theory and analysis. Recent progress in this area has been mainly in the displacement method of finite element analysis. We shall therefore concentrate our attention in this area. In order to follow the progress in this area we first trace the separate development of nonlinear analysis for material behavior. This has taken a clearly defined path since the early papers on the tangent modulus method by Pope [1], Swedlow and Yang [2], Marcal and King [3], and the initial strain method by Gallagher et. al. [4], Argyris et. al. [5], Jensen et. al. [6]. A linear incremental stress strain relation can be developed, and both the tangent modulus and initial strain method can be seen to be close together as shown by papers by Marcal [7] and Zienkiewicz et. al. [8]. There is general agreement that both methods produce equally good results as evidenced by the recent works using either method. (Furner et. al. [9], Kamel et. al. [10]) The differences can be summed up as differences in development of techniques for solving the same nonlinear problems in a number of piecewise linear steps.

Much progress has been made in the nonlinear geometric problem. Here the earlier papers were based on a physical and intuitive approach to the problem, gradually transferring to a firmer base by drawing on the energy theorems. This is in accord with developments in other areas of finite element analysis. Thus, from the earlier paper of Furner et. al. [11] and Argyris [12] we see a gradual transference to energy approaches in papers by Gallagher et. al. [13], Hartz and Kapur [14], and Martin [15]. More recently, the dependence of nonlinear geometric analysis on the methods of continuum mechanics have been brought out by Wissman [16], Besseling [17], Oden [18], Popov and Yaghmai [19], and Hibbitt et. al. [20]. In this area there is less overall agreement on general procedures and methods. Like nonlinear material analysis, preferences have developed on placing the nonlinearity either on the left hand or the right hand side of the equation. We do not refer to the choice of solution method but we do refer to the choice of retaining one or more stiffness matrices in the analysis. The problem is somewhat clouded by the adoption either of an updating or nonupdating procedure in time, i.e. by either an Eulerian (current coordinates) or a Lagrangian (initial coordinates) point of view.

In this paper we shall follow both approaches in order to understand more fully the relevance of each of the incremental stiffness terms. We restrict our attention to static analysis of large displacement small strain problems, since it is this area which has been well studied in the literature.

Before we leave the area of shell analysis we should note the progress in the development of compatible shell and plate elements. The understanding and analysis of these shell elements has stimulated the viewing of the finite element method as part of continuum mechanics and energy theorems since it was in shell problems that the importance of compatibility of displacements and rigid body motion was brought out. In the class of compatible elements we have the piecewise function method of De Veubeke [21], the isoparametric methods of Ergatoudis [22], the Hermitian polynomials of Bognor, et. al. [23], and also the rational polynomial functions of Goel and Dupuis [24]. Superimposed on all this we have the isoparametric procedures which allow the distortion of shell elements to any arbitrary shell surface. More recently Ahmad et. al. [25] have approached the shell analysis problem by degenerating a full three-dimensional element in one of its coordinate directions. Finally we mention the development of general purpose programs which have allowed the pyramiding of previous development in finite element analysis (see Melosh et. al. [26], and Marcal [27]). This has led to an easy combination of both the nonlinear material and geometric methods together with the developed compatible shell elements which provide a valuable tool for shell analysis. Because of the broader use of these general purpose programs it is easy to justify the development of special procedures for tying nodal points and degrees of freedom together and this has allowed the combined analysis with shell and solid elements. This is particularly important at intersection areas such as those studied by Hibbitt and Marcal. [28]

Theoretical Considerations

In this section we summarize the essential components of a finite element analysis by the matrix displacement method. We develop our formulation simultaneously on both an Eulerian (current coordinate x) and a Lagrangian (initial coordinate X) basis. We shall first develop our equations in global coordinates and then show the simplifications that can be achieved by working in local coordinates.

We first select a conforming displacement function for an increment of displacement $\{du\}$

$$\{du\} = [f(x \text{ or } X)] \{da\} \quad (1)$$

where a are the undertermined coefficients.

$[f]$ is a function of position in the element and is shown as a function of x or X depending on the formulation axis.

d is a prefix denoting an increment of the quantity.

The undetermined coefficients are related to the nodal displacements $\{d\bar{u}\}$ by

$$\{da\} = [a(x \text{ or } X)] \{d\bar{u}\} \quad (2)$$

The increment of strain is given by

$$\{de\} = [B(x)] \{da\} \quad (3a)$$

for an increment of deformation in the Eulerian coordinate and by

$$\{dE\} = [B(X, u)] \{da\} \quad (3b)$$

for an increment of Green's or Lagrangian strain.

For an increment of stress we use the linearized and generalized incremental stress-strain relation for an elastic-plastic material as summarized by Marcal [29].

$$\{d\sigma\} = [D] \{de\} \quad (4a)$$

This relation is formed for shells by integrating the Eulerian stress-strain relations $\{d\sigma\} = [p] \{de\}$ through the thickness for the direct force N and bending moment M and by separating the strains into mid-wall strains \bar{e} and rotations k

$$\left\{ \frac{dN}{dh} \right\} = \int_{-H}^H \left[\frac{p}{zp} + \frac{zp}{z^2 p} \right] dz \left\{ \frac{d\bar{e}}{dk} \right\} \quad (5)$$

where N is the direct force per unit length

M is the bending moment per unit length

and the integration is performed over the thickness of the plate or shell.

For small strains and following Hibbitt et. al. [20] we may use an orthogonal transformation matrix to write the stress-strain relations of (4a) in Lagrangian terms. Since this discussion is best carried out in tensor notation

we shall let D_{mnkl} replace the matrix $[D]$ of (4a) so that the Kirchhoff stress increment dS_{ij} is given by

$$dS_{ij} = T_{im} T_{jn} T_{rk} T_{sl} D_{mnkl} dE_{rs} \quad (4b)$$

and T_{im} is an orthogonal rotation that carries the reference axis from a direction parallel to an initial material line element to a new direction parallel to the current position of the same material line element.

In equation (4b) we have used the assumption of small strain and the familiar double transformation to convert the increment of Eulerian stress to a Kirchhoff stress increment. A similar double transformation converts the Eulerian strain increment to a Lagrangian strain increment. In a continuum the double rotations do not affect the incremental stress-strain matrix $[D]$. However, this is not so for shells, because of its directional properties along the shell plane. We can trace many of the difficulties in geometric nonlinear analysis to this fact, since most writers have intuitively attempted to achieve a realignment of stresses and strains by updating of geometry. In subsequent discussion we shall replace (4b) by its matrix form

$$\{dS\} = [D]_0 \{dE\} \quad (6)$$

We now use the principle of virtual work to define equivalent forces $\{P\}$ at the nodes. For a virtual and non-zero displacement $[\delta \bar{u}]$ we have

$$[\delta \bar{u}]\{P\} = \int_V [\delta e]\{\sigma\} dV \quad (7a)$$

$$= \int_{V_0} [\delta E]\{S\} dV_0 \quad (7b)$$

We thus arrive at nonlinear equations which define equilibrium in an integral sense

$$\{P\} = \int_A [\alpha(x)]^T [B(x)]^T \{\sigma\} dA \quad (8a)$$

$$\{P\} = \int_{A_0} [\alpha(x)]^T [B(x,u)]^T \{S\} dA \quad (8b)$$

Some writers have chosen to solve (8) by a Newton-Raphson approach (Bogner et al. [30] and Oden and Kubitza [31]). However, it seems more feasible to solve large-

scale problems in this area by a linearized and incremental approach. Such a method of solution is a necessity when the material law includes some form of deformation history dependence. An interesting linearized and iterative procedure to solving this nonlinear equation has been described by Murray and Wilson [32]. Similar approaches have also been adopted by Purdy and Przemieniecki [33] and Stricklin et. al. [34].

We now cast the nonlinear equations in incremental form in order to solve the equations as a series of piecewise linear equations.

$$\begin{aligned} \{dP\} = & \int_A [\alpha(x)]^T [B(x)]^T [D] [B(x)] [\alpha(x)] dA (d\bar{u}) \\ & + \int_A d[\alpha(x)]^T [B(x)]^T \{\sigma\} dA \\ & + \int_A [\alpha(x)]^T d[B(x)]^T \{\sigma\} dA \end{aligned} \quad (9a)$$

Because of the small strain assumption and the observation, that the differential operator $[B]$ is not dependent on rigid body motion

$$d[R(x)]^T = \{0\} \quad (10)$$

and we may neglect the third term in (9a).

To understand the physics embodied in the second term we expand the $[\alpha]$ matrix so that we work in local coordinates

$$[\alpha(x)]^T = [T]_L^T [\alpha(x)]_L^T \quad (11)$$

where $[T]_L$ is a global to local transformation matrix. Thus we see that

$$d[\alpha(x)]^T = d[T(x)]_L^T [\alpha(x)]_L^T + [T(x)]_L^T d[\alpha(x)]_L^T \quad (12)$$

$d[T(x)]_L^T$ is the increment of rotation while $d[\alpha(x)]_L^T$ measures the change in shape of a shell element, i.e., its "bowing." We note that $d[\alpha(x)]_L^T = 0$ when the element is sufficiently small and small strain is assumed.

The Eulerian approach therefore gives rise to an incremental stiffness relation

$$\{dP\} = [k^{(0)}] \{d\bar{u}\} + [k^{(1)}] \{d\bar{u}\} \quad (13a)$$

where $[k^{(0)}]$ is the small displacement stiffness matrix and $[k^{(1)}]$ is the initial stress matrix accounting for both the effects described by (12).

This formulation was used by Argyris et. al. [12] for beam columns and described for a triangular constant stress element by Zienkiewicz [35]. The first writers [12] have used an approximation which neglected the change in $[\alpha]$ and Martin [15] has shown the importance of terms derived from it. However, the important point that was missed in this and subsequent discussions on [12] and [35] was that the equations being used were part of a proper Eulerian formulation. Similarly we obtain the incremental equations for a Lagrangian approach.

$$\{dP\} = \int_{A_0} [\alpha(X)]^T [B(X,u)]^T [D] [B(X,u)] [\alpha(X)] dA (du) + \int_{A_0} [\alpha(X)]^T \Delta [B(X,u)]^T \{S\} dA \quad (9b)$$

The first term on the right may be separated into two stiffness terms, one of which is the small displacement stiffness $[k^{(0)}]$ and the other is the initial displacement stiffness matrix $[k^{(2)}]$. Thus (9b) may be rewritten

$$\{dP\} = [k^{(0)}] \{d\bar{u}\} + [k^{(2)}] \{d\bar{u}\} + [k^{(1)}] \{d\bar{u}\} \quad (13b)$$

It can be seen that since (13b) is written for initial global coordinates $[k^{(2)}]$ it includes the effect of changes of geometry due to both rotation and "bowing."

In the Lagrangian approach it is also advantageous to use a local coordinate system. Then (to terms of order strain and hence small) increments of Kirchhoff stress and Lagrange strain, oriented in the initial directions of this local coordinate system, correspond to increment of 'true' stress and increments of deformation aligned with the current directions of the same local coordinate system. Thus by considering the usual incremental stress-strain relation (4a) as a relationship between increments of Kirchhoff stress and Lagrange strain, we have a properly aligned plane stress condition. This result was obtained from a full finite strain formulation of the equations in a Lagrangian frame of reference by Hibbitt et. al. [20] with certain approximations on the form of the $[D]$ matrix in the elastic-plastic case.

Now that both the Eulerian and Lagrangian approaches have been completed, we return to equation (13) and compare the resulting element stiffnesses. We expect that for the same level of approximation adopted we shall obtain the same

quantities by either approach so that in global coordinates

Eulerian	Lagrangian	
$[k^{(0)}(x)]$	$= [k^{(0)}] + [k^{(2)}(u)]$	
and	$[k^{(1)}(\sigma, x)] = [k^{(1)}(s)]$	(14)

where in (14) we note that the stiffnesses derived by an Eulerian approach are a function of the current geometry and thus a function of the developing curvature in a plate or shell element, i.e., its "bowing." This latter effect can be neglected, however, if the elements are made sufficiently small so that arcs of circles can be compared to straight lines. Many writers have used $[k^{(0)}(x)]$ in combination with $[k^{(1)}(s)]$ with an updated nodal system and also assuming a linear connection between nodes, e.g., Martin [25], Murray and Wilson [32] and Armen et. al. [37]. The explanation for the success of this combination is of course the small elements used. It may be noted that the same results could have been expected by using the true Eulerian initial stress matrix $[k^{(1)}(\sigma, x)]$ with a smaller number of elements. This matter will be discussed further when results comparing analysis with the different combinations of the element stiffnesses have been presented.

Case Studies

In this section we shall present examples of beam, plate and shell analysis to illustrate various aspects of the theory discussed earlier and to demonstrate analysis that may be applied to practice. The first example is concerned with the use of an arbitrary doubly curved triangular shell element. Hartung [38] has discussed the need for such an element. The second example is one concerned with stresses at shell junctions and brings out the need for a change to solid elements at shell discontinuities.

The remaining examples illustrate the different large displacement formulations in several sensitive cases. In these examples we compare two formulations; the full Lagrangian formulation and the usually adopted approach of updating without the stiffness resulting from the increment of the $[u]$ matrix. Three problems are considered; a shallow arch under concentrated load, a spherical cap under a concentrated load and a flat plate, simply supported under a uniform pressure load.

Cylindrical Shell Roof

In this example we examine the small displacement elastic-plastic behavior of a cylindrical shell roof subjected to uniform vertical load. This is the shell that has been much studied e.g. in [50,51]. This shell was modeled with the arbitrary doubly curved triangular shell element of Dupuis [40]. Though no experimental work is available for comparison of this elastic-plastic study, it is hoped that the results will provide a comparison for other non-linear analysis.

The shell geometry is defined as triangles in the region of the Gaussian coordinates (θ^1, θ^2) and is then mapped onto curved triangular elements which fit the cylindrical shell at the nodal points. The actual shell surface is thus approximated by a smooth surface which has the same Cartesian coordinates and the same tangent plane as the cylinder at each nodal point. Nine degrees of freedom are associated with each nodal point viz. the three Cartesian components of displacements and their first derivatives with respect to the curvilinear coordinates θ^1 and θ^2 . The displacement functions are polynomials of the third order in θ^1 and θ^2 , corrected by rational functions to insure compatibility between adjacent elements. The strain displacement relations used are those of the Koiter-Sanders shell theory. Because the coordinates of the undeformed middle surface are defined as linear combinations of the displacement functions, the differential operator $[B]$ vanishes exactly for all rigid-body motions. The properties of this element, i.e. compatibility and rigid-body motion were found to be important with respect to the rate of convergence for the elastic analysis of this shell by Dupuis [40].

The analysis of the cylindrical shell shown in Fig. 1 was performed with an elastic-perfectly plastic Mises material with the following properties:

$$\text{Young's Modulus } E = 3 \times 10^6 \text{ lb./in.}^2$$

$$\text{Equivalent Yield Stress } \bar{\sigma} = 6 \times 10^2 \text{ lb./in.}^2$$

$$\text{Poisson's ratio } \nu = 0$$

The analysis was carried out for one quadrant of the shell together with the following load schedule. A load was first applied which caused first yielding in the most severely strained element in the shell viz. the center element. Then eleven increments of a tenth of that value were applied successively. As shown in Fig. 2, the shell is very close to its limit load. Figure 3 gives the

load maximum strain curve for the shell. Curiously the maximum strain developed in a transverse direction which suggests substantial ovalization of the shell at the center. This is borne out by the plot of the progressive yielding at the surface of the shell shown on Figs. 4 and 5. The numbers in each zone indicate the load increment after first yield in which plasticity developed at the surface..

In concluding this case study we note that other features in the program such as strain hardening and large displacement effects [41] though available have not been exercised. Together these form a powerful tool for the study of realistic shell problems. On the other hand this study is but a first step and many points of interest have still to be investigated, for instance, the comparison of incremental elastic-plastic analysis and the limit analysis of shells; in particular the influence of the large displacement effects. While it is well known that those terms have a tremendous influence on the elastic-plastic behavior of plates [29], there is less overall knowledge of the behavior of shells. In addition to this it is also of interest to study the behavior of the shell due to strain hardening according to an isotropic hardening law with that due to a kinematic strain hardening law. This is of particular interest in an example with cyclic loading. It is hoped to report further on these points in a future report.

Analysis of Shell-Nozzle Junction with Combined Shell and Triangular Ring Elements

This example is included to show a combination of shell and solid elements by the method of linear constraints [28]. A mild steel shell nozzle junction under pressure was studied experimentally by Dinno and Gill [42]. This same problem was analyzed using the mesh in Fig. 6. Triangular ring elements are used in and around the weld section, and shell elements are used throughout the main body of the shell and nozzle. Comparison of the finite element results with experimental data is shown in Fig. 7. The actual differences between the predicted yield loads can be seen in Table 1. The hybrid finite element results show considerable improvement over a previous modified shell theory approach using a band of pressure for the junction [43]. That theory was itself a large improvement over the simple shell theory.

Shallow Arch Under Concentrated Load

In this example we investigate the convergence of both the updated (partial Eulerian) and the Lagrangian approach using curved beam elements. In the updated approach shown here and in subsequent examples, we merely update the nodal points but do not account for the 'bowing' effect. Figure 8 shows the load central deflection relation for the arch. Twelve equal load increments were used to obtain the results. The solutions can be seen to approach each other with increase in the number of elements until the results are indistinguishable at 32 elements. The predicted buckling loads are still too high when compared with the results of Mallet et. al. [44] for a four equilibrium element solution and also with the experimental result of Gjelsvik and Bodner [45]. In the writers opinion a better curved beam element than the element used here should be developed. The element used here is based on a specialization of the axisymmetric shell of [46].

Shell Cap Under Concentrated Load

In this example we study the behavior of a spherical cap subjected to a point load. This is the example studied by Stricklin et. al. [47] using an iterative nonlinear finite element approach. This example was also studied experimentally by Evan-Ivanowski et. al. [48].

The shell analysis was made with a Young's Modulus of 10.0×10^6 lbs./in.² and a Poisson's Ratio of 0.30. The shell parameter is defined by $\lambda^4 = a^4 12(1-\nu^2) / (Rt)^2$ which results in $\lambda = 6$. The actual experimental model of [48] had a shell parameter of $\lambda = 6.23$. The analysis was carried out with twenty equal elements subjected to twenty increments of load. Figure 9 shows the load central displacement behavior of the spherical cap. The updated solution though showing the same trends still do not quite agree with the Lagrangian solution. This example is highly nonlinear [47] so that it is possible that there is still a considerable bowing effect in the updated solution which has not been accounted for. The Lagrangian solution is in reasonable agreement with the results of Stricklin et. al. [47] and in better agreement with the experimental results of [48].

Simply Supported Square Plate With Uniform Pressure

In this example we investigate the large displacement behavior of a flat plate with both the updated and Lagrangian approach. The triangular element used is of the DeVeubeke type and is described in [36]. The analysis is carried out for the simply supported plate of Murray and Wilson [32] and of Levy [49]. The plate is $16 \times 16 \times 0.1$ ins. with a Young's Modulus of 30×10^6 lbs./in.² and a Poisson's ratio of 0.316. Analyses were carried out with two, four and eight elements respectively. The resulting pressure central deflection curves for the nonlinear elastic analysis are shown in Fig. 10. The two eight element solutions show a tendency for the updated and Lagrangian solutions to come together. Since these eight element runs took 30 mins. of IBM 360/67 time each, the writers did not continue with a sixteen element analysis. The results are only in moderate agreement with the results in the literature [32,49]. It is noted that in [36], an analysis with an update and a partial initial displacement matrix which accounted for the bowing effect produced better agreement with the results of [32,46]. We see in the present update of analysis results, the persistence of the bowing effect even at eight elements. Indeed Murray and Wilson [32], employing sixteen elements, resorted to a special iterative and residual correction procedure to include this effect. This effect is of course simply accounted for by the initial displacement matrix $[k^{(2)}]$ in the Lagrangian approach.

Discussion And Conclusions

In this paper we have summarized the nonlinear analysis of beams, plates and shells, tracing the separate developments of nonlinear material and geometric analysis. As shown elsewhere [36], both nonlinear effects are easily combined in an incremental analysis. More stress was placed on nonlinear geometric analysis in this paper in an effort to clarify the basis for the many methods in use. Our results suggest that though the full Eulerian approach is equivalent to the Lagrangian approach, the current use of the updated procedure may leave much to be desired. The 'bowing' effect in the displacing shell structure is not fully accounted for, unless many elements are used. In addition the use of flat plate elements in a nonlinear situation results in a discontinuous surface which may have an unpredictable effect. The amount of time taken to solve the simply supported plate problem is of some concern since many more elements will

have to be used in a realistic structure.

We conclude our discussion with a brief summary of the state-of-the-art in static nonlinear finite element analysis. It appears that good theories have been developed to account for both nonlinear material and geometric behavior. Compatible elements have been developed for most plate and shell like structures. Techniques have been developed to join the different types of elements together. Sufficient studies have been performed to indicate the more promising numerical methods. Much of the above has also been implemented in a few general purpose programs. (As far as is known to the authors the full range of the above features is available in ASKA and MARC 2). Therefore, the state-of-the-art is such that significant practical designs can be effected in the nonlinear regimes using the finite element method.

Acknowledgements:

Support by the Naval Ship Research and Development Center under Contract No. N00014-67-A-0191-0008 is gratefully acknowledged. The authors are indebted to Mr. Rembert Jones of that Laboratory for useful discussions.

REFERENCES

1. Pope, G., "A Discrete Element Method for Analysis of Plane Elastic-Plastic Stress Problems," Royal Aeronautical Establishment TR 65028, 1965.
2. Swedlow, J. L., and Yang, W. H., "Stiffness Analysis of Elastic-Plastic Plates," Graduate Aeronautical Lab., California Institute of Technology SM 65-10, 1965.
3. Marcal, P. V., and King, I. P., "Elastic-Plastic Analysis of Two-Dimensional Stress Systems by the Finite Element Method," Intern. J. Mech. Sci., Vol. 9, No. 3, 1967, pp. 143-155.
4. Gallagher, R. H., Padlog, J. and Bijlaard, P. P., "Stress Analysis of Heated Complex Shapes," ARS Journal, May 1962, pp. 700-707.
5. Argyris, J. H., Kelsey, S., and Kamel, W. H., "Matrix Methods of Structural Analysis. A Precis of Recent Developments," Proc. 14th Meeting of Structures and Materials Panel, AGARD, 1963.
6. Jensen, W. R., Falby, W. E., and Prince, N., "Matrix Analysis Methods for Anisotropic Inelastic Structures," AFFDL-TR-65-220, 1966.
7. Marcal, P. V., "Comparative Study of Numerical Methods of Elastic-Plastic Analysis," AIAA Journal, Vol. 6, No. 1, 1967, pp. 157-158.
8. Zienkiewicz, O. C., Valliappan, S., and King, I. P., "Elasto-Plastic Solutions of Engineering Problems 'Initial Stress', Finite Element Approach," Intern. J. for Numerical Methods in Eng., Vol. 1 75-100 (1969).
9. Armen, H. Jr., Isakson, G. and Pifko, A., "Discrete Element Methods for the Plastic Analysis of Structures Subjected to Cyclic Loading," Proc. AIAA/ASME 8th Structures, Structural Dynamics and Materials Conference, Palm Springs, March 1967.
10. Kamel, H. and Sack, R. L., "Computational Stability in Nonlinear Discrete Structural Systems," Proc. AIAA/ASME Structures, Structural Dynamics and Materials Conf., New Orleans, La., April 1969.
11. Turner, J. L., Clough, R. W., Martin, H. C., and Topp, L. J., "Stiffness and Deflection Analysis of Complex Structures," J. Aero Science, Vol. 23, No. 9, Sept. 1956, pp. 805-825.
12. Argyris, J. H., "Recent Advances in Matrix Methods of Structural Analysis," Progress in Aeronautical Sciences, 4, Pergamon Press, 1963.
13. Gallagher, R. H., Gellatly, R. A., Padlog, J., and Mallett, R. H., "Discrete Element Procedure for Thin-Shell Instability Analysis," AIAA Journal, Vol. 5, No. 1, 1967, pp. 138-144.
14. Kapur, K. K., and Hartz, B. J., "Stability of Plates Using the Finite Element Method," Journal Eng. Mech. Div., ASCE, Vol. 92, EM2, 1966, pp. 177-195.

REFERENCES (cont.)

15. Martin, H. C., "Derivation of Stiffness Matrices for the Analysis of Large Deflection and Stability Problems," Proc. 1st Conf. on Matrix Methods in Struct. Mech., AFFDL-TR-66-80, 1966, pp. 697-715.
16. Wissmann, J. W., "Nonlinear Structural Analysis; Tensor Formulation," Proc. 1st Conf. on Matrix Methods in Struct. Mech., AFFDL-TR-66-80, 1966, pp. 679-696.
17. Besseling, J. F., "Matrix Analysis of Creep and Plasticity Problems, J," Proc. 1st Conf. on Matrix Methods in Struct. Mech., AFFDL-TR-66-80, 1966, pp. 655-679.
18. Oden, J. T., "Numerical Formulation of Non-Linear Elasticity Problems," J. Struct. Div., ASCE, Vol. 93, No. ST3, June 1967, pp. 235-255.
19. Popov, E. P., and Yaghmai, S., "Linear and Nonlinear Static Analysis of Axisymmetrically Loaded Thin Shells of Revolution," Proc. 1st Int. Conf. on Pressure Vessel Technology, ASME/Roy. Netherlands Eng. Soc., Delft, Sept., 1969, pp. 237-245.
20. Hibbitt, H. D., Marcal, P. V., and Rice, J. R., "Finite Element Formulation for Problems of Large Strain and Large Displacement," Int. J. Solids and Structures, 6, 1970.
21. De Veubeke, B. F., "Bending and Stretching of Plates," Proc. 1st Conf. on Matrix Methods in Struct. Mech., AFFDL-TR-66-80, 1966, pp. 863-886.
22. Ergatoudis, I., "Quadrilateral Elements in Plane Analysis," M.Sc. thesis, University of Wales, Swansea, 1966.
23. Bogner, F. K., Fox, R. L., and Schmit, L. A., "The Generation of Inter Element-compatible Stiffness and Mass Matrices by the Use of Interpolation Formulae," Proc. 1st Conf. on Matrix Methods in Struct. Mech., AFFDL-TR-66-80, 1966, pp. 397-444.
24. Dupuis, G., and Goel, J. -J., "A Curved Finite Element for Thin Elastic Shells," Brown University Engineering Report M00014-0007/4, December 1969.
25. Ahmad, S., Irons, B. M. and Zienkiewicz, O. C., "Curved Thick Shell and Membrane Elements With Particular Reference to Axisymmetric Problems," Proc. 2nd Conf. on Matrix Methods in Struct. Mech., AFFDL-TR-68-150, 1968, pp. 539-572.
26. Melosh, R., Lang, T., Schmele, L., and Bamford, R., "Computer Analysis of Large Structural Systems," Proc. AIAA 4th Annual Meeting, Paper 67-955, 1967.
27. Marcal, P. V., "On General Purpose Programs for Finite Element Analysis, With Special Reference to Geometric and Material Nonlinearities," Brown University Engineering Report ARPA E-73, May 1970.

REFERENCES (cont.)

28. Hibbitt, H. D., and Marcal, P. V., "Hybrid Finite Element Analysis with Particular Reference to Axisymmetric Structures," Proc. AIAA 8th Aerospace Sciences Meeting, Paper No. 70-137, 1970.
29. Marcal, P. V., "Elastic-Plastic Analysis of Pressure Vessel Components," Proc. 1st Pressure Vessel and Piping Conf., ASME Computer Seminar, Dallas, Sept. 1968.
30. Bogner, F. K., Mallett, R. H., Minich, M. D., and Schmit, L. A. "Development and Evaluation of Energy Search Methods of Nonlinear Structural Analysis," AFFDL-TR-65-113, 1965.
31. Oden, J. T., and Kubitza, W. K., "Numerical Analysis of Nonlinear Pneumatic Structures," Proc. 1st International Colloquium on Pneumatic Structures, Stuttgart, May 1967.
32. Murray, D. W., and Wilson, E. L., "Finite Element Post Buckling Analysis of Thin Elastic Plates," Proc. 2nd Conf. Matrix Methods in Struct. Mech., AFFDL, Oct. 1968.
33. Purdy, D. M., and Przemieniecki, I. S., "Influence of Higher-Order Terms in the Large Deflection Analysis of Frameworks," Proc., ASCE, Joint Specialty Conf., Optimization and Nonlinear Problems, April 1968, pp. 142-152.
34. Stricklin, J. A., Haisler, W. E., MacDougall, H. R., and Stebbins, F. J., "Nonlinear Analysis of Shells of Revolution by the Matrix Displacement Method," AIAA Journal, Vol. 6, No. 12, Dec. 1968, pp. 2306-2312.
35. Zienkiewicz, O. C., "Non-linear Problems Chapter 12," Finite Element Method in Structural and Continuum Mechanics, McGraw-Hill, 1967, 99, pp. 192-211.
36. Marcal, P. V., "Finite Element Analysis of Combined Problems of Nonlinear Material and Geometric Behavior," Proc. ASME Computer Conference on Computational Approaches in Applied Mechanics, June 1969, pp. 133. Also, Brown University Engineering Report N00014-0007/1, March 1969.
37. Armen, H., Jr., Pifko, A., and Levine, H. S., "Finite Element Method for the Plastic Bending Analysis of Structures," Proc. 2nd Conf. on Matrix Methods in Struct. Mechanics, AFFDL-TR-68-150, October 1968, pp. 1301.
38. Jones, R. E., "A Generalization of the Direct Stiffness Method of Structural Analysis," AIAA Journal, 2, 1964, pp. 821-826.
39. Hartung, R. F., "Assessment of Current Capability for Computer Analysis of Shell Structures," Preliminary Draft, AFFDL-TR-67-194, Wright-Patterson Air Force Base, Ohio, February, 1970.

REFERENCES (cont.)

40. Dupuis, G. A., "Application of Ritz's Method to Thin Elastic Shell Analysis," Brown University Engineering Report N00014-0008/1, July 1970.
41. Dupuis, G. A. "Lagrangian Formulation for Large Elastic Deformation of Thin Shells," Brown University Engineering Report N00014-0008/2, August 1970.
42. Dinno, K. S., and Gill, S. S., "An Experimental Investigation into the Plastic Behavior of Flush Nozzles in Spherical Pressure Vessels," Int. J. Mech. Sci., 7, 1965, pp. 817-839.
43. Marcal, P. V., and Turner, C. E., "Elastic-Plastic Behavior of Flush Nozzles in Spherical Pressure Vessels," 9, 3, Journal Mech. Eng. Sci., 1967, p. 182.
44. Mallett, R. H. and Berke, L., "Automated Method for the Large Deflection and Instability Analysis of Three-Dimensional Truss and Frame Assemblies," AFFDL-TR-66-102, December, 1966.
45. Gjelsvik, A. and Bodner, S. R., "The Energy Criterion and Snap Buckling of Arches," Journal Engineering Mechanics Division, ASCE, 88, EM5, 1962, pp. 87-134.
46. Khojasteh-Bakht, H., "Analysis of Elastic-Plastic Shells of Revolution under Axisymmetric Loading by the Finite Element Method," Ph.D. Dissertation, University of California at Berkeley, SESH 67-8, April 1967.
47. Stricklin, J. A., Martinez, J. E., Tillerson, J. R., Hong, J. H., and Haisler, W. E., "Nonlinear Dynamic Analysis of Shells of Revolution by Matrix Displacement Method," Texas A & M University, Report 69-77, February, 1970.
48. Evan-Iwanowski, R. M., Cheng, H. S., and Loo, T. C., "Experimental Investigation of Deformations and Stability of Spherical Shells Subjected to Concentrated Load at the Apex," Proceedings of the Fourth U. S. National Congress of Applied Mechanics (American Society of Mechanical Engineers, New York, pp. 563-575, 1962
49. Levy, S., "Bending of Rectangular Plates with Large Deflection," NACA Technical Note 846, 1942.
50. Bonnes, G., Dhatt, G., Giroux, Y. H., and Robichaud, L. P. A., "Curved Triangular Elements for the Analysis of Shells," Proc. 2nd Conf. on Matrix Methods in Struct. Mechanics, AFFDL-TR-68-151, October 1968, p. 617.
51. Strickland, G. E. and Leden, W. A., "A Doubly Curved Triangular Shell Element," Proc. 2nd Conf. on Matrix Methods in Struct. Mechanics, AFFDL-TR-68-150, October 1968, p. 641.

TABLE 1. First Yield of Shell-Nozzle Junction
with Internal Pressure

	LIMIT OF PROPORTIONALITY (lb/in ²)
Experimental [42]	800
Simple shell theory [43]	340
Band theory [43]	630
Hybrid analysis	793

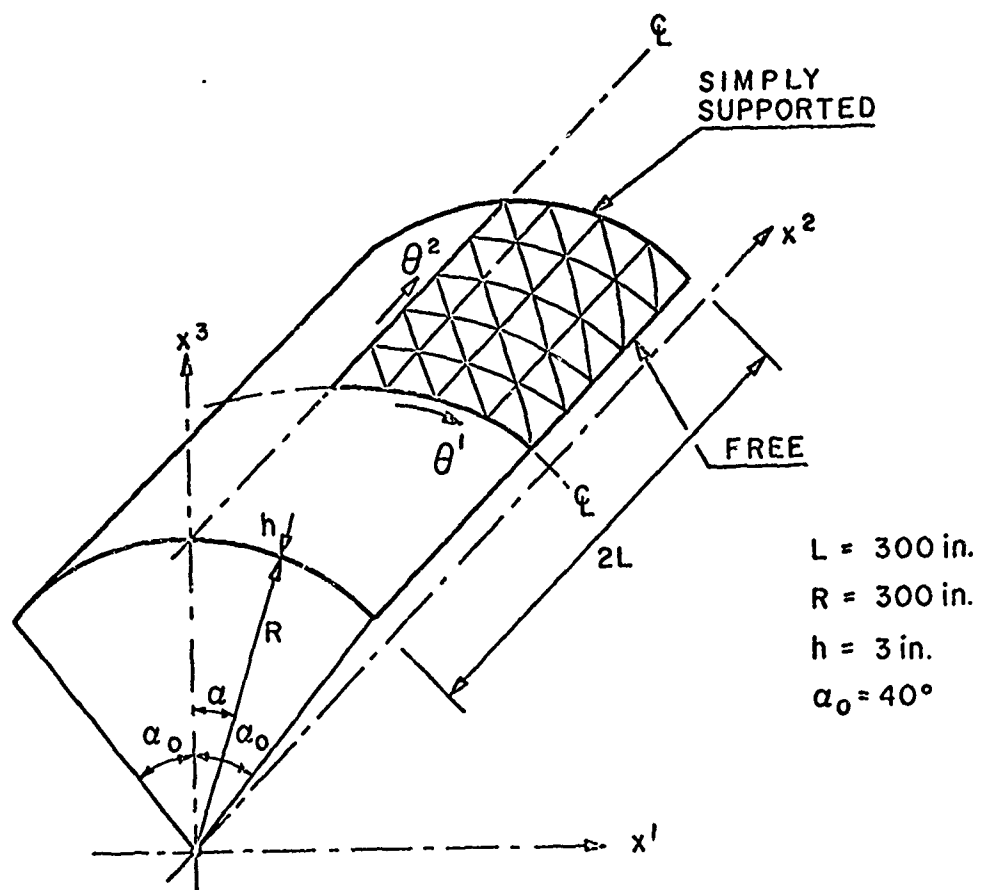


FIG. 1 CYLINDRICAL SHELL ROOF.

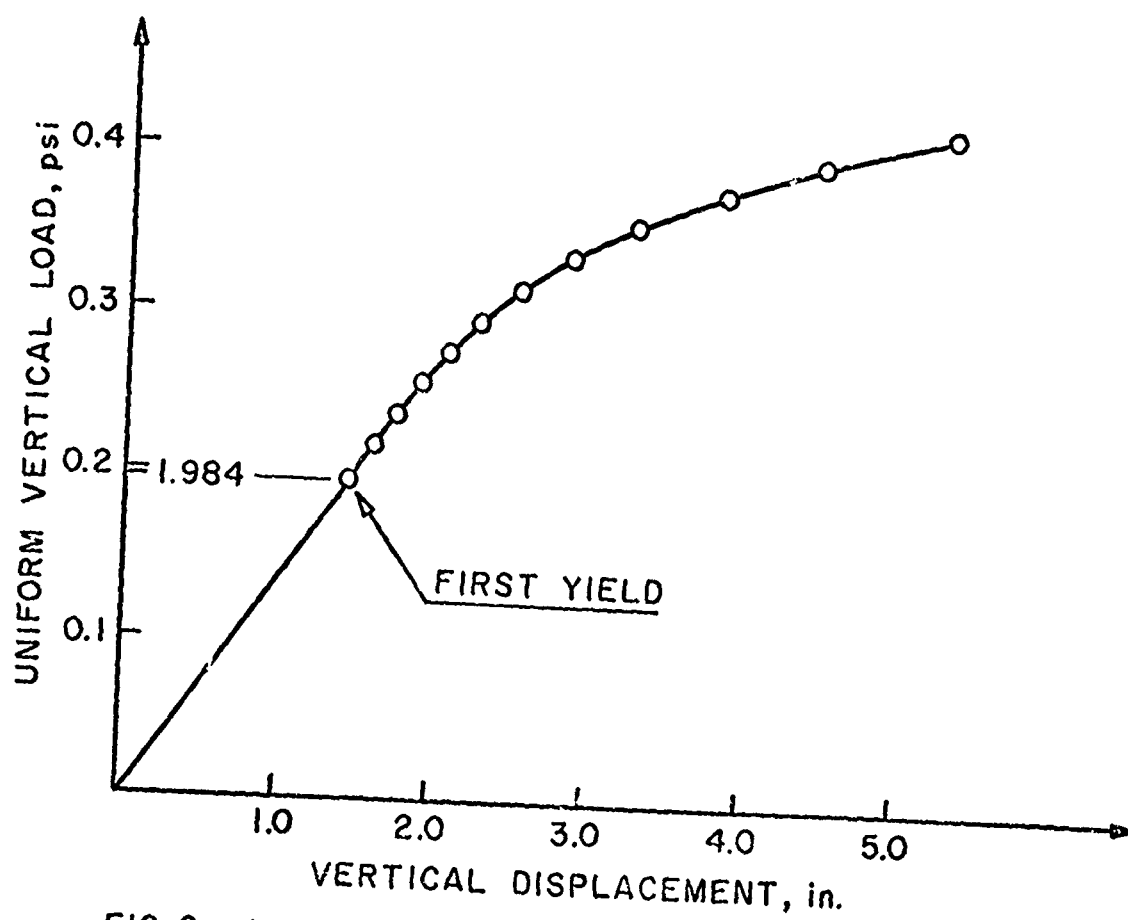


FIG. 2 LOAD DISPLACEMENT AT CENTER OF FREE EDGE.

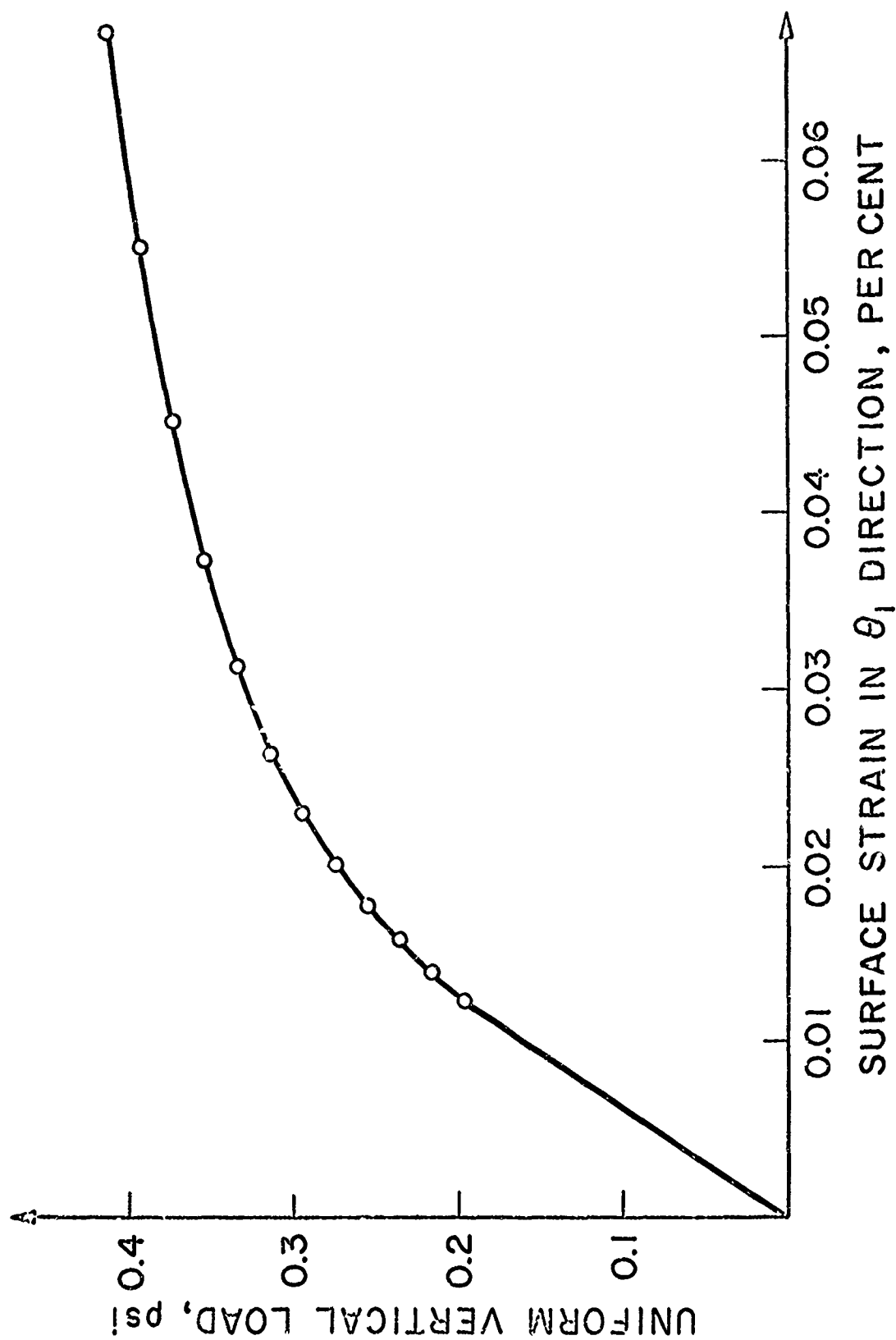
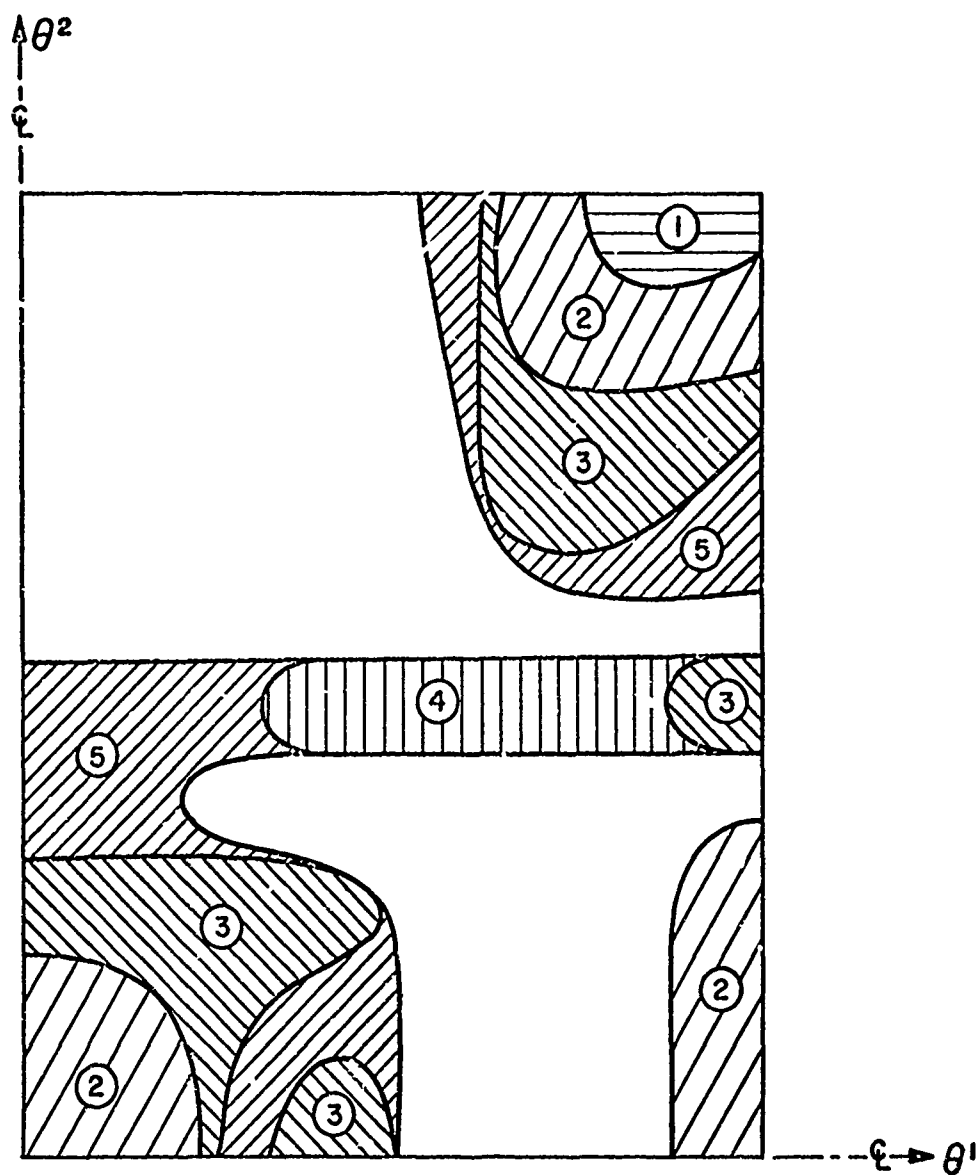
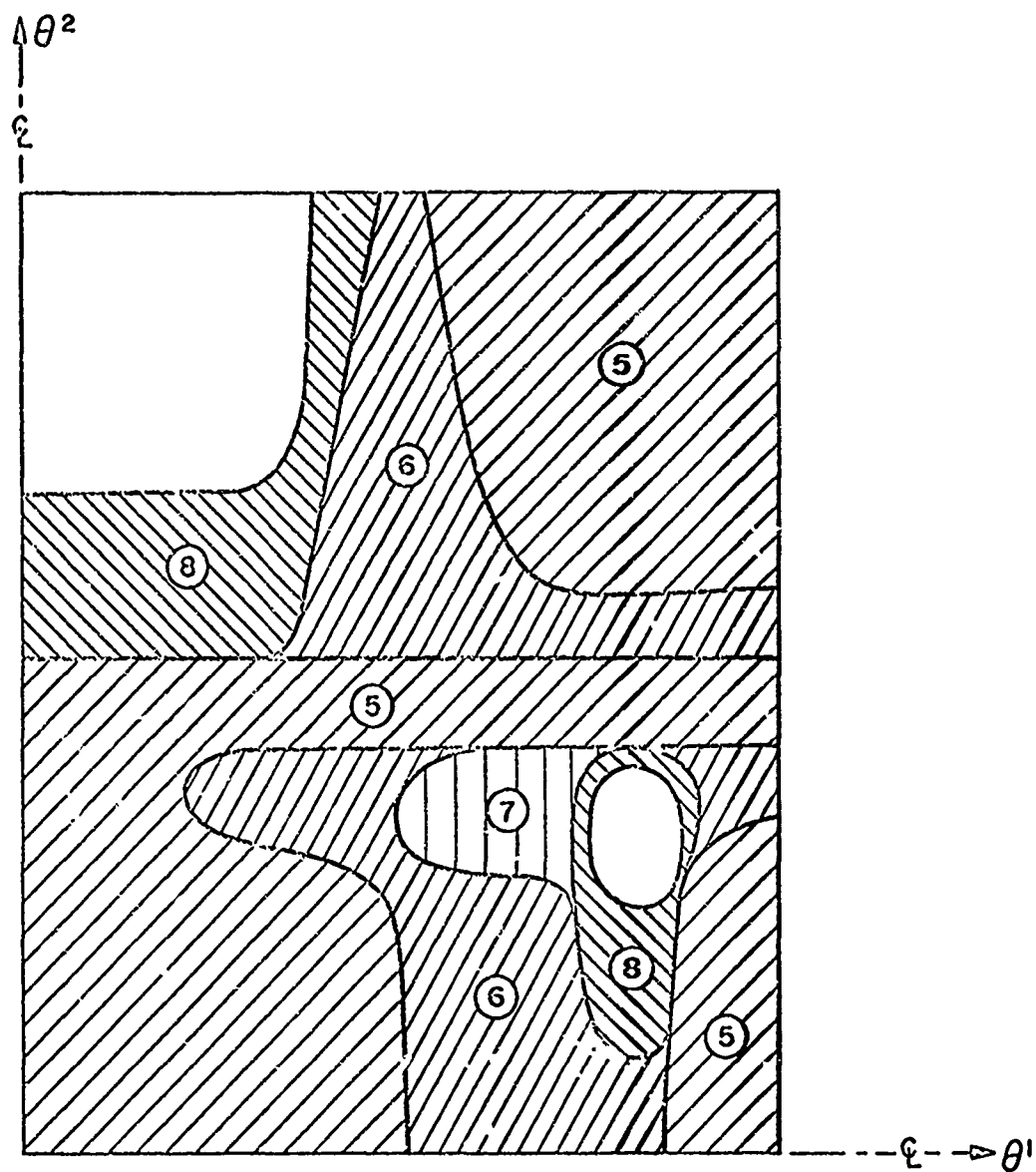


FIG. 3 LOAD - MAXIMUM STRAIN AT TOP SURFACE.



PLASTIC YIELDING FOR INCREMENTS 1 TO 5

FIG.4 PLASTIC YIELDING ON SURFACE



PLASTIC YIELDING FOR INCREMENTS 5 TO 8.

FIG. 5 PLASTIC YIELDING ON SURFACE.

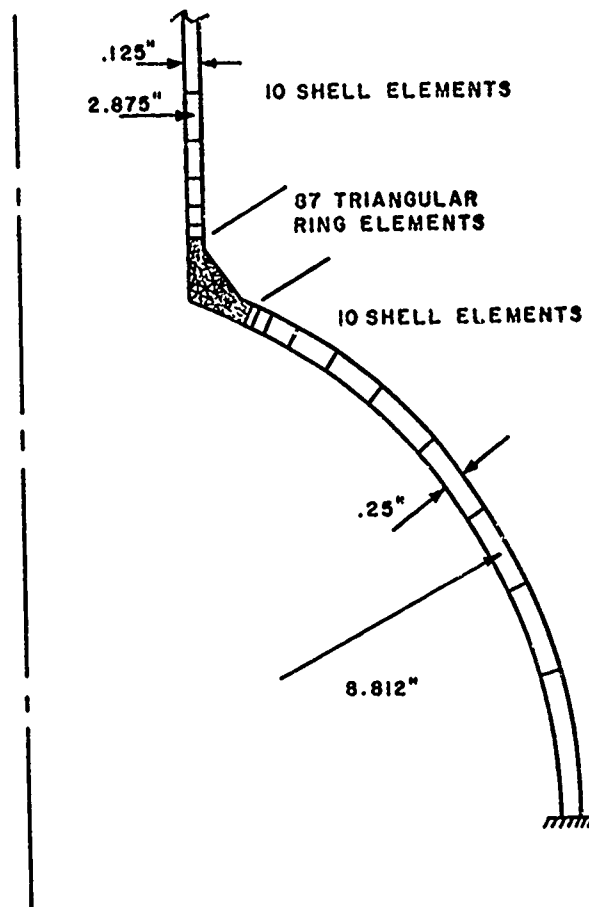


FIG. 6 MESH FOR SHELL-NOZZLE JUNCTION. (NOT TO SCALE)

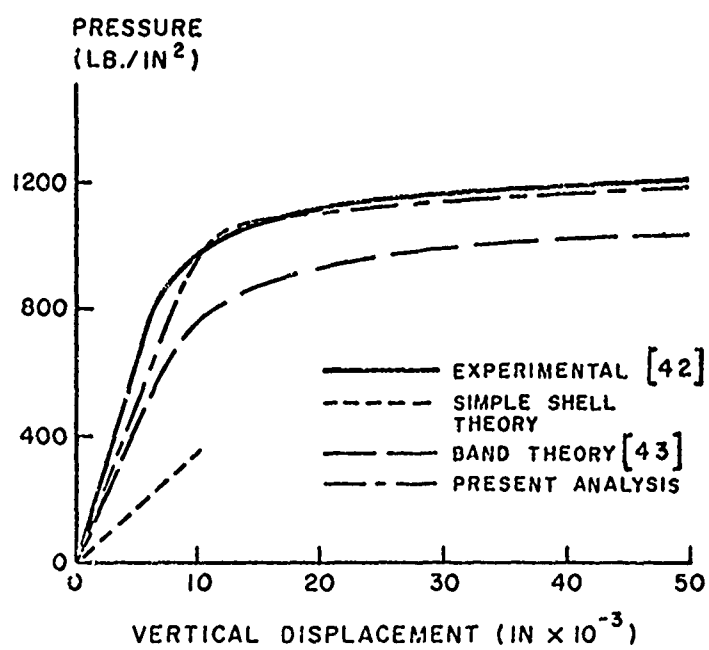


FIG.7 NOZZLE DISPLACEMENT

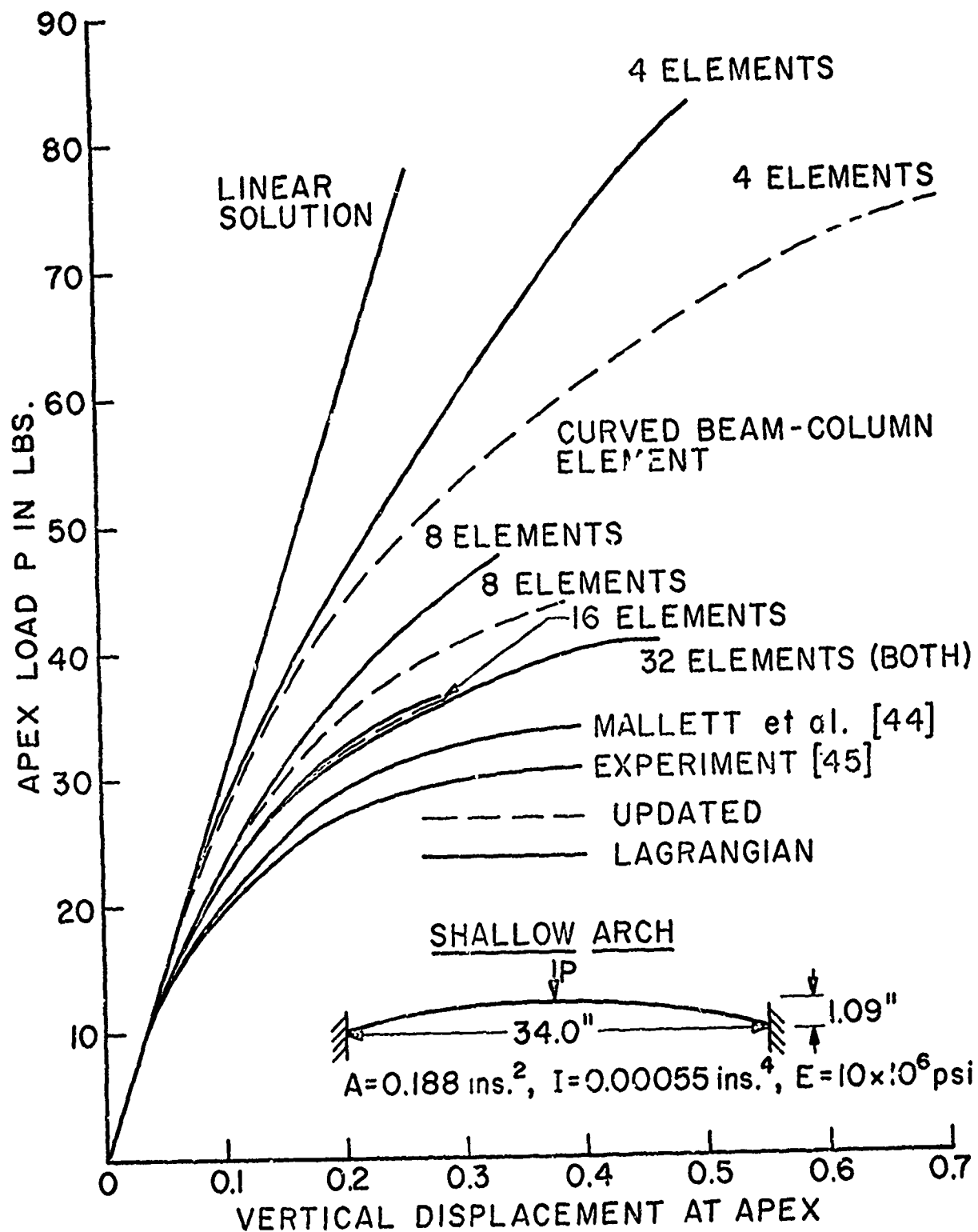


FIG.8 SHALLOW ARCH UNDER CONCENTRATED LOAD.

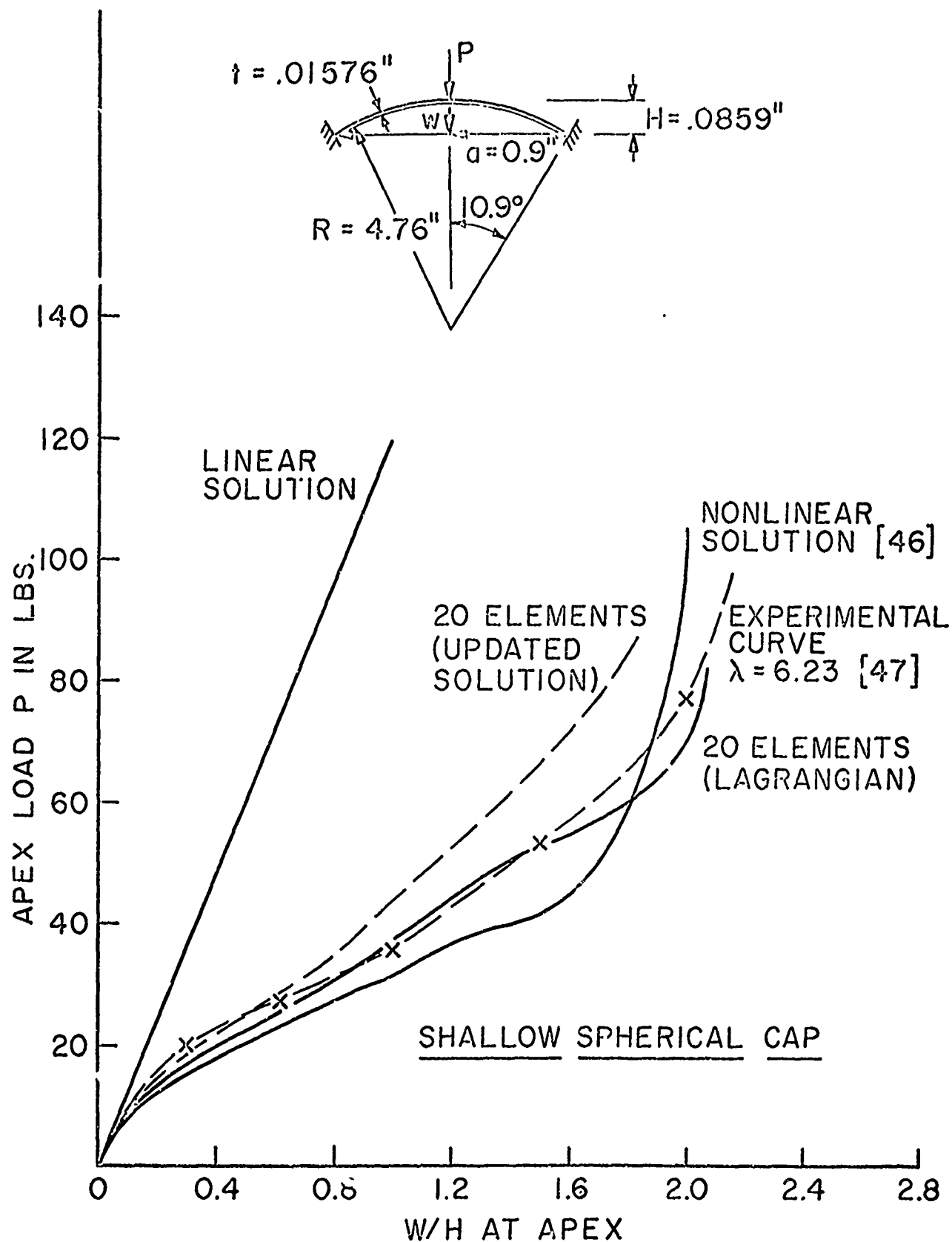


FIG. 9 RESPONSE OF SPHERICAL CAP TO CONCENTRATED LOAD.

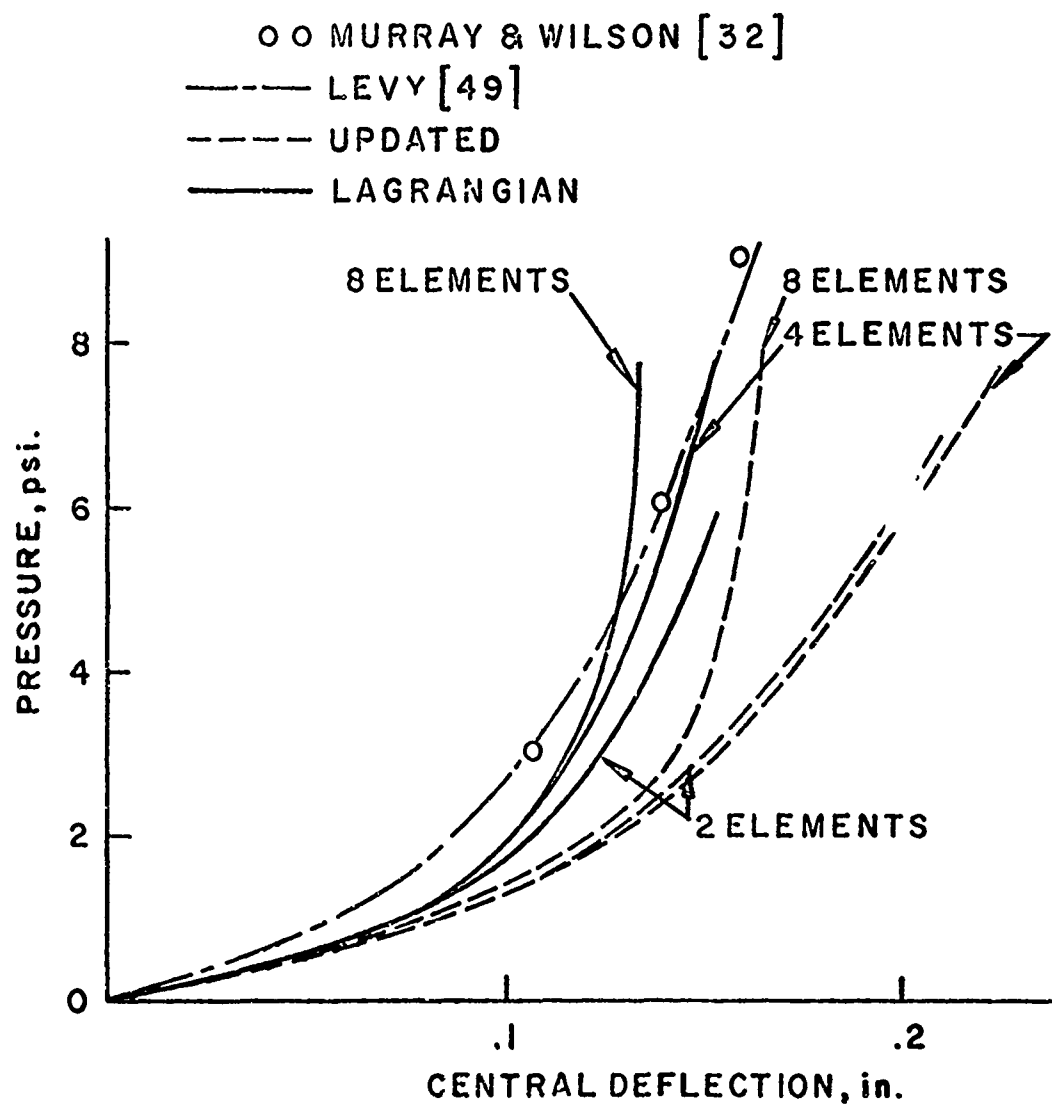


FIG.10 PRESSURE DEFLECTION CURVE FOR SIMPLY SUPPORTED PLATE

QUESTIONS AND COMMENTS FOLLOWING MARCAL'S PAPER

QUESTION: I'd like to ask Prof. Marcal if in the updated version or the Eulerian system, he additionally updated the geometry between nodal points. In other words, do you take into account the change of the curvature between the elements and reintegrate the element stiffness matrix again to get these new properties into account?

MARCAL: No, I do not.

QUESTION: Well, can I suggest that this may be one way of taking into account this bowing effect you mentioned. You can calculate the deflections by knowing the assumed displacement function between the nodes, find a new shell geometry surface from these results, and then form your new stiffness matrices in terms of this Eulerian approach.

I also have another question. You say you have solved problems both by modifying the geometric nonlinearity in the stiffness matrix and also by taking into account the geometric nonlinear effects as essentially an effective load. Would you comment on these two approaches as to their effect on computation time? This might be considerable since in one case apparently you don't have to recalculate the stiffness matrix.

MARCAL: We've shown that if you iterate you can show and prove convergence providing you're below the first buckling load. If you're below the buckling load, λ is bigger than 1, and your rate of convergence is proportional to the power of λ at each iteration. So, when you're below this buckling load, one would advise you to iterate, but as soon as you go up to

a load that's close to your buckling load, that's the time to switch to the tangent modulus method. So I place my bet on both sides.

QUESTION: The question arises here as whether to treat the plasticity as an effective load vector or via this tangent modulus method. I think you should be consistent in the way you handle plasticity and geometric nonlinearity to avoid any penalties of mixing two methods. For instance, if you treat the plastic effects as an effective load vector, then, in that case, you should try to treat the geometric nonlinear effects as an effective load vector to avoid recomputing the stiffness matrix as much as possible. However, if you're going to take into account the plasticity through the tangent stiffness matrix, then I believe you might as well update the geometry just as well, since you're going to have to reformulate stiffness matrices and integrate through the thickness and over the area again. Do you have any comment on this?

MARCAL: In some recent work with Dick Gallagher we've shown convergence of this plasticity thing and I think there I would use the same approach I outlined before. That is, when it's useful to me I will iterate on the right-hand side and when the iteration gets long I will switch. However, in doing this work we were stumped when we wanted to combine both the plastic nonlinear behavior and the geometric behavior together in the right-hand side iteration. We found it very difficult to form the constituent stiffnesses. Maybe you have found the way around this. We just looked at the equations and the corrections we had to make and just threw up our hands in horror. So, when you get the combined nonlinear geometry and material behavior, just use the tangent modulus method all the way through

because you've got it there anyway. Do you have some experience on this?

QUESTION: Up until now we have been using the plasticity as an effective load vector and accounting for the geometric nonlinearity by modifying the stiffness matrix. We don't know whether this is the best way of doing it. This is what I'd like to evoke some more comments on if anybody else has experience.

COMMENT: I'm doing a lot of work involving thermoplastic analysis in solid bodies and I've used the tangent stiffness approach basically because the temperature load is present and stiffness matrix changes anyway. But I found that the time that you spend to solve the equations is so much greater than generating the stiffness matrix itself that I'm looking for improvements in solving the equations and not so much in say this other iterative approach. Currently, the ratio is about 3 to 1; one second to generate the equations, three seconds to solve them. So I find we use the updated geometry and have no problems at all.

COMMENT: With regard to taking the loads to the right-hand side, I will say this. We have used the method with some success and some failures. In particular, if the nonlinear solution is about three times the linear solution, it will not converge, even though you use something like underrelaxation to help it. I might point out in the same regard that the present method which we are using is the incremental approach with a one step Newton Raphson corrector. The one step Newton Raphson corrector is quite significant in that it keeps the solution from drifting away from the true solution.

QUESTION: Could you comment on constitutive relations and which ones you should use?

MARCAL: I think here I'm just covering all bets. I have a student programming the Lee type constitutive relations for dynamic work, and we're just starting to do some work on kinematic hardening. This is just to put it into the equations. I guess my philosophy towards this general purpose program is that we shouldn't make decisions in advance as to what type of relationships we will have. Just allow flexibility to evolve some reasonable rules for certain problems as time goes on. For instance, if you're worried about thermal fatigue and low cycle fatigue, it appears you have to worry about kinematic hardening. But if you're not worried about that, you can get away with isotropic hardening.

THE ANALYSIS OF THIN SHELLS WITH A DOUBLY CURVED
ARBITRARY QUADRILATERAL FINITE ELEMENT^{*}

by

Samuel W. Key

Member of the Technical Staff

Sandia Laboratories

1. INTRODUCTION

The finite element method which is a numerical solution technique has been applied to the analysis of thin shells with considerable success. A recent review article by Gallagher [50] provides an excellent perspective of current efforts in the analysis of shells by the finite element method. Much of the current effort in shells has centered on the development of doubly curved quadrilateral and triangular elements for use in the analysis of arbitrary shell structures.

Compared to finite elements based on shallow shell equations and facet idealizations using flat plate elements, the elements based on non-shallow shell equations are rather limited in their extent of application to shell problems.

^{*}This work was supported by the United States Atomic Energy Commission.

For the most part, only finite length axisymmetric cylinders have been treated and only with elements aligned with the surface coordinates. Only three papers have looked at anything beyond the cylinder applications. A couple of papers only propose displacements to be used.

In a Ph.D. thesis, C. Visser[1] discusses a doubly curved triangular element based on linear membrane displacements and the constant bending strain but nonconforming normal deflection function of Bazeley, Cheung, Irons, and Zienkiewicz[2]. No computations based on this element are presented.

Gallagher[3] and Gallagher and Yang[4] examine a doubly curved quadrilateral element defined by lines in a principle coordinate system. The element has constant but distinct principle curvatures, and is based on bilinear membrane displacements and a bicubic normal deflection. Two shell problems are worked in Reference [3]. The first is a finite length circular cylinder with a line load around the midsection making it an axisymmetric problem. The second is a spherical dome of square planform with a concentrated load at the center.

Bogner, Fox and Schmit[5] develop a cylindrical shell element again aligned with the principal coordinates of the cylinder and based on bicubic displacement assumptions for both the membrane and normal displacements. They consider a finite length circular cylinder loaded on a diameter by concentrated forces.

Oden and Wempner[6] introduce the notion of a discrete Kirchhoff hypothesis and consider a shell element rectangular in the coordinates of the reference

surface. While they discuss rather general shells, only a cylindrical shell is used in the applications. The element derivation starts with a transverse shear shell theory where the reference surface displacements and fiber rotations are independent variables. At discrete points the Kirchhoff hypothesis is applied resulting in the fiber rotations being defined in terms of the reference surface behavior. The residual transverse shear energy is dropped from the elements. The calculations presented are for a finite circular cylindrical shell loaded at the midsection by a circumferentially uniform radial force.

In a note Oden[7] discusses a quadrilateral element defined by coordinate lines in a shell theory retaining general surface coordinates rather than orthogonal principle coordinates. He suggests bilinear polynomials for the membrane displacement and a bicubic polynomial for the normal displacement. No calculations are presented.

Cantin and Clough[8] provide a rectangular cylindrical shell element by using exact rigid body trigonometric terms in conjunction with polynomial terms for the displacement fields. When the element curvature vanishes or the size diminishes to zero, the membrane displacements reduce to bilinear polynomials while the normal displacement approaches a bicubic polynomial. Two applications are presented. One is a cylindrical panel supported at the ends by diaphragms and gravity loaded. The other is a finite length circular cylinder loaded across a diameter by concentrated forces. For this last problem they give the deflection under the load for various meshes for three different elements. One set of calculations are for the all bicubic polynomials of Bogner, Fox and Schmit[5], a set of calculations for their trigonometric/polynomial combination element, and a set of calculations for the bilinear/

bicubic displacements which are the same displacement assumptions as mentioned by Oden[7]. The results clearly show what the lack of explicit rigid body freedoms can do to the bilinear/bicubic polynomial element in this problem. However, the all bicubic polynomial element still maintains an edge in either a mesh size comparison or degree of freedom comparison for this problem.

Key and Beisinger[9] put forth an arbitrary doubly curved quadrilateral element. A transverse shear deformation shell theory is utilized to reduce the continuity requirements on the displacement assumptions at the expense of an increased number of unknowns. Extensive applications of this element to various shell problems show that the rigid body freedoms are not well represented in this approach and that the stiffness of the shear deformations slows convergence to an unacceptable degree.

Olsen and Lindberg[10] introduce a curved rectangular element for cylindrical shells. It is based on membrane displacement assumptions which are linear in the axial coordinate and cubic in the circumferential coordinate. The normal displacement is a 12 term cubic expansion used before for plate bending[11]. An extensive vibration analysis is performed on a cantilevered cylindrical panel.

Greene, Jones and Strome[12] treat a quadrilateral shell element defined by principle coordinate lines, again making it rectangular in the surface of the shell. Bicubic polynomials are utilized for all of the displacements. They consider edge bending of a hemisphere, the pressurization of an elliptic dome, both axisymmetric problems, and the vibration modes of a finite length circular cylinder and a spherical cap.

Argyris, Buck, Fried, Hilber, Mareczek, and Scharpf[13] discuss at great length without application a triangular shell element.

In a somewhat different approach to generating a stiffness matrix, Tsui, Massard and Loden[14] put forth a rectangular shell element again defined by coordinate lines. To generate the stiffness matrix, they start by using an 11×11 point finite difference mesh over the elements. In the interior the field equations for a transverse shear deformation shell theory are differenced and then solved subject to specified boundary deflections along the edges which are defined by displacement and rotation variables at the corner nodes. Thus, entry by entry, a stiffness matrix is generated. The major difficulty encountered is the generation of nonsymmetric stiffness matrices. As an application they examine a cylindrical panel idealization of a gravity loaded arch dam, but have no other solution to compare against.

In a recent paper, Herrmann[15] examines a cylindrical shell element based on a mixed formulation originally used in plate bending[16]. Considerable care has been exercised in including the rigid body freedoms for this element. Again, a finite length cylindrical problem is examined.

In a forthcoming paper, W. Visser[17] examines a doubly curved triangular element based on a mixed formulation due originally to Herrmann[16]. The element uses quadratic displacement assumptions along with linear bending moment assumptions.

In what follows, a doubly curved arbitrary quadrilateral element is developed based on the discrete Kirchhoff hypothesis notion put forth by Oden and Wempner[6]. The 12 term cubic polynomial used in plate bending, [11], forms the basis for the membrane and normal displacements. Biquadratic polynomials

are used for the fiber rotation descriptions. Extensive applications of the results show some of the features of this element.

2. SHELL THEORY

Shell Theory

The treatment is one presented by K. Washizu in a series of lectures at the University of Washington in 1962. A later treatment of this problem appears in his monograph [18]. Figure 1 shows the geometry of the reference surface.

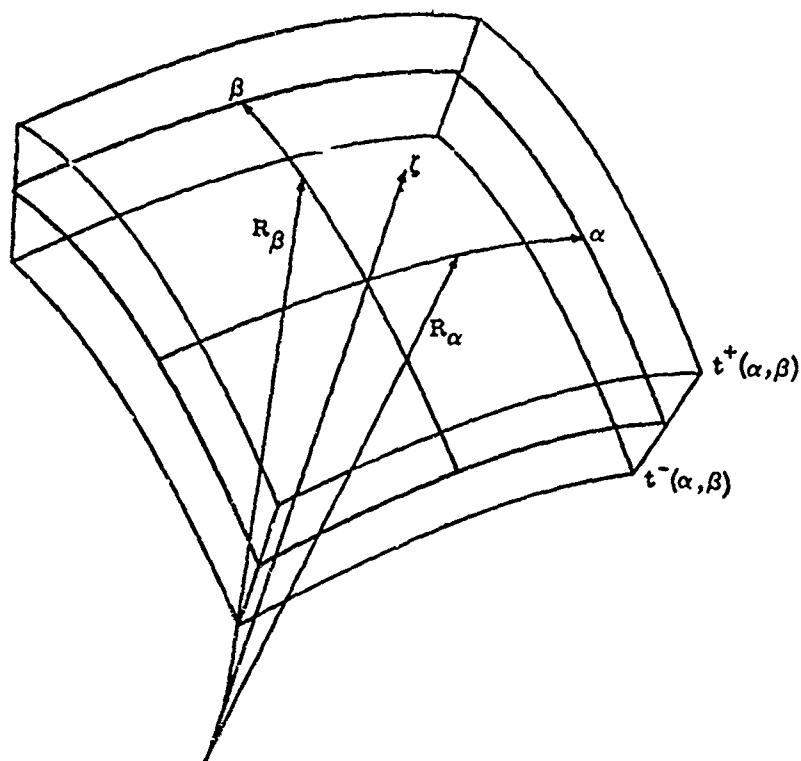


Figure 1.
Shell Geometry

The principal coordinates in the reference surface are α and β . Normal to the reference surface is the coordinate ζ . The principal curvatures of the reference surface, $1/R_\alpha$ and $1/R_\beta$, are positive as shown. The upper surface of the shell is given by $t^+(\alpha, \beta)$ and the lower surface by $t^-(\alpha, \beta)$. An element of length in the shell coordinate system is given by

$$ds^2 = A^2 \left(1 + \frac{\zeta}{R_\alpha}\right)^2 d\alpha^2 + B^2 \left(1 + \frac{\zeta}{R_\beta}\right)^2 d\beta^2 + d\zeta^2, \quad (1)$$

where A and B are the Lamé coefficients in the α, β -plane.

In terms of Cartesian components of the displacement vector, the deformations allowed in the shell are of the form

$$\begin{aligned} u_\alpha(\alpha, \beta, \zeta) &= u(\alpha, \beta) + \zeta f(\alpha, \beta) \\ u_\beta(\alpha, \beta, \zeta) &= v(\alpha, \beta) + \zeta g(\alpha, \beta) \\ u_\zeta(\alpha, \beta, \zeta) &= w(\alpha, \beta) \end{aligned} \quad (2)$$

where the rotations f and g are given by

$$\begin{aligned} f &= -\frac{1}{A} \frac{\partial w}{\partial \alpha} + \frac{u}{R_\alpha} \\ g &= -\frac{1}{B} \frac{\partial w}{\partial \beta} + \frac{v}{R_\beta} \end{aligned} \quad (3)$$

In a transverse shear deformation shell theory the fiber rotations f and g are independent deformation variables and equations (3) represent kinematic constraints reducing the theory to a Kirchhoff shell theory. It is this transition from a transverse shear deformation shell theory to a Kirchhoff theory that will be utilized below in the element derivation.

The resulting Cartesian components of the strain tensor are given by

$$e_{\alpha\alpha} = \frac{\epsilon_{\alpha\alpha} + \zeta_{\alpha}^{\kappa}}{\left(1 + \frac{\zeta}{R_{\alpha}}\right)}$$

$$e_{\beta\beta} = \frac{\epsilon_{\beta\beta} + \zeta_{\beta}^{\kappa}}{\left(1 + \frac{\zeta}{R_{\beta}}\right)} \quad (4)$$

$$2e_{\alpha\beta} = \frac{\gamma_{\alpha\beta} + 2\zeta_{\alpha\beta}^{\kappa}}{\left(1 + \frac{\zeta}{R_{\alpha}}\right)\left(1 + \frac{\zeta}{R_{\beta}}\right)}$$

$$e_{\zeta\zeta} = e_{\alpha\zeta} = e_{\beta\zeta} = 0$$

where

$$\epsilon_{\alpha\alpha} = \frac{1}{A} \frac{\partial u}{\partial \alpha} + \frac{v}{AB} \frac{\partial A}{\partial \beta} + \frac{w}{R_{\alpha}}$$

$$\epsilon_{\beta\beta} = \frac{1}{B} \frac{\partial v}{\partial \beta} + \frac{u}{AB} \frac{\partial B}{\partial \alpha} + \frac{w}{R_{\beta}}$$

$$\gamma_{\alpha\beta} = \frac{1}{B} \frac{\partial u}{\partial \beta} - \frac{v}{AB} \frac{\partial B}{\partial \alpha} + \frac{1}{A} \frac{\partial v}{\partial \alpha} - \frac{u}{AB} \frac{\partial A}{\partial \beta}$$

$$\kappa_{\alpha} = \frac{1}{A} \frac{\partial f}{\partial \alpha} + \frac{g}{AB} \frac{\partial A}{\partial \beta}$$

$$\kappa_{\beta} = \frac{1}{B} \frac{\partial g}{\partial \beta} + \frac{f}{AB} \frac{\partial B}{\partial \alpha} \quad (5)$$

$$2\kappa_{\alpha\beta} = \frac{1}{B} \frac{\partial f}{\partial \beta} - \frac{f}{AB} \frac{\partial A}{\partial \beta} + \frac{1}{A} \frac{\partial g}{\partial \alpha} - \frac{g}{AB} \frac{\partial B}{\partial \alpha} + \frac{1}{R_{\alpha}} \left(\frac{1}{B} \frac{\partial u}{\partial \beta} - \frac{v}{AB} \frac{\partial B}{\partial \alpha} \right) + \frac{1}{R_{\beta}} \left(\frac{1}{A} \frac{\partial v}{\partial \alpha} - \frac{u}{AB} \frac{\partial A}{\partial \beta} \right).$$

The equations of equilibrium in terms of the physical components of the stress resultants are

$$\begin{aligned} \frac{\partial}{\partial \alpha} \left(B N_{\alpha\alpha} \right) + \frac{\partial}{\partial \beta} \left(A N_{\beta\alpha} \right) + N_{\alpha\beta} \frac{\partial A}{\partial \beta} - N_{\beta\beta} \frac{\partial B}{\partial \alpha} + Q_{\alpha\zeta} \frac{AB}{R_\alpha} + AB \bar{Y}_\alpha &= 0 \\ \frac{\partial}{\partial \alpha} \left(B N_{\alpha\beta} \right) + \frac{\partial}{\partial \beta} \left(A N_{\beta\beta} \right) + N_{\beta\alpha} \frac{\partial B}{\partial \alpha} - N_{\alpha\alpha} \frac{\partial A}{\partial \beta} + Q_{\beta\zeta} \frac{AB}{R_\beta} + AB \bar{Y}_\beta &= 0 \\ \frac{\partial}{\partial \alpha} \left(B Q_{\alpha\zeta} \right) + \frac{\partial}{\partial \beta} \left(A Q_{\beta\zeta} \right) - AB \left(\frac{N_{\alpha\alpha}}{R_\alpha} + \frac{N_{\beta\beta}}{R_\beta} \right) + AB \bar{Y}_\zeta &= 0 \end{aligned} \quad (5)$$

where

$$\begin{aligned} Q_{\alpha\zeta}^{AB} &= \frac{\partial}{\partial \alpha} \left(B M_{\alpha\alpha} \right) + \frac{\partial}{\partial \beta} \left(A M_{\alpha\beta} \right) + M_{\alpha\beta} \frac{\partial A}{\partial \beta} - M_{\beta\beta} \frac{\partial B}{\partial \alpha} \\ Q_{\beta\zeta}^{AB} &= \frac{\partial}{\partial \alpha} \left(B M_{\alpha\beta} \right) + \frac{\partial}{\partial \beta} \left(A M_{\beta\beta} \right) + M_{\alpha\beta} \frac{\partial B}{\partial \alpha} - M_{\alpha\alpha} \frac{\partial A}{\partial \beta} \\ N_{\beta\alpha} &= S_{\alpha\beta} + \frac{M_{\alpha\beta}}{R_\alpha} \\ N_{\alpha\beta} &= S_{\alpha\beta} + \frac{M_{\alpha\beta}}{R_\beta} \end{aligned} \quad (7)$$

The reference surface tractions are denoted by \bar{Y}_α , \bar{Y}_β and \bar{Y}_ζ , and the stress resultants $N_{\alpha\alpha}$, $N_{\beta\beta}$, $S_{\alpha\beta}$, $M_{\alpha\alpha}$, $M_{\beta\beta}$ and $M_{\alpha\beta}$ are defined by

$$\begin{aligned}
 N_{\alpha\alpha} &= \int_{t-}^{t+} \sigma_{\alpha\alpha} \left(1 + \frac{\zeta}{R_\beta}\right) d\zeta \\
 N_{\beta\beta} &= \int_{t-}^{t+} \sigma_{\beta\beta} \left(1 + \frac{\zeta}{R_\alpha}\right) d\zeta \\
 S_{\alpha\beta} &= \int_{t-}^{t+} \sigma_{\alpha\beta} d\zeta \\
 M_{\alpha\alpha} &= \int_{t-}^{t+} \sigma_{\alpha\alpha} \zeta \left(1 + \frac{\zeta}{R_\beta}\right) d\zeta \\
 M_{\beta\beta} &= \int_{t-}^{t+} \sigma_{\beta\beta} \zeta \left(1 + \frac{\zeta}{R_\alpha}\right) d\zeta \\
 M_{\alpha\beta} &= \int_{t-}^{t+} \sigma_{\alpha\beta} \zeta d\zeta .
 \end{aligned} \tag{8}$$

On the curve C bounding the reference surface S, the boundary conditions are

$$\begin{aligned}
 u &= \bar{u} & \text{or } N_{\alpha} + \frac{M_{\alpha}}{R_{\alpha}} &= \bar{N}_{\alpha} + \frac{\bar{M}_{\alpha}}{R_{\alpha}} \\
 v &= \bar{v} & \text{or } N_{\beta} + \frac{M_{\beta}}{R_{\beta}} &= \bar{N}_{\beta} + \frac{\bar{M}_{\beta}}{R_{\beta}} \\
 w &= \bar{w} & \text{or } Q - \frac{\partial M_{\alpha}}{\partial \alpha} &= \bar{Q} - \frac{\partial \bar{M}_{\alpha}}{\partial \alpha} \\
 \frac{\partial w}{\partial n} &= \frac{\partial \bar{w}}{\partial n} & \text{or } -M_n &= -\bar{M}_n
 \end{aligned} \tag{9}$$

where the bar denotes a specified quantity, and, referring to Figure 2, the force resultants are defined by

$$\begin{aligned}
 N_{\alpha} &= N_{\alpha\alpha} \cos \theta + N_{\beta\alpha} \sin \theta \\
 N_{\beta} &= N_{\alpha\beta} \cos \theta + N_{\beta\beta} \sin \theta \\
 Q &= Q_{\alpha\zeta} \cos \theta + Q_{\beta\zeta} \sin \theta \\
 M_{\alpha} &= M_{\alpha\alpha} \cos \theta + M_{\alpha\beta} \sin \theta \\
 M_{\beta} &= M_{\alpha\beta} \cos \theta + M_{\beta\beta} \sin \theta \\
 M_{\alpha} &= -M_{\alpha} \sin \theta + M_{\beta} \cos \theta \\
 M_n &= M_{\alpha} \cos \theta + M_{\beta} \sin \theta
 \end{aligned} \tag{10}$$

In Figure 2, n and s are coordinates tangent to the reference surface which are perpendicular and tangent to the edge of the shell, respectively. Assuming the shell material to be anisotropic, the stress-strain-temperature relation is given by

$$e_{ij} = B_{ijrs} \sigma_{rs} + \alpha_{ij} \Delta T. \quad (11)$$

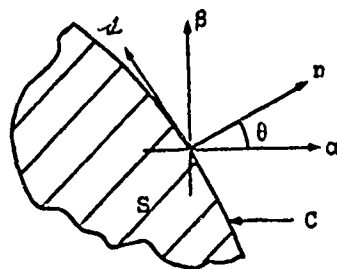


Figure 2. Boundary Condition Geometry

Here, B_{ijrs} are the Cartesian components of the elastic flexibility tensor, α_{ij} are the Cartesian components of the thermal expansion tensor, and ΔT is the temperature change. The elastic flexibility tensor has the symmetries

$$B_{ijrs} = B_{jirs} = B_{ijsr} = B_{rsij}.$$

Assuming the shell to be in a state of plane stress, $\sigma_{\zeta\zeta} = 0$, results in

$$\begin{bmatrix} \sigma_{\alpha\alpha} \\ \sigma_{\beta\beta} \\ \sigma_{\beta\zeta} \\ \sigma_{\alpha\zeta} \\ \sigma_{\alpha\beta} \end{bmatrix} = \begin{bmatrix} B_{1111} & B_{1122} & 2B_{1123} & 2B_{1113} & 2B_{1112} \\ B_{1122} & B_{2222} & 2B_{2223} & 2B_{2213} & 2B_{2212} \\ 2B_{1123} & 2B_{2223} & 4B_{2323} & 4B_{2313} & 4B_{2312} \\ 2B_{1113} & 2B_{2213} & 4B_{2313} & 4B_{1313} & 4B_{1312} \\ 2B_{1112} & 2B_{2212} & 4B_{2312} & 4B_{1312} & 4B_{1212} \end{bmatrix}^{-1} \begin{bmatrix} e_{\alpha\alpha} \\ e_{\beta\beta} \\ 2e_{\beta\zeta} \\ 2e_{\alpha\zeta} \\ 2e_{\alpha\beta} \end{bmatrix} - \begin{bmatrix} \alpha_{\alpha\alpha} \\ \alpha_{\beta\beta} \\ 2\alpha_{\beta\zeta} \\ 2\alpha_{\alpha\zeta} \\ 2\alpha_{\alpha\beta} \end{bmatrix} \Delta T \quad (12)$$

and carrying out the inversion gives

$$\begin{bmatrix} \sigma_{\alpha\alpha} \\ \sigma_{\beta\beta} \\ \sigma_{\beta\zeta} \\ \sigma_{\alpha\zeta} \\ \sigma_{\alpha\beta} \end{bmatrix} = \begin{bmatrix} C_{ij} \\ \text{sym.} \end{bmatrix} \begin{bmatrix} e_{\alpha\alpha} \\ e_{\beta\beta} \\ 2e_{\beta\zeta} \\ 2e_{\alpha\zeta} \\ 2e_{\alpha\beta} \end{bmatrix} - \begin{bmatrix} B_1 \end{bmatrix} \Delta T. \quad (13)$$

The stress resultant-strain-temperature relation for the shell is obtained by using the definition (8). It is

$$\begin{bmatrix} N_{\alpha\alpha} \\ N_{\beta\beta} \\ S_{\alpha\beta} \\ M_{\alpha\alpha} \\ M_{\beta\beta} \\ M_{\alpha\beta} \end{bmatrix} = \begin{bmatrix} D_{ij} \\ \text{sym.} \end{bmatrix} \begin{bmatrix} e_{\alpha\alpha} \\ e_{\beta\beta} \\ \gamma_{\alpha\beta} \\ \kappa_{\alpha} \\ \kappa_{\beta} \\ 2\kappa_{\alpha\beta} \end{bmatrix} - \begin{bmatrix} M_1 \end{bmatrix} \quad (14)$$

The equations of equilibrium (6), the stress resultant-strain-temperature equations (14), and the strain-displacement equations (5) combined result in a set of three fourth order partial differential equations in the three unknowns u , v and w to be satisfied in the region S subject to the boundary conditions (9). These equations form a self-adjoint system and are equivalent

to the following minimum potential energy principle. The functional

$\pi(u, v, w)$, given by

$$\pi = \int_S \left(\frac{1}{2} \begin{bmatrix} \epsilon_{\alpha\alpha} \\ \epsilon_{\beta\beta} \\ \gamma_{\alpha\beta} \\ \kappa_\alpha \\ \kappa_\beta \\ 2\kappa_{\alpha\beta} \end{bmatrix}^T [D_{ij}] \begin{bmatrix} \epsilon_{\alpha\alpha} \\ \epsilon_{\beta\beta} \\ \gamma_{\alpha\beta} \\ \kappa_\alpha \\ \kappa_\beta \\ 2\kappa_{\alpha\beta} \end{bmatrix} - \begin{bmatrix} \epsilon_{\alpha\alpha} \\ \epsilon_{\beta\beta} \\ \gamma_{\alpha\beta} \\ \kappa_\alpha \\ \kappa_\beta \\ 2\kappa_{\alpha\beta} \end{bmatrix}^T [M_i] \begin{bmatrix} u \\ v \\ w \end{bmatrix} - \begin{bmatrix} \bar{Y}_\alpha \\ \bar{Y}_\beta \\ \bar{Y}_\zeta \end{bmatrix} \right) A B d\alpha d\beta$$

$$- \int_{C_2} \begin{bmatrix} u \\ v \\ w \\ \frac{\partial w}{\partial n} \end{bmatrix} \begin{bmatrix} \bar{N}_\alpha + \frac{\bar{M}_\alpha}{R_\alpha} \\ \bar{N}_\beta + \frac{\bar{M}_\beta}{R_\beta} \\ \bar{Q} - \frac{\partial \bar{M}_\alpha}{\partial \alpha} \\ \bar{M}_n \end{bmatrix} ds \quad (15)$$

is to be minimized on those functions u , v , and w which satisfy

the displacement boundary conditions on $C_1 = C - C_2$ and which result in the

displacements u, v , and w together with the rotations $\left(-\frac{1}{A} \frac{\partial w}{\partial \alpha} + \frac{u}{R_\alpha} \right)$ and $\left(-\frac{1}{B} \frac{\partial w}{\partial \beta} + \frac{u}{R_\beta} \right)$ being continuous with piecewise continuous derivatives. Here,

the strains are interpreted as functions of u, v , and w .

It should be noted that these are the same continuity requirements as in a transverse shear shell theory. That is, the displacements and rotations are required to be continuous with piecewise continuous derivatives. In view of the Kirchhoff hypothesis (3) defining the rotations in terms of the displacements, it becomes apparent that an equivalent continuity statement would be ". . . the in-plane displacements u and v continuous with piecewise continuous derivatives together with the out of plane displacement w continuous with continuous derivatives and piecewise continuous second derivatives".

Axisymmetric Geometry

In what follows, the specialization is made for shells whose reference surfaces are portions of an axisymmetric surface. In Figure 3 the reference surface coordinates are $\alpha = \theta$ circumferentially and $\beta = s$, a length coordinate, meridionally.

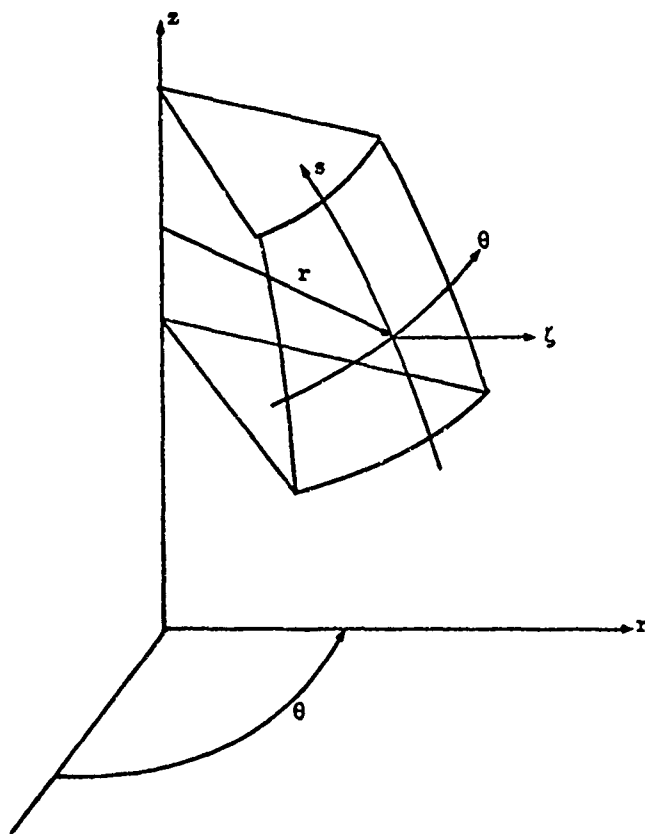


Figure 3. Axisymmetric Shell Geometry

The Lamé coefficients in this case become

$$A = r(s), \quad B = 1. \quad (16)$$

With the r and z coordinates of a meridional line in terms of s , the curvatures are given by the expressions

$$\frac{1}{R_\theta} = \frac{dz/ds}{r}$$

$$\frac{1}{R_s} = \frac{d^2 z}{ds^2} \frac{dr}{ds} - \frac{d^2 r}{ds^2} \frac{dz}{ds}. \quad (17)$$

3. PREVIOUS QUADRILATERAL SHELL ELEMENTS (KB0-KB5)

In the finite element method it is the displacement assumptions within an element which are the chief concern. There are rules and guidelines to follow in making element displacement assumptions [1, 19, 20, 21, 22, 23, 24, 25, 26]. These, of course, are dependent on the problem being treated but beyond that the choice of displacement behavior is arbitrary. The displacement assumptions that provide the best answers together with a reasonable amount of required computing are judged the best. In what follows, a brief account of the previous elements considered is given.

This history is based on the element displacement assumptions tried and the results of these assumptions. The element geometry is an arbitrary quadrilateral on the surface of the shell and within the element an oblique coordinate system is used based on the element geometry [27,28]; see Figure 4.

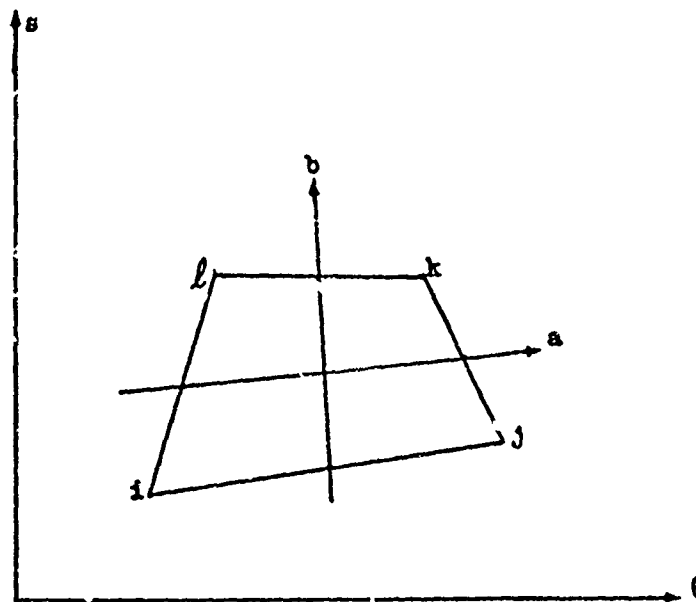


Figure 4
Oblique Element Coordinate System

A transverse shear strain shell theory was used and the displacements allowed in the shell were

$$\begin{aligned}u_{\theta}(\theta, s, \zeta) &= u(\theta, s) + \zeta r(\theta, s) \\u_s(\theta, s, \zeta) &= v(\theta, s) + \zeta s(\theta, s) \\u_{\zeta}(\theta, s, \zeta) &= w(\theta, s)\end{aligned}\tag{18}$$

The displacement assumptions used were:

KB0 (u,v,w,f,g bilinear in a and b.) (20 x 20)

This resulted in a shell element too stiff in bending behavior and requiring a very large number of elements. It was judged unsatisfactory.

KB1 (u,v,f,g bilinear and w bicubic in a and b.) (28 x 28)

This was satisfactory and was used for sometime in a working program, [29]. It is not completely practical, requiring a large number of elements.

KB2 (u,v,w bilinear and f,g bicubic in a and b.) (36 x 36)

This was less satisfactory than KB1 and was dropped.

KB3 A change in the shell theory was made so that $u, v, w, \gamma_{\theta\zeta}$, and $\gamma_{s\zeta}$ were the independent displacement variables;

$$\begin{aligned}u_{\theta}(\theta, s, \zeta) &= u(\theta, s) + \zeta \left(\gamma_{\theta\zeta} - \frac{1}{r} \frac{\partial w}{\partial \theta} + \frac{u}{R_{\theta}} \right) , \\u_s(\theta, s, \zeta) &= v(\theta, s) + \zeta \left(\gamma_{s\zeta} - \frac{\partial w}{\partial s} + \frac{v}{R_s} \right) , \\u_{\zeta}(\theta, s, \zeta) &= w(\theta, s).\end{aligned}\tag{19}$$

$u, v, \gamma_{s\zeta}$ and $\gamma_{\theta\zeta}$ were taken bilinear and w bicubic.

This theory requires that the assembled normal displacement field w be of class C_1 . Since this was impossible to achieve and still keep the element geometry arbitrary, it was abandoned.

KB4 (u, v, w, r , and g bicubic in a and b .) (60 x 60)

The results of these assumptions were excellent, however, excessive computer time made their use impractical.

KB5 (u & v bilinear, f & g biquadratic, and w bicubic in a and b .) (20 x 20)

In this element, the shear strain energy was dropped and a discrete version of the Kirchhoff hypothesis imposed, (zero transverse shear strain). On the basis of the normal deformation w the functions f and g are required to produce zero shear strain at selected points;

$$\gamma_{\theta\zeta} = f + \frac{1}{r} \frac{\partial w}{\partial \theta} - \frac{u}{R_\theta}$$

$$\gamma_{s\zeta} = g + \frac{\partial w}{\partial s} - \frac{v}{R_s}$$

This was an excellent element in bending and computationally very efficient. However, in the presence of curvature the rigid body behavior was restrained to the point of requiring an excessively large number of elements for a satisfactory solution in problems involving gross motion over part of the structure.

The characteristic feature running through all these elements is an increase in their complexity at each step of the way. The element KB6 developed below is again even more complex. All of this is brought on by the requirements of bending and rigid body motion. Experience indicates even in a transverse shear theory, solutions for thin shells can have a very complicated bending behavior and must be representable by the element displacement assumptions for satisfactory numerical behavior.

4. PRESENT QUADRILATERAL SHELL ELEMENT (KB6)

The quadrilateral shell element KB6 (36x36) is based on a "discrete" Kirchhoff hypothesis. The Kirchhoff hypothesis is applied, mesh point by mesh point, to independent reference surface displacement and fiber rotation assumptions. In essence, a shear deformation shell element is reduced to a Kirchhoff shell element by restraining the shear deformations to be zero at the mesh points and deleting the residual transverse shear energy between the mesh points.

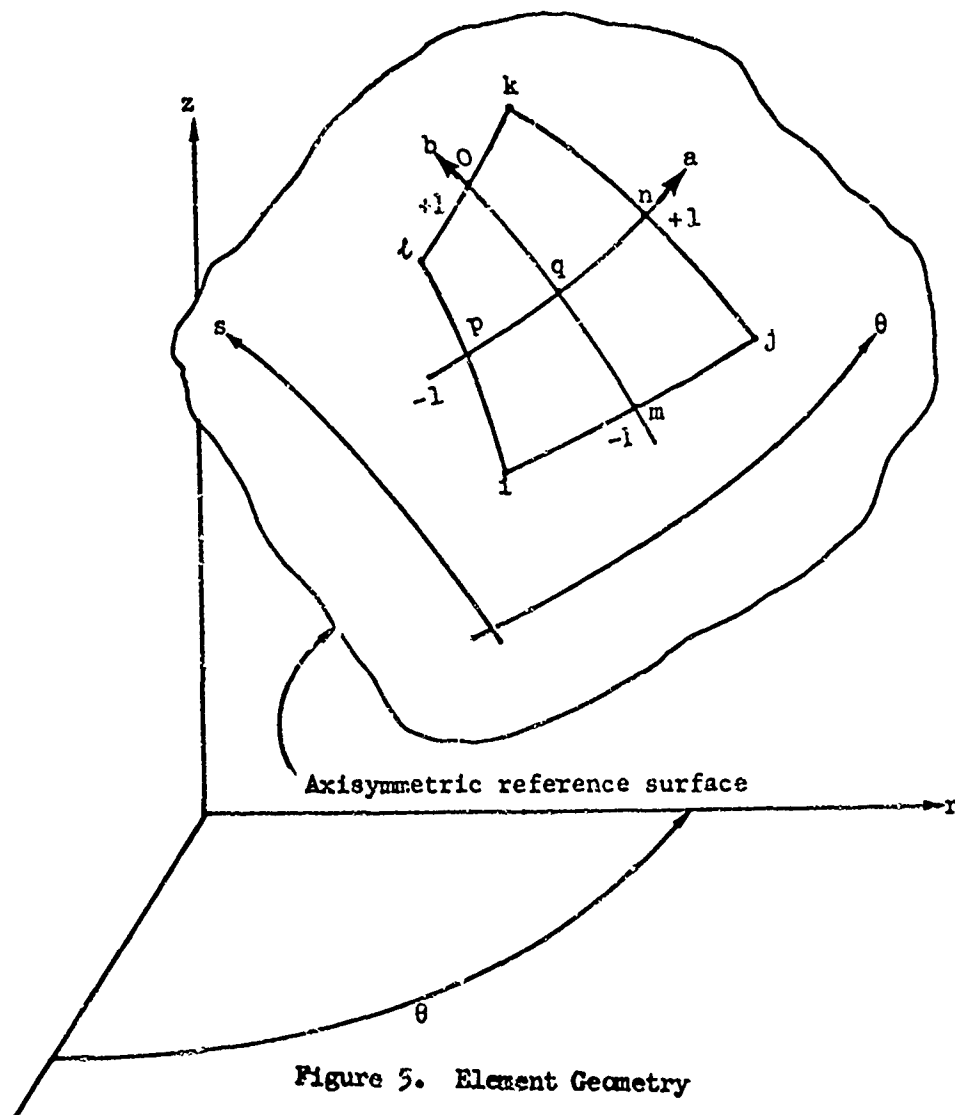


Figure 5. Element Geometry

Element Geometry

Referring to Figure 5, the element is a quadrilateral in the reference surface of the shell. Following Irons[27] and Ergatoudis, Irons and Zienkiewicz[28], an oblique coordinate system a, b is introduced in the quadrilateral element defined by the element geometry. The resulting coordinate transformation is

$$\begin{aligned}\theta(a,b) = & \theta_1 \frac{(1-a)(1-b)}{4} + \theta_j \frac{(1+a)(1-b)}{4} \\ & + \theta_k \frac{(1+a)(1+b)}{4} + \theta_l \frac{(1-a)(1+b)}{4}\end{aligned}\quad (20)$$

$$\begin{aligned}s(a,b) = & s_1 \frac{(1-a)(1-b)}{4} + s_j \frac{(1+a)(1-b)}{4} \\ & + s_k \frac{(1+a)(1+b)}{4} + s_l \frac{(1-a)(1+b)}{4}\end{aligned}$$

The axisymmetric reference surface for the element is given by

$$r = r(a,b) \qquad \theta = \theta(a,b) \qquad z = z(a,b) \qquad (21)$$

The function $\theta(a,b)$ is treated exactly and is given by Eq. (20). The functions $r(a,b)$ and $z(a,b)$ are treated approximately and replaced with bicubic polynomials in a and b . The result is

$$\begin{aligned}
q(a,b) = & h_1(a) h_1(b) q_1 + h_2(a) h_1(b) q_j \\
& + h_2(a) h_2(b) q_k + h_1(a) h_2(b) q_\ell \\
& + h_3(a) h_1(b) \left(\frac{\partial q}{\partial a} \right)_1 + h_4(a) h_1(b) \left(\frac{\partial q}{\partial a} \right)_j \\
& + h_4(a) h_2(b) \left(\frac{\partial q}{\partial a} \right)_k + h_3(a) h_2(b) \left(\frac{\partial q}{\partial a} \right)_\ell \\
& + h_1(a) h_3(b) \left(\frac{\partial q}{\partial b} \right)_1 + h_2(a) h_3(b) \left(\frac{\partial q}{\partial b} \right)_j \\
& + h_2(a) h_4(b) \left(\frac{\partial q}{\partial b} \right)_k + h_1(a) h_4(b) \left(\frac{\partial q}{\partial b} \right)_\ell \\
& + h_3(a) h_3(b) \left(\frac{\partial^2 q}{\partial a \partial b} \right)_1 + h_4(a) h_3(b) \left(\frac{\partial^2 q}{\partial a \partial b} \right)_j \\
& + h_4(a) h_4(b) \left(\frac{\partial^2 q}{\partial a \partial b} \right)_k + h_3(a) h_4(b) \left(\frac{\partial^2 q}{\partial a \partial b} \right)_\ell ,
\end{aligned} \tag{22}$$

where h_1, h_2, h_3 and h_4 are second order Hermite interpolation functions given for both a and b by

$$\begin{aligned}
h_1(\eta) &= \frac{1}{4} (\eta^3 - 3\eta + 2) \\
h_2(\eta) &= -\frac{1}{4} (\eta^3 - 3\eta - 2) \\
h_3(\eta) &= \frac{1}{4} (\eta^3 - \eta^2 - \eta + 1) \\
h_4(\eta) &= \frac{1}{4} (\eta^3 + \eta^2 - \eta - 1)
\end{aligned} \tag{23}$$

The functions h_1, h_2, h_3 , and h_4 are shown in Figure 6.

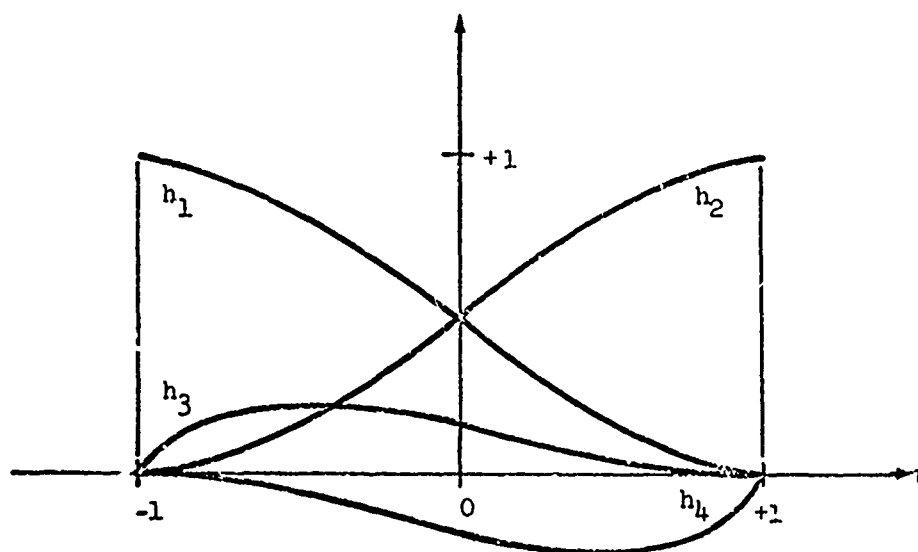


Figure 6. Interpolation functions h_1, h_2, h_3, h_4

The derivatives in a and b are obtained from

$$\left(\frac{\partial q}{\partial a}\right)_m = \left(\frac{\partial s}{\partial a}\right)_m \left(\frac{\partial q}{\partial s}\right)_m, \quad m = i, j, k, l$$

$$\left(\frac{\partial q}{\partial b}\right)_m = \left(\frac{\partial s}{\partial b}\right)_m \left(\frac{\partial q}{\partial s}\right)_m, \quad m = i, j, k, l \quad (24)$$

$$\left(\frac{\partial^2 q}{\partial a \partial b}\right)_m = \left(\frac{\partial^2 s}{\partial a \partial b}\right)_m \left(\frac{\partial q}{\partial s}\right)_m + \left(\frac{\partial s}{\partial a}\right)_m \left(\frac{\partial s}{\partial b}\right)_m \left(\frac{\partial^2 q}{\partial s^2}\right)_m, \quad m = i, j, k, l.$$

The function q represents either r or z . For the r coordinate the derivatives in s are obtained from

$$\left(\frac{\partial r}{\partial s}\right)_m = -\sin \varphi_m, \quad m = i, j, k, l \quad (25)$$

and for the z coordinate the derivatives in s are obtained from

$$\left(\frac{\partial z}{\partial s}\right)_m = \cos \eta_m, \quad m = 1, j, k, \ell \quad (26)$$

For the second derivatives in s, a value based on the change in η from mesh point to mesh point is used. The derivatives needed to calculate the curvatures are obtained from the bicubic expression (22). This treatment of the reference surface is suitable for arbitrary surfaces; however, the expressions (24) will then contain additional terms.

These steps provide the needed flexibility in element geometry and result in an approximate reference surface from which satisfactory curvatures are calculated.

KB6 Element Displacement Assumptions

In the a,b coordinate system a 12 term polynomial is used to define the behavior of the displacements u, v and w [30,31]:

$$\begin{aligned} &\alpha_1 + \alpha_2 a + \alpha_3 b + \alpha_4 a^2 + \alpha_5 ab + \alpha_6 b^2 + \alpha_7 a^3 \\ &+ \alpha_8 a^2 b + \alpha_9 ab^2 + \alpha_{10} b^3 + \alpha_{11} a^3 b + \alpha_{12} ab^3. \end{aligned}$$

In terms of interpolation functions, this deflection shape can be written

as

$$\begin{aligned} u = & \left(l_1(a)h_6(b) + h_6(a)l_1(b) \right) u_1 + \left(l_2(a)h_6(b) + h_7(a)l_1(b) \right) u_j \\ & + \left(l_2(a)h_7(b) + h_7(a)l_2(b) \right) u_k + \left(l_1(a)h_7(b) + h_6(a)l_2(b) \right) u_\ell \\ & + h_3(a)l_1(b)\left(\frac{\partial u}{\partial a}\right)_1 + h_4(a)l_1(b)\left(\frac{\partial u}{\partial a}\right)_j + h_4(a)l_2(b)\left(\frac{\partial u}{\partial a}\right)_k + h_3(a)l_2(b)\left(\frac{\partial u}{\partial a}\right)_\ell \\ & + l_1(a)h_3(b)\left(\frac{\partial u}{\partial b}\right)_1 + l_2(a)h_3(b)\left(\frac{\partial u}{\partial b}\right)_j + l_2(a)h_4(b)\left(\frac{\partial u}{\partial b}\right)_k + l_1(a)h_4(b)\left(\frac{\partial u}{\partial b}\right)_\ell \end{aligned} \quad (27)$$

The displacement v is treated the same. For the displacement w normal to the reference surface, the same polynomial is used plus additional higher order shapes to control the midside normal derivatives:

$$w = \left(l_1(a)h_6(b) + h_6(a)l_1(b) \right) w_1 + \dots + l_4(a)h_4(b) \left(\frac{\partial w}{\partial b} \right)_l \quad (28)$$

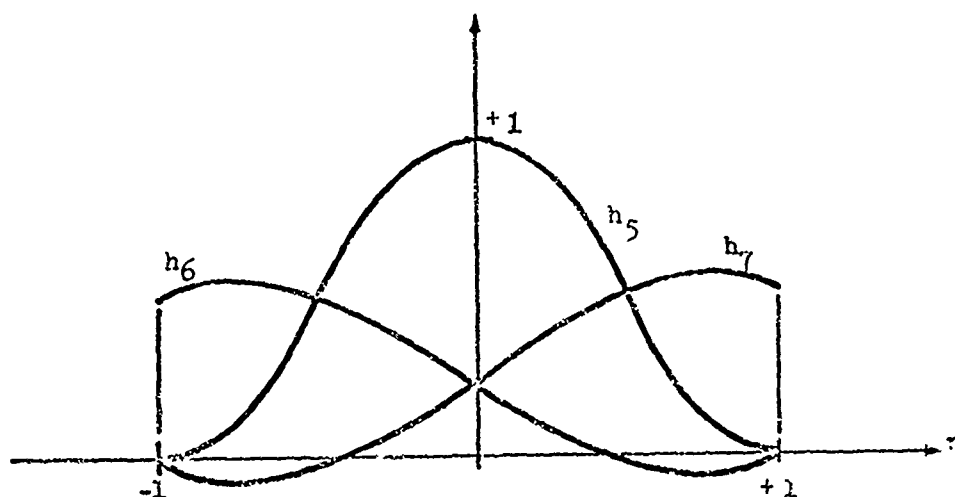
$$+ h_5(a)h_3(b)\gamma_1 + h_4(a)h_5(b)\gamma_2 + h_5(a)h_4(b)\gamma_3 + h_3(a)h_5(b)\gamma_4$$

The variables $\gamma_1, \gamma_2, \gamma_3$ and γ_4 contribute only to the normal derivatives along the sides ij, jk, kl and li , respectively. The values of $\gamma_1, \gamma_2, \gamma_3$ and γ_4 are chosen to make the normal derivative at the midside an average of the normal derivatives at the corners. This is an element by element process since it is geometry dependent. This step provides continuous derivatives of w at each midside node. Without such a correction, the normal derivative to any side would suffer a jump across the element interface for irregular geometries.

The functions h_3 and h_4 are given by eqs. (25). The functions l_1, l_2, h_5, h_6 and h_7 are defined for both a and b by

$$\begin{aligned} l_1(\eta) &= 1/2 (1 - \eta) \\ l_2(\eta) &= 1/2 (1 + \eta) \\ h_5(\eta) &= (\eta^4 - 2\eta^2 + 1) \\ h_6(\eta) &= 1/4 (\eta^3 - 2\eta + 1) \\ h_7(\eta) &= -1/4 (\eta^3 - 2\eta - 1) \end{aligned} \quad (29)$$

The functions h_5, h_6 and h_7 are shown in Figure 7.



Interpolation Functions h_5, h_6, h_7
Figure 7

The rotations f and g are taken to vary biquadratically, defined by their values at the mesh points i, j, k, l, m, n, o, p and q ,

$$\begin{aligned}
 f = & f_i \frac{(a^2 - a)(b^2 - b)}{4} + f_j \frac{(a^2 + a)(b^2 - b)}{4} + f_k \frac{(a^2 + a)(b^2 + b)}{4} \\
 & + f_l \frac{(a^2 - a)(b^2 + b)}{4} + f_m \frac{(1 - a^2)(b^2 - b)}{2} + f_n \frac{(a^2 + a)(1 - b^2)}{2} \\
 & + f_o \frac{(1 - a^2)(b^2 + b)}{2} + f_p \frac{(a^2 - a)(1 - b^2)}{2} + f_q \frac{(a^2 - 1)(b^2 - 1)}{2} \\
 g = & g_i \frac{(a^2 - a)(b^2 - b)}{4} + g_j \frac{(a^2 + a)(b^2 - b)}{4} + g_k \frac{(a^2 + a)(b^2 + b)}{4} \\
 & + g_l \frac{(a^2 - a)(b^2 + b)}{4} + g_m \frac{(1 - a^2)(b^2 - b)}{2} + g_n \frac{(a^2 + a)(1 - b^2)}{2} \\
 & + g_o \frac{(1 - a^2)(b^2 + b)}{2} + g_p \frac{(a^2 - a)(1 - b^2)}{2} + g_q \frac{(a^2 - 1)(b^2 - 1)}{2}
 \end{aligned} \tag{30}$$

Mesh point values of u , v , f and g are continuous and have piecewise continuous derivatives.

Discrete Kirchhoff Hypothesis

Rather than using the above displacement assumptions directly in a transverse shear deformation shell theory, a discrete version of the Kirchhoff hypothesis is used to define the nodal values of the rotations f and g after which the Kirchhoff functional (15) is used. Strictly speaking, the strain energy due to the transverse shear deformations between mesh points should be retained when only a discrete version of the Kirchhoff hypothesis is being employed. However, the convergent solution is a Kirchhoff solution with zero transverse shear deformation energy, so the energy is dropped from the start. This procedure has seen application in the past for various choices of element geometries and displacement shapes [6,32,33,34]. Finite elements which have retained the transverse shear deformations and the associated energy have also been derived [29,35,36,37]. They have been, in many cases, excessively stiff in their behavior and have proven to be only partially suitable for general shell problems.

Here, the pointwise usage of the Kirchhoff hypothesis consists of using Eqs. (3) at the nodal points, $i, j, k, \ell, m, n, o, p$ and q to define the nodal values of f and g in terms of the assumed behavior of u , v and w . In other words, the rotations f and g are forced to produce zero transverse shear strains at the discrete points i through q . In view of the continuity of the derivatives of w , the required continuity of the rotations is preserved. The element KB6 is completely compatible for all convex quadrilateral geometries. If $[u]$ represents the 18 nodal values of the rotations f and g , and if $[v]$ represents the 36 nodal values of u , v , w , and their first derivatives

$\frac{1}{r} \frac{\partial}{\partial \theta}$ and $\frac{\partial}{\partial s}$, the pointwise application of the Kirchhoff hypothesis (3)

can be written in matrix notation as

$$[u] = [BK] [v] \quad (31)$$

Element Stiffness Matrix and Load Vector

In evaluating the Kirchhoff functional (15) for a single element, it is necessary to express the element displacements and strains in terms of the nodal deformations. The displacements are given by

$$\begin{bmatrix} u \\ v \\ w \\ r \\ s \end{bmatrix} = \begin{bmatrix} 5 \times 54 & 54 \times 1 \\ AO & AX \end{bmatrix} \begin{bmatrix} v \\ u \end{bmatrix} \quad (32)$$

Here the displacement assumptions (27), (28) and (30) are being written in matrix form. The strain-displacement relations are given by

$$\begin{bmatrix} \epsilon_{\alpha\alpha} \\ \epsilon_{\beta\beta} \\ \gamma_{\alpha\beta} \\ \kappa_{\alpha} \\ \kappa_{\beta} \\ 2\kappa_{\alpha\beta} \end{bmatrix} = \begin{bmatrix} \frac{1}{r} \frac{\partial}{\partial \theta} & \frac{1}{r} \frac{\partial r}{\partial s} & -\frac{1}{R_{\theta}} & 0 & 0 \\ 0 & \frac{\partial}{\partial s} & -\frac{1}{R_s} & 0 & 0 \\ \frac{\partial}{\partial s} + \frac{1}{r} \frac{\partial r}{\partial s} & \frac{1}{r} \frac{\partial}{\partial \theta} & 0 & 0 & 0 \\ 0 & 0 & 0 & \frac{1}{r} \frac{\partial}{\partial \theta} & \frac{1}{r} \frac{\partial r}{\partial s} \\ 0 & 0 & 0 & 0 & \frac{\partial}{\partial s} \\ -\frac{1}{R_{\theta}} \frac{\partial}{\partial s} + \frac{1}{R_s r} \frac{\partial r}{\partial s} & -\frac{1}{R_s r} \frac{\partial}{\partial \theta} & 0 & \frac{\partial}{\partial s} - \frac{1}{r} \frac{\partial r}{\partial s} & \frac{1}{r} \frac{\partial}{\partial \theta} \end{bmatrix} \begin{bmatrix} u \\ v \\ w \\ r \\ s \end{bmatrix} \quad (33)$$

or in matrix notation

$${}_{6 \times 1} [\epsilon] = {}_{6 \times 5} [d] \begin{bmatrix} u \\ v \\ w \\ f \\ g \end{bmatrix} \quad (34)$$

Equations (32) and (34) are combined to give the strain in terms of the nodal deformations as

$${}_{6 \times 1} [\epsilon] = {}_{6 \times 5} [d] \quad {}_{5 \times 4} [A_0 | A_X] \quad {}_{4 \times 1} \begin{bmatrix} v \\ u \end{bmatrix} = {}_{6 \times 36} [B_0] \quad {}_{36 \times 1} [v] + {}_{6 \times 18} [B_X] \quad {}_{18 \times 1} [u] \quad (35)$$

Using the discrete Kirchhoff hypothesis (31), the nodal values of the rotations [u] may be expressed in terms of the displacements [v]; thus,

$${}_{6 \times 1} [\epsilon] = \begin{bmatrix} {}_{6 \times 36} [B_0] & {}_{6 \times 18} [B_X] & {}_{18 \times 36} [B_K] \end{bmatrix} \quad {}_{36 \times 1} [v] = \begin{bmatrix} {}_{6 \times 36} [B] & {}_{36 \times 1} [v] \end{bmatrix} \quad (36)$$

$$\begin{bmatrix} u \\ v \\ w \\ f \\ g \end{bmatrix} = \begin{bmatrix} {}_{5 \times 36} [A_0] & {}_{5 \times 18} [A_X] & {}_{18 \times 36} [A_K] \end{bmatrix} \quad {}_{36 \times 1} [v] = \begin{bmatrix} {}_{5 \times 36} [A] & {}_{36 \times 1} [v] \end{bmatrix}$$

Thus, for a given quadrilateral element, the functional (15) can be written as

$$\pi([v]) = \frac{1}{2} [v]^T \int_{S_0} [B]^T [D] [B] \, r d\theta ds \quad [v]^T - [v]^T \int_{S_0} [B]^T [M] \, r d\theta ds$$

$$- [v]^T \int_{S_0} [A]^T [\tilde{Y}] \, r d\theta ds - [v]^T \int_{C_0} [A]^T [\tilde{F}] \, d\mathcal{L}. \quad (37)$$

The quadratic form in the nodal deformations is identified as the element stiffness matrix $[k]$;

$$[k] = \iint_{S_0} [B]^T [D] [B] \, r d\Omega ds \quad (38)$$

The linear form in the nodal deformations is identified as the element load vector $[f]$;

$$[f] = \iint_{S_0} [B]^T [M] + [A]^T [\bar{Y}] \, r d\Omega ds + \int_{C_0} [A]^T [\bar{F}] \, d\mathcal{L}. \quad (39)$$

It is understood that the line integral in Eq. (39) is performed only on those elements whose boundaries are subjected to stress boundary conditions.

With this notation, the functional (37) can be written as

$$\pi([v]) = \frac{1}{2} [v]^T [k] [v] - [v]^T [f]. \quad (40)$$

By summing over the elements, the potential energy functional for the entire problem for this family of functions is obtained;

$$\pi([V]) = \frac{1}{2} [V]^T [K] [V] - [V]^T [F], \quad (41)$$

where $[V] = \sum_{\text{elements}} [v],$

$$[K] = \sum_{\text{elements}} [k],$$

$$[F] = \sum_{\text{elements}} [f]. \quad (42)$$

The best approximation is found by minimizing the potential energy functional (41) with respect to those generalized nodal deformations $[\bar{V}]$ that are not involved in the displacement boundary conditions;

$$\frac{\partial \pi}{\partial [\bar{V}]} = [\bar{K}] [\bar{V}] - [\bar{F}] = 0 . \quad (43)$$

After the displacement field has been found, the element strains, stresses and stress resultants are calculated. From Eq. (36), the reference surface strains and curvature are calculated based on the nodal deformations. With these the Cartesian components of the strain tensor (4) are evaluated. From the strains, the Cartesian components of the stress tensor are calculated with Eq. (12). Using the reference surface strain and the stress resultant strain relation (14), the element stress resultants are calculated.

Rigid Body Freedoms

The most difficult rigid body freedoms to obtain are the infinitesimal rotations. This difficulty can be illustrated by examining a square

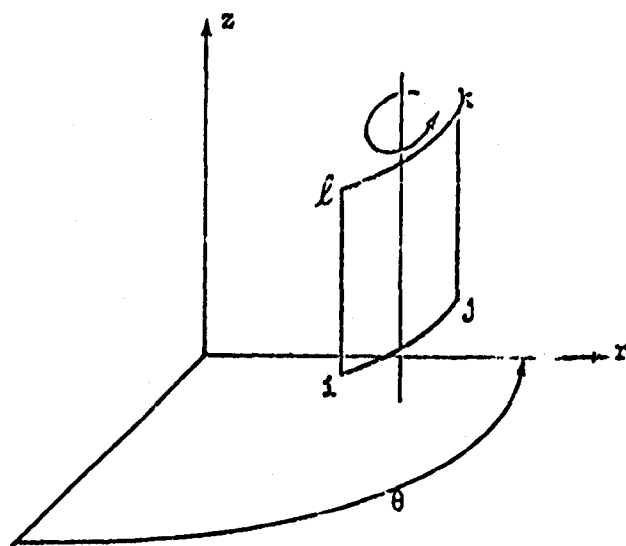


Figure 8
Square Cylindrical Element

cylindrical panel such as the one pictured in Figure 8. A rotation about a generator is one of the infinitesimal rotation freedoms that should produce zero strain energy. The circumferential membrane strain in Eq. (44) is

$$\epsilon_{\theta\theta} = \frac{1}{r} \frac{\partial u}{\partial \theta} + \frac{w}{R_\theta} \quad (44)$$

composed of both a contribution from the circumferential displacement u and the normal displacement w . The rotation about the generator requires at least a linear behavior in w for small angular spans in the circumference to approximate this rotation. If the membrane strain is to remain zero, then the circumferential derivative in u must also be linear and of opposite sign. To achieve this, the displacement u must then be at least quadratic in the circumferential variable θ . It is these rotations of doubly curved elements that preclude the use of the bilinear polynomials, the simplest admissible polynomials for the membrane displacements, found in element KB5. To avoid the practical difficulties of numbering, boundary condition specification and increased equation bandwidths associated with midside nodes and quadratic displacement assumptions, a cubic displacement assumption is used here for the membrane displacements u and v . This approach is comparable with that of Bogner, Fox and Schmit[5] and Greene, Jones and Strone[12] and contrasts to that of Cantin and Clough[8] and Herrmann[15] where explicit trigonometric terms are used for rigid body freedoms. The higher order polynomial is much more usable for arbitrary geometries.

5. NUMERICAL APPROXIMATIONS

In addition to the approximations inherent in the finite element method, additional computational approximations must be made. These are done in order to make the needed computations possible.

Integration

The integrations required for the element stiffness matrix (38) and the element load vector (39) are carried out numerically with a 5-point Gaussian quadrature in the a, b element coordinate system. Referring to Fig. 9, a function is integrated as follows

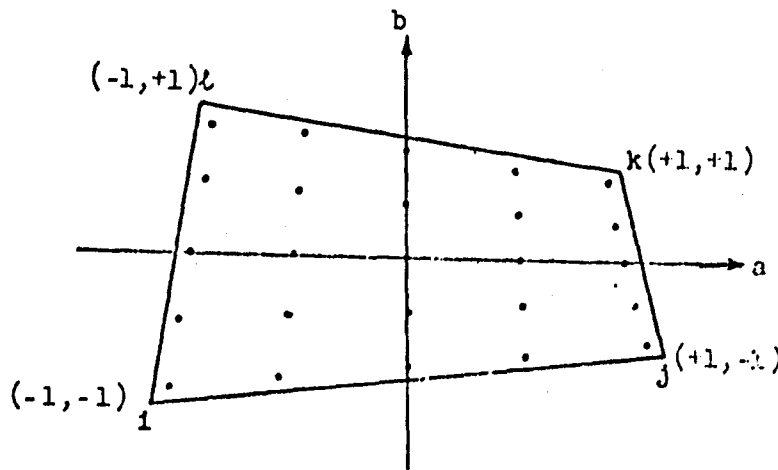


Figure 9. Integration Mesh

$$\iint f(\theta, s) d\theta ds = \iint f(\theta(a, b), s(a, b)) |\det J(a, b)| da db$$

$$= \sum_{m=1}^5 \sum_{n=1}^5 H_m H_n f(\theta(a_m b_n), s(a_m b_n)) |\det J(a_m b_n)| \quad (45)$$

Here the coordinates a_m and b_n , and the weighting coefficients H_m and H_n are specified by the Gaussian quadrature. The values used are shown in Table I.

TABLE I
Gaussian Quadrature Coordinates and Weights, Golub [38]

m, n	a_m, b_n	H_m, H_n
1	- 0.9061798459	0.2369268850
2	- 0.5384693101	0.4786286705
3	0.0	0.5688888889
4	+ 0.5384693101	0.4786286705
5	+ 0.9061798459	0.2369268850

Thickness and Temperature

Information about the thickness of the shell and the temperature at the inside and outside is supplied as data at the nodal points. In order to find the thicknesses and temperature at the interior points, a bilinear interpolation is used

$$\begin{aligned}
 t^+(a, b) &= t_1^+ \frac{(1-a)(1-b)}{4} + \dots + t_\ell^+ \frac{(1-a)(1+b)}{4} \\
 t^-(a, b) &= t_1^- \frac{(1-a)(1-b)}{4} + \dots + t_\ell^- \frac{(1-a)(1+b)}{4} \\
 \Delta T(a, b, \zeta) &= \Delta T_1(\zeta) \frac{(1-a)(1-b)}{4} + \dots + \Delta T_\ell(\zeta) \frac{(1-a)(1+b)}{4}
 \end{aligned} \tag{46}$$

When the elastic constants are temperature dependent, a value at the center of the element layer is used for that layer in the integrals in Eqs. (14).

Meridional Coordinates

For each quadrilateral element the meridional coordinate s is calculated from the nodal point r , z coordinates and the angle between the outward

normal and the positive r-axis at each node. Referring to Fig. 10, the arc length between two nodal points of the same element is approximated by a circular arc between them.

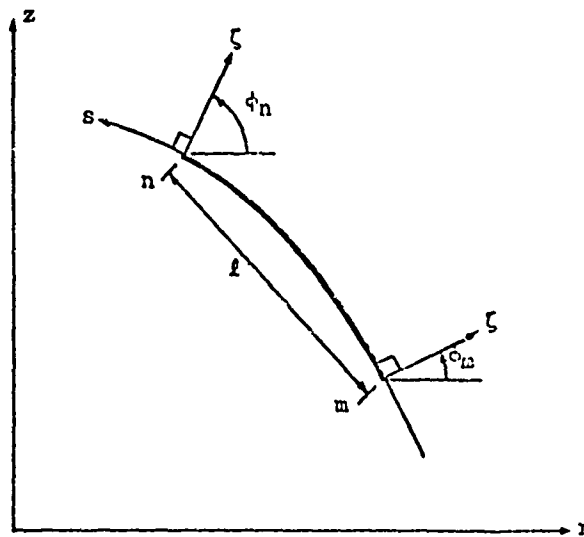


Figure 10. Reference Surface Arc Length

Thus, the meridional distance between m and n is given by

$$s_n - s_m = \frac{l}{(\sin \bar{\varphi}/\varphi)} \quad , \quad (47)$$

where

$$l = \left[(r_n - r_m)^2 + (z_n - z_m)^2 \right]^{1/2}$$

$$\sin \bar{\varphi}/\varphi \approx 1 - \frac{\bar{\varphi}^2}{3!} + \frac{\bar{\varphi}^4}{5!} - \frac{\bar{\varphi}^6}{7!} + \frac{\bar{\varphi}^8}{9!} \quad (48)$$

$$\bar{\varphi} = \frac{1}{2}(\varphi_n - \varphi_m) \quad .$$

For axisymmetric shells, numerous approaches have been taken in approximating

the meridional arc length, the curvatures, and the reference surface [39, 40, 41]. They all bear similarities to one another and to the treatment given here, since it is the same quantities which are being sought, based on a minimum of given information about the shell.

Elastic Constant Integrals

The integrals in Eqs. (14) are not easily evaluated. The following approximations are used.

$$D_{11} = \int_{t-}^{t+} C_{11} \left(1 - \frac{\zeta}{R_0} + \frac{\zeta}{R_s} + \frac{\zeta^2}{R_0^2} - \frac{\zeta^2}{R_0 R_s} + \frac{\zeta^3}{R_0^2 R_s} \right) d\zeta$$

$$D_{12} = \int_{t-}^{t+} C_{12} d\zeta$$

$$D_{13} = \int_{t-}^{t+} C_{15} \left(1 - \frac{\zeta}{R_0} + \frac{\zeta}{R_s} \right) d\zeta$$

$$D_{14} = \int_{t-}^{t+} C_{11} \left(\zeta - \frac{\zeta^2}{R_0} + \frac{\zeta^2}{R_s} + \frac{\zeta^3}{R_0^2} - \frac{\zeta^3}{R_0 R_s} + \frac{\zeta^4}{R_0^2 R_s} \right) d\zeta$$

$$D_{15} = \int_{t-}^{t+} C_{12} \zeta d\zeta$$

$$D_{16} = \int_{t-}^{t+} C_{15} \left(\zeta - \frac{\zeta^2}{R_0} + \frac{\zeta^3}{R_0^2} \right) d\zeta$$

$$D_{22} = \int_{t-}^{t+} C_{22} \left(1 + \frac{\zeta}{R_0} - \frac{\zeta}{R_s} + \frac{\zeta^2}{R_s^2} - \frac{\zeta^2}{R_0 R_s} + \frac{\zeta^3}{R_0 R_s^2} \right) d\zeta \quad (49)$$

$$D_{23} = \int_{t-}^{t+} C_{25} \left(1 - \frac{\zeta}{R_s} + \frac{\zeta^2}{R_s^2} \right) d\zeta$$

$$D_{24} = D_{15}$$

$$D_{25} = \int_{t-}^{t+} C_{22} \left(\zeta + \frac{\zeta^2}{R_\theta} - \frac{\zeta^2}{R_s} + \frac{\zeta^3}{R_\theta^2} - \frac{\zeta^3}{R_\theta R_s} + \frac{\zeta^4}{R_\theta^2 R_s^2} \right) d\zeta$$

$$D_{26} = \int_{t-}^{t+} C_{25} \left(\zeta - \frac{\zeta^2}{R_s} + \frac{\zeta^3}{R_s^2} \right) d\zeta$$

$$D_{33} = \int_{t-}^{t+} C_{55} \left(1 - \frac{\zeta}{R_\theta} - \frac{\zeta}{R_s} + \frac{\zeta^2}{R_\theta^2} + \frac{\zeta^2}{R_\theta R_s} + \frac{\zeta^2}{R_s^2} - \frac{\zeta^3}{R_\theta R_s^2} - \frac{\zeta^3}{R_\theta^2 R_s} + \frac{\zeta^4}{R_\theta^2 R_s^2} \right) d\zeta$$

$$D_{34} = D_{16}$$

$$D_{35} = D_{26}$$

$$D_{36} = \int_{t-}^{t+} C_{55} \left(\zeta - \frac{\zeta^2}{R_\theta} - \frac{\zeta^2}{R_s} + \frac{\zeta^3}{R_\theta^2} + \frac{\zeta^3}{R_\theta R_s} + \frac{\zeta^3}{R_s^2} - \frac{\zeta^4}{R_\theta R_s^2} - \frac{\zeta^4}{R_\theta^2 R_s} + \frac{\zeta^5}{R_\theta^2 R_s^2} \right) d\zeta$$

$$D_{44} = \int_{t-}^{t+} C_{11} \left(\zeta^2 - \frac{\zeta^3}{R_\theta} + \frac{\zeta^3}{R_s} - \frac{\zeta^4}{R_\theta R_s} \right) d\zeta$$

$$D_{45} = \int_{t-}^{t+} c_{12} \zeta^2 d\zeta$$

$$D_{46} = \int_{t-}^{t+} c_{15} \left(\zeta^2 - \frac{\zeta^3}{R_\theta} \right) d\zeta$$

$$D_{55} = \int_{t-}^{t+} c_{22} \left(\zeta^2 + \frac{\zeta^3}{R_\theta} - \frac{\zeta^3}{R_s} - \frac{\zeta^4}{R_\theta R_s} \right) d\zeta$$

$$D_{56} = \int_{t-}^{t+} c_{25} \left(\zeta^2 - \frac{\zeta^3}{R_s} \right) d\zeta$$

$$D_{66} = \int_{t-}^{t+} c_{55} \left(\zeta^2 - \frac{\zeta^3}{R_\theta} - \frac{\zeta^3}{R_s} + \frac{\zeta^4}{R_\theta R_s} \right) d\zeta$$

The thermal loads $[M_1]$ are integrated in the form they are obtained for Eq. (14).

6. EXAMPLE SOLUTIONS

The computer program based on the element KB6 is called SLADE. It is designed specifically for a shell whose reference surface is a portion of an axisymmetric surface; it allows up to five separate layers and up to five separate elastic anisotropic materials with temperature dependent properties. The program handles shells of variable thickness and allows thickness discontinuities along element boundaries; furthermore, it provides for both normal and tangential surface loads and for temperature changes through the

thickness as well as temperature variations over the reference surface. The problems that follow have been used to evaluate the program and the analysis.

Curvature Study

The curvatures resulting from the approximated reference surface are among the important parts of the analysis that must be examined. This can be done by considering a spherical shell. Figure 11 shows the maximum meridional curvature error occurring as a function of the number of finite elements used along the meridian of the sphere. It can be seen that, with eight elements spread over a 90-degree segment of a meridian, the curvature calculations begin to depend more on the accuracy of the input data than on the approximations to the reference surface. The input information for this study is accurate to five digits. The circumferential curvature errors are an order of magnitude smaller. A more difficult situation is encountered with an arbitrary element on a parabolic shell. Figure 12 shows such an element. For this element the outward normal turns through an angle of 9 degrees in the meridional direction and through an angle of 40 degrees in the circumferential direction. The maximum error in the meridional curvature is 3.95 percent, and the maximum error in the circumferential curvature is 0.070 percent.

Membrane Study

A relatively simple membrane problem requiring a curved element and involving a very nearly degenerate geometry is a sphere under internal pressure. Using the same geometry and mesh as in the curvature study, the errors in the radial displacement and the in-plane stress resultant are shown in Figures 13 and 14. The element at the pole is very nearly degenerate. The two nodal points at the pole have radial positions of $r = 10^{-4}$ inches. This situation does not present any difficulties for this problem.

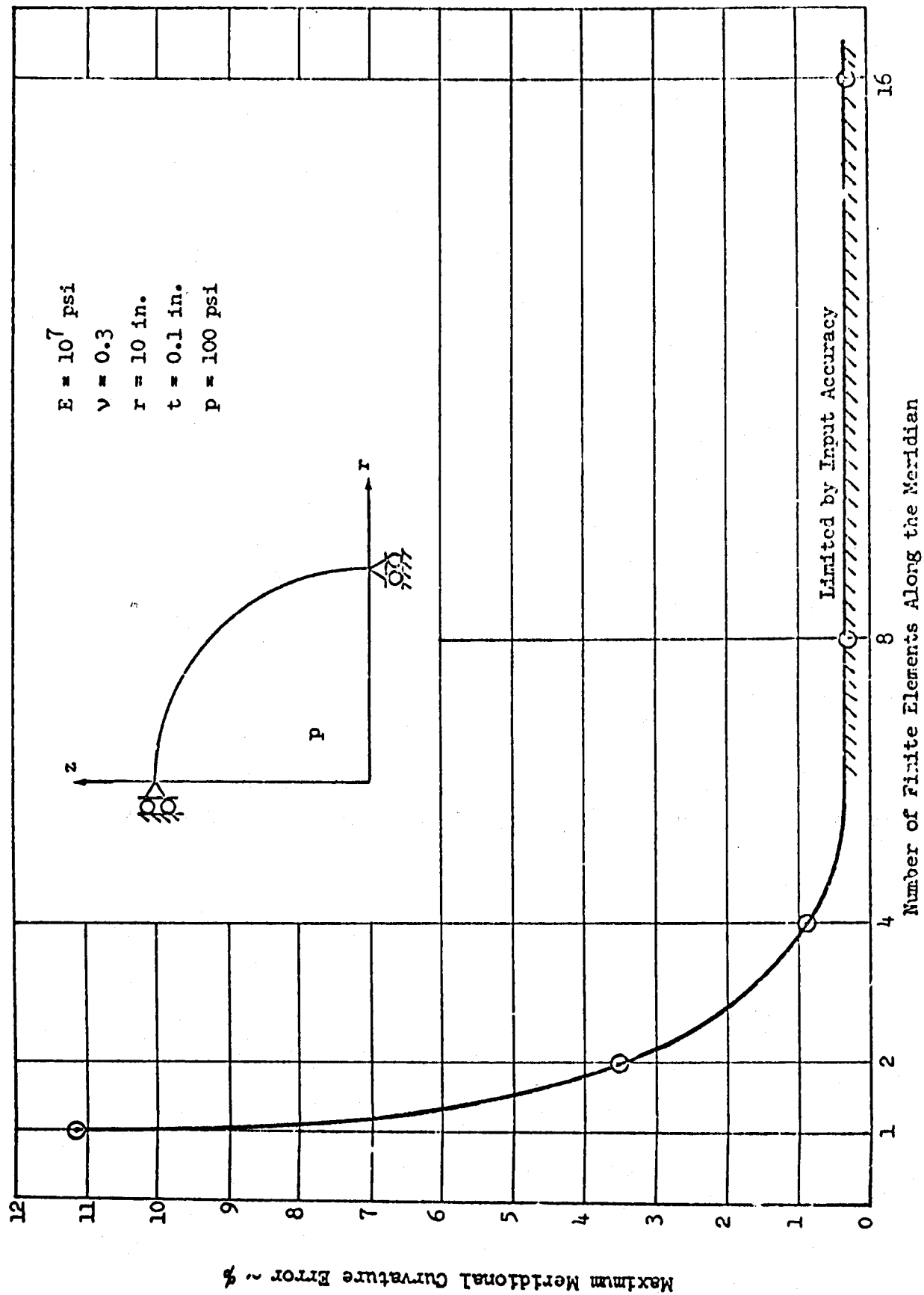
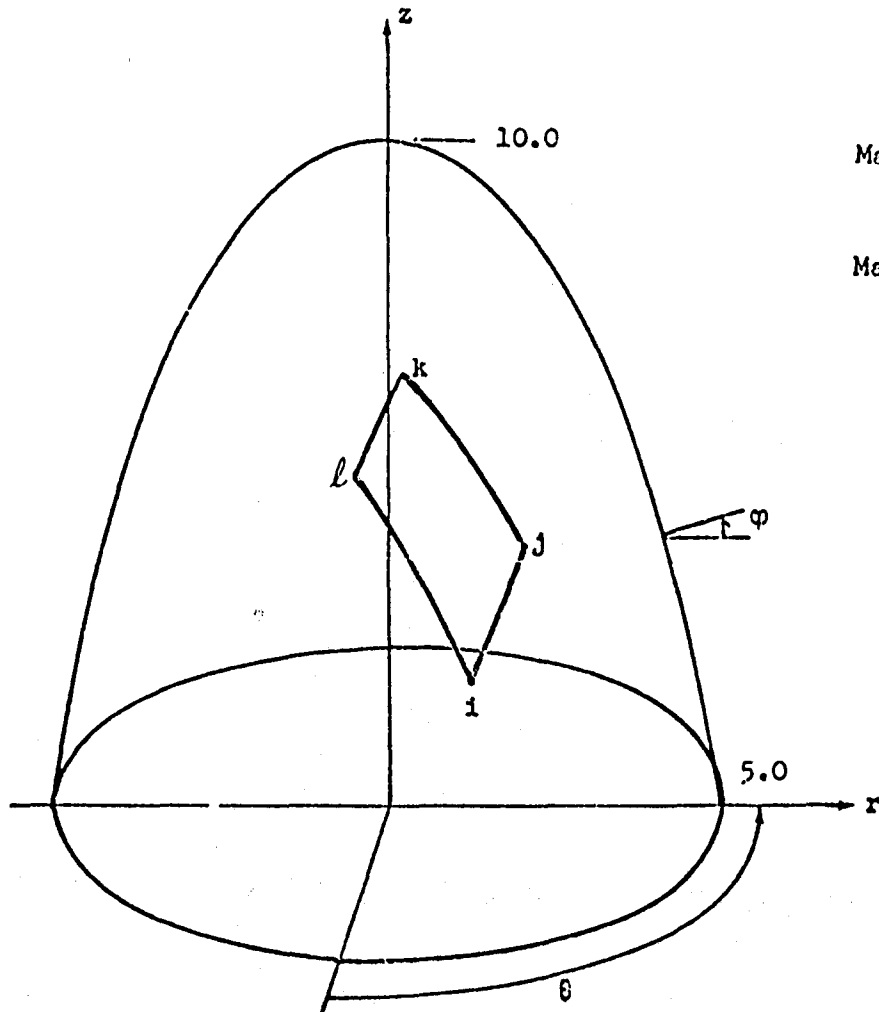


Figure 11. Curvature Behavior with Decreasing Element Size

Nodal Point Coordinates & Curvatures

	r	θ	z	φ	$\frac{1}{R_\theta}$	$\frac{1}{R_\varphi}$
i	4.0	25.0°	3.6	17.3°	.239	.021
j	3.5	40.0°	5.1	19.6°	.269	.030
k	2.5	15.0°	7.5	26.6°	.358	.072
l	3.0	0.0°	6.4	22.6°	.308	.046



Maximum error in $\frac{1}{R_\theta}$ is 0.070%

Maximum error in $\frac{1}{R_\varphi}$ is 3.95%

Figure 12 Curvature Study

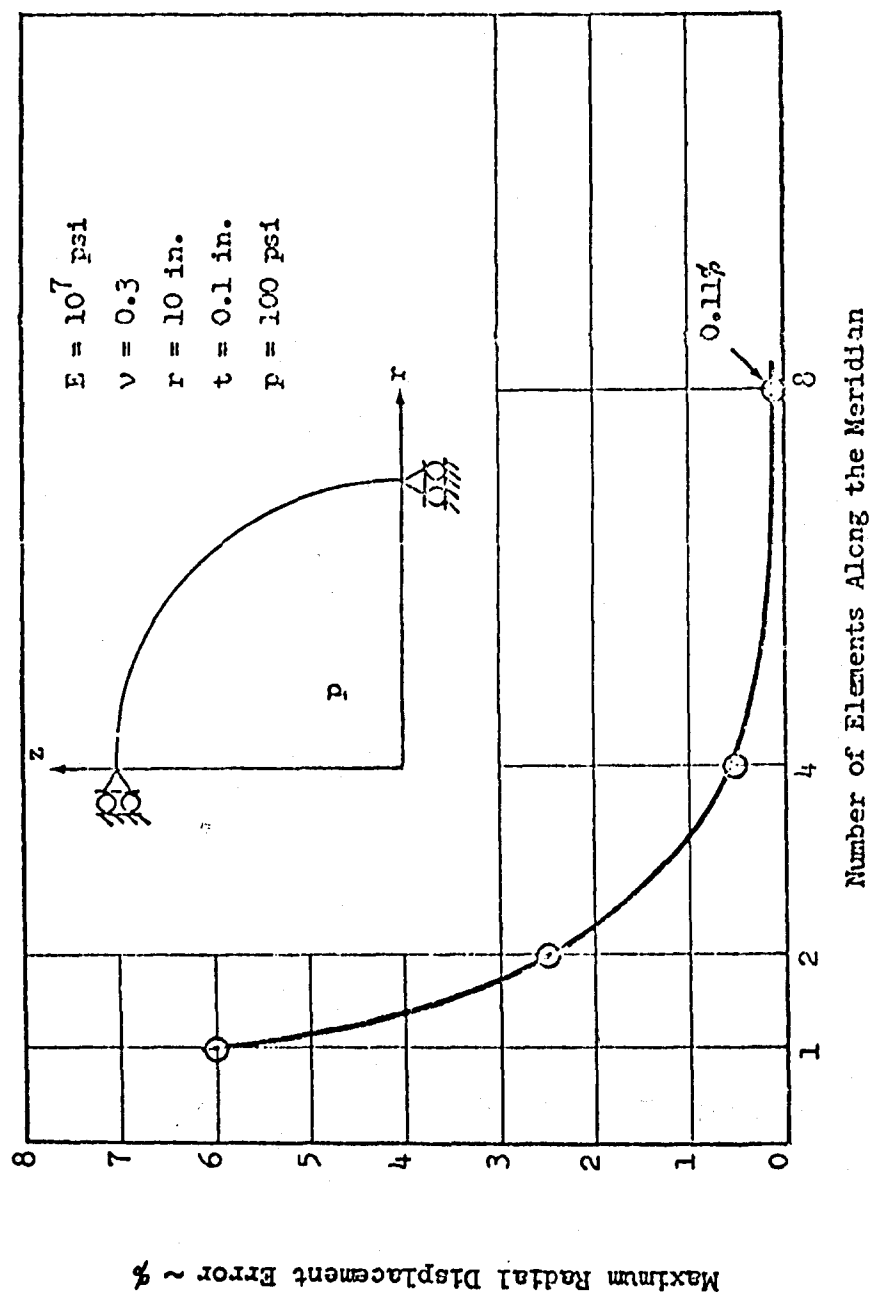


Figure 13. Displacement Errors for Decreasing Element Size

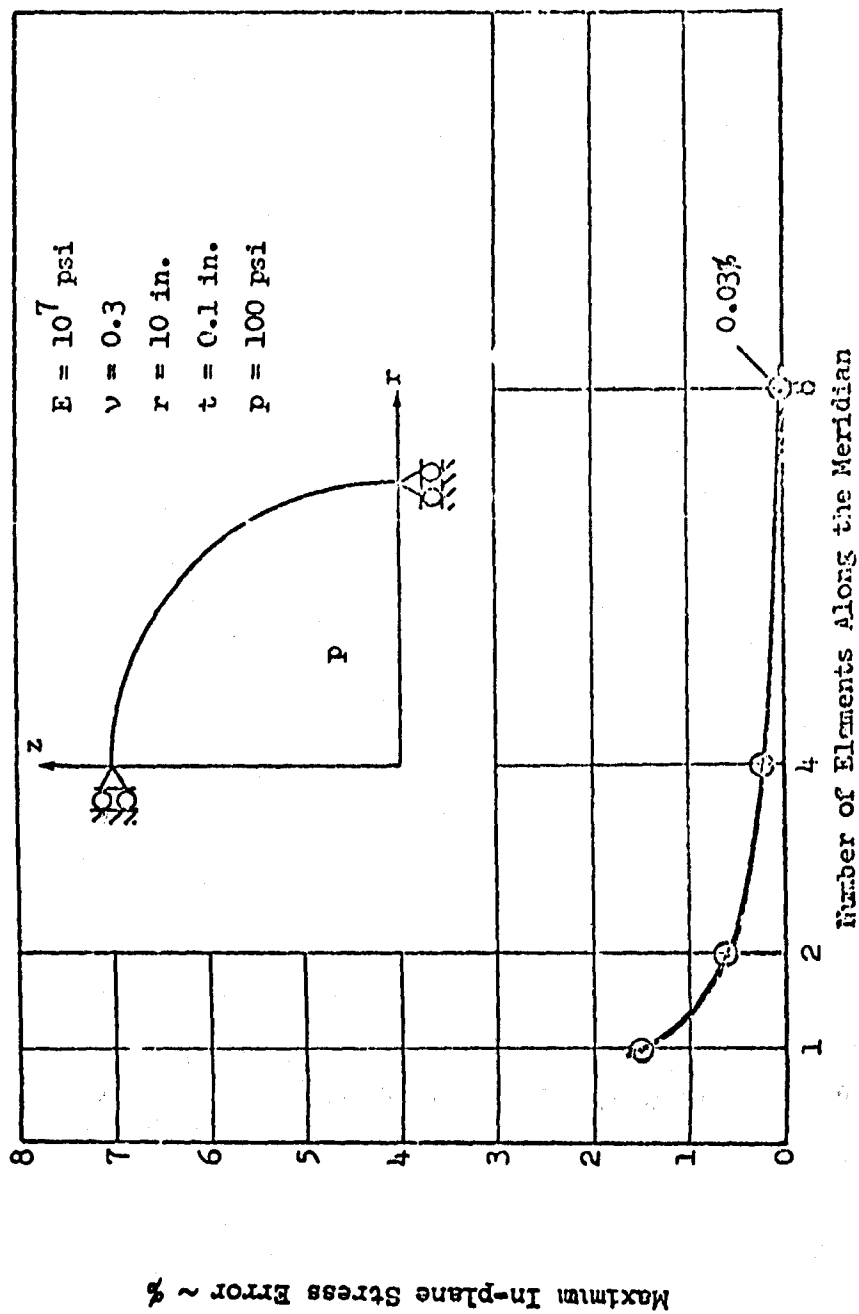


Figure 14. Stress Errors for Decreasing Element Size

Bending Study

Contained in this analysis as a special case is an arbitrary quadrilateral flat plate element. As a comparison with existing flat plate elements, a portion of the thorough study of Clough and Tocher [11] was repeated. Using the symmetry of the problem, a quadrant of a simply supported uniformly loaded square plate was analyzed. Shown in Fig. 15 is the convergence behavior of the KB6 element compared with the elements examined by Clough and Tocher. The ACM element, Adini-Clough-Melosh, is a rectangular element based on a 12-term polynomial. The M element, Melosh, is a rectangular element based on physical reasoning. The P element, Papenfuss, is a rectangular element based on an incomplete bicubic polynomial. The HCT element, Hsieh-Clough-Tocher, is a triangular element based on three subtriangles with preferred polynomial expansions leading to a continuous displacement w with continuous derivatives $\partial w/\partial x$ and $\partial w/\partial y$. The complete study and references to these elements are contained in Reference [11].

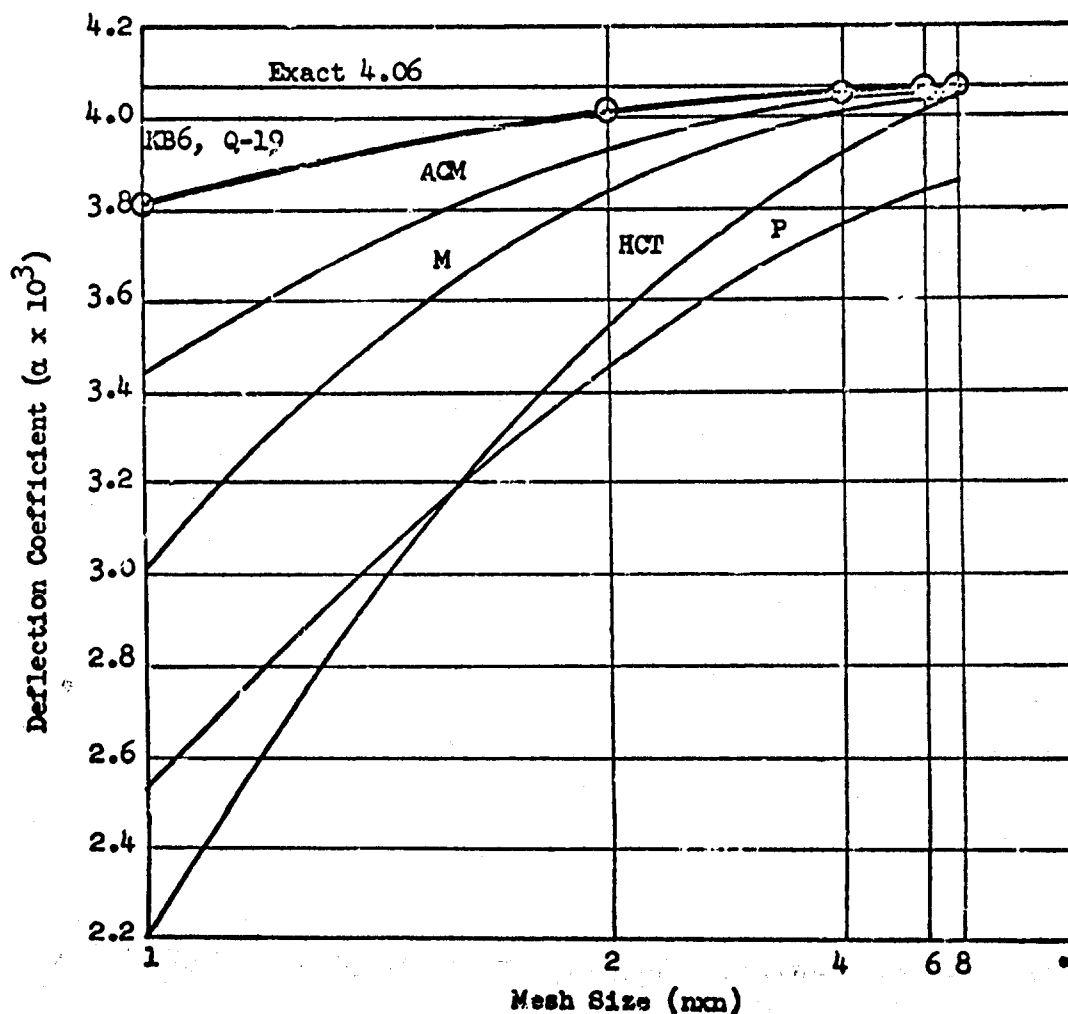


Fig. 15 Deflection Coefficient Behavior with Decreasing Element Size, $\alpha = \frac{w_0 D}{q a^4}$

Also contained on Figure 15 is a quadrilateral element Q-19, based on four triangles which in turn are composed of three subtriangles each. Midside nodes are employed on the interior sides and constraints on the four exterior sides to provide compatibility. The element is by Clough and Felippa [42].

The pinched cylinder is a relatively simple bending problem requiring a curved element. The simply supported cylinder, pictured in Figure 16, is loaded by point loads on a diameter midway along its length. Along the simply supported boundary the radial deflection w , the circumferential deflection u , the axial load N_s and the bending moment M_n are all zero. By using the symmetry of the problem only one eighth of the cylinder requires a mesh. The dimensions were selected to provide a square $n \times n$ mesh over the region. Figure 17 shows the deflection behavior both under a load and at 90° to a load when the mesh is refined. For the case of a 1×1 mesh and a 2×2 mesh the answers were very low reflecting the poor representation of rigid body modes for elements spanning 90 and 45 degree sectors. The closed form solution comes from Valsov[43], page 394, based on his exact theory of cylindrical shells, page 298. Although the deflection is plotted non-dimensionally, the problem cannot be nondimensionalized and depends on Poisson's ratio and the radius to thickness ratio.

Concentration Study

Lekkerkerker[44] and Van Dyke[45] have both analyzed an infinite cylinder under axial load with a circular cutout. The problem has two planes of symmetry which are utilized in the analysis (see Figure 18). The meshes used, shown in Figures 19 and 20, are irregular meshes on the surface of the cylinder with several nearly degenerate elements. They are located in relatively quiet regions of the problem and are not recommended for use

where the answers are of interest. The results of these analyses are shown in Table II along with the results of VanDyke[46]. In Table II, σ_m is the membrane stress, σ_b is the bending part and σ_∞ is the membrane stress at infinity. It should be noted that the plot programs connect the nodal points with straight lines and do not reflect the fact that the mesh is on the reference surface of the cylinder.

Table II
Stresses for a Cylinder Under Axial
Tension with a Circular Cutout

	VanDyke[46]	Finite Element Solution Coarse	Finite Element Solution Fine
σ_m/σ_∞ @ A	3.60	3.44 (4.6%)	3.59 (.3%)
σ_b/σ_∞ @ A	$\pm .59$	$\pm .55$ (7.4%)	$\pm .55$ (7.4%)
σ_m/σ_∞ @ B	-1.25	-1.08 (15.7%)	-1.18 (5.4%)
σ_b/σ_∞ @ B	$\pm .809$	$\pm .806$ (.4%)	$\pm .812$ (.4%)

A is at the side of the hole at $r\theta = 1.0$, $z = 0.0$

B is at the top of the hole at $r\theta = 0.0$, $z = 1.0$

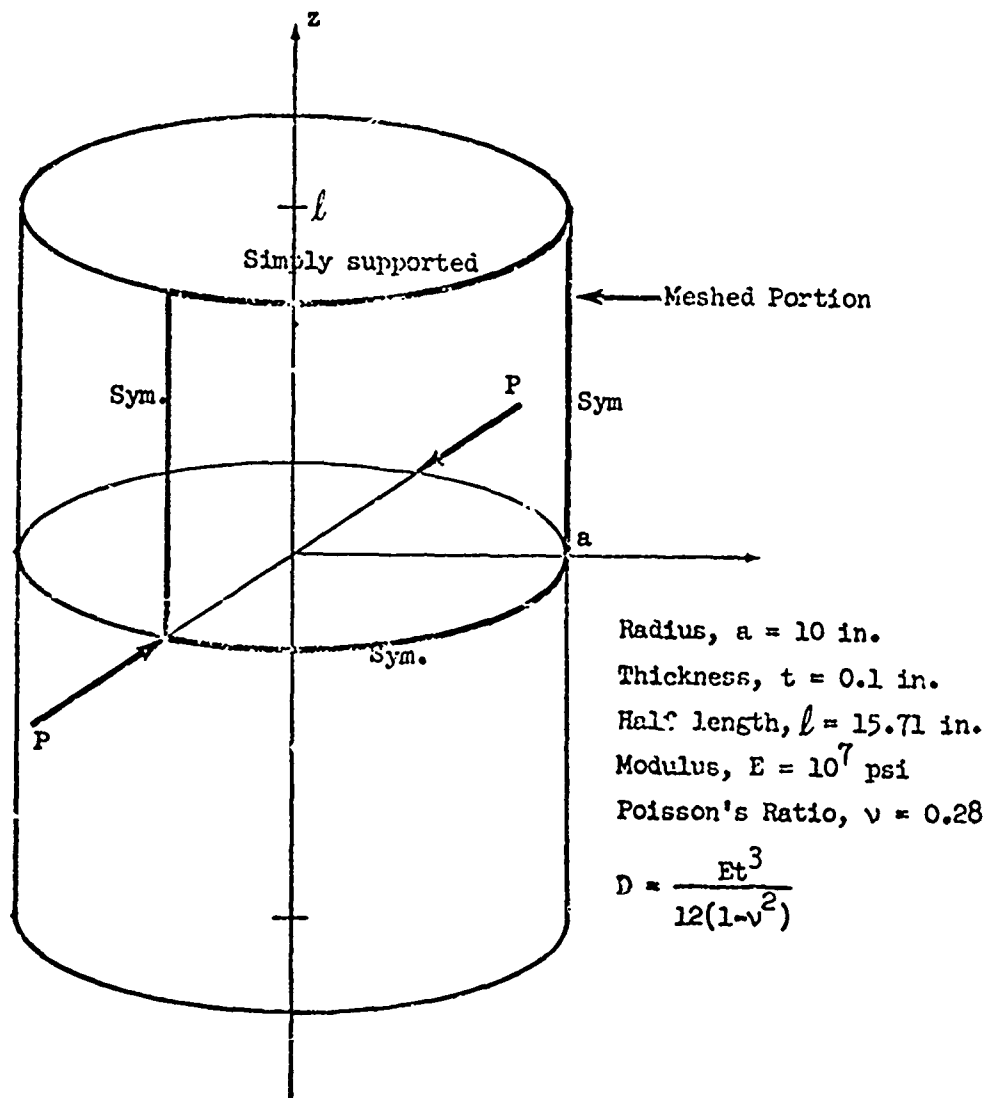


Figure 16.

Simply Supported Cylinder Meshed by Point Loads

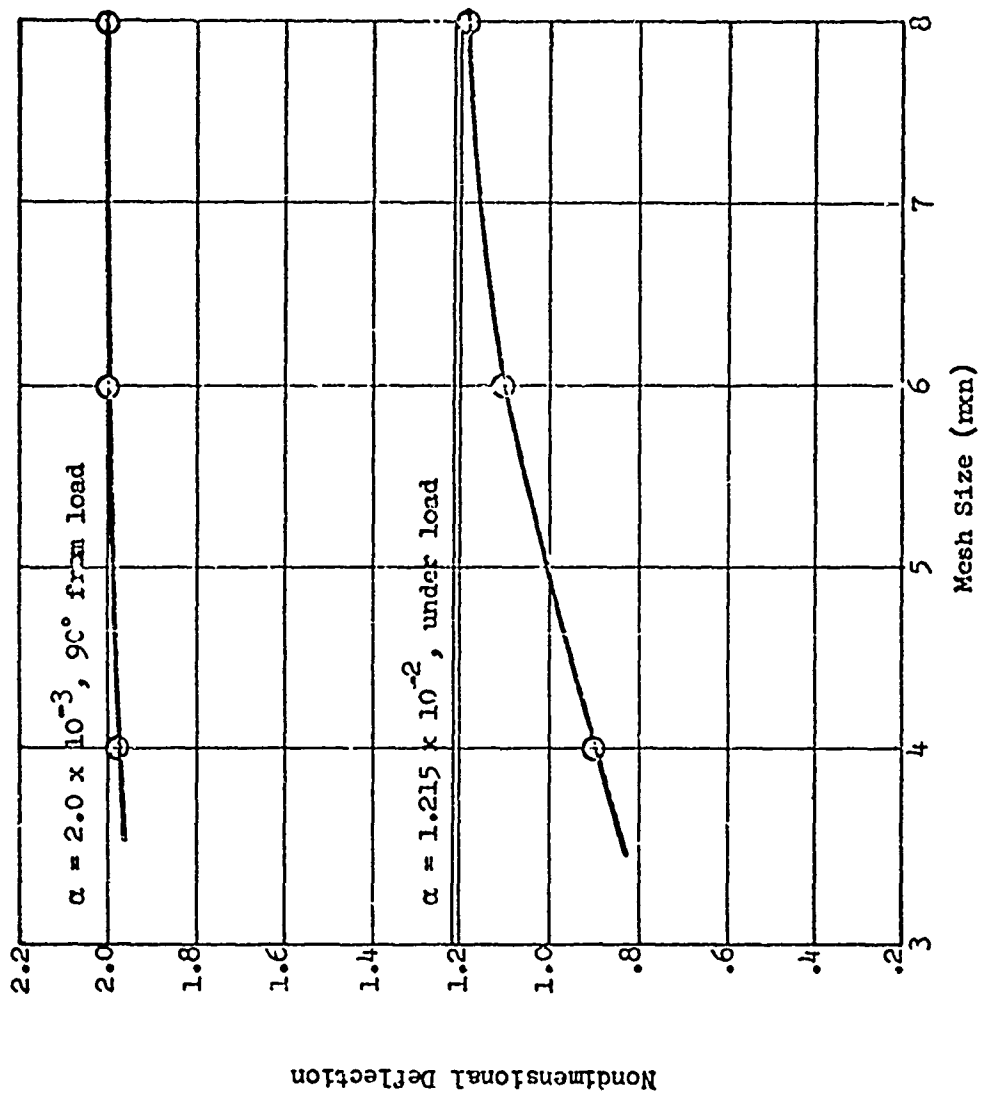


Figure 17.

Radial Deflection Behavior for Decreasing Mesh Size, $\alpha = \frac{4 D \ell^4}{a^3}$

Radius 9.1"
Thickness 0.091"
Half Length 45.0"
Hole Radius 1.0"
Loaded in Uniform
Tension
Poisson's ratio 0.28

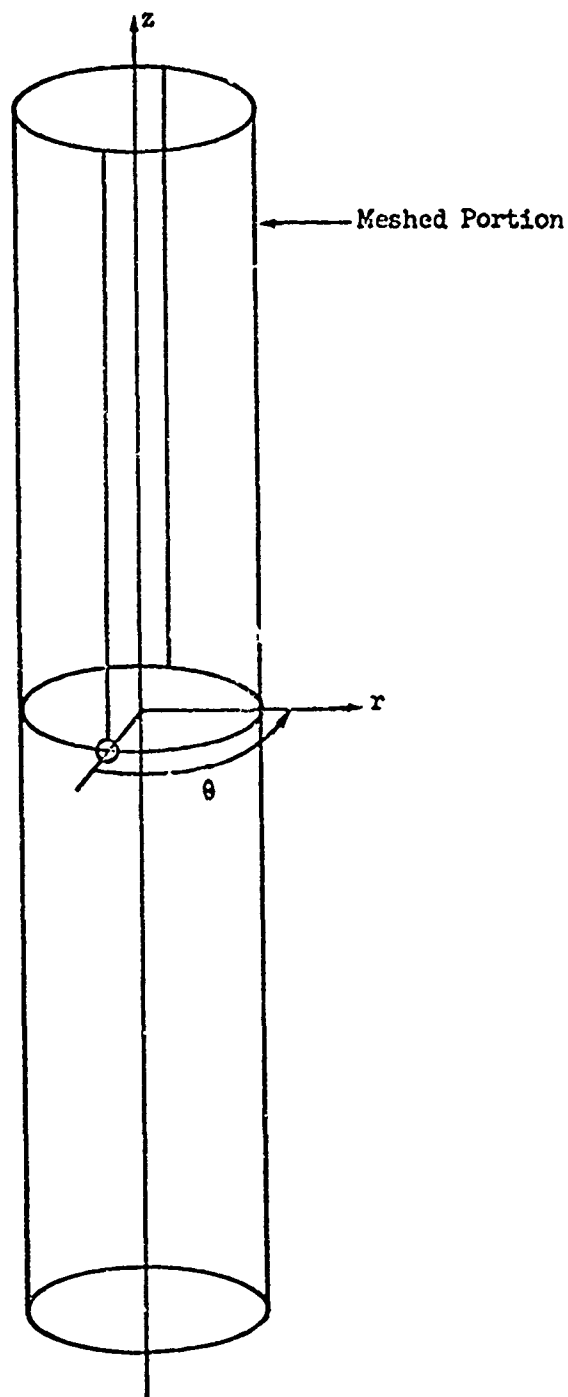
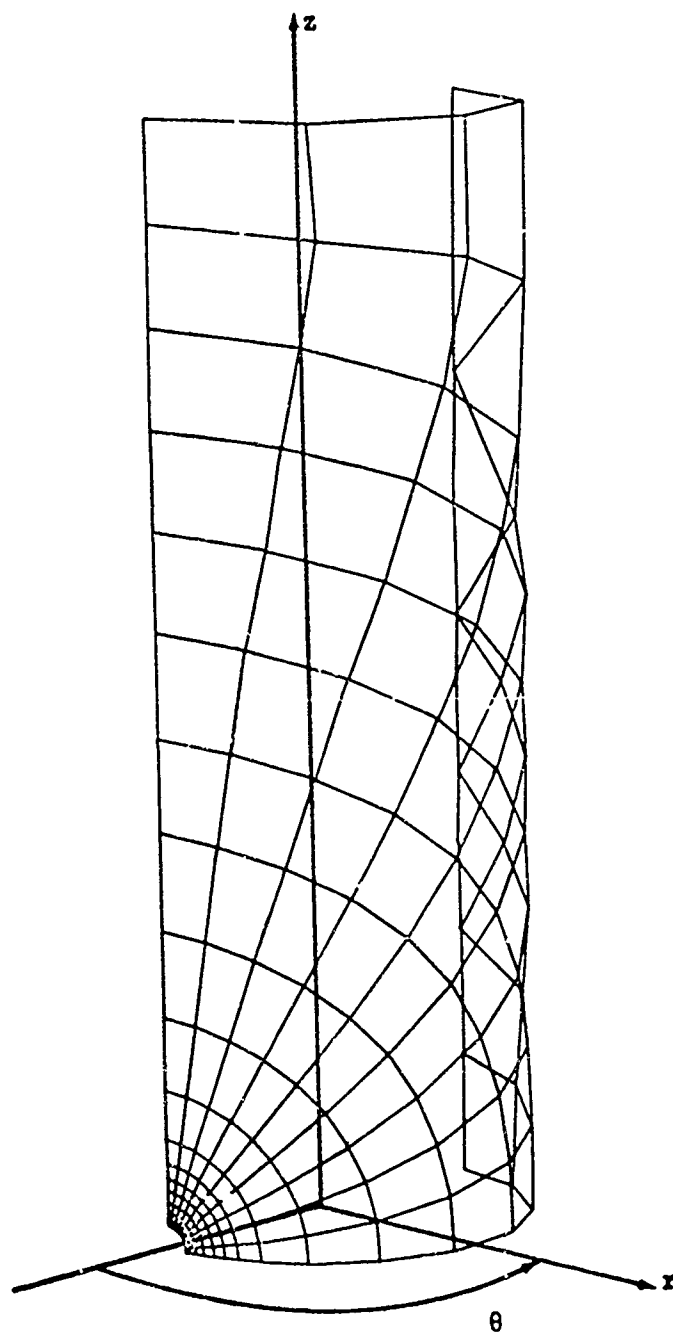


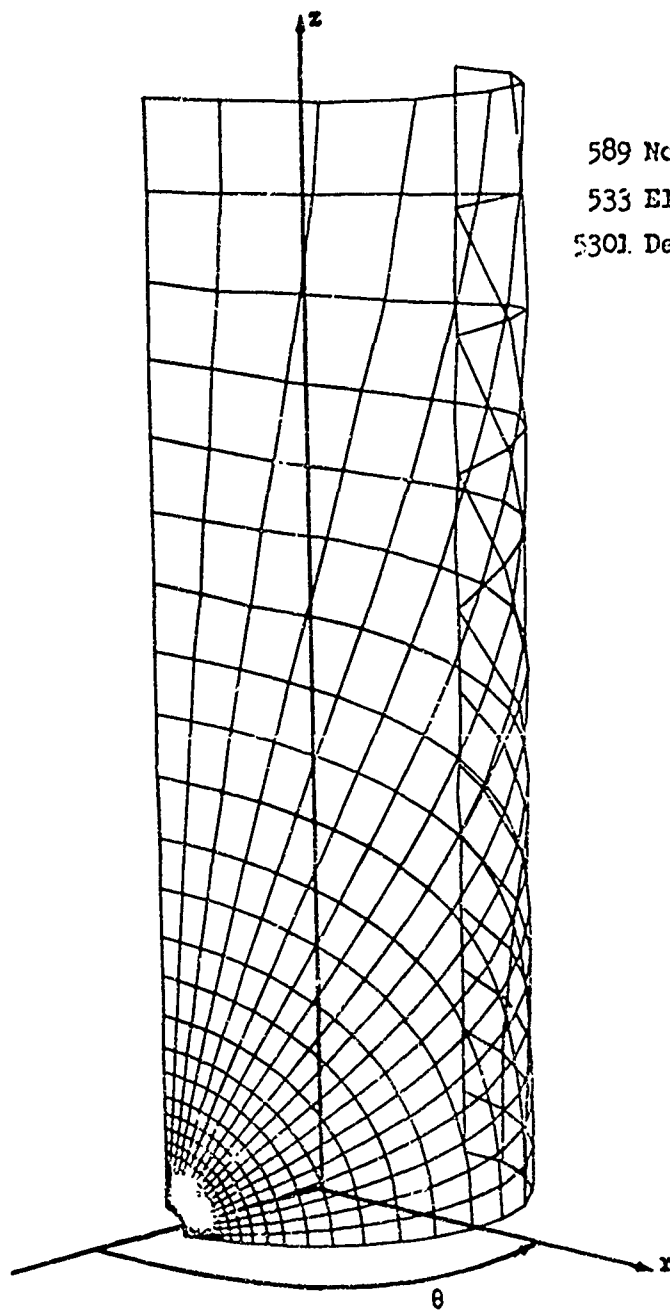
Figure 18.

Cylinder with a Circular Cutout Loaded in Tension



176 Nodal Points
148 Elements
1534 Degrees of Freedom

Figure 19. Coarse Mesh Layout



589 Nodal Points
533 Elements
5301 Degrees of Freedom

Fig. 20. Fine Mesh Layout

A relatively simple stress concentration bending problem requiring a doubly curved element and involving a very nearly degenerate geometry is the point loaded sphere. Using the same geometry and mesh as in the curvature and membrane studies, the membrane stress resultants for sixteen uniformly spaced elements are shown in Figure 23. The element at the pole is very nearly degenerate. The two nodal points at the pole have radial positions of $r = 10^{-4}$ inches and the point load is applied as a distributed shear load on this circle. The closed form solution was obtained from Flugge [47], page 350.

Chernyshev [48] has provided an approximate value for the deflection under the point load. His expression gives -4.13×10^{-4} inches as an upper bound for this problem and the numerical value from SLADE for sixteen elements is -3.91×10^{-4} inches.

Reference Surface Location Study

Of considerable interest is the effect the location of the reference surface has on the answers for small radius to thickness ratios. The plane strain ring in Figure 24 has been analyzed for a half cosine temperature load. Three cases are considered; one with the reference surface on the inside, one with the reference surface in the middle and one with the reference surface on the outside. The results are presented in Table VII along with a closed form solution. The results indicate a very slight sensitivity to reference surface location. The displacements vary by something less than 1%, while the stresses vary by about a half a percent.

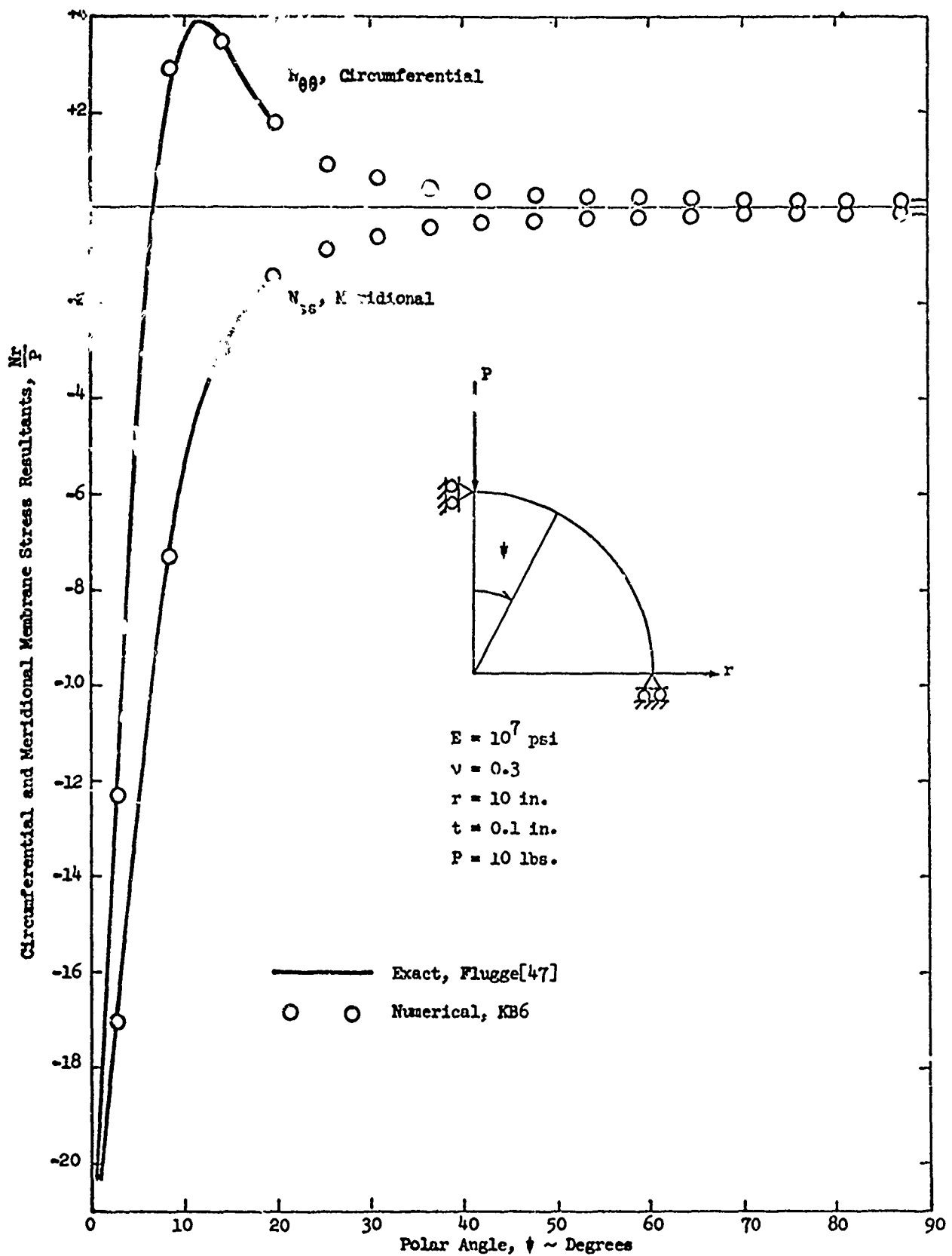
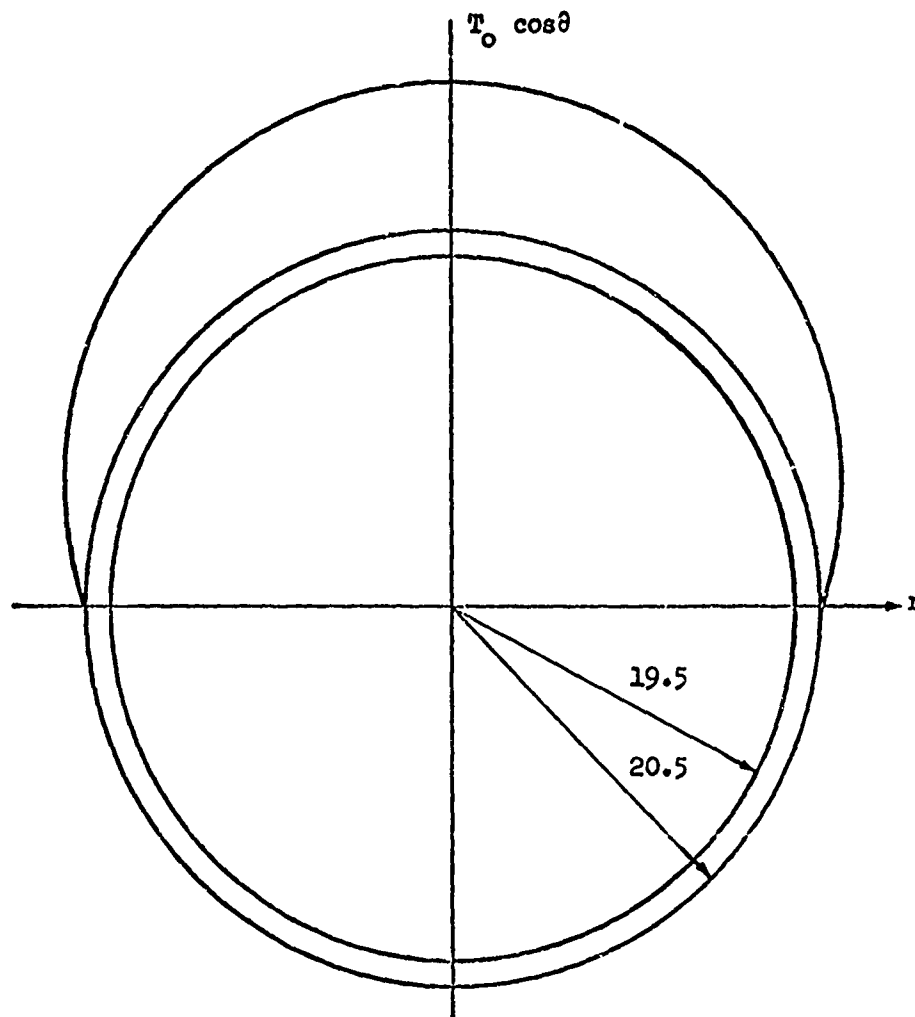


Figure 21. Sphere Stressed by Point Loads



Modulus, $E = 10^7$ psi

Poisson's Ratio, $\nu = 0.3$

Coef. of Thermal Expansion, $\alpha = 10^{-6}$

Peak Outside Temperature, $T_0 = 100^\circ\text{F}$

Inside Temperature = 0

(temperature linear in r)

Figure 22

Circular Ring Loaded by a Half Cosine Temperature
Distribution on the Outside

Table III

The Effect of Reference Surface Location
on
Deflection and Stress Predictions in a Thick Ring

Reference Surface on the Inside

	Diameter Change Under Peak Temperature	Outside Stress Under Peak Temperature	Inside Stress Under Peak Temperature
16 Elements @ 11.25°	.00795 in.	-584 psi	586 psi
Exact Solution	.00798 in.	-587. psi	589. psi

Reference Surface in the Middle

	Diameter Change Under Peak Temperature	Outside Stress Under Peak Temperature	Inside Stress Under Peak Temperature
16 Elements @ 11.25°	.00791 in.	-585. psi	587 psi
Exact Solution	.00794 in.	-587. psi	589. psi

Reference Surface on the Outside

	Diameter Change Under Peak Temperature	Outside Stress Under Peak Temperature	Inside Stress Under Peak Temperature
16 Elements @ 11.25°	.00794 in.	-584. psi	586. psi
Exact Solution	.00796 in.	-587. psi	589. psi

Rigid Body Mode Study

The deformation assumptions used to derive an element stiffness matrix may not contain exact rigid body deformations. Rigid body deformations are trigonometric in character and are only approximated by polynomials. As a result, a stiffness matrix can predict restoring forces for rigid body displacements. The strain-displacement relations used in KB6 give zero strains for rigid body translations and infinitesimal rotations for any geometry. An eigenvalue examination of a stiffness matrix will reveal the energy associated with given deformations as well as with rigid body motions. Three KB6 elements in each of three thicknesses were examined. In all cases six zero eigenvalues were present, one for each of the six rigid body motions. This study is summarized in Table IV.

Table IV

A Summary of the Non-Zero and Zero Eigenvalues
Occurring for Various Element Curvatures

	1"x1" Flat Plate Element $R = \infty$				1"x1" Cylindrical Element $R = 10"$			1"x1" Spherical Element $R = 10"$		
	$t = 1.0"$	$t = 0.5"$	$t = 0.1"$		$t = 1.0"$	$t = 0.5"$	$t = 0.1"$	$t = 1.0"$	$t = 0.5"$	$t = 0.1"$
Maximum Straining	1.69×10^7	8.47×10^6	1.69×10^6		1.69×10^7	8.48×10^6	1.69×10^6	1.70×10^7	8.50×10^6	1.70×10^6
Minimum Straining	4.48×10^4	2.24×10^4	4.02×10^2		4.49×10^4	2.24×10^4	4.02×10^2	4.47×10^4	2.23×10^4	4.02×10^2
Maximum Rigid Body	10^{-7}	10^{-8}	10^{-9}		10^{-1}	10^{-2}	10^{-4}	10^{-2}	10^{-3}	10^{-5}
Minimum Rigid Body	10^{-9}	10^{-9}	10^{-11}		10^{-9}	10^{-8}	10^{-10}	10^{-7}	10^{-8}	10^{-8}

7. CONCLUSIONS AND OBSERVATIONS

The element KB6 represents a workable shell element. Its geometry is an arbitrary quadrilateral allowing irregular boundaries. It is a compatible element corresponding to physical reality. It accounts for the coupling behavior induced by the reference surface curvature by using shell theory strain displacement relations in the strain energy computations. It is an efficient element requiring only the formation of a single element per quadrilateral, since it has no subelement breakdown.

In retrospect, the advice offered by Greene, Jones and Strone[12] in the selection of shell element displacement assumptions is excellent. "The rigid body motion of an element must be represented, at least approximately, in the displacement functions. The membrane and normal displacements should all be represented with equal accuracy. The displacement functions should be at least of the competence of the bicubic. The continuity of displacement and slope must be enforced, at least approximately, at the inter-element boundaries."

Probably one of the most striking comparisons that can be made is with the Fourier series/finite element analysis of asymmetrically loaded axisymmetric shells. In this approach the equations are first decomposed into circumferential harmonics leaving only the meridional behavior to be determined. A one-dimensional finite element solution along the meridian is then used for each harmonic. The one dimensional finite element mesh provides the smallest possible bandwidth which results in minimum storage requirements and execution times. Even for a large number of circumferential harmonics it is computational more efficient to use the Fourier series approach than to employ a two dimensional gridwork over the reference surface of the shell.

However, the advantages disappear whenever symmetry is lost by cutouts, circumferential changes in modulus or thickness, or circumferential changes in boundary conditions. These asymmetries serve to couple the harmonics requiring the simultaneous solution of the meridional behavior in each harmonic. In this circumstance, the two dimensional mesh is competitive and in many cases necessary in obtaining a solution.

With regard to an extension to general shells, the problem appears to be one of geometric specification rather than a limitation in the element itself. The shell theory in Section 2 has already been simplified by assuming that the coordinates α and β are principle surface coordinates coinciding with the directions of minimum and maximum curvature. For a free form shell, it is highly unlikely that it will come with the principle surface coordinates already defined. The best alternative would be to start with a shell theory that does not assume the use of principle coordinates[49], then any convenient set of surface variables would suffice. Next, it is necessary to locate the shell reference surface in space and after selecting the mesh to specify the outward normal or any other convenient parameter at each mesh point. All of this will require the most sophisticated mesh generators yet devised to prevent a return to hand inputting. It should be remarked that the essence of shell theory is the geometry of the reference surface and only a faithful representation of the true shell will provide meaningful results. Once these difficulties have been overcome, the above treatment of the reference surface and the displacement assumptions used will provide a suitable element.

In terms of alternate displacement derivations, there are currently three other approaches that are being used. One is to use a transverse shear

deformation shell theory. Here, the primary motivation is to obtain lower order continuity requirements on the finite element displacement assumptions albeit at the expense of a greater number of unknown functions. This has provided a great deal of freedom in element shapes but two things have emerged from this work; (1) the transverse shear deformations are very stiff in relation to the bending behavior and distort the solution badly until they have converged under element refinement, and (2) for thin shells the solutions are sufficiently complicated that higher order polynomials are required anyway to resolve the detail in the solution[29,35,36,37].

Another approach is to start with a Kirchhoff shell theory with the three displacement variables u , v and w and attempt to cope with the requirements of having continuous derivatives in the normal deflection w and yet retain sufficient freedom of geometry and deformation that realistic problems can be worked. With the exception of the flat geometry of the plate, this has proven to be rather elusive with only elements along coordinate lines having been developed[3,5,7,12].

The third approach is based on a finite difference solution of the equations in the interior of an element subjected to certain boundary displacements along the edges[14].

The most difficult analysis for all of the elements investigated here has been the infinite cylinder under axial tension with a circular cutout. The solution to this problem is very complicated but is confined to within a couple of hole radii of the cutout. Near the hole the fine mesh is required to resolve the membrane portion of the solution but away from the hole it is more than is required. The bending part of the solution appears to be

adequately characterized by the coarse mesh. Part of the difficulty in examining this problem arises from the inadequate presentations of the closed form solutions by Lekkerkerker[44] and Van Dyke[45]. They are no more accurate than plus or minus 5% making a 1% comparison impossible. Their bending solutions are not nondimensional, since they depend on Poisson's ratio.

Of the two element geometries that are widely used, the quadrilateral is more efficient, both from a data preparation or generation standpoint and internally from a numerical standpoint. However, the triangle is much more flexible in terms of matching the problem geometry. It also has the advantage of not requiring an auxiliary coordinate system for its use. The "triangular coordinates" frequently introduced are in reality interpolation polynomials in the original coordinates.

A related problem area which may limit the current use of this element is in the area of computer requirements. While the computer program written for this element is virtually machine independent, it has been written using random access input/output routines. More and more computers are having this kind of input and output routine written for them, but they are frequently awkward to use or unreliable. The present routines that are being used for this element on the CDC 6600 are used with standard FORTRAN call statements, and it is straightforward to write sequential tape handling subroutines that would affect the data transfer. A second difficulty will occur on machines that do not have the core capacity, speed or 60 bit word length of a CDC 6600 computer. Problem sizes will become limited, running times will lengthen to

half hours, and double precision calculations will have to be undertaken to compensate for 24 bit business oriented word lengths.

Just as the formulation and solution of shell equations is an order of magnitude more difficult than elasticity equations, it appears the numerical solution of shell equations is going to remain an order of magnitude more difficult than elasticity equations.

REFERENCES

1. C. Visser, "The Approximate Analysis of Thin Shells by the Finite Element Method," Ph.D. Thesis, Department of Engineering Mechanics, Ohio State University, Columbus, Ohio, 1966.
 2. G. P. Bazeley, Y. K. Cheung, R. M. Irons and O. C. Zienkiewicz, "Triangular Elements in Plate Bending, Conforming and Nonconforming Solutions," Proceedings of the 1st Conference on Matrix Methods in Structural Mechanics, AFFDL-TR-66-80, Air Force Institute of Technology, October 1965.
 3. R. H. Gallagher, The Development and Evaluation of Matrix Methods for Thin Shell Structural Analysis, Bell Aerosystems, Buffalo, New York, Report No. 8500-902011, June 1966.
 4. R. H. Gallagher and H. T. Y. Yang, "Elastic Instability Predictions for Doubly Curved Shells," Proceedings of the 2nd Conference on Matrix Methods in Structural Mechanics, AFFDL-TR-68-150, Air Force Institute of Technology, October 1968.
 5. F. K. Bogner, R. L. Fox, and L. A. Schmit, "A Cylindrical Shell Discrete Element," AIAA Journal, Vol. 5, No. 4, April 1967.
 6. J. T. Oden and G. A. Wempner, Numerical Analysis of Arbitrary Shell Structures Under Arbitrary Static Loadings, University of Alabama Research Institute RR-47, November 1967.
- G. A. Wempner, "New Concepts for Finite Elements of Shells," ZAMM, Vol. 48, August 1968.

G. A. Wempner, J. T. Oden, D. A. Kross, "Finite Element Analysis of Thin Shells," Journal of the Engineering Mechanics Division, Proceedings ASCE, EM6, (December 1968).

G. A. Wempner, "Finite Elements, Finite Rotations, and Small Strains of Flexible Shells," Int. Journal Solids Structures, Vol. 5, No. 2, (February 1969).

7. J. T. Oden, "Calculation of Stiffness Matrices for Finite Elements of Thin Shells of Arbitrary Shape," Technical Note AIAA Journal, Vol. 6, No. 5, May 1968.
8. G. Cantin and R. W. Clough, "A Curved, Cylindrical-Shell, Finite Element," AIAA Journal, Vol. 6, No. 6, June 1968.
9. S. W. Key and Z. E. Beisinger, "The Analysis of Thin Shells with Transverse Shear Strains by the Finite Element Method," Proceedings of the 2nd Conference on Matrix Methods in Structural Mechanics, AFFDL-TR-68-150, Air Force Institute of Technology, October 1968.
10. M. D. Olson and G. M. Lindberg, "Vibration Analysis of Cantilevered Curved Plates Using a New Cylindrical Shell Finite Element," Proceedings of the 2nd Conference on Matrix Methods in Structural Mechanics, AFFDL-TR-68-150, Air Force Institute of Technology, October 1968.
11. R. W. Clough and J. L. Tocher, "Finite Element Stiffness Matrices for Analysis of Plate Bending," A paper presented at the Second Conference on Matrix Structural Analysis Methods, Wright-Patterson AFB, Ohio, October 1965.
12. B. E. Greene, R. E. Jones and D. R. Strome, "Dynamic Analysis of Shells Using Doubly-Curved Finite Elements," Proceedings of the 2nd Conference on Matrix Methods of Structural Mechanics, AFFDL-TR-68-150, Air Force Institute of Technology, October 1968.

13. J. H. Argyris, K. E. Buck, I. Fried, H. M. Hilber, G. Mareczek and D. W. Scharpf, "Some New Elements for the Matrix Displacement Method," Proceedings of the 2nd Conference on Matrix Methods of Structural Mechanics, AFFDL-TR-68-150, Air Force Institute of Technology, October 1968.
14. E. Y. W. Tsui, J. M. Massard and W. A. Loden, "Element Stiffness Matrices of Thick-walled Orthotropic Shells with Applications," Proceedings of the Symposium on Application of Finite Element Methods in Civil Engineering, School of Engineering, Vanderbilt University, November 1969.
15. L. R. Herrmann, "Mixed Formulations for Finite Element Shell Analysis," Conference on Computer Oriented Analysis of Shell Structures, Lockheed Palo Alto Research Laboratory, Palo Alto, California, August 1970.
16. L. R. Herrmann, "A Bending Analysis for Plates," Proceedings of the 1st Conference on Matrix Methods in Structural Mechanics, AFFDL-TR-66-80, Air Force Institute of Technology, October 1965.
17. W. Visser, "Application of a Mixed Type Shell Element," IUTAM Symposium on High Speed Computing of Elastic Structures, Liege, Belgium, August 1970.
18. K. Washizu, Variational Methods in Elasticity and Plasticity, Pergamon Press, 1968.
19. R. J. Melosh, Development of the Stiffness Method to Define Bounds on Elastic Behavior of Structures, Ph.D. Thesis, Department of Civil Engineering, University of Washington, Seattle, Washington, June 1962.

20. R. W. McLay, An Investigation into the Theory of the Displacement Method of Analysis for Linear Elasticity, Ph.D. Thesis, Department of Engineering Mechanics, University of Wisconsin, Madison, August 1963.
21. S. W. Key, A Convergence Investigation of the Direct Stiffness Method, Ph.D. Thesis, Department of Aeronautics and Astronautics, University of Washington, Seattle, Washington, March 1966.
22. M. W. Johnson, Jr. and R. W. McLay, "On the Finite Element Method in the Theory of Elasticity," The Boeing Company, Seattle, Washington, D2-125154-1, September 1966.
ASME Journal of Applied Mechanics, Vol. 35, June 1968.
23. R. W. McLay, "Completeness and Convergence Properties of Finite Element Displacement Functions - A General Treatment," D2-125271-1, November 1966, The Boeing Company, Seattle, Washington.
AIAA 5th Aerospace Sciences Meeting, New York, New York, January 1967.
24. P. Tong and T. H. H. Pian, "The Convergence of Finite Element Method in Solving Linear Elastic Problems," Int. Journal Solids Structures, Vol. 3, 1967.
25. C. A. Felippa and R. W. Clough, "The Finite Element Method in Solid Mechanics," AMS Symposium on the Numerical Solution of Field Problems in Continuum Mechanics, Durham, North Carolina, April 1968.
26. E. R. de Arantes e Oliveira, "Completeness and Convergence in the Finite Element Method," Proceedings of the 2nd Conference on Matrix Methods in Structural Mechanics, AFFDL-TR-68-150, Air Force Institute of Technology, October 1968.

27. B. M. Irons, "Engineering Applications of Numerical Integration in Stiffness Methods," AIAA Journal, Vol. 4, No. 11, November 1966.
28. I. Ergatoudis, B. M. Irons, and O. C. Zienkiewicz, "Curved, Isoparametric, 'Quadrilateral' Elements for Finite Element Analysis," Int. Journal Solids Structures, Vol. 4, 1968.
29. S. W. Key and Z. E. Beisinger, "The Analysis of Thin Shells with Transverse Shear Strains by the Finite Element Method," Proceedings of the 2nd. Conference on Matrix Methods in Structural Mechanics, Air Force Institute of Technology, Dayton, Ohio, AFFDL-TR-68-150, October 1968.
30. A. Adini and R. W. Clough, "Analysis of Plate Bending by the Finite Element Method," Report submitted to the Nat. Sci. Foundation, Grant G7337, 1960.
31. R. J. Melosh, "Basis for Derivation of Matrices for the Direct Stiffness Method," AIAA Journal, Vol. 1, 1631, 1963.
32. J. A. Stricklin, W. E. Haisler, P. R. Tisdale and R. Gunderson, "A Rapidly Converging Triangular Plate Element," AIAA Journal, Vol. 7, No. 1, pp. 180-181, January 1969.
33. P. R. Tisdale, "Triangular Plate Element Based on Higher Order Displacement Functions," AIAA Southwest Student Paper Competition, Fort Worth, Texas, March 1969.
34. G. S. Dhatt, "Numerical Analysis of Thin Shells by Curved Triangular Elements Based on Discrete Kirchhoff Hypothesis," Proc. of Symposium on Application of Finite Element Methods in Civil Engineering, Vanderbilt University, November 13-14, 1969.

42. R. W. Clough and C. A. Felippa, "A Refined Quadrilateral Element for Analysis of Plate Bending," 2nd Air Force Conference on Matrix Methods in Structural Mechanics, Dayton, Ohio, October 1968.
43. V. Z. Valsov, "General Theory of Shells and Its Applications in Engineering," NASA Technical Translation TTF-99, April 1964.
44. J. G. Lekkerkerker, "Stress Concentration Around Circular Holes in Cylindrical Shells," Proceedings of the 11th International Congress of Applied Mechanics, Munich, 1964.
45. P. Van Dyke, "Stresses About a Circular Hole in A Cylindrical Shell," AIAA Journal, Vol. 3, No. 9, September 1965.
46. P. Van Dyke, private communication.
47. W. Flugge, "Stresses in Shells," Springer-Verlag, New York, 1967.
48. G. N. Chernyshev, "Bending of Shells with Positive Curvature Under A Concentrated Load," PMM, Vol. 31, No. 5, 1967.
49. A. E. Green and W. Zerna, "Theoretical Elasticity," Oxford University Press, London (1960).
50. R. H. Gallagher, "Analysis of Plate and Shell Structures," Proc. Symposium on Application of Finite Element Methods in Civil Engineering, Vanderbilt University, Nashville, Tennessee, November 13-14, 1969.

35. R. J. Melosh, "A Flat Triangular Shell Element Stiffness Matrix,"
Proceedings of the 1st Conference on Matrix Methods in Structural
Mechanics, AFFDL-TR-60-80, Air Force Institute of Technology,
October 1965.
36. S. Utku, "Stiffness Matrices for Thin Triangular Elements of Nonzero
Gaussian Curvature," AIAA Paper No. 66-530, AIAA 4th Aerospace Sciences
Meeting, Los Angeles, California, June 1966.
37. S. Utku and R. J. Melosh, "Behavior of Triangular Shell Element Stiff-
ness Matrices Associated with Polyhedral Deflection Distributions,"
AIAA Paper No. 67-114, AIAA 5th Aerospace Sciences Meeting, New York,
New York, January 1967.
38. Z. Kopal, "Numerical Analysis," 2nd Edition, Chapman & Hall Ltd.,
London, 1961.
39. R. E. Jones and D. R. Strome, "Direct Stiffness Metho. Analysis of
Shells of Revolution Utilizing Curved Elements," AIAA Journal, Vol. 4,
No. 9, September 1966
40. J. A. Stricklin, D. R. Navaratna, and T. H. H. Pian, "Improvements on
the Analysis of Shells of Revolution by the Matrix Displacement Method,"
AIAA Journal, Vol. 4, No. 11, November 1966.
41. M. Khojasteh-Bakht, Analysis of Elastic-Plastic Shells of Revolution
Under Axisymmetric Loading by the Finite Element Method, Structures
and Materials Research, Department of Civil Engineering, University
of California, Berkeley, SESM 67-8, April 1967.

QUESTIONS AND COMMENTS FOLLOWING KEY'S PAPER

COMMENT: I think you should expand your list of other types of curved elements to include the Ahman/Irons element which was recorded at the 1968 Wright Patterson Air Force Conference. This is a degenerate version of their three-dimensionalized iso-parametric elements and it has a number of similarities to the type of element that you're describing. The most recent paper they've presented describing that type of element is in the July issue of the International Journal for Numerical Methods in Engineering. In that paper, they describe both the quadratically curved and also a cubically curved degenerate 3D element, which I think has many of the capabilities of the type of element that you're describing here. I think both your element and theirs have tremendous potential in future developments of sophisticated shell analysis programs and I think both of them should be considered simultaneously.

QUESTION: I'm trying to fathom these fast times. Do you know anything about the difference between the lowest frequency and the highest frequency of this idealized shell? This is lower bending mode behavior we're seeing in movies of the Lockheed cone problem. These waves we see are, I would say, comparable to the period of the lower bending modes, is that correct? (Yes). Normally we would see high frequency response from the very high modes of the shell superimposed on the low frequency response and normally our integration time intervals have to be small compared to the periods of even these high frequency responses for stability. I don't see any high frequency wiggles on your major mode responses. How short is this two microsecond time interval compared to the high fre-

quency modes of this system?

KEY: The highest frequency modes in this system are the membrane modes. If you watch that movie closely on a smaller screen, you'll see the meshes moving in a membrane manner with very high frequency. The two microsecond time step is smaller than the period of the highest natural frequency of the idealized system.

QUESTION: Well, how high is that highest natural frequency compared with the first mode bending frequency? What I'm driving at is the period of that very highest frequency sets the size of the time interval we have to use while the period of the low frequencies generally sets the length of time we wish to investigate. And in many dynamics problems, the ratio between that high frequency and the low frequency is so big that with direct integration methods it would take a long computer time to run. These times seem very short; that's why I was trying to get at some of that information.

KEY: The highest natural frequency present is governed by the mesh size and for this problem is 1.6×10^5 c/s. The first mode bending is approximately 2×10^3 c/s. The stability of the central difference time integration scheme used here is governed by the highest frequency in the system with Δt less than one over π times the maximum frequency. The result is 750 time steps required to calculate the 1500 μ sec of response shown. The time I quoted for the calculation was that required for those 750 steps.

QUESTION: You have a 36 degree of freedom element and you use 18 nodal points around the semi-circle in that cone problem. That leads to

a bandwidth in excess of 400. And there were a total of many, many equations. So, you had to use auxiliary storage, didn't you?

KEY: That's correct.

COMMENT: And even with that you had such a very fast solution for 750 steps; just 17 minutes CP time for the entire problem. It's amazing!

KEY: It took 17 minutes to integrate the equations. There's also a setup time which I didn't include in that 17 minutes. The storage scheme we use requires only the nonzero terms in each row and an index telling you the column it comes from; all we're doing is carrying out a matrix product for each time step.

COMMENT: The question has been brought up about the integration step time in terms of the shortest period of the system. It's been our experience and I think the experience of most everybody working in stress wave calculation in solids that what you want to do is to make the integration step time less than some fraction, like $7/10$, of the transit time of the fastest wave in the system. That could be the longitudinal wave, that is, it could be the bulk wave; it could possibly be a thickness shear wave in some systems if you don't have the longitudinal wave represented. What puzzles me about these calculations is the fact that such a wave did not show up as higher frequency oscillation on these graphs. The only explanation I can think of is that the frequency shown on the graph is the highest frequency of the system. Newmark has shown that with that central difference scheme you've got to have a semi-stable response of the highest frequency in the system. It has to oscillate. There's no other way.

KEY: If you look at the complete set of computations for this problem, there is also a graph showing the axial membrane displacement at the same nodal point and it clearly indicates the presence of membrane modes and it has a very high frequency. And, if you look at the meshes pinching on that closeup movie, you'll see the membrane in there as a very high frequency. Everything that has been said about the highest natural frequency in the numerical system is correct. People have unnecessarily been panicked by "conditional stability." Conditional stable integration schemes have a critical time step below which the scheme is stable and above which the scheme is unstable and diverges exponentially. For the linear elastic problem presented, only frequencies present in the initial conditions will be evident in the solution.

A PROGRAM FOR THE NONLINEAR STATIC AND DYNAMIC
ANALYSIS OF ARBITRARILY LOADED SHELLS OF REVOLUTION

R. E. Ball, Associate Professor
Naval Postgraduate School
Monterey, California

INTRODUCTION

The design of many shell structures is influenced by the geometrically nonlinear response of the shell when subjected to static and/or dynamic loads. As a consequence, a number of investigations have been devoted to the study of the buckling phenomenon exhibited by shells. Most of the early works examine the behavior of the shallow spherical cap, the truncated cone, and the cylinder under axisymmetric loads. As a consequence of the lack of information on the axisymmetric response of shells with other meridional geometries and on the response of shells subjected to asymmetric loads, a computer program for the geometrically nonlinear static and dynamic response of arbitrarily loaded shells of revolution has been developed. The dynamic analysis capability is a recent extension of the program developed by the author for the nonlinear static analysis of arbitrarily loaded shells of revolution¹. The program can be used to analyze any shell of revolution for which the following conditions hold:

- 1) The geometric and material properties of the shell are axisymmetric, but may vary along the shell meridian.
- 2) The applied pressure and temperature distributions are symmetric about, but may vary along, a meridian.
- 3) The shell material is isotropic, but the modulus of elasticity may vary through the thickness. Poisson's ratio is constant.
- 4) The boundaries of the shell may be closed, free, fixed, or elastically restrained.

The governing partial differential equations are based upon Sanders' nonlinear thin shell theory for the condition of small strains and moderately small rotations². The inplane and normal inertial forces are accounted for, but the rotary inertial terms are neglected. The set of governing nonlinear partial differential equations is reduced to an infinite number of sets of four second-order differential equations in the meridional and time coordinates by expanding all dependent variables in a sine or cosine series in terms of the circumferential coordinate. The sets are uncoupled by utilizing appropriate trigonometric identities and by treating the nonlinear coupling terms as pseudo loads. The meridional derivatives are replaced by the conventional central finite difference approximations, and the displacement accelerations are approximated by the implicit Houbolt backward differencing scheme³.

This leads to sets of algebraic equations in terms of the dependent variables and the Fourier index. At each load or time step, an estimate of the solution is obtained by extrapolation from the solutions at the previous load or time steps. The sets of algebraic equations are repeatedly solved using Potters'⁴ form of Gaussian elimination, and the pseudo loads are recomputed, until the solution converges.

Basically, there are four fundamental features of the method of solution; (1) circumferential series, (2) meridional finite differences, (3) pseudo load concept, and (4) the Houbolt timewise differencing scheme. Obviously there are many other ways to solve the problem considered here, and there are physical features common to many shell structures that have not been considered. Thus, it is not surprising that there are several other computer programs currently available, or under development, that have approximately the same, or more advanced, capabilities for a nonlinear static and/or dynamic analysis*. The purpose of this paper is to compare results with previously published solutions from some of these programs in order to illustrate the ability, or inability, of the program to treat specific problem areas. In this manner, the advantages, and disadvantages, of the method of solution will hopefully become evident.

*Refer to reference 5 for an assessment of these programs.

THEORY

Shell Geometry

Consider the general shell of revolution shown in figure 1. Located within this shell is a reference surface. All material points of the shell can be located using the orthogonal coordinate system s, θ, ζ , where s is the meridional distance along the reference surface measured from one boundary, θ is the circumferential angle measured from a datum meridian plane, and ζ is the normal distance from the reference surface. The positive direction of each coordinate is indicated in figure 1. For convenience, let the reference surface be positioned so that

$$\int \zeta E d\zeta = 0 \quad (1)$$

where E is the elastic modulus and the integration is carried out through the thickness of the shell. Thus, when E is independent of ζ the reference surface coincides with the middle surface of the shell. Further, let the location of the reference surface be described by the dependent variable r , the normal distance from the axis of the shell. Accordingly, the principal radii of curvature of the reference surface are

$$\begin{aligned} R_\theta &= r / [1 - (r')^2]^{3/2} \\ R_s &= - [1 - (r')^2]^{1/2} / r' \end{aligned} \quad (2)$$

where a prime denotes differentiation with respect to s . Further, note the Codazzi identity

$$\left(\frac{1}{R_\theta} \right)' = r' (R_s^{-1} - R_\theta^{-1}) / r \quad (3)$$

and the relation

$$r'' = -r / R_s R_\theta \quad (4)$$

Strain-displacement Relations

For a shell of revolution, the strain-displacement relations derived by Sanders take the form

$$\begin{aligned} \epsilon_s &= U' + W/R_s + (\phi_s^2 + \phi_\theta^2)/2 \\ \epsilon_\theta &= V'/r + r' U/r + W/R_\theta + (\phi_\theta^2 + \phi_s^2)/2 \\ \epsilon_{s\theta} &= (V' + U'/r - r'V/r + \phi_s \phi_\theta)/2 \end{aligned} \quad (5)$$

and

$$\begin{aligned}\kappa_s &= \dot{\phi}_s \\ \kappa_\theta &= \dot{\phi}_\theta / r + r' \dot{\phi}_s / r \\ \kappa_{s\theta} &= [\dot{\phi}_\theta' + \dot{\phi}_s' / r - r' \dot{\phi}_\theta / r + (R_\theta^{-1} - R_s^{-1}) \dot{\phi}] / 2\end{aligned}\quad (6)$$

where ϵ_s , ϵ_θ , and $\epsilon_{s\theta}$ are the reference surface strains, κ_s , κ_θ , and $\kappa_{s\theta}$ are the bending strains, U and V are the displacements in the directions tangent to the meridian and to the parallel circle respectively, W is the displacement normal to the reference surface, and ϕ_s , ϕ_θ , and ϕ are rotations defined by

$$\begin{aligned}\phi_s &= -W' + U/R_s \\ \phi_\theta &= -W' / r + V/R_\theta \\ \phi &= (V' + r'V/r - U' / r) / 2\end{aligned}\quad (7)$$

In these equations, and henceforth, a superscript dot denotes differentiation with respect to θ .

Equations of Motion

Converting Sanders' equilibrium equations to the equations of motion for a shell of revolution leads to

$$\begin{aligned}(rN_s)' + N_{s\theta}' - r'N_\theta + rQ_s/R_s + (R_s^{-1} - R_\theta^{-1}) M_{s\theta}' / 2 &= r(\int m d\zeta) \partial^2 U / \partial T^2 \\ - r\dot{q}_s + r(\dot{\phi}_s N_s + \dot{\phi}_\theta N_{s\theta}) / R_s + [\dot{\phi}(N_s + N_\theta)]' / 2 \\ N_\theta' + (rN_{s\theta})' + r'N_{s\theta} + rQ_\theta/R_\theta + r[(R_\theta^{-1} - R_s^{-1}) M_{s\theta}]' / 2 &= r(\int m d\zeta) \partial^2 V / \partial T^2 \quad (8) \\ - r\dot{q}_\theta + r(\dot{\phi}_\theta N_\theta + \dot{\phi}_s N_{s\theta}) / R_\theta - r[\dot{\phi}(N_s + N_\theta)]' / 2 \\ (rQ_s)' + Q_\theta' - rN_s/R_s - rN_\theta/R_\theta &= r(\int m d\zeta) \partial^2 W / \partial T^2 \\ - r\dot{q} + (r\dot{\phi}_s N_s + r\dot{\phi}_\theta N_{s\theta})' + (\dot{\phi}_s N_{s\theta} + \dot{\phi}_\theta N_\theta)' &\end{aligned}$$

and

$$(rM_s)' + M_{s\theta}' - r' M_\theta - rQ_s = 0. \quad (9)$$

$$M_\theta' + (rM_{s\theta})' + r'M_{s\theta} - rQ_\theta = 0 \quad (10)$$

when the effects of rotary inertia are neglected. In equations (8) - (10), m is the density of the shell material, T is time, q_s , q_θ , and q are the meridional, circumferential, and normal components of the applied pressure load, Q_s and Q_θ are the transverse forces per unit length, N_s , N_θ and $N_{s\theta}$ are the membrane forces per unit length, and M_s , M_θ , and $M_{s\theta}$ are the bending and twisting moments per unit length.

Constitutive Relations

The constitutive relations used in Sanders' nonlinear theory are the same as those proposed by Love in his first approximation to the linear, small strain theory of thin elastic shells. Noting equation (1), these can be given in the form

$$N_s = B (\epsilon_s + \nu \epsilon_\theta) - \epsilon_T \quad (11a)$$

$$N_\theta = B (\epsilon_\theta + \nu \epsilon_s) - \epsilon_T \quad (11b)$$

$$N_{s\theta} = B(1 - \nu) \epsilon_{s\theta} \quad (11c)$$

$$M_s = D (\kappa_s + \nu \kappa_\theta) - \kappa_T \quad (11d)$$

$$M_\theta = D (\kappa_\theta + \nu \kappa_s) - \kappa_T \quad (11e)$$

$$M_{s\theta} = D (1 - \nu) \kappa_{s\theta} \quad (11f)$$

where ν is Poisson's ratio, assumed constant through the thickness, and

$$B = \int E d\zeta / (1 - \nu^2) \quad (12a)$$

$$D = \int \zeta^2 E d\zeta / (1 - \nu^2) \quad (12b)$$

$$\epsilon_T = \int \alpha \tau E d\zeta / (1 - \nu) \quad (12c)$$

$$\kappa_T = \int \zeta \alpha \tau E d\zeta / (1 - \nu) \quad (12d)$$

In equations (12c) and (12d), τ is the local temperature change and α is the coefficient of thermal expansion.

Boundary Conditions

In Sanders' nonlinear theory, the conditions to prescribe on the edges of a shell of revolution are

$$\begin{array}{ll} N_s \text{ or } U & \hat{N}_{s\theta} \text{ or } V \\ \hat{Q}_s \text{ or } W & M_s \text{ or } \phi_s \end{array} \quad (13)$$

where $\hat{N}_{s\theta}$ and \hat{Q}_s are the effective shear and transverse forces per unit length defined by

$$\hat{N}_{s\theta} = N_{s\theta} + (3 R_\theta^{-1} - R_s^{-1}) M_{s\theta} / 2 + (N_s + N_\theta) \phi / 2 \quad (14)$$

$$\hat{Q}_s = Q_s + M'_{s\theta} / r - \phi_s N_s - \phi_\theta N_{s\theta} \quad (15a)$$

Using the equilibrium equation (9) to eliminate Q_s from equation (15a) leads to

$$\hat{Q}_s = [(r M_s)' + 2 M'_{s\theta} - r' M_\theta] / r - \phi_s N_s - \phi_\theta N_{s\theta} \quad (15b)$$

Elastic restraints at the edge of a shell can be provided for by linearly relating the forces or moment to the appropriate displacements or rotation. Consequently, the boundary conditions may be given in the matrix form

$$\bar{\Omega} \begin{Bmatrix} N_s \\ \hat{N}_{s\theta} \\ \hat{Q}_s \\ \phi_s \end{Bmatrix} + \bar{\Lambda} \begin{Bmatrix} U \\ V \\ W \\ M_s \end{Bmatrix} = \ell \quad (16)$$

where $\bar{\Omega}$ and $\bar{\Lambda}$ are 4×4 matrices and ℓ is a column matrix. The values of the elements of these matrices are determined by the conditions prescribed at the shell boundary.

METHOD OF SOLUTION

Fourier Expansions

The crux of the method used here to solve the nonlinear field equations is the elimination of the independent variable θ by expanding all dependent variables into sine or cosine series in the circumferential direction. Only loading conditions that are symmetric about a datum meridian plane will be considered. Thus, the variable ϕ_s can be expressed in the form*

$$\phi_s = \frac{\sigma_o}{E_o} \sum_{n=0}^{\infty} \psi_s^{(n)} \cos n\theta \quad (17)$$

where σ_o is a reference stress level, E_o is a reference elastic modulus, and the nondimensional series coefficient $\psi_s^{(n)}$ is a function of the independent variables s and T . Similar series expansions can be made for the remaining dependent variables.

Modal Uncoupling

In order to eliminate the independent variable θ from the problem, and convert the partial differential equations to sets of uncoupled partial differential equations, the nonlinear terms are treated as known quantities or pseudo loads. Since every nonlinear term is the product of two Fourier series, each product can be reduced to a single trigonometric series wherein the coefficient is itself a series. For example, using equation (17) ϕ_s^2 can be expressed as

$$\phi_s^2 = \left(\frac{\sigma_o}{E_o}\right)^2 \sum_{m=0}^{\infty} \sum_{n=0}^{\infty} \psi_s^{(m)} \psi_s^{(n)} \cos m\theta \cos n\theta \quad (18)$$

Since

$$\cos m\theta \cos n\theta = \frac{1}{2} [\cos (m-n)\theta + \cos (m+n)\theta] \quad (19)$$

equation (18) can be given in the form

$$\phi_s^2 = \frac{\sigma_o}{E_o} \sum_{n=0}^{\infty} \beta_s^{(n)} \cos n\theta \quad (20a)$$

*Theoretically, the complete Fourier series including both the sine and cosine expansions should be used because of the possibility of "odd" displacements occurring under "even" loads, i.e. a bifurcation phenomenon. This aspect is not considered here.

where

$$\beta_s^{(n)} = \frac{\sigma_0}{2E_0} \sum_{i=0}^{\infty} \varphi_s^{(i)} [\eta \varphi_s^{(i+n)} + \mu \varphi_s^{|i-n|}] \quad (20b)$$

with

$$\eta = \begin{cases} 0 & \text{for } n = 0 \\ 1 & \text{for } n > 0 \end{cases}, \quad \mu = \begin{cases} 1 & \text{for } i \neq n \\ 2 & \text{for } i = n \end{cases}$$

Similar series expressions can be derived for the other nonlinear terms in equations (5), (8), (14) and (15b).

As a result of the trigonometric series expansions, there is one set of governing equations for each value of n considered; when only the linear terms are considered the sets are uncoupled. The presence of the nonlinear terms couples the sets through terms like $\beta_s^{(n)}$ as given by equation (20b). However, by treating the nonlinear terms as known quantities and grouping them with the load terms, the sets of equations become uncoupled.

Final Equations

Budiansky and Radkowski⁶ have shown that for the linear shell problem each set of Sanders' uncoupled field equations can be reduced to four second order differential equations provided M_θ is replaced by the equality obtained from the constitutive relations (11d) and (11e)

$$M_\theta = \nu M_s + D(1-\nu^2)\kappa_\theta - (1-\nu)\epsilon_T \quad (21)$$

to prevent derivatives of w higher than two from appearing. The same procedure is used here. The four unknown dependent variables are the nondimensional series coefficients $u^{(n)}$, $v^{(n)}$, $w^{(n)}$, and $m_s^{(n)}$ corresponding to U , V , W , and M_s respectively. Three of the final four equations are derived from the equations of motion (8) by applying the rotational equilibrium equations (9) and (10), the constitutive relations (11) and (21), and the strain-displacement relations (5), (6), and (7). The fourth equation is derived from the meridional bending moment-curvature relationship given by (11d) with κ_s and κ_θ expressed in terms of the displacements.

A convenient representation of these four equations is the nondimensional matrix form

$$E^{(n)} z^{(n)''} + F^{(n)} z^{(n)'} + G^{(n)} z^{(n)} = e^{(n)} + \bar{\mu} \partial^2 z^{(n)} / \partial t^2 \quad (22)$$

where

$$z^{(n)} = \begin{Bmatrix} u^{(n)} \\ v^{(n)} \\ w^{(n)} \\ m_s^{(n)} \end{Bmatrix}$$

and primes denote differentiation with respect to the nondimensional meridional coordinate $\bar{s} = s/a$, a is a reference length,

t is the nondimensional time T/T_0 , T_0 is a reference time, and $\bar{\mu}$ is the mass matrix given by

$$\bar{\mu} = \mu \begin{bmatrix} 1 & 0 & 0 & 0 \\ 0 & 1 & 0 & 0 \\ 0 & 0 & 1 & 0 \\ 0 & 0 & 0 & 0 \end{bmatrix}$$

The scalar mass μ is defined by

$$\mu = \frac{a^2}{h_0 E_0 T_0^2} \int_0^1 \rho d\zeta$$

where h_0 is a reference thickness. Henceforth, the superscript n will be dropped for convenience.

The E , F , G , and e in equation (22) are matrices defined in reference 1. The elements of E , F , and G are identical with those given in reference 6 for the linear shell analysis, but the e matrix contains both the load and thermal terms and the nonlinear terms.

The boundary conditions on z are obtained by applying the constitutive relations (11) and (21), and the strain-displacement relations (5), (6), and (7) to equation (16). This leads to the matrix equation

$$\Omega H z' + (\Lambda + \Omega J) z = l - \Omega f \quad (23)$$

where Ω and Λ are the nondimensional form of $\bar{\Omega}$ and $\bar{\Lambda}$. Matrices H and J are identical with those given in reference 6 for the linear shell problem, and matrix f , as defined in reference 1, contains the thermal and nonlinear terms. In this formulation, Ω and Λ are not functions of n , and hence, the same set of boundary conditions applies for each value of n considered.

Spatial Finite Difference Formulation

Let the shell meridian be divided into $K - 1$ equal increments, and denote the end of each increment or station by the index i . Thus, $i = 1$ corresponds to the initial edge of the shell and $i = K$ corresponds to the final edge. A fictitious station is added off each end of the shell at $i = 0$ and $i = K + 1$.

Let the first and second derivatives of z at station i be approximated by

$$z'_i = (z_{i+1} - z_{i-1}) / 2\Delta \quad (24a)$$

$$z''_i = (z_{i+1} - 2z_i + z_{i-1}) / \Delta^2 \quad (24b)$$

where Δ is the nondimensional distance between stations. Substituting equations (24a) and (24b) into equation (22) leads to

$$A_i z_{i+1} + B_i z_i + C_i z_{i-1} = g_i + 2\Delta \bar{\mu}_i (\partial^2 z / \partial t^2)_i \quad (25)$$

where

$$A_i = 2E_i / \Delta + F_i$$

$$B_i = -4E_i / \Delta + 2\Delta G_i$$

$$C_i = 2E_i / \Delta - F_i$$

$$g_i = 2\Delta e_i$$

and $i = 1, 2, \dots, K$ to insure equilibrium over the total length of the shell.

At the boundaries equation (23) must be satisfied. Thus, substituting equation (24a) into equation (23) leads to

$$\frac{1}{2\Delta} \Omega_{11} z_2 + (\Omega_{11} J_1 + \Lambda_1) z_1 - \frac{1}{2\Delta} \Omega_{11} z_0 = l_1 - \Omega_{11} f_1 \quad (26a)$$

at the initial edge, and

$$\frac{1}{2\Delta} \Omega_{KK} z_{K+1} + (\Omega_{KK} J_K + \Lambda_K) z_K - \frac{1}{2\Delta} \Omega_{KK} z_{K-1} = l_K - \Omega_{KK} f_K \quad (26b)$$

at the final edge.

Timewise Differencing Scheme

The inertial terms that appear in equations (25) can be approximated by Houbolt's backward differencing scheme. Accordingly,

$$\left(\frac{\partial^2 z}{\partial t^2} \right)_{i,j} = (2z_{i,j} - 5z_{i,j-1} + 4z_{i,j-2} - z_{i,j-3}) / (\delta t)^2 \quad (27)$$

where j denotes the time step and δt is the nondimensional time interval. Thus, substituting equation (27) into equation (25) yields

$$A_i z_{i+1,j} + \bar{B}_i z_{i,j} + C_i z_{i-1,j} = \bar{g}_{i,j} \quad (28)$$

where

$$\bar{B}_i = B_i - \frac{4\Delta \bar{\mu}_i}{(\delta t)^2}$$

$$\bar{g}_{i,j} = g_{i,j} + \frac{2\Delta \bar{\mu}_1}{(\delta t)^2} (-5 z_{i,j-1} + 4 z_{i,j-2} - z_{i,j-3})$$

and $i = 1, 2, \dots K$.

Solution: by Elimination

Equations (26a), (26b), and (28) constitute a set of simultaneous algebraic equations in the unknowns $z_{i,j}$ provided $g_{i,j}$, $z_{i,j-1}$, $z_{i,j-2}$, and $z_{i,j-3}$ are known. There is one such set for each value of n considered. The equations can be arranged in the form shown in figure 2. Since these equations are tridiagonal in the matrix sense, Potters' form of Gaussian elimination can be used to solve for the $z_{i,j}$. In this method, recursion relationships of the form

$$x_{i,j} = \bar{P}_i \bar{g}_{i,j} - \hat{P}_i x_{i-1,j} \quad (29)$$

$$z_{i,j} = -P_i z_{i+1,j} + x_{i,j}$$

are developed. A forward pass from the initial edge to the final edge computes the $x_{i,j}$, and a back substitution determines the $z_{i,j}$. The matrices P_i , \bar{P}_i , and \hat{P}_i are independent of the load and solution. Hence, they are computed only once.

Poles

The equations (26a) and (26b) are applicable when the shell has edges. If the shell has a pole, $r=0$, and special "boundary" conditions are required to assure finite stresses and strains at the pole. These conditions are derived in reference 1.

SOLUTION PROCEDURE

As a consequence of the selection of the Houbolt timewise differencing scheme, both static and dynamic analyses can be carried out using essentially the same set of equations and solution procedure.

Static Analysis

For a static analysis, $\mu=0$, and the applied load is increased monotonically. Thus, the index j denotes the load step.

The procedure used to determine z for the monotonically increasing load is illustrated in figure 3 and described below:

- 1) The matrices P_1 , \bar{P}_1 , and \hat{P}_1 are computed.
- 2) A solution is obtained for a specified increment of each Fourier coefficient of the design load. All pseudo loads are taken as zero.
- 3) The new solution is used to calculate the nonlinear terms, and a new value of the load vector \bar{g} is obtained for each n . Additional values of n may be introduced by the nonlinear terms.
- 4) A solution is obtained for the new value of \bar{g} , for each n , and is compared with the previous solution.
- 5) If the difference between two consecutive solutions, at any station and for any n , is greater than a specified percentage of the maximum solution in that mode then step #3 is repeated. However, if the number of iterations has exceeded a specified maximum, the total load is reduced by one load increment, the increment is reduced by a factor of 5, and this new increment is added to the load. If a specified number of load reductions have been made, the program ends.
- 6) If the two consecutive solutions have converged, another load increment is added, provided the number of load steps is less than a specified maximum. An estimate of the solution for this new load is made by linear extrapolation using the two preceeding converged solutions, and step #3 is repeated.

Since the method of solution is based on a nonlinear pseudo load approach, the shell reacts equally, in a linear fashion, to any change in either the applied load or the pseudo load. Thus, failure of the solution to converge in any mode can be attributed to two types of nonlinear behavior. Both types are illustrated in figure 3. The existence of a maximum or an inflection point on the softening load-deflection curve A represents a type of behavior for which a solution can be obtained only below the point of zero or nearly zero slope.

$$\bar{\epsilon}_{i,j} = \epsilon_{i,j} + \frac{2\Delta \bar{\mu}_i}{(\delta t)^2} (-5 z_{i,j-1} + 4 z_{i,j-2} - z_{i,j-3})$$

and $i = 1, 2, \dots, K$.

Solution by Elimination

Equations (26a), (26b), and (28) constitute a set of simultaneous algebraic equations in the unknowns $z_{i,j}$ provided $\bar{\epsilon}_{i,j}$, $z_{i,j-1}$, $z_{i,j-2}$, and $z_{i,j-3}$ are known. There is one such set for each value of n considered. The equations can be arranged in the form shown in figure 2. Since these equations are tridiagonal in the matrix sense, Potters' form of Gaussian elimination can be used to solve for the $z_{i,j}$. In this method, recursion relationships of the form

$$\begin{aligned} x_{i,j} &= \bar{P}_i \bar{\epsilon}_{i,j} - \hat{P}_i z_{i-1,j} \\ z_{i,j} &= -P_i z_{i+1,j} + x_{i,j} \end{aligned} \quad (29)$$

are developed. A forward pass from the initial edge to the final edge computes the $x_{i,j}$, and a back substitution determines the $z_{i,j}$. The matrices P_i , \bar{P}_i , and \hat{P}_i are independent of the load and solution. Hence, they are computed only once.

Poles

The equations (26a) and (26b) are applicable when the shell has edges. If the shell has a pole, $r=0$, and special "boundary" conditions are required to assure finite stresses and strains at the pole. These conditions are derived in reference 1.

On the other hand, the existence of a stiffening nonlinearity, as illustrated by curve B of figure 3, can also cause a convergence failure whenever the slope becomes too steep. Thus, in general, it is necessary to examine the load-displacement behavior of the shell in order to determine the cause of the convergence failure.

Dynamic Analysis

The dynamic analysis proceeds in essentially the same manner as the static analysis. The only differences are due to the fact that; (1) the applied load is not monotonically increased, but instead is a function of the time step j ; and (2) initial conditions on z and $\partial z/\partial t$ are required to start the procedure. A brief description of the procedure used to obtain the response of the shell for a specified period of time and time increment is given below:

- 1) The matrices P_i , \bar{P}_i , and \hat{P}_i are computed.
- 2) The solutions at $j = 0, -1$ and -2 are computed for each n from the specified initial conditions using the expressions

$$z_{i,0} = \text{initial condition on } z \text{ supplied by user,}$$

$$(\partial z/\partial t)_{i,0} = \text{initial condition on } \partial z/\partial t \text{ supplied by user}$$

$$z_{i,-1} = z_{i,0} - \delta t (\partial z/\partial t)_{i,0}$$

$$z_{i,-2} = z_{i,0} - 2\delta t (\partial z/\partial t)_{i,0}$$

$$\left. \begin{array}{l} \\ \\ \end{array} \right\} i = 0, 1, \dots, K+1$$

An estimate of the solution at $j=1$ is obtained for each n from

$$z_{i,1} = z_{i,0} + \delta t (\partial z/\partial t)_{i,0}$$

for $i = 0, 1, 2, \dots, K+1$.

- 3) This new solution is used to calculate the nonlinear terms, and a new value of \bar{g} is obtained for each n using the estimated nonlinear terms and applied loads at j and the solutions at $j-1, j-2$, and $j-3$.
- 4) A solution is obtained for the new value of \bar{g} for each n and is compared with the previous solution at j .
- 5) If the difference between two consecutive solutions, at any station and for any n , is greater than a specified percentage of the maximum solution in that mode then step #3 is repeated. However, if the number of iterations has exceeded a specified maximum the program ends.
- 6) If the two consecutive solutions are sufficiently close, an estimate of the solution at $j+1$ is obtained by quadratic extrapolation from the solution at $j, j-1$, and $j-2$. The preceding solutions are updated, and step #3 is repeated for the new time step $j=j+1$, provided the number of time steps is less than a specified maximum.

Two comments are in order here. First, the approximations used to obtain the solutions at $j=-1$ and -2 are not the ones suggested by Houbolt. Houbolt's approximations require a change in the \bar{B} matrix at the first time step. This is time consuming since it necessitates the recomputation of the P_i , P_i , and \hat{P}_i matrices, and does not appear to be worth the extra effort. Second, the time interval is usually so small no iteration is required since the difference between the estimated solution and computed solution is generally negligible. However, when the shell becomes dynamically unstable, the solution may not converge, even with iteration. Thus, the maximum number of iterations allowed should be small.

BRIEF DESCRIPTION OF THE COMPUTER PROGRAM

The program described in this paper is a modified version of the program described in reference 1. The revisions were made by personnel at the NASA Langley Research Center and by the original author. The main difference between the two versions is the addition of the capability for dynamic analysis. Another difference is in the manner in which core storage is allocated for the solution vector z . The solution vector is now handled as a two dimensional array instead of a three dimensional array, allowing the user the freedom of prescribing almost any combination of meridional and circumferential unknowns within the dimensions of the array. In the modified program up to 200 unknowns may be specified so that the product of the total number of meridional stations and the total number of Fourier harmonics must be less than 201. However, the maximum number of Fourier harmonics that can be considered is still 10. Any combination of harmonics may be used. For example, $n = 5, 0, 22$ and 91 is allowed; there is no restriction on the order nor on the number.

A change was also made in the test for convergence. The original program required two consecutive solutions to differ by less than a specified percentage of the latest solution. This test was made at every station, for every mode, except when the solution was less than 10^{-6} . Experience with this routine showed it to be too restrictive. Consequently, it was replaced with the requirement that for each harmonic the difference between two consecutive solutions at each station must be less than a specified percentage of the maximum solution in that harmonic, considering all the stations, except when the solution is less than 10^{-6} . This new test for convergence appears to provide converged, accurate solutions in fewer iterations than the original scheme. The significance of the convergence test is discussed in the Applications section.

The output subroutine was also modified in order to present the data in more compact form; the `COMMON` and `DIMENSION` statements were changed to allow the compilation of the program in any order; and several bugs were detected and eliminated. The operational parameters of the program and the boundary conditions are still read in on cards, but the geometry and mass of the shell, the inplane and bending stiffnesses, and the pressure and thermal loads are introduced through user-prepared subroutines. The input and output data may be in either dimensional form or nondimensional form, and no special tapes, discs, or routines are required for execution. All of these changes have enlarged the program to the extent that it now requires a core space of approximately 150,000 bytes on an IBM 360/67 digital computer and can no longer be executed on a 32,000 word computer.

APPLICATIONS

The computer program has been used to solve a number of static and dynamic problems for both axisymmetric and asymmetric loads. Several of these solutions are presented here to illustrate either the capability or the inability of the program to treat a specific problem area. All of the solutions are for shallow spherical caps since that's the shell for which several published solutions are available. The geometry of the spherical cap can be specified by the single nondimensional parameter λ . The value of λ is increased when either the rise of the shell H is increased or the thickness of the shell h is decreased. The classical buckling pressure of a complete sphere is denoted by q_0 . The reference time is taken as $T_0 = R_s \sqrt{m/E}$. Unless specified otherwise, forty finite difference stations were used.

Static, Axisymmetric Examples

The first example is the clamped cap subjected to a uniform pressure q . A typical load-displacement curve is shown in figure 4 for $\lambda = 8$. The displacement is the maximum displacement of the shell and occurs at a station approximately half-way between the pole and the outer edge. Note that the nonlinearity is the softening type and that axisymmetric snap buckling appears to be imminent. The maximum load at which a converged solution can be obtained is referred to as the final load, and in this case the final load appears to be the axisymmetric snap buckling load. The final loads obtained for several values of λ are presented in figure 5 along with the critical pressures for axisymmetric snap buckling presented by Huang⁷ and Weinitzschke⁸. Forty, eighty, and one hundred stations were used for $\lambda < 10$, $10 \leq \lambda \leq 16$, and $\lambda > 16$ respectively. A stringent convergence criterion of .002 was used for all runs. There is very good agreement with the published results except for $\lambda = 4, 9$, and 10 , where the present results are about ten percent high.

The second axisymmetric example is the clamped cap subjected to a centrally distributed uniform pressure approximating a point load at the pole. The final nondimensional loads P^* are shown in figure 6 for several values of λ . Experimental results for axisymmetric snap buckling due to a small finite area load given by Penning and Thurston⁹ and Penning¹⁰ are also presented in figure 6. The experimental load-displacement curves for $\lambda > 15$ show a well-defined, abrupt discontinuity in the displacement at the pole when $2 \leq P^* \leq 3$. The region of buckling for this range of P^* is in the neighborhood of the pole. Below a value of $\lambda = 15$, the experimental results show no axisymmetric snap, but a large majority of the load-displacement curves show significant decreases in slope in the vicinity of $P^* = 2.0$. Figure 7 shows the theoretical load-displacement curve for $\lambda = 12$, and a reasonably accurate reproduction of the experimental results given in reference 10 for $\lambda = 12.56$ and a small finite area load. Note that although the solution failed to converge for $P^* > 2.27$, snap buckling apparently is not imminent since the experimental results indicate that no snap occurs at this value of load, and the theoretical load-displacement curve does not show the significant decrease

in slope that appears in figure 4 for the pressure loaded cap. Thus, the final load is not a snap buckling load for $\lambda < 15$. The cause of the convergence failure is probably associated with a rapid decrease in slope.

Static, Asymmetric Examples

Liepins¹¹ has published static and dynamic nonlinear solutions for the simply supported cap subjected to the load $q(1 - \frac{r}{r_{\max}} \cos \theta)$. His analysis uses finite differences for all derivatives and the Houbolt implicit differencing scheme. The nonlinear algebraic equations are solved by the Newton - Raphson technique in conjunction with an extension of Potters' method. Plots of q/q_0 versus \bar{V} , an average axisymmetric deflection parameter, are given in figure 8 for a static analysis for $\lambda = 4$ and 8. In the present analysis, fifteen stations and seven and nine modes were used for the two values of λ respectively. This discretization is approximately the same as that of Liepins. Note that for $\lambda = 4$, the present solution compares favorably with Liepins' results, and the final load appears to be a buckling load. However, for $\lambda = 8$, the present solution failed to converge at a load approximately ten percent below Liepins' final load, and buckling does not appear to be imminent since there is very little softening. On the other hand, plots of W/h at $r = .71r_{\max}$ and $\theta = \pi/2$ and π versus q/q_0 , figure 9, reveal that the portion of the shell under the maximum value of the load is definitely softening. Since this appears to be a local effect, the average axisymmetric displacement parameter \bar{V} is not significantly influenced by this large nonlinearity. The convergence criterion used obviously has some influence on the final load*. The present program failed to converge because of the softening nonlinearity in one of the high mode numbers. Perhaps Liepins' convergence criterion, which is based on the square root of the sum of the squares of the solution at each mesh point, is more desirable since it might diminish the significance of local effects. On the other hand, knowledge of local buckling is certainly desirable.

The program has also been used to estimate the bifurcation buckling loads of the clamped cap subjected to an axisymmetric uniform pressure. This was accomplished by applying a nearly axisymmetric load** to the shell and introducing one or more asymmetric modes to the total response. As the load approached the minimum bifurcation load of the modes considered, the response in the critical mode grew very large. Eventually, the solution failed to converge due to softening in the asymmetric mode. The final loads obtained in this manner are shown in figure 10 for several values of λ . Also shown in figure 10 are the unsymmetrical bifurcation buckling loads obtained by Huang⁷ using an eigenvalue formulation. The agreement is very good for all values of λ considered. By varying the amount of asymmetry of the load it was possible to estimate the sensitivity of the pressure loaded

* The final load obtained by the program of reference 1 using the original convergence criterion was .336 and .304 for $\lambda = 4$ and 8 respectively. Figure 8 shows final loads of .342 and .384 for the new convergence criterion.

**Very little asymmetric load was required. A typical value used was .0002 of the axisymmetric load.

shell to imperfections. Figure 11 shows a plot of the normal displacement in the axisymmetric mode at $r = .59r_{\max}$ versus q/q_0 for several values of ϵ , the measure of the amount of asymmetry in the load. Note that as the asymmetry grows, the final load is reduced. Thus, the pressure loaded cap appears to be imperfection sensitive. Also shown in figure 11 is the initial slope of the bifurcation branch of the equilibrium path predicted by Fitch and Budiansky¹² in their study of the initial post buckling behavior of spherical caps based on Koiter's initial post buckling theory*. Apparently, as the asymmetry in the load grows, the solution fails to converge when it reaches the bifurcation branch.

Dynamic, Axisymmetric Example

The program has been used to obtain the dynamic buckling loads of clamped spherical caps subjected to a step uniform pressure loading. A plot of the peak of the deflection parameter \bar{V} versus q/q_0 is given in figure 12 for $\lambda = 5, 8$, and 11. Also shown in figure 12 are the results for $\lambda = 5$ presented by Huang¹³ and by Stephens and Fulton¹⁴. The present solution was carried out to $t = 50$ for $\lambda = 5$, and $t = 120$ for $\lambda = 8$ and 11, with $\delta t = .05$. The maximum load for which a converged solution was obtained is given in figure 13 with the critical pressures presented by Huang¹³, by Stephens and Fulton¹⁴, and by Stricklin, et al.¹⁵. Stricklin's computer program is quite similar to this one; the main difference is that Stricklin uses a finite element formulation for the meridional coordinate. Huang and Stephens and Fulton analyses are for axisymmetric loads only, and they use finite differences and the 'bolt scheme. Stephens and Fulton use the Newton-Raphson procedure. The present results are in very good agreement with Stricklin's results.

Dynamic, Asymmetric Example

The final example is a comparison of the present results with Liepins¹¹ solution for the nonlinear dynamic response of the simply supported cap with $\lambda = 4$ subjected to the finite duration step loading $q(1 - \frac{r}{r_{\max}} \cos \theta)$. The results for the peak \bar{V} versus q/q_0 are presented in figure 14 for the case where the load is on the shell from $0 \leq t \leq 5$. Fifteen finite difference stations and 5 harmonics were used. This was the same discretization as that used by Liepins. Both solutions were carried out to $t = 15$. Liepins' time increment was .1; the ones used here were .1 and .025. Both programs used a convergence criterion of .01. The predicted buckling loads are in fair agreement. Note that the present solution did not experience a convergence failure when the smaller time increment was used. This raises some questions concerning the effect of the time increment and the value of the convergence criterion upon the ability of the solution to converge. The numerical stability of the scheme needs to be examined in the context of the nonlinear problem. Further study is needed in this area.

*The load-displacement relationship used in reference 12 is based on an average deflection parameter.

PROGRAM EVALUATION

The examples presented in this paper demonstrate that the program can accurately predict axisymmetric snap buckling loads and asymmetric buckling loads for both static and dynamic loading conditions. It can also be used to predict bifurcation buckling loads and to estimate imperfection sensitivity. However, the program cannot enter the static post-buckling region*, and in some instances, the point load for example, the final load is not a buckling load. Thus, it may be necessary to examine the solution in some detail to ascertain whether or not buckling is imminent.

The cause of these convergence difficulties is the pseudo load method of solution. On the other hand, this method of solution is efficient. For example, consider the dynamic, axisymmetric example. Each data point in figure 12 required approximately 2 minutes of execution time** to march out 1000 time steps at $\delta t = .05$. A static asymmetric solution to Liepins' problem, figure 8, required approximately 1.5 minutes for 11 load steps for $\lambda = 4$ and 3.0 minutes for 20 load steps for $\lambda = 8$. The dynamic, asymmetric solution to Liepins' problem, figure 14, required approximately 2.5 minutes to march out 600 time steps at $\delta t = .025$. All of these times are based on the FORTRAN H Compiler with OPT = 2. Thus, if this program is applicable to the problem under consideration, it can compute the buckling load in a relatively short time.

One interesting feature of the program is its ability to predict bifurcation loads. Because it uses circumferential series expansions, it can find the buckling load of each harmonic by considering only two modes at a time, $n = 0$ and $n = n$. Or, it can find the minimum buckling load when several modes are considered simultaneously. On the other hand, when finite elements or finite differences are used for the circumferential discretization, there must be many meridians in the network when the critical mode number is high. No computation times are available for comparison with the traditional eigenvalue approach to the problem, so it is not apparent whether or not this procedure is a desirable one.

There are other aspects besides accuracy and efficiency to take into consideration when selecting a program. Ease of usage is very important. Does it take one hour or many to prepare the input data? Is the program easy to modify, with confidence? These questions cannot be answered by the author, since he is biased and is too familiar with the program to make a valid judgement. Other users must provide the answers to these questions. The author welcomes any comments regarding improvements that should be made.

* The Newton-Raphson procedure is supposed to allow the solution to progress into the post-buckling region. Studies of the nonlinear axisymmetric behavior of the point loaded cap show this to be the case. However, Liepins' notes that he was not always able to obtain a solution in the post-buckling region. For example, note in figure 8 the absence of a post buckling solution for $\lambda = 8$. Similar difficulties were encountered in some of the dynamic problems. Thus, it appears that the use of the Newton-Raphson procedure does not guarantee post-buckling solutions.

** Execution time does not include compilation and linkage time.

There are several features of the program that need additional study. For example, is it more efficient in a static analysis to use very small load increments and few iterations or larger load increments and more iterations? What kind of load extrapolation is best for estimating the new solution at each load or time step? Should over or under relaxation be used? What is the significance of the value of the time increment on the convergence failure? What is the best convergence criterion to use?

Future plans for the program include extending it to treat:

- 1) segmented shells,
- 2) complete Fourier series in solution,
- 3) orthotropic material behavior,
- 4) boundary conditions as a function of mode number and time,
- 5) discrete rings,
- 6) use of disc storage,
- 7) post-buckling behavior,
- 8) initial imperfections in shell geometry.

All of the above extensions are straight forward and should be incorporated with little difficulty, except item #7; post-buckling behavior. That extension is going to take some ingenuity. The use of the Newton-Raphson procedure does not appear promising since the governing matrix would not be banded. Perhaps the modified Newton-Raphson technique developed by Greenbaum and Conroy¹⁶ for a conical shell of revolution will work for the general problem considered here. Greenbaum and Conroy also use circumferential series expansions, but they place the nonlinear terms that do not couple the sets of equations, i.e. the terms involving the axisymmetric mod $n = 0$, on the left hand side and use the Newton incremental procedure.

ACKNOWLEDGEMENTS

The author gratefully acknowledges the financial support provided by the NASA-Langley Research Center under Contract No. NAS 1-5804 and grant L-16,438. The technical monitors have been H. G. Schaeffer and R. E. Fulton. The author also acknowledges the contributions of LCDR W. C. Stilwell. Figures 3 - 7, 10 and 11 are taken from Stilwell's thesis, reference 17.

REFERENCES

1. Ball, R. E., "A Geometrically Nonlinear Analysis of Arbitrarily Loaded Shells of Revolution," NASA CR-909, Jan. 1968.
2. Sanders, J. Lyell, Jr., "Nonlinear Theories for Thin Shells," Quart. Appl. Math., Vol. 21, No. 1, 1963, pp. 21-36.
3. Houbolt, John C., "A Recurrence Matrix Solution for the Dynamic Response of Aircraft in Gusts," NACA Rpt. 1010, 1951.
4. Potters, M. L., "A Matrix Method for the Solution of a Second Order Difference Equation in Two Variables," Mathematics Centrum, Amsterdam Holland, Report MR 19, 1955.
5. Hartung, Richard F., "An Assessment of Current Capability for Computer Analysis of Shell Structures," Tech. Rpt. AFFDL-TR- to be published.
6. Budiansky, B., and Radkowski, P., "Numerical Analysis of Unsymmetrical Bending of Shells of Revolution," AIAA Journal, Vol. 1, No. 8, Aug. 1963, pp. 1833-1842. (Discussion by G. A. Greenbaum, Vol. 2, No. 3, Mar. 1964, pp. 590-592.
7. Huang, N. C., "Unsymmetrical Buckling of Thin Shallow Shells," ASME Journal Appl. Mech., Vol. 31, Sept. 1964, pp. 447-457.
8. Weinitschke, H. J., "On Asymmetric Buckling of Shallow Spherical Shells," Journal of Math. and Phy., Vol. 44, Jun. 1965, pp. 141-163.
9. Penning, F. A., and Thurston, G. A., "The Stability of Shallow Spherical Shells Under Concentrated Load," NASA CR-265, Jul. 1965.
10. Penning, F. A., "Experimental Buckling Modes of Clamped Shallow Shells Under Concentrated Load," ASME Journal Appl. Mech., Vol. 33, Jun. 1966, pp. 297-304.
11. Liepins, Atis A., "Asymmetric Nonlinear Dynamic Response and Buckling of Shallow Spherical Shells," NASA CR-1376, Jun. 1969.
12. Fitch, J. R., and Budiansky, B., "Buckling and Postbuckling Behavior of Spherical Caps Under Axisymmetric Load," AIAA Journal, Vol. 8, No. 4, Jun. 1970, pp. 686-693.
13. Huang, N. C., "Axisymmetric Dynamic Snap-Through of Elastic Clamped Shallow Spherical Shells," AIAA Journal, Vol. 7, No. 2, Feb. 1969, pp. 215-220. (Erratum: Vol. 7, No. 8, Aug. 1969, pg. 1664)

14. Stephens, W. B., and Fulton, R. E., "Axisymmetric Static and Dynamic Buckling of Spherical Caps Due to Centrally Distributed Pressures," AIAA Journal, Vol. 7, No. 11, Nov. 1969, pp. 2120-2126.
15. Stricklin, J. A., Martinez, J. E., Tillerson, J. R., Hong, J. H., and Haisler, W. E., "Nonlinear Dynamic Analysis of Shells of Revolution by Matrix Displacement Method," Texas A. and M., Aerospace Eng. Dept., Rpt. 69-77, Feb. 1970.
16. Greenbaum, G. A., and Conroy, D. C., "Postwrinkling Behavior of a Conical Shell of Revolution Subjected to Bending Loads," AIAA Journal, Vol. 8, No. 4, Apr. 1970, pp. 700-707.
17. Stilwell, W. C., "A Digital Computer Study of the Buckling of Shallow Spherical Caps and Truncated Hemispheres," A.E. Thesis, Naval Postgraduate School, Jun. 1970.

QUESTIONS AND COMMENTS FOLLOWING BALL'S PAPER

QUESTION: What does your simplification 2 or assumption 2 mean? I don't understand what you mean when you say the applied pressure and temperature distributions are symmetric about but may vary along the meridian.

BALL: What I'm saying there is that we have not an axis of symmetry but a plane of symmetry. I have ruled out the opportunity of a bifurcation about that particular plane.

QUESTION: Do I understand you correctly to say that essentially your application of additional small load in any mode harmonic is equivalent to the imperfection in that particular mode.

BALL: No, I said that I can use an asymmetric load to estimate the sensitivity of the shell to imperfections.

COMMENT: Well, I think that you really do the same thing. I think it's the same thing because you get the deformation corresponding to that load and it really should mean the same thing.

BALL: It's a triggering mechanism in the nonlinear portion. I've actually gone through an analytical study showing that in the limit my program does indeed give a bifurcation load.

COMMENT: A comment on this last point on the asymmetric buckling. It does appear you've put in this imperfection of geometry, but I believe you've also put in an imperfection of stress which may or may not

be important. Now, sometimes you find that stresses are not important, but you have put this stress imperfection in there.

BALL: You're absolutely right. The stresses are not insignificant in part of the shell. So, in that sense, I do tend to deviate from a stress-free state of a shell which has a very large imperfection. But as the asymmetry of the load gets smaller and smaller, that stress gets very small and looking at the results and the analytical work I've done, it can be shown that the stress is insignificant when compared to the axisymmetric stress.

COMMENT: I think Archer solved this problem of a spherical cap with a point load some years ago and his solution failed to converge at the same point your's did. He concluded that the shell fails there. It's since been discovered that the reason it fails to converge is that the method you use to solve the nonlinear equation is not a quadratically convergent process. When you throw all the nonlinear terms on the right-hand side, the rate of convergence is too weak to achieve convergence beyond the knee of that load deflection curve. I tried to solve the problem by throwing the nonlinear terms on the right-hand side and found it didn't converge and that's what made me go to the Newton Raphson method.

BALL: I said that when two solutions are sufficiently close, I've converged. But what's sufficiently close? I can put in a very relaxed convergence criterion and I can fool you all. Or I could put in a very stringent one and I could hurt myself, since it won't converge simply because of the fact that the machine operates only on a finite number of digits. So, the question of what is the best or most realistic convergence criterion is some-

thing that none of us to my knowledge has really looked into. All of my results are in single precision. The question has been raised by Prof. Stricklin that maybe we ought to go to double precision and he may be right. I'm not sure. I use single precision on the linear dynamic Lockheed sample problem and I got what I consider to be excellent results. But on the nonlinear problem maybe I'll have to go to double precision. I don't know.

COMMENT: I tried both single and double precision with the method of throwing the terms on the right-hand side and the order of the precision has nothing to do with it. It just doesn't converge. You can't get around that bend even in double precision. But even in single precision the Newton Raphson method does converge.

COMMENT: A further comment on this question of convergence and non-convergence. If you look at the succeeding substitution of the nonlinear terms on the right-hand side, you see that you are essentially doing a power sweep method and the convergence is one over λ . When you go beyond the buckling load, the λ is less than one and, in fact, you will diverge. The interesting thing is that the equations tell you not only that you diverge but also that you oscillate in a plus and minus fashion. One interesting observation here is that if you realize that you're essentially doing the power sweep method, then you can pull out from your successive iteration at any load while you're climbing up this nonlinear curve. You can pull out this λ and tell you where you're going to buckle at the very beginning.

COMMENT: I'd like to point out that the method Ball uses to solve this equation is not far fetched. In fact, it is one of the methods that Bushnell and Almroth use whenever they are solving problems and it is a modified Newton Raphson approach. If you take the second derivatives and evaluate them in the undeformed state of the body, then this particular solution technique reduces this exactly to the Newton Raphson approach.

BALL: I'll let Bushnell and Almroth comment on that.

BUSHNELL: Well, from what I understand in your method, you don't refactor the stiffness matrix and in the modified Newton Raphson method you have to refactor the stiffness matrix every once in awhile. You don't do it every time but if you applied it to the particular problem of a sphere with a point load, you certainly would have to refactor the stiffness matrix maybe about 3 or 4 times while you were going around the knee in the load deflection curve.

ALMROTH: I think the essential difference is that when you use a modified Newton Raphson method, you probably use the same scheme, but when you refactor what you do is to take a new reference point instead of the zero point and then put the nonlinear terms into the left-hand side and continue the calculation and you get convergence at higher loads.

BALL: Yes, you're using a local slope. That's essentially how I view the Newton Raphson procedure--as a local slope-local stiffness method.

QUESTION: Evidently your program is user-oriented. Is there a user's manual with this that other people can obtain?

BALL: There is for the static version. It's been available for about six months and can be obtained from NASA Langley Research Center. The dynamic program user's manual will be ready within the next six months.

QUESTION: And would this program handle such things as concentrate loads on cylinders or other shells of revolution?

BALL: Yes, it will, but of course it suffers from the fact that the evaluation of the concentrated load with the Fourier series would require the full ten modes that I can accommodate which then limits me, with my present dimension statements, to 20 meridional stations. However, this can be increased for use on the CDC 6600 or any larger machine that has, say, 64,000 words.

FINITE DIFFERENCE TECHNIQUES FOR VARIABLE GRIDS

Paul S. Jensen
Research Scientist
Lockheed Palo Alto Research Laboratory

Finite difference analysis of shells has commonly been carried out using discretization grids having rectangular mesh elements (rectangular grids). Such grids are quite convenient to implement in a computer program because the coefficients in the finite difference expressions are relatively easy to calculate and the truncation error of the expressions is quite small. The situation is particularly convenient when the dimensions of the mesh elements are fixed. In that case the difference coefficients are constants, and the truncation error is particularly small.

The major difficulty one encounters when using grids with fixed rectangular mesh elements is that of covering a non-rectangular problem domain with his grid. Finite difference expressions corresponding to grid nodes on or near a curved boundary require special treatment. Good general discussions of this are presented in Chapter 6 of Reference 1 and Sections 20.9 and 20.10 of Reference 2. As indicated in both of these discussions, it is advantageous to have nodes of the grid lying on the curved boundary. But this cannot be accomplished in general with grids having fixed mesh elements. Consequently, it is necessary in practical analysis programs using grids with rectangular mesh elements to permit variability in the sizes of the mesh elements.

The first difficulty one encounters when using a rectangular grid with variably sized mesh elements is the calculation of coefficients for each differential expression at each node. These coefficients depend in a non-trivial way upon the distances to neighboring nodes in the grid and thus, because of the variability in the grid, vary from node to node. Because the calculation of these coefficients can require a significant amount of computer time, it is prudent to calculate them only once for a given grid and save them for subsequent application in the solution of the finite difference equations.

A second difficulty arising from the use of a general rectangular grid is the need for substantially more nodes in the grid than is actually necessary to achieve a particular accuracy in the solution. The reason for this inefficiency is illustrated in the two dimensional example of Figure 1.1. The nature of the boundary between points (x_2, y_{j+1}) and (x_3, y_j) is such that the difference $y_{j+1} - y_j$ must be very small. This results in an unnecessarily close spacing between nodes (x_1, y_j) and (x_1, y_{j+1}) for each interior coordinate x_1 .

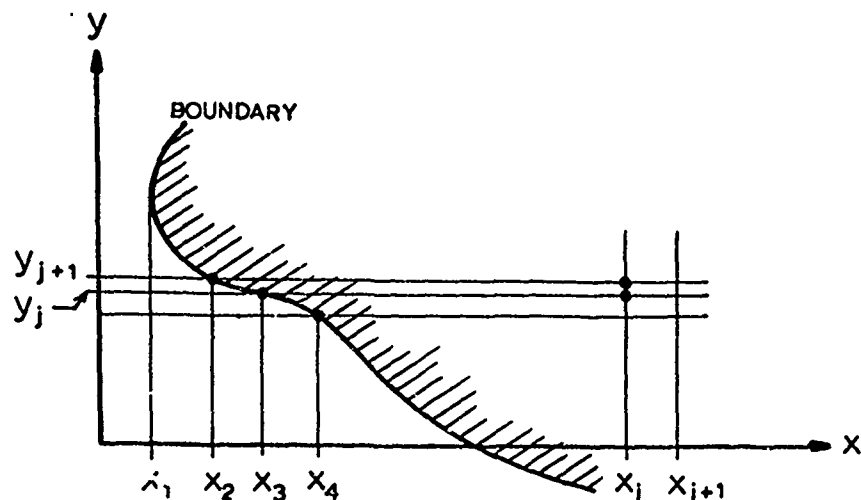


Fig. 1.1 Illustration of Rectangular Grid Inefficiency

Because of the size and complexity of most of the current structural analysis problems being encountered, it is imperative that the inefficiency described above be eliminated. The only apparent way to eliminate this inefficiency is to drop the requirement that the grid be rectangular.

Since the nodes of any two dimensional grid can be interconnected so as to produce all triangular mesh elements, any general two dimensional grid can be called a triangular grid. Note, however, that the interconnection of nodes to form triangles is not unique.

Triangular grids have been used for the finite difference solution of second order partial differential equations for a number of years. Apparently the earliest such application was in 1953 by MacNeal³ in connection with a study of current flow through a thin sheet. Since then it appears that the major application of triangular grids has been to the solution of the neutron diffusion equation. Most of these results and references to other studies in this area can be found in the works by Kellogg, Refs. 4,5,6 and 7. The methods of solution employed in these works were difference methods derived by the variational approach (see Sec. 20.5 of Ref. 2) and the Ritz method. The latter is analogous in several ways to the finite element methods used in mechanics.

There does not appear to have been appreciable application of triangular grids to finite difference analysis of structures. Other than the difficulties associated with calculating and handling the difference coefficients, there appears to be no reason for not using them in transient response programs utilizing explicit time integration.

For solution of structural problems by means of an energy formulation, however, an apparent difficulty does give one pause. The classical solution of second order problems using an energy formulation entails the application of Green's formula (see Ref. 8, page 280) to replace elemental area integration by line integration around an elemental boundary. This results in rather

nice simplifications which, unfortunately, do not readily extend to the higher order equations of structural analysis. The significance of this, however, is just that the classical approach does not readily apply to structural analysis.

Fortunately, there are other methods for obtaining a minimum for the energy functional, or more generally, extremals of functionals. The most obvious approach is to cast the entire functional into discrete form (the discrete finite difference approximation of the functional) and determine extremals of that functional. The major question that has to be investigated then is whether or not the discrete extremals converge to the extremals of the continuous problem. This basic approach has been discussed in some length by D. Greenspan (Refs. 9, 10) and has been applied by him to biharmonic problems (Ref. 11).

The triangular grids that have been used in finite difference computer programs appear to have been of a somewhat restricted nature. Hexagonal grids (each interior node is common to 6 triangular mesh elements) appear to be popular for second order problems and halves of rectangles for higher orders. The ideal is to have a "node generator" which would sprinkle nodes on the problem domain with a density varying according to some given "density function". This density function should then be an approximation to the truncation error in the finite difference expressions used, which of course depends upon the solution. If such a grid construction scheme were realizable, then one could produce a grid possessing the minimum number of nodes required for a given truncation error for any problem. As bonuses, this minimality would both minimize the effects of round off error and maximize the program efficiency (to the extent resulting from having fewer discrete equations to solve).

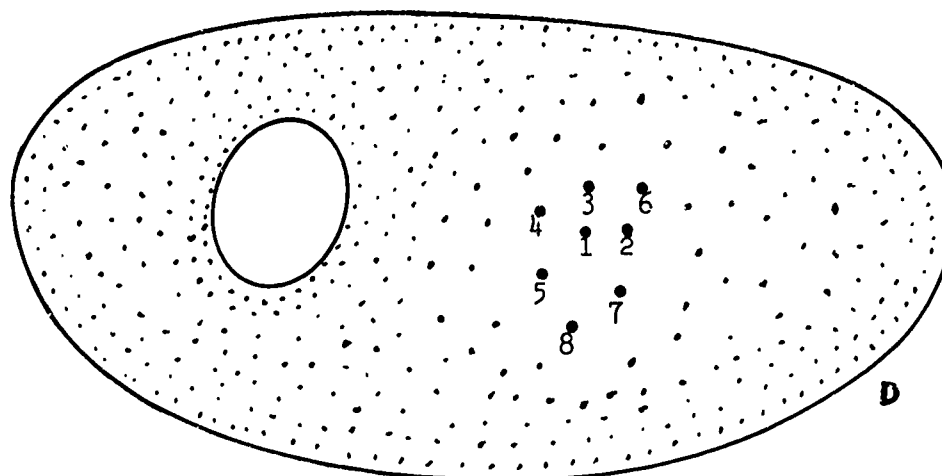
Because of the dependence of the ideal density function upon the solution, it is very likely that the ideal will never be achieved. Nevertheless in structural problems one can go a long way toward the ideal by intuition. For example, given a cylinder under compression with a square cutout, it is intuitively obvious that the nodal density of the grid should be highest in the vicinity of the corners of the cutout, fairly high in the general vicinity of the cutout and relatively low away from the cutout. Using a rough initial density description (function) such as this, a well planned analysis program should be able to cheaply produce a rough solution on the basis of which a more refined density function and solution could be constructed.

In studies involving the propagation of a wave or disturbance through a structure, one can fairly readily determine a region R_1 in the vicinity of the disturbance origin within which motion is going to be restricted for some time period T_1 . Thus for analysis during the period $0 \leq t \leq T_1$ a grid with high nodal density in R_1 and very low density outside of R_1 can effectively be used. Regions R_2, R_3, \dots can of course be determined for subsequent time periods T_2, T_3, \dots as appropriate. For complex problems, the nodal distribution within each region could very well be determined iteratively as described earlier.

DIFFERENCE COEFFICIENTS

Crucial to the success of general triangular grids is the ability to calculate coefficients for difference expressions which have convergent truncation error. Fortunately this can be done, in fact, as one would expect difference expressions of as high order as desired can be formed under mild density and distribution restrictions.

Consider a domain D with a set of n nodes sprinkled on it.



For any sufficiently differentiable function $f(x,y)$ on D and a node (x_1, y_1) one can obtain values of the function at neighboring* nodes by formal Taylor expansion with respect to the node (x_1, y_1) . As will become clearer later on in connection with truncation error, it is convenient to denote neighboring nodes by $(x_1 + \alpha_i h, y_1 + \beta_i h)$ where we assume $|\alpha_i| \leq 1$, $|\beta_i| \leq 1$ and $0 \leq h < 1$. Under this assumption, there exists a constant δ_i such that the value g_i of function at the i^{th} neighbor is given by

$$\begin{aligned} g_i &\equiv f(x_1 + \alpha_i h, y_1 + \beta_i h) = \\ &= f(x_1, y_1) + h(\alpha_i \frac{\partial}{\partial x} + \beta_i \frac{\partial}{\partial y}) f(x_1, y_1) + \dots \\ &\quad + h^m (\alpha_i \frac{\partial}{\partial x} + \beta_i \frac{\partial}{\partial y})^m f(x_1, y_1) \frac{1}{m!} \\ &\quad - h^{m+1} \delta_i \end{aligned} \tag{2}$$

In order to put equations (2) into matrix form it is convenient to introduce the notation:

$$\begin{aligned} \underset{\sim}{F}_m &= (f \quad \frac{\partial f}{\partial x} \quad \dots \quad \frac{1}{i!} \frac{\partial^i f}{\partial x^{i-j} \partial y^j} \quad \dots \quad \frac{1}{m!} \frac{\partial^m f}{\partial x^m})^T \\ i &= 0, 1, \dots, m \quad \text{and} \quad j = 0, 1, \dots, i \end{aligned} \tag{3a}$$

*The word neighbor is loosely used in this context to mean "near-by". The nearest neighbor to any node is the node itself.

where $(\quad)^T$ denotes the vector transpose,

$$H_m = \text{diag} (h^{[a_i]}) \Big|_{i=1}^{n_m}$$

$$= \begin{bmatrix} 1 & h & h & h^2 & h^2 & & 0 \\ 0 & & & & & & h^m \end{bmatrix} \quad (3b)$$

where $a_i = (\sqrt{8 \cdot i - 7} - 1)/2$, $n_m = (m+1)(m+2)/2$ and $[a_i]$ denotes the largest integer not exceeding a_i ,

$$T_m = \begin{bmatrix} 1 & \alpha_1 & \beta_1 & \alpha_1^2 & 2\alpha_1\beta_1 & \dots & \beta_1^m \\ 1 & \alpha_2 & \beta_2 & \alpha_2^2 & 2\alpha_2\beta_2 & \dots & \beta_2^m \\ \cdot & \cdot & \cdot & \cdot & \cdot & \cdot & \cdot \\ \cdot & \cdot & \cdot & \cdot & \cdot & \cdot & \cdot \\ 1 & \alpha_{n_m} & \beta_{n_m} & \alpha_{n_m}^2 & \cdot & \dots & \beta_{n_m}^m \end{bmatrix}, \quad (3c)$$

and

$$\underset{\sim}{G}_m = (g_1 \ g_2 \ \cdot \ \cdot \ \cdot \ g_{n_m})^T \quad (3d)$$

Then there exists a constant vector

$$\underset{\sim}{e}_m = (\delta_1 \ \delta_2 \ \cdot \ \cdot \ \cdot \ \delta_{n_m})^T \quad (3e)$$

such that, as in (2),

$$T_m H_m \underset{\sim}{F}_m = \underset{\sim}{G}_m + h^{m+1} \underset{\sim}{e}_m \quad (4)$$

If the neighbor nodes are chosen so that the nodal matrix T_m is non-singular, then the finite difference expressions for the derivatives of f at the point (x_1, y_1) which appear in the derivative vector $\underset{\sim}{F}_m$ can be obtained from (4) by

$$\tilde{F}_m = H_m^{-1} T_m^{-1} \tilde{G}_m + \tilde{E}_m \quad (5)$$

where the error vector

$$\tilde{E}_m = (h^{m+1}.e_1 \quad h^m.e_2 \quad h^m.e_3 \quad . \quad . \quad . \quad h.e_{n_m})^T$$

with

$$\begin{bmatrix} e_1 \\ . \\ . \\ . \\ e_{n_m} \end{bmatrix} = T_m^{-1} \tilde{e}_m$$

The critical point here is that all of the terms of the error vector $\tilde{E}_m \rightarrow 0$ as $h \rightarrow 0$ so that from (5) it is clear that as the grid spacing $h \rightarrow 0$, the finite difference vector $H_m^{-1} T_m^{-1} \tilde{G}_m$ approaches the derivative vector \tilde{F} . In general (5) shows that with this formulation the derivatives of order m can be calculated with an accuracy $O(h^{m+1-i})$ by using $n_m = (m+1)(m+2)/2$ neighboring values. Thus for example the difference expressions for all derivatives up to the fourth order require at least $n_4 = 15$ neighboring values and consequently the inversion of a 15×15 nodal matrix for each point! In view of the computational effort required to invert a 15×15 matrix it is now appropriate to mention some ways of alleviating this problem.

In most problems encountered in practice, not all of the derivatives up to the given order appear and consequently finite difference terms for all of the derivative terms are not required. For example in the solution of Poisson's equation $\Delta f = -v$, finite difference expressions for only f_2 and f_4 are required. In such cases the order of the nodal matrices can often be reduced.

For shell problems with derivative terms up to the fourth order which satisfy a variational principle, the order of the nodal matrices can be reduced by minimizing the energy expression

$$I(f) = \int_D H(f, f^{(1)}, f^{(2)}) d\sigma \quad (6)$$

to obtain the solution since no derivatives of order higher than two appear in the integrand H (the superscripts on the arguments of H indicate orders of differentiation). Thus if the finite difference approximation to the integrand of equation (6) is

$$H(\bar{f}, \bar{f}^{(1)}, \bar{f}^{(2)}) = H(f, f^{(1)}, f^{(2)}) + O(h^j)$$

then

$$\begin{aligned} I(\bar{f}) &= \int_D H(\bar{f}, \bar{f}^{(1)}, \bar{f}^{(2)}) d\sigma \\ &= I(f) + O_1(h^j) \end{aligned}$$

Consequently convergence is assured for $j \geq 1$ which can be achieved using $n \geq n_2 = 3 \cdot 4/2 = 6$ neighbors, even when all second order derivatives of f appear in H .

BOUNDARY CONDITIONS

The nodal matrices for points on the boundary of the domain are constructed differently from those in the interior in order to satisfy the imposed boundary conditions. For linear analysis the boundary conditions at a boundary node p can be expressed in terms of the derivative vector \tilde{F}_{m-1} of equation (3a) by a set of r_p linear equations

$$\tilde{B}_p \cdot \tilde{F}_{m-1} = \tilde{K}_p$$

where matrix \tilde{B}_p is of order $r_p \times n_{m-1}$ and rank $r_p \leq n_{m-1}$. If $r_p = n_{m-1}$ then \tilde{B}_p is the nodal matrix at point p and the vector \tilde{F}_{m-1} is fully determined there. When $r_p < n_{m-1}$ the nodal matrix \tilde{T}_{m-1} is formed by adjoining $n_{m-1} - r_p$ rows of the form

$$(1 \quad \alpha_1 h \quad \beta_1 h \quad \dots \quad \epsilon_1^{m-1, m-1} h^{m-1})$$

to the matrix \tilde{B}_p corresponding to $n_{m-1} - r_p$ neighboring nodes and the right hand nodal vector \tilde{G}_{m-1} is obtained by adjoining the unknown function values g_i to the vector \tilde{K}_p . Thus at a boundary point when the boundary conditions do not fully determine the vector \tilde{F}_{m-1} , it is determined as in (5) relative to its neighbors. Because of the boundary conditions, fewer neighbors are required for the finite difference expressions at boundary points which indeed is a happy situation since boundary points quite naturally have fewer neighboring nodes inside the domain. Nonlinear boundary conditions need to be linearized and solved iteratively using the linear technique discussed above with an appropriate iterative algorithm.

CURRENT STATUS OF INVESTIGATION

Besides the theoretical investigation presented above, several key programs for studying the feasibility of the finite differences for arbitrary

grids (FIDAG) method have been written. The following is a list of the routines for analyzing a given grid that are operational:

1. A routine for locating a user specified number of neighbors for each node,
2. A routine for classifying nodes according to the neighbor pattern (two nodes are of the same class if the normalized locations of all of their neighbors are the same),
3. A routine for calculating and storing the inverse nodal matrix for each class of node,
4. A routine for testing the condition (non-singularity) of each nodal matrix,
5. Input-output routines for reading in node point locations and displaying the results.

Results for a sample grid are presented in the last section.

Occasionally one finds that the set of nearest neighbors in a given grid is insufficient to determine all of the difference expressions needed. For example, if the set of neighbors lie on a line with the given node it is impossible to determine a difference expression for a derivative normal to that line. This situation is manifested in the analysis by a singular nodal matrix T_m (see Equation 3c). Whenever the nodal matrix is singular or nearly singular for a given node, the node must be reclassified, i.e., a new set of neighbor nodes must be selected. Nodal reclassification is accomplished by simply replacing nodes corresponding to rows of the nodal matrix which are linear combinations of previous rows. This algorithm has not yet been incorporated in our program.

FUTURE POTENTIAL AND WORK

Through the use of variable grids, there appears to be a potential for substantial improvement in efficiency and capacity together with moderate improvement in accuracy of finite difference methods for structural analysis. There remains, however, more research effort to be done before variable grids can be widely used.

The construction and handling of difference coefficients for a given grid is reasonably well in hand. Although grids can presently be generated which are superior to rectangular grids, more work is required in grid generation. For analyses based on a variational approach (energy minimization), research in grid triangularization is required. Numerical integration over a very skew triangular mesh element tends to be somewhat less accurate than over one having all acute angles. An algorithm is needed which, for a given triangularization of a grid, will modify the nodal connections so as to minimize elemental skewness existing in the grid.

SAMPLE PROBLEM

To illustrate the processes involved in analyzing an arbitrary grid in order to produce finite difference coefficients, the FIDAG program in its present form was applied to the grid shown in Fig. 1.

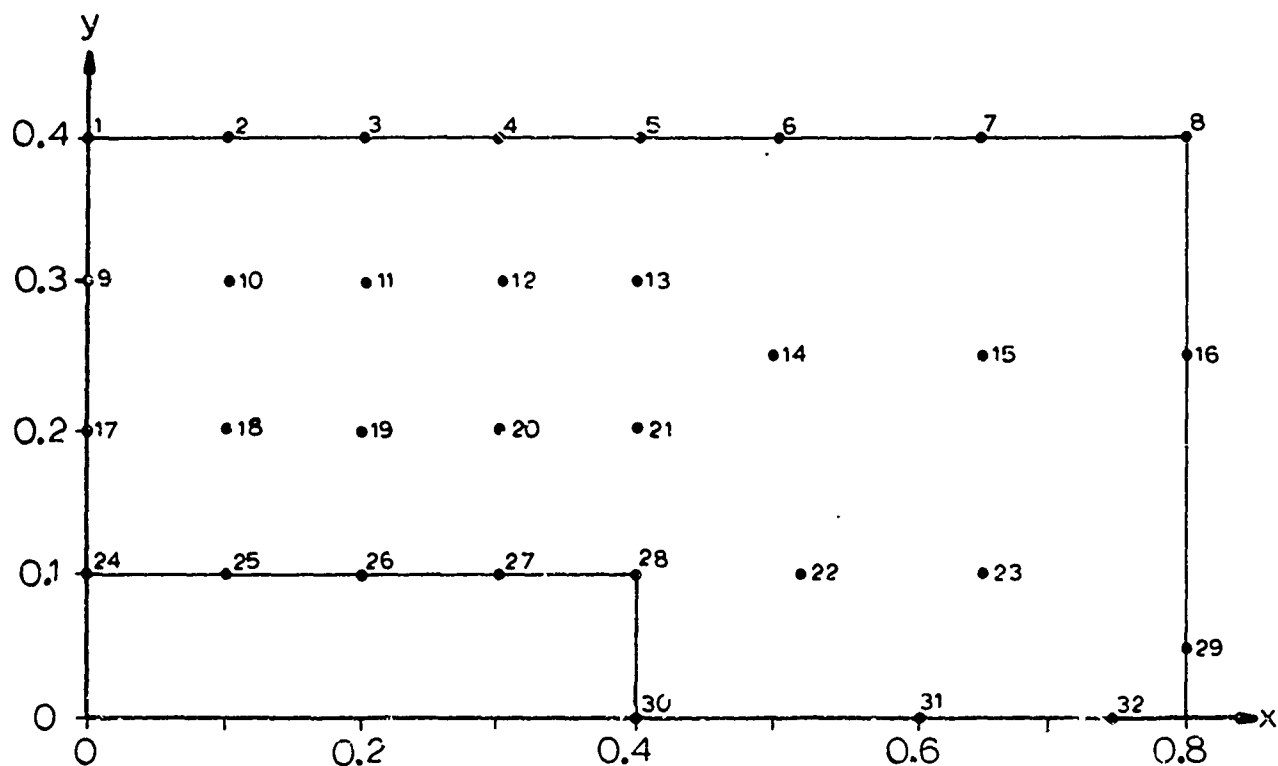


Fig. 1 Sample 32 Node Grid

Comments pertaining to the computer output have been included right on the output where appropriate for reading convenience.

FINITE DIFFERENCES FOR ARBITRARY GRIDS

N = 32 NBI = 5 NBB = 5

LOC	32	58	256	283	443	608
I	X(I)	Y(I)	CLASS			
1	0.000	4.000-01	-1			
2	1.000-01	4.000-01	-1			
3	2.000-01	4.000-01	-1			
4	3.000-01	4.000-01	-1			
5	4.000-01	4.000-01	-1			
6	5.000-01	4.000-01	-1			
7	6.500-01	4.000-01	-1			
8	8.000-01	4.000-01	-1			
9	0.000	3.000-01	-1			
10	1.000-01	3.000-01	1			
11	2.000-01	3.000-01	1			
12	3.000-01	3.000-01	1			
13	4.000-01	3.000-01	1			
14	5.000-01	2.500-01	1			
15	6.500-01	2.500-01	1			
16	8.000-01	2.500-01	-1			
17	0.000	2.000-01	-1			
18	1.000-01	2.000-01	1			
19	2.000-01	2.000-01	1			
20	3.000-01	2.000-01	1			
21	4.000-01	2.000-01	1			
22	5.200-01	1.000-01	1			
23	6.500-01	1.000-01	1			
24	0.000	1.000-01	-1			
25	1.000-01	1.000-01	-1			
26	2.000-01	1.000-01	-1			
27	3.000-01	1.000-01	-1			
28	4.000-01	1.000-01	-1			
29	8.000-01	5.000-02	-1			
30	4.000-01	0.000	-1			
31	6.000-01	0.000	-1			
32	7.500-01	0.000	-1			

N is the total number of nodes in the grid and NBI and NBB are the numbers of neighboring nodes to be used for interior and boundary nodes of the grid. This program utilizes a completely dynamic storage allocation scheme. The array LOC is used to hold the memory allocation for the present problem.

As indicated in the grid definition table above, each node is initially classified -1 if it is a boundary node and +1 if it is an interior node.

FINITE DIFFERENCES FOR ARBITRARY GRIDS

POINTERS TO THE NEIGHBORING NODES FOR EACH NODE OF THE GRID

NODE	POINTERS					
1	2	9	10	3	17	11
2	1	3	10	9	11	4
3	2	4	11	10	12	1
4	3	5	12	11	13	2
5	4	6	13	12	14	3
6	5	13	7	14	4	15
7	6	8	15	14	16	5
8	7	16	15	6	14	23
9	1	10	17	2	18	11
10	2	9	17	18	1	3
11	3	10	12	19	2	4
12	11	20	4	13	3	19
13	21	5	12	14	4	6
14	13	21	6	15	22	5
15	7	14	16	23	22	6
16	8	15	29	7	23	32
17	9	18	24	10	25	1
18	10	17	19	25	9	11
19	11	18	20	26	10	12
20	12	19	21	27	11	13
21	13	20	28	14	12	27
22	28	31	23	14	21	30
23	31	22	32	15	29	14
24	17	25	18	9	26	10
25	18	24	26	17	19	10
26	19	25	27	18	20	11
27	20	26	28	19	21	31
28	21	27	30	22	20	14
29	32	23	16	31	15	22
30	28	27	22	21	31	20
31	23	22	32	30	29	28
32	29	23	31	22	16	15

The routine for locating neighboring nodes finds one more neighbor than is requested by the user (variables NBI and NBB). The extra neighbor is to be used for nodal reclassification if it is required later on in the analysis.

FINITE DIFFERENCES FOR ARBITRARY GRIDS

NODAL CLASSIFICATION

THE NUMBER OF CLASSES IS 21

NODE CLASS	NEIGHBOR	ALPHA BETA	COORDINATES	COORDINATES	
1 -1	5.0-01 0.0	0.0 -5.0-01	5.0-01 -5.0-01	1.0+00 0.0	0.0 -1.0+00
2 -2	-1.0+00 0.0	1.0+00 0.0	0.0 -1.0+00	-1.0+00 -1.0+00	1.0+00 -1.0+00
3 -2	-1.0+00 0.0	1.0+00 0.0	0.0 -1.0+00	-1.0+00 -1.0+00	1.0+00 -1.0+00
4 -2	-1.0+00 0.0	1.0+00 0.0	0.0 -1.0+00	-1.0+00 -1.0+00	1.0+00 -1.0+00
5 -3	-6.7-01 0.0	6.7-01 0.0	0.0 -6.7-01	-6.7-01 -6.7-01	6.7-01 -1.0+00
6 -4	-5.0-01 0.0	-5.0-01 -5.0-01	7.5-01 0.0	0.0 -7.5-01	-1.0+00 0.0
7 -2	-1.0+00 0.0	1.0+00 0.0	0.0 -1.0+00	-1.0+00 -1.0+00	1.0+00 -1.0+00
8 -5	-5.0-01 0.0	0.0 -5.0-01	-5.0-01 -5.0-01	-1.0+00 0.0	-1.0+00 -5.0-01
9 -4	0.0 1.0+00	1.0+00 0.0	0.0 -1.0+00	1.0+00 1.0+00	1.0+00 -1.0+00
10 7	0.0 1.0+00	-1.0+00 0.0	1.0+00 0.0	0.0 -1.0+00	-1.0+00 1.0+00
11 7	0.0 1.0+00	-1.0+00 0.0	1.0+00 0.0	0.0 -1.0+00	-1.0+00 1.0+00
12 7	0.0 1.0+00	-1.0+00 0.0	1.0+00 0.0	0.0 -1.0+00	-1.0+00 1.0+00
13 8	0.0 -1.0+00	0.0 1.0+00	-1.0+00 0.0	1.0+00 -5.0-01	-1.0+00 1.0+00
14 9	-6.7-01 3.3-01	-6.7-01 -3.3-01	0.0 1.0+00	1.0+00 0.0	1.3-01 -1.0+00
15 10	0.0 1.0+00	-1.0+00 0.0	1.0+00 0.0	0.0 -1.0+00	-6.7-01 -1.0+00
16 -11	0.0 7.5-01	-7.5-01 0.0	0.0 -1.0+00	-7.5-01 7.5-01	-7.5-01 -7.5-01
17 -6	0.0 1.0+00	1.0+00 0.0	0.0 -1.0+00	1.0+00 1.0+00	1.0+00 -1.0+00

FINITE DIFFERENCES FOR ARBITRARY GRIDS

18	0.0	-1.0+00	1.0+00	0.0	-1.0+00
7	1.0+00	0.0	0.0	-1.0+00	1.0+00
19	0.0	-1.0+00	1.0+00	0.0	-1.0+00
7	1.0+00	0.0	0.0	-1.0+00	1.0+00
20	0.0	-1.0+00	1.0+00	0.0	-1.0+00
7	1.0+00	0.0	0.0	-1.0+00	1.0+00
21	0.0	-1.0+00	0.0	1.0+00	-1.0+00
12	1.0+00	0.0	-1.0+00	5.0-01	1.0+00
22	-8.0-01	5.3-01	8.7-01	-1.3-01	-8.0-01
13	0.0	-6.7-01	0.0	1.0+00	6.7-01
23	-3.3-01	-8.7-01	6.7-01	0.0	1.0+00
14	-6.7-01	0.0	-6.7-01	1.0+00	-3.3-01
24	0.0	5.0-01	5.0-01	0.0	1.0+00
-15	5.0-01	0.0	5.0-01	1.0+00	0.0
25	0.0	-1.0+00	1.0+00	-1.0+00	1.0+00
-16	1.0+00	0.0	0.0	1.0+00	1.0+00
26	0.0	-1.0+00	1.0+00	-1.0+00	1.0+00
-16	1.0+00	0.0	0.0	1.0+00	1.0+00
27	0.0	-1.0+00	1.0+00	-1.0+00	1.0+00
-16	1.0+00	0.0	0.0	1.0+00	1.0+00
28	0.0	-8.3-01	0.0	1.0+00	-8.3-01
-17	8.3-01	0.0	-8.3-01	0.0	8.3-01
29	-2.5-01	-7.5-01	0.0	-1.0+00	-7.5-01
-18	-2.5-01	2.5-01	1.0+00	-2.5-01	1.0+00
30	0.0	-5.0-01	6.0-01	0.0	1.0+00
-19	5.0-01	5.0-01	5.0-01	1.0+00	0.0
31	2.5-01	-4.0-01	7.5-01	-1.0+00	1.0+00
-20	5.0-01	5.0-01	0.0	0.0	2.5-01
32	2.0-01	-4.0-01	-6.0-01	-9.2-01	2.0-01
-21	2.0-01	4.0-01	0.0	4.0-01	1.0+00

After the neighboring nodes have been found, the local coordinates (α_i, β_i) of the neighbors for each node are calculated and normalized so that the largest component $\max(\alpha_1, \beta_1, \dots, \alpha_m, \beta_m) = 1$, where here m represents either NBI or NBB. The neighbor coordinate set $C_1 \equiv \{(\alpha_1, \beta_1), (\alpha_2, \beta_2), \dots, (\alpha_m, \beta_m)\}_1$ for node 1 is now used to define node class 1. Then for $k = 2, 3, \dots, n$ the neighbor coordinate set C_k for node k is compared with the previously defined sets and if for some $i < k$, $C_i = C_k$ then node k is declared to be of the same class as node i . Otherwise a new class is defined by C_k .

Note that the output verifies the facts, obvious from Fig. 1, that nodes 2, 3, 4 and 7 form one class, nodes 9 and 17 form another, nodes 10, 11, 12, 18, 19 and 20 form a third and nodes 25, 26 and 27 form a fourth class of nodes.

Having classified all of the nodes, one nodal matrix for each class of nodes is constructed and inverted. Since the nearest neighbor to any node is the node itself, the local coordinates of this neighbor are (0, 0). Thus in general the nodal matrix (see Equation 3c) will be of the form

$$T = \begin{bmatrix} 1 & 0 \\ u & B \end{bmatrix}$$

where $u^T = (1 \ 1 \ \dots \ 1)$. Consequently the inverse will be of the form

$$T^{-1} = \begin{bmatrix} 1 & 0 \\ -B^{-1}u & B^{-1} \end{bmatrix}$$

and so it is sufficient just to store the inverse B^{-1} . The quality of the calculated inverse is ascertained by comparing $B^{-1} \cdot B$ with I .

FINITE DIFFERENCES FOR ARBITRARY GRIDS

THE NODAL MATRIX FOR POINT CLASS 1

5.00000+01	0.00000	2.50000-01	0.00000	0.00000
0.00000	-5.00000-01	0.00000	0.00000	2.50000-01
5.00000+01	-5.00000-01	2.50000-01	-5.00000-01	2.50000-01
1.00000+00	0.00000	1.00000+00	0.00000	0.00000
0.00000	-1.00000+00	0.00000	0.00000	1.00000+00

ITS INVERSE

4.00000+00	-5.96046-08	5.96046-08	-1.00000+00	-0.00000
-0.00000	-4.00000+00	-0.00000	-0.00000	1.00000+00
-4.00000+00	5.96046-08	-5.96046-08	2.00000+00	-0.00000
2.00000+00	2.00000+00	-2.00000+00	-0.00000	-0.00000
0.00000	-4.00000+00	0.00000	0.00000	2.00000+00

INVERSE 1 IS STORED STARTING AT 1

THE PRODUCT OF THE INVERSE AND THE MATRIX

1.0+00	-1.5-08	1.5-08	0.0	0.0
0.0	1.0+00	0.0	0.0	0.0
1.5-08	0.0	1.0+00	0.0	0.0
0.0	0.0	0.0	1.0+00	0.0
0.0	0.0	0.0	0.0	1.0+00

Thus for node 1 the finite difference expressions are

$$\begin{bmatrix} f \\ h \cdot f_x \\ h \cdot f_y \\ .5 h^2 \cdot f_{xx} \\ .5 h^2 \cdot f_{xy} \\ .5 h^2 \cdot f_{yy} \end{bmatrix} = \begin{bmatrix} 1 & 0 & 0 & 0 & 0 & 0 \\ -3 & 4 & 0 & 0 & -1 & 0 \\ 3 & 0 & -4 & 0 & 0 & 1 \\ 2 & -4 & 0 & 0 & 2 & 0 \\ -2 & 2 & 2 & -2 & 0 & 0 \\ 2 & 0 & -4 & 0 & 0 & 2 \end{bmatrix} \begin{bmatrix} f_1 \\ f_2 \\ f_9 \\ f_{10} \\ f_3 \\ f_{17} \end{bmatrix}$$

FINITE DIFFERENCES FOR ARBITRARY GRIDS

THE NODAL MATRIX FOR POINT CLASS 2

-1.00000+00	0.00000	1.00000+00	0.00000	0.00000
1.00000+00	0.00000	1.00000+00	0.00000	0.00000
0.00000	-1.00000+00	0.00000	0.00000	1.00000+00
-1.00000+00	-1.00000+00	1.00000+00	2.00000+00	1.00000+00
1.00000+00	-1.00000+00	1.00000+00	-2.00000+00	1.00000+00

ATTEMPTED TO RECLASSIFY CLASS 2

Occasionally the neighbor set C for a particular class of nodes will be insufficient to define all of the derivatives required. This situation is indicated by a singular nodal matrix. In such a case a different neighbor set must be defined for each node in the class and new classes must be formed as needed. The reclassification algorithm has not yet been incorporated in FIDAG.

FINITE DIFFERENCES FOR ARBITRARY GRIDS

THE NODAL MATRIX FOR POINT CLASS 3

-6.66667-01	0.00000	4.44444-01	0.00000	0.00000
-6.66667-01	0.00000	4.44444-01	0.00000	0.00000
0.00000	-6.66667-01	0.00000	0.00000	4.44444-01
-6.66667-01	-6.66667-01	4.44444-01	8.88889-01	4.44444-01
6.66667-01	-1.00000+00	4.44444-01	-1.33333+00	1.00000+00

ITS INVERSE

-7.50000-01	7.50000-01	-0.00000	-0.00000	-0.00000
-3.00000+00	-2.00000+00	-7.50000+00	3.00000+00	2.00000+00
1.12500+00	1.12500+00	-0.00000	-0.00000	-0.00000
-1.12500+00	-3.72529-09	-1.12500+00	1.12500+00	3.72529-09
-4.50000+00	-3.00000+00	-9.00000+00	4.50000+00	3.00000+00

INVERSE 3 IS STORED STARTING AT 26

THE PRODUCT OF THE INVERSE AND THE MATRIX

1.0+00	7.5-09	0.0	0.0	0.0
-1.5-08	1.0+00	0.0	0.0	0.0
-3.0-08	0.0	1.0+00	0.0	1.5-09
-1.5-08	1.5-08	6.0-08	1.0+00	1.5-09
-6.0-08	0.0	0.0	0.0	1.0+00

FINITE DIFFERENCES FOR ARBITRARY GRIDS

THE NODAL MATRIX FOR POINT CLASS 7

0.00000	1.00000+00	0.00000	0.00000	1.00000+00
-1.00000+01	0.00000	1.00000+00	0.00000	0.00000
1.00000+00	0.00000	1.00000+00	0.00000	0.00000
0.00000	-1.00000+00	0.00000	0.00000	1.00000+00
-1.00000+00	1.00000+00	1.00000+00	-2.00000+00	1.00000+00

ITS INVERSE

-0.00000	-5.00000-01	5.00000-01	-0.00000	-0.00000
5.00000-01	0.00000	-0.00000	-5.00000-01	-0.00000
-0.00000	5.00000-01	5.00000-01	-0.00000	-0.00000
5.00000-01	5.00000-01	3.72529-02	-0.00000	-5.00000-01
5.00000-01	0.00000	0.00000	5.00000-01	0.00000

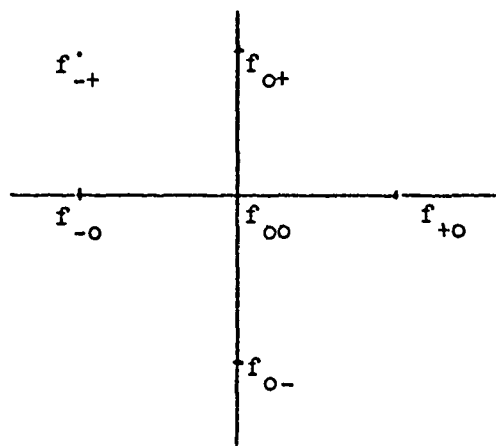
INVERSE 7 IS STORED STARTING AT 76

THE PRODUCT OF THE INVERSE AND THE MATRIX

1.0+00	0.0	0.0	0.0	0.0
0.0	1.0+00	7.5-02	0.0	0.0
0.0	-3.7-08	1.0+00	0.0	0.0
-1.5-08	0.0	0.0	1.0+00	0.0
2.2-08	1.5-08	-2.2-16	0.0	1.0+00

Node 10 (class 7) coupled expression

$$\frac{h^2}{2} f_{xy} = \frac{1}{2} (f_{ot} - f_{-+}) - \frac{1}{2} (f_{oo} - f_{-o})$$



FINITE DIFFERENCES FOR ARBITRARY GRIDS

THE NODAL MATRIX FOR POINT CLASS 10

0.00000	1.00000+00	0.00000	0.00000	1.00000+00
-1.00000+00	0.00000	1.00000+00	0.00000	0.00000
1.00000+00	0.00000	1.00000+00	0.00000	0.00000
0.00000	-1.00000+00	0.00000	0.00000	1.00000+00
-8.66667-01	-1.00000+00	7.51111-01	1.73333+00	1.00000+00

ITS INVERSE

-0.00000	-5.00000-01	5.00000-01	-0.00000	-0.00000
5.00000-01	0.00000	-0.00000	-5.00000-01	-0.00000
-0.00000	5.00000-01	5.00000-01	-0.00000	-0.00000
-0.00000	-4.66667-01	3.33333-02	-5.76923-01	5.76923-01
5.00000-01	0.00000	0.00000	5.00000-01	0.00000

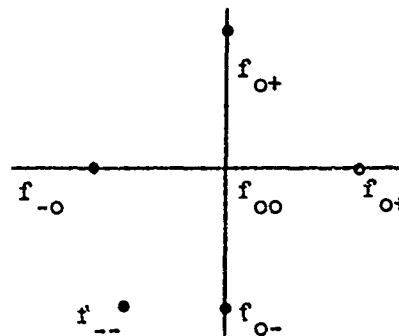
INVERSE 10 IS STORED STARTING AT 151

THE PRODUCT OF THE INVERSE AND THE MATRIX

1.0+00	0.0	0.0	-1.5-08	0.0
0.0	1.0+00	7.5-09	0.0	0.0
0.0	-2.2-08	1.0+00	0.0	0.0
0.0	0.0	0.0	1.0+00	0.0
0.0	7.5-09	1.2-09	7.5-09	1.0+00

Node 15 (class 10) coupled expression

$$\frac{h^2}{2} f_{xy} = (0.0333 f_{+o} + 0.4333 f_{oo} - 0.4667 f_{-o}) - 0.5769 (f_{o-} - f_{--})$$



FINITE DIFFERENCES FOR ARBITRARY GRIDS

THE NODAL MATRIX FOR POINT CLASS 11

0.00000	7.50000-01	0.00000	0.00000	5.62500-01
-7.50000-01	0.00000	5.62500-01	0.00000	0.00000
0.00000	-1.00000+00	0.00000	0.00000	1.00000+00
-7.50000-01	7.50000-01	5.62500-01	-1.12500+00	5.62500-01
-7.50000-01	-7.50000-01	5.62500-01	1.12500+00	5.62500-01

ITS INVERSE

-4.31414+07	-1.00663+08	-3.23541+07	5.03316+07	5.03316+07
7.61905-01	0.00000	-4.28571-01	-0.00000	-0.00000
-5.75219+07	-1.34218+08	-4.31414+07	6.71089+07	6.71089+07
5.07937-01	0.00000	-2.85714-01	-4.44444-01	4.44444-01
7.61905-01	0.00000	5.71429-01	0.00000	0.00000

INVERSE 11 IS STORED STARTING AT 176

THE PRODUCT OF THE INVERSE AND THE MATRIX

1.0+00	0.0	-1.5-08	0.0	0.0
0.0	0.0	0.0	5.0-01	5.0-01
0.0	0.0	1.0+00	0.0	0.0
3.6-01	0.0	3.9-01	1.0+00	1.5-08
5.0-01	0.0	2.5-01	0.0	1.0+00

CLASS 11 HAS AN ILL-CONDITIONED NODAL MATRIX

Occasionally the neighbor set C for a class of nodes is insufficient to produce an accurate set of finite difference expressions. The quality of the set is indicated by the variance of $B^{-1} \cdot B$ from the identity I. In normal operation the user will provide the program with a parameter indicating what degree of ill-condition in the nodal matrix will be accepted without reclassification.

FINITE DIFFERENCES FOR ARBITRARY GRIDS

THE NODAL MATRIX FOR POINT CLASS 21

2.00000-01	2.00000-01	4.00000-02	8.00000-02	4.00000-02
-4.00000-01	4.00000-01	1.60000-01	-3.20000-01	1.60000-01
-6.00000-01	0.00000	3.60000-01	0.00000	0.00000
-9.20000-01	4.00000-01	8.46400-01	-7.36000-01	1.60000-01
2.00000-01	1.00000+00	4.00000-02	4.00000-01	1.00000+00

ITS INVERSE

1.17128+00	-1.68269+00	-1.51042+00	9.01442-01	7.81250-02
3.67188+00	2.74038+00	8.22917-01	-1.02163+00	-4.21875-01
1.95313+00	-2.80449+00	2.60417-01	1.50240+00	1.30208-01
1.75781+00	-1.20192-01	2.31771+00	-1.05168+00	1.17188-01
-4.68750+00	-2.24359+00	-1.45833+00	1.20192+00	1.35417+00

INVERSE 21 IS STORED STARTING AT 401

THE PRODUCT OF THE INVERSE AND THE MATRIX

1.0+00	-2.6-08	-1.6-08	1.4-08	9.8-09	<div>hours</div> <div>minutes</div> <div>seconds</div> <div>milliseconds</div>
0.0	1.0+00	-1.3-08	1.9-09	0.0	
0.0	0.0	1.0+00	7.5-09	-3.3-09	
1.5-08	-2.6-08	-4.3-08	1.0+00	1.9-09	
-6.0-08	3.0-08	-3.0-08	1.5-08	1.0+00	

THE TOTAL ELAPSED TIME IS 00:00:01.387

Notice that many of the nodal matrices have been omitted for brevity.

REFERENCES

1. Varga, R. S., Matrix Iterative Analysis, Prentice-Hall, Inc., New Jersey (1962)
2. Forsythe, G. E. and W. R. Wasow, Finite Difference Methods for Partial Differential Equations, John Wiley & Sons, Inc., New York (1960)
3. MacNeal, R. H., "An Asymmetrical Finite Difference Network", Quart. Appl. Math., 11 (1953) pp 295-310
4. Kellogg, R. B., "A Finite Difference Approximation to the Diffusion Equation in Hexagonal Geometry", Report MPC-21, Combustion Engineering, Inc., Windsor, Conn. (1959)
5. _____, "A Ritz Finite Difference Approximation to the Neutron Diffusion Equation", Bettis Tech. Rev., WAPD-BT-31, (1964) pp 51-58
6. _____, "The Errors for Finite Difference Approximations to the Diffusion Equation", Report MPC-24, Combustion Engineering, Inc., Windsor, Conn. (1960)
7. _____, "Difference Equations on a Mesh Arising from a General Triangulation", Math. of Comp., Vol. 18 (1964), pp 203-210
8. Courant, R. and D. Hilbert, Methods of Mathematical Physics, Vol. 1, Interscience Publishers, Inc., New York, (1937)
9. Greenspan, D., "On Approximating Extremals of Functionals - I. The Method and Examples for Boundary Value Problems," Bull. Int. Comp. Centre, Vol. 4, University of Rome (1965), pp 99-120
10. _____, "On Approximating Extremals of Functionals - II. Theory and Generalizations Related to Boundary Value Problems for Nonlinear Differential Equations", Int. J. Engng. Sci., Vol. 5 (1967), pp 571-588.
11. _____, "A Numerical Approach to Biharmonic Problems," Computer J., Vol. 10, No. 2 (1967), pp 198-201

QUESTIONS AND COMMENTS FOLLOWING JENSEN'S PAPER

QUESTION: Surely you've been tempted to try and write small programs and exercise some of these ideas. What kind of experiences have you had in trying to write mesh generators and grid generators and meshing routines?

JENSEN: I haven't done anything in the grid generation, but I've used a few of the techniques which are around. You consider a domain and assume that it's made out of very thin rubber. You then distort it into a nice tractable domain and draw on it a nice rectangular grid. Then you let go of it and it comes back to the shape of the original domain with a very fancy grid. Sometimes you're really surprised with what you get and may be tempted to call it a mess generator.

COMMENT: Compared to what you're talking about, those mesh generators are extremely confining.

QUESTION: Since your alphas and betas have to be less than one, will it not inherently produce lower accuracy near the boundaries where you just can't get as many points as you want?

JENSEN: No, it won't necessarily. Happily, at the boundaries you don't need as many neighbors because you're applying boundary conditions.

COMMENT: At AVCO we have a two-dimensional shell code that uses grid techniques that are similar in philosophy to the ones that you

talk about. At present it utilizes non-uniform quadrilaterals. I was very interested to see the kinds of approaches that you took.

QUESTION: Have you attempted to rotate the grids at the boundaries? In fluid flow problems, they use this technique whenever they flow past an object. Has there been any work on this idea?

JENSEN: I haven't done that. I tend to shun that because it seems a little restrictive since you have to find a mapping function. If you're going to try and find an analytical mapping function, then you're going to restrict the kinds of curved boundaries you're going to allow. If you're going to use a numerical mapping function, I intuitively suspect that you would have some mighty tight clusters of nodes near sharp corners.

I might make one further comment. I have produced some results for a test grid just to see if this really does produce differences that we know are true and indeed it does. They came out very accurately. I was using all single precision for inverting these matrices. A person can look at the results for several hours if he's interested in really understanding how different neighboring patterns affect the coefficients in these differences expressions. In fact, one can draw a lot of intuitive conclusions, one of which might be that you wish to have a sort of circular nature in your neighbor patterns. The reason for this is that basically the Taylor series is a very local expansion and the error grows very rapidly as you get far from a node. So, if you can have as many nodes in close as possible, you're naturally going to improve your accuracy. And it turns out that when you follow a circular like pattern, you get coefficients that are all of approximately the same size and this is very appealing because you are,

in a sense, putting equal weights on the value at neighboring nodes rather than giving heavy emphasis to some neighbors and very low emphasis to others.

QUESTION: I'm curious to know if you've programmed any plate or shell equations on this basis and what the experience might be. Also, would you comment on the comparison of your ideas with those posed by Budianski in his paper, "Nodes Without Elements," of a couple of years ago.

JENSEN: I have started a program in this area but I haven't really gotten it to the point where it can be used. With regard to your second question, I haven't read Budianski's paper, but he was visiting here not long ago and I talked with him. He mentioned the problem of these coefficient matrices and said that he was bogged down in handling all of the coefficients. One approach is to calculate the coefficients each time you need them. But that clearly wipes you out because it takes so much time. What you really want to do is calculate the coefficients for the grid once and save them to use whenever you need them. As a result of that conversation, I got very interested in manipulation of coefficients and, as I mentioned before, I discovered that it can actually be handled in a very efficient fashion, even on a dedicated computer.

FORSBERG: I might give a little bit of background as to the motivation for this work. We've done quite a bit of work with finite differences. We have used variable grids but they still use orthogonal meshes, or in the case of an elliptic cone, they may be non-orthogonal but they still exhibit a regular pattern. As a result, when you vary the spacing, that

variable spacing runs the entire length of the shell and this causes a great deal of inefficiency since you have a large number of points where you really don't want concentrations. That's what Stan alluded to here somewhat earlier. The present work is really an attempt to broaden the capability of the finite difference method for shell analysis. Variable methods have been used extensively in other systems of lower order and this is an essential step in broadening the scope of the finite difference method to apply to types of problems that are solved every day with the finite element technique. The next step is to take this work and tie it in with the existing shell codes that we have already developed.

QUESTION: I would like to ask Forsberg if he foresees any difficulties at the juncture of two shells.

FORSBERG: No difficulty, we have been using variable meshes for solving problems of fuel slosh in the low gravity environment. These are highly nonlinear motions and the nets are very distorted and much of that work has provided background for the present work. The difference is, of course, that the differential equations for the slosh problem are of lower order.

QUESTION: I feel as though your lecture this morning is one of the most exciting I've heard in a long time. I think the ideas that you present hold great potential, both for the finite difference and for the finite element methods, especially in the area of remeshing during the problem. How much work has been done in deciding how to remesh? You suggested that perhaps a stress gradient might be the way to remesh, i. e., in areas of high stress gradients. Is this as far as it's gone?

JENSEN: On the point of remeshing or regridding, one can approximate the truncation error in his differential equations simply by calculating the derivatives of the next higher order. If you're using fourth order derivatives, then if you calculate the fifth order derivatives, you really are calculating approximately your truncation error. You can calculate these derivatives in exactly the same way you calculate the others, namely, from rows out of your coefficient matrices. I envision using these calculated truncation errors of the rough solution over the domain as the density function for the next grid pass rather than exact the stress gradients.

COMMENT: I looked at your equation 2 and it reminds me of some equations put up by Strang who is at MIT and Fitz at Harvard. They've been able to use this type of expression, together with the Ritz-Galerkin procedure to form bounds on the error.

JENSEN: I'm not really assuming a function and in Ritz methods or Galerkin methods you do assume a function and it's in essence a method of undetermined coefficients.

COMMENT: That's true, but your undetermined coefficients are already implied in your expansion of the Taylor's theories. You might say you can attack differential equations directly but I think it's better to have something--some minimum potential--some function you can get hold of and exploit with the intuition that you have.

COMMENT: One of the reasons we wanted to switch to a variable grid, I believe, is to perhaps save on the total number of grid points we

have to use and at the same time be able to have a very dense concentration of grid points in the vicinity of a discontinuity. This would be particularly helpful in a dynamics code where computer times that we're up against now are very high. What bothers me a little bit is, if the people insist on using explicit schemes where the time step is governed by the grid size, might we not be getting ourselves into a situation here where, because we use a very fine grid over some portion of the shell, we are then stuck with a very small time step for the entire analysis. Maybe we have to attack this on two fronts and look for ways of varying the time step as well as varying the spatial step. Does anybody have any comments on that?

COMMENT: My impression is that you will have to use implicit methods. You will not be able to practically use explicit methods if you have small grid spacing. But there are also problems with the implicit method. As you go implicit, you have to solve a set of simultaneous equations to get from time 1 to time 2 and those equations will become more and more poorly conditioned as the nodal point density increases.

NUMERICAL METHODS FOR MIXED BOUNDARY VALUE PROBLEMS OF SHELLS OF REVOLUTION*

BY

ARTURS KALNINS**

ABSTRACT

For the solution of a mixed boundary value problem of an axisymmetric shell, for which different variables are prescribed over portions of the circular boundaries, methods are required which are applicable to boundary value problems governed by two-dimensional partial differential equations. Two such methods are discussed in this paper. One uses a truncated series expansion in terms of separable solutions, and the other employs finite difference expressions in the circumferential direction. Using these two techniques, the problem is brought to a one-dimensional form, and then solved with the multisegment method of direct numerical integration. An example of pure bending of a cylindrical shell with a semicircular slit is solved by both methods, and numerical results are given.

* A part of this work has been supported by the National Aeronautics and Space Administration Grant NGR-39-007-017.

** Professor of Mechanics, Lehigh University, Bethlehem, Pennsylvania 18015.

I. INTRODUCTION

Linear boundary value problems of thin, elastic shells of revolution can be readily solved with available methods when the same set of boundary variables is prescribed at every point along each of the two circular edges of the shell. For some problems, however, it is necessary to prescribe different sets of boundary variables over different portions of the circular edges. Numerical methods for the solution of such mixed boundary value problems are discussed in this paper.

Since a shell is represented by a two-dimensional reference surface, its behavior is governed by a system of two-dimensional partial differential equations. For a shell of revolution with axisymmetric geometrical and physical properties, these equations are separable by means of solutions which are expressible as products of functions of the meridional and circumferential coordinates. For an exact solution of the mixed boundary value problem, however, an infinite number of such separable solutions must be combined. Therefore, the techniques of solving such a mixed boundary value problem must be those which are applicable for solving systems of partial differential equations.

Two different numerical methods of solving the mixed boundary value problem are discussed in this paper. The methods are based on two different reduction techniques of a boundary value problem governed by partial differential equations to

one governed by ordinary differential equations, which for both methods are then solved by the multisegment direct numerical integration technique [1]*.

The first method employs the technique applied to the analysis of shells of revolution with a curved axis of symmetry (curved tube) [2], for which circumferential derivatives are eliminated by means of finite difference expressions. The second method uses a truncated expansion of separable solutions, and the satisfaction of the mixed boundary conditions is enforced by the standard point-matching technique. An example problem of the bending of a cylindrical shell is solved by both methods, and the results are compared.

*Numbers in brackets denote references listed at end of paper. Numbers in parentheses refer to equations.

II. REDUCTION TO ORDINARY DIFFERENTIAL EQUATIONS

1. Governing Equations

The mixed boundary value problems considered in this paper are governed in a two-dimensional region, defined by $a \leq x \leq b$ and $0 \leq \theta \leq 2\pi$, by a system of linear differential equations in the form

$$\partial y / \partial x = F(x, \theta, y, \partial y / \partial \theta, \partial^2 y / \partial \theta^2) \quad (1)$$

where $y = y(x, \theta)$ denotes an $(m, 1)$ column matrix whose elements are m unknown dependent variables; F denotes m linear functions, arranged in a column matrix form; and x, θ are the coordinates.

For the two methods proposed in this paper, the boundary conditions at the ends of the interval of x will be stated in the form

$$T_a(\theta_i) y(a, \theta_i) = u_a(\theta_i) \quad (2a)$$

$$T_b(\theta_i) y(b, \theta_i) = u_b(\theta_i) \quad (2b)$$

where θ_i are N selected points*, called pivotal points, on

*The selected points θ_i need not be the same on $x = a$ as on $x = b$, but the total number of such points on each edge must equal N .

each of the two edges of the region, defined by $x = \text{constant}$ (Figure 1); $T_a(\theta_i)$ and $T_b(\theta_i)$ are given (m,m) matrices which identify the $m/2$ prescribed elements of y or their linear combinations, and u_a, u_b are $(m,1)$ column matrices which contain the values of the $m/2$ prescribed elements. The feature of mixed boundary conditions is revealed by the fact that on the edges $x = \text{constant}$ the boundary conditions, as represented by the T matrices, can change from point to point along the θ -coordinate curve. The θ -coordinate curve is assumed a closed circle, so that continuity of all variables at the endpoints of the interval on θ is enforced for all values of x .

2. Expansion in Separable Solutions

For axisymmetric shells, which have a straight axis of symmetry in the geometric and physical properties, the solution of (1) can be expressed as a term of a Fourier series

$$y(x, \theta) = y_n(x) T_n(\theta) \quad (3)$$

with a wave number n , where

$$T_n(\theta) = \begin{Bmatrix} \cos n\theta \\ \sin n\theta \end{Bmatrix} \quad (4)$$

for any integral value of n . The meaning of $T_n(\theta)$ is that, depending on symmetry and the particular element of y , the top or bottom trigonometric function in (4) is applicable.

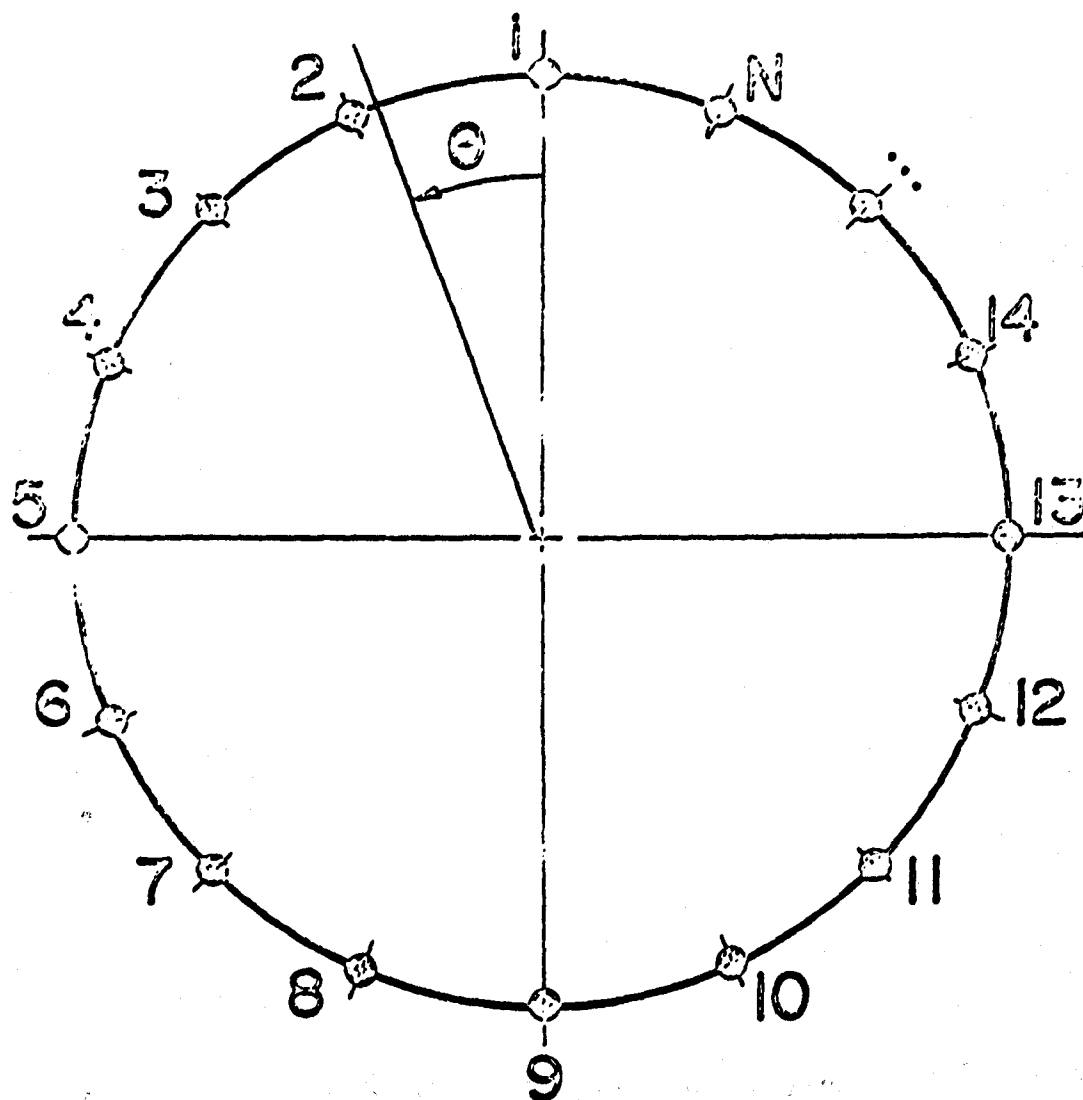


FIGURE 1. Pivotal points around a latitude circle.

If the load terms, contained in (1), are chosen in a similarly separable form, i.e.,

$$b(x, \theta) = b_n(x)T_n(\theta) \quad (5)$$

then the x-dependent Fourier coefficients of y are governed by the system of m linear ordinary differential equations given by

$$dy_n(x)/dx = F_n(x, y_n) + b_n(x) \quad (6)$$

for any integral value of n.

If the boundary conditions at the ends of the x-interval were not mixed, i.e., the T_a and T_b matrices in (2) were the same over all values of θ , then the boundary value problem would be uncoupled with respect to the Fourier coefficients of the solution. Then the nth Fourier coefficient of the load would produce only the nth Fourier coefficient of the solution. The mixed boundary value problem, however, requires that an infinite number of Fourier coefficients be included in the solution for each nth Fourier coefficient of the load.

To solve such a mixed boundary value problem approximately, we shall assume that the solution is expressed by the truncated series

$$y(x, \theta) = \sum_{n=0}^N y_n(x) T_n(\theta) \quad (7)$$

where the number of terms N must be identical to the number of boundary points chosen in (2a) at which the boundary conditions are enforced. Although the solution (7) satisfies exactly the governing differential equations, it is only approximate because the boundary conditions away from the N pivotal points are not exactly satisfied.

It should be also remarked that the indices n in (7) need be neither consecutive nor start with $n = 0$. Owing to symmetry or other considerations, a specially selected list of N wave numbers can be chosen to participate in the solution. For the purpose of illustrating the technique and for the example worked out in the last section, the form of the solution given by (7) is employed.

When the solution in the form of (7) is evaluated at $\theta = \theta_1$ and then substituted into (2a), the resulting form

$$T_a(\theta_1)[y_0 T_0(\theta_1) + \dots + y_N T_N(\theta_1)] = u_a(\theta_1) \quad (8)$$

suggests that the problem be formulated in terms of an extended solution matrix y^* having mN elements. The first N elements of this matrix are the N Fourier coefficients of the first unknown variable of y , the second N elements are the N Fourier coefficients of the second variable of y , and so on. Then the

boundary conditions (2) can be restated in the form

$$T_a^* y^*(a) = u_a^* \quad (9)$$

$$T_b^* y^*(b) = u_b^*$$

where T_a^* , T_b^* and u_a^* , u_b^* are similarly extended (mN, mN) and $(mN, 1)$ matrices, respectively.

With this formulation, the mixed boundary value problem has been brought to the form in which it can be solved by means of the multisegment direct numerical integration technique. Before discussing some details of this method, we shall consider another technique of bringing the problem to the same formulation.

3. Finite Difference Technique

The partial derivatives with respect to θ in (1) can also be removed by replacing them with their finite difference expressions. Such a solution technique has been proposed for the analysis of curved tubes [2], but it can be also applied to the solution of the mixed boundary value problem of a shell of revolution.

In analogy to the separable solution expansion technique, the finite difference method also requires the selection of N pivotal points on the θ -coordinate curve. Then the first and second partial derivatives with respect to θ , occurring in (1),

are replaced at every value of x by their finite difference expressions in terms of the pivotal values of the unknown variables contained in y , which themselves remain functions of x . Since the θ -coordinate curve for a shell of revolution is a closed circle, the partial derivatives can be expressed easily by central differences based on five point formulas. According to such formulas, the derivatives at a point θ_0 are given by

$$\partial y / \partial \theta = [8(y_1 - y_{-1}) - y_2 + y_{-2}] / 12\Delta \quad (10a)$$

$$\partial^2 y / \partial \theta^2 = [16(y_1 - y_{-1}) - (y_2 + y_{-2}) - 30y_0] / 24\Delta^2 \quad (10b)$$

where the plus indices denote points ahead of θ_0 and the minus indices mean points behind θ_0 ; Δ denotes the interval of θ between the pivotal points, which here is assumed constant.

Once such replacement of the derivatives is achieved and N pivotal points around the θ -coordinate curve are selected, then it is convenient again to augment the $(m, 1)$ column matrix $y(x, \theta)$ to include as its elements the N pivotal values of each of the m unknown variables. Thus a new $(mN, 1)$ column matrix y^* is constructed which has as its first N elements the N pivotal values of the first unknown variable of y , the second N elements are the N pivotal values of the second unknown variable of y , and so on. Similarly, the boundary conditions (2) can be stated in the form of (9) where now, obviously, at every pivotal point a different set of boundary variables can be

prescribed, which can lead to a mixed boundary value problem. As before, such a solution to the mixed boundary value problem is only approximate, because now the differential equations (1) are only satisfied approximately.

Thus, it has been shown that the two techniques lead to an identical formulation of the mixed boundary value problem, but there are some differences in the obtaining of the solution. If the number of Fourier components in (7) is the same as the number of pivotal points in the finite difference technique, then the extended solution matrix y^* is of the same size in both methods. The boundary conditions are also stated by the same type of equations (9), but for the finite difference technique usually the pivotal values themselves are prescribed, while in the expansion method linear combinations of the Fourier coefficients are prescribed. Both ways can be handled by the multisegment method of direct numerical integration, but the latter is slightly more complicated than the former. Moreover, the differential equations (6) for the expansion method are uncoupled for each wave number n , while those for the difference method, obtained from (1), are coupled in all pivotal values of the unknown variables. This means that for one set of initial value problems by classical shell theory (when $m = 8$), $8N$ initial value problems with 8 differential equations must be solved with the expansion method, while 8 initial value problems with $8N$ differential equations must be solved with the finite difference technique.

III. METHOD OF SOLUTION

The multisegment method of direct numerical integration will be applied to solve the two-point boundary value problem governed by the system of linear first-order ordinary differential equations

$$dy/dx = A(x)y + b(x) \quad (11)$$

within $a \leq x \leq b$ and subject to the boundary conditions

$$T_a y = u_a \quad (12)$$

$$T_b y = u_b$$

As before, the elements of y denote the unknowns, mN in number, and T_a , T_b , u_a , u_b have the same meaning as in (9), except that the asterisks have been omitted. The statement of the boundary value problem by (11) and (12) is of the form which was used in [1] and later also in [3]. However, in these earlier formulations, the size of the matrices was meant to be $(8,1)$ and $(8,8)$, but now they are enlarged to $(8N,1)$ and $(8N,8N)$. The method, of course, is equally well applicable to systems of equations of any size.

According to the multisegment method, initial value problems in the form

$$dY_i(x)/dx = A(x)Y_i(x) \quad (13a)$$

$$Y_i(x_i) = I \quad (13b)$$

and

$$dz_i(x)/dx = A(x)z_i(x) + b(x) \quad (14)$$

$$z_i(x_i) = 0$$

are defined for $x_i \leq x \leq x_{i+1}$ over the segments S_i of the shell, M in number, whose endpoints have the coordinates x_i and x_{i+1} (see Figure 2). $Y_i(x)$ is an $(8N, 8N)$ and $z_i(x)$ an $(8N, 1)$ matrix, which relate the solution at any x within S_i to the solution at the beginning of the segment by

$$y(x) = Y_i(x)y(x_i) + z_i(x) \quad (15)$$

According to this method, only the elements of $Y_i(x)$ at the end of the segment must be retained, and the intermediate values can be forgotten. Thus, to obtain the solution, it is required to perform the initial value integrations defined by (13) and (14) from the beginning of each segment to its end. We shall now examine how this integration is carried out over one segment S_i for the specific purpose of solving the mixed boundary value problem formulated with the two techniques

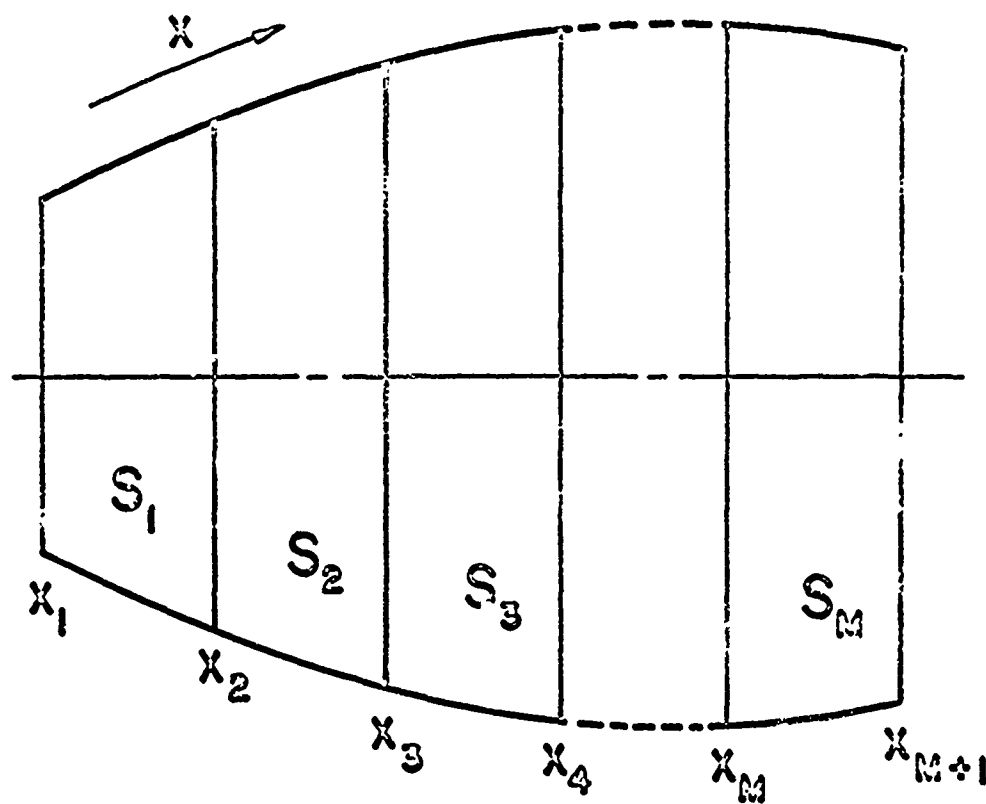


FIGURE 2. Division of shell into segments.

given in the preceding section.

The initial value problems defined by (13) can be interpreted as follows: find the y 's by (13a) at the end of the segment ($x = x_{i+1}$) when y at the beginning of the segment ($x = x_i$) has its first element equal 1 and the rest 0, then the second element of y equal 1 and the rest 0, and so on, until $8N$ initial value problems have been solved and all columns of $Y_i(x_{i+1})$ filled. Each of these initial value problems has a physical meaning.

If the first element of $y(x, \theta)$ is the transverse deflection w , then, using the finite difference technique in the θ direction, the first initial value problem defined by (13) means to find all variables at all pivotal points at the end of the segment when at the beginning of the segment all variables at all pivotal points are prescribed* zero except that at point No. 1 (Figure 1) $w = 1$. Clearly, if the shell is axisymmetric, the solution with $w = 1$ at point No. 2 need not be repeated, because it will be the same as with $w = 1$ at point No. 1, except that all values of variables must be shifted by one pivotal point. Consequently, for an axisymmetric shell, only

*One should not be alarmed by such a statement of a "boundary" value problem in structural mechanics. It does amount to asking for the solution of a beam for which the shear force, bending moment, slope, and normal deflection are all prescribed at one end of the beam and nothing is prescribed at the other end. It clearly violates the deeply rooted belief that the "natural" boundary conditions must be specified to get a unique solution. The fact that the natural boundary conditions are only sufficient but not necessary to ensure the uniqueness of a solution, if it does exist, was discussed in [4].

8 columns of $Y_i(x_{i+1})$ must be calculated, and the others are filled in by shifting the pivotal points. However, the $8N$ elements of y for each initial value problem are coupled, so that in total 8 initial value problems, of $8N$ differential equations each, must be solved over each of the segments.

With the separable solution expansion technique, the interpretation of the initial value solutions is similar. The first initial value problem defined by (13) now means to find all N Fourier coefficients of the solution (7) at the end of the segment when at the beginning of the segment all Fourier coefficients are prescribed zero except that $w_n = 1$ when $n = 0$. Since (6) are uncoupled with respect to the n th Fourier coefficients, then only 8 differential equations must be solved for each initial value integration. The solution at the end of the segment will be such that only those elements of y which represent the n th coefficients of the variables will be nonzero when $w_n = 1$ at the beginning of the segment. However, now all $8N$ initial value problems defined by (13) must be solved over each of the segments.

Once the matrices $Y_i(x_{i+1})$ are obtained for every segment of the shell, the solutions at the ends of segments are then obtained by following the same procedure as given in [1]. First, continuity conditions* at ends of segments are written

*It has been assumed here that the shell has a continuously turning normal. If it does not, then transformed variables must be made continuous, as shown in [3].

from (15) as

$$y(x_{i+1}) = Y_i(x_{i+1})y(x_i) + z_i(x_{i+1}) \quad (16)$$

and the unknown variables at the ends of the shell are changed from $y(x_1)$ and $y(x_{M+1})$ to u_a and u_b , which requires that the initial value solutions in the first segment must be replaced by the rule

$$Y_1(x_2)T_a^{-1} \rightarrow Y_1(x_2) \quad (17)$$

and those of the last segment by

$$T_b Y_M(x_{M+1}) \rightarrow Y_M(x_{M+1}) \quad (18)$$

$$T_b z_M(x_{M+1}) \rightarrow z_M(x_{M+1})$$

After this replacement is carried out, the continuity equations (16) are rewritten as a partitioned matrix product in the form

$$\begin{bmatrix} y_1(x_{i+1}) \\ y_2(x_{i+1}) \end{bmatrix} = \begin{bmatrix} Y_i^1(x_{i+1}) & Y_i^2(x_{i+1}) \\ Y_i^3(x_{i+1}) & Y_i^4(x_{i+1}) \end{bmatrix} \begin{bmatrix} y_1(x_i) \\ y_2(x_i) \end{bmatrix} + \begin{bmatrix} z_i^1(x_{i+1}) \\ z_i^2(x_{i+1}) \end{bmatrix} \quad (19)$$

If the boundary condition matrices in (12) are arranged so that the upper $4N$ elements of u_a and the lower $4N$ elements of u_b are the prescribed elements, then the partitioned equations (19) can be displayed in the form

$$\begin{bmatrix}
 Y_1^2 & -I & 0 & 0 & 0 & 0 \\
 Y_1^4 & 0 & -I & 0 & 0 & 0 \\
 0 & Y_2^1 & Y_2^2 & -I & 0 & 0 \\
 0 & Y_2^3 & Y_2^4 & 0 & -I & 0 \\
 0 & 0 & 0 & Y_M^1 & Y_M^2 & -I \\
 0 & 0 & 0 & Y_M^3 & Y_M^4 & 0
 \end{bmatrix}
 \begin{bmatrix}
 y_2(x_1) \\
 y_1(x_2) \\
 y_2(x_2) \\
 y_1(x_M) \\
 y_2(x_M) \\
 y_1(x_{M+1})
 \end{bmatrix}
 =
 \begin{bmatrix}
 -z_1^1 - Y_1^1 y_1(x_1) \\
 -z_1^2 - Y_1^3 y_1(x_1) \\
 -z_2^1 \\
 -z_2^2 \\
 -z_M^1 \\
 -z_M^2 + y_2(x_{M+1})
 \end{bmatrix}
 \quad (20)$$

where, for brevity, in place of $Y_i^j(x_{i+1})$ and $z_i^j(x_{i+1})$ the symbols Y_i^j and z_i^j have been used. It should also be kept in mind that, because of (17) and (18), $y(x_i)$ is really u_a and $y(x_{M+1})$ is really u_b .

While in [1] each of the square matrices in (20) were of the size $(4,4)$, here they are $(4N,4N)$. Similarly, the column matrices are $(4N,1)$. Equations (20) represent a system of $2M$ matrix equations with $2M$ unknowns: $y_1(x_2)$, $y_1(x_{M+1})$, and $y_j(x_i)$, for $j=1,2$, $i=2,3,\dots,M$. Regardless of the size of the elements, the system of matrix equations (20) can be solved by following the same procedure and formulas given in [1] and [3].

IV. EQUATIONS FOR CYLINDRICAL SHELL

The governing equations for thin shells of revolution can be obtained by various theories and stated in various forms. A system of first-order differential equations which fits the form of (11) and describes the behavior of an arbitrary shell of revolution is written out in detail in [1]. Since the example given at the end of this paper will involve a cylindrical shell and since some of the equations will be needed to discuss the total resultants, therefore we shall present here the governing differential equations needed for the solution of a mixed boundary value problem of the cylindrical shell. These equations can be stated as follows.

$$\epsilon_{\theta} = (u_{\theta,\theta} + w)/a \quad (21a)$$

$$k_{\theta} = (u_{\theta,\theta} - w_{,\theta\theta})/a^2 \quad (21b)$$

$$\epsilon_x = N_x/K - \nu\epsilon_{\theta} \quad (21c)$$

$$k_x = M_x/D - \nu k_{\theta} \quad (21d)$$

$$w_{,x} = -\beta_x \quad (21e)$$

$$u_{,x} = \epsilon_x \quad (21f)$$

$$u_{\theta,x} = 2N_{x\theta}/(1-\nu)K - u_{x,\theta}/a - 2D\beta_{x,\theta}/Ka^2 \quad (21g)$$

$$\beta_{x,x} = k_x \quad (21h)$$

$$N_{\theta} = K(\epsilon_{\theta} + \nu\epsilon_x) \quad (21i)$$

$$M_{\theta} = D(k_{\theta} + \nu k_x) \quad (21j)$$

$$Q_{x,x}^* = N_{\theta}/a - M_{\theta,\theta\theta}/a^2 - p \quad (21k)$$

$$M_{x\theta} = (1-\nu)D(\beta_{x,\theta} + \frac{1}{2} u_{\theta,x})/a \quad (21l)$$

$$N_{x,x} = M_{x\theta,\theta}/a^2 - N_{x\theta,\theta}^*/a \quad (21m)$$

$$N_{x\theta,x}^* = -N_{\theta,\theta}/a - M_{\theta,\theta}/a^2 \quad (21n)$$

$$M_{x,x} = Q_x^* - 2M_{x\theta,\theta}/a \quad (21o)$$

These equations are based on a classical theory of shells in which the transverse shear strain is set equal to zero. The meaning of the symbols is as follows:

u_x, u_θ, w = deflections

β_x = rotation of normal

$N_x, N_\theta, N_{x\theta}$ = membrane stress resultants

$M_x, M_\theta, M_{x\theta}$ = stress couples

Q_x = transverse shear resultant

$Q_x^* = Q_x + M_{x\theta,\theta}/a$

$N_{x\theta}^* = N_{x\theta} + M_{x\theta}/a$

$K = Eh/(1-\nu^2)$

$D = Kh^2/12$

h = thickness

E = Young's modulus

ν = Poisson's ratio

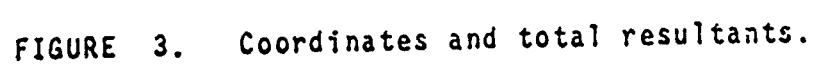
a = mean radius

The subscripts have the usual meaning, with x designating the axial and θ the circumferential direction (Figure 3).

Equations (21) are arranged in the special form as required by the multisegment method of direct numerical integration, so that the derivative with respect to x of every fundamental variable can be calculated at a required value of x when the fundamental variables themselves and the properties of the shell are known at that value of x . The fundamental variables are the elements of the y matrix in (1), and for a cylindrical shell they are defined as

$$y = \begin{bmatrix} w \\ u_x \\ u_\theta \\ \beta_x \\ Q_x^* \\ N_x \\ N_{x\theta}^* \\ M_x \end{bmatrix} \quad (22)$$

Equations (21) correspond to the scalar representation of (1) as governing equations of the system. After the θ -derivatives are eliminated, either by means of (7) or (10), they



are turned into the system of first-order, ordinary differential equations represented by (11).

V. TOTAL RESULTANTS

The usual stress resultants in shell theory are defined as forces and couples per unit length of the reference surface. For shells of revolution, it is also useful to calculate the components of the force and couple vectors obtained by integrating the usual stress resultants around a latitude circle, defined by the intersection of the reference surface and the plane $x = \text{constant}$. Such resultants will be called total resultants. They produce an averaged effect on whole axisymmetric sections of a shell of revolution, cut out by two planes $x = \text{constant}$, and are similar to the shear force and bending moment employed in beam theory.

Taking as an example the cylindrical shell, it follows from Figure 3 that the components of the total resultant force vector at some value of x are given by

$$R_1 = \int_0^{2\pi} (Q_x^* \cos \theta - N_{x\theta}^* \sin \theta) a d\theta \quad (23a)$$

$$R_2 = \int_0^{2\pi} (Q_x^* \sin \theta + N_{x\theta}^* \cos \theta) a d\theta \quad (23b)$$

$$R_3 = \int_0^{2\pi} N_x a d\theta \quad (23c)$$

and the components of the total couple vector by

$$M_1 = \int_0^{2\pi} (aN_x + M_x) \sin \theta a d\theta \quad (24a)$$

$$M_2 = \int_0^{2\pi} (aN_x + M_x) \cos \theta a d\theta \quad (24b)$$

$$M_3 = \int_0^{2\pi} N_{x\theta}^* a^2 d\theta \quad (24c)$$

We shall now calculate the derivatives of the total resultants with respect to x with the use of the governing equations (21) for a cylindrical shell. For example, taking a derivative of (23a) with respect to x , we get

$$R_{1,x} = \int_0^{2\pi} (Q_{x,x}^* \cos \theta - N_{x\theta,x}^* \sin \theta) a d\theta \quad (25)$$

Replacing the derivatives in the integrand by (21k) and (21n), we get

$$\begin{aligned} R_{1,x} = \int_0^{2\pi} (N_\theta \cos \theta / a - M_{\theta,\theta\theta} \cos \theta / a^2 - p \cos \theta \\ + N_{c,\theta} \sin \theta / a + M_{\theta,\theta} \sin \theta / a^2) a d\theta \end{aligned} \quad (26)$$

Assuming constant pressure with respect to θ and then integrating (26) by parts leads to

$$R_{1,x} = 0 \quad (27a)$$

Similarly

$$R_{2,x} = 0 \quad (27b)$$

$$R_{3,x} = 0 \quad (27c)$$

and

$$M_{1,x} = -R_2 - \int_0^{2\pi} M_{x\theta} \cos \theta d\theta \quad (28a)$$

$$M_{2,x} = -R_1 + \int_0^{2\pi} M_{x\theta} \sin \theta d\theta \quad (28b)$$

$$M_{3,x} = 0 \quad (28c)$$

Equations (27) and (28c) are exactly the relations expected from elementary equilibrium considerations. However, the two integrals on the right-hand sides of (28a) and (28b) are not expected, because they violate the fundamental moment equilibrium requirement of a section of a cylindrical shell. Such a violation of moment equilibrium in bending problems of shells of revolution is discussed in detail in [5], and it is blamed on the well-known fact that the classical shell theory, from which equations (21) have been obtained, does not satisfy moment equilibrium of a shell element about its normal. The integrals in (28a) and (28b) represent the projections of an extraneous surface couple about the normal which, as shown in

[5], must be included in moment equilibrium consideration, whenever a classical shell theory is employed. However, it has also been shown in [5] that if the shell is reasonably thin and not very long, the effect of the extraneous surface couple is indeed negligible.

Another source of error in the total resultant relations is possible, and that is concerned with the approximations admitted in solving the mixed boundary value problem. It will now be examined whether or not the two proposed solution techniques violate any of the equilibrium relations (27) or (28).

Considering first the separable solution expansion technique, it can be easily shown that when the variables in the form of (7) are used in the derivation of (27) and (28), none of the equations is violated. However, since the mixed boundary conditions are satisfied at certain pivotal points only and may be violated between the points, the actual total resultants on an edge must be calculated from the Fourier components of the solution on that edge and not by some numerical integration of the values of the forces or couples at the pivotal points. What this means is that a given component of a total resultant cannot be exactly prescribed on an edge, and that the shell will not maintain total equilibrium of total resultants with respect to the forces specified at pivotal points and integrated numerically around the circumference. It will maintain total equilibrium if the total resultants are

calculated from the Fourier components given by the solution on the edge.

More difficulties arise when the circumferential derivatives are replaced by finite difference expressions with respect to N pivotal points around the circumference. This can be illustrated by considering the step when going from (25) to (26) in the calculation of $R_{1,x}$. The expected result of (27a) depends on identities of the type

$$\int_0^{2\pi} N_{\theta,\theta} \sin \theta d\theta = - \int_0^{2\pi} N_{\theta} \cos \theta d\theta \quad (29)$$

which are verified through integration by parts. If the θ -derivative in (29) is replaced by a finite difference expression, such as (10a), then the integrands of both sides of (29) must be expressed in terms of the pivotal values of N_{θ} and integrated numerically. If the expressions of the pivotal values of N_{θ} after integration are equal, then indeed we shall have (27a) satisfied. This, however, does not happen. Whatever finite differences and integration formulas were tried, the author was not successful in making both sides of (29) exactly equal. From this experience, it was concluded that the separable solution expansion technique is better than the finite difference technique, because it does satisfy the differential equations exactly and violates only the prescribed boundary conditions.

VI. EXAMPLE: CYLINDRICAL SHELL WITH A SEMICIRCULAR SLIT

As an example, we consider the shell shown in Figure 4 subjected to a total moment $M_2 = -M$ at both ends. The problem is symmetric with respect to the plane $x = 0$ passing through the slit. It is also symmetric circumferentially with respect to the diameter connecting the points 1 and 9 (Figure 1). Therefore, only the pivotal points from 1 to 9 and the region $0 \leq x \leq 60$ must be considered.

Owing to the circumferential symmetry, the trigonometric functions, according to (7), are assigned such that w , u_x , β_x , Q_x^* , N_x , M_x are multiplied by $\cos \theta$ and u_θ , $N_{x\theta}^*$ by $\sin \theta$.

The boundary value problem has mixed boundary conditions at $x = 0$ to simulate the open slit. The specific variables which are prescribed at the nine chosen pivotal points at $x = 0$ are given in Table 1. At the other end, $x = 60$, the boundary conditions are not mixed, but consist of

$$Q_x^* = N_{x\theta}^* = M_x = 0 \quad (30a)$$

and

$$N_x = -\cos \theta \quad (30b)$$

Such boundary conditions, according to (24b), produce a total moment in the section $x = 60$ in the amount

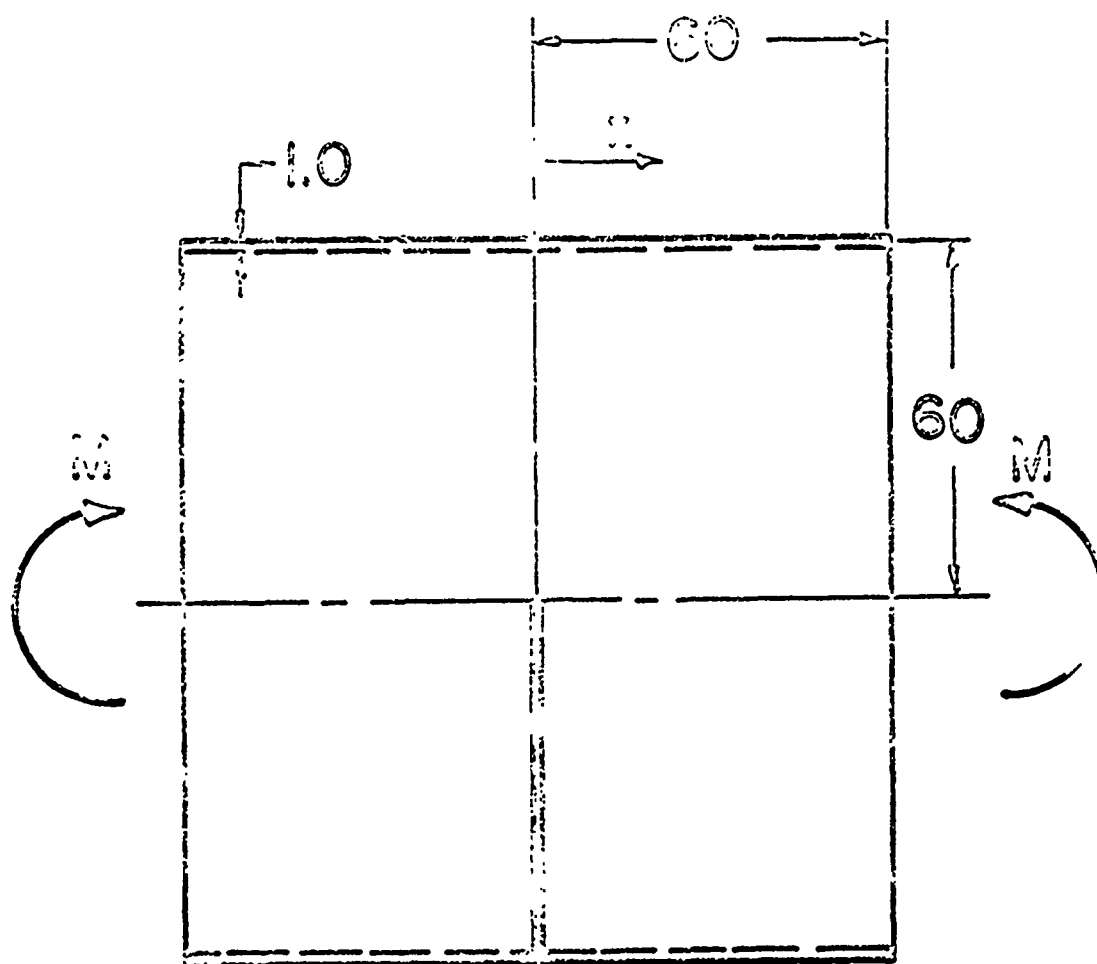


FIGURE 4. Cylindrical shell with slit.

Table 1. Boundary Conditions in Example

<u>Point</u>	<u>At $x = 0$</u>	<u>At $x = 60$</u>
1	$w = u_x = u_\theta = \beta_x = 0$	$N_x = 1.0$
2	$u_x = u_\theta = \beta_x = Q_x^* = 0$	$N_x = 0.9239$
3	$u_x = u_\theta = \beta_x = Q_x^* = 0$	$N_x = 0.7071$
4	$u_x = u_\theta = \beta_x = Q_x^* = 0$	$N_x = 0.3827$
5	$u_x = u_\theta = \beta_x = Q_x^* = 0$	$N_x = 0.0$
6	$Q_x^* = N_x = N_{x\theta}^* = M_x = 0$	$N_x = -0.3827$
7	$Q_x^* = N_x = N_{x\theta}^* = M_x = 0$	$N_x = -0.7071$
8	$Q_x^* = N_x = N_{x\theta}^* = M_x = 0$	$N_x = -0.9239$
9	$Q_x^* = N_x = N_{x\theta}^* = M_x = 0$	$N_x = -1.0$

$$M = \pi a^2 \quad (31)$$

which for our example is

$$M = 11,310$$

For the finite difference technique, we must prescribe the boundary conditions point by point and then, while (30a) holds for all points, N_x is prescribed the values at the 9 pivotal points as given in Table 1.

The mixed boundary value problem was solved by the multi-segment direct numerical integration method, using the two techniques described in the preceding sections. The half-length of the cylinder, $L = 60$, was divided into 10 segments, and 9 pivotal points were chosen around the circumference, which required 9 Fourier components (from $n = 0$ to $n = 8$) for the separable solution expansion technique. The computer time needed to solve this example with these two techniques was about the same. The computer program was run on Lehigh University's CDC 6400; it required about 100K (in octal) word core and temporary auxiliary storage on disks. It took 3 minutes of computer time to run each case.

Some results obtained by both techniques are displayed in Figures 5, 6, and 7. The full lines mean the solution given by the expansion technique, while the points represent the solution obtained by the finite difference technique, whenever the results from the two methods differed substantially.

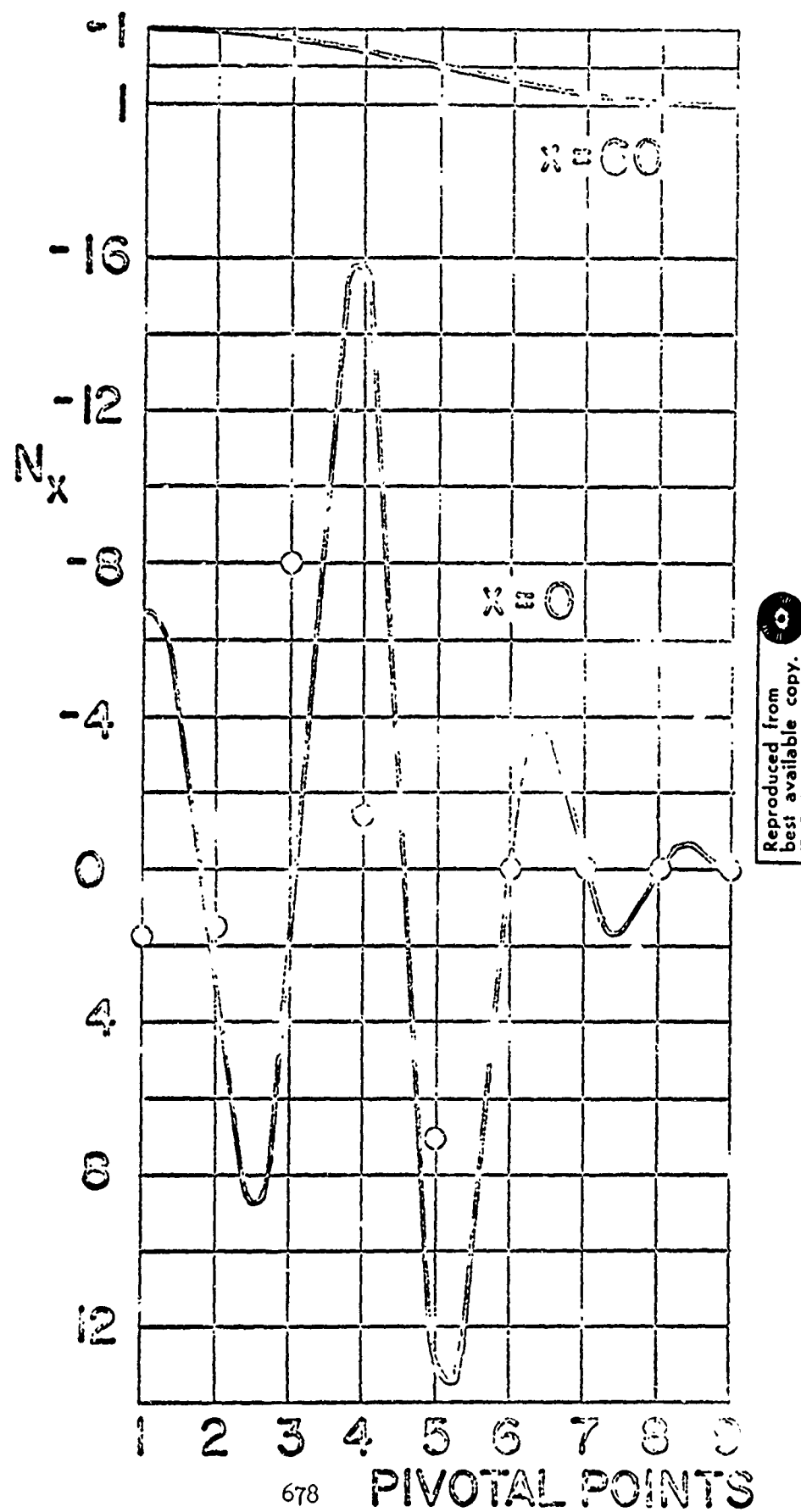


FIGURE 5.

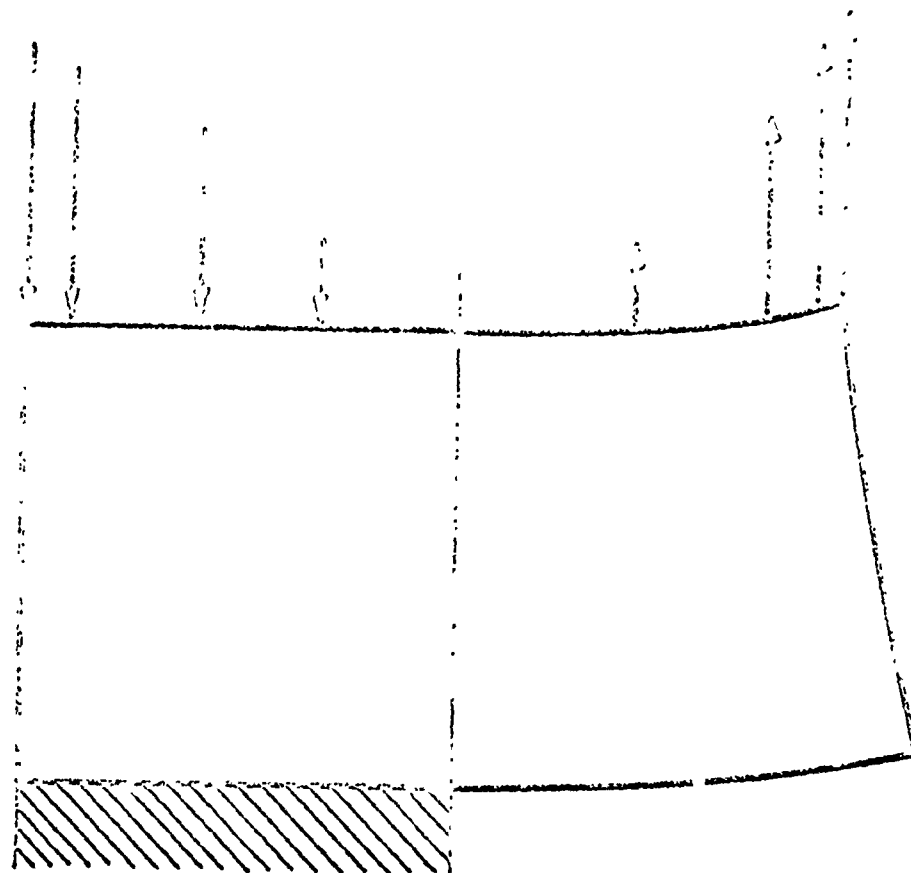


FIGURE 6. Deformed profile of cylindrical shell

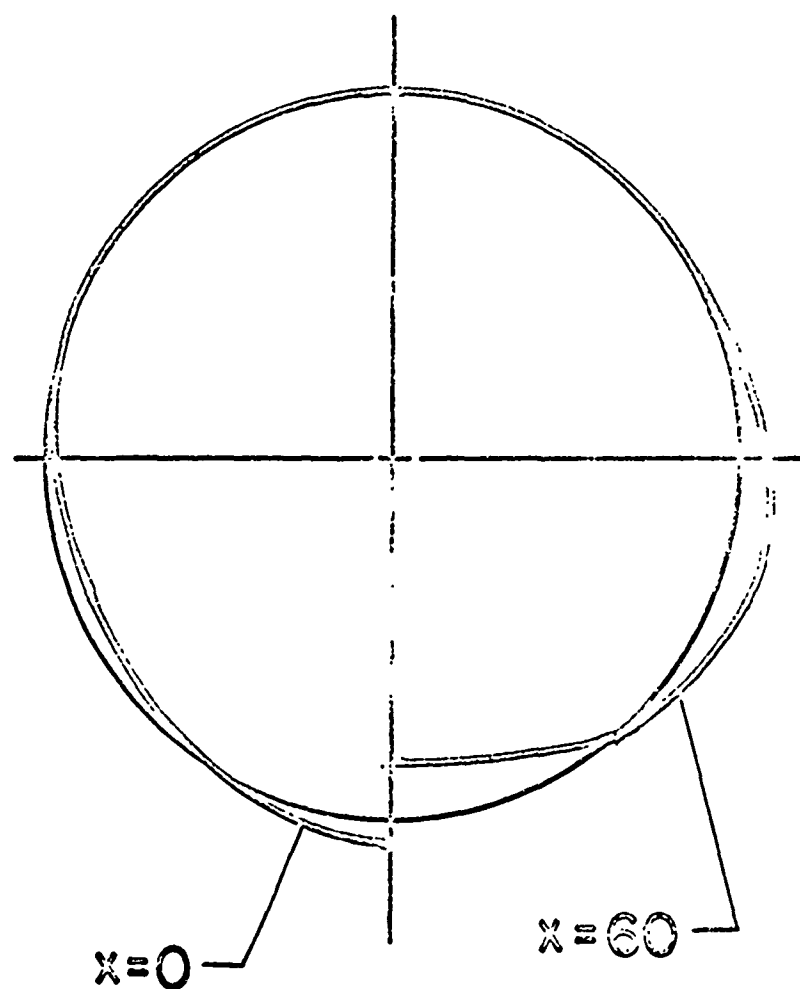


FIGURE 7. Deformed latitude circles.

Figure 5 shows the circumferential variation of N_x at $x=0$ and 60 of the cylinder. Since N_x produces the maximum stress in the shell, it is significant that it is increased from 1.0 at $x = 60$ to a maximum absolute value of 15.6 at $x = 0$. If the slit were absent, then the distribution of N_x given at $x = 60$ would have remained the same at any value of x . The reason why N_x must have larger values when approaching the slit is that the same total moment M_2 must be present at any x as applied at $x = 60$. Since N_x is prescribed zero at points 6-9, larger values of N_x are expected at points 1-5.

The error in the analysis by means of the separable solution expansion technique is illustrated by the fact that N_x at $x = 0$ goes through zero at the points 6-9, as prescribed, but it is not zero between them. The actual boundary values of N_x , which are present at $x = 0$, are shown in Figure 5. No such interpretation can be made for the finite difference technique, because the forces only at the pivotal points can be calculated.

It might be argued that infinitesimal elasticity theory predicts infinite stress at point 5 and $x = 0$, i.e., at the tip of the slit, and that the results of this paper in the vicinity of point 5 are not realistic. This of course is true, because in the vicinity of point 5, the stress state is significantly affected by the actual shape of the tip of the slit in a real manufactured cylindrical shell. Even if the

slit were a perfectly true semicircle, the prediction of infinite stress is caused by the, in this case faulty, mathematical model of infinitesimal elasticity theory, in which equilibrium is satisfied in the undeformed state. If the same problem were solved with respect to the deformed state, no infinite stress would be predicted. To be sure, the solution in the vicinity of the tip of the slit given in this paper, as the solution obtained with any infinitesimal theory, is not to be taken seriously.

Figure 6 shows the deformed profile of the cylindrical shell, illustrating the opening of the crack, and Figure 7 shows the deformed latitude circle at $x = 0$ and $x = 60$, respectively. With respect to Figure 6, it seems that the shell does not deform very much throughout the sector of the shell which does not have the slit; most of the deformation takes place in the sector with the slit.

VII. CONCLUSIONS

While the finding of the solution of a boundary value problem governed by a system of ordinary differential equations has by now become a routine procedure, the situation is not at all that way for problems requiring a true two-dimensional solution. While the mixed boundary value problem of a shell of revolution is somewhat of a degenerate case, because each term of the separable solution expansion (7) satisfies the governing equations exactly, the procedures applied here can be regarded as a step, however small, toward the solution of the general boundary value problem governed by a system of two-dimensional partial differential equations. This, then, was the motivation of this paper, rather than the value of the actual results displayed here.

After all the results were studied and the curves plotted, it had to be admitted that the separable solution expansion seemed preferable to the finite differences. Two reasons stand out to support this statement. First, with the expansion technique, the only approximation lies in the prescribed boundary values. However, the actual boundary values given by the solution can be calculated, and then a judgement can be made whether or not such boundary data are acceptable. No such physical interpretation can be made with the results obtained from the finite difference technique. Second, this may be a very minor point, but the solution obtained from the ex-

pansion technique can be calculated as a continuous function of θ . If the actual boundary data are acceptable, then (7) does give the actual solution at all values of θ . There is no danger of missing any peaks in some critical stress distribution. Again, no such interpretation of the solution between the pivotal points is possible with the finite difference technique.

Finally, the results given in this paper have been only checked with the common-sense expectations, simply because no other sources of comparison were available to the author.

VIII. REFERENCES

1. A. Kalnins, "Analysis of Shells of Revolution Subjected to Symmetrical and Nonsymmetrical Loads", Journal of Applied Mechanics, V. 31, 1964, pp. 467-476.
2. A. Kalnins, "Analysis of Curved Thin-Walled Shells of Revolution", AIAA Journal, V. 6, 1968, pp. 584-588.
3. A. Kalnins, "Static, Free Vibration, and Stability Analysis of Thin, Elastic Shells of Revolution", Wright-Patterson Air Force Base, Report No. AFFDL-TR-68-144, 1969.
4. A. Kalnins, "On the Boundary Conditions Obtained from the Principle of Minimum Potential Energy for an Elastic Shell", Lehigh University Report No. MECH-69-1, 1969.
5. A. Kalnins, "On the Violation of Moment Equilibrium About Normal in Shell Theory", Lehigh University Report No. MECH-69-AK-5, 1969.

QUESTIONS AND COMMENTS FOLLOWING KALNIN'S PAPER

QUESTION: It must be that all these $nx8$ equations are uncoupled in groups of 8. So you really don't have to solve $nx8$ equations corresponding to your Fourier coefficients; you only have to solve n sets of 8. Correct?

KALNINS: Yes. It is explained in the paper.

QUESTION: Is this method of solution dependent upon the computer that you're operating with?

KALNINS: Well, that's very hard to say. The only thing that could affect it would be the number of significant digits kept. That has not seemed to be a problem. I have not encountered any breakdown on account of accuracy.

QUESTION: How many significant figures do you think you need to carry to maintain this accuracy.

KALNINS: Well, I prefer the CDC machine with thirteen figures.

QUESTION: Have you any experimental verification of the accuracy of your technique?

KALNINS: Yes, I have. I have had a paper at the Delft Congress where a comparison was made between experimental data and data generated by the code and the conclusion was that everything was all right.

COMMENT: I just wanted to make a comment. I've found that another possible way of satisfying the boundary conditions which appears to

be more reliable than point matching is to expand these boundary conditions in some complete set and truncate this expansion at the number of coefficients that you have available and then satisfy these truncated series term by term. You could do this over each portion for the mixed boundary value problem. It appears that it is more reliable and less numerically sensitive than the point matching procedure.

KALNINS: I already have the expansion which is truncated.

COMMENT: You re-expand that in another series over each of these intervals and then satisfy this truncated series.

KALNINS: What kind of series could it be that you could expand in?

COMMENT: Just any complete set, it doesn't really matter. Just whatever happens to be convenient. You have a series which you'd like to satisfy displacements, for example, over part of a boundary and another series expansion you'd like to satisfy for stresses on the second part of the boundary. You take these equations and expand both sides in some other complete set over the proper intervals. You then truncate these series expansions to the number of terms that you have available. For example, if you have ten terms and you wish to use five of these in each of the two regions, you truncate each of the series after five terms and then satisfy those truncated series term by term. It's sort of a way of applying a weighted average to your point matching and you take every point into consideration.

KALNINS: Wouldn't least squares do the same thing?

COMMENT: If you integrated, yes.

COMMENT: We analyzed an oblique nozzle using this technique and we found that by the series expansion method, one can develop fairly good accuracy with a low order harmonic, simply by stating the conditions at each of these points you've selected in the circumferential direction and then by over specifying the boundary conditions at intermediate points. That is, points along the boundary but between the circumferential stations, so you add more stations. What you're doing, in a least squares sense, is satisfying those boundary conditions. With this technique, we've agreed with experimental data to within five percent for an oblique 45 degree nozzle.

KALNINS: Yes, I agree that would be a definite improvement.

COMMENT: In this problem you've selected, namely, the cylinder with a slit, a fracture mechanic would be interested in the stress intensity factor. Now I have a feeling that no matter how far you carry your solution in terms of number of mesh points and so forth, you wouldn't be able to come up with it.

KALNINS: That's correct. But the analysis is based on linear theory which would predict infinite stress at the tip of the slit. I don't really want to get into it what the stress is in the vicinity of the tip; it's not going to be realistic anyway. You're absolutely correct, this is not the way to do fracture problems.

LIESSA: I'd like to add a couple of comments of my own here. Having worked with point matching and boundary point least squares methods quite a bit, I can see some of the difficulties and why they happened in

the results. One of them has already been mentioned by Prof. Kalnins. If you force the functions to go through the points by point matching, then you'll get this wildly oscillating type of behavior as we saw in the plot for N_x . If you recall, from the slide, the function had to go through a few points having zero values and then as it got into the body of the shell where you did not have a free edge, this oscillation continued to build up. And one way to cut down on this oscillation is, of course, to use this least squares method which numerically is done very simply by taking additional points, or as someone else mentioned, by actually adding additional supplementary boundary conditions at points and coming up with a non-square set of equations, then multiplying through by the transpose to get a least square fit.

Now another key point. You can do even better in eliminating this wild oscillation if you can add some type of singularity function at the base of this crack and thereby remove the singularity and get rid of the residual on the smooth function that's left over. Now, of course, guessing the form of the singularity has to be based upon some other analysis.

STRUCTURAL SHELL ANALYSIS

THE INTERACTION OF ASYMPTOTIC AND COMPUTER METHODS OF SHELL ANALYSIS

by

C. R. STEELE

Associate Professor, Aeronautics and
Astronautics, Stanford University

ABSTRACT

Before the comparatively recent developments in computer capability, the complexity of the thin shell equations made necessary the utilization of various approximate solutions, which usually are leading terms of appropriate "asymptotic" expansions of exact solutions. Even today, asymptotic solutions are useful, since they provide simple formulas for preliminary design and exact solutions for limiting cases in which straightforward numerical procedures encounter difficulty. Moreover, the asymptotic and numerical approaches can have a healthy interaction in an investigation of a particular problem. Various problems are discussed which show some of the strengths and weaknesses of each approach, some past fruitful interactions, and some possibilities for future interaction.

- I. Introduction
- II. Some Advantages and Disadvantages
 - 1. Bending of Curved Tube
 - 2. Dome with Tilting Moment
 - 3. Heated Slab with Stress Pulse
- III. Examples of Interaction
 - 1. Pressure Vessels with Slope Discontinuity
 - 2. Vibration of Cones
- IV. Further Possibilities for Interaction
 - 1. Stress Pulses in Inhomogeneous Solids
 - 2. Moving Load Problems
 - 3. Shells with Holes and Concentrated Loads

¹Work performed with the support of National Science Foundation Grant GK2701.

I. INTRODUCTION

Various asymptotic expansions have been used by countless investigators of the behavior of thin shells. For the basic problem of shell statics, one type of expansion gives the "membrane" and "inextensional" solutions for the leading terms while another expansion gives the "edge effect bending" solution. However, these expansions are invalid in numerous situations of practical importance; for instance, when a boundary curve is tangent to an asymptotic line of the surface, which occurs at a cutout on a cylinder, when a toroid is considered, when the spatial derivative of the load distribution or geometric parameters is too large, and so on. Each type of difficulty seems to require a different, basic modification in the expansion. Airy functions are used for the toroid, Bessel functions for the sphere, and completely different terms are taken into consideration in the expansion depending on the "index of variation" of the load. Furthermore, knowing when to apply these modifications requires what appears to be mysticism to the uninitiated. It is little cause for wonder that most of the current effort in shell analysis is in the development of computer programs that can provide answers for a given problem without an undue amount of analysis. However, the straightforward numerical methods remain fundamentally inefficient for shell analysis, since a considerable expenditure of effort is required for regions of the shell where the solution has little interest.

It now seems, at least remotely possible, the asymptotic techniques may develop to the point that they might be used directly in a general purpose computer program for shell analysis. Such would be the ideal situation, in which all the known analytical simplifications could be utilized together with the high speed computing capabilities for an analysis of maximum efficiency. For the near future, however, the explorations of asymptotic and direct numerical methods will continue to be rather distinct.

The usual situation is that the investigator, after completion of an asymptotic analysis, might seek a direct numerical result for confirmation, while the developer of a computer program likewise looks for asymptotic results for check cases. For illustration, we discuss the problems of the bending of a curved tube [1], the dome with a tilting moment [2,3], and the propagation of a stress pulse through a heated slab [4,5]. These problems show the inherent advantages and disadvantages of the asymptotic and numerical methods.

The objective of this paper, however, is to show that, in the course of an

investigation of a particular problem, the simultaneous utilization of the asymptotic and numerical methods can lead to very satisfactory conclusions. Furthermore, these conclusions would, very likely, not have been obtained with either approach alone. The examples are the recent investigations of pressure vessels with "weld sinkages" [6,7] and the modes of vibration of the conical shell [8,9].

Of interest is a problem somewhat analogous to the vibration of a conical shell in a fluid — the mechanical behavior of the cochlea of the inner ear. Many direct computational approaches have been used and have failed to provide a basic understanding which would resolve the conflicting theories [10,11]. However, a simple asymptotic result has been recently obtained which seems to clear up many things, and should give guidance for future, more precise, computations.

Finally, some recent asymptotic results [12-16], are briefly discussed which would seem to be helpful, when combined with direct numerical calculations, in various problems of shell statics and transient dynamics.

The problems discussed in this paper strongly reflect the interest and recent work of the author. No attempt is made to give a general survey or to acknowledge all the significant results of other investigators.

II. SOME ADVANTAGES AND DISADVANTAGES

The basic notion underlying most "asymptotic" methods is that a feature of a problem, which causes an undue amount of difficulty for a direct numerical calculation, can be turned to an advantage by suitable analytical manipulation. Indeed, there are numerous examples of such tricks used on power series, integrals, matrix inversions, and so on. Many features of the thin shell equations are in the standard equation

$$y'' + p(x)y' + \left[-\lambda^2 q(x) + r(x) \right] y = -\lambda^2 f(x) \quad (1)$$

Where p , q , r , and f are prescribed functions and λ can be taken as the radius-to-thickness parameter, which is usually large. For moderate values of λ , there is no difficulty in obtaining an approximate solution with the use of any direct numerical or energy method. But as λ becomes very large, the direct methods all encounter severe difficulties; the capacity of any finite computer will be exceeded by a sufficiently large λ . The reason is that the finite difference or finite element grid spacing must become very small, or the approximating polynomial must have a high degree to adequately represent the solution. This feature can be turned to an advantage, however, by finding the appropriate forms of the asymptotic expansions of the solution.

The particular solution can be obtained as a usual perturbation expansion

$$y(x) = y_0(x) + \frac{1}{\lambda} y_1(x) + \frac{1}{\lambda^2} y_2(x) + \dots \quad (2)$$

in which it is assumed that each $y_i(x)$ is completely independent of λ . After substituting the expansion into the equation and equating the terms multiplied by each power of λ to zero, a set of equations is obtained for the successive computation of y_0 , y_1 , \dots . The first is

$$y_0 = f(x)/q(x)$$

For shells, such an expansion gives the "membrane" and "inextensional" solutions. Thus

many of the terms of the equation have a secondary effect on this particular solution. This, however, is not a general solution since no arbitrary constants are obtained. When the perturbation expansion does not give enough arbitrary constants, we have a "singular perturbation" problem [12].

To find the missing complementary solution, which supplies the arbitrary constants, an expansion must be used which gives a "rapidly varying" solution for which the second derivative term is significant. The simplest form is

$$y = e^{\lambda \xi(x)} \left[\alpha_0(x) + \frac{1}{\lambda} \alpha_1(x) + \frac{1}{\lambda^2} \alpha_2(x) + \dots \right] \quad (3)$$

where ξ and all the $\alpha_i(x)$ are assumed to be independent of the large parameter λ . Substituting into the equation and equating the coefficient of each power of λ to zero gives an "eiconel" equation for the argument function

$$(\xi')^2 - q(x) = 0$$

and a "transport" equation for the first coefficient

$$2\xi'\alpha_0' + (\xi'' + p\xi')\alpha_0 = 0$$

then a recursive set of equations for the $\alpha_1, \alpha_2, \dots$. When $q(x)$ is positive, or, more generally, when $|\arg q| < \pi$, then the solution will increase, or decrease, exponentially giving an "edge effect" or "boundary layer" type of solution. When q is negative, the solution is oscillatory and $\xi(x)$ is the "phase integral" and the coefficient $\alpha_0(x)$ gives the variation in the envelope of the waves. Although this solution was obtained by Louville (1836) and independently developed for shell theory by H. Reissner and Blumenthal (1912), it is commonly, but erroneously, referred to as the WKBJ (1928-1940) solution. When used on a partial differential equation, this type of expansion gives the "geometric optics" solution [12].

To come to the question of advantages and disadvantages, the most important point is that the direct numerical and asymptotic approaches are not

competing methods for doing the same thing, but are most complementary. The direct numerical computation gives answers for the low and moderate values of λ but becomes unreliable and/or expensive for large λ , while the asymptotic result is simple and accurate for very large, but is unreliable for moderate, values of λ . Then we have the possibilities for interaction. For instance, with the general features indicated by the asymptotic solution, the appropriate mesh size could be used, fine in the "edge zones" and coarse in the interior, to improve the efficiency of the computer program.

Unfortunately, the situations in which these simple expansions are invalid are all too frequently encountered. The modifications in the asymptotic solution for "transition points", are indicated in the following examples.

1. Bending of Curved Tubes - Several points can be illustrated by the analysis of the bending of a curved tube [1]. The simplified equation is

$$\psi''(\varphi) - i\mu \sin\varphi \psi(\varphi) = \mu k \cos\varphi \quad (4)$$

where μ is the change in curvature and the parameter is

$$\mu = [12(1-\nu^2)]^{1/2} b^2/ah$$

where a^{-1} and b^{-1} are the curvatures of the tube and the cross section, respectively, and h is the thickness. In this situation, the parameter μ could be small or large. When the tube is initially straight $\mu = 0$, and the dimensionless rigidity factor ρ is unity. So the early investigators considered a solution for a slightly curved tube, for which a perturbation expansion in μ could be used. Since ψ must be periodic,

$$\psi = \mu k \rho \left[\cos\varphi + \sum_{n=1,2,\dots}^{\infty} \mu^{2n-1} a_n \sin 2n\varphi + \mu^{2n} b_n \cos(2n+1)\varphi \right]$$

If only one term is retained, the result for the straight tube is obtained

$$\rho = 1$$

If two terms are retained, the result is

$$\rho = \frac{16}{16 + \mu^2}$$

If three terms are retained

$$\rho = \frac{16 + \frac{\mu^2}{9}}{16 + \frac{10\mu^2}{9}}$$

while the four term result is

$$\rho = \frac{16 + \frac{5}{36}\mu^2}{16 + \frac{41}{36}\mu^2 + \frac{1}{576}\mu^4}$$

Any of several existing computer programs using direct numerical methods should easily be able to improve on the perturbation results by using more exact equations including the nonlinearities, etc. However, as μ becomes large, the algebra for carrying out more terms in the perturbation expansion or the computer time becomes excessive. On the other hand, the simple asymptotic expansions (2,3) are useless for (4) since the term multiplied by the large parameter has a zero, producing singularities in the leading terms of (2,3) at points at which the equation is perfectly well-behaved.

So, a certain amount of trickery was required. Clark and Reissner [1] came up with an extension of the Langer "comparison equation" approach [12]. Instead of (2) or (3) it is necessary to use, for the simplest uniformly valid asymptotic solution, the solution of

$$T''(x) - ixT(x) = 1$$

$$(T(x) \sim ix^{-1} \text{ for } |x| \rightarrow \infty)$$

in the expansion

$$\begin{aligned} \psi(\varphi) = & T(\mu^{1/3} \xi(\varphi)) \left[\alpha_0(\varphi) + \frac{1}{\mu} \alpha_2(\varphi) + \dots \right] \\ & + \mu^{-2/3} T'(\mu^{1/3} \xi(\varphi)) \left[\alpha_1(\varphi) + \frac{1}{\mu} \alpha_3(\varphi) + \dots \right] \end{aligned}$$

Once the correct form of the expansion is obtained, it is straightforward to obtain the functions

$$\begin{aligned} \xi(\varphi) &= \left(\frac{3}{2} \int_0^\varphi \sin^{1/2} \varphi \, d\varphi \right)^{2/3} \\ \alpha_0(\varphi) &= \mu^{1/3} \xi \cot \varphi \end{aligned}$$

The argument function $\xi(\varphi)$ has a simple zero at the transition point $\varphi = 0$, so $\alpha_0(\varphi)$ and all the other terms in the expansion are well-behaved.

It often seems that those considered the greatest mathematicians are those who can make simple things the most obscure. But the attractive feature of asymptotic analysis is that "obscure manipulation" can end in simple results. The above use of the $T(x)$ function gives for the rigidity of the tube

$$\rho \sim 2/\mu \quad \text{for } \mu \gg 1$$

Fig. 1, from [1], shows the three term perturbation curve (A) and the asymptotic result (B). The two curves are quite close for the moderate values of μ , so this is almost a case of "matched asymptotic expansions". Generally, however, the expansions for small and large values of a parameter will not overlap, but this is the region easily handled by direct numerical methods.

2. Dome with Tilting Moment - For the shell of revolution whose meridian is a second degree curve at the apex (sphere, ellipsoid, paraboloid) the equation is

$$\frac{1}{rR_2R_1} \frac{d}{d\varphi} \left(\frac{rR_2}{R_1} \frac{d\psi}{d\varphi} \right) + \left[\frac{1}{RR_2} - \frac{n^2}{r^2} \left(2 - \frac{R_2}{R_1} \right) \right] \psi = 0 \quad (5)$$

where $R = R_1 = R_2$ and $r \approx R\varphi$ near the apex $s = 0$, the large parameter is

$$\kappa = [12(1-\nu^2)]^{1/4} (R/h)^{1/2}$$

and n is the Fourier harmonic index. Again the expansion (2) is not valid near $\varphi = 0$ since the coefficients of (5) are singular. However, very near $\varphi = 0$ (5) has the form of Bessel's equation, so the "comparison equation" method can be used. The expansion is

$$\begin{aligned} \psi(\varphi) = \eta(\zeta(\varphi)) & \left\{ \alpha_0(\varphi) + \frac{1}{\kappa^2} \alpha_1(\varphi) + \dots \right\} \\ & + \eta'(\zeta(\varphi)) \left\{ \frac{1}{\kappa} \alpha_1(\varphi) + \dots \right\} \end{aligned}$$

where η is the appropriate Bessel function

$$\eta(\zeta) = C_1(\text{ber}_n \zeta - i \text{bei}_n \zeta) + C_2(\text{ker}_n \zeta - i \text{kei}_n \zeta)$$

and we find

$$\zeta(\varphi) = \kappa \int_0^\varphi (R_1^2 \sin \varphi / rR)^{1/2} d\varphi$$

$$\alpha_0(\varphi) = (\zeta / rR_2^{1/2})^{1/2}$$

and so on.

An advantage of the asymptotic solution is that some problems can be solved in terms of the transformation variable ζ . One curve Fig. 5 from [3] gives ζ for a variety of geometry. For the dome shown in Fig. 4, the stress at the upper edge is given in Fig. 6 by the value of ζ at that edge. The dotted lines in Fig. 6 give the typical decrease in stress away from the edge. This asymptotic result was used for a check case for the computer program developed by Cohen [2], who found the agreement shown in Fig. 7.

3. Heated Slab with Stress Pulse - The direct numerical and asymptotic methods also play complementary roles in dynamic problems. For the transient plane stress in a slab with a variable speed of sound, due to, for instance, high heating of one face of the slab, the equation is

$$c^2(x) \frac{\partial^2 u}{\partial x^2} = \frac{\partial^2 u}{\partial t^2}$$

After a Laplace transformation in time, the equation is of the form of (1)

$$\frac{\partial^2 \bar{u}}{\partial x^2} - \frac{p^2}{c^2} \bar{u} = 0$$

so for large values of the transform variable p , the asymptotic solution given in [5] is

$$\sigma(x, p) = C e^{-p \xi(x)} \left[\alpha_0(x) + \frac{1}{p} \alpha_1(x) + \dots \right]$$

where we find

$$\xi(x) = \int_0^x dx/c(x)$$

$$\alpha_0(x) = [c(x)/c(0)]^{1/2}$$

For a pressure pulse on the face

$$\sigma(0, t) = \begin{cases} \sigma_0 f(t) & \text{for } 0 < t < t_0 \\ 0 & \text{for } t < 0, t > t_0 \end{cases}$$

the constant C can be evaluated and the inversion integration performed giving for a first approximation for the internal stress pulse

$$\frac{\sigma(x, t)}{\sigma_0} \sim \begin{cases} \alpha_0(x) f(t - \xi(x)) & \text{for } t - t_0 < \xi < t \\ 0 & \text{for } \xi \text{ elsewhere} \end{cases}$$

This simple approximation is valid for a sufficiently high frequency pulse, for which the internal reflections from the inhomogeneity is negligible. The function $\alpha_0(x)$ gives the amplitude modulation and the function $\xi(x)$ gives the distortion in the pulse shape.

Thus for a slab with the variation in speed of sound shown by the smooth solid curve in Fig. 3d, subjected to a triangular pulse, the asymptotic result gives the compressional pulse traveling through the slab in Fig. 2 (a-d) and the tensile pulse reflected from the free surface in Fig. 3 (a-c). A comparison with the finite difference numerical solution obtained by Massard [4] is also shown in Figs. 3, 4.

For advantages and disadvantages, the asymptotic result is very good for the high frequency part of the pulse, so the sharp peak should be accurate. However, the main part of the pulse has a spatial wave length which is long in comparison with the distance over which c varies significantly, so a significant internal reflection is missing from the asymptotic result. On the other hand, in the numerical approach, the actual variation in c was approximated by the step curve shown in Fig. 3d, which should cause more internal reflections than are actually there.

This is compensated by the artificial damping that must be used for numerical stability. Thus the peak of the pulse, which is accurately given by the asymptotic solution, is quickly lost in the numerical solution. The conclusion is that the actual pulse is somewhere between the two results. Actually, if the two term asymptotic solution, which gives the internal reflections, and the improved numerical solution with less internal damping are used, quite good agreement is obtained.

One interesting feature, is that the curve for α_0 (Fig. 3d), seems to give the internal stress envelope even for this long wavelength pulse. If we take only the half sine wave portion of the incident pulse, assume that the peak is all lost in the numerical solution, then the maximum tensile and compressive stress envelopes from $\alpha_0(x)$ and the computer results are close.

III. EXAMPLES OF INTERACTION

In the previous examples, the direct numerical and asymptotic results were obtained independently. Now examples are considered in which both approaches were used simultaneously in the investigation of a particular type of problem.

1. Pressure Vessel with Slope Discontinuity - When a pressure vessel is formed from segments of shells of revolution welded together, often there can be seen a very small deviation in the nominal geometry near each weld seam. For simplification, this "weld sinkage" was approximated by a meridian with a discontinuity in slope, as indicated in Fig. 8.

Instead of a scalar formulation, the vector form of the static shell equations were used

$$-\frac{d}{dx} \underline{y} + \left(\lambda \underline{A}_0 + \underline{A}_1 + \frac{1}{\lambda} \underline{A}_2 \right) \cdot \underline{y} = \lambda^2 \underline{a}_0 + \lambda \underline{a}_1 + \underline{a}_2 \quad (6)$$

where the components of \underline{y} are the physical variables, x is the dimensionless arclength, λ is the radius-to-thickness parameter, the \underline{A}_i are matrices and the \underline{a}_i are vectors due to the surface and axial loading. The usual perturbation expansion (2) now is of the form

$$\underline{y} = \lambda \underline{\delta}_0 + \underline{\delta}_1 + \frac{1}{\lambda} \underline{\delta}_2 + \dots \quad (7)$$

Substitution into (6) gives

$$\underline{A}_0 \cdot \underline{\delta}_0 = \underline{a}_0$$

$$\underline{A}_0 \cdot \underline{\delta}_1 = \underline{a}_1 - \underline{A}_1 \cdot \underline{\delta}_0$$

...

Since \underline{A}_0 is nonsingular, all the $\underline{\delta}_i$ can be computed; $\underline{\delta}_0$ gives the membrane stress, $\underline{\delta}_1$ the corresponding radial displacement, $\underline{\delta}_2$ the rotation, $\underline{\delta}_3$ the corresponding (small) bending stress, and so on. The complementary solution (3) is now of the form

$$\underline{y} = e^{\lambda \xi(x)} \left[\underline{a}_0 + \frac{1}{\lambda} \underline{a}_1 + \frac{1}{\lambda^2} \underline{a}_2 + \dots \right] \quad (8)$$

Substitution into (6) gives

$$(-\xi' I + A_0) \cdot \alpha_0 = 0$$

$$(-\xi' I + A_0) \cdot \alpha_1 = \alpha_0' - A_1 \cdot \alpha_0$$

. . .

Thus ξ' is an eigenvalue of A_0 and α_0 is the corresponding eigenvector. For α_1 to exist, the right-hand-side of the second equation must be orthogonal to the solutions of the homogeneous transpose equation, which gives the "transport equation" for the amplitude of the eigenvalue α_0 .

If these "membrane" and "edge-effect" solutions (7,8) are applied to a pressure vessel with the slope discontinuity shown in Fig. 8, the maximum meridional stress at the seam is found to be

$$\sigma = \frac{pR}{2h \sin \varphi} [1 + g] \quad (9)$$

where the stress concentration factor is

$$g = \left[\frac{27}{16(1-\sqrt{2})} \right]^{1/4} \left(\frac{r}{h \sin \varphi} \right) (\varphi^- - \varphi^+)$$

where φ is the nominal angle

$$\varphi = (\varphi^- + \varphi^+)/2$$

This "classical" asymptotic result gives a convenient grouping of the many variables of the problem into the one significant parameter g .

Then comes the question of the range of validity of the analytic result. Although error estimates can sometimes be obtained for an asymptotic result, the information gained is usually not worth the work required. Therefore, the direct finite difference solution of Reissner's nonlinear equations [7] was utilized. The computer results, as expected, agreed very well with (9), except, however, when the edges became tightly curled or when the pressure load was excessive. The tightly curled edge is a situation in which the geometry varies significantly in the edge zone, a situation which is not considered in the literature of asymptotic methods. However, the computer results showed such a smooth deviation from (9) as the curvature increased, that we were sufficiently intrigued to seek an analytical explanation. Indeed, an investigation of the cylinder, with its very simple nominal geometry, revealed that an appropriate modification of the membrane and edge

effect solutions could be obtained, which gave a result that agreed with the computer results. Then the computer analysis showed that the same modification held for the sphere with the seam at any angle. This in turn motivated the effort to find a solution for the general nominal meridian.

For a meridian given by

$$r(s) = R(s) - \alpha \lambda^{-2} \exp \lambda \zeta(s)$$

where $R(s)$ is the nominal radius, α is a constant, and $\zeta(s)$ is a given function of the arclength with the expansion

$$\zeta = \frac{\mu s}{R(0)} \sin \varphi_0 + O(s^2)$$

where μ is a constant, then the equation can be written in a form displaying explicitly the dependence on λ

$$\begin{aligned} -\underline{y}' + (\lambda \underline{A}_0 + \underline{A}_1 + \dots + e^{\lambda \zeta} \underline{B}_1 + \frac{1}{\lambda} e^{2\lambda \zeta} \underline{B}_2 + \dots) \cdot \underline{y} \\ = \lambda^2 \underline{a}_0 + \lambda \underline{a}_1 + \dots + \lambda e^{\lambda \zeta} \underline{b}_1 + e^{2\lambda \zeta} \underline{b}_2 + \dots \end{aligned}$$

where the \underline{A}_i and \underline{a}_i are from the nominal geometry, while the \underline{B}_i and \underline{b}_i are due to the deviation from nominal. For the particular solution the expansion is

$$\begin{aligned} \underline{y} = \lambda \underline{\delta}_0 + \frac{1}{\lambda} \underline{\delta}_1 + \dots \\ + e^{\lambda \zeta} \left[\underline{\eta}_1 + \frac{1}{\lambda} \underline{\eta}_2 + \dots \right] \\ + e^{2\lambda \zeta} \left[\frac{1}{\lambda} \underline{\theta}_2 + \frac{1}{\lambda^2} \underline{\theta}_3 + \dots \right] + \dots \end{aligned}$$

while the expansion which works for the complementary solution is

$$\begin{aligned} \underline{y} = \exp(\lambda \xi) \left[\underline{\alpha}_0 + \frac{1}{\lambda} \underline{\alpha}_1 + \dots \right] \\ + \exp(\lambda \xi + \lambda \zeta) \left[\frac{1}{\lambda} \underline{\beta}_1 + \frac{1}{\lambda^2} \underline{\beta}_2 + \dots \right] \\ + \exp(\lambda \xi + 2\lambda \zeta) \left[\frac{1}{\lambda^2} \underline{\gamma}_2 + \dots \right] + \dots \end{aligned}$$

The result of retaining only the first term giving the deviation from nominal is that the stress concentration factor g in (9) is multiplied by $F(\mu, \rho)$ where

$$F(\mu, \rho) = \frac{1 + \mu[2(1 + \rho)]^{1/2}}{(1 + \rho)^{1/2} \{1 + \mu[2(1 + \rho)]^{1/2} + \mu^2\}} \quad (10)$$

where μ is the curvature parameter and ρ is the ratio of the internal pressure to the external classical buckling pressure.

The curves for $F(\mu, \rho)$ are shown in Fig. 9, with points from the direct numerical computation, for a nominal cylinder with $R/h = 100$. The agreement is reasonably good, even for excessive values of pressure. The agreement remains reasonable, even for $R/t = 10$ and a large discontinuity in angle, as shown by the table in Fig. 10. The computer results for geometric deviations other than the smooth exponential, show that (10) holds if μ is taken as the measure of the edge curvature deviation.

Thus a simple result valid over a wide range of the problem variables was obtained, which would, very probably, never have been obtained by either an independent analytical or numerical investigation. Without the guidance of the asymptotic solution, the significant parameters would be very difficult to determine out of the numerical output. On the other hand, without the motivation of the computer results, the asymptotic solution for rapidly varying coefficients would not have been attempted.

The analysis of [6], involving only geometric nonlinearity, was extended to an elastic-plastic material. Again a fruitful interaction took place. The computer program, using a detailed elastic-plastic material model, fails to converge as the limit load is reached. However, the estimated limit load was in reasonable agreement with the analytic result, using an oversimplified elastic-plastic model. So each solution by itself would be subject to doubt, but together give a conclusive result — that the local plastic collapse at the slope discontinuity can occur well before the pressure for overall collapse of the shell is attained.

2. Vibration of Cones — The ability of the asymptotic analysis to provide a simple qualitative understanding of a complex problem is shown in the investigations of shell vibrations [8,9]. The significant feature is in

the simpler equation for a beam on a foundation with variable properties

$$\frac{\partial^2}{\partial x^2} \left(EI \frac{\partial^2 w}{\partial x^2} \right) + ky + \rho A \frac{\partial^2 w}{\partial t^2} = 0$$

The expansion (3) is modified to the form

$$w(x, t) = e^{i\omega(t - \xi(x))} [\alpha_0(x) + \frac{1}{\omega} \alpha_1(x) + \dots]$$

The first term is the exact solution for constant properties, so for the general case, this expansion should give a valid approximation for wave lengths which are sufficiently small compared to the distance over which the properties vary. Substitution into the equation gives the "phase integral"

$$\xi(x) = \int_0^x \left(\frac{\rho A \omega^2 - k}{\omega^4 EI} \right)^{1/4} dx$$

and the "transport function"

$$\alpha_0 = (\xi')^{-3/2} (EI)^{-1/2}$$

Therefore, in a region for which

$$\omega^2 > k/\rho A$$

there will occur sinusoidal modes which are similar to those for the constant property beam, but with a distortion in amplitude and mode points. In a region for which $\omega^2 < k/\rho A$, ξ will be complex valued, so no sinusoidal modes can exist, i.e., ω is below the resonance frequency. The dramatic deviation of the variable from the constant property beam occurs when $\omega^2 = k/\rho A$ at a point on the beam. Then a transition takes place from a sinusoidal mode in the more flexible region to an almost negligible response in the stiffer region of the beam (or cone).

Past efforts to find the vibrational and buckling modes for conical shells by an energy method, using a series of cylinder modes, have been puzzling. In some situations convergence occurred with only a few terms, while in other cases, hundreds of cylinder modes would be required for

convergence to one mode of the cone. From the asymptotic result comes the explanation; when the transition point is on the cone, the mode shape is drastically different from any cylinder mode.

Thus in [9] the knowledge of the location of the transition point was used to conveniently categorize the results from a finite element computer program for some 3000 different configurations. Fig. 11 shows the frequency spectrum for a cylinder, while Fig. 12 is for a 60° cone. Fig. 13 shows the regimes I for which the transition point is off the truncated cone toward the apex, III for which the transition point is off the big end of the cone, and II for which the transition point is on the cone. Some deviation is seen as the curves enter the region II on Fig. 12. More pronounced is the effect on mode shapes shown in Fig. 14; the upper curves showing "cylinder" modes are from region I, while the lower curves are well into region II.

An interesting problem that turns out to be analogous to the cone vibration problem, concerns the analysis of the cochlea of the middle ear. The simplified mechanical model consists of a long, slightly tapered thin plate (the basilar "membrane") immersed in a fluid. The means by which a single nerve might be excited by a single frequency tone remains a controversial subject [10,11], even though several extensive programs for numerical analysis have been utilized. It would appear that an asymptotic analysis may offer some clarity for the situation. The taper of the plate, as the taper of the cone, causes a transition point to occur whose location is dependent on the frequency. Thus a simple formula using elastic properties from the deflection of the plate under a static concentrated load at three points along the cochlea, gives the curve shown in Fig. 15. The agreement with the experimental evidence over most of the significant frequency range indicates that something is going on at the transition point which excites the local nerve. A satisfying resolution will likely depend on an interaction between the asymptotic and numerical methods.

IV. FURTHER POSSIBILITIES FOR INTERACTION

There are numerous problems treated by the direct numerical methods which are beyond reach of any analytical effort. On the other hand, recent asymptotic results may offer some assistance for certain difficult problems.

1. Stress Pulses in Inhomogeneous Solids - For transient pulse propagation in a solid with variation in material properties in two or three directions, it is difficult to determine the points in space and time that maximum stresses occur. The geometric optics approximation can be applied in some cases. In [5], the bending of a stress ray due to the inhomogeneity is discussed (Fig. 16), and applied to the slab heated on one face but nonuniformly along the face. Thus an incident pressure pulse will not travel as a plane wave across the slab but will have an effect focused on the caustics, the envelopes of the rays. The caustics can be obtained from a relatively simple geometric construction and the time of arrival of the peak stress at the cusp easily computed, but the details are more difficult to obtain. Thus there should be a tie-in with the direct methods.

2. Moving Load Problems - The recent asymptotic results for shells of revolution with axisymmetric moving loads [14,15] show the development of the "steady-state" out of the complete transient solution. Furthermore, the behavior at the "critical" load speeds and the general behavior is obtained, as shown in Fig. 18, for the cylinder. When the load speed and/or the geometry varies, the asymptotic results become less useful, however, the general features can be obtained. In Fig. 19, the load position ξ is shown as a function of time τ for an increasing and a decreasing load speed. When the speed exceeds the minimum phase velocity, waves are generated which travel at their group velocity, giving the influence lines in Fig. 19. Again caustics form as the envelope of these influence lines, which give the locus of an accumulation of stress. Just how significant this view might be, remains to be established by direct numerical methods.

3. Shells with Holes and Concentrated Loads - The notions from geometric optics of rays and wave fronts can be applied to shell statics. In [16] the shell equations are reduced to the one equation

$$\nabla \cdot (\underline{p} + \lambda^{-2} \nabla p \otimes \underline{a}_3) + \underline{L} = 0$$

where \underline{p} is a symmetric tensor, which has the tangential stress resultants for its real part and the curvature changes for its imaginary part. p is the trace of \underline{p} , \underline{a}_3 is the unit normal to the surface, \underline{L} is a load vector, and \otimes denotes the tensor product. The "geometric optics" solution is

$$\underline{p} = e^{\lambda \xi} \left[\underline{\alpha} + \frac{1}{\lambda} \underline{\beta} + \frac{1}{\lambda^2} \underline{\gamma} + \dots \right]$$

Substitution into the equation gives the "eiconel" equation

$$(\nabla \xi \cdot \nabla \xi)^2 - \nabla \xi \cdot \underline{\epsilon} \cdot \underline{b} \cdot \underline{\epsilon} \cdot \nabla \xi = 0$$

where \underline{b} is the curvature and $\underline{\epsilon}$ the rotation tensor. This equation states that the gradient of ξ is equal to the square root of the normal curvature of the contour lines. Since this equation is a first order nonlinear partial differential equation, it can be solved by the method of characteristics. The characteristics turn out to be, generally, not in the direction of the gradient lines. Thus a nonorthogonal coordinate system consisting of the characteristics and the contour lines, on which ξ is constant, is used.

For the cylindrical shell, the characteristics are straight lines (i.e. geodesics) and the intrinsic part of $\nabla \xi$ does not change along the characteristic. Thus for a circular rigid insert in the wall of a cylinder, the picture is indicated in Fig. 20. The zone of significant bending propagates a considerable distance along the generators tangent to the hole. However, the maximum bending stress is about the same all around the hole. In contrast, the usual "boundary layer" analysis utilizes orthogonal coordinates and leads to a singularity at the points of the insert tangent to the generators.

There seem to be many possibilities for this type of solution. In particular, it should be possible to investigate shells with lightly stiffened holes for which membrane and inextensional solutions are important. Also problems of nearly concentrated loading should be amenable. Finally, it should be possible to obtain the generalization to orthotropic shells and to the dynamic problems. Since all these are problems which are far from resolution by the direct numerical methods, it would seem that there remains a broad area of significant practical problems in which a very interesting interaction of methods can and should take place.

REFERENCES

1. R. A. Clark and E. Reissner, "Bending of Curved Tubes", Advances in Applied Mechanics, Vol. II, Academic Press, 1951, pp. 93-122.
2. G. A. Cohen, "Computer Analysis of Asymmetrical Deformation of Orthotropic Shells of Revolution", AIAA Journal, Vol. 2, No. 5, May 1964, pp. 932-934.
3. C. R. Steele, "Nonsymmetric Deformation of Dome-Shaped Shells of Revolution", J. Appl. Mech., Vol. 29, No. 2, June 1962, pp. 353-361.
4. J. M. Massard, "HARTS III Final Report", Lockheed Missiles and Space Company, Report LMSC-B130725, Vol. II, Sec. 4, 1967.
5. C. R. Steele, "Asymptotic Analysis of Stress Waves in Inhomogeneous Solids", AIAA Journal, Vol. 7, No. 5, May 1969, pp. 896-902.
6. C. R. Steele and J. Skogh, "Slope Discontinuities in Pressure Vessels", to appear in J. Appl. Mech.
7. D. Bushnell, "Nonlinear Analysis for Axisymmetric Elastic Stresses in Ring-Stiffened Segmented Shells of Revolution", Proceedings of the AIAA/ASME 10th SDM Meeting, New Orleans, 1969.
8. E. W. Ross, Jr., "Transition Solutions for Axisymmetric Shell Vibration", J. Math. and Physics, No. 4, 1966, 335-355.
9. R. F. Hartung, and W. A. Loden, "Axisymmetric Vibration of Conical Shells", Proceedings of the AIAA/ASME 10th SDM Meeting, New Orleans, 1969.
10. C. von Békésy, "Traveling Waves As Frequency Analysers in the Cochlea", Nature, Vol. 225, March 28, 1970, pp. 1207-1209
11. A. F. Huxley, "Is Resonance Possible in the Cochlea After All?", Nature, Vol. 221, March 8, 1969, pp. 935-940.
12. C. H. Wilcox, Asymptotic Solutions of Differential Equations and Their Applications, Wiley, 1964.
13. Yu. A. Kravtsov, "Two New Asymptotic Methods in the Theory of Wave Propagation in Inhomogeneous Media", Soviet Physics - Acoustics - Vol. 14, No. 1, July-Sept. 1968.
14. C. R. Steele, "Beams and Shells with Moving Loads", Dynamics Symposium, Western Applied Mechanics Conference, Albuquerque, 1969, submitted for publication.
15. K. Schiffner and C. R. Steele, "The Cylindrical Shell with an Axisymmetric Moving Load", to appear in AIAA Journal.
16. C. R. Steele, "A Geometric Optics Solution for the Thin Shell Equation", submitted for publication.

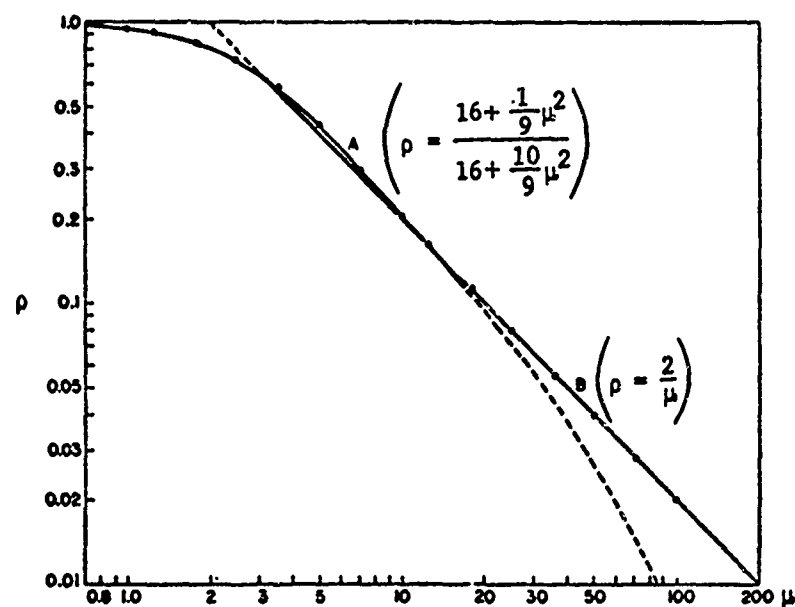


Fig. 1 Rigidity factor ρ for bending of curved tube. Curve A for $\mu^2 \ll 1$; Curve B for $\mu \gg 1$; Points from computation using 12 terms.

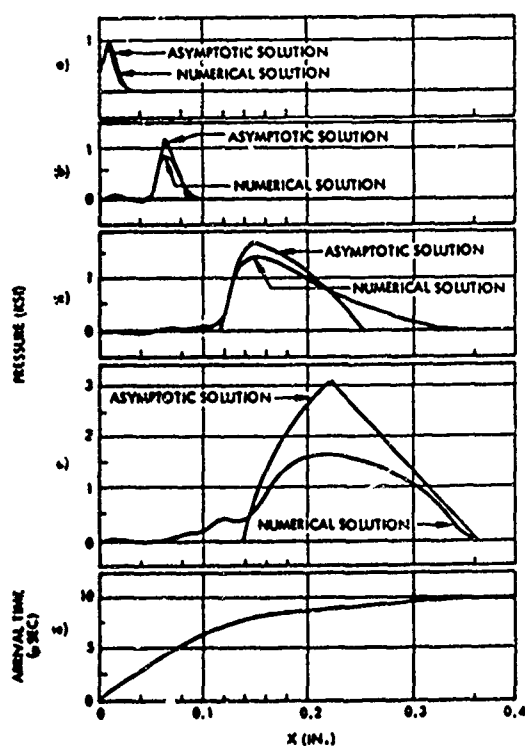


Fig. 2 Pressure profiles due to triangular pulse, asymptotic and numerical results.

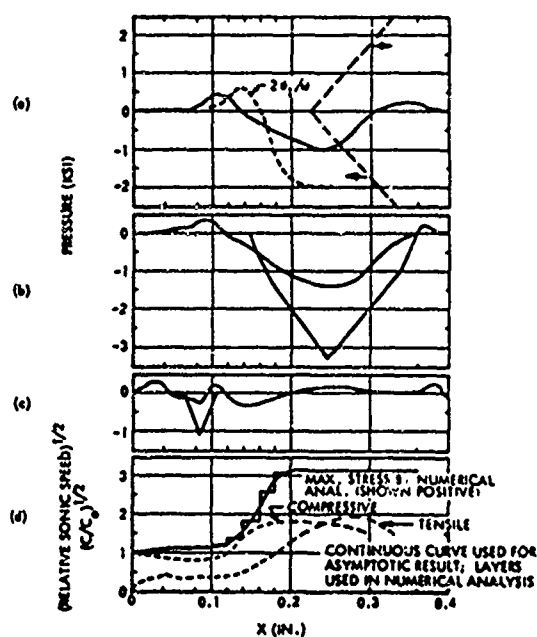


Fig. 3 Reflected pressure profiles, asymptotic and numerical results.

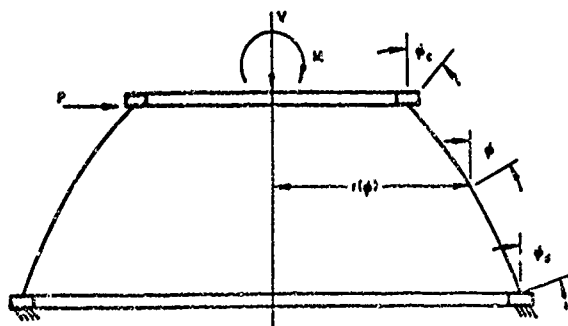


Fig. 4 Dome with rigid rings clamped to edges

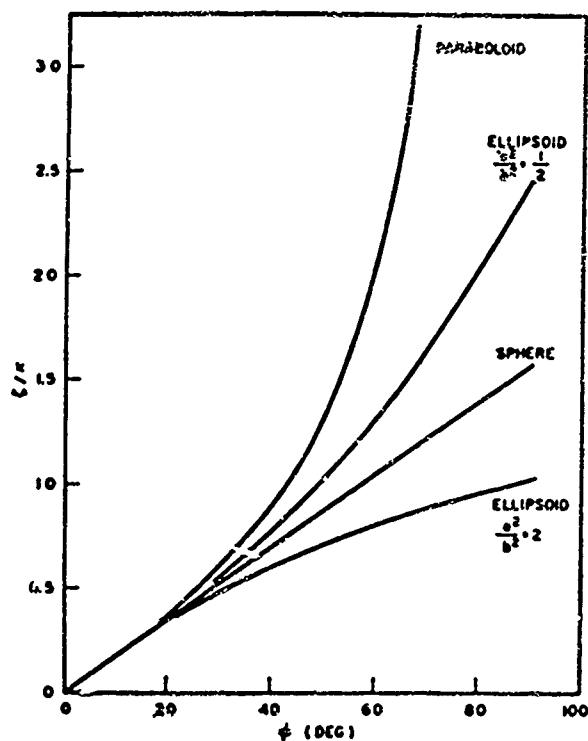


Fig. 5 Transformation function $\zeta/\kappa = \int_0^\varphi (r_1^2 \sin \psi / r_1^2) / d\psi$ for typical meridian curves

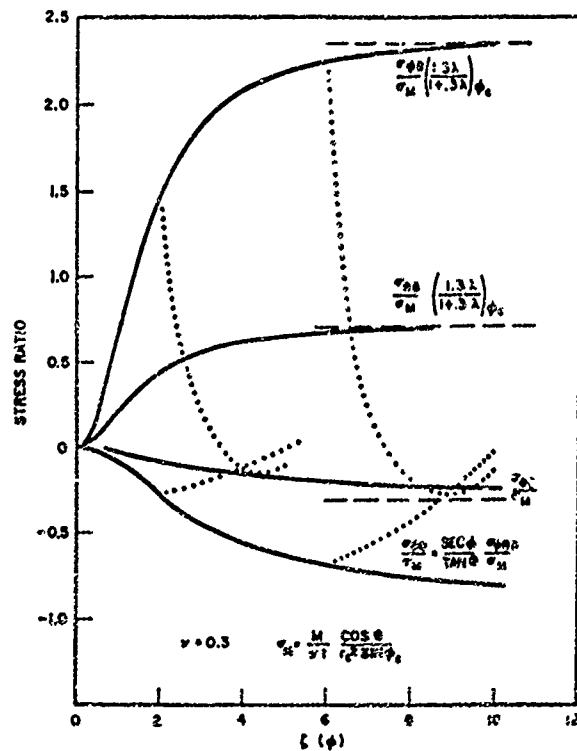


Fig. 6 Stresses due to tilting moment M

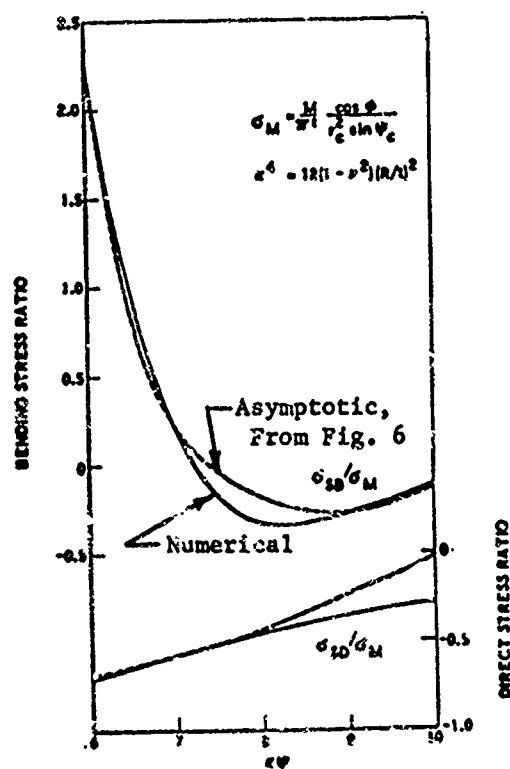


Fig. 7 Stresses due to tilting moment M .

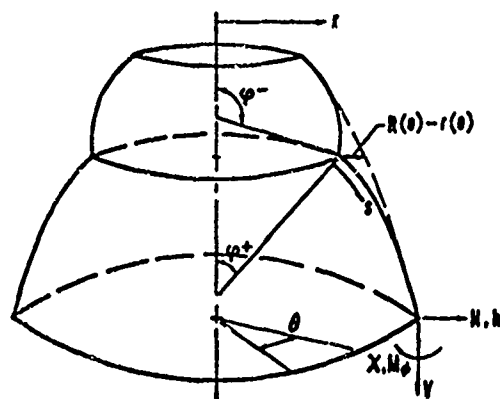


Fig. 8 Shell with discontinuity in slope of meridian

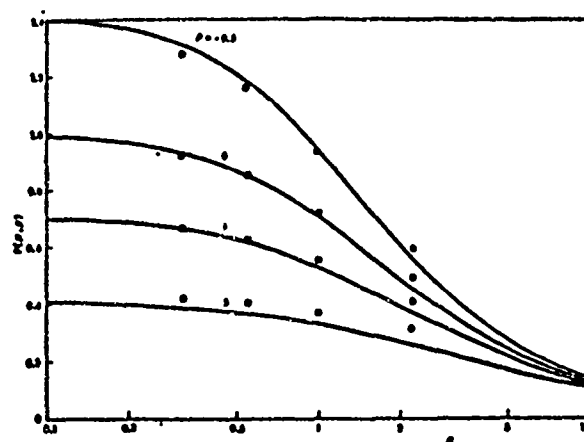


Fig. 9 Function $F(\mu, \rho)$, curves from equation (10), points from numerical analysis

Fig. 10 Maximum stress for thick shell: comparison between analytical and numerical analysis, $\lambda/t = 10$, $\nu = 0.3$

θ°		0.1°		1°	
$\theta^\circ - \alpha^\circ$		10.1°		69.8°	
		Eqs. 10	Numerical	Eqs. 10	Numerical
$\rho = 0.5$	$\sigma_p/(m/z)$	1.870	1.876	3.210	3.070
	$\sigma_g/(m/z)$	2.630	2.710	3.040	2.890
$\rho = 0.6$	$\sigma_p/(m/z)$	1.622	1.636	2.800	2.770
	$\sigma_g/(m/z)$	2.326	2.320	2.769	2.805
$\rho = 0.7$	$\sigma_p/(m/z)$	1.333	1.340	2.610	2.570
	$\sigma_g/(m/z)$	2.337	2.360	2.676	2.705

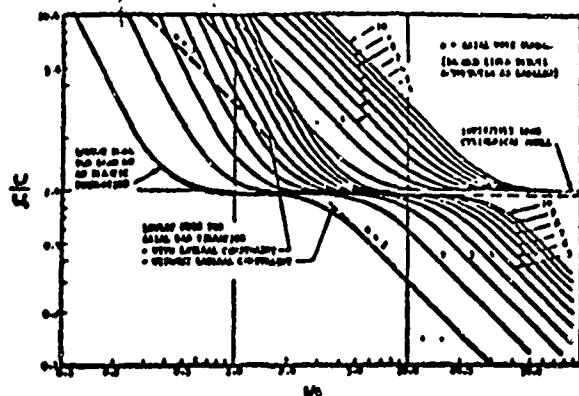


Fig. 11 Axisymmetric Frequency Spectrum for a Freely-Supported Cylinder for $A/H = 20$

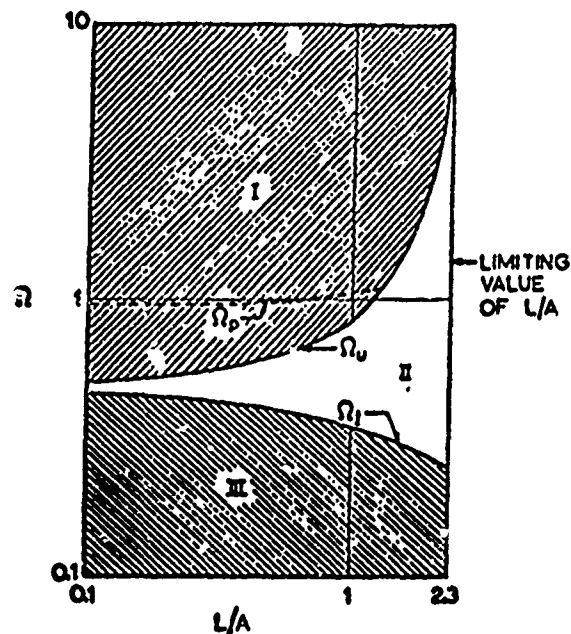


Fig. 13 Regimes on the Frequency Spectrum for a 60° Cone

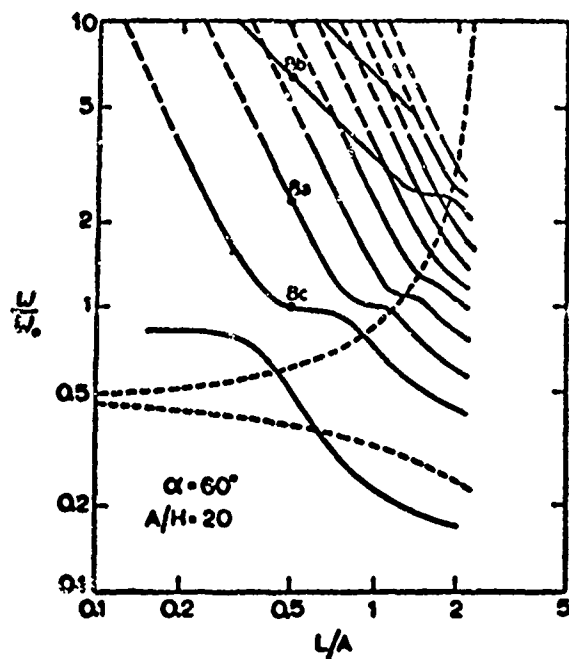


Fig. 12 Frequency Spectrum for a Simply Supported 60° Cone with $A/H = 20$

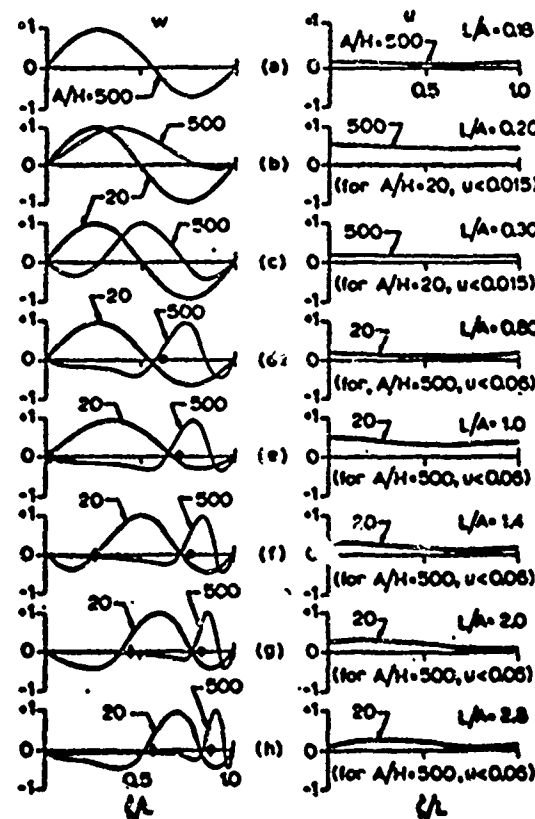


Fig. 14 Evolution of the third mode of a 45° freely supported cone as L/A is varied

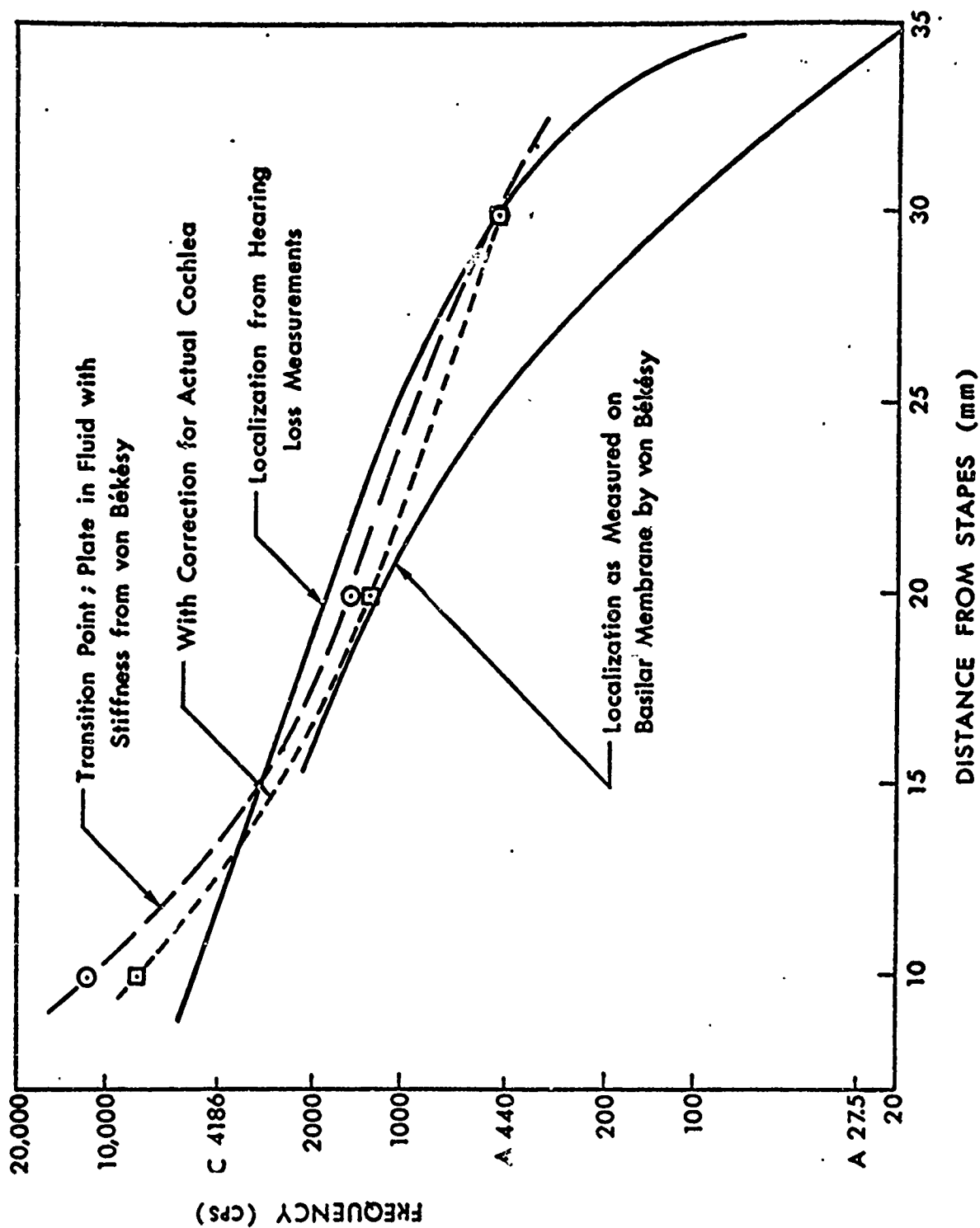


Fig. 15 - Localization of Nerve Excitation along Cochlea due to Monochromatic Sound at Eardrum

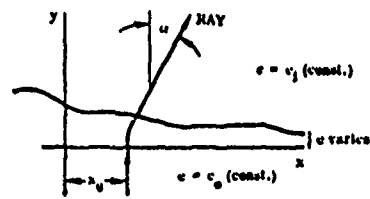


Fig. 16 Bending of ray in inhomogeneous layer.

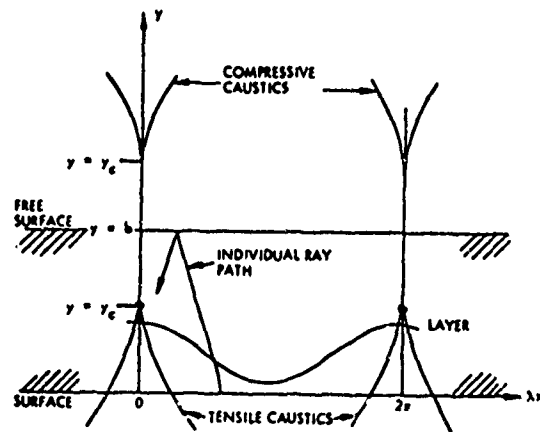


Fig. 17 Caustics formed by reflected waves.

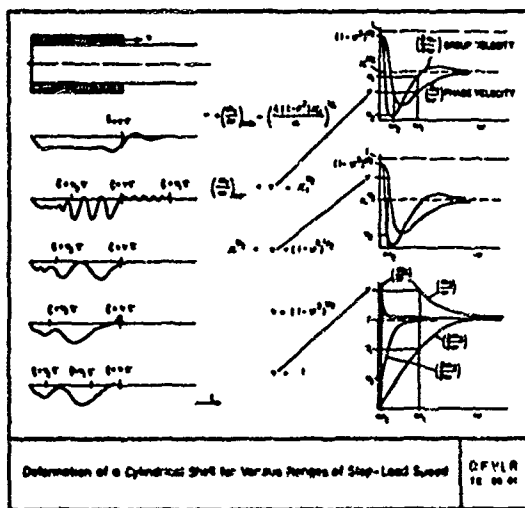


Fig. 18

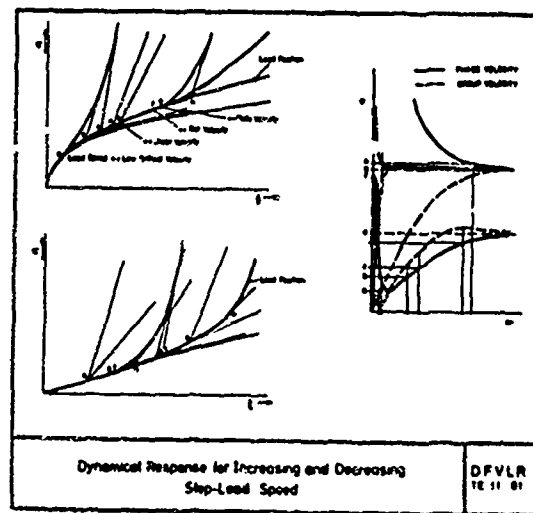


Fig. 19

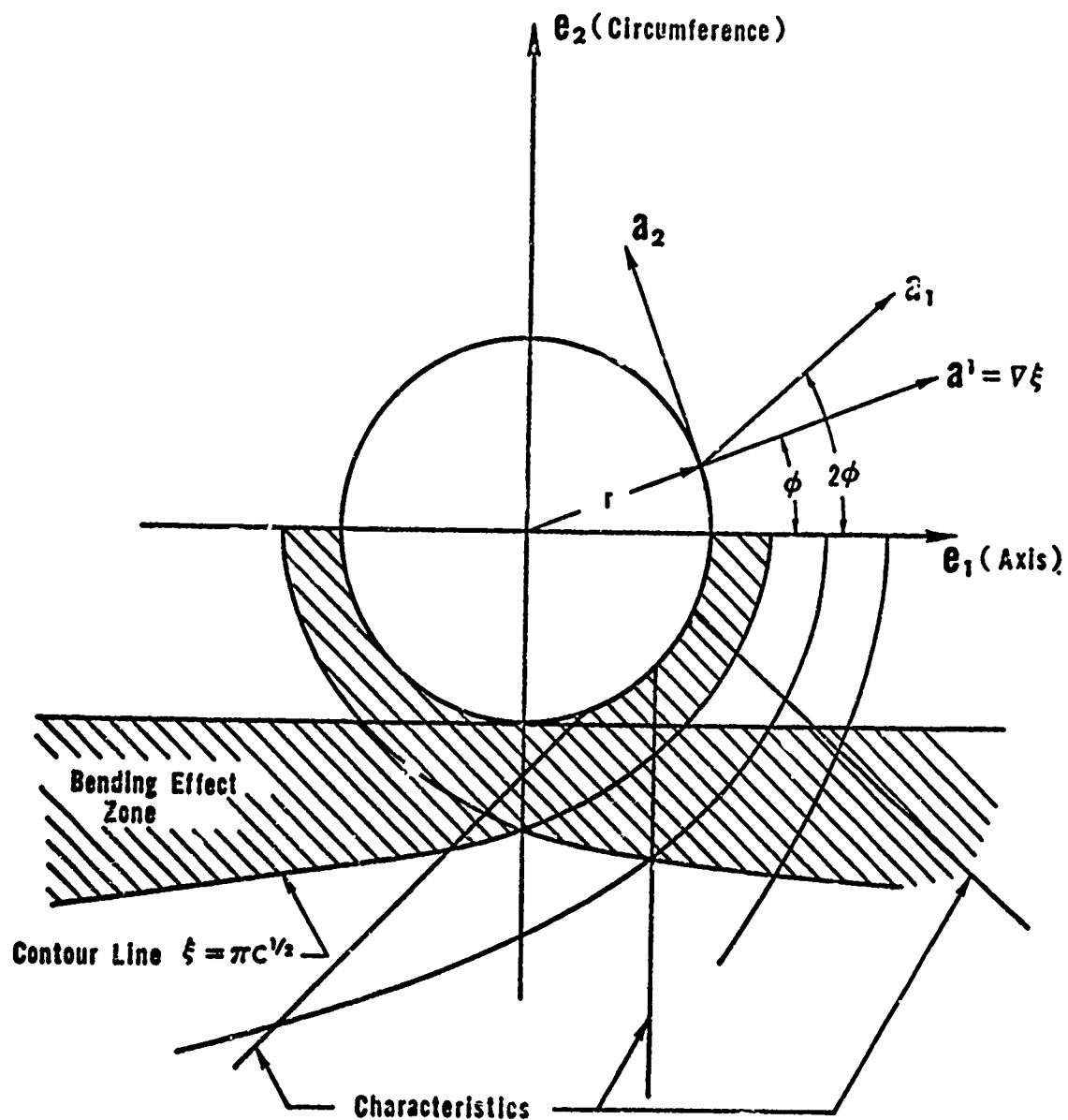


FIG.20- CYLINDER WITH RIGID INSERT

QUESTIONS AND COMMENTS FOLLOWING STEELE'S PAPER

COMMENT: I really don't have a question but I would like to make some comments. You were talking about the cylindrical shell with a hole in it and about the bending effects which may propagate it at long distance. In a recent experimental program we put a nozzle in a cylindrical shell similar to the one you discussed and we had great difficulty locating where the strain gages should be to find the so-called membrane stress part of the cylindrical shell. Your paper provides us insight as to why this was the case and I think your work will be of advantage to many if it is developed further.

STEELE: Well, I must say that by using a rigid insert, I've intentionally restricted the problem to avoid the membrane and inextensional solutions. If you really consider a flexible boundary, then the problem becomes more difficult. I really haven't looked at it yet but I'm very optimistic about this approach being able to do something definite about this more difficult problem of the hole, or a hole lightly reinforced.

COMMENT: I want to make a comment rather than ask a question. I think the work that Steele has done, especially that with Skogh most recently, is very exciting. Too often numerical analysts and people with large computer codes become so enmeshed in the numerical details that they don't look up every now and then and try to see the physics involved. For instance, in the conical shell problem which was discussed, modes were very hard to interpret. You don't know whether you have a bug in the program or whether to believe the results, and I think this interaction of numerical solutions with

the analytical solutions as provided by methods described here is an extremely powerful marriage--one that should be used much more frequently than it is.

QUESTION: The use of analytical techniques in combination with numerical techniques seem promising but do you think you'll be able to obtain analytical results for shells other than shells of revolution?

STEELE: Well, this last solution presented was for a general shell surface. The problem comes in computing these rays. If you have an arbitrary boundary curve on the general surface, then you can't get a closed form solution. You must use a numerical solution. But the fact is the large parameter is out of the problem, so you can use a fairly coarse grid to compute step by step into the interior and thus can easily compute all the rays emitting from an arbitrary boundary on an arbitrary surface. I think it's a very feasible approach.

LIESSA: There's just a couple of points I would like to make in summary. Regarding Prof. Kalnin's paper, I think the important thing here is that we realize two types of methods or techniques are being used. The numerical integration technique that probably most of you associate with Prof. Kalnin was not really necessary for that problem at all. What he was attempting to do was to extend the technique into the circumferential direction by means of the finite difference, least square or some other method. And, of course, the direct integration procedure as he presented is adaptable to those types of shells for which it is virtually impossible to solve using some exact technique.

Regarding Prof. Steele's paper, I think the important message there is

that asymptotic methods are certainly a very strong complement to the traditional numerical methods we're all familiar with. It gives us information that is extremely valuable if, for example, we want to change a parameter and see what happens. In particular, I'd like to quote from Prof. Steele's abstract where he says "asymptotic solutions are useful because they provide simple formulas for preliminary design and exact solutions for limiting cases in which straightforward numerical procedures encounter difficulty." I certainly agree with that and I would add that if you're trying to solve a design problem using finite elements, for example, you all know which direction to change some variable to get a better design. I think also that Prof. Steele showed us a number of directions where asymptotic methods can be used.

ON THE POSTBUCKLING BEHAVIOR OF IMPERFECTION-SENSITIVE
STRUCTURES IN THE PLASTIC RANGE^{*}

John W. Hutchinson
Harvard University
Cambridge, Massachusetts

ABSTRACT

Aspects of postbuckling behavior are investigated for structures undergoing plastic deformation. The structures singled out are characterized by a highly imperfection-sensitive behavior where buckling takes place in the elastic range. A simple model study is carried out and is followed by an analysis of the plastic buckling of a complete spherical shell under external pressure. In both instances, the bifurcation behavior and subsequent deformation of the perfect structure as well as the influence which geometric imperfections have on buckling are studied.

1. INTRODUCTION

Elastic structures which are labeled imperfection-sensitive have the property that when a perfect realization of the structure undergoes bifurcation the load carrying capacity diminishes, and the bifurcation load is the (local) maximum load that can be supported. Small imperfections arising from various sources usually have an appreciable effect on the maximum load such a structure can support. On the other hand, when bifurcation occurs in the plastic range it is generally true that bifurcation must take place under increasing applied load. At least this is what happens according to the Shanley concept [1-4], and Hill's [5, 6] general study of the bifurcation behavior of elastic-plastic solids suggests that this is the rule rather than the exception.

For an elastic system, a study of the equilibrium configurations in the neighborhood of the bifurcation point reveals its stability characteristics. If the structure is imperfection-sensitive and if small imperfections are accounted for in the analysis, then exact asymptotic results relating the buckling load (local maximum) to the imperfection amplitude can be obtained (Koiter [7, 8], [9]). An analysis of the plastic buckling of imperfection-sensitive structures, similar in spirit to Koiter's analysis of elastic systems, has not been accomplished in part, no doubt, due to the considerable complications which accompany the introduction of elastic-plastic behavior. In fact, it seems unlikely that results as general and concise as those for elastic systems will be obtainable.

^{*} Presented at Conference on Computer-Oriented Analysis of Shell Structures, August 10-14, 1970, Palo Alto, California.

This work was supported in part by the National Aeronautics and Space Administration under Grant NGL 22-007-012, and by the Division of Engineering and Applied Physics, Harvard University.

In this paper we focus on the postbuckling behavior of structures which are imperfection-sensitive when buckling takes place in the elastic range. First, a simple model study is carried out which does yield some simple and revealing formulas for the effect of small imperfections. The model study is followed by an analysis of the plastic buckling of a complete spherical shell. A brief review of the bifurcation behavior of the perfect sphere is given, and a numerical analysis of the axisymmetric postbuckling deformation of perfect and imperfect spherical shells is reported.

2. BUCKLING OF AN IMPERFECTION-SENSITIVE SIMPLE MODEL IN THE PLASTIC RANGE

Significant imperfection-sensitivity of elastic structures is due to strong geometric, or structural, nonlinearities. These nonlinearities will be equally important when buckling takes place in the plastic range. The simple model investigated here combines the essential features of Shanley's [1] model of plastic column buckling and Kármán, Dunn and Tsien's [10] model of elastic buckling of imperfection-sensitive structures. It is similar in a number of respects to models studied by Sewell [11] and Augusti [12] but differs in that the model possesses a strong geometric nonlinearity and this property is exploited in the analysis. An elastic version of the model was used to study dynamic buckling in Ref. [13].

The rigid-rod model, which is shown in Fig. 1, can displace vertically as measured by u and can rotate as measured by θ . An initial rotation from the vertical in the unload state is called the imperfection and is denoted by $\bar{\theta}$ so that the total rotation is $\bar{\theta} + \theta$. The load-deflection behavior of each of the supporting springs, #1 and #2, is also shown in Fig. 1 and is given by

$$\dot{F} = E\dot{\Delta} \quad \text{for} \quad \begin{cases} F < F^{\max} \\ F = F^{\max} \quad \text{and} \quad \dot{F} < 0 \end{cases}, \quad \text{or} \quad (1)$$

$$\dot{F} = E_c \dot{\Delta} \quad \text{for} \quad F = F^{\max} \quad \text{and} \quad \dot{F} > 0$$

where $F^{\max} = F_y$ for initial yield. Spring #3 is introduced to bring in a strong geometric nonlinearity. Under a rotation θ the force which develops in this spring is $Q = \beta\theta^2$. We shall assume that the parameter $\beta/(EL_1)$ is large compared to unity. This insures that Q is the only significant geometric nonlinearity and permits us to replace $\sin \theta$ and $\cos \theta$ by θ and 1, respectively.

The equations of equilibrium and the deflection-displacement relations are

$$F_1 + F_2 = P \quad (2)$$

$$(F_2 - F_1)L_1 + PL_2(\bar{\theta} + \theta) + \beta L_2 \theta^2 = 0 \quad (3)$$

$$\begin{aligned}\Delta_1 &= u + L_1 \theta \\ \Delta_2 &= u - L_1 \theta\end{aligned}\quad (4)$$

where subscripts denote springs #1 and #2.

The behavior of the model for a purely elastic response ($E_c = E$) is shown in Fig. 2. Bifurcation of the perfect structure occurs at $P_C = 2ErL_1$; and the maximum support load in the presence of an imperfection, $\bar{\theta} > 0$, is given by

$$\left(1 - \frac{P^{\max}}{P_C}\right)^2 = \left(\frac{2\beta}{ErL_1} \bar{\theta}\right) \frac{P^{\max}}{P_C} \quad (5)$$

For $\bar{\theta}$ sufficiently small,

$$\frac{P^{\max}}{P_C} = 1 - \left(\frac{2\beta}{ErL_1} \bar{\theta}\right)^{\frac{1}{2}} + \dots \quad (6)$$

Turning to plastic buckling, we first consider the bifurcation behavior of the model with no imperfection. The lowest value of P at which bifurcation is possible is $P^{\tan} = 2E_c r L_1$, the so-called tangent modulus load; but bifurcation is possible for any $P \geq P^{\tan}$. It is readily verified that the conditions (1) of loading and unloading can be satisfied at the bifurcation point only if one spring loads and the other unloads. The interesting case is when $\theta \geq 0$ for which spring #1 continues to load and spring #2 unloads coincident with bifurcation. If bifurcation occurs at $P = P_C$ then the load-deflection relation is

$$P = \left[P_C + \frac{1}{r} \left(\frac{1+\lambda}{1-\lambda}\right) P^{\tan} \theta - \frac{\beta}{r} \left(\frac{1+\lambda}{1-\lambda}\right) \theta^2\right] \left[1 + \frac{1}{r} \left(\frac{1+\lambda}{1-\lambda}\right) \theta\right]^{-1} \quad (7)$$

$$= P_C + \theta \left[\frac{1}{r} \left(\frac{1+\lambda}{1-\lambda}\right) (P^{\tan} - P_C)\right] - \theta^2 \left[\frac{1}{2} \left(\frac{1+\lambda}{1-\lambda}\right)^2 (P^{\tan} - P_C) + \frac{\beta}{r} \left(\frac{1+\lambda}{1-\lambda}\right)\right] + \dots \quad (8)$$

where $\lambda = E_c/E$. The reduced modulus load where bifurcation takes place with no change in the applied load, to first order, is given by

$$P^{\tan} = \frac{2P^{\tan}}{1+\lambda}$$

For $P_C < P^{\tan}$, bifurcation takes place under increasing load. The maximum load which the perfect structure can support when bifurcation occurs at $P_C = P^{\tan}$ satisfies the equation

$$(P^{\tan} - P_0^{\max})^2 + 4\beta r \left(\frac{1-\lambda}{1+\lambda}\right) (P^{\tan} - P_0^{\max}) = 0 \quad (9)$$

or

$$P_0^{\max} = P^{\tan} \left[1 + \frac{E L_1}{2\beta} \left(\frac{1-\lambda}{1+\lambda} \right) + \dots \right]$$

This value is only very slightly above the bifurcation load.

An example of the load-deflection relation (7) is plotted in Fig. 3 for three different bifurcation values. In this figure P is normalized by $P_C = P^{\tan}$ and this curve is shown as a solid line ($\bar{\theta}=0$). The upper dashed curve corresponds to bifurcation at the reduced modulus load, while bifurcation takes place half way between P^{\tan} and P^{\tan} for the lower dashed curve. On each curve, the maximum load occurs at the point marked by a cross. Our discussion this far follows that given in more detail by Sewell [11] for a similar model.

In the presence of a small imperfection, $\bar{\theta} > 0$, the load-deflection behavior is considerably more complicated. There are three distinct sequences of loading and unloading which can take place depending on the magnitude of $\bar{\theta}$. First, consider the case for which $\bar{\theta}$ is sufficiently small so that the resulting formulae will be valid in the limit as $\bar{\theta}$ vanishes. In this case, it is found that there are four separate steps to the loading history. With the first application of load both springs are elastic. Next, spring #1 starts deforming plastically and is followed by spring #2 at a slightly higher load. The load continues to rise. At a value of θ , denoted by $\hat{\theta}$, spring #2 unloads. From this point on spring #1 loads while #2 stays in the elastic range.

The maximum value of P occurs at a value of θ slightly larger than $\hat{\theta}$. Some of the formulas for the values of P and θ at the various stages of the history are rather lengthy and will not be listed here.[†] On the other hand, the expressions for $\hat{\theta}$ and P^{\max} are relatively simple. They are independent of F_y and are given by

$$\hat{\theta} = -\bar{\theta} + \left\{ \bar{\theta}^2 + \frac{r\bar{\theta} - \bar{\theta}^2}{1 + \beta/(2E_c L_1)} \right\}^{\frac{1}{2}} \quad (10)$$

and

$$P^{\max} = P_0^{\max} - 2\beta \left[\hat{\theta} + \left\{ \left(1 + \frac{2E_c L_1}{\beta} \right)^{\frac{1}{2}} - 1 \right\} (\hat{\theta} + \bar{\theta}) \right] \quad (11)$$

Asymptotically for small $\bar{\theta}$, Eq. (11) becomes

$$\frac{P^{\max}}{P_0^{\max}} = 1 - \left(\frac{2\beta}{E_c r L_1} \bar{\theta} \right)^{\frac{1}{2}} + \dots \quad (12)$$

[†] I am indebted to N. L. Goldman for a careful check of the analysis of the simple model.

where it is recalled that P_0^{\max} is the maximum support load (9) of the perfect structure when bifurcation occurs at $P_C = P^{\tan}$.

The asymptotic result (12) is particularly expressive in that it is very similar to the analogous result (6) for the purely elastic model. The important difference is the presence of Z_t in (12) rather than E . Thus, for small imperfections the model is more imperfection-sensitive in the plastic range than in the elastic range in the sense that an imperfection amplitude $\lambda\bar{\theta}$ results in the same relative reduction of the buckling load as does $\bar{\theta}$ in the elastic case.

Equation (11) ceases to hold when $\bar{\theta}$ is sufficiently large such that spring #2 does not become plastic at all. In this sequence of loading, spring #1 yields at a value of P just under $2F_y$ and the model deflects readily under only slightly increasing load until the maximum load occurs at a value which is given very closely by

$$P^{\max} \approx 2F_y \quad (13)$$

Curves of P vs. $\bar{\theta}$ for the example of Fig. 3 are also shown for non-zero values of $\bar{\theta}$. The parameters of the model have been chosen such that P^{\tan} (P_C in Fig. 3) is forty percent higher than $2F_y$, the initial yield value for the perfect model. Curves of the maximum load as a function of the imperfection $\bar{\theta}$ are shown on the right in Fig. 3. The asymptotic prediction (12) is shown as a dashed curve and agrees very closely with the exact result until second branch (13) governs.

If the 'elastic buckling load', $2ErL_1$, is only slightly higher than the plastic value, $2E_t rL_1$, a third possibility arises in which for sufficiently large imperfections neither spring becomes plastic before the maximum load occurs. On this branch (6) holds. Thus, for example, if a structure is highly imperfection-sensitive an imperfection of modest size may trigger buckling before any plastic deformation sets in even though the perfect structure would buckle in the plastic range.* The example shown in Fig. 4 illustrates this behavior. Here $E_t/E = 3/4$ so that the elastic buckling load is only one third greater than the tangent modulus load. Branch A-B displays the strong imperfection-sensitivity associated with Eq. (11), while on B-C (13) holds. On C-D the maximum load is attained before any plastic deformation takes place as discussed.

*

Some specific calculations for cylindrical shells under axial compression suggest that the opposite can be true [14]. Namely, that an imperfection may induce high local stresses and plastic deformation (which tend to reduce the buckling load) even though the perfect shell would buckle in the elastic range.

3. BIFURCATION BEHAVIOR OF A PERFECT SPHERICAL SHELL IN THE PLASTIC RANGE

The critical external pressure for elastic buckling of a perfect complete spherical shell is

$$p_C = \frac{2E}{[3(1-\nu^2)]^{\frac{1}{2}}} \left(\frac{t}{R}\right)^2 \quad (14)$$

where t is the shell thickness, R is its radius and the isotropic elastic properties are specified by the Young's modulus E and Poisson's ratio ν . The principle in-plane stresses are equal and are given by $\sigma_C = -p_C R / (2t)$.

Associated with this critical pressure is a multiplicity of $(2n+1)$ linearly independent buckling modes whose displacements normal to the shell middle surface are given in terms of the spherical surface harmonics of degree n :

$$w = S_n(\theta, \phi) = a_0 P_n(\cos \theta) + \sum_{m=1}^n P_n^{(m)}(\cos \theta) [a_m \cos m\phi + b_m \sin m\phi] \quad (15)$$

where θ is the polar angle and ϕ is the longitudinal coordinate. The degree n is the integer which most closely satisfies

$$n(n+1) = 2[3(1-\nu^2)]^{\frac{1}{2}} \frac{R}{t} \quad (16)$$

and P_n is the Legendre polynomial of degree n and $P_n^{(m)}$ is the associated polynomial of degree n and order m .

This result in its general form is due to van der Neut [15]. We have taken the above formulas from a recent paper by Koiter [16] who has rederived these results using the simpler Donnell-Mushtari-Vlasov shell equations which are entirely adequate for this problem due to the shallow character of the buckling deformations.

The state of stress in a perfect spherical shell prior to bifurcation is a purely membrane one with equal principle in-plane stresses whether or not the shell has undergone plastic deformation. Thus, the relationship between the in-plane stress rates and strain rates at bifurcation is necessarily isotropic for any plasticity theory with a single plastic branch as long as no elastic unloading occurs. Therefore, it is possible to introduce an effective tensile modulus E_e and Poisson's ratio ν_e relating in-plane stress and strain rate quantities. Under the usual assumptions for thin shells that the Kirchhoff-Love hypotheses apply, the lowest bifurcation pressure in the plastic range is still given by (14) but with E replaced by E_e and ν by ν_e ; i.e.,

$$p_C = \frac{2E_e}{[3(1-\nu_e^2)]^{\frac{1}{2}}} \left(\frac{t}{R}\right)^2 \quad (14a)$$

where $C_e = [3(1-\nu_e^2)]^{\frac{1}{2}}$. The same axisymmetric and non-axisymmetric bifurcation modes (15) are possible (coupled with a uniform radial displacement rate) if ν is replaced by ν_e in (16). Bijlaard [17] was apparently the first to note that (14), appropriately modified, holds in the plastic range. It is rigorously valid within the context of first order shell theory as long as the bifurcation modes are sufficiently shallow, that is, as long as n given by (16) is sufficiently large ($n \geq 5$ or 7 is probably a reasonable cutoff).

Bifurcation at the value p_C given by (14a) is only possible if no elastic unloading occurs anywhere in the shell [1, 6]. The rate of change of the J_2 stress invariant at the bifurcation point with loading everywhere can be obtained by a straightforward analysis which employs the bifurcation rate of the normal displacement (15) and the associated Airy stress function rate of Donnell-Muskhvishvili-Vlasov shell theory. The details of this calculation are not given here. Consistent with the assumptions of thin shell theory, the J_2 invariant is taken to depend only on the in-plane stresses so that with $s_{ij} = \sigma_{ij} - \frac{1}{3}\sigma_{kk}\delta_{ij}$,

$$J_2 \equiv \frac{1}{2}s_{ij}s_{ij} = \frac{1}{3}(\sigma_{11}^2 + \sigma_{22}^2 + 3\sigma_{12}^2 - \sigma_{11}\sigma_{22}) \quad (17)$$

We find that at a distance z measured outward from the middle surface of the shell J_2 is given by

$$\dot{J}_2 = -\frac{1}{6}(p_C \frac{R}{t})^2 \left\{ C_e \left[\frac{1}{2} + \left(\frac{z}{t} \right) \frac{C_e}{1-\nu_e} \frac{\dot{S}_n}{t} - \frac{\dot{p}}{p_C} \right] \right\} \quad (18)$$

where \dot{p} is the pressure rate and \dot{S}_n is the bifurcation mode rate given by (15). For any plasticity theory based on the J_2 invariant alone, such as simple flow theory and deformation theory discussed below, the loading condition requires $\dot{J}_2 \geq 0$ everywhere in the shell. If the buckling amplitude rate at bifurcation is denoted by $\dot{\delta}$ (i.e., $\dot{\delta} = \max[\dot{S}_n]$), then no unloading occurs as long as

$$\frac{\dot{p}}{p_C} \geq \frac{C_e}{2} \left(1 + \frac{C_e}{1-\nu_e} \right) \frac{\dot{\delta}}{t} \quad (19)$$

For J_2 flow theory, for example, the effective Young's modulus and Poisson's ratio for the perfect sphere in the prebifurcation state are given by

$$\frac{1}{E_e} = \frac{1}{E} \left[1 + \frac{1}{4} \left(\frac{E}{E_t} - 1 \right) \right] \quad \text{and} \quad \frac{\nu_e}{E_e} = \frac{1}{E} \left[\nu - \frac{1}{4} \left(\frac{E}{E_t} - 1 \right) \right] \quad (20)$$

where the tangent modulus E_t is a function of J_2 and is defined in the usual way by $\dot{\sigma} = E_t \dot{\epsilon}$ for a uniaxial tensile history. The critical pressure is

$$p_c = \frac{4E}{[6(1+\nu)(1-2\nu+E/E_t)]^{\frac{1}{2}}} \left(\frac{t}{R}\right)^2 \quad (21)$$

This formula, which was originally due to Bijlaard, was rederived by Batterman [18] under the restriction of axisymmetric deformations using equations for shells of revolution given in [19]. Batterman [18] also gives a formula similar to (19) derived specifically for J_2 flow theory and under the restriction of axially symmetric deformations.

For a J_2 deformation theory of plasticity:

$$\frac{1}{E_e} = \frac{1}{4} \left(\frac{1}{E_t} + \frac{3}{E_s} \right), \quad \frac{\nu_e}{E_e} = \frac{1}{4} \left[\frac{2(1-2\nu)}{E} + \frac{1}{E_t} - \frac{3}{E_s} \right] \quad (22)$$

and

$$p_c = \frac{4E}{\left\{ 3 \left[\frac{E}{E_t} \frac{E}{E_s} - (1-2\nu)(1-2\nu + \frac{E}{E_t} - \frac{3E}{E_s}) \right] \right\}^{\frac{1}{2}}} \left(\frac{t}{R}\right)^2 \quad (23)$$

where E_s is a function of J_2 and is defined in uniaxial tension to be $E_s = \sigma/\epsilon$.

4. PLASTIC POSTBUCKLING BEHAVIOR AND IMPERFECTION-SENSITIVITY OF A SPHERICAL SHELL UNDERGOING AXISYMMETRIC DEFORMATIONS

Formulation of the rate equations and numerical analysis

In this section a numerical analysis of the postbuckling behavior of perfect and imperfect complete spherical shells is carried out. Our investigation is restricted to deformations and imperfections which are rotationally symmetric with respect to some axis. Interaction between the axisymmetric bifurcation mode and the many non-axisymmetric modes (15) is likely to be important particularly if non-axisymmetric imperfections are present; but for elastic buckling at least, there is now little doubt that the strong imperfection-sensitivity of the spherical shell is uncovered by an axisymmetric analysis [16, 20-22].

Reissner's [23] nonlinear equations for the axisymmetric deformation of shells of revolution are employed in the analysis. The strain-displacement and equilibrium equations of this shell theory are left in their uncombined form in which no dependent variable is differentiated more than once with respect to the polar coordinate θ . As discussed in more detail below, the equations governing an incremental step in the deformation history are reduced to a set of six first order ordinary differential equations.

A small strain theory of plasticity is used in which the relation between the stress rates and strain rates for the material in the shell is assumed to be of the form

$$\dot{\sigma}_{ij} = L_{ijkl} \dot{\epsilon}_{kl} \quad (24)$$

with $L_{ijkl} = L_{jikl} = L_{ijlk} = L_{klij}$. These instantaneous moduli depend, in general, on the stress history and here it is assumed that there are two branches to L depending on whether loading or unloading occurs. In an approximately plane state of stress only the in-plane stresses enter into the constitutive relation and it is convenient to introduce the in-plane moduli according to

$$\dot{\sigma}_{\alpha\beta} = \hat{L}_{\alpha\beta\gamma\mu} \dot{\epsilon}_{\gamma\mu} \quad (25)$$

where the Greek indices take on only the values 1 and 2. The in-plane moduli are related to the 3-D moduli by

$$\hat{L}_{\alpha\beta\gamma\mu} = L_{\alpha\beta\gamma\mu} - \frac{L_{\alpha\beta 33} L_{\gamma\mu 33}}{L_{3333}} \quad (26)$$

Strain rate components a distance z outward from the shell middle surface are given in terms of the middle surface strain rates $\dot{E}_{\alpha\beta}$ and the bending strain rates $\dot{K}_{\alpha\beta}$ by

$$\dot{\epsilon}_{\alpha\beta} = \dot{E}_{\alpha\beta} + z \dot{K}_{\alpha\beta} \quad (27)$$

Using the usual definitions of the resultant stress tensor $N_{\alpha\beta}$ and the bending moment tensor $M_{\alpha\beta}$, we find

$$\dot{N}_{\alpha\beta} = H_{\alpha\beta\gamma\mu}^{(1)} \dot{E}_{\gamma\mu} + H_{\alpha\beta\gamma\mu}^{(2)} \dot{K}_{\gamma\mu} \quad \text{and} \quad \dot{M}_{\alpha\beta} = H_{\alpha\beta\gamma\mu}^{(2)} \dot{E}_{\gamma\mu} + H_{\alpha\beta\gamma\mu}^{(3)} \dot{K}_{\gamma\mu} \quad (28)$$

where

$$H_{\alpha\beta\gamma\mu}^{(1)} = \int_{-\frac{t}{2}}^{\frac{t}{2}} \hat{L}_{\alpha\beta\gamma\mu} z^{i-1} dz \quad (29)$$

Two phenomenological theories of plasticity will be used in the present analysis. In each of them the plastic deformation depends only on J_2 invariant (17). The instantaneous moduli for J_2 flow theory with isotropic elastic properties are

$$L_{ijkl} = \frac{E}{1+\nu} \left\{ \frac{1}{2} (\delta_{ik} \delta_{jl} + \delta_{il} \delta_{jk}) + \frac{\nu}{1-2\nu} \delta_{ij} \delta_{kl} - \frac{f s_{ij} s_{kl}}{1+\nu+2fJ_2} \right\} \quad (30)$$

where for $\dot{J}_2 < 0$ or $J_2 < (J_2)_{\max}$, $f = 0$; while for $J_2 = (J_2)_{\max}$ and $\dot{J}_2 \geq 0$,

$$f = \frac{3}{4J_2} \left(\frac{E}{E_t} - 1 \right) \quad (31)$$

For J_2 deformation theory (with unloading incorporated),

$$L_{ijkl} = \frac{E}{1 + \nu + g} \left\{ \frac{1}{2} (\delta_{ik} \delta_{jl} + \delta_{il} \delta_{jk}) + \frac{3\nu + g}{3(1-2\nu)} \delta_{ij} \delta_{kl} - \frac{g' s_{ij} s_{kl}}{1 + \nu + g + 2g' J_2} \right\} \quad (32)$$

where $g' \equiv \frac{dg}{dJ_2}$. For unloading, $g = g' = 0$; while for loading,

$$g = \frac{3}{2} \left(\frac{E}{E_g} - 1 \right) \quad (33)$$

Rate equations of equilibrium for shells of revolution undergoing axisymmetric deformations involve five stress quantities -- M_{11} , M_{22} , N_{11} , N_{22} and Q_1 -- in the usual notation with the indice 1 associated with the polar coordinate θ . The strain rate-displacement rate equations involve four strain quantities, \dot{E}_{11} , \dot{E}_{22} , \dot{K}_{11} and \dot{K}_{22} , two displacement rates, \dot{u} and \dot{w} , and one rotation rate $\dot{\phi}_1$. Six of these rate quantities can be eliminated from the governing Reissner equations with the aid of the constitutive relations (28) to give a set of six first order differential equations which in matrix notation take the form

$$\frac{d}{d\theta} \bar{X} + A \bar{X} = \bar{p} \quad (34)$$

In this equation $\bar{X} \equiv (\dot{N}_{11}, \dot{Q}_1, \dot{M}_{11}, \dot{u}, \dot{w}, \dot{\phi}_1)$. The column vector \bar{p} depends on the loading rates and the current state of deformation of the shell through \bar{X} , and the 6×6 matrix A depends on the instantaneous moduli (29) and on \bar{X} . This choice of dependent variables has been used previously with success in the analysis of elastic shells of revolution [24-26] and a detailed discussion of the numerical analysis of this system of equations is given in [27].*

The great advantage of dealing with a system of first order differential equations in a plasticity analysis is that no differentiation of the stiffness quantities is required. Equation (34) is cast into finite difference form by dividing the polar coordinate, θ , into N equally spaced intervals with $N+1$ stations at which \bar{X} is defined running from the pole to the equator. Equation (34) is replaced by

$$\frac{\bar{X}_{i+1} - \bar{X}_i}{\Delta\theta} + A_i \left(\frac{\bar{X}_{i+1} + \bar{X}_i}{2} \right) = \bar{p}_i \quad (35)$$

where A_i and \bar{p}_i are evaluated halfway between the i^{th} and the $i+1^{\text{th}}$ station.

* A Potters-type routine for the solution of the banded matrix which arises when the equations are finite differenced was kindly supplied by W. B. Stephens.

As discussed in [27], the boundary conditions at the pole are $Q_1 = u = \phi_1 = 0$ and these same conditions hold at the equator if the deformation is symmetric with respect to the equator.

At any stage in the loading history, instantaneous bending and stretching stiffnesses (29) are calculated by integrating the 'local' moduli $\hat{L}_{\alpha\beta\gamma\mu}$ through the shell thickness. This can be accomplished in a number of ways. Here, the distance through the thickness is divided into M equal intervals and the local moduli are taken to be constant within each interval. As the deformation proceeds the stresses and $(J_2)_{\max}$ are calculated (and stored) at the midpoint of each of these intervals using (25), (27), (30) or (32). In this way, the $\hat{L}_{\alpha\beta\gamma\mu}$ are known in the M intervals through the thickness. So, for example,

$$H_{\alpha\beta\gamma\mu}^{(3)} = \sum_{j=1}^M \frac{t}{M} [z_j^2 + \frac{1}{12}(\frac{t}{M})^2] \hat{L}_{\alpha\beta\gamma\mu}^{(j)} \quad (36)$$

where z_j is the midpoint of the j^{th} interval.

To evaluate (36) at a particular stage of the deformation history it is necessary to anticipate whether the elastic branch or the plastic branch of each $\hat{L}_{\alpha\beta\gamma\mu}^{(i)}$ will be active. Of course, if $J_2 < (J_2)_{\max}$ the elastic branch is active; but if $J_2 = (J_2)_{\max}$, the actual branch depends on the stress rates from the solution to (35). A correct solution for any increment of the deformation history requires an iterative procedure to finally obtain the branches which are everywhere consistent with the sign of \dot{J}_2 which does occur. If the history is sufficiently smooth so that the transition from loading to unloading, or vice versa, at any point of the shell occurs only once or twice, a more straightforward approach is possible which eliminates the iterations at each step. If $J_2 = (J_2)_{\max}$ at any stage of the history, then the plastic branch is taken to be active. If \dot{J}_2 turns out to be negative, elastic unloading will occur in the next increment of the history. This procedure will only be accurate if the incremental steps making up an entire history are very small; but anyway, this is consistent with the necessity of taking small increments to approximate nonlinear behavior by a series of piecewise linear steps. The simpler procedure was used in calculating the results reported here. An indication of the accuracy of the method and the number of stations required, both through the thickness and along the longitude, is discussed in conjunction with the numerical results.

Numerical results

A Ramberg-Osgood-type relation between the tensile stress and strain is used in the examples studied. The form used here is

$$\frac{\epsilon}{\epsilon_y} = \frac{\sigma}{\sigma_y} + \alpha \left(\frac{\sigma}{\sigma_y} \right)^n \quad (37)$$

where σ_y will be referred to as the yield stress in tension and the 'yield strain' is defined as $\epsilon_y = \sigma_y/E$. Note that if $\sigma = \sigma_y$, then $\epsilon = (1+\alpha)\epsilon_y$ so that σ_y is only a reasonable measure of the yield stress if α is small. The tensile curve for $\alpha = 0.1$ and a fairly high hardening rate, $n = 6$, is plotted in Fig. 5 together with the predictions for the critical bifurcation stress, $\sigma_C = -p_C R/(2t)$, as predicted by (21) for J_2 flow theory and (23) for J_2 deformation theory. The ordinate for the bifurcation results (dashed curves) is σ_C/σ_y while the abscissa is $[3(1-\nu^2)]^{-1/2} t/(\epsilon_y R)$ and with this choice the bifurcation curves fall on the stress-strain curve in the elastic (linear) range. As is typical for plates and shells, the deformation theory predictions fall below those of flow theory.

The example chosen to illustrate the axisymmetric postbuckling behavior is a shell made of material with the stress-strain curve of Fig. 5 and characterized by the additional parameters:

$$[3(1-\nu^2)]^{-1/2} \frac{t}{\epsilon_y R} = 3, \quad \frac{R}{t} = 64.5, \quad \epsilon_y = 0.00318 \quad \text{and} \quad \nu = \frac{1}{3} \quad (38)$$

The ratio of the bifurcation pressure to the elastic critical pressure for a shell of the same thickness to radius ratio is 0.492 according to the flow theory formula (21) and 0.455 from the deformation theory result (23). In each case the axisymmetric bifurcation mode is a Legendre polynomial of degree 14.

An imperfection in the form of an axisymmetric initial deflection of the middle surface \bar{w} is taken proportional to the bifurcation mode of the perfect sphere so that

$$\bar{w} = -\bar{\delta} P_{14}(\cos \theta) \quad (39)$$

where $\bar{\delta}$ represents the amplitude of the inward initial deflection at the pole of the sphere. Plots of pressure vs. the buckling deflection at the pole are shown in Fig. 6 for various imperfection amplitudes according to the predictions of J_2

flow theory. In this plot, the pressure is normalized by the bifurcation pressure p_C of the perfect shell (21), and ΔW_{pole} is defined to be the difference between the actual deflection at the pole and the deflection of a perfect sphere in the unbifurcated state at the same pressure.

The curve labeled 'perfect shell' is really the result of a calculation using an extremely small imperfection, $\bar{\delta} = 10^{-5} t$. The maximum support load is only very slightly above the bifurcation value (21) and it occurs at a buckling deflection of almost one tenth of a thickness as indicated by a cross on the curve. Sketched in Fig. 6 is the lowest possible initial slope of this curve which is consistent with the condition no unloading at bifurcation as predicted by (19). This initial slope for the perfect sphere is rather large; obviously, it can only be a good approximation to the slope in an exceedingly small neighborhood of the bifurcation point. For all practical purposes the maximum support load of the perfect shell,

just as in the case of the simple model, is the lowest bifurcation pressure.

Elastic and plastic regions of the shell at two stages of the loading history are given in Fig. 7 along with the middle surface deflection at the corresponding stages for the 'perfect' shell just discussed. Prior to the point at which the maximum pressure is attained the elastic zones have grown from nothing (before bifurcation) to the shapes shown at the top of the figure. Once the pressure starts to fall all of the shell but the region near the pole unloads. As shown at the bottom of Fig. 7 the region near the pole dimples inward and continues to deform plastically.

The character of the load-deflection curves for the imperfect spheres in Fig. 6, including the location of the maximum points, is very similar to the analogous curves for the simple model. A plot of the maximum support pressure normalized by p_0^{\max} , the maximum support pressure of the 'perfect' shell, as a function of the imperfection amplitude normalized by the shell thickness is given in Fig. 8. The effect of small axisymmetric imperfections on buckling in the plastic range is comparable to their effect in elastic buckling [16, 20-22].

Results based on J_2 deformation theory are also included in Fig. 8, except now p_0^{\max} is still normalized by the maximum support pressure of the perfect shell as predicted by J_2 flow theory. As discussed above, deformation theory predictions for the perfect shell fall about seven percent below those of flow theory. However, once the imperfection amplitude becomes about one tenth of a shell thickness there is virtually no difference in the buckling pressure predictions. A similar observation was made by Onat and Drucker [28] with respect to the buckling of a cruciform column in compression where the disparity between the bifurcation results of the two plasticity theories was much greater.

The curve of buckling pressure as a function of the imperfection amplitude does not level out at a pressure corresponding to the effective yield pressure of the perfect sphere in the way that the simple model does as discussed in conjunction with Fig. 3. Of course, the shell material in this example has a high hardening rate with a very smooth transition from the elastic to the plastic regime. Instead, the buckling pressure falls steadily with increasing imperfection amplitude and at a value of $\bar{\delta}/t = 0.4$ the buckling load has been reduced by a factor of two.

Some indication of the extent to which the computed buckling pressures are sensitive to the discretization parameters is shown in the following table. There, N is the number of finite difference stations from the pole to the equator, M is the number of intervals through the thickness as in (36), I is the number of linear steps in the computation history taken to reach the maximum pressure and the fourth column is the ratio of the computed maximum pressure to the elastic buckling load (14). The numerical values are for the shell of (38) and Fig. 6 with J_2 flow theory and with $\bar{\delta} \approx 0.15t$. Most of the graphical results were calculated with $N = 50$, $M = 10$ and I between 25 and 30.

TABLE

N	M	I	$p^{\max}/p_c^{\text{elastic}}$
30	6	17	0.338
30	10	17	0.337
50	10	21	0.333
50	10	27	0.331
90	14	27	0.328

We have chosen our second example to illustrate buckling behavior under circumstances in which buckling takes place just outside the elastic range. In practice this might be expected to happen when a structure is inadvertently overloaded or when the yield stress is overestimated. We will also investigate another imperfection shape, the flat spot considered by Budiansky [29] and Koga and Hoff [22]. In this case a flat spot of radius \bar{r} and maximum inward deflection $\bar{\delta}$ is located at each pole. The imperfection shape is given by (at the upper pole)

$$\bar{w} = -\bar{\delta}\{1 - 3(\frac{\theta}{\gamma})^2[1 - (\frac{\theta}{\gamma})^2 + \frac{1}{3}(\frac{\theta}{\gamma})^4]\} \quad , \quad |\theta| < \gamma$$

$$= 0 \quad , \quad |\theta| > \gamma$$
(40)

where $\sin \gamma = \bar{r}/R$. With this choice the slope and the radii of curvatures of the imperfect shell vary continuously across $\theta = \gamma$. A convenient measure of the width of the imperfection is

$$\bar{\lambda} = [12(1-\nu^2)]^{\frac{1}{4}} \frac{\bar{r}}{\sqrt{Rt}}$$
(41)

For elastic buckling, Koga and Hoff [22] found that the critical value of $\bar{\lambda}$ for a given imperfection amplitude was about 4.

In our study, J_2 flow theory is used with the stress-strain relation (37) with $\alpha = 0.1$ and $n = 12$ together with the following shell parameters

$$[3(1-\nu^2)]^{-\frac{1}{2}} \frac{t}{\epsilon_y R} = 1.2 \quad , \quad \frac{R}{t} = 64.5 \quad , \quad \epsilon_y = 0.00793 \quad , \quad \bar{\lambda} = 4 \quad \text{and} \quad \nu = \frac{1}{3}$$
(42)

For this choice the bifurcation pressure of the perfect shell (21) occurs at 80% of the elastic critical pressure (14). As before, the maximum support pressure

of the 'perfect' sphere ($\bar{\delta} = 10^{-5}t$) is only very slightly above the bifurcation value p_c . A plot of maximum pressure as a function of the imperfection amplitude is shown in Fig. 9. The results are not unlike those of Fig. 8 for the other imperfection shape (39) except that for very small imperfection amplitudes the bifurcation mode imperfection (39) causes larger relative reductions.

Included in Fig. 9 is a plot of the elastic buckling pressure (i.e., calculated with $\alpha = 0$) in the presence of the same flat spot imperfections. This curve is virtually identical to one given by Koga and Hoff [22] which was obtained by a rather different method of computation for a flat spot at only one pole. Once the buckling pressure has been reduced by about 30%, the discrepancy between the elastic predictions and those which account for plastic deformation is very small. Analogous to the behavior observed with respect to the simple model, the imperfection reduces the buckling pressure to the point where plastic deformation plays a less important role in the buckling process.

5. CONCLUDING REMARKS

If it is possible to generalize from the two examples investigated here, it would appear that imperfection-sensitivity is potentially as much of a problem for buckling in the plastic range as it is in elastic buckling. In practice, however, it is not likely to cause the large reductions in buckling loads that have to be lived with in some elastic shell structures. This is because, for shell structures made of engineering materials for example, plastic buckling usually requires relatively high thickness to radius ratios and in such circumstances the problem of manufacturing 'reasonably perfect' shells is much less difficult than when the thickness to radius ratio is very low.

Although there are some similarities between the analytic features of bifurcation and buckling in the plastic range and the initial postbuckling behavior of elastic structures, plastic buckling has some distinct characteristics which make an analytic treatment of imperfection-sensitivity very difficult. Not the least of these is the fact that the maximum support load of the perfect structure is not the bifurcation load.

Finally, we mention that we have purposely included predictions based on both of the two popular phenomenological theories of plasticity to emphasize that, for the examples studied here, the predictions are qualitatively the same and our conclusions are not subject to the controversy concerning the use of one of these theories rather than the other.

of the 'perfect' sphere ($\bar{\delta} = 10^{-5}t$) is only very slightly above the bifurcation value p_C . A plot of maximum pressure as a function of the imperfection amplitude is shown in Fig. 9. The results are not unlike those of Fig. 8 for the other imperfection shape (39) except that for very small imperfection amplitudes the bifurcation mode imperfection (39) causes larger relative reductions.

Included in Fig. 9 is a plot of the elastic buckling pressure (i.e., calculated with $\alpha = 0$) in the presence of the same flat spot imperfections. This curve is virtually identical to one given by Koga and Hoff [22] which was obtained by a rather different method of computation for a flat spot at only one pole. Once the buckling pressure has been reduced by about 30%, the discrepancy between the elastic predictions and those which account for plastic deformation is very small. Analogous to the behavior observed with respect to the simple model, the imperfection reduces the buckling pressure to the point where plastic deformation plays a less important role in the buckling process.

5. CONCLUDING REMARKS

If it is possible to generalize from the two examples investigated here, it would appear that imperfection-sensitivity is potentially as much of a problem for buckling in the plastic range as it is in elastic buckling. In practice, however, it is not likely to cause the large reductions in buckling loads that have to be lived with in some elastic shell structures. This is because, for shell structures made of engineering materials for example, plastic buckling usually requires relatively high thickness to radius ratios and in such circumstances the problem of manufacturing 'reasonably perfect' shells is much less difficult than when the thickness to radius ratio is very low.

Although there are some similarities between the analytic features of bifurcation and buckling in the plastic range and the initial postbuckling behavior of elastic structures, plastic buckling has some distinct characteristics which make an analytic treatment of imperfection-sensitivity very difficult. Not the least of these is the fact that the maximum support load of the perfect structure is not the bifurcation load.

Finally, we mention that we have purposely included predictions based on both of the two popular phenomenological theories of plasticity to emphasize that, for the examples studied here, the predictions are qualitatively the same and our conclusions are not subject to the controversy concerning the use of one of these theories rather than the other.

REFERENCES

1. Shanley, F. R., "Inelastic Column Theory", J. Aero. Sci., 14, 261-267, 1947.
2. Duberg, J. E. and Wilder, T. W., "Inelastic Column Behavior", NACA Report 1072, 1952.
3. Pearson, C. E., "Bifurcation Criterion and Plastic Buckling of Plates and Columns", J. Aero. Sci., 417-424, 1950.
4. Hill, R. and Sewell, M. J., "A General Theory of Inelastic Column Failure", J. Mech. Phys. Solids, 8, 105-118, 1960 and, 10, 285-300, 1962.
5. Hill, R., "A General Theory of Uniqueness and Stability in Elastic-Plastic Solids", J. Mech. Phys. Solids, 6, 236-249, 1958.
6. Hill, R., "Some Basic Principles in the Mechanics of Solids Without a Natural Time", J. Mech. Phys. Solids, 7, 209-225, 1959.
7. Koiter, W. T., "Over de Stabiliteit van het Elastisch Evenwicht" ("On the Stability of Elastic Equilibrium"), Thesis, Delft, H. J. Paris, Amsterdam, 1945. English translation issued as NASA TT F-10, 833, 1967.
8. Koiter, W. T., "Elastic Stability and Post-Buckling Behavior", Proc. Symp. Nonlinear Problems, 257-275, Univ. of Wisconsin Press, Madison, 1963.
9. Thompson, J. M. T., "A General Theory for the Equilibrium and Stability of Discrete Conservative Systems", Zeit. für Math. und Phys., 20, 797-846, 1969.
10. Kármán, Th. von, Dunn, L. G. and Tsien, H. S., "The Influence of Curvature on the Buckling Characteristics of Structures", J. Aero. Sci., 7, 276, 1940.
11. Sewell, M. J., "The Static Perturbation Technique in Buckling Problems", J. Mech. Phys. Solids, 13, 247-265, 1965.
12. Augusti, G., "Buckling of Inelastic Arches: A Simple Model", Meccanica, 2, 102-105, 1968.
13. Budiansky, B. and Hutchinson, J. W., "Dynamic Buckling of Imperfection-Sensitive Structures", Proc. XI Internat. Congr. Appl. Mech., Munich, 636-651, Julius Springer-Verlag, Berlin, 1964.
14. Mayers, J. and Wesenberg, D. L., "The Maximum Strength of Initially Imperfect Axially Compressed, Circular Cylindrical Shells", Report, Dept. of Aero. and Astro., Stanford Univ., August 1969.
15. Neut, A. van der, "De Elastische Stabiliteit van den Dunwandigen Bol" ("The Elastic Stability of the Spherical Shell"), Thesis, Delft, H. J. Paris, Amsterdam, 1932.
16. Koiter, W. T., "The Nonlinear Buckling Problem of a Complete Spherical Shell Under Uniform External Pressure", I, II, III and IV, Proc. Kon. Ned. Ak. Wet., B72, 40-123, 1969.

17. Bijlaard, P. P., "Theory and Tests on the Plastic Stability of Plates and Shells", J. Aero. Sci., 16, 529-541, 1949.
18. Batterman, S. C., "Plastic Stability of Spherical Shells", ASCE, J. Eng. Mech., EM2, 433-446, 1969.
19. Batterman, S. C., "Load-Deformation Behavior of Shells of Revolution", ASCE, J. Eng. Mech., EM6, 1-19, 1964.
20. Bushnell, D., "Nonlinear Axisymmetric Behavior of Shells of Revolution", AIAA J., 5, 432-439, 1967.
21. Thurston, G. A. and Penning, F. A., "Effect of Axisymmetric Imperfections on the Buckling of Spherical Caps under Uniform Pressure", AIAA J., 4, 319-327, 1966.
22. Koga, T. and Hoff, N. J., "The Axisymmetric Snap-Through Buckling of Thin-Walled Spherical Shells", Int. J. Solids Struct., 5, 679, 1969.
23. Reissner, E., "On Axisymmetrical Deformations of Thin Shells of Revolution", Proc. of Symp. in Appl. Math., 3, 27-52, McGraw-Hill, 1950.
24. Kalnins, A., "Analysis of Shells of Revolution Subject to Symmetrical and Nonsymmetrical Loads", J. Appl. Mech., 33, 467-476, 1964.
25. Stephens, W. B. and Fulton, R. E., "Axisymmetric Static and Dynamic Buckling of Spherical Caps Due to Centrally Distributed Pressures", AIAA J., 7, 2120-2126, 1969.
26. Greenbaum, G. A. and Conroy, D. C., "Postwrinkling Behavior of a Conical Shell of Revolution Subject to Bending Loads", AIAA J., 8, 700-707, 1970.
27. Stephens, W. B., "Computer Program for Static and Dynamic Analysis of Symmetrically Loaded Orthotropic Shells of Revolution", to be published as NASA TN.
28. Onat, E. T. and Drucker, D. C., "Inelastic Instability and Incremental Theories of Plasticity", J. Aero. Sci., 20, 181-186, 1953.
29. Budiansky, B., "Buckling of Clamped Shallow Spherical Shells", Proc. Symp. Theory of Thin Elastic Shells, Delft, 64-94, North Holland Publishing Company, Amsterdam, 1960.

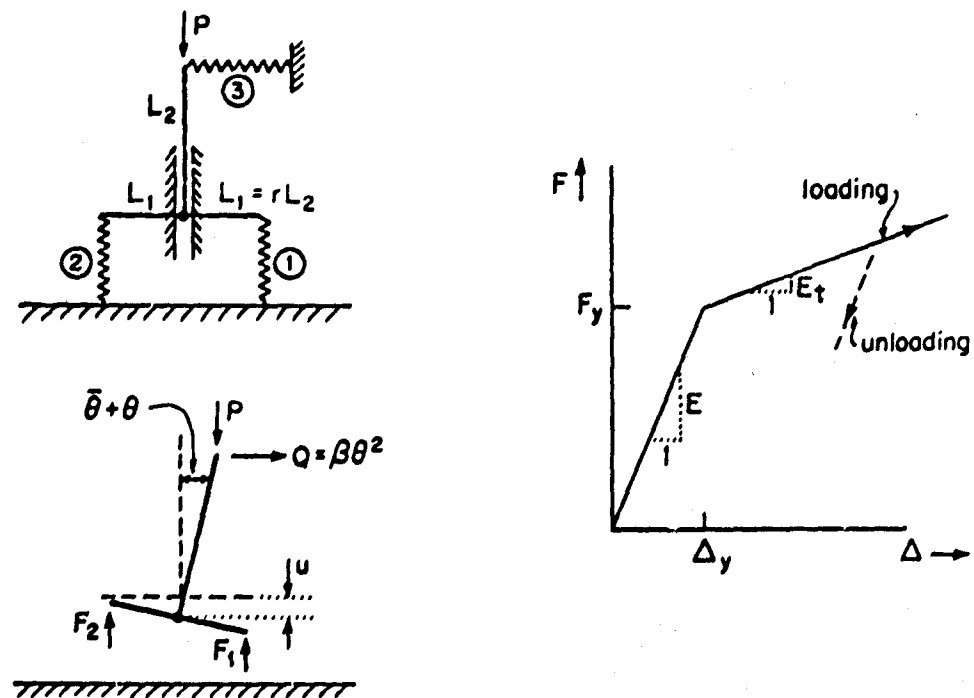


FIG. 1 SIMPLE MODEL AND LOAD-DEFLECTION RELATION FOR SPRINGS #1 AND #2

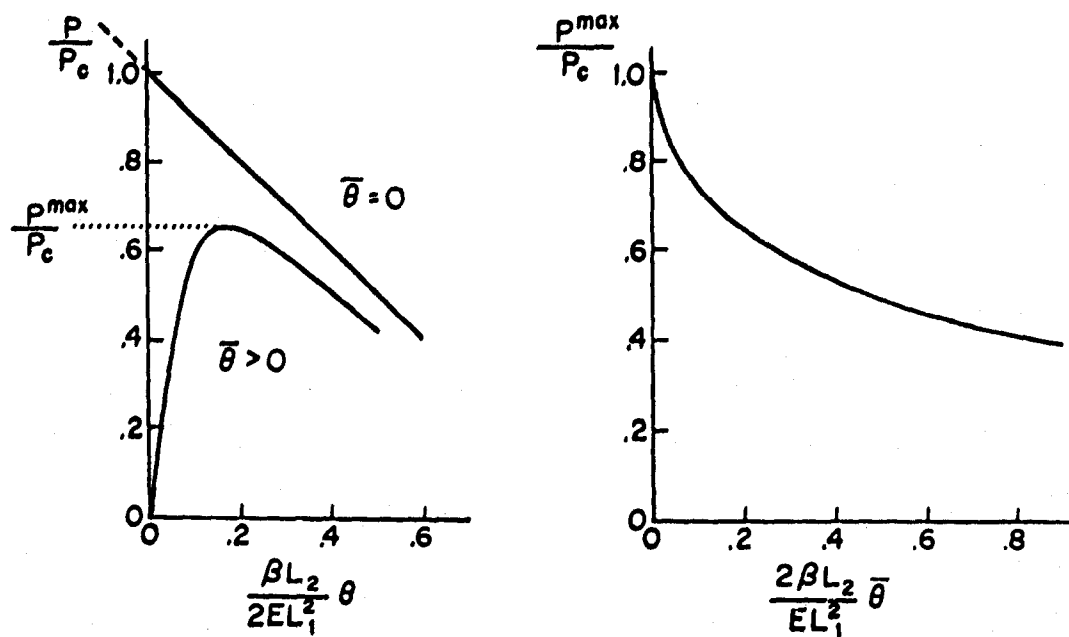


FIG. 2 BUCKLING BEHAVIOR OF MODEL IN THE ELASTIC RANGE

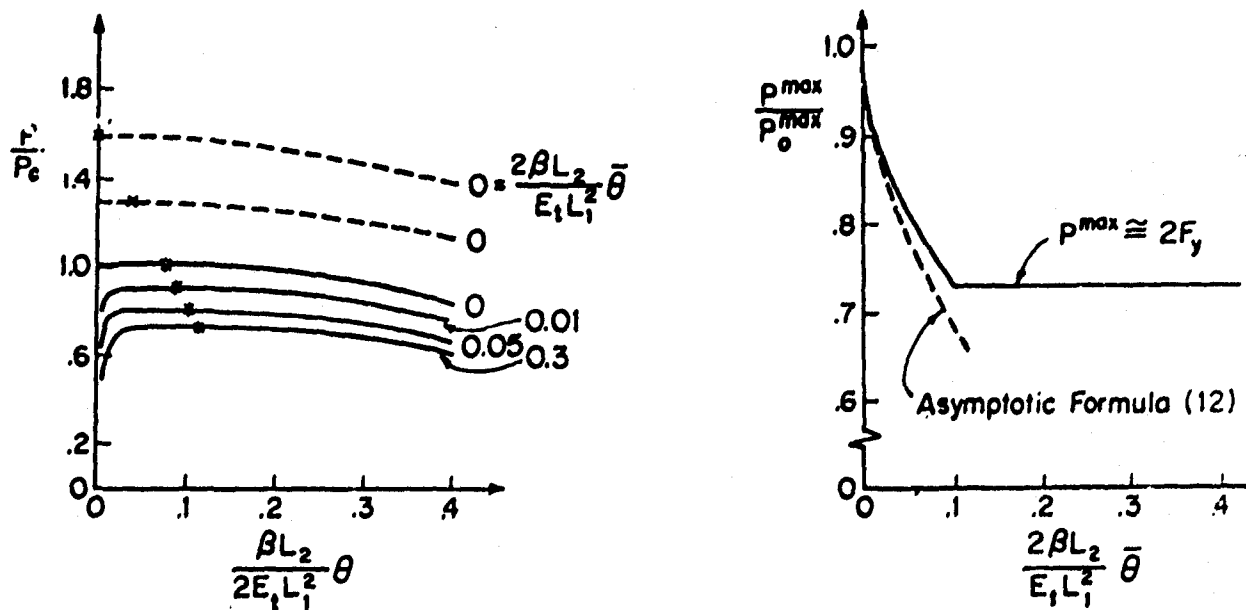


FIG. 3 BUCKLING BEHAVIOR OF MODEL IN THE PLASTIC RANGE WITH $E_1/E = 0.25$, $\delta/(E_1 L_1^2) = 10$ AND $\delta_1 L_2/L_1^2 = 0.16$ ($\bar{\theta}$ DENOTES MAX. LOAD, $P_c = 2E_1 \gamma L_1$ AND P_0^{max} IS THE MAX. SUPPORT LOAD FOR $\bar{\theta} = 0$)

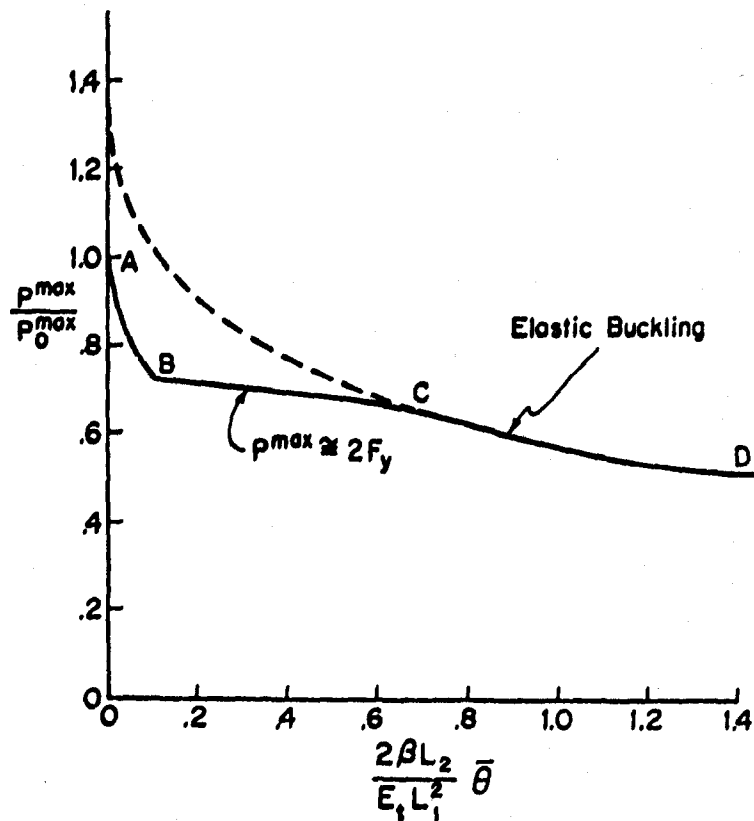


FIG. 4 BUCKLING OF MODEL FOR A CASE IN WHICH THE PLASTIC BUCKLING LOAD OF THE PERFECT MODEL IS ONLY SLIGHTLY BELOW THE ELASTIC BUCKLING LOAD ($E_1/E = 0.75$, $\delta/(E_1 L_1^2) = 10$ AND $\delta_1 L_2/L_1^2 = 0.325$)

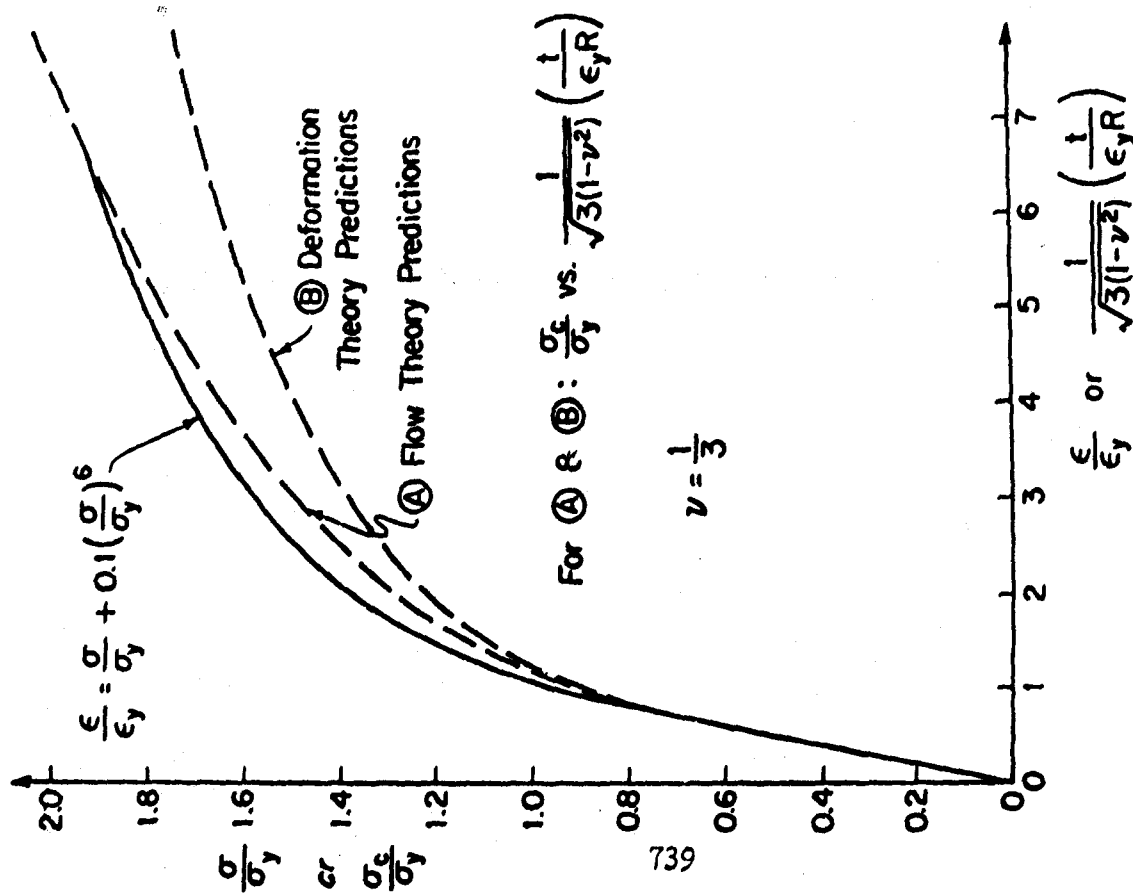


FIG. 3 TENSILE STRESS-STRAIN CURVE AND BIFURCATION STRESSES FOR A PERFECT SPHERICAL SHELL UNDER EXTERNAL PRESSURE

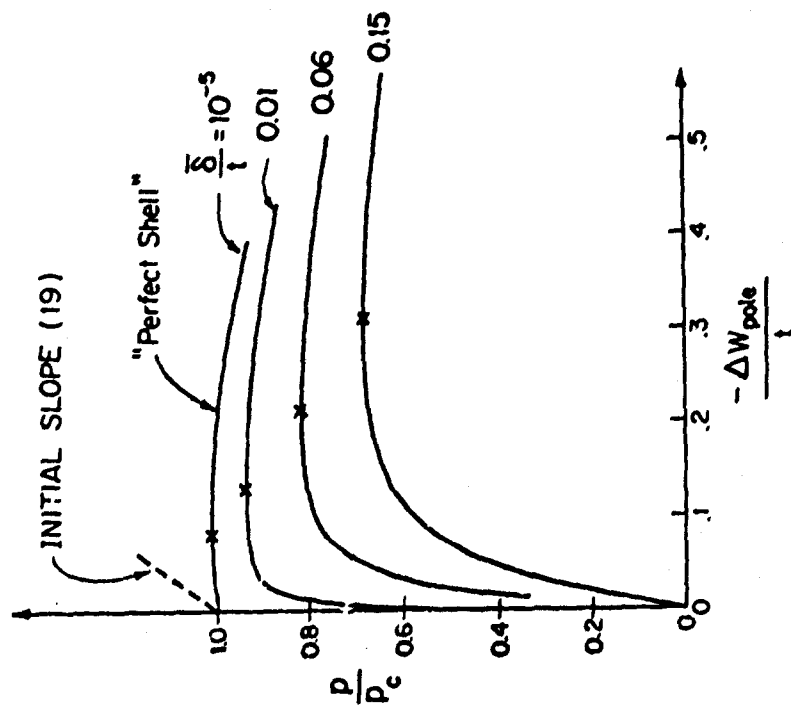


FIG. 6 CURVES OF PRESSURE VS. POLE BUCKLING DEFLECTION FOR 'PERFECT' AND IMPERFECT SPHERICAL SHELLS (SHELL PARAMETERS ARE GIVEN IN THE BODY OF THE PAPER)

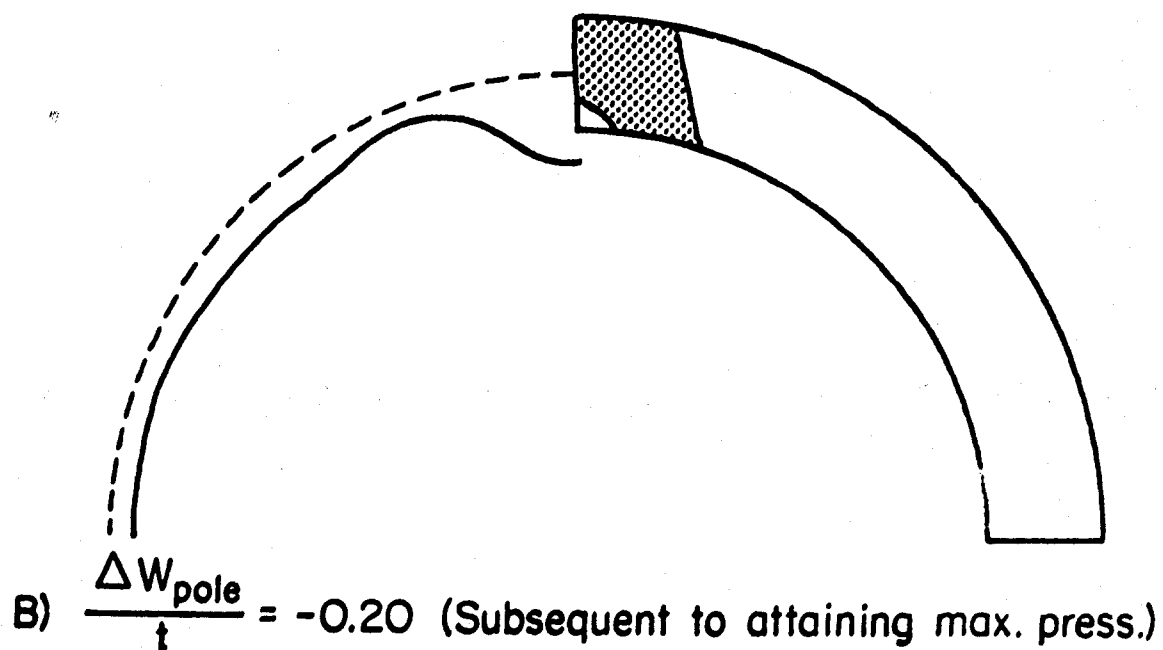
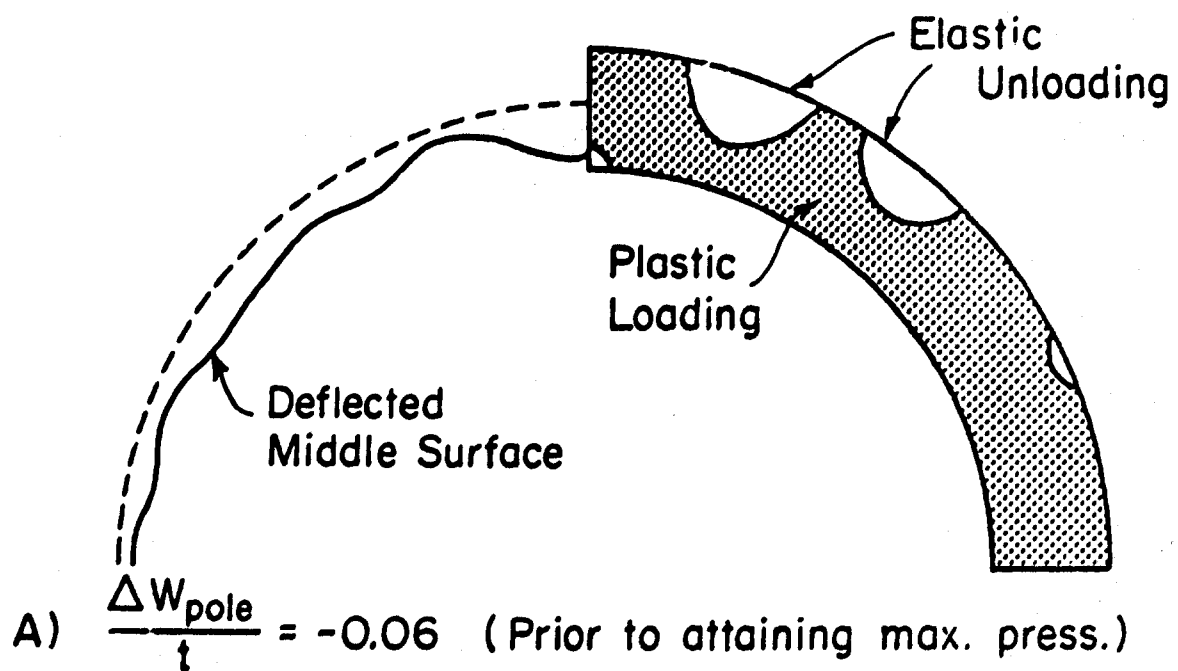


FIG. 7 CURRENT ELASTIC AND PLASTIC REGIONS FOR THE 'PERFECT' SPHERICAL SHELL OF FIG. 6 AT TWO POINTS OF THE DEFORMATION HISTORY (EXAGGERATED SHELL THICKNESS AND DEFLECTION)

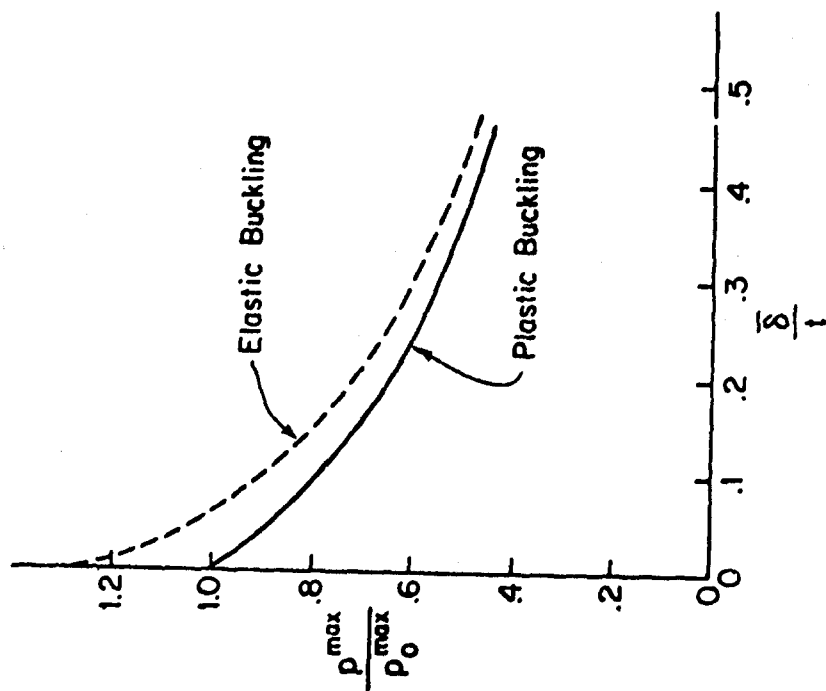


FIG. 9 BUCKLING PRESSURES FOR SPHERICAL SHELLS WITH FLAT SPOT IMPERFECTIONS. FOR BOTH CURVES, p_0^{\max} IS THE MAXIMUM SUPPORT PRESSURE OF THE 'PERFECT' SHELL AS PREDICTED BY J_2 FLOW THEORY (SHELL PARAMETERS ARE GIVEN IN THE BODY OF THE PAPER)

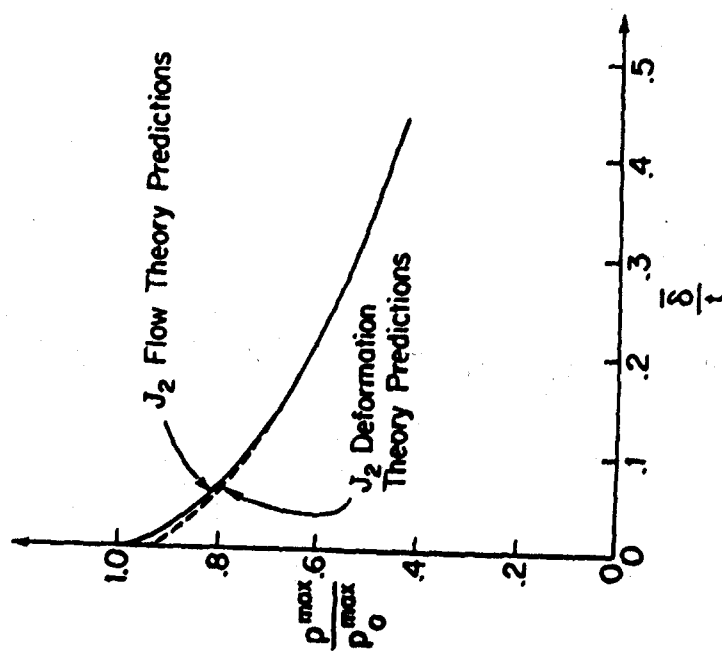


FIG. 8 BUCKLING PRESSURES FOR IMPERFECT SPHERICAL SHELLS. FOR BOTH CURVES p_0^{\max} IS THE MAXIMUM SUPPORT PRESSURE OF THE 'PERFECT' SHELL AS PREDICTED BY THE J_2 FLOW THEORY CALCULATION (SHELL PARAMETERS ARE GIVEN IN THE BODY OF THE PAPER)

QUESTIONS AND COMMENTS FOLLOWING HUTCHINSON'S PAPER

QUESTION: Did I understand you to say that as the imperfection increases the difference between plastic buckling and elastic buckling disappears.

HUTCHINSON: I didn't mean that as a general rule. In the model case it did disappear and in the one example I looked at, namely the last one, it didn't disappear but it diminished. There are further remarks concerning this on pages 5 and 15 of my paper.

QUESTION: In practical cases (R/t 600-1000) we do have imperfections. As you said, the plastic buckling analysis is much more complicated than elastic analysis. Would it be reasonable to make a design estimate that elastic buckling analysis gives a good approximation to the behavior of this shell or do we have to have a plastic buckling analysis?

HUTCHINSON: That's a very tough question. For fairly imperfect shells, it might be reasonable although there is not much experience that I know of to back it up. In my paper I refer to recent work on this question by Mayers; you might take a look at that.

QUESTION: That was a very interesting lecture indeed on the effect of plastic analysis and buckling. When I look at the curves, I note that Koiter's theory predicts that the slope of the imperfection curves becomes infinite. Doesn't that happen in a plastic analysis?

HUTCHINSON: I don't know. For the two degree of freedom model, it is, but for a "continuum" structure my guess is that it will be quite finite.

As far as I can see, it's going to be very difficult and perhaps impossible to do the asymptotic work to determine analytically the behavior on the part of the curve you're talking about.

COMMENT: I would like to comment on a couple of things. First, you use the name bifurcation buckling for the flow theory and in my opinion this is a misnomer because if you have a flow theory you have a path dependent relation between deformation and stress. Bifurcation implies an intersection between a fundamental branch and a branch for buckle equilibrium. A branch for buckle equilibrium cannot be defined unless you have defined the path γ which you get there; so it doesn't exist. Nevertheless, you can use bifurcation theory as was used with a flow theory, but you don't really have a bifurcation point there. It's not really defined and I think that would relate to the difficulties involved if one wanted to apply a Koiter theory.

HUTCHINSON: Well, there is a genuine bifurcation at that point. I hope I didn't use the word bifurcation buckling in the plastic range, because it is not the buckling load. I wanted to emphasize that bifurcation takes place there, then after further deformation takes place, the maximum load occurs; that is what we would call the buckling load.

COMMENT: I would like to say that you would find the bifurcation point if you analyze a shell with an imperfection and make the imperfection smaller and smaller. In your case you can actually analyze with zero imperfection, but if you have a numerical analysis you get closer and closer to something which is a bifurcation point and this may and may not be the same as the presently applied flow theory bifurcation buckling gives.

The next comment concerns the curve you show that indicates when the imperfection becomes bigger and bigger the discrepancy between flow theory and deformation theory almost disappears. This is what you might expect since, because the bigger the imperfections you have, the smoother the curve in the stress plane; and we know that if we have a smooth curve in the stress plane, then we won't get any difference between the two theories.

COMMENT: I'm not quite clear here whether you're saying that there is a question between the flow and deformation theories or in the numerical procedures associated with each.

HUTCHINSON: It has nothing to do with numerical methods. In fact, in my analysis, I treated deformation theory as a rate theory. It wasn't necessary but I did it anyway, so both theories are treated identically. The difference really is in the theories themselves. Simple flow theory is idealized in the sense that it in no way accounts for corners (or regions of high curvature) on the yield surface whereas deformation theory, in a very approximate way, does incorporate a corner or an effective corner and this is where the difference lies.

QUESTION: Yes, I know, but why the suspicion on analysis with the flow theory?

HUTCHINSON: I'm not suspicious of the buckling analysis. I'm suspicious of comparing the analysis with experiments. The experience of the 1950's, and there's a lot of it, was that the agreement between experiment and deformation theory was in general quite good, but flow theory gave con-

sistently high predictions.

COMMENT: I think that it depends upon the type of experiment and how the data is collected and how the comparison is made when you're talking about whether the theory fits comparatively well. I would like to see plots of distributions across surfaces of shells to decide whether the method was adequate or not. What I have seen in the literature is that one point is picked and followed through time as it goes from the elastic to plastic regime and this is compared to an experimental point. I really don't think this can be used as verification for theory without taking many points and many positions on the model.

SOLUTION OF STRUCTURAL EIGENVALUE
PROBLEMS USING SPARSELY POPULATED MATRICES

Hussein A. Kamel* and Russell L. Lambert†
University of Arizona, Tucson, Arizona

ABSTRACT

Eigenvalue problems in the area of structural analysis occur in structural vibrations and elastic instability problems. Computer methods so far have involved a decomposition or an inversion of the basic matrices. With systems involving a large number of freedoms these procedures are lengthy and alternatives must be sought. This is particularly so for three-dimensional problems which exhibit a large band width. The paper describes methods for dealing with structural vibrations, both lumped and kinematically consistent mass matrix approaches, as well as the problem of critical buckling using the finite element method. All pertinent matrices are stored in a sparsely populated form. The procedures described do not necessitate an inversion or decomposition of any of the matrices utilized. Preliminary investigations involving over 350 degrees of freedom systems show favorable behavior.

* Professor of Aerospace and Mechanical Engineering, Aerospace and Mechanical Engineering Department.

† Graduate Assistant, Department of Aerospace and Mechanical Engineering; presently employed by LOCKHEED MISSILES & SPACE COMPANY, Sunnyvale, California.

ACKNOWLEDGMENTS

This research was supported by LOCKHEED MISSILES AND SPACE COMPANY and the UNIVERSITY OF ARIZONA Engineering Experiment Station and Computer Center. The authors are in particular grateful to Mr. Derek N. Yates of LMSC for his continuous encouragement. Mr. Gary Adkins contributed to the examples shown. The authors are grateful to Miss Diana McLane for typing the manuscript and to Mr. George Taylor for preparing the drawings.

NOMENCLATURE

$\underline{\underline{A}}_{(m \times n)}$ = $[A_{ij}]$, is a rectangular matrix with m rows and n columns.

$A_{i,j}$ = element of matrix \underline{A} in the i^{th} row and j^{th} column.

$\underline{\underline{d}}_{(n \times n)}$ = $[\underline{d}_1, \underline{d}_2, \dots, \underline{d}_n]$ is an $(n \times n)$ diagonal matrix.

\underline{d}_i = i^{th} diagonal element of \underline{d} .

\underline{A}^t = transpose of matrix \underline{A} .

\underline{B}^{-1} = inverse of matrix \underline{B} .

\underline{I} = a unit matrix.

\underline{O} = a zero matrix.

\underline{B}^n = n^{th} power of matrix \underline{B} .

\underline{K} = stiffness matrix for structure.

\underline{K}_E = Elastic stiffness matrix of a structure.

\underline{K}_G = Geometric stiffness matrix of a structure.

\underline{r} = Displacement vector of a structure.

\underline{R} = Load vector of a structure.

\underline{M} = Mass matrix of a structure.

I. INTRODUCTION

The problem of structural vibrations can be formulated using either the force or the displacement methods.¹ Of the two approaches, the displacement method has become increasingly the more popular due to its generality, simplicity of approach, and therefore its great programmability on an electronic digital computer. This paper will, therefore, be confined to the displacement method formulation.

A finite element model with n degrees of freedom will yield n eigenvalues representing the natural frequencies of the system and n corresponding eigenvectors giving the vibrational modes. In the case of free free body vibrations some of the eigenvalues will be zero and the associated eigenvectors will represent rigid body movements.

Of all the vibrational modes, only those corresponding to the lowest frequencies are of interest; the higher modes are inherently inaccurate due to their sensitivity to the modeling procedure. The power method² in conjunction with the displacement method yields the least important modes first. To overcome this difficulty one of three procedures is usually utilized. An inversion of the matrix of stiffness coefficients provides a formulation which will deliver the lowest eigenvalues first. This is time-consuming and becomes prohibitive with a large system. An improvement on this procedure is the inverse power method². It necessitates a decomposition of the stiffness matrix. The third procedure involves a condensation of the dynamic matrix³. It involves a solution of a large system of simultaneous equations. This paper describes first a technique which obtains the vibrational mode in the correct order without inversion, decomposition or solution of a matrix equation. The basic technique utilizes the power method together with a simple matrix origin-shift and is applicable to the finite element lumped mass approach. Due to the absence of a matrix inversion or decomposition the basic matrices may be stored

in a sparsely populated form. This results in great savings in computer storage and at the same time a speed up of the iteration cycle time. Since the power method is iterative, the method proves to be perfectly suitable for application of the power method using a computer. It is estimated that 1000 degrees of freedom problem can be handled in a 64 K core, and 2000 with a 131 K core.

The problem of elastic instability of structures consists of seeking critical load levels under which the structure becomes unstable⁴. Mathematically it is formulated in terms of two large sparsely populated matrices, one of which represents the structural stiffness matrix and the other includes the effect of deflections on geometry and therefore on the equations of equilibrium. The second matrix, often called the geometrical stiffness matrix, depends on the element stresses due to the loading in question.

The traditional procedure⁵ involves the solution for deflections and stresses within the model. Subsequently the geometrical stiffness matrix can be computed and it remains to find the lowest load level under which instability occurs together with the associated buckling mode. In order to find these results an eigenvalue problem has to be solved which involves inverting one of the matrices or using the results of previous decomposition prior to application of the inverse power method. In either case the storage requirement increases considerably.

In this paper, it is argued that for the critical load

level the combined stiffness matrix becomes singular. A method is developed by which the variation of the lowest eigenvalue of the combined stiffness matrix is observed as a function of the load level and, using the slope interval method, the value for which this root disappears is determined. Convergence to the desired mode is rapid.

The mathematical formulation of the kinematically consistent mass matrix approach⁶ to structural vibrations is identical to that of the buckling problem. It can be shown that the method suggested for the solution of the instability problem would also apply.

II. THE ORIGIN SHIFT TECHNIQUE

If a matrix \underline{A} , order $(n \times n)$ has the n eigenvalues

$$\lambda_1, \lambda_2, \dots, \lambda_1, \dots, \lambda_n$$

and the corresponding n column eigenvectors

$$\underline{v}_1, \underline{v}_2, \dots, \underline{v}_1, \dots, \underline{v}_n$$

then, by definition

$$\underline{A} \underline{v}_1 = \lambda_1 \underline{v}_1 \quad (1)$$

If we combine all eigenvalues λ_i into one diagonal matrix

$$\underline{\Lambda} = \begin{bmatrix} \lambda_1 & & & \\ & \lambda_2 & & \\ & & \ddots & \\ & & & \lambda_n \end{bmatrix}, \quad (2)$$

and the column eigenvectors into an $n \times n$ square matrix

$$\underline{V} = [\underline{v}_1 \quad \underline{v}_2 \quad \dots \quad \underline{v}_1 \quad \dots \quad \underline{v}_n] \quad (3)$$

we may rewrite Eq. (1) in a form that considers all eigenvalues and vectors simultaneously.

$$\underline{A} \underline{v} = \underline{v} \underline{A} \quad (4)$$

Note that the multiplication by \underline{A} is a post-multiplication since it represents operations on the columns of \underline{v} .

If we define the matrix \underline{B} as,

$$\underline{B} = \underline{A} - \alpha \underline{I}, \quad (5)$$

where α is an arbitrary constant and \underline{I} is an $(n \times n)$ unit matrix, then the eigenvalues and vectors of \underline{B} are given by,

$$(\lambda_1 - \alpha), (\lambda_2 - \alpha) \dots (\lambda_n - \alpha)$$

and

$$\underline{v}_1 \quad \underline{v}_2 \quad \dots \quad \underline{v}_n.$$

The eigenvectors are the same as those of \underline{A} and the eigenvalues are shifted by the value α . This process is called a shift of origin, since it represents a displacement of the datum associated with the eigenvalue spectrum, see Fig. 1.

A slightly different form of this procedure, which is going to be used throughout this paper is that of the matrix

$$\underline{C} = \alpha \underline{I} - \underline{A} \quad (6)$$

which has the eigenvalues

$$(\alpha - \lambda_1) \quad (\alpha - \lambda_2) \quad \dots \quad (\alpha - \lambda_n)$$

and the eigenvectors

$$\underline{v}_1 \quad \underline{v}_2 \quad \cdot \cdot \cdot \quad \underline{v}_n$$

This is identical to an origin shift followed by a reversal of a sign.

The shift of origin process is usually used to influence the convergence of the power method iterative procedure for obtaining eigenvalues and eigenvectors of a matrix. In this paper it will be used extensively to obtain simple and efficient methods of solution to basic eigenvalue problems in structural engineering.

III. THE POWER METHOD

1. Determination of the Highest Root and the Corresponding Vector.

To find the highest eigenvalue and the corresponding eigenvector of a matrix \underline{A} , an arbitrary vector, \underline{u} , is assumed at the start. Through successive pre-multiplication with the matrix \underline{A} , followed by normalization so that

$$\underline{u}^t \underline{u} = 1 \quad (7)$$

The vector finally converges to \underline{v}_1 , and the normalizing factor to λ_1 , where λ_1 is the largest eigenvalue of \underline{A} .

To prove this² let us express \underline{u} as a linear combination of \underline{v}_1 ---- \underline{v}_n .

$$\underline{u} = \sum_{i=1}^n a_i \underline{v}_i \quad (8)$$

After m multiplications with \underline{A} , using (1)

$$\begin{aligned}\underline{A}^m \underline{u} &= \sum_{i=1}^n a_i \underline{A}^m \underline{v}_i = \sum_{i=1}^n a_i \lambda_i^m \underline{v}_i \\ &= \sum_{i=1}^n a_i \left(\frac{\lambda_i}{\lambda_1} \right)^m \underline{v}_i.\end{aligned}\tag{9}$$

if λ_1 is the dominant eigenvalue, so that

$$\left| \frac{\lambda_i}{\lambda_1} \right| < 1,$$

the first term of the series will predominate as m tends to infinity. Since a computer has a limited word length, however, the convergence is accomplished with a finite number of iterations to a satisfactory degree of accuracy.

It is generally accepted that the speed of convergence depends on the ratios (λ_i/λ_1) .

2. Sweeping of Modes. (Deflation)

Once a root λ_1 and the corresponding vector \underline{v}_1 of a matrix \underline{A} have been obtained, it is possible to construct a matrix \underline{B} which has all eigenvalues and vectors of \underline{A} except λ_1 and \underline{v}_1 . This process is termed sweeping or deflation. \underline{B} is given by:

$$\underline{B} = \underline{A} - \lambda_1 \underline{v}_1 \underline{v}_1^t\tag{10}$$

where \underline{v}_1 is normalized according to Eq. (7).

proof:

$$\underline{B} \underline{v}_j = (\underline{A} \underline{v}_j - \lambda_1 \underline{v}_1 \underline{v}_1^t \underline{v}_j)$$

Case 1 $i = j$

$$\therefore \underline{v}_i^t \underline{v}_j = 1$$

and

$$\underline{B} \underline{v}_j = \lambda_i \underline{v}_i - \lambda_i \underline{v}_i = 0$$

Case 2 $i \neq j$

$$\underline{v}_i^t \underline{v}_j = 0$$

$$\underline{B} \underline{v}_j = \lambda_j \underline{v}_j$$

The procedure is also applied for sweeping more than one eigenvalue. If, for example, all eigenvalues $\lambda_1, \lambda_2, \dots, \lambda_i$ have been found, and the next largest, $\lambda(i+1)$, is desired, we construct the matrix

$$\underline{B} = \underline{A} - \sum_{j=1}^i \lambda_j \underline{v}_j \underline{v}_j^t \quad (11)$$

which has all eigenvalues and vectors of \underline{A} except for the subset corresponding to $\lambda_1, \dots, \lambda_i$.

The process of sweeping will be used repeatedly in this paper.

IV. APPLICATION OF THE POWER METHOD TO STRUCTURAL VIBRATIONS

The equation of vibration of a structure is given by:

$$(\underline{K} - \omega^2 \underline{M}) \underline{r} = \underline{0} \quad (12)$$

where

\underline{K} is the stiffness matrix of the structure, and

\underline{M} is its mass matrix.

ω is the equivalent angular velocity of vibration and \underline{r} is the corresponding vibration mode vector representing the displacement pattern.

It must be noted that the highest value for ω^2 is of least interest since it corresponds to the highest mode of vibration. Correspondingly, the lowest value of ω^2 is the most important.

There are basically two methods for converting Eq. (12) to a standard form that can be handled by an eigenvalue program. The first is obtained by premultiplying by \underline{M}^{-1} .

$$(\underline{M}^{-1} \underline{K} - \omega^2 \underline{I}) \underline{r} = 0 \quad (13)$$

This has an advantage if \underline{M} is diagonal, since the inversion procedure is trivial. The matrix $\underline{M}^{-1} \underline{K}$ retains the original bandedness of \underline{K} .

The disadvantage lies in convergence of the process to the highest ω^2 first.

The alternative form is the inverse of that in Eq. (13),

$$(\frac{1}{\omega^2} \underline{I} - \underline{K}^{-1} \underline{M}) \underline{r} = 0 \quad (14)$$

and has the advantage of convergence to the lowest, more interesting, modes first. On the other hand the inversion of \underline{K} is computationally forbidding. The matrix $\underline{K}^{-1} \underline{M}$ is fully populated, and requires a large storage capacity. Since the solution is an iterative one, the constant transfer from and to mass storage and the amount of computation necessary for each iteration slows the operation. The inverse power method² avoids forming an inverse but requires the decomposition of

the \underline{K} matrix, thus destroying its sparsely populated nature.

Most standard computer eigenvalue programs are more efficient in handling the special case of symmetric matrices. It is possible to reformulate Eq. (12) in order to achieve symmetry if \underline{M} is diagonal (lumped mass approach). Eq. (12) may be rewritten as

$$(\underline{K} - \omega^2 \underline{M}^{\frac{1}{2}} \underline{M}^{\frac{1}{2}}) \underline{r} = \underline{0}.$$

Pre-multiplying by $\underline{M}^{-\frac{1}{2}}$,

$$(\underline{M}^{-\frac{1}{2}} \underline{K} - \omega^2 \underline{M}^{\frac{1}{2}}) \underline{r} = \underline{0}.$$

Introducing a unit matrix to the right of \underline{K} ,

$$(\underline{M}^{-\frac{1}{2}} \underline{K} \underline{M}^{-\frac{1}{2}} \underline{M}^{\frac{1}{2}} - \omega^2 \underline{M}^{\frac{1}{2}}) \underline{r} = \underline{0}.$$

In other words

$$(\underline{M}^{-\frac{1}{2}} \underline{K} \underline{M}^{-\frac{1}{2}} - \omega^2 \underline{I}) \underline{M}^{\frac{1}{2}} \underline{r} = 0$$

which may be written as

$$(\underline{K}^* - \omega^2 \underline{I}) \underline{u} = 0 \quad (15)$$

where

$$\underline{K}^* = \underline{M}^{-\frac{1}{2}} \underline{K} \underline{M}^{-\frac{1}{2}} \quad (\text{Symmetric}) \quad (16)$$

and

$$\underline{u} = \underline{M}^{\frac{1}{2}} \underline{r} \quad (17)$$

Thus the problem is transformed to a symmetric form, simplifying the process of eigenvalue and vector determination.

V. ORIGIN SHIFT AND THE LUMPED MASS APPROACH

In this section a procedure is described by which the origin shift technique is applied to solve the structural

vibration problem using a lumped mass representation. We start with the symmetric dynamic matrix \underline{K}^* defined by Eq. (16).

$$\underline{K}^* = \underline{M}^{-\frac{1}{2}} \underline{K} \underline{M}^{-\frac{1}{2}}$$

Using the power method, the highest eigenvalue, ω_1^2 is obtained. It must be emphasized that we do NOT seek an exact value, but only the approximate position of this relatively uninteresting quantity to within, say, 3 decimal figures. Let the approximate value of this value be $\omega_1'^2$. Subsequently the matrix

$$\underline{K}^{**} = (\omega_1'^2 \underline{I} - \underline{K}^*) \quad (18)$$

is considered. Its eigenvalues will be given by

$$(\omega_1'^2 - \omega_1^2), (\omega_1'^2 - \omega_2^2), \dots, (\omega_1'^2 - \omega_n^2).$$

The largest eigenvalue is now $(\omega_1'^2 - \omega_n^2)$, which corresponds to the lowest frequency of vibration. The first value, $(\omega_1'^2 - \omega_1^2)$ is approximately equal to zero.

We denote a typical eigenvalue of \underline{K}^{**} by β_1 , where

$$\beta_1 = (\omega_1'^2 - \omega_{n-1+1}^2), \quad (19)$$

so that

$$\beta_1 > \beta_2 > \beta_3 \dots \beta_n. \quad (20)$$

The corresponding eigenvector is \underline{u}_1 , where

$$\underline{u}_1 = \underline{M}^{\frac{1}{2}} \underline{r}_{n-1+1} \quad (21)$$

To obtain the m eigenvalues $\omega_n^2, \dots, \omega_{n-m+1}^2$ corresponding to the lowest frequencies and the associated eigenvectors, we proceed by obtaining β_1, \underline{u}_1 , sweeping it to obtain β_2 and \underline{u}_2 , etc., until β_m and \underline{u}_m . In order to obtain β_1 and \underline{u}_1 we iterate

with the matrix

$$\begin{aligned}\underline{K}_1^{**} &= \underline{K}^{**} - \sum_{j=1}^{i-1} \beta_j \underline{u}_j \underline{u}_j^t \\ &= \omega_n'^2 \underline{I} - \underline{K}^* - \sum_{j=1}^{i-1} \beta_j \underline{u}_j \underline{u}_j^t\end{aligned}\quad (22)$$

in the standard power method fashion.

We observe, however, that \underline{K}_1^{**} is no longer a banded matrix as \underline{K}^{**} is. This will result in all the disadvantages associated with the form given by Eq. (14).

In order to retain the efficiency of the method, a close look at the matrix product $\underline{K}_1^{**} \underline{v}$, which represents the basic iterative step in the method, is necessary. If \underline{v} is an $(n \times 1)$ iterative vector, then

$$\begin{aligned}\underline{K}_1^{**} \underline{v} &= (\omega_n'^2 \underline{I} - \underline{K}^* - \sum_{j=1}^{i-1} \beta_j \underline{u}_j \underline{u}_j^t) \underline{v} \\ &= \omega_n'^2 \underline{v} - \underline{K}^* \underline{v} - \sum_{j=1}^{i-1} \beta_j \underline{u}_j (\underline{u}_j^t \underline{v})\end{aligned}\quad (23)$$

Since $\underline{u}_j^t \underline{v}$ is a scalar, the product becomes a linear combination of $(n \times 1)$ vectors that may be computed separately, and subsequently superimposed.

$$\underline{K}_1^{**} \underline{v} = \omega_n'^2 \underline{v} - \underline{K}^* \underline{v} - \sum_{j=1}^{i-1} \beta_j (\underline{u}_j^t \underline{v}) \underline{u}_j \quad (24)$$

It is only necessary to store the \underline{K}^* matrix in the most economical fashion, as well as the previously obtained eigenvalues and vectors in full.

We must be clear at this point that the inner loop time will be increased, since the sweeping has to be repeated

during every iteration. On the other hand, the faster multiplication using the sparsely populated matrix representation combined with the saving in storage space provides a distinct advantage. The pay-off increases with problem size and half band width, which renders the method particularly suitable for large systems.

VI. STRUCTURAL VIBRATION - TEST CASES

In order to evaluate the method, the axial vibration of a long elastic bar under different methods of support as well as two dimensional frameworks were chosen as examples. In spite of the simplicity of the problems many interesting results lead to clarification of questions relating to convergence of this method in particular, and of iterative structural procedures in general. The largest system handled was a two dimensional framework with 364 freedoms. The computation was performed using 64 K of core, and the program was capable of handling one thousand degrees of freedom in that space.

1. Vibrations of a Bar Between Two Rigid Supports - Effect of Problem Size.

A uniform axial bar supported between two rigid supports, Fig. 2, is divided up into a number of equal segments. Constant strain rods were used as elements. The mass of each element was lumped and shared equally between the two adjacent nodes. The number of nodes was varied from 12 to 47 (10 to 45 degrees of freedom). In determining the highest value necessary to com-

pute the origin shift three figures of accuracy were considered satisfactory. In obtaining the subsequent eigenvalues and vectors six figures of accuracy were prescribed. The first five modes were computed in each case. Tables 1 and 2 show details of the computations for both 10 and 45 degrees of freedom on a CDC 6400. Figure 3 shows the variation of the number of iterations necessary for convergence against the number of degrees of freedom for all five roots. Figure 4 shows the variation of the basic iteration time for all modes against the number of degrees of freedom.

2. Conclusions.

The following conclusions may be drawn from the results:

- a. No convergence problems were encountered.
- b. The first mode was always the slowest to converge. Higher modes required successively less iterations.
- c. The basic iteration time increases linearly with problem size, see Fig. 4. This is an extremely important characteristic of a sparsely populated matrix representation.
- d. The basic iteration time increases with the mode number, see Fig. 5, due to the necessary sweeping. However, the increase is linear and the value relative to the first mode is practically independent of the number of degrees of freedom. The third and fourth modes need approximately 50% more CP time per iteration than the first mode and the sixth mode needs twice the time.

TABLE 1. CONVERGENCE CHARACTERISTICS
VIBRATIONS OF A UNIFORM ELASTIC BAR BETWEEN TWO RIGID SUPPORTS
10 DEGREES OF FREEDOM

Root No.	No. of Necessary iterations	CP Time/iteration sec.	Total CP Time sec.
Shift	--	--	.146
1	199	.00234	.465
2	137	.00286	.392
3	93	.00341	.317
4	75	.00395	.296
5	55	.00457	.251
<hr/>			
No. of Nodes	= 12	Shift Accuracy	= 3 figures
No. of Elements	= 11	Subsequent Root accuracy	= 6 figures
No. of Freedoms	= 10	Subsequent Vector accuracy	= 6 figures

TABLE 2. CONVERGENCE CHARACTERISTICS
VIBRATIONS OF A UNIFORM ELASTIC BAR BETWEEN TWO RIGID SUPPORTS
45 DEGREES OF FREEDOM

Root No.	No. of Necessary iterations	CP Time/iteration sec.	Total CP Time sec.
Shift	--	--	2.685
1	2743	.0088	24.139
2	2037	.0105	21.362
3	1401	.0122	17.096
4	1244	.0139	17.256
5	963	.0155	14.950
<hr/>			
No. of Nodes	= 47	Shift Accuracy	= 3 figures
No. of Elements	= 11	Subsequent Root accuracy	= 6 figures
No. of Freedoms	= 10	Subsequent Vector accuracy	= 6 figures

- e. The number of iterations necessary for convergence decreases monotonically with mode number, see Fig. 6. This compensates for the increase in the basic iteration time, and the net result is a decrease in total mode time, see Tables 1 and 2.
- f. By comparing the total time required for the most time consuming mode, the first, between the 10 and 45 freedom systems, we observe that the time ratio was 52 for a freedom ratio of 4.5. This indicates a variation with somewhere between the square and the cube of the number of degrees of freedom. Should we extrapolate these values, it would appear that a problem involving 350 freedoms would require 3 hours of CP time for the first mode, and a 2000 freedom system 600 CP hours. While this may be correct for a one-dimensional system, it is an erroneous conclusion for two and three dimensional cases. We know that the increase in time is due to the increase of number of iterations rather than the cycle time. It is reasonable to assume that the number of iterations is primarily affected by the number of stations encountered from one end of the structure to the other. Ignoring secondary effects therefore, a 20 degree of freedom rod (22 nodes) is comparable to a 484 node, 800 degrees of freedom two dimensional framework or a 10648 node 24000 freedom three dimensional

framework system. This is supported by results of a two-dimensional frame vibration analysis discussed in the next section. As an example, the number of iterations necessary for convergence of a 12 node rod compares with a (12 x 12) two-dimensional framework as follows:

In the first mode 199 iterations against 677

In the second mode 137 iterations against 513.

Should we have extrapolated using the number of degrees of freedom as the only parameter we would have arrived at the figures 40,000 and 25,000 iterations. Admittedly, the number of iterations seems to be consistently three times as large, but this is still of the same order of magnitude. It would be safe to assume that structural models with a large slenderness ratio will tend to require more iterations than equally partitioned grids. All times given here are based on a FORTRAN IV program using the CDC 6400 computer. No attempt was made so far to speed the program up by many of the techniques for optimizing inner loops.

3. Effect of Method of Support on Convergence.

Figure 7 shows an elastic rod model made of six elements of equal stiffness (unity) and a seventh element of stiffness α . As α is varied from unity to zero, the problem changes from that of a built-in rod to that of free-free vibration. Figure 8 shows the effect of α on the number of iterations

necessary for convergence. We observe that the computation of the first mode becomes longer as we approach the free-free case. On the other hand, the other modes hardly seem to be affected.

4. Application to two-Dimensional Frameworks.

Figure 9 shows a two-dimensional framework, built-in at all edge points. If the number of nodes along any one direction is n , the total number of nodes is n^2 . The number of active nodes is $(n-2)^2$ and the number of degrees of freedom is $2(n-2)^2$.

At first a series of computations were performed using values for n from 4 (8 unknowns) to 12 (200 unknowns). The number of iterations necessary for some modes as a function of size is shown in Figure 10. Convergence difficulties were encountered in all cases with the second mode. Therefore, it is absent from the figure. This should have no substantial effect on the accuracy of the subsequent modes (see Section 11). The fifth mode also met occasional difficulties. The time per iteration is plotted in Figure 11. The results seem to confirm the behavioral tendencies observed in the one-dimensional case.

5. Effect of Symmetry.

Some convergence difficulties were consistently encountered in the two-dimensional framework example of VI. 4. It was felt that the slow convergence was due to closely spaced eigenvalue pairs. By using the symmetry of the structure, the modes may

be separated into four subgroups of modes and vectors, symmetric and antisymmetric in turn about the horizontal and vertical axes. Convergence difficulties disappeared. Results are given in Table 3 for a (6 x 6) grid representing a quarter of a (13 x 13) framework.

VII. IMPROVEMENT OF THE RATE OF CONVERGENCE

Let us consider an iterative process designed to obtain a variable starting with a value v_0 and converging to v_∞ after an infinite number of iterations. We may express the result of the p th iteration, v_p , in the form:

$$v_p = a_0 + \sum_{j=1}^{\infty} \frac{a_j}{p^j} = a_0 + \frac{a_1}{p} + \frac{a_2}{p^2} + \dots \quad (25)$$

It is clear that as $p \rightarrow \infty$,

$$v_p \rightarrow a_0$$

$$\therefore a_0 = v_\infty \quad (26)$$

We may apply equation (25), with a finite number of terms m , to the results of $(m + 1)$ consecutive iterations, obtaining $(m + 1)$ equations in $(m + 1)$ unknown coefficients of which only a_0 is of interest to us, since it gives an improved estimate of v_∞ .

This process has been applied to both the vibrations problem, and the buckling of a framework for $m = 2, 3$ and 4 . The value of $m = 3$ delivered the best result, cutting the number of iterations by almost one half.

TABLE 3. VIBRATIONS OF (6 x 6) FRAMEWORK

		MODE No.	No. of Iterations	EIGENVALUE
Symmetric	(x)	1	272	1.71374367×10^6
		2	281	1.78750610×10^6
	(y)	3	83	1.85149498×10^6
		4	194	2.03002336×10^6
		5	125	2.10428310×10^6
Symmetric	(x)	1	143	1.44456879×10^6
		2	98	1.57882136×10^6
	(y)	3	251	1.78836755×10^6
		4	257	1.84714666×10^6
		5	287	1.89707520×10^6
Antisymmetric	(x)	1	89	1.57001619×10^6
		2	101	1.67225707×10^6
	(y)	3	161	1.82149131×10^6
		4	107	1.85910349×10^6
		5	179	2.00221913×10^6
Antisymmetric	(x)	1	92	1.43814781×10^6
		2	185	1.60442560×10^6
	(y)	3	56	1.62676316×10^6
		4	185	1.79548117×10^6
		5	68	1.82334918×10^6

The three equations in this case are:

$$\begin{aligned}v_1 &= a_0 + a_1 + a_2 \\v_2 &= a_0 + a_{1/2} + a_{2/4} \\u_3 &= a_0 + a_{1/3} + a_{2/9}\end{aligned}\tag{27}$$

giving

$$a_0 = (v_1 - 8 v_2 + 9 v_3)/2$$

The second order extrapolation is now a standard general purpose part of the program and has so far caused great improvements in convergence speed, and no difficulties of any kind. The maximum problem handled was a (29 x 29) framework. By taking symmetry into account, only a quarter of the structure was studied, resulting in a (15 x 15) grid with 364 unknowns for the doubly symmetric case. For example, the first mode converged after 692 iterations and 141 CP seconds. The second mode needed 347 iterations and 76 CP seconds. The third mode needed 254 iterations and 59 CP seconds. In all cases the root converged to 10 significant figures.

The procedure described above can be applied in general to any iterative procedure. However, it was found, as in the case of most such methods, that it may not produce the desired effect under all circumstances. It appears to speed up monotonically convergent iterative processes (buckling, dynamics, Gauss-Seidel matrix solution) while presenting a positive danger if any oscillation, however small, is present (Jacobi Iterative matrix equation solution). To circumvent this difficulty,

two suggestions are given:

1. Eq. (27) can be rewritten in matrix form as:

$$\underline{v} = \underline{P} \underline{a} \quad (29)$$

We may apply Eq. (29) to more iteration steps than $(m + 1)$, and thereby obtain a rectangular \underline{P} matrix. Next we apply the least square method to obtain

$$\underline{a} = (\underline{P}^t \underline{P})^{-1} \underline{P}^t \underline{v} \quad (30)$$

This has been applied to the iterative matrix solution technique and has been found to behave well only for 3 equations and 2 coefficients.

2. To use every second iteration, or use the mean values of each two successive iterations as input to the improvement scheme. This is applicable to oscillating processes with a period of two iterations, as is usually the case.

VIII. FREE-FREE VIBRATIONS

To study the vibrations of an unsupported structure, a singular matrix \underline{K} is formed. The singularity will show itself in the presence of up to 6 zero eigenvalues $\omega_1^2 \text{ --- } \omega_6^2$. When operating with the matrix \underline{K}^{**} , of Eq. (18), they will correspond to the highest eigenvalues of the matrix. In order to avoid unnecessary computations, it is possible to include facilities in the program to construct rigid-body vectors as needed, resulting in immediate convergence, and hence elimination of the unwanted freedoms so that the effort may be directed to the subsequent elastic modes.

IX. ELASTIC INSTABILITY

The basic equation⁵ for elastic instability of a structure is given by

$$(\underline{K}_E + \lambda \underline{K}_G) \underline{r} = \underline{0} \quad (31)$$

where \underline{K}_E is the elastic stiffness of the structure

\underline{K}_G is a geometric stiffness representing a first order correction term accounting for the effect of change of structure geometry on equilibrium. It is dependent on the initial stress distribution in the structure due to the applied loading.

λ is a factor denoting the load level at which instability occurs

and \underline{r} is the displacement form associated with λ .

Equation (31) represents an eigenvalue problem possessing n possible solutions $(\lambda_1, \underline{r}_1)$, $(\lambda_2, \underline{r}_2)$, ----- $(\lambda_n, \underline{r}_n)$. The most interesting of these is $(\lambda_1, \underline{r}_1)$, representing the lowest value at which instability occurs.

One suggested method for solution of the problem⁵ has been to convert (24) to the form:

$$(\underline{K}_E^{-1} \underline{K}_G + \frac{1}{\lambda} \underline{I}) \underline{r} = \underline{0} \quad (32)$$

for which the highest value $\frac{1}{\lambda_1}$, corresponds to the lowest load value desired. Other methods involve decomposition of the matrix \underline{K}_E .

It is apparent that this form of solution suffers from the disadvantages associated with Eq. (14) in the vibrations problem. The matrix $(\underline{K}_E^{-1} \underline{K}_G)$ becomes fully populated requiring excessive

storage and slowing down the basic iteration time. A new method is suggested here which should overcome these problems.

1. The λ Search Technique.

In order to predict the initial load level, it is necessary to find the lowest value of λ for which the matrix

$$\underline{K}^* = (\underline{K}_E + \lambda \underline{K}_G) \quad (33)$$

becomes singular.

The matrix \underline{K}^* has n eigenvalues

$$\omega_1, \omega_2, \dots, \omega_1, \dots, \omega_n$$

mentioned in descending order.

Each root, ω_1 , is a function of λ . If λ is zero, all eigenvalues ω_1 are positive since \underline{K}_E is positive definite. As λ increases in value, the spectrum of ω_1 starts to shift with each ω_1 passing through the origin one at a time, each time causing \underline{K}^* to be singular. The lowest value of λ for which \underline{K}^* becomes singular is therefore that required for $\omega_n = 0$.

In order to find the required λ , it would seem reasonable to solve the equation

$$\omega_n(\lambda) = 0 \quad (34)$$

using an iterative scheme such as the slope-interval method.

First we assume $\lambda = 0$. For this case

$$\underline{K}^*(0) = \underline{K}_E$$

Using the power method, one finds an approximation to the value of ω_1, ω_1' , followed by application of the origin shift technique to obtain a value $\omega_n(0)$. This value corresponds to the highest

$$(\omega_1^2 \mathbf{I} - \mathbf{K}_0^*)$$

Next we assume a small positive value for λ , $\lambda_{(1)}$. If the original load is chosen to be larger than the buckling load, but within the same order of magnitude, a value of $\lambda_{(1)} = 0.1$ is reasonable.

The process is then repeated for

$$\mathbf{K}^* = (\mathbf{K}_E + \lambda_{(1)} \mathbf{K}_G)$$

with a resultant smallest eigenvalue $\omega_n(\lambda_{(1)})$.

Now the iterative process has been initiated and should continue according to the following scheme:

$$\lambda_{(p+1)} = \lambda_{(p)} - \omega_n(\lambda_{(p)}) \cdot \frac{[\lambda_{(p)} - \lambda_{(p-1)}]}{[\omega_n(\lambda_{(p)}) - \omega_n(\lambda_{(p-1)})]} \quad (35)$$

until convergence is achieved to a satisfactory degree of accuracy. The eigenvector \mathbf{r}_1 associated with $\omega_n(\lambda_1)$, where λ_1 is the value $\lambda_{(p)}$ at convergence, is the correct buckling mode associated with the value λ_1 since

$$(\mathbf{K}_E + \lambda_1 \mathbf{K}_G) \mathbf{r}_1 = \mathbf{0} \quad (36)$$

2. Higher Order Buckling Modes.

Although the lowest buckling load, λ_1 , is the primary objective of the analysis, it is still possible to obtain any number of higher modes.

Should it be desired to find the eigenvalue and corresponding vector of buckling mode i , λ_i and \mathbf{r}_i , it would be necessary to find the value λ_i such that the i th root of \mathbf{K}^* , λ_i ,

disappears. For that purpose the following procedure is followed:

- i - Assume a value of λ . Start with zero, then a small number, then let the iteration proceed automatically as before, though in a generalized form as explained below.
- ii - For each value of λ , find the approximate value for the maximum eigenvalue ω_1 of the matrix \underline{K}^* , ω_1 .
- iii - Form $\underline{K}_{(\lambda)}^{**} = (\omega_1 \underline{I} - \underline{K}^*(\lambda))$ (37)
- iv - Find the highest $(i-1)$ eigenvalues $(\omega_1 - \omega_n)$, $(\omega_1 - \omega_{n-1})$ ----- $(\omega_1 - \omega_{n-i+1})$ of \underline{K}^{**} using the power method, and sweeping the appropriate values and vectors as needed to obtain the following ones. The corresponding eigenvectors are then \underline{u}_1 , \underline{u}_2 ----- \underline{u}_{i-1} .
- v - Finally obtain $(\omega_1 - \omega_{n-i+1})$ as the highest eigenvalue of the matrix

$$\underline{K}_{(\lambda)}^{**} = \omega_n \underline{I} - \underline{K}_{(\lambda)}^* - \sum_{j=1}^{n-i} (\omega_1 - \omega_j) \underline{u}_j \underline{u}_j^t \quad (38)$$

- vi - Study the variation of ω_{n-i+1} with λ , and use the slope interval method to improve its value till convergence to zero. Upon convergence, \underline{u}_i will be identical to \underline{r}_i , the i th buckling mode.

3. Solved Example.

As a preliminary study, a simple two-dimensional framework, Figure 13, was chosen. The method functioned as expected and produced a load level λ of 0.1964 and a buckling mode as shown by the dotted line.

Figure 14 shows some data describing the convergence of the process. With $\lambda = 0$, 8 iterations were used to obtain the approximate highest eigenvalue $\omega_1^!$, and 21 to obtain the lowest. The second trial, with $\lambda = 0.1$, took only 2 and 8 iterations respectively. The speed up was due to the fact that vectors obtained in the first process were used as starting vectors for the second. The third trial value obtained using the slope interval method required similar computational effort. Afterwards convergence was fast and the fifth trial value resulted in satisfactory convergence of the root.

X. COMPARISON OF LUMPED MASS AND KINEMATICALLY CONSISTENT SYSTEMS

The question of whether to use a simple lumped mass representation, resulting in a diagonal \underline{M} matrix, or the kinematically consistent mass matrix approach, resulting in a banded \underline{M} matrix with an identical pattern to that of the \underline{K} matrix, can only be determined on the basis of the computational effort involved. A kinematically consistent mass matrix gives a better representation of the inertia of the structure, and allows rotational freedoms but requires a lengthy matrix inversion. The lumped approach is cruder, but it is computationally faster.

One of the arguments in favor of the lumped system is based on the fact that the values of the frequencies obtained by both methods are nearly the same, and that the difference in accuracy, if any, hardly justifies the additional computational effort involved.

The method suggested for the solution of the buckling problem is again applicable in this case. In obtaining higher modes than the first, however, we expect more effort than that in dealing with the lumped mass system. The process is similar to that suggested in IX. 2.

In order to speed up the application in this particular case, it is suggested that a first approximation to the roots and vectors be obtained using the lumped mass approach, followed by the λ search technique described for the buckling problem. This should ensure fast convergence.

Since the procedures described in this paper are capable of handling both cases, a preliminary study was undertaken to compare the two approaches. Again a uniform elastic rod between two rigid supports was chosen, for which the exact solution is known. Table (4) shows a comparison of results obtained from both approaches with the exact value for the first root. Figure (15) shows both first and second mode convergence as functions of degrees of freedom. It was most surprising to find the first mode accuracy practically the same with both approaches, the lumped mass system having a slight edge. For the second mode the lumped mass system is definitely the more accurate and the fastest converging.

XI. THE CASE OF THE NEAR OR EQUAL ROOTS

The basic iterative step in the power method is described by the equation:

$$\underline{A}^m \underline{u} = \lambda_1^m \sum_{i=1}^n a_i \left(\frac{\lambda_i}{\lambda_1} \right)^m \underline{v}_i \quad (39)$$

TABLE 4. COMPARISON BETWEEN LUMPED MASS
AND KINEMATICALLY CONSISTENT MASS MATRIX APPROACHES
FOR THE VIBRATIONS OF A UNIFORM ELASTIC ROD

No. of Elements	No. of Freedoms	K.C.M. ω_1^2	L.M. ω_1^2	Error	
				$\Delta\omega_{K.C.M.}^2$	$\Delta\omega_{L.M.}^2$
2	1	.3333	.2222	.0592	.0519
3	2	.3000	.2500	.0258	.0242
4	3	.2885	.2604	.0143	.0138
5	4	.2833	.2653	.0091	.0089
6	5	.2805	.2680	.0063	.0062
ω_1^2 exact = 0.27416					

The process will converge to the vector \underline{v}_1 and the value λ_1 if repeated sufficiently, each step being followed by a normalization procedure.

The speed of convergence depends largely on the ratios between the roots nearest to λ_1 and λ_1 itself. Assuming λ_2 is close to λ_1 , convergence will be slow, and may have to be interrupted for reasons of economy. It is suggested here that, in spite of that, one may proceed to higher modes and indeed obtain accurate results there in spite of any local convergence problems. Let us rewrite Eq. (39) as

$$\underline{A}^m \underline{u} = \lambda_1^m \left[a_1 \underline{v}_1 + \left(\frac{\lambda_2}{\lambda_1} \right)^m \underline{v}_2 + \sum_{i=3}^n a_i \left(\frac{\lambda_i}{\lambda_1} \right)^m \underline{v}_i \right] \quad (40)$$

If m is large enough, \underline{u} will be mainly composed of vectors \underline{v}_1 and \underline{v}_2 so that \underline{u} is orthogonal to all other subsequent vectors. If \underline{u}_1 is frozen at this point, at value \underline{u} , then \underline{u}_2 will follow immediately from the arbitrarily chosen \underline{u}_1 . All other values and vectors should not be affected.

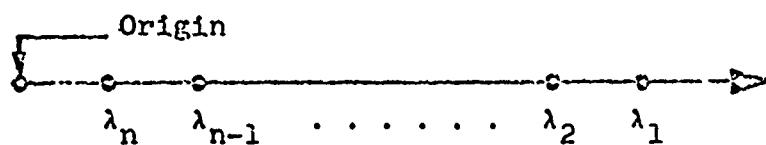
A physical interpretation of this mathematical phenomenon is possible. If we were dealing with a vibrations problem, for example, there would be two possible modes that occur practically at the same frequency, so that it would be very hard in the physical situation to excite one mode without the other. The process will be extremely sensitive to the method of excitation.

REFERENCES

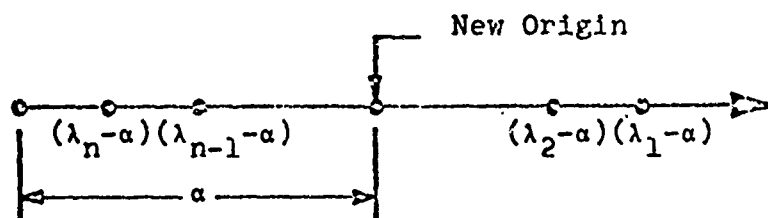
- 1) Argyris, J. H., Energy Theorems and Structural Analysis, Butterworth Scientific Publications, London, 1960.
- 2) Wilkinson, J. H., The Algebraic Eigenvalue Problem, Clarendon Press, Oxford University Press, London, 1965, pp. 570-647.
- 3) Guyan, R. J., "Reduction of Stiffness and Mass Matrices," AIAA Journal, Vol. 3, 1965, pp. 380.
- 4) Turner, J. J., Dill, E. H., and Melosh, R. J., "Large Deflections of Structures Subjected to Heating and External Loads," Journal of Aerospace Sciences, Vol. 27, 1960, pp. 97-102, 127.
- 5) Argyris, J. H., Kelsey, S., and Kamel, H., "Matrix Methods of Structural Analysis," AGARDograph 72, Ed. De Veubeke, F., Pergamon Press, 1964, pp. 159-163.
- 6) Archer, J. S., "Consistent Matrix Formulation for Structural Analysis Using Finite-element Techniques," AIAA Journal, Vol. 3, 1965, pp. 1910-1918.

FIGURE 1
ORIGIN SHIFT OF EIGENVALUE SPECTRUM

EIGENVALUE SPECTRUM OF MATRIX \underline{A}



EIGENVALUE SPECTRUM OF MATRIX $(\underline{A} - \sigma \underline{I})$



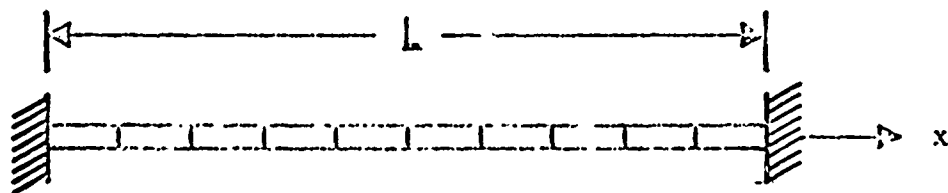
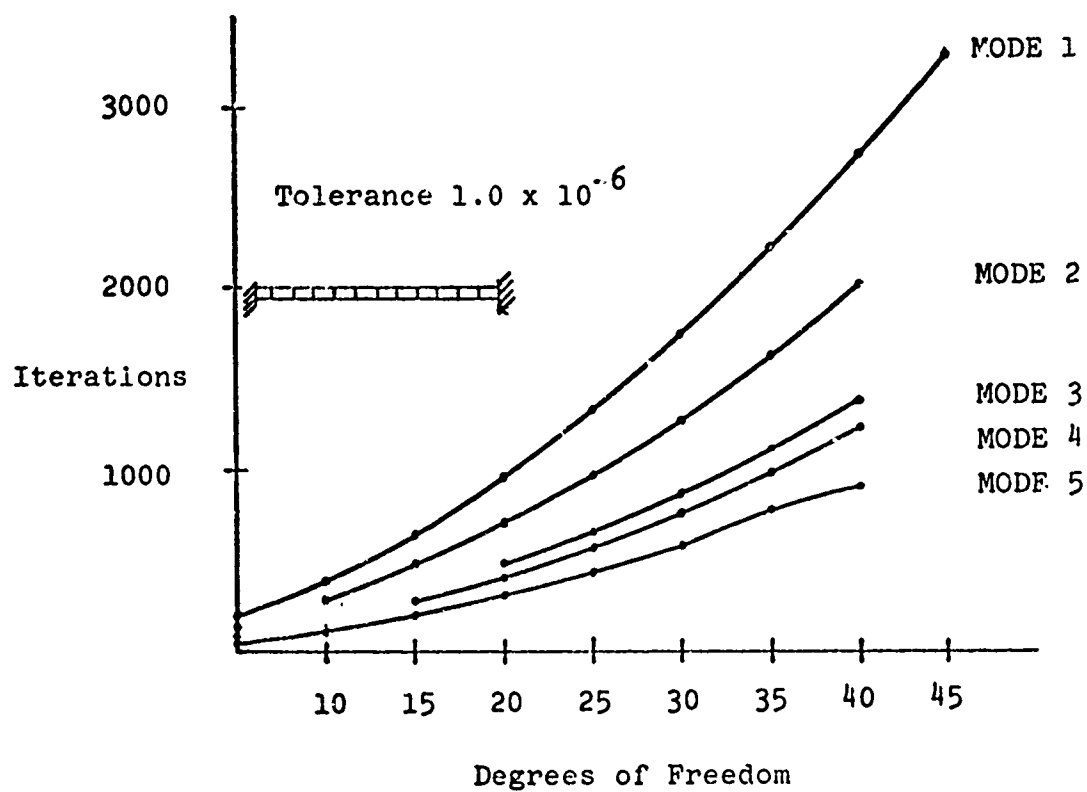


FIGURE 2
UNIFORM AXIAL BAR BETWEEN RIGID SUPPORTS



VIBRATIONS OF A UNIFORM ELASTIC BAR
FIGURE 3

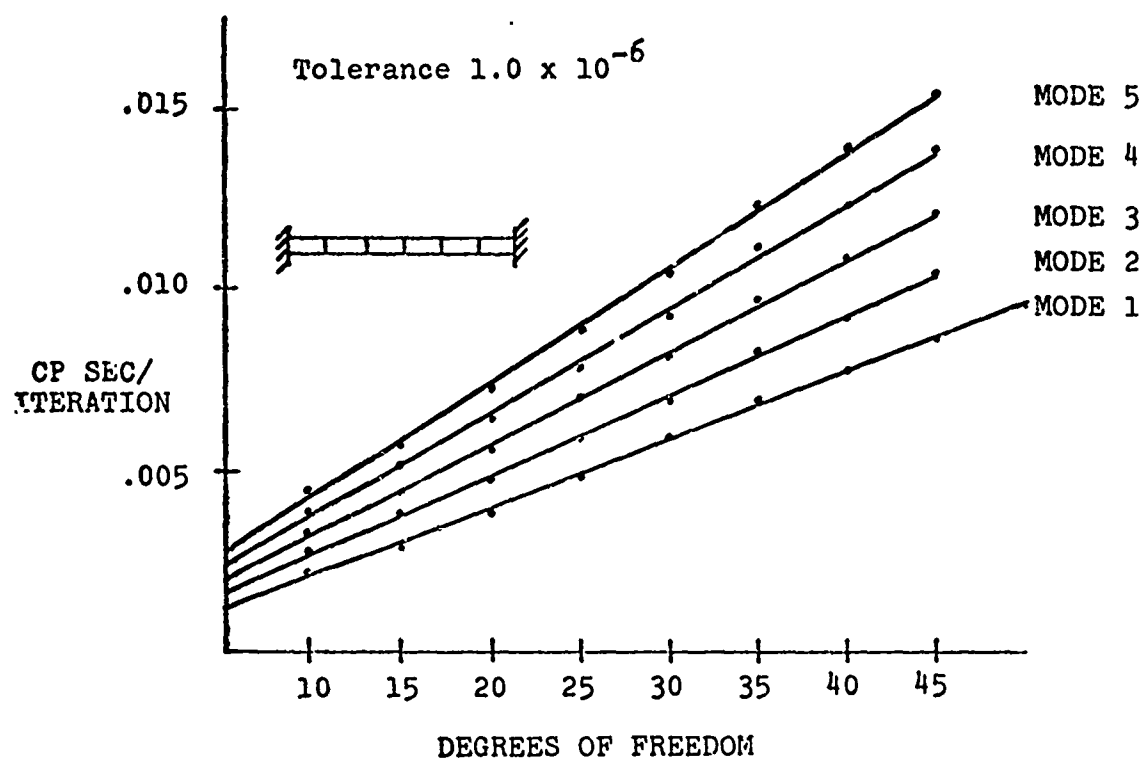


FIGURE 4
VIBRATIONS OF A UNIFORM ELASTIC BAR

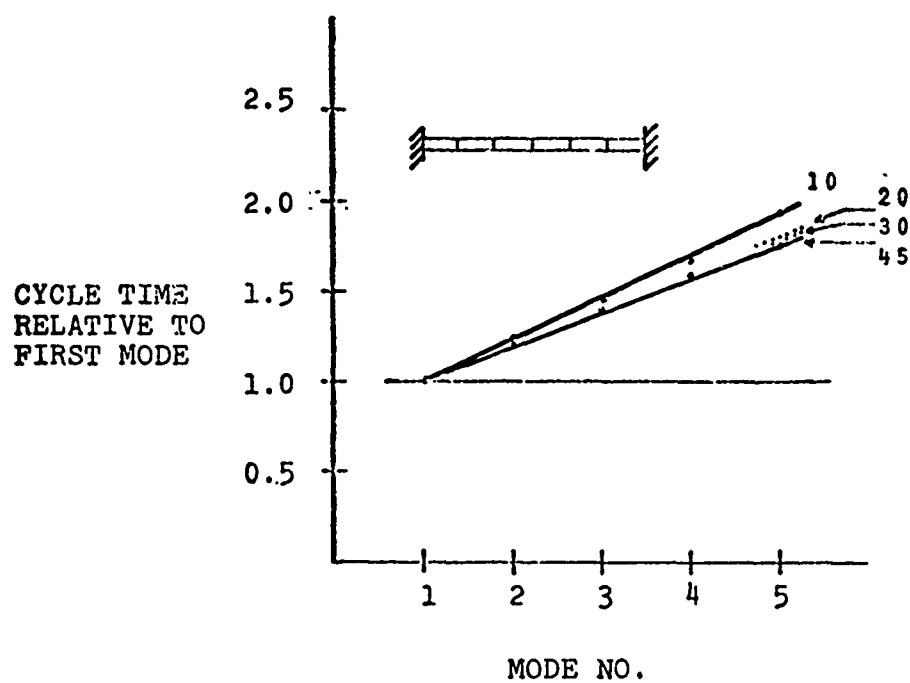


FIGURE 5
CYCLE TIME RELATIVE TO FIRST MODE
FOR VARIOUS DEGREE OF FREEDOM SYSTEMS

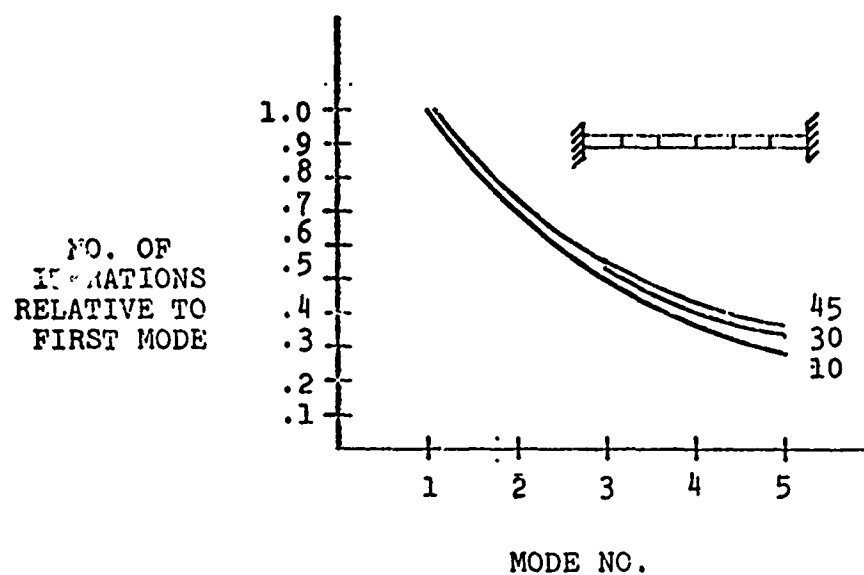


FIGURE 6
NO. OF ITERATIONS RELATIVE TO FIRST MODE
FOR DIFFERENT DEGREES OF FREEDOM

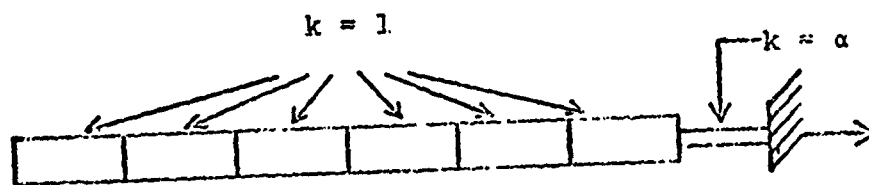


FIGURE 7
ELASTIC ROD MODEL WITH A WEAK END ELEMENT

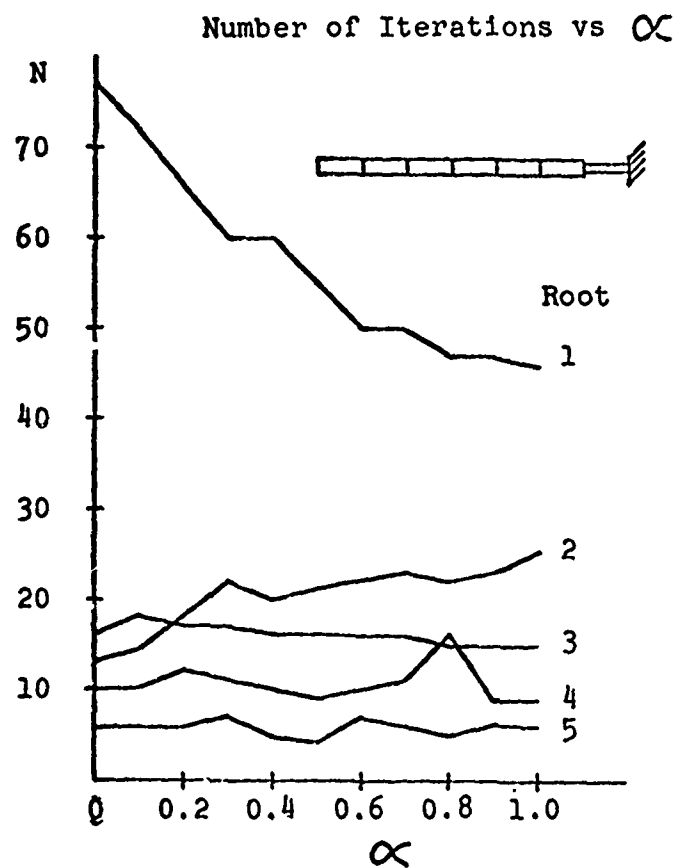


FIGURE 8
EFFECT OF METHOD OF SUPPORT OF THE
STRUCTURE ON CONVERGENCE OF THE METHOD

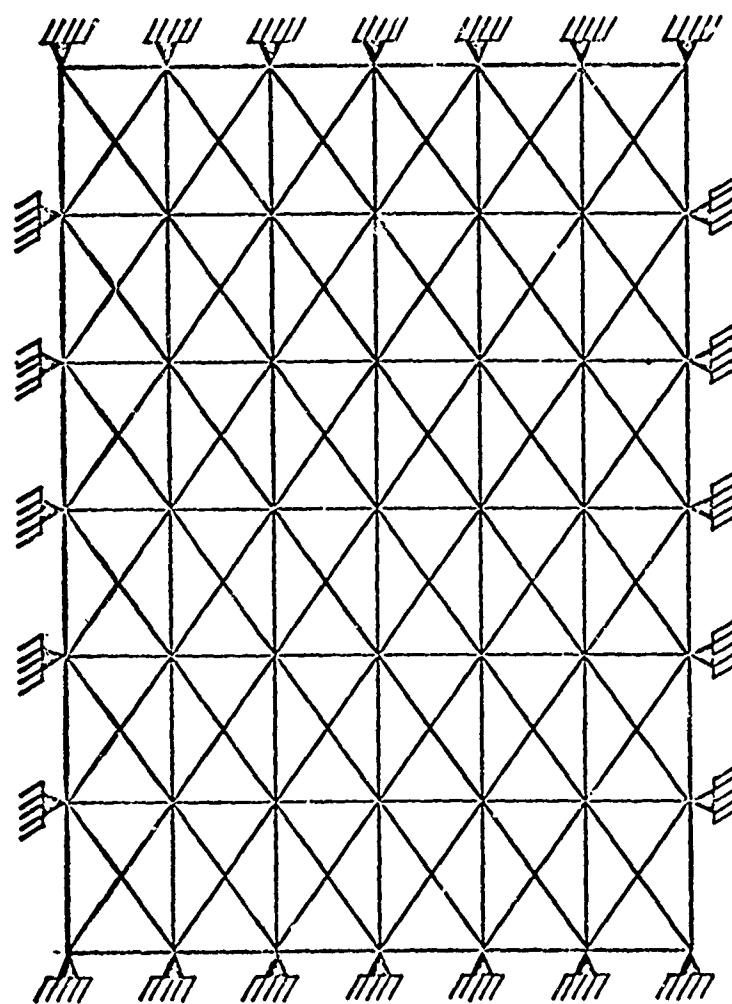


FIGURE 9
TWO DIMENSIONAL FRAMEWORK WITH BUILT-IN EDGES

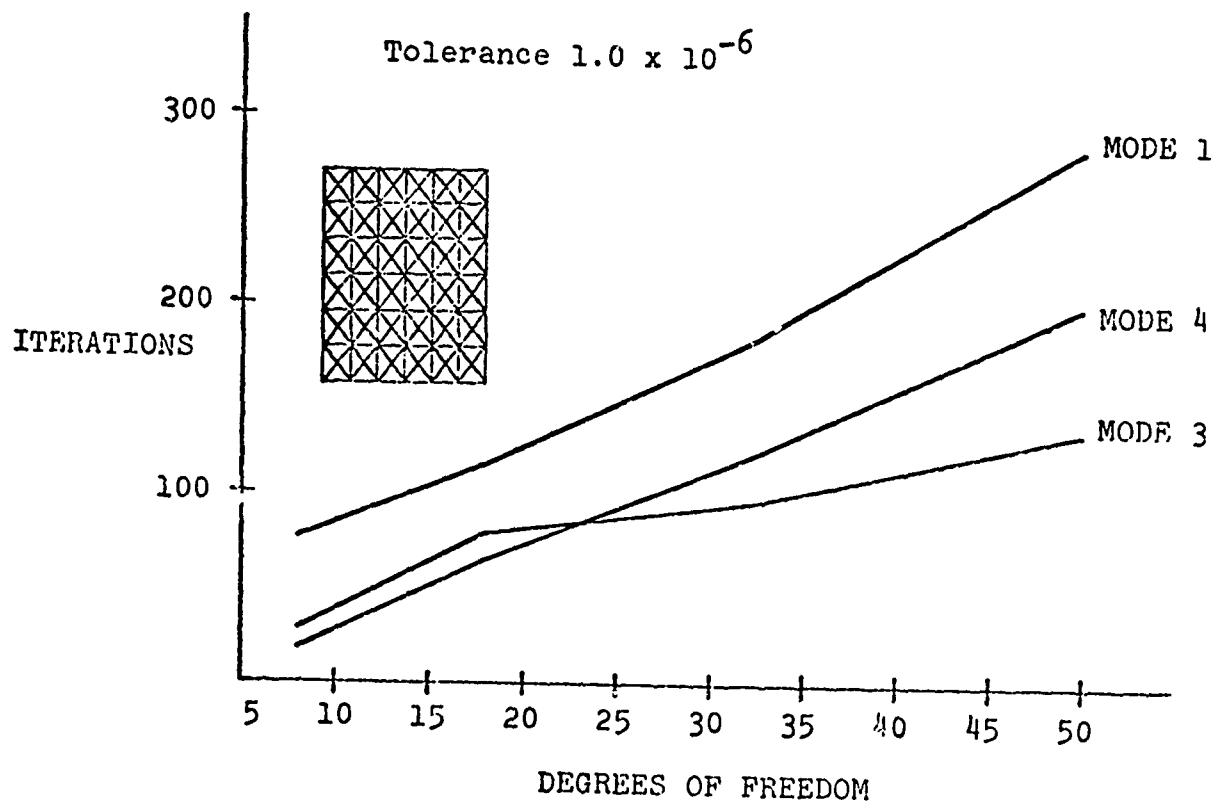


FIGURE 10
TWO-DIMENSIONAL FRAMEWORK,
NUMBER OF ITERATIONS

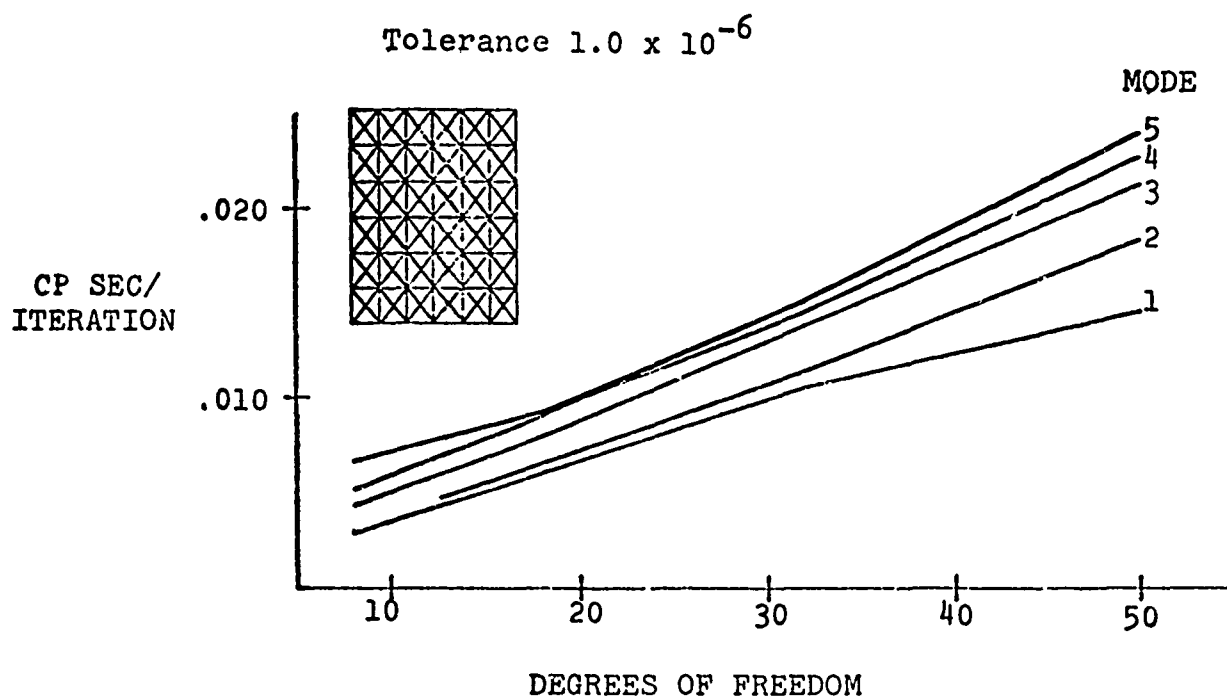


FIGURE 11
TWO-DIMENSIONAL FRAMEWORK,
TIME PER ITERATION

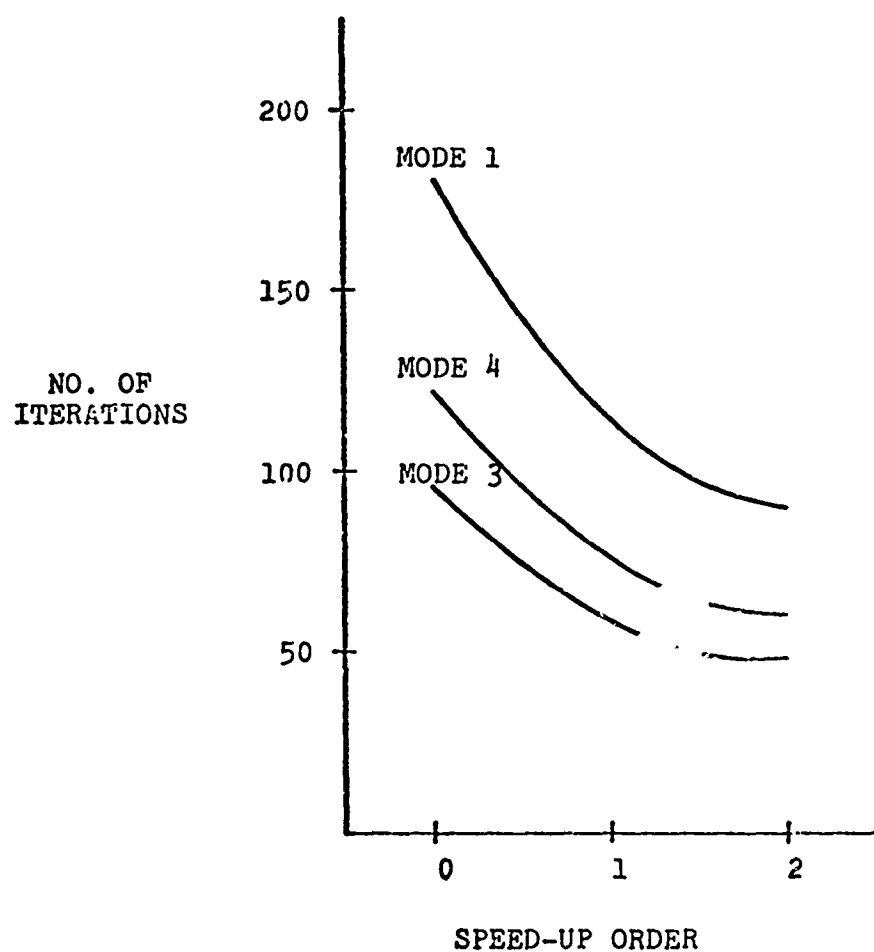
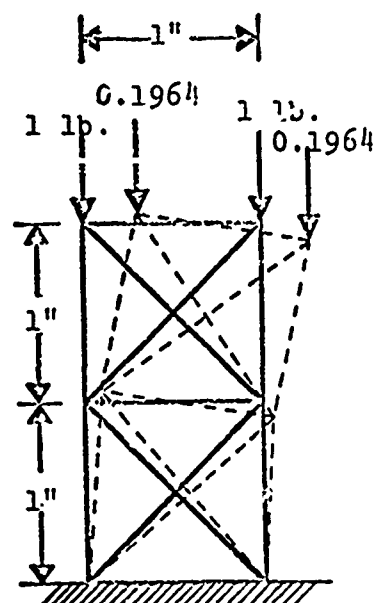


FIGURE 12
EFFECT OF SPEED-UP ON CONVERGENCE

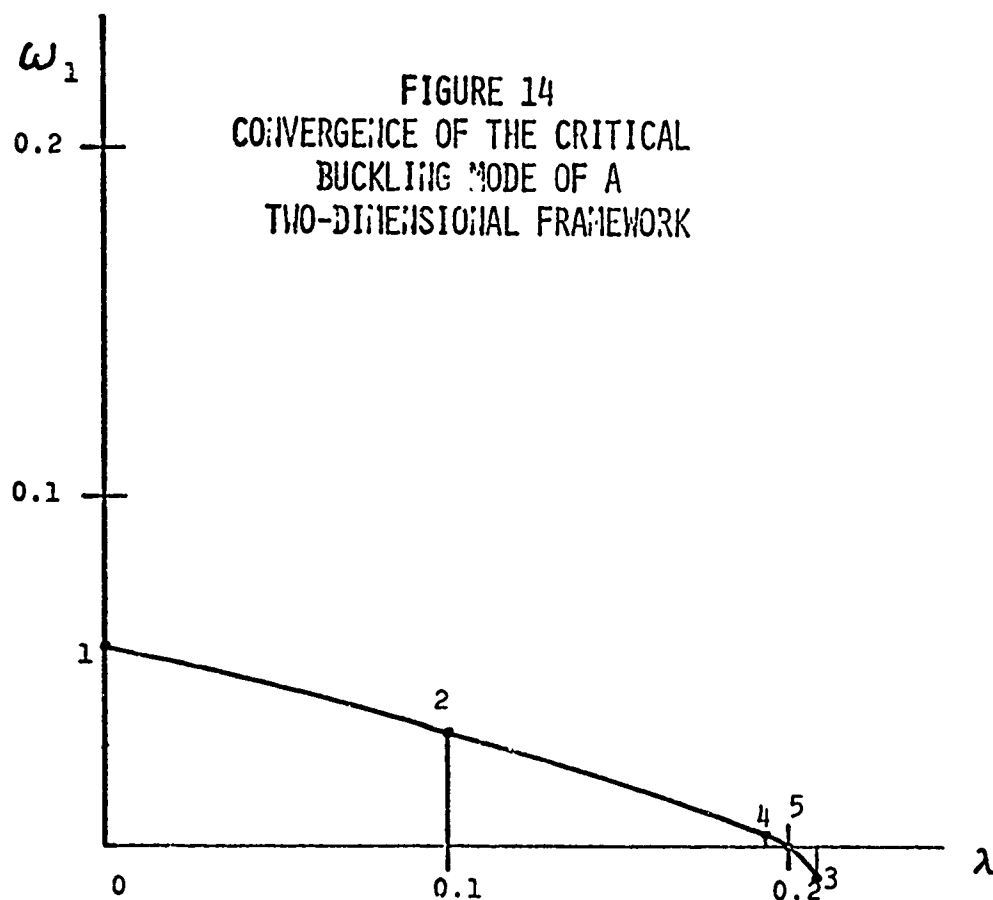


Young's Modulus $E = 1 \text{ lb/in}^2$

A for Diagonals $= (2)^{\frac{1}{2}} \text{ in}^2$

All others $= 1 \text{ in}^2$

FIGURE 13
CRITICAL BUCKLING MODE FOR TWO DIMENSIONAL FRAMEWORK



λ	No. of Its. ω_1'	No. of Its. ω_n	ω_n
0.0	8	21	5.7×10^{-2}
0.1	2	8	3.0×10^{-2}
0.2158	2	11	-7.1×10^{-3}
0.1938	2	2	9.37×10^{-4}
0.1964	2	2	-8×10^{-6}

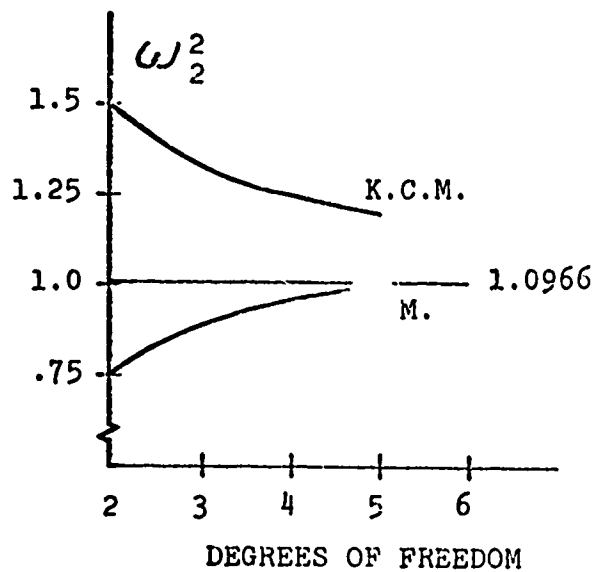
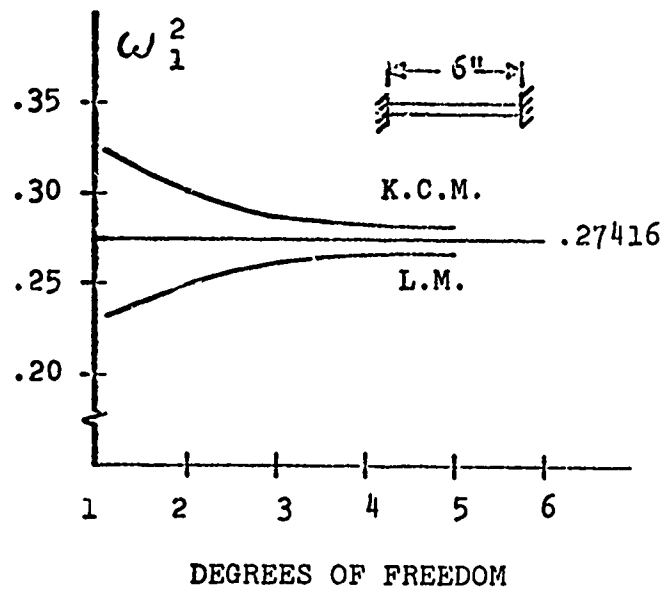


FIGURE 15
COMPARISON BETWEEN LUMPED MASS
AND KINEMATICALLY CONSISTENT MASS SUPPORT, 3

QUESTIONS AND COMMENTS FOLLOWING KAMEL'S PAPER

QUESTION: When you do your elastic instability analysis, it seems to me that in order to find the incremental matrix you either have to equation solve or invert the stiffness matrix to find the stress distribution. But in your solution here you don't imply that.

KAMEL: I didn't mention it, that's true, because we are still experimenting. There is now so much incentive to keep matrices in the sparsely populated form. Until about one year ago, I avoided iterative techniques. I wanted to have something that definitely would converge and I wanted to be able to estimate how long it was going to take. But in view of the advantages in time that you gain from iterative schemes, I'm beginning to think that one should put in an effort to try to find a fast iterative technique or to find how to speed up the iterative solution using a method such as Gauss-Seidel. You can apply such a scheme to a sparsely populated matrix and keep it in sparsely populated form.

COMMENT: I have a few comments to make about this type of eigenvalue problem since I have been working in this area. First of all, I regret that Dr. Kamel has not given any comparisons of his method with transformation schemes such as Householder-QR or with special techniques for large systems, such as inverse power iteration with spectral shifts. I mention this because for problems involving less than 300 degrees of freedom complete solution by transformation methods can be obtained in a matter of seconds. The power method you presented does not work if you have multiple roots as in free-free vibration. If two roots are not equal but

very close, the deflation scheme is strongly unstable. This fact has been well known to engineers who have used the Stodola and mode-sweeping methods and have experienced rapid loss of significance as one proceeds to compute intermediate modes. So I would like to ask if you have encountered some of those numerical problems and if comparison with other methods has been made.

KAMEL: First of all, let me point out that the purpose of the paper is not to say that the method is superior to others. I believe that this method is sufficiently different and worth looking at. In the second place, it has the advantage of saving computer storage. With a 65K memory, you can do over 1000 degrees of freedom and I don't think that is possible with the other methods. The method is attractive if you have a small fast computer, and you want to solve very large problems but cannot afford decomposition techniques. The methods you describe did not reach that speed until a high level of programming effort has been put into them. We are just making a preliminary study of the method and the results presented simply describe the current state of the code. No attempts have been made to speed things up.

COMMENT: This type of direct power iteration for solving vibration problems has been extensively used previously and a lot of experience gathered so far.

KAMEL: Are you talking about the vibration analysis part of the paper.

COMMENT: Yes.

KAMEL: Yes, it has been used but in the setup that one has to get your highest or lowest frequency first. The difference lies in the use of the shift.

COMMENT: The shift has always been used as a means of speeding convergence.

KAMEL: That is right. And that is how I came across it. I used it on another computer in order to try to speed up convergence. However, no one has described how much to shift by. It has been a sort of try your luck thing.

COMMENT: I just wanted to caution about the numerical problems. I understand the reluctance in trying to code inverse iteration which requires a good out of core equation solver.

KAMEL: Your computer time increases as you fill up the non-zero elements inside the band.

COMMENT: Yes, it is a band-squared cycle time, but in inverse iteration you normally need 5 to 10 iterations per eigenvalue, whereas you are talking about thousands in your method.

KAMEL: I agree, but think again of the advantages of small storage in large problems. The number of iterations will still remain the same using this method. For the method you are talking about, they will increase with the square or cube of the size of the problem. I am not saying that this method will supersede all others. We tried to find a method in which the structural matrices can be kept in a sparsely populated form.

The method works and the next step is to compare and investigate.

QUESTION: When you extrapolate to find the intersection with the axis and if you happen to have two close roots, do you run the risk of hitting the wrong one.

KAMEL: Yes.

COMMENT: I have solved a number of bar and beam problems using both consistent mass and lump mass approaches and I found that consistent mass has always come up with much better results than the lump mass especially for higher order displacement functions. So I definitely disagree with those results you presented.

JORDAN: Thank you, Prof. Kamel. I'd like to summarize today's session. I think Prof. Hutchinson in his presentation pointed out two significant facts. One was his discussion of the history of the conflicts between the deformation and flow theories of plasticity. He contends, with some dissent, that this conflict will continue and it must be resolved and he suggested looking into this stress-strain relationship. Indications from Prof. Hutchinson's work also reinforce the fact that the same types of problems that are encountered with imperfection sensitive structures in the elastic range will also be encountered with the same type of structures which buckle in the plastic range.

In Prof. Kamel's talk, I think he has presented at least a different method of finding eigenvalues and eigenvectors for both vibration and buckling problems.

PANEL DISCUSSION B

FINITE ELEMENTS VERSUS FINITE DIFFERENCES

Chairman: R. M. Jones, Aerospace Corporation,
San Bernardino, California

D. Bushnell, Lockheed Missiles & Space
Company, Palo Alto, California

S. W. Key, Sandia Corporation,
Albuquerque, New Mexico

R. D. Krieg, Sandia Corporation,
Albuquerque, New Mexico

E. L. Stanton, McDonnell Douglas
Astronautics, Huntington Beach, California

JONES: The objectives of this panel are to examine the finite element and finite difference methods relative to the advantages that each of these methods might have as illustrated by the successes that people have had. We also want to look at some of the disadvantages and the failures of the methods. By way of an agenda, each of the panel members will make some opening remarks. Then we will direct some questions in panel to one another. Afterwards we will have some prepared comments prior to the panel convening and then we will open the floor to discussion.

BUSHNELL: I have prepared comments in two areas. The first area I call numerical methods continuum. The second area has to do with various nonlinear methods applicable to both finite difference and finite element methods.

I can describe this numerical methods continuum with reference to Figure 1. Let's put finite differences based on equilibrium equations on the left side. A typical example in this category is the derivation of a general shell of revolution analyzer which is currently underway at NASA-Langley. This effort is based on the finite difference method in which the governing differ-

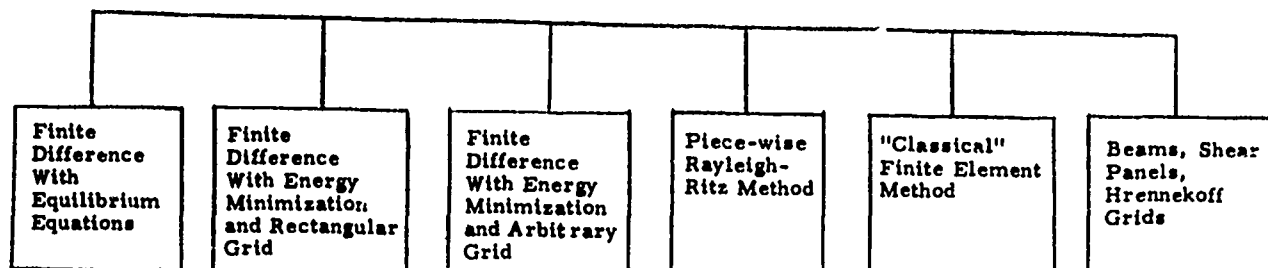


Figure 1. NUMERICAL ANALYSIS CONTINUUM

ential equations are expressed in finite difference form. On the right-hand end of the continuum, I would put the old beam and shear panel models of aircraft analyses in which complex structures are divided into very simple types of elements. Now in the middle of this continuum we have, for example, the finite difference method used in connection with energy methods with a regular grid. We're beginning now to resemble the finite element method because we use more matrix operations. The actual programming and structure of programs based on the finite-difference energy method are rather similar to those based on the finite element method. Let's now locate on this continuum a point which I'll call finite difference energy method with arbitrary grid. We heard a paper this morning by Stan Jensen on that subject. These finite difference methods begin more and more to resemble finite element methods. We approach the situation where we can analyze an arbitrary structure by maintaining complete generality in grid. Eventually this method can be applied to three-dimensional structures as well as two-dimensional.

Now approximately in the middle of the continuum is a fuzzy area where nobody talks to one another. Here I'm going to identify a point called the "Piece-wise Rayleigh-Ritz method." In this method, we take some arbitrary

shell and draw chalk marks on it. I'm not replacing the areas bounded by chalk marks with flat elements or curved elements. I'm just drawing boundaries within which I want to describe displacements in some functional form--polynomials with undetermined coefficients, for example. Essentially, I want to go now from a finite difference, in other words a point definition formulation, to a representation in which the functions are continuous and differentiable within the bounded regions, and in which, through constraint conditions, the appropriate displacement and rotation compatibility conditions are satisfied on the boundaries. We'll refer to this model without reference to, say, a finite element but rather a finite function form. I'm not convinced that the "piece-wise Rayleigh-Ritz" method is exactly the same as a finite element method, mainly because the energy functional now consists of strain energy plus appropriate constraint conditions. Further to the right on the continuum we have the "classical" finite element method which is the mainstay of the modern structural analysis. By means of a very simple procedure, this method can be applied to very complex structures and can be computerized in such a way that designers and engineers can use these tools very effectively, as we've seen during the course of this conference. I encourage comments from the audience about other methods that are different from these. My own feeling is that the tendency is to move toward the middle of the continuum. Somewhere we'll meet and have a really great general analysis for linear and nonlinear problems.

The second comment has to do with nonlinear methods. I want to outline very quickly which methods these are. All of them have been brought up at this conference. In my discussion I'm following a very good summary by Hoffmeister, Greenbaum and Evensen, presented in a paper at the 11th AIAA/ASME Structures, Structural Dynamics and Materials Conference in Denver in April 1970. It's the best discussion I've seen on various nonlinear methods. For the overall structure of my comment, I therefore give credit to them.

The first method involves putting the nonlinear terms on the right-hand side with no change in the stiffness matrix. We had an example in a paper by

Dr. Ball this morning in which the linear stiffness matrix is used and non-linear terms are included in the analysis as equivalent loads.

The second method is what I'll call an incremental method without equilibrium check. You take small load steps. The analysis for each step is linear, but there is no iteration to guarantee equilibrium. However, if you take small enough steps, you get a reasonable picture of what goes on in nature. The fact that you do get a reasonably good picture is evident from the work of Pedro Marcal, who has obtained good agreement between theory and experiment in a variety of applications.

The third method I call the modified Newton method. What I mean by "modified Newton method" is a method in which loads are increased incrementally and every once in a while the stiffness matrix is refactored; that is, the stiffness of the structure is recalculated in order to get more rapid convergence. Between these loads for which the stiffness matrix is refactored, the nonlinear terms are thrown on the right-hand side. The modified method is sort of a halfway station between putting the nonlinear terms on the right-hand side and a full Newton method. There is another method in here which Hoffmeister, Greenbaum and Evensen mentioned and, in fact, which I think they use in their own work. It's what has been called a one-step Newton method--an incremental method in which equilibrium unbalance in each step is taken into account. The unbalance in one load step is introduced as a pseudo-load in the next load step. In this way you keep close to the proper load-deflection curve.

The fifth method would be the full Newton method in which you recalculate the stiffness matrix for every load step and for every iteration at a given load. This method is used in the BOSOR3 program, which is a shell-of-revolution analyzer. You might say the full Newton method is needlessly inefficient in the sense that you're getting a lot more accuracy than you need. However, in a one-dimensional numerical analysis, it really doesn't matter much because the computer times are so small.

The sixth method would be a direct search method for the solution of non-

linear problems. For more on this, I refer you to the work of Schmit at Case Western Reserve (now at UCLA).

KEY: Well, I like very much the way Dave Bushnell has described his continuum of numerical methods and I believe that, in principle, any of these methods are applicable to the problems we are doing. However, there are certain practical features about the various approaches that either limit them in their application or actually enhance their application. I'd like to attempt to describe those types of problems for which I feel finite element and finite difference methods are currently most applicable.

Figure 2 shows a two-dimensional grid work. Vertically, I've put Material

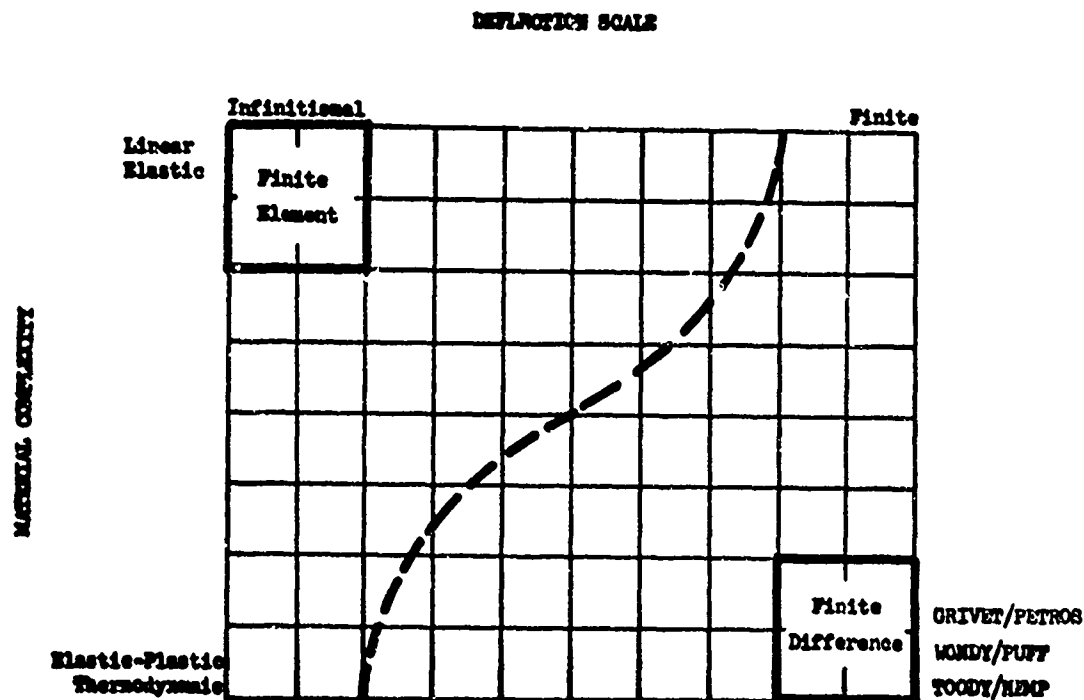


Figure 2. Complexity Space for Shell Problems

Complexity ranging from linear elastic material behavior to the extreme, elastic plastic, thermodynamic material descriptions found in shock wave

codes. Horizontally I've indicated a Deflection Scale. On the left end is the infinitesimal deflection, classical shell work. Going over to the extreme right, we have finite or large deflections. I've indicated regions in this grid where one particular method seems to be used with greater prevalence. For example, in the upper left-hand corner, the finite element method tends to predominate while over in the opposite corner you have the finite difference method. Now I don't mean to infer that the other methods can't be used in these corners, but due to either practical features or personal preference of the investigator, the designated methods have come to dominate these regions. The other corners I tend to view as neutral corners. It depends on an individual's tastes, how he approaches a problem and the formulations involved as to which method is really going to provide results. The dashed line across the middle is really sort of a neutral dividing line. If you're a finite element type, you'll tend to move the line to the right while the finite difference people will tend to move it left. One of the things you see is both sides tending to carry the battle to the other's camp and when they do this they find that the method they're practicing tends to look a lot like the other method that was already there.

KRIEG: I think that shell analysis using finite difference and finite element methods is reaching some sort of plateau at which we can solve a large number of really practical problems. I think this situation compares with that which prevailed in the area of stress wave propagation just a few years back. Now that we have reached this plateau, we have the time to sit back and examine other methods, to look at them very critically, and to start tweaking on them. The wave propagation people thought that in doing so they could achieve something like a ten percent improvement in computer time. But in examining other methods and re-examining their own methods, they were able to come up with improvements like factors of five in running times. I'm hoping that shell theory might be able to do this same thing.

We've seen a simultaneous development of two methods, finite difference and finite element, and I think that each of these methods has areas of application in which the other will find it very difficult to compete as out-

lined by Sam Key. The two methods share some common problems and deficiencies. I would like to see more research devoted to these common areas. For example, a good mesh generator and initialization scheme is needed and virtually the same one could be used for both methods. Also, whether you set up the stiffness matrix using finite elements or finite differences, it still must be solved. Improvements in equation solving routines and eigenvalue routines will benefit both methods. Time integration procedures need to be developed. Transient response problems are generally costly to solve by either method and development of dynamic remeshing procedures in which remeshing occurs as the solution proceeds may lead to considerable improvements in efficiency for both methods. To effectively use remeshing techniques, you must be able to anticipate areas of high stress gradients. If this could be automated, the same process will perhaps work for both finite element and finite difference methods. Ideally, the user would specify an allowable error in a given quantity and the code would then automatically generate a mesh for him that would do that job. This intimate knowledge of truncation error could probably be applied to both finite element and finite difference methods.

Another problem is that of determining how to compare and evaluate different programs; programs with different degrees of freedom, with different unknowns, different accuracies, different capabilities. We need some set of norms to compare programs and check them out and to evaluate them. Finally, we need to answer the question, "Are few high-order elements better than many low-order elements, or alternately, is high-order differencing with a coarse mesh work better than low-order differencing with a fine mesh?"

STANTON: I'd like to begin by saying that the title of the session, Finite Elements Versus Finite Differences, may imply to some people that one or the other will prove to be intrinsically better. I don't believe that is the case. I started out using finite differences in thermal stress problems and dynamic response analyses and the thought that Sam Key expressed here just a moment ago was one of the first things that occurred to me. Namely, is there one to oneness in the methods or are there areas of speci-

alization in which one or the other is not applicable in its present state of development? There are areas of practical interest where the two methods do not overlap significantly and areas where they seem to overlap fairly strongly. In the latter case, the question of computational efficiency is certainly one of practical importance. The finite element methods seems to be increasingly used for nonlinear shell problems where the finite difference method had an earlier start and one thought that occurs to me is the rather mundane issue of generation times for the math model. I've been interested in and am working with incremental stiffness matrices for a higher-order shell element including prebuckling deformations in its interior, that has 48 degrees of freedom. Variations in the membrane stresses and bending displacements causes the generation time for these elements to become substantial and I wonder if the generation time for the coefficient matrices in the finite difference method may not be substantially less assuming, of course, that you have comparable accuracy. These are two thoughts that I would suggest for discussion.

JONES: That concludes the opening statements. What I'd like to do now is address several questions in panel and then turn questions over to the floor. Dr. Stanton, will you lead off?

STANTON: I'm sure the finite difference method applies to built-up structures, but many of the hardware stress analysts that I've worked with, especially the ones that have been steeped in the finite element method, are not familiar with all of the modeling techniques that are available to the finite difference method. Dave, will you enlighten me and maybe some of the rest of us on the modeling techniques that are available in the finite difference method--things like smearing out stiffeners?

BUSHNELL: Well, my experience with analysis of built-up structures is mostly with the BOSOR program applicable to shells of revolution. We have two ways of treating built-up shells of revolution: smearing out rings and strings, and/or treating rings as discrete. These models have nothing really to do with which numerical method you use--finite difference or finite element. "Smeared" stiffeners affect the constitutive law, or the

relation of stress resultants and moment resultants to strains and changes of curvature. The geometric and material properties of a stiffened structure are first taken into account in this law, the decision to use finite differences or finite elements can be made after that point in the modeling. The discrete ring is considered to be attached to the shell at a single point, and it has the same displacements and rotations as the shell at that point. The displacements of the centroid of the ring are expressed in terms of the shell wall displacements at the attachment point by means of simple transfer matrices. The ring cross section is assumed to be rigid. It can rotate and translate, but it is rigid. In this way each discrete ring is introduced into the structure as a stiffness coefficient matrix.

KEY: One of the beauties of a finite element code is the generality of geometry that is invariably contained in it. I'd like Roy Krieg to comment about how the finite difference method is going to be able to obtain the flexibility of mesh geometry inherent in the finite element method.

KRIEG: This conference has helped to dispel the old wife's tale that finite difference methods can't have flexibility of mesh geometry. I think all of the finite difference papers presented here have had variable size mesh in their finite difference grid work. However, there is one limitation with my own and most other finite difference codes and that is that we've been using rectangular meshes. As Jensen pointed out this morning, a triangular mesh does give you more flexibility in the actual shape and his work shows or explains how you can get around the limitations of a rectangular mesh.

I want to return to the dynamic remeshing concept. The details for the one-dimensional case have been worked out and are now operational in several wave propagation codes, in particular WONDY and PUFF. For example, consider the problem of a shock wave moving down a one-dimensional space. With dynamic remeshing you anticipate that a shock wave is approaching and automatically put nodes in front of the shock wave. After the shock wave has already passed and things are smooth, you remove nodes. In essence, it is an attempt to keep the finest mesh in the area of the greatest

action as it progresses with time. However, WONDY is a finite difference code. Sam Key, would you care to comment on how the finite element method can achieve that sort of flexibility?

KEY: Actually, there are two kinds of rezoning that go on in the finite difference method and one of them is deleting and inserting meshes or nodal points as you mentioned. The other approach that's available is a floating grid work. The coordinate system is moving relative to the material or relative to the problem and that's an extremely nasty problem mathematically. It's about all you can do to formulate the equations of motion, leave alone actually implement them. I don't know that the finite element method is going to have a very easy time of coming up with this capability. One of the things that you've got to do is actively create and destroy meshes and that means creating and destroying entries in a finite element stiffness matrix. I don't see any way to do it in the finite element context. You really have to bend the finite element method into what appears to be a finite difference method in order to get this kind of flexibility.

Let me change the subject. One of the things that occurs automatically in the finite element method is the symmetric stiffness matrix which reflects the fact that you start out with a self-adjoint system of differential equations. One of the most difficult things to obtain in the finite difference method is a symmetric stiffness matrix and, in my opinion, I think you've committed a transgression to come up with a nonsymmetric stiffness matrix in the finite difference method because you've altered the character of the problem. I'd like to know from either Ray Krieg or Dave Bushnell how you're going to resolve this problem in the finite difference method.

KRIEG: Ordinarily the finite difference method attacks a differential equation directly. If you hold onto that stubbornness and persist in it, I think you'll have a rough time. On the other hand, I think the way to go about it is as Bushnell and Almroth have done. Would you comment on that, Dave?

BUSHNELL: All you're doing with the energy method is taking an integro-differential form and making an algebraic form out of it. When you minimize or differentiate with respect to the dependent variables, you've got a symmetric matrix, sometimes positive definite and sometimes not, but symmetric in any case. As far as making self-adjoint differential equations have symmetric matrices, I guess they do until you get to the boundaries and then you have problems. You have boundary conditions and constraint conditions. That's what destroys the symmetry. But if the differential equation is self-adjoint and you use a uniform mesh with constant spacing, then you would get a symmetric matrix, wouldn't you--in the absence of boundary conditions?

KEY: Well, part of a self-adjoint system of differential equations are the boundary conditions that go with the differential equations. So what you're saying is that the real trouble comes in the finite difference method when you get to the boundary where the symmetry winds up being destroyed grossly.

STANTON: Very often in static stress analysis the variables that are of interest to the analyst are primarily the forces and not so much the displacements. They may not even be calculated in some applications, particularly if the force method is used. I think that given proper elements the redundant force method is a viable analysis tool for shell problems and there are elements, possibly even hybrid elements, that could be used in the force method without letting the number of degrees of freedom per node get out of hand. How would you formulate a finite difference procedure to compute the redundant forces in a shell structure?

KRIEG: I can't answer directly, but I think the way that I would attack the problem is through an energy principle. Whether you would have success in that regard, I'm not sure. But as far as attacking it directly from a differential equation standpoint, I'm not sure how to proceed.

JONES: Dave, would you like to add anything?

BUSHNELL: I would say you express some set of equations in terms of forces instead of displacements and apply finite difference techniques to these equations. There's nothing about either technique that says you can't use either displacements or stresses as unknowns. I guess it hasn't been done for the reason the force method just doesn't seem to be as popular as the displacement method. Complementary energy principles just don't seem to be as popular as minimum potential energy principles. In principle, there's nothing wrong with using either method applied to either technique. It just depends on what information you want out. I guess a lot actually depends on tradition--how much of a body of literature exists in a certain area. The straightforward physical aspect of the displacement method is more appealing than the force method and hence there is much more work in that area.

I'd also like to ask what is the state of the art in the application of the finite element method to problems involving composite structures and materials? For example, eccentrically stiffened or layered shells. We've seen a lot of literature on elements where there's a bending element and an extensional element but for built-up structures, we often have coupling between membrane and bending effects. For example, an eccentrically stiffened shell has what I would call coupling terms, that is, terms which couple bending moments and direct strains and direct stress resultants and changes in curvature. These coupling terms can be very important, indeed, as we've seen from the classical effect that external stiffeners on an axially compressed cylinder may increase the buckling load by a factor of two or more over internal stiffeners. I'm wondering how would one do a finite element analysis of an eccentrically stiffened shell?

STANTON: In yesterday's session, Warren Gibson from the Case Institute talked a little bit about FESTRAN which is a program with the capability of using discrete stiffener elements which have nodal degrees of freedom off the midsurface of the shell being analyzed. That particular stiffener element has been used at Case to look at things such as the effect of putting the stiffening on the inside of the shell as opposed to the outside. Also, Dr.

Montforton, while at Case, presented some work at the 1968 Dayton conference, in which he had a flat plate element with the stress resultants coupled in membrane and bending and he was able to correlate well with an elasticity solution for an unbalanced laminate. And in his presentation yesterday, I think that Warren Gibson solved thermal stress problems for a laminated strip and used a straightforward integration through the thickness giving an unbalanced laminate type coupling between the membrane and the bending action. At MDAC we are also doing some work along these lines very much similar to what Montforton had done. The materials people provide us with the coefficient matrices relating the stress resultants. Once these data are provided, we're able to use them in generating element stiffness matrices.

KEY: I think the answer is that we'll simply have to abandon isotropic shell theories that utilize a middle surface of constant thickness shell theories. That's really not very serious because there's plenty of information in the shell literature on how you develop a shell theory where the reference surface is arbitrary. It's relatively straightforward and to incorporate it in the finite element method simply means dealing with more coding and a lot more algebra in generating the element.

QUESTION: I'd like to direct my question to Sam Key. I was somewhat surprised with your answer to Bushnell's question. Such things as layered shells and variable thickness are very common. In the direct integration technique, the idea of a middle surface is now regarded as ancient. Is the finite element method really bound to a middle surface?

KEY: Not at all. What I was referring to when I said that we'd have to abandon the middle surface concept is that in doing development or research work in the finite element method, the question of isotropic or orthotropic materials is completely irrelevant. So, for convenience, most of the research work is based on isotropic materials. Among the codes in production use, you'll invariably find orthotropic materials and variable reference surfaces. That is, a reference surface whose location is arbitrary.*

JONES: The knowledge of just what material properties are independent is a big educational barrier to get across. For example, an orthotropic material doesn't just have one E and one ν . The shear modulus in a composite material is completely independent, yet it's surprising how little information is available on physical measurements of shear moduli. I think that we have to take the principal role in educating the materials people in perhaps just what to measure.

I also want to ask a question. How do the finite element and finite difference methods compare in required computer running time for solution of nonlinear problems such as in large deflection problems and plastic deformations? There are many other ways this question could be stated and many aspects of the problem, some of which already have been alluded to in the panel discussion, but I'd like each panel member to make an additional comment on this question because I think this is where one of the principal differences between the methods does arise.

BUSHNELL: Well, really this is a very difficult question and my reply to the question is six more questions. The first of these questions is how many degrees of freedom are required for a given accuracy? Obviously, the computer time depends on that. The second question is how much computer time or cost per degree of freedom is required for each formation of the stiffness matrix? That sounds like sort of a funny way to ask it, but sometimes stiffness matrices are formed while they are being decomposed in some programs and so the effective cost is less. A third question is how much computer time or cost per degree of freedom is required for factoring the linear equation system for each iteration? There are many methods around for factoring these systems. Given a matrix of a certain size, which methods costs the least? The fourth question is how many times per case must the stiffness matrix be formed? In various nonlinear methods, such as those referred to earlier, this might be a different number and obviously it's case dependent. A fifth question is how many times must the linear system be factored in a given case? The sixth question involves numerical conditions. Is double precision required for desired accuracy? In forward integration techniques, for instance, one can often get

by with single precision. However, in finite difference or finite element techniques, double precision is often needed.

JONES: I think these questions you raise point out just exactly how complicated the overall question is. It's not easy to sit down and make a simple statement comparing the methods. There are many aspects to the entire question.

KEY: I'd like to answer the question using specific numbers taken from a specific example. There was a very nice finite element thesis done at UC-Davis by Mark Hartsman. He used a two-dimensional finite element analysis, including nonlinear deformations and nonlinear material behavior, to solve shock wave propagation problems. I'd like to describe one particular problem that was tackled which involved wave propagation through a slab. Mark used elements arranged as shown in Figure 3. Symmetry boundaries on both sides of this mesh produce a one dimensional problem. A wave was initiated at $x=0$ and propagated into the region to $x=L$ and allowed to reflect from the boundary. The analysis was continued for a couple of transmit times and the computer time for that was about nine minutes of CDC 6600 CPU time. Well, the equivalent two-dimensional finite difference code, called TOODY, which can be used to solve the same problem is forced to use three rows of meshes as shown in Figure 3, in order to handle the boundary conditions. I have an estimate that seven minutes of CDC 6600 CPU time would be required for this problem. So you can see the finite element method is about 20 percent slower at this point. This really isn't the kind of problem that you want to do with a two-dimensional code. The one-dimensional finite difference code for this problem using the same mesh would take about two minutes and when you go to the dynamic rezoning where you're taking out meshes and putting them in as needed the time would drop to two-tenths of a minute. If you're going to write a one-dimensional wave propagation code with the finite element method, these are the execution times you're going to have to shoot for and the kinds of features these codes should have.

KRIEG: I think, as Sam Key does, that finite displacements

cient in terms of accuracy per unit of computer cost.

STANTON: I want to take minor exception with Ray's comments. In earlier experiences with plasticity problems, I had occasion to solve the same problem both with the finite difference technique and the finite element technique. It was a strip problem with a parabolically varying temperature field, one that Mendelson had studied. In that particular application, the finite element method for a given level of accuracy in the stress resultants was a little faster than the finite difference method. You may discount that somewhat because solution procedure used in the finite difference code was different, but this was a specific elastoplastic thermal stress problem in which a higher-order finite element, one that was bicubic, was able to do a fairly nice job on the stresses with a coarse mesh, whereas a central difference operator in the finite difference approach required that I use a fine mesh to get the similar stress accuracy. I'm not having the same sort of experience in the geometrically nonlinear area where I'm coming up with long generator times on some of these incremental stiffness matrices. I would have to agree with the general opinion that the finite element method is usually longer running, especially for problems that are essentially one-dimensional in nature.

JONES: Before we open the discussion to the audience, I would like to ask Dr. Gerald Wempner and Dr. Liessa to present their prepared comments.

(Edited versions of comments by Wempner and by Liessa appear at the end of this panel discussion.)

COMMENT: I would like to comment on the efficiency of the two methods. If we confine ourselves to problems which have neatly defined surfaces and easily defined regular grid, then some comparisons on the run time between what we consider an efficient finite element and efficient finite difference program are useful. The regular grid helps the finite differences in terms of setting up the matrix. It takes hardly any time. The time for factoring is about the same as the finite element method

with elements having the lowest possible numbers of freedom. For some different cases, including the vibration of a cylinder with a cutout and the pear-shaped cylinder which Dave Bushnell discussed in his paper and one more case, we found a factor of between two and a half and three in run times between finite elements and finite differences with the finite difference being the faster. Those times apply if the grid is the same in the two cases. We have made a much more restricted comparison between the convergence of the two methods and Bushnell's paper illustrates that we needed twice as fine spacing for the finite elements to achieve comparable accuracy with finite differences.

When you use the finite difference/energy method, you must determine the coefficients of the first and second fundamental forms of the shell surface. The analytical expression for the energy contains these coefficients of the fundamental form and derivatives of the displacements. For both finite elements and finite differences, the derivatives of displacements are determined numerically but when we use finite differences, in the way we generally apply it, we use analytically determined coefficients in the fundamental form while in finite elements we define only the coordinate points and I assume that means we are taking these derivatives numerically. If we go to more complicated structures, with more complicated boundaries, but still nice and smooth, or mathematically well defined surface, or if you want to concentrate the points, we can still determine the coefficients of the fundamental form analytically provided that the shell surface is smooth or mathematically defined, and I think we'll continue to be more efficient with finite differences. If you go still further and say the surface is not suitable to mathematical definition, then we would have to determine also the Lamé' coefficients by taking numerical derivatives and I think it's an open competition between the two methods. I probably would put my bet still on finite differences.

Finally, if we go to a structure which really is not a continuum but is discontinuous to start with, I'll say that finite differences are generally out.

QUESTION: My question refers to the bread and butter problem-- static stress and deflection analysis of linear structures. I don't ask it of the finite difference people because I accept it is the same as the finite element and I've already asked the finite element people. We do get production stops in the stiffness approach due to loss of numerical significance. A number of years ago, Denke was able to point to production runs approaching 1000 with no stops due to loss of numerical significance. This is with the force method of finite element analysis. I'd like to ask the panel to comment on that subject in general.

STANTON: First of all, let me say that I'm sure in that problem of 1000 that the number of redundants was probably no where near that, but Dale Warren is here in the audience and he is a lot more familiar with the latest developments. Would you like to take a shot at that, Dale?

WARREN: I have a slide to show tomorrow that summarizes the production analysis done on the DC-10 using the force method. As I recall them right now, the structure was divided into two major areas, each totaling in excess of 20,000 unknowns. These were further divided into substructures, five I believe, each having on the order of 1,000 to 6,000 unknowns. This required solution of simultaneous equations in the structure cutter of the force method of roughly two-thirds of these sizes total. We found only one instance of a job failure associated with any kind of conditioning problem. This is all done with single precision on a 36 bit machine. This one occasion was where a substructure was unwisely selected--a boundary on a unit of the complete composite was not well chosen; it was not more than a one-week exercise to correct that and proceed.

QUESTION: My question is addressed to the whole panel. In finite element methods there exist many hybrid models where you can start a problem assuming stress and finally using displacements as unknowns mixed together in the regular displacement method. Is there an equivalent method in finite difference?

BUSHNELL: It sounds, at least this late in the afternoon, like the

other question: can you use the complementary energy method or mixed energy method with finite differences? Again, I don't see why not. And as to whether it's been done or not, I don't know.

COMMENT: I think anything the finite element method can do, the finite difference/energy method discussed by Dr. Bushnell can also do, and vice versa. Both are concerned with evaluating a functional. In the finite element method, you use explicit interpolation functions; in the finite difference/energy method, you use implicit interpolation functions in a sense that you replace the first derivative by a difference expression and which implies a linear function and so forth. In fact, if you take the plane stress, constant strain triangle finite element and use Dr. Bushnell's method, you come up with exactly a finite element method, if you choose your finite differences in the right way. So I might suggest a better division of the topic is differential equation method versus direct variational method instead of finite elements versus finite differences. Now what I think distinguishes the finite element method from others is that you deal with that region you call an element. You may think of it as a physical element or a mathematical region, but what we do for the element does not depend on anything else outside. Then, you build up your whole structure just by superimposing one element after another. I think this is an essential feature of the finite element method. Now Dr. Bushnell's method may include this and may go beyond it actually because when he evaluates his integrals in the domain, he integrates over an area. That area may be considered a finite element provided all his derivatives depend on things in or on a boundary of that area. But if he goes beyond, then his method would be different. But both fall, I think, into the domain of direct variational methods.

BUSHNELL: Well, I'll just make a quick comment. It does go beyond and, in fact, this was the reason for Budiansky's title on his paper "Nodes Without Elements." There are, of course, node points outside the elemental areas of integration.

JONES: I don't think we've resolved whether there will be any

survivor of the battle between finite elements and finite differences. I'm sure they will both continue. Hopefully, I think we have a better perspective of what some of the advantages and disadvantages of each of the methods are. It is not a simple comparison to make. There are many aspects of numerical computation and material models and so on to consider. Without considering each and every one of those aspects, I don't think the question can be answered yes or no. Thank you very much.

STATEMENT FOR PANEL B

by

Arthur Leissa

Professor of Engineering Mechanics
Ohio State University

The attention of this conference has been primarily focused on those methods of computer-oriented shell analysis which deal with discrete models, namely the finite element and finite difference methods. While these methods have great versatility and capability, there are many types of problems which can be analyzed more accurately and with less computer time and cost by methods using continuous variables.

Two methods which depend upon using continuous variables are point matching and its generalization, the method of boundary point least squares. These two methods are examples of a class of weighted residual methods which use exact solutions of governing field equations while satisfying boundary conditions either exactly or in the least squares sense at a finite number of boundary points. These methods have been used with great success on various boundary value and eigenvalue problems of structural analysis, including the analysis of shells. They rely heavily upon the digital computer for the formulation of the pointwise boundary conditions, the solution of the resulting large sets of simultaneous equations or characteristic determinants, and evaluation of the solutions at desired points throughout the shell.

The point matching and boundary point least squares method have been used by the author to determine:

1. Stresses and deflections in shallow spherical shells having edges which are non-circular and non-rectangular and having various types of edge restraint.

2. Stresses and deflections in the vicinity of a rigid insert in a shell. The insert is loaded and of arbitrary configuration.
3. Stress concentrations in the vicinity of cutouts in shells. The cutouts may be noncircular.

Some of the advantages of these methods over the finite element and finite difference procedures include:

1. Capability of fitting irregular boundaries simply and straightforwardly.
2. Satisfaction of the shell equilibrium equations exactly at every point in the structure.
3. Capability of representing rapidly changing functions (including load singularities) such as bending stress in a shell smoothly and with no particular difficulty.

The greatest disadvantage of the methods occurs when a general set of solution functions to the equilibrium equations cannot be obtained, such as in the case of a shell having continuously varying thickness or for the nonlinear, large deflection shell equations.

FINITE-DIFFERENCES VIA FINITE-ELEMENTS

by

G Wempner

The University of Alabama in Huntsville

A discussion of:

"Finite-differences versus finite-elements"

The following comments are offered in the hope that they will place "finite-differences" and "finite-elements" in a certain perspective. From our viewpoint, the method of finite-elements appears as a means to derive finite-difference equations of a particular kind. Hopefully, the advantages and disadvantages will be more evident from such a vantage point.

The technique of finite-elements provides a means to approximate a continuous field by discrete values. Usually, the desired function(s) belongs to a particular class and provides a stationary value of a given functional. The approximation provides a stationary value among a subclass of spline functions, i.e., functions defined by nodal values and prescribed interpolating functions. The algebraic equations which determine the approximation must approach the Euler equations of the continuum theory as the element diminishes. In other words, the resulting algebraic equations are difference equations.

To illustrate the point, consider an equilibrium condition of "Plane-stress" as required by the expression of virtual work:

$$\iint_S (S_{,1}^{11} + S_{,2}^{12} + f^1) \delta u \, dS = 0 \quad (1)$$

Now, in the method of "finite-elements", the function δu is approximated by a spline function. For example, if Lagrangian interpolation is used, then the function is expressed in terms of nodal values:

$$\delta u = \delta u_{MN} f^{MN}(x_1, x_2) \quad (2)$$

Here the suffix signifies the node $(x_1 = x_M, x_2 = x_N)$ and summation is implied by the repeated suffix. In the manner of Ritz, the functional is rendered stationary with respect to variations of the nodal values. The stationary conditions follow:

$$\iint_S (s_{,1}^{11} + s_{,2}^{12} + f^1) f^{MN} dS = 0 \quad (3)$$

Observe that the discrete conditions are a weighted average of the Euler equation. Moreover, the averaging extends over a finite subregion about the node $(x_1 = x_M, x_2 = x_N)$ since the weighting function f^{MN} is nonzero only in the region of elements adjacent to the node.

If the condition (3) is obtained by the stationary theorem of E. Reissner, then the stress and displacement are treated as independent variables and each is approximated by a spline function. If Lagrangian interpolation is used, then the stresses and load are approximated in the form of (2), and the condition (3) takes the following form:

$$s_{MQ}^{11} \iint_S f_{,1}^{MQ} f^{NP} dS + s_{MQ}^{12} \iint_S f_{,2}^{MQ} f^{NP} dS + f_{MQ}^1 \iint_S f^{MQ} f^{NP} dS = 0 \quad (4a)$$

For simplicity, we can normalize the coordinates and utilize an element of unit length and width. Then, (4a) takes the explicit form:

$$\begin{aligned} & \frac{4}{3} \left(s_{(M+1)Q}^{11} - s_{(M-1)Q}^{11} \right) + \frac{1}{3} \left(s_{(M+1)(Q+1)}^{11} - s_{(M-1)(Q+1)}^{11} \right) \\ & + \frac{1}{3} \left(s_{(M+1)(Q-1)}^{11} - s_{(M-1)(Q-1)}^{11} \right) + \frac{4}{3} \left(s_{M(Q+1)}^{12} - s_{M(Q-1)}^{12} \right) \\ & + \frac{1}{3} \left(s_{(M+1)(Q+1)}^{12} - s_{(M+1)(Q-1)}^{12} \right) + \frac{1}{3} \left(s_{(M-1)(Q+1)}^{12} - s_{(M-1)(Q-1)}^{12} \right) \end{aligned}$$

$$\begin{aligned}
& + \frac{4}{9} f_{MQ}^1 + \frac{1}{9} \left(f_{(M+1)Q}^1 + f_{(M-1)Q}^1 + f_{M(Q+1)}^1 + f_{M(Q-1)}^1 \right) \\
& + \frac{1}{36} \left(f_{(M+1)(Q+1)}^1 + f_{(M+1)(Q-1)}^1 + f_{(M-1)(Q+1)}^1 + f_{(M-1)(Q-1)}^1 \right) = 0
\end{aligned}
\tag{4b}$$

Equation (4b) is our discrete counterpart of the Euler equation and approaches that differential equation as the elements shrink.

We may ask: What is the distinguishing feature(s) of the difference equations obtained via finite-elements? Firstly, the equations are obtained by a consistent application of the Ritz technique. The stationary conditions are imposed upon a subclass which approximates the continuous field as closely as computer time and storage permit. Secondly, a higher-order approximation usually entails the introduction of higher-derivatives (rather than additional nodal values).

To illustrate the higher-order approximation of finite-elements, consider a one-dimensional problem wherein we seek an approximation $S(x)$ satisfying the stationary condition:

$$\int_0^L \frac{dS}{dx} \delta u \, dx = 0$$

The simplest difference-equation is achieved by a linear interpolation between adjacent nodes ($x = x_M, x_{M+1}$). Usually, the higher-order difference-equation is obtained by quadratic, then cubic approximations, etc., accompanied by one, then two, or more, intermediate nodal values of the function 'S'. In the method of finite-elements, no additional nodes accompany the cubic interpolation; instead, nodal values of the derivatives are introduced. Then the stationary theorem provides two difference equations for each node as the nodal values of the function and derivative are variable. The additional difference equation is the discrete approximation of $d^2S/dx^2 = 0$. The result is quite natural, for we introduce the derivative(s) because the continuum theory requires the

existence of the derivative(s), e.g., in the Kirchhoff theory of plates the continuum theory requires the first and second derivatives and so our approximation must possess the discrete counterparts, the nodal values of the function, first and second derivatives. Stated otherwise, as the class of functions in the continuum theory requires derivatives, so the subclass of spline functions requires the corresponding nodal values.

SHELL ANALYSIS WITH LARGE GENERAL PURPOSE PROGRAMS

by

Caieb W. McCormick

Director of Engineering Analysis
The MacNeal-Schwendler Corporation

Introduction

During the last several years a number of general purpose programs for structural analysis have been developed. Many of these programs treat both static and dynamic analyses. While several of these general purpose programs include a restricted nonlinear capability, they are basically programs for linear structural analysis. Most of the nonlinear analysis capability still resides in the smaller, special purpose codes. Although these programs have used finite element methods for model definition, there is no fundamental reason why finite difference procedures could not be included in a well-designed general purpose program. Most of these programs, particularly the most recently developed ones, use the displacement method of problem formulation and solution.

This paper discusses the development and use of large general purpose computer programs for structural analysis. The use of finite element modeling procedures and the displacement method of problem solution are assumed for the following discussion. The main additional requirement of a general purpose program to make it suitable for shell analysis, is that it include an adequate library of finite elements for the representation of shell structures.

General Purpose Requirements

The most important requirement of a general purpose program is that it have a modular design. The modularity allows one to make modifications and additions to the program in a reasonable amount of time and for a reasonable cost. The ability to make modifications and additions is important if a program is to maintain its usefulness for an extended period of time. Since the initial cost of a general purpose program is high, it is desirable to maintain the usefulness of the program over as long a period as possible. This means that one must be able to substitute new matrix routines and add new finite elements as the state of the art develops, to modify routines to take advantage of new hardware developments in secondary storage and arithmetic processors, and to extend the program to include new problem areas, perhaps even outside the field of structural analysis.

There are a number of considerations in the design of a modular program, but the primary requirement is that the calculations and data processing be accomplished by independent subprograms that are not allowed to communicate directly with each other. This requirement suggests the need

for an executive program to control the execution sequence of the independent subprograms and to manage all communication. Small amounts of frequently used information can be held in main memory, but most of the data will have to be stored on secondary devices (disks, drums, tapes), in order to preserve the main memory for working space. In any case, the executive program must store and retrieve information for the subprograms upon their request.

The control of the sequence of execution of the individual subprograms may be either under user control or program control, using a finite number of stored tables. The most generality is achieved by allowing the user to control the sequence of module executions. However, it is time consuming for the user to prepare the necessary instructions and there is a high probability of failure on the first attempt for a given problem. The use of rigid formats, in the form of stored tables, relieves the user of the responsibility of controlling the sequence of operations. It is believed that a general purpose program should provide both the generality of direct user control and the ease and reliability associated with the use of rigid formats. The generation of rigid formats imposes an additional burden on program development, while direct user control requires greater understanding of the program and additional input preparation on the part of the user.

The success of any general purpose program is largely dependent on the quality of the basic matrix operations that are available in the program. The matrix routines must be reliable and efficient. The following list of matrix operations should be available:

1. Decomposition
2. Multiply-Add
3. Add
4. Partition and Merge
5. Transpose
6. Solution of Linear Algebraic Equations
7. Extraction of all of the eigenvalues and eigenvectors
8. Extraction of all eigenvalues and eigenvectors in a specified range
9. Integration of Linear Differential Equations

All matrix operations should allow for single, double, or perhaps higher precision arithmetic. All routines, except the integration of equations, should be available for both real and complex arithmetic. The decomposition routines should be available in both symmetric and unsymmetric versions.

The preliminary draft of a survey on shell analysis was distributed as background information for this conference¹. It is stated in this survey that an efficient and reliable technique is needed for the extraction of all eigenvalues in a specified range. The inverse power method with shifts² is an effective procedure for extracting all eigenvalues in a specified range. This procedure has been operational in the NASTRAN program since August 1968.

The success of a general purpose program is also dependent on the quality and variety of finite elements that are available. Since there are wide differences of opinion among structural analysts regarding the use of finite elements, it is important that the library of elements be as inclusive as possible and that provision be made to add elements to the library. The following is a list of elements that are useful in shell analysis:

1. Flat triangular and quadrilateral shell elements
2. Doubly curved triangular and quadrilateral shell elements
3. Beam elements with offsets
4. Solid elements - tetrahedron, wedge, and hexahedron
5. Conical shell elements
6. Doubly curved axisymmetric elements
7. Solid axisymmetric elements.

In order to model stiffened shells and other more complex shell structures, it must be possible to combine elements in the above list. In particular, the combination of axisymmetric elements of different types, and axisymmetric elements with nonaxisymmetric elements is desirable. The latter may require the use of multipoint constraints (linear relationship among selected degrees of freedom). The use of multipoint constraints permits the use of one-dimensional shell elements for problems that are basically axisymmetric, but have loads, masses, boundary conditions or limited amounts of structure that are not axisymmetric. This procedure permits the treatment of problems that have only modest departures from axisymmetry as modified one-dimensional problems. If the structure departs radically from axisymmetry, it should be modeled as a two-dimensional problem.

1 Hartung, Richard F., "An Assessment of Current Capability for Computer Analysis of Shell Structures", AFFDL Technical Report, February 1970.

2 MacNeal, Richard H., Editor, NASTRAN THEORETICAL MANUAL, NASA SP-221, Section 10.4.

Some of the more recently developed finite elements use derivatives of displacements as degrees of freedom in the formulation of the stiffness matrix. In order to include these elements, provision must be made for more than the usual six degrees of freedom at each grid point. Provision must also be made to accommodate the larger than usual number of grid points that are used in the formulation of the stiffness matrices for some of the recently developed finite elements.

Since there are a number of different computers that are suitable for the execution of general purpose programs, it is desirable that the program be written in a language that is acceptable to as wide a range of computers as possible. This imposes an additional burden on the development of the program, but a program cannot be considered to be truly general purpose if it is designed for a single piece of hardware. The program should not only be designed to take full advantage of the kinds of hardware that are available, but also to modify the instructions to the executive program at execution time in order to take full advantage of the hardware that is available for a particular run. These modifications are associated with such things as, the amount of main memory available, the amount and type of secondary storage available, the size of physical blocks to be written on secondary devices, and the type of plotter that is available.

Large Problem Requirements

The solution of very large problems imposes additional requirements on a general purpose program. Probably the most important requirement for a general purpose program, that is intended to solve large problems, is that it must include effective sparse matrix routines. Both the storage requirements and the computing times are excessive if full matrices are used in the solution of large problems. A full tape or a complete disk pack is required to store a single full matrix of 2,000 order. Even the largest and fastest computer requires about five hours to multiply two matrices of 2,000 order and about half as much time to make a symmetric decomposition of a matrix of 2,000 order. The average third generation computer would require more than an order of magnitude longer to perform these operations on 2,000 order full matrices. This means that if problems of several thousand order are to be solved in a reasonable amount of time and for reasonable cost, the problems must be formulated in terms of sparse matrices, and either reasonable sparsity must be maintained, or effective matrix reduction techniques must be used to reduce the order of the problem.

In addition to routines for sparse matrix operation, utility routines must be provided to pack the sparse matrices so that only nonzero terms are stored on secondary devices. These utility routines assemble the data into physical blocks that are appropriate for the particular type of secondary device that is being used. The efficiency of the packing routines is particularly important for large problems, as all intermediate results should be placed on secondary storage devices in order to reserve the main memory for current matrix operations. This results in extensive use of the packing routines with resulting significant effect on total computing time.

it is important in shell analysis that the matrix operations be performed with truly sparse routines, and not be limited to operations within a defined band. There are many shell problems for which the matrices are reasonably well banded, but have a few widely scattered coupling terms. Some examples are branch shells, axisymmetric shells in which multipoint constraints have been used to couple some or all of the harmonics, and two dimensional shells with a modest amount of internal structure.

In order to minimize computing time for large problems, it is necessary to have as large a fraction as possible of the main storage available for each matrix operation and thereby minimize the use of secondary storage. This dynamic use of main storage can be accomplished if the executable program is well overlaid, and the executive program monitors the available core storage and advises each subprogram at execution time as to the amount and location of main storage that is currently available. The matrix routines must in turn be designed to utilize whatever storage is available in the most effective way.

It is important in shell analysis that arbitrary limits not be placed on the order of problems that can be handled by the matrix routines. Some problems, such as axisymmetric shells with a large number of harmonics or when a large number of simple shells are connected in series, result in large order, but rather narrowly banded matrices. In such cases, the core requirements and computing times are not great, but arbitrary limits on problem size frequently preclude their solution.

Since main storage must be preserved for current matrix operations, all of the intermediate and final results generated by the program must be written on secondary storage devices. Moreover, a very large number of separate data blocks are generated in each problem solution, and since many of these data blocks are needed only during a portion of the solution process, it is desirable to use the secondary storage space in a dynamic manner. The dynamic allocation of secondary storage, as well as the reading and writing of information on secondary devices, are tasks that must be reserved for the executive program. The executive program must be prepared to handle data blocks that vary widely in size. In order to effectively handle files of varying size dynamically, it is necessary for the executive program to maintain a pool of secondary storage space, unless this service can be provided by the resident operating system. In any event, problem size may be limited by the availability of sufficient secondary storage space. Moreover, the extensive use of secondary storage requires that efficient input/output routines be provided for the executive program if large problems are to be efficiently solved.

The formulation of stiffness matrices (also mass matrices in the case of consistent mass formulation) may consume a large fraction of the total computing time. This is particularly true for the newer, more sophisticated finite elements. On the other hand, the longer computing time per element is at least partially offset by the fact that fewer elements are required

in the model. In any event the computing time is significant, and for large problems consideration must be given to the fact that only a portion of the stiffness matrix can be held in main memory.

The general question of matrix assembly will be discussed with reference to Figure 1. The initial, straight portion of the solid line indicates the linear growth of matrix assembly time with problem size when the complete stiffness matrix can be held in main memory. The curved portion of the solid line indicates the rapid growth in matrix assembly time with problem size, when the stiffness matrix is assembled from element stiffness matrices that are stored on a sequential access secondary storage device.

The dashed line in Figure 1 indicates a linear growth in matrix assembly time for the case when the required partitions of the element stiffness matrices are regenerated at each grid point. The slope of this line is proportional to the number of grid points connected to each finite element. This procedure will be superior to the use of sequential access devices for large problems. The location of the crossover point will depend on the ratio of the time to generate an element stiffness matrix and the time required to retrieve the same information from a secondary storage device.

The dotted line in Figure 1 indicates a linear growth in matrix assembly time when the element stiffness matrices are retrieved from a direct access secondary storage device. The slope of this line is proportional to the time to generate the stiffness matrix for a single element plus the time required to retrieve the element stiffness from a direct access device. The total time to generate a stiffness matrix, using direct access devices should be only slightly greater than when the entire stiffness matrix can be held in main memory.

It has been shown³ that double precision (60-70 bits) floating point arithmetic is necessary for both stiffness matrix formulation and static solutions if problems containing more than a few hundred grid points are to be solved with reasonable accuracy. Examination of Figure 2 indicates that, if double precision arithmetic is used in the formulation of the stiffness matrix, one-dimensional problems having a thousand grid points, and two-dimensional problems having a hundred thousand grid points, can be solved with an accuracy of several decimal digits in the solution. On the other hand, the use of single precision arithmetic would restrict one-dimensional problems to less than a hundred grid points and two-dimensional problems to not much over a hundred grid points. Examination of Figure 3 results in similar conclusions for errors associated with the solution of the equilibrium equations. The error in the equation solution is largely in the decomposition of the stiffness matrix.

Substantially greater errors than those indicated above will result if isolated finite elements are significantly stiffer than the rest of the structural model. An isolated element that is two or three times stiffer than the rest of the model can cause an additional loss of two or three

3 MacNeal, Richard H., Editor, NASTRAN THEORETICAL MANUAL, NASA CP-221, Section 15.1.

decimal digits in the solution. Errors associated with extremely stiff elements can be avoided if such elements are replaced with rigid elements in the structural model. Consequently, provision should be made in all general purpose programs, using the displacement formulation, for the use of rigid elements.

Provision must also be made to guard against errors associated with solutions obtained from poorly conditioned stiffness matrices. If the equation to be solved is

$$[K]\{u\} = \{P\} \quad (1)$$

where $[K]$ = stiffness matrix

$\{P\}$ = applied load vector

$\{u\}$ = displacement solution vector

a residual vector, $\{\delta P\}$, can be determined for each solution vector as follows:

$$\{\delta P\} = \{P\} - [K]\{u\} \quad (2)$$

The residual vector can be used to calculate the following error ratio.

$$\epsilon = \frac{\{u\}^T \{\delta P\}}{\{u\}^T \{P\}} \quad (3)$$

This error ratio is the ratio of the energy associated with the residual load vector to the energy associated with the applied load vector. The magnitude of this error ratio gives an indication of the numerical accuracy of the solution vector. A somewhat more time consuming operation is to solve the equation

$$[K]\{\delta u\} = \{\delta P\} \quad (4)$$

where $\{\delta u\}$ gives a direct indication of the roundoff errors associated with the solution of Equation 1. In any event, none of the results associated with the use of the residual vector can be any more accurate than the residual vector itself. The residual vector will only have order of magnitude significance, unless higher precision is used in Equation 2 than is used in the solution of Equation 1.

Under many circumstances, parts of previous solutions can be used in succeeding solutions. This suggests that the executive program should contain some form of checkpoint and restart capability. The use of previous

Intermediate results is particularly important in large problems where substantial amounts of time may have been invested in the initial solution. In the case of unscheduled exits due to program errors, machine failure, or user errors, restarts can be made following correction of the error. This restart procedure will usually result in the saving of most of the time already invested in the partial solution. Scheduled exits, followed by restarts, may be made to examine intermediate results before proceeding with the solution. Following completed solutions modified restarts may be made to request additional output, or to obtain solutions for new boundary conditions and/or new loading conditions. These modified restarts can be completed by using only a fraction of the computer time required for the initial solution.

The restart capability may be considered in two parts. First, the executive program must write all data blocks that may be needed for restart on a secondary storage medium that can be saved, probably a tape. The second, and far more difficult task, is for the executive program to select those data blocks that are useful under any particular set of restart conditions. In order to make this selection, the executive program must consider such things as, was the previous solution completed, have any changes been made in the finite element model, have any changes been made in the boundary conditions or loading conditions, and has a change been made in the type of solution to be made, such as statics the first time and dynamics the second time.

The basic input for large problems may easily consist of several thousand cards. Most of this information is usually associated with the geometry of the finite element model. There are two serious problems associated with the preparation of large amounts of input data. First, it is time consuming, and secondly, it is difficult to detect errors in the data. Therefore, it is highly desirable to provide procedures that will take advantage of any regularity or special characteristics of the model, and generate the bulk of the input data with the program. For example, in the case of two-dimensional structures, it is convenient to specify the locations of the grid points at the boundary and allow an input generator to generate the geometrical information for the interior points. These input generators may either be part of the general purpose program or they may operate as auxiliary routines.

The presentation of the results is an important consideration where large problems are concerned. In particular, the user must be able to select only that output which he wishes from the large volume that may be available. Since it is difficult for the user to interpret large volumes of printed results, graphic output is an important consideration. Structural plots of the undeformed and deformed structure should be available as well as curve plots for various structural responses. Punched output is frequently useful as input to other programs. These auxiliary programs may themselves be concerned with the presentation of results in a more meaningful form.

Solution of Large Problems

Any well-designed general purpose program will probably solve shell problems larger than one is willing to pay for. Although the amount of available secondary storage may limit problem size, the most likely limit is computing time. Static solutions for shell structures having a few thousand grid points can be completed in about one hour on the larger third generation computers. For larger problems and limited main storage availability, it may be necessary to use structural partitioning in order to avoid excessive use of secondary storage devices during the triangular decomposition of the stiffness matrix. Assuming double precision arithmetic, structural partitioning will not reduce the computing time unless the main storage available for the triangular decomposition is less than the square of the semiband of the stiffness matrix, or more generally, less than the square of the maximum number of nonzero columns that exist at any stage of the decomposition. Structural partitioning may also be required because insufficient secondary storage is available for intermediate results.

If only a few vibration modes are required in a specified range or ranges, the inverse power method with shifts is the most effective procedure. It requires about twice as long to extract a single eigenvalue as to complete a static analysis. If a large number of eigenvalues are required, it is far more efficient for large problems to reduce the stiffness and mass matrices to five or 10 per cent of their initial size, and extract all the eigenvalues, after first reducing the dynamic matrix to tridiagonal form. The inverse power method with shifts is particularly effective for buckling problems where usually only one, or at most a few, buckling modes are required.

In dynamic response problems, the user should have the choice of a direct formulation or a modal formulation. In the direct method, the dynamic degrees of freedom are the displacements of the grid points in the finite element model. This procedure is satisfactory for large problems if the number of frequencies or the number of time steps to be considered is small. If the number of time steps or frequencies to be considered are large, it may be more efficient to reduce the stiffness, mass, and damping matrices to five or ten per cent of their initial size, and then proceed with the response calculations using the smaller dense matrices, rather than the larger sparse matrices.

In the modal method of dynamic problem formulation, the vibration modes of the structure, in a selected frequency range, are used as degrees of freedom, thereby reducing the number of degrees of freedom while maintaining accuracy in the selected frequency range. The modal method will usually be more efficient in problems where a small fraction of all the modes are sufficient to produce the desired accuracy and where the number of frequencies or time steps to be considered are large. For very large problems, it may be desirable to use a modal combination procedure, wherein the vibration modes are determined for a number of substructures rather than for the structure as a whole. The modal results are then combined to form a complete model for which response calculations are performed.

Advantages and Disadvantages of General Purpose Programs

Large general purpose programs for structural analysis have a number of advantages as well as disadvantages. The following lists conclude this paper:

Advantages of general purpose programs.

1. Only have to learn how to use a single program in order to solve a large class of problems.
2. General purpose programs are more likely to be user oriented, whereas special purpose programs are frequently low budget, and hence less likely to be user oriented.
3. Easy to add new capability to the program, while taking full advantage of all utility routines, matrix operations, and other services provided by the basic general purpose program.
4. If, through wide use and/or government support, the cost of obtaining the program is small enough, the smaller organizations can have a far greater problem solving capability.
5. Proper modular design allows quick implementation of the latest in the state of the art for matrix operations, finite elements, new solution techniques, etc., without expending effort to modify unneeded parts of the program.

Disadvantages of general purpose programs.

1. High initial cost of program development.
2. Requires continuous centralized maintenance to correct errors, make additions, and maintain the integrity of the program.
3. Special purpose programs are faster in execution. However, the advantage is likely to be greatest on small problems where the total computing time is small. In any event, good program development can minimize this difference.
4. Most users have to use the program as delivered, as it is unlikely that the average programming staff can make changes in a large sophisticated program.
5. Some form of initial training in the use of a general purpose program is likely to be required.
6. Even if the initial cost of the program is low, a budget must be provided to keep the program operational at any particular facility.

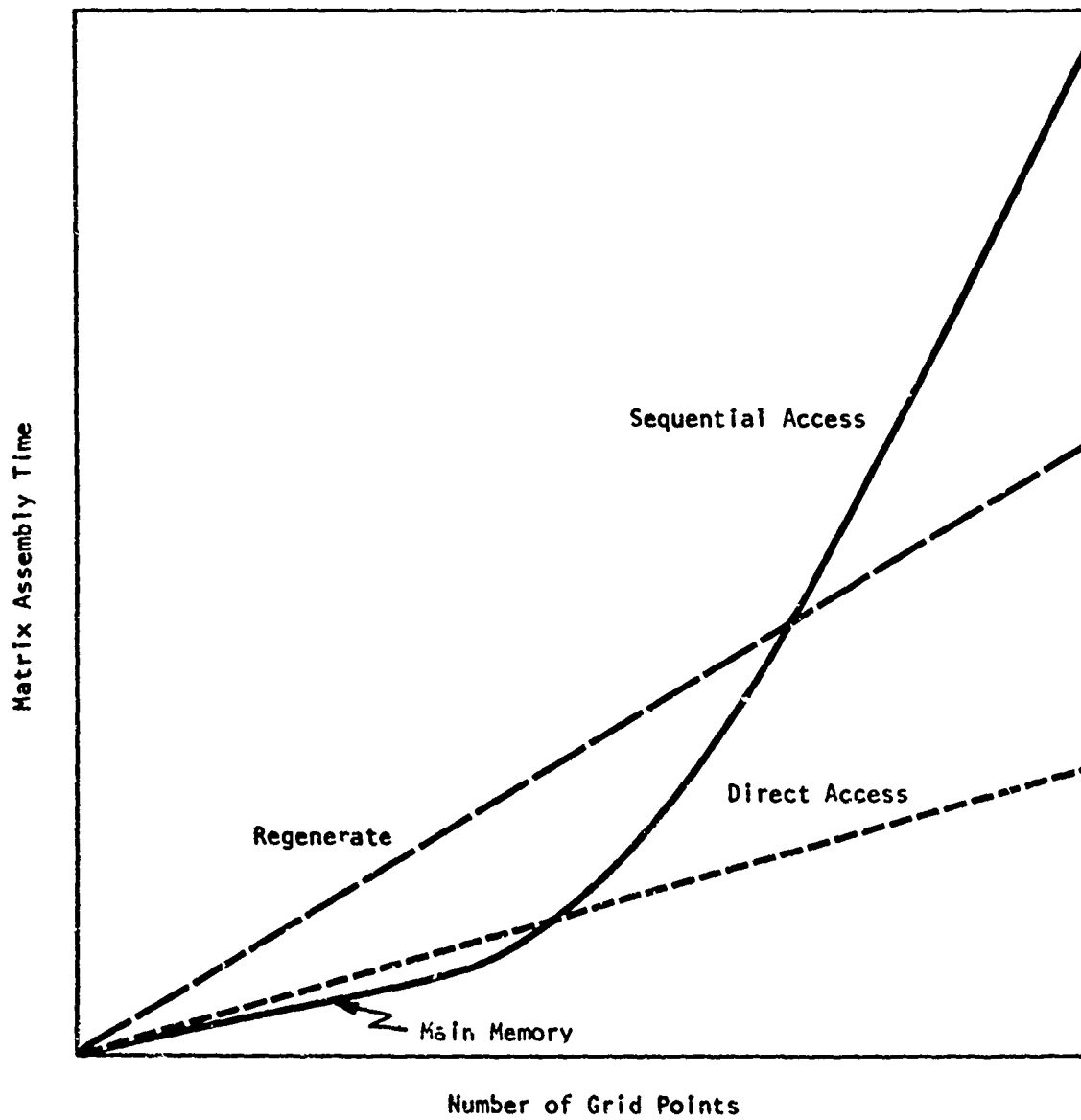


Figure 1. Comparison of Matrix Assembly Procedures.

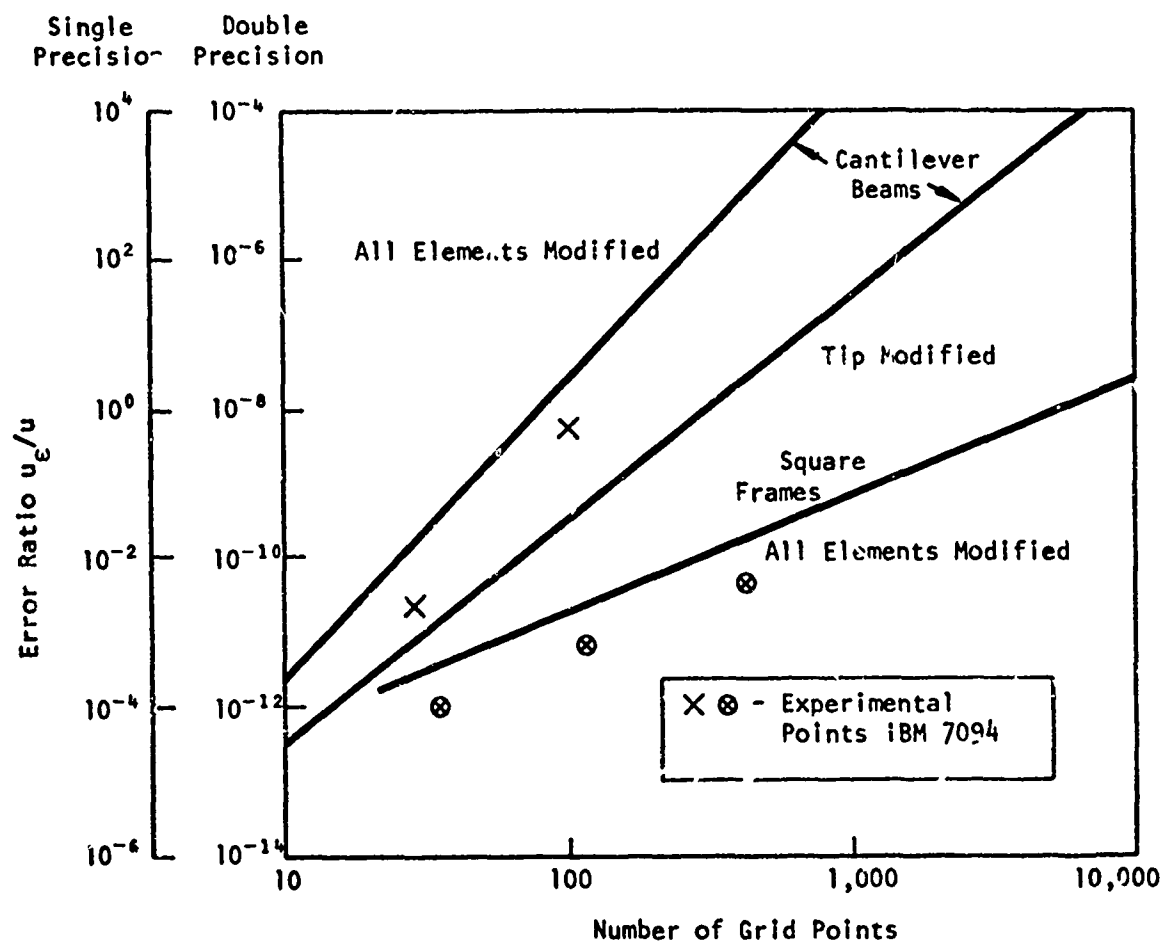


Figure 2. Effect of Stiffness Matrix Error in Static Solutions.

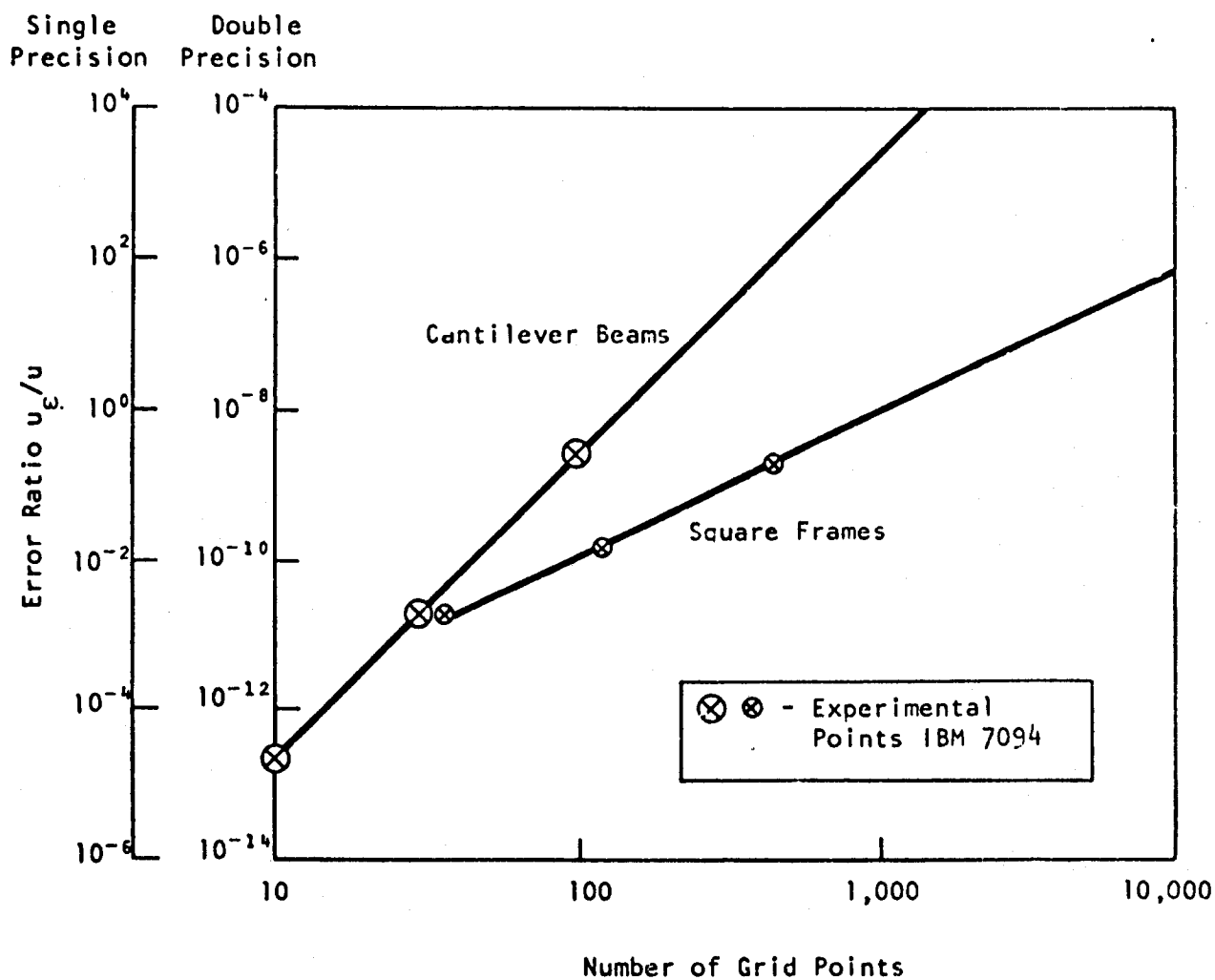


Figure 3. Effect of Roundoff Error in Static Solutions.

QUESTIONS AND COMMENTS FOLLOWING MCCORMICK'S PAPER

QUESTION: I'd be interested to hear your comments on what the best way would be to make a capability like this available. Do you have one single copy of the program and make the capability available through some kind of a network or do you make thousands of copies and everybody in every small shop has one? The optimum must be somewhere in between there and I'm sure you've given it a great deal of thought at this point.

MCCORMICK: I'm not sure I can answer it, but I'll give you my thoughts. First, I would preface my answer by the fact that, in general, the larger computers are more effective and less costly for solving large problems. This means that you would like to run on the larger, and preferably the largest, computer available. This tends to lead away from running the programs in your own shop because most shops can't have the largest computer available. So I think there's a lot to be said for having central facilities where the program is maintained, particularly now with the hardware terminals being as good as they are. You can have line printers, card readers and everything in your own shop. Even though a lot of outfits have that big machine, I believe that the tendency will be in the direction of the central facility.

QUESTION: I'm interested in these accuracies you've been talking about. As a user of an IBM 360, this worries me considerably. I can't acquire the accuracy you're discussing here without very expensive

modifications such as multiple precisions. What about 16 bits?

MCCORMICK: You've got to get out to 60 or 70 bits before you can do problems of any size at all. Even then you can get into difficulty but generally 60 to 70 bits will carry you quite a ways. Remember we all like to look at the one dimensional structures because they're easy to understand but what you're really trying to solve are the big two and three dimensional problems.

QUESTION: I've looked very carefully at that curve you presented. In most large problems, you're talking about two to five thousand elements. This is what we're really aiming for. And with the type of accuracy we can get on 360, do we have a chance?

MCCORMICK: Well, the 360 operating in double precision has 64 bits. That's about the same as 60 bits on the CDC. You just can't use the IBM single precision, 32 bits, for problems of any size.

QUESTION: Your equation (2) indicates that the residual on the equilibrium or the residual forces are not necessarily sufficient indicators of quality of solution. I wonder if you would expand a little bit on that? Perhaps something like sum of the squares of residuals would be a better indicator?

MCCORMICK: Well, I think I gave my answer to that question by indicating that I prefer to dot the residuals with the displacement vector

and calculate this energy ratio. That gives me a number to look at and I think a better overall feel for what's going on. It's been my experience that this is a good physical indicator.

QUESTION: This question relates to stiffness variation. You said that when you have a large order of magnitude differences in different elements or different entries in the stiffness matrix, it might create a problem. I wonder what, in your opinion or by your experience, is an acceptable range for such variation.

MCCORMICK: The rough rule that I sort of use is that if the entries vary by an order of magnitude, I figure I'm going to lose something like a decimal digit. That's very crude and very rough but that's sort of a rule that I use.

COMMENT: We have run problems with ratios of elements to the 10^6 power for systems of 4500 by 4500. I don't know whether that's good or not and it's probably structure dependent. Now you said that if you lose a digit per 10 power it would mean that I would have lost 6 digits in accuracy. But that didn't seem to be the case.

MCCORMICK: Well, I have run some problems of this sort and in the worst cases that is what I have found. But my experience is very limited, so I guess I can't really help you too much.

QUESTION: You mentioned in your paper, although you didn't

discuss it this morning, the solution of large eigenvalue problems and you mentioned where you want to get a large number of mode shapes and frequencies in a large system that you recommend reducing the number of degrees of freedom down to 10% or 15%. I wonder if you would discuss the technique that you would use for this reduction and how you would automate it in your regular program procedures.

MCCORMICK: The reduction technique that I use is what I prefer to call a stiffness reduction, although some people call it Guyan reduction. The procedure is well documented in the NASTRAN theoretical manual. It's a well known procedure. It simply amounts to partitioning the stiffness matrix, making a decomposition and calculating a transformation matrix and then operating on the stiffness and mass matrices to get them reduced. These matrices will generally be full. One of the reasons for a significant reduction--I think I said 5 to 10 percent--is that computing times may well get out of hand and be more than would occur without reduction if you're careless and reduce to about half size. You have to come well down in order to keep the computing times within range and then my tendency is to use a tridiagonalization technique or something similar which is most effective as long as you can hold the matrices in core.

QUESTION: In the Guyan type of reduction, how do you choose the degrees of freedom to be retained?

MCCORMICK: Well, this, of course, requires judgment on the part of the user, and in general you have to look at the dynamic degrees of freedom and decide how many you think you need to adequately describe the problem.

This depends on the nature of the problem, the kind of response, what the forcing functions are and all this sort of thing. But in general what you're trying to do is to keep a courser mesh and, in particular, be careful to retain those points that have big masses on them. This sort of thing is well known among structural dynamicists, isn't it?

COMMENT: I think there is more to that question because it costs you quite a bit to reduce that matrix to begin with, you gain something in solution time of the reduced system, and you lose something in accuracy of the final solution. So there probably are a number of questions involved.

MCCORMICK: Let me just say one thing. If you're going to do large dynamic problems, you have to find some way of handling them. This is one way to do it. It may not be the best, but we have found it can be reasonably effective. If there are other ideas here, I'd like to learn about them.

THE IMPACT OF FUTURE DEVELOPMENTS IN COMPUTER TECHNOLOGY

William R. Graham^{*}

The RAND Corporation, Santa Monica, California

June 1970

Computer hardware design is progressing at such a rate that it is difficult to understand where it is now, much less where it is going. On the other hand, computer software still exists only as a pre-science technology, and therefore it is very difficult to make any generalization about its status, other than to say that it is a sufficiently primitive art to require the name "Computer Sciences" in most centers of research.

This paper will make an attempt to move away from analyzing computer capability only in terms of raw hardware speeds, and will try to give a rounded picture of the disadvantages as well as the advantages of some radically new machine designs. The point of view will be that of a person interested in solving very large and complex problems.

HARDWARE

The current state of the art in computer hardware may be summarized in terms of switching speed as follows [Ware, 1969]:

Device	Switching Time (Seconds)
Magnetic cores	10^{-7}
Magnetic films	10^{-9}
Transistor	10^{-9}

Projecting what lies ahead is a particularly risky undertaking in the electronics business. However, a few things can be said. If a transistor is to be built using light, then the base width is constrained

^{*}Any views expressed in this paper are those of the author. They should not be interpreted as reflecting the views of The RAND Corporation or the official opinion or policy of any of its governmental or private research sponsors. Papers are reproduced by The RAND Corporation as a courtesy to members of its staff.

This paper was prepared for presentation at the Joint Air Force and Lockheed Aircraft Conference on Computer-Oriented Analysis of Shell Structures on 13 August 1970.

by diffraction to be greater than a wavelength--about 3000 angstroms. This width would give a switching time of about 10^{-10} seconds. If an electron microscope is used for constructing the device, the base width might be reduced an order of magnitude, decreasing the switching time to about 10^{-12} seconds [Linvill and Gibbons, 1961].

There appears to be another speed limit which is both considerably more general and considerably more distant [Ware, 1969]. If a state of a switching device is to be stable in an environment at temperature T , then an energy of at least a few times kT (where k is Boltzman's constant) must be transferred to the device to switch it. After switching, the energy must be dissipated [Landauer, 1961]. To keep the energy dissipation requirements low so that the device density can be large, not a great deal more energy than is required for switching should be provided. To determine the switching energy within kT , the Heisenberg uncertainty principle tells us that a time of at least h/kT (where h is Planck's constant) is required. This gives an ultimate room temperature switching time of 1.6×10^{-13} seconds. Note that $5 kT$ is a switching energy of 2×10^{-20} joules, which could appear, for example, as 11 millivolts at 11 microamps for the 1.6×10^{-13} seconds. At cryogenic temperatures, the switching time would be decreased in the same ratio as the absolute temperature, with a corresponding decrease in the total switching energy.

To summarize, in the future we may expect a probable switching speed increase of one order of magnitude, a possible increase of an additional one to two more orders of magnitude with small semiconductor devices, and an ultimate switching speed at least another order of magnitude faster still.

THE SOFTWARE OF ELEMENTARY OPERATIONS

The software of elementary operations in a computer is the collection of wired-in algorithms for executing the operational code of the computer. It was not until many years after electronic computers were built and operating that a theory of the minimum time required to perform simple arithmetic operations was developed [Winograd, 1965, 1967]. When the Winograd limit is compared with the speed of good present-day machines, we find that addition is performed at roughly 60% to 80% of the Winograd limit, and that multiplication goes at 30% of the limit [Ware, 1969]. This means that we can expect at most an improvement of a factor of 3 in speed from algorithm improvements in these elementary operations. Proper design of the more complicated algorithms which calculate exponentials, trigonometric functions, etc. may result in considerably greater increases in speed.

If elementary hardware and software improvements were the only means to increase machine speed, then obtaining another two or three orders of magnitude in speed would probably be a rather slow, expensive, and difficult process. However, there is another way to increase speed. It is to make basic changes in the overall organization of the computer.

Two examples of radically new machine organization plans are those used in the University of Illinois' parallel-organized ILLIAC IV and the Control Data Corporation's pipeline-organized STAR. The price paid for the speed improvement in these machines is extracted from the user in a subtle but definite way [Chen, 1969]. To understand the drawbacks and advantages of these machines, one must first understand their organization plans [Graham, 1970].

THE PARALLEL COMPUTER

The parallel computer, such as the University of Illinois' ILLIAC IV, is based on the notion that two conventional computing machines can work at twice the rate of one machine. The major deficiency in this approach is that two machines also cost twice as much as one machine.

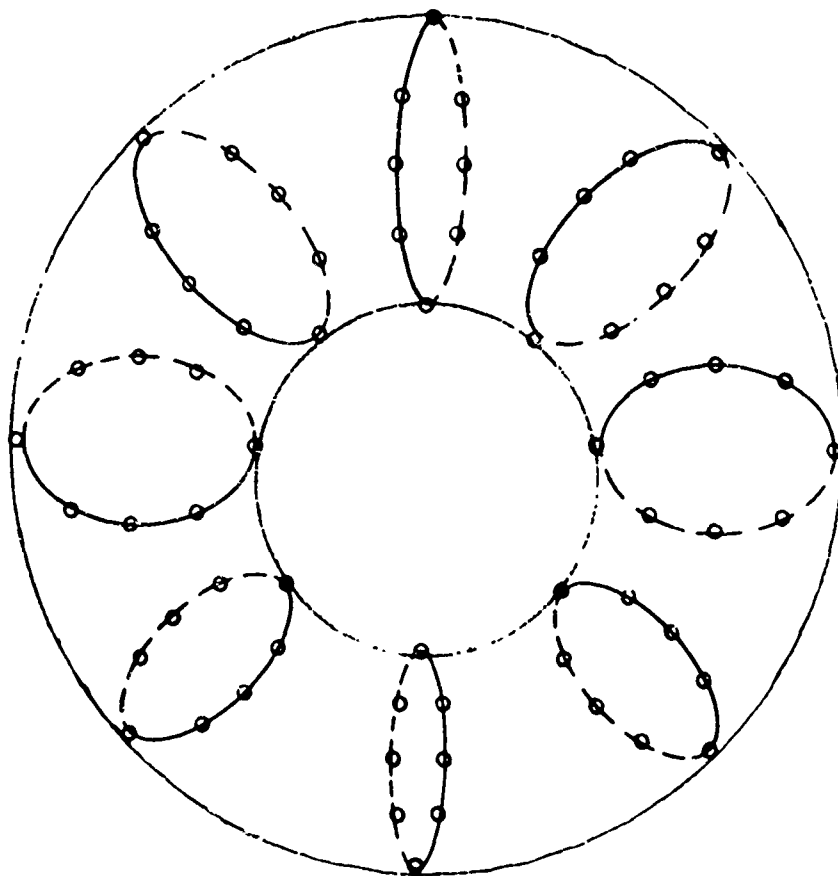


Fig. 1. ILLIAC IV Memory Interconnection

To overcome so fundamental a drawback, the parallel design has many identical copies of the conventional computer's arithmetic unit driven with only one control unit. The control unit is responsible for obtaining, decoding, and issuing instructions, and generally assuring that the machine will do what it is supposed to do. Since the control unit is rather sophisticated and expensive, a considerable amount of money is saved by having only a single control unit in charge of W identical arithmetic units. (W is called the "width" of the parallel processor.) The price paid for getting by with only a single control unit is that each of the arithmetic units must do the same thing at the same time or else be inhibited and do nothing, a condition which somewhat limits the flexibility of the computer.

The parallel processor must be organized so that it is impossible for two or more arithmetic units to attempt to change the same number in memory at the same time. This is achieved most simply by allocating to each arithmetic unit an exclusive block of memory, not directly accessible to any other arithmetic unit. The result is that if arithmetic unit J needs a number stored in the memory of arithmetic unit K , the control unit must have K recall the number and then transmit it, over specially provided channels, to J . The number of channels that would be required to interconnect directly all of the arithmetic units is $W^2 - W$. If the designer wishes to sacrifice transmittal time, a smaller number of channels may be used. For example, in the ILLIAC IV, if one imagines the arithmetic units strung on a circle, then only the two nearest units and the two seven units away are in direct communication. Another way to visualize the interties is to arrange the arithmetic units on a toroid as shown in Fig. 1. Then only the four nearest neighbors (two on the circles shown and two along the toroid) can communicate directly. In this arrangement, eight transmissions are required for communications between the most distant arithmetic units.

THE PIPELINE PROCESSOR

A quite different approach underlies the design of the pipeline processor such as the STAR, which is under development at the Control Data Corporation. In the conventional computer, the time required to retrieve operands from the memory, execute the operation, and return the result to memory must be greater than a time equal to the distance traveled by the information divided by the speed of light, and several other less inevitable factors. The pipeline processor, shown schematically in Fig. 2, gains its advantage by starting the retrieval of a second set of operands, each located in memory adjacent to the first, before the first result has been returned to the memory. Thus, a pipeline begins to fill, and the round-trip distance divided by the speed of light no longer limits the apparent cycle time.

So that the arithmetic unit will not be an obstruction to the flow, it too is built as a pipeline. It can receive and start working on a second set of operands before finishing the calculation for the first set. The hardware required to make the arithmetic and memory units

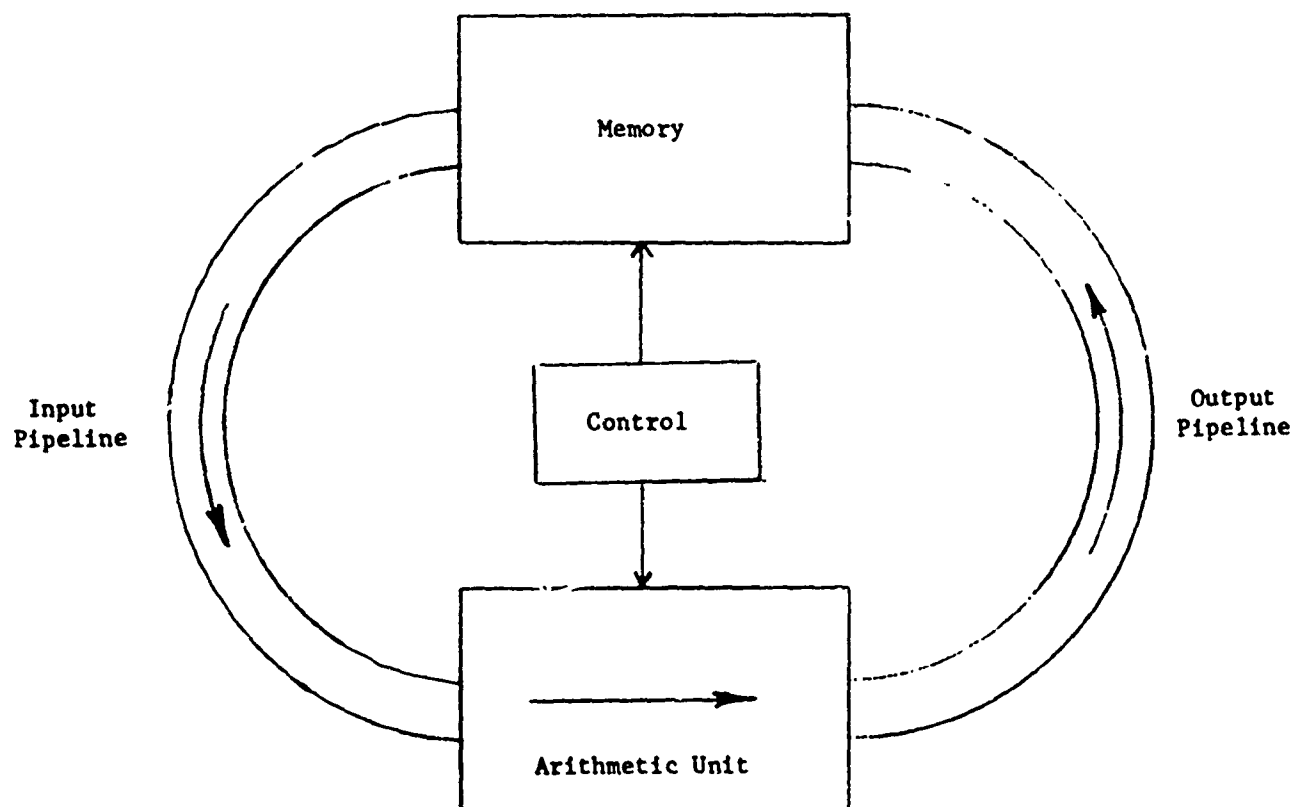


Fig. 2. The Pipeline Processor

work as a pipeline is elaborate and expensive, so that if the pipeline processor is to be economical, the pipe must be kept full a substantial part of the time.

To complete the memory-to-memory pipeline, the arithmetic unit must deliver the results back into memory at the same time and rate that it is receiving new pairs of operands from the memory. It is sometimes desirable to skip an operation on certain operands in the pipeline. This is done through the use of a control vector which contains one bit that is associated with each operand set in the pipeline. Depending on whether the associated control vector bit is one or zero, the operation is either performed or skipped. If no operation is performed, the memory location for the result does not have its previous content changed.

The logical control processes that must take place for the number stream in the pipeline to flow smoothly are collectively referred to as a Boolean Orgy, and are sufficiently difficult that the foreseeable pipeline machines will permit only one type of arithmetic operation per stream (e.g., add or multiply or divide) and only one stream at a time. (A rather amazing exception to this is the vector inner product operation, which may be implemented on the STAR.) Furthermore, the pipeline memory retrieval and storage locations for each operand string are constrained to lie on a consecutive linear sweep through the memory. As with the parallel processor, both the maximum computing rate and the opportunities for inefficient operation are greatly increased by this design.

PARALLEL AND PIPELINE

To compare the two types of machines, it is first necessary to have a clear idea of what computation can proceed in parallel and what in pipeline.

The hierarchy of computer activities starts with the basic step; the retrieval of a set of operands from memory, the operation, and the return of the results to memory. At the next level is the parallel or pipeline stage. The stage is the collection of all of the program steps which could be done in parallel or in the same pipeline stream without creating a dilemma in the logic of the program execution. A stage is a property of the logic of the problem, but not of the computer width or pipeline capacity. Finally, all of the stages connected in the proper order constitute a computer program.

The following conditions result from the constraints of logical simplicity being imposed in present computer designs. N computing steps, S_1, S_2, \dots, S_N , form a parallel stage if (1) no step depends upon the result of any other in the stage, (2) all steps require the same operation to be performed, and (3) the operands are properly distributed among the arithmetic unit memories.

N computing steps form a pipeline stage if (1) no step depends upon the result of any other in the stage, (2) all steps require the same operation to be performed, and (3) the members of each operand string are packed in successive memory locations. Comparing these two sets of conditions, one sees that (1) and (2) are the same, only (3), memory location assignment, is different for the parallel and pipeline machines.

A world of trouble is hidden in these three conditions. The first condition means that many implicit differencing schemes, including, for example, the usual two-pass algorithm for solving the Crank-Nicholson equation, will reduce pipeline and parallel computers to conventional one step per stage operation, with a corresponding long execution time and low machine efficiency. The third condition, proper storage allocation, makes performing such a simple operation as multiplying a matrix by itself a substantial problem in parallel or pipeline operation. The

parallel computer requires that the operands for a stage be distributed throughout its arithmetic units' memories in a two dimensional arrangement, while the pipeline computer requires that the same operands be packed together tightly in the one-dimensional memory. This difference in memory allocation and the ability of the parallel arithmetic units to communicate with each other are the dominant differences that the user sees between the two types of computers.

Assuming that the three conditions have been met (a non-trivial assumption), one may then proceed to compare the machines on the basis of execution time and the efficiency with which resources are used. One overriding fact to keep in mind through the following discussion is that one step at a time sequential operations will greatly diminish the computers' performance. If half of the operations executed are so well matched to the machine that they take essentially no time to execute, but the other half must be done one step at a time, then the total program execution time is at best an unimpressive factor of two less than that for a conventional machine. As a first approximation, the ratio of the parallel or pipeline program execution time to the conventional computer's time is the ratio of the number of steps that must be performed sequentially, one at a time, to the total number of steps. To make efficient use of the parallel or pipeline computer's resources, it is not sufficient that a few steps of the program be suited to the machine; the majority of the program steps must be part of large stages--ones which each contain many steps.

PARALLEL VS PIPELINE: EXECUTION TIME

In a parallel processor, the three parts of a computing step--the memory retrieval, the operation, and the memory storage--may be diagrammed as follows:

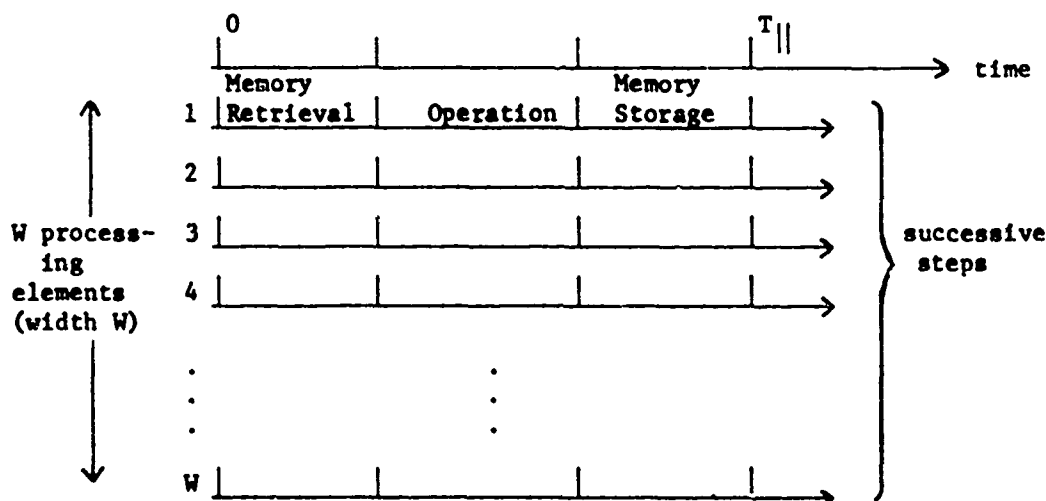


Fig. 3

Here, the step time $T_{||}$ depends upon the specific operation being performed. For a stage of N steps, the time required for execution by a parallel machine is $T_{||}$ times the integer part of $(N-1+W)/W$, usually written as $T_{||} \cdot [(N-1+W)/W]$.

The operation of the pipeline machine may be diagrammed:

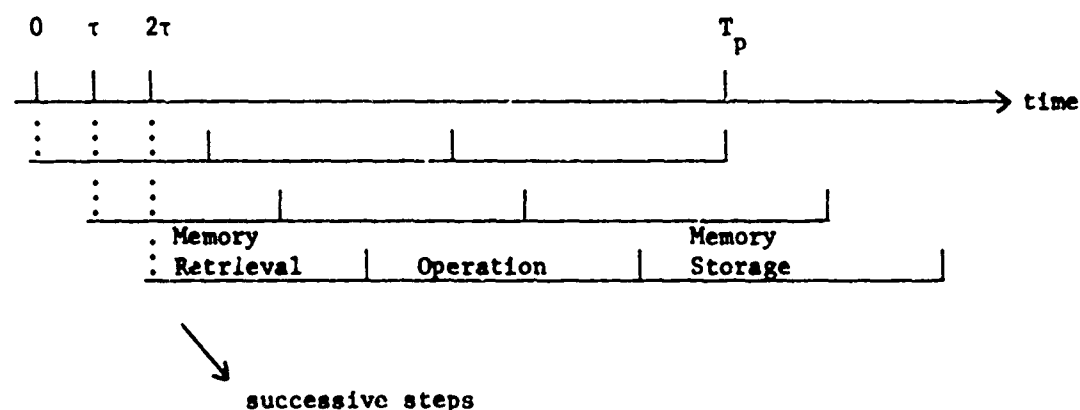


Fig. 4

The time required for the pipeline computer to execute a stage of N steps is $T_p + \tau(N-1)$. Knowing the parameters $T_{||}$, T_p , W , and τ of two machines, these times may be calculated as a function of N . For example, when $N=1$, the parallel machine time is just $T_{||}$ and the pipeline machine time is T_p . At the other extreme, as N tends to infinity, the parallel machine time per step tends to $T_{||}/W$, and the pipeline machine time per step tends to τ .

With a parallel machine, the execution of a stage of N steps takes a time that is always less than or equal to $T_{||} \cdot (N+W-1)/W$. Thus, if $T_{||}/W$ is less than τ and $T_{||}$ is less than T_p , then the parallel machine will execute any stage, of whatever size N , more rapidly than will the pipeline machine.

For a stage of N steps, the parallel machine will always take a time greater than or equal to the larger of the times $T_{||}$ and $T_{||} \cdot N/W$. If $T_{||}$ is greater than $T_p + (W-1)\tau$, then the pipeline machine will execute any stage faster than the parallel machine. In general, the results can be more mixed, and it is quite possible for the advantage to shift back and forth between the two machines as N increases.

Table 1
64 BIT PRECISION CHARACTERISTIC PARAMETERS*
FOR THE CDC STAR AND THE ILLIAC IV

Operation	CDC STAR		ILLIAC IV	
	T_p	τ	$T_{ }$	W (one quadrant)
Addition	1.76 μ sec	20 ns.	1.28 μ sec	64
Multiplication	1.76 μ sec	40 ns.	1.45 μ sec	64
Division	1.80 μ sec	80 ns.	3.76 μ sec	64

Using the preliminary information in Table 1 (shown here for illustrative purposes) one may deduce that the STAR and an ILLIAC IV quadrant have comparable speeds for performing addition, with the ILLIAC having the edge when only a few sums are to be formed. In multiplication, the ILLIAC IV is always faster than the STAR, while in division, the STAR is about twice as fast as the ILLIAC in finding a single quotient, but the ILLIAC is about 1.4 times as fast as the STAR in calculating a long sequence of quotients. Of course, accurate determinations of the hardware speeds must await the final stages of machine development.

Computing rates are also shown in Table 2 for the IBM 360/75, the CDC 7600, and the IBM 360/195.

Table 2
64 BIT PRECISION COMPUTATION SPEEDS** (MEMORY TO MEMORY)
IN MILLIONS OF OPERATIONS PER SECOND

Operation	Steps per Stage	IBM	IBM	CDC	CDC	ILLIAC IV
		360/75	360/195	7600	STAR	(One Quadrant)
Addition	N=∞	.24	4.6	5.2	10	50
	N=1	.24	.55	1.6	.57	.78
Multiplication	N=∞	.14	4.6	5.2	25	44
	N=1	.14	.53	1.5	.57	.69
Division	N=∞	.096	1.7	2.0	12.5	17
	N=1	.096	.43	.93	.56	.27

*The figures are preliminary and for illustrative purposes only.

**For the ILLIAC IV and the STAR, the figures are preliminary and for illustrative purposes only.

Although the 7600 and 195 are much faster than the familiar 360/75, they are obviously not in the same league as the STAR and the ILLIAC IV when it comes to performing long sequences of identical calculations. However, except for problems well suited to parallel or pipeline manipulation, the 7600 and 195 are as fast or even faster than the STAR and ILLIAC IV.

PARALLEL VS PIPELINE: EFFICIENCY

The cost of executing a stage is more closely related to the efficiency with which each computer's resources are used than it is to the execution time. For the parallel computer, maximum computing rate is reached when all processors are used. At the maximum W/T_p steps per second are executed. For the pipeline machine, the maximum computing rate is reached when the pipeline is filled; then the rate is $1/\tau$ steps per second.

Efficiency for a stage may be defined as the ratio of the actual computing rate in steps per unit time to the maximum computing rate; this efficiency always lies between zero and one. For a stage of one step, the efficiency of the parallel machine is $1/W$ and that of the pipeline machine is τ/T_p . For a stage of N steps, the efficiency of the parallel machine is $N/(W \cdot [(N-1+W)/W])$ and the efficiency of the pipeline machine is $N/(T_p/\tau + N-1)$.

It is useful to remember when formulating a problem that the efficiency of the parallel computer reaches unity whenever N is an integer times W but is not monotonic in N , whereas the efficiency of the pipeline processor increases monotonically with N but approaches unity only asymptotically as N tends to infinity. The ILLIAC IV has a quadrant width W of sixty-four, so it would execute a stage of sixty-four steps with unit efficiency. The STAR would execute a stage of this size with an efficiency lying between .42 (for addition) and .75 (for division). For a stage of 65 steps, the STAR efficiency would increase slightly, while the ILLIAC IV efficiency would drop to about .5.

To see what the efficiencies are in the worst case, note from Table 1 that the one step efficiency for the STAR is between 1% and 4 1/2%, depending on the operation, and for the ILLIAC IV is always about 1 1/2%. The license for inefficient use of computer resources which the parallel and pipeline designs give to the programmer and to the compiler far exceeds any habitual excess yet seen in the computing world.

The efficiency with which a complete program is executed is the average of the efficiency E_i of each stage weighted by the total time T_i required to complete that stage:

$$\text{Program Efficiency} = \sum_i T_i E_i / \sum_i T_i.$$

Stated most simply, the program efficiency is the ratio of the time required to execute a program if the computer is operating at unit efficiency as defined above to the actual execution time. For a program which has half of its operations executed at unit parallel or pipeline efficiency, and the other half executed one step per stage, memory to memory, the overall program efficiency would lie between 2% and 9% for the STAR and be 3% for the ILLIAC IV.

The parallel and pipeline designs will produce computers that when used to their maximum, unquestionably will be faster than more conventional computers. However, formulating problems and writing programs which will use the new machines to anything approaching their maximum capabilities will prove a severe and perhaps on occasion an overwhelming challenge to the creativity of all concerned. Whether these huge machines will become the workhorses of computing hardware or go the way of the dinosaurs has yet to be seen. Their future hinges upon the skill of the users.

PERFORMANCE ON PRACTICAL PROBLEMS

To understand how well the parallel and the pipeline machines work in practice, the Air Force Weapons Laboratory had a series of programs written for solving the same problems on the 64 P.E. one quadrant ILLIAC [Wirsching, Alberts, McIntyre, Carroll, 1970] and the STAR [Wirsching, Alberts, 1970]. Parts of two large running programs, HEMP and SC, were coded in ASK, the ILLIAC IV assembly language, and PL/*, the STAR assembly language. Only the central 5% of the total HEMP and SC program was coded for the parallel and pipeline machines, but this 5% accounts for 95% of the running time on the present generation machine.

HEMP is an electromagnetic source and field calculation involving the time dimension and one spatial dimension. Its five sections break down as follows:

- Section 1: Combination of input and intermediate values which result in input to section 2.
- Section 2: Search for match and subsequent interpolation on values resulting from section 1. This is a logistics problem which is not directly related to the mathematical algorithm.
- Section 3: Convolution integrals.
- Section 4: Interpolation or restructuring of data resulting from convolution. This is also a logistics problem not directly related to the algorithm.
- Section 5: Calculation of the electric fields.

After the same parts of these sections were coded for the ILLIAC IV and STAR, the execution times were determined to be the values shown in Table 3. The efficiency as well was calculated for the ILLIAC IV, and has been derived approximately for the STAR from the data given. These efficiencies are also shown in Table 3.

Table 3
HEMP TIMING AND EFFICIENCY

HEMP Section	ILLIAC IV (64 P.E.'s)		STAR (50 ns. cycle)		Present Generation Machine (~6600)
	Time (Sec)	Efficiency (%)	Time (Sec)	Efficiency (%)	Time (Sec)
1	0.11	90	.301	93	
2	8.80	22	1.539	99.8	
3	6.40	51	8.067	98	
4	0.22	2	.009	67	
5	0.35	29	.672	74	
Totals	5.88	32 overall	10.59	98	688

For the HEMP problem, the STAR is about 65 times as fast as the present generation machine (PGM), while the ILLIAC IV is about 43 times as fast. The high efficiency of the STAR is due in part to the very powerful operation code of the machine, and in part to "brute force" techniques that are natural to use on the STAR for some operations, such as linear search table lookups. This last point is substantiated by the closeness in the total execution times in light of the similar hardware speeds of the two machines. The variation in the ILLIAC IV efficiency among the various sections of HEMP gives some notion of the control which the programmer and the algorithm have on the computer performance.

SC is an electrodynamics program that solves Maxwell's equations in the time dimension and two spatial dimensions. Some of the variables are defined recursively by the equation

$$T_{IJ} = T_{I(J-1)} * C_J$$

Straightforward iteration of this formula for a fixed I would seriously degrade the performance of both the pipeline and the parallel computers. Fortunately, it was found that the equations were uncoupled for fixed J over an appropriate choice of I's, so that by performing the operation for a range of I's and a fixed J efficient use could be made of the

machines. The results of the SC coding are shown in Table 4:

Table 4
SC TIMING AND EFFICIENCY

ILLIAC IV (64 P.E.'s)		STAR (50 ns. cycle)		Present Generation Machine (~6600)
Time (Sec)	Efficiency (%)	Time (Sec)	Efficiency (%)	Time (Sec)
6.55	85	15.2	90	590

For the SC problem, the STAR is about 39 times as fast as the PGM, while the ILLIAC IV is about 90 times as fast. The overall efficiency of the ILLIAC IV is considerably improved over its value for the HEMP code, while the efficiency of the STAR is slightly decreased. It was pointed out in the original work that a slight change in the ILLIAC IV memory allocation scheme would double the total SC running time and halve the efficiency, and it is probable that similar small errors in allocation would greatly reduce the STAR program efficiency. This again demonstrates the sensitivity of these machines to the user's skill.

LANGUAGES

The ILLIAC IV has two machine languages: one for the CONTROL UNIT and another for the PROCESSING ELEMENT. Both of these languages must be mastered by the assembly language programmer. Both operate on a rather conventional elementary level: fetch A, add B, store SUM, conditional branch, etc. A language called Glypnir now exists which is above AJK but below something like FORTRAN.

The STAR language, PL/*, is at once a high level language and nearly a machine language. This is the result of the very high-level operation code which is wired into the machine. For example, one single instruction in the STAR will transpose an 8x8 matrix, another will perform a dot product, another a vector average, another will evaluate a polynomial, and another will multiply one string by another conditionally dependent upon a control vector and place the product string back in the designated area of memory.

The programming for the STAR required about 1/6 as many instructions as the programming for the ILLIAC IV. The STAR instructions were considerably more complicated than the ILLIAC instructions, and each required on the average about six times as long for execution. Although

it is not explicitly stated in the reports, the programmers seemed to give the impression that the STAR was somewhat easier to program than the ILLIAC IV, at least in assembly language.

FINAL CAUTION

One last word should be said concerning the interpretation of the results reviewed above. Only the central 5% of the HEMP and SC programs were coded for the ILLIAC and the STAR. Although these portions of the programs required 95% of the running time on the present generation machine, the division of time may be considerably different on the parallel and pipeline machines, as was noted earlier. It is not inconceivable that if the remaining 95% of the programs were to be coded, it might result that the additional code would dominate the running time, reducing the overall efficiency to something in the range of 10% to 40%. Such are the curiosities of these machines.

BIBLIOGRAPHY

Chen, T. C., The fact that the parallel and pipeline computer designs have inherent limitations which render their performance very sensitive to problem and programming formulation was first pointed out to the author by Dr. Tien Chi Chen, a result which Dr. Chen derived from his extensive unpublished research on the subject, Private Communication, 1969.

Graham, W. R., "The Parallel and the Pipeline Computers," Datamation, April 1970, pp. 68-71.

Landauer, R., "Irreversibility and Heat Generation in the Computing Process," IBM J. Res. and Develop., Vol. 5, No. 3, July 1961, pp. 183-191.

Linville, J. G., and J. F. Gibbons, Transistors and Active Circuits, McGraw-Hill, New York, 1961, 515 p.

Ware, W. H., On Limits in Computing Power, The Rand Corporation, P-4208, October 1969.

Winograd, S., "On the Time Required to Perform Addition," J. Assoc. Comput. Mach., Vol. 12, No. 2, April 1965, pp. 277-285; idem, "On the Time Required to Perform Multiplication," J. Assoc. Comput. Mach., Vol. 14, No. 4, October 1967, pp. 793-802.

Wirsching, J. E., and A. A. Alberts, Application of the Star Computer to Problems in the Numerical Calculation of Electromagnetic Fields, Air Force Weapons Laboratory, Technical Report No. AFWL-TR-69-165, April 1970.

Wirsching, J. E., A. A. Alberts, D. E. McIntyre, and A. E. Carrol, Application of the ILLIAC IV Computer to Problems in the Numerical Calculation of Electromagnetic fields, Air Force Weapons Laboratory, Technical Report No. AFWL-TR-69-91, March 1970.

QUESTIONS AND COMMENTS FOLLOWING GRAHAM'S PAPER

QUESTION: You mentioned that these machines don't do to well with inner products, but structural analysis, as we know it today, consists primarily of taking lengthy inner products over and over again. Would you care to comment on that particular point a little further.

GRAHAM: If I chose my words correctly, I said that a single dot product isn't done terribly efficiently on these machines. Now it's not done as poorly as you would think. For example, the inner product is a hard-wired instruction on the STAR as is almost everything else you can imagine, like polynomial evaluation, matrix transposition and so on. The designers have tried to take that programming out of your hands and put in the most efficient algorithm they can. On the ILLIAC IV, doing an $A \cdot B$ is somewhat inefficient, but doing a matrix multiply which requires a lot of inner products is very efficient. The reason is that the ILLIAC starts forming 64 inner products at the same time and carries them all through together. It doesn't have any one finished until it's got 64 finished, but it can do those at peak machine speeds. So, if you want to do more than one inner product as you would for a matrix multiply, then the machines will work pretty well. I hope those are the inner products you were mostly concerned with.

COMMENT: I realize that in the ILLIAC IV every parallel processor has to do the same thing at the same time; but conceptually I wonder why this is necessary. Why couldn't you have a number of processors sitting around and hand each one a stage where the stage itself is independent of

the other stages. Perhaps the control unit could be just a super shuffler that could hand these things out and take them back.

GRAHAM: The control unit is already a kind of super shuffler compared with decoders in the present machines. I think there's no basic reason one can't do what you suggest. A practical concern has to do with the complexity of the control unit. One of the drawbacks of the ILLIAC IV type of design is that the control unit is so complex that at the machine language level you have to use two languages, one of which is the control unit language and the other of which is the processing element language. The control unit tries to do a lot of look-ahead and also does fixed point control arithmetic operations inside itself.

If one goes far enough in the direction you suggest, one obtains N independent machines. There's no reason that you can't run N entirely independent machines that just talk to each other once in a while. In fact, a weather code exists that runs on four CDC 6400's which communicate through a common extended core memory.

COMMENT: One reason the control unit is so complicated may be that all of the processors are doing the same thing. You must continually think to yourself, "Well, do I want all those elements doing the same thing," and you have to say, "Gee, just because I'm moving data from A to B, I'm also moving it from D to E and do I really want to do that?" So, it's complicated.

GRAHAM: It makes the machine less complicated to do that but it makes the programming more complicated. You're always juggling a 64 bit vector where each element of the vector is a yes or a no on whether or

not you want the correspondingly numbered processing element on. As you issue each instruction, you've got to go consider all your processing elements and decide which ones you want on and which ones you want off. A good deal of the programming time goes into that process.

QUESTION: I'm somewhat concerned about not the theoretical speed of the machine, but rather the practical speed of the machine. Does the machine have many registers or do you store everything in core? What are the speeds of the peripheral equipment and how do they influence the calculation speed of the machine?

GRAHAM: The operations I was discussing were all core to core. The STAR also has a 256 word very high speed register memory. The typical size of STAR memories will be half million to million words while ILLIAC will have 128,000 words per quadrant. Each of these machines is designed with careful attention to the I/O so that you can be shuffling things in and out of the memory while the machine is also doing arithmetic. The total rate of all the memory fringes on the ILLIAC or on the STAR is about a billion bits per second. Both machines have peripheral storage devices that operate at several hundred million bits per second. The addressing on the STAR will be from a logical address through a table lookup to a physical address. If the table happens to say that the physical address is on the drum, then you pay whatever the drum access time is to start moving the numbers into the core.

QUESTION: Using a machine like the CDC 6600 in a multiprocessing environment, there's a large amount of software programming that resides in core or is being handed in and out of peripheral devices. A large amount

of time is now devoted just to systems operations for looking after everything. Can we expect this kind of overhead or extra cost to go up or down with these next generation machines?

GRAHAM: The ILLIAC IV does not presently have memory boundary protection; if a memory address calculation gets out of hand, any part of the memory could be changed. Therefore, only one problem at a time will be permitted in core. An average overhead of about 73 milliseconds must be paid each time the core is reloaded. Most of the rest of the ILLIAC IV's overhead operations will be performed by the associated B-6500 computer. Since the B-6500 also does all the program compiling, it may become the ILLIAC IV's bottleneck.

The STAR was designed to serve as the pinnacle of an interconnected pyramid of time-sharing computers. In this scheme, much of the overhead would be handled by lower-level computers. Nonetheless, the STAR's logical to physical address table lookup could slow down the computing in some cases.

THE OPTIMUM APPROACH TO
ANALYSIS OF ELASTIC CONTINUA

R. J. Melosh, Staff Scientist
Philco-Ford Corporation

ABSTRACT

The optimization of structures requires many analyses. This provides the incentive to reassess analysis approaches and select one which insures that complex numerical analyses of structures are performed efficiently.

This paper classifies the decisions of analysis which, in turn, classify analysis methods. By example and rationale it examines analysis alternatives and selects the more attractive ones for maximizing analysis accuracy per unit of analysis effort. In the process, it reviews some important analysis issues. New arguments are furnished on the question of the force versus the displacement method, coarse versus refined models, and finite elements versus finite differences.

The paper identifies error control as the key issue. It indicates that lack of a theoretical basis for directly controlling undesirable errors makes published comparisons of methods and operators of questionable value. This lack insures that arguments for one alternative over another must often be less than rigorous.

It is concluded that the optimum unmixed analysis approach uses an integral equation formulation, displacement behavior states, intersecting operators, low order extra degree articulation, and determinate error control.

INTRODUCTION

Optimizing structural designs incurs calculations for redesign and for design analysis. Redesign calculations produce new variable assignments for a design of improved merit. These calculations have high leverage. They determine the number of design analyses required before the sequence of improved designs converge. Design analysis provides measures of the effect on behavior of changing design variables (influence analysis) and evaluations of the integrity of given designs (reanalysis). Efficient performance of these operations is important because it requires most of the effort in an optimization cycle. Thus, the desire to optimize structures places incentives on developing an efficient analysis approach.

This paper addresses itself to identifying such an approach. Attention is restricted to numerical analysis methods in which generalized behavior coordinates are associated with control points (joints) on the structure. It is only incidentally concerned with mesh refinement and convergence.

Many researchers have examined aspects of this subject. By examining various finite element models, Pian and Tong⁽¹⁾ have scrutinized the effect of various integral equation formulations on response predictions. Leissa et al.⁽²⁾ have asked similar questions for the differential equation methods. A few papers show rigorous concern for the adequacy of models. Reference 3, Key,⁽⁴⁾ and a series of papers by Walz et.al,⁽⁵⁾ are cited as examples in the engineering literature. Papers reporting results of numerical experiments showing the effect of articulation of the structural system on solution accuracy are too numerous to list here. Some of these are found in Ref. 6 and many more are referenced there.

This paper presents an assessment of the classes of decisions made in analysis of linear elastic continua under static loadings. The next section defines the classes of decisions involved. The third section examines the effects of each choice on analysis efficiency. The fourth section relates other issues of analysis to the context. The last section lists conclusions.

This study was stimulated by the need for a strategy for designing complex multicomponent structural systems using the finite element method. Thus it is closely associated with a Goddard Space Flight Center study on this subject. Acknowledgement is made to Dr. Richard McConnell and Mr. Thomas Butler of GSFC for their contributions in discussions of analysis strategy.

DECISIONS OF APPROXIMATE ANALYSIS

In general, analysis decisions are those involved in defining the mathematical and numerical models of the structure and in translating the numerical results into predictions of behavior of the real system. This encompasses decisions which are regarded as prerogatives of the engineer as opposed to computer configuration decisions. The analysis decisions are complementary to solution decisions, i.e., the decisions and approximations made in solving the equations which model the structure.

Analysis decisions fall into two classes: numerical modelling and mathematical modelling. Loosely speaking, numerical modelling decisions are implicit in the set of numbers modelling the structure and in interpreting results. Mathematical modelling decisions involve the basis selected for the computer program and options exercised in its use.

Though numerical modelling decisions will not be considered in detail here, their importance is not discounted. They include approximations, with bounded errors, in the idealization of geometric and material anisotropy and joint force and displacement boundary conditions. They may include unbounded errors incurred in modelling geometry. Despite the importance of the numerical modelling decisions, definition of this strategy must still be regarded as an art, rather than a science.

Some modelling decisions interact with mathematical modelling decisions. As examples, selection of the number and disposition of mesh points, and selection of material anisotropy to model geometric anisotropy are interactive. The best decisions in these cases depend on the mathematical model as well as the system being analyzed.

Mathematical modelling decisions are of concern here. These decisions incur bounded errors. Their importance is due largely to their strong effect on analysis accuracy per calculation.

In the approximate analyses of interest structural behavior is assumed to comply with a set of interpolating functions related to mesh point generalized coordinates:

$$\alpha_g = \sum_{i=1,2,\dots,N} \lambda_i f_i(x, y, z), \quad g = 1, 2, 3 \dots G$$

where α_g are components of response,

λ_i are generalized coordinates scalars,

f_i are interpolating functions in the spatial coordinates x, y, z ,

N is the number of generalized coordinates and interpolating functions,

G is the number of response components required to completely define system behavior.

Suppose the set of f_i is mathematically complete and satisfies certain continuity conditions (see Ref. 7). Then, with appropriate choices of the λ_i , Eqs. (1) can represent the solution of the equations of elasticity as accurately as desired as N approaches infinity.

When N is finite, response predictions will usually be approximate. Then the λ_i are evaluated, as pointed out by Crandall, (8) by choosing to minimize some weighted measure of analysis error. The mathematical modelling decisions of concern here involve selection of the interpolating functions, f_i , and the error criteria used for quantifying the λ_i .

Table I provides a decision ladder which groups mathematical modelling decisions. The top three rungs of the ladder involve mainly selection of interpolating functions; the lower two, selection of error criteria. Decisions at all levels, however, affect analysis efficiency.

Decisions at the highest rung fix the analyst's goal by identifying the equations whose solution is being sought. Either a differential (D. E.) or integral equation (I.E.) approach may be taken. The differential equations will be the equilibrium, constitutive, and compatibility equations. The I. E. approach involves finding the solution of these equations by minimizing an integral (variational approach) or solution of a Fredholm integral equation. Since it is always possible to transform from the differential equation form to the integral, and conversely, the analyst can always choose either formulation for his analysis.

The selection of formulation identifies specifications for the f functions. The D. E. approach requires functions which can be differentiated and will provide good estimates of the variation of the differentials over the structure. The I. E. approach requires functions which are integrable and whose integral are good estimates of the corresponding exact integral of structure behavior.

The analyst can also choose to use any of a spectrum of hybrid approaches. In these approaches, functions are chosen which can be both differentiated and integrated. The approach can be to choose functions which would make zero particular terms of the integral and find the λ_i to satisfy differential equations. Alternately, the approach could be to minimize the integral subject to differential equation conditions of the functions. These hybrid approaches are not popular, though they offer a great deal of analysis flexibility.

Though not usually done, the analyst could choose to mix the two approaches. He could use the differential equation approach for part of the structure and the integral for another part, and hybrid over a third part.

The second decision level limits the type and form of the behavior functions. The most important of these decisions is the choice of the α_i . These may be stress components, strain components, or hybrid functions both stress and strain components. The selection can also be spatially mixed over the structure.

This decision establishes the form of the equations and additional conditions on the f_i . For example, if the differential equation approach is taken and the α_i are stresses, the equations take the Beltrami-Mitchell form. The functions must be differentiable through the second derivatives. If the corresponding integral equation approach is taken, the functions must have integrable second order derivatives, satisfy the differential equations in the regions of definition, and satisfy the homogeneous conditions at the boundaries. If the differential equation approach is taken, and the α_i are displacement components, the equations take the Navier form.

Table I

Analysis Decision Ladder

Formulation:	Differential Equations	Integral Equation	Mixed Equations	Hybrid Equations
Behavior Model:	Stress of Force	Strain or Displacements	Mixed Functions	Hybrid Functions
Operators:	Intersecting	Disjoint	Both	
Articulation:	Sub Degree	Least Degree	Extra Degree	Mixed
Total Error Criterion:	Uniform Weighting	Galerkin Weighting	Positive Weighting	Mixed Weighting

If both stress and displacement functions are included, the differential equations of elasticity in unreduced form are to be solved. Alternately, in the I.E approach nonextremum variational principles (such as Reissner Energy) define the equations of interest.

The behavior model is further particularized by the decision to attack the equations in microscopic or macroscopic form. In microscopic form, stress or strain (or displacement) variables are retained. To write the equations in macroscopic form, they are integrated over some of the dimensions of the structure. Stress variables are replaced by force resultants and strains with displacements.

The third decision level involves the selection of difference and integral operators. The difference operators will transform the differential equations into difference equations. The integral operators will replace the integration with a summation. These operators will form a collection from which operators will be picked for given systems.

At this level, an important decision is whether the collection will contain disjoint, intersecting, or both types of operators. Each disjoint operator can be uniquely identified with a particular region of a structure. The region can be delineated by fictitious cuts. Inclusion of only these operators limits the analysis method to finite element operators. The collection must include an operator model for every element topology and material model that may arise. Intersecting operators, on the other hand, are defined among mesh points. They need not be based on functions which are uniquely defined over a region nor be associated with fictitious cuts. A complete set of these operators requires subsets of operators for the boundaries of the structure and for the interior. The finite difference method uses intersecting operators.

The operators may also be classified by characteristics of the functions upon which they are based. This, in turn, can distinguish between analysis methods. Use of only harmonic functions is a hallmark of the Trefftz and Rafelson methods. Finite difference methods are based on first order estimates of the derivatives based on their definitions, which, using Taylor's series, is comparable to a polynomial basis. The complementary energy method restricts operators to those based on functions which satisfy the stress equations of equilibrium everywhere in the interior and match surface tractions across boundaries. The potential energy approach requires functions which satisfy displacement continuity (not compatibility) everywhere. Except for the finite difference method, specialization of the basis in these methods insures a solution bound. If the analyst will forego bounding, practically any piecewise continuous functions can be used.

The fourth level of decisions establishes the difference equations which model the structure. Consider that numerical modelling identifies mesh points on the system and the requirement to produce specific data at these points, say displacements. Then, in the differential equation approach, the fourth level of decisions defines at what points, across what lines, or over what regions the difference equations will be expressed. In the integral equation approach, this level of decisions determines where and how many fictitious cuts will interlace the mesh points. These cuts delineate the integration boundaries.

Minimizing the sum of the parts with respect to the generalized coordinates produces the difference equations. (It is noted that a direct minimization attack could be used to find the generalized coordinates, but this is a solution decision rather than an analysis one).

One important decision is what degree operators shall be used. The method is called sub-degree if the number of degrees of freedom in the analysis is less than that specified by the idealization. In this case, interpolation must be used on the numerical results to obtain response evaluations at points specified by the analyst. In least degree analysis, generalized coordinates are only associated with idealization points. In extra degree, the operators are based on additional coordinates to those specified. In the finite element approach, these elements have been referred to as superelements. Of course, the analyst may choose to vary the degree of operator over the structure, using a mixed approach.

Another articulation decision determines the order of the operators to be used. These may be least order or refined. Least order operators are based on functions which imply the simplest elastic behavior. The rod, beam, and Turner⁽⁸⁾ triangular membrane finite elements are least order. Refined operators involve higher order behavior states. The six joint triangular membrane model of Argyris⁽⁹⁾ illustrates this type of operator.

The final analysis decisions concern the basis for minimizing analysis errors. The errors may be considered components of an error vector.

The analyst must decide how many error components to use. He can define as many as there are generalized coordinates (determined set) or more (over determined set). The analyst can also choose to evaluate the λ_i to minimize any norm measure of this error vector. If there are an equal number of error components (difference equations) and λ_i , the system of equations is determinate and the λ_i can be evaluated so all components of the vector vanish. If there are more error components than λ_i , the λ_i can be found so the sum of the squares of the error is minimum (Euclidean vector norm), the maximum error is minimum (min-max norm), or the sum of the absolute value of the error is minimum.

A more important error decision defines how the error shall be weighted over the system. All methods evaluate error by measuring an inadequacy of the assumed behavior in satisfying the equations of elasticity, but they differ on how these errors shall be weighted in combining them into a single error criterion. Uniform weighting may be used (finite difference and Biezeno-Koch methods), weighting the error by the behavior states, Eq.(1), may be used (Galerkin's method), other positive weightings can be used, or these weightings can be mixed over the structure.

Table II catalogs a number of analysis methods based on decisions made at each ladder level. The decision ladder permits classifying 768 analysis methods. Thus, the 12 given in Table II are a small sample of the possibilities. Detailed description of these 12 methods can be found in Ref. 7. In this table, "open" means that the relevant decision may be any of the alternatives suggested at that level in Table I.

This table shows that, except for methods 1, 2, and 3, and 8 and 9, the group decisions are sufficient to discriminate among the methods. Methods 1, 2, and 3 differ in their choice of function and weighting of the integral of

Table II
Catalog of Methods

<u>Method</u>	<u>Formulation</u>	<u>Behavior</u>	<u>Differences</u>	<u>Articulation</u>	<u>Criterion</u>
1. Ritz, Rayleigh Ritz, Galerkin	Integral	Displacements	Undefined	Open	Galerkin
2. Trefftz	Integral	Displacements	Undefined	Open	Galerkin
3. Rafelson	Integral	Displacements	Undefined	Open	Galerkin
4. Biezeno-Koch	Integral	Displacements	Undefined	Open	Uniform
5. Complementary Energy	Integral	Stresses	Undefined	Open	Galerkin
6. Reissner Energy	Integral	Stresses and Displacements	Undefined	Open	Uniform
7. Collocation	Differential	Displacements	Intersecting	Least Order	Uniform
8. Boundary Point Least Squares (Mikhlen)	Differential	Displacements	Intersecting	Extra Order	Uniform
9. Interior Least Squares	Differential	Displacements	Intersecting	Extra Order	Uniform
10. Airy Stress Function	Differential	Stresses	Intersecting	Least Order	Uniform
11. Maxwell-Mohr	Differential	Stresses and Displacements	Intersecting	Least Order	Uniform
12. Finite Difference (Navier Eqs.)	Differential	Displacements	Intersecting	Least Order	Uniform

the error. In method 8, functions are restricted to those which satisfy the differential equations in the interior. In 9, they must satisfy the boundary conditions exactly. Thus, these methods would be distinctly characterized if details of the basis of the difference operators were included. This is not indicated as an independent ladder level because selection is so diverse.

Assuming the methods given are representative, additional conclusions can be drawn. Most methods use displacement variables. No methods are restricted to use of only disjoint operators. In integral methods, selection of operators is always open. The uniform error criterion is most popular.

ANALYSIS OF ELASTIC CONTINUA

This section considers the effect of decisions on analysis economy accuracy calculation. Alternate decisions at each ladder level are considered independently.

To make the discussion less abstract, it illustrates points of view using approximate solutions of the membrane shown in Fig. 1a. This 100 x 140 rectangular uniformly thick panel is composed of an isotropic material with a Poisson's ratio of 1/3. The left and right edges are stress free. The upper edge is clamped. The lower edge is welded to a rigid stiffener which is translated in the direction of its length 0.001 units. The panel is considered sufficiently thin so that it behaves as a linearly elastic membrane (plane stress). Deformations are required for points on the 4 x 8 uniform mesh shown.

The "exact" solution predicts the structure will deform as depicted in Fig. 1b. This shows that the central region distorts in, predominately, shear action. Near the free edges, the strain pattern is complex.

This solution was developed by a finite difference analysis of the problem. A regular 15 x 35 mesh was used. The 1050 equations were solved, by a relaxation process, to five significant digits of accuracy.

In the sequel, the accuracy of a given analysis will be measured by defining an error vector ϵ ,

$$\begin{Bmatrix} \epsilon_{u_i} \\ \epsilon_{v_i} \end{Bmatrix} = \begin{Bmatrix} u_{Ei} - u_{Ai} \\ v_{Ei} - v_{Ai} \end{Bmatrix} \quad (1)$$

where ϵ_{u_i} and ϵ_{v_i} are component errors for displacements in the x and y directions as illustrated in Fig. 1.

u_{Ei} and v_{Ei} are the displacement components from the "exact" analysis

u_{Ai} and v_{Ai} are displacement components from the approximate analysis.

Thus, the ϵ vector is null for the exact analysis.

A single error measure is given by

$$e = \sqrt{\frac{1}{2N}} \left[\sum_{i=1,2,\dots,N} (\epsilon_{u_i}^2 + \epsilon_{v_i}^2) \right]^{1/2} \quad (2)$$

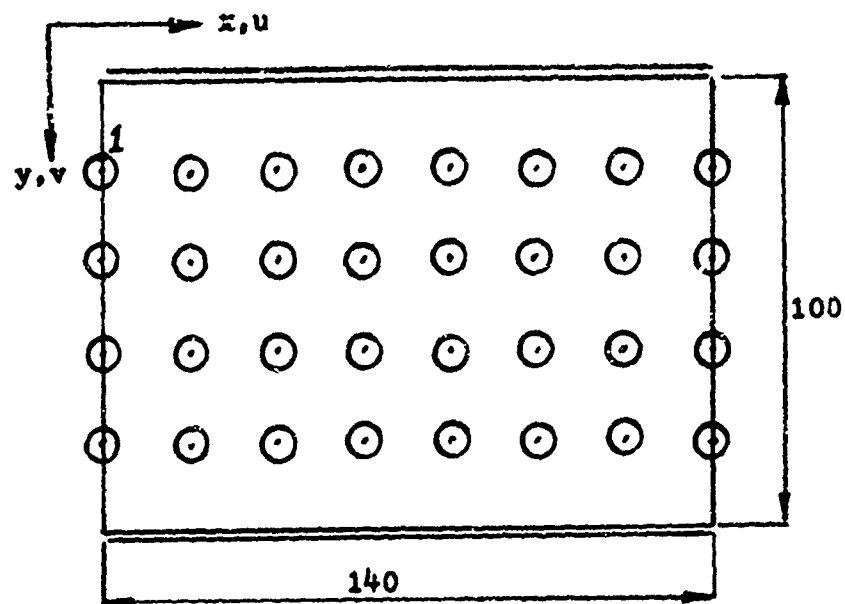
where e is the "mean component error"

Formulation

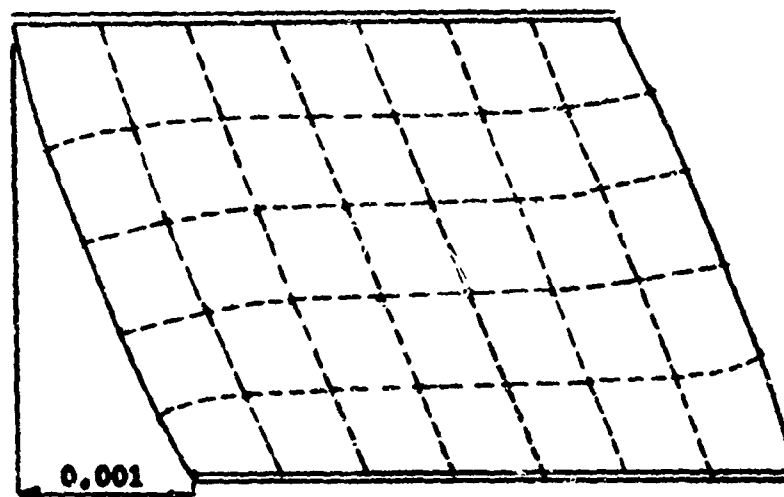
To particularize a comparison between D. E. and I. E. formulations, consider the articulation illustrated schematically in the upper panel of Fig. 2a. In the model, the u and displacements are assumed to vary linearly over each triangular region. i.e.

$$\alpha_g = \begin{Bmatrix} u \\ v \end{Bmatrix} = \begin{Bmatrix} \lambda_1 + \lambda_2 x + \lambda_3 y \\ \lambda_4 + \lambda_5 x + \lambda_6 y \end{Bmatrix} \quad (3)$$

At issue is whether the λ 's shall be determined by minimizing the errors in satisfying the differential equations of elasticity or by minimizing weighted integrals of the error.

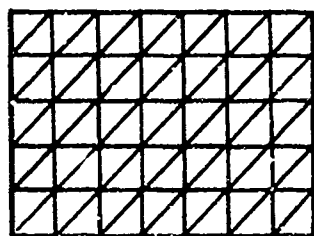


a. Panel Undeformed Geometry

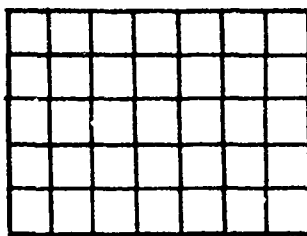


b. Panel Deformed Geometry

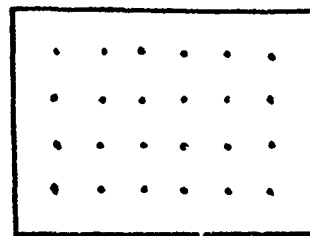
Figure 1. Illustrative Membrane Structure



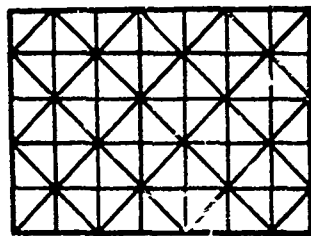
a. Parallel



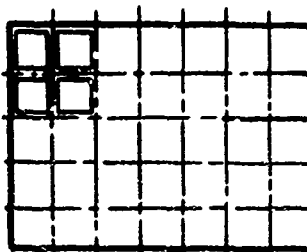
b. Square Module



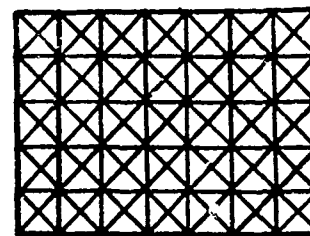
c. Basic Model



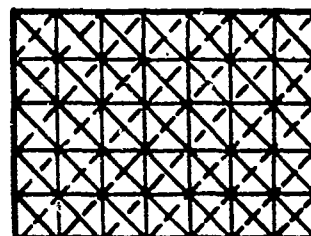
d. Alternating



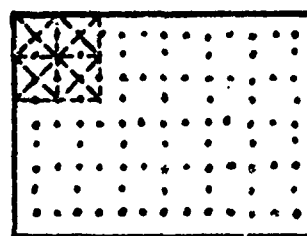
e. Sheet Analog



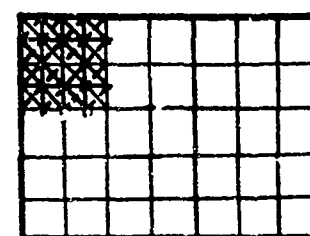
f. Crossed



g. Laminated



h. Stress Model



i. Refined

Figure 2. Schematics of Membrane Models

The D. E. alternative is represented by writing equilibrium equations across all the unfixed boundaries of the membrane. This is a collocation solution. Across the real free boundaries, stresses are required to be zero. Across fictitious boundaries it is required that the stresses be continuous at the midpoint of triangle sides. This results in 206 equations in the 64 unknown displacements. The unknown displacements are then found such that the sum of the squares of the residuals in each equation is minimized.

The I. E. alternative is represented by a potential energy analysis of the system. This involves direct use of the Turner triangular element membrane stiffness matrix for the mesh chosen. It results in 64 equations in the 64 unknown displacements. In this approach, the method corresponds to evaluating displacements so the integral of the error in satisfying the differential equations of equilibrium, when weighted by the assumed displacement functions, will be a minimum. ⁽⁹⁾

These analyses indicate the error norm for the potential energy method is less than half that for the differential equation model. As would be expected, the fact that all diagonal cuts are made in the same direction makes it difficult to interpret the error pattern over the planform.

Figure 2b shows a different mesh for the same membrane. Two analyses like the above were made of this model using, as assumed displacements,

$$\alpha_g = \left\{ \begin{array}{l} \lambda_1 + \lambda_2 u + \lambda_3 y + \lambda_4 u y \\ \lambda_5 + \lambda_6 u + \lambda_7 y + \lambda_8 u y \end{array} \right\} \quad (4)$$

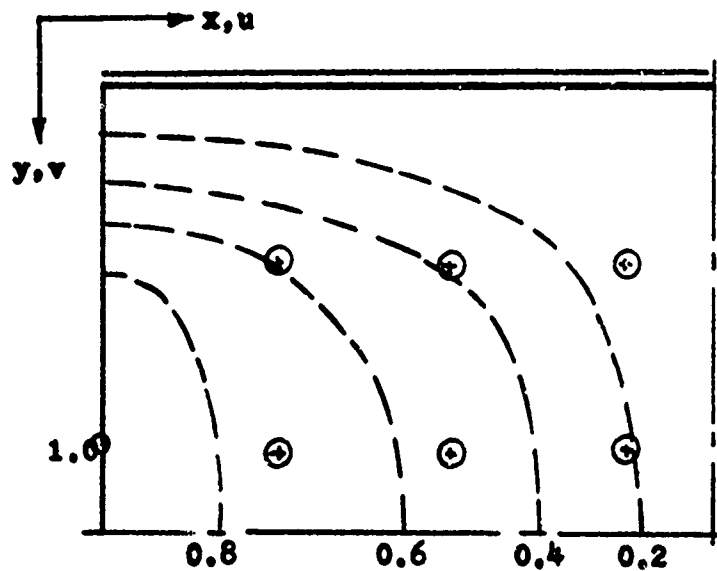
The collocation solution involves only 136 equations and the potential energy 64, in the 64 unknowns. The finite element stiffness matrix is given in Ref. 10.

These analyses indicate the error norm for the potential energy solution is less than one third that of the differential equation solution. Figure 3 shows analysis error contours for these last two solutions. These have been normalized to the maximum error to facilitate interpretation. Because of the deformation asymmetries, one quadrant of the system is representative of all. Only errors in v displacement components are plotted, since these are twice as big as u displacement errors. Both analyses given errors indicating predicted displacements are less than exact.

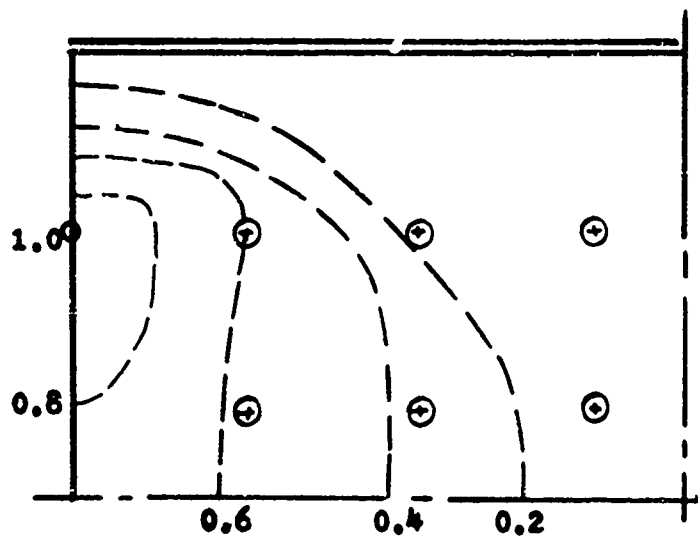
Both analyses have the largest errors at the free edges. The spacing of contours for the collocation analysis is more regular than for the potential energy. This suggests the collocation analysis will yield better estimates of the distribution of stresses if the difference in deflections is dominated by the errors. Nevertheless, since the potential energy solution has smaller u and v errors at every joint, it is more accurate.

In these analyses, the potential energy approach is more efficient than the collocation. The potential approach is not burdened with the extra calculations of the least square error evaluation and is more accurate.

If this argument for the integral approach is not convincing, a more compelling argument may be found in the analysis of determinate structures. Consider the prismatic, tip-loaded cantilevered beam shown in Fig. 4. The displacements for this beam obtained by solving the beam equation are shown in continuous curve in Fig. 4.



a. Collocation Analysis



b. Potential Energy Analysis

Figure 3. Relative Error Contours of Formulation Alternatives

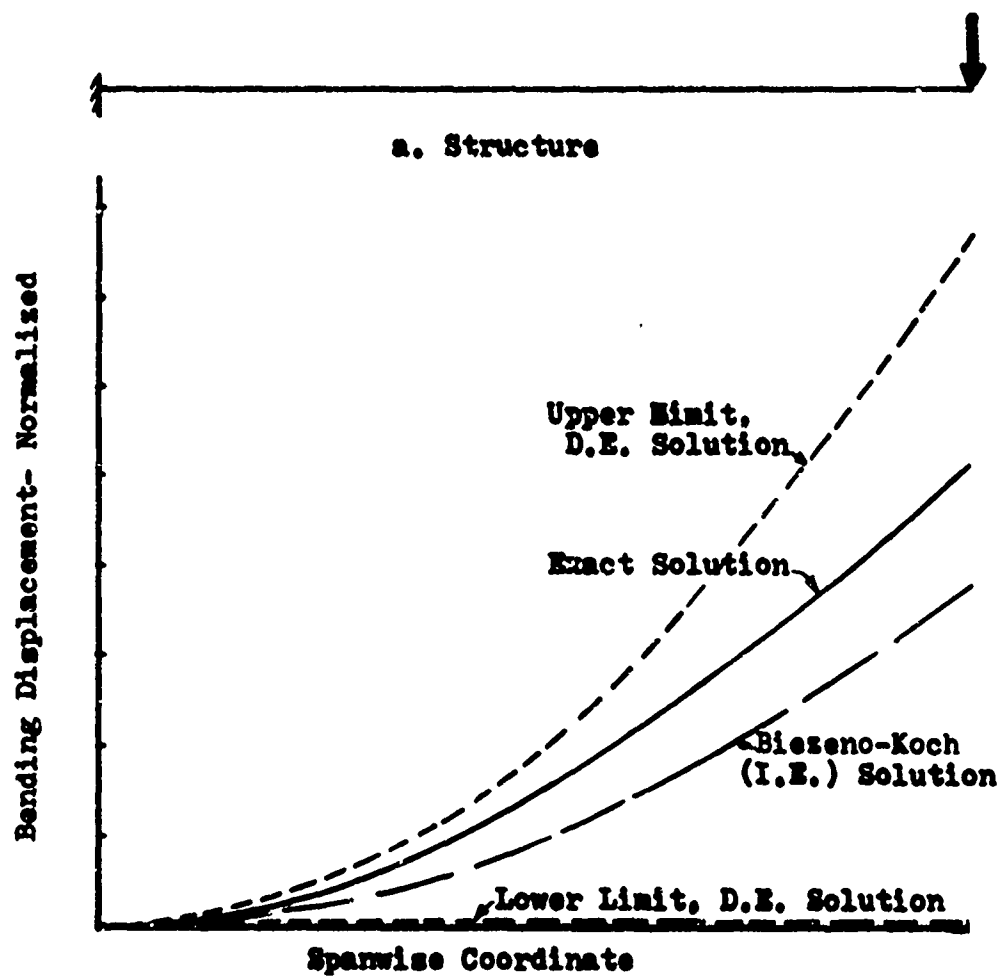


Figure 4. Analysis Results for Simple Beam

Assume displacements vary with x^2 , the coordinate measured along the beam from the root toward the tip. Then the displacement estimate for the Biezeno-Koch is shown as the long dashed curve in the figure.

The two short dashed curves bound the predicted behavior when the generalized coordinate is chosen so the beam equation is satisfied. The upper curve occurs when collocation is made at the root. The curve lying on the x axis is the predicted behavior when collocation occurs at the tip. The span between the curves is indicative of the relatively high sensitivity of the D. E. approach to selection of collocation positions. Even if the optimum collocation point were known ab initio, a different point would be required for each loading, thus requiring a complete analysis for each load. Then even if both approaches had the same accuracy, the differential will carry excessive calculation penalties for multiple loadings.

For the same number of generalized coordinates the I. E. approach requires more calculations than the differential. In the integral formulation more effort is required in developing equation coefficients. Irregular regions are usually treated by performing integrations numerically. Difficulty is experienced in the differential equation approach with defining the equations in regions of geometric anisotropy and mesh irregularity. The first difficulty is masked by allowing the analyst to select from a limited number of non-uniform geometry models at no significant calculation penalty. The second can be overcome by choosing functions identified with regions rather than points, as was done in the analyses described above.

It is concluded that the I. E. approach is intrinsically the more efficient approach, as long as excessive penalties for integration can be avoided.

Behavior Model

Figure 2g, 2h, and 2i show three articulations used to compare the affect of the selection of the behavior model on analysis efficiency. The Fig. 2g and Fig. 2i representations provide the bases for analyses using assumed displacement functions and the potential energy approach. The Fig. 2h model pertains to use of assumed stress functions and the complementary energy approach.

The displacement analyses uses a square membrane finite element matrix based on the Turner triangle model. Two stiffness matrices are developed for a square region. Each is for one-half the membrane stiffness. One has an upward slanting diagonal and the other, a downward. These matrices are added to define an "unbiased" stiffness matrix. Use of this matrix insures displacement predictions with the desirable deformation asymmetries.

This element model is used in the two displacement method analyses. The Fig. 2g articulation results in 64 equations and unknowns. The articulation of Fig. 2i leads to 270 equations and unknowns. Despite the added degrees of freedom in this model, the components of the error vector are taken as only those which also exist in the Fig. 2c model.

The stress variable analysis is also based on a triangular finite element model which is formed by adding two stiffness matrices. As DeVeubeke⁽¹¹⁾ has shown, complementary energy solutions can be developed by the direct stiffness method using the Turner triangle if joints are located at the middle of the sides of the triangle. Then, because the displacement function given by Eq. (3) implies uniform stress distributions, matching displacement components corresponds to satisfying the microscopic equations of equilibrium across each boundary of the triangle.

Accordingly, stiffness matrices were developed for the diagonal-slanting-down and a diagonal-slanting-up square. These matrices were added. Then the equations associated with center joint were reduced out.

Applying this model to the arrangement of squares shown in Fig. 2h leads to a set of 206 equations in 206 unknowns. Evaluations of these unknowns produces the desired displacements.

Unfortunately, a direct comparison of the norms of the error vector for the two types of analysis cannot be made. The stress approach does not yield unique values for displacements at the points of interest. (Note that a corresponding deficiency exists in the displacement method for stresses). This difficulty is circumvented by defining displacement errors components at the mesh points shown in Fig. 2h.

Values of the mean component error for articulations associated with Fig. 2g, 2h, and 2i are, respectively, .0136, and .0131, .0050. These data do not show that the stress variable has intrinsic accuracy advantages over the displacement for a given number of degrees of freedom and comparable assumed behavior functions.

This triangular membrane stress model avoids the calculation penalties usually associated with use of stress variables. These arise because it is necessary to develop coefficients of the total set of structural equations to

maintain stress continuity.

Usually, the equations are written and solved choosing the force method of manipulations. Then, as Bamford also points out, the number of calculations can be increased by several orders of magnitude over those required in the displacement method due to calculation penalties associated with redundant selection. A minimum of a factor of four is projected. Table III reproduces data from Ref. 13. These data are indicative of the calculation penalty in practical problems for stress variables selection when comparable articulations are used.

To examine the desirability of using both displacement and stress variables, consider a system with "d" displacement redundants or "s" stress redundants. To obtain the exact problem solution requires, in general, either d displacement states or s stress states. Using both sets of states must always result in more equations than the minimum. Thus, the two variable approach cannot be as efficient as the better of the stress and displacement approaches.

Thus, displacement variables should be used to maximize analysis efficiency. Their efficiency is attributed to the relatively few calculations required in solving the associated reduced set of structural equations.

Table III
Calculation Effort for Practical Analyses

<u>Structure</u>	<u>Method</u>	<u>No. of Equations</u>	<u>No. of Redundants</u>	<u>No. of Calculations</u>	<u>Relative No. of Calculations</u>
Swept Wing	Displacement Force	360	---	0.45×10^6	1.0
		390	101	1.71×10^6	4.3
Unswept Box	Displacement Force	300	---	0.26×10^6	1.0
		390	161	3.58×10^6	13.8

Table IV
Relative Calculation Effort

<u>No. of Equations</u>	<u>Disjoint Mesh</u>	<u>Operator Wavefront</u>	<u>Intersecting Mesh</u>	<u>Operator Wavefront</u>	<u>Calc. Disj./Inter.</u>
300	6 x 8	36	9 x 16	18	3.8
1000	11 x 15	66	20 x 25	40	2.6
3600	21 x 29	126	35 x 52	70	3.3
14000	41 x 57	246	70 x 100	140	3.2

Operators

To compare the efficiency of disjoint and intersecting operators, consider deformations on cross sections taken through the membrane. The continuous curve in Fig. 6 shows the exact v (y direction) deflections for a cross section along the first line of mesh points (see insert).

Now consider a disjoint and an intersecting operator, each based on a cubic displacement function. The disjoint operator uses the deflection and its first derivative at each end as generalized coordinates. It involves a Hermite polynomial. The intersecting uses the deflection at the ends, $1/3$, and $2/3$ points.

The relative accuracy of these two operators can be compared by comparing their fidelity in interpolation for structural problems. The two dashed curves in Fig. 6 permit this comparison for line 1 of the membrane. These curves show, separately, the interpolation curves. These data suggest that the intersecting operator will be more accurate than the disjoint.

Table IV cites the value of the solution wavefront as a function of the number of equations for the membrane, using increasingly finer meshes. The number of calculations is given by,

$$N_g = 2Nw^2 + 4Nwc \quad (5)$$

where N_g is the number of calculations for equation solution for $N \gg 1$,

w is the wavefront, and

c is the number of loadings (1.0).

Meshes are chosen so both analyses will have the same number of equations.

The number of calculations to develop operator coefficients is,

$$N_g = \beta D^2 \quad (6)$$

where N_g is the number of generation calculations for $N \gg 1$,

β is a scalar, and

D is the number of degrees of freedom referenced.

Since, in this comparison, D is the same for both operators, the difference in the number of calculations is dependent only on the number of equations and wavefront.

These data show disjoint operators involve about three times as many calculations for equation solution as intersecting for this membrane. Though the factor will vary with the problem and basic articulation, the conclusion that the use of disjoint operators will involve a calculation penalty is valid in general. Since the intersecting operator requires fewer calculations and will be as accurate as the disjoint, it is more efficient. (The complications in implementing intersecting operators, however, may not justify the small gains expected.)

The only requirement for each operator is that it be based on a function which faithfully represents the structural behavior over its domain of application. Since the behavior is unknown, *ab initio*, this requirement is that the function be an adequate interpolation function, i.e., that the error associated with its use vanish as the number of mesh points approaches infinity. This is the requirement of mathematical completeness.

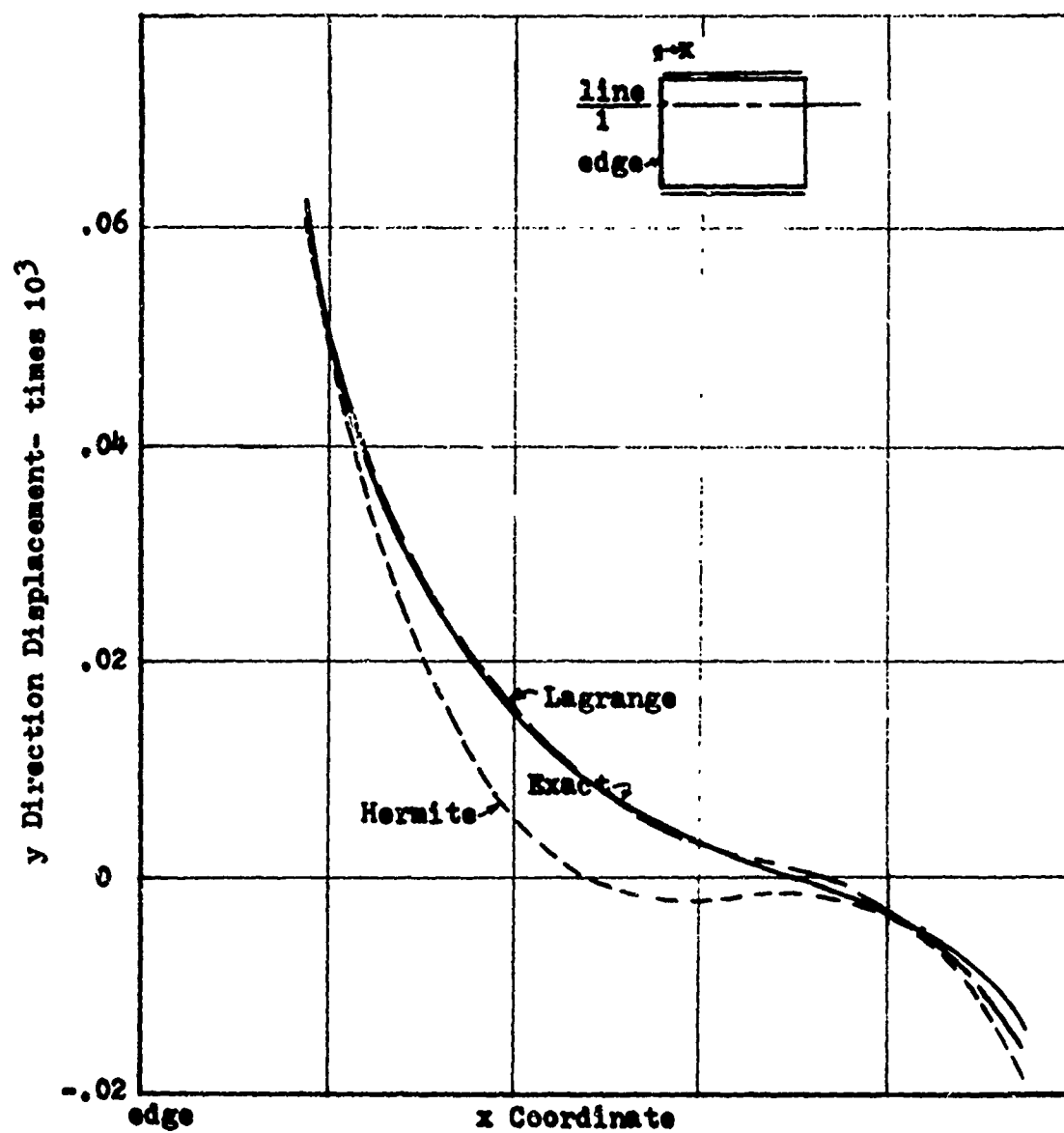


Figure 6. Interpolation of Membrane Behavior

If this requirement is met, the exact solution may be developed by choosing a sufficiently refined mesh, barring manipulation errors. Functions need not satisfy compatibility, equilibrium, nor Hooke's law when the mesh is finite. Functions may contain singularities.

It might be inferred from the study by Walton et al⁽¹⁴⁾ that the manner in which the structure is articulated can destroy the adequacy of an operator. The reader could infer that if difference equations characteristic of a point in a triangulated mesh are typical, the Turner triangle in the limit, does not solve the differential equations of elastic equilibrium. This is false. The proof given by Synge⁽¹⁵⁾ of the adequacy of the triangular interpolating function is sufficient to insure convergence to the elastic solution regardless of the mesh model.

Assuming the solution to the problem of interest is unknown, and restricting selection to ones with mesh-size dependent error terms, there are still many possibilities. The most attractive from an efficiency standpoint will -

1. have invariance of strains with translations and rotations of coordinates. This property will improve efficiency by permitting reuse of operators for similar geometries, by permitting macroscopic equilibrium checks on the solution,⁽¹⁰⁾ and by improving accuracy for a given number of generalized coordinates⁽¹⁶⁾
2. insure monotonic convergence with mesh refinement. Use of operators with this property will admit solution extrapolation with a minimum number of solutions. It will guarantee that refined mesh models will yield improved answers.
3. be easy to differentiate and integrate. This will minimize the need for numerical differentiation and integration, thus eliminating calculations and a potential source of error.
4. depend only on elementary operations. This will avoid relatively costly series evaluations.

As in interpolation, polynomials provide the most popular basis for assumed functions. Harmonic functions are used when response must be periodic. Particular forms of these functions can easily be chosen to meet the completeness requirement and satisfy the desirability requirements listed above.

Thus, intersecting operators are more efficient than disjoint. Subject to the requirement that operators have error terms that vanish as mesh points become infinite, all operators can be included in the operator collection.

Articulation

To suggest guidelines for articulation, consider the 14 articulations of the membrane cited in Table V. Seven of these use a triangulated mesh so are given code names containing the letter "T". They are based on a linear displacement field over the triangle of the form of Eq. (3). The last seven use a rectangular mesh.

The articulation details for the first seven are represented schematically by the drawings in Fig. 2. The first three use the Turner stiffness matrix for a triangular membrane. They differ only in the manner in which the fictitious cuts are made. The first uses parallel diagonal cuts (Fig. 2a) recommended by Walton et al.⁽¹⁴⁾ The second uses alternating diagonals (Fig. 2d). The third uses crossed diagonals, (Fig. 2f) resulting in an added mesh point at the center of each square. Number 4 and 5 use the laminated model described in discussing behavior models. These two articulations differ only in the mesh refinement. Analysis 4 uses the least order mesh (Fig. 2a), analysis 5, a mesh with four times as many mesh points (Fig. 2i). The mid-side model (Fig. 2h) is the mesh for the complementary energy articulation. The boundary (Fig. 2a) models have been described in comparing formulations.

The last seven articulations are all based on a square module mesh. Numbers 8, 13, and 14 assume a hyperbolic displacement field (Eq. 3) over the square but evaluate generalized coordinates using different error measures. Number 8 is a potential energy model. Number 13 and 14 are differential equation models: 13 using collocation points at element and free edge boundaries, 14 collocating at the midpoint of each square and at the free edge boundaries. Number 9 uses the rectangular panel stiffness matrix given by Turner⁽⁸⁾. Number 10 (Fig. 2f) uses the analog operator of Hrennikoff⁽¹⁷⁾. This replaces each square panel by six rods. The area of the rods are selected so that the truss model will have the correct stiffness when the membrane is under a uniform stress state. Number 11 is also an analog model. It replaces each square module by a shear panel bounded by four rods. Number 12, the finite difference articulation, (Fig. 2c), uses point operators based on second order polynomials. Operators for free edge boundary points use backward differences.

Results of analyses using these articulations are summarized in Table VI. This table cites the number of equations and unknowns. The "trend" notes whether predicted deflections tend to be less (stiff) or greater (soft) than the exact values. None of the analyses were too stiff or too soft everywhere.

Figure 7 is a bar chart of the mean component error for the 14 analyses. The error has been plotted on a log scale to compress data. These data show error predictions span two orders of magnitude. The results fall roughly into three groups: good, fair, and poor. Good results have relative mean component errors ranging from .0059 to .0085; fair, from .0130 to .0175; and poor, from .0413 to .1620. The relative error is defined as the absolute divided by the largest deflection, .001. In the figure, the ones in each region are keyed differently.

The good results are associated with the square module and refined triangular meshes. Fair results arise from the simple triangular meshes and the finite difference square mesh model. All the poor results arise in collocation analyses. Thus, these results confirm the desirability of using an integral approach.

Table V

Membrane Analysis Articulations

<u>Articulation No.</u>	<u>Name</u>	<u>Code Name</u>	<u>Mesh Model</u>	<u>Operator and Basis</u>
1	Parallel diagonal	PT	a	Triangle - linear displacement field
2	Alternating diagonal	AT	d	Triangle - linear displacement field
3	Crossed diagonal	CT	f	"
4	Laminated square	LT	g	"
5	Refined laminated	RT	i	"
6	Mid-side	MT	h	"
7	Boundaries	BT	a	"
8	Hyperbolic	HR	b	Rectangle-hyperbolic displacement field
9	Moment	MR	b	Rectangle-limited linear stress field
10	Truss analog	TR	f	Rectangle-Hrennikoff analogy
11	Shear panel	SR	e	Rectangle-panel stringer analog
12	Finite difference	DR	c	Point-quadratic polynomials
13	Boundaries	BR	b	Square and line-hyperbolic displacement field
14	Panel-edge	ER	b	Square and line-hyperbolic displacement field

Table VI

Membrane Analysis Results

<u>Analysis No.</u>	<u>Code Name</u>	<u>No. of Equations</u>	<u>No. of Unknowns</u>	<u>Trend in Results</u>	<u>ex10</u>
1	PT	64	64	Stiff	0.138
2	AT	64	64	Stiff	0.130
3	CT	134	134	Stiff	0.071
4	LT	64	64	Stiff	0.136
5	RT	270	270	Stiff	0.050
6	MT	206	206	Soft	0.131
7	BT	206	64	Mixed	1.620
8	HR	64	64	Stiff	0.068
9	MR	64	64	Mixed	0.059
10	TR	64	64	Stiff	0.085
11	SR	64	64	Mixed	0.081
12	DR	64	64	Mixed	0.175
13	BR	136	64	Mixed	0.413
14	ER	90	64	Mixed	1.050

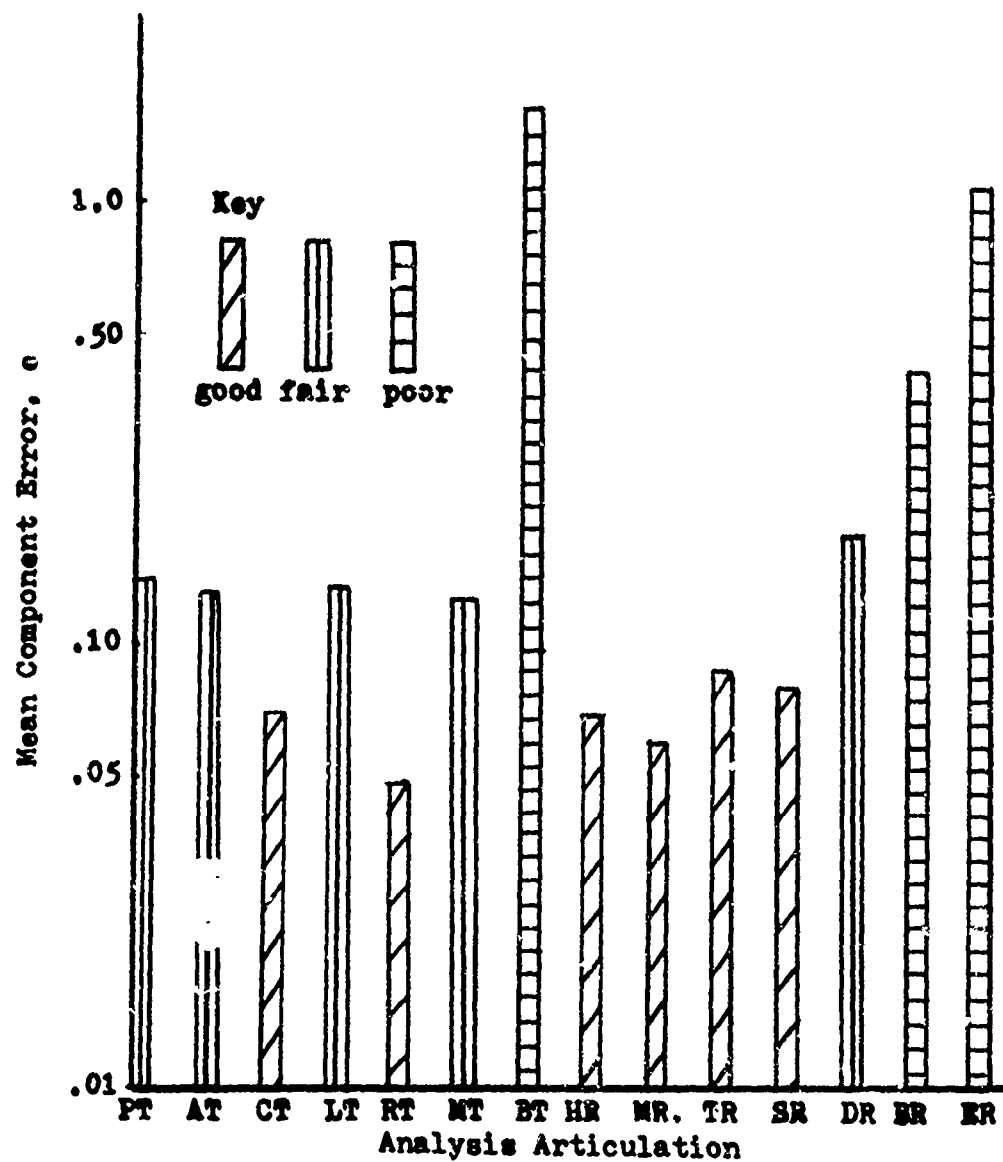


Figure 7. Bar Chart of Mean Component Error

Articulation Order

The decision on the order of articulation is solely an accuracy decision. The choice of idealization defines the mesh points. The choice of behavior states identifies the least number of α_g to be evaluated. Fewer, an equal number or more generalized coordinates should be used in each region as required to attain the accuracy needed by the analyst. Thus, this is a decision that must be made adaptively, i.e., to suit the problem at hand.

Experience with the displacement method suggests that the number of points required for describing the structural geometry is less than that required for the desired accuracy. Thus extra order articulation is the mode.

The membrane problem illustrates this condition. Table VII lists the strain in the y direction at point 1, as shown in Fig. 1a. Data are given for analyses 3 through 5. These data can be compared with the exact estimate of strain given, based on the 1050 degree of freedom finite difference analysis.

These data show that the error with the least order models is excessive. The accuracy of the extra order models improves as more coordinates are added, but still is not within engineering requirements, five percent, for the finest (RT) articulation.

Operator Degree

These analyses show that the efficiency of operators for triangles is low compared with rectangular. The accuracy of the crossed diagonal model (CT) is comparable to the square models (HR, MR, TR, and SR). The CT analyses, however, incurs more calculations because it involves more equations and more generation arithmetic. Conversely, when the number of calculations is comparable for the triangle (PT, AT, and LT analyses) and square, the accuracy of the triangle models is worse. The data in Ref. 18 illustrates that this conclusion extends to three dimensional analyses. Here prisms are more efficient than tetrahedra.

Table VIII lists data for comparing calculations in least and higher degree membrane models. The first four columns summarize problem calculation data for five levels of mesh refinement. For each, each square in the mesh of Fig. 2b is replaced by the square module shown in Table VIII. Similar data is given in the last four columns for increasingly higher degree modules.





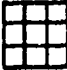





These data exhibit the calculation penalty due to the increased wavefront associated with the higher degree operators. The higher degree operators involve no generation calculation penalty, but all required more calculations than use of a comparable least degree operator. Moreover, this calculation penalty is incurred even though the higher degree models have fewer degrees of freedom.

With respect to accuracy, there is no reason to believe the higher degree operators have higher accuracy than corresponding least order. Comparisons based on an equal number of degrees of freedom are discounted because the least degree operators can be applied with much finer meshes for a given number of calculations.

Table VII
Strain Estimates from Various Analyses

<u>Analysis:</u>	<u>LT</u>	<u>CT</u>	<u>RT</u>	<u>Exact</u>
No. of Equations:	64	134	270	1050
Strain:	1.8293	1.0741	0.9629	0.7354
Error:	149%	46%	31%	0%

Table VIII
Least and Higher Degree Membrane Calculations

<u>Set</u>	<u>Least Module</u>	<u>N</u>	<u>W</u>	<u>Calcs.</u>	<u>Higher Module</u>	<u>N</u>	<u>W</u>	<u>Calcs.</u>
1		96	16	$560\beta + .05^6$		96	16	$560\beta + .05^6$
2		330	26	$2240\beta + .48^6$		260	34	$2240\beta + .63^6$
3		704	36	$5040\beta + 1.9^6$		412	56	$5040\beta + 3.5^6$
4		1220	46	$8960\beta + 5.4^6$		588	80	$8960\beta + 7.7^6$
5		1860	56	$13,900\beta + 12.3^6$		752	104	$13,900\beta + 16.7^6$

Comparison of results for the set two modules of Table VIII could illustrate that no accuracy advantages lie with higher degree models. Analyses PT and CT provide similar results for a triangular module. These data show that increasing the number of cuts does not, per se, result in reduced accuracy.

Higher degree operators are desirable when it means replacing rectangles with triangles. However, higher degree operators are undesirable if they result in increased wavefronts.

Operator Basis

These analyses suggest that analysis efficiency is not sensitive to the operator basis used. Effectiveness of the four square mesh operators are comparable though they involve two different analogs, a potential energy, and a non-conforming rectangle. Efficiency of using the laminated (averaged) and parallel diagonal triangular based operators are comparable.

Comparing results of the triangular mesh patterns provides no justification for selecting one over the other. Parallel, and alternating, models yield results with similar accuracy. Since they require the same number of calculations, they are equally efficient.

These analyses give significantly different distributions of the error components, however. The bias introduced by the irregularity of the mesh results in a lack of the v deflection asymmetry about the y centerline and u symmetry about the x . Though these dissymmetries can be avoided using the laminated model, a more efficient approach is to analyze only $\frac{1}{2}$ of the membrane and superimpose symmetric and asymmetric solutions.

Thus extra degree articulations can be expected. Refined but not high degree operators should be used. The criterion of maximum accuracy per calculation leads to no preference for one articulation over another.

Total Error Criterion

To examine the significance of the choice of the weighting of errors, consider a general analysis based on Eqs. (4). In this general analysis expressions for error are written at the panel central points, and at the midpoints of each side. Since there are more error equations than unknowns, the variables are assigned to minimize the sum of the errors squared.

The mean component error in these analyses varies as a function of the ratio of weighting between the panel and midside points. As the relative weighting of panel equilibrium error varies from zero (non-uniform) to 1.0 (uniform) the error increases by more than twenty-five percent and then diminishes to nine percent. Not surprisingly, lower error is associated with non-uniform weighting.

Adding the panel equilibrium equations to the HR model and using a least squares analysis provides a similar test of Galerkin weighting. In this case, the mean component error is reduced by about four percent by introducing the panel equilibrium conditions. This confirms that Galerkin weighting is not the most efficient weighting.

Thus the weighting involving the most accuracy per calculation is a non-uniform positive weighting. Both uniform and Galerkin weighting can be considered special cases of the non-uniform, but neither offers special advantages. (Even the bounding capability identified with Galerkin weighting can be disassociated from it). Thus mixed uniform and Galerkin weighting is excluded.

Unfortunately there is no best way known to choose the weighting if the solution is unknown. The analyst may require that peak stresses be predicted with less than five percent error, or he may be interested in accurate deflection distributions. The analysis, however, only directly controls the error in satisfying equilibrium, compatibility and/or Hooke's law. This inconsistency between error that is controlled and the analyst's requirements make comparisons of experimental results and exact solutions speculative. A statement that operator A is better than B because it gets better results for a particular problem is largely meaningless.

If the analyst desires to bound his solution, weightings can be selected adaptively. The weighting which provides the narrowest solution range must be the most accurate. The analysis problem becomes then an optimization problem, viz: select the positive weighting which will result in the minimum bounds on predicted behavior.

If the analyst's objective is to obtain the best possible answers then the analysis can still be viewed as an optimization problem; viz: select the positive weighting which results in the minimum error from a statistical viewpoint.

Thus, selection of weighting can transform the analysis problem into an optimization. Whether this will produce a more efficient analysis approach requires study.

Even if the weighting can be selected, what measure of all the errors to minimize is still a question for the problem with an overdetermined equation set. Of the norm measures, the least square measure is most efficient because it permits selection of the generalized coordinates by solving linear simultaneous equations. The maximum component and absolute error sum methods require iterative solution algorithms and can involve non-unique solutions.

The inefficiency of the least square error approach is illustrated by reconsidering the finite difference analysis, DR. Consider two new variants of the DR analysis. In the first, the panel equilibrium equations supplement the finite difference equations. Thus, it is required that equilibrium be satisfied at the panel central points and the mesh points of the basic grid, Fig. 2c. Then there are 134 equations and 64 unknown displacements. Solving these equations using least squares produces a solution with $e = 0.0080$.

In the second variant, an additional mesh point is taken at the center of each panel. Writing equilibrium equations at these and the basic mesh points, Fig. 2c, results in 134 equations in 134 unknowns. Solution of these equations produces answers with $e = 0.0123$.

The accuracy of these two solutions is comparable. In addition, both problems involve the same number of calculations. The reduced order of the least square analysis is balanced by the increased calculations in generation as long as the known symmetry of the final matrix is exploited. Thus, the choice between minimizing the sum of the squares of the error components so all will be made zero is not one of efficiency.

The least square approach can be rejected because it introduces a supernumary error control. In the limit this control is immaterial. For approximate analysis, however, this control complicates the interpretation of solution accuracy and may introduce an analysis inconsistency.

To maximize efficiency, a general positive weighting should be selected. Overdetermined sets of equations should be avoided.

EXISTING ANALYSIS APPROACHES

The most efficient analysis has been one identified by an integral equation approach, displacement variables, intersecting operators, and low degree low order articulation. In the paragraphs that follow, some current issues of analysis will be resolved in this context.

Force or Displacement Method?

Two features distinguish force method analysis from displacement: choice of behavior states and the sequence in which variables of the structural equations are evaluated. The force method uses stress or generalized forces as independent variables and writes microscopic equations of equilibrium across element boundaries. The displacements and dependent forces are eliminated from the structural equations first and then redundant forces evaluated.

In the displacement method, approximate equilibrium equations are expressed in terms of the assumed displacement states by eliminating all force unknowns from the structural equations. The reduced equations are solved for displacements.

Compared with the ideal, both methods have the disadvantage of using disjoint operators. Compared with each other, the force method, as previously discussed, involves large calculation penalties with no concomitant accuracy advantage.

Finite Differences or Finite Elements?

The finite difference method uses the D. E. approach, intersecting operators and low degree, low order operators. The finite element approach, however, is only distinguished by use of disjoint operators. As such, a finite element analysis of a regular structure can become a finite difference analysis. Thus, without defining other decisions, finite difference analysis and finite element approaches cannot be compared since finite difference analysis can be a subset of finite element.

As most commonly practised, the finite element method uses the I. E. approach, disjoint operators and low degree low order operators. As such its formulation is superior to the finite difference, but its operator basis less efficient. The membrane analyses suggest that the efficiency advantages of the I. E. approach outweigh the disadvantages of disjoint operators. Therefore the finite element method is better than the finite difference.

Should Reanalysis use the Best Analysis Method?

The simulation environmental conditions for reanalysis are different from the analysis environment. Thus, the reanalysis method can be expected to take a different form. In particular, each reanalysis is one of a series of analyses of a group of closely related configurations. Moreover, reanalysis need not be as accurate as the usual analysis. It need only be as accurate as the accuracy of current estimates of the design variables. The first condition admits special initializing calculations to accelerate the multiple configuration analysis, since these calculations will be amortized over a number of reanalyses. The second condition suggests the use of fewer degrees of freedom in reanalysis than in a baseline analysis of the system.

The analysis decision vulnerable to this environment is selection of assumed behavior states. For all structures for which St. Venant's principle applies, use of stress states offers large savings in reanalysis costs. This is, in fact, the basis for the efficient fully-stressed and uniform-strain-energy-density optimization approaches. (19), (20).

CONCLUSIONS

This review of analysis decisions leads to the following conclusions:

1. Published analysis methods are but a small sampling of the possible analysis methods that can be defined based on the basic analysis decisions: formulation, behavior states, operators, articulation, and error criterion.
2. To maximize analysis accuracy per calculation, the integral equation formulation, displacement behavior states, intersecting operators, and low degree-low order articulation should be selected.
3. Neither uniform nor Galerkin error weighting is optimum. The most efficient approach involves non-uniform (positive) weighting.
4. Overdetermined sets of error equations should be avoided. Their use may obscure analysis predictions and complicate interpretation of results.
5. The displacement method is better than the force method, not because of accuracy differences, but due to calculation penalties in the force method.
6. The popular version of the finite element method is better than the finite difference method.

References

1. Pian, T. H. and Tong, P. "Rationalization in Deriving Element Stiffness Matrix by Assumed Stress Approach", Reference 6, p. 441-471.
2. Leissa, A. W., Halbert, L. E., Hopper, A. T., and Clausen, W. E., "A Comparison of Approximate Methods for Solution of Plate Bending Problems," AIAA Jour., Vol. 7, No. 5, May, 1969. pp. 920-928.
3. Melosh, R. J. "Basis for Derivation of Matrices for the Direct Stiffness Matrix," AIAA Jour. Vol. 1, No. 7, July 1963, pp 1631-1637.
4. Key, S. N., A Convergence Investigation of the Direct Stiffness Method, Ph.D. Dissertation, University of Washington, 1966.
5. Walz, T. E. et al., "Accuracy of Finite Element Approximations to Structural Problems," TND-5728, 1970, NASA
6. Proceeding of the Second Conference on Matrix Methods in Structural Mechanics, AFFDL-TR-68-150, Wright-Patterson AFB, Ohio, December 1969.
7. Sokolnikov, I. S. Mathematical Theory of Elasticity, McGraw-Hill Book Co., New York, 1956.
8. Crandall, S. H., Engineering Analysis, McGraw-Hill, New York, 1956.
9. Turner, M. J., Clough, R. W., Martin, H. C. and Topp, L. J. "Stiffness and Deflection Analysis of Complex Structures," Jour. Aero. Sci, Vol. 23, No. 9, September 1948, pp 805-823.
10. Argyris, J. H. and Kelsey, S. Modern Fuselage Analysis and Elastic Aircraft, Butterworths, London, 1963, p.101.
11. Fraeijls de Venbeke, B., "Bending and Stretching of Plates Special Models for Upper and Lower Bounds", Proceedings of Conference on Matrix Methods in Structural Mechanics, AFDDL-TR-66-80, Wright-Patterson AFB, Ohio, December 1965.
12. Bamford, R. M., "Force Method versus the Displacement Method," JPL memo dated April 12, 1970.
13. Melosh, R. J and Palacol, E. L. "Manipulation Errors in Finite Element Analyses of Structures," NASA CR-1385, National Aeronautics and Space Administration, Washington, August 1969, 141 p.
14. Waltz, J. E., Fulton, R. E., and Cyrus, N J. "Accuracy and Convergence of Finite Element Approximations," Reference 6, pp 995-1028.
15. Synge, J. L. The Hypercircle in Mathematical Physics, Cambridge University Press, 1957.
16. Murray, K. H. "Comments on Convergence of Finite Element Solutions," AIAA Journal, April, 1970, Vol. 8, No. 4, pp 815-816.

17. Hrennikoff, A. "Solution of Problems of Elasticity by the Framework Method," Jour. Appl. Mech., ASME, December 1941.
18. Melosh, R. J. "Structural Analysis of Solids," Jour. Struct. Div. ASCE, Vol. 89, No ST4, August 1963, pp 205-224.
19. Melosh, R. J., "Convergence in Fully-Stressed Designing," AGARD Symposium on Structural Optimization, Istanbul, October 1969.
20. Venkayya, V. B., Khot, N. S., and Reddy, V. S. "Optimization of Structures Based on the Study of Energy Distribution," Reference 6, pp 111-164.

QUESTIONS AND COMMENTS FOLLOWING MELOSH'S PAPER

COMMENT: You start out with what looked like an exact and invariant study of a very difficult problem and end up with the demonstration of a numerical example. It's neither exact nor invariant and I believe the conclusions you drew are only valid for that example.

MELOSH: I tried to point out that you can't prove very much but negative hypotheses by examples. This game can be played in many ways; however, there's no way to prove that one method is better with respect to efficiency than another. If we choose to prove which is the best method, we need to do an infinite number of problems to guarantee the right conclusion.

COMMENT: On the chart that you have there showing the Lagrange and the Hermite comparisons, it looked like the particular function involved was approaching a slope singularity at the left which is part of the reason why the Hermite function, using slope variables, was poor. I think that the decision between lower order and higher order operators generally depends a great deal upon the smoothness of the function and the presence of singularities or near singularities. The lower order operators will look very good to you when you have a stress gradient that gets very large or near singularity.

MELOSH: Well, there's no question about it. If you know how your structure behaves, you ought to assume functions that will simulate that behavior. However, there's no way to argue which function is better than another without some kind of an evaluation of the problems that people solve on the average or problems that occupy people's minds most of the time.

That's the way you want to address the selection of the operators.

QUESTION: In your conclusion you said that displacements as the primary variables are better than stresses. Do you mean that if you assume a stress hybrid model, it would not be as good as the displacement model?

MELOSH: What I meant by hybrid was the Reissner formulation. In the case of the Reissner formulation, there's no doubt in my mind that it costs you more to get good answers than using a potential or complementary energy strategy.

DESIGN OF OPTIMUM STRUCTURES

V. B. VENKAYYA

FLIGHT DYNAMICS LABORATORY, WRIGHT-PATTERSON AFB, OHIO

ABSTRACT

A method for optimal design of structures is presented. It is based on an energy criteria and a search procedure for design of structures subjected to static loading. The method can handle very efficiently, (a) design for multiple loading conditions, (b) stress constraints, (c) constraints on displacements, (d) constraints on sizes of the elements. Examples of bar and beam structures are presented to illustrate the effectiveness of the method. Some of these examples are compared with the designs obtained by linear and nonlinear programming methods. The method is extremely efficient in obtaining minimum weight structures and in a small fraction of the computer time required by linear and nonlinear programming methods.

DESIGN OF OPTIMUM STRUCTURES

V. B. VENKAYYA

FLIGHT DYNAMICS LABORATORY, WRIGHT-PATTERSON AFB, OHIO

1. INTRODUCTION

The development of efficient structural analysis and design methods in the last decade is unprecedented and gratifying. Much of this progress was made possible by even more impressive developments in the field of digital computer technology. The result of this progress is the proliferation of large scale structural analysis computer programs such as "FORMAT", "MAGIC", "NASTRAN" and a host of others developed by industry. Many of these are finite element based but there are others which use finite differences, Raleigh-Ritz, Galerkin methods, etc. These programs can analyze structures with several thousand degrees of freedom and structural elements. The advantage of discrete modelling approaches lies in their ability to handle complex situations arising from discontinuities in structure as well as the loading conditions. However, this increased capability is invariably accompanied by the need for analysing problems with large number of variables and degrees of freedom.

With the aid of these large computer programs it is possible to analyze, as single units with all their discontinuities, an entire wing or fuselage and be able to predict quite accurately the displacements, stresses, frequencies and other information necessary to

understand the behavior of the structure. The development of design methods that can efficiently utilize the full capability of the analysis methods is only at an infant stage. This lag is expected because the design problem is several orders of magnitude more complex than analysis. The vast number of papers published in recent years on structural optimization underscore the need for an optimization algorithm that can handle efficiently design problems with large number of variables. The efficiency of the algorithm should be measured by its ability to arrive at an optimum design with least amount of computational effort.

Numerous review papers on the subject of optimization have been published in recent years assessing the state of the art. The papers by Wasiutynski and Brandt [1] and Sheu and Prager [2] made a comprehensive survey of the state of the art up to 1968. A more recent paper by Schmit [3] makes an assessment of the value of nonlinear programming methods to structural optimization.

Structural optimization problems are generally characterized by a) a large number of design variables, b) a simple objective function and c) an indirect but well behaved constraint functions. The constraint functions are indirect in the sense that they cannot be expressed explicitly as functions of the design variables. Attempts to optimize structures by nonlinear programming methods have met with varying degree of success. These methods are extremely useful in defining the design problem in proper mathematical terms. When the design variables are few (say less than 50) the non-linear programming

methods can be used quite effectively for optimization. However, in the presence of a large number of variables these methods are painfully slow and erratic in obtaining a solution. The examples presented in sections 7 and 8 substantiate this conclusion. The situation can be improved to some extent by introducing such empirical procedures as linking the variables and extrapolation techniques. The successful application of the modified stress ratio method for the design of practical aerospace structures is presented in [4-6]. This approach has the advantage of simplicity and computational efficiency over mathematical programming approaches.

The present effort is a continuation of the work started in 1968 with the object of developing design methods that can efficiently optimize structures with a large number of variables. An optimization procedure based on an energy criterion and a search procedure based on constraint gradient values was presented in [7]. The reference contains a large number of bar structures designed by this approach. This design procedure considered such practical design requirements as:

1. Design for multiple loading conditions
2. Stress-constraints
3. Displacement Constraints
4. Limits on sizes of the elements

In a subsequent paper [8] the author considered design examples with local instability considerations.

This report contains the detailed study of the method presented

in [7], extension to structures with beam and plate elements and modifications to the search algorithm for improved convergence. Experience with the iterative algorithms derived in this paper indicate the following beneficial trends when used for the design of indeterminate bar structures under single loading condition.

a) When the indeterminate structure degenerates to a determinate structure it goes to the one with the lowest weight.

b) If an indeterminate structure which satisfies the optimality criteria exists then it will have the same weight as the lowest of the determinate structures.

2. STRAIN ENERGY CRITERION FOR AN OPTIMUM DESIGN

An optimality condition based on a strain energy criterion is mathematically established here for the case of a design for a single loading condition. This criterion with some modifications will be used later for constructing an efficient path for the optimum design of more complex cases.

A structure with m structural elements and specified configuration is subjected to a generalized force vector \underline{R} . The problem is to obtain optimum sizes for the elements such that the weight of the structure is a minimum. To simplify the derivation of the criteria the following restrictions are imposed:

- a) The structure is subjected to a single load vector
- b) The load vector does not change during design
- c) The structure is made of the same material
- d) No restrictions on the sizes of the elements
- e) No limits on displacements

Suppose A and A' are two designs in the neighborhood of the minimum weight design. Since the density of the material is assumed to be the same, the weights of the structure corresponding to the two designs are proportional to W and W' which are defined as

$$W = \sum_{i=1}^m A_i l_i \quad (1)$$

$$W' = \sum_{i=1}^m A'_i l_i \quad (2)$$

For beams and bars A and l are areas and lengths, respectively. For plate elements these parameters will be defined in Section 3. If the geometrical configuration is fixed, the parameter l is same in both designs.

The strain energies of the i th element corresponding to the two designs are given by

$$u_i = 1/2 \underline{s}_i^t \underline{v}_i \quad (3)$$

$$u'_i = 1/2 \underline{s}'_i{}^t \underline{v}'_i \quad (4)$$

\underline{s}_i and \underline{v}_i are the internal force and displacement vectors of the i th element in the first design. Similarly \underline{s}'_i and \underline{v}'_i are the corresponding vectors of the second design.

The average strain energy density of the i th element in the two designs is defined as

$$\rho_i(u) = u_i / v_i \quad (5)$$

$$\rho'_i(u) = u'_i / v'_i \quad (6)$$

v_i and v'_i are the volumes of the i th element in the two designs.

$\rho_i(u)$ and $\rho'_i(u)$ are strain energy densities of the element in two cases. The difference in the total strain energies of the two designs may be written as

$$\sum_{i=1}^m A_i l_i \rho_i(u) - \sum_{i=1}^m A'_i l_i \rho'_i(u) = \Delta P \quad (7)$$

where ΔP is the difference in the potential of the external forces in the two cases. Since both designs are assumed to be in the neighborhood of the optimum, in the limiting case equation (7) may be written as

$$\lim_{\Delta A \rightarrow 0} \left[\sum_{i=1}^m A_i l_i \rho_i(u) - \sum_{i=1}^m A'_i l_i \rho'_i(u) \right] = \lim_{\Delta A \rightarrow 0} \Delta P = 0 \quad (8)$$

ΔA is the difference vector in the sizes of the elements in the two cases.

Let \underline{r} and \underline{r}' be the actual generalized displacement vectors corresponding to the first and second designs, respectively. Since the

geometric configuration of the structure is the same in both cases the displacement vector \underline{r} is kinematically admissible for the second design and vice-versa. If the second design is forced to have the displacement configuration of the first design, then from the principle of minimum potential energy the following inequality can be written,

$$\sum_{i=1}^m A_i' l_i \rho_i(u) \geq \sum_{i=1}^m A_i l_i \rho_i'(u) \quad (9)$$

The use of $\rho_i(u)$ on the left side of the inequality is valid for the following reasons. In the case of bar structures the strain energy density depends on the displacement configuration only and not on the sizes of the elements. In the case of beam elements the strain energy density is again independent of the areas of the elements provided the radius of gyration of each element in the first design is the same as in the second design. One should not confuse this assumption with the condition of having the same radius of gyration for all elements. It simply means an i th element has the same radius of gyration both in the first and in the second design. Since the two designs are assumed to be in the neighborhood of each other this assumption is not unreasonable.

Invoking the limiting condition stated in equation (8) the inequality (9) may be written as

$$\sum_{i=1}^m A_i' l_i \rho_i(u) \geq \sum_{i=1}^m A_i l_i \rho_i(u) \quad (10)$$

The same inequality may be written also as

$$\sum_{i=1}^m (A_i' - A_i) l_i \rho_i(u) \geq 0 \quad (11)$$

It should be remembered that $\rho_i(u)$ is the average strain energy density and A_i is the area of the i th element in the first design. If all the elements in the first design have same average strain energy density, i.e. $\rho_1(u) = \rho_2(u) = \dots = \rho_m(u)$, then inequality (11) may be written as

$$\sum_{i=1}^m A_i' l_i \geq \sum_{i=1}^m A_i l_i \quad (12)$$

From equations (1) and (2) and inequality (12) it is evident that

$$W' \geq W \quad (13)$$

This means, the design that has the same average strain energy density in all its elements is a lower weight design than the one in which this condition is not satisfied. Now the statement of the optimality criteria is as follows:

"The optimum structure is the one in which the average strain energy density is the same in all its elements."

If the change in potential of the applied forces is considered as a measure of the stiffness of the structure then it can be shown that the structure that satisfies the above strain energy criteria will also be the stiffest structure for that loading condition.

In the case of determinate structures the above optimality criteria is both a necessary and a sufficient condition for global minimum provided the stress constraints on the elements are fixed. In the case of indeterminate structures it is possible to have more than

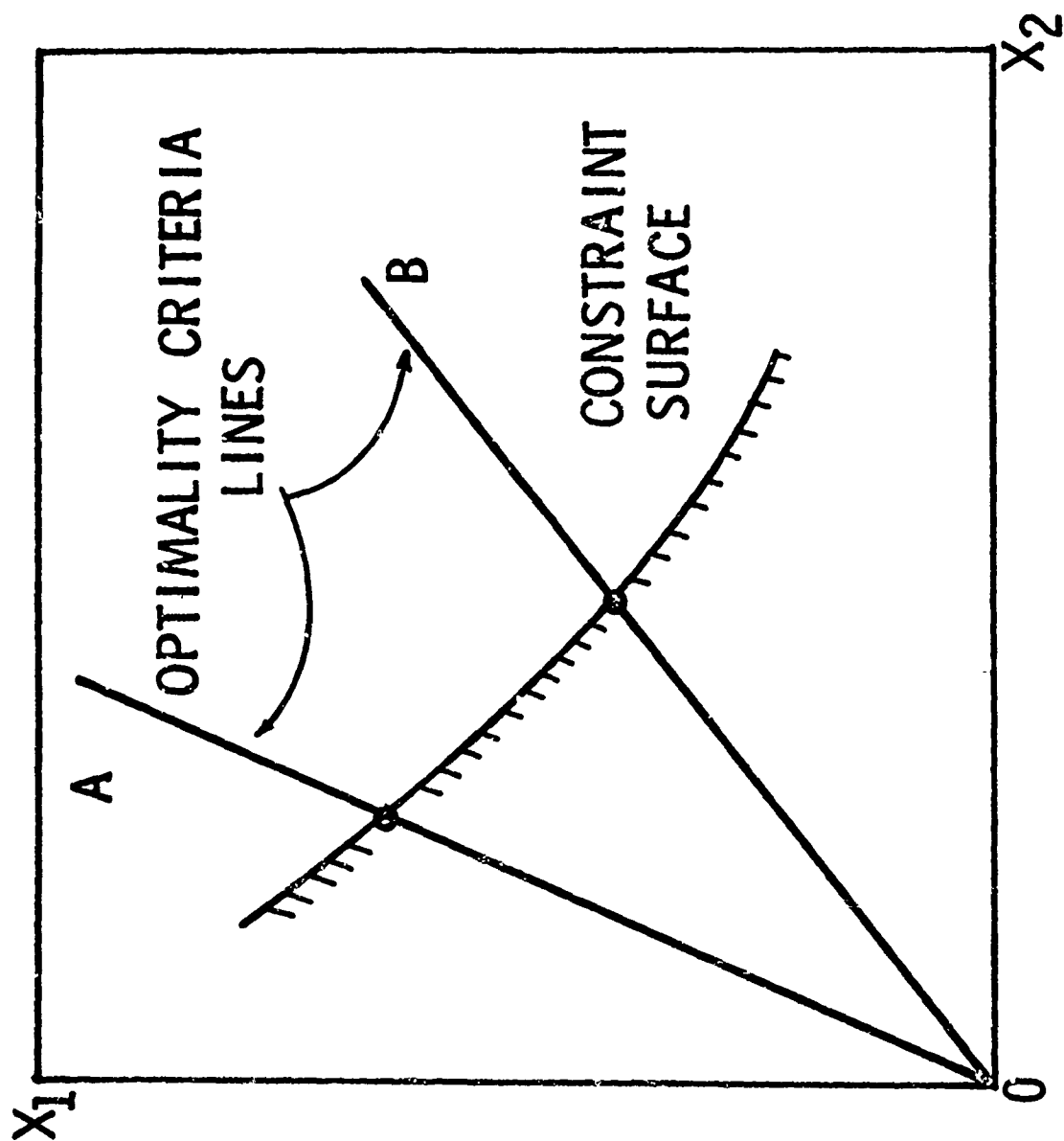


FIGURE 1. TWO VARIABLE DESIGN SPACE

one design that satisfies the optimality criteria. This indicates the existence of multiple minima. The validity of these statements can be examined with the aid of a two variable design space (Fig. 1).

Suppose point A in the design space represents a design that satisfies the optimality criteria. In case of bar structures then every design on line OA and its extension satisfies the optimality criteria. In case of beam structures with the radius of gyration of each element fixed, all designs on line OA would satisfy the optimality criteria. Some of the designs on line OA are feasible and others are not in view of the stress constraints. The point on line OA that separates feasible and non-feasible designs is the desired optimum.

If OA is defined as the optimality criteria line (all the designs on line OA satisfy the optimality criteria) two cases can arise.

- 1) If the line OA is unique (i.e. no other lines satisfy the optimality criteria) then the lowest feasible design that satisfies the optimality criteria is the global minimum.

- 2) If more than one optimality criteria line OB exists then corresponding to each line there will be a design which will be a relative optimum.

In case of determinate structures it is shown that the optimality criteria line is unique [9] and the optimum obtained is a global optimum. In general this is not true for indeterminate structures. This can be shown with the aid of a four bar truss (Fig. 2).

This three dimensional truss is statically indeterminate to the

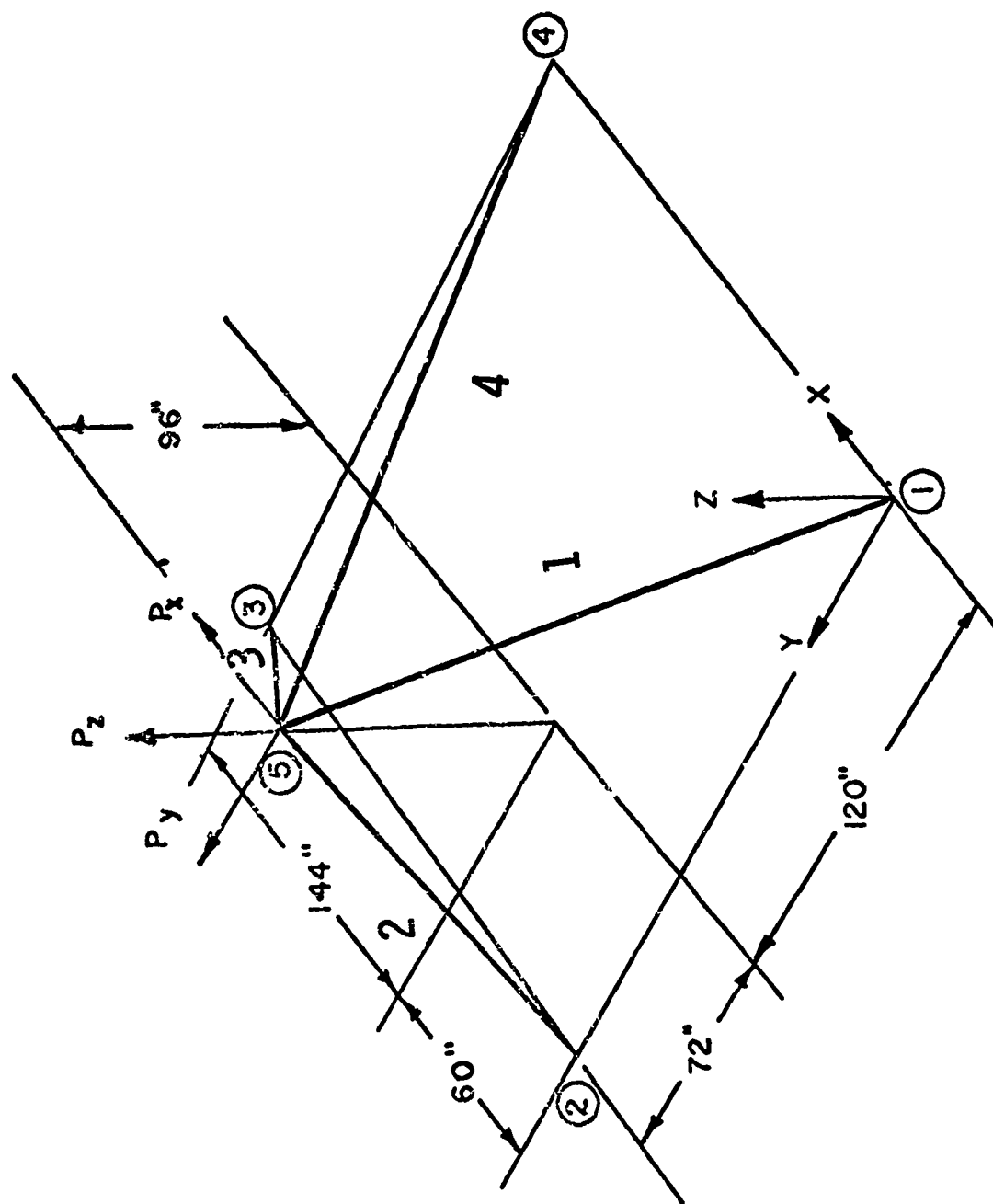


FIGURE 2 FOUR BAR TRUSS

first degree. By removing one member at a time one can obtain four kinematically stable determinate structures. If removing a member is interpreted as assigning a zero area, in the limiting sense, then the four determinate structures are a subset of the original indeterminate structure. In addition a fifth case, in which all the areas greater than zero can also exist. In each of the four determinate cases it is possible to obtain a design that satisfies the optimality criteria. In the fifth case two possibilities exist:

a) No design with all areas greater than zero satisfies the optimality criteria i.e., the indeterminate structure degenerates to one of the determinate cases when the optimality criteria is enforced.

b) An indeterminate structure satisfying the optimality criteria can be found.

Which one of these two cases is valid for a given indeterminate structure appears to depend on the nature of the loading on the structure.

The above discussion shows at least four or more optimality criteria lines exist for the four bar truss in question. Corresponding to each of these lines there will be one relative minimum. Of all these minimums the design that has the lowest strain energy will be the global minimum [9]. However, this statement is not of much help in locating the global minimum since it involves investigation of all the possible minimums which is not practical in a large structure. Additional discussion of this problem can be found in Section 7.

3. RECURSION RELATION BASED ON STRAIN ENERGY CRITERIA

In an indeterminate system, statement of the optimality criteria does not complete the task of obtaining an optimum design. An effective iterative algorithm is necessary for achieving the optimality condition. This section contains the derivation of such an algorithm. It is intended for design under more general conditions than the restricted case considered in the previous section and as such contains certain terms and definitions which are not essential for that case. Justification of this extension to a more general case will be discussed later with the aid of a two variable design space.

The optimality criteria modified for the general case is as follows:

"The optimum design is the one in which the strain energy of each element bears a constant ratio to its energy capacity."

The energy capacity is defined as total strain energy stored if the entire element is stressed to its limiting normal stress. The limiting normal stress can be different from the actual stress limit as long as it does not exceed it. The step size in iteration, based on energy criteria, can be altered by varying the magnitude of the limiting normal stress. It should be pointed out that the definition of energy capacity is independent of the actual state of stress in the element and depends only on the volume and on the limiting normal stress of the elements. It is determined from the same basis for bars, beams, plates and every other structural element. When the

design conditions are the same, the modified optimality criteria differs from the one stated in the last section only by a scaling factor.

The expression for the energy capacity of the i th element is given by

$$\tau_i = \frac{1}{2} \sigma_i^{(U)} \epsilon_i^{(U)} V_i \quad (14)$$

where $\sigma_i^{(U)}$ and $\epsilon_i^{(U)}$ are the limiting normal stress and strain respectively, and V_i is the volume of the element. Assuming the material to be linearly elastic the relation between limiting normal stress and strain is written as

$$\sigma_i^{(U)} = E_i \epsilon_i^{(U)} \quad (15)$$

Substitution of equation (15) in (14) gives the expression for energy capacity in the form

$$\tau_i = \frac{1}{2} (\epsilon_i^{(U)})^2 \Lambda \alpha_i l_i \quad (16)$$

The quantity l_i is defined as

$$l_i = \frac{V_i E_i}{\Lambda \alpha_i} \quad (17)$$

The scalar Λ is the base parameter for all the elements and α_i is the relative value of the i th design variable. In the case of bar elements l_i is simply the length of the element and $\Lambda \alpha_i$ is the product of the area and the modulus of elasticity of the element. In the case

of elements in bending, torsion, etc. appropriate variable definitions are given in Section 6. The actual design variable vector may be written as $\Lambda \underline{\alpha}$. The vector $\underline{\alpha}$ alone will be referred to as the relative design variable vector or normalized vector. The scalar Λ is then the normalizing factor.

The relative response of the structure depends on the vector $\underline{\alpha}$ and the absolute response can be manipulated by simply changing the scalar Λ . In a two variable design space (see Fig. 1) the normalized vector $\underline{\alpha}$ represents a line (such as OA) and the value of Λ fixes the point on the line. Movement on the line OA may be considered as scaling. The implications of scaling in case of multi-variable elements is discussed in section 6.

The strain energy in the element is written in terms of its internal forces and displacements as

$$u_i = \frac{1}{2} \underline{s}_i^T \underline{v}_i \quad (18)$$

where \underline{s}_i is the generalized force vector of the i th element and \underline{v}_i is the corresponding relative displacement vector. It is related to the actual displacement vector \underline{v}_i by

$$\underline{v}_i = \Lambda \underline{v}_i \quad (19)$$

According to the modified optimality criteria the strain energy of each element should bear a constant ratio to its energy capacity.

Equations (16), (18) and the optimality criteria yield

$$\Lambda^2 = c^2 \frac{u_1'}{\tau_1'} \quad (20)$$

where c is the constant of proportionality and u_1' and τ_1' are given by

$$u_1' = \frac{1}{2} s_1^t v_1' \quad (21)$$

$$\tau_1' = \frac{1}{2} (\epsilon_1^{(u)})^2 \alpha_1 \lambda_1 \quad (22)$$

Multiplying both sides of equation (20) by α_1^2 and taking the square root yields

$$\alpha_1 \Lambda = c \alpha_1 \left[\frac{u_1'}{\tau_1'} \right]^{\frac{1}{2}} \quad (23)$$

where $\alpha_1 \Lambda$ is the i th design variable which is expressed as a function of α_1 . The form of Equation (23) suggests the following recursion relation for determining the design variable in each cycle.

$$(\alpha_1 \Lambda)_{\nu+1} = c (\alpha_1)_{\nu} \left[\left[\frac{u_1'}{\tau_1'} \right]_{\nu} \right]^{\frac{1}{2}} \quad (24)$$

Where the subscripts ν and $\nu+1$ refer to the cycles of iteration.

When the design conditions include multiple loading case equation (24) will be modified to read

$$(\alpha_1 \Lambda)_{\nu+1} = c (\alpha_1)_{\nu} \left[\left[\frac{u_{1\max}'}{\tau_1'} \right]_{\nu} \right]^{\frac{1}{2}} \quad (25)$$

Where $u'_{1\max}$ is a measure of the maximum strain energy of the i th element due to any of the loading conditions.

The usefulness of the recursion relation (25) and its limitations can be explained with the aid of a two variable design space, Fig. 3, where X_1 and X_2 are the two design variables. Every point in this space represents a design. The line $c-c$ is the boundary between the feasible and nonfeasible regions and is referred to as the constraint surface. The straight lines $w-w$ represent the constant weight planes. All designs in the region R and its boundary are feasible designs. Suppose the point OP represents the optimum design. The function of a design algorithm is to chart a path from an arbitrary point A_1 to the optimum point OP .

The point A_1 (Fig. 3) represents a preliminary or a starting design. The line joining point A_1 and the origin O (line OA_1) will be called the design line. In the case of bar structures every point on line OA_1 will have the same normalized design variable vector. In such a case movement on line OA_1 simply involves changing the value of the scalar λ . The movement on line OA_1 will be referred to as scaling the design. Similarly every line passing through the origin is a design line and the movement on each of these lines can be accomplished in a single step (one analysis). On a given design line, such as OA_1 , the point B_1 , which is at the intersection of OA_1 and the constraint surface, is the lowest weight feasible design. The procedure for locating this point is as follows:

The structure is first analyzed with the relative design variable

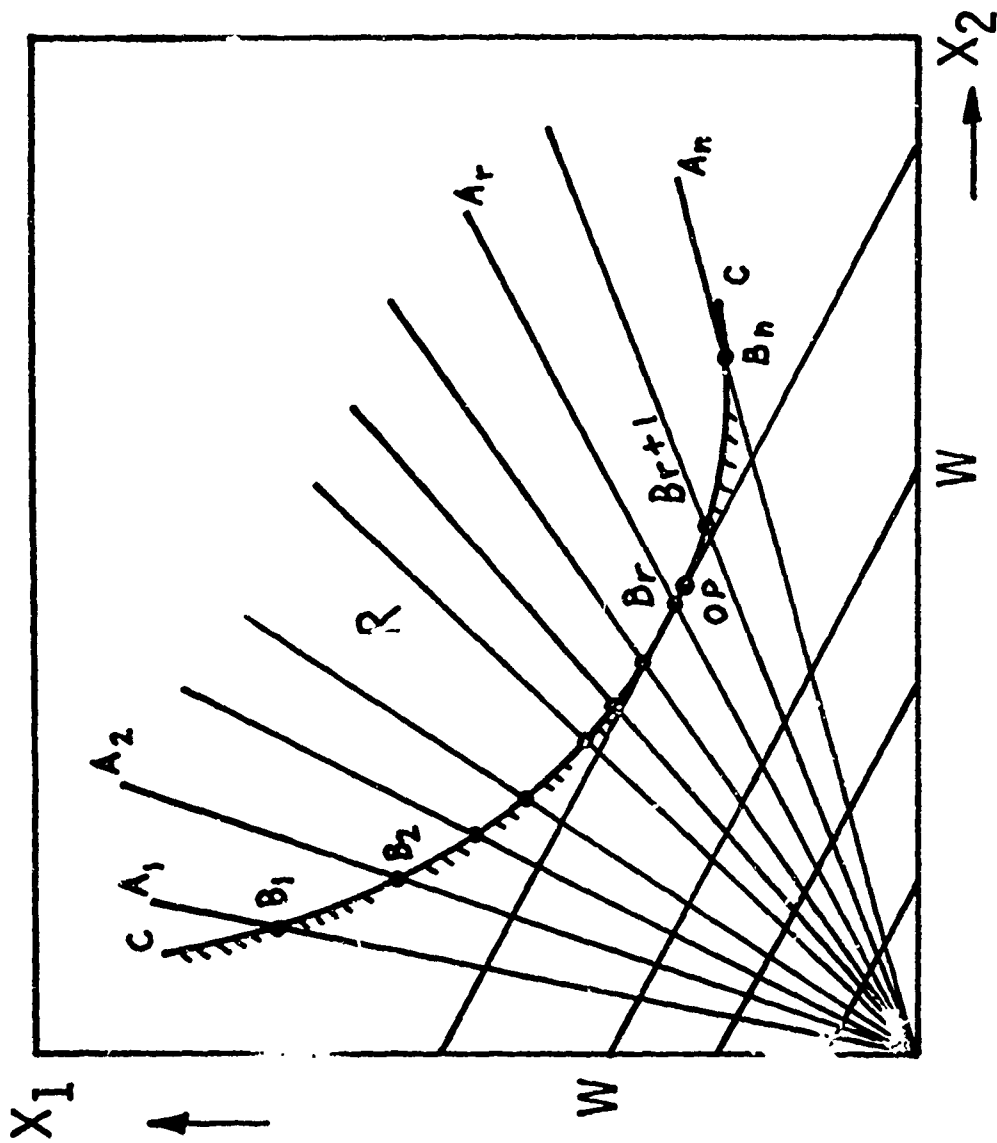


FIGURE 3. DESIGN LINES IN TWO VARIABLE SPACE

vector corresponding to the line OA_1 . From the relative response the active constraints can be identified. From this information the magnitude of the scalar λ corresponding to the point B_1 can be determined.

In case of elements in bending and torsion a similar procedure can be used but not necessarily in a single step. This problem and the necessary modifications are discussed in detail in section 6.

By iteration using equation (25) in conjunction with the scaling procedure discussed in this section an efficient path to the optimum can be constructed. In the case of a single loading condition with stress constraints only, the design that satisfies the optimality criteria is the lowest weight design. Iteration using equation (25) produces such a design. When there are constraints on the sizes of the elements and multiple loading conditions the design satisfying the optimality criteria may not be the lowest weight design. In such cases equation (25) will be used to simply generate design lines and in conjunction with the scaling procedure a directed search for the lowest weight design can be made. This procedure was successfully used for the design of a number of bar structures in [7]. Some additional examples of bar structures are presented in Section 7.

It should be recognized at the outset that the objective is to obtain the lowest weight design and not just satisfying the optimality criteria and as such one should not force the design to satisfy the criteria, when the design conditions include constraints on sizes and multiple loading conditions. The optimum design and a design that

satisfies the optimality criteria are synonymous only in the case of a single loading condition and no constraints on member sizes. Failure to recognize this fact has led to various misinterpretations and premature rejection of the optimality criteria approaches to minimum weight design of structures. The optimum design usually lies on the path to the design satisfying the optimality criteria. As a result the optimum design is reached before the optimality criteria is satisfied. When there are constraints on displacements in addition to stress constraints the recursion relation based on energy criteria is used in the initial stages and the design is further improved with the aid of an iterative algorithm based constraint gradient information. The next two sections contain the derivation of such an algorithm.

4. GRADIENT CALCULATIONS USING BANDED MATRIX SOLUTION SCHEME

An approximate procedure for calculating the displacement gradients was presented in [7]. The procedure is equivalent to taking the first two terms of the Taylor's Series expansion of the original displacement vector. The gradients are expressed in terms of the inverse of the stiffness matrix. Stiffness matrices of structures are in general sparsely populated and in such cases finding an inverse is uneconomical in terms of computer time as well as storage requirements. To take advantage of the sparsity, a procedure for calculating gradients using a banded matrix solution scheme is presented in this section.

If \underline{r} is the actual displacement vector due to the applied

forces and \underline{dr}_i is the change in \underline{r} due to a change in the variable X_i then the Taylor's series for \underline{dr}_i is given by

$$\underline{dr}_i = \frac{\partial}{\partial x_i} \underline{r} dx_i + \frac{1}{2!} \frac{\partial^2}{\partial x_i^2} \underline{r} dx_i^2 + \dots \quad (26)$$

Premultiplying both sides of equation (26) by the stiffness matrix and neglecting the terms beyond the first yields

$$\underline{K} \underline{dr}_i = \underline{K} \frac{\partial}{\partial x_i} \underline{r} dx_i \quad (27)$$

The relation between the applied force vector \underline{R} and the displacement vector \underline{r} is given by

$$\underline{R} = \underline{K} \underline{r} \quad (28)$$

Differentiation of equation (28) with respect to the variable X_i yields

$$\frac{\partial}{\partial x_i} \underline{R} = \left(\frac{\partial}{\partial x_i} \underline{K} \right) \underline{r} + \underline{K} \frac{\partial}{\partial x_i} \underline{r} \quad (29)$$

If the applied forces are assumed to be constant during the design, the left side of equation (29) will be zero and thus it can be written as

$$\underline{K} \frac{\partial}{\partial x_i} \underline{r} = - \left(\frac{\partial}{\partial x_i} \underline{K} \right) \underline{r} \quad (30)$$

Substitution of equation (30) in (27) yields

$$\underline{K} \underline{dr}_i = -\underline{\Delta K}_i \underline{r} \quad (31)$$

Where $\underline{\Delta K}_i$ is given by

$$\underline{\Delta K}_i = \frac{\partial}{\partial x_i} \underline{K} dx_i \quad (32)$$

Equations (28) and (31) are similar in form when $-\underline{\Delta K}_i \underline{r}$ is considered

as a load vector.

Analysis of the structure requires solution of equation (28). This solution is obtained by decomposition using standard Gauss elimination. This scheme consists of decomposition of the stiffness matrix by using the relation

$$\underline{K} = \underline{L} \underline{D} \underline{L}^t \quad (33)$$

where \underline{L} is the unit lower triangular matrix and \underline{D} is a diagonal matrix. Substitution of equation (33) into equation (28) gives

$$\underline{L} \underline{Y} = \underline{R} \quad (34)$$

where the vector \underline{Y} is given by

$$\underline{Y} = \underline{D} \underline{L}^t \underline{r} \quad (35)$$

Now the solution of load deflection equations (28) is accomplished in three stages:

1. Decomposition of the stiffness matrix. This involves determination of the elements of the matrices \underline{L} and \underline{D} and it can be accomplished by equation (33).
2. Forward substitution: In this step the elements of the vector \underline{Y} are determined by equation (34).
3. Back substitution: From Equation (35) the elements of the displacement vector \underline{r} are determined.

When a structure is subjected to more than one load vector, only the last two steps have to be repeated. The decomposed matrices \underline{L} and \underline{D} would be the same in all cases. If the quantity $\underline{\Delta K}_i \underline{r}$

is treated as an additional load vector in equation (31), only the last two steps have to be repeated for determining the vector \underline{dr}_i . Using this procedure the change in the displacement vectors corresponding to the change in each design variable can be determined. The vectors \underline{dr}_i will be referred to as displacement gradients. The purpose of \underline{dr}_i calculations will be explained in the next section.

The advantage of the solution scheme is that the decomposed matrix \underline{L} retains some of the sparseness characteristics of the original stiffness matrix and many arithmetic operations involving zero elements can be eliminated [5, 10].

The procedure presented here for gradient calculations differs from the one presented in [7] in the following respects:

a) In [7] the expression for \underline{dr}_i contains an additional term which is equivalent to the second term in Taylor's series expansion. The effect of this term was evaluated by an iterative procedure and was found to be insignificant.

b) The change in the stiffness matrix $\underline{\Delta K}$ was assumed to be due to unit change in the size of the element in [7]. This was found to have the disadvantage of exaggerating the effect of elements with small sizes. In the present work the change in size of the element is assumed to be proportional to its actual size in that cycle in calculating the vector \underline{dr}_i . This has produced improvement in some designs and a discussion of this can be found in section 7.

c) The need for finding the inverse of the stiffness matrix is eliminated.

STRESS GRADIENTS:

The changes in the displacement vector due to changes in the sizes of the elements can be determined by equation (31). This displacement vector \underline{dr}_i can be used to determine the changes in the stresses of the elements due to a change in size of one element at a time. The necessary stress-gradient relations are as follows [7]:

$$\underline{dv}_{ij} = \underline{a}_j \underline{dr}_j \quad (36)$$

where \underline{dv}_{ij} is the i th element displacement vector due to change in the size of the element j and \underline{a}_j is a kinematic matrix which relates the structure and element generalized displacements.

From the force displacement relations of the element

$$\underline{ds}_{ij} = \underline{k}_i \underline{dv}_{ij} \quad (37)$$

where the vector \underline{ds}_{ij} is the change in i th element generalized forces. Corresponding changes in element stresses are given by

$$\underline{d\sigma}_{ij} = \underline{\beta}_i \underline{ds}_{ij} \quad (38)$$

The changes in structure displacements (31) and stresses (38) due to a change in size of each element provide information regarding the influence of each element on the total response of the structure. Using this information a recursion relation is derived for the resizing of the elements in the next section.

5. RECURSION RELATION BASED ON CONSTRAINT GRADIENTS

In section 3 a recursion relation based on strain energy criterion was derived for the generation of design lines. This relation in conjunction with the scaling procedure presented is sufficient to design minimum weight structures with constraints on stresses and sizes. When there are constraints on displacements in addition, the design obtained by equation (25) can be further improved by an iterative algorithm based on constraint gradients which is derived in this section.

The algorithm is of the following form

$$\underline{\alpha}_{\nu+1} = \underline{\alpha}_{\nu} + \Delta \underline{D} \quad (39)$$

where ν and $\nu+1$ refer to the cycles of iteration and $\underline{\alpha}$ is the normalized design variable vector. Δ is the step size which determines the rate of approach to the optimum. If Δ equal to 1.0 is considered as the normal step size, then the value greater than 1.0 increases the rate of approach to the optimum while a value less than 1.0 slows the iteration. However, a larger step size increases the possibility of missing the optimum between two steps. The vector \underline{D} represents the departure of the new design from the present design. The elements of \underline{D} are determined by the influence of each variable on the active constraints. The procedure for determining the elements of \underline{D} is presented first in case of active displacement constraints.

When the design is at the boundary of the feasible and non-feasible regions, the generalized displacements that are at their limiting values are called active displacement constraints (see Fig. 4). The influence of each element on all the generalized displacements can be determined by equation (31). If "j" is the direction corresponding to the active displacement constraint then only the j^{th} elements of \underline{dr}_i are of interest and need to be stored. Depending on their influence on the active constraints, the elements of the structure are grouped into those having negative and positive influence. If an increase in the size of the element increases the displacement in the constraint direction, then it is called negative influence and vice versa. The sizes of the elements that have negative effect, or zero effect, on active constraints can be reduced. This is only a qualitative description of the procedure. It does not specify the magnitude of the change nor does it assure that the constraints at other locations are not activated by this change. The following procedure is adopted to overcome this problem.

The displacements are allowed to increase arbitrarily by a certain percentage (say 10% to 20%). This can be accomplished by simple scaling on the design line. This means movement from point C_1 to B_1 on line OA in Fig. 4. From point B_1 the design is moved to point E_1 by changing the normalized design variable vector by equation (39) with the elements of \underline{D} given by

$$D_i = C \frac{dr_j^{(i)}}{l_i} \quad (40)$$

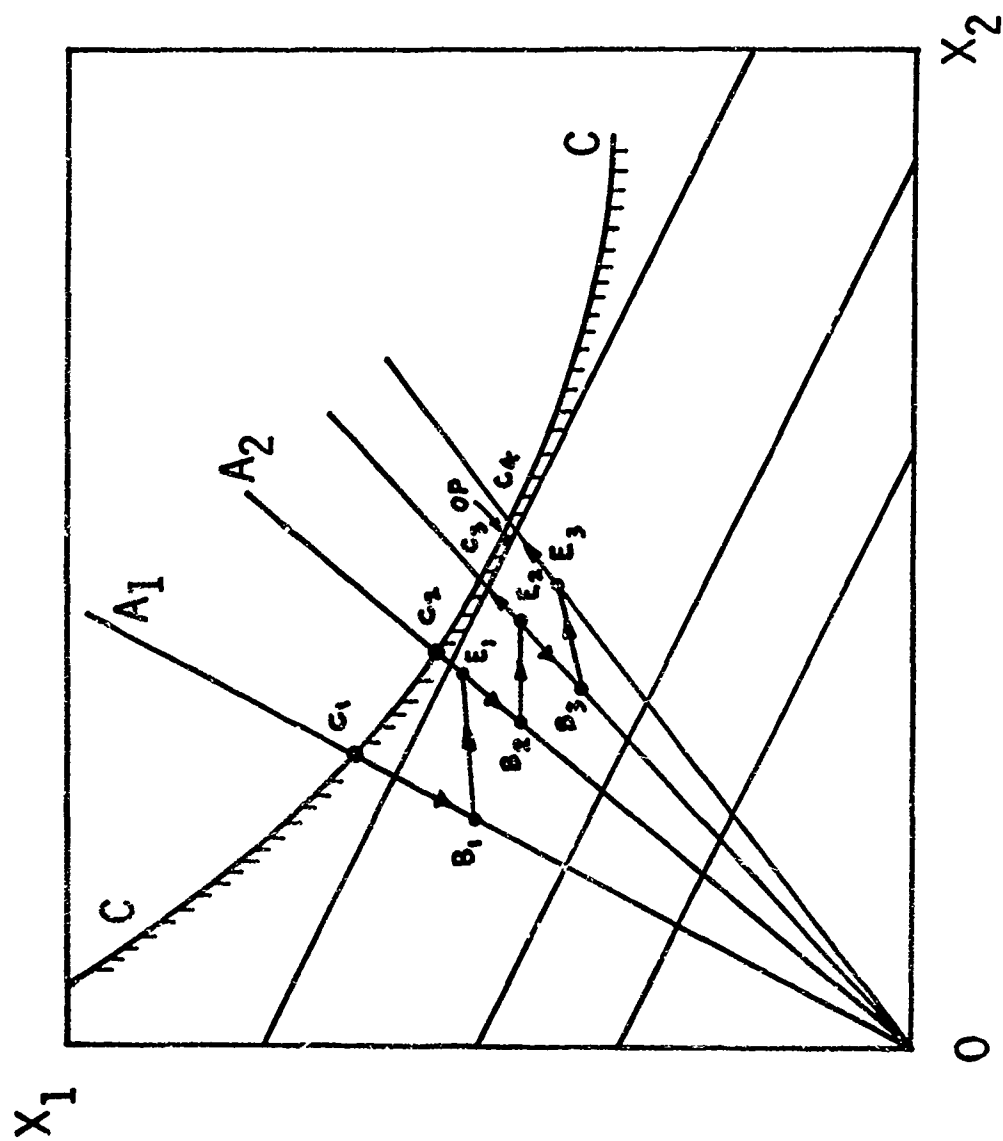


FIGURE 4. PATH OF SEARCH ALGORITHM

where C is the constant of proportionality, "j" is the direction of the active displacement constraint and $dr_j^{(i)}$ is the influence of the i^{th} variable on the active constraint displacement r_j . This influence can be determined by equation (31). In determining $d r_j^{(i)}$ the change in size of the element is assumed to be proportional to its actual size. The change in r_j due to D_i is $\delta r_j^{(i)}$ and is given by

$$\delta r_j^{(i)} = \frac{dr_j^{(i)}}{\alpha_i} D_i \quad (41)$$

Substitution of equation (40) in (41) gives

$$\delta r_j^{(i)} = \frac{C}{\alpha_i} \frac{(dr_j^{(i)})^2}{l_i} \quad (42)$$

The constant of proportionality C may be determined from the condition that the displacement r_j should be brought to its limiting value by changing the sizes of the elements according to equation (40). This condition is equivalent to

$$\Psi_j = \sum_{i=1}^m \delta r_j^{(i)} = C \sum_{i=1}^m \frac{1}{\alpha_i} \frac{(dr_j^{(i)})^2}{l_i} \quad (43)$$

In the summation only the elements that have positive influence on

the constraints are included. From equation (43), C is given by

$$C = \frac{\Psi_j}{\sum_{p=1}^m \frac{1}{\alpha_p} \frac{(dr_j^{(p)})^2}{l_p}} \quad (44)$$

Then D_i is given by

$$D_i = \frac{\Psi_j}{\sum_{p=1}^m \frac{1}{\alpha_p} \frac{(dr_j^{(p)})^2}{l_p}} \left[\frac{dr_j^{(i)}}{l_i} \right] \quad (45)$$

When the value of D_i is negative it is assumed to be zero. If more than one displacement exceeded the limit, then the necessary change in each element size is determined separately for each constraint using equation (45). The largest D_i was used in [7] for the actual change in the size of the i th element. However, slightly lighter weight designs, and in a fewer number of cycles, are obtained, in some cases, by using sum of all the changes for each element.

The procedure consists of the following three steps:

1. The first step involves movement from point C_1 to B_1 (Fig. 4). This movement can be accomplished by scaling.
2. Then movement from B_1 to E_1 is achieved by equations (39) and (45).
3. Then E_1 is joined to the origin and the movement to C_2 is accomplished by scaling. By repeating this procedure an efficient

path to the optimum is charted. This combined procedure is used to solve the examples in sections 7 and 8.

6. MULTIVARIABLE STRUCTURAL ELEMENTS

So far the design procedure is explained in the context of structural elements possessing one variable such as area of the element. In such cases, the scaling procedure and the recursion relations can be used as they are explained in the foregoing sections. However, most structural elements have more than one variable. For example, in case of a beam element, the response of the structure is dependent both on the area and the moment of inertia of the element. These two variables are semi-dependent in the sense that for the same area there can be elements with different values of moment of inertia. At the same time they cannot be treated as completely independent variables, because it may not be possible to construct a practical element with two arbitrary values of area and moment of inertia. Also the effect of these two variables is not of the same order of magnitude on the response.

It is convenient to introduce the idea of primary and secondary variables. The variable that has the largest effect on the response of the structure will be considered as a primary variable. All others will be treated as secondary variables. The design variable vector will contain only the primary variables and the secondary variables will be handled by implicit or empirical relations. Fig 5 lists six commonly used structural elements and the associated variables.

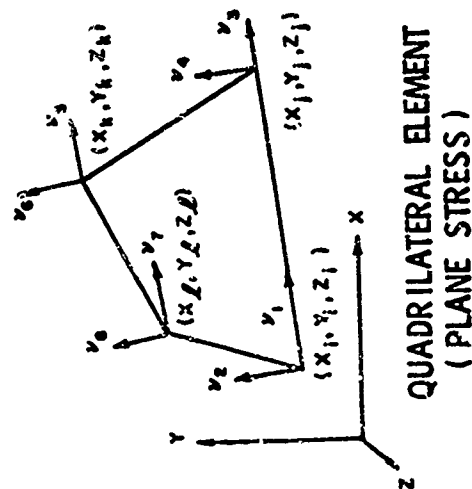
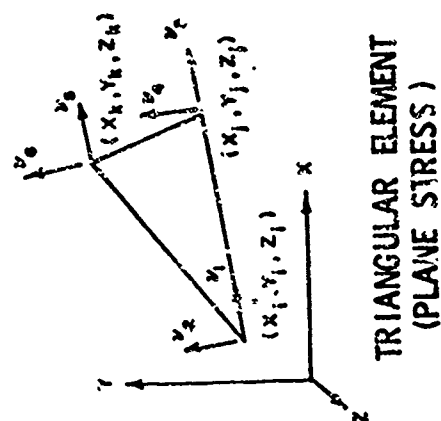
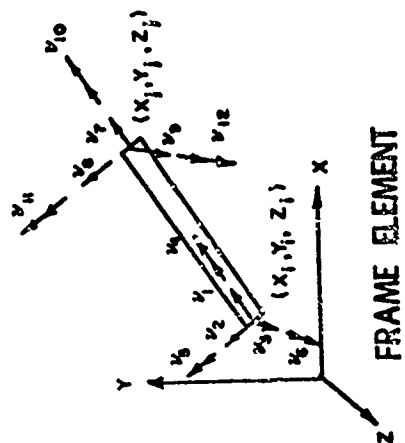
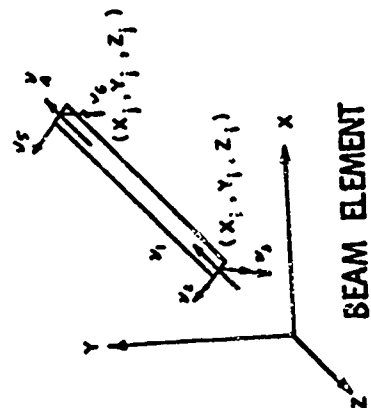
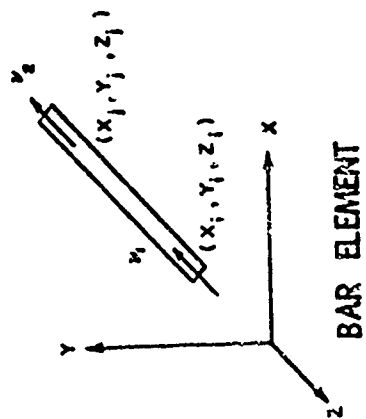


FIGURE 5. ELEMENTS

The necessary modifications and the implications of the scaling procedure in case of multivariable elements is discussed next.

1. BAR ELEMENTS:

The area of the element is the only variable in this case. If the members are braced against local instabilities, the scaling procedure and the recursion relations can be used as they are without any modifications. When this is not the case the scaling procedure can be handled by implicit relations between buckling stresses and the areas of the elements [8]. Recursion relations, however, need no modifications.

2. BEAM ELEMENTS IN PLANE FRAMES:

The cross-sectional areas and the moments of inertia are the two variables for a beam element in a plane frame. Box-beams, I-beams and sandwich beams are some of the examples of plane frame elements. Since the response is primarily governed by moment of inertia, it will be considered as the primary variable and area as the secondary variable. In this case both the scaling procedure and the recursion relations need modifications.

When the ratio of area to moment of inertia (A/I) is the same for all the elements (the depth of the elements is the same for all elements), then scaling can be done in a single step. When this is not the case, large changes in the scaling parameter Λ produce deviations during movement on the intended straight line. This may also be viewed as a problem of a non-stationary constraint surface. This means that when the design is moved from an arbitrary point on the design line to the

constraint surface by simply changing the scalar parameter Λ the constraint surface has moved from its assumed position and needs correction to locate its new position. This correction may need one or more analysis steps. However, in a practical structure the response is insensitive to the changes in A/I ratio and the scaling can be accomplished in a single step.

When the primary variable is moment of inertia, the quantity $\alpha_i \Lambda$ would give the moment of inertia times the modulus of elasticity of the element, $E_i I_i$. In that case the expression for energy capacity, equation (16) becomes

$$\tau_i = \frac{1}{2} (\epsilon_i^{(U)})^2 \alpha_i \left(\frac{A_i}{I_i} \right) I_i \quad (46)$$

Then τ_i' in equation (22) becomes

$$\tau_i' = \frac{1}{2} (\epsilon_i^{(U)})^2 \alpha_i \left(\frac{A_i}{I_i} \right) I_i \quad (47)$$

Except for this change the form and use of the recursion relation based on the strain energy criteria remains the same as before.

The recursion relation based on constraint gradients (equation 40) retains its original form except the expression for the elements of D_i becomes

$$D_i = \frac{\Psi_j}{\sum_{p=1}^m \frac{1}{\alpha_p} \frac{(\frac{dr_j^{(p)}}{dr_j^{(1)}})^2}{I_p}} \left(\frac{\Omega_i}{\Omega_{\max.}} \right)^2 \left[\frac{(\frac{dr_j^{(1)}}{dr_j^{(1)}})}{I_i} \right] \quad (48)$$

where Ω_j and Ω_{\max} are the radius of gyration of the j^{th} element and the element that has the maximum moment of inertia. It is assumed that the design variable vector was normalized by dividing the vector by its largest element.

3. THREE DIMENSIONAL FRAME ELEMENT:

In the case of the three-dimensional frame element modifications to the scaling procedure and the recursion relations are similar to those indicated for the plane frame element. The primary variable in this case would be the moment of inertia about the strong axis of the element. In addition to the above modifications a failure criteria has to be defined to determine the stress constraints. The axial force, bending, shear and torsion in a three-dimensional element produce more than one stress component at every point of the section. To determine the effective stress constraint in the section, the distortion energy criterion (or Von Mises criterion) will be used. According to this criterion the effective stress $\sigma_{\text{EFF.}}$ of an element in a general state of stress is given by

$$\sigma_{\text{EFF.}} = \sqrt{\frac{1}{2} \left[(\sigma_1 - \sigma_2)^2 + (\sigma_2 - \sigma_3)^2 + (\sigma_3 - \sigma_1)^2 \right]} \leq \sigma_A \quad (49)$$

where σ_1 , σ_2 and σ_3 are the principal stresses at the point of interest in the element and σ_A is the stress constraint in simple tension or compression.

4. SANDWICH PLATE ELEMENTS IN BENDING:

The depth and the thickness of the skin are two variables in this case. These two variables can be replaced by area and moment of inertia of the element. The modifications to the scaling and recursion relations are similar to that of the plane frame element.

5. MEMBRANE ELEMENTS:

In this case only the thickness of the element is variable and it can be replaced by an equivalent area in which case the recursion relations can be used as they are given in section 3 and 5.

6. PLATE BENDING ELEMENT:

Area and the moment of inertia are the two variables and the modifications indicated for plane frame element are applicable to this case.

7. PROBLEMS OF MULTIPLE MINIMA AND COMPARISON OF DESIGNS

Based on the behavioral constraints the design problems are categorized into two types, a) Problems with stress constraints only, b) Problems with stress and displacement constraints. Constraints on sizes can be present in both cases. In the first case the design is completed by iteration using equation (25). There is no need for the calculation of constraint gradients and equation (39) need not be used. When there are constraints on both stresses and displacements, however, iteration is carried out, by equation (25) as long as it improves the design. Then this design becomes a starting design for iteration using equation (39). This two stage approach has a better chance of

converging to an absolute minimum when there are stress and displacement constraints.

The rationale in using iterative algorithms based on strain energy criteria, equation (25) can be explained with the aid of Fig. 6. A distinction between an optimum design and a design that satisfies the optimality criteria is essential for understanding the mechanics of the algorithm. When a structure is subjected to a single loading condition and there are only constraints on stresses, the optimum design and the design that satisfies the optimality criteria are synonymous. In Fig. 6 the point C_n represents the design that satisfies the optimality criteria. Assuming that the iterative algorithm started from the point C_1 , it reached the point C_n in "n" steps (represented by the radial lines). In an ideal case, when no interference from disturbing constraints are encountered, the optimum design and the design that satisfies the optimality criteria are both represented by the same point C_n . In a more practical case this path is interrupted at point I by some additional constraints and the constraint surface is shifted to the dotted line. In this case iteration using equation (25) moves the designs on the dotted line after the point I. If there are no other interruptions the design ends at C'_n where the optimality criteria is satisfied. Here I represents the optimum design while C'_n represents the design satisfying the optimality criteria. Since the object is to find the optimum and not satisfaction of the optimality criteria the design

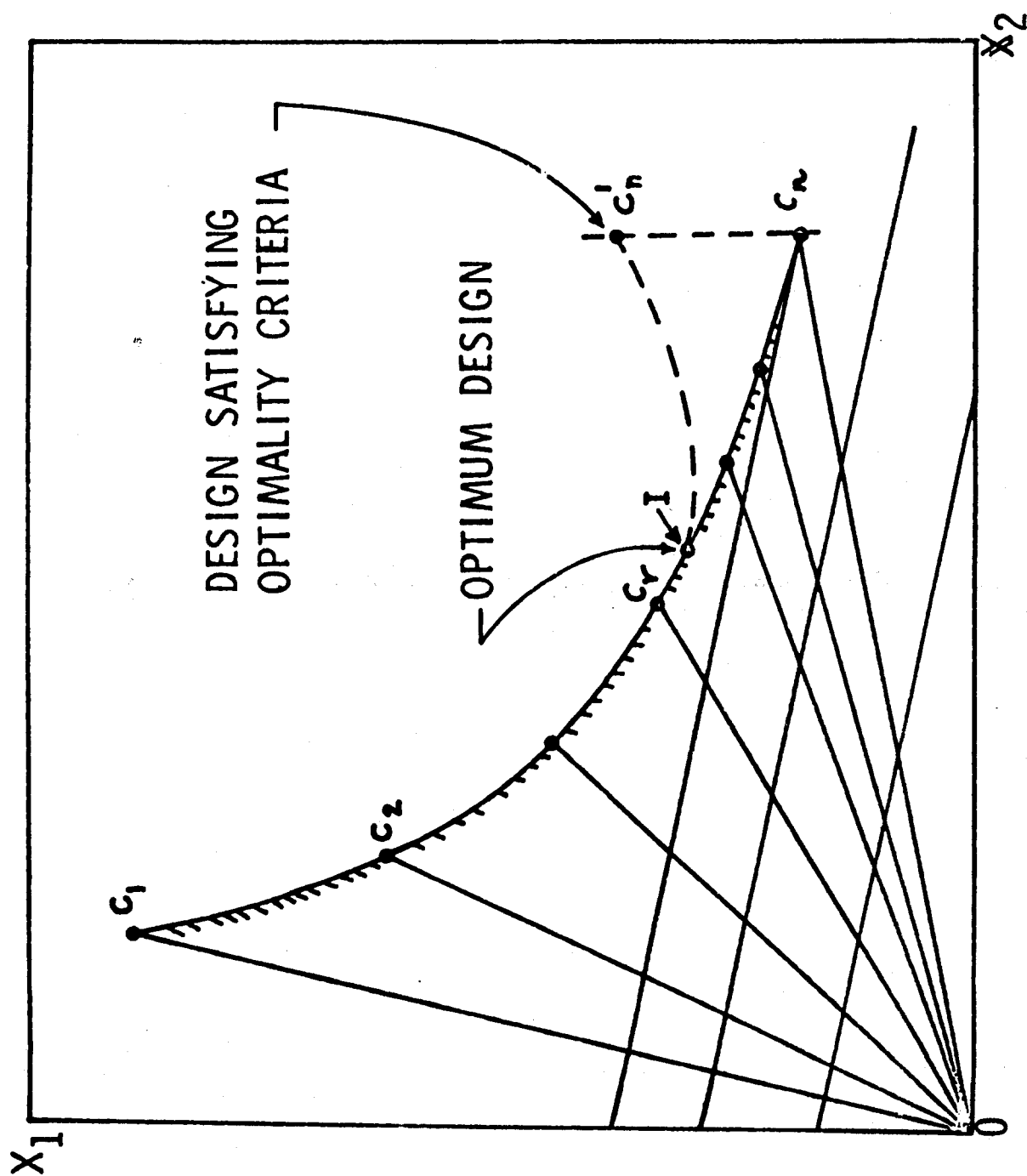


FIGURE 6. OPTIMUM AND OPTIMALITY CRITERIA DESIGNS

should be terminated at I and should not be forced to C_n^I . The validity of the optimality criteria approach to optimum design is due to the fact that, in general, the optimum point lies on the path to the optimality criteria. As stated before failure to recognize this distinction has often led to a misunderstanding of optimality criteria approaches to the design of optimum structures.

Another important point to be recognized is that iteration using equation (25) proceeds in finite steps and it is possible to miss the point I between two steps C_r and C_{r+1} (Fig. 6). There are two ways to avoid this situation.

a) A line between the lowest and the next design can be drawn by averaging the two relative design vectors. Then the scaling procedure gives a point nearer the optimum. Repetition of this procedure will lead to as close to the optimum as one wishes.

b) A better approach is to adjust the step size in the iteration. The step size can be altered by adjusting the magnitude of the limiting normal stress in the expression for the energy capacity of the elements. This adjustment can be done effectively on the elements whose actual stresses are below the stress limits. This does not imply a change in the actual stress limits. As long as the limiting normal stress in the energy capacity is lower than the stress limit, it is acceptable. The latter procedure is used in Example 2, (Three Bar Truss) for reducing the step size.

When there are both stress and displacement constraints the

optimum design, in general, lies beyond the range of the recursion relation based on the energy criteria. In such cases equation (39) extends the range of investigation to include the optimum. This combined approach was used for the design of a large number of bar and beam structures. The results of five of these bar structures are presented in this Section. The first example was used to study the problem of multiple minima in structural design. The designs of examples two and four were compared with those obtained by the mathematical programming approach.

All problems reported in this paper were designed using computer programs written in FORTRAN IV and ran on IBM 7094-II-7044-DCS.

Example 1: Four Bar Pyramid Truss

Fig. 2 gives the geometry and dimensions of the truss. Eight different design conditions were considered for this truss. The details of the loading and other design information are given in Table 1 for all these cases.

Case 1: Four Bar Truss - Single Loading - Stress Constraints

Since there are only stress constraints, the design can be completed using the recursion relation based on the strain energy criteria (equation (25)). The results of this iteration are given in Table 1 under Case 1. The optimum design weighing 65.76 lbs was obtained in two steps. In this case the optimum design is also the design satisfying the optimality criteria. It does not degenerate to any determinate structure.

TABLE 1

EXAMPLE 1: Four Bar TrussDesign Information

Material:	Aluminum
Stress Limits:	25,000 psi
Modulus of Elasticity:	$E = 10^7$ psi
Specific Weight:	0.1 lbs/cubic inch
Lower Limits:	None
Upper Limits:	None

Displacement Limits

Case	Node	Direction		
		x	y	z
5 and 6	5	None	None	$\pm 0.3''$
7 and 8	5	$\pm 0.3''$	$\pm 0.5''$	$\pm 0.4''$

Number of Loading Conditions: Single loading (in pounds)

Loading Information:

Load Condition	Node	Direction of Load		
		x	y	z
<u>Cases</u> 1, 2, 5 and 6	5	10,000	20,000	-60,000
<u>Cases</u> 3, 4, 7 and 8	5	40,000	100,000	-30,000

Example 1

Case 1. Four Bar Truss - Single Loading - Stress Constraints

Cycle No.	Areas of Members in Sq. In.				Weight in Pounds
	1	2	3	4	
1	1.755	1.755	1.755	1.755	122.35
2	0.430	1.755	1.258	0.548	65.76

Case 2. Four Bar Truss - Single Loading - Stress Constraints
Multiple Minima

Member Removed	Areas of Members in Sq. In.				Final Weight in Pounds
	1	2	3	4	
1	0	2.105	0.770	1.097	65.76
2	2.588	0	3.710	2.207	158.70
3	0.677	2.655	0	1.961	88.11
4	0.859	1.406	1.746	0	65.76
None	0.430	1.755	1.258	0.548	65.76

Case 2: Four Bar Truss - Single Loading - Stress Constraints -

Multiple Minima

The loading condition on the structure is the same as in Case 1. The four bar truss is indeterminate to one degree. Since there are no limits on the sizes of the element, all the stable determinate structures are subsets of the original truss in the limiting sense. In this case four such determinate structures are possible, each derived by removing one member at a time. The fifth case is the original structure with all members present. The optimum designs for all the five cases are given in Table 1, Case 2. Interestingly, the designs one, four and five have the same weight even though they are distinctly different designs. The design weight of 65.76 appears to be the absolute minimum for this structure and there are three designs having the absolute minimum weight. The other two may be considered as relative minimums. It should be noted that the design of the indeterminate structure using Equation 25 converged to the absolute minimum without degenerating to any of the determinate structures. This is a simple example of a structural design problem with multiple minimums.

Case 3: Four Bar Truss - Single Loading - Stress Constraints

The same four bar truss is designed, but for a different loading condition. The details of this loading condition are given in Table 1. By iteration, using equation (25), the design converged to 115.27 lbs in seven steps. The details are given in Table 1, Case 3.

Example 1

Case 3. Four Bar Truss - Single Loading - Stress Constraints

Cycle No.	Relative Areas of Members				Scalar Multiplier	Weight Pounds
	1	2	3	4		
1	1.0000	1.0000	1.0000	1.0000	2.4711	172.28
2	0.9668	0.8395	1.0000	0.1418	2.6518	129.79
3	1.0000	0.8646	0.8864	0.0497	2.6353	120.59
4	1.0000	0.8632	0.8316	0.0137	2.6567	116.77
5	1.0000	0.8628	0.8157	0.0033	2.6620	115.62
6	1.0000	0.8627	0.8118	0.0008	2.6633	115.33
*7	1.0000	0.8626	0.8109	0.0004	2.6634	115.27

* There was minimum size limit of 0.001 sq. in. If this is removed, the structure degenerates to a determinate structure with member four removed.

Case 4. Four Bar Truss - Single Loading - Stress Constraints - Multiple Minima

Member Removed	Areas of Members in sq. in.				Final Weight lbs.
	1	2	3	4	
1	0	0.132	5.186	3.400	170.58
2	0.162	0	5.370	3.607	179.28
3	4.564	3.843	0	2.426	177.95
4	2.664	2.298	2.159	0	115.25
NONE	2.663	2.298	2.160	0.001	115.27

If there was no limit on the size of the fourth member it would have degenerated to the determinate structure with member four removed.

Case 4: Four Bar Truss - Single Loading - Stress Constraints -

Multiple Minima

The truss and the loading condition are the same as Case 3. To study the multiple minima problem, four determinate structures and the original indeterminate structure are considered. Table 1, Case 4 gives the details of the minimum weight designs obtained in each of these cases. In this case the fourth determinate structure (member four removed) has the lowest design weight of 115.25 lbs. It is interesting to note that iteration on the original indeterminate structure using equation (25) degenerated to the determinate structure that has the lowest weight.

Case 5: Four Bar Truss - Single Loading - Stress and Displacement

Constraints

This is the same as Case 1 except the vertical displacement of node five is limited to 0.3 inches. The details of the design in each cycle are given in Table 1, Case 5. Since there are both stress and displacement constraints, the combined approach was used for design. From the initial design to the next design the elements were resized by equation (25). Further iteration was carried out by equation (39). In the first five cycles the reduction in weight was quite significant. Then in the subsequent cycles the design creeps along slowly until it reaches 137 lbs., a reduction of about 7 lbs in more than 20 cycles.

Example 1

Case 5. Four Bar Truss - Single Loading - Stress & Displacement Constraints

Cycle No.	Relative Areas of Members				Scalar Multiplier	Weight in Pounds
	1	2	3	4		
1	1.0000	1.0000	1.000	1.0000	2.4166	168.48
*2	0.2449	1.0000	0.7168	0.3123	4.0364	151.25
3	0.3137	1.0000	0.6596	0.3464	3.8016	145.41
4	0.3456	1.0000	0.6253	0.3628	3.7423	144.00
5	0.3600	1.0000	0.6029	0.3732	3.7271	143.55
6	0.3651	1.0000	0.5867	0.3809	3.7272	143.35
7	0.3652	1.0000	0.5740	0.3873	3.7340	143.23
8	0.3622	1.0000	0.5631	0.3931	3.7442	143.12
9	0.3576	1.0000	0.5531	0.3985	3.7553	142.03
10	0.3518	1.0000	0.5437	0.4038	3.7696	142.93
11	0.3454	1.0000	0.5344	0.4090	3.7838	142.82
12	0.3384	1.0000	0.5252	0.4143	3.7986	142.71
13	0.3312	1.0000	0.5158	0.4196	3.8141	142.59
14	0.3236	1.0000	0.5064	0.4250	3.8300	142.46
15	0.3158	1.0000	0.4967	0.4304	3.8464	142.33
16	0.3078	1.0000	0.4869	0.4360	3.8633	142.18
17	0.2996	1.0000	0.4768	0.4417	3.8807	142.03
18	0.2911	1.0000	0.4664	0.4476	3.8985	141.86
19	0.2824	1.0000	0.4558	0.4536	3.9167	141.67
20	0.2735	1.0000	0.4449	0.4597	3.9354	141.48
21	0.2643	1.0000	0.4337	0.4660	3.9546	141.26
22	0.2549	1.0000	0.4222	0.4724	3.9743	141.02
23	0.2452	1.0000	0.4107	0.4790	3.9943	140.76
24	0.2352	1.0000	0.3981	0.4858	4.0148	140.47
25	0.2249	1.0000	0.3855	0.4928	4.0357	140.15
26	0.2142	1.0000	0.3724	0.4999	4.0568	139.80
27	0.2032	1.0000	0.3589	0.5073	4.0782	139.39
28	0.1918	1.000	0.3449	0.5149	4.0956	138.93
29	0.1799	1.0000	0.3303	0.5228	4.1209	138.40
30	0.1676	1.0000	0.3151	0.5309	4.1417	137.78
31	0.1548	1.0000	0.2991	0.5392	4.1615	137.06
32	0.1414	1.0000	0.2824	0.5479	4.1796	136.18
33	0.1274	1.0000	0.2647	0.5569	4.1947	135.11
34	0.1127	1.0000	0.2460	0.5662	4.2047	133.75
35	0.00	1.0000	0.2258	0.5759	4.2059	131.98

Example 1 - Case 5 (cont'd)

Cycle No.	Relative Areas of Members				Scalar Multiplier	Weight in Pounds
	1	2	3	4		
36	0.0807	1.0000	0.2039	0.5860	4.1911	129.55
37	0.0668	1.0000	0.1797	0.5964	4.1527	126.43
**	0.01	3.8960	0.7700	2.443	1.0000	118.91

* This is the last cycle using equation (25). The remaining designs are obtained by equations (39) and (45).

** This design was not obtained by continuation of the above iteration, but nevertheless, a feasible design. It was one of the determinate cases with 0.01 sq. inches added to the first member and scaled to satisfy the constraints.

Case 6. Four Bar Truss - Single Loading - Stress and Displacement Limits Multiple Minima

Member Removed	Areas of Members in Sq. In.				Final Weight lbs.
	1	2	3	4	
1	0	3.894	0.770	2.443	118.13
2	14.138	0	16.981	10.100	764.27
3	0.755	4.781	0	3.532	150.98
4	2.596	2.813	3.493	0	146.04
NONE	0.01	3.896	0.770	2.443	118.91

Then in the next five cycles the weight reduces to 126.43 lbs. At this point stress in one of the members and the node displacement become active at the same time. Stress gradient calculations (equation (38)) are not incorporated into the present program and the design could not proceed further. If this capability is included, it is anticipated that the design would degenerate to the determinate structure with member one removed. The last line of the table gives such a design.

Case 6: Four Bar Truss - Single Loading - Stress and Displacement

Limits - Multiple Minima

The truss, loading condition and the displacement limits are the same as in Case 5. To study the multiple minima problem, four determinate structures and the original indeterminate structure are considered. Table 1, Case 6 gives the details of the optimum designs obtained in each case. In this case the first determinate structure (member one removed) has the lowest weight design of 118.13 lbs. The indeterminate structure with 126.4 lbs has a tendency to degenerate to this design.

Case 7: Four Bar Truss - Single Loading - Stress and Displacement

Limits.

This is the same as Case 3 except the displacements of node 5 are limited in all three directions. The details of the displacement limits are given in Table 1. The same table under Case 7 gives the details of the designs in each cycle.

Example 1

Case 7 - Four Bar Truss - Single Loading - Stress & Displacement Constraints

Cycle No	Relative Areas of Members				Scalar Multiplier	Weight in Pounds
	1	2	3	4		
1	1.0000	1.0000	1.000	1.000	2.6658	185.85
2	0.9668	0.8395	1.000	0.1417	3.1171	152.56
3	1.0000	0.8646	0.8864	0.0497	3.1011	141.90
4	1.0000	0.8632	0.8316	0.0137	3.1277	137.47
5	1.0000	0.8628	0.8157	0.0033	3.1343	136.13
6	1.0000	0.8627	0.8118	0.0008	3.1360	135.80
7	1.0000	0.8626	0.8109	0.0003	3.1362	135.73
8	3.147	2.691	2.163	0.001	1.000	128.59

Case 8. Four Bar Truss - Single Loading - Stress and Displacement Constraints - Multiple Minima

Member Removed	Area of Members in Sq. In.				Final Weight
	1	2	3	4	
1	0	0.132	9.581	7.781	345.219
2	2.486	0	14.291	9.035	499.143
3	10.382	3.844	0	8.597	403.906
4	3.147	2.691	2.162	0	128.561
NONE	3.147	2.691	2.163	0.001	128.594

Case 8: Four Bar Truss - Single Loading - Stress and Displacement

Limits - Multiple Minima.

The truss, loading condition and the displacement limits are the same as in Case 7. The optimum designs of the four determinate structures and the original indeterminate structure are given in Table 1, Case 8. The fourth determinate structure (member four removed) has the lowest weight design of 128.56 lbs. The original indeterminate structure, on iteration using equations (25) and (39), degenerates to the determinate structure with lowest weight design.

Example 2: Three Bar Truss - Three Loadings - Stress Constraints

The design of this truss (Fig. 5) was first reported by Schmit in 1960 [11]. The conclusions drawn in this reference had a significant impact on the research on structural optimization in subsequent years. The second case, in which the method of alternate steps gave an 8% lighter design than the one obtained by the stress ratio design, was selected to test the algorithm based on the strain energy criteria (equation (25)).

The truss is subjected to three independent loading conditions and the details of the loading are given in Table 2. The stress limits are 5000 psi on members 1 and 3 and 20,000 psi on member 2. When this information was submitted to the algorithm based on the strain energy criteria (equation (25)), a design weighing 16.7 lbs was obtained in two steps. This design was about 4.5% heavier than the design reported in [11]. An examination of the stresses in the members

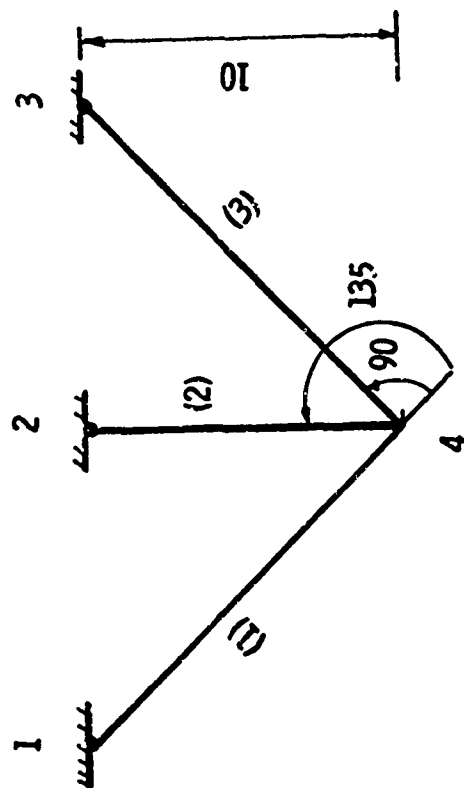


FIGURE 7. THREE BAR TRUSS

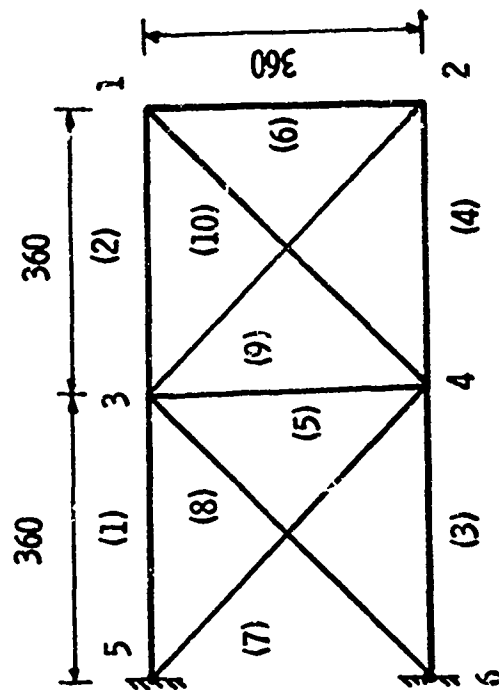


FIGURE 8. CANTILEVER TRUSS

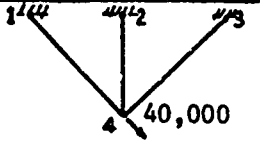
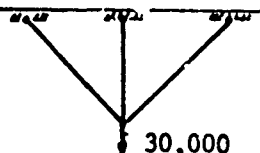
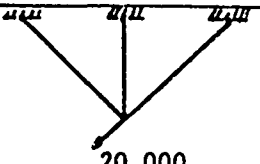
TABLE 2

EXAMPLE 2: Three Bar Truss - Comparison

Design Information

Material:	Aluminum
Stress Limits:	See the Table
Modulus of Elasticity:	$E = 1.0 \times 10^7$
Specific Weight:	0.1 lbs/cu. inch
Lower Limits:	None
Upper Limits:	None
Displacement Limits:	None
Number of Loading Conditions:	Three

Loading Information:

Load Condition	Node	Direction of Load	
		x	y
	4	28,284	-28,284
	4	—	-30,000
	4	-14,142	-14,142

Three Bar Truss (Cont'd)

Stress Limits.

Member	1	2	3
Stress Limits	5,000	20,000	5,000

Design Obtained by Iteration Using Equation (25)

Cycle No	Areas of Members in Sq. In.			Weight in Pounds
	1	2	3	
1	5.6568	5.6568	5.6568	21.6567
2	6.7917	2.6523	3.3959	17.0597
3	7.1164	1.7903	2.9252	15.9912

Comparison

Source	Areas of Members			Final Weight in Pounds	No. of Steps
	1	2	3		
Design Given in Ref. 11	7.0990	1.8490	2.8970	15.986	13
By Eq. (25)	7.116	1.790	2.925	15.991	3

revealed that the stress in member 2 is less than 7000 psi, while the other two members are close to their limits. For some obscure reason a disproportionately large stress limit (20,000 psi) was specified for member 2 in this problem. The large stress limit on member 2 has the effect of increasing the step size in the optimality criteria approach. The increase step size has the beneficial effect of arriving at the near optimum very rapidly (only two steps). This benefit is accompanied by the possibility of missing the optimum between two steps (See Fig. 6).

To reduce the step size, the same problem was submitted with the limiting normal stress values of 5000 psi for members 1 and 3 and 8000 psi for member 2. Iteration using equation (25) gave a design weighing 16.0 lbs in three steps. It should be noted that the limiting normal stress of 8000 psi was used to evaluate the energy capacity but the stress limit was left at 20,000 psi. When the energy capacity of member 2 was evaluated by using 7955 psi as the limiting normal stress, a design weight of 15.991 lbs was obtained again in three steps. The details of the design in each step is given in Table 2. The method of alternate steps gave the optimum design in 13 steps [11]. This comparison was made just to show the relevance of the energy criteria approach in the design of optimum structures.

Example 3: Cantilever Truss

The cantilever truss shown in Fig. 8 was designed for four different cases. The details of the loading and other information are given in Table 3. This truss exhibits interesting behavior which

is pointed out while discussing each case.

Case 1: Cantilever Truss - Single Loading - Stress Constraints

This problem has stress limits and a limit on the sizes of the members. The optimum design weighing 1593.2 lbs was obtained in 17 steps using equation (25). Four members were at the minimum size limit of 0.1 square inches. All members except the ones governed by the minimum size have satisfied the optimality criteria. The large proportion of members at the minimum size appears to contribute to the slow convergence. The details of the optimum design are given in Table 3, Case 1.

Case 2: Cantilever Truss - Single Loading - Stress and Displacement

Limits

The geometry and loading were the same as in Case 1. In addition to stress constraints, a displacement limit of ± 2.0 " was imposed on all nodes in the vertical direction. An optimum design weighing 5084.9 lbs was obtained in 25 steps. Twenty of these steps were based on the energy criteria (equation (25)) and the remaining steps used equation (39). The details of the design are given in Table 3.

Case 3: Cantilever truss - Single loading - Stress limits

The truss is the same as in the last two cases but the loading at the bottom nodes was increased to 150,000 lbs., and on the top nodes 50,000 lbs was placed in the opposite direction. The net downward load is still 200,000 lbs as in Case 1. An optimum design weighing 1664.6 lbs was obtained in 11 steps. In this case three members were

TABLE 3

EXAMPLE 3: Cantilever Truss - Single Loading

Design Information

Material:	Aluminum
Stress Limits:	25,000 psi
Modulus of Elasticity:	$E = 1.0 \times 10^7$ psi
Specific Weight:	0.1 lbs/cu. inch
Lower Limits:	0.1 Sq. Inches on all Members
Upper Limits:	None
Displacement Limits:	± 2.0 " in y-direction Cases 2 & 4 None in Cases 1 & 3
Number of Loading Conditions:	Single Loading

Loading Information:

Load Condition	Node	Direction of Load		
		x	y	z
<u>Cases 1 & 2</u> 	2		-100,000	
	4		-100,000	
<u>Cases 3 & 4</u> 	1		+50,000	
	2		-150,000	
	3		+50,000	
	4		-150,000	

Example 3

Case 1. Cantilever Truss - Single Loading - Stress Constraints

Cycle	1	2	3	4	5	6	7
Weight	3435.0	1969.2	1821.8	1721.5	1680.2	1664.1	1650.9
Cycle	8	9	10	11	12	13	14
Weight	1639.0	1628.9	1620.3	1613.3	1607.6	1603.1	1598.9
Cycle	15	16	17	Computer Time (7094) 2 sec.			
Weight	1595.9	1593.6	1593.2				

Final Design

Member	1	2	3	4	5
Area	7.938	0.100	8.062	3.938	0.100
Member	6	7	8	9	10
Area	0.100	5.745	5.569	5.569	0.100

Case 2. Cantilever Truss - Single Loading - Stress & Displacement Limits

Cycle	1	2	3	4	5	6	7
Weight	8266.1	6281.7	6065.2	5984.5	5963.1	5920.1	5881.6
Cycle	8	9	10	11	12	13	14
Weight	5848.1	5819.7	5795.9	5776.4	5760.7	5748.2	5738.3
Cycle	15	16	17	18	19	20	* 21
Weight	5730.7	5724.7	5720.2	5716.7	5713.7	5712.2	5502.9
Cycle	22	23	24	25	Computer Time 3 seconds.		
Weight	5343.8	5221.5	5127.0	5084.9			

* First Cycle in Search

Example 3 - Case 2 (Cont'd)

Final Design

Member	1	2	3	4	5
Area	30.416	0.128	23.408	14.904	0.101
Member	6	7	8	9	10
Area	0.101	8.696	21.084	21.077	0.186

Example 3

Case 3. Cantilever Truss - Single Loading - Stress Constraints

Cycle	1	2	3	4	5	6	7
Weight	3512.8	2079.6	1920.6	1828.8	1758.2	1699.8	1677.3
Cycle	8	9	10	11	Computer Time 2 Seconds		
Weight	1675.3	1666.8	1664.7	1664.6			

Final Design

Member	1	2	3	4	5
Area	5.948	0.100	10.053	3.948	0.100
Member	6	7	8	9	10
Area	2.052	8.559	2.755	5.583	0.100

Case 4. Cantilever Truss - Single Loading - Stress and Displacement Constraints

Cycle	1	2	3	4	5	*6	7
Weight	8417.7	6565.2	6242.8	6031.6	5935.4	5686.3	5505.2
Cycle	8	9	10	11	12	13	Time
Weight	5354.9	5220.0	5099.0	4991.4	5099.0	4895.6	2 Sec

* First Cycle in Search

Final Design

Member	1	2	3	4	5
Area	25.190	0.363	25.419	14.327	0.417
Member	6	7	8	9	10
Area	3.144	12.083	14.612	20.261	0.513

at the minimum size and this may have partly contributed to the reduction in the number of steps. Except for these three members all others satisfied the optimality criteria. The design weight of 1664.6 lbs appears to be reasonable compared with 1593.2 lbs in Case 1. The details of the design are given in Table 3, Case 3.

Case 4: Cantilever Truss - Single Loading - Stress and Displacement Limits.

The truss and the loading condition are the same as in Case 3. In addition to the stress limits, a displacement limit of ± 2.0 " is on all nodes. This limit is the same as in Case 2. An optimum design weighing 4895.6 lbs was obtained in 13 steps. Six of these were based on the energy criteria). This design is about 200 lbs lighter than the design obtained in Case 2 and it was obtained in about half the number of cycles. None of the members were governed by the minimum size in this case. The design weight in Case 3 is heavier than Case 1 while this case is lighter than Case 2. The design obtained in Case 4 is not acceptable for Case 2.

These four cases conclude the discussion of Example 3.

Example 4: Transmission Tower

The design of this tower was first reported by Fox and Schmit in [12]. Later the same tower was designed by Gellatly [13], Marcal and Gellatly [14], Venkayya, Khot and Reddy [7], Dwyer, Emerton and Ojalvo [15]. In the first three references mathematical programming methods were used and in [15] a combined approach based on modified fully stressed design and a search procedure were used. This problem

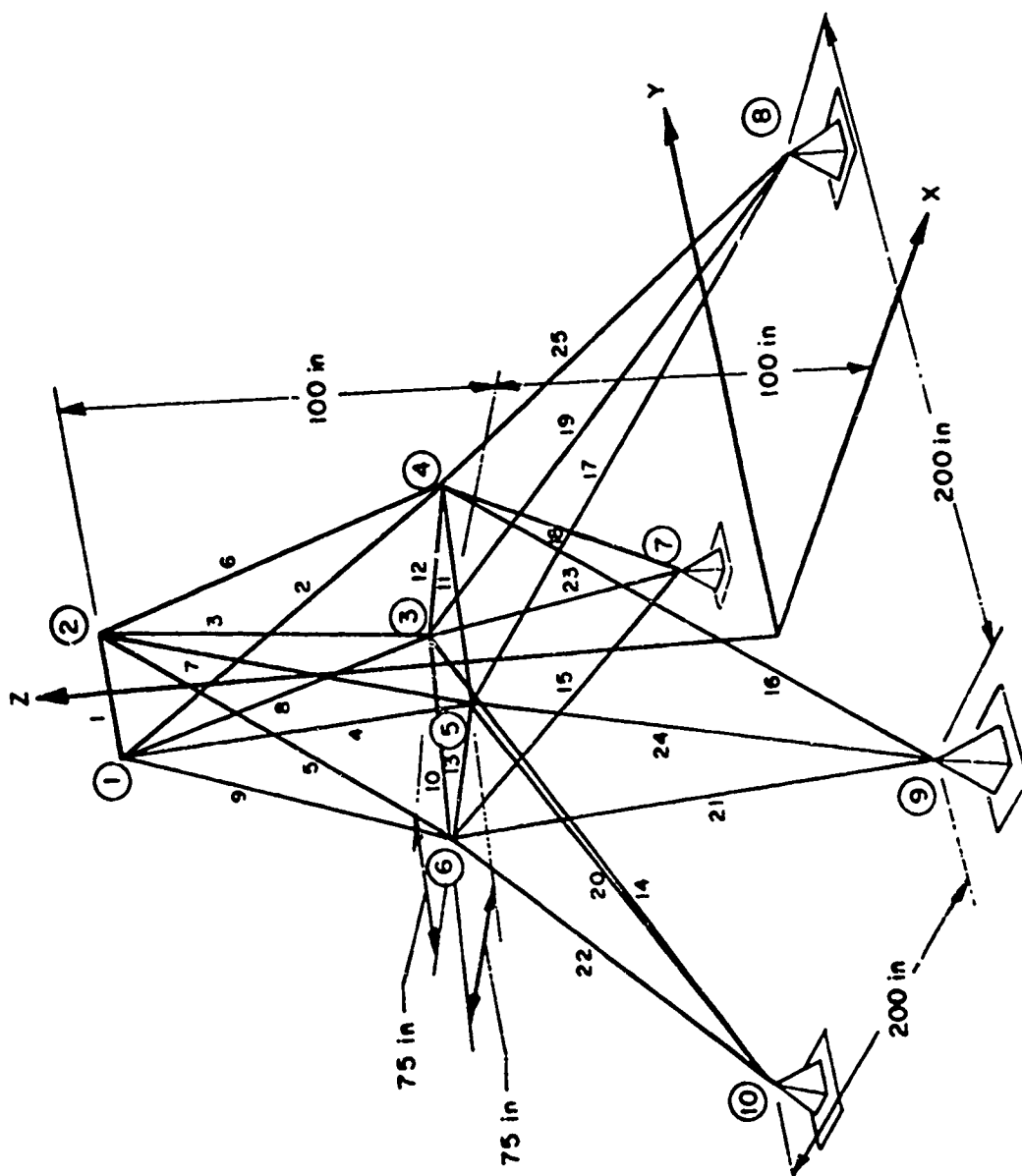


FIGURE 9. TRANSMISSION TOWER

was selected in order to make an exact comparison of the designs obtained by the mathematical programming method and the combined approach presented in this paper. The design conditions, as reported in [12], were reproduced in Table 4. Two cases were considered. In the first case the design conditions were strictly those given in [12]. In the second case the design conditions are still the same except the lower and upper limits on the diameter of the tube were relaxed.

Case 1: Transmission Tower - Stress and Displacement Constraints

Under the design conditions specified in [12], the combined approach gave an optimum design weighing 553.4 lbs in 6 cycles. Two of these cycles used the recursion relation based on the energy criteria and the remaining four cycles used equation (39). The total computational time for this design on the IBM-7094-II-7044-DCS was 20 seconds.

Fox and Schmit reported [12] as an optimum, a design weighing 570.4 lbs. This design was obtained in 360 seconds on the Univac 1107, using a variable metric minimizer (Fletcher-Powell method). Table 4 contains the details of the designs obtained by the combined approach and the one reported in [12].

It is significant to note that the combined approach arrived at a lighter design in a small fraction of the computer time required by the mathematical programming approach. The difference between the two designs is about 17 lbs. However, in the case of the design reported in [12], the displacements exceed the specified limits by 1.5% while

Table 4

Example 4 - Transmission Tower

Design Information

Material: Aluminum

Stress Limits: 40,000 psi in Tension Buckling Stress in Comp

Modulus of Elasticity: 10^7 psi

Specific Weight: 0.1 lbs/cubic inch

Lower Limits: Area 0.01 sq. in. for additional limits see after loading table

Upper Limits: On Diameters and Thickness see after load

Displacement Limits: 0.35" on all nodes and all directions

Number of Loading Conditions: 6 (All loads are in lbs.)

Load Condition	Node	Direction of Load		
		x	y	z
1	1	1,000	10,000	-5,000
	2	0	10,000	-5,000
	3	500	0	0
	6	500	0	0
2	1	0	10,000	-5,000
	2	-1,000	10,000	-5,000
	4	- 500	0	0
	5	- 500	0	0
3	1	1,000	-10,000	-5,000
	2	0	-10,000	-5,000
	3	500	0	0
	6	500	0	0

Table 4 (Cont'd)

Loading Condition	Node	Direction of Load		
		x	y	z
4	1	0	-10,000	-5,000
	2	-1,000	-10,000	-5,000
	4	- 500	0	0
	5	- 500	0	0
5	1	0	20,000	-5,000
	2	0	-20,000	-5,000
6	1	0	-20,000	-5,000
	2	0	20,000	-5,000

Additional Limits on Sizes of Elements

Members are all made of circular tubes, subject to the following limitations:

1. Mean Diameter D $0.5" \leq D \leq 4.0"$
2. Thickness t $0 \leq t \leq 1.0$
3. D/t $10.0 \leq D/t \leq 100.0$

Case 1: Transmission Tower - Six Loadings - Stress and Displacement Limits - Comparison

Design conditions are as given in [12]

Cycle	1	2	*3	4	5	6	Time
Weight	734.4	670.8	613.1	584.1	566.0	553.4	20 Sec.

Case 2: Same as in Case 1, except upper and lower limits on diameter of the tubes are relaxed

Cycle	1	2	3	4	*5	6	Time
Weight	734.4	589.2	578.3	577.3	555.6	545.5	13 sec.

* First cycle in Search, Equation (39)

Transmission Tower: Details of Designs in Two Cases and Design from Ref. 12

Design Case	Description of Design	Members									Weight	Time Sec.
		1	2, 3, 4, 5	6, 7, 8, 9	10, 11	12, 13	14, 15 16, 17	18, 19 20, 21	22, 23 24, 25			
* Case 1	Area Sq. In	0.021	1.726	2.965	0.044	0.155	0.725	2.007	2.540	553.44	* 20	
	Diam. In.	0.668	4.000	4.000	1.000	1.000	4.000	4.000	4.000			
	Thickness In.	0.010	0.1373	0.2359	0.014	0.049	0.0576	0.1597	0.2021			
	D/t	66.84	29.13	16.956	71.92	20.284	69.444	25.047	19.792			
	Max. Comp.	—	7606	6883	1331	1350	5078	5893	5735			
	Max Tension	4139	7517	5125	—	—	3653	4640	4145			
	Allowable	—	11590	17306	2200	2200	6016	6016	11082			
Case 2	Area Sq. In.	0.028	1.942	3.081	0.010	0.010	0.693	1.678	2.627	545.49	* 13	
**Ref. 12	Area Sq. In.	0.783	2.398	2.199	0.092	0.358	0.918	1.871	2.560	570.40	** 360	

Nodes 1 and 2 are at the displacement limit, 0.35 inches in the first 4 loadings and very close to the limit in the other two loads, (IBM 7094)

** Nodes 1 and 2 exceed displacement limits in the first four loading conditions and at limits in the other two loading conditions (UNIVAC 1107).

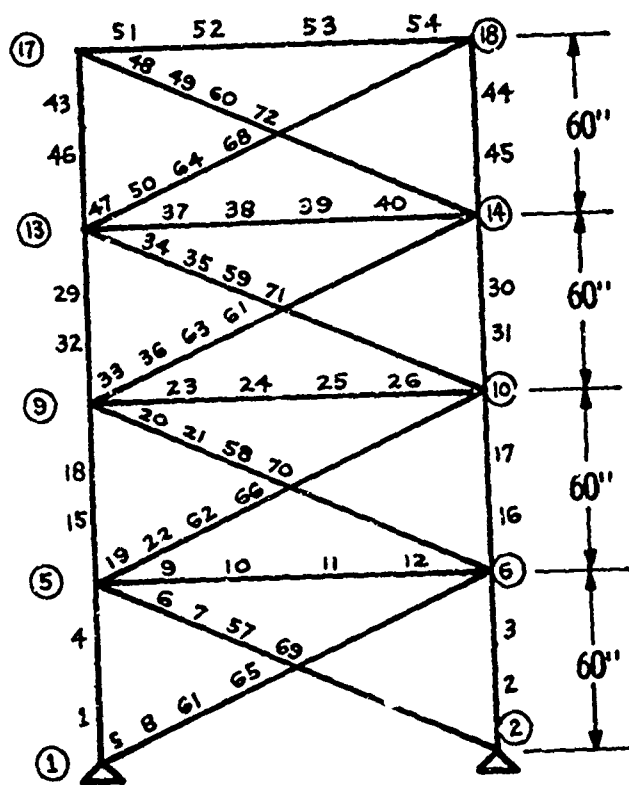
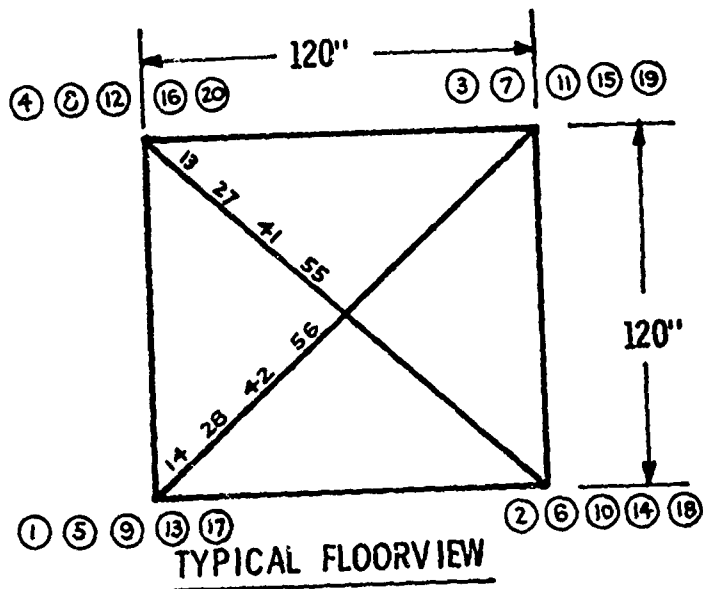
the author's design adheres strictly to the specified limits. Ref.[12] takes advantage of the symmetry of the tower and designs only for two loading conditions. The author's design was obtained by considering six independent loading conditions. These differences, particularly computer times, become even more significant as the number of variables increase.

Case 2: Transmission Tower - Stress and Displacement Limits

The geometry of the structure and the loading conditions were the same as in Case 1. The lower and upper limits on the diameter of the tubes were relaxed in this case. A minimum size limit of 0.01 sq. in. was placed on all members. Under these conditions the combined approach gave an optimum design weighing 545.5 lbs. in six cycles. Four of these cycles used the recursion relation based on the energy criteria and two were in the search (equation (39)). The computer time was 15 seconds in this case. The details of this design are given in Table 4, Case 2.

Example 5: 72 Bar Truss - Stress and Displacement Limits

The design of this truss was first reported by Venkayya, Khot and Reddy in [7]. The design conditions are given in Table 5. An optimum design weighing 381.2 lbs was obtained in 15 cycles. The details of the design are given in Table 5. The weight of the design presented in Reference[7] was 425.8 lbs. The improvement in the design was due to two reasons. In Reference[7] iteration using optimality criteria was terminated too soon. The second reason was due to the modifications



FRONT VIEW

FIGURE 10. FOUR LEVEL TOWER

Table 5

Example 5 - 72 Bar Truss

Design Information

Material:	Aluminum
Stress - Limits:	25,000 psi
Modulus of Elasticity:	$E = 10^7$ psi
Specific Weight:	0.1 lb/cu in.
Lower Limit:	0.1 square inch
Upper Limits:	None
Displacement Limits:	0.25 on all nodes and all directions

NUMBER OF LOADING CONDITIONS 5

Load Condition	Node	Direction of Load		
		x	y	z
1	17	5,000	5,000	-5,000
2	18	-5,000	5,000	-5,000
3	19	-5,000	-5,000	-5,000
4	20	5,000	-5,000	-5,000
5	17	0	0	-5,000
	18	0	0	-5,000
	19	0	0	-5,000
	20	0	0	-5,000

Example 5 - 72 Bar Truss

Cycle	1	2	3	4	5	6	*7
Weight	656.8	478.6	455.0	446.9	445.5	445.4	401.7
Cycle	8	9	10	11	Computer Time 240 Sec.		
Weight	391.5	383.6	381.6	381.2			

* First cycle in search, equation (39).

Details of Final Design:

El. Nos	1,2,3,4	5,6,7,8	15,16,17,18	19,20,21,22	29,30,31,32
Area Sq. In.	1.818	0.523	1.246	0.524	0.611
El. Nos	33,34,35,36	43,44,45,46	47,48,49,50	51,52,53,54	55,56
Area Sq. In.	0.532	0.161	0.557	0.377	0.506
El. Nos	57,61,65,69	58,62,66,70	59,63,67,71	60,64,68,72	Remaining
Area Sq. In.	0.523	0.524	0.532	0.557	0.100

discussed in section 5 and 6. It is interesting to note that a cycle using equation (25) took 2 seconds of computer time while a cycle in search took about 37 seconds. The number of cycles in search can be reduced to half by increasing the step size Δ to 2.0 in Eq. (39).

This 72 bar truss was also designed by Dwyer, Emerton and Ojalvo [15], weighed 384.9 lbs. Except for this small difference (3.7 lbs), their design is similar to the one presented in table 5.

8. DESIGN OF PLANE FRAMES

The energy criterion method estimates the participation of each element more realistically than an approach like the stress ratio design. For example, the four elements shown in Figure 11 are subjected to different states of bending, but they all have the same maximum bending moment and cross-sectional dimensions. The stress ratio design treats them alike while the energy criteria method distinguishes them by evaluating the total energy and not just the maximum stress point. However, the stress-ratio method can be improved by averaging the stresses along the element.

Three structures were selected to illustrate the method. In all cases box sections were used for members. The design started with elements having the same relative moment of inertia (1.0). Analysis in the first cycle started with the assumption of constant depth for all the elements. The actual depth for each element was determined prior to the determination of weight in this cycle. The compatibility

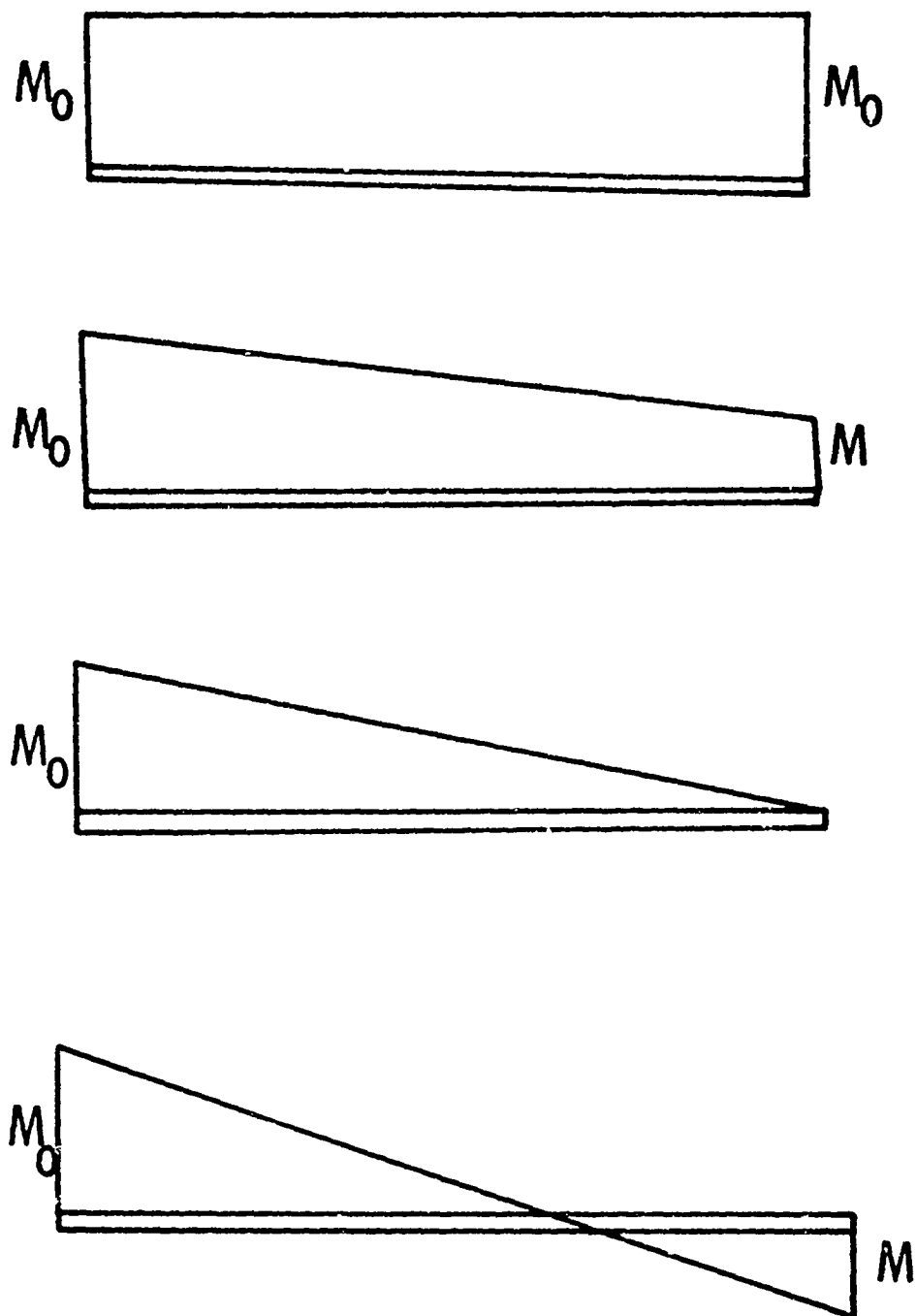


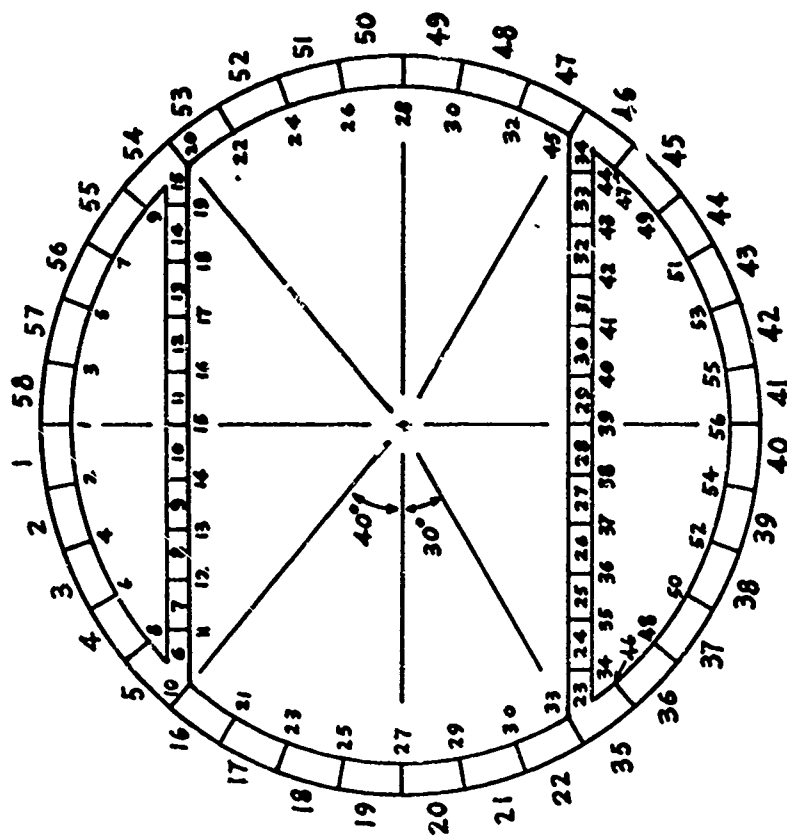
FIGURE 11. MOMENT VARIATION

between the primary (moment of inertia in this case) and the secondary variable was established by the implicit relations and iteration. This iteration involved more than one analysis in some cycles. The design obtained at the end of each cycle is a feasible design and does not violate any design conditions.

Example 6: Ring Frame - Four Loadings - Stress Constraints

Figure 12 shows the schematic diagram and the idealization of the ring frame. It is a circular ring with a mean diameter of 360 inches. It has two floors along the chord lines, at 40 and 30 degrees from the horizontal line passing through the center. The frame was divided into 58 elements. The 36 elements along the circumference were at 10 degree intervals. The top floor is divided into 10 equal elements and the bottom floor into 12 equal elements. The curved elements along the circumference were approximated by straight line elements. This idealization gave a structure with 168 degrees of freedom and 58 structural elements. The frame is subjected to four independent loading conditions. The loading and other design information are given in Table 6.

The optimum design weighing 830 lbs was obtained in two cycles using Equation(25) with the modifications indicated in Section 6. The computer time was 59 seconds for the complete design. The structure was analyzed four times to complete the design. The node numbering scheme, shown in Figure 12, gave a stiffness matrix with a very favorable distribution on non-zero elements for the solution scheme



MEAN DIAMETER 360"

FIGURE 12. RING FRAME

BOUNDARIES

NODES	DISP X	DISP Y	ROTATION
1, 56	0	-	0
33, 45	-	0	-

Table 6

Example 6: Ring Frame

Design Information

Material:	Aluminum
Stress Limits:	25,000 psi
Modulus of Elasticity:	10^7 psi
Specific Weight:	0.1 lbs/cubic inch
Lower Limits:	See after loading information
Upper Limits:	
Displacement Limits:	None
Number of Loading Conditions:	Four

Loading Information

Loading Condition 1:

Outer ring is subjected to uniform internal pressure of 1440 lbs/ft

Loading Condition 2:

The space bounded by the two floors and the ring is subjected to internal pressure of 1440 lbs/ft

Loading Condition 3:

Floors are subjected to 100 lbs/ft acting vertically downwards.

Loading Condition 4:

Loading Conditions 2 and 3 are combined

Limits on Box Beam

D = Mean Depth, B = Mean Width

$$4" \leq D \leq 12"$$

$$B = 6"$$

$$* 0.023 \leq t_F/D \leq 0.034$$

$$t_W/D = 0.009$$

* Allowed to exceed when the depth is at limit

Example 6

Ring Frame - Four Loadings - Stress Limits

Final Design Weight 829.5 lbs
Design Weight in First Cycle 1380.4 lbs
Total Number of Cycles 2
Computer Time (IBM 7094) 59 Sec

Final Design

Members	Area	I	Depth Inches	Members	Area	I	Depth Inches
1,58	3.598	50.258	8.395	20,49	4.373	74.197	9.496
2,57	3.021	31.176	7.213	21,48	4.640	85.006	9.912
3,56	2.918	28.689	7.024	22,47	4.979	99.898	10.428
4,55	4.594	83.096	9.841	23,34	8.701	251.132	12.00
5,54	6.246	162.678	12.00	24,33	4.860	94.534	10.249
6,15	6.400	168.198	12.00	25,32	3.847	55.109	8.644
7,14	3.475	43.431	8.015	26,31	5.835	142.921	11.661
8,13	4.504	79.390	9.701	27,30	7.447	205.930	12.00
9,12	5.858	144.154	11.692	28,29	8.329	237.727	12.00
10,11	6.656	177.424	12.00	35,46	7.022	190.622	12.00
16,53	3.598	46.937	8.215	36,45	5.269	113.594	10.858
17,52	3.780	52.915	8.533	37,44	3.695	50.146	8.389
18,51	3.979	59.623	8.862	38,43	2.925	28.842	7.036
19,50	4.179	66.810	9.187	39,42	3.403	41.342	7.890
				40,41	3.928	57.874	8.779

used in the computer program (see the authors discussion of Reference [10] . The small computer time was partly due to the favorable distribution of non-zero elements.

The design weight in the first cycle was 1380 lbs and it was reduced to 830 lbs, a weight saving of 40%. It involved resizing only once. This rapid reduction, in the initial stages, is characteristic of most optimality criteria approaches. This property makes them very attractive for the optimization of practical structures with a large number of variables.

Example 7: Symmetrical Rectangular Frame

The details of this frame are given in Figure 13. The design of this frame was reported in References [16] and [17], using Rosen's gradient projection method. Reference [17] contains an excellent discussion and interpretation of the gradient projection method for structural optimization problems.

This frame was optimized by the combined approach presented in this paper with the following modifications: a) Each horizontal member was divided into four equal parts and the distributed forces were replaced by equivalent concentrated forces. b) The design conditions were not exactly those given by the AISC Code. c) The analysis scheme in References [16] and [17] did not consider the deformations in the axial direction. These modifications were necessitated by the limitations of the computer program. Because of these differences it is difficult to compare the designs exactly.

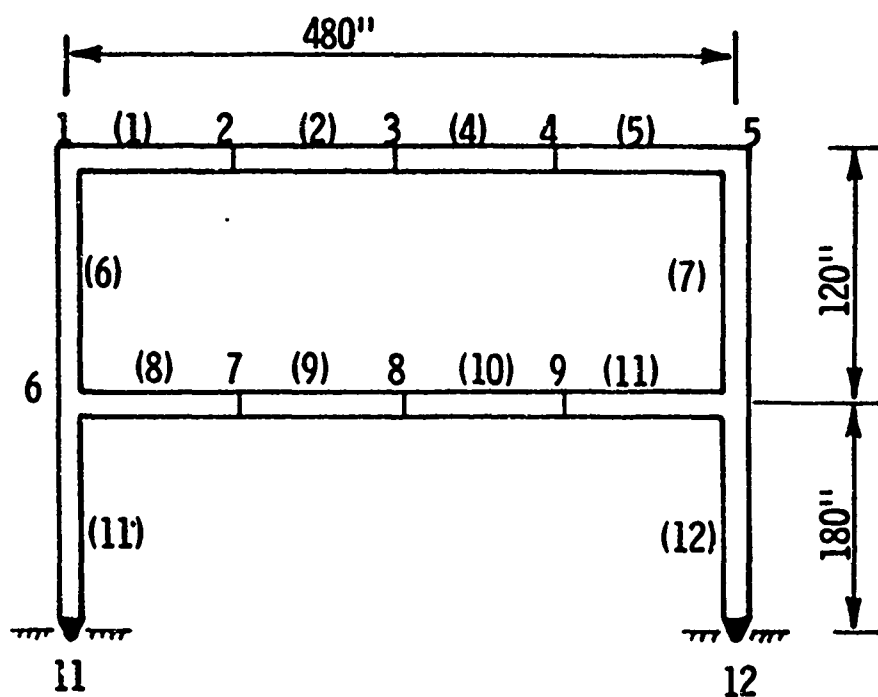


FIGURE 13. SYMMETRIC FRAME

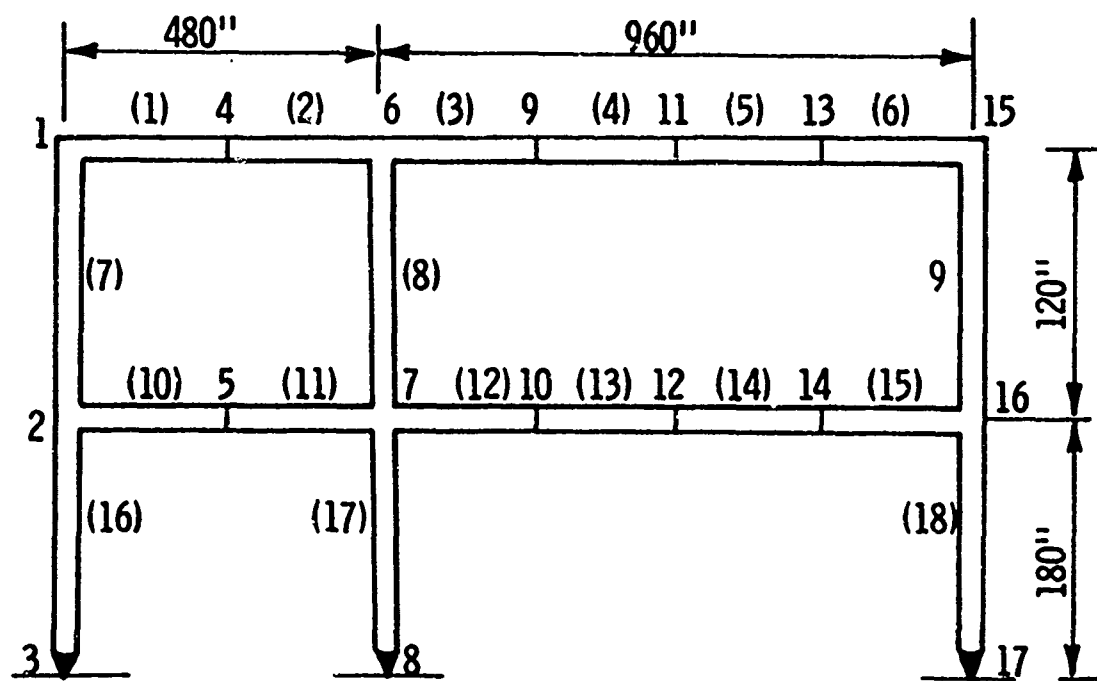


FIGURE 14. UNSYMMETRIC FRAME

Table 7

Example 7: 12 Element Plane Frame

Design Information

Material: Steel

Stress Limits: 29,000 psi

Modulus of Elasticity: 29.0×10^6 psi

Specific Weight: 0.283 lbs/cu inch

Lower Limits: Depth 8", Additional Info, see after loading

Upper Limits: Depth 21" (Case 1) 36" (Case 2)

Displacement Limits: Case 1: None; Case 2: 0.3" x-direction

Number of Loading Conditions: Three

Loading Information: Same for Cases 1 and 2

Load Condition	Node	Direction of Load lbs		
		x	y	Moment
1	1,5		-5,000	
	2,3,4		-10,000	
	6,10			
	7,8,9		-20,000	
Vertical Load		Same as above in addition		
2	1	3,570		
	6	8,920		
Vertical Load		Same as above in addition		
3	5	-3670		
	10	-8920		

Example 7

Limits on Box Beam

D = Mean Depth; B = Mean Width

B = 10"

Case 1. $8" \leq D \leq 21"$

Case 2. $8" \leq D \leq 30"$

$0.023 \leq t_F/D \leq 0.034$ *

$t_W/D = 0.009$

* Allowed to exceed when the depth is at limit

Case 1: 12 Element Plane Frame - Three Loadings - Stress Limits

Final Design Weight 6268 lbs

Design Weight in First Cycle 8083 lbs

Total Number of Cycles (Eq. (25)) 6

Computer Time (IBM 7094) 8 Sec.

Final Design

Members	1,4	2,3	5,6	7,10	8,9	11,12
Area Sq. In.	11.781	10.106	12.038	20.440	16.804	14.076
I (in ⁴)	524.0	365.9	550.9	1626.4	1169.4	790.0
Depth in	15.27	13.63	15.51	20.57	19.57	17.38
t_F/D	0.0248	0.0248	0.0248	0.0312	0.0253	0.0248
Sec. Mod	66.96	52.40	69.30	153.36	116.58	88.69

Example 7

Case 2: 12 Element Plane Frame - Three Loadings - Stress & Disp. Limits

Final Design Weight	10,638 lbs
Design Weight in First Cycle	13,328 lbs
Design Weight Entering Search	11,386 lbs
Total Number of Cycles	12
Number of Cycles Using Eq. (25)	5
Computer Time (IBM 7094)	29 Seconds

Final Design:

Members	1,4	2,3	5,6	7,10	8,9	11,12
Area (Sq. In.)	19.362	10.640	17.441	41.280	22.883	30.016
I (in ⁴)	1611.3	413.1	1282.5	6878.0	2347.0	3786.0
Depth (in)	21.63	14.15	20.20	30.00	24.39	26.42
t_F/D	0.0253	0.0249	0.0250	0.0418	0.0250	0.0330
Sec. Mod	145.35	56.99	123.91	440.10	187.76	277.46

Case 1: Symmetrical Frame - Three Loadings - Stress Constraints:

An optimum design weighing 6268 lbs was obtained in 4 cycles. The details of the design are given in Table 7, Case 1. The computer time for this design was 8 seconds.

Case 2: Symmetrical Frame - Three Loadings - Stress and Displacement Constraints:

An optimum design weighing 10,638 lbs was obtained in 12 cycles. Five of these cycles were based on the energy criteria and the remainder of the cycles used Equation 39 with the modifications given in Section 6. The computer time was 29 seconds. The details of the design are given in Table 7, Case 2.

Example 8: Unsymmetrical Frame - Three Loadings - Stress Constraints:

The schematic diagram of this frame and its dimensions are given in Figure 14. The design of this frame was also reported in Reference [16]. Because of the differences in the design conditions (as mentioned in the previous example) an accurate comparison with the design presented in Reference [16] is not possible. The distributed loads were replaced by equivalent concentrated forces. The frame was designed as an eighteen variable problem. An optimum design weighing 26,873 lbs was obtained in 6 cycles. The computer time was 17 seconds. The details of the design are given in Table 8. Reference [16] reports 6 minutes as the computer time required by the gradient projection method.

Table 8

Example 8: 18 Element Plane Frame

Design Information

Material: Steel

Stress Limits: 29,000 psi

Modulus of Elasticity: 29.0×10^6

Specific Weight: 0.283 lbs/cubic inch

Lower Limits: Depth 8" Additional Info see after loading

Upper Limits: Depth 36"

Displacement Limits: None

Number of Loading Conditions: Three

Loading Information:

Load Condition	Nodes	Direction of Load		
		x	y	Moment
1	1,15		-10,000	
	2,4,6			
	9,11,13		-20,000	
	16			
	5,7,10		-40,000	
	12,14			
Vertical Loads		Same as above. In addition		
2	1	3,570		
	2	8,920		
Vertical Loads		Same as above. In addition		
3	15	-3,570		
	16	-8,920		

Example 8

18 Element Plane Frame - Three Loadings - Stress Limits

Limits on Box Beams

D = Mean Depth; B = Mean Width

B = 10"

8" \leq D \leq 36"

0.023 \leq t_F/D \leq 0.034*

t_w/D = 0.009

*Allowed to exceed when depth is at limit

Final Design Weight 26,873 lbs

Design Weight in First Cycle 45,289 lbs

Total Number of Cycles (Eq. 25) 6

Computer Time (IBM 7094) 17 Seconds

Final Design

Member	1	2	3	4	5	6
Area	9.373	11.862	31.086	22.553	23.969	26.219
I	298.5	515.5	4461.8	2267.8	2592.2	3152.8
Depth	12.66	15.00	29.30	24.15	25.17	26.73
Member	7	8	9	10	11	12
Area	7.482	27.265	29.001	13.509	20.578	46.913
I	177.0	3432.7	3923.4	716.1	1816.3	10166.5
Depth	10.79	27.44	28.60	16.83	22.30	36.00
Member	13	14	15	16	17	18
Area	37.688	39.988	38.355	7.451	24.662	23.472
I	6874.8	7793.7	7135.3	175.4	2758.6	2475.8
Depth	33.94	35.26	34.33	10.76	25.65	24.81

9. SUMMARY AND CONCLUSIONS

The combined method discussed in this paper was first presented in Reference[7]. A more detailed proof of the energy criteria was presented in Section 2. A brief discussion of the problem of multiple minima in structural design was also included in that section. The derivation and interpretation of the recursion relation based on the energy criteria was given in Section 3. A method for the stress and displacement gradient calculations was presented in Section 4 in the context of the symmetrical Gaussian elimination scheme for the solution of equations. A semi-sparse matrix scheme (Reference[10]) was used for the elimination of many of the arithmetic operations involving zero elements.

A recursion relation based on constraint gradients was derived in Section 5. This relation is similar to the one derived in Reference[7] except that the change in variable was assumed to be proportional to its actual value instead of a unit value. This modification has produced 2 to 3% lower weight designs in some cases. Section 5 also contains additional discussion and interpretation of the search algorithm.

The necessary modifications to the recursion relations in the case of multivariable elements were discussed in Section 6. The problems of multiple minima in structural design were discussed in Section 7. That section also contains designs of some interesting bar structures. Some of these designs were compared with the designs

obtained by the mathematical programming methods. The design of plane frames with beam elements was presented in Section 8.

The iterative algorithms derived in this paper indicate the following beneficial trends when used for the design of indeterminate bar structures under a single loading condition.

a) When the indeterminate structure degenerates to a determinate structure, it goes to the one with the lowest weight.

b) If an indeterminate structure that satisfies the optimality criteria exists, then it will have the same weight as the lowest of the determinate structures.

The above conclusions were based on the tests of a large number of bar structures. If these conclusions are valid, the need for investigating a large number of determinate structures for finding the absolute minimum can be eliminated.

The combined approach, presented in this paper, charts an efficient path to the optimum and this makes it attractive for the optimization of structures with a large number of variables. Dwyer Emerton and Ojalvo have developed a combined approach based on the modified stress ratio design and a search algorithm for the optimization of practical aerospace structures in Reference [15].

The algorithm based on the energy criteria is far more efficient, when it is applicable, than the search algorithm (See the discussion after example 5).

Barnett and Hermann [18] have derived an optimality condition for

minimum weight design of statically determinate trusses subjected to single loading condition and specified nodal displacement. Berke [19] has suggested the possibility of extending this approach, in an iterative fashion, for the design of indeterminate structures subjected to multiple loading conditions and displacement constraints. Following this suggestion, Gellatly [20] has successfully applied this approach for the design of Cantilever Truss, Transmission Tower and the 72 Bar Truss and obtained the designs similar to the ones presented in Section 7. Reference [20] also contains examples of plate structures.

Algorithms based on optimality criteria are much more attractive, from the point of computational efficiency, than the search techniques. However, the validity of the optimality criteria approaches have been established only for restrictive cases and need to be extended to more general design conditions.

REFERENCES

1. Wasiutynski, Z., and Brandt, A., "The Present State of Knowledge in the Field of Optimum Design of Structures", Applied Mechanics Reviews, Vol. 16, P341-350, 1963.
2. Sheu, C.Y., and Prager, W., "Recent Developments in Optimal Structural Design", Applied Mechanics Reviews, Vol. 21, No. 10, P355-992, 1968.
3. Schmit, L.A., "Structural Synthesis", 1959-1969 A Decade of Progress", A Paper Presented at Japan-U.S. Seminar on Matrix Methods of Structural Analysis and Design, August 25-30, 1969, Tokyo, Japan.
4. Lansing, W., Dwyer, W., Emerton, R., and Randall, "Application of Fully Stressed Design Procedures to Wing Empennage Structures", A Paper Presented at AIAA/ASME 11th Structures, Structural Dynamics and Materials Conference, April 22-24, 1970, Colo. Denver.
5. Batdorf, W.J., "Applications of Computer Graphics in Structural Design" AGARD Structures and Materials Panel Conference, October 8, 1969, Istanbul, Turkey.
6. Losh, R.J., "Structural Analysis, Frailty Evaluation and Redesign", (SAFER Technical Document), AFFDL-TR-70-15, July 1970.
7. Venkayya, V.B., Khot, N.S., and Reddy, V.S., "Optimization of Structures Based on the Study of Strain Energy Distribution", 2nd Conference on Matrix Methods in Structural Mechanics, October 1968, AFFDL-TR-68-150.

8. Venkayya, V.B., "An Energy Criteria and A Search Procedure For Automated Design of Minimum Weight Structures", A Paper Presented at 28th Annual Meeting of SAWE, San Francisco, California, May 1969.
9. Venkayya, V.B., and Khot, N.S., "An Examination of Optimum Structural Designs", AFFDL-TR-70-
10. Melosh, R., and Bamford, R., "Efficient Solution of Load-Deflection Equations", J. of The Structural Division, ASCE Vol. 95, April 1969.
11. Schmit, L.A., "Structural Design By Systematic Synthesis", Second Conference on Electronic Computation, ASCE Structural Division, Pittsburgh, Pennsylvania 1960, PP105-132.
12. Fox, R.L. and Schmit, L.A., "Advances in the Integrated Approach to Structural Synthesis", J. of Spacecraft and Rockets, Vol. 3, No. 6, June 1966, pp 858-866.
13. Gellatly, R.A., "Development of Procedures for Large Scale Automated Minimum Weight Structural Design", AFFDL-TR-66-180, December 1966.
14. Marcal, P.V. and Gellatly, R. A., "Application of the Created Response Surface Technique to Structural Optimization", 2nd Conference on Matrix Methods in Structural Mechanics, Wright-Patterson AFB, Ohio, October 1968, AFFDL-TR-68-150.
15. Dwyer, W., Emerton, R., and Ojalvo, I., "An Automated Procedure for the Optimization of Practical Aerospace Structures" Vol. I and II AFFDL-TR-70-118.

16. Brown, D.M. and Ang, A.H.S., "A Nonlinear Programming Approach to the Minimum Weight Elastic Design of Steel Structures", Structural Research Series No. 298, University of Illinois, Civil Engineering Studies, Urbana, Ill., 1965.
17. Brown, D.M., and Ang, A.H.S., "Structural Optimization by Nonlinear Programming", J. of the Structural Division, ASCE, Vol. 92, No. ST 6, December 1966, pp 319-340.
18. Barnett, R. L., and Hermann, P. C., "High Performance Structures," NASA CR-1038, May 1968.
19. Berke, L. "An Efficient Approach to the Minimum Weight Design of Deflection Limited Structures", AF Flight Dynamics Laboratory Technical Memorandum, TM-70-4-FDTR. July 1970
20. Gellatly, R. A., "Optimal Structural Design" AFFDL-TR-70 (In preparation).

QUESTIONS AND DISCUSSION FOLLOWING VENKAYYA'S PAPER

QUESTION: What you've shown us today has been limited to minimum weight design. I think it was you yourself the other day that brought up the need for introducing more realistic and complicated cost functions in our optimization efforts. The math programming approach has its drawbacks, of course, but an arbitrary cost function can be handled without any particular difficulty. Would you comment on determining some optimality criteria for arbitrary cost functions.

VENKAYYA: You don't have to make a new optimality criterion for cost functions. It's simple to include it in the present analysis. You can use the same iterative procedure given by Eq. 25 in the paper. I didn't do it because nobody has defined a proper cost function. If you give me one, I don't see any problems putting in my analysis.

COMMENT: I'd like to make a few comments with respect to the mathematical programming approach. I'd like to point out here that the comparisons in the paper with mathematical programming approaches are made with rather primitive methods; in one instance, a method that was employed in 1965, reported in 1966. I think that before one draws any sweeping conclusions about the potential of the mathematical programming method, whether you talk cost or weight or other objective functions, it is important to consider the more modern algorithms which were alluded to in your paper, such as the feasible direction methods and penalty function methods using approximation schemes. I would like to bring out a point

that Dr. Venkayya and I have discussed previously and that is there are two ways to play the approximations game. He, in this paper, has presented the use of the optimality criteria, which is in general an approximation, although in some cases does give the optimum design. So you can use optimality criteria by way of an approximation to the basic optimization problem and seek designs which satisfy the optimality criterion. Alternatively you can formulate the problem as a mathematical programming problem and introduce approximations in the analysis. Very little work has been done in using rather radical and drastic approximations in the analysis which would speed up the math programming approach tremendously. The point I wish to make is that to draw a general conclusion with respect to the efficiency of the mathematical programming method based on a comparison with two rather primitive and ancient papers with which I had something to do is dangerous at this time because I think mathematical programming still has a future.

VENKAYYA: Since Professors Fox and Schmit presented the tower design in 1965, five or six other solutions appeared for the same problem. The methods used in obtaining these solutions include all the old and modern methods Professor Schmit alluded to. For example, Dr. Tocher at Boeing has obtained a solution using the method of feasible directions which Professor Schmit considers as being modern. Mr. Echleman at Douglas solved the same problem in 1969. He appeared to have used an approximate procedure based on optimality criteria. Dr. Gellatly at Bell Aerosystems used three methods to solve the same problem: First he obtained a solution using steepest descent and side step method in 1965. Then he obtained a solution by unconstrained minimization with a penalty function.

Most recently he obtained an extremely efficient solution by optimality criteria approach. This problem has six loading conditions. By taking advantage of symmetry one can consider it as having two loading conditions and treat it as a smaller eight variable problem. However, we treated it as a problem with twenty-five independent variables. The design reported by Professors Fox and Schmit weighs 570 pounds and required 360 seconds on Univac 1107. We obtained a design weighing 553 pounds and it was on IBM 7094. Dr. Tocher reported a design weighing 552 pounds and it was obtained in 30 seconds of CPU time on CDC 6600.

I would like to make a second comment. Professor Schmit mentioned approximate analysis and approximate design. If I had a choice I would keep the exact analysis because using an approximate analysis one can get a completely irrelevant optimum. Here, in every cycle, we are examining the behavior of the structure exactly. But if a structure is optimized by using approximate analysis, there is no evidence to show that that structure actually conforms to the constraints imposed. Mathematical programming should be used when there is no other alternative; otherwise, I think the optimality criteria is far superior in obtaining solutions economically. One can handle very large numbers of variables without any linking and do it with reasonable computer time. This is very difficult to do in the case of mathematical programming except in specific problems where one can use a linking procedure or something similar to reduce the number of variables.

COMMENT: I'd like to identify one thing that I think is important that you didn't bring out strongly enough in your paper. That was that a device used in this optimization procedure is to perform analysis by scaling.

We know when a structure is changed in size--the whole structure is scaled so that the generalized forces don't change a bit and that can accelerate the analysis process very greatly. This procedure is not incorporated in non-linear programming techniques. The second point I'd like to make is that the number of cycles that you have to do in an optimization process is very critical in problems for which members disappear on your criteria for cutoff, and I'd like to ask you what your cutoff criterion was?

VENKAYYA: Thus far, we have solved problems including a three bar truss to trusses having 300 variables and beams having about 60 variables and 168 degrees of freedom. In a well behaved structure we normally end up with anywhere from 6 to 15 cycles regardless of the number of variables. The worst case is the single loading case where a tremendous amount of readjustment of the structure takes place. Such cases take a larger number of cycles where this readjustment is not limited by the conflicting loads as it is in the single loading case and we generally get a design in about 6 to 12 cycles. It doesn't seem to depend on the number of variables. There are pathological cases where the number of cycles is higher. For example, a four bar truss with displacement limits required 35 cycles.

MCINTOSH: In summary, I want to say that progress in the field is extremely rapid and that what was a good method yesterday may not be a good method tomorrow. We have to be very careful about making too broad projections in the particular method that you have used and the particular problem you have solved. I think many people are finding that you are going to need a number of different techniques in your arsenal and furthermore that each one of these techniques may have to be tailored very care-

fully to the specific problem at hand to produce really efficient optimum computation for that particular problem.

INTEGRATION OPERATORS FOR
TRANSIENT STRUCTURAL RESPONSE

by

R. S. Dunham

Captain, United States Army
Redstone Arsenal, Alabama;

R. E. Nickell
Bell Telephone Laboratories, Inc.
Whippany, New Jersey;

and

D. C. Stickler
Bell Telephone Laboratories, Inc.
Whippany, New Jersey

I. Introduction

The structural analyst can choose among a number of alternatives when making transient response calculations. If the dynamical system is linear and has small dimension, a proper choice might be to find the undamped natural frequencies and mode shapes; then, to compute the forced response for each mode by way of the Duhamel integral, or any equivalent method, and use superposition to obtain the total response. This approach would be especially attractive if low frequency bands of excitation, which such a truncated system might represent adequately, dominate the applied loading. Even for

systems of large dimension, condensation or component modal reduction schemes can reduce the problem to manageable size, without significant loss in accuracy, provided the applied loading has this low frequency domination.

When high frequency excitation is significant, however, the analyst might choose to solve the coupled equations of motion of the system by direct integration, regardless of the number of degrees of freedom. Such a decision is dependent upon many factors - chiefly, the relative cost of direct integration and mode superposition, and the numerical characteristics of the integration operators to be used to implement either procedure. It should be kept in mind that there is no truncation advantage in using one procedure over the other; the number of degrees of freedom is the same, and, therefore, the cut-off frequency is the same. For the sake of completeness, we note that truncation error is the difference between the exact solution of the governing partial differential equation for the continuous system and the exact solution of the governing equations for the discretized system. The cut-off frequency represents the highest frequency to which the discretized system is able to respond. Excitation at frequencies higher than the cut-off frequency is manifested by noise in the discretized system response.

As an example of such a decision-making process, consider the structural system of Figure 1. Suppose that the masses A and B represent complex electronic packages with far too many components for any practical, economic mathematical modeling exercise. Then, if the structure is excited by motion of the embedment region C or is acoustically driven by the gas D, the best that can be done is to model the inertia of the masses and to examine the load transmission characteristics of the primary structural members. If the integrity of the system requires that the electronics function continuously in these dynamic environments, qualification tests based on such analyses will be required. Interpretation of the results of the analyses and the development of the test program will be meaningless: (a) if the integration operator generates excessive noise in frequency bands of interest; (b) if the cut-off frequency of the mathematical model of the primary structure is below excitation frequency bands of interest; or (c) if the integration operator has excessive artificial damping (due to what could be called approximation viscosity) such that signal amplitudes are heavily attenuated and vibrational periods are distorted.

During the rest of the discussion emphasis will be placed on resolving these issues and putting the alternatives of action for the analyst on a more rational footing.

II. Integration Operators

For this discussion, the governing equations of the discretized system will be taken to be

$$[K]\{u(t)\} + [C]\{\dot{u}(t)\} + [M]\{\ddot{u}(t)\} = \{F(t)\}, \quad (\text{II.1})$$

where $[K]$, $[C]$ and $[M]$ are the stiffness, damping and mass matrices, respectively; $\{u(t)\}$, $\{\dot{u}(t)\}$ and $\{\ddot{u}(t)\}$ are the displacement, velocity and acceleration vectors, respectively; and $\{F(t)\}$ is the force vector. These equations can be derived in a number of ways, such as by a finite-difference or a finite element formulation, but the mass matrix will be assumed to be positive definite.

An integration operator will be defined as a transformation on the displacement, velocity and acceleration vectors at time t_n (and, possibly, at time t_{n-1} , t_{n-2} , ...) to the displacement, velocity and acceleration vectors at time t_{n+1} . If the mass, damping and stiffness matrices do not depend on the displacements, or their space and time derivatives, the transformation will be linear. An integration operator will, in general, depend on the time step size, $\Delta t = t_{n+1} - t_n$, the matrices $[K]$, $[C]$ and $[M]$, and the inverse of the mass matrix.

Approximate integration operators for (II.1) can be derived in many different ways. Generalization, therefore, is virtually impossible. Typically, however, approximate expressions for two of the three kinematic variables (e.g., the displacement and velocity vectors) at time t_{n+1} are derived and used, in conjunction with (II.1), to form a determinate system. This ensemble can be written in the form

$$\underline{K}_1 \underline{\bar{u}}(t_{n+1}) = \underline{F} + \underline{K}_0 \underline{\bar{u}}(t_n, t_{n-1}, \dots), \quad (\text{II.2})$$

where

$$\underline{\bar{u}}^T(t_{n+1}) = \langle \underline{u}(t_{n+1}) : \dot{\underline{u}}(t_{n+1}) : \ddot{\underline{u}}(t_{n+1}) \rangle, \quad (\text{II.3a})$$

$$\underline{\bar{u}}^T(t_n, t_{n-1}, \dots) = \langle \underline{u}(t_n) : \dot{\underline{u}}(t_n) : \ddot{\underline{u}}(t_n) : \dots \rangle, \quad (\text{II.3b})$$

and the superscript T indicates the transpose of a vector or matrix.

If the matrix \underline{K}_1 can be put in upper or lower triangular form, (II.2) is referred to as an explicit integration operator; otherwise, it is implicit. The amplification matrix of the approximate integration operator is seen to be

$$\underline{A} = \underline{K}_1^{-1} \underline{K}_0, \quad (\text{II.4})$$

where the superscript indicates the matrix inverse, assuming that the inverse exists. Then

$$\bar{u}(t_{n+1}) = G + A \bar{u}(t_n, t_{n-1}, \dots), \quad (\text{II.5})$$

where

$$G = K_1^{-1} F. \quad (\text{II.6})$$

As an example, consider the central difference approximation for the acceleration and velocity vectors. This operator is obtained by writing an expression for the velocity vector in forward difference form:

$$\dot{u}(t_n) = \frac{1}{\Delta t} u(t_{n+1}) - \frac{1}{\Delta t} u(t_n); \quad (\text{II.7})$$

an expression for the acceleration vector in backward difference form:

$$\ddot{u}(t_{n+1}) = \frac{1}{\Delta t} \dot{u}(t_{n+1}) - \frac{1}{\Delta t} \dot{u}(t_n); \quad (\text{II.8})$$

and using (II.1) at time t_{n+1} . It can easily be verified that the substitution of (II.7) into (II.8) will yield the conventional central difference operator. If the vectors

$$\bar{u}^T(t_{n+1}) = \langle u(t_{n+1}) : \ddot{u}(t_{n+1}) : \dot{u}(t_{n+1}) \rangle \quad (\text{II.9a})$$

and

$$\bar{u}^T(t_n) = \langle u(t_n) : \ddot{u}(t_n) : \dot{u}(t_n) \rangle, \quad (\text{II.9b})$$

then

$$K_1 = \begin{bmatrix} I & 0 & 0 \\ K & M & 0 \\ 0 & -\Delta t I & I \end{bmatrix} \quad (\text{II.10a})$$

and

$$K_0 = \begin{bmatrix} I & 0 & \Delta t I \\ 0 & 0 & 0 \\ 0 & 0 & I \end{bmatrix}, \quad (\text{II.10b})$$

where I and 0 are the identity matrix and the null matrix, respectively. Note that the damping matrix has been neglected and that the partitioned matrix K_1 would be in lower triangular

form if the mass matrix is diagonal. To find K^{-1} requires only that the mass matrix have an inverse; the amplification matrix is thus seen to be

$$A = \begin{bmatrix} I & 0 & \Delta t I \\ -D & 0 & -\Delta t D \\ -\Delta t D & 0 & I - (\Delta t)^2 D \end{bmatrix}, \quad (\text{II.11})$$

where

$$D = M^{-1} K. \quad (\text{II.12})$$

The spectrum of the amplification matrix can easily be shown to be identical to that deduced in Reference 1, where the central-difference operator was found to be conditionally stable; i.e., for a step size Δt larger than 4π times the shortest natural period of the structure, the method is unstable.

Several other approximate integration operators were examined in References 2 and 3 with regard to stability limitations and other characteristics, such as artificial attenuation and vibration periodicity error as a function of frequency, using the Lax-Richtmyer procedure described here⁴ or the von Neuman procedure⁵. The Houbolt backward difference operator⁶

is implicit and has been found to be unconditionally stable.² Qualitative discussions of the attenuation characteristics have been given in References 7, 8 and 9. The Newmark generalized acceleration operator¹⁰ has been extensively studied³ and has been found to be unconditionally stable for values of the parameters $\gamma = 1/2$ and $\beta \geq 1/4$. For these values the operator is implicit; a recent study indicates an explicit unconditionally stable form ($\beta = \gamma = 0$) which uses compensatory damping.¹¹ The Wilson averaging operator,¹² apparently derived independently in Reference 13 and cited in Reference 14, is also implicit and was found to be unconditionally stable.³ This operator and a similar method called the Gurtin averaging operator¹⁵, have been found to exhibit substantial artificial damping and vibrational period error for higher modes of excitation.³ The Gurtin averaging operator is also implicit and unconditionally stable.

III. A Precise Integration Operator

For linear problems, a significant improvement in the accuracy of integration operators has been noted.¹⁶ In an analogous manner, an integration operator has been derived which is numerically precise in three important ways: (a) there is no artificial attenuation for any excited frequency up to, and including, the cut-off frequency; (b) there is no

artificial growth in the vibrational periods of these frequencies; and (c) the operator is unconditionally stable. This combination of properties insures that numerical errors are propagated harmonically with a mean value of zero. The operator is derived by first solving the free vibration eigenvalue problem for equation (II.1). The undamped equations of motion are

$$[K]\{u(t)\} + [M]\{\ddot{u}(t)\} = \{F(t)\}, \quad (\text{III.1})$$

where, in general, $[K]$ and $[M]$ are large $(\rho \times \rho)$, banded, symmetric matrices; $[M]$ need not be diagonal. Let $\{\omega^2\}$ be the vector of natural, undamped frequencies of the homogeneous system and $[Z]$ the corresponding mode shape matrix; $\{\omega^2\}$ is of dimension $1 \times q$, where $1 \leq q \leq \rho$, and $[Z]$ is of dimension $q \times \rho$.

Then, define

$$\{u(t)\} = [Z]\{v(t)\}, \quad (\text{III.2})$$

so that

$$[K^*]\{v(t)\} + [M^*]\{\ddot{v}(t)\} = \{F^*(t)\}, \quad (\text{III.3})$$

where

$$[K^*] = [Z]^T[K][Z], \quad [M^*] = [Z]^T[M][Z],$$

and

(III.4)

$$\{F^*(t)\} = [Z]^T\{F(t)\}$$

are the generalized stiffnesses, masses, and forces of the system. Therefore, the multiple-degree-of-freedom problem (second-order, coupled, ordinary differential equations) is reduced to q second-order, uncoupled ordinary differential equations, each of which has the form

$$\omega_i^2 v_i(t) + \ddot{v}_i(t) = f_i(t), \quad i = 1, 2, \dots, q. \quad (\text{III.5})$$

These simple equations can be solved by a variety of methods, either by the formal integral representation of Duhamel or by an approximate integration operator. Many of these operators can be represented by the recursion formula

$$\begin{Bmatrix} v_i(t_{n+1}) \\ \dot{v}_i(t_{n+1}) \\ \ddot{v}_i(t_{n+1}) \end{Bmatrix} = [A] \begin{Bmatrix} v_i(t_n) \\ \dot{v}_i(t_n) \\ \ddot{v}_i(t_n) \end{Bmatrix} + \{G\} f_i(t_{n+1}). \quad (\text{III.6})$$

The usual technique is to subdivide the time domain into segments over which the loading can be approximated by piecewise linear functions and then proceed with the marching recipe (III.6). With such approximation of the load, an amplification matrix $[A]$ which matches the desired response precisely should be derivable. Consider the parametric representation of the integration operator:

$$[A] = \begin{bmatrix} a_1 & a_2 & a_3 \\ a_4 & a_5 & a_6 \\ a_7 & a_8 & a_9 \end{bmatrix}; \{G\} = \begin{Bmatrix} g_1 \\ g_2 \\ g_3 \end{Bmatrix}. \quad (\text{III.7})$$

The first requirement for the integration operator is that harmonic motion must be matched; i.e.,

$$v_1(t) = \sin \omega_1 t$$

and

$$\dot{v}_1(t) = \cos \omega_1 t,$$

or

$$\begin{Bmatrix} v_1(0) \\ \dot{v}_1(0) \\ \ddot{v}_1(0) \end{Bmatrix} = \begin{Bmatrix} 0 \\ \omega_1 \\ 0 \end{Bmatrix}, \quad \begin{Bmatrix} v_1(\Delta t) \\ \dot{v}_1(\Delta t) \\ \ddot{v}_1(\Delta t) \end{Bmatrix} = \begin{Bmatrix} \sin(\omega_1 \Delta t) \\ \omega_1 \cos(\omega_1 \Delta t) \\ -\omega_1^2 \sin(\omega_1 \Delta t) \end{Bmatrix}, \quad (\text{III.8})$$

and

$$\begin{Bmatrix} v_1(0) \\ \dot{v}_1(0) \\ \ddot{v}_1(0) \end{Bmatrix} = \begin{Bmatrix} 1 \\ 0 \\ -\omega_1^2 \end{Bmatrix}, \quad \begin{Bmatrix} v_1(\Delta t) \\ \dot{v}_1(\Delta t) \\ \ddot{v}_1(\Delta t) \end{Bmatrix} = \begin{Bmatrix} \cos(\omega_1 \Delta t) \\ -\omega_1 \sin(\omega_1 \Delta t) \\ -\omega_1^2 \cos(\omega_1 \Delta t) \end{Bmatrix}.$$

This requires that

$$[A] = [A(\omega_1, \Delta t)] = \begin{bmatrix} a_1 & \frac{\sin(\omega_1 \Delta t)}{\omega_1} & \frac{a_1 - \cos(\omega_1 \Delta t)}{\omega_1^2} \\ a_4 \omega_1 & \cos(\omega_1 \Delta t) & \frac{a_4 + \sin(\omega_1 \Delta t)}{\omega_1} \\ -a_1 \omega_1^2 & -\omega_1 \sin(\omega_1 \Delta t) & -a_1 + \cos(\omega_1 \Delta t) \end{bmatrix}. \quad (\text{III.9})$$

The second requirement is that the solution of (III.5) to a linearized forcing function with homogeneous initial conditions be satisfied identically; i.e.,

$$\omega_i^2 v_i(t) + \ddot{v}_i(t) = 1 + t, \quad (\text{III.10})$$

which implies that

$$v_i(t) = \frac{1}{\omega_i^2} \left[(1+t) - \cos(\omega_i t) - \frac{1}{\omega_i} \sin(\omega_i t) \right], \quad (\text{III.11})$$

or

$$\begin{pmatrix} v_i(0) \\ \dot{v}_i(0) \\ \ddot{v}_i(0) \end{pmatrix} = \begin{pmatrix} 0 \\ 0 \\ 0 \end{pmatrix}; \quad \begin{pmatrix} v_i(\Delta t) \\ \dot{v}_i(\Delta t) \\ \ddot{v}_i(\Delta t) \end{pmatrix} = \begin{pmatrix} \frac{1}{\omega_i^2} \left[(1+\Delta t) - \cos(\omega_i \Delta t) - \frac{1}{\omega_i} \sin(\omega_i \Delta t) \right] \\ \frac{1}{\omega_i^2} \left[1 + \omega_i \sin(\omega_i \Delta t) - \cos(\omega_i \Delta t) \right] \\ \frac{1}{\omega_i} \left[\omega_i \cos(\omega_i \Delta t) + \sin(\omega_i \Delta t) \right] \end{pmatrix} \quad (\text{III.12})$$

This requires that

$$[A(\omega_i, \Delta t)] = \begin{bmatrix} \frac{\sin(\omega_i \Delta t)}{\omega_i \Delta t} & \frac{\sin(\omega_i \Delta t)}{\omega_i} & \frac{1}{\omega_i^2} \left[\frac{\sin(\omega_i \Delta t)}{\omega_i \Delta t} - \cos(\omega_i \Delta t) \right] \\ \frac{\cos(\omega_i \Delta t) - 1}{\Delta t} & \cos(\omega_i \Delta t) & \frac{1}{\omega_i} \left[\sin(\omega_i \Delta t) + \frac{\cos(\omega_i \Delta t) - 1}{\omega_i \Delta t} \right] \\ -\frac{\omega_i \sin(\omega_i \Delta t)}{\Delta t} & -\omega_i \sin(\omega_i \Delta t) & \cos(\omega_i \Delta t) - \frac{\sin(\omega_i \Delta t)}{\omega_i \Delta t} \end{bmatrix}$$

and

$$\{G(\omega_1, \Delta t)\} = \begin{pmatrix} \frac{1}{\omega_1^2} \left[1 - \frac{\sin(\omega_1 \Delta t)}{\omega_1 \Delta t} \right] \\ \frac{1}{\omega_1^2 \Delta t} \left[1 - \cos(\omega_1 \Delta t) \right] \\ \frac{\sin(\omega_1 \Delta t)}{\omega_1 \Delta t} \end{pmatrix}. \quad (\text{III.13})$$

The spectral characteristics of the precise amplification matrix are found to be

$$\lambda_{1,2} = \cos(\omega_1 \Delta t) \pm j \sin(\omega_1 \Delta t) = e^{\pm j \omega_1 \Delta t}$$

and

$$\lambda_3 = 0.$$

(III.14)

where $j = \sqrt{-1}$. The operator is therefore seen to be unconditionally stable with no artificial damping or error in vibrational period.

As a consequence of the foregoing, the amplification matrix depends on the natural frequency ω_1 and a linearized modal participation forcing function $f_1(t)$. However, since the amplification matrix was deduced directly, the K_0 and K_1 matrices are undefined; therefore, the precise marching algorithm is suitable for modally uncoupled systems only.

Through equations (III.13), the time marching algorithm is carried out precisely. In fact, during the verification process, the procedure was found to be more accurate than an evaluation of the trigonometric functions with large argument (see the discussion by Bellman [17]). The precise amplification matrix can also be derived directly from the Duhamel integral; however, the marching algorithm should be considered as a computationally advantageous representation of the formal solution.

IV. Numerical Results

An example problem was chosen in order to illustrate the arguments presented here. The requisite features of the problem were: (a) simplicity; (b) the ease with which the exact solution could be found; and (c) convenient representation as a multiple-degree-of-freedom system. A uniform free-free beam, suddenly loaded at midspan, meets all the criteria.

The exact solution for the displacement of the free-free beam was calculated by using a conventional eigenfunction expansion for the spatial displacement function. The differential equation, boundary conditions, and initial conditions are given by

$$\frac{\partial^4 w}{\partial x^4} + \lambda^4 \frac{\partial^2 w}{\partial t^2} = \frac{P}{EI} \delta(x) s(t), \quad -l < x < l, \quad (IV.1)$$

$$0 < t;$$

$$\frac{\partial^2 w}{\partial x^2} = \frac{\partial^3 w}{\partial x^3} = 0; \quad x = \pm l; \quad (IV.2)$$

and

$$w(x,0) = \frac{\partial w}{\partial t}(x,0) = 0; \quad (IV.3)$$

where $\lambda^4 = m/EI$, $w(x,t)$ is the displacement as a function of space x and time t , $\delta(x)$ is the Dirac delta function, $s(t)$ is the Heaviside step function, and l is the half-length of the beam.

Since the load is applied at the center ($x = 0$), only the even spatial eigenfunctions are needed; these are given by

$$w_n(x) = A_n \left[\cosh(\mu_n) \cos\left(\mu_n \frac{x}{l}\right) + \cos(\mu_n) \cosh\left(\mu_n \frac{x}{l}\right) \right], \quad (\text{IV.4})$$

where the

$$A_n = \left\{ l \left[\cosh^2(\mu_n) + \cos^2(\mu_n) \right] \right\}^{-1/2} \quad (\text{IV.5})$$

are chosen so that

$$\int_{-l}^l w_n^2(x) dx = 1, \quad n = 1, 2, \dots \quad (\text{IV.6})$$

The eigenvalues are given by the approximate expression

$$\mu_n = \beta_n + \varepsilon_n, \quad (\text{IV.7})$$

where

$$\beta_n = (n-1)\pi + \frac{3}{4}\pi \quad (\text{IV.8})$$

and

$$\epsilon_n = \frac{\sqrt{2 - \tanh^2(\beta_n)} - 1}{1 + \tanh(\beta_n)}, \quad (\text{IV.9})$$

which was derived from the characteristic equation

$$\tan(\mu_n) + \tanh(\mu_n) = 0 \quad (\text{IV.10})$$

by assuming ϵ_n to be small.

Computer calculations show that, for all n , Eq. (IV.7) yields accurate eigenvalues with the accuracy increasing with increasing n . Using the eigenfunctions (IV.4), the displacement is found to be

$$w(x, t) = \frac{2P\ell^4}{EI} \sum_{n=1}^{\infty} \frac{w_n(0)w_n(x)}{\mu_n^4} \sin^2\left(\frac{1}{2} \mu_n^2 \tau\right), \quad (\text{IV.11})$$

where

$$\tau = \frac{t}{\lambda^2 \ell^2}. \quad (\text{IV.12})$$

A plot of (IV.11) as a function of the dimensionless time is shown in Figure 2. Nearly three cycles of the fundamental period are included, and response corresponding to

frequencies higher than the fundamental is clearly noticeable near the peaks and troughs of the plot.

For the comparison studies using approximate integration operators, the beam was modeled with six and twelve finite elements (fourteen and twenty-six degrees of freedom, respectively) in order to assess the truncation accuracy; in this way, primary concern could then be focused on the time integration and the spatial discretization could be assumed to be practically exact. Consistent mass matrices were used throughout to remove this point as a source of contention.* The characteristic frequencies and mode shapes for the symmetrically deformed beam were found by using successive Householder transformations on the consistent mass and reduced stiffness matrices. A comparison of the exact and approximate frequencies is given below:

<u>Mode</u>	<u>Exact</u>	<u>6-Elem. Approx.</u>	<u>12-Elem. Approx.</u>
1	31.29	31.30	31.29
3	913.6	924.1	914.4
5	5571.	5700.	5600.
7	19263.	24700.	19580.

* Since the beam stiffness is exact, the only approximation here is the spatial distribution of the inertial forces.

From this table it can be deduced that noticeable error in periodicity of response is not apparent for the first three harmonics. Some slight error might possibly be noticeable in second-overtone response for the coarser model.

In order to check this point, the Newmark Method, with $\beta = 0.25$ and $\Delta\tau = 0.05$, was exercised for both models and any difference in the two calculations is not discernible within plotting accuracy. Such agreement indicated that essentially all of the response is contained in the first three harmonics. The comparison between the Newmark results and the exact solution is shown in Figure 3. Areas of substantial agreement can be seen, primarily in the first harmonic response, but some behavioral differences can be seen in the higher order response. To examine these differences we recall some results from Reference 3 - namely, that the modulus of Newmark spectrum is unity (no attenuation for any mode of response) and that the incremental phase is given by

$$\theta_1 = \tan^{-1} \left[\frac{\omega_1 \Delta\tau}{1 - \frac{1}{4} (\Delta\tau)^2 \omega_1^2} \right], \quad (\text{IV.12})$$

where ω_1 is the "1th" structural frequency. We are concerned with making the comparison, at time $\tau_n = n\Delta\tau$, between $\sin(\omega_1 \tau_n)$, from equation (IV.11), and $\sin(n\theta_1)$. If we look at $\tau_{60} = 3.0$, then, for the first mode,

$$\theta_1 = 0.2787 \text{ radians}; 60 \theta_1 = 16.722 \text{ radians};$$

(IV.13)

$$\omega_1 = 5.60 \text{ rad/sec}; \tau_{60} \omega_1 = 16.80 \text{ radians}.$$

The error is seen to be less than 0.1 radians after nearly three periods of vibration for the first mode. For the second mode,

$$\theta_2 = 1.295 \text{ radians}; 60 \theta_2 = 77.7 \text{ radians};$$

(IV.14)

$$\omega_2 = 30.23 \text{ rad/sec}; \tau_{60} \omega_2 = 90.69 \text{ radians}.$$

The error here is substantial, nearly 4π radians, indicating that the response in mode two has been steadily going in and out of phase with the first mode, compared to the exact solution. This explains the anomalous behavior in the peaks and valleys of Figure 3.

Another comparison, this time between the Wilson averaging operator, with $\Delta\tau = 0.01$, and the exact solution, is shown in Figure 4. The smaller time step was required in order to get any meaningful response definition in the modes higher than the first. Substantial attenuation in modal amplitude is evident, but, since the characteristic equation for the Wilson operator has three non-trivial eigenvalues

that are functions of the time step and the structural frequencies, no attempt was made to correlate the results in Figure 4 with modal data.

The Gurtin averaging operator, with $\Delta\tau = 0.01$, is compared to the exact solution in Figure 5. Once again, the attenuation in the operator dominates the comparison. From Reference 3 we note that the modulus of the approximate modal response in the Gurtin operator is

$$R_1^2 = \frac{1 + \frac{1}{24} (\Delta\tau)^2 \omega_1^2}{1 + \frac{1}{12} (\Delta\tau)^2 \omega_1^2} \quad (\text{IV.15})$$

and that the phase increment is

$$\theta_1 = \tan^{-1} \left\{ \frac{\left[\frac{1}{4} (\Delta\tau)^2 \omega_1^2 - \frac{1}{2304} (\Delta\tau)^4 \omega_1^4 \right]^{1/2}}{1 - \frac{1}{16} (\Delta\tau)^2 \omega_1^2} \right\}. \quad (\text{IV.16})$$

Going through the calculations for mode one, we find that

$$(R_1)^{300} = 0.922, \quad (\text{IV.17})$$

which indicates the attenuation in the first mode response, while the error in phase is negligible. Clearly, the attenuation is a first order effect and the phase error a second order effect. For mode two,

$$(R_2)^{300} = 0.106 \quad (\text{IV.18})$$

and the error in phase is 0.66 radians ($\pm 38^\circ$ out-of-phase). For higher modes the response $n = 3.0$ has essentially vanished. These calculations confirm the increasing harmonic purity of the approximate response obtained via the Gurtin averaging operator.

The last comparison shows the results obtained with the precise marching algorithm and the exact solution in Figure 6. This comparison is demonstrable proof of the accuracy inherent in this operator.

V. Conclusions

As stated in the beginning, the object of this investigation is to provide guidance to the analyst concerned with specifying qualification tests for sensitive internal components of dynamically loaded structures. In order for an analyst to plan such tests in a meaningful way, using a combination of environmental sampling (if such sampling is feasible) and results from numerical simulation studies, the

digital filtering characteristics of the analytical tools must be understood.

The general behavior common to all finite-degree-of-freedom mathematical models that are consistently derived is: (a) the cut-off frequency - that frequency which represents the upper excitation limit of the structure; excitation at frequencies higher than this result in noisy response; and (b) a tendency for the accuracy of the response to deteriorate as the excitation frequencies tend toward the cut-off frequency. The fundamental cause of the deterioration is the monotonic increase of error in the calculation of mode shapes and frequencies (as a function of increasing frequency). Very little can be done by the analyst to improve on the general situation except to model the structure carefully in critical regions so as to widen the bandwidth of accurate frequency response.

Particular behavior of the integration operator used by the analyst to obtain the forced structural response is another matter. The major concerns are: (a) signal attenuation and (b) error in vibrational period as a function of (the approximate) structural frequency; (c) instability in the computational algorithm triggered by noise and round-off; and (d) the cost of using the algorithm. These factors form the necessary ingredients for a choice of an integration operator.

For the example used here, which is typical of the problems encountered in practice (though not nearly as complex), the clear choice would be the precise marching algorithm, especially if the analyst is concerned about broad-band excitation. When the system becomes too large for modal decoupling to be economical, or when nonlinear behavior is introduced, the choice would seem to be the Newmark operator with $\beta = 1/4$ and $\gamma = 1/2$. (Other possibilities might be to use the precise marching algorithm in conjunction with condensation or component mode synthesis techniques). When the structure to be analyzed clearly overdamps higher modes of excitation, such as the case when soil or fluid interacts with a structure, then the Wilson or Gurtin averaging operators are strong candidates. The Houbolt operator also fits into this category. Other special needs might require the analyst to use a combination of methods, such as the precise marching algorithm for the first few response cycles and the Wilson averaging operator for the long-time response.

There seems to be little question that explicit operators are more economical than implicit operators; there also seems to be strong evidence indicating the desirability of an unconditionally stable operator - such as the implicit methods described herein. Needless to say, the search for

the unconditionally stable explicit operator goes on. A better investment of effort might be to investigate iteration schemes based on implicit, unconditionally stable operators. At any given time t_{n+1} , the values of the dependent variables at the previous time t_n ought to be a good prediction for the beginning of the iteration cycle.

For nonlinear problems, the most promising approach has been described in Reference 18. The method, called "piecewise linearization," would use the values of the dependent variables at time t_n to describe the behavior of the structure during the interval (t_n, t_{n+1}) ; then a high-accuracy algorithm, such as the precise marching algorithm, based on modal decomposition would be used to find the solution at t_{n+1} . With these new values of the dependent variables, the behavior of the structure during the interval (t_{n+1}, t_{n+2}) would be describe, and the process repeated. The expense might be prohibitive, but the accuracy might justify the expense.

REFERENCES

1. Leech, J. W., Hsu, P. T., and Mack, E. W., "Stability of a Finite-Difference Method for Solving Matrix Equations," AIAA J. 3, pp. 2172-2173 (1965).
2. Johnson, D. E., "A Proof of the Stability of the Houbolt Method," AIAA J. 4, pp. 1450-1451 (1966).
3. Nickell, R. E., "On the Stability of Approximation Operators for Problems of Structural Dynamics," Technical Memorandum MM 69-4116-14, Bell Telephone Laboratories, Inc. (November 14, 1969).
4. Lax, P. D. and Richtmyer, R. D., "Survey of the Stability of Finite Difference Equations," Comm. on Pure and Appl. Math. 9, pp. 267-293 (1956).
5. O'Brien, G. G., Hyman, M. A., and Kaplan, S., "A Study of the Numerical Solution of Partial Differential Equations," J. Math. Phys. 29, pp. 223-251 (1951).
6. Houbolt, J. C., "A Recurrence Matrix Solution for the Dynamic Response of Elastic Aircraft," J. Aero. Sci. 17, pp. 540-550 (1950).
7. Levy, S. and Kroll, W. D., "Errors Introduced by Finite Space and Time Increments in Dynamic Response Computation," J. Res. NBS 51, 1, pp. 57-68 (July 1953).
8. Johnson, D. E. and Greif, R., "Dynamic Response of a Cylindrical Shell: Two Numerical Methods," AIAA J. 4, pp. 486-494 (1966).
9. Stricklin, J. A., et al., "Nonlinear Dynamic Analysis of Shells of Revolution By Matrix Displacement Method," "AIAA/ASME 11th Structures, Structural Dynamics, and Materials Conference, Denver, Colorado (April 22-24, 1970).
10. Newmark, N. M., "A Method of Computation for Structural Dynamics," Proc. ASCE 85, EM3, pp. 67-94 (1959).
11. Grant, J. and Gabrielson, V. K., "Newmark's Numerical Integration Technique with γ and β Equal to Zero," Sandia Laboratories Report SCL-DC-69-32 (June 1969).

12. Wilson, E. L., "A Computer Program for the Dynamic Stress Analysis of Underground Structures," Report No. 68-1, Univ. of Calif., Berkeley (1968).
13. Chaudhury, N. K., Brotton, D. M., and Merchant, W., "A Numerical Method for Dynamic Analysis of Structural Frameworks," Int. J. Mech. Sci. 8, pp. 149-162 (1966).
14. Wilson, E. N. and Herrmann, T. P., "Nonlinear Structural Vibrations by the Linear Acceleration Method," Report No. S-69-1, New York University (January 1969). NASA N69-30236.
15. Becker, E. B. and Nickell, R. E., "Stress Wave Propagation Using the Extended Ritz Method," AIAA/ASME 10th Structures, Structural Dynamics, and Materials Conference, New Orleans, Louisiana (April 14-16, 1969).
16. Bettis, D. G., "Numerical Integration of Products of Fourier and Ordinary Polynomials," Numer. Math. 14, pp. 421-434 (1970).
17. Bellman, R., "The Roles of the Mathematician in Applied Mathematics", Proc. 5th U.S. National Congress of Applied Mechanics, pp. 195-204, ASME, New York (1966).
18. Destefano, G. P., "Causes of Instabilities in Numerical Integration Techniques," Int. J. Comp. Math. 2, pp. 123-142 (1968).

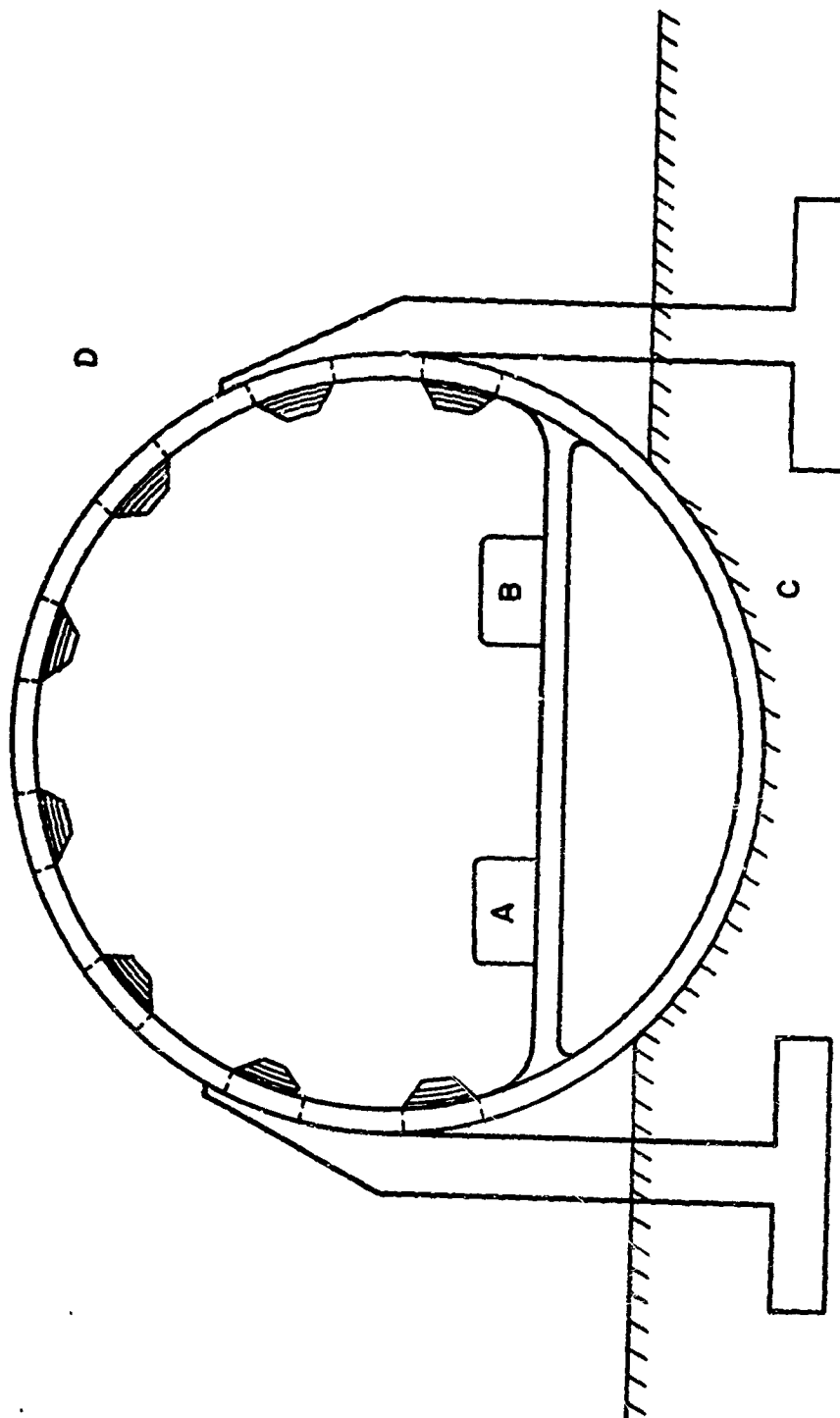


FIGURE 1. CROSS SECTION OF A TYPICAL STRUCTURE WITH SENSITIVE INTERNAL COMPONENTS

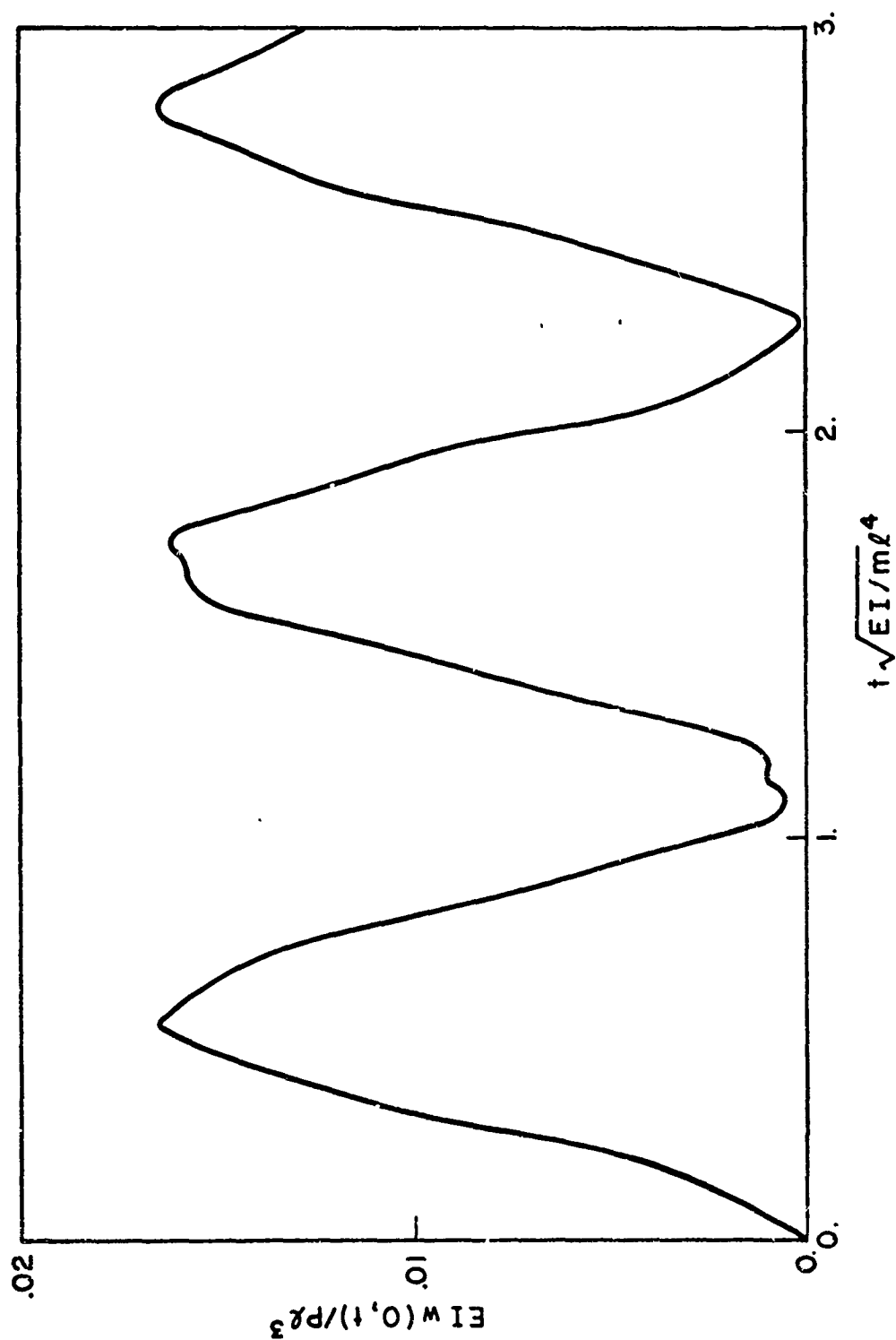


FIGURE 2. EXACT SOLUTION FOR THE MID-SPAN DEFLECTION OF A FREE-FREE BEAM UNDER STEP LOADING

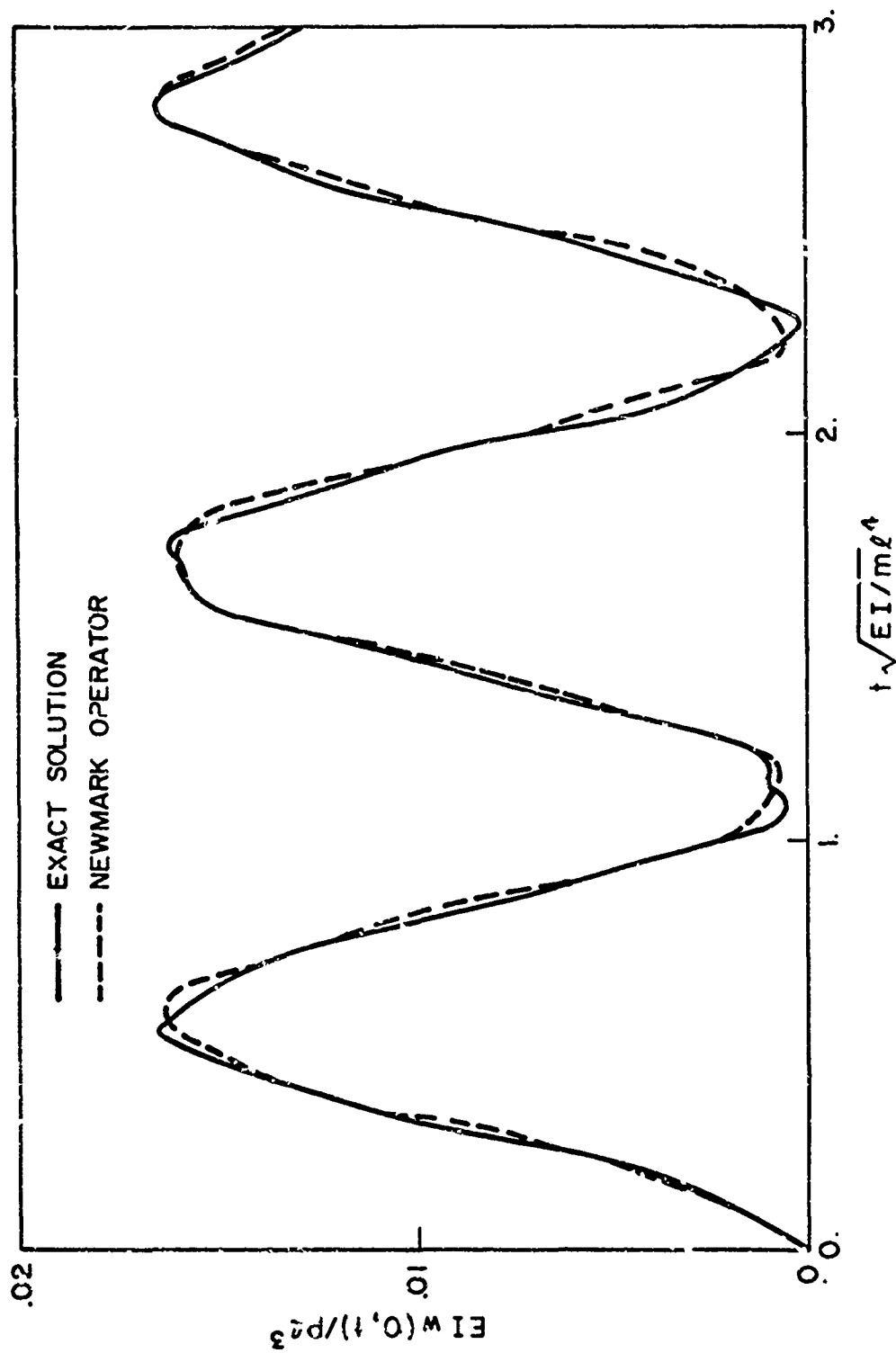


FIGURE 3. COMPARISON OF NEWMARK OPERATOR ($\beta=0.25, \gamma=0.5$)
WITH EXACT SOLUTION FOR $\Delta t=0.05$

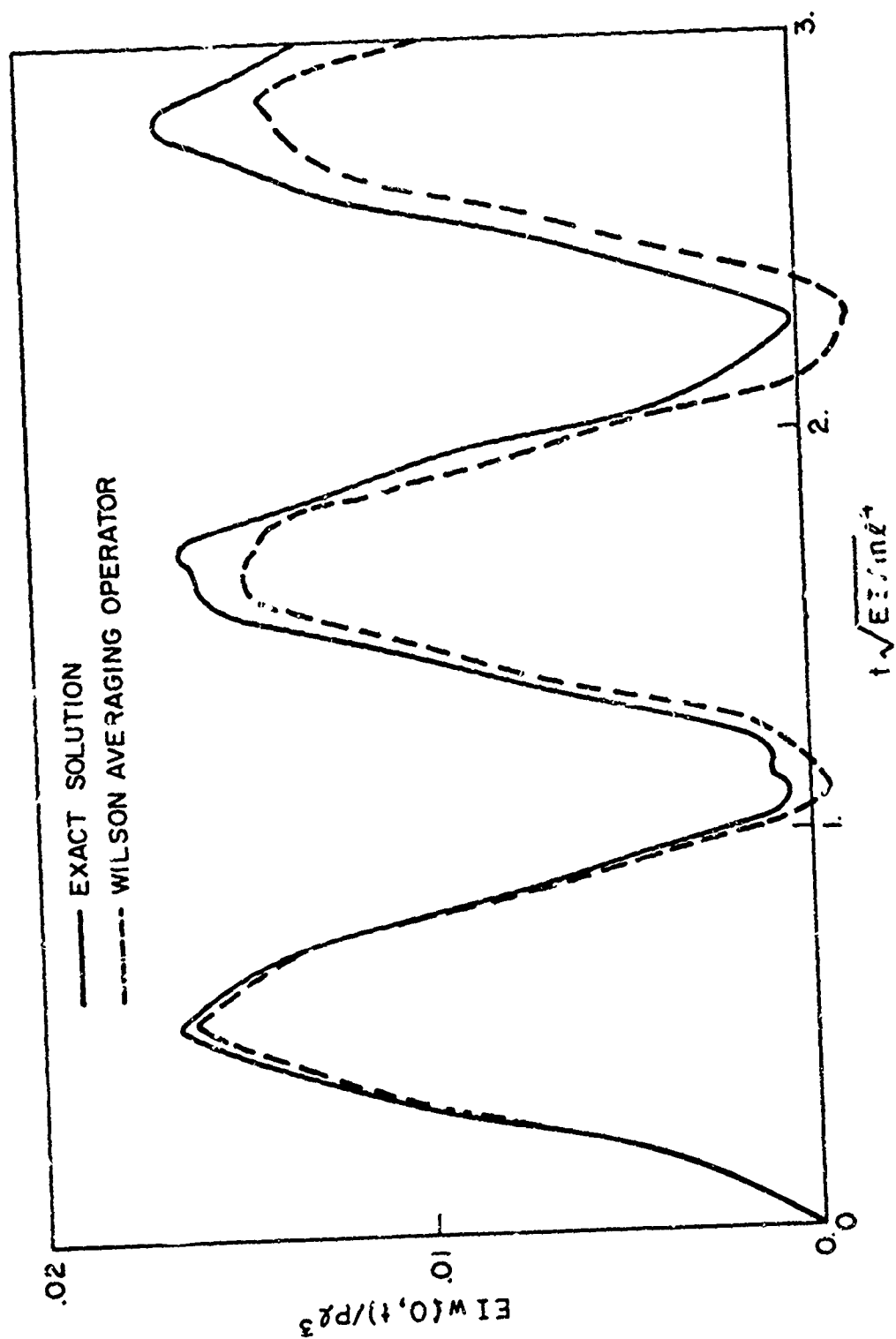


FIGURE 4. COMPARISON OF WILSON AVERAGING OPERATOR WITH EXACT SOLUTION FOR $\Delta t = 0.01$

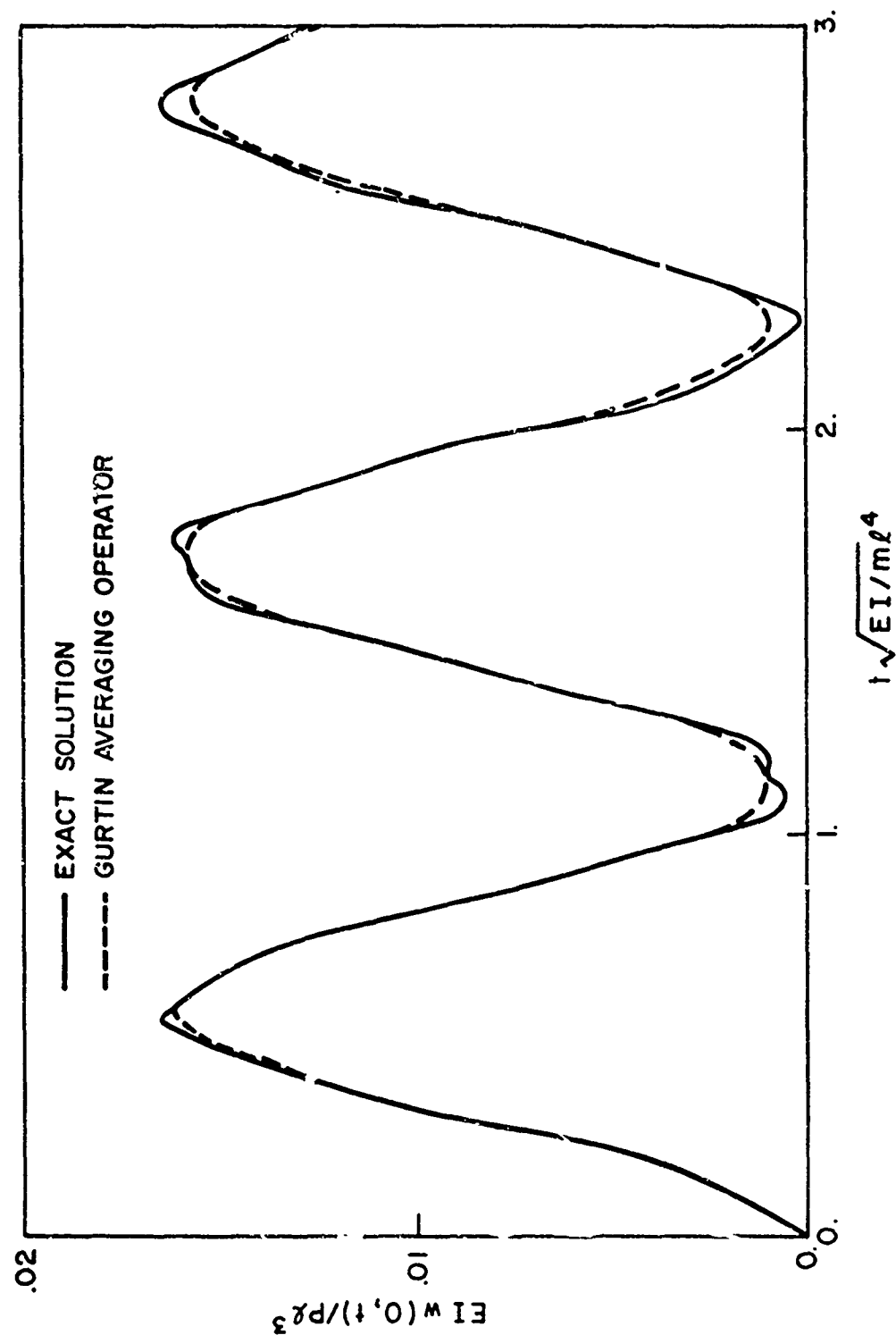


FIGURE 5. COMPARISON OF GURTIN AVERAGING OPERATOR WITH EXACT SOLUTION FOR $\Delta t = 0.01$

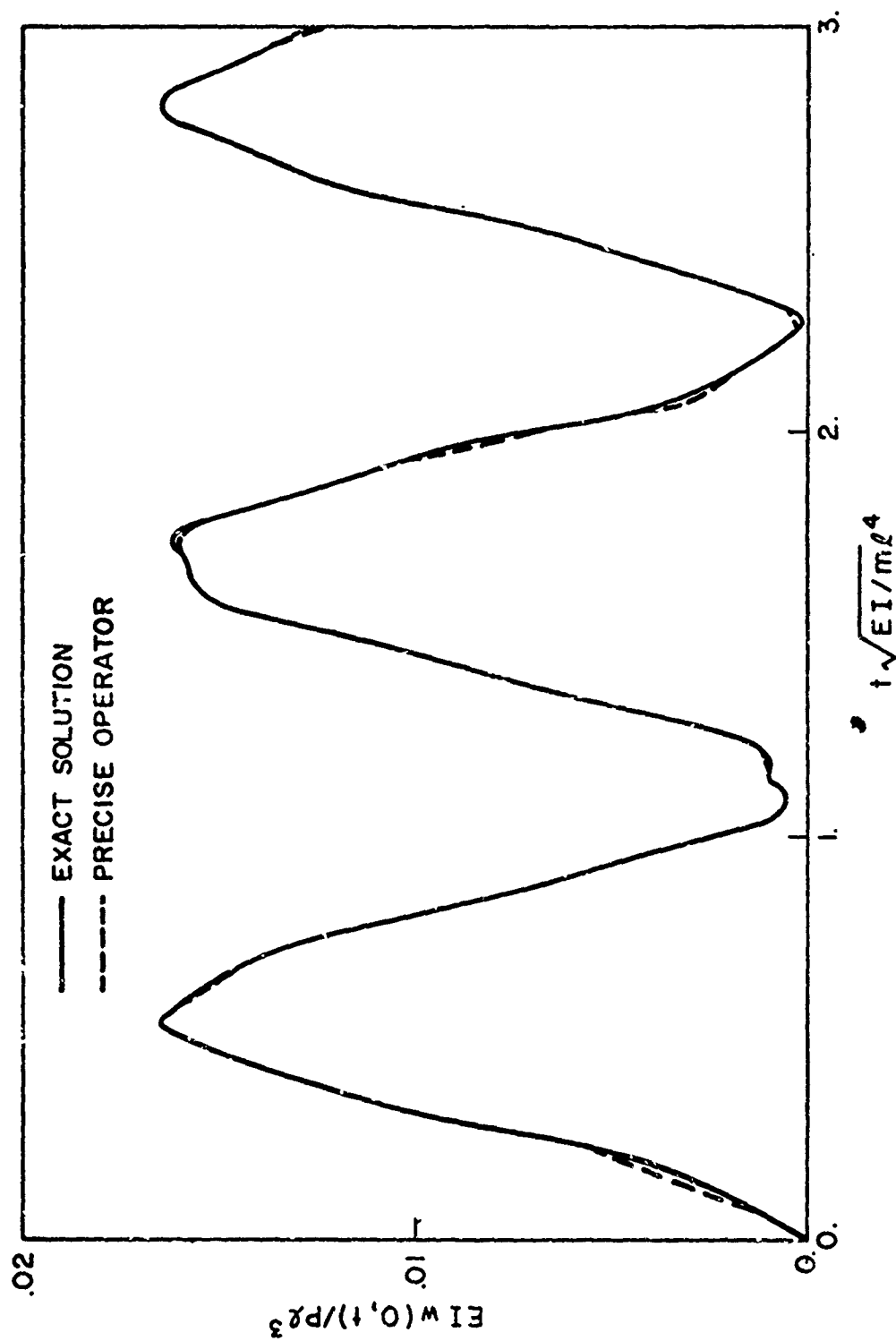


FIGURE 6. COMPARISON OF PRECISE INTEGRATION OPERATOR WITH EXACT SOLUTION FOR $\Delta t = 0.05$

QUESTIONS AND COMMENTS FOLLOWING NICKELL'S PAPER

QUESTION: You talked about exciting a structure with loads that contain high frequencies. In the example, you indicated that even though it was subjected to a point load or point velocity the response really is contained in the fundamental modes of the structure and then you did all your comparisons of all your integration operators based on these very fundamental modes. Now what's going to happen when you hit the structure with a signal or the response that does involve the higher modes?

NICKELL: The loading for the problem was a suddenly applied load, i. e., a step load at mid-span that excited all the structural frequencies up to the cutoff frequency. The fact that most of the response is contained in the first four modes may be significant; e. g., the conclusion might be that the first few modes always dominate the response unless there are wide differences in flexibility between parts of the structure.

COMMENT: Okay, but you could have, for example, struck the beam on the end and the response should have been a sharp wave front going down it.

NICKELL: (author misunderstood question and assumed that question referred to flexural waves excited by striking the beam transversely on the end) Bernoulli-Euler beam theory is being used here so that the governing equation is elliptic, rather than hyperbolic, in the transient response regime. Timoshenko beam theory would have to be used to get wave propagation effects.

QUESTION: Okay, would your results still hold if you did have a wave propagation problem?

NICKELL: My opinion would be that the results are still valid; i. e., one would still do a frequency scan and find out that all structural modes are being excited and that extreme deterioration of the higher frequency response would occur for integration operators other than the mode superposition approach.

COMMENT: We did an experiment using a beam ten inches long and one eighth inch thick loaded by sheet explosive over the central two inches and we got excellent correlation with results obtained using the one dimensional shell code, UNIVALVE. We made movies of it and the displacement as a function of time looked nice but the moment distribution as a function of position exhibited sharp fronts. We were using a central difference operator. There were sharp spikes that propagated to the boundary, bounced off and as I recall they made it back to the inside and interfered with each other and were eventually damped by dispersion effects and, of course, some plasticity. When we changed the mesh size, we got higher frequencies which, of course, traveled to the edge, bounced off and came back. I think those things were physically meaningful; we saw transient noise in our strain gages along the beam. I think the response was really there and if we had used an integration operator which had damping on it, I think we wouldn't have seen those things which I think are part of the physical problem.

NICKELL: I agree. If your operator had contained artificial damping, you would not likely have seen these effects at all.

QUESTION: You identified two types of error--one is truncation and one is roundoff. You said you eliminated truncation error by choosing two different meshes which produced the same results. Did you discuss the influence of roundoff error in your analysis? How do you avoid that?

NICKELL: The assumption made here is that the roundoff error present would have caused instability in a conditionally stable integration operator unless the step size had been chosen extremely small.

QUESTION: Does it have any significance? Did you try two different precision arithmetics, for example, to isolate and investigate the effect?

NICKELL: No. I think that such a comparison would be interesting but we did not do it.

COMMENT: Since my algorithm looked rather bad up there, I thought I'd better comment that it has been improved considerably and much of the damping has been reduced. The algorithm that Prof. Clough and I presented at this conference is a much better operator. I think, however, that when you have an arbitrary structure, one for which you really don't know much about the frequency content, you need an unconditionally stable integration scheme. Then you can actually plot up a damping ratio as a function of your time step and look at the components of your load, decide what you're interested in, then determine the time step you must choose in order to have an acceptable level of damping. So, from an engineering standpoint, I think you can very successfully use these algorithms which contain damping.

NICKELL: We concur on that point. When waves are being propagated in media, such as soils, where damping effects are large but not well understood, the Wilson Averaging Operator has some advantages.

COMMENT: The examples you have presented seems to indicate that by including damping you eliminate parts of the solution that you don't want or at least you don't believe are very important and you keep the lion's share of the things you do want. But sometimes what I really want to keep in the solution is the sharpness itself as in the case of a pulse problem in longitudinal waves.

NICKELL: I think that any of these methods that contain artificial damping are going to be undesirable when the primary interest is in shock strength and pulse shape. A great deal of care must be taken for these cases.

THE ROLE OF COMPONENT MODAL TECHNIQUES
IN DYNAMIC ANALYSIS OF ENGINEERING STRUCTURES

C. W. Coale*
W. A. Loden**
Lockheed Palo Alto Research Laboratory
Palo Alto, California

ABSTRACT

Following a brief description of the standard theory of the component modal analysis technique, some useful extensions to the standard theory are outlined. Several investigations that have been and are currently being carried out at Lockheed Missiles & Space Company using the REXBAT finite element program in combination with the COMPOS composite modes program are described. The paper concludes with comments on the method.

*Senior Staff Scientist

**Research Scientist

1. Introduction

The component modes method provides a systematic and orderly means of setting up generalized functions for analysis of a complex structure by means of a generalized Rayleigh-Ritz or energy approach. If only a few functions are used, the solution may be highly approximate. However, it is possible using functions carefully chosen from a complete set of functions for the problem at hand to obtain any desired degree of accuracy in the solution. In its essence the method can be considered a distillation process whereby the most essential information concerning behavior of the structure for the problem at hand is obtained and used in the analysis. The critical questions are those of rate of convergence to the desired accuracy of the solution and of the computer time required to obtain these solutions.

With ever larger computers and general purpose finite element programs available, the question arises: What advantages if any are to be gained by using component modes analysis instead of making direct calculation of modal behavior of the multicomponent structure with a finite element program?

Although the component modes method has been neither fully evaluated nor exploited, several potentially potent advantages exist. Basically, there are always benefits to reducing computer time for solution of a given problem. In the final estimate the useful engineering information obtained per dollar spent is, or should be, the controlling factor. The component modes method offers the possibility of greatly reduced computer run times through the reduction of coordinates. A possible secondary benefit of the method, which should not be minimized, is the potential for better physical insight into the dynamic behavior of the structure.

This paper outlines some extensions to the standard method of component modes and describes some investigations performed in this area. Some opinions of the authors are also expressed concerning the role of this method in engineering structural analysis.

2. Component Modes - Standard Theory

The original theory of component modes as expounded by Hurty and by Craig and Bampton (Refs. 1, 2, 3) may be summarized as follows: To determine the dynamic behavior (usually modal behavior) of a linearly-behaving structure

composed of two or more components (Fig. 1a) each component is first treated separately. The component is constrained at the connection boundaries, in addition to any constraints applicable to the structure as a whole (Fig. 1b). A representative set of normal modes of the component under these constraints is then determined. Additionally, a series of static solutions called constraint modes or boundary functions are calculated. These functions are created by freeing one degree of boundary constraint at a time and giving that degree of freedom a unit deflection with no other applied loads present. The result is a set of functions equal to the number of boundary degrees of freedom.

The combined set of normal modes and boundary functions constitute a set of generalized functions adequate for representing any arbitrary displacement configuration of the component with external loads applied at the connection boundary. As shown in Fig. 2, a transformation to generalized coordinates can be set up using these functions. The calculation of the reduced mass and stiffness matrices in generalized coordinates is facilitated by the orthogonality of the normal modes and by the lack of stiffness coupling between the boundary functions and normal modes.

The several components are then combined to form the complete structure by directly associating corresponding boundary functions in the different components. Fig. 3 shows the connection process (in generalized coordinates) which can be expressed in transformation form and involves a reduction of coordinates through application of the connection constraint equations. The resulting transformation for the displacements is displayed in Fig. 4, which illustrates the relation of the component displacements to the generalized coordinates of the connected structure. The functions ψ are the desired generalized functions for the entire structure. These functions are of two types:

- (1) a normal mode in one component with the remainder of the structure at rest,
- (2) a connection boundary displacement function consisting of displacements in the two components adjacent to that boundary with the other components at rest.

This set of generalized functions for the complete structure constitutes a subset of an ordered complete set of functions for describing arbitrary displacements of the structure.

A standard Rayleigh-Ritz analysis of the structure can now be made to determine its modal behavior. The eigenvalue problem is set up in terms of the generalized coordinates of the connected structure. Once the modes have been determined in terms of the generalized coordinates, the modal displacement vectors can be obtained by linear combination of the generalized functions. For details of the method the reader is referred to the paper by Craig and Bampton (Ref. 3).

3. Component Modes - Modifications to the Theory

The standard theory allows use only of component modes with the connection boundary constrained and with the same other constraints on the component as it experiences as a part of the complete structure. Furthermore, the orthogonality of the modes is assumed and utilized in forming the reduced mass and stiffness matrices in terms of generalized coordinates. Both of these requirements can be relieved.

If the orthogonality of the component internal functions is not assumed, the calculation of the entire reduced stiffness and mass matrices must be made with the formulas of Fig. 2 (which may be somewhat more costly for large problems). It then becomes possible to use generalized functions other than modes to describe behavior of the component.

It is still desirable, however, to retain the ordered character and the completeness characteristics provided by a set of normal modes.

With orthogonality of the component internal functions no longer assumed, the other requirement mentioned above can be bypassed in the following way. Consider any set of modes of the component under specified arbitrary constraints. By linear combination with suitable boundary functions these modes can be transformed to non-orthogonal generalized functions clamped at the connection boundary and satisfying any other component constraints (Fig. 5). The component modes method is then pursued as usual, excepting that orthogonality of the component internal functions is not assumed. These component generalized functions, because they are derived from a set

of modes of the component still retain an ordered and completeness characteristic.

Another extension of the component modes method which can be made is that of utilizing symmetries of the component which are not symmetries of the entire structure. (If a symmetry of the component were a symmetry of the complete structure then the standard method would be applicable to a half body model of the structure.) If a component symmetry is present then a half body model of the component can be analyzed, first with symmetric boundary conditions on the plane of symmetry and then with antisymmetric conditions. The resulting modes and boundary functions can then be used to form the same reduced mass and stiffness matrices in terms of generalized coordinates as would have been generated if the full component had been analyzed ignoring the plane of symmetry (Fig. 6).

These extensions while not major in nature greatly expand the applicability and usefulness of the component modes method.

4. Computer Programs

For initial implementation of the component modes method, the COMPOS program (Ref. 4) has been developed at Lockheed's Palo Alto Research Laboratory. This program is designed to join two components to form a larger structure. The connection can involve any degree of redundancy. COMPOS incorporates the features of the standard component modes method as well as the extensions described in this paper, namely, half body component capability and the ability to utilize non-orthogonal internal functions. The program is designed to operate both accurately and efficiently on the Univac 1108 system currently operational at Lockheed Missiles & Space Company. The program can handle components having any number of degrees of freedom, but for most efficient operation the component mass, stiffness, and two copies of the modal data should fit on drum storage or other suitable peripheral storage devices which permit random access to this information. The sum of the number of connection degrees of freedom and of the component modes used cannot presently exceed 200. This limitation is imposed by the eigenvalue solver used with the program. The solver must be able to handle full mass and stiffness matrices.

Although the COMPOS program is designed to be general in form so as to accept data from any source (finite element, finite difference, analytical, experimental) it has been used in practice only with the REXBAT finite element program (Ref. 5). The REXBAT program uses a finite element approach based on the direct displacement (stiffness) method of matrix structural analysis for linear static and dynamic analyses of complex general structural configurations and has been tailored to handle the class of structures most often encountered in the aerospace industry -- i.e., aircraft, booster vehicles, spacecraft, etc. REXBAT has a large library of useful discrete elements and currently treats structural systems having up to 6000 simultaneous equations with virtually unlimited bandwidth restrictions. (The program is limited to 3500 degrees of freedom for eigensolution analyses.)

As is probably typical the interfacing of these two programs required both some modifications to the REXBAT program and an intermediate processor program. Modifications to REXBAT consisted of providing for automatic generation of a series of static boundary functions. Without this feature the input data requirements for generation of boundary functions were at least tedious and for larger problems, stifling. The intermediate processor provides for sorting and selection of both boundary functions and modes, for forming linear combinations of these functions, and for storage of component information on tape for introduction to COMPOS.

5. Structural Studies

The REXBAT-COMPOS program set has been and is being used to analyze several configurations, both simple and complex. Discussions of some of these studies follow.

Rectangular Plate

In the paper published in 1968 (Ref. 3) Craig and Rampton applied the component modes method to a cantilevered rectangular plate (Fig. 7). To check out the REXBAT-COMPOS computer program combination and to evaluate its capabilities, several plate problems have been solved using this same configuration. The plate chosen is shown in Fig. 7a. It consists of a rectangular plate of aspect ratio 2 which is clamped along one of the

longer sides. A finite element model of the plate (identical with that of Ref. 3) was set up as shown in Fig. 7b. This model has 78 free nodal points and 234 degrees of freedom. At each nodal point transverse displacement and rotation about two orthogonal axes in the plane of the plate can occur. No inplane displacements are considered. Using REXBAT, the frequencies and mode shapes for the lowest ten modes were determined. Following the example of Ref. 3, the plate was then cut along an asymmetric line perpendicular to the clamped edge (Fig. 8a) thus dividing the plate into two unequal components (Fig. 8b). Using corresponding finite element models, REXBAT was applied to each component to find and store (1) fifteen normal modes with two edges clamped (the originally constrained edge plus the connection boundary), and (2) eighteen boundary functions obtained by releasing one boundary degree of freedom at a time and giving that degree of freedom a unit displacement.

The COMPOS program was then fed the stored information, proceeded to rejoin the two components to form the full plate, and find modal frequencies and displacements. The generalized degrees of freedom in this modal analysis consisted of 18 boundary function coordinates, 15 modal coordinates for component 1, and 15 modal coordinates for component 2. The frequency results of both the direct REXBAT and the REXBAT-COMPOS analyses are given below:

Modal Frequencies - Cantilevered Rectangular Plate

Mode Number	Direct Finite Element Analysis REXBAT 234 variables	Component Mode Analysis REXBAT-COMPOS 15 modes per component 48 variables
1	29.14 cps	29.14 cps
2	44.10	44.10
3	83.01	83.01
4	153.2	153.2
5	176.9	176.9
6	198.9	199.0
7	248.1	248.2
8	272.7	272.7
9	336.5	337.0
10	415.4	416.1

The mode shapes of the plate obtained by both methods were also compared and showed close agreement. The results are also in fairly close agreement with those obtained by Craig and Bampton. Differences can be traced primarily to the different plate element formulations used in the two studies.

A second solution of the plate problem was obtained by using the two components shown in Fig. 9a. Here component 2 is the same as previously, while component 1 is clamped on three edges. In this problem a set of normal modes and 36 boundary functions are determined for component 1. Eighteen of the boundary functions are employed in the connection to component 2. The remaining eighteen boundary functions are left as free functions together with the normal modes. Again extremely good agreement in both frequency and mode shape was obtained.

The third problem which was solved illustrates the half body feature of the COMPOS program. In this problem component 2 was again treated in the same manner. However only half of component 1 was analyzed by the REXBAT⁴ program (Fig. 9b). Normal modes and boundary functions were obtained for each of two boundary conditions on the plane of symmetry of the component. This half body data was fed to COMPOS. In COMPOS the required matrices for component 1 were generated from the half body data and joined to component 2 to form the full plate. The results were identical with those of the previous case where the full component 1 with three edges clamped was utilized.

Space Shuttle

As part of space shuttle preliminary design work performed this year at IMSC, three-dimensional models of several space shuttle vehicles were developed. Figure 10 shows one of these models - a half body model of a symmetric delta-wing orbiter vehicle. A number of free body modes such as the one shown in this figure were obtained. For development and demonstration of the ability to join two vehicles to form a combined vehicle, a model was needed. In the absence of a three-dimensional model of the booster, a double orbiter model was used, as shown in Figure 11. This model has no significance except for demonstration and evaluation purposes. A statically determinate connection was used which preserves the symmetry present

in each of the two vehicles (Fig. 12). Using the REXBAT-COMPOS programs, this structure was analyzed both directly with REXBAT and also with REXBAT-COMPOS. The results obtained in this case show the same close agreement obtained in the previous study.

Modal Frequencies - Double Orbiter - Symmetric Modes

Direct Finite Element Analysis REXBAT 1149 variables	Component Modes Analysis REXBAT-COMPOS 10 modes/component 23 variables
3.137 cps	3.141 cps
3.630	3.632
4.355	4.365
4.908	4.916
5.366	5.367
5.452	5.452

The mode shapes have been spot checked and appear to be closely similar (one of the mode shapes obtained is shown in Fig. 13). An even more significant check would be a comparison of internal forces (e.g., the connection forces), but this capability is not presently available in the COMPOS program.

Space Vehicle Shroud

In an investigation underway at the present time, an aerospace structure which must be designed to operate properly and without structural failure in a dynamic response environment, is being used to further demonstrate and evaluate the utilization of component modal techniques. The structure under consideration is a space vehicle shroud. This is a light shell structure which is fitted onto the forward end of a booster launch vehicle to encase and protect a space vehicle from air flow and aerodynamic heating during ascent through the atmosphere (Fig. 14a). After the vehicle leaves the atmosphere the shroud is split into two halves by a pyrotechnic separation joint, rotated on hinges and thruster springs away from the space vehicle, and discarded (Fig. 14b).

As can be seen in Fig. 15 the shroud has a fairly regular structure consisting of orthotropic shell construction with equally spaced reinforcing rings. The construction becomes progressively lighter (through use of thinner shell gauges) in progressing from the base of the shroud toward the nose. The longitudinal separation joints including stiffening stringers are located 180° apart. These joints destroy the axisymmetry of the structure both because of the mass and stiffness of the stringers and because the separation joint is for all practical purposes a hinged joint. Thus we have two longitudinally hinged half shells rather than a single shell. At the base the shroud is clamped to the launch vehicle through a circumferential separation joint.

This shroud is of particular interest for several reasons. First, it is a specific engineering structure for which dynamic analysis is required. Second, it is regular enough in configuration and construction to allow rapid evaluation of solutions obtained. Finally, for analysis of shroud behavior both before and after separation, modal behavior of the shroud under several highly different boundary conditions is required.

Although the pre-separated shroud is not axisymmetric it retains two planes of symmetry - the separation plane and the plane at 90° to the separation plane. Thus either a half-body model or a quarter-body model can be used for analysis of shroud behavior.

Some of the configurations for which modal sets are required are shown in Fig. 16. It is of considerable advantage to analyze the pre-separated shroud as a separate structure with a constrained base, as shown in Fig. 16a. After verification of the model and evaluation of behavior of the shroud as a separate structure, it can be incorporated into the entire launch vehicle for modal analysis (Fig. 16b).

Ideally, upon separation the shroud halves separate cleanly and become independent structures (Fig. 16c). However because of aerodynamic heating, internal thermal stresses build up during ascent. This prestressing can cause the shroud to remain in contact at the tips for a short time after separation. For analysis of the separation, modes of the structure in this condition are needed.

There are various possible applications of component modes techniques in this problem:

(1) The most obvious application perhaps is the use of modes of the pre-separated shroud in modal analysis of the entire launch vehicle. If the joint between shroud and vehicle can be considered rigid the problem is simplified and engineering computer programs are available for this purpose. If, however, the joint is flexible a full component modes analysis is required.

(2) A common problem which arises in engineering structural dynamic analysis is the following. A model of the structure is formulated, checked out, and used to find a set of modes for use in forced response calculations. This modal analysis can require a significant amount of computer time. At this point the designers make some changes in the mass, stiffness, or configuration of the structure. Often the significance of the changes in structural dynamic behavior is uncertain so a new modal analysis is made. If the structural model has a large number of degrees of freedom and design changes occur frequently, the computer costs skyrocket. The use of component modes analysis in this situation is twofold. If the changes to the structure are not too widespread, the modes of the structure already available can be used in a rough component modal analysis to evaluate the influence of the changes on modal behavior of the structure. If the changes are significant, accurate new modes can be generated using the same analysis.

(3) Finally when several modal sets for the same structure under different constraints are required, as in Fig. 16, it is theoretically possible to calculate one set with a basic structural analysis program using a large degree of freedom model and then to determine all of the other modal sets by component modal analysis. The practicality of this concept is being evaluated in the present investigation.

The investigation has proceeded to the point where both half and quarter body models of the complete shroud have been set up, checked out, and rather thoroughly evaluated. These same models represent full and half body models of the independent post-separated shroud halves. Modes of the shroud under several of the boundary conditions of Fig. 16 have been obtained with the REXBAT program and are stored on tape. Plots of

two of the modes of the post separated shroud on hinges and springs are shown in Fig. 17. The various modes exhibit symmetric beam and ring behavior (or alternatively symmetric half-shell behavior) as well as antisymmetric torsion and sideways.

Work is being conducted at present using the REXBAT-COMPOS program to determine one set of shroud modes making use of another set (e.g., determining the modes of Fig. 16c using the modes of 16b). It is hoped that several results of this type will be available at an early date.

6. Comments on Component Modal Techniques

At the present state of evaluation of the method of component modes the following comments appear to be in order. Some of these statements will require further verification for full acceptance.

- (1) The component modes method has a definite role to play as a basic tool of the engineering analyst in the area of structural dynamics. It provides a flexibility in analysis not otherwise obtainable.
- (2) The method is best employed as a companion to a basic structural analysis program (such as a large-scale, finite element program). This program must be operational and accurate and the analyst must have knowledge of how to use it efficiently. The program must include a good eigenvalue solver and boundary function generator.
- (3) The component modes method requires considerable engineering judgment for skillful use. This is not particularly unique - so do all complex multipurpose methods and programs.
- (4) The method is not always better than direct analysis for a given problem to which both are applicable. The criteria for making a decision as to which path to follow are the engineering time required and the computer time required.
- (5) There is more to component modes than meets the eye. It has many uses that appear only with experience.

- (6) There is a basic need for a means of generating functional boundary functions to supplement the point boundary functions. At present, although the internal behavior of the component can be and is approximated to whatever degree of accuracy is desired, the point boundary functions cannot be truncated. Thus no approximation is possible. Functional boundary functions should be truncatable, ordered, and have the completeness feature of normal modes.
- (7) The key to accurate use of the component modes method in any application is consideration of the internal forces which occur in the component acting as part of the larger structure.

7. References

1. Hurty, W. C., "Dynamic Analysis of Structural Systems by Component Mode Synthesis," TR 32-530, January 1964, Jet Propulsion Laboratory, California.
2. Hurty, W. C., "Dynamic Analysis of Structural Systems Using Component Modes," AIAA Journal, Vol. 3, No. 4, April 1965.
3. Craig, R. R., and Bampton, M. C. C., "Coupling of Substructures for Dynamic Analysis," AIAA Journal, Vol. 6, No. 2, 1313-19, July 1968.
4. Jensen, P. S., "COMPOS - Program for Composite Structure Analysis," LMSC Internal Memorandum, January 1970.
5. Loden, W. A., "User's Manual for the REXBAT Program," LMSC Report 6-80-70-24, August 1970.

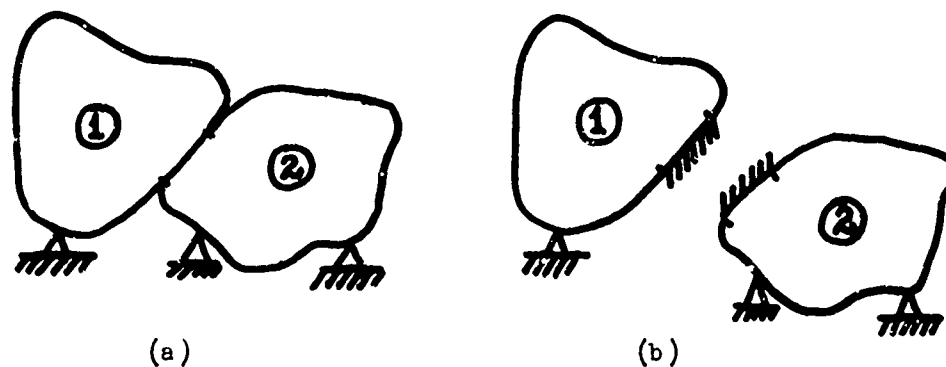


Fig. 1. Multicomponent Structure - Component Modes Analysis

$$\left\{ u^{(i)} \right\} \left[K^{(i)} \right] \left[M^{(i)} \right]$$

$$\left\{ u^{(i)} \right\} = \begin{pmatrix} I & 0 \\ \phi_{BI}^{(i)} & \phi_{NE}^{(i)} \end{pmatrix} \begin{Bmatrix} P_R^{(i)} \\ P_N^{(i)} \end{Bmatrix} = \begin{pmatrix} \phi^{(i)} \end{pmatrix} \left\{ P^{(i)} \right\}$$

$$\left\{ P^{(i)} \right\} \left[\begin{matrix} \vdots \\ \bar{K}^{(i)} \\ \vdots \end{matrix} \right] \left[\begin{matrix} \vdots \\ \bar{M}^{(i)} \\ \vdots \end{matrix} \right]$$

$$\bar{K}^{(i)} = \phi^{(i)T} K^{(i)} \phi^{(i)} \quad \bar{M}^{(i)} = \phi^{(i)T} M^{(i)} \phi^{(i)}$$

Fig. 2. Component Modes Analysis - Transformation to Generalized Coordinates

$$\begin{Bmatrix} b^{(1)} \\ p^{(2)} \end{Bmatrix} \quad \begin{bmatrix} \bar{K}^{(1)} & 0 \\ 0 & \bar{K}^{(2)} \end{bmatrix} \quad \begin{bmatrix} \bar{M}^{(1)} & 0 \\ 0 & \bar{M}^{(2)} \end{bmatrix}$$

$$\begin{Bmatrix} p^{(1)} \\ p^{(2)} \end{Bmatrix} = \begin{pmatrix} \beta \end{pmatrix} \begin{Bmatrix} q \end{Bmatrix}$$

$$\begin{Bmatrix} q \end{Bmatrix} \quad \begin{bmatrix} \bar{K} \\ \bar{M} \end{bmatrix}$$

Fig. 3. Component Connection - Transformation to Structure Generalized Coordinates

$$\begin{Bmatrix} u^{(1)} \\ u^{(2)} \end{Bmatrix} = \begin{bmatrix} \varphi^{(1)} & 0 \\ 0 & \varphi^{(2)} \end{bmatrix} \begin{Bmatrix} p^{(1)} \\ p^{(2)} \end{Bmatrix} = \begin{pmatrix} \varphi \beta \end{pmatrix} \begin{Bmatrix} q \end{Bmatrix}$$

Fig. 4. Final Transformation - Generalized Functions of Complete Structure

$$\begin{pmatrix} \mathbf{I} & \mathcal{P}_{NB} \\ \mathcal{P}_{BI} & \mathcal{P}_{NI} \end{pmatrix} \begin{pmatrix} -\mathcal{P}_{NB} \\ \mathbf{I} \end{pmatrix} = \begin{pmatrix} \mathbf{0} \\ \mathcal{P}_{GI} \end{pmatrix}$$

$$\mathcal{P}_{GI} = \mathcal{P}_{NI} - \mathcal{P}_{BI} \mathcal{P}_{NB}$$

$$\begin{Bmatrix} u \end{Bmatrix} = \begin{pmatrix} \mathbf{I} & \mathbf{0} \\ \mathcal{P}_{BI} & \mathcal{P}_{GI} \end{pmatrix} \begin{Bmatrix} p \end{Bmatrix}$$

Fig. 5. Transformation of Component Normal Modes to Non-Orthogonal Generalized Functions

$$\begin{array}{c} u_H \\ \left\{ \begin{array}{c} u \\ u_{PS} \\ u_{PA} \end{array} \right\} \end{array} \quad \begin{array}{c} K_H \\ \left[\begin{array}{c|cc} K_{11} & K_{12} & K_{13} \\ \hline K_{12}^T & K_{22} & 0 \\ K_{13}^T & 0 & K_{33} \end{array} \right] \end{array} \quad \begin{array}{c} M_H \\ \left[\begin{array}{c|cc} M_{11} & M_{12} & M_{13} \\ \hline M_{12}^T & M_{22} & 0 \\ M_{13}^T & 0 & M_{33} \end{array} \right] \end{array}$$

$$\begin{array}{c} u_H \\ \left\{ \begin{array}{c} u \\ u_{PS} \\ u_{PA} \end{array} \right\} \end{array} = \begin{array}{c} \varphi_H \\ \left[\begin{array}{c|cc} \varphi_S & \varphi_A \\ \hline \varphi_{PS} & 0 \\ 0 & \varphi_{PA} \end{array} \right] \end{array} \begin{array}{c} p \\ \left\{ \begin{array}{c} p_S \\ p_A \end{array} \right\} \end{array}$$

$$\begin{array}{c} p \\ \left\{ \begin{array}{c} p_S \\ p_A \end{array} \right\} \end{array} \quad \begin{array}{c} \bar{K} \\ \left[\begin{array}{c|cc} \bar{K}_{11} & \bar{K}_{12} & 0 \\ \hline \bar{K}_{12}^T & \bar{K}_{22} & 0 \end{array} \right] \end{array} \quad \begin{array}{c} \bar{M} \\ \left[\begin{array}{c|cc} \bar{M}_{11} & \bar{M}_{12} & 0 \\ \hline \bar{M}_{12}^T & \bar{M}_{22} & 0 \end{array} \right] \end{array}$$

$$\bar{K}^* = 2 \varphi_H^T K \varphi_H$$

$$\bar{M}^* = 2 \varphi_H^T M \varphi_H$$

Fig. 6. Component with Planar Symmetry - Half Body Analysis

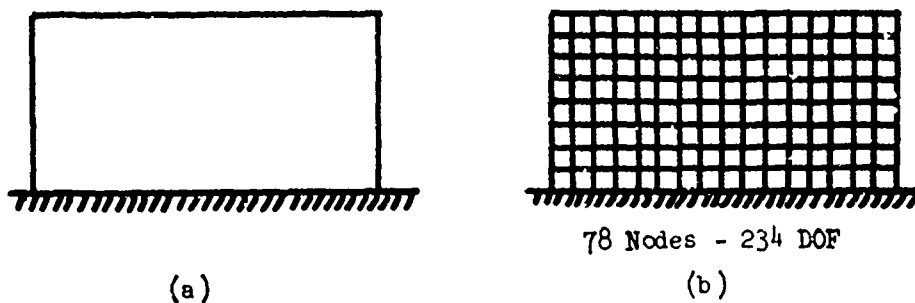


Fig. 7. Cantilevered Rectangular Plate

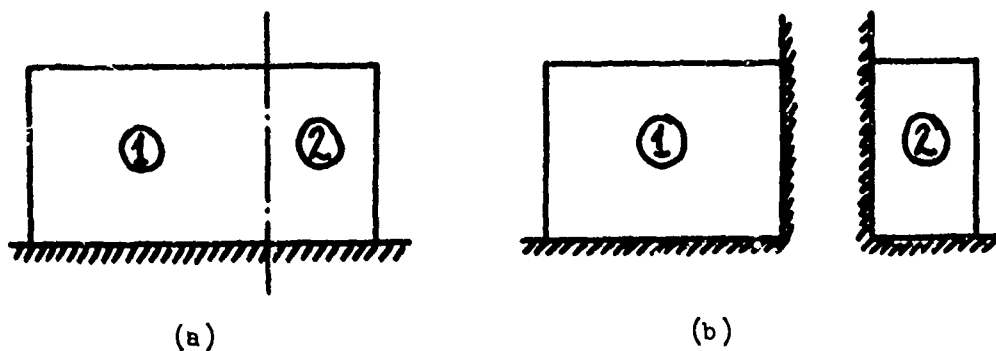


Fig. 8. Two Components - Cantilevered Rectangular Plate

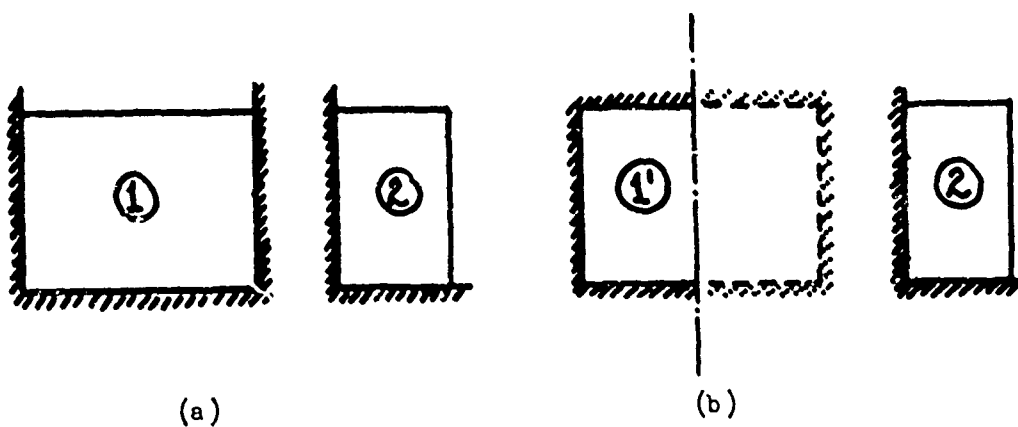


Fig. 9. Alternate Plate Components for Component Mode Analysis

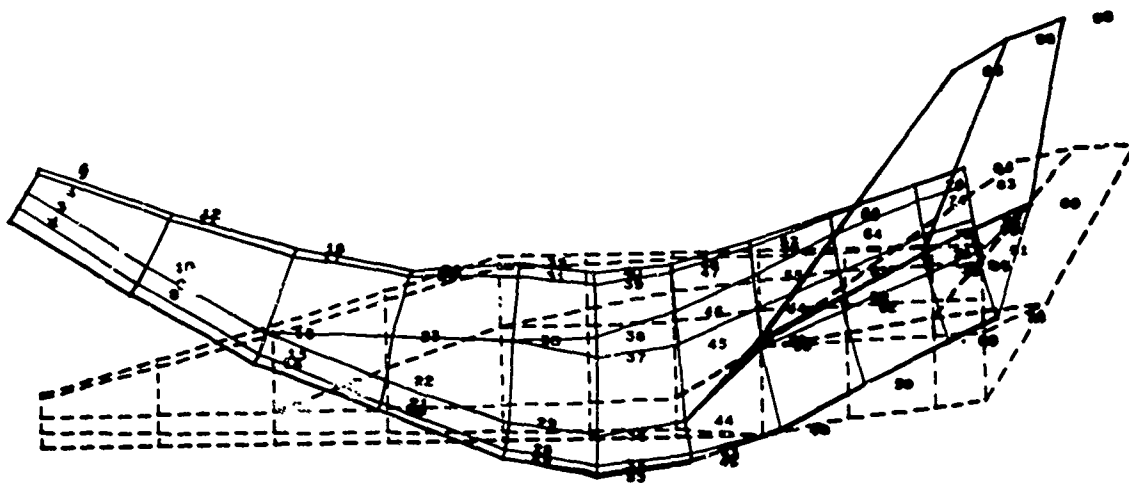
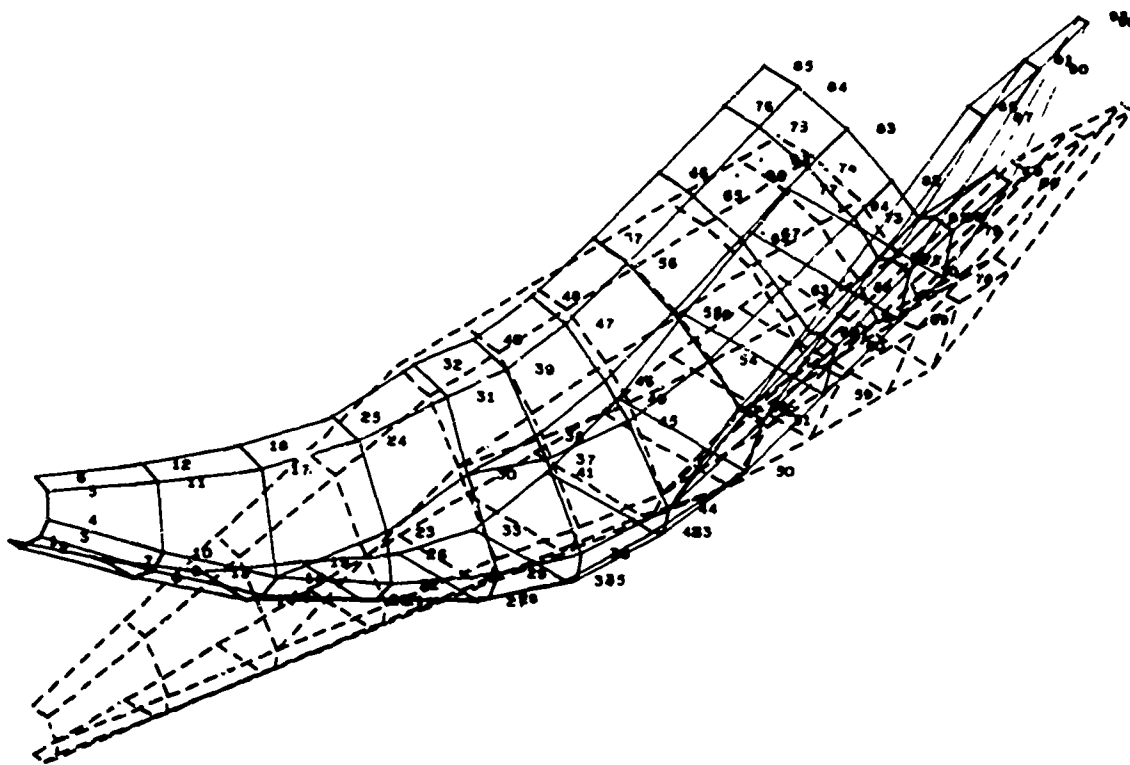


Fig. 10. Space Shuttle - Delta Orbiter Vehicle

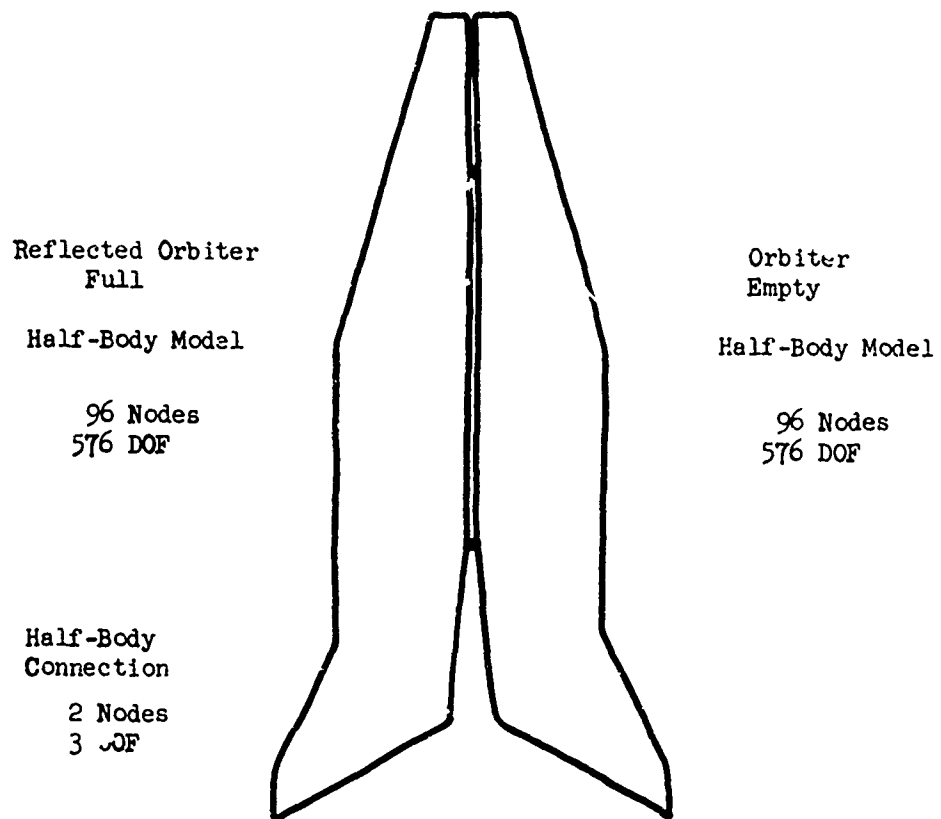


Fig. 11. Space Shuttle - Double Orbiter Configuration

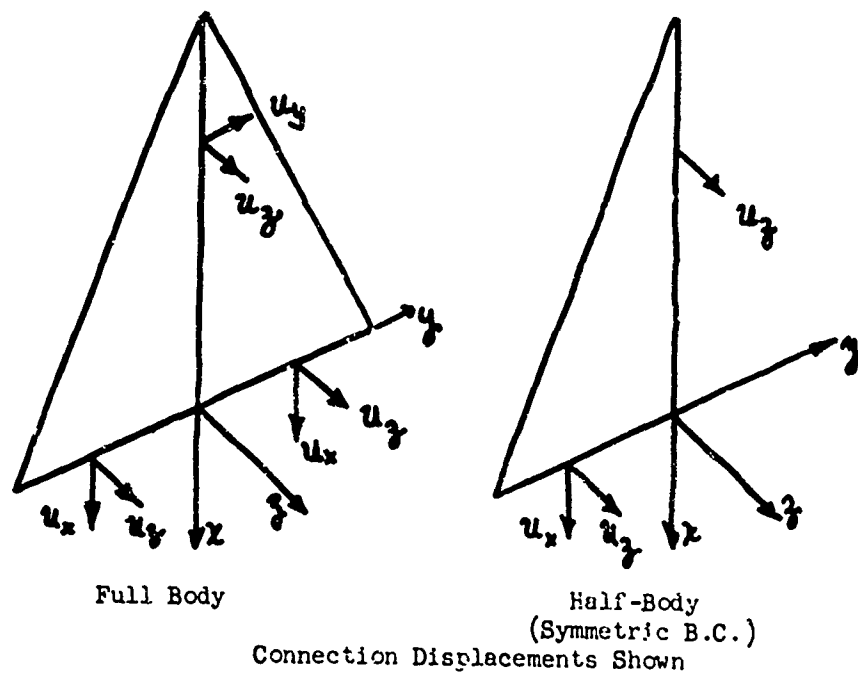


Fig. 12. Connection Conditions - Double Orbiter

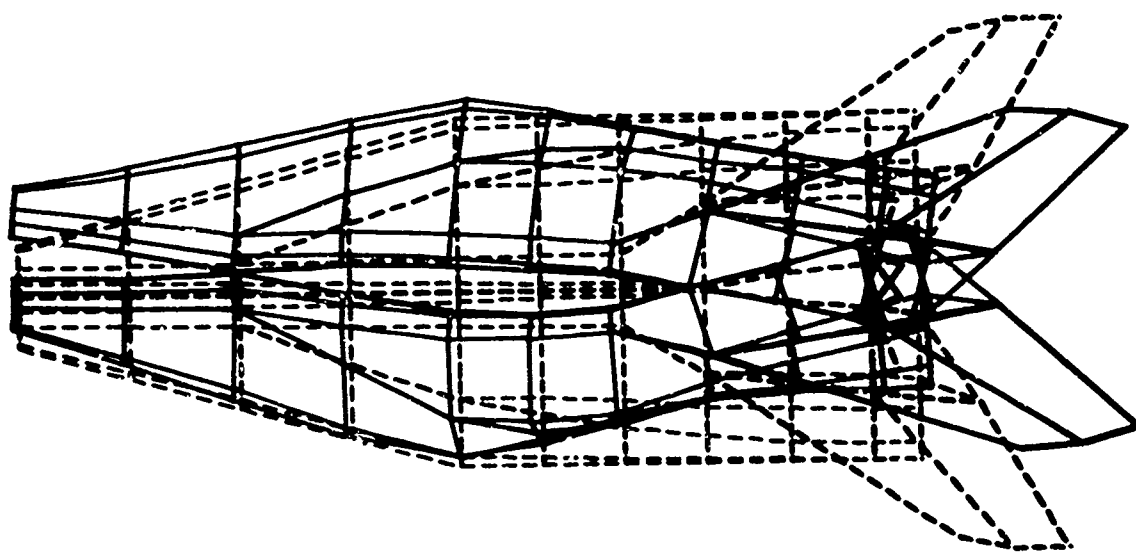
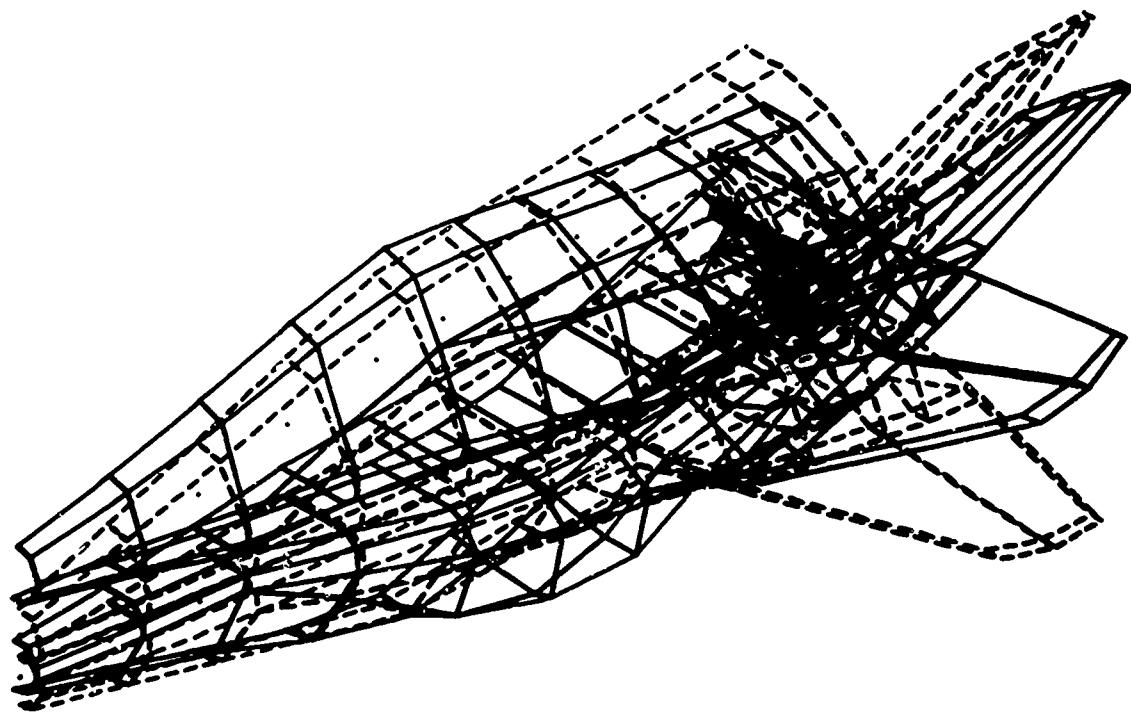


Fig. 13. Mode No. 1 - Unconstrained Double Orbiter

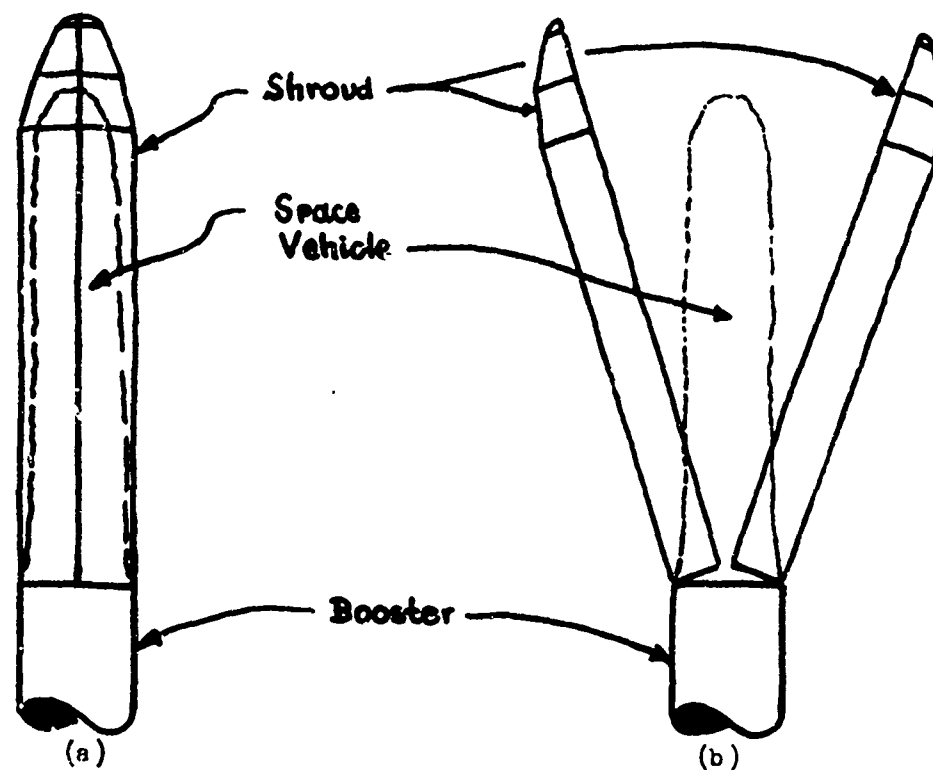


Fig. 14. Space Vehicle with Separable Shroud

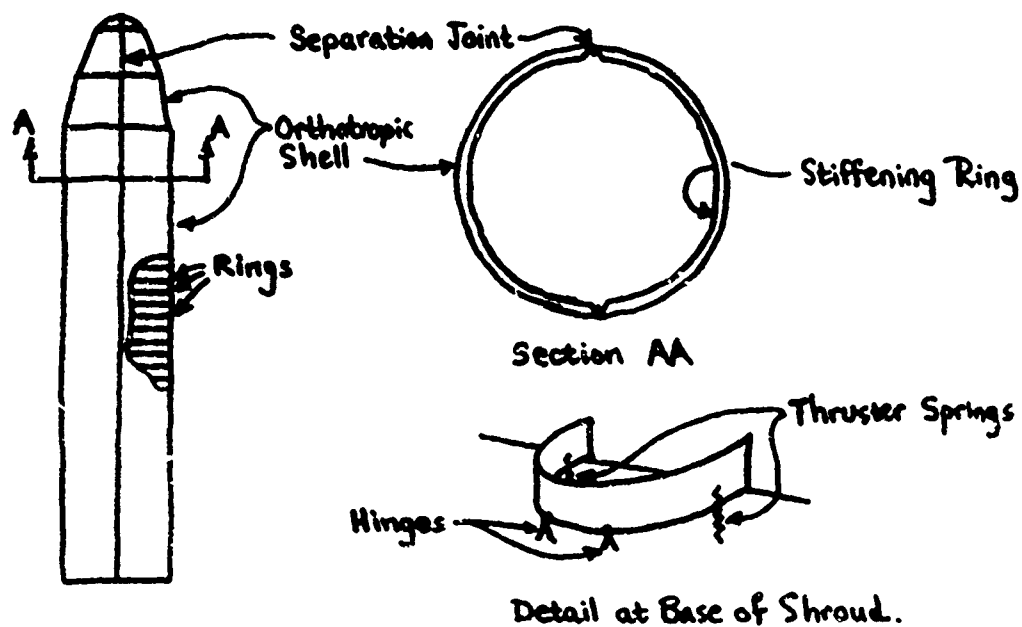
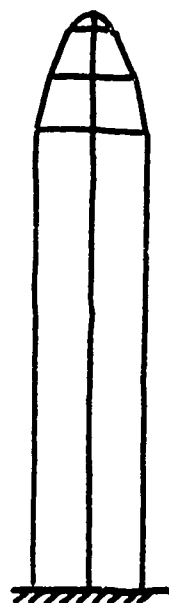
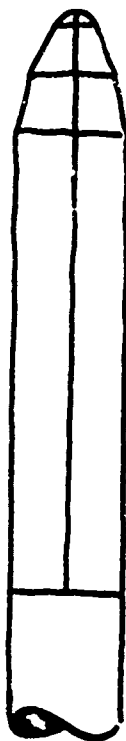


Fig. 15. Space Vehicle Shroud - Construction



(a)

Pre-separated Shroud Clamped
Base, Hinged Longitudinal Joints



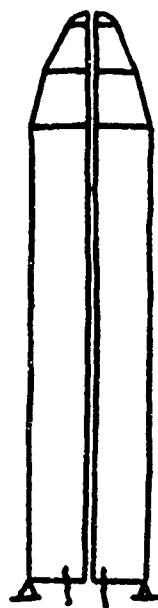
(b)

Launch Vehicle with Space Vehicle
and Pre-separated Shroud



(c)

Post Separated Shroud with
Tip Contact
Base Hinges and Springs



(d)

Independent Shroud Halves
Base Hinges and Springs

Fig. 16. Shroud Modes Required for Analysis

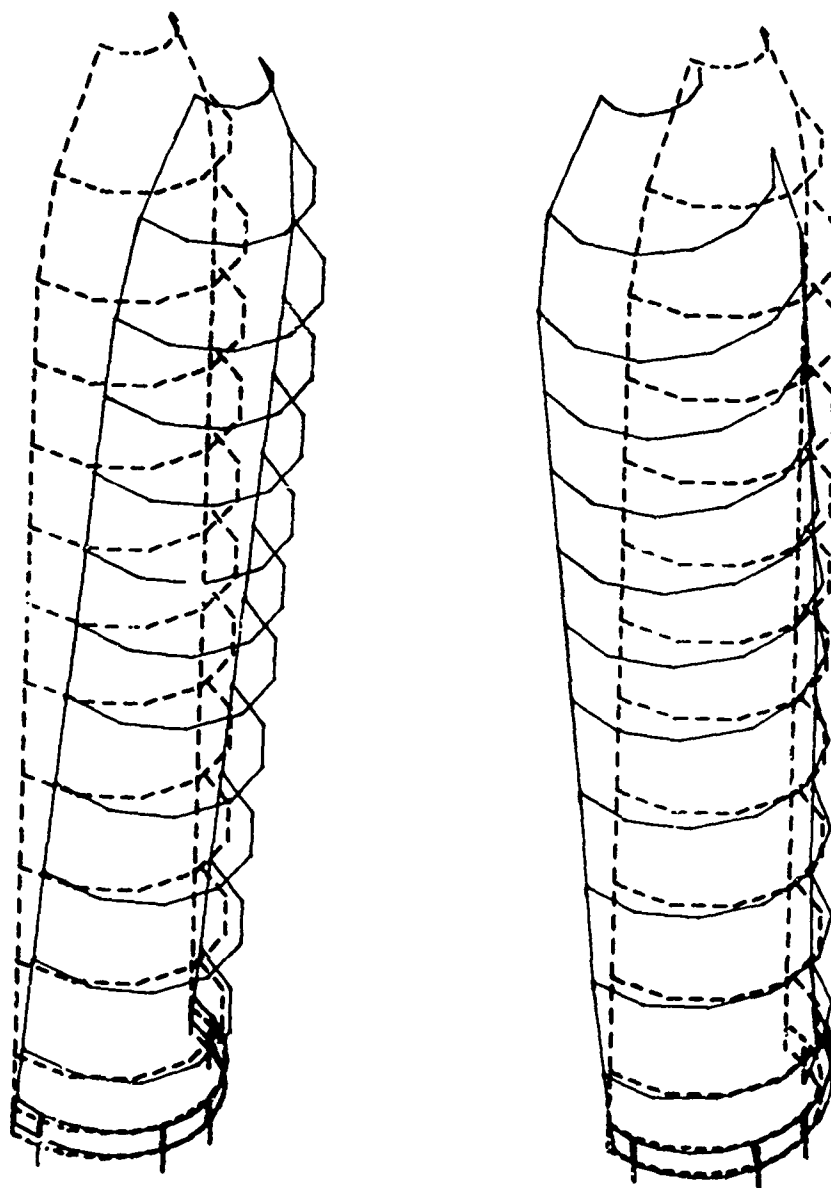


Fig. 17. Two Modes - Post-Separated Shroud on Springs and Hinges

QUESTIONS AND COMMENTS FOLLOWING COALE'S PAPER

QUESTION: You compare the frequencies on these test cases involving plates; did you also compare the mode shapes in these cases to the exact mode shapes?

COALE: Yes, we have gotten very good comparisons with the mode shapes. The ultimate way of comparing would be to compare the internal forces since they, of course, diverge more quickly than either the mode shape, the modal displacements, or certainly the modal frequencies. I believe that good internal force agreement would be obtained with the method but I don't have figures to verify that.

QUESTION: In some cases you have some of these component modes unrestrained. What are the specific steps that you take to account for possible rigid body motion?

COALE: This is included. If you take a body that is completely unconstrained except on a connection boundary, then you release each degree of freedom of the connection boundary separately so no rigid body modes occur. The rigid body motions of the components turn out to be a linear combination of the boundary deformation functions. As a matter of fact, Hurty pulled rigid body motions out and used them separately. You can do this and in some cases it's a good idea.

QUESTION: What if your boundary or connecting points would only consist of the constraints required for rigid body motion?

COALE: Even then you can include the rigid body motions or equivalent motion of one constraint at a time and it still works. The double orbiter example was a case of that. That was a statically determinate constraint.

COMMENT: The problem of having an excessive number of degrees of freedom along the boundary between these substructures is indeed a problem but this is something that's readily handled by the so-called Guyan reduction. Let's suppose, for example, that you had initially cast your sub-surfaces for stress analysis. You may well want to use the Guyan reduction before you take the modes of the individual substructures. Then, after you've assembled the individual substructures and have this excess number of interface degrees of freedom, they are really rather handily removed by Guyan reduction applied again at that level.

COALE: In some cases, that's a good idea. However, there are cases where we do not wish to remove the excess degrees of freedom but we wish to describe them by functions. When you reduce in the component as you're talking about, you no longer are able to connect those degrees of freedom to the other structure. Is that right?

COMMENT: Perhaps I shouldn't have mentioned this first stage that one person can do. But at the second stage, the problem is that you have an excess of degrees of freedom and certainly you don't want at that level to try to eliminate all of these interface degrees of freedom. If, for example, you have a linear point along which two substructures are stitched together you might keep as your undetermined coefficients every tenth one or something like that.

COALE: Yes, you're talking about this reduction after connection rather than before.

COMMENT: I was trying to address the problem of having an excess number of physical degrees of freedom left on the boundary after having assembled the substructures.

COMMENT: I agree completely with those last comments about reduction. You have the appropriate back substitution matrices on hand presumably to calculate the so-called slave displacements in that method.

I also want to ask about terminology. You kept saying standard approach and I think you meant the Craig and Bampton approach, which does bypass the complexity that is usually incorporated in Hurty's original component load method. In fact, I think that's one of the things that has prevented it from becoming very popular, up until Craig and Bampton did their work. But I myself would say that Hurty's method is the standard and Craig and Bampton would be a modification of the standard.

COALE: The only modification that I recall is the elimination of the rigid body modes and merely using boundary functions.

COMMENT: Yes, the rigid modes are still there, but they're incorporated within all the degrees of freedom that you have in your connections. I also wanted to say that I think this method has a very good future and it does help to answer the question of how do you determine what degrees of freedom to retain in a reduced system. The answer here is to retain the connecting degrees between the substructures and the lower normal modes as generalized displacements in each of the substructures.

Since the decision is automatically made about what is to be retained, the important question then is how do you cut your structure up into parts? Everything, of course, hinges on that decision!

QUESTION: My question concerns efficiency. In the selection of the modes for the element, it seems unreal to consider idealized boundary conditions like clamped conditions when we know that in reality the structure will have some spring effect on the support. It seems to me that rather than choose idealized conditions, we ought to make some wild guess as to what the restraint conditions will be. Even though it's wild, it will be better than assuming clamped conditions. So that when we truncate the modes, the lower modes will more naturally represent how the structure wants to behave and hence we'll get better accuracy with fewer modes.

COALE: I agree with you; but there are two possible cases. One is where you know much about the problem ahead of time and therefore can make estimates. You would like to build into the program the ability to take into account these estimates. There are other cases, however, where you don't know to what other structure the structure is going to be joined. It may be joined to several things and you don't know enough about the characteristics of them to make that prediction ahead of time. Then I think you have to go to something like this. You can't make estimates if you don't know the characteristics of the structure or of the boundary or the structure you're joining it to.

COMMENT: I think there is a place for component mode synthesis in the situation which you described in these practical structures where the

design process actually was based on substructuring principles. In other words, different people probably design different components and you assemble the components in the development of the actual structure. But I think there is no benefit in applying the component mode approach to a structure which in itself is a single unit. All you're using is a standard Rayleigh-Ritz analysis procedure. You're using the component modes as a means of defining a set of shapes and the particular set of shapes that you're using is not a particularly well adapted one. In one case you mentioned getting 14 modes from 15 shapes but you had an additional 18 boundary conditions so you had 33 Rayleigh Ritz inputs and this should obviously be very good for calculating 14 modes if you've any kind of intuition. I think the operation of calculating a bunch of component modes as a means of choosing appropriate input functions for your complete structure is a point that I would definitely question.

COALE: Well, the question that I must bring up then is what method would you advocate for getting these functions in a very complex structure?

COMMENT: That's where the real ingenuity lies. We generally use unit loads applied to various nodes to define a mode shape.

COALE: They're not very good in general either.

COMMENT: It depends on the problem.

COMMENT: I'd like to caution against the idea of always being able to get away with putting in the lower modes of a structure. It's been our experience with shells which exhibit three classes of modes (extensional,

bending and torsional) that you can't just put in lower frequency modes. You may have to put in a lower frequency bending and then perhaps one or two membrane modes. If you really got nasty, you might have to put in a torsional mode too. It depends on how the structure is behaving. You may have to look through the spectrum and not just pick the lower modes.

COALE: Let me make one final comment and that is that I like to use engineering judgment as well as anybody and I believe it should be used wherever it can be. I'm interested, however, in a method that will work for a structure where engineering judgment is difficult to apply.

PANEL DISCUSSION C

THE LARGE GENERAL PURPOSE CODE

Chairman: D. Warren, Douglas Aircraft Company,
Long Beach, California
C. W. McCormick, MacNeal-Schwendler Corp.,
Los Angeles, California
Y. Rashid, General Electric Company,
San Jose, California
R. Melosh, Philco-Ford Western Development
Laboratory, Palo Alto, California
S. Jordan, Bell Aerosystems,
Buffalo, New York

WARREN: Our objective is to discuss large general purpose computer programs in terms of their advantages and disadvantages and to describe some features of several of the well known programs. Four of our panelists have been involved in the development of large programs: McCormick with NASTRAN, Jordan with MAGIC, Melosh with SAMIS, and Warren with FORMAT. Our fifth panelist, Rashid, represents the single purpose computer program as opposed to the large general purpose program.

The discussion will begin with a brief introduction by me followed by opening remarks by each of the other panelists. We will then open the discussion to questions from the audience.

I'd like to kick off the discussion with a slide (see Figure 1) that describes my idea of a complex problem in shell analysis. This is a Douglas DC-10 and is somewhat different than the shells we have been hearing about for the last few days. It is a fantastically large structure. Probably one of the most astounding things about it is that only 18 months elapsed from the decision to build to the first flight. This schedule put a tremendous burden on the analysts because the first airplane had to be right. It is a \$15,000,000 item

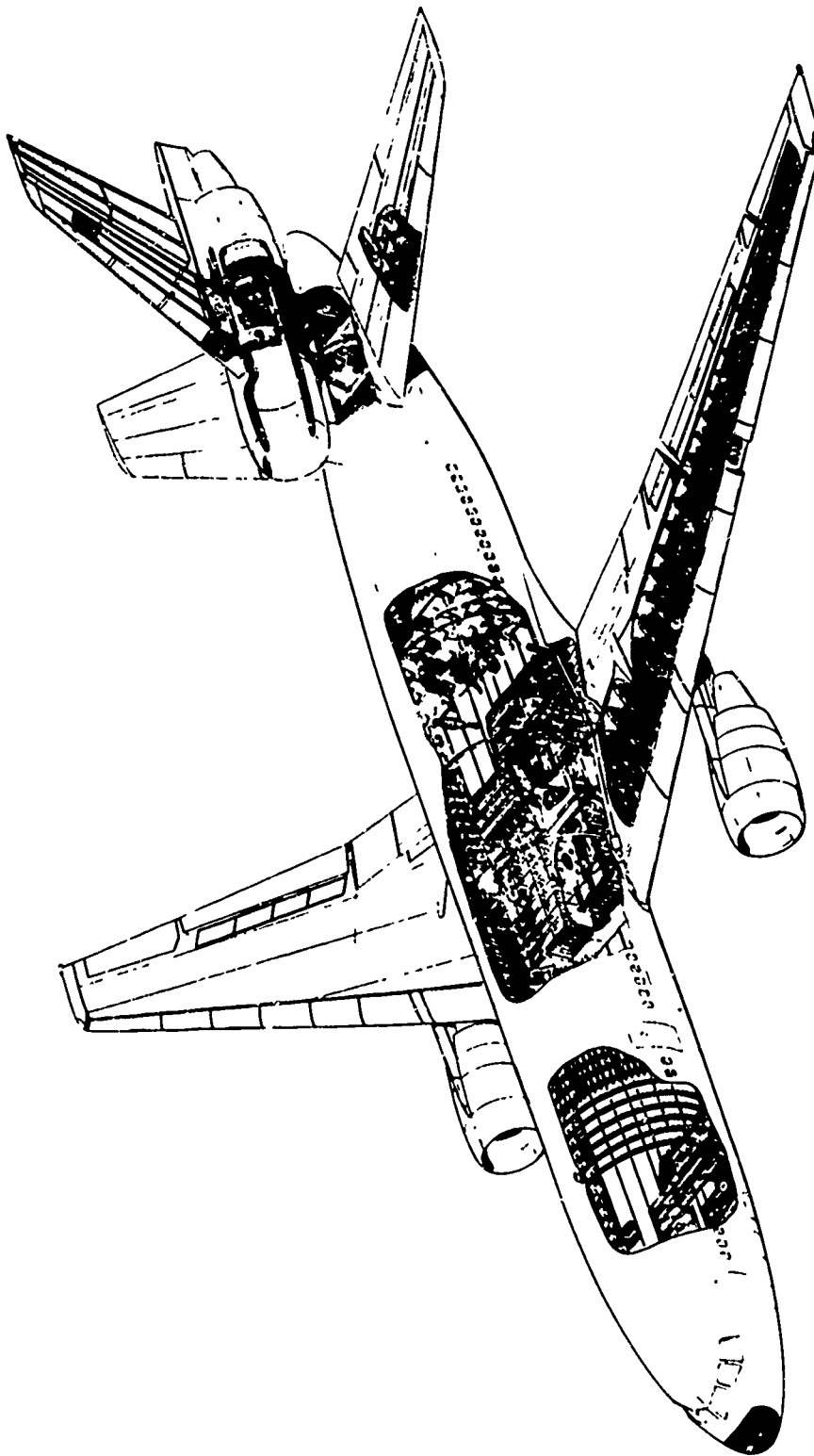


Figure 1. DC-10 STRUCTURAL ARRANGEMENT

and it can't be rebuilt or scrapped because of crude assumptions made in the analysis. Another significant point is that the airframe has a warranty for fatigue life. This also implies a very severe demand on the structural analysis used to design the airplane.

This type of shell problem is not easily attacked with anything but a general purpose computer program and in this case a very large one. One of the more sophisticated elements of the structure is the aft-fuselage/empennage assembly with the third engine supported by a pylon cantilevered from the base of the vertical fin. The loads from the engine go through the pylon and are added to the loads from the vertical fin, then through a system of rings around the inlet duct for the third engine and down into the shell. Loads are transferred into the fuselage shell by frames rather than bulkheads. This aft fuselage structure is complicated further by a thruway access for the movable horizontal stabilizer. The decision to have a straight-through air inlet duct with ring frames rather than a bifurcated duct with straight-through structure was made at an early stage of design based on elaborate analyses including fail-safe studies. There are similar systems of very complicated mechanisms elsewhere: large storage compartments under the floor for the landing gear, large doors for access to the lower level and the passenger level, and some trickery in the structural design in the side of the fuselage aft of the wing root to more evenly distribute the loads of the wing into the fuselage shell structure. Such configurations are very difficult to handle with any computer code specialized for particular structural geometry.

Finally, I'd like to offer a few remarks to help clarify what we mean when we speak of a large general purpose computer program. McCormick provided an excellent definition earlier today: "A large computer program is one whose capacity is limited by the user's pocketbook and not the program." If that definition proves to be too vague, we can resort to the following. A large program is one which requires at least five boxes of cards for the source deck, at least three levels in the overlay structure, at least two levels of storage throughout the program, and coding that provides automatic piecewise segmentation of data. For example, in matrix operations, a com-

plete matrix need not fit into core at one time. Also, by general purpose we mean without restriction as to geometry.

RASHID: A single special purpose computer program and a general purpose program are difficult to compare directly. In those cases where the special purpose program can be used, it often has decided advantages over the general purpose code. For cases where the specific purpose program can't be used, there is nothing to compare. Thus, I think that we must consider that the alternative to the general purpose program is not a single special purpose program, but a library of them. I propose then that we compare the general purpose program with a library of special purpose programs. There are seven advantages I have listed that accrue to such a library and I'd like to mention these briefly.

1. First of all, as individual programs they offer great flexibility to a large number of users. As a collective system they can be assembled in such a way as to produce an analysis capability of a size tailored to the problem at hand.
2. They are readily made user oriented. Graphics capabilities are easily incorporated and user instructions are generally quite simple compared with a general purpose program. It's hard for me to believe that the general purpose program could be made more user oriented than the special purpose program.
3. Efficiency and economy are important advantages. Special purpose programs are tailored for a single class of programs and therefore they utilize the computer hardware in a most efficient way. This provides for short running time, of course, minimum storage requirements and a greater overall economy. There is not a great deal of bookkeeping necessary as is required to bring the large general purpose program in and out of the computer. Furthermore, we see computer data centers around the country are each utilizing their own bookkeeping systems and accounting procedures. It is possible that a short running program may cost more than a long running program since the charges are a function of the special

accounting systems of data centers.

4. Reliability is another important consideration. A library of special purpose programs are separate systems internally. Thus, one does not mix, for example, the coding for a complex inelastic, finite displacement nonlinear analysis with simple linear dynamic analysis in the same program. This helps to reduce the chance of misapplication by an inexperienced user and therefore maintains reliability and confidence in the results. Furthermore, the fact that the relatively large size of general purpose programs leads to the concentration of skills for operating the programs in only a few individuals.

5. They are more convenient than general purpose programs. For example, different coordinate systems may be required to specify different shell problems conveniently. A global system might be fine in one case but a local coordinate system is useful when one tries to interpret results or input boundary conditions. I know of some general purpose computer programs which utilize only on a global coordinate system, thus making them inconvenient to use for boundary conditions which are naturally expressed in local coordinates. If the general purpose program provides options for using several schemes, then it clutters the program for those users who don't need such options. Furthermore, from the computational point of view, different theories require different computational schemes. Take, for example, the memory theory in creep versus the equation of state theory. If we try to build both into the same computer program, it gets very clumsy and inconvenient to use.

6. The sixth point concerns accessibility of special or general purpose programs. A large general purpose program may be too complex and expensive to be acquired and operated by many concerns which need computerized structural analysis capability. They are forced to do without it or turn to someone else to perform their analysis. However, these same firms can compile a library of special purpose programs which will effectively and economically satisfy their analysis needs.

7. The special purpose program can be readily adapted and modified to one's own special needs; that is a very important consideration. Special purpose programs form excellent building blocks by which one progresses from a linear problem to a nonlinear problem and so forth or from a static problem to a dynamic problem and so forth. They are less costly to debug and can be carried out by personnel within the same organization without the need to rely on other organizations to develop slight or major modifications.

MCCORMICK: I want to make several remarks concerning large general purpose computer programs. Most of what I have to say here today is based on my experience in the development of NASTRAN. I regard myself as kind of an analytical tool maker and it's my feeling that in this role I must try to make the most available to the most people. Large general purpose computer programs are a good way to accomplish this. NASTRAN could actually be considered a collection of programs although not in the same sense that was previously discussed. If you were doing a static problem, the computations performed in the computer are really in no way influenced by the computations which would be required if you were doing vibration problems or transient response problems. The same matrix routines and certainly the same input-output routines would be used, but I really don't believe that the efficiency of the static computations are adversely affected by the fact that the program also has dynamic capability. In fact, I think they are aided by the fact that they are all a part of the same family. I think I would prefer to call NASTRAN a large general purpose system which is really a collection of programs which exists in executable form in a library. The load time is essentially zero and you start an execution immediately. The fact that it is a large system means simply that it takes more library space. But as far as executing a statics problem is concerned, the fact that other capabilities such as transient response or flutter analysis exist in the program has essentially no effect whatsoever on the execution of the statics problem as far as the core you use or anything else.

I view developing a program such as NASTRAN as a job of looking at the available computer hardware and looking at the problems you have to solve and figuring out the best way to go about it. The hardware as you all know

changes very rapidly and NASTRAN had far too long a development period. I guess almost five years, and we practically have gone through another generation. We are now in the third and if we're not careful we are liable to get to the fourth generation before NASTRAN becomes fully operational.

Documentation of these large general purpose systems, of course, is extremely important and it's never done very well according to anybody except the guy who wrote the documents; maybe even he won't think it's very good. We have considerable documentation for NASTRAN and we've certainly made efforts to make it at least reasonably complete and accurate. I believe I'll refrain from further comment at this time since I had an opportunity to talk at some length earlier when I presented my paper.

MELOSH: The advantages and disadvantages of special and general purpose programs have been well covered. However, I'd like to add that one role that the general purpose program serves better than the special purpose is the role of communicating technology. General purpose program developers are forced to adopt a unified approach to all structural analyses. Thus approximations for special cases must be identified, classified, and regimented for orderly program development and use. In the special purpose program the technology transmitted may involve black box approximations. Unaware of the approximations, the user may apply the code when it is inappropriate.

Now, I'd like to say a few words about SAMIS; the oldest nonproprietary general purpose program. It has a thoroughly debugged capability and most of the program inefficiencies have been eliminated. Because it is one of the first general purpose structural analysis programs, it is the simplest. It does all the things that McCormick mentioned this morning that a general purpose code should do with respect to packing of data, management of core, etc. Moreover, these housekeeping tasks are done in a straightforward way. An engineer can modify the logic without the help of a systems programmer. Finally, it's responsive. There's no black magic in the program; the user has complete control over every macro-operation. He controls disposition of data, management of the sequence of calculations, and

the approximations and error checks. This, in turn, imposes a responsibility upon the user to understand his problems solution steps. Bearing this responsibility makes the user better prepared to interpret and verify solution results.

With respect to accuracy, let's take a quick survey of the state of the art. Table I delineates the major error classes in any numerical analysis. The principal errors we will discuss are quantification and manipulation errors. Quantification error includes idealization, discretization and mapping errors. Idealization errors are the most important of these because errors may be unbounded and are not well understood. Manipulation errors involve either gradual erosion of the mantissa (from the right) due to the sequence of arithmetic steps (mantissa distortion error) or rapid deterioration of accuracy due to an operation which destroys vital information contained in the lower bits (critical arithmetic). These errors are important whenever low precision arithmetic is used relative to problem size.

As program developers, we have a responsibility with respect to idealization error. We must include low error guaranteed operators (finite element models); guaranteed in the sense that Sam Key discussed earlier. We must guarantee that the included operators will yield correct answers when the mesh is made sufficiently fine. We have a responsibility to provide generality in the material modeling; a responsibility to insure that the representations lead to bounded error in representing the geometry of interest; and a responsibility to simulate simple common boundary conditions--uniform distributions of pressure, temperature, and mass, for example.

With respect to the state of the art, available programs are remiss primarily with respect to operators. Many programs contain operators that are not guaranteed. Some are even known to be unacceptable. Emphasis should be placed on assuring that guaranteed operators exist in all general purpose codes both to avoid structural design calamities and to fulfill responsibilities as technology disseminators.

With respect to manipulation errors, the program developer has three

Table I. Numerical Analysis Errors

<u>Error Class</u>	<u>Error Order</u>	<u>Error Family</u>
1. <u>Quantification</u>	Modelling (Idealization)	Mapping Discretization
	Citation	Transcription Transmission Truncation
2. <u>Input-Output</u>	Conversion	Number base Number format Algorithm
	Rendition	Truncation Transmission
3. <u>Process</u>	Iteration	Convergence Accuracy criterion
	Approximation	Algorithm Software
4. <u>Manipulation</u>	Exponent exceedance	Overflow Underflow
	Mantissa distortion	Attrition Critical arithmetic
5. <u>Interpretation</u>	Unmodelling	Unmapping Smoothing

responsibilities: (1) he must include low error algorithms; (2) he must include meaningful error reports; and (3) for the sake of efficient utilization of the computer, he should strive for consistent precision management.

The state of the art indicates deficiencies in meeting the last two responsibilities. No current program has meaningful error reports; although we are addressing ourselves to attaining them in SAMIS. In this regard, a Goddard study stimulated by Tom Butler shows that equilibrium, reaction, and Maxwell Reciprocity checks are often meaningless. To my knowledge, no program developers other than those involved with NASTRAN have attempted consistent precision management. The failure to attain the goal cannot be severely criticized.

This review indicates that existing general (and special) purpose programs are deficient with respect to measuring idealization and manipulation errors and noting implications on the accuracy of solution results. These deficiencies impose upon the engineer the burden of being a numerical analyst; a burden which belongs on the program developers and which the engineer is often unprepared to assume.

JORDAN: A good measure of the reliability of a general purpose computer program, or any program for that matter, is the confidence that the user can place in the results which are generated through his day to day applications of the particular program.

The reliability spectrum is made up of many components; some of those which apply to a General Purpose Structural Analysis System are shown in Figure 2.

One of the first measures of reliability is the type of element library contained in the program. Figure 3 shows the element library available to MAGIC users. It must be adequate to attack the class of problem which you would like to solve. The way I view it, it's the heart of the analysis system, and even the most sophisticated software and graphics or similar things will produce less than acceptable results without an adequate element library. A

SUMMARY

- SOPHISTICATED ELEMENT LIBRARY
- ADEQUATE ELEMENT MATRICES
- LIBRARY OF SPECIALIZED COMPUTATIONAL PROCEDURES
 - STATIC SUBSTRUCTURING
 - DYNAMIC SUBSTRUCTURING
 - CONDENSATION
- PREPRINTED INPUT DATA FORMS
 - INTERNALLY GENERATED TRANSFORMATIONS
- INPUT DATA CONFIRMATION PHASE
 - PLOTTING
- READABLE OUTPUT DATA
 - DISPLACEMENTS, STRESSES, ELEMENT FORCES, REACTIONS
- INTERNAL ERROR CHECKS (DIAGNOSTICS)
 - NEGATIVE MAIN DIAGONALS
 - MATRIX, POSITIVE DEFINITENESS
 - USE OF NON COMPATIBLE ELEMENTS
- MODULAR CONSTRUCTION OF SYSTEM
- DETAILED AND EASILY UNDERSTOOD DOCUMENTATION

Figure 2. Reliability Summary

IDENT. NO.	DESIGNATION
10	TRUSS
11	FRAME
20	HELLE TRIANGULAR THIN SHELL
21	MALLETT QUADRILATERAL THIN SHELL
22	BELL TRIANGULAR THIN SHELL
23	BELL QUADRILATERAL THIN SHELL
24	QUADRILATERAL SHEAR PANEL
30	TOROIDAL THIN SHELL RING
40	TRIANGULAR CROSS SECTION RING
41	TRAPEZOIDAL CROSS SECTION RING
42	CORE
50	TETRAHEDRON
51	TRIANGULAR PRISM
52	RECTANGULAR PRISM

FIGURE 3. FINITE ELEMENT LIBRARY

set of element matrices can be associated with the library as shown in Figure 4. These are basically consistent matrices and can at the option of the analyst be generated internally at the element level in the program. These provide considerable flexibility in the type of operations that can be performed.

When you want to handle large scale problems on the order of over 1000 degrees of freedom, you need a library of specialized computational procedures such as static and dynamic substructuring (Figure 5). Substructuring allows you to handle the data which may become unmanageable with large degree of freedom systems or to more readily interact with design groups within your organization if a change in the structure were to come about. Furthermore, condensation techniques (e. g. , Guyan reduction) in conjunction with substructuring are also very useful. Condensation, however, needs a logical rationale for selection of degrees of freedom which are to be condensed in any particular application. The use of energy based methods or simple interrogation of the diagonals of the stiffness and the mass matrix, examination of the ratios, and then using these values to decide which degrees of freedom to keep or condense, is under investigation.

Reliability is also related to how the input and output data is handled. From my experience, preprinted input data forms (Figures 6 and 7) are very important. Furthermore, you need an input data confirmation phase so that you are able to check input data before you execute your problems. Output should be in a condensed form, if possible, and if it is to be meaningful, it should include at least displacements, stresses, element forces and system reactions. I guess this last point is disputed somewhat by Bob Melosh. Some programs don't give you reactions and it has been our experience at Bell Aerospace Company that after we solve the problem the first thing we turn to are the reactions for examination. Internal error checks such as a negative main diagonal checks or a check on positive definiteness are a very simple thing to implement and can save a lot of wasted time. Checks to assure that the user has not linked two incompatible elements or failed to define certain elements are also quite useful.

MATRIX	IDENTIFICATION
$[M]$	CONSISTENT MASS
$[D_v]$	VISCOUS DAMPING
$[D_s]$	STRUCTURAL DAMPING
$[K]$	STIFFNESS
$[N]$	INCREMENTAL STIFFNESS
$\{F_{pf}\}$	FIELD PRESSURE LOAD
$\{F_{pc}\}$	BOUNDARY PRESSURE LOAD
$\{F_e\}$	PRESTRAIN LOAD
$\{F_T\}$	THERMAL LOAD
$\{F_\sigma\}$	PRESTRESS LOAD
$[S]$	STRESS
$\{A\}$	STRESS CORRECTION

FIGURE 4. FINITE ELEMENT MATRICES

COMPUTATIONAL PROCEDURES UTILIZED
TO SUPPORT ANALYSES

- STATIC SUBSTRUCTURING
- DYNAMIC SUBSTRUCTURING
- CONDENSATION TECHNIQUES
- AUTOMATIC DATA GENERATION AND
REDUCTION
- LARGE ORDER EIGENVALUE PACKAGE

Figure 5. Computational Procedures

MAGIC STRUCTURAL ANALYSIS SYSTEM INPUT DATA FORMAT

BOUNDARY CONDITIONS

INPUT CODE - 0 - No Displacement Allowed
1 - Unknown Displacement
2 - Known Displacement

1	2	3	4	5	6
B	O	U	N	D	

(/)

PRE-SET MODE

1	2	3	4	5	6
M	O	U	A	L	

TRANSLATIONS			ROTATIONS			GENERALIZED		
U	V	W	θ_x	θ_y	θ_z	1	2	3
13	14	15	16	17	18	19	20	21

(/)

LISTED INPUT

Grid Point Number						Repeat									
7	8	9	10	11	12	13	14	15	16	17	18	19	20	21	
															(/)
															(/)
															(/)
															(/)
															(/)
															(/)
															(/)
															(/)
															(/)
															(/)
															(/)
															(/)
															(/)
															(/)
															(/)
															(/)
															(/)
															(/)
															(/)
															(/)
															(/)
															(/)
															(/)
															(/)
															(/)
															(/)
															(/)
															(/)
															(/)
															(/)
															(/)
															(/)
															(/)
															(/)
															(/)
															(/)
															(/)
															(/)
															(/)
															(/)
															(/)
															(/)
															(/)
															(/)
															(/)
															(/)
															(/)
															(/)
															(/)
															(/)
															(/)
															(/)
															(/)
															(/)
															(/)
															(/)
															(/)
															(/)
															(/)
															(/)
															(/)
															(/)
															(/)
															(/)
															(/)
															(/)
															(/)
															(/)
															(/)
															(/)
															(/)
															(/)
															(/)
															(/)
															(/)
															(/)
															(/)
															(/)

MAGIC STRUCTURAL ANALYSIS SYSTEM INPUT DATA FORMAT	ELEMENT CONTROL DATA
1. TITLE PAGE	1. ELEMENT NUMBER
2. MATERIAL PROPERTIES	2. ELEMENT TYPE
3. GEOMETRY	3. ELEMENT COORDINATES
4. BOUNDARY CONDITIONS	4. ELEMENT SHAPE
5. LOADS	5. ELEMENT STRESS
6. RESULTS	6. ELEMENT STRAIN
7. POST-PROCESSING	7. ELEMENT DISPLACEMENT
8. OUTPUT	8. ELEMENT ROTATION
9. ERROR CHECKS	9. ELEMENT TORSION
10. SUMMARY	10. ELEMENT BUCKLING
11. REFERENCES	11. ELEMENT STABILITY
12. APPENDICES	12. ELEMENT DYNAMICS
13. INDEX	13. ELEMENT THERMAL
14. GLOSSARY	14. ELEMENT ACoustics
15. BIBLIOGRAPHY	15. ELEMENT OPTICS
16. REFERENCES	16. ELEMENT ELECTROMAGNETICS
17. APPENDICES	17. ELEMENT FLUID MECHANICS
18. INDEX	18. ELEMENT PLASMA
19. GLOSSARY	19. ELEMENT PARTICLES
20. BIBLIOGRAPHY	20. ELEMENT ATOMS
21. REFERENCES	21. ELEMENT MOLECULES
22. APPENDICES	22. ELEMENT SOLIDS
23. INDEX	23. ELEMENT LIQUIDS
24. GLOSSARY	24. ELEMENT GASES
25. BIBLIOGRAPHY	25. ELEMENT PLASMA
26. REFERENCES	26. ELEMENT PARTICLES
27. APPENDICES	27. ELEMENT ATOMS
28. INDEX	28. ELEMENT MOLECULES
29. GLOSSARY	29. ELEMENT SOLIDS
30. BIBLIOGRAPHY	30. ELEMENT LIQUIDS
31. REFERENCES	31. ELEMENT GASES
32. APPENDICES	32. ELEMENT PLASMA
33. INDEX	33. ELEMENT PARTICLES
34. GLOSSARY	34. ELEMENT ATOMS
35. BIBLIOGRAPHY	35. ELEMENT MOLECULES
36. REFERENCES	36. ELEMENT SOLIDS
37. APPENDICES	37. ELEMENT LIQUIDS
38. INDEX	38. ELEMENT GASES
39. GLOSSARY	39. ELEMENT PLASMA
40. BIBLIOGRAPHY	40. ELEMENT PARTICLES
41. REFERENCES	41. ELEMENT ATOMS
42. APPENDICES	42. ELEMENT MOLECULES
43. INDEX	43. ELEMENT SOLIDS
44. GLOSSARY	44. ELEMENT LIQUIDS
45. BIBLIOGRAPHY	45. ELEMENT GASES
46. REFERENCES	46. ELEMENT PLASMA
47. APPENDICES	47. ELEMENT PARTICLES
48. INDEX	48. ELEMENT ATOMS
49. GLOSSARY	49. ELEMENT MOLECULES
50. BIBLIOGRAPHY	50. ELEMENT SOLIDS
51. REFERENCES	51. ELEMENT LIQUIDS
52. APPENDICES	52. ELEMENT GASES
53. INDEX	53. ELEMENT PLASMA
54. GLOSSARY	54. ELEMENT PARTICLES
55. BIBLIOGRAPHY	55. ELEMENT ATOMS
56. REFERENCES	56. ELEMENT MOLECULES
57. APPENDICES	57. ELEMENT SOLIDS
58. INDEX	58. ELEMENT LIQUIDS
59. GLOSSARY	59. ELEMENT GASES
60. BIBLIOGRAPHY	60. ELEMENT PLASMA
61. REFERENCES	61. ELEMENT PARTICLES
62. APPENDICES	62. ELEMENT ATOMS
63. INDEX	63. ELEMENT MOLECULES
64. GLOSSARY	64. ELEMENT SOLIDS
65. BIBLIOGRAPHY	65. ELEMENT LIQUIDS
66. REFERENCES	66. ELEMENT GASES
67. APPENDICES	67. ELEMENT PLASMA
68. INDEX	68. ELEMENT PARTICLES
69. GLOSSARY	69. ELEMENT ATOMS
70. BIBLIOGRAPHY	70. ELEMENT MOLECULES
71. REFERENCES	71. ELEMENT SOLIDS
72. APPENDICES	72. ELEMENT LIQUIDS
73. INDEX	73. ELEMENT GASES
74. GLOSSARY	74. ELEMENT PLASMA
75. BIBLIOGRAPHY	75. ELEMENT PARTICLES
76. REFERENCES	76. ELEMENT ATOMS
77. APPENDICES	77. ELEMENT MOLECULES
78. INDEX	78. ELEMENT SOLIDS
79. GLOSSARY	79. ELEMENT LIQUIDS
80. BIBLIOGRAPHY	80. ELEMENT GASES
81. REFERENCES	81. ELEMENT PLASMA
82. APPENDICES	82. ELEMENT PARTICLES
83. INDEX	83. ELEMENT ATOMS
84. GLOSSARY	84. ELEMENT MOLECULES
85. BIBLIOGRAPHY	85. ELEMENT SOLIDS
86. REFERENCES	86. ELEMENT LIQUIDS
87. APPENDICES	87. ELEMENT GASES
88. INDEX	88. ELEMENT PLASMA
89. GLOSSARY	89. ELEMENT PARTICLES
90. BIBLIOGRAPHY	90. ELEMENT ATOMS
91. REFERENCES	91. ELEMENT MOLECULES
92. APPENDICES	92. ELEMENT SOLIDS
93. INDEX	93. ELEMENT LIQUIDS
94. GLOSSARY	94. ELEMENT GASES
95. BIBLIOGRAPHY	95. ELEMENT PLASMA
96. REFERENCES	96. ELEMENT PARTICLES
97. APPENDICES	97. ELEMENT ATOMS
98. INDEX	98. ELEMENT MOLECULES
99. GLOSSARY	99. ELEMENT SOLIDS
100. BIBLIOGRAPHY	100. ELEMENT LIQUIDS
101. REFERENCES	101. ELEMENT GASES
102. APPENDICES	102. ELEMENT PLASMA
103. INDEX	103. ELEMENT PARTICLES
104. GLOSSARY	104. ELEMENT ATOMS
105. BIBLIOGRAPHY	105. ELEMENT MOLECULES
106. REFERENCES	106. ELEMENT SOLIDS
107. APPENDICES	107. ELEMENT LIQUIDS
108. INDEX	108. ELEMENT GASES
109. GLOSSARY	109. ELEMENT PLASMA
110. BIBLIOGRAPHY	110. ELEMENT PARTICLES
111. REFERENCES	111. ELEMENT ATOMS
112. APPENDICES	112. ELEMENT MOLECULES
113. INDEX	113. ELEMENT SOLIDS
114. GLOSSARY	114. ELEMENT LIQUIDS
115. BIBLIOGRAPHY	115. ELEMENT GASES
116. REFERENCES	116. ELEMENT PLASMA
117. APPENDICES	117. ELEMENT PARTICLES
118. INDEX	118. ELEMENT ATOMS
119. GLOSSARY	119. ELEMENT MOLECULES
120. BIBLIOGRAPHY	120. ELEMENT SOLIDS
121. REFERENCES	121. ELEMENT LIQUIDS
122. APPENDICES	122. ELEMENT GASES
123. INDEX	123. ELEMENT PLASMA
124. GLOSSARY	124. ELEMENT PARTICLES
125. BIBLIOGRAPHY	125. ELEMENT ATOMS
126. REFERENCES	126. ELEMENT MOLECULES
127. APPENDICES	127. ELEMENT SOLIDS
128. INDEX	128. ELEMENT LIQUIDS
129. GLOSSARY	129. ELEMENT GASES

ELEMENT NUMBER	PLUG NO.	MATERIAL NUMBER	INTERPOLATE OPTION	MATERIAL TEMPERATURE	Repeat Elem. Matrices	Elem. Input	PRINT			Number of Input Nodes	No. of Assoc. Nodes	NODE POINTS											
							Print Elem.	Mat. Elem.	Full			1	2	3	4	5	6	7	8	9	10	11	12
1	1		2		28	29	30	31	32	33	3	3	6	7	8	9	10	11	12	7			
7	8	3	1	1						35	6	7	8	9	10	11	12	13	14	15			
8	9	4	2	2							4	4	5	6	7	8	9	10	11	12			
9	0	5	3	3							5	5	6	7	8	9	10	11	12	13			
0	1	6	4	4							6	6	7	8	9	10	11	12	13	14			
1	2	7	5	5							7	7	8	9	10	11	12	13	14	15			
2	3	8	6	6							8	8	9	10	11	12	13	14	15	16			
3	4	9	7	7							9	9	10	11	12	13	14	15	16	17			
4	5	0	8	8							0	0	1	2	3	4	5	6	7	8			
5	6	1	9	9							1	1	2	3	4	5	6	7	8	9			
6	7	2	0	0							2	2	3	4	5	6	7	8	9	10			
7	8	3	1	1							3	3	4	5	6	7	8	9	10	11			
8	9	4	2	2							4	4	5	6	7	8	9	10	11	12			
9	0	5	3	3							5	5	6	7	8	9	10	11	12	13			
0	1	6	4	4							6	6	7	8	9	10	11	12	13	14			
1	2	7	5	5							7	7	8	9	10	11	12	13	14	15			
2	3	8	6	6							8	8	9	10	11	12	13	14	15	16			
3	4	9	7	7							9	9	10	11	12	13	14	15	16	17			
4	5	0	8	8							0	0	1	2	3	4	5	6	7	8			
5	6	1	9	9							1	1	2	3	4	5	6	7	8	9			
6	7	2	0	0							2	2	3	4	5	6	7	8	9	10			
7	8	3	1	1							3	3	4	5	6	7	8	9	10	11			
8	9	4	2	2							4	4	5	6	7	8	9	10	11	12			
9	0	5	3	3							5	5	6	7	8	9	10	11	12	13			
0	1	6	4	4							6	6	7	8	9	10	11	12	13	14			
1	2	7	5	5							7	7	8	9	10	11	12	13	14	15			
2	3	8	6	6							8	8	9	10	11	12	13	14	15	16			
3	4	9	7	7							9	9	10	11	12	13	14	15	16	17			
4	5	0	8	8							0	0	1	2	3	4	5	6	7	8			
5	6	1	9	9							1	1	2	3	4	5	6	7	8	9			
6	7	2	0	0							2	2	3	4	5	6	7	8	9	10			
7	8	3	1	1							3	3	4	5	6	7	8	9	10	11			
8	9	4	2	2							4	4	5	6	7	8	9	10	11	12			
9	0	5	3	3							5	5	6	7	8	9	10	11	12	13			
0	1	6	4	4							6	6	7	8	9	10	11	12	13	14			
1	2	7	5	5							7	7	8	9	10	11	12	13	14	15			
2	3	8	6	6							8	8	9	10	11	12	13	14	15	16			
3	4	9	7	7							9	9	10	11	12	13	14	15	16	17			
4	5	0	8	8							0	0	1	2	3	4	5	6	7	8			
5	6	1	9	9							1	1	2	3	4	5	6	7	8	9			
6	7	2	0	0							2	2	3	4	5	6	7	8	9	10			
7	8	3	1	1							3	3	4	5	6	7	8	9	10	11			
8	9	4	2	2							4	4	5	6	7	8	9	10	11	12			
9	0	5	3	3							5	5	6	7	8	9	10	11	12	13			
0	1	6	4	4							6	6	7	8	9	10	11	12	13	14			
1	2	7	5	5							7	7	8	9	10	11	12	13	14	15			
2	3	8	6	6							8	8	9	10	11	12	13	14	15	16			
3	4	9	7	7							9	9	10	11	12	13	14	15	16	17			
4	5	0	8	8							0	0	1	2	3	4	5	6	7	8			
5	6	1	9	9							1	1	2	3	4	5	6	7	8	9			
6	7	2	0	0							2	2	3	4	5	6	7	8	9	10			
7	8	3	1	1							3	3	4	5	6	7	8	9	10	11			
8	9	4	2	2							4	4	5	6	7	8	9	10	11	12			
9	0	5	3	3							5	5	6	7	8	9	10	11	12	13			
0	1	6	4	4							6	6	7	8	9	10	11	12	13	14			
1	2	7	5	5							7	7	8	9	10	11	12	13	14	15			
2	3	8	6	6							8	8	9	10	11	12	13	14	15	16			
3	4	9	7	7							9	9	10	11	12	13	14	15	16	17			
4	5	0	8	8							0	0	1	2	3	4	5	6	7	8			
5	6	1	9	9							1	1	2	3	4	5	6	7	8	9			
6	7	2	0	0							2	2	3	4	5	6	7	8	9	10			
7	8	3	1	1							3	3	4	5	6	7	8	9	10	11			
8	9	4	2	2							4	4	5	6	7	8	9	10	11	12			
9	0	5	3	3							5	5	6	7	8	9	10	11	12	13			
0	1	6	4	4							6	6	7	8	9	10	11	12	13	14			
1	2	7	5	5							7	7	8	9	10	11	12	13	14	15			
2	3	8	6	6							8	8	9	10	11	12	13	14	15	16			
3	4	9	7	7							9	9	10	11	12	13	14	15	16	17			
4	5	0	8	8							0	0	1	2	3	4	5	6	7	8			
5	6	1	9	9							1	1	2	3	4	5	6	7	8	9			
6	7	2	0	0							2	2	3	4	5	6	7	8	9	10			
7	8	3	1	1							3	3	4	5	6	7	8	9	10	11			
8	9	4	2	2							4	4	5	6	7	8	9	10	11	12			
9	0	5	3	3							5	5	6	7	8	9	10	11	12	13			
0	1	6	4	4							6	6	7	8	9	10	11	12	13	14			
1	2	7	5	5							7	7	8	9	10	11	12	13	14	15			
2	3	8	6	6							8	8	9	10	11	12	13	14	15	16			
3	4	9	7	7							9	9	10	11	12	13	14	15	16	17			
4	5	0	8	8							0	0	1	2	3	4	5	6	7	8			
5	6	1	9	9							1	1	2	3	4	5	6	7	8	9			
6	7	2	0	0							2	2	3	4	5	6	7	8	9	10			
7	8	3	1	1							3	3	4	5	6	7	8	9	10	11			
8	9	4	2	2							4	4	5	6	7	8	9	10	11	12			
9	0	5	3	3							5	5	6	7	8	9	10	11	12	13			
0	1	6	4	4							6	6	7	8	9	10	11	12	13	14			
1	2	7	5	5							7	7	8	9	10	11	12	13	14	15			
2	3	8	6	6							8	8	9	10	11	12	13	14	15	16			
3	4	9	7	7							9	9	10	11	12	13	14	15	16	17			
4	5	0	8	8							0	0	1	2	3	4	5	6	7	8			
5	6	1	9	9							1	1	2	3	4	5	6	7	8	9			
6	7	2	0	0							2	2	3	4	5	6	7	8	9	10			
7	8	3	1	1							3	3	4	5	6	7	8	9	10	11			
8	9	4	2	2							4	4	5	6	7	8	9	10	11	12			
9	0	5	3	3							5	5	6	7	8	9	10	11	12	13			
0	1	6	4	4							6	6	7	8	9	10	11	12	13	14			
1	2	7	5	5							7	7	8	9	10	11	12	13	14	15			
2	3	8	6	6							8	8	9	10	11	12	13	14	15	16			
3	4	9	7	7							9	9	10	11	12	13	14	15	16	17			
4	5	0	8	8							0	0	1	2	3	4	5	6	7	8			
5	6	1</																					

IF ELEMENT CONTROL DATA MUST BE CONTINUED ON SECOND SHEET, USER MUST DELETE ELEM LABEL CARD FROM SECOND SHEET.

Another very important reliability factor is modular construction of the system. The main reasons for the modularity is that if the finite element program is to be a viable tool you have to be able to take advantage of advances in the state of the art very quickly. With the use of modular construction in the MAGIC system, we at Bell have been able to implement new advances in the program very quickly.

Finally, and this point has been discussed previously, detailed and easily understood documentation is a must. I feel that the more a computer program is used, both within an organization and by other interested users, the more reliable it tends to become. Documentation is probably the first key step toward extended usage.

WARREN: I'd like to talk for a moment about my favorite program, FORMAT. It is organized distinctly different than most other general purpose programs (Figure 8). Basically, it is a three part program consisting of a matrix abstraction package with interpreters at the front and back. User oriented input data is processed by Phase 1 which includes an elaborate file data/edit capability and a matrix generation capability. The output of this phase is a system of matrices on tape; these matrices are used as input to Phase 2. The Phase 2 processing is completely controlled by the user and is stipulated in a matrix abstraction sequence. The available operations include processes for solving simultaneous equations, matrix multiplication, pseudo matrix operations and some special operations. A "structure-cutter" is included primarily for the force method of analysis and provides for concurrent solution of the equilibrium equations and automatic selection of redundants. It is usable for other purposes, one of which is to determine the optimum location for strain gages for a flight test article. There are currently three ways to determine eigenvalues and eigenvectors, including one for 2000 order systems. There are also operations such as print matrices, save matrices, etc. Results of Phase 2 are more matrices on tape which are translated by Phase 3 into a form directly usable by the engineer without any auxiliary tables. Final output options are report pages and pictorials, including isometrics of structures and plots of matrix data.

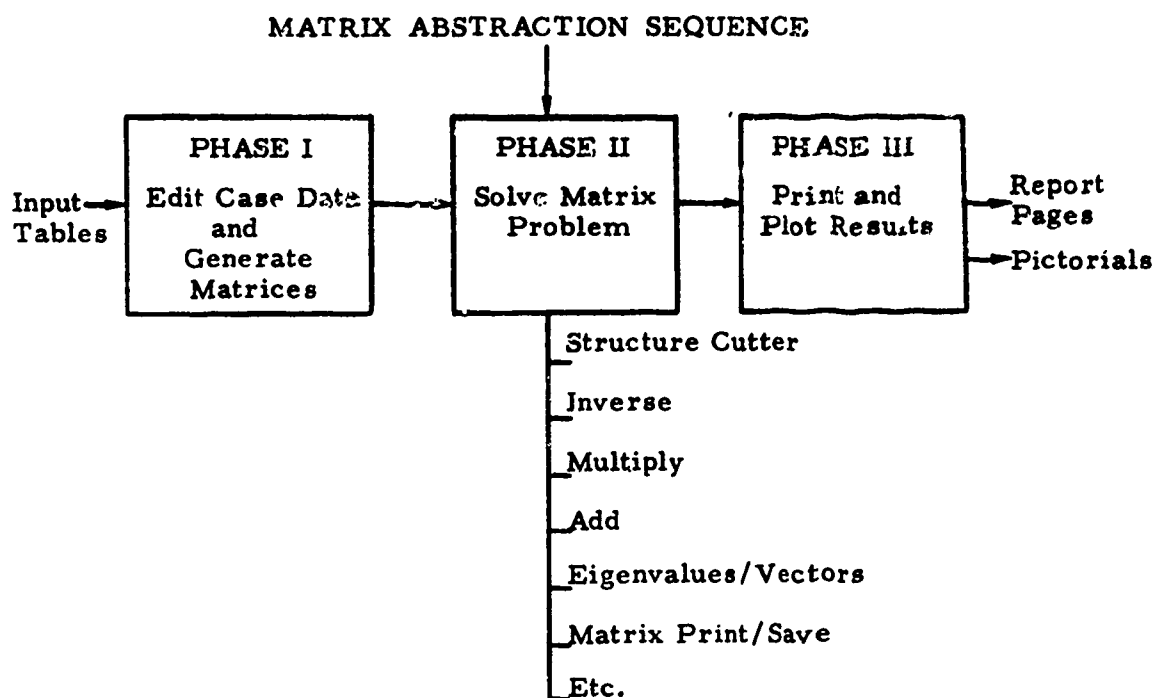


Figure 8. Operation of the FORMAT System

One of the objectives of FORMAT is to eliminate the delays associated with communications between special purpose programs. The idea is to take maximum advantage of the generality and flexibility of matrix abstraction techniques and the creativity of skilled engineers to apply the latest technology and most efficient approach to each analysis problem. This may not be optimum use of machines but it is best use of calendar time, technology and manpower in system development. We are currently adding other interpreters to provide for the aerodynamic influence coefficients and static aeroelastic solutions.

Figure 9 summarizes application of FORMAT in a production operation. Three large analyses are included: approximately 22,000 unknowns or equations in the aft section, and 12,000 unknowns each in the center section and the forward section. Each one of these major sections was analyzed as a series of substructures and at no time did we solve 12,000 equations at one time. The forward section, for example, was done in 9 substructures. Symmetry was accounted for in every substructure where it was applicable. A rather unique idea was used in the aft section: multiple layer substructuring and joining. There are 16 substructures altogether; each one required approximately 2/3 of the FORMAT 7094 capacity. Eight substructures were joined to form a super-substructure A. Another 8 structures were then formed to join a super-substructure B. Then A and B were joined to form the final solution. The complete solution was developed for unit loads on the structure because final external loads were not determined at that time. All of this information is on file as part of a library of 30,000 tapes for use in analysis of future variations of this structure.

Figure 10 is the basis for some remarks regarding the economics of large general purpose programs. Everyone emphasizes machine costs and I find myself very frustrated because I don't believe that is really our problem. The big problem in my job is to design airplanes, and it is very frustrating to see all of the available talent apparently dedicated solely toward reducing computer time. In any case, there are two completely different views of machine costs. One is the cost algorithm; the other is the rental agreement. The two are completely different but related concepts. Two

DOUGLAS DC-10 STRUCTURAL ANALYSIS

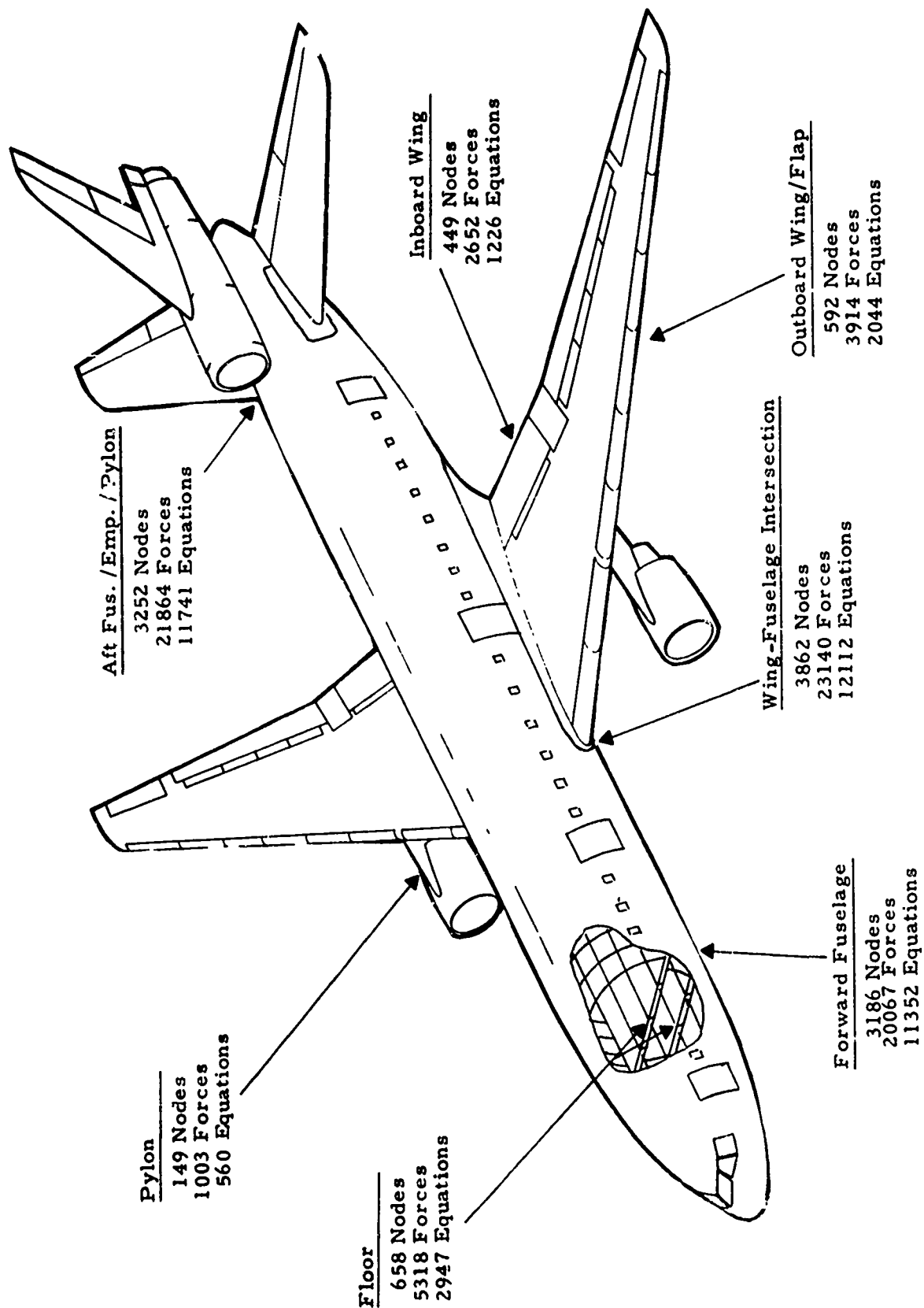


Figure 9. Douglas DC-10 Structural Analysis

MACHINE COSTS

Cost Algorithms

$$\textcircled{1} \quad \$ = f [\text{CPU} + (\text{CORE} + \text{DISK}) (\text{CPU} + \text{I/O})]$$

$$\textcircled{2} \quad \$ = f [\text{CPU} + \text{CORE (CPU)} + \text{DISK} + \text{DRUM}]$$

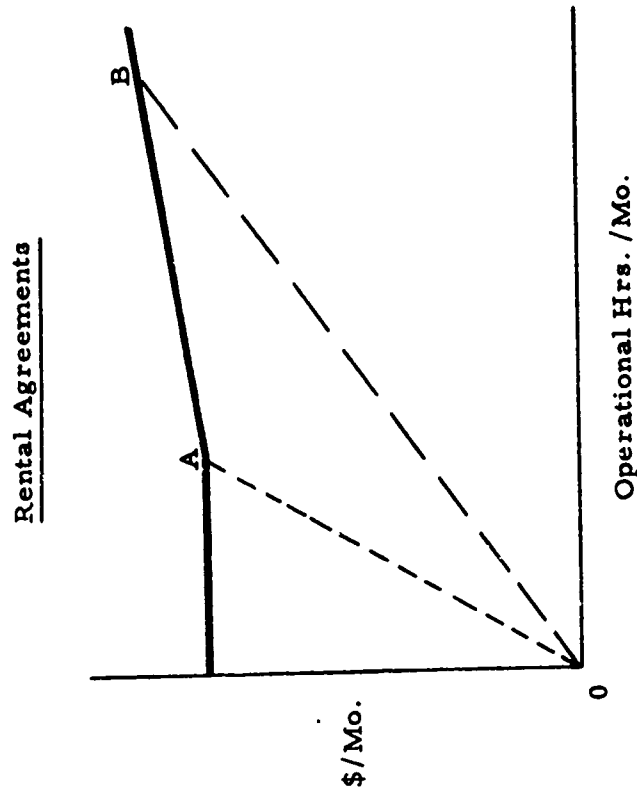


Figure 10. Economics of Large General Purpose Computer Program

families of algorithms are in use, and presumably they reflect the actual performance of the available hardware and software systems. The first algorithm includes a product of two binomials. The result includes coupling terms that don't exist in the other system. The implication of the coupling terms is a charge for resources which are not actually in use but held in reserve during various other activities. The meaning of the cost computed from the algorithm is complicated further by the fact that each term contains an arbitrary factor. The primary criterion in determination of these factors is that total algorithm "cost" for an accounting period must be greater than the actual operational cost.

The rental agreement is the basis of actual machine costs. The most popular agreement is depicted by the solid line. There is a fixed base cost for utilization up to point "A" which represents prime time for a month. Beyond that utilization is an increment of cost based on a rate equal to 10% of the rate indicated by the line \overline{OA} . Most computer installations operate more than one shift and the marginal cost rate applicable for "one more job" is indicated by the line \overline{AB} . For simplicity in allocation of costs, large companies establish the factors in cost algorithms corresponding to the rate indicated by the line \overline{OB} . It is interesting to note that the large general purpose computer program is typically run on Saturdays, Sundays, and at night. This means that the user is served in a manner corresponding to the rate \overline{AB} but "charged" at the overall average rate \overline{OB} . This inequity compensates for the "service \overline{OA} " given to the user of special purpose programs at the "bargain rate \overline{OB} ."

An integrated view of the idiosyncracies of the current machine cost procedures is provided by the following example. We found recently on our latest implementation of FORMAT on the IBM 360 that we could revise the JCL and very significantly alter the apparent cost. In reality we did not change the amount of time that the company was billed for computer utilization, however the algorithm cost that appeared at the end of the output was reduced by 75%. This value certainly cannot be construed as an actual cost savings.

Figure 11 shows data that are more basic to the economics of large computer

ECONOMIC OVERVIEW

<u>Fixed Cost</u>	
• Development	- 500 K\$
• Training	- 50 K\$
<u>Direct Cost (One System)</u>	
• Application	- Computer 500 K\$ Manpower 5,000 K\$
• Maintenance	- 100 K\$
<u>Payoff (Unit)</u>	
• System	- One DC-10 @ 10% = One computer
• Testing	- One Test Condition = 1000 computer hours
<u>Other Factors</u>	
• Generality	
• Flexibility	

Figure 11. An Economic Overview of Large Computer Program Utilization

program utilization. First, it should be noted that these values are indicated with one significant figure. This degree of precision is perhaps an optimistic description of their accuracy, however, there are some very definite trends. In general, these values are an estimate of the cost to develop and use a large general purpose program on an actual production system, and in addition, to provide rationalization for these large expenditures. The FORMAT system development costs were of the order of \$500,000 over a period of three years. Training costs for introduction of this system into our office were of the order of \$50,000. Application of this capability to the first version of the DC-10 involved up to 150 engineers for design analysis and documentation at an approximate cost of \$5,000,000. The computer cost during that same time for all analysis work was approximately \$500,000. The 10:1 ratio applies to every project that we have evaluated. This ratio is my objection to the preoccupation with computer costs. It suggests that we could better invest our efforts by attacking the problem of high manpower cost.

For the sake of perspective regarding computer cost rates in general and the \$500,000 computer application cost above, it is worthwhile to compare unit payoff values to other high rate development considerations. The most significant system consideration is a possible delay in delivery schedule. As indicated, the time value of a DC-10 at current investment rates is approximately equal to the total operating cost rate for a third generation machine.

As a further comparison, an estimate of the relative cost for one test condition on the DC-10 is 1000 computer hours. These comparisons show that computing probably is not the most significant cost consideration in system development. Further, they suggest that method development objectives should give at least equal emphasis to system development schedule and product reliability.

From the viewpoint of overall economics, generality and flexibility in the computer code are intangible but significant. People are the most valuable

resource of an organization and if you provide them with programs that have flexibility and generality, they will find ways to save money and to do better analyses. This reservoir of capability is wasted if they are provided only a black box with restricted input and output slots.

RASHID: I'd like to ask Mac two questions. First, what level of skill and degree of training is required for NASTRAN users; and second, since NASTRAN is not complete, what are the plans for NASTRAN's future development?

MCCORMICK As far as level of training required to use NASTRAN is concerned, that depends a lot on what you're trying to do. I have trained a lot of people at NASA centers and a few people in industry to use NASTRAN (somewhat limited because NASTRAN is not yet widely distributed). My limited experience has been that people can learn to use NASTRAN fairly easily up to the level of their ability and by this I mean that you can't get away from the need for engineering judgment in order to model the structure and understand what you're doing. But as far as learning to use NASTRAN itself, I have really not seen any serious difficulty. NASTRAN is not completed, and never will be of course, since continuing development is envisioned. As far as NASA's plans for NASTRAN I, it was released last December (1969) to a limited number of primary government agencies and aerospace contractors for the purpose of evaluation. The evaluation is now complete and a new level is being prepared which I presume will be released sometime this fall (1970). Recently, Langley Research Center has agreed to accept the management of NASTRAN and I presume it will continue to be distributed by COSMIC in the usual way for NASA programs.

Earlier today Bob Melosh commented that no computer programs make decent checks on whether the answers are any good. What checks should be made to insure that the answers are meaningful?

MELOSH: With respect to the checks that should be used, let me say that there should be sufficient checks to perform three functions:

(1) to identify magnitudes of the errors due to the various source of the error; (2) to identify from the user's point of view the magnitude of the errors of displacements and the magnitudes of errors in stresses, eigenvalues, eigenvectors, etc; and (3) there ought to be error measures that provide some information for future correlation regarding the errors which may be found in future problems. That is, some kind of measure which tells you that if you solve a problem of such and such order of such and such complexity that then you can expect, based upon a statistical study, that the errors will be of such and such a magnitude based upon the precision that you are using in your installation.

The checks I like are energy checks for displacements, and a combined energy and generalized force precision check for stresses. The effectiveness of these checks is reported in a Contractor's Report to NASA/GSFC to be published soon.

Well, now I think I'd like to ask a question of Steve. How should structural input be organized to minimize user errors?

JORDAN: In the MAGIC system we felt that input data should be organized on the concept of preprinted or permanently labeled printed input data forms. Figure 12 shows the kind of concept that I mean. I might note that the keypunchers punch directly from these forms. This particular form is used for input into our material library and I'll just go through it real quickly. It's prelabeled at the top MATER. The slash next to that block and these blocks down here are what indicate to the keypuncher to proceed to the next IBM card for punching of subsequent data. The sheets are permanently layed out in this manner and the analyst has an exact position in which to delineate each input item. The computer output for this particular form is shown in Figure 13.

I have a question which Dale has partially answered already. In your experience have you found that FORMAT in effect has a major impact on design or something like the DC-10 and really does it save money for the

MAGIC STRUCTURAL ANALYSIS SYSTEM

INPUT DATA FORMAT

7 8 9
No. of Requests
(1)

MATERIAL TAPE INPUT

[illegible]

MATERIAL PROPERTIES TABLE

TEMPERATURE									
1									
3	4	5	6	7	8	9	0	1	2

Direction

23

[illegible][illegible][illegible]

2X

[illegible]

22

POISSONS RATIOS					
	3	4	5	6	7
1	3	4	5	6	7
2					
3					
4					
5					
6					
7					
8					
9					
10					
11					
12					
13					
14					
15					
16					
17					
18					
19					
20					
21					
22					
23					
24					
25					
26					
27					
28					
29					
30					
31					
32					
33					
34					
35					
36					
37					
38					
39					
40					
41					
42					
43					
44					
45					
46					
47					
48					
49					
50					
51					
52					
53					
54					
55					
56					
57					
58					
59					
60					
61					
62					
63					
64					
65					
66					
67					
68					
69					
70					
71					
72					
73					
74					
75					
76					
77					
78					
79					
80					
81					
82					
83					
84					
85					
86					
87					
88					
89					
90					
91					
92					
93					
94					
95					
96					
97					
98					
99					
100					

3

[illegible]

11

[illegible]

Figure 12 Material Tape Input

RELATIONSHIP OF THE

[illegible]

1 77390 5.28104

Reproduced from
ship copy.

0101131

501-252-0000

62-1177-1-Sub C-1134

[illegible]

75-13698	66	1000011-9
75-13697	66	1000011-9
75-13696	66	1000011-9
75-13695	66	1000011-9
75-13694	66	1000011-9
75-13693	66	1000011-9
75-13692	66	1000011-9
75-13691	66	1000011-9
75-13690	66	1000011-9
75-13689	66	1000011-9
75-13688	66	1000011-9
75-13687	66	1000011-9
75-13686	66	1000011-9
75-13685	66	1000011-9
75-13684	66	1000011-9
75-13683	66	1000011-9
75-13682	66	1000011-9
75-13681	66	1000011-9
75-13680	66	1000011-9
75-13679	66	1000011-9
75-13678	66	1000011-9
75-13677	66	1000011-9
75-13676	66	1000011-9
75-13675	66	1000011-9
75-13674	66	1000011-9
75-13673	66	1000011-9
75-13672	66	1000011-9
75-13671	66	1000011-9
75-13670	66	1000011-9
75-13669	66	1000011-9
75-13668	66	1000011-9
75-13667	66	1000011-9
75-13666	66	1000011-9
75-13665	66	1000011-9
75-13664	66	1000011-9
75-13663	66	1000011-9
75-13662	66	1000011-9
75-13661	66	1000011-9
75-13660	66	1000011-9
75-13659	66	1000011-9
75-13658	66	1000011-9
75-13657	66	1000011-9
75-13656	66	1000011-9
75-13655	66	1000011-9
75-13654	66	1000011-9
75-13653	66	1000011-9
75-13652	66	1000011-9
75-13651	66	1000011-9
75-13650	66	1000011-9
75-13649	66	1000011-9
75-13648	66	1000011-9
75-13647	66	1000011-9
75-13646	66	1000011-9
75-13645	66	1000011-9
75-13644	66	1000011-9
75-13643	66	1000011-9
75-13642	66	1000011-9
75-13641	66	1000011-9
75-13640	66	1000011-9
75-13639	66	1000011-9
75-13638	66	1000011-9
75-13637	66	1000011-9
75-13636	66	1000011-9
75-13635	66	1000011-9
75-13634	66	1000011-9
75-13633	66	1000011-9
75-13632	66	1000011-9
75-13631	66	1000011-9
75-13630	66	1000011-9
75-13629	66	1000011-9
75-13628	66	1000011-9
75-13627	66	1000011-9
75-13626	66	1000011-9
75-13625	66	1000011-9
75-13624	66	1000011-9
75-13623	66	1000011-9
75-13622	66	1000011-9
75-13621	66	1000011-9
75-13620	66	1000011-9
75-13619	66	1000011-9
75-13618	66	1000011-9
75-13617	66	1000011-9
75-13616	66	1000011-9
75-13615	66	1000011-9
75-13614	66	1000011-9
75-13613	66	1000011-9
75-13612	66	1000011-9
75-13611	66	1000011-9
75-13610	66	1000011-9
75-13609	66	1000011-9
75-13608	66	1000011-9
75-13607	66	1000011-9
75-13606	66	1000011-9
75-13605	66	1000011-9
75-13604	66	1000011-9
75-13603	66	1000011-9
75-13602	66	1000011-9
75-13601	66	1000011-9
75-13600	66	1000011-9
75-13599	66	1000011-9
75-13598	66	1000011-9
75-13597	66	1000011-9
75-13		

1968 A13124 B

卷一

INDEX

[illegible][illegible]

~~It may be noted that the above information is confidential and its disclosure would be injurious to the national defense.~~

company or is analysis still done to a large extent after the fact?

WARREN: I'm glad you asked that question. Yes, the analysis work that we are doing on this system does have a direct impact on the design. Every piece of the structure has been analyzed at least twice: the first time with a rough grid system to make very basic design decisions, and a second time to make refinements such as selection of material gages. For example, the rough grid case on the aft section of the DC-10 determined the number of vertical spars in the vertical stabilizer which corresponds to the number of rings in the inlet tube; this was a very fundamental decision in the structural design. The wing fuselage intersection was studied in detail using a rough grid system prior to the decision to proceed on the program. Using the method of subsequent modifications, 46 configurations were studied parametrically to optimize the detailed framing of the fuselage intersection.

I have a question for Joe. I would think that as a consultant that occasionally you have a customer asking for a capability outside the family of special purpose programs that you have. Don't you on these occasions wish that you had a general purpose program handy so that you could grind out some numbers rather than write a program on the spot?

RASHID: If I don't have among the family of programs in my possession a special purpose program that handles the problem, then I must do with what I have using my engineering judgment and intuition. Moreover, if such a problem occurs very often, then I must develop a special purpose program for the class of problems, in which that particular problem belongs.

WARREN: I think it's time to open the discussion to the floor.

QUESTION: We operate in the environment most of these gentlemen in the room operate in and it's been our experience to have programs running today and they won't run tomorrow because we have a system change. What problems do you have getting a big code like NASTRAN from one system

to another?

COMMENT: NASTRAN is written almost entirely in FORTRAN IV. You need to do something like this just to be able to operate on the number of computers that we run across. We use a subset of FORTRAN IV actually. We had to do that in order to get across the machines. Furthermore, we tried to hold down machine dependent FORTRAN operations that programmers like to use so that we would have minimum effect from changes of one sort or another when they change levels. Not only do operating systems change, the FORTRAN compilers change too. We looked at this very carefully in the beginning and we've had minimum difficulty with it in NASTRAN, but it could cause you trouble. Originally, I felt that we needed more assembly language in NASTRAN than we currently have. There is no assembly language in any of the functional modules in NASTRAN. The only machine language in NASTRAN in the released versions from NASA are in places where we have to interface with the resident operating system for such things as the date and time, availability and kind of secondary storage, and so forth. On the other hand, I have found that, while it isn't necessary, you can certainly improve the efficiency of the program if you're willing to do one or two other things in assembly language. For instance, in the 360 version, the IO package is all FORTRAN and the packing is all FORTRAN. We have recently been playing around with some assembly language for the IO package and it substantially improves things.

QUESTION: I wanted to ask Mr. Warren a question. How can you sleep peacefully knowing that you have 30,000 tapes that you might have to read tomorrow? And what are the chances that just one of these tapes won't read and all your two months effort is wasted?

WARREN: We have a calculated risk procedure that we use on tapes and when we do update tapes we use the same concept that is used by systems people; that is we maintain a father and grandfather according to a standard plan. We do this as a calculated risk based on how much it costs to generate a tape. If it's not too much, we may not maintain backups. To my knowledge, the only times we have ever suffered were because a tape was

lost in the library system, not because it was unreadable.

QUESTION: I have a particular question for Bob Melosh. I want to congratulate you, Bob, for spending a large part of the day in making a lot of people feel nervous about what they have been doing in the past. Many who have been more or less deluding themselves are exposed in a certain way. I feel a little bit exposed about a comment that you made earlier about the reaction check in general not being a worthwhile thing put into a general or special purpose program. I've found it to be a pretty valuable tool myself so I'm one of those who has been deluding himself for quite awhile. Would you explain why?

MELOSH: The central idea is that when you calculate the reactions you are differencing displacements that are generally small because those are the displacements near the reactions. Essentially you are doing something comparable to an estimation of strain by differencing displacements, or if you like, you are predicting a stress even though it looks like a generalized force. Take a simple problem like a cantilevered beam. When you consider the differencing of displacements at the root, these data give you no idea what the accuracy will be when you differentiate displacements at the tip. It is much better, of course, to take a complete residual check and check it over the whole structure. Unfortunately, that doesn't test whether the displacements are meaningful or not, it only tests whether there is any meaningful data for differentiation. You can have very accurate displacements and still get very poor stresses.

QUESTION: Regarding the element library and a general purpose program being as general as possible, I would like to know why so many general purpose programs wind up with fixed numbers of degrees of freedom usually built into the coding?

MCCORMICK: In NASTRAN it's going to be changed as soon as possible in order to accommodate the newer elements.

COMMENT: Earlier the question was raised as to how much effort is required to train a man to use NASTRAN. I guess I'm one of those who attended a two week class with others having levels of sophistication ranging from very experienced people to people who had never used a general purpose program. Within the rigid format part of NASTRAN, they all now use it with reasonable success. It's a good self-teacher too. When you do make a mistake, the diagnostics generally guide you to the correct input. I would say it teaches rather easily on the superficial level and people are now beginning to get more aggressive and have begun rearranging it themselves.

QUESTION: I want to direct a question to Dr. Melosh. In the beginning I was almost in agreement with you not to check the reactions, however, I think this story has gone a little bit in the wrong direction. My understanding of any problem of structural analysis is that one of the very first prerequisites that must be satisfied in order to have at least a chance for a unique solution is the equilibrium of the entire system. Now if you don't go through the equations, don't compare them to applied loading, then you really don't know anything about the solution. I think the first prerequisite for a solution to be unique is the equilibrium, so I consistently check it. I wonder why you insist that we don't have to check reactions?

MELOSH: Well, reaction checks may be good confidence builders but they don't necessarily correlate with accuracy. You can satisfy reaction checks very well and have very bad results and the converse can be true. So, if you want a reliable indicator that sometimes will make you feel happy, then stay with reaction checks. Reaction checks are checks on your ability to predict strains, not your ability to predict displacements, and if you're interested in displacements you may throw out a good analysis because you made a reaction check that you didn't like.

COMMENT: I disagree for the reason that the finite element method for each joint actually solves equilibrium equations. If you turn to your original stiffness matrix, put in displacements, then compute the reactions based on discrete equilibrium, it has nothing to do with the strains. Strains are the consequences of that. As a matter of fact, if you compute strains

near the boundaries where these reactions are computed, they are worthless because you almost never predict stresses correctly except some place in the middle of the element. Yet the reactions very correctly satisfy the equilibrium at each of these nodal points. Therefore, they are not related to strains at all at their particular boundary.

MELOSH: Since reactions are calculated by differencing deflections, they are comparable to strains in a numerical sense. It is in this sense that I have used the term strain. It is true that the "closure" of the analysis does not depend on approximations used to relate strain (or stress) to the generalized forces (reaction) of the element.

JORDAN: I think we're missing one important point. Regardless of the accuracy check aspects, reactions are very useful information to the stress analyst along with element forces, and it doesn't hurt him to point them out. In fact in most cases, they serve as viable equilibrium checks. I don't feel that we should throw them out just because they might be inaccurate in some cases.

MELOSH: We shouldn't use that for our criterion for accuracy. That's what I'm saying.

JORDAN: I agree; however, they can act as a criteria for accuracy.

WARREN: I'd like to briefly summarize. You should be aware that most of the members of the panel have mentioned privately that they believe that this issue of special purpose versus general purpose computer programs is a fabricated one. There is a place for each kind of program, and there is a place for each kind of analysis work. From my point of view, in the final analysis it's all based on cost effectiveness of the whole system and that means the people, the available computers, and the problem at hand. This certainly puts the demand on the special analytical approaches that provide more guidance for the user in modeling his problems to analyze them either by special purpose or general purpose programs. I'd like to close the meeting and thank the members of the panel.

The following statement was prepared by Dr. Neil Prince of Gulf General Atomic to support the position of Dr. Rashid and to demonstrate some of the benefits of special purpose programs.

Statement by N. Prince on

Special Purpose Shell Program SHELL-3D

The production version, SHELL9, of the special purpose finite element shell analysis program SHELL-3D developed at Gulf General Atomic is operational. Very briefly, SHELL9 is particularly well suited for intersecting three-dimensional thin shells with any desired loading distributions. The basic element is a triangular plate with cubic membrane and cubic bending polynomial displacement fields. SHELL9 results in 3 displacements, 3 rotations, and 3 membrane strains computed in the nodal surface coordinate directions.

Some interesting and informative analysis results have been obtained with SHELL9. Fig. 1 shows the computer graphics generated finite element mesh for a quarter of a nozzle-to-cylinder intersection structure that has been experimentally investigated at Oak Ridge National Laboratory for an internal pressure of 50 psi. The idealization consists of 291 nodal points and 493 elements.

Comparison of the SHELL9 model inside and outside surface axial and circumferential stresses with experimental data in the vicinity of the intersection for the longitudinal and transverse planes are shown in Figs. 2, 3, 4 and 5.

These plots are useful for observing the stresses as a function of one parameter but they do not show the distribution of the stresses throughout the shell. The capability of visualizing the surface stress distribution, for instance, in the vicinity of an intersection, is a very important consideration in fully utilizing a special purpose three-dimensional shell program. For this reason, orthographic projection plotting of the surface stress contours has been included as a necessary adjunct to the SHELL-3D program.

Typical examples of computer generated plots for the nozzle-to-cylinder problem are shown in Figs. 6, 7, 8 and 9. The projection of different viewing planes, magnifications, and removal of hidden lines allows a wide variety of options for the analyst to use in viewing the numerical results at critical regions of interest.

SHELL-3D NOZZLE-TO-CYLINDER INTERSECTION MESH

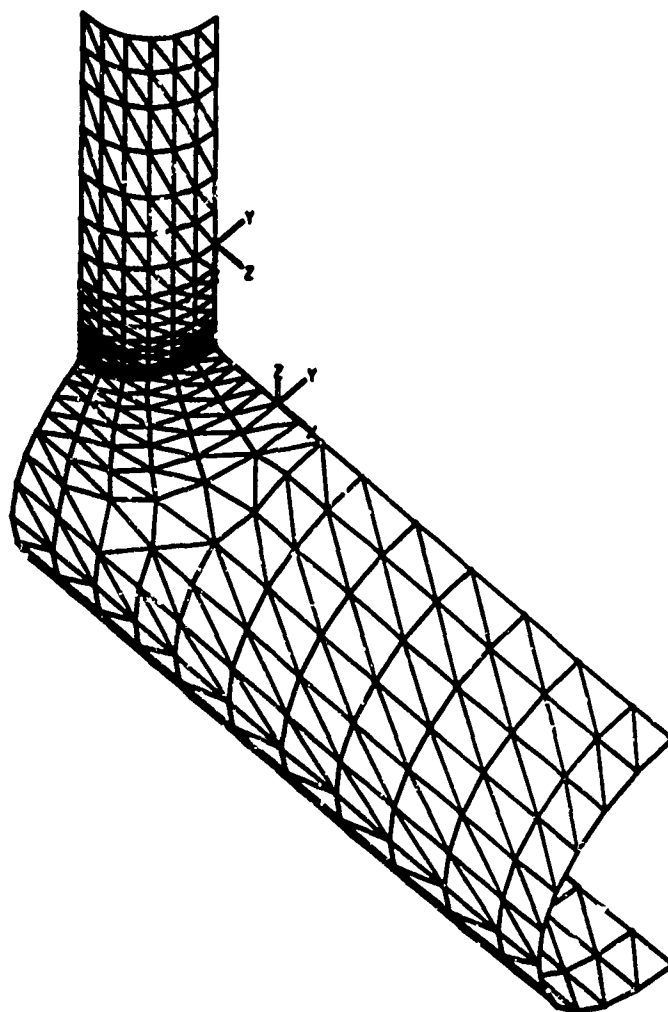


Fig. 1

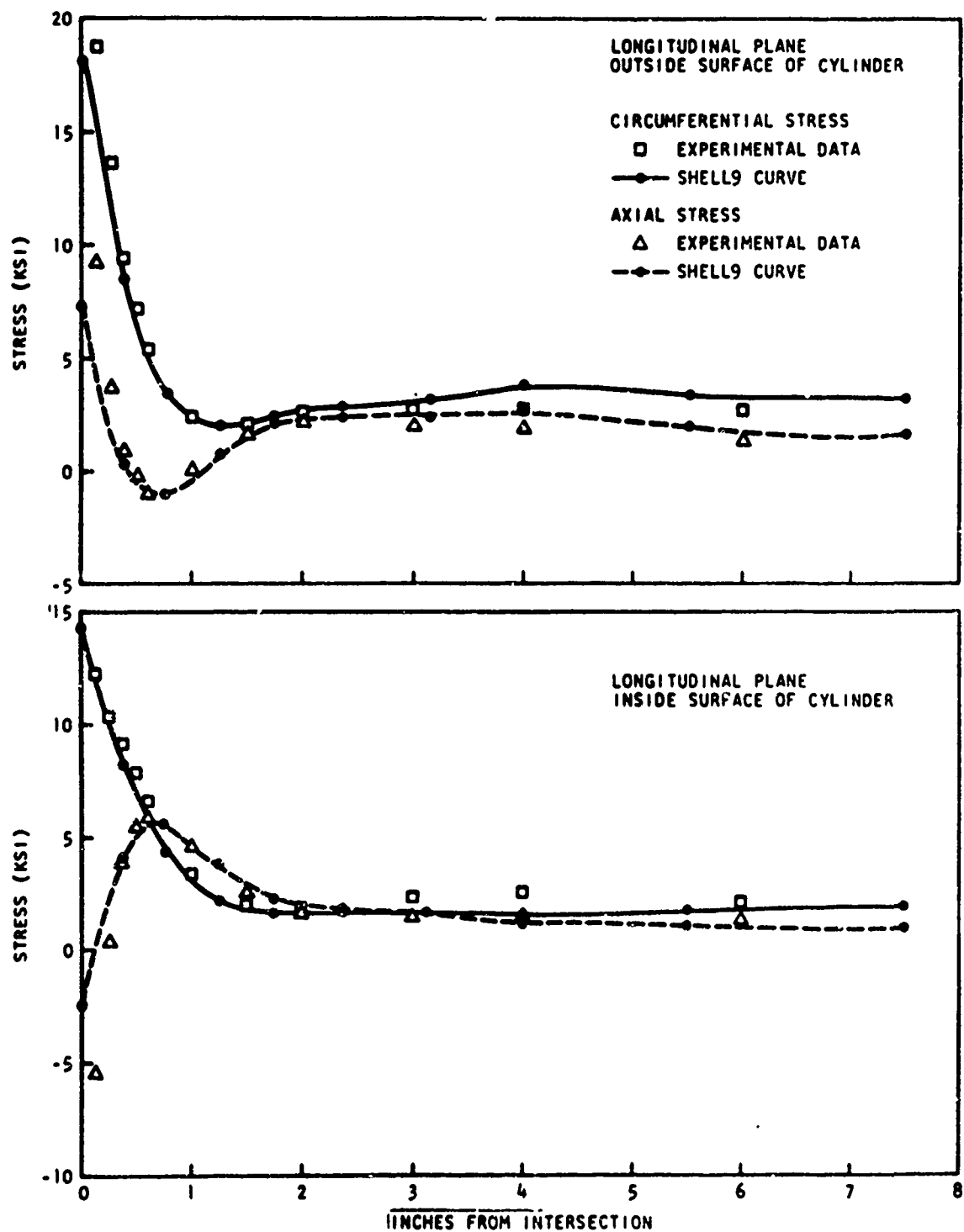


Fig. 2 - Cylinder stresses along longitudinal plane

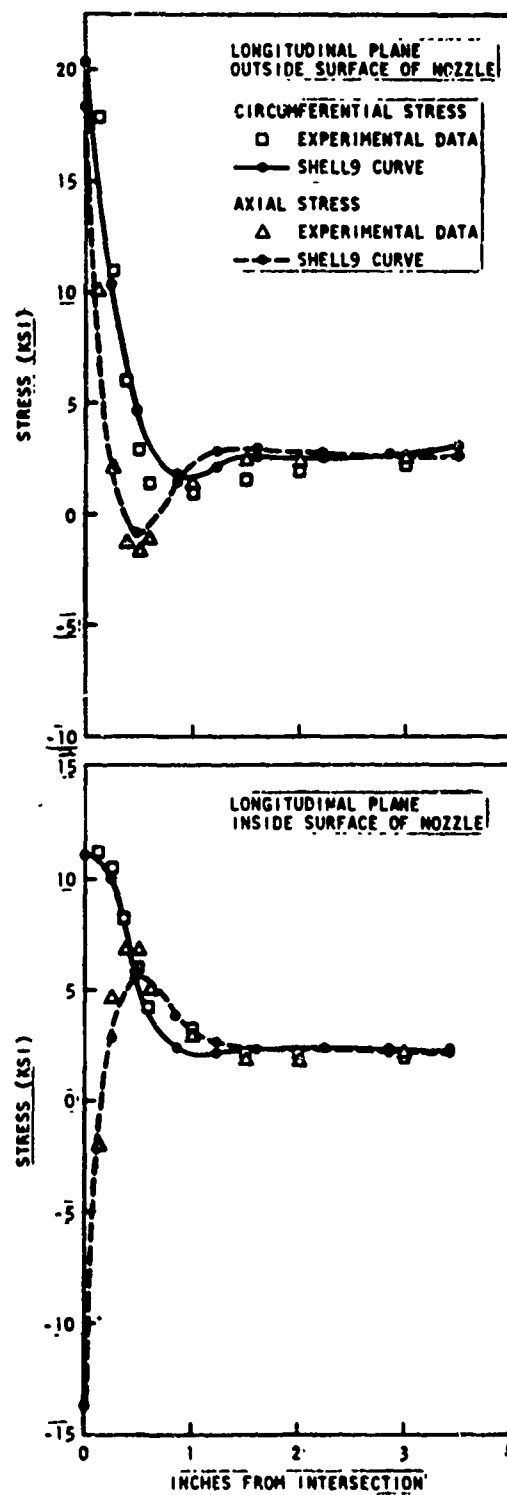


Fig.3 - Nozzle stresses along longitudinal plane

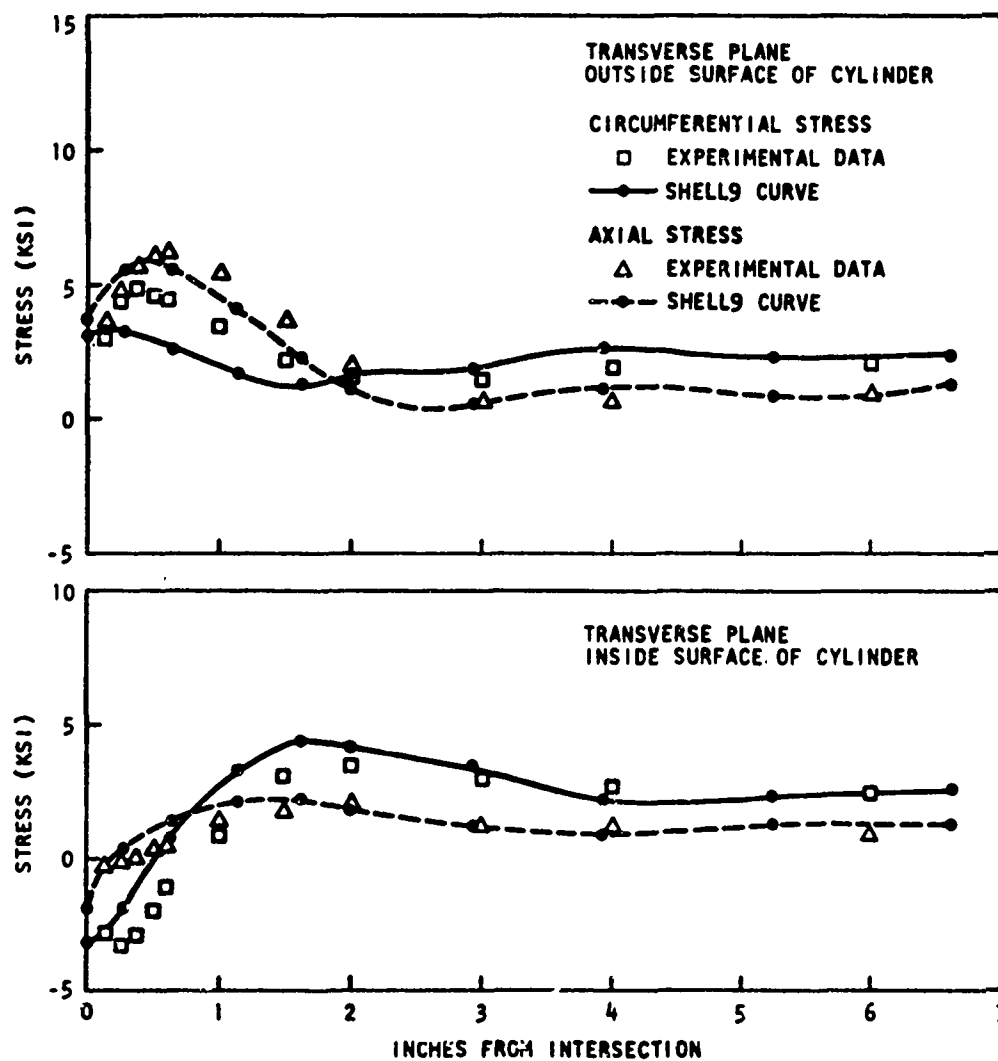


Fig. 4 - Cylinder stresses along transverse plane

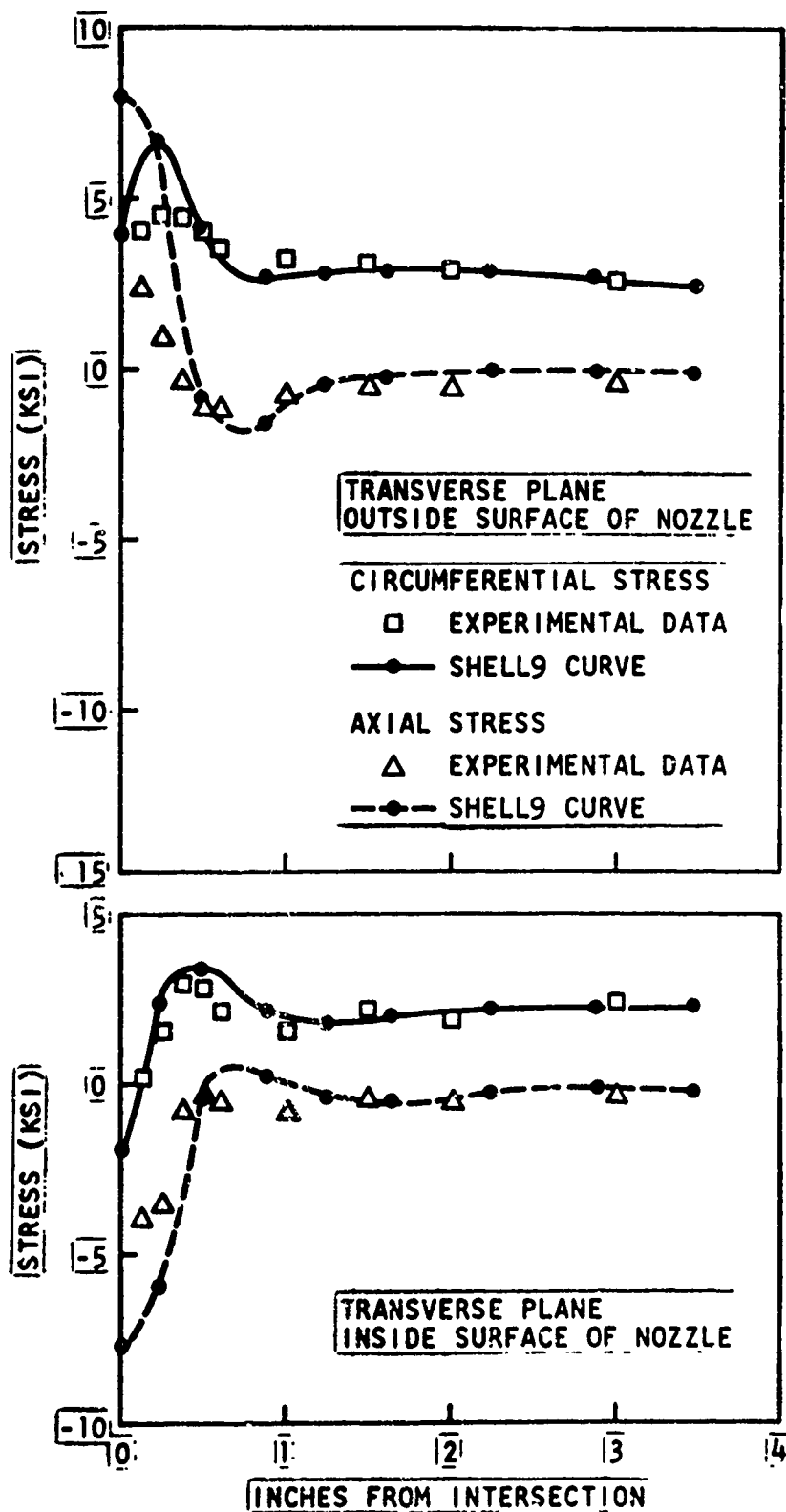


Fig. 5 ~ Nozzle stresses along transverse plane

NOZZLE-TO-CYLINDER INTERSECTION STRESSES

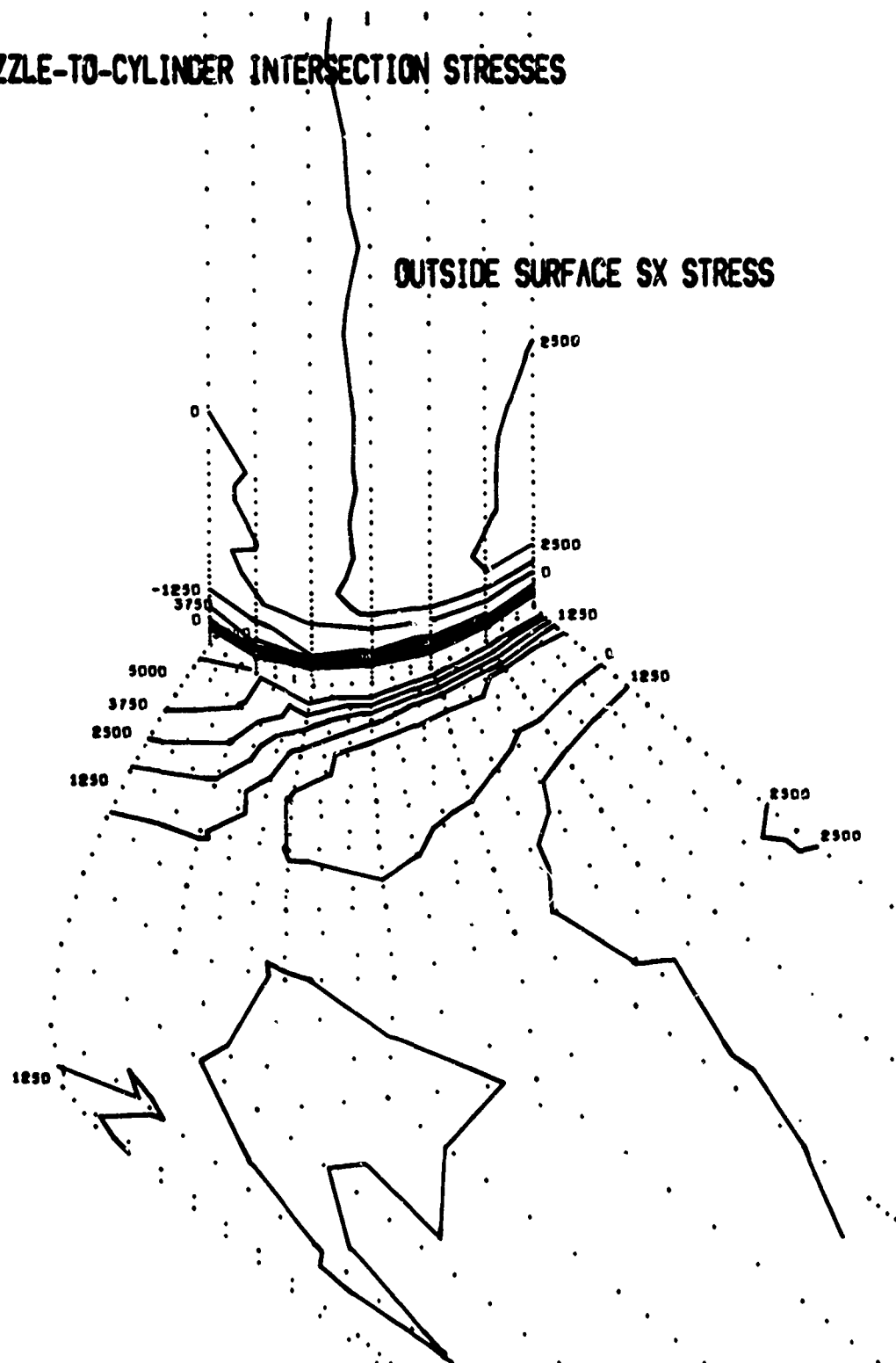


Fig.6 - Outside surface axial stress contours

NOZZLE-TO-CYLINDER INTERSECTION STRESSES

INSIDE SURFACE SX STRESS

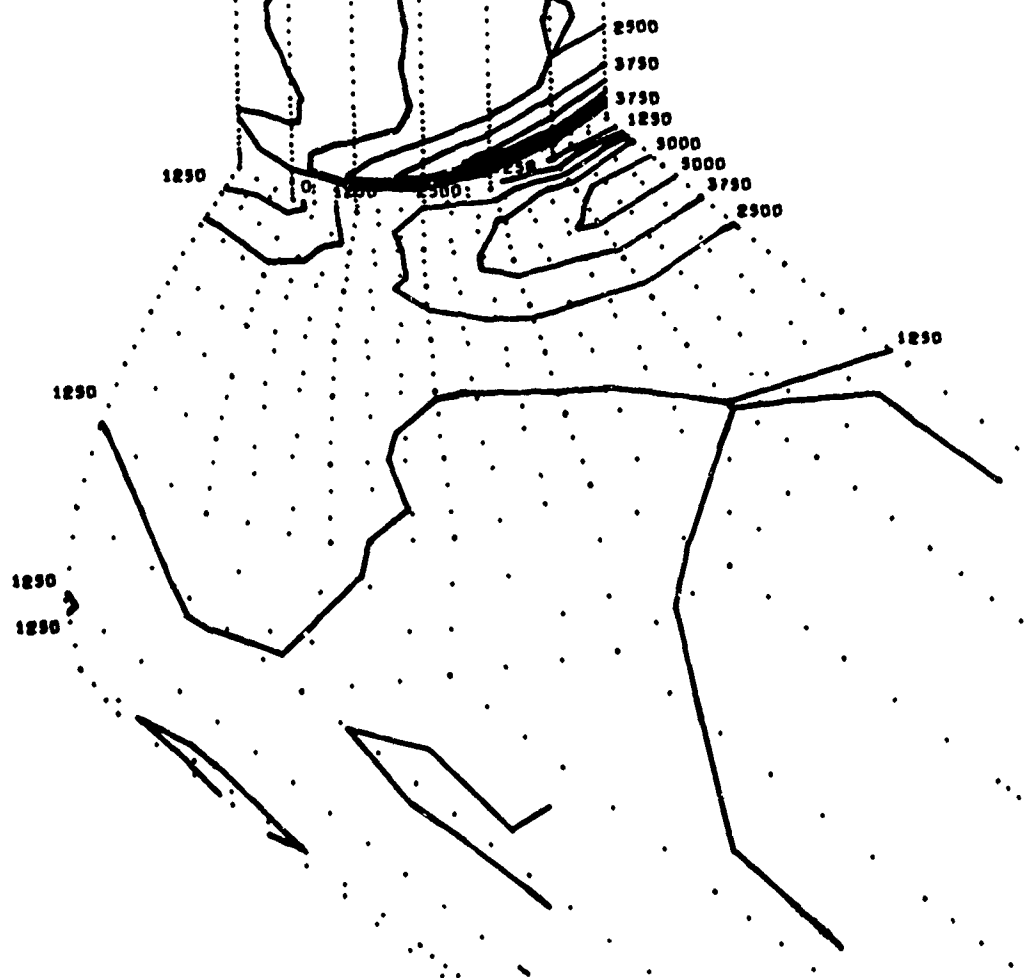


Fig.7 - Inside surface axial stress contours

NOZZLE-TO-CYLINDER INTERSECTION STRESSES

OUTSIDE SURFACE SY STRESS

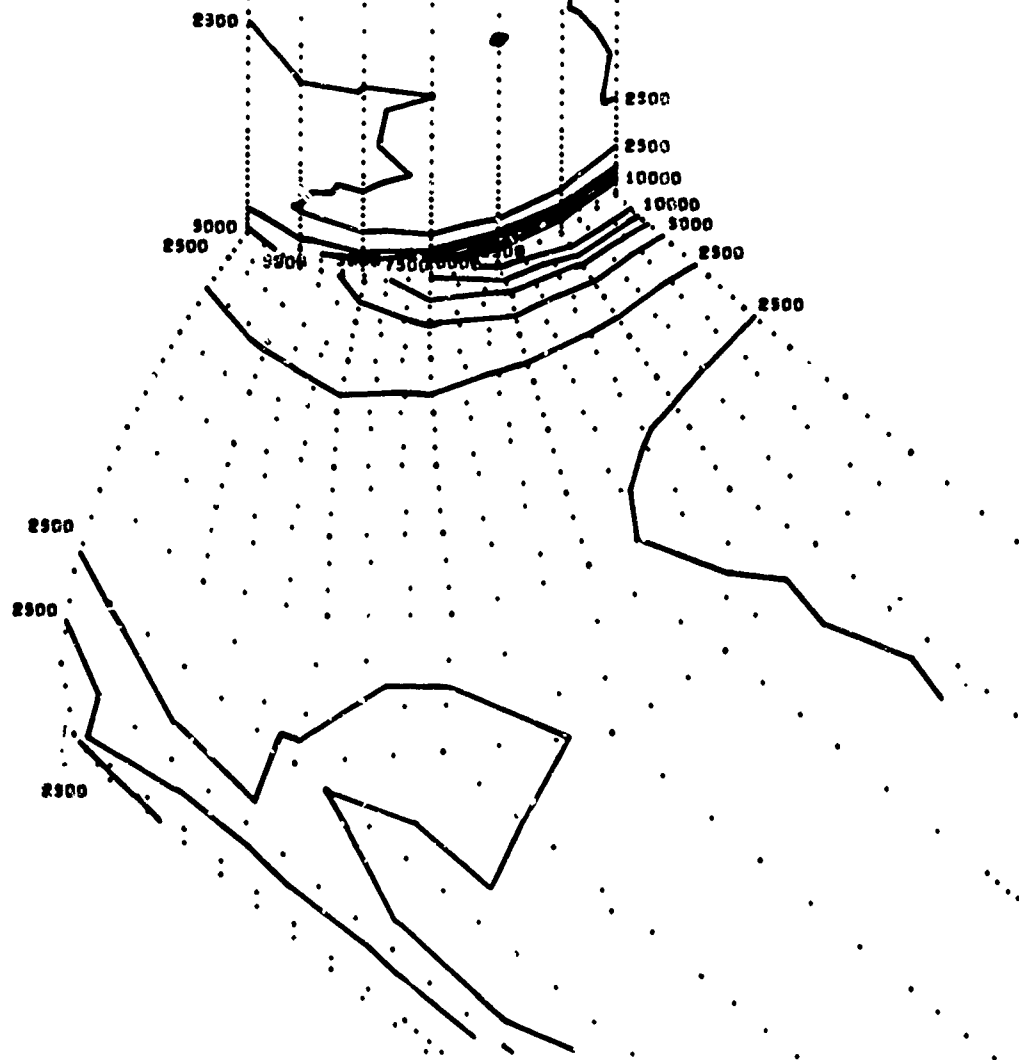
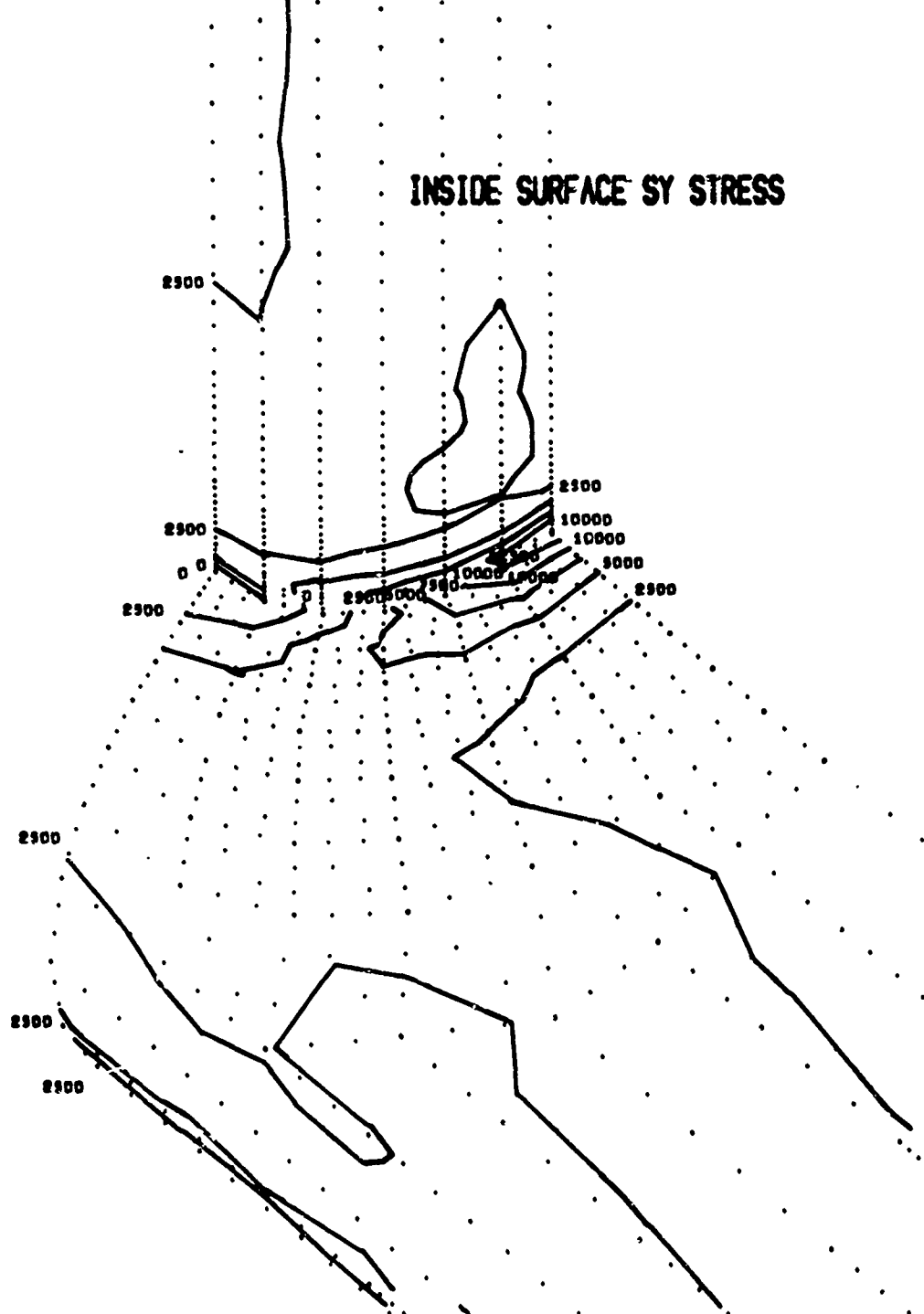


Fig.8 - Outside surface circumferential stress contours

INSIDE SURFACE SY STRESS



1106

IMPERFECTION SENSITIVITY OF ELASTIC STRUCTURES:
THE SECOND APPROXIMATION FOR UNIQUE MODE BUCKLING

Gerald A. Cohen
Structures Research Associates
Newport Beach, California

Abstract

It is shown that the usual Koiter-type expansion relating the load factor to the amplitude of the bifurcation mode contribution to equilibrium displacements becomes ambiguous when higher order terms are retained. In order to obtain a second approximation for limit loads associated with small finite imperfections in axisymmetric structures with unique harmonic bifurcation modes, a relationship between the load factor and the work deflection, valid for imperfect structures at loads in the vicinity of the bifurcation load of the perfect structure, is derived. Since the work deflection has physical meaning, this relation is unique and can be used to obtain the limit load as the maximum value of the load factor. The resulting expression for the limit load factor is of the same form as that obtained in a previous paper in which a second imperfection parameter β was introduced but was obtained without consideration of all the contributing terms. Thus, the present result corrects the formula for β given previously. An interesting aspect of the result relates to the special case of a linear prebuckling state with negligible prebuckling deformations of the perfect structure, and imperfection displacements proportional to its buckling mode displacements. In this case, the parameter β reduces to zero, so that the second approximation coincides with the first approximation. In contrast, the generally accepted result for this case, given by Budiansky and Hutchinson, implies a β -value of unity. In light of the present result, their result does not appear to be a self-consistent approximation.

I. Introduction

In a previous paper (Ref. 1) Koiter's asymptotic imperfection theory for unique mode buckling was rederived using the series expansion approach of Budiansky and Hutchinson (Ref. 2). This theory allows, through an analysis of the perfect structure, the approximate calculation of limit buckling loads of geometrically imperfect structures in the vicinity of simple bifurcation loads of the corresponding perfect structure. The first-order results presented there for the limit load [Eqs. (37) and (38) of Ref. 1] are included in Koiter's somewhat more general formulas [Eqs. (45.5) and (45.10) of Ref. 3]. In an attempt to improve the

To be presented at the Conference on Computer-Oriented Analysis of
Shell Structures, Palo Alto, August 1970

accuracy of these formulas when the limit load is not in the immediate vicinity of the bifurcation load, a second imperfection parameter β was introduced in Ref. 1. However, as noted there, this did not constitute a consistent second approximation, since terms tacitly neglected in the assumed displacement expansion contribute to this approximation. On the other hand, computer results (Refs. 4 and 5) based on the β -formula of Ref. 1 suggest that for many shells, for imperfections large enough to produce realistic buckling load knockdowns of 0.6 or less, a second approximation is necessary for an accurate calculation of the limit load.

In this paper, a consistent second approximation for limit loads due to imperfections in axisymmetric structures having unique harmonic bifurcation modes is derived. In the usual Koiter theory only the dominant terms are retained in the equilibrium relation between load factor λ and expansion parameter ξ , where ξ is the amplitude of the contribution of the perfect structure buckling mode to equilibrium states of the imperfect structure, and the maximum value of λ with respect to ξ defines the limit load. When higher order terms are retained, the λ - ξ relation becomes ambiguous, since the coefficients of these terms are not uniquely defined, and therefore cannot be used directly to obtain the limit load. Instead, the mathematical parameter ξ is eliminated in favor of the "work deflection" Δ , defined so that the area under the λ - Δ curve represents the work of the external loads. The λ - Δ relation, being a relation between physically meaningful quantities, is unique, and the limit load can then be determined as the maximum value of λ with respect to Δ .

The analysis of this paper is divided into five parts: 1) Development of a consistent second approximation λ - ξ relation, by a straightforward extension of Koiter's original method; 2) Rederivation of this approximation by extending the series expansion method of Ref. 1; 3) Reconciliation of the results of parts 1 and 2; 4) Derivation of the corresponding λ - Δ relation for axisymmetric structures; and 5) Calculation of the limit load and deflection from this relation.

II. Koiter Theory for Unique Mode Buckling

As in Ref. 3, the potential energy Π of an imperfect structure is expressed in terms of the potential energy P of a model or perfect structure as

$$\Pi(U) = P(U) + \bar{\xi}Q(U) + O(\bar{\xi}^2) \quad (1)$$

Here U represents the displacement field of the structure due to load, $\bar{\xi}$ is an imperfection amplitude, and Q is a functional of U which also depends on the imperfection shape \bar{U} . For an investigation of equilibrium states for which the displacements differ only slightly from the prebuckling displacements u_0 of the model, it is convenient to express U by

$$U = u_0(\lambda) + u \quad (2)$$

where λ is the load factor for a proportional load system. As discussed in Ref. 3, the integrands of the functionals $P(u_0+u)$ and $Q(u_0+u)$ may be expanded to give

$$\begin{aligned} \Pi(u_0(\lambda)+u) = & P(u_0(\lambda)) + \bar{\xi}Q(u_0(\lambda)) + P_1^\lambda[u] + P_2^\lambda[u] + P_3^\lambda[u] + P_4^\lambda[u] \\ & + \bar{\xi}\{Q_1^\lambda[u] + Q_2^\lambda[u] + Q_3^\lambda[u] + Q_4^\lambda[u]\} + O(\bar{\xi}^2) \end{aligned} \quad (3)$$

where $P_m^\lambda[u]$ and $Q_m^\lambda[u]$ are homogeneous functionals of degree m in the displacements u and their derivatives. The dependence of these functionals on λ is indicated by the superscript λ ; henceforth the symbols P and Q without the superscript λ will denote evaluation of these functionals at the bifurcation load $\lambda = \lambda_c$ of the model.

According to the principle of minimum potential energy, of all the kinematically admissible displacement fields u , those which extremize Π at a constant value of λ determine equilibrium states of the structure. Since for a given value of λ , the first two terms on the right-hand side of Eq. (3) are constant, they do not affect the extremization of Π and can therefore be disregarded. Furthermore, since $u_0(\lambda)$ is an equilibrium state of the model, the first-order change in its potential energy, viz. $P_1^\lambda[u]$, vanishes. For an investigation of the equilibrium states at loads in the vicinity of $\lambda = \lambda_c$, the remaining terms of Eq. (3) are expanded in a Taylor series about $\lambda = \lambda_c$, to give

$$\begin{aligned} F^\lambda[u] \equiv \Pi(u_0+u) - \Pi(u_0) \\ = P_2[u] + (\lambda - \lambda_c)P_2'[u] + (1/2)(\lambda - \lambda_c)^2P_2''[u] + \dots \\ + P_3[u] + (\lambda - \lambda_c)P_3'[u] + \dots + P_4[u] + \dots + \bar{\xi}\{Q_1[u] \\ + (\lambda - \lambda_c)Q_1'[u] + \dots + Q_2[u] + \dots + O(u^3)\} + O(\bar{\xi}^2u) \end{aligned} \quad (4)$$

where the omitted terms are higher degree in $(\lambda - \lambda_c)$.

Following Koiter, the extremization of $F^\lambda[u]$ with respect to u is performed in two steps. For this purpose, u is decomposed into a component proportional to u_1 , the buckling mode displacements of the model, and a kinematically admissible component \bar{u} orthogonal to u_1 in some sense but otherwise arbitrary, i.e.

$$u = \xi u_1 + \bar{u} \quad (5)$$

The orthogonality of \bar{u} and u_1 is expressed in terms of a bilinear functional $T_{11}[u, v]$ by

$$T_{11}[u_1, \bar{u}] = 0 \quad (6)$$

The quadratic functional $T_2[u]$ from which $T_{11}[u,v]$ is derived is supposed to contain all the arguments of $P_2[u]$ and should be positive-definite but is otherwise arbitrary. In general, doubly-subscripted functionals are defined by the expansion

$$S_m[u+v] = S_m[u] + S_m[v] + \sum_{k=1}^{m-1} S_{m-k,k}[u,v] \quad (7)$$

which implies the relation

$$S_{m-k,k}[u,u] = \binom{m}{k} S_m[u] \quad (8)$$

where $\binom{m}{k}$ are the usual binomial coefficients. Note also that $S_{m,n}[u,v]$ is homogeneous of degree m in u and its derivatives and of degree n in v and its derivatives. With this notation the variational equation for the buckling mode u_1 takes the compact form

$$P_{11}[u_1, \delta u] = 0 \quad (9)$$

where δu represents arbitrary kinematically admissible displacement variations. Setting $\delta u = u_1$ in Eq. (9) gives

$$P_2[u_1] = 0 \quad (10)$$

For unique mode buckling, Eq. (9) is not satisfied by any kinematically admissible function orthogonal to u_1 and further

$$P_2[\eta] > 0 \quad \text{if} \quad T_{11}[u_1, \eta] = 0 \quad (11)$$

In the first step of the extremization process, $F^\lambda[u]$ is minimized with respect to u for an arbitrary constant value of the coefficient ξ . The resulting function $F(F; \lambda)$ is then extremized with respect to ξ to give the desired equilibrium relation between λ and ξ . Introduction of Eq. (5) into Eq. (4), expansion according to Eq. (7), and arrangement of the result in ascending degree in u gives

$$\begin{aligned}
F^\lambda[\xi u_1 + \bar{u}] = & \xi^2 \{ (\lambda - \lambda_c) P_2[u_1] + (1/2)(\lambda - \lambda_c)^2 P_2'[u_1] + \dots \} \\
& + \xi^3 \{ P_3[u_1] + (\lambda - \lambda_c) P_3'[u_1] + \dots \} + \xi^4 \{ P_4[u_1] + \dots \} \\
& + \bar{\xi} \xi \{ Q_1[u_1] + (\lambda - \lambda_c) Q_1'[u_1] + \dots \} + \bar{\xi} \xi^2 \{ Q_2[u_1] + \dots \} \\
& + O(\bar{\xi} \xi^3) + O(\bar{\xi}^2 \xi) \\
& + \xi \{ (\lambda - \lambda_c) P_{11}[u_1, \bar{u}] + (1/2)(\lambda - \lambda_c)^2 P_{11}'[u_1, \bar{u}] + \dots \} \\
& + \xi^2 \{ P_{21}[u_1, \bar{u}] + (\lambda - \lambda_c) P_{21}'[u_1, \bar{u}] + \dots \} + \xi^3 \{ P_{31}[u_1, \bar{u}] + \dots \} \\
& + \bar{\xi} \{ Q_1[\bar{u}] + (\lambda - \lambda_c) Q_1'[\bar{u}] + \dots \} + \bar{\xi} \xi \{ Q_{11}[u_1, \bar{u}] + \dots \} \\
& + O(\bar{\xi} \xi^2 \bar{u}) + O(\bar{\xi}^2 \bar{u}) \\
& + P_2[\bar{u}] + (\lambda - \lambda_c) P_2'[\bar{u}] + \dots + \xi \{ P_{12}[u_1, \bar{u}] + \dots \} \\
& + \xi^2 \{ P_{22}[u_1, \bar{u}] + \dots \} + \bar{\xi} \{ Q_2[\bar{u}] + \dots \} + O(\bar{\xi} \xi \bar{u}^2) \\
& + P_3[\bar{u}] + \dots + \xi \{ P_{13}[u_1, \bar{u}] + \dots \} + O(\bar{\xi} \bar{u}^3) + P_4[\bar{u}] \quad (12)
\end{aligned}$$

In obtaining Eq. (12), use has already been made of Eq. (10) and Eq. (9) with $\delta u = \bar{u}$. In the approximation to be obtained it is unnecessary to retain terms following $P_2[\bar{u}]$ in Eq. (12). The neglect of these terms will be justified after obtaining the minimizing solution for \bar{u} . For this purpose, it is noted that the dominant terms following $P_2[\bar{u}]$ are - for small values of $\bar{\xi}$, $\lambda - \lambda_c$, ξ , and \bar{u} - $(\lambda - \lambda_c) P_{11}'[\bar{u}]$, $\xi P_{12}[u_1, \bar{u}]$, $\bar{\xi} Q_2[\bar{u}]$, and $P_3[\bar{u}]$. The remaining expression is the same as that used by Koiter [Eq. (43.7) of Ref. 3] with the exception of the two additional terms underlined in Eq. (12). To minimize $F^\lambda[\xi u_1 + \bar{u}]$ with respect to \bar{u} , one computes the difference

$$\begin{aligned}
F^\lambda[\xi u_1 + \bar{u} + \eta] - F^\lambda[\xi u_1 + \bar{u}] = & \xi \{ (\lambda - \lambda_c) P_{11}[u_1, \eta] + (1/2)(\lambda - \lambda_c)^2 P_{11}'[u_1, \eta] + \dots \} \\
& + \xi^2 \{ P_{21}[u_1, \eta] + (\lambda - \lambda_c) P_{21}'[u_1, \eta] + \dots \} + \xi^3 \{ P_{31}[u_1, \eta] + \dots \} \\
& + \bar{\xi} \{ Q_1[\eta] + (\lambda - \lambda_c) Q_1'[\eta] + \dots \} + \bar{\xi} \xi \{ Q_{11}[u_1, \eta] + \dots \} \\
& + O(\bar{\xi} \xi^2 \eta) + O(\bar{\xi}^2 \eta) + P_{11}[\bar{u}, \eta] + P_2[\eta] \quad (13)
\end{aligned}$$

For \bar{u} to be the minimizing solution, the terms of Eq. (13) which are first-degree in η must vanish for all kinematically admissible η orthogonal to u_1 . For if there exists such a displacement field, say η^* , for which these linear terms did not vanish, then the difference given by Eq. (13) would be negative for either $\eta = \eta^*$ or $-\eta^*$ for sufficiently small η^* . Furthermore, in view of Eq. (11), \bar{u} satisfying this condition does indeed minimize $F^\lambda[\xi u_1 + \bar{u}]$. To obtain a variational equation for \bar{u}

with an unconstrained variation $\zeta = \delta u$, $\zeta - tu_1$ is substituted for η . Because of the condition $T_{11}[u_1, \eta] = 0$, it follows that

$$t = T_{11}[u_1, \zeta]/2T_2[u_1] \quad (14)$$

After substitution, the resulting equation for \bar{u} is

$$\begin{aligned} & \xi(\lambda - \lambda_c) \{P_{11}'[u_1, \zeta] - 2tP_2'[u_1]\} + (1/2)\xi(\lambda - \lambda_c)^2 \{P_{11}''[u_1, \zeta] - 2tP_2''[u_1]\} + \dots \\ & + \xi^2 \{P_{21}[u_1, \zeta] - 3tP_3[u_1]\} + \xi^2(\lambda - \lambda_c) \{P_{21}'[u_1, \zeta] - 3tP_3'[u_1]\} + \dots \\ & + \xi^3 \{P_{31}[u_1, \zeta] - 4tP_4[u_1]\} + \dots + \bar{\xi} \{Q_1[\zeta] - tQ_1[u_1]\} \\ & + \bar{\xi}(\lambda - \lambda_c) \{Q_1'[\zeta] - tQ_1'[u_1]\} + \dots + \bar{\xi}\xi \{0 - 2tQ_2[u_1]\} + \dots \\ & + O(\bar{\xi}\xi^2\zeta) + O(\bar{\xi}^2\zeta) + P_{11}[\bar{u}, \zeta] = 0 \end{aligned} \quad (15)$$

where use has again been made of Eq. (9) with $\delta u = \bar{u}$.

Equations (15) and (6) uniquely determine \bar{u} , since the difference of two solutions for u would satisfy Eq. (9), contradicting the hypothesis of a unique buckling mode. Because of the linearity of Eqs. (6) and (15), the solution for \bar{u} can be written as

$$\begin{aligned} \bar{u} = & \xi(\lambda - \lambda_c)\phi_1' + (1/2)\xi(\lambda - \lambda_c)^2\phi_1'' + \dots + \xi^2\phi_2 + \xi^2(\lambda - \lambda_c)\phi_2' + \dots \\ & + \xi^3\phi_3 + \dots + \bar{\xi}\phi_0 + \bar{\xi}(\lambda - \lambda_c)\phi_0' + \dots + \bar{\xi}\xi\phi_{11} + \dots \\ & + O(\bar{\xi}\xi^2) + O(\bar{\xi}^2) \end{aligned} \quad (16)$$

For $\zeta = \bar{u}$, Eqs. (6) and (14) show that $t = 0$, and hence Eq. (15) shows that the sum of the terms of Eq. (12) which are linear in u is equal to $-2P_2[\bar{u}]$. Making this substitution in Eq. (12) gives the following expression for the minimized function $F(\xi; \lambda)$

$$\begin{aligned} F(\xi; \lambda) = & \xi^2 \{(\lambda - \lambda_c)P_2'[u_1] + (1/2)(\lambda - \lambda_c)^2P_2''[u_1] + \dots\} \\ & + \xi^3 \{P_3[u_1] + (\lambda - \lambda_c)P_3'[u_1] + \dots\} + \xi^4 \{P_4[u_1] + \dots\} \\ & + \bar{\xi}\xi \{Q_1[u_1] + (\lambda - \lambda_c)Q_1'[u_1] + \dots\} + \bar{\xi}\xi^2 \{Q_2[u_1] + \dots\} \\ & + O(\bar{\xi}\xi^3) + O(\bar{\xi}^2\xi) - P_2[\bar{u}] \end{aligned} \quad (17)$$

where \bar{u} is given by Eq. (16). From the terms of Eq. (12) which were neglected and Eq. (16), it may be seen that the lowest order terms neglected in Eq. (17) are those which are fifth degree in ξ and $\lambda - \lambda_c$ [i.e., $\xi^2(\lambda - \lambda_c)^3$, $\xi^3(\lambda - \lambda_c)^2$, $\xi^4(\lambda - \lambda_c)$, and ξ^5], those of order $\bar{\xi}$ which are third degree in ξ and $\lambda - \lambda_c$ [i.e., $\bar{\xi}\xi(\lambda - \lambda_c)^2$, $\bar{\xi}\xi^2(\lambda - \lambda_c)$, and $\bar{\xi}\xi^3$],

those of order $\bar{\xi}^2$ which are linear in ξ and $\lambda - \lambda_c$ [i.e., $\bar{\xi}^2\xi$ and $\bar{\xi}^2(\lambda - \lambda_c)$], and those of order $\bar{\xi}^3$. Therefore, upon substitution of Eq. (16) into Eq. (17), terms of these orders should be consistently neglected. As a consequence, the only terms of Eq. (16) which contribute to this approximation are $\xi(\lambda - \lambda_c)\phi_1^i$, $\xi^2\phi_2$, and $\bar{\xi}\phi_0$; the corresponding result for $F(\xi; \lambda)$ is

$$F(\xi; \lambda) = (\lambda - \lambda_c)A_2^i\xi^2 + (\lambda - \lambda_c)^2A_2^{i'}\xi^2 + A_3\xi^3 + (\lambda - \lambda_c)A_3^i\xi^3 + A_4\xi^4 + \bar{\xi}B_1\xi + \bar{\xi}(\lambda - \lambda_c)B_1^i\xi + \bar{\xi}B_2\xi^2 - \bar{\xi}^2P_2[\phi_0] \quad (18)$$

where

$$\begin{aligned} A_2^i &= P_2^i[u_1] \\ A_2^{i'} &= (1/2)P_2^{i'}[u_1] - P_2[\phi_1^i] \\ A_3 &= P_3[u_1] \\ A_3^i &= P_3^i[u_1] - P_{11}[\phi_1^i, \phi_2] \\ A_4 &= P_4[u_1] - P_2[\phi_2] \\ B_1 &= Q_1[u_1] \\ B_1^i &= Q_1^i[u_1] - P_{11}[\phi_0, \phi_1^i] \\ B_2 &= Q_2[u_1] - P_{11}[\phi_0, \phi_2] \end{aligned} \quad (19)$$

Variational equations for the functions ϕ_0 , ϕ_1^i , and ϕ_2 are, from Eqs. (6), (14), (15), and (16).

$$\begin{aligned} P_{11}[\phi_0, \zeta] + Q_1[\zeta] - T_{11}[u_1, \zeta]Q_1[u_1]/2T_2[u_1] &= 0 ; T_{11}[u_1, \phi_0] = 0 \\ P_{11}[\phi_1^i, \zeta] + P_{11}^i[u_1, \zeta] - T_{11}[u_1, \zeta]P_2^i[u_1]/T_2[u_1] &= 0 ; T_{11}[u_1, \phi_1^i] = 0 \\ P_{11}[\phi_2, \zeta] + P_{21}[u_1, \zeta] - 3T_{11}[u_1, \zeta]P_3[u_1]/2T_2[u_1] &= 0 ; T_{11}[u_1, \phi_2] = 0 \end{aligned} \quad (20)$$

Equilibrium states at the load λ are determined by stationary values of $F(\xi; \lambda)$ with respect to ξ . Thus, the equilibrium λ - ξ relation is

$$\begin{aligned} \partial F / \partial \xi &= 2(\lambda - \lambda_c)A_2^i\xi + 2(\lambda - \lambda_c)^2A_2^{i'}\xi + 3A_3\xi^2 + 3(\lambda - \lambda_c)A_3^i\xi^2 + 4A_4\xi^3 \\ &+ \bar{\xi}B_1 + \bar{\xi}(\lambda - \lambda_c)B_1^i + 2\bar{\xi}B_2\xi = 0 \end{aligned} \quad (21)$$

The lowest orders neglected in this relation are $\xi(\lambda - \lambda_c)^3$, $\xi^2(\lambda - \lambda_c)^2$, $\xi^3(\lambda - \lambda_c)$, ξ^4 , $\bar{\xi}(\lambda - \lambda_c)^2$, $\bar{\xi}\xi(\lambda - \lambda_c)$, $\bar{\xi}\xi^2$, and $\bar{\xi}^2$. In Ref. 3, Koiter retains

only the three dominant terms on the right-hand side of Eq. (21), viz. $2(\lambda - \lambda_c)A_2^1\xi$, $\bar{\xi}B_1$, and the lowest degree monomial in ξ with a nonzero coefficient. However, it should be noted that Eq. (21), with all terms retained, is a consistent approximation and is developed further in the remainder of this paper.

From Eqs. (19), the coefficients in Eq. (21) are seen to depend on the three functions ϕ_0 , ϕ_1^1 , and ϕ_2 , in addition to the buckling mode u_1 . Equation (21) can, however, be reduced to a simpler form depending on only two additional functions in place of the above three. Rewriting Eq. (21) slightly, one has

$$(\lambda - \lambda_c)\xi = -\bar{\xi}B_1/2A_2^1 - 3A_3\xi^2/2A_2^1 - \dots \quad (22)$$

Substituting Eq. (22) back into Eq. (21) and neglecting terms of the orders already neglected gives

$$(\lambda - \lambda_c)\xi - a\lambda_c\xi^2 - b\lambda_c\xi^3 = -\bar{\xi}[\alpha\lambda_c + \beta(\lambda - \lambda_c) + \gamma\lambda_c\xi] \quad (23)$$

where

$$\begin{aligned} a &= -3A_3/2\lambda_c A_2^1 \\ b &= -[4A_4 + 3a\lambda_c A_3^1 + 2(a\lambda_c)^2 A_2^{1'}]/2\lambda_c A_2^1 \\ \alpha &= B_1/2\lambda_c A_2^1 \\ \beta &= (\bar{u}_1^1 - 2a\lambda_c A_2^{1'})/2A_2^1 \\ \gamma &= (2B_2 - 3a\lambda_c A_3^1 - 2a\alpha\lambda_c^2 A_2^{1'})/2\lambda_c A_2^1 \end{aligned} \quad (24)$$

Similarly, substitution of Eq. (22) into Eq. (16) and retaining only those terms which contribute to this approximation gives

$$\bar{u} = \xi^2 u_2 + \bar{\xi} u_{01} \quad (25)$$

where

$$\begin{aligned} u_2 &= \phi_2 + a\lambda_c \phi_1^1 \\ u_{01} &= \phi_0 - \alpha\lambda_c \phi_1^1 \end{aligned} \quad (26)$$

From Eqs. (19), (20), (24), and (26), the equations which determine u_2 and u_{01} are

$$\begin{aligned} P_{11}[u_2, \xi] + P_{21}[u_1, \xi] + a\lambda_c P_{11}'[u_1, \xi] &= 0 \\ P_{11}[u_{01}, \xi] + Q_1[\xi] - \alpha\lambda_c P_{11}'[u_1, \xi] &= 0 \end{aligned} \quad (27)$$

and

$$T_{11}[u_1, u_2] = T_{11}[u_1, u_{01}] = 0 \quad (27a)$$

In contrast to the functions ϕ_0 , ϕ_1' , and ϕ_2 [see Eqs. (20)], the dependence of u_2 and u_{01} on the choice of $T_2[u]$ is only through the supplemental conditions (27a). Given the functional $T_2[u]$, these conditions would make u_2 and u_{01} unique. However, u_2 and u_{01} will in general change with the choice of $T_2[u]$. From the fact that, for unique mode buckling, Eq. (9) had only solutions proportional to u_1 , it follows that Eqs. (27) alone determine u_2 and u_{01} to within additional functions proportional to u_1 . Since the choice of $T_2[u]$ cannot affect results of the analysis with physical meaning, it will be of interest to verify that such results are not affected by this degree of arbitrariness in u_2 and u_{01} .

In order to show that b , β , and γ depend only on u_2 and u_{01} , in place of ϕ_0 , ϕ_1' , and ϕ_2 , several auxiliary relations derivable from Eqs. (20) by choosing $\zeta = \phi_0$, ϕ_1' , and ϕ_2 are useful. These are

$$\begin{aligned} P_2[\phi_1'] &= -P_{11}'[u_1, \phi_1']/2 \\ P_2[\phi_2] &= -P_{21}[u_1, \phi_2]/2 \\ P_{11}[\phi_1', \phi_2] &= -P_{11}'[u_1, \phi_2] = -P_{21}[u_1, \phi_1'] \\ P_{11}[\phi_0, \phi_1'] &= -P_{11}'[u_1, \phi_0] \\ P_{11}[\phi_0, \phi_2] &= -P_{21}[u_1, \phi_0] \end{aligned} \quad (28)$$

Using Eqs. (19), (24), (26), and (28), one obtains the results

$$\begin{aligned} a &= -3P_3[u_1]/2\lambda_c P_2'[u_1] \\ b &= -\{4P_4[u_1] + 2P_{21}[u_1, u_2] + a\lambda_c(3P_3'[u_1] + P_{11}'[u_1, u_2]) \\ &\quad + (a\lambda_c)^2 P_2''[u_1]\}/2\lambda_c P_2'[u_1] \\ \alpha &= Q_1[u_1]/2\lambda_c P_2'[u_1] \\ \beta &= \{Q_1'[u_1] + P_{11}'[u_1, u_{01}] - \alpha\lambda_c P_2''[u_1]\}/2P_2'[u_1] \\ \gamma &= \{2Q_2[u_1] + 2P_{21}[u_1, u_{01}] - \alpha\lambda_c(3P_3'[u_1] + P_{11}'[u_1, u_2]) \\ &\quad - a\lambda_c^2 P_2''[u_1]\}/2\lambda_c P_2'[u_1] \end{aligned} \quad (29)$$

An alternate expression for γ , independent of u_{01} if $a = 0$, can be obtained by setting $\zeta = u_{01}$ in the first of Eqs. (27), $\zeta = u_2$ in the

second of Eqs. (27), subtracting the resulting equations, and using the result to eliminate $P_{21}[u_1, u_{01}]$ from the above expression for γ . This gives

$$\gamma = \{2Q_2[u_1] + 2Q_1[u_2] - 3\alpha\lambda_c(P_3'[u_1] + P_{11}'[u_1, u_2]) - 2\alpha\lambda_c P_{11}'[u_1, u_{01}] - \alpha\lambda_c^2 P_2'[u_1]\} / 2\lambda_c P_2'[u_1] \quad (30)$$

As noted previously, the functions u_2 and u_{01} are only determined to within additional functions proportional to u_1 , and consequently Eqs. (29) do not uniquely determine the coefficients b , β , and γ . In particular, if in Eqs. (29) u_2 and u_{01} are replaced by $u_2 + C_2 u_1$ and $u_{01} + C_{01} u_1$, respectively, then b , β , and γ change by the amounts $C_2 \alpha$, C_{01} , and $-(2C_{01} \alpha + C_2 \alpha)$, respectively. The consequent ambiguous nature of Eq. (23), when all terms are retained, makes the determination of limit loads from it unfeasible. This problem is treated in Section V of this paper.

III. Series Expansion Method

As a prelude to the determination of buckling loads of imperfect structures, equivalent results to those of the preceding section are derived in this section using the method of Ref. 1. It may be noted that, although the notation used in this method is somewhat less abstract than that of Section II, this development is somewhat less general in that it is based on the assumption of small strains.

A displacement expansion is assumed in the form [cf. Eqs. (2), (5), and (25)]

$$U = u_0(\lambda) + \xi u_1 + \xi^2 u_2 + \xi^3 u_3 + \dots + \bar{\xi}[u_{01} + (\lambda - \lambda_c) u_{01}' + \xi u_{11} + \dots] + O(\bar{\xi}^2) \quad (31)$$

In contrast to Eq. (25) of Section II, it will be necessary to retain all the terms shown in Eq. (31), since the equations for the coefficients a , b , \dots , α , β , γ , \dots of the expansion corresponding to Eq. (23), viz.

$$(\lambda - \lambda_c) \xi - a \lambda_c \xi^2 - b \lambda_c \xi^3 - \dots = -\bar{\xi}[\alpha \lambda_c + \beta(\lambda - \lambda_c) + \gamma \lambda_c \xi + \dots] + O(\bar{\xi}^2) \quad (32)$$

are to be derived from the compatibility conditions for the functions u_2 , u_3 , \dots , u_{01} , u_{01}' , u_{11} , \dots , respectively. These compatibility conditions are necessary since the homogeneous forms of the equations for these functions are identical to the eigenvalue equations for the buckling mode and therefore have the nontrivial solution u_1 .

If the strains are small compared to displacement gradients (as is consistent with a small strain, moderate rotation shell theory), then

the strains of an imperfect structure may be expressed in terms of the strains of the model by†

$$\epsilon = L_1(U) + (1/2)L_2(U) + \bar{\xi}L_{11}(\bar{U}, U) \quad (33)$$

Substituting Eq. (31) into Eq. (33) and using Eq. (32) and the Taylor series expansion of the prebuckling displacements about $\lambda = \lambda_c$

$$u_0 = u_0^* + (\lambda - \lambda_c)u_0^{(1)*} + (1/2)(\lambda - \lambda_c)^2 u_0^{(2)*} + \dots \quad (34)$$

give the strain expansion

$$\begin{aligned} \epsilon = \epsilon_0 + \xi\epsilon_1 + \xi^2\epsilon_2 + \xi^3\epsilon_3 + \dots + \bar{\xi}[\epsilon_{01} + (\lambda - \lambda_c)\epsilon_{01}' \\ + \xi\epsilon_{11} + \dots] + O(\bar{\xi}^2) \end{aligned} \quad (35)$$

where expressions for ϵ_1 , ϵ_2 , and ϵ_3 are given in Ref. 1, and

$$\begin{aligned} \epsilon_{01} &= L_1(u_{01}) + L_{11}(u_0^*, u_{01}) + L_{11}(u_0^*, \bar{U}) - \alpha\lambda_c L_{11}(u_0^{(1)*}, u_1) \\ \epsilon_{01}' &= L_1(u_{01}') + L_{11}(u_0^*, u_{01}') + L_{11}(u_0^{(1)*}, \bar{U}) + L_{11}(u_0^{(1)*}, u_{01}) \\ &\quad - \beta L_{11}(u_0^{(1)*}, u_1) - (1/2)\alpha\lambda_c L_{11}(u_0^{(2)*}, u_1) \\ \epsilon_{11} &= L_1(u_{11}) + L_{11}(u_0^*, u_{11}) + L_{11}(u_1, u_{01}) + L_{11}(u_1, \bar{U}) \\ &\quad - \gamma\lambda_c L_{11}(u_0^{(1)*}, u_1) - \alpha\lambda_c L_{11}(u_0^{(1)*}, u_2) - (1/2)\alpha\lambda_c^2 L_{11}(u_0^{(2)*}, u_1) \end{aligned} \quad (36)$$

Substitution of Eq. (35) into the constitutive relation

$$\sigma = H(\epsilon) \quad (37)$$

gives the stress expansion

$$\begin{aligned} \sigma = \sigma_0 + \xi\sigma_1 + \xi^2\sigma_2 + \xi^3\sigma_3 + \dots + \bar{\xi}[\sigma_{01} + (\lambda - \lambda_c)\sigma_{01}' \\ + \xi\sigma_{11} + \dots] + O(\bar{\xi}^2) \end{aligned} \quad (38)$$

where each stress component in Eq. (38) is related to the corresponding strain component in Eq. (35) through Eq. (37). Substituting the variation of Eq. (33) and Eq. (38) into the equation of virtual work

$$\sigma \cdot \delta \epsilon = \lambda[q_0 + q_1(U) + \bar{\xi}q_1(\bar{U})] \cdot \delta u \quad (39)$$

using the expansion (34) (and a similar expansion for the prebuckling

† Note that the definition of the operator $L_{11}(u, v)$, viz. $L_2(u+v) = L_2(u) + 2L_{11}(u, v) + L_2(v)$, differs by a factor of 2 with the definition, Eq. (7), of doubly-subscripted functionals.

stress σ_0 and Eq. (32), then equating to zero coefficients of ξ^k , $\bar{\epsilon}$, $\bar{\xi}(\lambda - \lambda_c)^k$, and $\bar{\xi}\xi^k$ for $k = 1, 2, \dots$ give the variational equations satisfied by the stress components of Eq. (38). These equations for σ_1 , σ_2 , and σ_3 have been presented as Eqs. (8c), (13c), and (14c) in Ref. 1. In addition, one obtains

$$\begin{aligned} \sigma_{01} \cdot \delta \epsilon_0^* + \sigma_0^* \cdot L_{11}(u_{01} + \bar{U}, \delta u) - \lambda_c q_1(u_{01} + \bar{U}) \cdot \delta u - \alpha \lambda_c E^{(1)}(u_1, \delta u) &= 0 \\ \sigma_{01}' \cdot \delta \epsilon_0^* + \sigma_0^* \cdot L_{11}(u_{01}', \delta u) - \lambda_c q_1(u_{01}') \cdot \delta u - \beta E^{(1)}(u_1, \delta u) \\ - (1/2) \alpha \lambda_c E^{(2)}(u_1, \delta u) + E^{(1)}(u_{01}, \delta u) + \sigma_0^{(1)*} \cdot L_{11}(\bar{U}, \delta u) \\ - q_1(\bar{U}) \cdot \delta u &= 0 \\ \sigma_{11} \cdot \delta \epsilon_0^* + \sigma_0^* \cdot L_{11}(u_{11}, \delta u) - \lambda_c q_1(u_{11}) \cdot \delta u + \sigma_{01} \cdot L_{11}(u_1, \delta u) \\ + \sigma_1 \cdot L_{11}(u_{01} + \bar{U}, \delta u) - \gamma \lambda_c E^{(1)}(u_1, \delta u) - \alpha \lambda_c E^{(1)}(u_2, \delta u) \\ - (1/2) \alpha \lambda_c^2 E^{(2)}(u_1, \delta u) &= 0 \end{aligned} \quad (40)$$

Equations (36), (37), and (40) constitute the field equations for the displacement states u_{01} , u_{01}' , and u_{11} . Comparison with Eqs. (8) of Ref. 1 shows that the homogeneous forms of these field equations, as well as the equations for u_2 and u_3 , are satisfied by the buckling mode u_1 . Just as the compatibility conditions for the functions u_2, u_3, \dots yield expressions for the postbuckling coefficients a, b, \dots , the compatibility conditions for $u_{01}, u_{01}', u_{11}, \dots$ yield expressions for the imperfection parameters $\alpha, \beta, \gamma, \dots$. For example, setting $\delta u = u_1$ in the first of Eqs. (40) and $\delta u = u_{01}$ in the corresponding buckling mode equation [Eq. (8c) of Ref. 1], and subtracting the results give

$$\begin{aligned} \sigma_{01} \cdot \epsilon_1 - \sigma_1 \cdot [L_1(u_{01}) + L_{11}(u_0^*, u_{01})] + \sigma_0^* \cdot L_{11}(\bar{U}, u_1) - \lambda_c q_1(\bar{U}) \cdot u_1 \\ - \alpha \lambda_c E^{(1)}(u_1, u_1) &= 0 \end{aligned} \quad (41)$$

Replacing $\sigma_{01} \cdot \epsilon_1$ by $\sigma_1 \cdot \epsilon_{01}$ and elimination of ϵ_{01} through use of the first of Eqs. (36) give, upon collection of terms, the result [cf. Eq. (34a) of Ref. 1]

$$\alpha = [\sigma_0^* \cdot L_{11}(\bar{U}, u_1) + \sigma_1 \cdot L_{11}(\bar{U}, u_0^*) - \lambda_c q_1(\bar{U}) \cdot u_1] / \lambda_c F^{(1)}(u_1, u_1) \quad (42a)$$

In a similar way, one obtains for β and γ the following expressions†

† The expression for β given in Ref. 1 is that part of Eq. (42b) which is independent of u_{01} , which was tacitly neglected in Ref. 1.

$$\beta = [\sigma_0^{(1)*} \cdot L_{11}(\bar{U}, u_1) + \sigma_1 \cdot L_{11}(\bar{U}, u_0^{(1)*}) - q_1(\bar{U}) \cdot u_1 - (1/2)\alpha\lambda_c F_c^{(2)}(u_1, u_1) + F_c^{(1)}(u_{01}, u_1)]/F_c^{(1)}(u_1, u_1) \quad (42b)$$

$$\gamma = [2\sigma_1 \cdot L_{11}(u_{01}, u_1) + 2\sigma_1 \cdot L_{11}(\bar{U}, u_1) + \sigma_{01} \cdot L_2(u_1) - \alpha\lambda_c F_c^{(1)}(u_1, u_2) - (1/2)\alpha\lambda_c^2 F_c^{(2)}(u_1, u_1)]/\lambda_c F_c^{(1)}(u_1, u_1) \quad (42c)$$

An alternate expression for γ , dependent on u_{01} only if a is nonzero, can be derived through use of the field equations for u_{01} and u_2 . This expression is

$$\gamma = [2\sigma_2 \cdot L_{11}(u_0^*, \bar{U}) + 2\sigma_0^* \cdot L_{11}(u_2, \bar{U}) - 2\lambda_c q_1(\bar{U}) \cdot u_2 + 2\sigma_1 \cdot L_{11}(u_1, \bar{U}) - 3\alpha\lambda_c F_c^{(1)}(u_1, u_2) - 2\alpha\lambda_c F_c^{(1)}(u_1, u_{01}) - (1/2)\alpha\lambda_c^2 F_c^{(2)}(u_1, u_1)]/\lambda_c F_c^{(1)}(u_1, u_1) \quad (43)$$

IV. Reconciliation of the Results of Sections II and III

In Section II variational equations (27) for the expansion states u_2 and u_{01} and expressions (29) for expansion coefficients a , b , α , β , and γ were derived in terms of potential energy functionals. Upon specialization to a small strain theory, as in Section III, these results should reduce to the corresponding formulas derived in Section III. This reduction will serve as a check on both sets of formulas.

In order to accomplish this reduction it is necessary to expand the potential energy, expressed in terms of the variables of Section III, in terms of a displacement increment u about the prebuckling state $u_0(\lambda)$. In terms of the variables of Section III, the potential energy Π of an imperfect structure may be written in the form

$$\Pi = (1/2)\epsilon \cdot H(\epsilon) - \lambda[q_0 + \bar{\xi}q_1(\bar{U}) + (1/2)q_1(U)] \cdot U \quad (44)$$

where the strain ϵ is given by Eq. (33). Substituting Eq. (2) for U in Eq. (33) and expanding in terms of functions which are homogeneous in u gives†

$$\epsilon(u_0+u) = \epsilon_0 + \epsilon_I + \epsilon_{II} + \bar{\xi}\eta_0 + \bar{\xi}\eta_I \quad (45)$$

where

† In order to avoid confusion with the already defined variables ϵ_1 and ϵ_2 , the roman numeral subscripts are used to indicate degree of the strain operators ϵ, η in the displacements u and their derivatives.

$$\begin{aligned}
\varepsilon_0 &= L_1(u_0) + (1/2)L_2(u_0) \\
\varepsilon_I &= L_1(u) + L_{11}(u_0, u) \\
\varepsilon_{II} &= (1/2)L_2(u) \\
\eta_0 &= L_{11}(u_0, \bar{u}) \\
\eta_I &= L_{11}(u, \bar{u})
\end{aligned} \tag{46}$$

Substituting Eqs. (2) and (45) into Eq. (44), expanding, and comparing the results with Eq. (3) give

$$\begin{aligned}
P_1^\lambda[u] &= \sigma_0 \cdot \varepsilon_I - \lambda[q_0 + q_1(u_0)] \cdot u \\
P_2^\lambda[u] &= \sigma_0 \cdot \varepsilon_{II} + (1/2)\varepsilon_I \cdot H(\varepsilon_I) - (1/2)\lambda q_1(u) \cdot u \\
P_3^\lambda[u] &= \varepsilon_{II} \cdot H(\varepsilon_I) \\
P_4^\lambda[u] &= (1/2)\varepsilon_{II} \cdot H(\varepsilon_{II})
\end{aligned} \tag{47}$$

and

$$\begin{aligned}
Q_1^\lambda[u] &= \eta_0 \cdot H(\varepsilon_I) + \sigma_0 \cdot \eta_I - \lambda q_1(\bar{u}) \cdot u \\
Q_2^\lambda[u] &= \eta_0 \cdot H(\varepsilon_{II}) + \eta_I \cdot H(\varepsilon_I) \\
Q_3^\lambda[u] &= \eta_I \cdot H(\varepsilon_{II}) \\
Q_4^\lambda[u] &= 0
\end{aligned} \tag{48}$$

where use has been made of the relation $\sigma_0 = H(\varepsilon_0)$.

Doubly-subscripted functionals are obtained from Eqs. (47) and (48) through the definition Eq. (7). From Eqs. (46), one has

$$\begin{aligned}
\varepsilon_I(u+v) &= \varepsilon_I(u) + \varepsilon_I(v) \\
\varepsilon_{II}(u+v) &= \varepsilon_{II}(u) + \varepsilon_{II}(v) + L_{11}(u, v)
\end{aligned} \tag{49}$$

Forming $P_2^\lambda[u+v]$ from the second of Eqs. (47) and using Eqs. (49) give

$$P_2^\lambda[u+v] = P_2^\lambda[u] + P_2^\lambda[v] + \sigma_0 \cdot L_{11}(u, v) + \varepsilon_I(u) \cdot H[\varepsilon_I(v)] - \lambda q_1(u) \cdot v \tag{50}$$

Comparing Eq. (50) with the definition

$$P_2^\lambda[u+v] = P_2^\lambda[u] + P_2^\lambda[v] + P_{11}^\lambda[u, v] \tag{51}$$

gives

$$P_{11}^\lambda[u, v] = \sigma_0 \cdot L_{11}(u, v) + \epsilon_I(u) \cdot H[\epsilon_I(v)] - \lambda q_1(u) \cdot v \quad (52a)$$

In a similar manner, one obtains

$$P_{21}^\lambda[u, v] = \epsilon_{II}(u) \cdot H[\epsilon_I(v)] + L_{11}(u, v) \cdot H[\epsilon_I(u)] \quad (52b)$$

Primed functionals are obtained by taking derivatives with respect to λ of the corresponding unprimed functionals. Noting that the λ -dependence of these functionals arises only through the prebuckling state variables $u_0(\lambda)$, $\sigma_0(\lambda)$ and λ itself, one obtains from Eqs. (46), (47), (48), and (52)

$$\begin{aligned} P_2^{\lambda'}[u] &= (1/2)\sigma_0^{(1)} \cdot L_2(u) + L_{11}(u_0^{(1)}, u) \cdot H(\epsilon_I) - (1/2)q_1(u) \cdot u \\ P_2^{\lambda''}[u] &= (1/2)\sigma_0^{(2)} \cdot L_2(u) + L_{11}(u_0^{(2)}, u) \cdot H(\epsilon_I) \\ &\quad + L_{11}(u_0^{(1)}, u) \cdot H[L_{11}(u_0^{(1)}, u)] \\ P_{11}^{\lambda'}[u, v] &= \sigma_0^{(1)} \cdot L_{11}(u, v) + L_{11}(u_0^{(1)}, u) \cdot H[\epsilon_I(v)] \\ &\quad + L_{11}(u_0^{(1)}, v) \cdot H[\epsilon_I(u)] - q_1(u) \cdot v \\ P_3^{\lambda'}[u] &= L_{11}(u_0^{(1)}, u) \cdot H(\epsilon_{II}) \\ Q_1^{\lambda'}[u] &= L_{11}(u_0^{(1)}, \bar{u}) \cdot H(\epsilon_I) + L_{11}(u_0^{(1)}, u) \cdot H(n_0) \\ &\quad + \sigma_0^{(1)} \cdot L_{11}(u, \bar{u}) - q_1(\bar{u}) \cdot u \end{aligned} \quad (53)$$

Finally, the corresponding functionals without the superscript λ are obtained from Eqs. (47), (48), (52), and (53) simply by setting $\lambda = \lambda_c$ and u_0 , σ_0 and their derivatives $u_0^{(p)}$, $\sigma_0^{(p)}$ to u_0^* , σ_0^* and $u_0^{(p)*}$, $\sigma_0^{(p)*}$, respectively. Using these expressions for the P, Q-functionals, it is easy to show the equivalence of the results of Sections II and III, viz. that Eqs. (27) reduce to Eqs. (13) of Ref. 1 for u_2 , and to Eq. (37) and the first of Eqs. (36) and (40) for u_{01} ; Eqs. (29) reduce to Eqs. (22) of Ref. 1 for a and b , and to Eqs. (42) for α , β , and γ ; and Eq. (30) reduces to Eq. (43).

V. The λ - Δ Relationship for Axisymmetric Structures

As noted previously, the λ - ξ relation, Eq. (32), is not in general a unique relation, since, from Eqs. (29), the coefficients b , β , and γ change by the amounts C_{2a} , C_{01} , and $-(2C_{01}a + C_{2a})$ when u_2 and u_{01} change by $C_2 u_1$ and $C_{01} u_1$, respectively, where C_2 and C_{01} are arbitrary constants. This change corresponds to a transformation of the coordinate ξ and can be verified independently of Eqs. (29) by noting

that both Eqs. (31) and (32) must be invariant with respect to such transformations. First, note that the above changes in u_2 and u_{01} imply through Eqs. (14) of Ref. 1 and Eqs. (36), (37), and (40) certain changes in u_3 and u_{11} (and higher order states). Thus, consistent with the transformations

$$\begin{aligned} u_2 &= \bar{u}_2 + C_2 u_1 \\ u_{01} &= \bar{u}_{01} + C_{01} u_1 \end{aligned} \quad (54)$$

are the transformations

$$\begin{aligned} u_3 &= \bar{u}_3 + 2C_2 \bar{u}_2 + C_3 u_1 \\ u'_{01} &= \bar{u}'_{01} + C'_{01} u_1 \\ u_{11} &= \bar{u}_{11} + 2C_{01} \bar{u}_2 + C_{11} u_1 \end{aligned} \quad (55)$$

where C_3 , C'_{01} , and C_{11} are additional arbitrary constants. Substituting Eqs. (54) and (55) into Eq. (31) and collecting terms give, upon comparison with Eq. (31) for the tilda system,

$$\bar{\xi} = \xi + C_2 \xi^2 + C_3 \xi^3 + C_{01} \bar{\xi} + C'_{01} \bar{\xi}(\lambda - \lambda_c) + C_{11} \bar{\xi} \xi \quad (56)$$

and

$$\bar{\xi}^2 = \xi^2 + 2C_2 \xi^3 + 2C_{01} \bar{\xi} \xi + \dots \quad (56a)$$

which is consistent with Eq. (56). If Eq. (56) is substituted into Eq. (32) for the tilda system, comparison with Eq. (32) gives the stated changes in b , β , and γ , previously obtained from Eqs. (29), viz.

$$\begin{aligned} b &= \bar{b} + C_2 a \\ \beta &= \bar{\beta} + C_{01} \\ \gamma &= \bar{\gamma} - (2C_{01} a + C_2 \alpha) \end{aligned} \quad (57)$$

Since the coefficients in the λ - ξ relation are ambiguous, it cannot be used, beyond Koiter's first approximation, to determine the maximum value of λ , which is the buckling load of the imperfect structure. On the other hand, the relationship between λ and the work deflection Δ must be unique, since both λ and Δ have physical meaning. This relation is derived in this section for the technically important case of axisymmetric loading of axisymmetric structures with a unique harmonic bifurcation mode. It will be further assumed that the distribution of imperfection displacements \bar{U} is also harmonic with the same circum-

ferential wave number n_c as the bifurcation mode.[†] In this case

$$a \equiv 0 \quad (53)$$

and it can be deduced by consideration of the nonhomogeneous terms in the equations for u_2 , u_3 [Eqs. (13) and (14) of Ref. 1] and u_{01} , u_{01}' [Eqs. (36), (37), and (40)] that a tilda coordinate system may be chosen such that

$$\begin{aligned} \tilde{u}_2 &\text{ contains only the harmonics } n = 0 \text{ and } 2n_c \\ \tilde{u}_3 &\text{ contains only the harmonics } n = n_c \text{ and } 3n_c \\ \tilde{u}_{01} \text{ and } \tilde{u}_{01}' &\text{ contain only the harmonic } n = n_c \end{aligned} \quad (59)$$

It follows that, for this coordinate system,

$$\tilde{\gamma} = 0 \quad (60)$$

since the numerator of Eq. (42c) reduces to the sum of integrals of the form

$$\int_0^{2\pi} P_{2k-1}(\cos n_c \phi, \sin n_c \phi) d\phi \equiv 0 \quad (61)$$

where $P_{2k-1}(x, y)$ is a homogeneous polynomial of degree $2k-1$ and k is a positive integer. The equations for u_{11} [Eqs. (36), (37), and (40)] then determine, in view of Eqs. (58), (59), and (60), that

$$\tilde{u}_{11} \text{ contains only the harmonics } n = 0 \text{ and } 2n_c \quad (62)$$

It should be noted that \tilde{u}_2 is a unique state since it does not contain the harmonic n_c of u_1 . On the other hand, the states \tilde{u}_{01} , \tilde{u}_3 , \tilde{u}_{01}' , and \tilde{u}_{11} are themselves ambiguous by virtue of the facts that \tilde{u}_{01} , \tilde{u}_3 , and \tilde{u}_{01}' contain the harmonic n_c , and \tilde{u}_{11} contains the same harmonics as \tilde{u}_2 [cf. Eqs. (54) and (55)]. It will be convenient in the following to make all calculations in the tilda system and then to verify that the results (after elimination of $\tilde{\xi}$) are invariant with respect to the arbitrariness of these states in the tilda system. This arbitrariness is characterized by Eqs. (54), (55), and (57) with $a = C_2 = C_{11} = 0$.

The work deflection Δ is defined by the following relation expressing conservation of energy

$$\lambda(d\Delta/d\tilde{\xi}) = \sigma \cdot (d\epsilon/d\tilde{\xi}) \quad (63)$$

[†] This is clearly the critical case since other harmonics do not contribute to the value of the first imperfection parameter α .

The right-hand side of Eq. (63) can be calculated from Eqs. (35) and (38). Taking the derivative of Eq. (35) gives

$$d\epsilon/d\tilde{\xi} = [\epsilon_0^{(1)*} + (\lambda - \lambda_c)\epsilon_0^{(2)*} + (1/2)(\lambda - \lambda_c)^2\epsilon_0^{(3)*} + \dots]d\lambda/d\tilde{\xi} + \epsilon_1 + 2\tilde{\xi}\tilde{\epsilon}_2 + 3\tilde{\xi}^2\tilde{\epsilon}_3 + \dots + \tilde{\xi}(\tilde{\epsilon}_{01}d\lambda/d\tilde{\xi} + \tilde{\epsilon}_{11} + \dots) + \dots \quad (64)$$

where $d\epsilon_0/d\lambda = \epsilon_0^{(1)}$ has been expanded in a Taylor series about $\lambda = \lambda_c$. Similarly expanding σ_0 , Eq. (38) may be written as

$$\sigma = \sigma_0* + (\lambda - \lambda_c)\sigma_0^{(1)*} + (1/2)(\lambda - \lambda_c)^2\sigma_0^{(2)*} + \dots + \tilde{\xi}\sigma_1 + \tilde{\xi}^2\sigma_2 + \dots + \tilde{\xi}(\tilde{\sigma}_{01} + \dots) + \dots \quad (65)$$

Forming the inner product from Eqs. (64) and (65) gives†

$$\sigma \cdot d\epsilon/d\tilde{\xi} = \{\sigma_0* \cdot \epsilon_0^{(1)*} + (\lambda - \lambda_c)[\sigma_0* \cdot \epsilon_0^{(2)*} + \sigma_0^{(1)*} \cdot \epsilon_0^{(1)*}] + (1/2)(\lambda - \lambda_c)^2[3\sigma_0^{(2)*} \cdot \epsilon_0^{(1)*} + \sigma_0* \cdot \epsilon_0^{(3)*}]\}d\lambda/d\tilde{\xi} + \tilde{\xi}(2\sigma_0* \cdot \tilde{\epsilon}_2 + \sigma_1 \cdot \epsilon_1) + [\tilde{\xi}(\lambda - \lambda_c) + \tilde{\xi}^2d\lambda/d\tilde{\xi}]\sigma_0^{(1)*} \cdot \tilde{\epsilon}_2 + \tilde{\xi}(\sigma_0* \cdot \tilde{\epsilon}_{11} + \tilde{\sigma}_{01} \cdot \epsilon_1) + \dots \quad (66)$$

The lowest orders omitted in Eq. (66) are $\tilde{\xi}^3$, $\tilde{\xi}^2(\lambda - \lambda_c)$, $\tilde{\xi}(\lambda - \lambda_c)^2$, $(\lambda - \lambda_c)^3$, $\tilde{\xi}\tilde{\epsilon}_3$, $\tilde{\xi}(\lambda - \lambda_c)\tilde{\epsilon}_2$, and $\tilde{\xi}^2$. Equation (66) can be simplified somewhat making use of Eq. (32), which may be written for the tilda system as

$$(\lambda - \lambda_c)\tilde{\xi} = -\alpha\lambda_c\tilde{\xi} - \beta(\lambda - \lambda_c)\tilde{\xi} - \dots + b\lambda_c\tilde{\xi}^3 + \dots \quad (67)$$

Differentiation of Eq. (67) with respect to $\tilde{\xi}$, multiplication of the result by $\tilde{\xi}$, and elimination of $(\lambda - \lambda_c)\tilde{\xi}$ by substitution of Eq. (67) gives

$$\tilde{\xi}^2d\lambda/d\tilde{\xi} = \alpha\lambda_c\tilde{\xi} + \beta\tilde{\xi}[(\lambda - \lambda_c) - \tilde{\xi}d\lambda/d\tilde{\xi}] + \dots + 2b\lambda_c\tilde{\xi}^3 + \dots \quad (68)$$

Only the first terms on the right-hand sides of Eqs. (67) and (68) should be retained upon substituting these equations into Eq. (66). Since the remaining terms are of orders already neglected. The result of this substitution is

$$\sigma \cdot d\epsilon/d\tilde{\xi} = \{\sigma_0* \cdot \epsilon_0^{(1)*} + (\lambda - \lambda_c)[\sigma_0* \cdot \epsilon_0^{(2)*} + \sigma_0^{(1)*} \cdot \epsilon_0^{(1)*}] + \dots\}d\lambda/d\tilde{\xi} + \tilde{\xi}[2\sigma_0* \cdot \tilde{\epsilon}_2 + \sigma_1 \cdot \epsilon_1] + \tilde{\xi}[\sigma_0* \cdot \tilde{\epsilon}_{11} + \tilde{\sigma}_{01} \cdot \epsilon_1 - \alpha\lambda_c\sigma_0^{(1)*} \cdot \tilde{\epsilon}_2] + \dots \quad (69)$$

† It is not necessary to use the tilda system in deriving Eq. (66). If an expression for $\sigma \cdot d\epsilon/d\tilde{\xi}$ is derived in a general coordinate system and the transformations (54), (55), and (56) are made, Eq. (66) will result.

Equations (63) and (69) suggest that Δ may be expressed as the sum of several power series, viz.

$$\Delta - \Delta_c = A_1 \bar{\xi}^2 + A_2 \bar{\xi}^4 + \dots + B_1 (\lambda - \lambda_c) + B_2 (\lambda - \lambda_c)^2 + \dots + \bar{\xi} [C_1 \bar{\xi} + C_2 \bar{\xi}^2 + \dots + D_1 (\lambda - \lambda_c) + D_2 (\lambda - \lambda_c)^2 + \dots] + O(\bar{\xi}^2) \quad (70)$$

where Δ_c is the value of Δ of the model (for which $\bar{\xi} = 0$) at the bifurcation load λ_c . For the class of structures considered, it may be inferred, by consideration of higher order terms of Eq. (69), that the power series in $\bar{\xi}$ shown on the first line of Eq. (70) is, in fact, a power series in $\bar{\xi}^2$. Taking the derivative of Eq. (70), forming the product $\lambda d\Delta/d\bar{\xi}$, and using Eq. (67) to eliminate $(\lambda - \lambda_c)\bar{\xi}$ give

$$\begin{aligned} \lambda d\Delta/d\bar{\xi} &= [\lambda_c + (\lambda - \lambda_c)] d\Delta/d\bar{\xi} \\ &= 2A_1 \lambda_c \bar{\xi} + \dots + B_1 \lambda_c d\lambda/d\bar{\xi} + (B_1 + 2B_2 \lambda_c) (\lambda - \lambda_c) d\lambda/d\bar{\xi} + \dots \\ &+ \bar{\xi} (C_1 \lambda_c - 2A_1 \alpha \lambda_c + \dots + D_1 \lambda_c d\lambda/d\bar{\xi} + \dots) + O(\bar{\xi}^2) \end{aligned} \quad (71)$$

Comparison of Eq. (71) with Eq. (69) gives the formulas

$$\begin{aligned} 2\lambda_c A_1 &= 2\sigma_0^* \cdot \bar{\epsilon}_2 + \sigma_1 \cdot \epsilon_1 \\ \lambda_c B_1 &= \sigma_0^* \cdot \epsilon_0^{(1)*} \\ 2\lambda_c B_2 &= \sigma_0^* \cdot \epsilon_0^{(2)*} + \sigma_0^{(1)*} \cdot \epsilon_0^{(1)*} - B_1 \\ \lambda_c C_1 &= \sigma_0^* \cdot \bar{\epsilon}_{11} + \sigma_{01} \cdot \epsilon_1 - \alpha \lambda_c \sigma_0^{(2)*} \cdot \bar{\epsilon}_2 + 2\alpha \lambda_c A_1 \\ D_1 &= 0 \end{aligned} \quad (72)$$

The coefficients A_1 , B_1 , and B_2 given in Eqs. (72) can be expressed in terms of the prebuckling and postbuckling stiffnesses of the model. The prebuckling stiffness K_0 is given by [see Eq. (25) of Ref. 1]

$$K_0 = \lambda / \sigma_0 \cdot \epsilon_0^{(1)} \quad (73)$$

Differentiation of Eq. (73) with respect to λ gives

$$K_0^{(1)} = \{1 - K_0 [\sigma_0 \cdot \epsilon_0^{(2)} + \sigma_0^{(1)} \cdot \epsilon_0^{(1)}]\} K_0 / \lambda \quad (74)$$

The initial postbuckling stiffness K^* is given by [see Eq. (31) of Ref. 1]†

$$K^* = K_0^* / [1 + (K_0^* / 2b\lambda_c^2) (\sigma_1 \cdot \epsilon_1 + 2\sigma_0^* \cdot \bar{\epsilon}_2)] \quad (75)$$

† Note that $\sigma_0^* \cdot \epsilon_2 = \sigma_0^* \cdot \bar{\epsilon}_2$ since $\sigma_0^* \cdot \epsilon_1 = 0$.

From Eqs. (72) through (75), one obtains

$$\begin{aligned} A_1 &= b\lambda_c(K_0^* - K^*)/K_0^*K^* \\ B_1 &= 1/K_0^* \\ B_2 &= -K_0^{(1)*}/2K_0^{*2} \end{aligned} \quad (76)$$

In order to derive the λ - Δ relation, Eq. (70) is rearranged slightly to the form

$$\begin{aligned} A_1\tilde{\xi}^2 + A_2\tilde{\xi}^4 + \dots &= \Delta - \Delta_c - B_1(\lambda - \lambda_c) - B_2(\lambda - \lambda_c)^2 - \dots \\ &- C_1\tilde{\xi}\tilde{\xi} - \dots \end{aligned} \quad (77)$$

If the right-hand side of Eq. (77) is denoted by η , reversal of the $\tilde{\xi}^2$ -series gives

$$\tilde{\xi}^2 = \eta/A_1 - A_2\eta^2/A_1^3 + \dots \quad (78)$$

Since the term $A_2\eta^2/A_1^3$ in Eq. (78) contributes a term of order $(\lambda - \lambda_c)^2$, it would be inconsistent to retain the term $B_2(\lambda - \lambda_c)^2$ in Eq. (77) when neglecting the term $A_2\tilde{\xi}^4$. Therefore, a consistent approximation relating $\tilde{\xi}$ and Δ is

$$A_1\tilde{\xi}^2 + C_1\tilde{\xi}\tilde{\xi} - [\Delta - \Delta_c - B_1(\lambda - \lambda_c)] = 0 \quad (79)$$

Equation (79) is a quadratic equation in $\tilde{\xi}$ with the solution

$$\tilde{\xi} = -(C_1/2A_1)\tilde{\xi} \pm [K^*/b\lambda_c(K_0^* - K^*)]^{1/2}[K_0^*(\Delta - \Delta_c) - (\lambda - \lambda_c)]^{1/2} \quad (80)$$

where, in accordance with Eq. (70), the order of $\tilde{\xi}^2$ has been neglected as compared to the quantity $[\Delta - \Delta_c - B_1(\lambda - \lambda_c)]$, and Eqs. (76) have been used. It may be noted that, in the case of interest, viz. $b < 0$, both radicals in Eq. (80) are real, regardless of the sign of K^* or $\Delta - \Delta_c$. Rearranging Eq. (67) to the form

$$\tilde{\xi}[\lambda - \lambda_c - b\lambda_c\tilde{\xi}^2 - \dots] = -[\alpha\lambda_c + \beta(\lambda - \lambda_c) + \dots]\tilde{\xi} + O(\tilde{\xi}^2) \quad (81)$$

and substituting Eq. (80) for $\tilde{\xi}$, Eq. (79) for $\tilde{\xi}^2$, and neglecting $O(\tilde{\xi}^2)$ as is consistent with Eq. (81), gives the result

$$\kappa[K_0^*(\Delta - \Delta_c) - (\lambda - \lambda_c)]^{1/2}[\lambda - \lambda_c - K^*(\Delta - \Delta_c)] = -[\alpha\lambda_c + \hat{\beta}(\lambda - \lambda_c)]\tilde{\xi} \quad (82)$$

where the \pm sign has been absorbed in $\tilde{\xi}$ and

$$\begin{aligned} \kappa &= [K_0^*/(K_0^* - K^*)][K^*/b\lambda_c(K_0^* - K^*)]^{1/2} \\ \hat{\beta} &= \tilde{\beta} - C_1/2A_1 \end{aligned} \quad (83)$$

As noted previously, although the \bar{u}_2 -state is uniquely defined, the remaining states upon which $\hat{\beta}$ is dependent [see Eqs. (42b) and (72)], viz. \bar{u}_{01} and \bar{u}_{11} , are not. From Eqs. (54) and (55), \bar{u}_{01} and \bar{u}_{11} are only determined to within the amounts $C_{01}u_1$ and $2C_{01}\bar{u}_2$, where C_{01} is an arbitrary constant. Consequently, from Eqs. (57), $\hat{\beta}$ is only determined to within the arbitrary constant C_{01} . On the other hand, the coefficients in Eq. (82) must be invariant with respect to these changes, since the quantities λ and Δ have physical meaning. The only coefficient which needs to be checked is $\hat{\beta}$, since the others are obviously invariant, being independent of \bar{u}_{01} and \bar{u}_{11} .† Equations (72) show that when \bar{u}_{01} and \bar{u}_{11} change by $C_{01}u_1$ and $2C_{01}\bar{u}_2$, respectively, C_1 changes by

$$C_{01}[2\sigma_0 \cdot \bar{\epsilon}_2 + \sigma_1 \cdot \epsilon_1]/\lambda_c = 2C_{01}A_1 \quad (84)$$

so that $\hat{\beta} = \beta - C_1/2A_1$ changes by $C_{01} - 2C_{01}A_1/2A_1 = 0$, that is, $\hat{\beta}$ is invariant. This result serves as a qualitative check of the validity of Eq. (82).

VI. Buckling of Imperfection Sensitive Axisymmetric Structures

If the coefficient b is negative, the structure will buckle, for sufficiently small imperfections, at a limit load λ smaller than the bifurcation load λ_c of the model. This limit load λ^s is the maximum value of λ for equilibrium states at loads in the vicinity of λ_c , and therefore can be determined from Eq. (82). Differentiating Eq. (82) with respect to Δ and setting $d\lambda/d\Delta = 0$ give, after simplification,

$$\Delta_s - \Delta_c = (\lambda_s - \lambda_c)(K_0^* + 2K^*)/3K_0^*K^* \quad (85)$$

where Δ_s is the value of Δ at the limit load. Substituting Eq. (85) into Eq. (82)⁸ evaluated at the limit load, and using the first of Eq. (83) for κ give the equation for λ_s , viz.

$$(1 - \lambda_s/\lambda_c)^{3/2} + 3\hat{\beta}(-3b\bar{\epsilon}^2)^{1/2}(1 - \lambda_s/\lambda_c)/2 - 3\alpha(-3b\bar{\epsilon}^2)^{1/2}/2 = 0 \quad (86)$$

Equation (86) is of the same form as Eq. (36) of Ref. 1, the only difference being the replacement of β by $\hat{\beta}$. Therefore, Fig. 1 of Ref. 4, which is a graphical representation of Eq. (36) of Ref. 1, remains valid if β is interpreted to be $\hat{\beta}$. This figure is reproduced here as Fig. 1.

It is of interest to evaluate α and $\hat{\beta}$ for the special case of a linear prebuckling state neglecting prebuckling deformations and imperfection displacements \bar{U} equal to the buckling mode u_1 . This case was previously treated by Budiansky and Hutchinson (Refs. 2 and 6). It is noted that Eq. (86) would reduce to their result, Eq. (15) of Ref. 2, if, for this case, α and $\hat{\beta}$ both reduce to unity. In this case, the function-

† Note also, from Eqs. (57), that $\bar{\gamma} = 0$ is invariant for $a = C_2 = 0$.

als $E^{(1)}(u,v)$ and $F^{(1)}(u,v)$, given by Eqs. (15) and (20) of Ref. 1, reduce to

$$\lambda_c E^{(1)}(u,v) = \lambda_c F^{(1)}(u,v) = \sigma_0^* \cdot L_{11}(u,v) - \lambda_c q_1(u) \cdot v \quad (87)$$

From Eq. (42a), it is then clear that, neglecting the term containing the prebuckling displacements u_0^* , $\alpha = 1$. Setting $\delta u = u_1$ in the variational equation for u_1 , Eq. (8c) of Ref. 1, gives, in view of Eqs. (87)

$$\lambda_c F^{(1)}(u_1, u_1) = \sigma_0^* \cdot L_2(u_1) - \lambda_c q_1(u_1) \cdot u_1 = -\sigma_1 \cdot \epsilon_1 \quad (88)$$

Similarly, setting $\delta u = u_1$ in the first of Eqs. (40), and using $\alpha = 1$ and Eqs. (87) give

$$\lambda_c F^{(1)}(\bar{u}_{01}, u_1) = \sigma_0^* \cdot L_{11}(\bar{u}_{01}, u_1) - \lambda_c q_1(\bar{u}_{01}) \cdot u_1 = -\bar{\sigma}_{01} \cdot \epsilon_1 \quad (89)$$

Hence, from Eq. (42b), neglecting $F^{(2)}(u_1, u_1)$ for linear prebuckling, one obtains

$$\bar{\beta} = 1 + \bar{\sigma}_{01} \cdot \epsilon_1 / \sigma_1 \cdot \epsilon_1 \quad (90)$$

The remaining contribution to $\hat{\beta}$, $C_1/2A_1$ [see Eqs. (83)], may then be written from Eqs. (72)

$$C_1/2A_1 = 1 + (\bar{\sigma}_{01} \cdot \epsilon_1 + \sigma_0^* \cdot \bar{\epsilon}_{11} - \sigma_0^* \cdot \bar{\epsilon}_2) / (\sigma_1 \cdot \epsilon_1 + 2\sigma_0^* \cdot \bar{\epsilon}_2) \quad (91)$$

However, setting $\delta u = u_0^*$ in the third of Eqs. (40) shows that when the effect of prebuckling deformations is neglected

$$\sigma_0^* \cdot \bar{\epsilon}_{11} = \bar{\sigma}_{11} \cdot \epsilon_0^* = 0 \quad (92)$$

Similarly, one obtains from the variational equation for \bar{u}_2 [Eq. (13c) of Ref. 1]

$$\sigma_0^* \cdot \bar{\epsilon}_2 = \bar{\sigma}_2 \cdot \epsilon_0^* = 0 \quad (93)$$

Consequently, $C_1/2A_1$ reduces to

$$C_1/2A_1 = 1 + \bar{\sigma}_{01} \cdot \epsilon_1 / \sigma_1 \cdot \epsilon_1 \quad (94)$$

From Eqs. (90) and (94), it follows that

$$\hat{\beta} = \bar{\beta} - C_1/2A_1 = 0 \quad (95)$$

giving the curious result that in this special case, Koiter's first approximation includes the second approximation. Setting $\alpha = 1$ and $\hat{\beta} = 0$ in Eq. (86) gives the buckling load relation

$$(1 - \lambda_s/\lambda_c)^{3/2} - 3(-3b\bar{\xi}^2)^{1/2}/2 = 0 \quad (96)$$

In contrast, the generally accepted relation for this case, Eq. (15) of Ref. 2 or Eq. (25) of Ref. 6, is

$$(1 - \lambda_s/\lambda_c)^{3/2} - 3(-3b\bar{\xi}^2)^{1/2}(\lambda_s/\lambda_c)/2 = 0 \quad (97)$$

Equation (97) was obtained from the λ - ξ relation without consideration of terms in the displacement expansion associated with the imperfection [cf. Eq. (31)]. It would therefore appear that the extra term (λ_s/λ_c) in Eq. (97) is not justified and that no real gain in accuracy is achieved by including it.

VII. Concluding Remarks

The essential result of the foregoing analysis is the corrected formula for the second imperfection parameter $\hat{\beta}$. When $\hat{\beta}$ is neglected, as in Koiter's first approximation, the theory is strictly valid only for infinitesimal imperfections, and may predict erroneous or, in some cases, even negative buckling loads for reasonable finite imperfections. For buckling load knockdowns of roughly 0.6 or less, the curves of Fig. 1 for different values of $\hat{\beta}$ have diverged sufficiently to suggest that the effect of $\hat{\beta}$ should not be neglected.

A digital computer program (Ref. 4) exists which computes for stiffened shells of revolution the second postbuckling coefficient b , the first imperfection parameter α , and that part of $\hat{\beta}$ which is given in Ref. 1. At the present time, two imperfection shapes are treated by this program - one proportional to the buckling mode shape u_1 and the other being the shape which maximizes α for constant values of the mean square angular imperfection amplitude. Both of these imperfections contain only the circumferential harmonic n of the buckling mode. The computer work done in this calculation is roughly equivalent to two linear shell statics problems of the perfect shell of revolution with pure harmonic loading, corresponding to the two harmonic components of the \bar{u}_2 -state required in the evaluation of b . To complete the evaluation of $\hat{\beta}$, two additional displacement states, \bar{u}_{01} and \bar{u}_{11} , must be obtained. The state \bar{u}_{01} contains only the harmonic n , and although \bar{u}_{11} , like \bar{u}_2 , contains both axisymmetric and $2n$ harmonics, only its axisymmetric component is required to evaluate $\hat{\beta}$. Note that the homogeneous forms of the equations for all the perturbation states contributing to the physical equilibrium state, i.e., u_1 , \bar{u}_2 , \bar{u}_{01} , \bar{u}_{11} , etc., are identical. Thus, components of these states in the same circumferential harmonic differ only by virtue of different nonhomogeneous terms. Consequently, relatively little extra work is required to compute \bar{u}_{11} over and above that already required to compute \bar{u}_2 . For example, if these states are being computed by a superposition of complementary and particular solutions, only the particular solution need be recomputed for \bar{u}_{11} , since the complementary

solutions computed for \bar{u}_2 apply to \bar{u}_{11} as well. Although \bar{u}_{01} and \bar{u}_{11} depend on the imperfection shape \bar{u} assumed, changes in this shape also require only the recalculation of the particular solution. Thus, the calculation of b , α , and β for a given buckling mode is roughly equivalent to that required for the solution of three linear shell statics problems with pure harmonic loading.

Since such problems are executed very rapidly with modern computers, the determination of a limit load, once the bifurcation mode of the perfect structure has been obtained, will require a relatively small amount of computer time. On the other hand, the unique mode theory employed does not account for the interaction of bifurcation modes, which can be important for closely spaced eigenvalues or in case of a higher mode being much more sensitive to imperfections than the fundamental mode. It may be feasible to include in the computer program the calculation of the extra coefficients involved when two modes are assumed to be active. However, there is clearly a practical limit to the number of interactive modes one would want to treat with this approach.

An alternate approach to the problem of computing limit loads of shells of revolution is the direct nonlinear two-dimensional finite difference (or finite element) approach as in Ref. 7. In contrast to the Koiter-type approach, in this method the imperfection is included in the shape of the shell numerically treated, so that, in general, the structure input to the computer is nonaxisymmetric. This approach, has the advantage that it automatically accounts for the nonlinear interaction of bifurcation modes and also imperfections of finite size. On the other hand, the basic simplicity of the Koiter-type approach, which requires only one-dimensional numerical calculations is lost. Programs based on direct solution of the nonlinear equations require very much more computer time and storage, and therefore although in principle applying to a larger class of problems, in practice the complexity of axisymmetric structures treatable may be more limited. Inclusion of the β -calculation in the Koiter-type program should serve to reduce any discrepancies attributable to finite imperfections found in a comparison of numerical results of these two different methods.

The basic idea employed in this paper, namely that of obtaining a physically meaningful load-deflection relation, can be employed to obtain still higher approximations within the context of Koiter's theory. For example, consideration of the third and fourth postbuckling coefficients should give some insight into the behavior of those structures which have a very shallow postbuckling load drop-off. In such cases, a real structure with small but finite imperfections may exhibit no limit load behavior, but rather a monotonically increasing load-deflection curve.

References

1. Cohen, G.A., "Effect of a Nonlinear Prebuckling State on the Postbuckling Behavior and Imperfection Sensitivity of Elastic Structures," AIAA J., vol. 6, no. 8, 1968, pp. 1616-1619; also "Reply by Author to J.R. Fitch and J.W. Hutchinson," AIAA J., vol. 7, no. 7, 1969, pp. 1407-1408.
2. Budiansky, B. and Hutchinson, J.W., "Dynamic Buckling of Imperfection-Sensitive Structures," Proceedings of the XI International Congress of Applied Mechanics, edited by H. Gortler, Springer-Verlag, Berlin, 1964, pp. 636-651.
3. Koiter, W.T., "On the Stability of Elastic Equilibrium," thesis, Polytechnic Institute at Delft, H.J. Paris, Amsterdam, 1945 (in Dutch); English translation, NASA TT F-10,833, 1967.
4. Cohen, G.A., "Computer Analysis of Imperfection Sensitivity of Ring-Stiffened Orthotropic Shells of Revolution," Proceedings of the AIAA/ASME 11th Structures, Structural Dynamics, and Materials Conference, vol. 1, April 1970, pp. 185-195.
5. Cohen, G.A., "Imperfection Sensitivity of Optimum Structural Designs for a Mars Entry Capsule," NASA CR (number to be assigned), 1970.
6. Budiansky, B., "Dynamic Buckling of Elastic Structures: Criteria and Estimates," Proceedings, International Conference on Dynamic Stability of Structures, Pergamon, New York, 1966, pp. 83-106.
7. Brogan F. and Almroth B., "Buckling of Cylinder with Cutouts," AIAA J. vol. 8, no. 2, 1970, pp. 236-240.

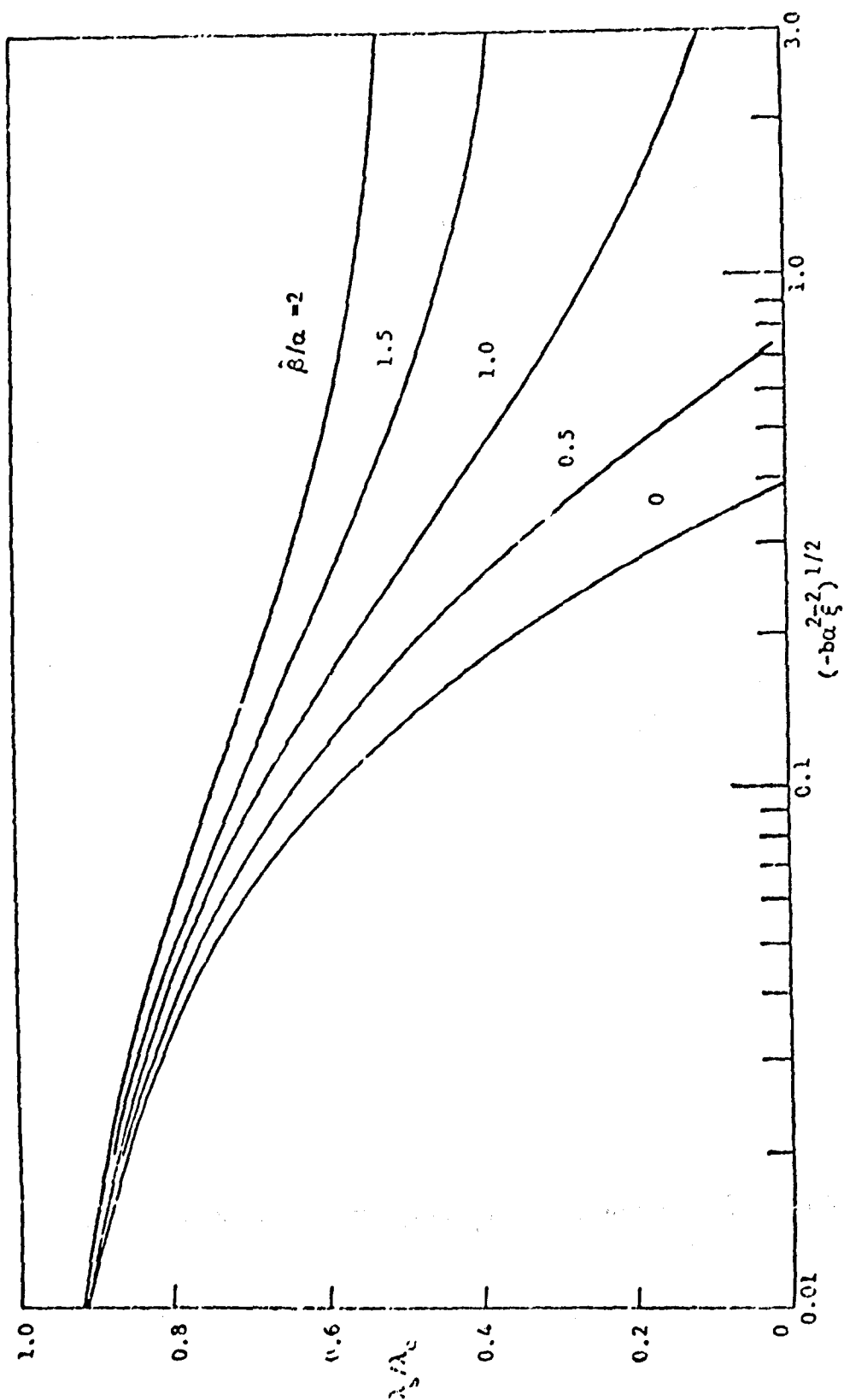


FIGURE 1. CRITICAL LOADS OF IMPERFECTION SENSITIVE STRUCTURES

QUESTIONS AND COMMENTS FOLLOWING COHEN'S PAPER

BALL: At the Wednesday morning session I talked briefly about this particular problem of determining imperfection sensitivity of shells and I agree with Dr. Cohen that his program is 1-D and that the STAGS program is 2-D. I'd like to classify mine as maybe several 1-D programs in which I do essentially what Dr. Cohen has talked about here, but I am not restricted to any one mode or two modes. I could select a number of modes and take into account the full coupling between these modes with no approximations. If these modes in themselves excite other modes, they could also be taken into account. So the complications that you mentioned, I feel, have been overcome in my particular program. I will have to admit, however, that my particular program does not handle the stringers or other features present in more practical shells. I will also say that the present program as such does not contain provisions for inserting geometric imperfections of a measured shell. However, this is very simply done.

COHEN: Well, I don't believe that you're obtaining a stress-free imperfection in your approach.

BALL: No, I mentioned I could. I agree that at the present time the program does not contain a mechanism for inserting geometric imperfections. However, this is a simple matter to do and slip them on the right-hand side.

COHEN: Okay, but then you've got the problem of coupled harmonics.

BALL: I've already taken that into account.

COHEN: It's clearly a more complicated approach. It's like you say, two or three one-dimensional problems.

NACHBAR: This past year, R. T. Haftka, R. H. Mallett and I have been working on application of Koiter's theory to finite element analysis of structures.* We have shown that the principal limitation of Koiter's method, which is the restriction to snap-through only in the imperfection neighborhood of bifurcating structures, can be eliminated. We can take general structures which do not necessarily have any adjacent bifurcating structure and apply Koiter's asymptotic expansion method. Moreover, our method can be used in conjunction with a linear finite element analysis; it need not be a nonlinear program.

One difficulty with asymptotic methods, however, is that it is possible to predict an effect which in practice isn't there because the expansion is valid in too restricted a regime. In other words, if the expansion is really valid only for such extremely small imperfections that have no practical meaning, we can actually lose this effect in the experiment. A resolution of this, we think, is to use the Koiter analysis as a warning signal. With our method, we can attach the Koiter analysis to a linear finite element analysis and use it to show a flag as to where trouble can occur. Then we go to a direct nonlinear analysis to actually plot the load-deflection curve and see the post-

*See Technical Report AFFDL-TR-130, November 1970; also "Adaption of Koiter's Method to Finite Element Analysis of Snap-Through Buckling Behavior," by R. T. Haftka, R. H. Mallett and W. Nachbar, in press, Int. J. Solids Structures.

buckling portion for finite imperfections.

I bring this up with reference to the graph you showed for the Koiter analysis of the conical shell for NASA. There were no dimensions shown on this graph, but I assume that little dip there is actually a very small one if plotted out on a nonlinear analysis and, as you stated in your talk, with any sort of a finite imperfection this dip was just bypassed in the direct nonlinear analysis results. You just saw a little increase in deflection; that was it. Well, for this case, I rather doubt that you can do anything with the Koiter analysis with high-order terms. You said that the term $(\beta/\alpha) (\lambda - \lambda_c)$ may be of order 1 even though $(\lambda - \lambda_c)$ is presumed to be small. This is a dangerous assumption, because there are no error estimates on asymptotic expansions. These terms are neglected compared to 1 regardless of the coefficients, no assumptions are made as to the relative order between $(\lambda - \lambda_c)$ and ξ itself. We expand in them independently.

If you are going to include the term $(\beta/\alpha) (\lambda - \lambda_c)$, this may have meaning experimentally. In other words, you can try cases in which it does have meaning, but your example of the NASA cone appears to show that improvement of the prediction for finite imperfections is not likely. I would like your comments on this.

COHEN: I think that the excellent agreement for the stringer-stiffened cylinder obtained by Frank Brogan using the STAGS program and myself using my program shows the usefulness of the Koiter analysis to obtain quantitative results. As you know, STAGS is a nonlinear response program, and in the comparison the knockdowns obtained, although not great, are as much as 0.8.

NACHBAR: The Koiter analysis can be extremely accurate. I'm saying that it also can be misleading for finite imperfections. In other words, from one example to another you can have different results.

COHEN: In his thesis, Koiter does show the order of the error terms that are being neglected and the expanded λ - ξ relationship that I showed is a consistent relationship. That is, all the terms that have been neglected are of higher order than the terms that have been retained. I feel that if this is done consistently and a careful tracking maintained of the order of the terms that are neglected, then one can go to higher approximations. The proof of the pudding seems to me to lie in this example involving a comparison with STAGS. I purposely took a small imperfection so the effect of high order terms is obviously negligible from the results. What we intend to do is take increasingly large imperfections and we should show a greater divergence between the results when just the α approximation is included. What I'm hoping is that by including the corrected β , we'll show that reduces the difference between the results. To me that will be some form of a numerical verification of inclusion of the β parameter. I would like to say one other thing. From your discussion, it appears that you have extended a Koiter type analysis to limit load buckling and Koiter analysis shows a drastic reduction in bifurcation load to a limit load for very small imperfections, but I doubt whether the same thing would occur in going from a limit load to another limit load.

BUSHNELL: I think in considering this question of whether the Koiter theory will ever be able to predict the initial post buckling instability and subsequent stability, it might be a good idea to look at the physics of the prob-

lem. For instance, if we try to relate this to buckling of an oval cylinder under uniform end shortening, what happens is that the low curvature areas buckle and the stresses are redistributed in the shell. It seems that the Koiter theory is tied to the prebuckling state at the bifurcation point and this problem is changing drastically as the loading continues. The oval cylinder carries load above the bifurcation load because the prebuckling problem has changed. I think it's probably a little bit optimistic to hope to predict this with the Koiter theory.

COHEN: It seems to me to be a question of how far away you get from the bifurcation point. If a shallow post-buckling dropoff is close enough, the theory may predict it, but clearly there must be a limit. You're not going to go way out into the post-buckling range with the Koiter theory and maybe you don't have to.

THE APPLICATION OF GRADIENT MINIMIZATION
METHODS AND HIGHER ORDER
DISCRETE ELEMENTS TO SHELL BUCKLING
AND VIBRATION EIGENPROBLEMS

Edward L. Stanton
and
Dennis J. McGovern

McDonnell Douglas Astronautics Company - West
Huntington Beach, California

ABSTRACT

Gradient minimization methods have been successfully applied to the discrete element analysis of shells with geometric nonlinearities and to plates with material nonlinearities. More recently, the feasibility of using such methods for the lower buckling and vibration modes of large eigenproblems has been established. The present investigation extends this work by developing scaling criteria and rescaling strategies based on the second variation of the discretized Rayleigh quotient. The importance of scaling to the efficiency of the conjugate gradient algorithm is found to be similar to that reported for potential energy minimization. Several shell vibration and shell buckling problems are then analyzed using the forty eight degree of freedom Bogner cylindrical panel element reformulated to include an incremental stiffness matrix. This element is based on bicubic Hermite polynomials for which discretization error bounds indicate rapid eigenvalue and eigenvector convergence in certain elliptic boundary value problems. These convergence rates are numerically tested in both shell buckling and vibration eigenproblems.

INTRODUCTION

Plate and shell discrete elements using $\mathcal{O}(\Delta^4)$ bicubic interpolation polynomials for the transverse displacement, w , are now widely available (References 1-4) and several also use the same polynomials for the in-plane displacements, u and v (References 1 and 2). The stress and displacement results obtained with these elements in standard reference problems exhibit rapid convergence to the true solutions. In the case of the 16-parameter plate element (Reference 1), convergence rates of $\mathcal{O}(\Delta^4)$ for displacement and $\mathcal{O}(\Delta^2)$ for stress have been obtained (Reference 5). This element has also been evaluated in buckling applications (Reference 6) and the results obtained indicate excellent convergence for the lowest eigenvalue. Recently, shell vibration (Reference 7) and shell buckling (Reference 4) results have been obtained using cylindrical panel elements of 48 and 24 degrees of freedom, respectively. The large size of the associated element matrices results in rather large eigenproblems, even for coarse idealizations. Thus, while improvements in discrete element technology permit more accurate analysis of many shell vibration and shell buckling problems, these analyses require the solution of eigenproblems near, if not beyond, the state of the art. In some cases, the size of the eigenproblem can be reduced without serious loss of accuracy by introducing constraint equations among the displacement variables. This is possible in vibration problems, more often than with buckling problems, although the technique was used to advantage in Reference 4. When the assembled structural matrices for a particular discrete element idealization are tightly banded, it may be possible to efficiently compute the lower modes by inverse iteration. This method has been used very successfully to compute the lower vibration modes of a cylinder with a cutout analyzed by the finite difference method (Reference 8). When the assembled structural matrices are sparse but not banded, a gradient minimization method has been suggested for the structural dynamics eigenproblem (Reference 9). A similar approach has also been applied to plate buckling eigenproblems (Reference 10). The present investigation extends this work to include scaling and applies the method to shell vibration and buckling analyses, using the 48 degree of freedom cylindrical panel element of Reference 1, reformulated to obtain first and second order incremental stiffness matrices. A linear bifurcation buckling analysis is employed with the prebuckling displacements obtained from a

efficiency of the scaled gradient minimization algorithm for the eigenproblem are compared with solutions from a Householder matrix eigenvalue routine and an inverse iteration eigenvalue routine. The latter routine uses a non-square-root Cholesky decomposition procedure (Reference 11) that takes advantage of any banded sparsity in the stiffness matrix. After evaluating eigenvalue routines, the cylindrical panel element convergence properties for buckling problems is evaluated and several analyses that include bending effects are presented.

AN ENERGY FORMULATION OF CONSISTENT ELEMENT MATRICES

The phrase "consistent element matrix" will be used to imply (1) that the assumed displacement functions used to discretize strain energy are also used to discretize kinetic energy or any other physical quantity present and (2) that the quadrature scheme used to generate these matrices does not change the order of the discretization error. Consistent first and second order incremental stiffness matrices are derived for a cylindrical panel discrete element originally formulated in Reference 1. The original formulation accounts for geometric nonlinearities through quartic terms in the strain energy in a consistent manner but not in a way that lends itself to a bifurcation buckling analysis. The present formulation may be used for either bifurcation buckling or nonlinear load deflection analyses.

Stiffness Matrices - K_2 , K_3 , K_4

Several discrete element formulations of geometric nonlinearity are possible (References 1, 2, 12, 13, and 14). The present formulation is similar to that in Reference 12 and mathematically begins with the selection of strain-displacement equations and a stress-strain law for the material. These are used to define the potential energy which is then discretized, using assumed displacement functions defined locally over the middle surface of a discrete element. The local element displacement functions are linked at nodes to obtain a global displacement function that satisfies the admissibility (i. e., smoothness) requirements of the energy derived variational principles. These variational principles are then used to define discretized equilibrium equations and stability criteria. Since the stability criteria used is in terms of the second variation of the potential energy it is convenient to define the K_2 , K_3 and K_4 matrices in terms of second partial derivatives.

Let U_2 be that portion of the strain energy quadratic in the displacements, U_3 the portion cubic in the displacements and U_4 the portion quartic in the displacements. If X_i denotes a nodal displacement parameter in the assumed displacement function where $i = 1, 2, \dots, N$ then

$$K_2 = \frac{\partial^2}{\partial X_m \partial X_n} U_2 (X_1, X_2, \dots, X_N) \quad (2.1)$$

$$K_3 = \frac{\partial^2}{\partial X_m \partial X_n} U_3 (X_1, X_2, \dots, X_N) \quad (2.2)$$

$$K_4 = \frac{\partial^2}{\partial X_m \partial X_n} U_4 (X_1, X_2, \dots, X_N) \quad (2.3)$$

This definition of K_2 is one of several equivalent ways of expressing the usual linear elastic stiffness matrix. The K_3 and K_4 matrices are equivalent to N1 and N2 of Reference 12 in the present analysis. Using the vector, $X = (X_1, X_2, \dots, X_N)^T$, the discretized potential energy is

$$\pi(X) = X^T \left[\frac{1}{2} K_2 + \frac{1}{6} K_3 (X) + \frac{1}{12} K_4 (X) \right] X - X^T F \quad (2.4)$$

with first variation

$$\nabla \pi(X)^T \cdot \delta X = \left[K_2 + \frac{1}{2} K_3 (X) + \frac{1}{3} K_4 (X) \right] X - F^T \cdot \delta X \quad (2.5)$$

and second variation

$$\delta X^T \cdot \nabla^2 \pi(X) \cdot \delta X = \delta X^T [K_2 + K_3 (X) + K_4 (X)] \delta X \quad (2.6)$$

These equations assume a linear elastic stress-strain law. The stability criteria assumes a conservative holonomic system and specifies an equilibrium position, X_E , as stable if $[K_2 + K_3 (X_E) + K_4 (X_E)]$ is positive definite (Reference 15). This formulation will now be used to derive specific K_3 and

K_4 matrices for the cylindrical panel element of Reference 1. The strain-displacement equations used are repeated here*

$$\epsilon_s = u_{,s} + \frac{1}{2} w_{,s}^2 - z w_{,ss} \quad (2.7)$$

$$\epsilon_\theta = \frac{1}{r} (v_{,\theta} + w) + \frac{1}{r^2} \left[\frac{1}{2} w_{,\theta}^2 - z (w_{,\theta\theta} - v_{,\theta}) \right] \quad (2.8)$$

$$\epsilon_{s\theta} = \frac{1}{r} \left(v_{,s} - \frac{u_{,\theta}}{r} \right) + \frac{1}{2r} w_{,s} w_{,\theta} - \frac{z}{r} (w_{,s\theta} - v_{,s}) \quad (2.9)$$

and the strain energy functions U_3 and U_4 for a linear elastic material are

$$U_{3C} = \frac{D}{2} \int_0^1 \int_0^{r\Delta\theta} \frac{12}{h^2} \left\{ u_{,s} \left[w_{,s}^2 + \nu w_{,\eta}^2 \right] + \nu \eta \left[w_{,\eta}^2 + \nu w_{,s}^2 \right] \right. \\ \left. + (1-\nu) (u_{,\eta} + v_{,s}) w_{,s} w_{,\eta} + \frac{w}{r} \left[w_{,\eta}^2 + \nu w_{,s}^2 \right] \right\} d\eta ds \quad (2.10)$$

$$U_{4C} = \frac{D}{2} \int_0^1 \int_0^{r\Delta\theta} \frac{12}{h^2} \left\{ \frac{1}{4} \left[w_{,s}^4 + w_{,\eta}^4 \right] + \frac{1}{2} w_{,s}^2 w_{,\eta}^2 \right\} d\eta ds \quad (2.11)$$

where D is the flexural rigidity, $Eh^3/12(1-\nu^2)$, and $\eta = r\theta$. The quadratic term, U_2 , is not repeated as the K_2 matrix is unchanged from the formulation in Reference 1. The displacements u , v and w are each approximated using 16 parameter bicubic Hermite polynomials $H_{kj}^{(1)}(s)H_{li}^{(1)}(\eta)$; $k, l = 0, 1$ for $i, j = 1, 2$. The component polynomials, $H_{kj}^{(1)}(s)$, are simply the beam functions and are tabulated in Reference 1. Let $P_m(s, \eta)$ denote a component of the 16 degree

*The comma notation denotes differentiation with respect to the coordinate variables indicated by subscripts to the right of the comma.

of freedom vector $P(s, \eta)$ generated from the $H_{kj}^{(1)}(s)H_{li}^{(1)}(\eta)$ by varying k, l, i and j in that order through their respective ranges. Then

$$u(s, \eta) = \sum_{m=1}^{16} U_m P_m(s, \eta) = U^T P \quad (2.12)$$

$$v(s, \eta) = \sum_{m=1}^{16} V_m P_m(s, \eta) = V^T P \quad (2.13)$$

$$w(s, \eta) = \sum_{m=1}^{16} W_m P_m(s, \eta) = W^T P \quad (2.14)$$

where U_m, V_m and W_m are the 48 scalar nodal parameters of the discrete element. These nodal parameters are $U, U_s, U_\eta, U_{s\eta}, V, V_s, V_\eta, V_{s\eta}, W, W_s, W_\eta$ and $W_{s\eta}$ at each of the four element nodes. Substituting the assumed displacement functions into Eq (2.2) and differentiating gives the K_3 matrix

$$K_3 = \begin{bmatrix} 0 & 0 & K^{WU^T} \\ 0 & 0 & K^{WV^T} \\ K_3^{WU} & K_3^{WV} & K_3^W \end{bmatrix} \quad (2.15)$$

where

$$\begin{aligned} (K_3^W)_{ij} = & \frac{12D}{h^2} \int_0^1 \int_0^{r\Delta\theta} \left\{ (\sum_k U_k P_{k,s}) (P_{i,s} P_{j,s} + \nu P_{i,\eta} P_{j,\eta}) \right. \\ & + (\sum_k V_k P_{k,\eta} + \frac{1}{r} \sum_k W_k P_k) (P_{i,\eta} P_{j,\eta} + \nu P_{i,s} P_{j,s}) \\ & + (1/r) (\sum_k W_k P_{k,\eta}) (P_i P_{j,\eta} + P_{i,\eta} P_j) \\ & + (\nu/r) (\sum_k W_k P_{k,s}) (P_i P_{j,s} + P_{i,s} P_j) \\ & \left. + 1/2(1-\nu)(\sum_k U_k P_{k,\eta} + \sum_k V_k P_{k,s})(P_{i,s} P_{j,\eta} + P_{i,\eta} P_{j,s}) \right\} d\eta ds \end{aligned} \quad (2.16)$$

$$\begin{aligned}
(K_3^{WU})_{ij} = & \frac{12D}{h^2} \int_0^1 \int_0^{r\Delta\theta} \left\{ (\sum W_k P_{k,s}) [P_{i,s} P_{j,s} \right. \\
& + \frac{1}{2} (1-\nu) P_{i,\eta} P_{j,\eta}] + (\sum W_k P_{k,n}) [\nu P_{i,\eta} P_{j,s} \\
& \left. + \frac{1}{2} (1-\nu) P_{i,s} P_{j,\eta}] \right\} d\eta ds
\end{aligned} \tag{2.17}$$

$$\begin{aligned}
(K_3^{WV})_{ij} = & \frac{12D}{h^2} \int_0^1 \int_0^{r\Delta\theta} \left\{ (\sum W_k P_{k,\eta}) [P_{i,\eta} P_{j,\eta} \right. \\
& + \frac{1}{2} (1-\nu) P_{i,s} P_{j,s}] + (\sum W_k P_{k,s}) [\nu P_{i,s} P_{j,\eta} \\
& \left. + \frac{1}{2} (1-\nu) P_{i,\eta} P_{j,s}] \right\} d\eta ds
\end{aligned} \tag{2.18}$$

The K_3 matrix is a linear function of the nodal parameters as these equations demonstrate explicitly. In a linearized bifurcation buckling analysis, these nodal parameters are assumed to increase linearly, $X = \lambda X_0$, until buckling. However, even in this case, the prebuckling solution, X_0 , produces non-uniform membrane stresses and bending displacements within each element. These are accounted for in K_3 , using X_0 to make the integrations in Eq (2.16-2.18). The integrations can be made economically by observing that they are always a linear combination of a relatively small number of reference integrals that can be made once and stored. The K_4 matrix is derived using the same assumed displacement functions as

$$K_4 = \begin{bmatrix} 0 & 0 & 0 \\ 0 & 0 & 0 \\ 0 & 0 & K_4^W \end{bmatrix} \tag{2.19}$$

where

$$\begin{aligned}
 (K_4^W)_{ij} = & \frac{18D}{h^2} \int_0^1 \int_0^{\Delta\theta} \left\{ (\sum_k \sum_s W_k W_l P_{k,s} P_{l,s}) (P_{i,s} P_{j,s}) \right. \\
 & + (\sum_k \sum_\eta W_k W_l P_{k,\eta} P_{l,\eta}) (P_{i,\eta} P_{j,\eta}) \\
 & \left. + (\sum_k \sum_s W_k W_l P_{k,s} P_{l,\eta}) (P_{i,s} P_{j,\eta} + P_{i,\eta} P_{j,s}) \right\} d\eta ds
 \end{aligned} \tag{2.20}$$

The K_4 matrix is a quadratic function of the nodal parameters, as this equation demonstrates explicitly. Although this second order incremental stiffness matrix could be included in a generalized bifurcation buckling analysis ($K_2 + \lambda K_3 + \lambda^2 K_4$) the results presented later are limited to the first order incremental stiffness matrix K_3 . The formulation of K_3 in Eq (2.16-2.18) was used to generate this matrix in numerical calculations presented later. These equations (2.16-2.18) can be written in a more compact form using Eq (2.12-2.14) in reverse and the linear membrane stress displacement equations. Let σ_s^m , σ_θ^m and $\sigma_{s\theta}^m$ denote the linear membrane stresses

$$\sigma_s^m = \frac{E}{1-\nu^2} [u_{,s} + (\nu/r)(v_{,\theta} + w)] \tag{2.21}$$

$$\sigma_\theta^m = \frac{E}{1-\nu^2} [(v_{,\theta} + w)/r + \nu u_{,s}] \tag{2.22}$$

$$\sigma_{s\theta}^m = \frac{E}{2(1+\nu)} [v_{,s} + u_{,\theta}/r] \tag{2.23}$$

then the K_3^W matrix can be written

$$\begin{aligned}
 (K_3^W)_{ij} = & h \int_0^1 \int_0^{\Delta\theta} \left[\sigma_s^m (P_{i,s} P_{j,s}) + \sigma_\theta^m (P_{i,\eta} P_{j,\eta}) + \sigma_{s\theta}^m (P_{i,s} P_{j,\eta} \right. \\
 & \left. + P_{i,\eta} P_{j,s}) + \frac{E}{1-\nu^2} [(W_{,\eta}/r) (P_i P_{j,\eta} + P_{i,\eta} P_j) \right. \\
 & \left. + \nu (W_{,s}/r) (P_i P_{j,s} + P_{i,s} P_j)] \right] d\eta ds
 \end{aligned} \quad (2.24)$$

The stresses and bending rotations in Eq (2.24) must be obtained from the assumed displacement functions if this form of K_3^W is to be consistent with Eq (2.16). The present analysis uses Eq (2.16-2.18) and, for bifurcation buckling, obtains the prebuckling displacements, hence stresses from a linear bending theory solution. Reference 16 defines a conventional analysis as one using membrane theory for the prebuckling stresses. To obtain a K_3^W for this case, Eq (2.24) can be used with the bending rotation terms omitted. To perform a nonlinear load deflection analysis, the equilibrium equations are obtained from Eq (2.5) where, unless the structure is loaded into the post buckled region, the $K_4(X)$ term can usually be omitted.

Mass Matrix - M

The kinetic energy expression for a body

$$T = \frac{1}{2} \int_V \rho (\dot{u}^2 + \dot{v}^2 + \dot{w}^2) dV$$

(using the dot notation for time differentiation) and the displacement variations through the thickness implicit in the strain-displacement equations, Eq (2.7-2.9), result in

$$\begin{aligned}
 T = & \frac{1}{2} \int_0^1 \int_0^{\Delta\theta} \rho \left[h(\dot{u}^2 + \dot{v}^2 + \dot{w}^2) + \frac{h^3}{12} (\dot{w}_{,s}^2 + (\dot{w}_{,\theta}/r)^2 \right. \\
 & \left. + (\dot{v}/r)^2 - 2\dot{v} \dot{w}_{,\theta}/r^2) \right] r d\theta ds
 \end{aligned} \quad (2.25)$$

Neglecting the rotary terms associated with \dot{v} and substituting the assumed displacement functions in Eq (2.25) gives

$$T = \frac{1}{2} [U^T M^U U + V^T M^V V + W^T M^W W] \quad (2.26)$$

where

$$(M^U)_{ij} = (M^V)_{ij} = \int_0^1 \int_0^{r\Delta\theta} \rho h (P_i P_j) d\eta ds \quad (2.27)$$

$$(M^W)_{ij} = \int_0^1 \int_0^{r\Delta\theta} \rho h \left[P_i P_j + \frac{h^2}{12} (F_{i,s} P_{j,s} + P_{i,\eta} P_{j,\eta}) \right] d\eta ds \quad (2.28)$$

This is the element mass matrix used for the vibration results presented later. It is identical to the one defined in Reference 1.

A SCALED GRADIENT MINIMIZATION METHOD FOR VIBRATION AND BUCKLING EIGENPROBLEMS

Several recent investigations (References 9, 10, and 17) have applied modern function minimization methods to a matrix Rayleigh quotient formulation of discrete vibration and buckling eigenproblems. These studies demonstrate the feasibility of using numerical minimization methods for computing the lower modes. References 9 and 10 suggest that very large discrete element eigenproblems arising from displacement formulations can be solved for the lower modes, using the conjugate gradient algorithm. In part this is a result of taking advantage of sparsity in the displacement method coefficient matrices when computing the gradient of the Rayleigh quotient. Using such procedures and the conjugate gradient algorithm, a 281 degree of freedom vibration eigenproblem is solved in Reference 9 and a 400 degree of freedom buckling eigenproblem is solved in Reference 10. The size of these problems is large by most standards (Reference 4), although small in comparison to a recent inverse iteration solution of a 4,029 degree of freedom shell of revolution vibration

problem (Reference 8). This rather remarkable solution was obtained by virtue of the coefficient matrices being tightly banded, which is typical of shells of revolution. In structures with less geometric regularity, the coefficient matrices may be equally sparse but have considerable variations in bandwidth. It is for such structures that minimization methods offer possible advantages, in that they are not directly influenced by bandwidth.

Rayleigh Quotient Formulation of Vibration and Buckling Eigenproblems

Linear elastic matrix vibration and buckling eigenproblems are of the form $AX = \lambda BX$, where both A and B are independent of X, both are symmetric and at least one of the coefficient matrices is positive definite. The minimizing properties of the eigenvectors, X_k , for such coefficient matrices are well known (cf. Reference 18, pp 317-331) and are briefly summarized here for reference. Let the eigenvalues be arranged in non-decreasing order, $\lambda_1 \leq \lambda_2 \leq \dots \leq \lambda_N$, then

$$\lambda_k = \frac{\text{Min}_X \frac{X^T A X}{X^T B X}}{\quad} \quad (3.1)$$

subject to the constraints

$$X \neq 0 \quad (3.2)$$

$$X^T B X_j = 0 \quad ; \quad j = 1, 2, \dots, k-1 \quad (3.3)$$

where A and B are symmetric and B is positive definite. The vibration eigenproblem is directly $A = K_2$, $B = M$ and $\lambda = \omega^2$. The linear buckling eigenproblem from Eq (2.6) has $A = K_2$, $B = -K_3$ and Eq (3.1) does not directly apply as B is not positive definite. The buckling eigenproblem may also have both positive and negative eigenvalues. To obtain the smallest positive eigenvalue, Λ_c , of $K_2 + \Lambda K_3$ take $A = K_3$ and $B = K_2$ which gives $\Lambda_c = (-1/\lambda_1)$. This is the Rayleigh quotient formulation of the buckling eigenproblem used in the numerical work presented later.

Scaled Conjugate Gradient Minimization of the Rayleigh Quotient

The minimization problem posed in Eq (3.1-3.3) is a constrained minimization problem for a function that is not convex. This usually implies a difficult if not intractable computational problem especially when X contains many degrees of freedom. Fortunately this is not the case for Eq (3.1-3.3) and the lower modes which involve few constraint equations. Let $R(X)$ denote the Rayleigh quotient

$$R(X) = \frac{X^T A X}{X^T B X} \quad (3.4)$$

which is indeterminate at the point $X = 0$ giving rise to the first constraint. This constraint can be implemented in many different ways

$$X^T B X = 1 \quad (3.5)$$

$$X^T X = 1 \quad (3.6)$$

$$\text{Max}_i |X_i| = 1 \quad (3.7)$$

and the particular form the constraint takes corresponds to a particular normalization of the eigenvectors. The relative merits of Eq (3.5-3.7) are discussed in Reference 17 and Eq (3.7), recommended for its computational simplicity. This constraint and the eigenvector orthogonality constraints, Eq (3.3), were appended to the Rayleigh quotient in Reference 9, using Lagrange multipliers. Reference 10 uses the previously found eigenvalues to append the orthogonality constraints. This latter procedure results in quadratic terms, $(X^T K_2 Z_i)^2$, which may adversely effect the conditioning of the minimization problem. Using the Lagrange multiplier approach, Eq (3.4) becomes

$$L_k(X, \alpha_i) = R(X) - \sum_{i=1}^{k-1} \alpha_i X^T Y_i - \alpha_k (X^T e_j - 1) \quad (3.8)$$

where the α_i are Lagrange multipliers, $Y_i = B Z_i$ and e_j is the unit vector associated with using Eq (3.7) for normalization. The Euler-Lagrange equations associated with variations in X

$$\nabla R - \sum_{i=1}^{k-1} \alpha_i Y_i - \alpha_k e_j = 0 \quad (3.9)$$

expressed in matrix notation

$$\nabla R - N_k \alpha = 0 \quad (3.10)$$

can be used to express α in terms of ∇R

$$\alpha = [N_k^T N_k]^{-1} N_k^T \nabla R \quad (3.11)$$

giving

$$\nabla_{X_k} L_k = \nabla R - N_k [N_k^T N_k]^{-1} N_k^T \nabla R = [P_k] \nabla R \quad (3.12)$$

This projection matrix formulation was successfully used in Reference 9 to minimize $R(X)$ in the subspace defined by the constraints. The procedure used was to first obtain a starting vector, X_0 , in this subspace and then use the conjugate gradient algorithm to minimize $L_k(X, \alpha_i)$ which is identically equal to $R(X)$ in the subspace defined by the constraints. Each step, i , in this minimization requires a one dimensional minimization

$$\text{Min}_t R(X_i + t S_i) \quad (3.13)$$

where S_i is the direction of travel determined by the conjugate gradient algorithm. The non-convexity of $R(X)$ could make this a formidable computation if $R(X)$ were not the ratio of quadratics. This property was used in Reference 17 to solve the one dimensional search problem in closed form. This solution was used in References 9 and 10, and also in the present work.

Use of the conjugate gradient algorithm to minimize other functions has demonstrated that scaling can significantly improve the convergence of the algorithm (References 19 and 20). The scaling used in these References is based on the diagonal elements of the matrix of second partial derivatives. The objective of this scaling is the improvement of the conditioning number of the matrix of second partial derivatives which directly influences the convergence of the conjugate gradient algorithm (Reference 21). In the case of the Rayleigh quotient, this matrix is

$$\nabla_x^2 L = \nabla^2 R = \frac{2}{b} [bA - aB - 2A X X^T B^T - 2B X X^T A^T + 4(\frac{a}{b})B X X^T B^T] \quad (3.14)$$

where

$$a = X^T A X \quad (3.15)$$

$$b = X^T B X \quad (3.16)$$

It is important to note that AX , BX , a and b are available from the computation of the gradient. As a consequence, the computation of the diagonal elements of the $\nabla^2 R$ matrix is simple. This matrix is of course a function of X so that any scaling procedure based on $\nabla^2 R$ is itself dependent on X . The diagonal scaling suggested in Reference 19 uses the square root of the diagonal elements which may be negative in the case of $\nabla^2 R$. A simple modification that avoids this is the use of the absolute value of the diagonal elements as in Reference 20. The rationale for this is the same Gerschgorin circle argument advanced in Reference 19. Instead of the Gerschgorin circles having one common center at $1/c^2$, they now have two possible centers at $\pm 1/c^2$, where the scaling transformation D is

$$d_{ij} = \frac{\delta_{ij}}{c |\nabla^2 R_{ij}|^{1/2}} \quad (3.17)$$

Another consequence of $\nabla^2 R$ not necessarily being positive definite is that the radii of the circles cannot be bounded as in Reference 19. However, the submatrix of $\nabla^2 R$ associated with the $N-1$ independent X_i in the first mode search is positive definite near Z_1 . This submatrix is obtained by deleting the row and column of $\nabla^2 R$ associated with the X_i prescribed to unity for the constraint given by Eq (3.2). At least for the first mode then, the scaling criteria of Reference 19 is applicable. In addition to a scaling criteria it is also necessary to decide how often to scale, as $\nabla^2 R$ may change considerably during the minimization. Experience with the scaling criteria of Eq (3.17) in a weight minimization problem (Reference 20) indicates that frequent rescaling helps in the beginning but not at the end of the search. A rational strategy based on the current $\nabla^2 R$, tempered by this experience is presented in Reference 20. The results of the present investigation indicate an ad hoc procedure that rescales at cycles 2, 4, 8, ... 2^M is effective in both vibration and buckling problems. The choice of a good starting vector X_0 can also significantly improve convergence. The unit vector e_j associated with the minimum (a_{ii}/b_{ii}) as suggested in Reference 17 worked well for buckling problems. Even with this starting vector, however, it was necessary to change normalizing components and restart the search at least once in most problems. The normalizing component need not be the maximum magnitude, X_i , but for best convergence it should be.

A COMPARATIVE EVALUATION OF GRADIENT MINIMIZATION AND MATRIX EIGENVALUE PROCEDURES

The potential of gradient minimization methods for structural eigenproblems was discussed in Section 3 and a scaling procedure suggested that should aid in realization of this potential. Taking the conjugate gradient algorithm with this scaling as representative of the current state of the art, this section makes a comparative evaluation of gradient minimization and matrix eigenvalue procedures. Specifically, a matrix transformation method using Householder's reduction to tridiagonal form and a banded matrix inverse iteration procedure are used in the comparison. A simply-supported, cylindrical panel serves as a representative structure for the vibration and buckling eigenproblems. The panel is idealized, using the consistent element matrices of Section 2 so that neither the A or B matrix is diagonal.

Panel Vibration Mode Comparisons

The first three symmetric modes of a simply supported panel were computed, using a standard matrix eigenvalue routine based on Householder's reduction to tridiagonal form (BIGMAT) and using a Rayleigh quotient minimization routine based on the conjugate gradient algorithm with scaling. The four element idealization of the panel and the u, v, w boundary conditions are shown in Figure 1. This idealization required 48 degrees of freedom. A symmetric matrix eigenvalue routine like BIGMAT requires transforming the $AX = \lambda BX$ problem to $DY = \lambda Y$, where D is symmetric. This was accomplished as in Reference 7, using the positive definite property of B . The frequency comparisons shown in Table 1 indicate agreement through five digits for the first three symmetric modes. The computational difficulty in obtaining the minimization results increased appreciably after the first mode, although the number of cycles actually decreased between modes one and two. The increased computations were required to purge the search vector of lower mode contamination before every function and gradient evaluation. If this was not done, Rayleigh quotient values slightly below the minimum were obtained with a relatively large gradient, indicating a poor eigenvector. However, the eigenvectors obtained with purging were far superior to those found by BIGMAT and will be discussed later. These results were obtained using the scaling criteria of Eq (3.17) for all three modes with rescaling every ten cycles. The convergence improvement achieved by this scaling procedure is illustrated in Table 2 for the first two modes. These data demonstrate that the importance of scaling for eigenproblems is similar to that reported in Reference 19 for systems of linear equations. It is interesting to note that

Table 1
FREQUENCY COMPARISONS

$\omega = \sqrt{\lambda}$	$AX = \lambda X$	$\lambda = X^T AX / X^T BX$
ω_1	2947.750	2947.732
ω_2	6051.968	6051.937
ω_3	7792.212	7792.200

Table 2
FREQUENCY CONVERGENCE COMPARISONS

Cycle	$\omega_1^2 \times 10^{-7}$		$\omega_2^2 \times 10^{-7}$	
	Unscaled	Scaled	Unscaled	Scaled
10	1.90273	1.68612	7.89168	5.58873
20	1.18910	0.87181	4.97172	3.66284
30	0.99351	0.86892	4.24870	3.66259
40	0.91413	0.86891	3.90426	---
50	0.88957	---	3.76853	---
100	0.86909	---	3.66411	---

the second mode convergence is improved even more than the first. This is somewhat surprising, since the criteria of Eq (3.17) do not reflect the constraints of Eq (3.3). Unfortunately, comparisons are not available for the third mode to determine if the trend continues. The Rayleigh quotient function values during the scaled minimization for all three modes are graphed in Figure 2. The cycles at which rescaling occurred and the cycles at which the search was restarted with a new normalizing component are also shown in Figure 2. The first mode search found the frequency to eight significant digits in 41 cycles, while the unscaled search was aborted at cycle 151 after converging to only six places. The second mode search found the frequency to eight places in 33 cycles, while the unscaled search was aborted at cycle 108 after converging to only four places.

The third mode search found the frequency to six places in 58 cycles and was not attempted without scaling. The influence of the constraints of Eq (3.3) may have appeared in the third mode search when unscaling was required at cycles 21 and 35 to reduce the Rayleigh quotient. Reference 5 indicates that constraint equations should be included in a scaling criteria for potential energy minimization to avoid this type of behavior. In the present situation, a projection matrix like P_k that transforms an arbitrary X vector into one satisfying the constraint equations might be used to congruently transform $\nabla^2 R$ into a metric that reflects the constraints.

The eigenvectors found by minimization can be computed to any desired accuracy by continuing the iteration using sufficiently precise arithmetic. In practice, this could be inefficient if an accurate eigenvector required many additional cycles after the eigenvalue converged to the desired accuracy. Error analyses (Reference 22) indicate bounds on eigenvector accuracy can be established from the norm of the Rayleigh quotient gradient. The Euclidean norm of the gradient is a convenient mathematical measure that approaches zero as the trial vector and associated Rayleigh quotient approach the eigenvector and eigenvalue. The relative change in this norm during the minimization is a practical measure of the approximate number of significant digits in the current trial eigenvector. Table 3 lists this norm at several cycles during the minimization for each eigenvector in scaled coordinates.

The missing entries in the listing for the third mode are cycles for which only the unscaled norm is available. A closed form solution for the cylindrical panel vibration problem (Reference 23) indicates that the eigenfunctions for $W(s, \theta)$ are $\sin(\eta\pi\theta/\beta)\sin(m\pi s/l)$. This solution neglects in-plane inertia so that slightly higher frequencies are obtained (Reference 7), however, the $W(s, \theta)$ eigenfunctions change little, if any.

Table 3
EIGENVECTOR CONVERGENCE

Cycle	$\ \nabla R(X_i^1)\ _E$	$\ \nabla R(X_i^2)\ _E$	$\ \nabla R(X_i^3)\ _E$
1	$1.3 \times 10^{+4}$	$3.1 \times 10^{+4}$	$4.0 \times 10^{+4}$
10	$3.0 \times 10^{+3}$	$1.0 \times 10^{+4}$	$7.4 \times 10^{+4}$
20	$7.7 \times 10^{+1}$	$9.8 \times 10^{+1}$	$1.1 \times 10^{+4}$
30	8.5	2.2	---
40	2.5×10^{-1}	4.7×10^{-2}	---
50	8.7×10^{-4}	4.3×10^{-4}	$5.2 \times 10^{+1}$

Table 4 shows the comparison of the trigonometric eigenfunctions with the minimization and BIGMAT eigenvectors.

Table 4
EIGENVECTOR COMPARISONS

n	m	θ/β	s/l	$\sin \frac{n\pi\theta}{\beta}$	$\sin \frac{m\pi s}{l}$	$W(s, \theta)$ Minimization	$W(s, \theta)$ BIGMAT
1	1	1/4	1/4	0.500000		0.500000	0.179853
1	1	1/4	1/2	0.707107		0.707107	0.421944
1	1	1/2	1/4	0.707107		0.707107	0.393165
1	1	1/2	1/2	1.000000		1.000000	1.000000
3	1	1/4	1/4	0.500000		0.500000	0.179853
3	1	1/4	1/2	0.707107		0.707107	0.421944
3	1	1/2	1/4	-0.707107		-0.707107	-0.393165
3	1	1/2	1/2	-1.000000		-1.000000	-1.000000

The poor quality of the BIGMAT eigenvectors was not investigated, although the transformation from $AX = \lambda BX$ to $DY = \lambda Y$ is probably involved.

The CDC 6600 time required to generate all matrices and compute one mode was approximately 10 seconds for both BIGMAT and Rayleigh quotient minimization. To compute three modes by minimization required over 40 seconds while BIGMAT used less than 12 seconds. This difference would increase progressively with additional modes. Recalling the dimension of the matrices in the problem, $N = 48$, this indicates that for small vibration problems minimization may be practical for no more than the first mode. However, as the dimension of the problem increases, a transformation eigenvalue routine like BIGMAT is slowed by a full D matrix. Gradient minimization routines are able to take advantage of the sparsity in the A and B matrices (Reference 10) and to avoid even assembling these matrices in discrete element vibration problems. Using such procedures, a 16-element idealization of the panel with 192 degrees of freedom was analyzed for the first mode. The eigenvalue converged to eight significant digits in 76 cycles and the eigenvector converged to eight significant digits in 97 cycles. The problem was run on the

CDC 6500 computer, a change from the previous cases which were run on the CDC 6600, and the solution times were 186 seconds for 76 cycles and 230 seconds for 91 cycles. A BIGMAT solution would have required 1,200 seconds and was not run for this reason. These results indicate that large shell vibration problems ($N > 100$) can be analyzed accurately and efficiently by conjugate gradient minimization for at least the first mode. Several modes beyond the first can also be computed accurately but the efficiency drops off with present methods for purging the search vector of components from previously computed eigenvectors. The state of the art regarding scaling for the higher modes may also require improvement to reflect the constraint equations.

Panel Buckling Mode Comparisons

The critical buckling load for a simply supported cylindrical panel was computed using BIGMAT, an inverse iteration routine and Rayleigh quotient minimization. The same boundary conditions were used for the prebuckling solution and the buckling analysis. These boundary conditions and a four-element idealization of the panel requiring 55 degrees of freedom are shown in Figure 3. Several other grid idealizations of the panel were also used and the buckling results are summarized in Table 5.

Table 5
BUCKLING LOAD COMPARISONS

Grid	N	Buckling Load N_s (lb/in.)		
		BIGMAT	Minimization	Inverse Iteration
2 x 2	16	-1735.064	-1735.064	-1735.064
4 x 4	55	-869.030	-869.030	-869.030
6 x 6	118	---	---	-810.194
8 x 8	205	--	---	-809.859

The eigenvalues from the three solution methods agree to at least seven significant digits for the lowest root. Convergence of the minimization routine and inverse iteration both were slowed by the presence of a second root very close to the first. In the case of the 4 x 4 grid, the second root was -885.72 lb/in. or less than 2 percent greater than the critical buckling load. The inverse iteration procedure at first missed the lower root and converged to -885.72 lb/in. It was necessary to shift the origin five times to obtain the first mode. The conjugate gradient minimization routine converged to two places in less than 40 cycles but then required another 84 cycles to converge to seven places. This behavior and the eigenvector convergence are illustrated in Table 6.

These computations were made using rescaling at cycles 2, 4, 8, ..., 2^M on a CDC 6500 computer. The cycle times were, on the average, one second which compares with a BIGMAT solution time of approximately 30 seconds and an inverse iteration solution time of approximately 38 seconds. The BIGMAT eigenvectors were, again, poor in comparison to the minimization and inverse iteration eigenvectors as Table 7 demonstrates. The comparisons were, however, slightly better than the vibration eigenvector comparisons in Table 4. The small differences between the minimization and inverse iteration eigenvectors is partly the result of different equation solvers being used for

Table 6
MINIMIZATION BUCKLING MODE CONVERGENCE

Cycle	N_s (lb/in.)	$\ \nabla r(X_1)\ _E$
1	-1083.060	1.0
10	-887.575	5.5×10^{-2}
20	-879.667	2.7×10^{-2}
30	-876.101	2.1×10^{-2}
40	-873.390	2.7×10^{-2}
50	-870.677	3.6×10^{-2}
70	-869.244	4.8×10^{-3}
90	-869.033	1.0×10^{-3}
110	-869.031	1.3×10^{-4}
130	-869.031	4.0×10^{-5}

the prebuckling solution. This resulted in differences in the first place for some of the smaller components of the prebuckling displacement vector.

The finer grid idealizations of the panel in Table 6 were analyzed by inverse iteration and the 6×6 grid problem was also partially solved by minimization. The minimization run was aborted after converging to three places which require 57 cycles at slightly over three seconds per cycle. Considering the convergence behavior shown in Table 6, another 100 cycles or more would have been required for eight place eigenvalue accuracy. The inverse iteration procedure converged to eight places after three shifts of origin and approximately 75 seconds. This would indicate minimization is not efficient in comparison to inverse iteration when the second mode is very close to the first. The only mitigating factor in favor of minimization (at least in the case of the conjugate gradient algorithm with the present scaling) is the guarantee that it will converge to the lowest buckling load. The performance of the minimization routine was improved for cases with well separated roots but, in no buckling case, was it better than inverse iteration.

AN EVALUATION OF THE CYLINDRICAL PANEL ELEMENT IN VIBRATION AND BUCKLING PROBLEMS

The accuracy of higher order discrete elements in vibration and buckling eigenproblems has been noted in several recent studies (References 4, 6, 24, and 25). A basic reason for this performance is the interpolation accuracy of the assumed displacement functions used for the elements. In the case of displacement functions based on Hermite polynomials, $H_{ij}^{(N)}(s)$, sharp interpolation error bounds have been established (Reference 26). These

Table 7
BUCKLING EIGENVECTOR COMPARISONS

θ/β	s/l	$W(s, \theta)$ Minimization	$W(s, \theta)$ Inverse Iteration	$W(s, \theta)$ BIGMAT
1/4	1/4	0.158484	0.158588	0.057323
1/4	1/2	-0.101409	-0.101656	-0.054522
1/2	1/4	-0.262733	-0.262811	-0.213848
1/2	1/2	0.109157	0.109600	0.151487

bounds can in turn be used to bound the accuracy of eigenvalues and eigenvectors found by Rayleigh Ritz approximations of elliptic boundary value problems (References 27 and 28). To cite a specific example from Reference 28, the rectangular membrane vibration problem

$$\nabla^2 W(X, Y) + \lambda W(X, Y) = 0 \quad \text{in } A \quad (5.1)$$

$$W(X, Y) = 0 \quad \text{on } \partial A \quad (5.2)$$

approximated using discrete elements with $H_{ij}^{(N)}(X) H_{kl}^{(N)}(Y)$ displacement functions results in eigenvalues with error $O(\Delta^{4N+2})$ and eigenvectors with error $O(\Delta^{2N+1})$ where Δ is the grid size. These bounds have also been confirmed numerically for the rectangular membrane; however, as Reference 28 shows, they are not valid for membranes with reentrant corners. The reason they are not valid is because the eigenfunctions have singular derivatives at the reentrant corner. Even in this case, Reference 28 shows that, by the addition of certain singular functions to the polynomials, $H_{ij}^{(N)}(X) H_{kl}^{(N)}(Y)$, the convergence rates for smooth eigenfunctions can be retained. Plate and shell structures, unlike membranes, must have eigenfunctions with continuous first derivatives in $W(s, \theta)$ or the bending strains are undefined. The second derivatives may be discontinuous, in which case, the error bounds in Reference 26 can not be used for $N \geq 1$. The present investigation of the cylindrical panel element is limited to problems with eigenfunctions that have continuous fourth derivatives. In this case, order Δ^4 eigenvalue convergence is expected for vibration problems. The buckling problem with prebuckling stresses and displacements dependent on (s, θ) is not of the form considered in Reference 27 and the convergence rate of the present consistent incremental stiffness matrix formulation is uncertain. Empirical results are presented for both these problems in this section and the panel element is then applied to a cylinder buckling problem.

Panel Vibration Mode Convergence

The cylindrical panel vibration problem used to study eigenvalue solution procedures will be used to evaluate the discrete element. The solution in Reference 23 neglects in-plane inertia and gives a first mode frequency 1.3 percent higher than the present. A Rayleigh-Ritz solution in Reference 29

includes in-plane inertia and uses Fourier series displacement functions. Truncating the series at six terms, this solution gives a first mode frequency 0.13 percent higher than the present. As more terms are added, this comparison indicates that the two solutions will have vanishingly small differences, as they theoretically must. To empirically test the discrete element convergence rate with grid size, the data in Table 8 were computed. Since no exact

Table 8
FREQUENCY CONVERGENCE WITH GRID SIZE

Grid	N	ω
2 x 2	12	2949.80
4 x 4	48	2947.73
6 x 6	114	2947.65
8 x 8	192	2947.64

solution is available, the 8 x 8 grid results were used to estimate convergence rates with logarithmic ratios as in Reference 5. These calculations indicate an exponent of 3.6 between the 2 x 2 and 4 x 4 grids which is compatible with Δ^4 convergence. The frequency from the 6 x 6 grid is too close to the frequency from the 8 x 8 grid to consider the latter as reference in computing a convergence rate between the 4 x 4 and 6 x 6 grids. Eigenvector convergence rates were not estimated because of the lengthy calculations required. The $w(s, \theta)$ components of the eigenvector were converged to at least six places in the 4 x 4 grid solution, as Table 4 indicates. The smaller components of the eigenvector, such as the slope variables, are less accurate but should converge at the same rate. To illustrate this, the derivatives $w_{,s}(0, \beta/2)$ and $w_{,\eta}(1/2, 0)$ are given in Table 9 for each grid. The corresponding derivatives of $\sin(n\pi\theta/\beta) \sin(m\pi\theta/l)$ for this problem are both equal to $\pi/10$.

Table 9
VIBRATION MODE CONVERGENCE WITH GRID SIZE

Grid	N	$W_s(0, \beta/2)$	$W_\eta(1/2, 0)$
2 x 2	12	0.316431	0.316431
4 x 4	48	0.314175	0.314321
6 x 6	114	0.314160	0.314176
8 x 8	192	0.314159	0.314162

As these data demonstrate, the smaller components of the eigenvector also converge rapidly and, even for a coarse grid, are accurate enough for most applications.

Panel Buckling Mode Convergence

The panel buckling problem previously analyzed is considered here in more detail to describe the prebuckling displacements and stresses and to investigate the discrete element convergence characteristics. The boundary conditions, as shown in Figure 3, result in local hoop compression near each end, $\sigma_s^m(0, \theta) \doteq \nu \sigma_\theta^m(0, \theta)$, which decays very rapidly away from the loaded edges. The axial membrane stress varies between -15,600 psi and -15,000 psi which is within 2 percent of being constant. The membrane shear stress is less than 100 psi everywhere except near the corners of the loaded edges where it reaches 700 psi. The bending and axial displacements are shown in Figure 4 along the centerline of the panel. The maximum bending stresses occur on the loaded edges where $\sigma_s^B \doteq 2,500$ psi and $\sigma_\theta^B \doteq 750$ psi at the top surface. The bending shear stress has a maximum of $\sigma_{s\theta}^B = -2,580$ psi in each of the four corners and is approximately zero elsewhere. These prebuckling stresses and displacements were computed using the 8 x 8 grid idealization of the panel under a uniform axial load of $N_s = -758$ lb per inch. The buckling load from Table 5 is $N_{cr} = -810$ lb per inch and the buckled shape in the axial direction is shown in Figure 4. There appear to be 9 half waves in the axial direction with their amplitude decaying away from the ends. The magnitude of the buckling load is about 7 percent greater than $0.6 Eh^2/r$ and was obtained using consistent (i.e., the same) boundary conditions for the prebuckling and buckling analysis. The convergence with grid size of the buckling load is indicated in

Table 5. Using the 8 x 8 grid results as reference, logarithmic ratios between the 2 x 2 and 4 x 4 grids result in an exponent of 4.0 which is Δ^4 convergence. This indicates that the convergence rate for the cylindrical panel element in buckling analyses may be the same as in vibration analyses. However, even though the convergence rate may be the same, the vibration modes for a given grid size are considerably more accurate than the buckling modes.

Cylinder Buckling Results

A cylinder with a non-axisymmetric critical buckling mode ($n=3$, $m=1$) for the boundary conditions shown in Figure 5 was analyzed under a uniform axial load. Since consistent boundary conditions are used in the present analysis, the u boundary conditions do not correspond to the classical simple support conditions. The classical buckling load for this cylinder is $N_c = -9,960$ lb/in., with the w portion of the mode shape given by $\sin 3\theta \sin \pi z/l$. The discrete element analysis was made using eight elements around the circumference and either two or four elements along the length as shown in Figure 5 where axial symmetry has been used. These idealizations require 112 and 208 degrees of freedom, respectively, while the same idealizations with classical boundary conditions require 96 and 192 degrees of freedom. Results from the discrete element bending theory solution are shown in Figure 6 and comparisons with the membrane theory solution are presented in Table 10.

The bending results are lower than the membrane and both discrete element solutions are slightly higher than classical. The bending theory results also increase slightly with grid refinement. A possible cause for this is an appreciable change in the prebuckling bending displacements between the 8 x 2 grid solution and the 8 x 4 grid solution. The eigenvectors from the bending theory solution are in excellent agreement with classical, as Table 11 demonstrates.

Table 10
CYLINDER AXIAL BUCKLING LOAD COMPARISONS

	N_c	N	N_c	N
Bending Theory Solution	-10,277	112	-10,339	208
Membrane Theory Solution	-10,364	96	-10,357	192

Table 11
CYLINDER BENDING THEORY AXIAL
BUCKLING MODE COMPARISONS

n	m	θ/π	s/l	$\sin n\theta$	$\sin \frac{m\pi s}{l}$	$W_{B(s,\theta)_{8 \times 2}}$	$W_{B(s,\theta)_{8 \times 4}}$
3	1	0	1/2	0		$0(10^{-10})$	$0(10^{-11})$
3	1	1/4	1/2	0.707107		0.707107	0.707107
3	1	1/2	1/2	-1.000000		-1.000000	-1.000000
3	1	3/4	1/2	0.707107		0.707107	0.707107
3	1	1	1/2	0		$0(10^{-10})$	$0(10^{-11})$
3	1	5/4	1/2	-0.707107		-0.707107	-0.707107
3	1	3/2	1/2	1.000000		1.000000	1.000000
3	1	7/4	1/2	-0.707107		-0.707107	-0.707107
3	1	2	1/2	0		$0(10^{-10})$	$0(10^{-11})$

These results were obtained using inverse iteration and there was no problem with close second mode roots as in the panel problem.

CONCLUSIONS

A Rayleigh quotient minimization method for structural vibration and buckling eigenproblems was shown significantly improved by scaling. Results from a cylindrical panel vibration eigenproblem demonstrate that first and second mode convergence in less than N cycles, is possible. Vibration modes higher than the first required frequent purging of the search vector to satisfy orthogonality constraints and appreciably increased the cycle time. When the dimension of the vibration eigenproblem was small ($N < 100$) minimization was competitive with Householder's matrix transformation method for no more than the first mode. However, the ability of the minimization method to take advantage of sparsity in the K_2 and M matrices produced a 5 to 1 time reduction for the first mode of a 192 degree of freedom panel vibration eigenproblem. Application of the minimization approach to buckling eigenproblems was not as efficient and usually required more than N cycles to converge. The complexity of the prebuckling displacements appears to adversely effect the condition of the K_3 matrix. The accuracy of the minimization buckling modes was excellent but, in comparison to inverse iteration, it was not efficient, even for large

buckling eigenproblems. These conclusions are to some extent dependent on the particular shell element used and the test problems; however, it seems clear that minimization is better suited for the vibration, rather than the buckling, eigenproblem.

The vibration mode shapes and frequencies determined using the cylindrical panel element were accurate without requiring many degrees of freedom. Even a coarse 12 degree of freedom idealization was within 1 percent of Rayleigh-Ritz solution in Reference 29. Convergence with grid size indicates that the frequency is approximated with error order Δ^4 , as predicted by mathematical error analyses (Reference 27) where this higher order convergence rate applies only if the continuum mode shapes have continuous derivatives through order four. Panel buckling results also suggest order Δ^4 eigenvalue convergence for the consistent incremental stiffness matrix formulation. However, the buckling accuracy for a given grid size was significantly less than the frequency accuracy for the corresponding vibration problem. The most noticeable effect of linear prebuckling bending displacements on the panel demonstration problem was a decay in the amplitude of the axial waves, away from the loaded edges. In the case of an axially loaded cylinder ($l/r = 4$, $r/h = 64.6$) there was little difference, with the membrane discrete element solution, or classical. The mode shape in w was the same as classical with the buckling load 5 percent higher than classical. Although the applications presented have been for linear bifurcation buckling, the element formulation presented can be used for nonlinear stability analyses, and such applications are in progress.

REFERENCES

1. Bogner, F. K., Finite Deflection Discrete Element Analysis of Shells, AFFDL-TR-67-188, (1968).
2. Monforton, G. R., and Schmit, L. A., Finite Element Analysis of Sandwich Plates and Cylindrical Shells with Laminated Faces, AFFDL-TR-68-150, pp. 573-608, (1969).
3. Key, S. W., The Analysis of Thin Shells with Transverse Shear Strains by the Finite Element Method, AFFDL-TR-68-150, pp. 667-710, (1969).
4. Gallagher, R. H. and Yang, T. Y., Elastic Instability Predictions for Doubly-Curved Shells, AFFDL-TR-68-150, pp. 711-739, (1969).
5. Stanton, E. L. and Schmit, L. A., A Discrete Element Stress and Displacement Analysis of Elastoplastic Plates, Douglas Paper 10251, (to appear in the AIAA Journal).
6. Isakson, G., Armen, H., and Pifko, A., Discrete Element Analysis Methods for the Plastic Analysis of Structures, NASA CR-803, (1967).
7. Stanton, E. L. and Palacol, E. L., Additions to the MDAC Discrete Element Program Library-1969. McDonnell Douglas Report MDC G1157, (1969).
8. Brogan, F., Forsberg, K., and Smith, S., Dynamic Behavior of a Cylinder with a Cutout, AIAA Journal Vol. 7, No. 5, pp. 903-911, (1969).
9. Fox, R. L. and Kapoor, M. P., A Minimization Method for the Solution of the Eigenproblem Arising in Structural Dynamics, AFFDL-TR-68-150, pp. 271-306, (1969).
10. Fried, I., Gradient Methods for Finite Element Eigenproblems, AIAA Journal, Vol. 7, No. 4, pp. 739-741, (1969).
11. Klein, S., The Cholesky Equation Solver, Aerospace Report No. ATR-70(S9990)-2, (1970).
12. Mallett, R. H. and Marcal, P. V., Finite Element Analysis of Nonlinear Structures, Journal of the Structural Division ASCE, Vol. 94, ST-9, pp. 2081-2105, (1968).

13. Gallager, R. H., Gellatly, R. A., Padlog, J., and Mallett, R. H., A Discrete Element Procedure for Thin Shell Instability Analysis, AIAA Journal, Vol. 5, No. 1, pp. 138-145, (1967).
14. Thompson, J. M. T. and Hunt, G. W., Comparative Perturbation Studies of the Elastica, Int. Jour. of Mech. Sci., Vol. 11, pp. 999-1014, (1969).
15. Langhaar, H. L., Energy Methods in Applied Mechanics, John Wiley, New York, Appendix A-5, (1962).
16. Stein, M., Recent Advances in Shell Buckling, AIAA Paper No. 68-103, Sixth Aerospace Sciences Meeting, (1968).
17. Bradbury, W. W. and Fletcher, R., New Iterative Methods for Solution of the Eigenproblem, Numerische Mathematik 9, pp. 259-267, (1966).
18. Gantmacher, R. R., The Theory of Matrices, Chelsea, New York, Vol. 1, Chapter X, (1959).
19. Fox, R. L. and Stanton, E. L., Developments in Structural Analysis by Direct Energy Minimization, AIAA Journal, Vol. 6, No. 6, pp. 1036-1042, (1968).
20. Schrader, M., An Algorithm for the Minimum Weight Design of the General Truss, DSMSMD Report No. 24, Case Western Reserve University, (1968).
21. Greenstadt, J., On the Relative Efficiencies of Gradient Methods, Mathematics of Computation, Vol. 21, pp. 360-368, (1967).
22. Wilkinson, J. H., The Algebraic Eigenvalue Problem, Clarendon Press, Oxford, Chapter 3, (1965).
23. Nowacki, W., Dynamics of Elastic Systems, John Wiley and Sons, New York, page 267, (1963).
24. Webster, J. J., The Accuracy of Finite Element Solutions for the Modal Characteristics of Shells of Revolution, International Journal of Mechanical Sciences, Vol. 12, pp. 157-168, (1970).
25. Adelman, H. M., Catherines, D. S., and Walton, W. C., Accuracy of Modal Stress Calculations by the Finite Element Method, AIAA Journal, Vol. 8, No. 3, pp. 462-468, (1970).
26. Birkhoff, G., Schultz, H. H., and Varga, R. S., Piecewise Hermite Interpolation in One and Two Variables with Applications to Partial Differential Equations, Numerische Mathematik, Vol. 11, pp. 232-256, (1968).

27. Ciarlet, P. G., Schultz, H. H., and Varga, R. S., Numerical Methods of High-Order Accuracy for Nonlinear Boundary Value Problems. III Eigenvalue Problems, Numerische Mathematik, Vol. 12, pp. 120-133, (1968).
28. Fix, G., Higher Order Rayleigh-Ritz Approximations, Journal of Mathematics and Mechanics, Vol. 18, No. 7, pp. 645-657, (1969).
29. Chen, R., Vibrations of Cylindrical Panels and Rectangular Plates Carrying a Concentrated Mass, Douglas Paper No. 3702, (1965).

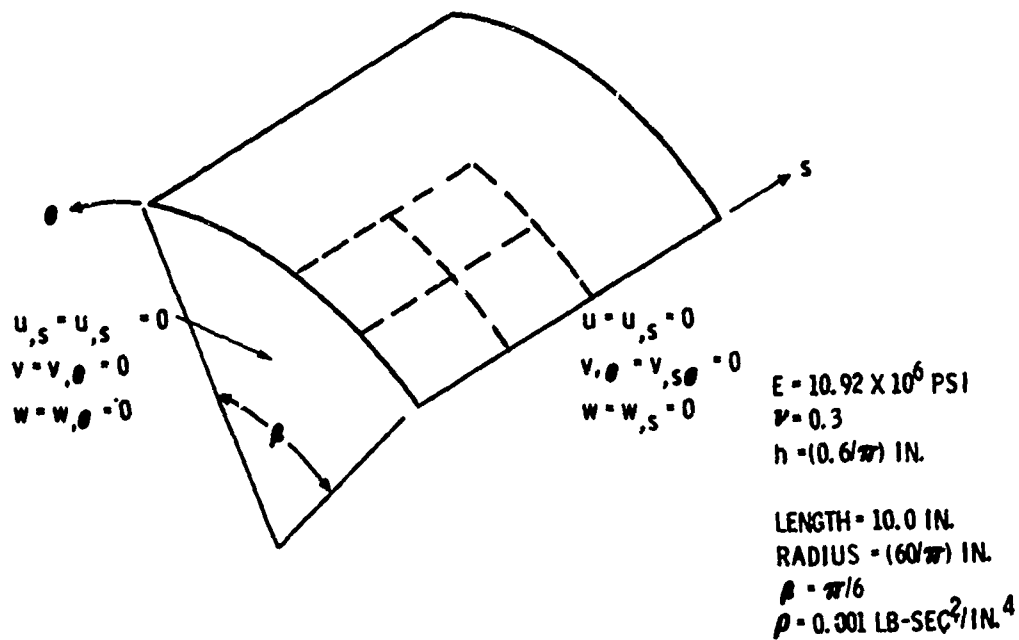


Figure 1. Cylindrical Panel Vibration Problem Idealization

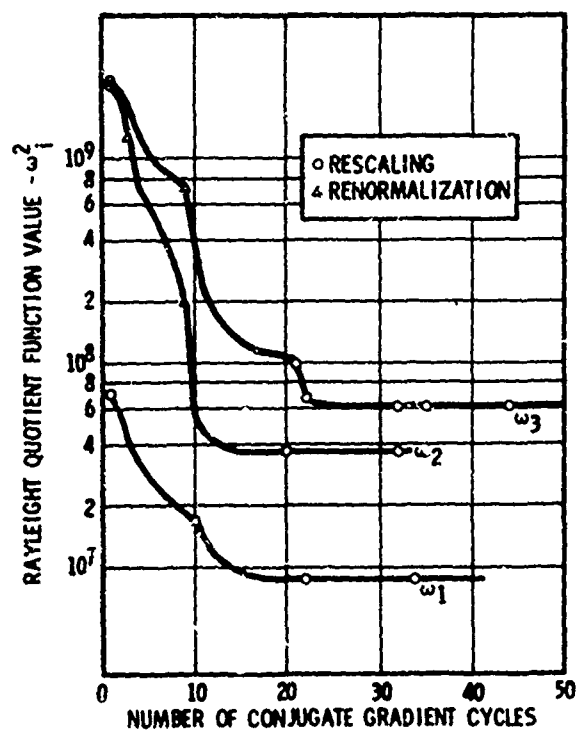


Figure 2. Rayleigh Quotient Convergence

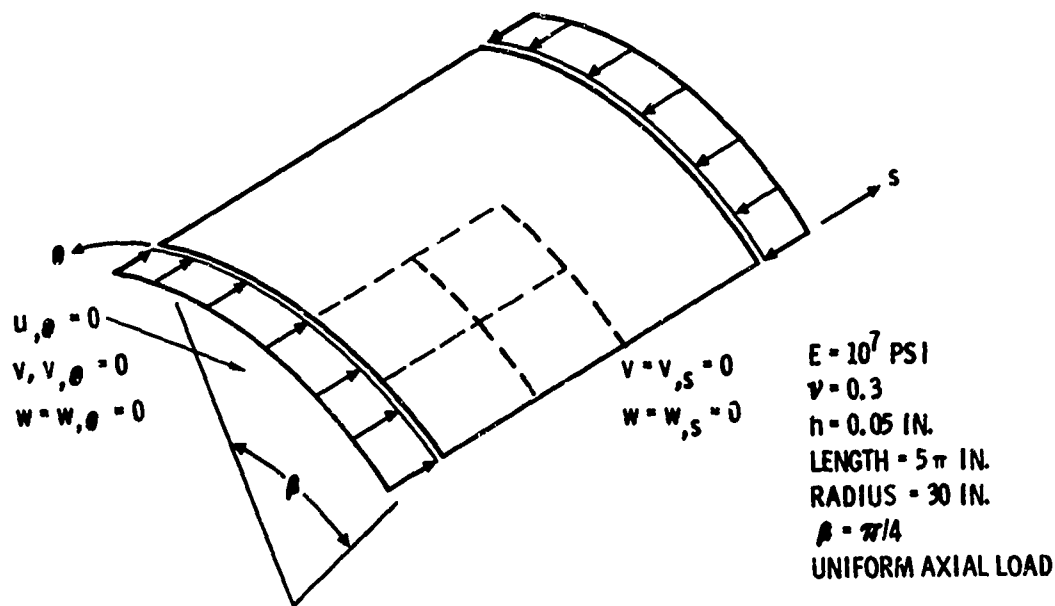


Figure 3. Cylindrical Panel Buckling Problem Idealization

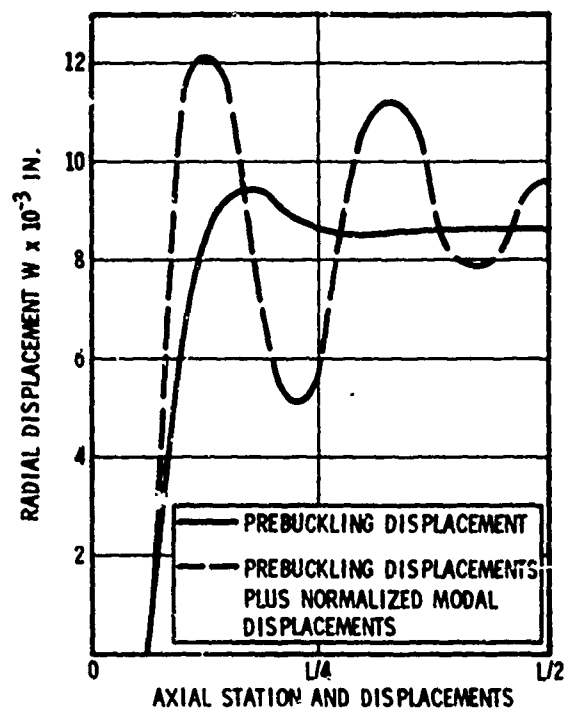


Figure 4. Panel Buckled and Prebuckled Shape

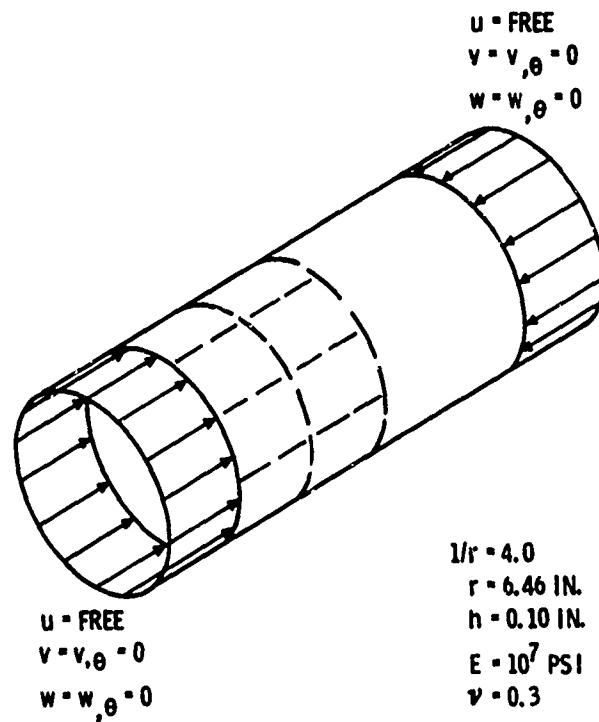


Figure 5. Cylinder Buckling Problem Idealization

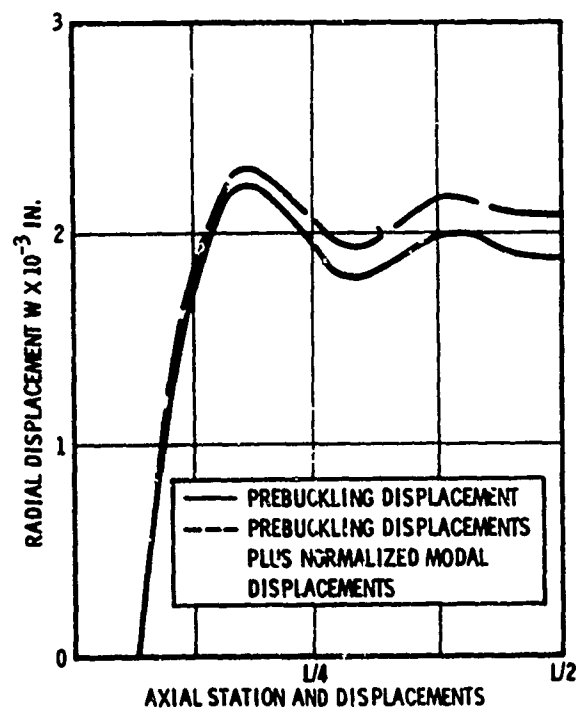


Figure 6. Cylinder Buckled and Prebuckled Shape

QUESTIONS AND COMMENTS FOLLOWING STANTON'S PAPER

QUESTION: Do I understand correctly that you really don't have to form these matrices K2, K3 and K4?

STANTON: That's right. What we do is take advantage of the fact that the assembly transformation for the element matrices is Boolean in locally consistent coordinates. The transformation associates a particular system degree of freedom with an element degree of freedom for each element matrix using a string of integers (in this case there are 48). It makes it rather easy to manage your data and very easy to avoid working with zeros in this fashion.

QUESTION: It wasn't clear to me whether in your scaling criterion you were using your normalization technique considering just the original stiffness matrix or both the incremental and the initial stiffness matrix. Could you answer the question I've implied by that statement?

STANTON: The scaling criteria was based on the second derivatives of the Rayleigh quotient which does include both the A and B matrices, one of them being the incremental stiffness matrix.

STRESS, BUCKLING, AND VIBRATION ANALYSIS OF SHELLS OF REVOLUTION

By M. S. Anderson*, R. E. Fulton*,
W. L. Heard, Jr.*, and J. E. Walz*
NASA Langley Research Center
Hampton, Virginia

SUMMARY

This paper summarizes the major computer programs in existence for the analysis of shells of revolution by numerical integration and finite difference procedures. The report describes programs for (1) linear and nonlinear analysis of shells subjected to axisymmetric and asymmetric static loads, (2) buckling and vibration behavior including effects of axisymmetric nonlinear prestress, and (3) transient response. Extensions of these programs which are currently underway and some of the primary assets of both the numerical integration and finite difference procedures are discussed. In addition, a summary of the shell theory formulation, the numerical approximation, and the solution techniques of a set of programs denoted SALORS (Structural Analysis of Layered Orthotropic Ring-Stiffened Shells), developed at the NASA Langley Research Center, are described. Stress, vibration, and buckling results from the SALORS program are given for several shell configurations having a variety of structural complexities that illustrate the current capability of shell of revolution programs.

INTRODUCTION

A substantial capability has been developed over the last 10 years for the numerical analysis of shells of revolution. Computer programs are now available, which are based on accurate shell theory, and are efficient in computer storage and computational speed, and are applicable to general shell shapes. Numerical analysis of such shells based on solution to the appropriate shell equations by numerical integration (e.g., see refs. 1-27) and finite differences (e.g., see refs. 28-59) have been developed. Finite element methods have also been used, but will not be discussed in this paper. Figure 1 shows a sketch of a shell structure and indicates some of the structural and load complexities that can be considered. The structure is an orthotropic shell of revolution having general meridional shape, structural rings, and discontinuities along the meridian and supported at the boundaries by a general elastic restraint. This type of shell can now be analyzed for a variety of loading conditions for stresses, buckling, free vibrations, and transient response. The purpose of the present paper is to summarize some of the major computer programs in existence for such analyses, to indicate the capability that is now generally available, and to identify areas of needed research. In addition, a summary of the shell theory formulation, the

*Aerospace Engineer, NASA Langley Research Center, Hampton, Virginia.

numerical approximation, and the solution techniques of a set of programs denoted SALORS (Structural Analysis of Layered Orthotropic Ring-Stiffened Shells), developed at the NASA Langley Research Center, are described and several example problems are presented. These examples indicate the structural detail which can be analyzed by numerical shell-of-revolution programs.

SUMMARY OF THE DEVELOPMENT OF NUMERICAL ANALYSIS OF SHELLS OF REVOLUTION

The numerical analysis of general shells of revolution has developed along three different lines: Methods based on numerical integration of the governing equations, methods based on finite difference approximations, and methods based on finite element approximations. Finite element methods are important tools in structural analysis, but are not discussed in the present paper. A survey of general shell computer programs is given in reference (60), and numerical analysis of shells of revolution is summarized in reference (61). A brief historical development and comparison of the numerical integration and finite difference methods will be given in the following sections. Table 1 is a listing according to programs which are in use or under development. The numbers in parentheses indicate the references associated with the programs. The programs listed generally have the capability of analyzing a shell of the type shown in Figure 1. However, in the more advanced analysis areas (asymmetric stiffness and dynamic stress analysis), there are no programs with this general capability, and the programs listed for these advanced areas are representative of the capability that is available or is under development. All the programs listed in Table 1 depend on a Fourier decomposition of the variables for the circumferential direction.

Numerical Integration Procedures

The earliest formalized procedure for solution of the differential equations for shells of revolution appears to have been presented by Goldberg(1), and was based on the numerical integration of a system of first-order shell equations as a two-point boundary value problem. This work was subsequently extended by Goldberg for numerous applications (see, e.g., refs. 1-3 and summary given in ref. 4).

The exponential growth and decay of the influence coefficients required in the two-point boundary value solution can lead to numerical difficulties for shell-of-revolution equations; thus, reliable solutions using this method require breaking a shell into an assemblage of shell segments. These modifications to the integration procedure, which have sometimes been denoted as the "multisegment integration procedure," were suggested by Goldberg(3), Kalnins(5), and Cohen(6). This integration procedure was subsequently used by the latter two authors and their collaborators to develop systems of computer programs for segmented shells of revolution for buckling, vibration, linear asymmetric stress analysis, and nonlinear axisymmetric stress analysis (see refs. 7-13 and Table 1).

A similar system of programs for linear and nonlinear stress analysis of shells of revolution denoted STARS was developed by Mason and his associates(14-18). References (14) and (16) were the first to outline (but not

program) a combined Fourier series - numerical integration procedure for nonlinear analysis of shells of revolution subjected to asymmetric loads. Swartz(19) developed a program similar to that contained in reference (14), and Thurston(20,21) developed a lesser known, but efficient numerical integration procedure for axisymmetric shell behavior wherein integration by parts is carried out prior to the numerical integration.

The above integration procedures for a linear asymmetric shell analysis require the calculation and storage of the particular solution and eight complimentary solutions for each segment. A major advance in the numerical integration procedure was made by Zarghamee and Robinson(22-24). Their approach requires calculation and storage of the particular solution and only four complimentary solutions for each shell segment. This numerical integration procedure appears to be the most efficient computational method developed to date for shells of revolution, and requires approximately half the computer storage and time of other integration procedures. To the writers' knowledge, however, this procedure has been used only for selected applications with classical boundary conditions and has not been incorporated in a complete system of general purpose programs for stress, vibration, and buckling analysis of orthotropic shells of revolution. In Appendix A the method presented by Zarghamee and Robinson is extended to the most general set of equations and boundary conditions that are currently being employed. Although these generalized equations have not, as yet, been programmed, the advantages in computer time and storage demonstrated in references (22-24) appear to be retained.

Finite Difference Procedures

Procedures based on finite difference solutions to the shell equations were developed simultaneously with the development of numerical integration procedures. The basic method of approach was presented by Radkowski, Davis, and Bolduc in 1960(28) for axisymmetric shell analysis. In this procedure the shell equations are formulated as second order equations and approximated by finite differences. The resulting tridiagonal equations are solved by a Gaussian elimination method suggested by Potters(29). This work formed the basis of a program by Hubka(30). It was also incorporated in a documented, nonproprietary computer program by Sepetoski, et al.(31), which was subsequently extended by Ball and Bodeen to include geometric nonlinearities(32).

A formulation of linear asymmetric stress analysis of shells of revolution was first given by Budiansky and Radkowski(33). The basic approach is to formulate the shell equations as four simultaneous second-order differential equations in terms of four basic variables - the three displacements and the meridional moment. Reference (33) describes the formulation of the problem for arbitrary boundary conditions, shell discontinuities, and branching. The Budiansky-Radkowski approach was implemented into an operational and documented computer program in reference (34), and similar such programs are given in references (35-37). Extension of the method to vibration and buckling problems was carried out in reference (38), and the modification of the shell-equation coefficients to account for orthotropic shell properties is given in reference (39).

The Budiansky-Radkowski procedure also served as the basis for two independent systems of programs for stress, vibration, and buckling analysis. One system, denoted SALORS, was developed at the NASA Langley Research Center and is described in Appendix B. The other system, denoted BOSOR(40-48), was developed by Bushnell and his associates. The original BOSOR program(40), was based on shallow shell theory for buckling and contained the effects of material orthotropy. Updating to BOSOR2(41-45), and finally to BOSOR3(46-48), led to a complete system of programs which provides essentially the same analysis capability as the SALORS system. The BOSOR2 and BOSOR3 programs differ from the other finite difference formulations in that the difference approximations are applied to the energy expression rather than to the differential equations. As a result, the finite difference equations are formulated in terms of only the three-shell displacement variables, and this method does not require use of the meridional moment as a fourth-basic variable. This method is similar to finite element methods in that the difference equations are symmetric and lend themselves to conventional finite element matrix manipulations.

Extensions to Asymmetric Problems, Dynamics, and Plasticity

The above computer programs are essentially one dimensional and the use of Fourier circumferential harmonics leads to uncoupled differential equations. As can be seen from Table 1, less work has been done for problems where coupled equations result, namely for nonlinear asymmetric geometry. A documented program has been developed by Ball(49) for the nonlinear elastic behavior of a shell of revolution subjected to asymmetric loads. A similar program has been developed by Greenbaum(51,52), but is applicable only to shells composed of cylindrical and conical segments. In these two programs the circumferential behavior is taken in the form of a finite number of Fourier terms, and finite difference approximations are used along the meridian. Extensions of linear analysis to include asymmetric thickness distributions for a shell of revolution have been obtained with the program described in references (53,54).

Some work has also been done to extend static analyses to account for transient loads. Neither the finite difference nor the numerical integration procedures are efficient for computing a large number of modes and frequencies for purposes of a modal-type transient response analysis. The most efficient application of the finite difference and numerical integration methods to such analyses is probably through direct integration of the equations of motion for a set of initial conditions. The use of an implicit integration scheme, such as the Houbolt method(62), appears to be very efficient for transient response, and each step forward in time is essentially a single-static solution. Programs which include transient response include one for axisymmetric, nonlinear dynamic response of orthotropic shells by Stephens and Fulton, denoted SADAOS(55,56). Schaeffer's linear static program for isotropic shells(34), has also been extended by Stephens to include dynamic response due to asymmetric loads(57), and the general Budiansky-Radkowski formulation for isotropic branched shells has been extended to asymmetric stiffness distributions and transient response in reference (54). In general, although the technology exists, transient response does not appear to be automated for the same level of structural complexity as exists for static loads. Shell of revolution programs which consider plasticity include the EPS program (ref. 58) for static loads and the GIRLS II program (ref. 59) for dynamic loads.

The following extensions are known to be underway and are denoted with dotted lines in Table 1:

(1) Ball's program(49) has been extended to nonlinear asymmetric dynamic response, but the program is not yet documented.

(2) Cohen is presently being funded by NASA to extend his programs to prestressed vibrations, bifurcation buckling due to asymmetric loads, and a shell-branching capability.

(3) Stephens and Fulton are extending the SADAOS program to include plasticity.

(4) R. E. Martin of Texas A & M University is extending the Ball nonlinear, asymmetric static-analysis program to anisotropic shells.

(5) Bushnell is funded by the Navy to extend the BOSOR program to include shell branching.

MAJOR PROGRAM SYSTEMS

From Table 1 it can be seen that four major program systems have been developed that cover the complete range of stress, buckling, and vibration. These four are BOSOR and SALORS and the programs by Cohen and Kalnins. The BOSOR system is available in COSMIC*. The more complete BOSOR3 is government property, is operational on the UNIVAC 1108 and IBM 360 computer systems in double precision, and is available from the Lockheed Missiles and Space Company, Palo Alto, California. The SALORS system, written in FORTRAN IV, is operational on CDC 6000 series computers, and various portions of it have already been made operational on most of the major computers, including the UNIVAC 1108, and IBM 360. It is planned for distribution through COSMIC upon completion of user documentation. Cohen's programs were originally written for operation on the Philco 2000 series computer, but have subsequently been made operational on the CDC 6000 series computer. They were originally proprietary in nature but, through government funding, will soon be generally available with distribution through COSMIC. Kalnins' programs have been well documented in reference (11) and are available from the Solid Mechanics Branch of the Air Force Flight Dynamics Laboratory at Wright-Patterson Air Force Base, Ohio.

These four programs are similar in that each has a segmentation capability to account for meridional variations and discontinuities in geometry, loading, and stiffness. In addition, each program can account for orthotropic shell properties, and thermal and mechanical loads. Some of the major differences in approach and capability are summarized in Table 2. The shell theories are all sufficiently accurate to obtain correct results for the first and second harmonics, where classical analysis using shallow-shell theory fails. The

*COSMIC - Computer Software Management & Information Center, University of Georgia, Athens, Georgia.

BOSOR, Cohen, and SALORS systems obtain eigenvalues by an iteration method which converges to the closest eigenvalue to a reference eigenvalue. The Kalnins system uses determinant plotting, which is unattractive for hardware problems because the analyst must know a priori the approximate value of the eigenvalue to obtain reliable results. For a given problem, the four programs can be expected to give the same numerical result. This is illustrated in Table 3 where the specific results for a diverse group of problems have been tabulated. Reasonable agreement is shown between all four programs for stress analysis, buckling, and vibration.

Comparison of Numerical Integration and Finite Difference Procedures

A comparison of some of the features in the numerical integration and finite difference procedures can be obtained by considering a representative program by each method. The discussion will focus on the Cohen (integration) and SALORS (difference) programs because of the authors' familiarity with the two programs. Portions of the discussion also apply to the other computer programs in the respective categories. The discussion will consider the areas of (1) formulation and programing of equations, (2) numerical approximation, and (3) input and output information.

Formulation and Programing of Shell Equations. The shell equations for the Cohen numerical integration procedure are the eight first-order differential equations composed of the equilibrium, the constitutive, and strain displacement equations. They are relatively easy to obtain and program. The SALORS finite difference procedure reduces the equations to four second-order differential equations before programing. This reduction facilitates application of difference approximations to the equations. However, the equations to be programed are long and complicated and lead to additional terms, such as derivatives of stiffnesses and other geometrical quantities.

Numerical Approximation and Solution. For the numerical solution of the differential equations, the Cohen integration procedure uses standard computer library integration routines for first-order differential equations. The routine automatically selects an increment size to assure accuracy to a prescribed input tolerance. However, the integration procedure becomes numerically unstable for long shells, and segmenting the shell is necessary. This requires the storage of a 9×8 matrix for each segment and the subsequent solution of a tridiagonal set of equations of the order of eight times the number of segments. Usually, discontinuities of practical structures serve to form convenient segment boundaries. The treatment of segmentation and boundary points are straightforward, since the first-order equations use edge force resultants and corresponding displacements as variables.

In the SALORS finite difference procedure, the user must select the difference stations in such a way as to achieve satisfactory numerical accuracy. In general, more difference stations are required than integration intervals for comparable accuracy. Also, fictitious exterior points, or forward differences at boundaries of discontinuity points, are required and the algebra and programing logic are fairly complex. On the other hand, the numerical solution is stable and no segmentation is required for long shells, although in some cases it is desirable. Boundary-layer effects which occur for very

thin shells are adequately handled with small, finite difference increments in the boundary-layer region.

Comparative computer time and storage requirements for analysis of the same shells by the SALORS and Cohen programs are reported in reference (61). These results are given in Table 4 for calculations of thermal buckling of a cylinder and the free vibrations of a conical shell. The programs have comparable computer requirements for these examples, and no clear advantage in numerical efficiency is demonstrated by either procedure.

Input and Output Details. The integration procedure inherently involves fewer input and output points than the difference procedure. Intermediate reference points are used in addition to segment end points to describe the meridional variation of quantities. This procedure may cause a loss in accuracy or may, in fact, be inadequate for buckling or vibration problems where the stress analysis provides the prestress input. Interpolation between reference points is required for these cases and interpolated prestress information is not as accurate as that calculated for reference points. This might be particularly important in the definition of the weakly oscillating prebuckling deformations in a ring-stiffened shell.

In the SALORS difference procedures, this problem does not arise because the information of interest is always defined in terms of the station variables, and all station variables are calculated and stored during a solution; thus they are automatically available. In a prestressed vibration or buckling problem, the input is precisely the output, station by station, of the stress analysis problem. This procedure gives a consistent numerical solution for the stress and eigenvalue problem.

Summary of Comparison. From a user point of view there are two significant differences between the two procedures; (1) an asset for the integration procedures is that criteria are included in the routines to automatically select integration intervals to achieve accurate results, whereas in the difference method the user must select a priori satisfactory station intervals, and (2) an asset for the difference procedure is that all difference station results having been calculated are subsequently used to advantage as point by point input for prestressed eigenvalue problems, whereas for the integration procedures interpolation between reference points (with possible loss in accuracy) is required.

From a programming point of view, other comments can be made. An asset for the integration procedure is the use of standard integration routines and simpler equations inherent in a first-order formulation of the shell equations. Boundary and discontinuity conditions are also relatively easy to program, and there can be a computer storage advantage, depending on the amount of output information required. An asset for the difference procedure is that no major numerical instability difficulties are apparent, whereas shell segmentation is required in the integration procedure.

An improvement in efficiency of the integration procedure appears to be possible by using the extension to the Zarghamee-Robinson procedure given in

Appendix A. Some of the differences between the integration and difference procedures due to equation order can be eliminated by using first, rather than second-order equations for the difference procedure, as was done in references (51) and (55). On the other hand, the first-order formulation requires the storage of twice as much information at every station and the inversion of twice as many matrices depreciating some of its conveniences. Derivatives of stiffness and geometrical data, as well as the use of fictitious boundary points in the difference procedure, can be eliminated, and a symmetric set of equations obtained by deriving the difference equations from the shell energy, as is done in the BOSOR program. The Kalnins and Cohen approaches appear to be very similar, and the comments and discussion generally apply to both programs.

On the basis of all the points considered, however, there appears to be no clear advantage to either the numerical integration or the finite difference procedure, provided both are well formulated and efficiently programmed; the choice is more likely to be based on personal preference, experience with a particular approach, or the availability of a program with certain checked-out subroutines.

APPLICATION OF PROGRAMS

The capabilities of these programs will be illustrated in the following section where stress, buckling, and vibration results will be given for several problems offering a wide variety of configurations and structural arrangement. The results are obtained with the SALORS system but illustrate the general capabilities of well developed shell-of-revolution programs. A summary of the shell theory formulation, the numerical approximation, and solution techniques used in SALORS are given in Appendix B.

Ring-Stiffened Cylinder

Progress in analytic capability is illustrated by attempts that have been made to predict the buckling pressure of the ring-stiffened cylinder shown in Figure 2. The cylinder, which was machined with 11 integral, external rectangular rings, was bolted to heavy end bulkheads. Bodner(63) reported the results of a theoretical analysis for this cylinder which had previously been tested(64). The primary utility of such tests is to establish the accuracy of analytical methods. The experimental buckling pressure and Bodner's prediction are shown in Table 5. Bodner's prediction was based on Donnell theory and orthotropic stiffness properties (ring area and moment of inertia were distributed uniformly), and resulted in a pressure of 796 psi. This prediction is much higher than the 675 psi obtained in the experiment. In an attempt to reduce this discrepancy between theory and experiment, he made a number of other predictions using different shell theories and different values of effective length of sheet acting with the rings. In the early 60's, investigators began to recognize that the eccentricity of rings and stringers could have a major effect in shell buckling. A Donnell theory was developed in reference (65) which accounts for stiffener eccentricity but still smears the ring stiffness uniformly over the length of the cylinder. When this theory was applied to the same problem, a buckling pressure of 739 psi was obtained. This result indicates that eccentricity reduces ring effectiveness, if the

rings are external. On the other hand, using the same theory of reference (65), but assuming the rings to be internal, yields a buckling pressure of 848 psi.

A comprehensive analysis of this cylinder has been made with the Langley shell-of-revolution programs (SALORS). First, the nonlinear behavior under an axisymmetric state of stress was determined and is shown in Figure 3. Plotted is external pressure against the unit shortening (total end shortening divided by length). As can be seen for pressures below 1000 psi, the nonlinear effects are negligible. The buckling pressure for this nonlinear state of stress was first calculated as 708 psi, assuming a dead pressure loading. This result reflects that for low harmonics (in this case $n = 3$) the more accurate shell theories predict lower buckling loads than Donnell's theory. However, the experiment was under a live pressure load (pressure force remains normal to surface during buckling), and for this condition a buckling pressure of 642 psi was calculated (Cohen, in ref. 13, calculated 644 psi for the same conditions). Thus, the effect of a live pressure loading was significant. All calculations to date have retained the original assumption of simply supported ends. This assumption appears unrealistic, due to the heavy bulkheads of the test cylinder and, particularly, since the most accurate calculation (in which the wall and discrete rings were accurately modeled with the Cohen or SALORS program), predicts a lower buckling load than obtained experimentally. For computer programs which handle discontinuities, it is not necessary to assume boundary conditions at the end of the cylinder, since the whole specimen, cylinder, plus end bulkheads can be analyzed routinely. Such an analysis was carried out with SALORS and predicts a buckling pressure of 860 psi. The experimental value is now approximately 20 percent less than the theoretical value (the difference probably due to imperfection sensitivity). As a result of the above study, a paradox occurs wherein the most accurate analysis to date increases the difference between theory and experiment. Nevertheless, it would be unrealistic to neglect the rather large effects of eccentric stiffening, live pressure load, and boundary restraints that apparently play a major role in the behavior of this specimen. Use of less accurate analyses in the past, which ignore such effects, has probably led, in many cases, to a false conclusion concerning the accuracy of theory.

Most experimental investigations of shell buckling are still restricted to shells of revolution. It is strongly recommended that the results of these investigations be analyzed with shell-of-revolution computer programs capable of handling all the parameters that might affect the result, including the supporting fixture. In many past programs, information on end bulkheads and attachments has been omitted. For example, the thickness of the bulkhead shown in Figure 2 had to be determined by scaling from a photograph. If complete information is available, a much better understanding of the relationship between theory and experiment can be made by using the current shell-of-revolution computer program capability.

Ring-Stiffened Cone

The SALORS system of programs has also been applied to the design and analysis of a blunt, conical planetary-entry body loaded by uniform pressure, as shown in Figure 4. The configuration shown is a ring-stiffened cone with a spherical nose cap. There are two large rings, one at the aft end, and one at

an interior location where the pressure load is reacted. Rings are of variable size and spacing. Table 6 gives the details of the ring and stringer properties and locations. The symbols used are given in Appendix B. The conventional analysis approach would probably consider an orthotropic cone under a membrane prestress, simply supported between the two larger rings. The cone stiffness would be based on average ring spacing and stiffness distributed uniformly over the length, and the portion of the shell forward of the reaction would be neglected. Local buckling of the skin would also be calculated, assuming simple support between the actual rings. Such calculations indicate the pressure required for general buckling is 2.9 psi, and that required for local buckling is 2.5 psi.

Applying the SALORS system of programs, the whole shell can be considered, and much more detailed and accurate information can be obtained. For example, the stress analysis program revealed a region of high circumferential stress in the vicinity of the load reaction. Longitudinal stiffeners were provided in this region, which limited the stress to acceptable values. The aft ring of circular cross section was sized by making buckling calculations for a wide range of ring sizes to determine the smallest ring with sufficient stiffness to provide the equivalent of simple support during buckling.

Calculations of the buckling pressure as a function of harmonic wave number are shown in Figure 5. These results give a more accurate picture of the buckling behavior than the simple analysis described above. Three different meridional buckling modes were observed. At low values of n , the predominant buckling deflections were confined to the region between the support ring and nose cap. This mode is denoted "local orthotropic buckling," since it involves deflection of several rings. The expected general buckling mode was critical for n between 4 and 10 with the critical harmonic $n = 6$. As n is increased beyond 10, buckling is of a local nature involving motion of one or a few bays between rings. The critical bays are those in which approximately square buckles occur for a particular value of n . The design was based on simultaneous occurrence of general and local bay buckling assuming a membrane state of stress. However, the computer solution shows the minimum pressure for local buckling to be 4.2 psi, which is significantly greater than the pressure of 2.7 psi required for general buckling. Thus, the accuracy and detail available with sophisticated shell-of-revolution programs provide a basis for redesign of the shell to closer margins, leading to a lighter structure.

Apollo-Saturn Short Stack

As an example of the extensive capability of current programs, consider the combined cylindrical, conical shell structure shown in Figure 6. On the left is shown the Apollo-Saturn vehicle. The circled portion has been denoted the "short stack" and will be considered for detailed analysis. Because of the structural complexities involved, this problem is proposed here as a basic checkout problem for shell-of-revolution computer programs. It is a problem representative of a real structure and has been studied in great detail by several aerospace groups. A description of the structure, together with results for selected loadings and structural modeling, are given in this section.

The conical part of the "short stack" (SLA) and the center, cylindrical section (IU) are of sandwich construction with unequal face sheets. The lower section (S-IVB forward skirt) is of skin-stringer construction. There are six rings located along the shell meridian. The pertinent structural properties are summarized in Table 7. A major detail which must be accounted for is the discontinuous character of the inner face sheet of the SLA sandwich just above ring 1 where the inner face sheet does not carry the load through to the lower structure (see detail A, Fig. 6). The boundary conditions at each end of the "short stack" are represented by stiffness matrices obtained from an analysis of the adjacent structure and are given in Table 8 for selected values of n . These boundary conditions apply for both stress and buckling analysis. The structure was analyzed for several loading conditions, and only a portion of the results can be given here. The loading considered herein is that described in Figure 6. There is an axisymmetric axial load of $0.764 P$ applied at the top, and an additional thrust of $0.236 P$ at ring 1 with eccentricity of -0.663 in. The reaction of these forces is taken out at the base.

The force at ring 1 will be considered in two different ways: First, as an axisymmetric line loading for both stress and buckling analysis, and second, as an asymmetric line loading applied at four points located 90° apart around the circumference, and having a total bearing length of $1/32$ of the circumference.

The structure was analyzed with the SALORS system of programs using 436 finite difference station points. The reference surface was taken at the continuous surface corresponding to the outer surface of the SLA, IU, and skin of the S-IVB forward skirt. Shell segments (portions of the shell bounded by discontinuities along the meridian) were divided into sufficiently small, finite difference spacings for highly accurate results. For example, 15 difference stations were used in the short cutout region above ring 1, shown in detail A.

For the case of axisymmetric loading at ring 1 and neglecting prebuckling deformations, the buckling load is $P_{cr} = 2.8365 \times 10^6$ lbs and corresponds to seven circumferential waves. Figure 7(a) shows a plot along the meridian of the axisymmetric meridional and circumferential prestress resultants \bar{T}_ξ and \bar{T}_θ and Figures 7(b) and 7(c) show, respectively, the $n = 0$ and $n = 7$ buckling mode displacements u_ξ , u_θ , and w . The mode shapes indicate that the primary buckling action occurs in the S-IVB forward skirt.

Figure 8 shows plots of the meridional stress on the inside and outside surfaces of the shell for the same axisymmetric load distribution and for $P = 500\,000$, which approximates design limit loads. Also shown in the figure are results for the case where the loading at ring 1 is asymmetric. The stresses are given along a meridian through the loading point and corresponds to the sum of the results for $n = 0, 4, 8, \dots, 64$. The stresses for the asymmetric loading grow in magnitude near the ring, but asymptote to the symmetric results away from the ring. The stress plots show several regions of sharp peaks and rapid variations caused by the discontinuities along the meridian. Thus, the importance of realistic modeling of the structural cut above ring 1 for an acceptable analysis is evident.

The vibration characteristics of the "short stack" are shown in Figure 9. The lowest free-vibration frequency corresponding to each n is shown in Figure 9(a) for the unloaded shell. The schematic mode shape shows that the interior rings do not form nodes, and points out the necessity of analyzing the whole "short stack" as a unit, rather than analyzing each component separately.

The effect of stress on vibration is shown in Figure 9(b). The figure gives the lowest frequency for $n = 5$ and a sketch of the corresponding mode shapes. Note how the maximum amplitude shifts from the conical sandwich to the cylindrical skirt of the S-IVB, as the stress approaches the buckling load. Again, the interaction of three separate structures is routinely handled where conventional analytic procedures would be difficult to apply.

For purposes of making more accurate comparisons of the above data with results of other programs, selected data on the stress, buckling, and vibration of the "short stack" are tabulated in Table 9. The central processing unit computer times required for the analyses are tabulated in Table 10.

CONCLUDING REMARKS

The characteristics of some of the major computer programs in existence for the analysis of shells of revolution have been summarized. Four separate systems have been developed on a comparable basis that can treat most of the complexities that occur for a shell of revolution. Two systems, Kalnins and Cohen, are based on numerical integration techniques, and the other two, BOSOR and SALORS, are based on finite difference solutions. The SALORS system, which has been developed at the NASA Langley Research Center, has been described in some detail, and results from the application of this system to several practical problems have been discussed. Based on this work, the following significant points can be noted:

(1) All four systems have the capability for the analysis of the stress, buckling, and vibration characteristics of complex shells of revolution. These systems of programs consider asymmetric loadings and permit detailed modeling of the structure, including meridional discontinuities in geometry and loading with little sacrifice in computing efficiency. The only restriction is that the shell be rotationally symmetric in stiffness, geometry, and prestress.

(2) The assets and liabilities of finite difference and numerical integration procedures are compared. There appears to be no clear advantage of one procedure over the other, provided both are well formulated and efficiently programmed.

(3) The use of the shell programs described makes possible a more accurate and meaningful comparison of experiment and theory, and should be a valuable tool in design for minimum weight.

(4) Stress, vibration, and buckling results for a complex shell of revolution, which has various structural and load complexities, have been

presented. The problem is well documented and is proposed as a checkout problem for other programs.

(5) Major difficulties in shell-of-revolution analysis occur when the behavior is not one dimensional, such as for asymmetric stiffness and nonlinear response to asymmetric loads. The most efficient means for moving into these areas would appear to be through extensions of the present four systems which have already been checked out and which have the appropriate system logic, rather than through the development of entirely new systems.

REFERENCES

Numerical Integration

1. Goldberg, J. E.; Bogdanoff, J. L.; and Marcus, L.: On the Calculation of the Axisymmetric Modes and Frequencies of Conical Shells. J. Acoust. Soc. Am., Vol. 32, 1960, pp. 738-742.
2. Goldberg, J. E.; and Bogdanoff, J. L.: Static and Dynamic Analysis of Conical Shells Under Symmetrical and Axisymmetrical Conditions. Proc. Sixth Symp. on Ballistic Missiles and Aerospace Technology, Vol. 1, Academic Press, N.Y., 1961, pp. 219-238.
3. Goldberg, J. E.; Bogdanoff, J. L.; and Alspaugh, D. W.: On the Calculations of the Modes and Frequencies of Vibration of Pressurized Conical Shells. AIAA Fifth Annual Structures and Materials Conference, Palm Springs, April 1-3, 1964, AIAA Publication CP-8, pp. 243-249.
4. Goldberg, John E.: Computer Analysis of Shells, In: Proceedings of Symposium on the Theory of Shells. Ed. by D. Muster, Univ. of Houston, Houston, Texas, April 4-6, 1966, pp. 5-22.
5. Kalnins, A.: "Analysis of Shells of Revolution Subjected to Symmetrical and Nonsymmetrical Loads." Appl. Mech., Trans. ASME, Series E, Vol. 31, 1964, pp. 467-476.
6. Cohen, G. A.: Computer Analysis of Asymmetrical Deformation of Orthotropic Shells of Revolution. AIAA J., Vol. 2, No. 5, May 1964, pp. 932-934.
7. Kalnins, A.: Free Vibration of Rotationally Symmetric Shells. Jour. Acoust. Soc. Am., Vol. 36, No. 7, July 1964, pp. 1355-1365.
8. Citerley, R. L.; Kalnins, A.; and Yamahara, S. T.: Analysis of Arbitrary Thin Elastic Shells of Revolution Subjected to Symmetrical or Nonsymmetrical Loads. Report TM 14-63-U38, United Technology Center, Nov. 1963. (User's Manual.)
9. Citerley, R. L.: Analysis of Arbitrary Layered Orthotropic Shells of Revolution Subjected to Symmetrical and Nonsymmetrical Loads. Report TM 14-65-U2, United Technology Center, Jan. 1965. (User's Manual.)
10. Kalnins, A.; and Lestingi, J. F.: On Nonlinear Analysis of Elastic Shells of Revolution. J. Appl. Mech., March 1967, pp. 59-64.
11. Kalnins, Arturs: Static, Free Vibration and Stability Analysis of Thin, Elastic Shells of Revolution. Report AFFDL-TR-68-144, Air Force Flight Dynamics Laboratory, Wright-Patterson Air Force Base, Ohio, March 1969. (User's Manual.)

12. Cohen, G. A.: Computer Analysis of Asymmetric Free Vibrations of Ring-Stiffened Orthotropic Shells of Revolution. AIAA J., Vol. 3, No. 12, Dec. 1965, pp. 2305-2312.
13. Cohen, G. A.: Computer Analysis of Asymmetric Buckling of Ring-Stiffened Orthotropic Shells of Revolution. AIAA J., Vol. 6, No. 1, Jan. 1968, pp. 141-149.
14. Mason, P.; Rung, R.; Rosenbaum, J.; and Ebrus, R.: Nonlinear Numerical Analysis of Axisymmetrically Loaded Arbitrary Shells of Revolution. AIAA J., Vol. 3, No. 7, July 1965, pp. 1307-1312.
15. Rung, Robert; Mason, Phillip; and Rosenbaum, J.: Unsymmetric Analysis of Shells of Revolution. Report ADR 02-11-65.3, Grumman Aircraft Engineering Corp., Dec. 1965.
16. Prince, Neil; Rung, Robert; and Svalbonas, Vytas: Unsymmetric Nonlinear First-Order Analysis of Layered Orthotropic Shells of Revolution. Report ADR 02-11-66.2, Grumman Aircraft Engineering Corp., May 1966.
17. Svalbonas, V.; and Shulman, M.: User's Manual for STARS - Shell Theory Automated for Rotational Structures. IBM 360/75 Digital Computer Program, NASA CR-98146, Feb. 1, 1968. (User's Manual.)
18. Svalbonas, V.; and Angrisano, N.: Numerical Analysis of Shells. Vol. 2, User's Manual for STARS-II, Shell Theory Automated for Rotational Structures-II, Digital Computer Program, NASA CR-61300, Sept. 1969. (User's Manual.)
19. Schwartz, R. W.: Nonlinear Analysis of Axisymmetrically Loaded Orthotropic Shells of Revolution. Report GDC-ERR-AN-776, General Dynamics Convair Division, Dec. 15, 1965. (User's Manual.)
20. Thurston, G. A.: Asymmetric Buckling of Shells of Revolution With Axisymmetric Initial Imputations. Report R62 FPD 426, Flight Propulsion Laboratory Department, General Electric Co., Cincinnati, Ohio, Dec. 18, 1962.
21. Thurston, Gaylen A.: Axisymmetric Bending and Buckling of Thin Shells of Revolution. Report SR-0530-64-2, Martin Marietta Company, April 1964.
22. Zarghamee, M. S.; and Robinson, A. R.: A Numerical Method for Analysis of Free Vibrations of Spherical Shells. AIAA J., Vol. 5, No. 7, July 1967, pp. 1256-1261.
23. Zarghamee, M. S.: Analysis of Shells of Revolution by Direct Numerical Integration. Presented at IASS International Congress on Application of Shell Structures to Architecture, Mexico City, Sept. 4-7, 1967.
24. Zarghamee, M. A.: A Numerical Method for Nonlinear Analysis of Shells. Report, Simpson, Gumpertz, and Heger, Inc., Cambridge, Mass., 1967.

25. Kalnins, A.: Analysis of Curved Thin-Walled Shells of Revolution. AIAA J., Vol. 6, 1968, pp. 584-588.
26. Zudans, Z.: Dynamic Response of Shell Type Structures Subjected to Impulsive Mechanical and Thermal Loadings. Nuclear Engineering and Design, Vol. 3, No. 1, 1966, pp. 117-127.
27. Zudans, Zenons; and Gregory, Frederick H.: Analysis of Shells of Revolution Formed of Closed Box Sections. Trans. ASME, J. Eng. for Industry, Paper No. 70-PVP-12.

Finite Difference Procedures

28. Radkowski, P.P.; Davis, R.M.; and Bolduc, M.R.: Numerical Analysis of Equations of Thin Shells of Revolution. American Pocket Society Journal, Vol. 32, Jan. 1962, pp. 36-41.
29. Potters, M.: A Matrix Method for the Solution of a Second Order Difference Equation in Two Variables. Report MR 19, Mathematisch Centrum, Amsterdam, Holland, 1955.
30. Hubka, Ralph E.: A Generalized Finite-Difference Solution of Axisymmetric Elastic Stress States in Thin Shells of Revolution. Report EM-11-19, Space Technology Labs., Inc., Los Angeles, Calif. June 1, 1961. Also Report AFBMD-TN-61-43, Cont. AF 04 (647)-619)), Air Force Ballistic Missile Division, Inglewood, California.
31. Sepetoski, W. K.; Pearson, C.E.; Dingwell, I.W.; and Adkins, A.W.: A Digital Computer Program for the General Axially Symmetric Thin Shell Problem. J. Appl. Mech., Trans. ASME, Series E, Vol. 29, Dec. 1962, pp. 655-661.
32. Ball, R. E.; and Bodeen, C.A.: A Digital Computer Program for the Geometrically Nonlinear Analysis of Axisymmetrically Loaded Thin Shells of Revolution. NASA CR-63703, March 22, 1965. (User's Manual.)
33. Budiansky, B.; and Radkowski, P.P.: Numerical Analysis of Unsymmetrical Bending of Shells of Revolution. AIAA J., Vol. 1, 1963, pp. 1833-1842.
34. Schaeffer, H.G.: Computer Program for Finite-Difference Solution of Shells of Revolution Under Asymmetric Loads. NASA TN D-3926, May 1967. (User's Manual.)
35. Roth, R.S.; Muskat, R.; and Grady, P.J.: Unsymmetrical Bending of Shells of Revolution, A Digital Computer Program. AVCO-RAD Report KHDR-6, Feb. 1965.

36. Capelli, A.P.; and Furuike, S.C.: Study of Apollo Water Impact. Vol. 10 User's Manual for Modification of Shell of Revolution Analysis, NASA CR-65862, May 1967. (User's Manual.)
37. Yen, Chi-Len: A Numerical Analysis of Orthotropic Shells of Revolution. Report AAS67-420(PS-10) Lockheed Missiles & Space Co., Huntsville, Ala., 1967. Also in Vol. 3, Transaction of National Symposium on Saturn V/ Apollo and Beyond, Huntsville, Ala., Jan. 11-14, 1967.
38. Cooper, Paul A.: Vibration and Buckling of Prestressed Shells of Revolution. NASA TN D-3831, March 1967.
39. Tene, Yair: Deformation of Asymmetrically Loaded, Symmetrically Prestressed Orthotropic Shells of Revolution. AIAA J., Vol. 6, No. 8, Aug. 1968, pp. 1599-1602.
40. Almroth, B.O.; Bushnell, D.; and Sobel, L.H.: Buckling of Shells of Revolution with Various Wall Constructions. Vol. 1, Numerical Results, NASA CR-1049; Vol. 2, Basic Equations, NASA CR-1050; Vol. 3, User's Manual for BOSOR, NASA CR-1051, 1968. (User's Manual.)
41. Bushnell, D.: Buckling and Vibration of Segmented Ring-Stiffened Shells of Revolution. User's Manual for BOSOR2, Report 6-78-68-40, Lockheed Missiles & Space Co., Sept. 1968. (User's Manual.)
42. Almroth, B.O.; and Bushnell, D.: Computer Analysis of Various Shells of Revolution. AIAA J., Vol. 6, Oct. 1968, pp. 1848-1855
43. Bushnell, D.: Buckling and Vibration of Ring-Stiffened, Segmented Shells of Revolution. Part 2, Numerical Results, presented at First International Piping and Pressure Vessel Technology Conference, Delft, Holland, 1969.
44. Bushnell, D.: Analysis of Buckling and Vibration of Ring-Stiffened, Segmented Shells of Revolution. Int. J. Solids Struct., Vol. 6, 1960, pp. 157-181.
45. Bushnell, David: Nonlinear Analysis for Axisymmetric Elastic Stresses in Ring-Stiffened Segmented Shells of Revolution. Report N-26-68-2, Lockheed Missiles & Space Co., September 1968, presented at AIAA/ASME 10th Structures, Structural Dynamics & Materials Conf., New Orleans, La., April 14-16, 1969.
46. Bushnell, D.: Computer Analysis of Complex Shell Structures. Presented at AIAA Eighth Aerospace Sciences Meeting, New York, N.Y., AIAA Paper No. 70-138, Jan. 19-21, 1970.
47. Bushnell, D.: Stress, Stability and Vibration of Complex Shells of Revolution. Analysis and User's Manual for BOSOR3, Lockheed Missiles & Space Co., Report N-5J-59-1, Sept. 1969. (User's Manual.)

48. Bushnell, D.: Analysis of Ring-Stiffened Shells of Revolution Under Combined Thermal and Mechanical Loading. AIAA 11th Structures, Structural Dynamics and Materials Conf., April 1970, p. 196.
49. Ball, R.E.: A Geometrically Nonlinear Analysis of Arbitrarily Loaded Shells of Revolution. NASA CR-909, Jan. 1968.
50. Schaeffer, Harry G.; and Ball, Robert E.: Nonlinear Deflections of Asymmetrically Loaded Shells of Revolution. Paper 68-292, presented at AIAA/ASME Ninth Structures, Structural Dynamics & Materials Conf., Palm Springs, California, April 1-3, 1968.
51. Greenbaum, G.A.; and Conroy, D.L.: Postwrinkling Behavior of a Conical Shell of Revolution Subjected to Bending Loads. AIAA Paper No. 69-90, presented at AIAA Seventh Aerospace Sciences Meeting, New York, N.Y., Jan. 20-22, 1969.
52. Greenbaum, G.A.; and Conroy, D.C.: Postwrinkling Analysis of Highly Pressurized Cylindrical and Conical Shells of Revolution Subjected to Bending Loads. Vol. 1 - Theory and Computer Program Description, Vol. 2 - Computer Program Listing, Report 07823-6011-R000, TRW Systems, Redondo Beach, California, Oct. 15, 1967. (User's Manual.)
53. Capelli, A.P.; Nishimoto, T.S.; and Radkowski, P. P.: Analysis of Shells of Revolution Having Arbitrary Stiffness Distributions. AIAA J., Vol. 7, No. 10, Oct. 1969, pp 1909-1915.
54. Carrion, E.; Furuike, S.C.; and Nishimoto, T.: Study of Apollo Water Impact. Vol. 11, User's Manual for Unsymmetric Shell of Revolution Analysis, NASA CR-65861, May 1967. (User's Manual.)
55. Stephens, W.B.; and Fulton, R.E.: Axisymmetric Static & Dynamic Buckling of Spherical Caps Due to Centrally Distributed Pressures. AIAA J., Vol. 7, No. 11, Nov. 1969, pp. 2120-2126.
56. Stephens, Wendell B.: Computer Program for Static and Dynamic Axisymmetric Nonlinear Response of Symmetrically Loaded Orthotropic Shells of Revolution. Proposed NASA TN (L-6299). (User's Manual.)
57. Stephens, Wendell B.; and Robinson, Martha P.: Dynamic Response of Asymmetrically Loaded Shells of Revolution. Proposed NASA TN (L-6298). (User's Manual.)
58. Stern, P.: Stress and Displacements in Elastic-Plastic Shells of Revolution with Temperature-Dependent Properties. Report 6-90-62-123, Lockheed Missiles & Space Co., Jan. 1963.
59. Massard, J.M.: GIRLS II - General Inelastic Response of Layered Shells, Hardening Technology Studies II. Report L-41-66-6, Lockheed Missiles & Space Co., Sept. 1966.

General

60. Bushnell, D.: Computer Analysis of Shell Structures. Paper No. 69-WA/PVP-13, presented at ASME Winter Annual Meeting, Los Angeles, California, Nov. 16-20, 1969.
61. Fulton, Robert E.: Numerical Analysis of Shells of Revolution. To be presented at IUTAM Symposium on High Speed Computing of Elastic Structures, Liege, Belgium, August 23-29, 1970.
62. Houbolt, John C.: A Recurrence Matrix Solution for the Dynamic Response of Aircraft in Gusts. NACA Report 1010, 1951.
63. Bodner, S.R.: General Instability of a Ring-Stiffened Circular Cylindrical Shell Under Hydrostatic Pressure. J. Appl. Mech., June 1957, pp. 269-277.
64. Wenk, E., Jr.; Slankard, R.C.; and Nash, W.A.: Experimental Analysis of the Buckling of Cylindrical Shells Subjected to External Hydrostatic Pressure. Proceedings Society for Experimental Stress Analysis, Vol. 12, No. 1, 1954, pp. 163-180.
65. Block, David L.; Card, Michael F.; and Mikulas, Martin, M., Jr.: Buckling of Eccentrically Stiffened Orthotropic Cylinders. NASA TN D-2960, August 1965.
66. Cohen, G.A.: Effect of Edge Constraint on the Buckling of Sandwich and Ring-Stiffened 120 Degree Conical Shells Subjected to External Pressure. NASA CR-795, 1967.

APPENDIX A

A NUMERICAL INTEGRATION PROCEDURE FOR ANALYSIS OF SHELLS OF REVOLUTION

Reference 6 presents a general set of first-order shell equations, and solves them with standard numerical integration techniques involving eight complimentary solutions and one particular solution. A generalization of the method of Zarghamee and Robinson(22-24), which involves only four complimentary solutions and one particular solution is given below for a quite general shell-of-revolution problem. The equations are (using the notation of ref. 6):

$$Y' = F(Y, S) \quad \text{differential equation} \quad (\text{A1a})$$

$$B_0 y_{10} + D_0 z_{10} = L_0 \quad \left. \begin{array}{l} \\ \\ \end{array} \right\} \text{boundary conditions at} \quad (\text{A1b})$$

$$B_m y_{m1} + D_m z_{m1} = L_m \quad \left. \begin{array}{l} \\ \\ \end{array} \right\} \text{station } 0 \text{ and } m \quad (\text{A1c})$$

with interior conditions (required to avoid numerical instabilities and at any points of discontinuity such as rings, abrupt changes in geometry or stiffness, line loadings, etc.)

$$B_1 (y_{i+1,0} - y_{i1} - y_{j1}) + D_1 z_{i1} = L_1 \quad (\text{A1d})$$

$$z_{i1} = z_{j1} = z_{i+1,0} \quad i = 1, m - 1 \quad (\text{A1e})$$

In these equations Y is the eighth-order harmonic vector of shell forces, moment, displacements, and rotation that is divided into the force and moment vector y and the displacement and rotation vector z . The first subscript is a segment number, and the second subscript 0, 1, indicates the beginning and end of the segment, respectively. The interior conditions include an open-branched shell (segment j) intersecting the end of segment 1. Equations for the branched shell were not included in reference (6). For each segment, one particular solution is obtained for the initial conditions,

$$B_1 y_{i+1,0} + G_1 z_{i+1,0} = H_1 \quad (\text{A2a})$$

$$-G_1 y_{i+1,0} + B_1 z_{i+1,0} = 0 \quad i = 0, m - 1 \quad (\text{A2b})$$

and four complementary solutions are obtained for

$$B_1 y_{i+1,0} + G_1 z_{i+1,0} = 0 \quad (\text{A3a})$$

$$-G_1 y_{i+1,0} + B_1 z_{i+1,0} = I \quad i = 0, m - 1 \quad (\text{A3b})$$

where

$$G_0 = D_0$$

$$H_0 = L_0$$

and

$$G_1 = D_1 - B_1 (U_{11} V_{11}^{-1} + U_{j1} V_{j1}^{-1})$$

$$H_1 = L_1 - B_1 (U_{11} V_{11}^{-1} T_{11} - S_{11} + U_{j1} V_{j1}^{-1} T_{j1} - S_{j1}) \quad i = 1, m-1$$

For each segment the solution is expressed as

$$y_i = S_i + U_i c_i \quad (A4a)$$

$$z_i = T_i + V_i c_i$$

where S_i and T_i are four element vectors generated from the particular solution, and U_i and V_i are 4×4 matrices formed from the four complementary solution vectors. The c_i are four element constant vectors which must be determined. The initial conditions for each segment (eqs. A2a and A3a) insure that the initial boundary condition and all interior conditions are satisfied providing

$$c_i = V_{11}^{-1} (V_{i+1,0} c_{i+1} + T_{i+1,0} - T_{11}) \quad i = 1, m-1 \quad (A5)$$

The additional initial conditions (eqs. A2b and A3b) are somewhat arbitrary and were formulated to satisfy the requirement that the system of equations be nonsingular.

The value of c_m is determined from the final boundary condition as

$$c_m = (B_m U_{m1} + D_m V_{m1})^{-1} (L_m - B_m S_{m1} - D_m T_{m1}) \quad (A6)$$

and the remaining c_i are determined from equation (A5).

The method involves inversion of the matrix V_{11} . This matrix is always nonsingular, even for arbitrary, rigid-body displacements which require special treatment by conventional numerical integration techniques, such as references (6) and (11). The only other matrix requiring inversion is in equation (A6). This matrix will be nonsingular for all correctly formulated boundary conditions.

APPENDIX B

SHELL ANALYSIS FORMULATION

Symbols

A	cross-sectional area of ring or stringer
$C_{11}, C_{12}, C_{22}, C_{33}$	membrane stiffness constants of shell wall (see eq. B11)
C_{1T}, C_{2T}	thermal forces (see eq. B11)
$D_{11}, D_{12}, D_{22}, D_{33}$	bending stiffness constants of shell wall (see eq. B11)
D_{1T}, D_{2T}	thermal moments (see eq. B11)
E	Young's modulus
$E, F, G, \bar{E}, \bar{F}, \bar{G}$	4×4 matrices associated with differential equations
E^*, F^*, G^*	of equilibrium (see Appendix C for nonzero terms)
e	4×1 matrix containing loads in differential equations of equilibrium (see Appendix C for elements of the matrix for stress analysis; elements of this matrix are zero for buckling or vibration)
$e_\xi, e_\theta, e_{\xi\theta}$	membrane meridional, circumferential, and shearing strain, respectively
f	4×1 matrix used in equation (B18) (elements of this matrix for stress analysis are defined in Appendix C)
f_ξ	shear stress resultant defined by equation (B16)
$f_{\xi\theta}$	circumferential shear stress resultant defined by equation (B15)
$H, J, \bar{H}, \bar{J}, H^*, J^*$	4×4 matrices used in equation (B18); nonzero terms given in Appendix C
I_s	centroidal moment of inertia of stringer cross section
I_x, I_y, I_{xy}	centroidal moments of inertia and product of inertia of ring cross section
$[I]$	unit matrix
J	torsional constant of ring or stringer
$[K], [K_0], [K_1], [K_2]$	stiffness matrices

$K_{11}, K_{12}, K_{22}, K_{33}$	interaction stiffness constants of shell wall (see eq. B11).
$k_{\xi}, k_{\theta}, k_{\xi\theta}$	meridional, circumferential, and twisting changes of curvatures
l	4×1 matrix of boundary loads
$[M]$	mass matrix
$m_{\xi}, m_{\theta}, m_{\xi\theta}$	meridional, circumferential, and twisting moment resultants, respectively
n	Fourier index
P	reaction at S-IVB end of "short stack" of Apollo-Saturn vehicle (see Fig. 6)
P_{cr}	magnitude of reaction at S-IVB end of "short stack" of Apollo-Saturn vehicle sufficient to cause buckling
P, P_{ξ}, P_{θ}	surface loads in normal, meridional, and circumferential directions, respectively
$S_{11}, S_{12}, S_{13}, S_{22}, S_{23}, S_{33}$	groupings of stiffness constants defined in Appendix C
u_{ξ}, u_{θ}	displacements in meridional and circumferential directions, respectively
$\{W\} = \lambda \{Z\}$	
w	normal displacement
x_r, y_r	coordinates of centroid of ring (measured from intersection of reference surface with a normal to the reference surface which passes through ring attachment point)
y	4×1 matrix whose elements are given by equation (B14) and related to displacements by equation (B18)
$\{Z\}$	column matrix composed of the z matrices at every station
z	4×1 matrix whose elements are given by equation (B13)
z_s	perpendicular distance from reference surface to centroid of stringer
$\gamma = \frac{\rho'}{\rho}$	

Δ	finite difference spacing
θ	angular circumferential coordinate
λ	eigenvalue
λ_e	effective eigenvalue
λ_s	eigenvalue shift
ν	mass per unit surface area
ξ	meridional coordinate, distance measured along surface
ρ	perpendicular distance from axis of shell of revolution to a particular point on the reference surface
σ_ξ	meridional stress
$\tau_\xi, \tau_\theta, \tau_{\xi\theta}$	meridional, circumferential, and shear stress resultants, respectively
$\varphi, \varphi_\xi, \varphi_\theta$	rotations about the normal, circumferential, and meridional coordinates, respectively
ω	circular frequency
$\omega_\xi, \omega_\theta$	curvatures of deformed shell in meridional and circumferential directions, respectively

Subscripts

max	maximum value
r	ring
s	stringer

Barred quantities refer to prestress variables.

Primes denote differentiation with respect to meridional coordinate.

Dots denote differentiation with respect to time.

Barred matrices contain prestress variables to the first power.

Starred matrices contain prestress variables to the second power.

Equations

This section summarizes the formulation of a suitable shell theory and an appropriate numerical solution for shells of revolution. The procedure and notation follow closely those of reference (33). The equations are based on Sanders' nonlinear shell equations specialized to the case of a shell of revolution. These equations are incremented and linearized to obtain, in the

usual manner, the equations for linear asymmetric motion of a shell of revolution from a general axisymmetric state of stress and deformation (see ref. 30). The linear asymmetric motion is assumed to vary harmonically in the circumferential direction (see Table 11).

$$\begin{aligned} \gamma \tau_{\xi} + \tau'_{\xi} + \frac{n}{\rho} \tau_{\xi\theta} - \gamma \tau_{\theta} + \omega_{\xi} \gamma m_{\xi} + \omega_{\xi} m'_{\xi} - \omega_{\xi} \gamma m_{\theta} + \frac{1}{2} \frac{n}{\rho} (3\omega_{\xi} - \omega_{\theta}) m_{\xi\theta} \\ - \omega_{\xi} \bar{\tau}_{\xi} \phi_{\xi} + \frac{1}{2} \frac{n}{\rho} (\bar{\tau}_{\xi} + \bar{\tau}_{\theta}) \phi + \omega_{\xi} \bar{\phi}_{\xi} \tau_{\xi} - \nu \ddot{u}_{\xi} + p_{\xi} = 0 \end{aligned} \quad (B1)$$

$$\begin{aligned} 2\gamma \tau_{\xi\theta} + \tau'_{\xi\theta} - \frac{n}{\rho} \tau'_{\theta} + \frac{1}{2} [(\omega_{\xi} + 3\omega_{\theta}) \gamma - \omega'_{\xi}] m_{\xi\theta} + \frac{1}{2} (3\omega_{\theta} - \omega_{\xi}) m'_{\xi\theta} \\ - \omega_{\theta} \frac{n}{\rho} m_{\theta} - \omega_{\theta} \bar{\tau}_{\theta} \phi_{\theta} - \frac{1}{2} (\bar{\tau}'_{\xi} + \bar{\tau}'_{\theta}) \phi - \frac{1}{2} (\bar{\tau}_{\xi} + \bar{\tau}_{\theta}) \phi' + \omega_{\theta} \bar{\phi}_{\xi} \tau_{\xi\theta} \\ - \nu \ddot{u}_{\theta} + p_{\theta} = 0 \end{aligned} \quad (B2)$$

$$\begin{aligned} - \omega_{\xi} \tau_{\xi} - \omega_{\theta} \tau_{\theta} - \omega_{\xi} \omega_{\theta} m'_{\xi} + 2\gamma m_{\xi} + m''_{\xi} + \left[\omega_{\xi} \omega_{\theta} - \left(\frac{n}{\rho} \right)^2 \right] m_{\theta} - \gamma m'_{\theta} \\ + 2\gamma \frac{n}{\rho} m_{\xi\theta} + \frac{2n}{\rho} m'_{\xi\theta} - (\gamma \bar{\tau}_{\xi} + \bar{\tau}'_{\xi}) \phi_{\xi} + \bar{\tau}_{\xi} \phi'_{\xi} + \frac{n}{\rho} \bar{\tau}_{\theta} \phi_{\theta} \\ + (\gamma \bar{\phi}_{\xi} + \bar{\phi}'_{\xi}) \tau_{\xi} + \bar{\phi}_{\xi} \tau'_{\xi} + \frac{n}{\rho} \bar{\phi}_{\xi} \tau_{\xi\theta} - \nu \ddot{w} + p = 0 \end{aligned} \quad (B3)$$

For stress analysis the barred variables are zero. For buckling and vibration they correspond to initial stress and deformation quantities. The primes denote differentiation with respect to the coordinate along the meridian, and dots denote differentiation with respect to time. The quantities τ_{ξ} , τ_{θ} , $\tau_{\xi\theta}$, are the amplitudes of the harmonically varying meridional, circumferential, and shear force resultants; m_{ξ} , m_{θ} , and $m_{\xi\theta}$ the amplitudes of the corresponding moments; and p_{ξ} , p_{θ} , p the amplitudes of applied surface loads in the meridional, circumferential, and normal directions. The quantities ϕ_{ξ} , ϕ_{θ} , and ϕ are the amplitudes of the rotations about the circumferential, meridional, and normal coordinate axes, and n is the Fourier harmonic.

The meridional and circumferential curvatures ω_{ξ} and ω_{θ} and the quantity γ are conveniently expressed in terms of the radial distance ρ as

$$\begin{aligned} \gamma &= \frac{\rho'}{\rho} \frac{1}{2} \\ \omega_{\theta} &= \frac{[1 - (\rho')^2]}{\rho} \\ \omega_{\xi} &= - \frac{(\gamma' + \gamma^2)}{\omega_{\theta}} \end{aligned} \quad (B4)$$

The corresponding Sanders' theory strain displacement relations for small, circumferentially harmonic motion about an axisymmetric stress and deformation state are

$$e_{\xi} = u'_{\xi} + \omega_{\xi} w + \bar{\phi}_{\xi} (\omega_{\xi} u_{\xi} - w') \quad (B5)$$

$$e_{\theta} = \gamma u_{\xi} + \frac{n}{\rho} u_{\theta}' + \omega_{\theta} w \quad (B6)$$

$$e_{\xi\theta} = -\frac{1}{2} \frac{n}{\rho} u_{\xi} + \frac{1}{2} u_{\theta}' - \frac{1}{2} \gamma u_{\theta} + \frac{1}{2} \bar{\phi}_{\xi} (\omega_{\theta} u_{\theta} + \frac{n}{\rho} w) \quad (B7)$$

$$k_{\xi} = \omega_{\xi} u'_{\xi} + \omega'_{\xi} u_{\xi} - w'' \quad (B8)$$

$$k_{\theta} = \gamma \omega_{\xi} u_{\xi} + \frac{n}{\rho} \omega_{\theta} u_{\theta} + \left(\frac{n}{\rho}\right)^2 w - \gamma w' \quad (B9)$$

$$k_{\xi\theta} = -\frac{1}{4} \frac{n}{\rho} (3\omega_{\xi} - \omega_{\theta}) u_{\xi} + \frac{1}{4} (3\omega_{\theta} - \omega_{\xi}) u_{\theta}' + \frac{1}{4} \gamma (\omega_{\xi} - 3\omega_{\theta}) u_{\theta} + \frac{n}{\rho} w' - \gamma \frac{n}{\rho} w \quad (B10)$$

The quantities e_{ξ} , e_{θ} , and $e_{\xi\theta}$ are the amplitudes of extensional and shearing strains, k_{ξ} , k_{θ} , and $k_{\xi\theta}$ the amplitudes of changes in curvature and twist, and u_{ξ} , u_{θ} , and w the amplitudes of shell displacements in the meridional, circumferential, and normal directions.

The constitutive stress-strain-temperature relations assumed for the elastic behavior of the shell along the meridian are the following equations relating the force and moment resultants and strain and curvature expressions.

$$\begin{Bmatrix} \tau_{\xi} \\ \tau_{\theta} \\ \tau_{\xi\theta} \\ m_{\xi} \\ m_{\theta} \\ m_{\xi\theta} \end{Bmatrix} = \begin{bmatrix} C_{11} & C_{12} & 0 & K_{11} & K_{12} & 0 \\ C_{12} & C_{22} & 0 & K_{12} & K_{22} & 0 \\ 0 & 0 & C_{33} & 0 & 0 & K_{33} \\ K_{11} & K_{12} & 0 & D_{11} & D_{12} & 0 \\ K_{12} & K_{22} & 0 & D_{12} & D_{22} & 0 \\ 0 & 0 & K_{33} & 0 & 0 & D_{33} \end{bmatrix} \begin{Bmatrix} e_{\xi} \\ e_{\theta} \\ e_{\xi\theta} \\ k_{\xi} \\ k_{\theta} \\ k_{\xi\theta} \end{Bmatrix} + \begin{Bmatrix} C_{1T} \\ C_{2T} \\ 0 \\ D_{1T} \\ D_{2T} \\ 0 \end{Bmatrix} \quad (B11)$$

where the stiffness constants C_{ij} , K_{ij} , and D_{ij} , and the thermal forces and moments C_{iT} and D_{iT} are allowed to vary along the meridian. Equations (B1)-(B3) and (B5)-(B11) are 15 equations in terms of the 15 unknowns τ_ξ , τ_θ , $\tau_{\xi\theta}$, m_ξ , m_θ , $m_{\xi\theta}$, e_ξ , e_θ , $e_{\xi\theta}$, k_ξ , k_θ , $k_{\xi\theta}$, u_ξ , u_θ , w . They may be combined in many ways to eliminate some of the intermediate variables. One such procedure is to reduce the system of equations to four simultaneous second-order differential equations (the three equilibrium equations and the fourth of equations (B11)) following the concepts of reference (33). As indicated in reference (33) m_θ must be eliminated in such a way that k_ξ does not appear in order to prevent the appearance of derivatives of w higher than two. From the fourth and fifth of equations (B11), the necessary relation can be obtained as

$$m_\theta = \frac{D_{12}}{D_{11}} m_\xi + \left(K_{12} - \frac{D_{12} K_{11}}{D_{11}} \right) e_\xi + \left(K_{12} - \frac{D_{12} K_{12}}{D_{11}} \right) e_\theta + \left(D_{22} - \frac{D_{12}^2}{D_{11}} \right) k_\theta + \left(D_{2T} - \frac{D_{12}}{D_{11}} D_{1T} \right)$$

and u_ξ , u_θ , w , and m_ξ are taken as the fundamental variables. The four simultaneous second-order differential equations can be written in matrix form as

$$Ez'' + Fz' + Gz + \bar{E}z'' + \bar{F}z' + \bar{G}z + E^*z'' + F^*z' + G^*z - \tilde{V}\ddot{z} = e \quad (B12)$$

where

$$z = \begin{Bmatrix} u_\xi \\ u_\theta \\ w \\ m_\xi \end{Bmatrix}, \quad \tilde{V} = \begin{bmatrix} 1 & 0 & 0 & 0 \\ 0 & 1 & 0 & 0 \\ 0 & 0 & 1 & 0 \\ 0 & 0 & 0 & 0 \end{bmatrix} \quad (B13)$$

and E , F , G , \bar{E} , \bar{F} , \bar{G} , E^* , F^* , and G^* are 4×4 matrices. The elements of these matrices are contained in Appendix C. The barred and starred matrices contain the initial stress and deformation quantities and vanish if the initial state is a zero state. The starred quantities reflect the contribution of the square of the initial rotations on the behavior of the problems. Equations (B12) may be applied to linear stress analysis problems by setting the barred and starred quantities to zero and letting $\ddot{z} = 0$, applied to buckling problems by setting $\ddot{z} = e = 0$, and applied to prestressed vibration problems with $e = 0$, and assuming z harmonic in time.

Boundary conditions are specified by use of the vector z and an additional vector y where

$$y = \begin{Bmatrix} \tau_{\xi} \\ f_{\xi\theta} \\ f_{\xi} \\ \phi_{\xi} \end{Bmatrix} \quad (B14)$$

and

$$f_{\xi\theta} = \tau_{\xi\theta} + \frac{1}{2} (\omega_{\theta} - \omega_{\xi}) m_{\xi\theta} + \left[\frac{1}{2} (\bar{\tau}_{\xi} + \bar{\tau}_{\theta}) \phi \right] \quad (B15)$$

$$f_{\xi} = m'_{\xi} + \gamma (m_{\xi} - m_{\theta}) + \frac{2n}{\rho} m_{\xi\theta} - \bar{\tau}_{\xi} \phi_{\xi} - \bar{\phi}_{\xi} \tau_{\xi} \quad (B16)$$

$$\phi_{\xi} = -w' + \omega_{\xi} u_{\xi} \quad (B17)$$

In matrix form

$$y = H z' + J z + \bar{H} z' + \bar{J} z + H^* z' + J^* z + f \quad (B18)$$

where $H, J, \bar{H}, \bar{J}, H^*, J^*$ are 4×4 matrices defined in Appendix C along with the vector f . Again, the barred and starred matrices contain only the prestress quantities, and the starred quantities reflect the contribution of the square of the prestress rotations.

For shell analysis problems, all admissible sets of linear boundary conditions at one boundary, including ring stiffeners, can be written in the form

$$(\Psi + \bar{\Psi}) y + (\Lambda + \bar{\Lambda} - \omega^2 \hat{M}) z = \gamma \quad (B19)$$

The quantities $\Psi, \bar{\Psi}, \Lambda, \bar{\Lambda}, \hat{M}$ are 4×4 matrices corresponding to prescribed boundary conditions, including any ring stiffness and mass contribution and γ is a vector of prescribed constants.

Numerical Procedure

Finite Difference Approximations. The governing shell equation and corresponding boundary conditions may be approximated by the standard central finite differences. Finite difference stations are selected with uniform spacing between discontinuities of the shell meridian, and the finite difference approximations at an i^{th} station are

$$z''_i = \frac{1}{\Delta^2} (z_{i-1} - 2 z_i + z_{i+1}) \quad (B20)$$

$$z'_i = \frac{1}{2\Delta} (-z_{i-1} + z_{i+1}) \quad (B21)$$

$$z_1 = z_1 \quad (\text{B22})$$

In order to compute derivatives at a boundary, introduction of fictitious exterior points or the use of forward (or backward) differences is required. Points of discontinuity along the meridian, due to sharp changes in geometry or finite difference spacing, should be treated as shell-edge points for both sides of the discontinuity.

Application of the difference approximations to the governing equations leads to tridiagonal simultaneous equations of the form

$$[K_0]\{Z\} + [K_1]\{Z\} + [K_2]\{Z\} - [M]\{\ddot{Z}\} = \{P\} \quad (\text{B23})$$

where $[K_0]$ contains the structural stiffness, $[K_1]$ contains the influence of prestress and prestress deformations to the first power, $[K_2]$ contains the influence of prestress deformations to the second power, and $[M]$ contains the mass contribution. The quantity $\{Z\}$ is the vector of unknowns composed of the subvectors z_1 at the various difference stations, and $\{P\}$ is the corresponding load vector.

Static Stress Analysis Problems. For static equilibrium problems $\{\ddot{Z}\}$ is zero, and the equations are solved by a tridiagonal Gaussian elimination procedure similar to that given in reference (33). For the special case of nonlinear axisymmetric behavior ($n = 0$), $\{P\}$ is a function of the $\{Z\}$ variables (see ref. 55, e.g.). These added axisymmetric nonlinearity effects are handled by a Newton-Raphson procedure in the SALORS program.

Free Vibration Problems. For free vibration problems $\{Z\}$ is assumed to vary harmonically with frequency ω . A prestress distribution, if needed, is first obtained from a static stress analysis, and this prestress state is then used to determine the coefficients in $[K_1]$ and $[K_2]$. The inertial contribution is treated as a load, and the eigenvalue problem is solved iteratively by the inverse power method as follows. Let the set of equations be compactly represented as

$$[K]\{Z\} = -\lambda [M]\{Z\} \quad (\text{B24})$$

where

$$[K] = [K_0] + [K_1] + [K_2]$$

and

$$\lambda = \omega^2$$

The lowest eigenvalue of equation (B24) is obtained by iteration, such that for the r th iteration the vector $\{Z^{r-1}\}$ is assumed and $\{Z^r\}$ determined by

$$[K] \left\{ \frac{1}{\lambda} Z^r \right\} = -[M] \{Z^{r-1}\} \quad (B25)$$

Again, taking advantage of the fact that $[K]$ is a banded tridiagonal matrix comprised of 4×4 submatrices, Gaussian elimination is used for each iteration.

An initial vector is automatically assumed to start the problem, and thereafter the previously determined $\{Z\}$ is used as the guess for the next cycle. When convergence has occurred, the ratio of the norm of the last assumed vector $\{Z^{r-1}\}$ to the norm of the final vector $\left\{ \frac{1}{\lambda} Z^r \right\}$ is

$$\frac{\left\{ \frac{1}{\lambda} Z^r \right\}^T \left\{ \frac{1}{\lambda} Z^r \right\}}{\{Z^{r-1}\}^T \{Z^{r-1}\}} = \frac{1}{\lambda^2} \quad (B26)$$

where the superscript T indicates the transpose of a matrix. If the vector $\{Z^{r-1}\}$ is normalized to 1 just prior to initiating an iteration cycle

$$\lambda^2 = \frac{1}{\left\{ \frac{1}{\lambda} Z^r \right\}^T \left\{ \frac{1}{\lambda} Z^r \right\}} \quad (B27)$$

The iteration procedure is continued until the eigenvalue determined from an iteration agrees with that obtained in the previous iteration to some prescribed degree of accuracy.

The iteration procedure converges to the eigenvalue lowest in absolute value (i.e., the eigenvalue closest to zero). If other eigenvalues are desired, the origin of the eigenvalue scale is shifted to some nonzero reference eigenvalue. Then the iteration procedure converges to the closest eigenvalue above or below this reference eigenvalue.

Let

$$\lambda = \lambda_g + \lambda_e \quad (B28)$$

where λ_g is some reference eigenvalue prescribed at the outset, and λ_e is an effective interim eigenvalue to be determined.

Substitution of equation (B28) into equation (B24), and rearranging terms gives

$$\left\{ \left[K \right] + \lambda_s \left[M \right] \right\} \{ Z \} = -\lambda_e \left[M \right] \{ Z \} \quad (B29)$$

This matrix equation is of the form

$$\left[K_e \right] \{ Z \} = -\lambda_e \left[M \right] \{ Z \} \quad (B30)$$

where

$$\left[K_e \right] = \left[K \right] + \lambda_s \left[M \right] \quad (B31)$$

The iteration procedure to determine λ_e is similar to that given by equations (B25) and (B27), and will converge to the eigenvalue closest to λ_s . The algebraic sign of λ_e can be determined from a Rayleigh quotient-type relationship.

$$\lambda_e = - \frac{\{ Z \}^T \left[K_e \right] \{ Z \}}{\{ Z \}^T \left[M \right] \{ Z \}} \quad (B32)$$

Buckling Problems. For buckling problems, a prestress distribution is first obtained from a static stress analysis. This prestress state is then used to determine the coefficients in $\left[K_1 \right]$ and $\left[K_2 \right]$. The resulting equations are

$$\left[K_0 \right] \{ Z \} + \lambda \left[K_1 \right] \{ Z \} + \lambda^2 \left[K_2 \right] \{ Z \} = 0 \quad (B33)$$

where λ is the eigenvalue corresponding to the multiplier of the prestress state required to cause buckling. For the case where quadratic prebuckling deformations are neglected $\left[K_2 \right] = 0$, and the eigenvalue solution is obtained by the inverse power method similar to that described for free vibrations, namely

$$\left[K_0 \right] \left\{ \frac{1}{\lambda} z^r \right\} = - \left[K_1 \right] \left\{ z^{r-1} \right\} \quad (B34)$$

It is particularly important to determine the sign of the converged buckling eigenvalue λ because of the possibility of negative eigenvalues. The sign of the eigenvalue is obtained from the Rayleigh quotient-type relationships

$$\lambda = - \frac{\{Z\}^T [K_0] \{Z\}}{\{Z\}^T [K_1] \{Z\}} \quad (B35)$$

If the quadratic prebuckling deformations are retained, the inverse power method may still be used; however, provisions must be included for handling the quadratic eigenvalue term. This is accomplished by introducing a new variable

$$\{W\} = \lambda \{Z\} \quad (B36)$$

Equation (B33), together with equation (B36), can be written as

$$\begin{bmatrix} K_0 & 0 \\ 0 & I \end{bmatrix} \begin{Bmatrix} Z \\ W \end{Bmatrix} = -\lambda \begin{bmatrix} K_1 & K_2 \\ -I & 0 \end{bmatrix} \begin{Bmatrix} Z \\ W \end{Bmatrix} \quad (B37)$$

which now is in the form of a linear eigenvalue problem and can be solved by the inverse power method as

$$\begin{aligned} [K_0] \begin{Bmatrix} \frac{1}{\lambda} & Z^r \end{Bmatrix} &= - [K_1] \begin{Bmatrix} Z^{r-1} \end{Bmatrix} - [K_2] \begin{Bmatrix} W^{r-1} \end{Bmatrix} \\ \begin{Bmatrix} \frac{1}{\lambda} & W^r \end{Bmatrix} &= \begin{Bmatrix} Z^{r-1} \end{Bmatrix} \end{aligned} \quad (B38)$$

The algebraic sign of the eigenvalue can be determined from

$$\lambda = - \frac{\{Z\}^T [K_0] \{Z\} + \{W\}^T \{W\}}{\{Z\}^T [K_1] \{Z\} + \{Z\}^T [K_2] \{W\} - \{W\}^T \{Z\}} \quad (B39)$$

The inclusion of the quadratic prebuckling deformation terms thus requires only minor additional calculations and the storage of two modal vectors, rather than one. The procedure can also be easily modified to include shifting the origin of the eigenvalue scale to obtain the closest eigenvalue to a reference value.

APPENDIX C

NONZERO COEFFICIENTS OF MATRICES

E, F, G, e, \bar{E} , \bar{F} , \bar{G} , E^* , F^* , and G^* Matrices

$$E_{11} = S_{11}$$

$$E_{13} = -\gamma S_{13}$$

$$E_{22} = \frac{1}{2} C_{33} + \frac{1}{8} (3\omega_\theta - \omega_\xi)^2 D_{33} + \frac{1}{2} (3\omega_\theta - \omega_\xi) K_{33}$$

$$E_{23} = \frac{n}{\rho} \left[\frac{1}{2} (3\omega_\theta - \omega_\xi) D_{33} + K_{33} \right]$$

$$E_{31} = E_{13}$$

$$E_{32} = E_{23}$$

$$E_{33} = \gamma^2 S_{33} + 2\left(\frac{n}{\rho}\right)^2 D_{33}$$

$$L_{34} = 1$$

$$E_{43} = -D_{11}$$

$$F_{11} = \gamma S_{11} + S'_{11}$$

$$F_{12} = \frac{n}{\rho} \left[s_{12} + \frac{1}{2} c_{33} + s_{13} \omega_{\theta} + \frac{1}{2} K_{33} (\omega_{\xi} + \omega_{\theta}) \right. \\ \left. + \frac{1}{8} (3\omega_{\xi} - \omega_{\theta}) (3\omega_{\theta} - \omega_{\xi}) D_{33} \right]$$

$$F_{13} = s_{11} \omega_{\xi} + s_{12} \omega_{\theta} + s_{13} \omega_{\xi} \omega_{\theta} + \gamma^2 (s_{23} + \omega_{\xi} s_{33}) \\ + \left(\frac{n}{\rho} \right)^2 \left[s_{13} + K_{33} + \frac{1}{2} (3\omega_{\xi} - \omega_{\theta}) D_{33} \right] - \gamma s'_{13}$$

$$F_{14} = \frac{K_{11}}{D_{11}} + \omega_{\xi}$$

$$F_{21} = -F_{12}$$

$$F_{22} = \frac{1}{2} \left\{ \gamma c_{33} - \frac{1}{4} (3\omega_{\theta} - \omega_{\xi}) \left[2\omega'_{\xi} - \gamma (5\omega_{\xi} - 3\omega_{\theta}) \right] D_{33} + K_{33} (2\gamma\omega_{\xi} - \omega'_{\xi}) \right. \\ \left. + c'_{33} + (3\omega_{\theta} - \omega_{\xi}) K'_{33} + \frac{1}{4} (3\omega_{\theta} - \omega_{\xi})^2 D'_{33} \right\}$$

$$F_{23} = \frac{n}{\rho} \left\{ \gamma (\omega_{\theta} s_{33} + s_{23}) - \frac{1}{2} \left[3\gamma (\omega_{\theta} - \omega_{\xi}) + \omega'_{\xi} \right] D_{33} \right. \\ \left. + \left[K'_{33} + \frac{1}{2} (3\omega_{\theta} - \omega_{\xi}) D'_{33} \right] \right\}$$

$$F_{31} = -\omega_{\xi} s_{11} - \omega_{\theta} s_{12} + \omega_{\xi} \omega_{\theta} s_{13} - \gamma^2 (s_{23} + \omega_{\xi} s_{33}) \\ - \left(\frac{n}{\rho} \right)^2 \left[s_{13} + K_{33} + \frac{1}{2} (3\omega_{\xi} - \omega_{\theta}) D_{33} \right] - \gamma s'_{13}$$

$$\begin{aligned} \Gamma_{32} = & -\frac{n}{\rho} \left\{ \gamma \left(s_{23} + \omega_{\theta} s_{33} \right) + \frac{1}{2} D_{33} \left[3\gamma(\omega_{\theta} - \omega_{\xi}) + \omega'_{\xi} \right] \right. \\ & \left. - \frac{1}{2} (3\omega_{\theta} - \omega_{\xi}) D'_{33} - K'_{33} \right\} \end{aligned}$$

$$F_{33} = -\gamma \left[s_{33} \left(\gamma^2 + 2\omega_{\xi} \omega_{\theta} \right) + 2\left(\frac{n}{\rho}\right)^2 D_{33} \right] + 2\left(\frac{n}{\rho}\right)^2 D'_{33} + \gamma^2 s'_{33}$$

$$F_{34} = \gamma \left(2 - \frac{D_{12}}{D_{11}} \right)$$

$$F_{41} = K_{11} + D_{11} \omega_{\xi}$$

$$F_{43} = -\gamma D_{12}$$

$$\begin{aligned} G_{11} = & -s_{13} \left(\omega_{\xi}^2 \omega_{\theta} - \gamma \omega'_{\xi} \right) - s_{12} \omega_{\xi} \omega_{\theta} - \gamma^2 \left(s_{22} + 2\omega_{\xi} s_{23} + \omega_{\xi}^2 s_{33} \right) \\ & - \frac{1}{2} \left(\frac{n}{\rho} \right)^2 \left[c_{33} + (3\omega_{\xi} - \omega_{\theta}) K_{33} + \frac{1}{4} (3\omega_{\xi} - \omega_{\theta})^2 D_{33} \right] \\ & + \gamma \omega_{\xi} s'_{13} + \gamma s'_{12} \end{aligned}$$

$$\begin{aligned} G_{12} = & \frac{n}{\rho} \left\{ -\gamma \left[s_{22} + \frac{1}{2} c_{33} + \left(s_{23} + \frac{1}{2} K_{33} \right) (\omega_{\xi} + \omega_{\theta}) \right. \right. \\ & \left. - s_{13} (\omega_{\xi} - \omega_{\theta}) + \frac{1}{8} (3\omega_{\xi} - \omega_{\theta}) (3\omega_{\theta} - \omega_{\xi}) D_{33} + \omega_{\xi} \omega_{\theta} s_{33} \right] \\ & \left. + s'_{12} + \omega_{\theta} s'_{13} \right\} \end{aligned}$$

$$\begin{aligned}
G_{13} = & s_{11} \omega_{\xi}' + \gamma (s_{11} \omega_{\xi} - s_{22} \omega_{\theta} - \omega_{\xi}^2 s_{13} - \omega_{\xi} \omega_{\theta} s_{23}) \\
& - \gamma \left(\frac{n}{\rho} \right)^2 \left[s_{23} + s_{13} + K_{33} + \omega_{\xi} s_{33} + \frac{1}{2} (3\omega_{\xi} - \omega_{\theta}) D_{33} \right] \\
& + \left(\frac{n}{\rho} \right)^2 s_{13}' + \omega_{\xi} s_{11}' + \omega_{\theta} s_{12}'
\end{aligned}$$

$$G_{14} = \gamma \left[\frac{K_{11}}{D_{11}} - \frac{K_{12}}{D_{11}} + \omega_{\xi} \left(1 - \frac{D_{12}}{D_{11}} \right) \right] + \frac{1}{D_{11}} \left(K_{11}' - \frac{K_{11} D_{11}'}{D_{11}} \right)$$

$$\begin{aligned}
G_{21} = & \frac{n}{\rho} \left\{ -\gamma \left[\frac{1}{2} C_{33} + s_{22} + s_{23} (\omega_{\xi} + \omega_{\theta}) + \omega_{\xi} \omega_{\theta} s_{33} \right] - \frac{1}{2} K_{33} (2\gamma \omega_{\xi} + \omega_{\xi}') \right. \\
& + \frac{1}{8} D_{33} \left[\gamma (6\omega_{\xi} \omega_{\theta} - 7\omega_{\xi}^2 - 3\omega_{\theta}^2) - 2\omega_{\xi}' (5\omega_{\theta} - 3\omega_{\xi}) \right] \\
& \left. - \frac{1}{2} C_{33}' - \frac{1}{2} (\omega_{\xi} + \omega_{\theta}) K_{33}' - \frac{1}{8} (3\omega_{\theta} - \omega_{\xi}) (3\omega_{\xi} - \omega_{\theta}) D_{33}' \right\}
\end{aligned}$$

$$\begin{aligned}
G_{22} = & \frac{1}{2} C_{33} \omega_{\xi} \omega_{\theta} - \frac{1}{2} \gamma^2 C_{33} - \left(\frac{n}{\rho} \right)^2 (s_{22} + \omega_{\theta}^2 s_{33} + 2\omega_{\theta} s_{23}) \\
& + \frac{1}{8} D_{33} (3\omega_{\theta} - \omega_{\xi}) \left[(3\omega_{\theta} - \omega_{\xi}) \omega_{\xi} \omega_{\theta} - \gamma^2 (5\omega_{\xi} - 3\omega_{\theta}) + 2\gamma \omega_{\xi}' \right] \\
& + \frac{1}{2} K_{33} \left\{ \gamma \omega_{\xi}' - \omega_{\xi} \left[2\gamma^2 - \omega_{\theta} (3\omega_{\theta} - \omega_{\xi}) \right] \right\} \\
& - \frac{\gamma}{2} \left\{ C_{33}' + \left[K_{33}' + \frac{1}{4} (3\omega_{\theta} - \omega_{\xi}) I_{33}' \right] (3\omega_{\theta} - \omega_{\xi}) \right\}
\end{aligned}$$

$$G_{23} = \frac{n}{\rho} \left\{ -\omega_{\xi} s_{12} - \omega_{\theta} s_{22} - \left(\frac{n}{\rho}\right)^2 (\omega_{\theta} s_{33} + s_{23}) \right. \\
- \omega_{\theta}^2 s_{23} + \omega_{\xi} \omega_{\theta} (-s_{13} + K_{33}) \\
+ \frac{1}{2} \left[3\gamma^2 (\omega_{\theta} - \omega_{\xi}) + \omega_{\xi} \omega_{\theta} (3\omega_{\theta} - \omega_{\xi}) + \gamma \omega_{\xi}' \right] D_{33} \\
\left. - \gamma \left[K_{33}' + \frac{1}{2} (3\omega_{\theta} - \omega_{\xi}) D_{33}' \right] \right\}$$

$$G_{24} = -\frac{n}{\rho} \left(\omega_{\theta} \frac{D_{12}}{D_{11}} + \frac{K_{12}}{D_{11}} \right)$$

$$G_{31} = \gamma \left[-\omega_{\xi} s_{12} - \omega_{\theta} s_{22} - \omega_{\xi}^2 s_{13} + (\omega_{\xi} \omega_{\theta} + \gamma^2) s_{23} \right. \\
+ (\gamma^2 \omega_{\xi} - \gamma \omega_{\xi}' + 2\omega_{\xi}^2 \omega_{\theta}) s_{33} - \gamma s_{23}' - \gamma \omega_{\xi} s_{33}' \\
+ \left(\frac{n}{\rho}\right)^2 \left\{ -\gamma (s_{23} + \omega_{\xi} s_{33}) + \frac{1}{2} \left[\gamma (\omega_{\xi} - \omega_{\theta}) - 3\omega_{\xi}' \right] D_{33} \right. \\
\left. \left. - \frac{1}{2} (3\omega_{\xi} - \omega_{\theta}) D_{33}' - K_{33}' \right\} \right]$$

$$G_{32} = -\frac{n}{\rho} \left\{ \omega_{\xi} s_{12} + \omega_{\theta} s_{22} + \omega_{\xi} \omega_{\theta} s_{13} + \omega_{\theta}^2 s_{23} \right. \\
- s_{33} \left[\omega_{\xi} \omega_{\theta}^2 - \omega_{\theta} \left(\frac{n}{\rho}\right)^2 - \gamma^2 (\omega_{\xi} - 2\omega_{\theta}) \right] \\
\left. - \frac{1}{2} D_{33} \left[3\gamma^2 (\omega_{\theta} - \omega_{\xi}) + \gamma \omega_{\xi}' + \omega_{\xi} \omega_{\theta} (3\omega_{\theta} - \omega_{\xi}) \right] \right\}$$

$$\begin{aligned}
& -\omega_{\xi}\omega_{\theta} (s_{23} + K_{33}) + s_{23} \left[\left(\frac{n}{\rho} \right)^2 - \gamma^2 \right] + \gamma s'_{23} \\
& + \gamma\omega_{\theta} s'_{33} + \frac{\gamma}{2} \left[(3\omega_{\theta} - \omega_{\xi}) D'_{33} + 2K'_{33} \right] \Big\}
\end{aligned}$$

$$\begin{aligned}
G_{33} = & -\omega_{\xi}^2 s_{11} - 2\omega_{\xi}\omega_{\theta} s_{12} - \omega_{\theta}^2 s_{22} + \omega_{\xi}\omega_{\theta} (\omega_{\xi} s_{13} + \omega_{\theta} s_{23}) \\
& - \gamma\omega_{\xi} s'_{13} - \gamma^2 (\omega_{\xi} - \omega_{\theta}) s_{23} + \left(\frac{n}{\rho} \right)^2 s_{33} \left[2\gamma^2 + \omega_{\xi}\omega_{\theta} - \left(\frac{n}{\rho} \right)^2 \right] \\
& + 2 \left(\frac{n}{\rho} \right)^2 \left[D_{33} (\gamma^2 + \omega_{\xi}\omega_{\theta}) - \omega_{\xi} s_{13} - \omega_{\theta} s_{23} \right] - \gamma\omega_{\xi} s'_{13} \\
& - \gamma\omega_{\theta} s'_{23} - \gamma \left(\frac{n}{\rho} \right)^2 (s'_{33} + 2 D'_{33})
\end{aligned}$$

$$G_{34} = -\omega_{\xi} \frac{K_{11}}{D_{11}} - \omega_{\theta} \frac{K_{12}}{D_{11}} - \omega_{\xi}\omega_{\theta} \left(1 - \frac{D_{12}}{D_{11}} \right) - \left(\frac{n}{\rho} \right)^2 \frac{D_{12}}{D_{11}} - \frac{\gamma}{D_{11}} \left(D'_{12} - \frac{D_{12} D'_{11}}{D_{11}} \right)$$

$$G_{41} = \gamma\omega_{\xi} D_{12} + D_{11} \omega'_{\xi} + \gamma K_{12}$$

$$G_{42} = \frac{n}{\rho} [D_{12} \omega_{\theta} + K_{12}]$$

$$G_{43} = K_{11} \omega_{\xi} + \left(\frac{n}{\rho} \right)^2 D_{12}$$

$$G_{44} = -1$$

$$e_1 = -\gamma \left[\frac{D_{1T}}{D_{11}} (K_{12} - K_{11}) + C_{1T} - C_{2T} - \omega_\xi \left(D_{2T} - \frac{D_{1T} D_{12}}{D_{11}} \right) \right] \\ + \frac{K_{11}}{D_{11}} \left(D_{1T}' - \frac{D_{11}' D_{1T}}{D_{11}} \right) + \frac{K_{11}' D_{1T}}{D_{11}} - C_{1T}' - p_\xi$$

$$e_2 = \frac{n}{\rho} \left[C_{2T} - \frac{K_{12} D_{1T}}{D_{11}} + \omega_\theta \left(D_{2T} - \frac{D_{12} D_{1T}}{D_{11}} \right) \right] - p_\theta$$

$$e_3 = \omega_\xi \left(C_{1T} - \frac{K_{11} D_{1T}}{D_{11}} \right) + \omega_\theta \left(C_{2T} - \frac{K_{12} D_{1T}}{D_{11}} \right) \\ - \left[\omega_\xi \omega_\theta - \left(\frac{n}{\rho} \right)^2 \right] \left(D_{2T} - \frac{D_{12} D_{1T}}{D_{11}} \right) \\ + \gamma \left[D_{2T}' - \frac{D_{12} D_{1T}'}{D_{11}} - \frac{D_{1T}}{D_{11}} \left(D_{12}' - \frac{D_{12} D_{11}'}{D_{11}} \right) \right] - p$$

$$e_4 = -D_{1T}$$

$$\bar{E}_{13} = -S_{11} \bar{\varphi}_\xi$$

$$\bar{E}_{22} = \frac{1}{4} (\bar{\tau}_\xi + \bar{\tau}_\theta)$$

$$\bar{E}_{31} = -S_{11} \bar{\varphi}_\xi$$

$$F_{33} = 2\gamma S_{13} \bar{\varphi}_\xi + \bar{\tau}_\xi$$

$$F_{12} = -\frac{1}{4} \frac{n}{\rho} (\bar{\tau}_\xi + \bar{\tau}_\theta)$$

$$F_{13} = -\gamma S_{11} \bar{\varphi}_\xi - S'_{11} \bar{\varphi}_\xi - S_{11} \bar{\varphi}'_\xi + \gamma S_{12} \bar{\varphi}_\xi + 2\gamma \omega_\xi S_{13} \bar{\varphi}_\xi$$

$$F_{21} = \frac{1}{4} \frac{n}{\rho} (\bar{\tau}_\xi + \bar{\tau}_\theta)$$

$$F_{22} = \frac{1}{4} (\bar{\tau}'_\xi + \bar{\tau}'_\theta) + \frac{1}{4} \gamma (\bar{\tau}_\xi + \bar{\tau}_\theta)$$

$$F_{23} = \frac{1}{2} \frac{n}{\rho} C_{33} \bar{\varphi}_\xi + \frac{n}{\rho} S_{12} \bar{\varphi}_\xi + \frac{1}{4} \frac{n}{\rho} (\gamma \omega_\theta - \omega_\xi) K_{33} \bar{\varphi}_\xi \\ + \frac{n}{\rho} \omega_\theta S_{13} \bar{\varphi}_\xi - \frac{n}{\rho} \omega_\theta K_{33} \bar{\varphi}_\xi$$

$$F_{31} = -2\gamma \omega_\xi S_{13} \bar{\varphi}_\xi - S_{11} (\gamma \bar{\varphi}_\xi + \bar{\varphi}'_\xi) - S'_{11} \bar{\varphi}_\xi - \gamma S_{12} \bar{\varphi}_\xi - \omega_\xi \bar{\tau}_\xi$$

$$F_{32} = \frac{n}{\rho} \omega_\theta K_{33} \bar{\varphi}_\xi - \frac{n}{\rho} S_{12} \bar{\varphi}_\xi - \frac{n}{\rho} \omega_\theta S_{13} \bar{\varphi}_\xi - \frac{1}{2} \frac{n}{\rho} C_{33} \bar{\varphi}_\xi \\ - \frac{1}{4} \frac{n}{\rho} (\gamma \omega_\theta - \omega_\xi) K_{33} \bar{\varphi}_\xi$$

$$F_{33} = -2\omega_{\xi}\omega_{\theta} s_{13} \bar{\varphi}_{\xi} + 2\gamma s'_{13} \bar{\varphi}_{\xi} + 2\gamma s_{13} \bar{\varphi}'_{\xi} + \gamma \bar{\tau}_{\xi} + \bar{\tau}'_{\xi}$$

$$F_{34} = -s_{14} \bar{\varphi}_{\xi}$$

$$\bar{F}_{43} = K_{11} \bar{\varphi}_{\xi}$$

$$\begin{aligned} G_{11} = & \gamma\omega_{\xi} s_{11} \bar{\varphi}_{\xi} + \omega_{\xi} s'_{11} \bar{\varphi}_{\xi} + \omega_{\xi} s_{11} \bar{\varphi}'_{\xi} + \omega'_{\xi} s_{11} \bar{\varphi}_{\xi} - 2\gamma\omega_{\xi} s_{12} \bar{\varphi}_{\xi} \\ & - 2\gamma\omega_{\xi}^2 s_{13} \bar{\varphi}_{\xi} - \omega_{\xi}^2 \bar{\tau}_{\xi} - \frac{1}{4} \left(\frac{n}{\rho} \right)^2 (\bar{\tau}_{\xi} + \bar{\tau}_{\theta}) \end{aligned}$$

$$\begin{aligned} G_{12} = & \frac{1}{2} \frac{n}{\rho} \omega_{\theta} c_{33} \bar{\varphi}_{\xi} + \frac{1}{4} \frac{n}{\rho} \omega_{\theta} (3\omega_{\xi} - \omega_{\theta}) K_{33} \bar{\varphi}_{\xi} - \frac{n}{\rho} \omega_{\xi} s_{12} \bar{\varphi}_{\xi} \\ & - \frac{n}{\rho} \omega_{\xi} \omega_{\theta} s_{13} \bar{\varphi}_{\xi} - \frac{1}{4} \gamma \frac{n}{\rho} (\bar{\tau}_{\xi} + \bar{\tau}_{\theta}) \end{aligned}$$

$$\begin{aligned} G_{13} = & \frac{1}{2} \left(\frac{n}{\rho} \right)^2 c_{33} \bar{\varphi}_{\xi} + \frac{1}{4} \left(\frac{n}{\rho} \right)^2 (3\omega_{\xi} - \omega_{\theta}) K_{33} \bar{\varphi}_{\xi} - \omega_{\xi}^2 s_{11} \bar{\varphi}_{\xi} \\ & - \omega_{\xi} \omega_{\theta} s_{12} \bar{\varphi}_{\xi} - \left(\frac{n}{\rho} \right)^2 \omega_{\xi} s_{13} \bar{\varphi}_{\xi} \end{aligned}$$

$$G_{14} = -\omega_{\xi} s_{14} \bar{\varphi}_{\xi}$$

$$\begin{aligned}\bar{G}_{21} = & -\frac{n}{\rho} \omega_{\xi} s_{12} \bar{\varphi}_{\xi} - \frac{n}{\rho} \omega_{\xi} \omega_{\theta} s_{13} \bar{\varphi}_{\xi} + \frac{1}{2} \frac{n}{\rho} \omega_{\theta} c_{33} \bar{\varphi}_{\xi} \\ & + \frac{1}{4} \frac{n}{\rho} \omega_{\theta} (3\omega_{\xi} - \omega_{\theta}) K_{33} \bar{\varphi}_{\xi} + \frac{1}{4} \frac{n}{\rho} (\bar{\tau}_{\xi}' + \bar{\tau}_{\theta}') \\ & - \frac{1}{4} \gamma \frac{n}{\rho} (\bar{\tau}_{\xi} + \bar{\tau}_{\theta})\end{aligned}$$

$$\begin{aligned}\bar{G}_{22} = & \gamma \omega_{\theta} c_{33} \bar{\varphi}_{\xi} + \frac{1}{2} \omega_{\theta} c_{33}' \bar{\varphi}_{\xi} + \frac{1}{2} \omega_{\theta} c_{33} \bar{\varphi}_{\xi}' + \frac{1}{2} \gamma \omega_{\xi} c_{33} \bar{\varphi}_{\xi} \\ & + \frac{1}{4} \omega_{\theta} \left[\gamma (\omega_{\xi} + 3\omega_{\theta}) - \omega_{\xi}' \right] K_{33} \bar{\varphi}_{\xi} + \frac{1}{4} \omega_{\theta} (3\omega_{\theta} - \omega_{\xi}) K_{33}' \bar{\varphi}_{\xi} \\ & + \frac{1}{4} \omega_{\theta} (3\omega_{\theta} - \omega_{\xi}) K_{33} \bar{\varphi}_{\xi}' + \frac{1}{4} \gamma \omega_{\xi} (3\omega_{\theta} - \omega_{\xi}) K_{33} \bar{\varphi}_{\xi} - \omega_{\theta}^2 \bar{\tau}_{\theta} \\ & + \frac{1}{4} \gamma (\bar{\tau}_{\xi}' + \bar{\tau}_{\theta}') - \frac{1}{4} (\omega_{\xi} \omega_{\theta} + \gamma^2) (\bar{\tau}_{\xi} + \bar{\tau}_{\theta})\end{aligned}$$

$$\begin{aligned}\bar{G}_{23} = & \frac{1}{2} \gamma \frac{n}{\rho} c_{33} \bar{\varphi}_{\xi} + \frac{1}{2} \frac{n}{\rho} c_{33}' \bar{\varphi}_{\xi} + \frac{1}{2} \frac{n}{\rho} c_{33} \bar{\varphi}_{\xi}' + \frac{1}{4} \frac{n}{\rho} \left[\gamma (\omega_{\xi} + 3\omega_{\theta}) - \omega_{\xi}' \right] K_{33} \bar{\varphi}_{\xi} \\ & + \frac{1}{4} \frac{n}{\rho} (3\omega_{\theta} - \omega_{\xi}) \left(K_{33}' \bar{\varphi}_{\xi} + K_{33} \bar{\varphi}_{\xi}' - \gamma K_{33} \bar{\varphi}_{\xi} \right) + \gamma \frac{n}{\rho} \omega_{\theta} K_{33} \bar{\varphi}_{\xi} - \frac{n}{\rho} \omega_{\theta} \bar{\tau}_{\theta}\end{aligned}$$

$$\begin{aligned}\bar{G}_{31} = & -\omega_{\xi}^2 s_{11} \bar{\varphi}_{\xi} + \omega_{\xi} \left[2\omega_{\xi} \omega_{\theta} - \left(\frac{n}{\rho} \right)^2 \right] s_{13} \bar{\varphi}_{\xi} - 2\gamma \omega_{\xi} s_{13}' \bar{\varphi}_{\xi} - 2\gamma \omega_{\xi} s_{13} \bar{\varphi}_{\xi}' \\ & - 2\gamma \omega_{\xi}' s_{13} \bar{\varphi}_{\xi} - \gamma s_{12} \bar{\varphi}_{\xi}' - \gamma s_{12}' \bar{\varphi}_{\xi} + \frac{1}{2} \left(\frac{n}{\rho} \right)^2 c_{33} \bar{\varphi}_{\xi} \\ & + \frac{1}{4} \left(\frac{n}{\rho} \right)^2 (3\omega_{\xi} - \omega_{\theta}) K_{33} \bar{\varphi}_{\xi} - \omega_{\xi} (\gamma \bar{\tau}_{\xi} + \bar{\tau}_{\xi}') - \omega_{\xi}' \bar{\tau}_{\xi}\end{aligned}$$

$$\begin{aligned}\bar{G}_{32} = & \frac{n}{\rho} \omega_{\theta} K'_{33} \bar{\varphi}_{\xi} + \frac{n}{\rho} \omega_{\theta} K_{33} \bar{\varphi}'_{\xi} + \gamma \frac{n}{\rho} \omega_{\xi} K_{33} \bar{\varphi}_{\xi} - \frac{n}{\rho} s_{12} \bar{\varphi}'_{\xi} - \frac{n}{\rho} \omega_{\theta} s_{13} \bar{\varphi}'_{\xi} \\ & - \frac{n}{\rho} s'_{12} \bar{\varphi}_{\xi} - \frac{n}{\rho} \omega_{\theta} s'_{13} \bar{\varphi}_{\xi} - \gamma \frac{n}{\rho} (\omega_{\xi} - \omega_{\theta}) s_{13} \bar{\varphi}_{\xi} - \frac{1}{2} \gamma \frac{n}{\rho} c_{33} \bar{\varphi}_{\xi} \\ & + \frac{1}{4} \gamma \frac{n}{\rho} (3\omega_{\theta} - \omega_{\xi}) K_{33} \bar{\varphi}_{\xi} - \frac{n}{\rho} \omega_{\theta} \bar{\tau}_{\theta}\end{aligned}$$

$$\begin{aligned}\bar{G}_{33} = & \left(\frac{n}{\rho}\right)^2 K'_{33} \bar{\varphi}_{\xi} + \left(\frac{n}{\rho}\right)^2 K_{33} \bar{\varphi}'_{\xi} - \omega_{\xi} s_{11} (\gamma \bar{\varphi}_{\xi} + \bar{\varphi}'_{\xi}) - \omega_{\theta} s_{12} \bar{\varphi}'_{\xi} - \left(\frac{n}{\rho}\right)^2 s_{13} \bar{\varphi}'_{\xi} \\ & - \omega_{\xi} s'_{11} \bar{\varphi}_{\xi} - \omega_{\xi} s_{11} \bar{\varphi}_{\xi} - \omega_{\theta} s'_{12} \bar{\varphi}_{\xi} - \gamma \omega_{\xi} s_{12} \bar{\varphi}_{\xi} - \left(\frac{n}{\rho}\right)^2 s'_{13} \bar{\varphi}_{\xi} \\ & + \gamma \left(\frac{n}{\rho}\right)^2 s_{13} \bar{\varphi}_{\xi} + \gamma \left(\frac{n}{\rho}\right)^2 K_{33} \bar{\varphi}_{\xi} - \left(\frac{n}{\rho}\right)^2 \bar{\tau}_{\theta}\end{aligned}$$

$$\bar{G}_{34} = -s_{14} (\gamma \bar{\varphi}_{\xi} + \bar{\varphi}'_{\xi}) - s'_{14} \bar{\varphi}_{\xi}$$

$$\bar{G}_{41} = \omega_{\xi} K_{11} \bar{\varphi}_{\xi}$$

$$E_{33}^* = s_{11} \bar{\varphi}_{\xi}^2$$

$$F_{13}^* = \omega_{\xi} s_{11} \bar{\varphi}_{\xi}^2$$

$$F_{31}^* = -\omega_{\xi} s_{11} \bar{\varphi}_{\xi}^2$$

$$F_{33}^* = \gamma s_{11} \bar{\varphi}_\xi^2 + s_{11}' \bar{\varphi}_\xi^2 + 2s_{11} \bar{\varphi}_\xi \bar{\varphi}_\xi'$$

$$G_{11}^* = -\omega_\xi^2 s_{11} \bar{\varphi}_\xi^2$$

$$G_{22}^* = -\frac{1}{2} \omega_\theta^2 c_{33} \bar{\varphi}_\xi^2$$

$$G_{23}^* = -\frac{1}{2} \frac{n}{\rho} \omega_\theta c_{33} \bar{\varphi}_\xi^2$$

$$G_{31}^* = -\omega_\xi s_{11} \left(\gamma \bar{\varphi}_\xi + 2\bar{\varphi}_\xi' \right) \bar{\varphi}_\xi - \omega_\xi s_{11}' \bar{\varphi}_\xi^2 - \omega_\xi' s_{11} \bar{\varphi}_\xi^2$$

$$G_{32}^* = -\frac{1}{2} \frac{n}{\rho} \omega_\theta c_{33} \bar{\varphi}_\xi^2$$

$$G_{33}^* = -\frac{1}{2} \left(\frac{n}{\rho} \right)^2 c_{33} \bar{\varphi}_\xi^2$$

where

$$s_{11} = c_{11} - \frac{k_{11}^2}{D_{11}}$$

$$s_{22} = c_{22} - \frac{k_{12}^2}{D_{11}}$$

$$s_{33} = D_{22} - \frac{D_{12}^2}{D_{11}}$$

$$S_{12} = C_{12} - \frac{K_{11} K_{12}}{D_{11}}$$

$$S_{13} = K_{12} - \frac{K_{11} D_{12}}{D_{11}}$$

$$S_{23} = K_{22} - \frac{K_{12} D_{12}}{D_{11}}$$

H, J, f, \bar{H} , \bar{J} , H^* , and J^* Matrices

$$H_{11} = S_{11}$$

$$H_{13} = -\gamma S_{13}$$

$$H_{22} = \frac{1}{2} \left\{ C_{33} + \left[K_{33} + (3\omega_\theta - \omega_\xi) \frac{D_{33}}{4} \right] (3\omega_\theta - \omega_\xi) \right\}$$

$$H_{23} = \frac{n}{\rho} \left[K_{33} + (3\omega_\theta - \omega_\xi) \frac{D_{33}}{2} \right]$$

$$H_{31} = H_{13}$$

$$H_{32} = H_{23}$$

$$H_{33} = \gamma^2 S_{33} + 2 \left(\frac{\gamma}{\rho} \right)^2 D_{33}$$

$$H_{34} = 1$$

$$H_{43} = -1$$

$$J_{11} = \gamma (s_{12} + \omega_{\xi} s_{13})$$

$$J_{12} = \frac{n}{\rho} (s_{12} + \omega_{\theta} s_{13})$$

$$J_{13} = \omega_{\xi} s_{11} + \omega_{\theta} s_{12} + \left(\frac{n}{\rho}\right)^2 s_{13}$$

$$J_{14} = \frac{K_{11}}{D_{11}}$$

$$J_{21} = -\frac{n}{2\rho} \left[c_{33} + K_{33} (\omega_{\xi} + \omega_{\theta}) + (3\omega_{\xi} - \omega_{\theta}) (3\omega_{\theta} - \omega_{\xi}) \frac{D_{33}}{4} \right]$$

$$J_{22} = -\frac{\gamma}{2} \left\{ c_{33} + \left[K_{33} + (3\omega_{\theta} - \omega_{\xi}) \frac{D_{33}}{4} \right] (3\omega_{\theta} - \omega_{\xi}) \right\}$$

$$J_{23} = -\frac{\gamma n}{\rho} \left[K_{33} + (3\omega_{\theta} - \omega_{\xi}) \frac{D_{33}}{2} \right]$$

$$J_{31} = -\gamma^2 (s_{23} + \omega_{\xi} s_{33}) \cdot \left(\frac{n}{\rho}\right)^2 \left[K_{33} + (3\omega_{\xi} - \omega_{\theta}) \frac{D_{33}}{2} \right]$$

$$J_{32} = -\frac{\gamma n}{\rho} \left[s_{23} + \omega_{\theta} s_{33} + K_{33} + (3\omega_{\theta} - \omega_{\xi}) \frac{D_{33}}{2} \right]$$

$$J_{33} = -\gamma \left[\omega_{\theta} s_{23} + \omega_{\xi} s_{13} + \left(\frac{n}{\rho}\right)^2 (s_{33} + 2D_{33}) \right]$$

$$J_{34} = \gamma \left(1 - \frac{D_{12}}{D_{11}} \right)$$

$$J_{41} = \omega_{\xi}$$

$$f_1 = c_{1T} - \frac{K_{11} D_{1T}}{D_{11}}$$

$$f_3 = -\gamma \left(D_{2T} - \frac{D_{12} D_{1T}}{D_{11}} \right)$$

$$\bar{H}_{13} = -s_{11} \bar{\varphi}_{\xi}$$

$$\bar{H}_{22} = \frac{1}{4} (\bar{\tau}_{\xi} + \bar{\tau}_{\theta})$$

$$\bar{H}_{31} = -s_{11} \bar{\varphi}_{\xi}$$

$$\bar{H}_{33} = \gamma s_{13} \bar{\varphi}_{\xi} + \bar{\tau}_{\xi} - \gamma s_{13} \bar{\varphi}_{\xi}$$

$$\bar{J}_{11} = \omega_{\xi} s_{11} \bar{\varphi}_{\xi}$$

$$J_{21} = \frac{1}{4} \frac{n}{\rho} (\bar{\tau}_{\xi} + \bar{\tau}_{\theta})$$

$$\bar{J}_{22} = \frac{1}{2} \omega_{\theta} c_{33} \bar{\varphi}_{\xi} + \frac{1}{4} \omega_{\theta} (3\omega_{\theta} - \omega_{\xi}) K_{33} \bar{\varphi}_{\xi} + \frac{1}{4} \gamma (\bar{\tau}_{\xi} + \bar{\tau}_{\theta})$$

$$\bar{J}_{23} = \frac{1}{2} \frac{n}{\rho} c_{33} \bar{\varphi}_{\xi} + \frac{1}{4} \frac{n}{\rho} (3\omega_{\theta} - \omega_{\xi}) K_{33} \bar{\varphi}_{\xi}$$

$$\bar{J}_{31} = -\gamma \omega_{\xi} s_{13} \bar{\varphi}_{\xi} - \omega_{\xi} \bar{\tau}_{\xi} - \gamma s_{12} \bar{\varphi}_{\xi} - \gamma \omega_{\xi} s_{13} \bar{\varphi}_{\xi}$$

$$\bar{J}_{32} = \frac{n}{\rho} \omega_{\theta} K_{33} \bar{\varphi}_{\xi} - \frac{n}{\rho} s_{12} \bar{\varphi}_{\xi} - \frac{n}{\rho} \omega_{\theta} s_{13} \bar{\varphi}_{\xi}$$

$$\bar{J}_{33} = \left(\frac{n}{\rho}\right)^2 K_{33} \bar{\varphi}_{\xi} - \omega_{\xi} s_{11} \bar{\varphi}_{\xi} - \omega_{\theta} s_{12} \bar{\varphi}_{\xi} - \left(\frac{n}{\rho}\right)^2 s_{13} \bar{\varphi}_{\xi}$$

$$\bar{J}_{34} = -s_{14} \bar{\varphi}_{\xi}$$

$$H_{33}^* = s_{11} \bar{\varphi}_{\xi}^2$$

$$J_{31}^* = -\omega_{\xi} s_{11} \bar{\varphi}_{\xi}^2$$

TABLE 1. COMPUTER PROGRAMS FOR ANALYSIS OF SHELLS OF REVOLUTION

Program function Structure	Static stress analysis			Buckling	Vibrations	Dynamic stress analysis		
	Linear	Geometric nonlinear	Plasticity			Linear	Geometric nonlinear	Plasticity
Sym. stiffness Dym. loads	SALORS Cohen(6) Kalinine(11) BOGOR(46-48) STANS(14-18)	SALORS Cohen(13) Kalinine(10) BOGOR(46-48) STANS(14-18)	[SALORS] [Cohen] [Kalinine(11)] [BOGOR(46-48)] [STANS(14-18)]	SALORS Cohen(13) Kalinine(11) BOGOR(46-48)	SALORS Cohen(12) Kalinine(11) BOGOR(46-48)	SALORS(55,56) Curran(54)	SALORS(55,56)	[SALORS] [Cohen] [Kalinine(11)] [BOGOR(46-48)] [STANS(14-18)]
Sym. stiffness Asym. loads	GENREL(26) BOISHL(27)		[GENREL(26)] [BOISHL(27)]	GENREL(26) BOISHL(27)	GENREL(26) BOISHL(27)	GENREL(26) BOISHL(27)		GENREL(26) BOISHL(27)
Sym. stiffness Asym. loads	SALORS Cohen(6) Kalinine(11) BOGOR(46-48) STANS(14-18)	Ball(49) Greenbaum(51,52) [Kalinine(11)]	[Cohen] [Kalinine(11)]			Stephens(37) Curran(54)	[Stephens(37)]	
Asym. stiffness Asym. loads	Cappelli-Curran(53,54)					Curran(54)		

() Denotes appropriate references

[] Under development

TABLE 2 COMPARISON OF FEATURES WITHIN FOUR MAJOR COMPUTER PROGRAMS

Feature	Computer program			
	SALORS	Cohen	BOSOR	Kalnins
Shell theory	Sanders	Novozhilov	Novozhilov-Sanders	Knowles and Reissner
Solution method	Finite difference	Forward integration	Finite difference	Forward integration
Discrete rings	Yes	Yes	Yes	No
Boundary conditions	Classical Ring Elastic Pole	Classical Ring Elastic Pole	Classical Ring Partial pole	Classical
Stringers (smeared)	Yes	Yes	Yes	Not automatically
Branching	No	Under development	Under development	Yes (major branches only)
Eigenvalue determination	Iteration (inverse power)	Iteration (Stodola)	Iteration (inverse power) Determinant plotting	Determinant plotting
Buckling under asymmetric loads	No	Under development	No	Limited capability
Live pressure loading	Yes	Yes	Yes	No

TABLE 3 COMPARISON OF SALORS WITH PUBLISHED RESULTS

Ring-stiffened cylinder (ref. 13, Tables 2 and 3)						
Analysis	Hydrostatic buckling pressures (psi), $n = 3$		Ring prebuckling hoop forces, T_{ϕ}/r^2 , at incipient buckling (nonlinear) (lb/in ²)			
	Prestress		Ring number			
	Linear	Nonlinear	1	4	6	
SALORS	641	642	-30.61	-28.523	-28.521	
Cohen	641	644	-30.62	-28.533	-28.533	
Ring-stiffened 120° cone (ref. 66, case 3)						
Analysis	External critical pressures (psi), $n = 7$, linear prestress		Ring prebuckling hoop forces (lb) for 1 lb/in ² external pressure			
	Prebuckling deformation		Ring number			
	Neglected	Included	1	8	16	24
SALORS	4.21	4.04	4419.4	-102.48	-109.86	-119.70
Cohen	4.21	4.05	4424.3	-102.72	-110.15	-120.03

TABLE 3 COMPARISON OF SALORS WITH PUBLISHED RESULTS - Concluded

Axisymmetric nondimensional frequencies of a 60°-spherical cap with simply supported edge			
Natural frequency \ Analysis	SALORS	Cohen (ref. 12)	Kalnins (ref. 7)
1st	0.960	0.959	0.959
2nd	1.332	1.325	1.328
3rd	1.650	1.646	—
4th	2.095	—	2.114

Natural frequencies in cps for various circumferential wave numbers for ring and stringer-stiffened cylinder (ref. 43, Table 4, discrete rings)					
n \ Analysis	3	5	7	9	11
SALORS	71.3	127	246	403	590
BOSOR2	71.7	129	251	411	603

TABLE 4 REPRESENTATIVE COMPUTER TIMES FOR EXAMPLE PROBLEMS
ON CDC 6600 COMPUTER
(CORE STORAGE = 70K OCTAL)

Problem	Calculation	Program	Number difference intervals or integration segments	Approximate computer time sec
Thermal buckling of cylinder	Axisymmetric prestress plus buckling load for one n	SALORS	100	28
		Cohen	3 segments	24
Vibration of conical shell	Vibration frequency for one value of n	SALORS	100	18
		Cohen	4 segments	18

TABLE 5 COMPARISON OF THEORY AND EXPERIMENT FOR RING-STIFFENED CYLINDER LOADED BY HYDROSTATIC PRESSURE

Boundary condition	Pressure	Method	Buckling pressure, psi	
			Theory	Experiment
Bulkhead	Live	—	—	675
Simple support	Dead	Bodner	796	
Simple support	Dead	Ref. (65)	739	
Simple support	Dead	SALORS	708	
Simple support	Live	SALORS	642	
Bulkhead	Live	SALORS	860	

TABLE 6 STRUCTURAL PROPERTIES FOR BLUNT CONICAL PLANETARY ENTRY BODY

Ring Properties

(The notation E ± x indicates × 10^{±x})

ρ (in.)	A_r (in ²)	I_x (in ⁴)	I_y (in ⁴)	I_{xy} (in ⁴)	J_r (in ⁴)	x_r (in.)	y_r (in.)
6.9000E + 01	3.7600E - 01	7.5280E - 01	7.5280E - 01	0.0000	1.5056E + 00	-1.8794E - 00	-6.8404E - 01
6.7389E + 01	3.1003E - 02	3.8938E - 04	3.4229E - 03	-2.9125E - 04	2.0669E - 06	-3.8414E - 01	7.1342E - 02
6.5754E + 01							
6.4097E + 01							
6.2415E + 01							
6.0706E + 01							
5.8968E + 01							
5.7299E + 01							
5.5595E + 01							
5.3553E + 01							
5.1669E + 01	3.1003E - 02	3.8938E - 04	3.4229E - 03	-2.9125E - 04	2.0669E - 06	-3.8414E - 01	7.1342E - 02
5.0000E + 01	2.4564E - 02	3.2129E - 04	2.1016E - 03	-3.0397E - 04	1.2540E - 06	-3.2238E - 01	7.9212E - 02
4.8086E + 01							
4.6110E + 01							
4.4065E + 01							
4.1938E + 01							
3.9710E + 01*							
3.7354E + 01**							
3.4822E + 01	2.4564E - 02	3.2129E - 04	2.1016E - 03	-3.0397E - 04	1.2540E - 06	-3.2238E - 01	7.9212E - 02
3.2000E + 01	6.7200E - 01	9.7440E - 02	3.5281E + 00	0.0000	3.5281E + 00	-3.0935E + 00	0.0000
3.0678E + 01	2.3678E - 02	2.9618E - 04	2.7363E - 03	-2.0602E - 04	8.8792E - 06	-3.9376E - 01	7.0458E - 02
2.9329E + 01							
2.7946E + 01**							
2.6534E + 01							
2.5083E + 01*							
2.3595E + 01							
2.2051E + 01							
2.0459E + 01							
1.8806E + 0							
1.7082E + 01							
1.5273E + 01							
1.3361E + 01							
1.1315E + 01							
1.0000E + 01	2.3678E - 02	2.9618E - 04	2.7363E - 03	-2.0602E - 04	8.8792E - 06	-3.9376E - 01	7.0458E - 02

* Denotes end points of 10 equally spaced long stringers

** Denotes end points of 10 equally spaced short stringers

Stringer Properties

A_s (in ²)	I_s (in ⁴)	J_s (in ⁴)	x_s (in)
0.081	0.0286	0.0000243	-0.75

$$x = x_r = x_s = 9.35E + 01 \text{ lb/in}^2$$

$$\mu = \mu_r = \mu_s = 0.32$$

TABLE 7 STRUCTURAL PROPERTIES FOR APOLLO-SATURN SHORT-STACK

Ring Properties

Ring no.	A_r (in^2)	I_x (in^4)	I_y (in^4)	I_{xy} (in^4)	J_r (in^4)	x_r (in.)	y_r (in.)	Mass density (lbm/in^3)
1	0.8090	1.2069	0.1590	0.0363	0.007927	0.3036	-1.8832	0.1
2	1.8050	6.2650	0.6190	0.1709	0.026600	-0.6670	-1.9990	0.1
3	1.0270	1.6130	0.1891	-0.1773	0.000666	0.1765	-1.1830	0.1
4	0.3975	0.8849	0.0635	-0.1644	0.000530	0.7440	-2.0490	0.1
5	0.3975	0.8849	0.0635	-0.1644	0.000530	0.7440	-2.0490	0.1
6	1.0467	0.7187	1.7261	0	0.538057	0	-1.0598	0.1

Stringer Properties of S-IVB Forward Skirt
(108 stringers equally spaced around circumference)

Location	A_s (in^2)	I_s (in^4)	J_s (in^4)	s (in.)	Mass density (lbm/in^3)
Inner bays	0.3293	0.08396	0.05	0.6365	0.1
Outer bays	0.3935	0.09867	0.05	0.5511	0.1

$$E = E_r = E_s = 10.5 \times 10^6 \text{ lb/in}^2$$

$$\mu = \mu_r = \mu_s = 0.32$$

$$\text{Mass density of skin} = 0.1 \text{ lbm/in}^3$$

$$\text{Mass density of core} = 0.003 \text{ lbm/in}^3$$

TABLE 8 BOUNDARY CONDITIONS FOR APOLLO-SATURN SHORT STACK

$$[\tilde{N}] \begin{Bmatrix} r_{\xi} \\ r_{\xi\theta} \\ r_{\xi} \\ m_{\xi} \end{Bmatrix} + \begin{bmatrix} 1 & 0 & 0 & 0 \\ 0 & 1 & 0 & 0 \\ 0 & 0 & 1 & 0 \\ 0 & 0 & 0 & 1 \end{bmatrix} \begin{Bmatrix} u_{\xi} \\ u_{\theta} \\ w \\ \phi_{\xi} \end{Bmatrix} = \begin{Bmatrix} l_1 \\ l_2 \\ l_3 \\ l_4 \end{Bmatrix}$$

$$n = 0$$

$$[\tilde{N}]_{\xi=0} = \begin{bmatrix} 0 & 0 & 0 & 0 \\ 0 & 0 & 0 & 0 \\ -1.966E-4 & 0 & -1.241E-3 & 1.088E-3 \\ 1.720E-4 & 0 & 1.088E-3 & -5.326E-3 \end{bmatrix}$$

$$[\tilde{N}]_{\xi = \xi_{\max}} = \begin{bmatrix} 0 & 0 & 0 & 0 \\ 0 & 0 & 0 & 0 \\ \text{Symmetric} & 8.588E-4 & -1.700E-4 & 1.403E-4 \end{bmatrix}$$

$$n = 4$$

$$[\tilde{N}]_{\xi=0} = \begin{bmatrix} -4.247E-3 & -1.635E-4 & 6.058E-5 & 2.555E-3 \\ -6.223E-5 & 1.396E-4 & -9.886E-5 & 7.516E-4 \\ \text{Symmetric} & -1.197E-3 & -5.358E-3 \end{bmatrix}$$

$$[\tilde{N}]_{\xi = \xi_{\max}} = \begin{bmatrix} 4.480E-5 & -2.511E-5 & 9.498E-5 & 1.578E-6 \\ 1.379E-4 & -5.011E-4 & -1.028E-5 & -1.118E-4 \\ \text{Symmetric} & 2.590E-3 & 1.350E-4 \end{bmatrix}$$

$$n = 7$$

$$[\tilde{N}]_{\xi=0} = \begin{bmatrix} -2.173E-3 & 3.770E-5 & -5.212E-4 & 2.720E-3 \\ -4.137E-5 & 1.324E-4 & -1.248E-4 & 7.456E-4 \\ \text{Symmetric} & -1.067E-3 & -5.365E-3 \end{bmatrix}$$

$$[\tilde{N}]_{\xi = \xi_{\max}} = \begin{bmatrix} 3.398E-5 & -2.354E-5 & 1.382E-4 & 1.161E-5 \\ 8.215E-5 & -4.638E-4 & -2.544E-5 & 2.929E-5 \\ \text{Symmetric} & 3.230E-3 & 1.363E-4 \end{bmatrix}$$

$$n = 8$$

$$[\tilde{N}]_{\xi=0} = \begin{bmatrix} -2.053E-3 & 6.308E-5 & -5.705E-4 & 2.740E-3 \\ -3.988E-5 & 1.386E-4 & -1.346E-4 & 7.463E-4 \\ \text{Symmetric} & 1.057E-3 & -5.363E-3 \end{bmatrix}$$

$$[\tilde{N}]_{\xi = \xi_{\max}} = \begin{bmatrix} 2.809E-5 & -1.753E-5 & 1.102E-4 & 1.232E-5 \\ 6.378E-5 & -3.879E-5 & -2.614E-5 & 5.717E-5 \\ \text{Symmetric} & 2.915E-3 & 1.372E-4 \end{bmatrix}$$

TABLE 9 NUMERICAL RESULTS FOR STRUCTURAL ANALYSIS OF
APOLLO-SATURN SHORT STACK

(a) Meridional stresses at innermost and outermost
fibers of shell wall

Station	ξ/ξ_{\max}	σ_{ξ} (lb/in ²)			
		Axysymmetric		Asymmetric*	
		Inner	Outer	Inner	Outer
838	0	9.941×10^2	-2.199×10^4	9.770×10^2	-2.196×10^4
583	0.518	6.923×10^3	-1.371×10^4	2.336×10^4	-6.760×10^3
	0.518	-2.324×10^3	-2.272×10^4	-7.568×10^4	-5.658×10^4
502	0.683	-1.132×10^4	-1.558×10^4	-1.292×10^4	-1.648×10^4
	0.683	-1.880×10^4	-7.294×10^3	-2.129×10^4	7.315×10^3
466	0.755	3.350×10^2	-2.043×10^4	8.212×10^2	-2.151×10^4
	0.755	-1.129×10^4	-1.093×10^4	-1.155×10^4	-1.121×10^4
437	0.813	-6.329×10^3	-6.401×10^3	-6.439×10^3	-6.521×10^3
	0.813	-7.302×10^3	-7.360×10^3	-7.355×10^3	-7.428×10^3
405	0.878	-7.924×10^3	-7.941×10^3	-7.890×10^3	-7.913×10^3
	0.878	-7.842×10^3	-7.865×10^3	-7.767×10^3	-7.801×10^3
373	0.942	-7.553×10^3	-7.430×10^3	-7.216×10^3	-7.285×10^3
	0.942	-6.298×10^3	-6.389×10^3	-6.148×10^3	-6.244×10^3
344	1.00	-1.057×10^4	-1.032×10^4	-1.027×10^4	-1.002×10^4

*Results for asymmetric loading are for a meridian passing through
a load point.

TABLE 9 NUMERICAL RESULTS FOR STRUCTURAL ANALYSIS OF
APOLLO-SATURN SHORT STACK

(a) Meridional stresses at innermost and outermost
fibers of shell wall

Station	ξ/ξ_{\max}	σ_{ξ} (lb/in ²)			
		Axisymmetric		Asymmetric*	
		Inner	Outer	Inner	Outer
838	0	9.941×10^2	-2.199×10^4	9.770×10^2	-2.196×10^4
583	0.518	6.923×10^3	-1.371×10^4	2.536×10^4	-6.760×10^3
	0.518	-2.324×10^3	-2.272×10^4	-7.568×10^4	-5.658×10^4
502	0.683	-1.132×10^4	-1.558×10^4	-1.292×10^4	-1.648×10^4
	0.683	-1.880×10^4	-7.294×10^3	-2.129×10^4	-7.313×10^3
466	0.755	3.350×10^2	-2.043×10^4	8.212×10^2	-2.151×10^4
	0.755	-1.129×10^4	-1.093×10^4	-1.155×10^4	-1.121×10^4
437	0.813	-6.329×10^3	-6.401×10^3	-6.439×10^3	-6.521×10^3
	0.813	-7.302×10^3	-7.360×10^3	-7.355×10^3	-7.428×10^3
405	0.878	-7.924×10^3	-7.941×10^3	-7.890×10^3	-7.913×10^3
	0.878	-7.842×10^3	-7.865×10^3	-7.767×10^3	-7.801×10^3
373	0.942	-7.363×10^3	-7.430×10^3	-7.216×10^3	-7.285×10^3
	0.942	-6.298×10^3	-6.389×10^3	-6.143×10^3	-6.244×10^3
344	1.00	-1.057×10^4	-1.032×10^4	-1.027×10^4	-1.002×10^4

*Results for asymmetric loading are for a meridian passing through
a load point.

TABLE 9 NUMERICAL RESULTS FOR STRUCTURAL ANALYSIS OF APOLLO-SATURN SHORT STACK - Continued
 (b) Buckling prestress input and $n = 7$ mode shape ($P_{cr} = 2.84 \times 10^6$ lb)

Station	$\frac{\xi}{\xi_{max}}$	Prestress					$n = 7$ Buckling mode			
		$\bar{\tau}_\xi$ ($\frac{lb}{in.}$)	$\bar{\tau}_\theta$ ($\frac{lb}{in.}$)	$\bar{\phi}_\xi$	$\frac{u_\xi}{v_{max}}$	$\frac{u_\theta}{v_{max}}$	$\frac{v}{v_{max}}$			
838	0	-7.697×10^2	-5.655×10^2	-1.022×10^{-3}	6.510×10^{-8}	-2.821×10^{-8}	1.530×10^{-7}			
583	0.518	-5.155×10^2	2.634×10^2	5.230×10^{-3}	4.648×10^{-4}	1.711×10^{-4}	-1.504×10^{-3}			
	0.518	-6.678×10^2	-9.435×10^1							
502	0.683	-6.054×10^2	6.307×10^1	-2.934×10^{-3}	-3.464×10^{-3}	-1.420×10^{-4}	2.772×10^{-3}			
	0.683	-5.979×10^2	1.062×10^2		-3.853×10^{-3}		2.198×10^{-3}			
466	0.755	-6.008×10^2	-1.180×10^2	-7.659×10^{-3}	-2.056×10^{-4}	8.129×10^{-3}	-1.335×10^{-1}			
	0.755		-6.630×10^1							
437	0.813	-6.015×10^2	1.143×10^1	1.152×10^{-3}	2.977×10^{-2}	-2.966×10^{-2}	2.581×10^{-1}			
	0.813		1.540							
405	0.878	-6.013×10^2	-2.760×10^1	8.260×10^{-5}	-2.229×10^{-2}	-4.126×10^{-3}	1.534×10^{-1}			
	0.878		-2.679×10^1							
373	0.942	-6.013×10^2	-2.633×10^1	-5.850×10^{-4}	1.262×10^{-2}	6.270×10^{-2}	-6.459×10^{-1}			
	0.942		-1.255×10^1							
344	1.00	-6.007×10^2	-1.345×10^2	7.305×10^{-3}	-9.349×10^{-4}	-3.592×10^{-3}	6.142×10^{-2}			

TABLE 9 NUMERICAL RESULTS FOR STRUCTURAL ANALYSIS OF
APOLLO-SATURN SHORT STACK - Concluded

(c) Vibration

Load, P lb	n	Frequency, ω rad/sec
0	0	365.1
0	2	147.2
0	3	128.3
0	4	185.3
0	5	277.8
0	6	367.6
0	7	450.2
0	8	538.6
0	9	634.0
981 3,1	5	269.0
1 962 674	5	256.7
2 453 342	5	245.5
2 649 609	5	235.6
2 747 743	5	228.7
2 845 877	5	184.2
2 914 570	5	67.0

TABLE 10 CDC 6600 SERIES COMPUTER RUN TIMES FOR SALORS ANALYSES OF
APOLLO-SATURN SHORT STACK

Analysis	Run time (sec)
Stress (Asymmetric analysis, 17 harmonic numbers)	104
Prestress and buckling (Calculates linear prestress and buckling for $n = 0$ and 7)	105
Vibration (Frequency for nine values of circumferential wave number)	282

TABLE 11 CIRCUMFERENTIAL VARIATION OF STRESS, BUCKLING,
AND VIBRATION VARIABLES

	<u>Circumferential variation</u>
<u>Prestress quantities</u>	
$\bar{\tau}_\xi, \bar{\tau}_\theta, \bar{\varphi}_\xi$	axisymmetric
<u>Linear asymmetric variables</u>	
$u_\xi, u_\theta, m_\xi, m_\theta, \tau_\xi, \tau_\theta, f_\xi, \varphi_\xi, e_\xi, e_\theta, k_\xi, k_\theta$	$\cos n\theta$
$u_\theta, f_{\xi\theta}, \tau_{\xi\theta}, m_{\xi\theta}, \varphi_\theta, \varphi, e_{\xi\theta}, k_{\xi\theta}$	$\sin n\theta$

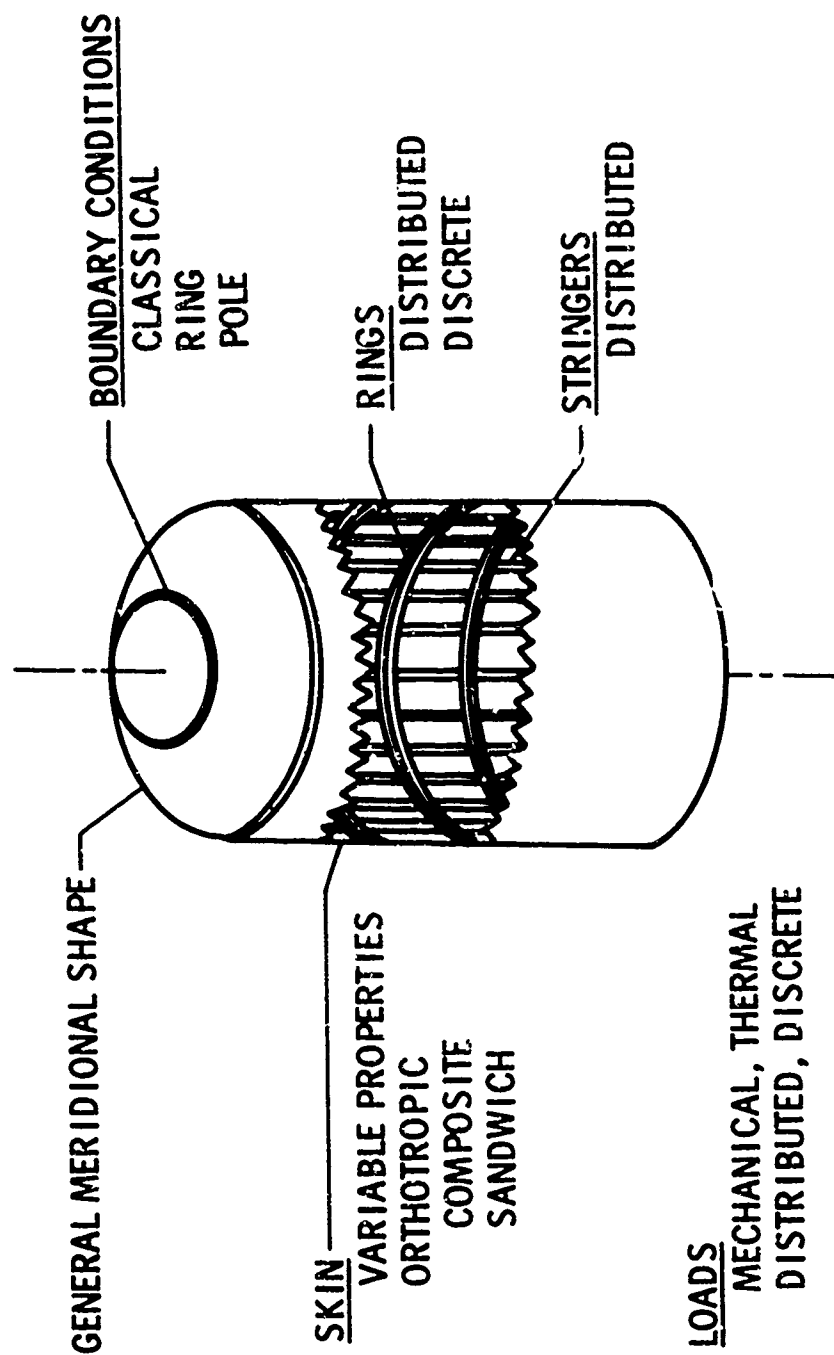


Figure 1.- Present capability for stress analysis including vibration and buckling of shells of revolution.

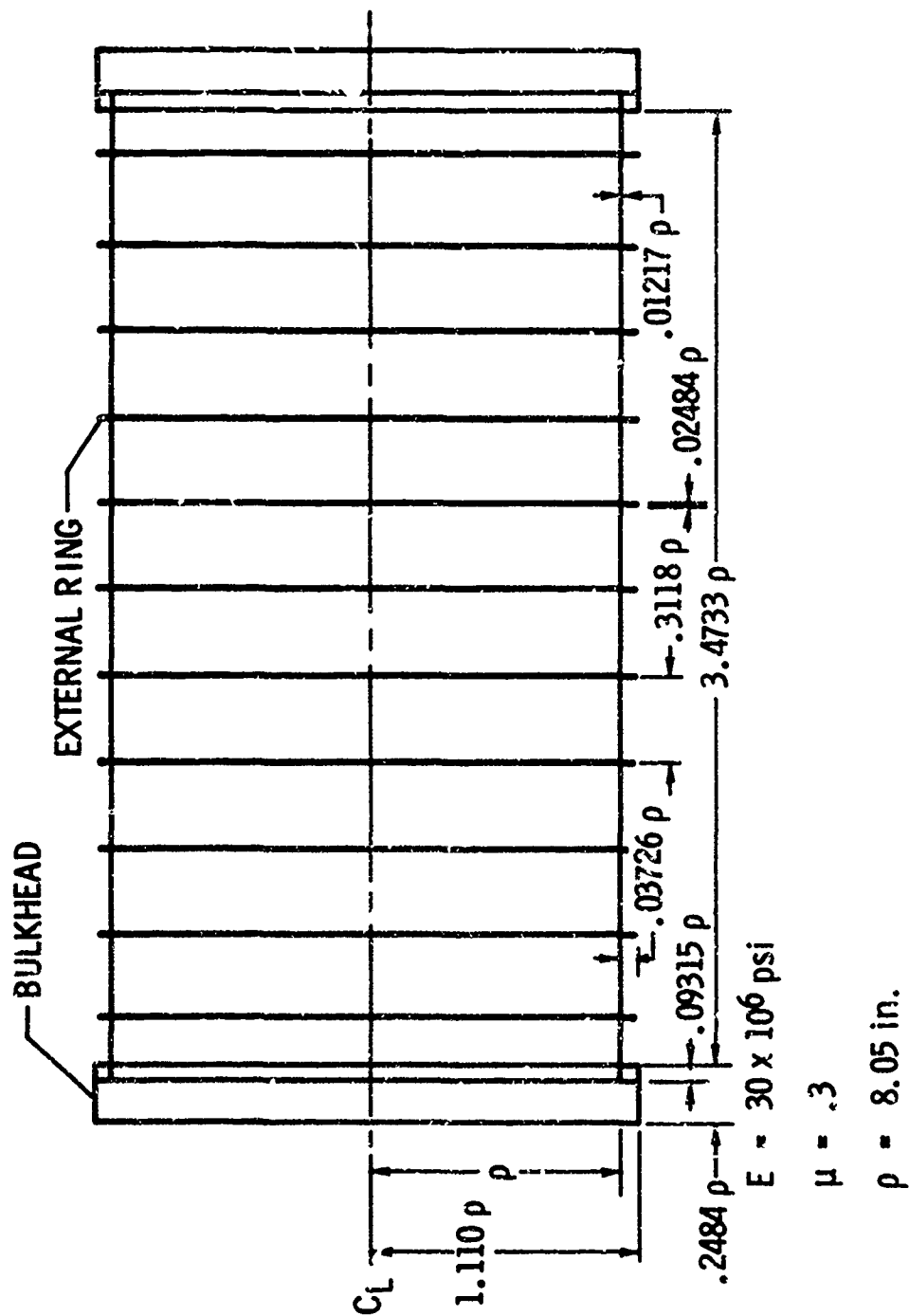


Figure 2.- Geometry of ring-stiffened cylinder.

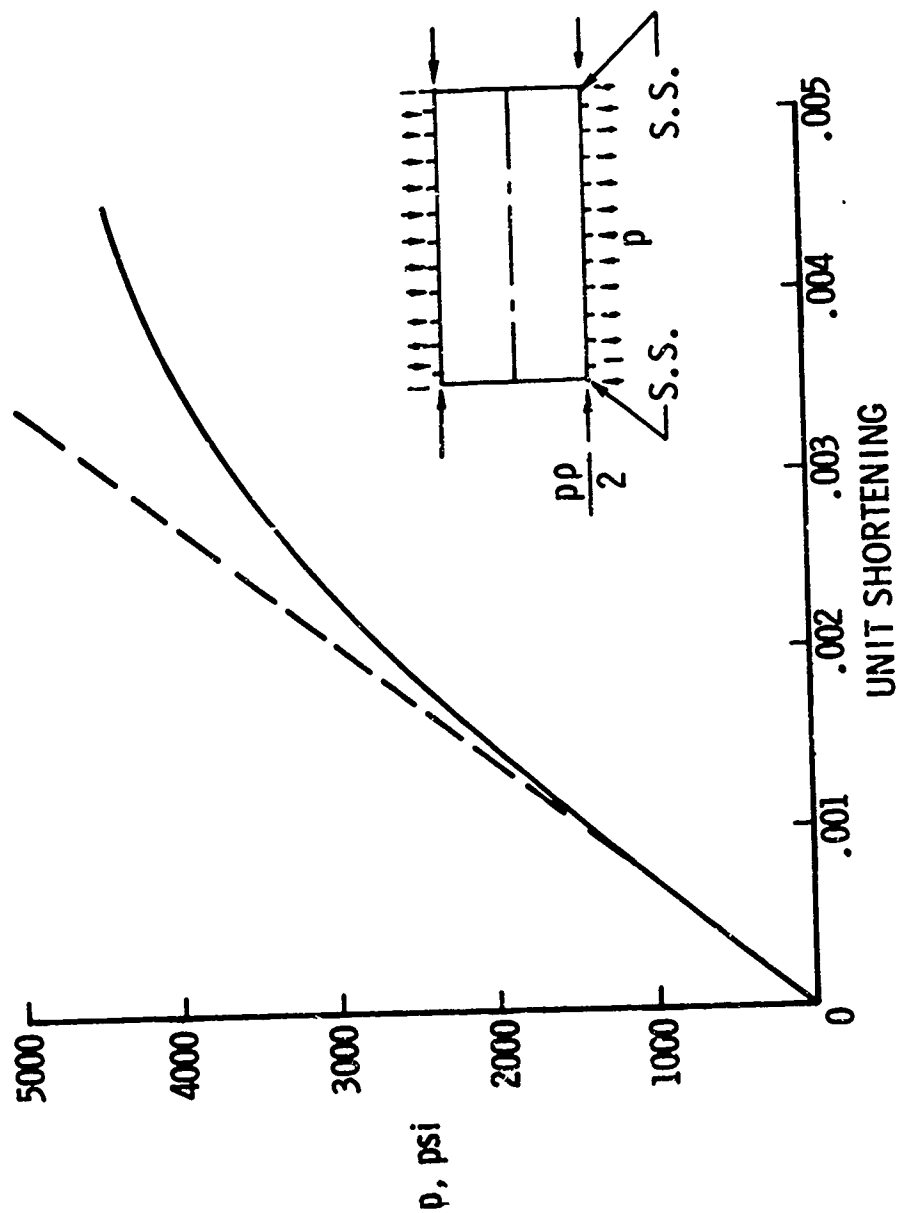


Figure 3.- Theoretical nonlinear load-shortening curve for ring-stiffened cylinder under hydrostatic pressure.

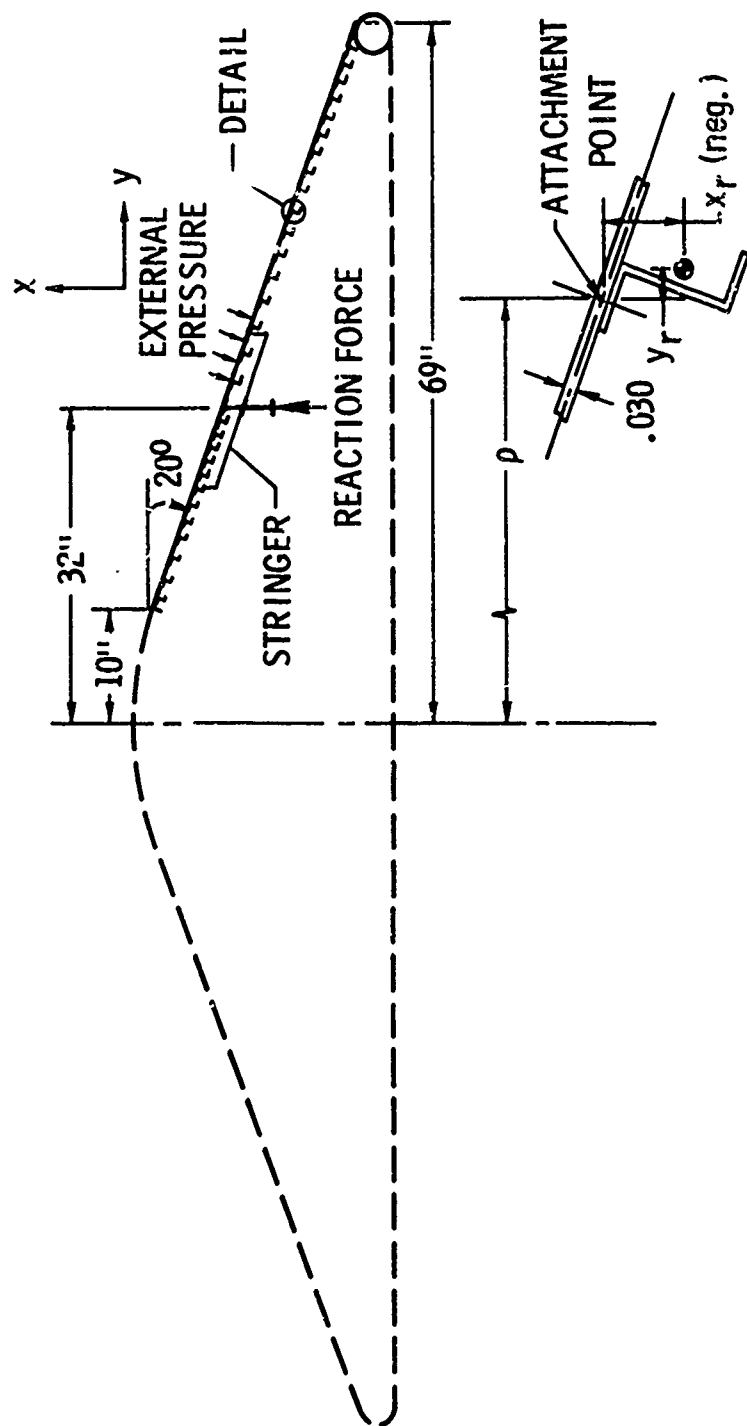


Figure 4.-- Blunt conical planetary entry body.

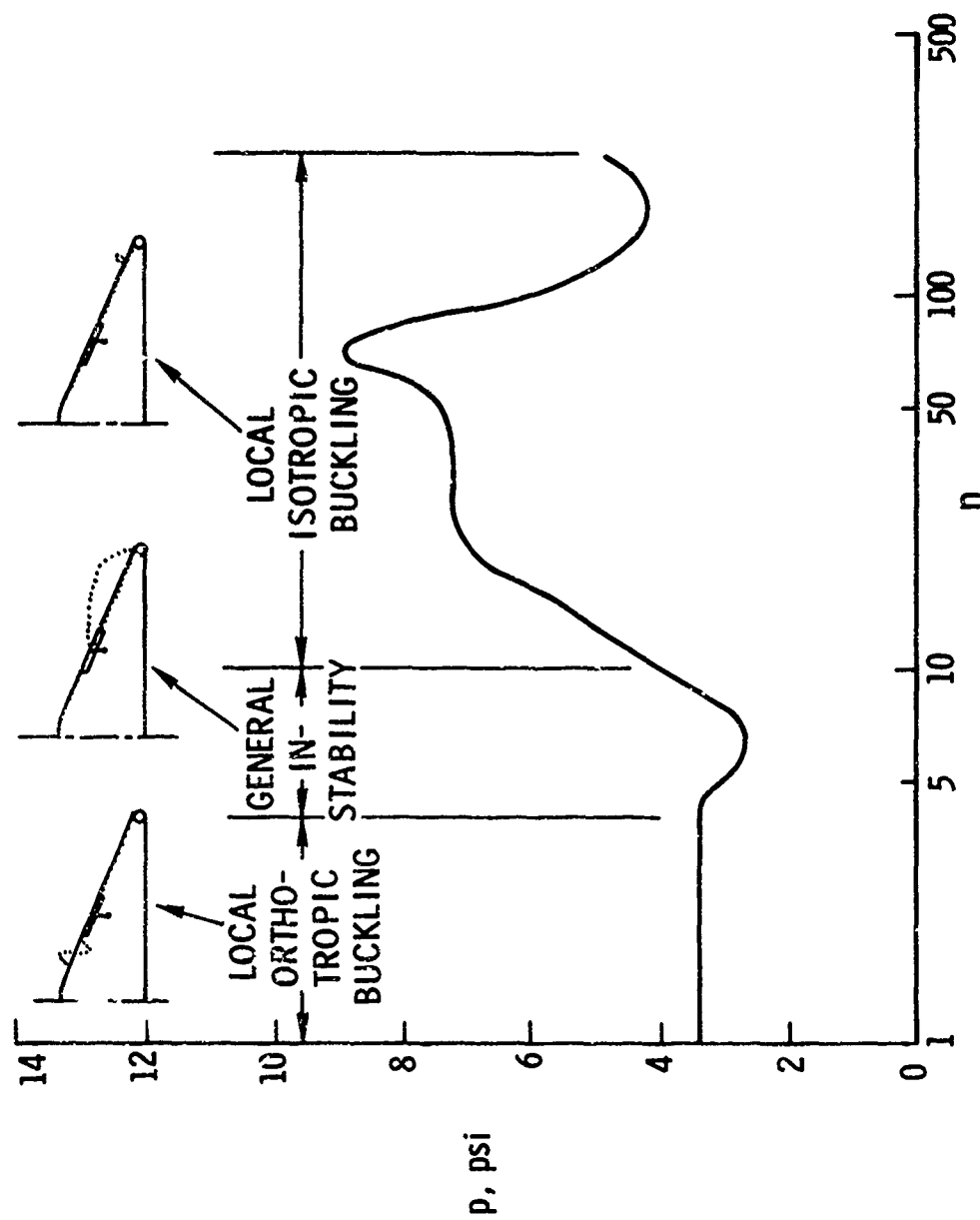
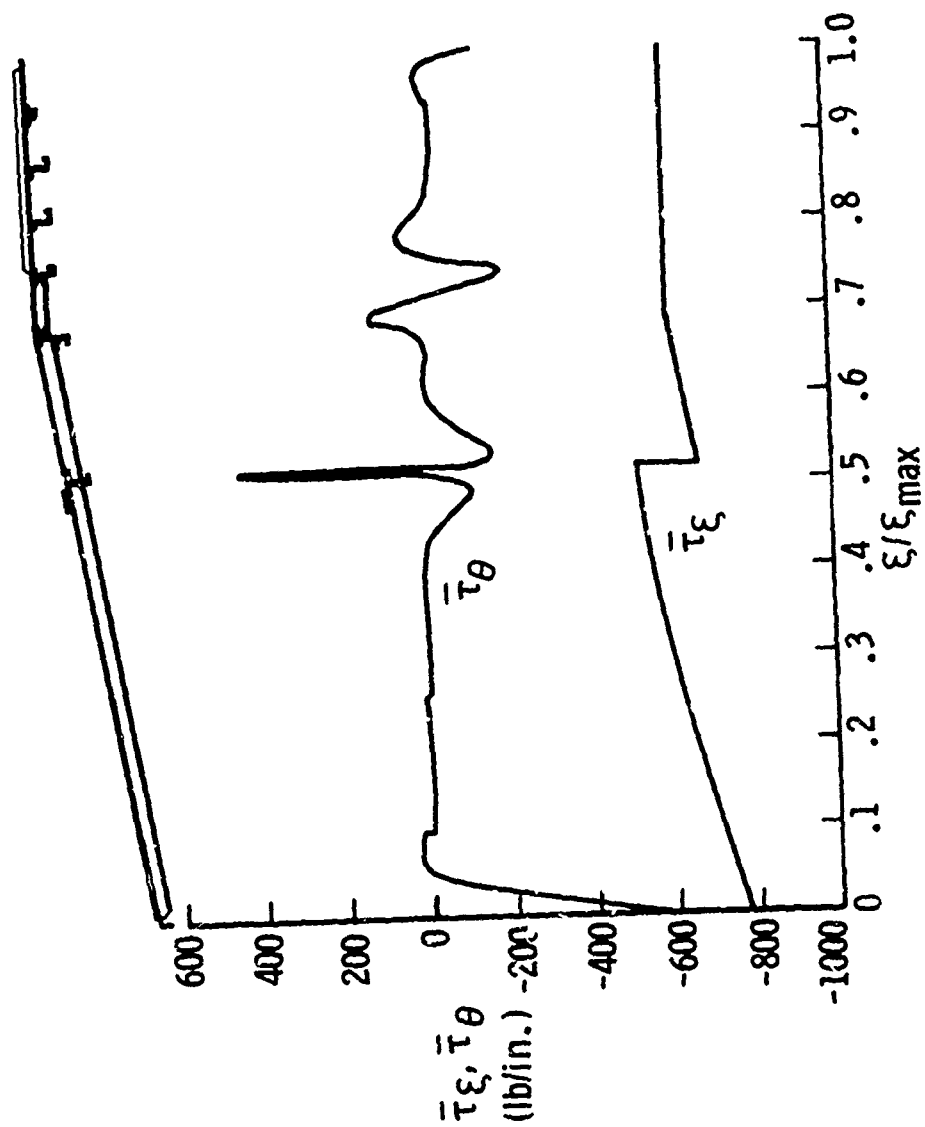
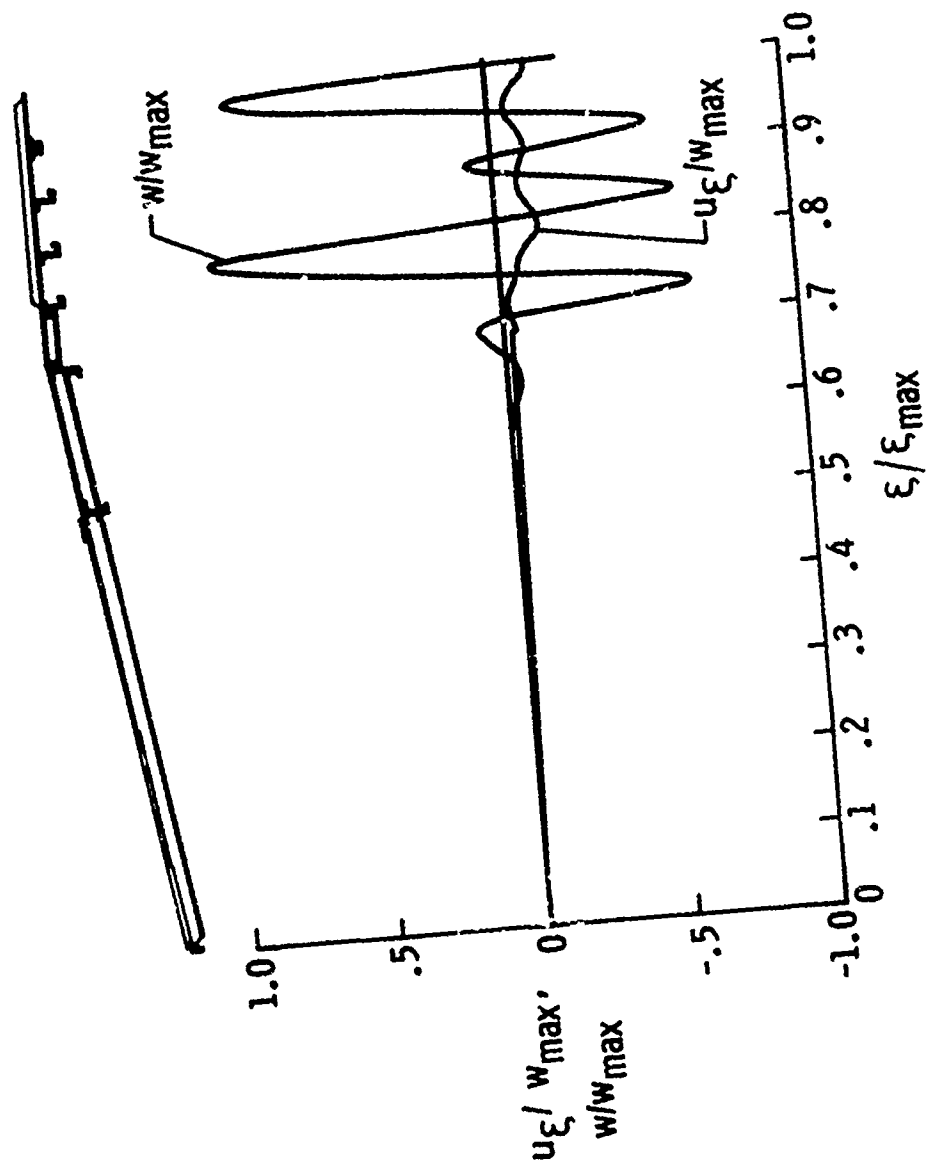


Figure 5.- Buckling pressure versus circumferential wave number for blunt conical planetary entry body.



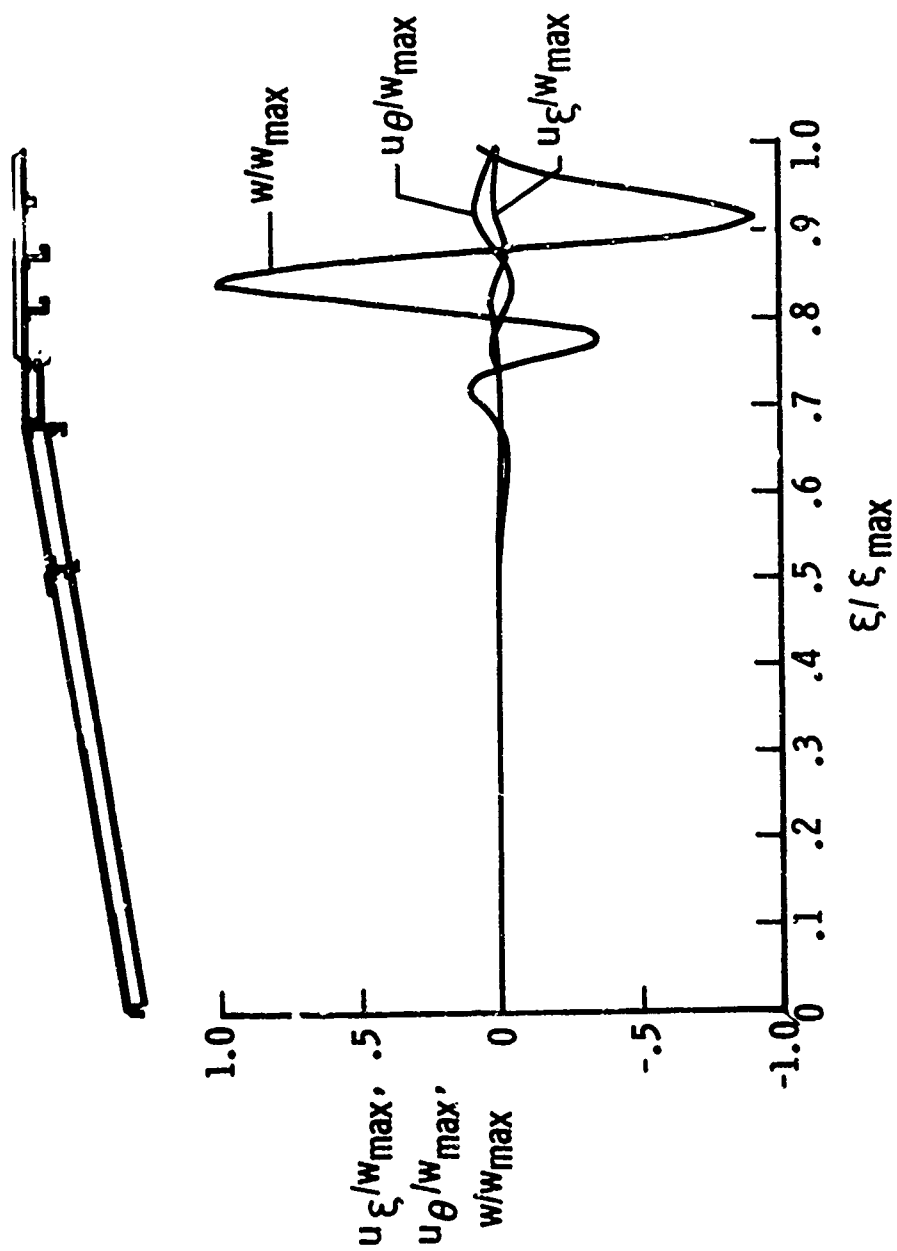
(a) Prebuckling stress resultants.

Figure 7.- Prebuckling stress resultants and buckling modes for Apollo-Saturn Short Stack.



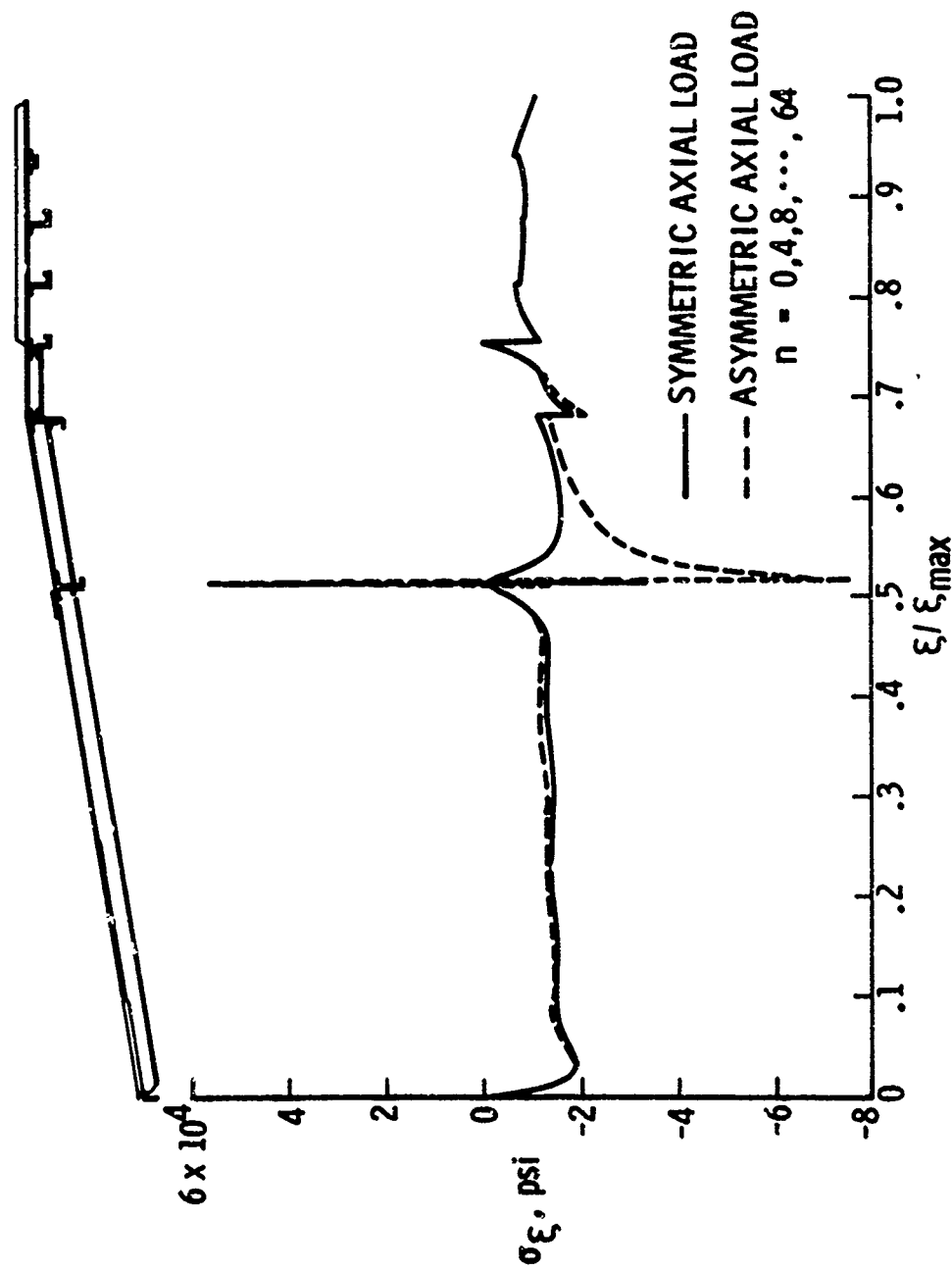
(b) Buckling mode, $n = 0$.

Figure 7.- Continued.



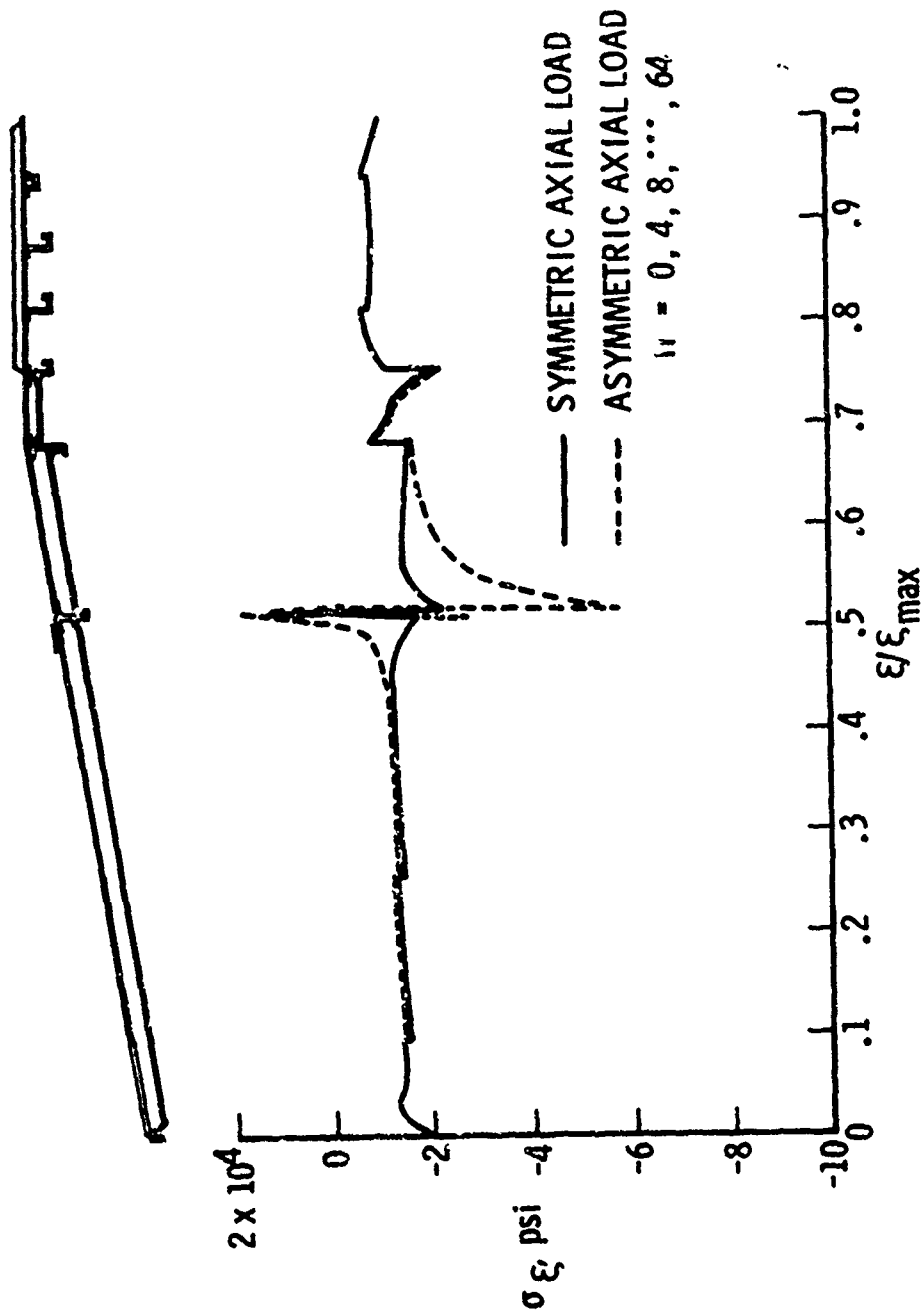
(c) Buckling mode, $n = 7$.

Figure 7.- Concluded.



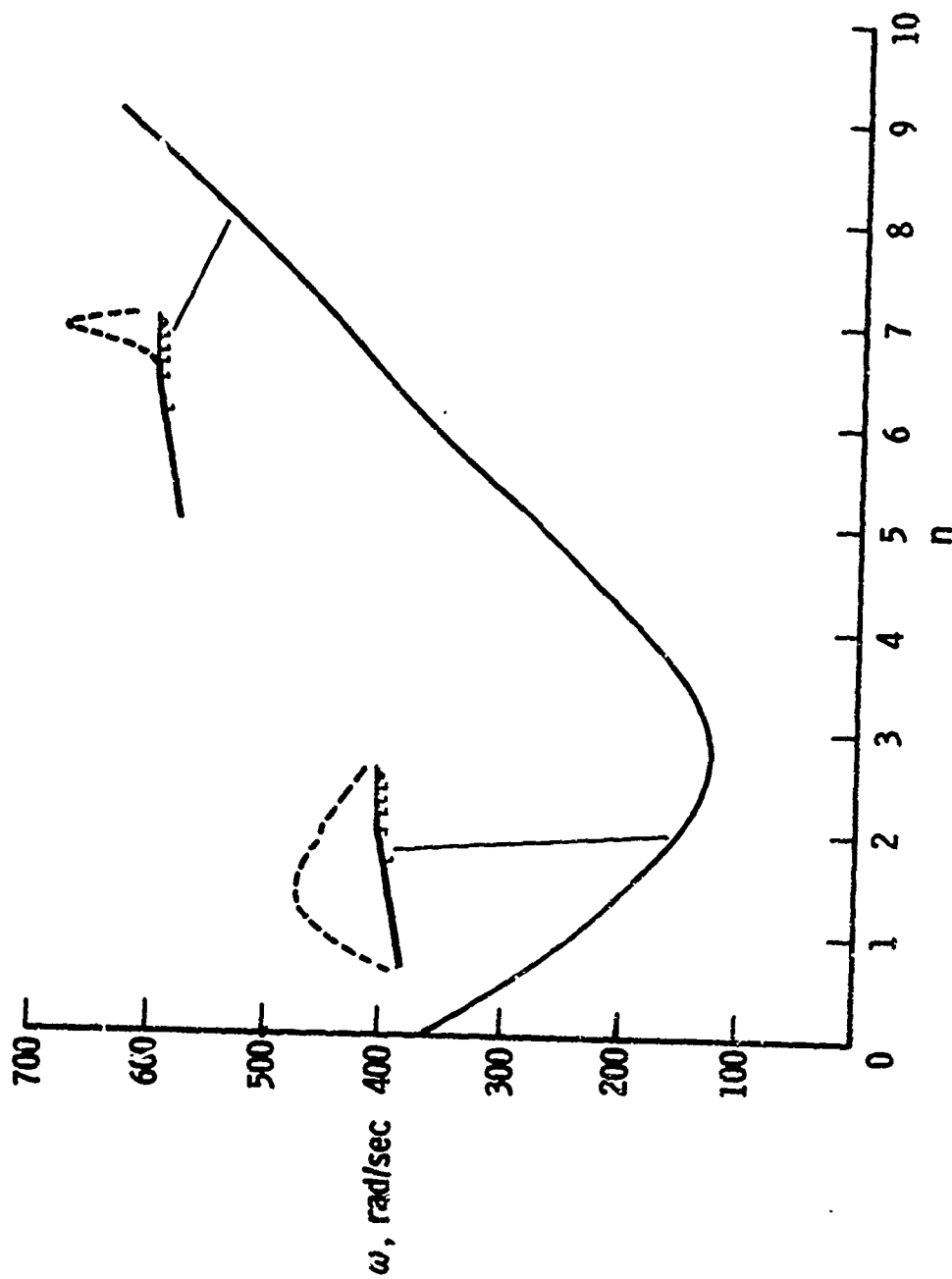
(a) Inside surface.

Figure 8.- Meridional stress for Apollo-Saturn Short Stack along a plane passing through load point.

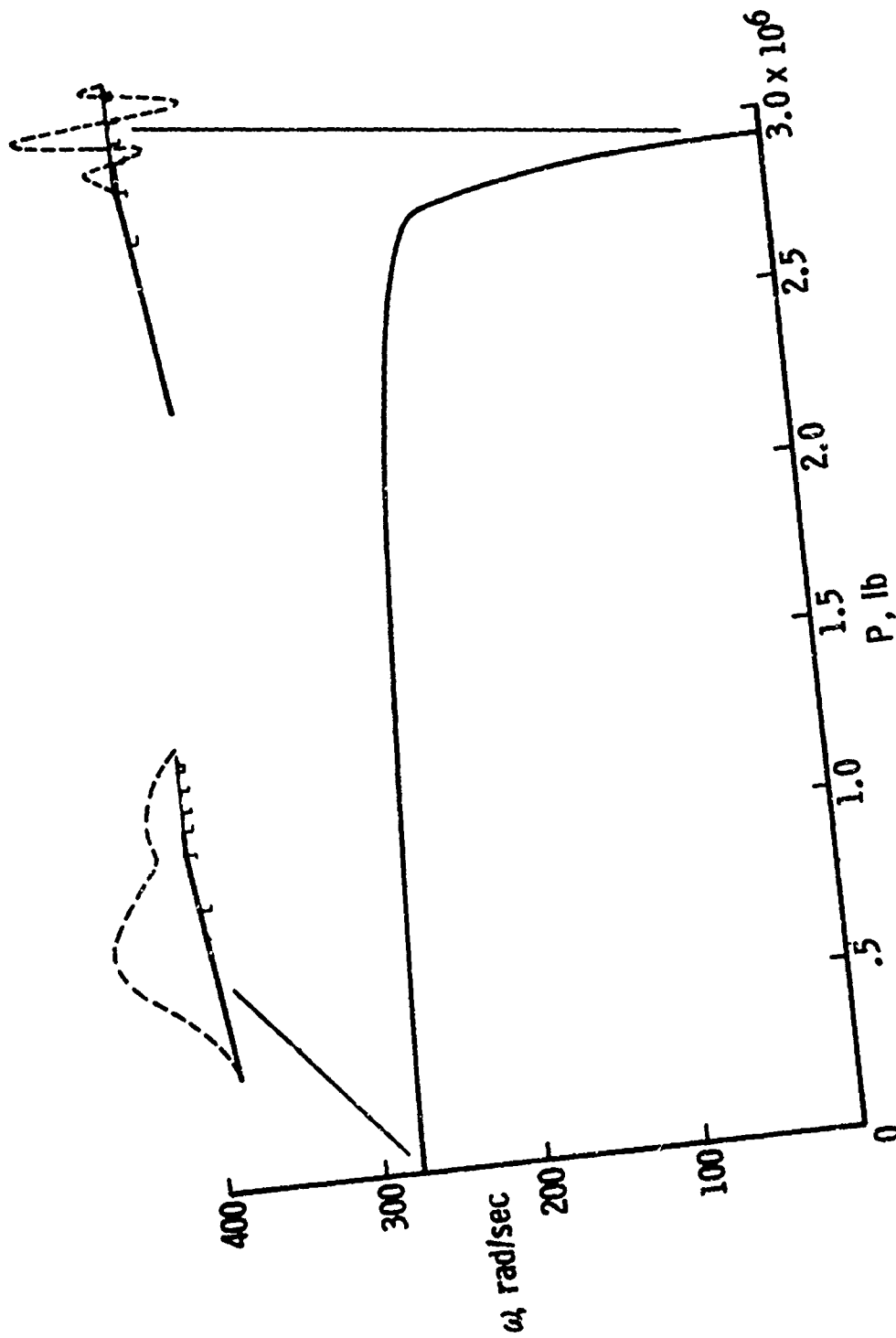


(b) Outside surface.

Figure 8.- Concluded.



(a) Frequency variation with circumferential wave number.
 Figure 9.- Vibration characteristics of Apollo-Saturn Short Stack.



(b) Effect of axial load on vibration frequency, $n = 5$.

Figure 9.- Concluded.

QUESTIONS AND COMMENTS FOLLOWING FULTON/ANDERSON PAPER

QUESTION: My thinking is stimulated by your slide showing the comparison of theoretical results with experiment. Here you present results for different "theories" showing a spread of something like 15% in the prediction of buckling. Do you believe the error lies in the theoretical assumptions made in each of the different theories or in the error made by the computer in manipulating the numbers or does it lie in the different levels of discretization used in the separate analyses?

ANDERSON: Well, I think the biggest difference is in assumption of the boundary condition. Another problem is trying to make accurate models of the whole specimen as well as any attachments and so forth that may affect the result. In this case, we had to scale the dimension of a bulkhead off a photograph because no information was given as to its thickness; this is a possible source of error. We scaled the bulkhead as somewhere between an inch and an inch and a quarter thick. We made a calculation for an inch thick bulkhead and the buckling pressure was 800 psi; for an inch and a quarter thick bulkhead, the buckling pressure was 860 psi.

QUESTION: Referring back to your comparison of finite difference and forward integration, you made a statement that forward integration provided less information with respect to prebuckling, prestress loading. I don't think this is true. It might be true of a specific problem that you are making reference to. Generally, I think the contrary is true because finite difference provides you with information only at your selected points. However, at the forward integration you can have any number of points if you

care to compute the stresses. Would you comment on that?

ANDERSON: Well, I think you're right and admittedly the abbreviated comment I made was a little unfair. You can calculate as many output points as you want in the forward integration method, but my point was that for stress problems in general forward integration methods don't require nearly as many points and for efficient solution of the problems you are likely not to use as many as you would in finite difference programs. But while it may not be necessary, you could go out of your way and calculate all these points and get all the information that you need using the forward integration method.

QUESTION: I have a question concerning the stress analysis of that cut in the sandwich where you have that very thin section. You made a shell theory approximation of this joint but you really don't know, with the shell theory, what the load path is through the sandwich, do you?

ANDERSON: That is correct and something I'm certainly aware of. I think the load picture in the sandwich is incorrect right at the discontinuity because the shell theory says that both face sheets are loaded right at the end of the cut while we know one face sheet is free. So there's kind of a shear lag effect here which possibly could be taken into account by adjusting your sandwich stiffness before you came to the cut. That might be a little better than using shell theory alone.

QUESTION: Were those tests you mentioned the DTMB tests-- the Bloomenbergs series of tests?

ANDERSON: No, these were done by Wink, I believe.

COMMENT: I was wondering how that bulkhead was attached to the shell. In the Bloomenberg series there was a rubber O ring which constrained the shell in such a way that end rotations were not permitted but axial displacements were permitted. I did a little study on the Bloomenberg tests. It wasn't really specified what the boundary stiffnesses in the various directions were but it turned out that if you allowed an axial displacement in the buckle pattern that had a very large effect and brought the thing right into agreement with the test results. In other words, you prevented rotations but allowed axial displacements in the buckle pattern. When you have long cylinders under external pressure the axial displacement boundary condition is rather important.

ANDERSON: We found the same thing. When we were looking at simple support, we were allowing axial displacement. The bulkhead tended to minimize that displacement. As far as I know, the bulkhead was bolted rather firmly through that rather heavy end ring on the cylinder and there probably was some form of a sealer there, too. I certainly hope in the future when we try to analyze these experiments with sophisticated programs that all the necessary information in test programs is provided.

COMMENT: I wonder whether I could suggest perhaps another reason why you're not getting such good comparisons in some cases. We've done several analyses on shells similar to those tested at DTMB and we've found that there was plastic yielding. In fact, these shells have been used pretty close to their stress limits.

ANDERSON: Yes, we haven't looked at that but I'm aware that often their tests are quite high stress levels.

GENERAL SUMMARY OF THE CONFERENCE

Kevin J. Forsberg*
Lockheed Palo Alto Research Laboratory
Palo Alto, California

Thank you Mr. Janik. The best one sentence summary of this conference was provided to me by Bo Almroth when he observed that 160 reasonably intelligent men spent an entire week arguing about which is the best method to determine the ultimate carrying capacity of a tin can. We really haven't resolved the issue, but I think we have had a lot of fun in trying. A number of very good papers have been presented; in fact some I consider to be quite outstanding. They have addressed problems that are of concern to the entire engineering community and they have pinpointed some of the difficulties in our present state of the art.

The objective of most of our research is to produce tools that can be of use in engineering analysis and hopefully in engineering design. I distinguish between the two in that analysis is done after the structure is really built, while des. consists of guiding the development of the structure through a number of parametric iterations in order to define the final configuration. The best design tool is engineering judgement, but the kind of problems with which we are currently dealing are highly complex and we don't have enough experience in handling these. Hence our engineering judgement isn't always a good guide. We must then rely on computer programs which we hope are reliable, easy to use and efficient. Many papers presented at the various matrix methods conferences dealing with finite elements are, in my opinion, mainly addressing the question of reliability. Whether you should use nine or twenty-four or thirty-six degrees of freedom to describe the bending behavior of a triangular plate element is in many ways a question of the reliability of a given formulation. We are also concerned about things like aspect ratio of the triangular elements (i.e., when does the accuracy begin to go to pct). Questions like this have been extensively examined in other symposia. The ease of use of a program is a very important consideration to the engineer. We have programs for which input can be prepared in a very simple format and for which the output can be displayed without the

* Asst. Director, Materials & Structures Directorate

blizzard of numbers referred to by Maney Stein in his opening remarks. This, however, is a problem that's totally independent of the method of solution.

The third criterion for computer program development is efficiency. I take exception to the opinion of Dale Warren that we are concentrating on the wrong thing when we look at the cost located in the computer run time. The ease of use of a computer program is really addressed at minimizing engineering costs which represent a major part of any computerized study. However the computer costs are very important because they determine the feasibility of performing parametric studies for detail design. I might also point out that we are minimally able to handle two dimensional problems right now and thus we must develop more efficient solution procedures if we are truly to have an engineering design tool for modern aerospace structures.

The question of computer efficiency depends not only on efficient equation solvers but also on the relative merits between various discretization methods. Thus although there has been a lot of talk about brotherhood and unity of finite difference and finite element methods, it is reasonable to raise the issue of whether or not there are distinctions between these methods. The distinction between them, in my opinion, should be on the basis of relative efficiency of a given method to achieve a given degree of accuracy. I believe that both finite element and finite difference techniques are suitable for solving most of the problems that we have at hand. They can be used in one-, two-, or three-dimensional static or dynamic linear or nonlinear problems, but I think there are areas where one technique stands out from the other.

I do not want to summarize the papers that have been presented this week either individually or in groups. I would rather touch on some of the topics that we have discussed and to state from my own unbiased point of view what I think the state of the art is. I would like to make the point rather strongly that there is a finite difference between what it is possible to do and what has been done. This difference is very significant. In fact, the realization of the potential of any method requires many years and the realization of the full engineering potential of both these techniques is still far into the future.

Let me start with an example of a two-dimensional structure (analyzed by Drs. M. Marlowe and T. Geers) where I think finite element techniques hold sway and where they will continue to hold sway for some time to come. This bastion of finite element application is represented by the highly complex fuselage of the Cheyenne helicopter. Figure 1 shows the triangular membrane and bending plate elements that were used in modeling the fuselage. Figure 2 shows the interior structure of this fuselage. This structure is complex enough that even skeptics like Bo Almroth would use finite element methods to solve this particular problem. I am appalled at the thought of trying to develop a suitable mathematical description of this surface, even in a piecewise fashion, for use in any of our existing finite difference codes. The deformed position of the fuselage in its first mode is shown superimposed on its undeformed position in Fig. 3. If we were to ask for tabular output for this 1200 degree of freedom problem, it is certain we could not make reasonable interpretation out of the blizzard of numbers to see what is going on. However I would also contend that you cannot make much sense out of this particular graph (Fig. 3). Even though many of the lines from the original model have been eliminated, we need at least this much definition to see the structure; yet when you have this much definition you cannot see what is going on. Thus even graphic displays can become so cluttered that it becomes a major task to interpret what is happening. For this reason we made a movie of the modal behavior of the forward fuselage. In the movie the behavior becomes very clear. In this analysis we wanted to assess the effects of the flexible access doors in the base of the fuselage. With stiff access doors the second mode of the fuselage is a lateral cantilever mode. The effect of flexible doors on the sidesway mode is to couple the lateral bending and torsional deformation. The pilot would be very much disturbed by this as it affects the controls of the aircraft. This change in behavior is very difficult to visualize in a static display. I think this demonstrates the power of the animation of a simple passive graphic display. The point was made on the first day by Mr. Vinson that graphic tools are great sales tools. You can go out and show them to somebody and say "wow, look what I've done!" I think that misses the point. The animated display is a powerful and vital engineering analysis tool as well. In this instance the engineers at our Lockheed-California Company had a very difficult time trying to visualize what was happening when they relaxed stiffness in the lower portion of the fuselage. The movie clearly demonstrates what's going on even to people who had never been exposed to the analysis before.

I would like now to make a comparison of finite difference and finite element techniques for other classes of problems where finite differences are more suitable or certainly can be used more readily. The cylindrical shell roof shown in Fig. 4 is of particular interest because we have numerical examples provided by our friends and neighbors in Canada. Dr. G. Lindberg and his colleagues at the National Research Council have developed solutions for this particular structure using their 36 degree of freedom doubly curved triangular element. The plot in Fig. 5 presents results from several solutions. As shown in Fig. 5a, the older finite element analyses (by Bonnes, et al.) converges slowly; it requires about 500 unknowns to obtain the correct answer for the vertical displacement at the mid-span of the free edge. With the improved doubly curved triangular element (with 36 degrees of freedom per node) the answer is very rapidly obtained with something like 200 unknowns. The STAGS code (a two-dimensional finite difference analysis) had an even faster rate of convergence. Thus the finite difference technique is very competitive with the finite element in terms of rate of convergence. Fig. 5b shows the normal displacement at the midpoint of this shell roof. The finite difference solution appears to be converging more rapidly than the finite element analysis. However one should note that in making comparisons between methods it is easy to draw erroneous conclusions. In Fig. 5b results are also shown from the same finite difference technique (the STAGS code) where the number of points in the axial direction (9 points) were kept constant and the number of points in the circumferential direction were increased. As can be seen the rate of convergence is much slower than it is when results are generated by simultaneously varying the grid in two directions. Since the rate of convergence is sensitive to the type of grid that is used, one has to be very careful in comparing different methods. In Fig. 5c results are compared for the moment M_{xx} . I'm sure Dr. Lindberg is unhappy with this particular comparison because it shows his method up to disadvantage. Since I could have the option of selecting the variables for comparison here, I have presented this graph even though the moment M_{yy} happens to be about 5 times larger (and hence more significant in terms of stresses). For M_{yy} both computer programs gave essentially the same results for a given number of unknowns. However Fig. 5c shows clearly that the finite difference method is better and if you want to lie with numbers this is the way to do it.

I want now to turn to another example. I'm trying to prove a point by going through a large number of numerical examples because I know of no other way to make any assessment of the finite difference and finite element methods. The example shown in Fig. 6 is a large cylindrical shell with many small rings, as well as several large rings and longitudinal stiffeners. We solved this problem with both finite difference and finite element techniques. The finite element model here was based on an Irons, et al. nonconforming bending triangle with a linear strain quadrilateral. The grid required to obtain a converged solution had 25 circumferential and 25 axial points. The finite difference solution with that grid has about 1800 degrees of freedom; the finite element grid has approximately 3100 degrees of freedom. The solution time for the finite element procedure is 6 minutes and 30 seconds for this particular case. The factoring of the matrix took approximately 2 minutes; the rest of the time was spent forming the stiffness matrices and then computing stresses. It also went through 3 cycles of iterative accuracy requirement. All solutions are done in single precision. The finite difference solution, on the other hand, took 2 minutes and 50 seconds; less than half the run time. When we ran the same problem with 3100 degrees of freedom in the finite difference approach, it still ran faster because the time to form the difference expressions was less than the time required to form the finite element expression. These comparisons, of course, all depend very much on how well you have written your program, how good your solution procedure is, what computers you are running on. Thus the comparisons given here have been generated at LMSC because this is the only way that we can guarantee that the equation solvers are the same and that the computer systems are the same.

Figure 7 presents a comparison of the rate of convergence for the first eigenvalue of a 30-inch long monocoque cylinder with a 60 degree cutout 6 inches high (similar to, but different from, the cylinder shown in Fig. 6). One set of curves show the finite element results for a constant number of axial points with increasing circumferential points. Another set of curves show the finite difference results. The rates of convergence are reasonably similar for the two methods. In fact for a given mesh you have essentially comparable accuracy for either of the techniques. However the finite element technique has more degrees of freedom at a node and hence a bigger problem size; thus it requires significantly more run time. Based on our experience to date this seems to be a general conclusion. I want now to turn to another problem. A typical configuration for the space shuttle orbiter is shown in Fig. 8. The point of presenting

it here is that in this vehicle we have other than circular cylindrical or conical shells. A typical cross-section (nondimensionalized) is shown in Fig. 9. It is of vital engineering importance to determine the collapse load of such a structure, and this can only be done by performing a nonlinear analysis. To the best of my knowledge the only code capable of such an analysis at present is the STAGS code. Typical results are shown in Fig. 9 of such an analysis at present in the STAGS code. We have also performed a linear analysis of the pear-shaped cylinder under uniform axial compression. Both finite difference (STAGS code) and finite element (REXBAT code) results give accurate information for the linear range. However as seen in Fig. 10 the rate of convergence of the finite difference scheme depends strongly on the formulation. When the whole station finite difference scheme showed such superior performance vis a vis the finite element (REXBAT) results, we were delighted because this meant that the finite difference method was clearly hands down winner compared to our own finite element formulation. Then we found the work by Linäberg and crew in Canada. The point is that both finite difference and finite element methods are sensitive to the type of discretization that is used.

The analysis of the Cheyenne fuselage is typical of a class of linear problems which are clearly in the domain of finite elements (and probably will remain so since there are so many finite element advocates). However the prediction of the nonlinear collapse of general shell structures (as typified by the problem illustrated in Fig. 9) is clearly in the domain of finite differences. In the example shown in Fig. 9 there is an initial linear range until the plates buckle. Then there is a dramatic redistribution of stresses as can be seen in the figure. I feel that it is the duty of a speaker summarizing a conference to avoid controversial statements, so that I'll only remark that finite elements are clearly unsuitable for solving a problem of this type.

I want to turn now to an area where we really are pushing the limits of our capabilities. Other speakers at this conference have demonstrated clearly that one-dimensional problems are in hand for linear static and dynamic problems. For problems involving nonlinear transient response, however, things are not completely resolved even for one-dimensional problems; for two dimensional problems our capabilities are limited indeed. Consider the problem of an isotropic monocoque circular cylindrical shell simply supported at the boundaries and subjected to a pressure pulse that varies as a half cosine over the top half, unloaded on the bottom

half of the circumference; the load is uniform in the axial direction. If we idealize the pressure pulse as an initial velocity we find that as we continually refine the time step for integration we pick up more and more of high frequency contributions (see Fig. 11). These are delightful; it's nice to pick them up if they're really there but I suspect that they actually come from numerical errors in the solution procedure. That is, a discrete undamped model of a continuous system does not respond correctly to truly impulsive loads. Fig. 12 shows the results for the same cylinder but with the load now modeled as a triangular pressure pulse rather than initial velocity. The duration of the loading is reasonably small - a fraction of the fundamental mode of this structure. Now you see as you refine the mesh the response converges nicely. The finest mesh ($\Delta x = 0.5h$) is approximately the limit of the convergence for the explicit scheme for this particular example. These comparisons were developed by Dr. L. Sobel of LMSC using the STAR code (which he helped develop). He has compared his solution with results of Bill Hubka from Kaman Nuclear.

One of the interesting things that was found in the course of this study is the accuracy obtained from different finite difference formulations. In Fig. 13 the linear response is presented for the same cylindrical shell discussed in the preceding paragraph. The solid lines are results that Hubka developed some time ago which he compared with an exact solution. Unfortunately, since we are using finite differences we cannot use Melosh's technique calling the finite difference solution exact, so we have chosen to use a modal expansion and call that the exact solution. The results from the STAR code (which is a two dimensional finite difference analog of the differential equations with an explicit numerical integration in time) are shown in Fig. 13. With the lower order difference schemes, which is the most commonly used formulation, we obtained results that began to diverge at reasonably early times; refining the mesh improved things somewhat but didn't solve the problem. By going to higher order finite difference expressions the results followed those developed by Hubka (he, too, uses higher order finite difference expressions in his code). Again this is a shell subjected to an idealized impulsive loading, and these results were generated in single precision. There are many questions that are left unanswered regarding the necessity for the (more complex) higher order formulation. The point I want to make is that although finite differences are great, we haven't solved all of the problems and particularly in the area of transient dynamic response.

Figure 14 presents a schematic of a conical shell having a large cutout, and indicates the kind of problems at which these codes (such as STAR) were initially directed. In such engineering problems (e.g., antenna windows in a conical shell) we are concerned about the early time nonlinear large deformation elastic plastic transient dynamic response. The STAR code developed by Dr. Sobel was used to solve such a problem. In Figure 14 a comparison between analysis and experiment is presented and I feel that this is a pretty good comparison. I must admit however that there were 28 or so other curves there of similar response quantities where there is no agreement at all. That's unfair to Dr. Sobel, however, because in the experimental model there were a lot of details which we cannot really model in our present finite difference program. And I think this is an important example because it shows the deficiencies of our present capability. Our primary difficulty is that we cannot model rings adequately with the equilibrium formulation. Rings are modeled by increasing the thickness of the shell since variable thickness and variable geometry are easily treated as part of a single set of differential equations while discrete stiffeners require a separate set of differential equations necessitating a very cumbersome matching at the boundaries. An energy formulation on the other hand is ideally adapted to addition of discrete stiffeners. This is the approach that has been used in the STAGS code which at present is only working for statics problems (collapse of shells). It is sobering to note that (as far as I can tell) the STAR code is the most advanced capability in the country for solving problems involving the nonlinear transient dynamic response; yet we are in a very primitive state of development. We must use a comparatively coarse mesh because a refined mesh costs too much in computer time; the run times get out of hand if plasticity is involved. We certainly are at the frontier of our capability with this simple two-dimensional problem.

I would like to point out some deficiencies in the state of the art. I think the deficiencies of finite elements are obvious to all, so I won't dwell on those but I'd like to indicate some of the limitations of our finite difference techniques. Of all of the current techniques in use these are the ones I'm most familiar with and can lie about most easily. Figure 15 depicts a typical example of the type of structure that can be analyzed on a routine basis now for linear or nonlinear static analyses. We have curved boundaries that can be contained as an interior boundary; we can treat partial or complete rings and stringers; we can include eccentricity effects. In short all of the good details that the finite element people love can be included in this type of modeling. These kinds of details

can be included whether you use an equilibrium formulation or an energy formulation, but life is much simpler when you model these problems using the energy formulation (as has been done in the STAGS code).

Consider a simple example of a flat plate with a circular cutout. The type of mesh that is generated to treat the curved boundary is shown in Fig. 16. You see immediately the tremendous disadvantage that we labor under in using finite difference procedures for this kind of problem at the present time. First of all, when the mesh is refined to get points equally spaced along the curved boundary, one obtains a concentration of mesh lines which extend throughout the region of interest. Second, while we are not restricted to an orthogonal mesh, we are reasonably restricted in the type of grid we can set up. We cannot do what the finite element method does so beautifully; that is, concentrate points just in the region of the reinforcement and leave other areas with a very coarse mesh since that's all you really require for your solution.

For the stiffened shell shown in Fig. 17a, a study was made of the axial membrane stress and axial moment comparing analytical results (circles in Fig. 18) with data from a photoelastic analysis (solid lines) done by Durelli at Catholic University. (This work was sponsored by Rembert Jones of the Naval Ship Research and Development Center.)

Earlier in this conference Mr. Stan Jensen talked about the use of arbitrary grids. This is perhaps the most exciting development in improving the capability of finite difference techniques. The thrust of his work is illustrated by the kind of thing being done in nonlinear fluid slosh problems using finite difference techniques with automated grid generators. Figure 19 is a finite difference grid for a second order partial differential equation. The problem is extending this capability from a second order to an eighth order system; life gets tough and that is the finite difference in capability I mentioned earlier. There is a long way to go between the potential capability and the realized capability in this area. Figure 19 is a model of a hemispherical closure on a cylindrical shell. During the course of the solution the tank is draining and the mesh is regenerated a number of times so that there is a dynamic rezoning of the mesh during solution.

All of the results that I have talked about today are things that we have developed here at Lockheed. This is because it is extremely hard to make valid comparisons between various techniques unless you have a common basis of comparison.

All too often problems available in the literature are fairly limited in the information that is given; you cannot make the detailed comparisons that you would like to make on quantities such as displacements, stresses, and computer run times. So what Nick Bernstein (AFFDL) and Dick Hartung (LMSC) have planned to do during the coming year is to generate a set of 5 sample problems which we hope to encourage as many people as possible here today to run on their codes. Then we will have a much broader basis of comparison for problems that are typical of those encountered in the aerospace industry. We have selected these problems because they are of practical interest. For instance, the first problem (Fig. 20a) considers a conical shell stiffened by rings and with an end closure. It is a very simple problem because it is a shell of revolution. Many people can handle shells of revolution very efficiently so we would like to throw in a few hookers like changing the wall construction, adding attached mass or cutouts, inducing non-linear material behavior, putting a liquid inside. We would then ask what happens to the solution procedure. An even simpler problem (that of a uniform isotropic homogeneous conical shell free or clamped at the boundaries subjected to an impulsive load) will also be considered. A second problem (shown in Fig. 20) is the pear-shaped cylinder. This is typical of the geometry encountered in the space shuttle. It's very important to get accurate descriptions of the buckling loads here because the simple approximations are really quite crummy in predicting the collapse load of such a structure.

Consider again the problem of the transient dynamic response of a simple conical shell. Figure 21 is an example of the type of data that we hope to generate. This figure presents the response of one of the parameters in the shell and the x's, dots and triangles represent solutions from four different investigators. Since all solutions agree, one has a high confidence that either everybody's getting either the wrong answers simultaneously or else we know how to solve this class of problems. It is this kind of comparison that we are looking for in detail over a wide spectrum of problems.

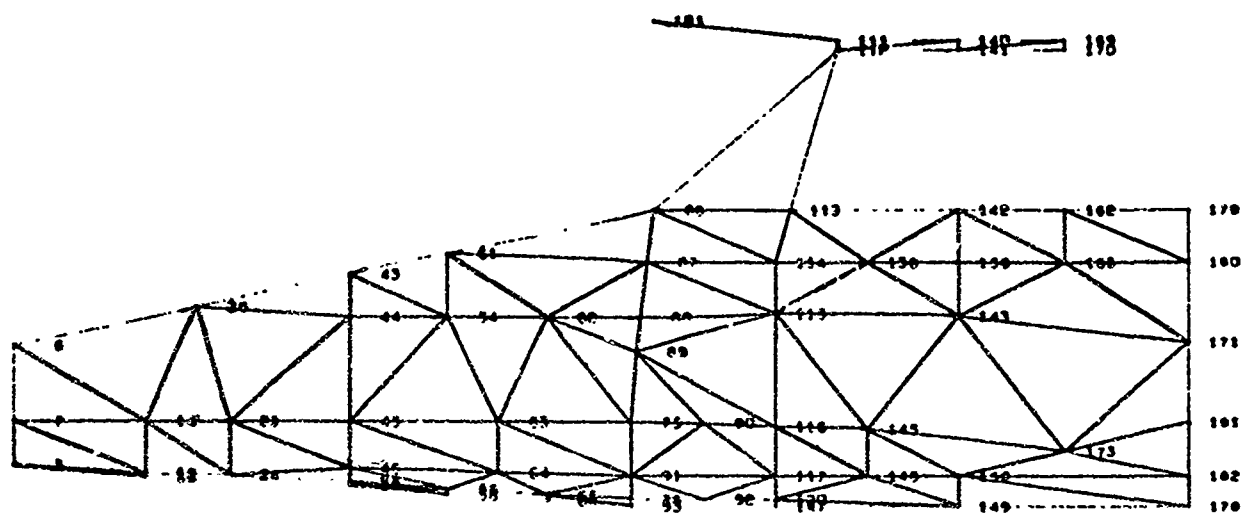
The third problem we want to consider is a circular cylindrical shell with a cutout (Fig. 22a). This is a problem encountered in all of our shroud designs and I'm sure other people have similar problems. Figure 22b is a spherical cap with a variable thickness. This is modeled on Apollo heatshield, again a realistic engineering problem. We would like you to predict the dynamic collapse of

such a structure. The fifth problem is the pinched cylinder (Fig. 23). This is a very nice example for showing the deficiencies of finite element techniques; finite differences I know will work very well for this problem (but we haven't tried it yet).

Now I've shown you the type of geometries. In Fig. 24 we have indicated the different types of problems from static down through dynamic, linear, non-linear, impulsive loads, distributed loads, etc., which we hope will be treated in the studies. We hope to have these problems formulated in the near future and to mail them to anybody who is willing to participate; unfortunately we can't pay to make these runs but we're hoping that the information exchange which we establish will be of benefit to the entire community in pinpointing the deficiencies of our current technology. Our intention then is to get people together again in a year perhaps to evaluate results of this study.

Thank you.

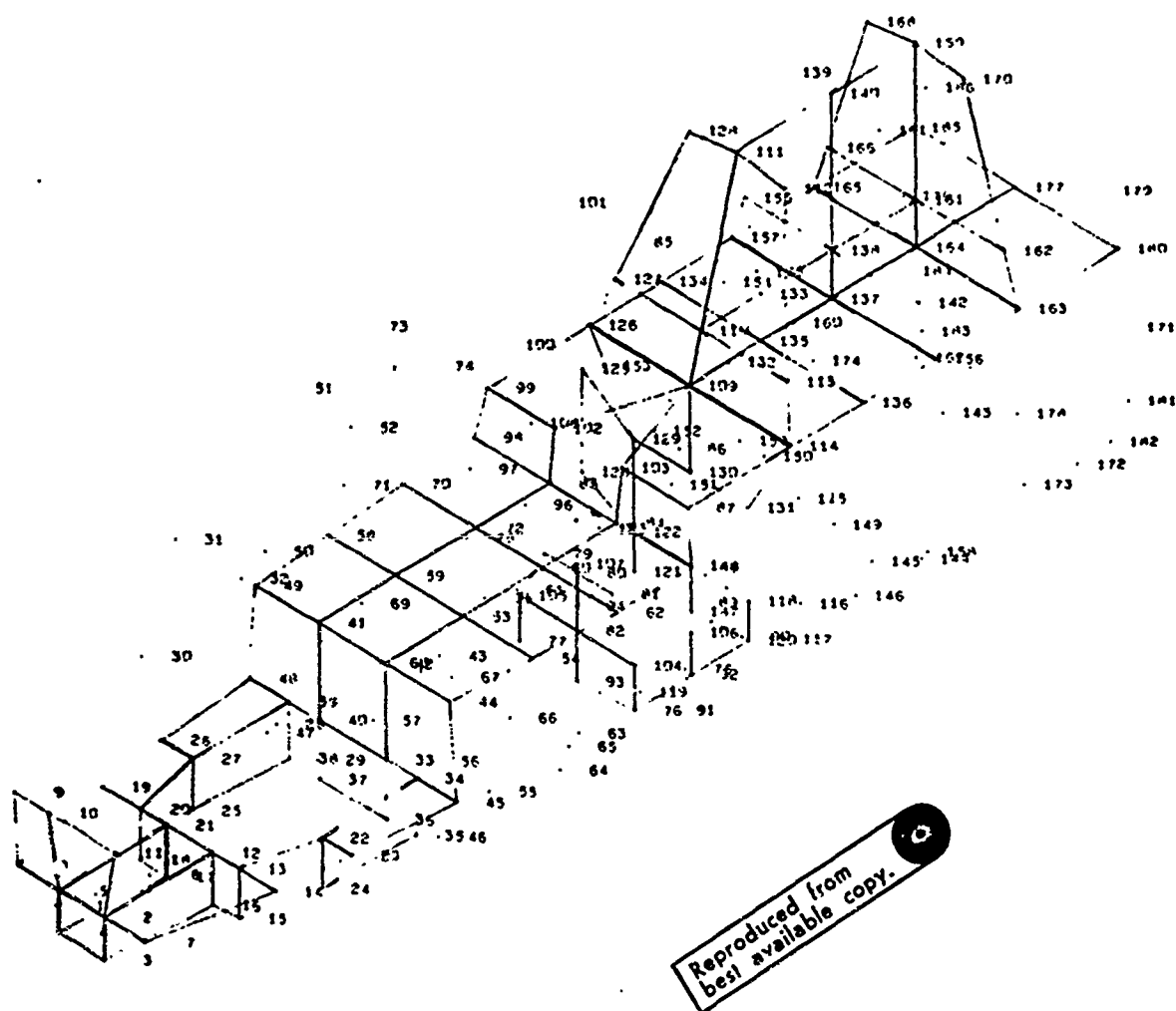
AH-56A FORWARD FUSelage TRIANGULAR BENDING ELEMENTS



PLANE VIEW

Figure 1 - AH-56A Forward Fuselage Modeled with Triangular Bending Elements

AM-56A FORWARD FUSELAGE QUADRILATERAL ELEMENTS



ISOMETRIC VIEW

Figure 2 - Interior of forward Fuselage Modeled with Quadrilateral Elements

AH-56A HELICOPTER (FIRST MODE)

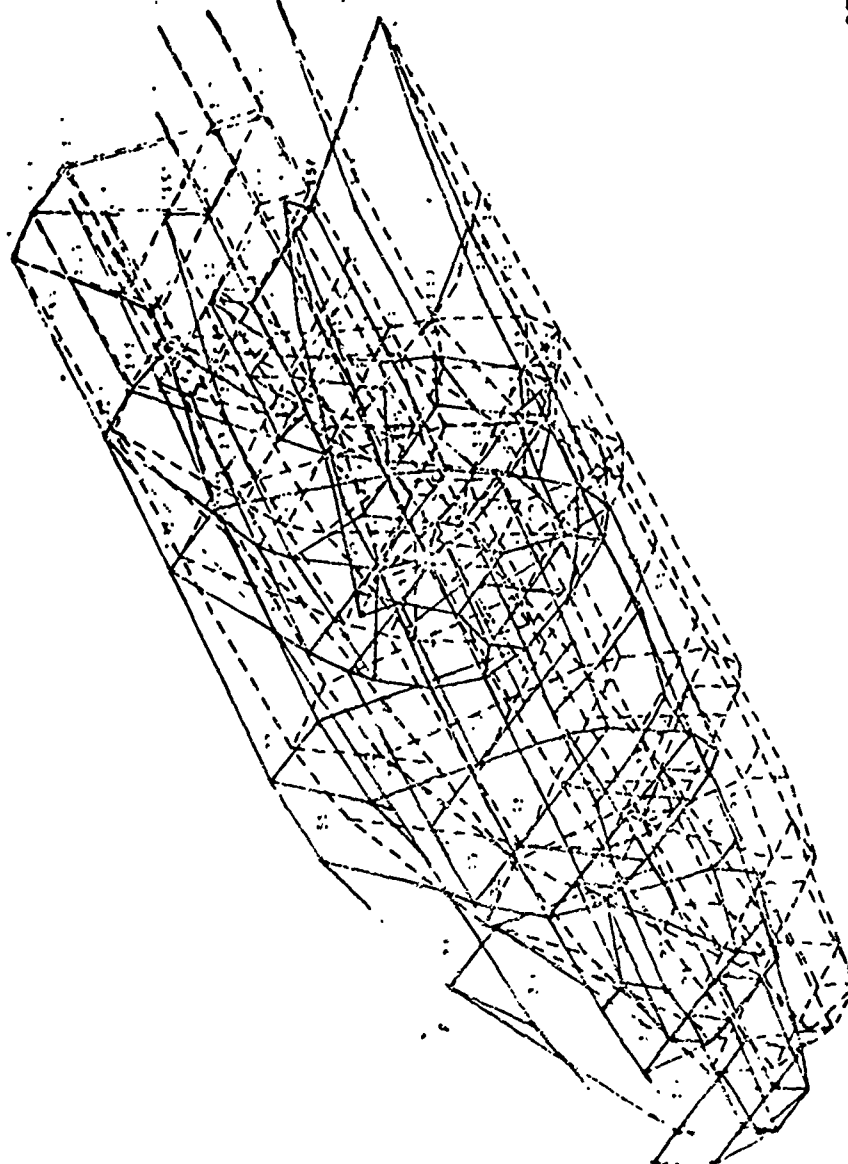


Figure 3 - First Mode of the AH-56A Forward Fuselage

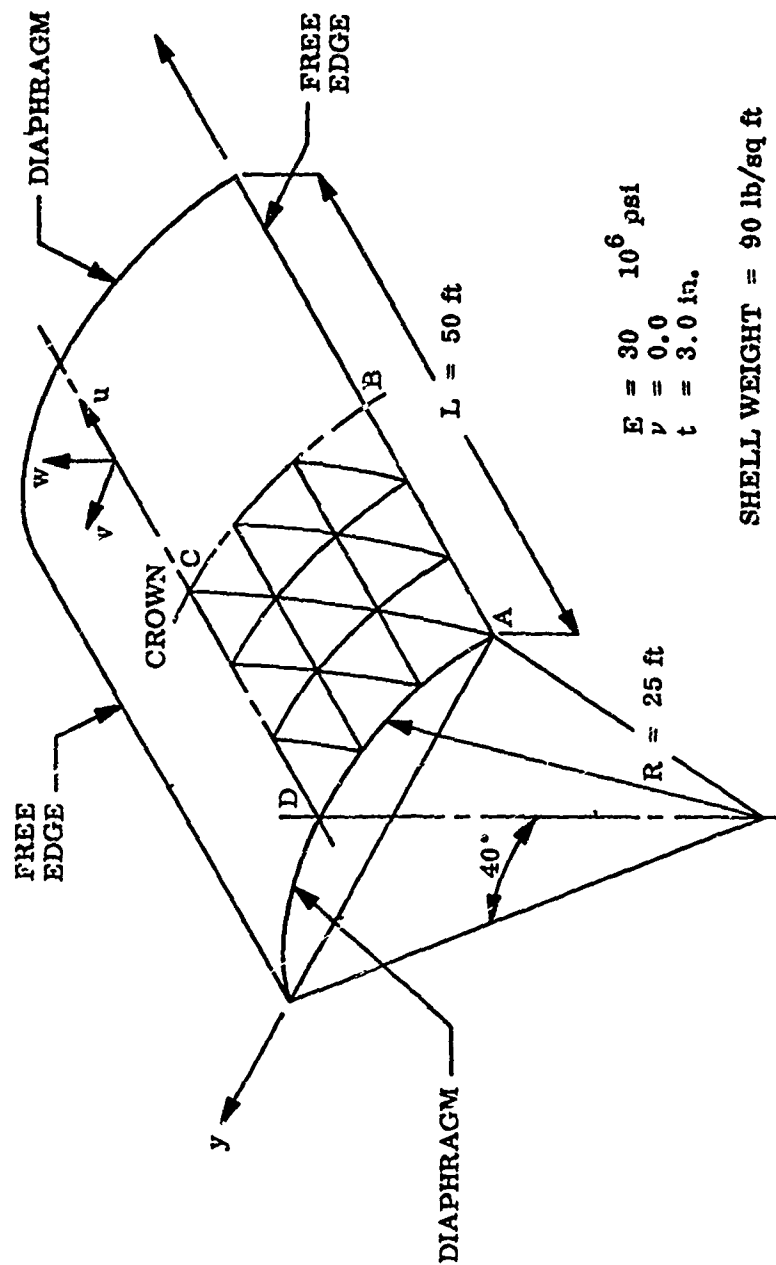


Figure 4 - Cylindrical Shell Roof Configuration

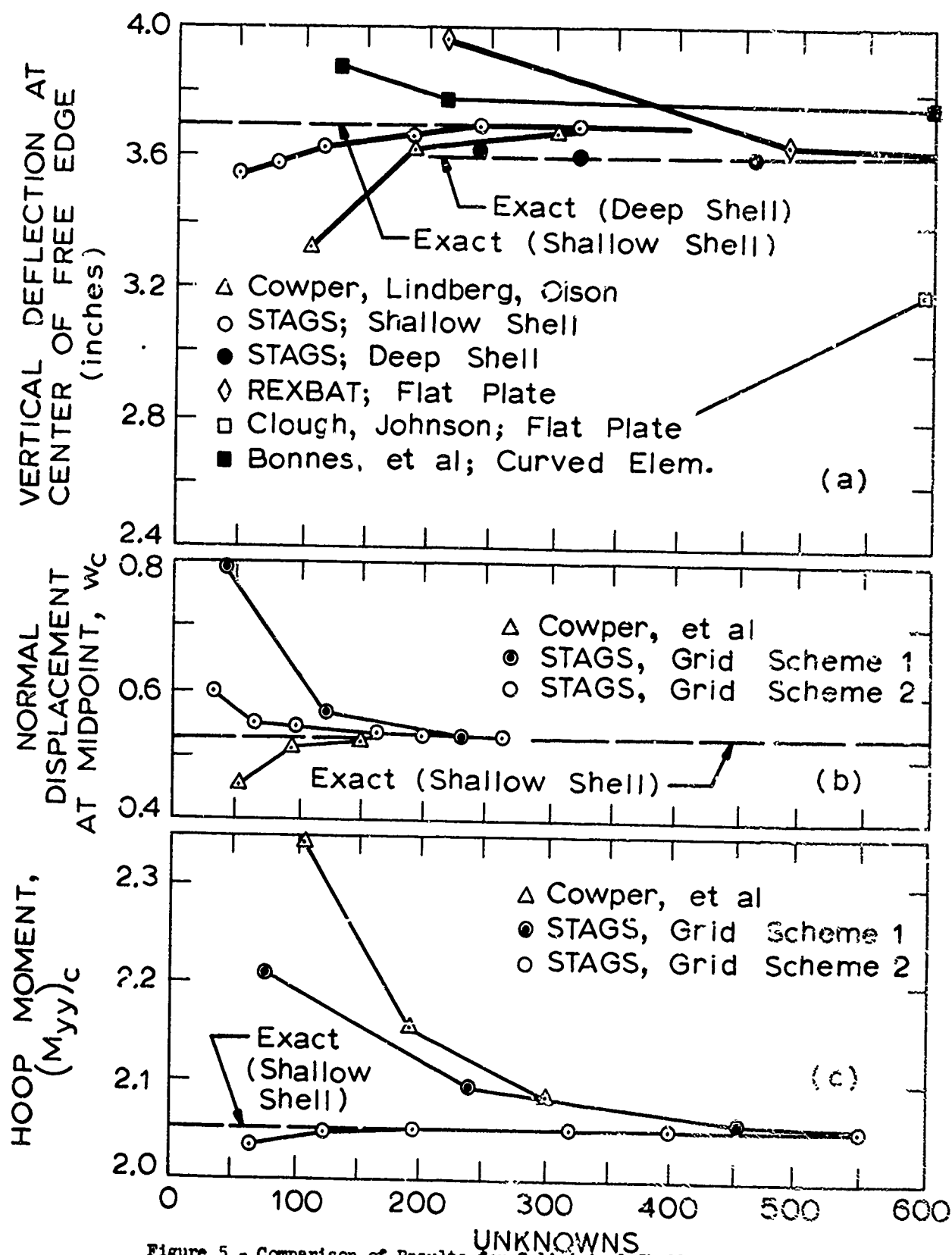


Figure 5 - Comparison of Results for Cylindrical Shell Roof Problem

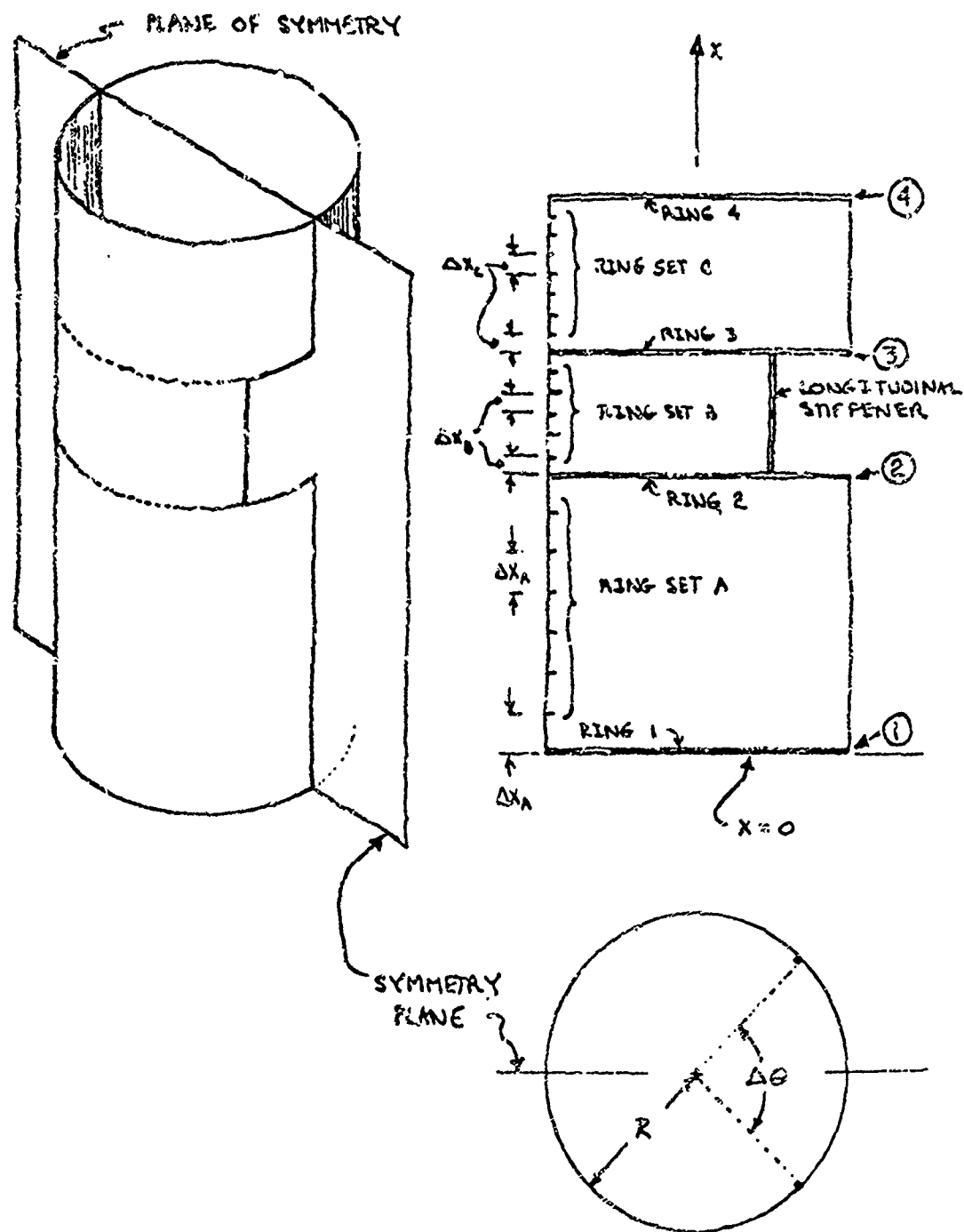


Figure 6 - Ring Stiffened Cylindrical Shell with Cutout

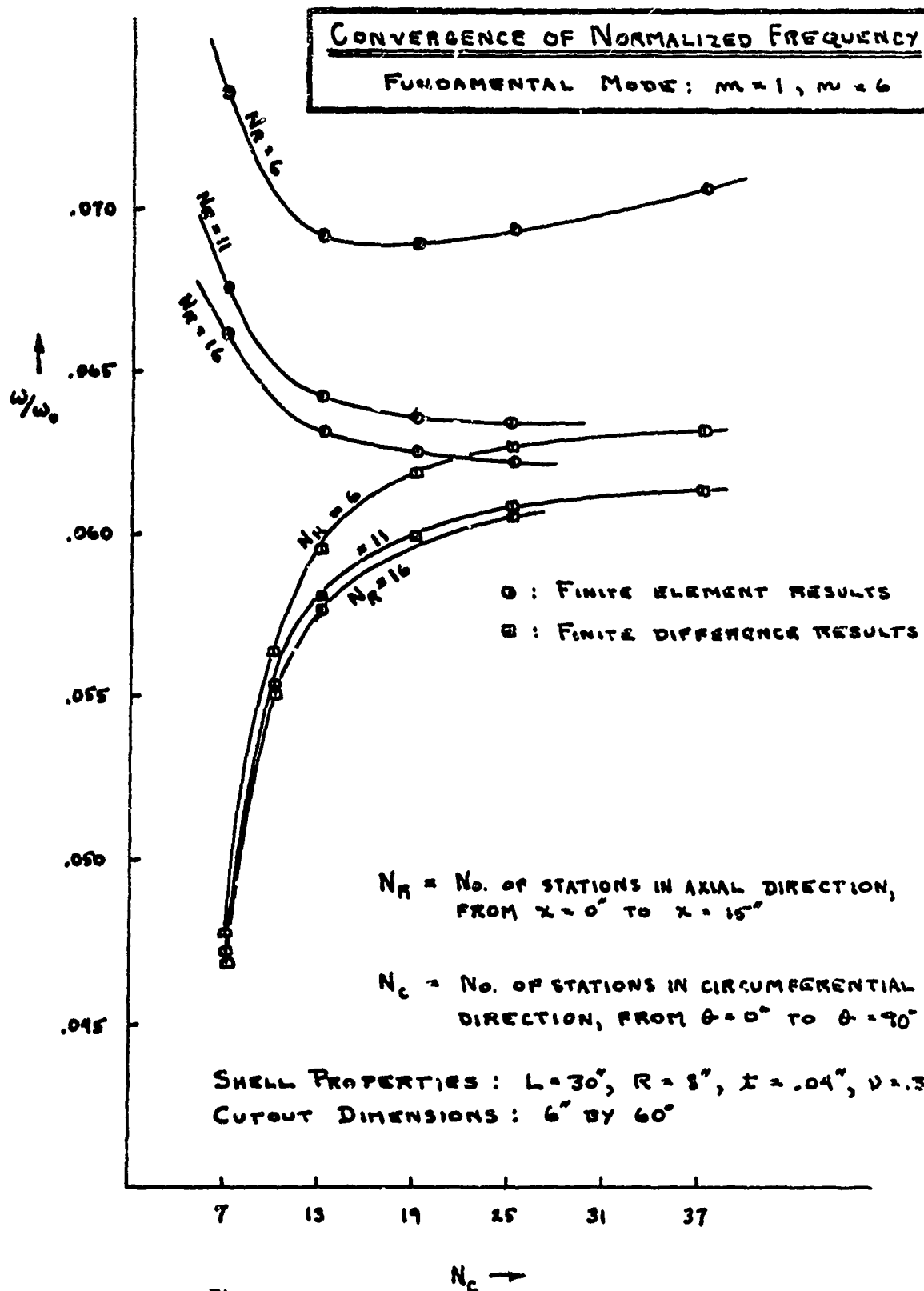


Figure 7 - Results of Eigenvalue Convergence Study

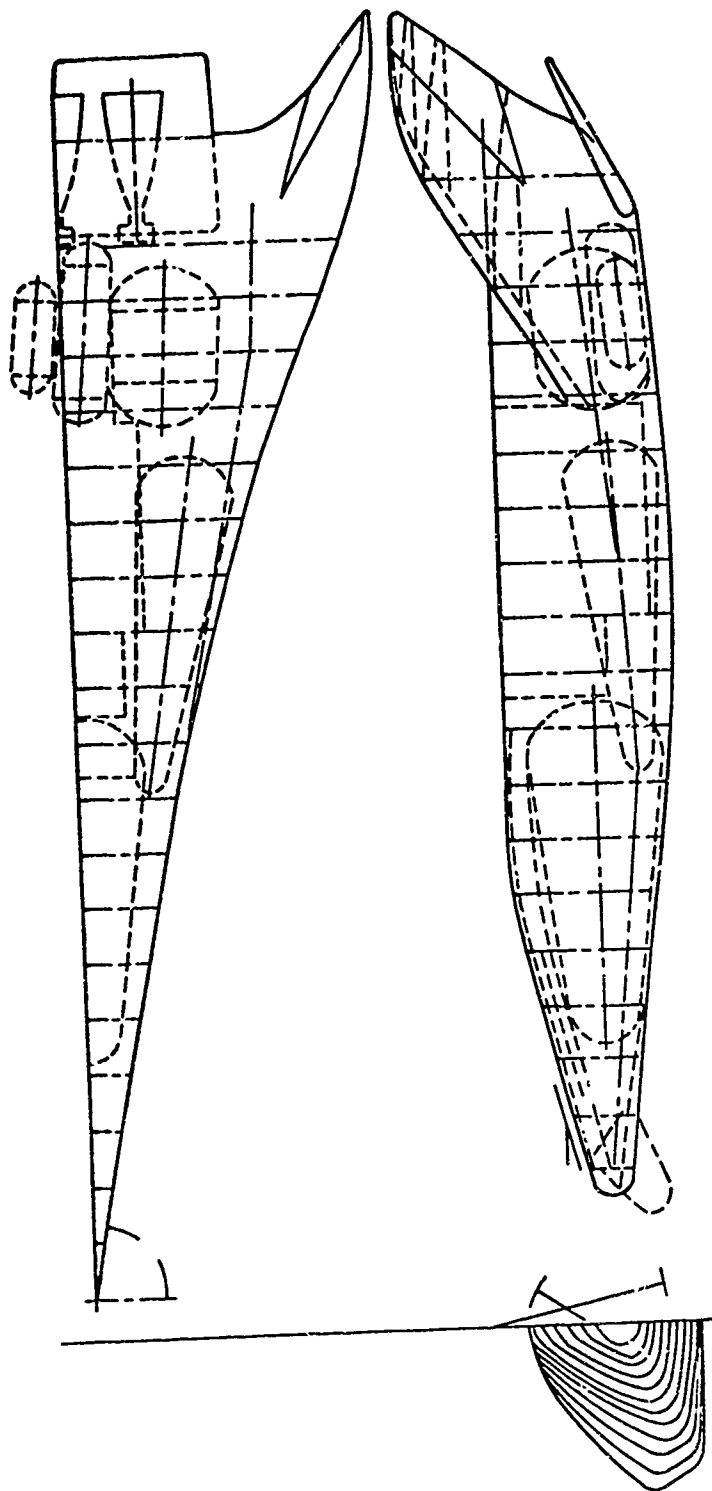


Figure 8 - Delta Body Orbiter Configuration

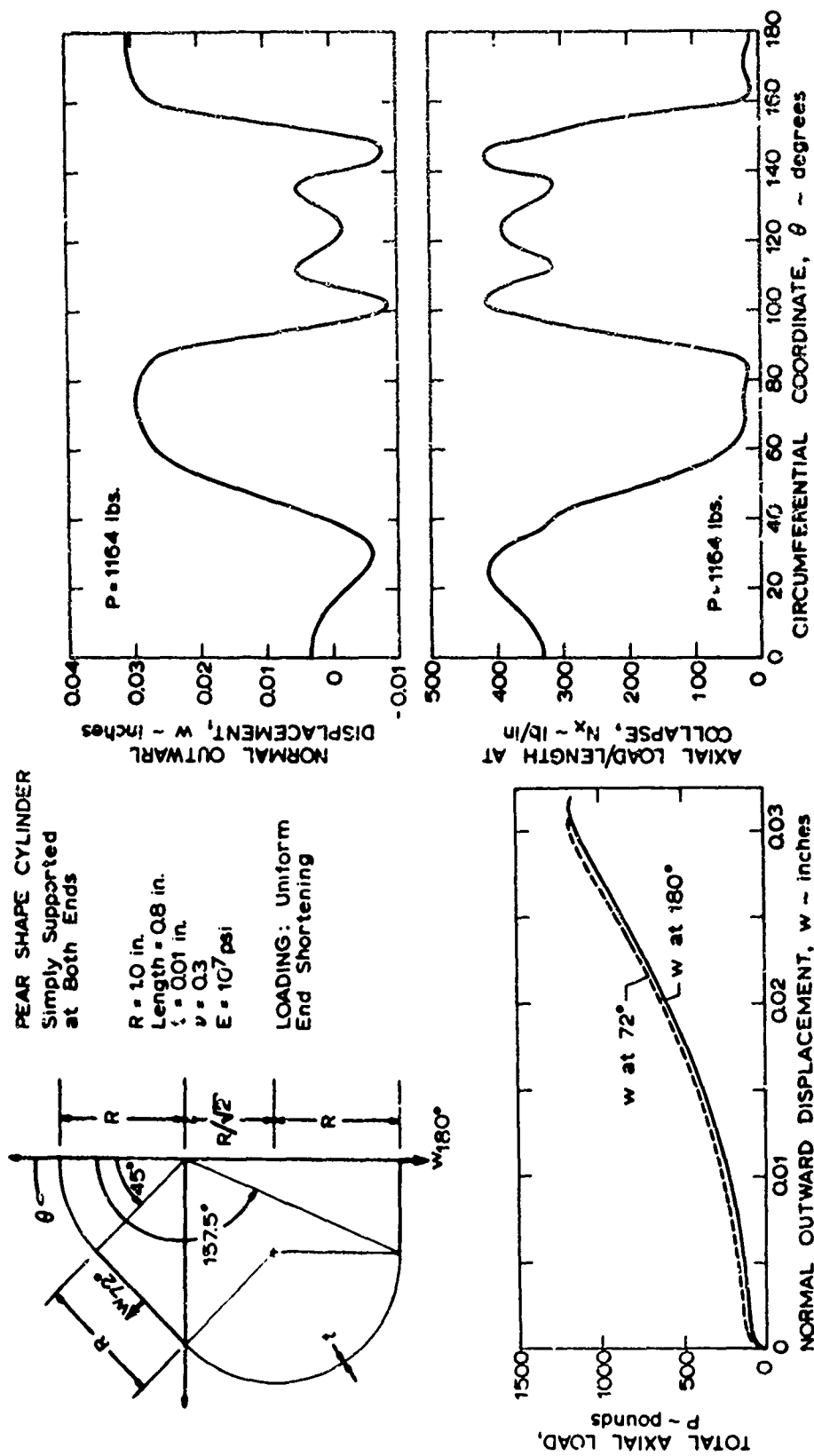


Figure 9 - Typical Results from Analysis of a Cylinder with Pear-Shape Cross-Section

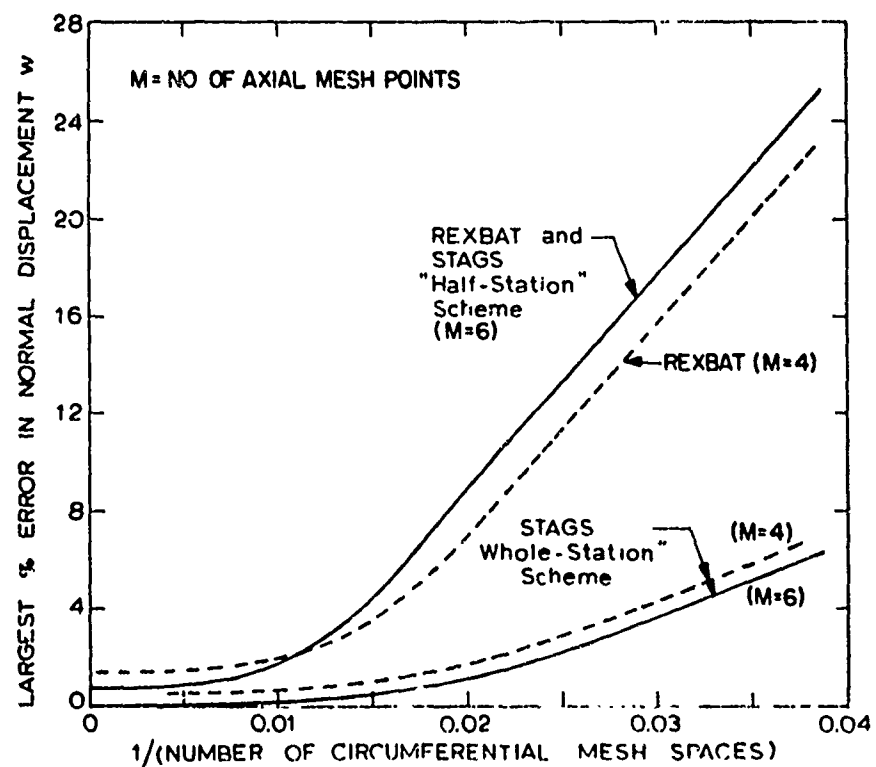
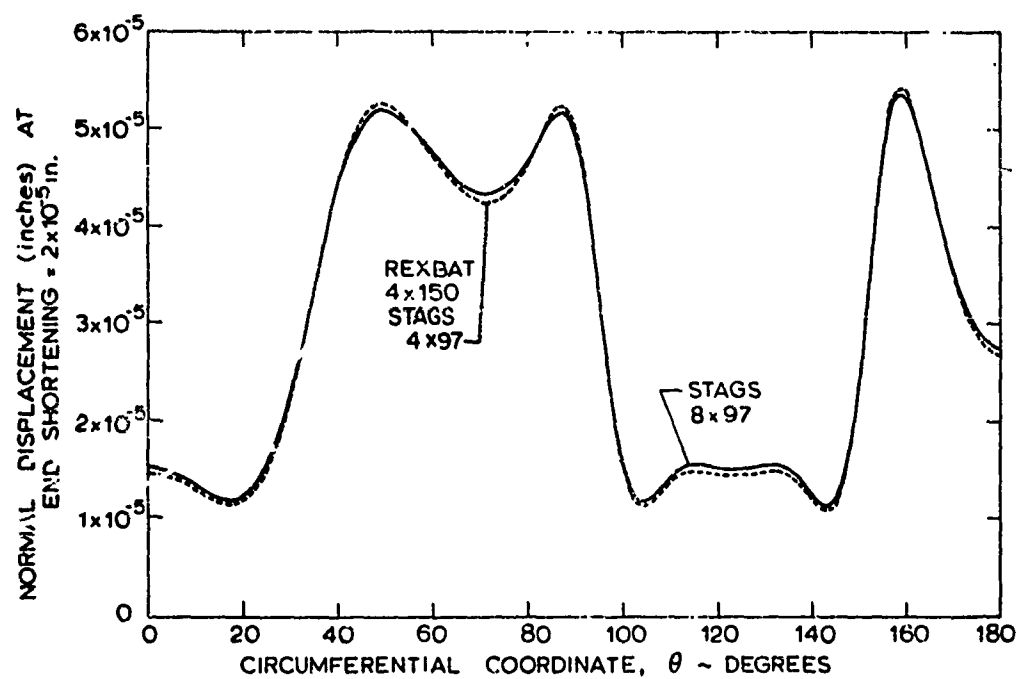


Figure 10 - Comparison of Finite Element and Finite Difference Results for Cylinder with Pear-Shape Cross-Section

..... $\Delta x/h = 0.50$

— $\Delta x/h = 1.00$

--- $\Delta x/h = 1.33$

- - - $\Delta x/h = 1.6$

o $\Delta x/h = 2.0$

* $\Delta x/h = 3.0$

OUTER SURFACE AXIAL STRAIN AT $x = L/2$

1271

Reproduced from
best available copy.

STRAIN (%)

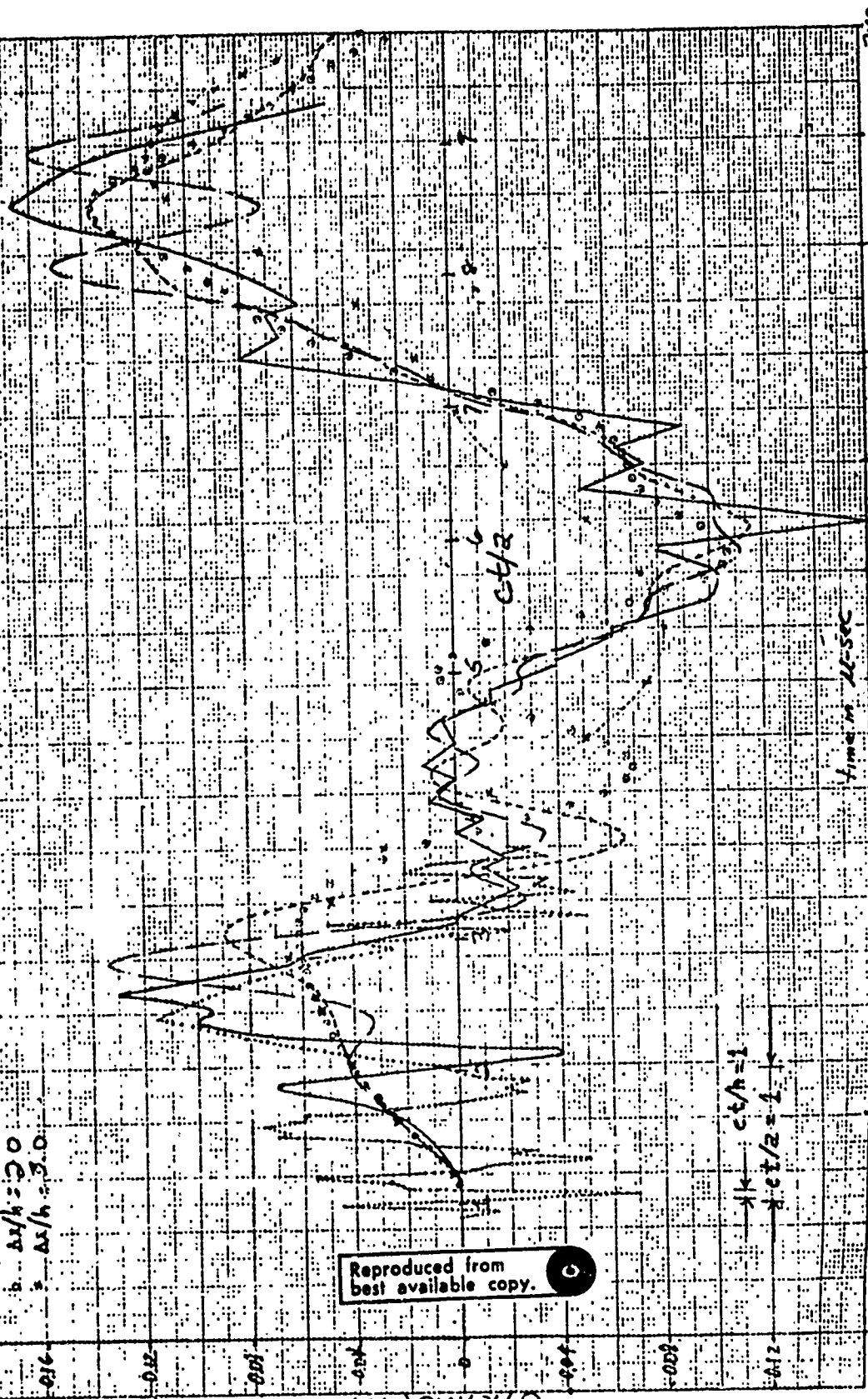


Figure 11 - Effect of Finite Difference Mesh Size on the Results of a Transient Response Analysis of a Cylinder Subjected to Initial Velocity that Varies Cosinusoidally Over Half the Circumference and Vanishes Over the Other Half

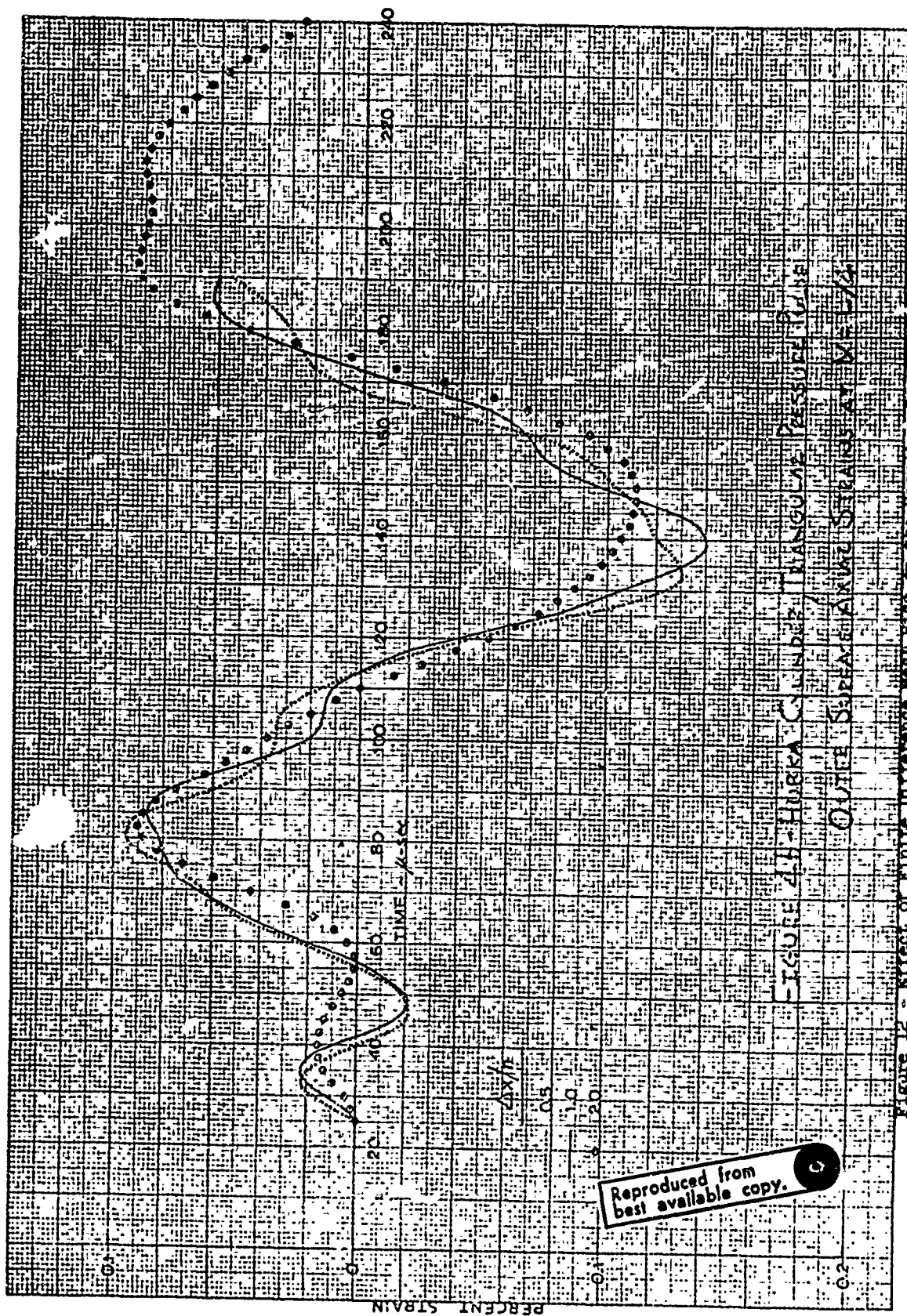


Figure 12 - Effect of finite difference mesh size on the results of a transient response analysis of a cylinder subjected to a triangular pressure pulse that varies cosinusoidally over half the circumference and vanishes over the other half

FIGURE 12 - EFFECT OF FINITE DIFFERENCE MESH SIZE ON THE RESULTS OF A TRANSIENT RESPONSE ANALYSIS OF A CYLINDER SUBJECTED TO A TRIANGULAR PRESSURE PULSE THAT VARIES COSINUSOIDALLY OVER HALF THE CIRCUMFERENCE AND VANISHES OVER THE OTHER HALF

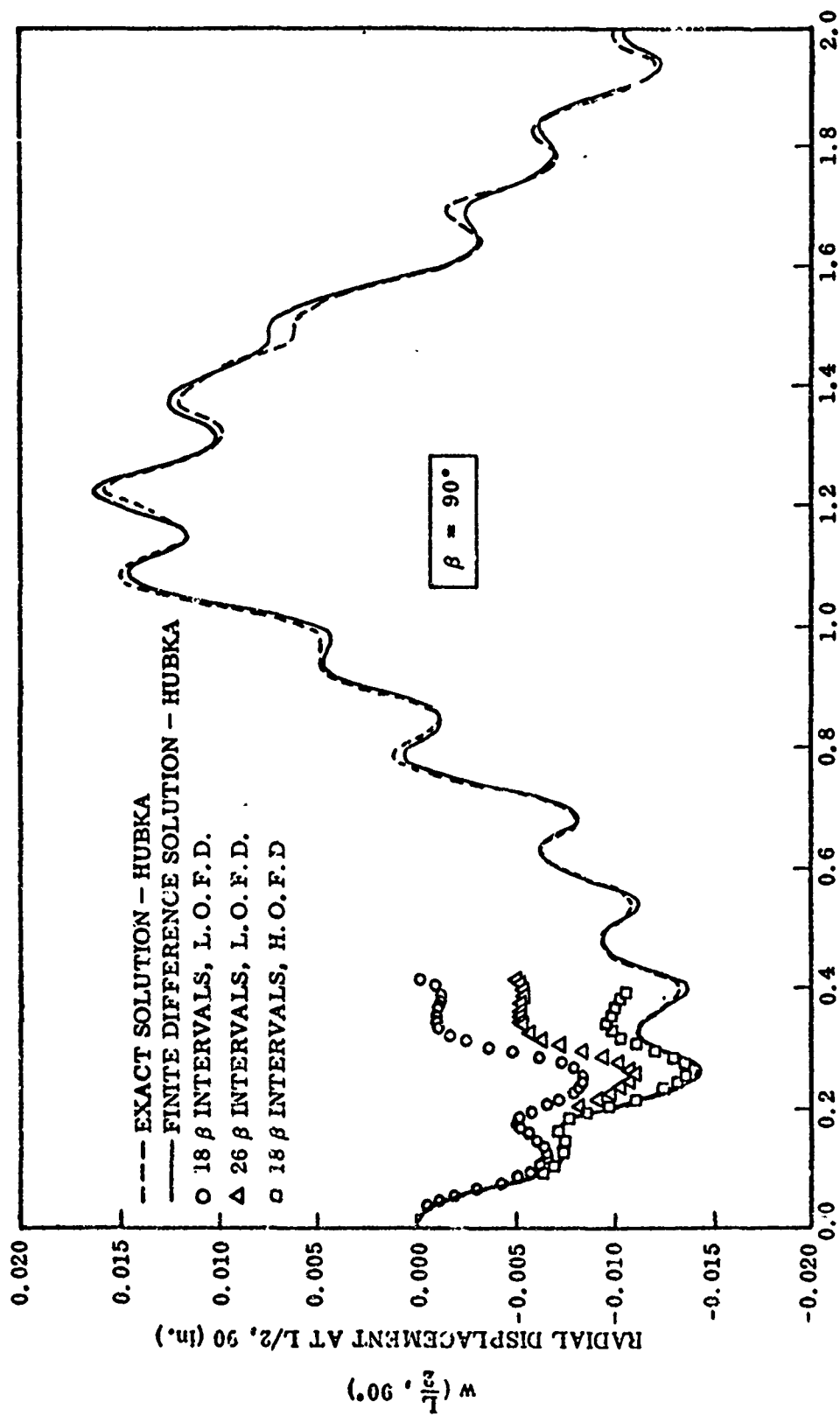


Figure 13 - Effect of Higher Order Finite Difference Expressions on the Results of a Transient Response Analysis of a Cylinder Subjected to Initial Velocity that Varies Cosinusoidally Over Half the Circumference and Vanishes Over the Other Half

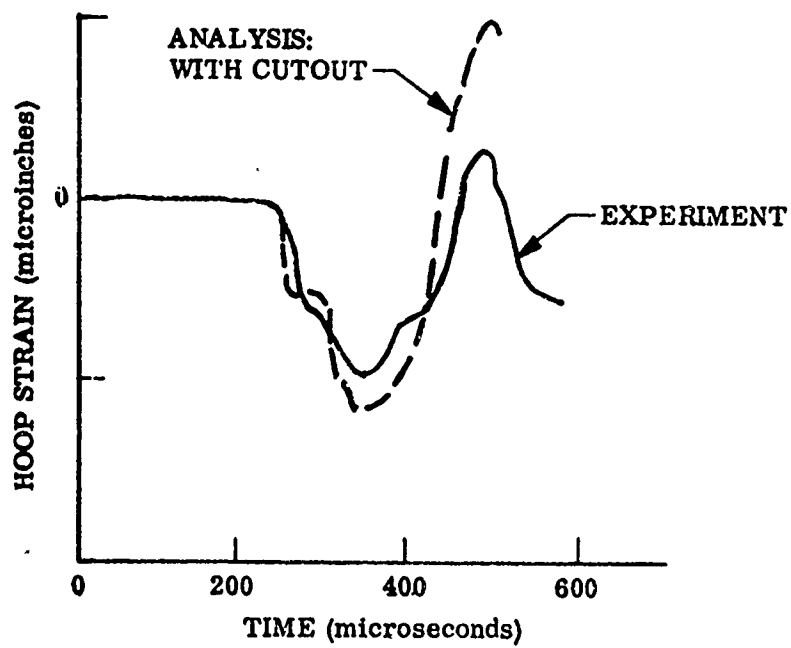
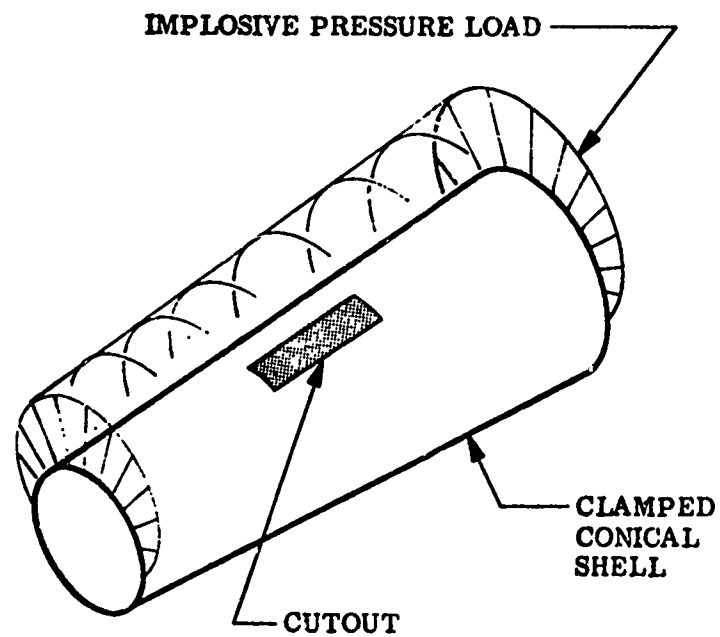


Figure 14 - Comparison of STAR Code Results and Test Data

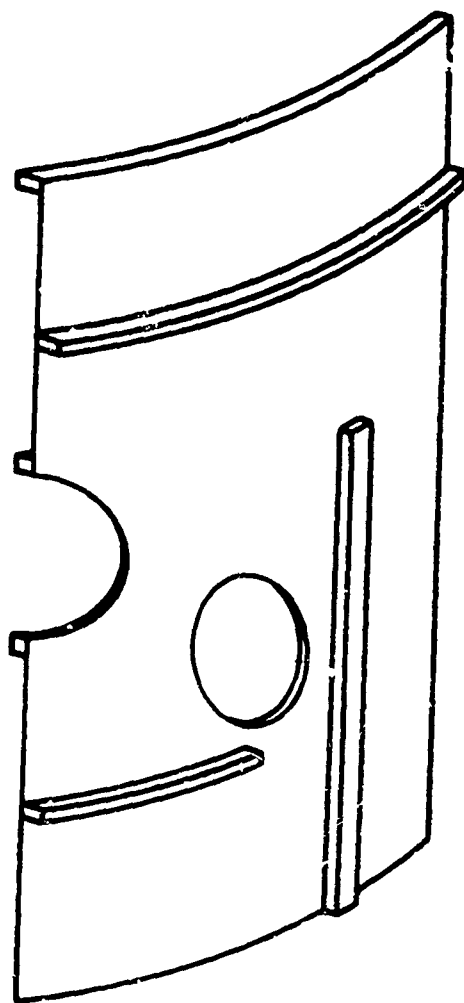


Figure 15 - Example of a Shell Panel with Discrete Reinforcement and Cutouts

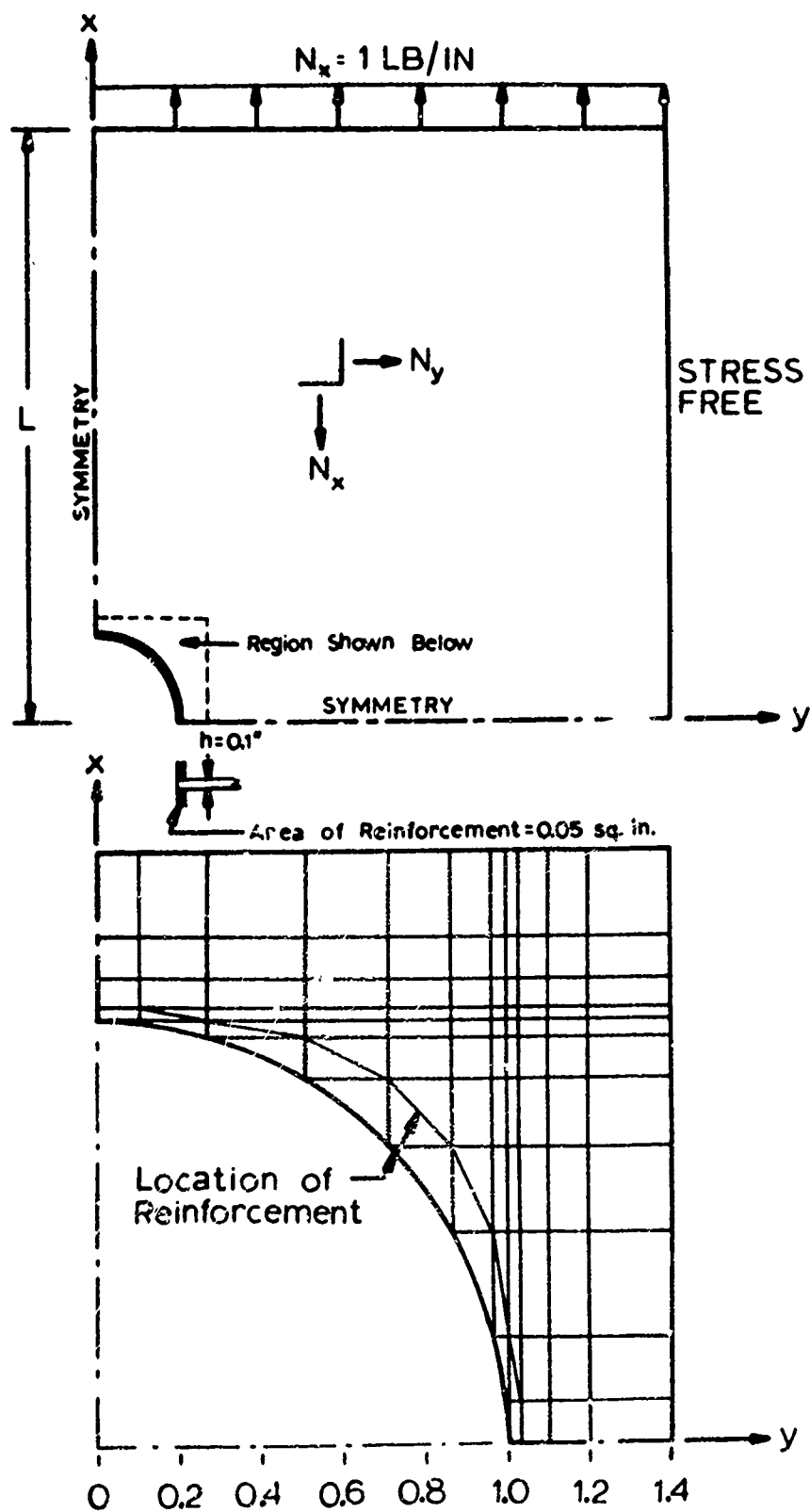
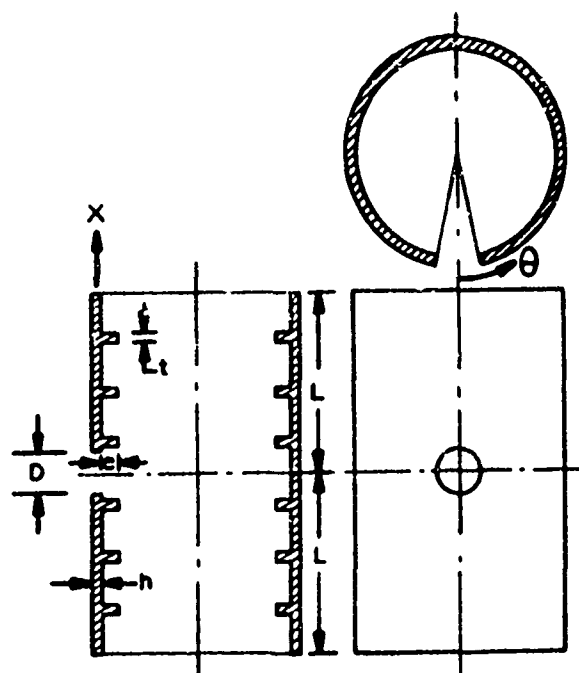


Figure 16 - Square Plate with Circular Hole and Finite Difference Mesh Around the Hole



	EM1	EM2
L =	10."	10.5"
R =	5.875"	5.875"
h =	0.25"	0.25"
D =	2.375"	1.5"
e =		1.125"
t =		.313"
E =	1.0 psi	1.0 psi
ν =	0.36	0.36

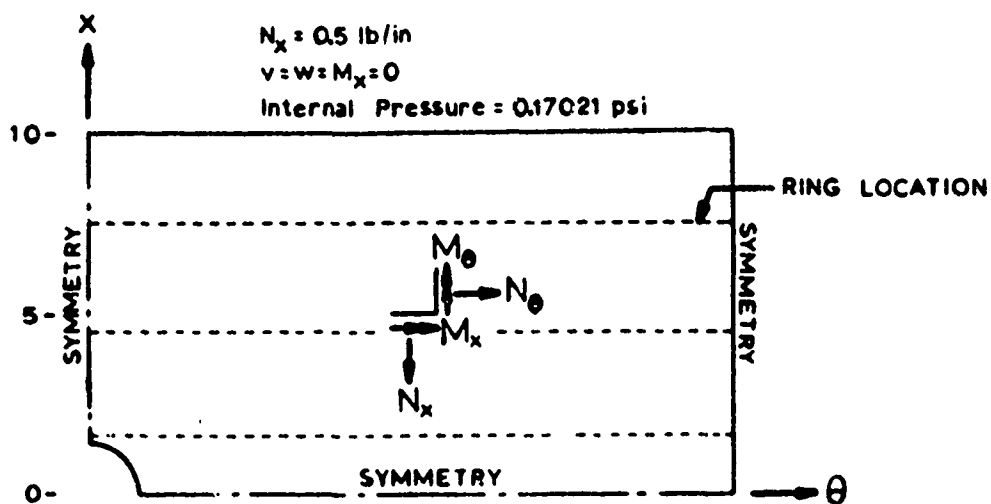


Figure 17 - Geometry, Loads and Boundary Conditions for an Unstiffened, Ring Reinforced Cylinder with Circular Hole Subjected to Hydrostatic Pressure

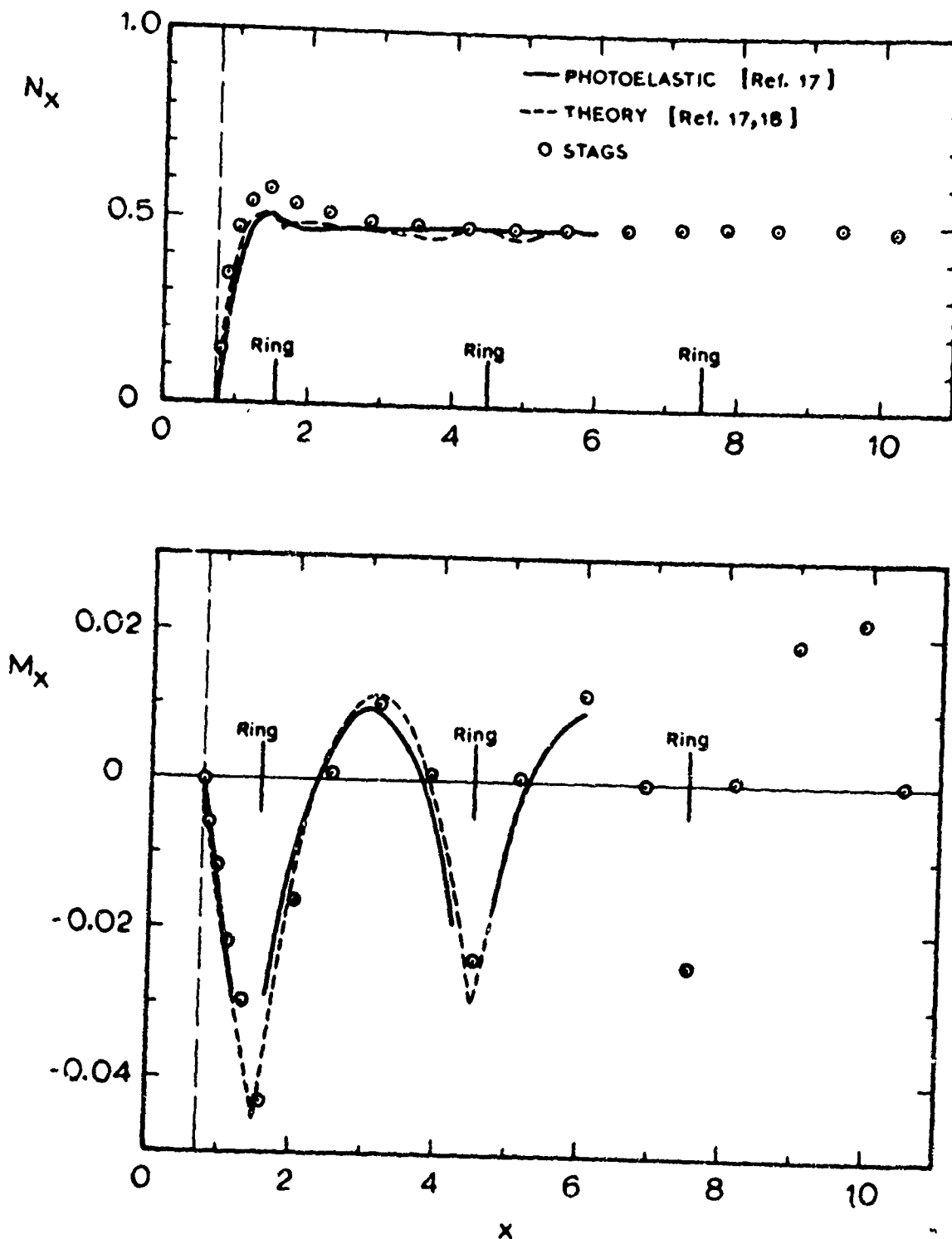


Figure 18 - Stress Resultant (N_x , M_x) along $x = 0$ for a Ring Stiffened Cylinder with Circular Hole (KM2)^x Subjected to Hydrostatic Test

STEP TIME STEP TIME

VIDEO/STANDARD
8000 8001

BONE NO. = 10.82
WEIBER NO. = 3.41
BRAIN RADIUS = 0.111
CENTER LINE M = 2.001

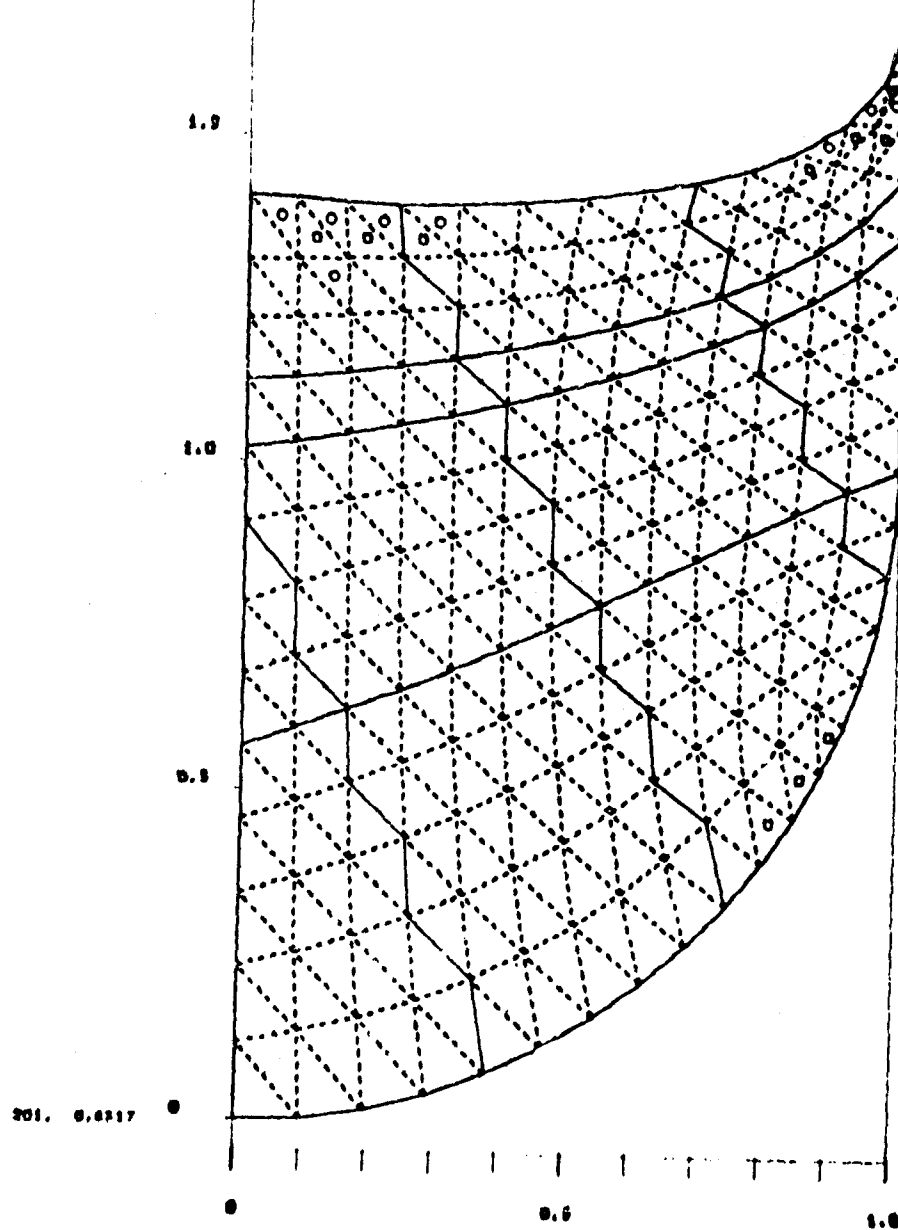
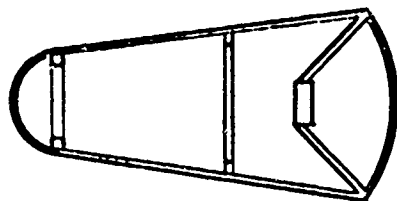
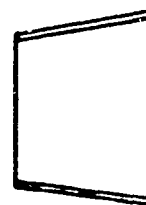


Figure 19 - Finite Difference Grid for a Second Order Partial Differential Equation

1. SHELL OF REVOLUTION



a.

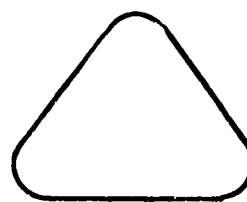
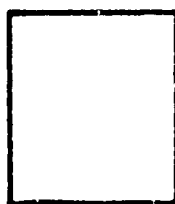


b.

VARIATIONS:

- Ring and Stringer Stiffeners
- Wall Construction
- Attached Mass
- Cutouts
- Material Behavior
- Contained Liquid

2. PEAR SHAPE CYLINDER



VARIATIONS

- Discrete Stiffeners
- Material Behavior
- Wall Construction
- Cutouts

Figure 20 - Two Sample Problems used in IMSC Studies

PROGRAM DYNAMIC OUTPUT
CONICAL AIR-BODY SECTION COMPUTER STATIONS 50.50 - 65.33 CLAMPED

SERIAL 910146

0000 00

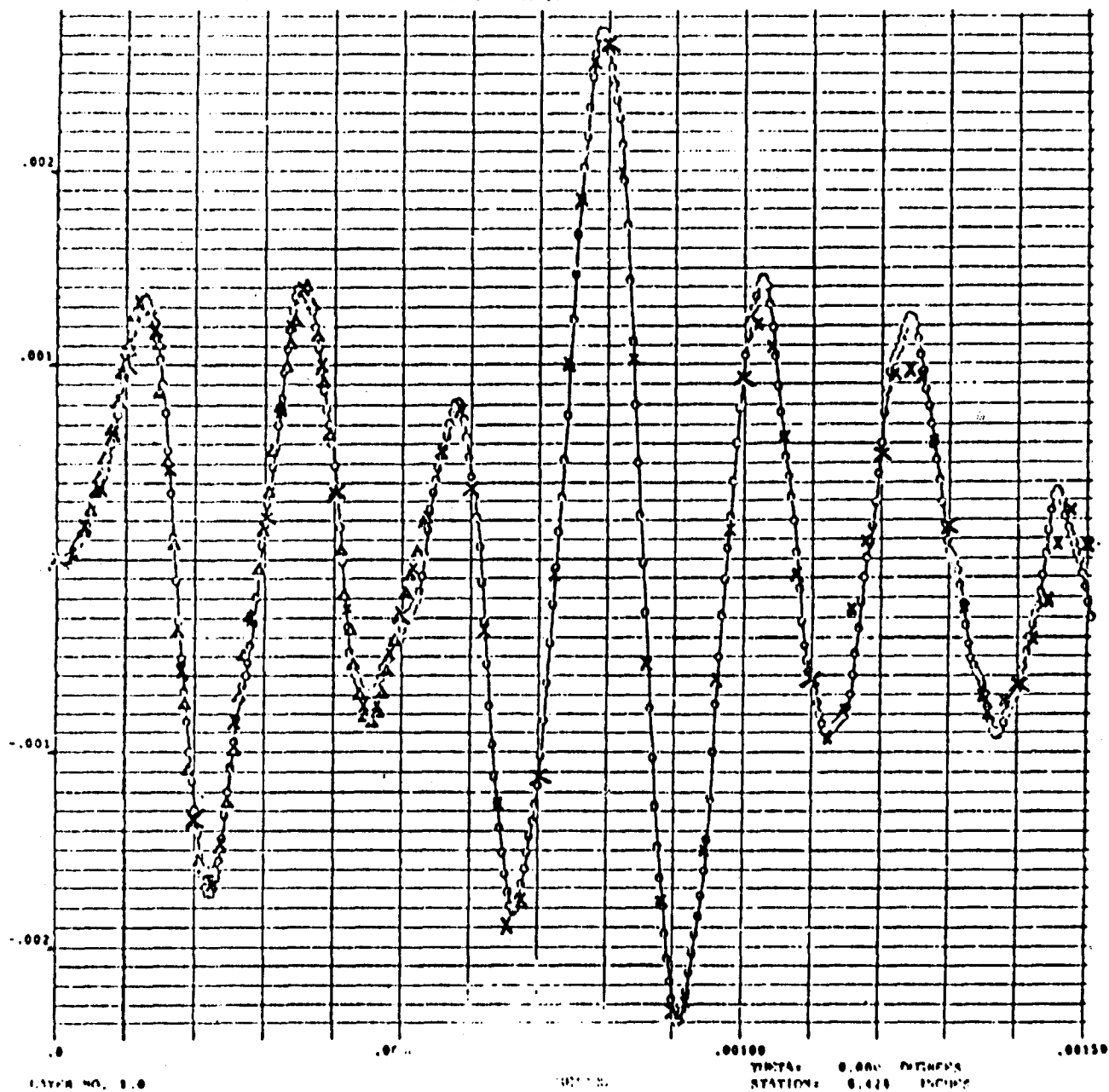
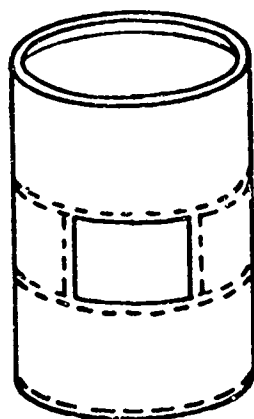


Figure 21 - Mechanical Displacement vs. Time for a Conical Shell Subjected to Asymmetrical Impulse Load

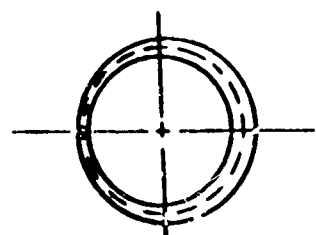
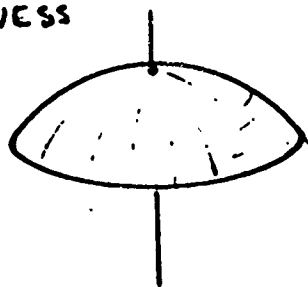
3. CIRCULAR CYLINDRICAL SHELL WITH CUTOUT



VARIATIONS:

- Cutout shape
- Cutout Reinforcement
- Material Behavior
- Cutout Boundary Conditions

4. SPHERICAL CAP WITH CIRCUMFERENTIALLY VARYING THICKNESS



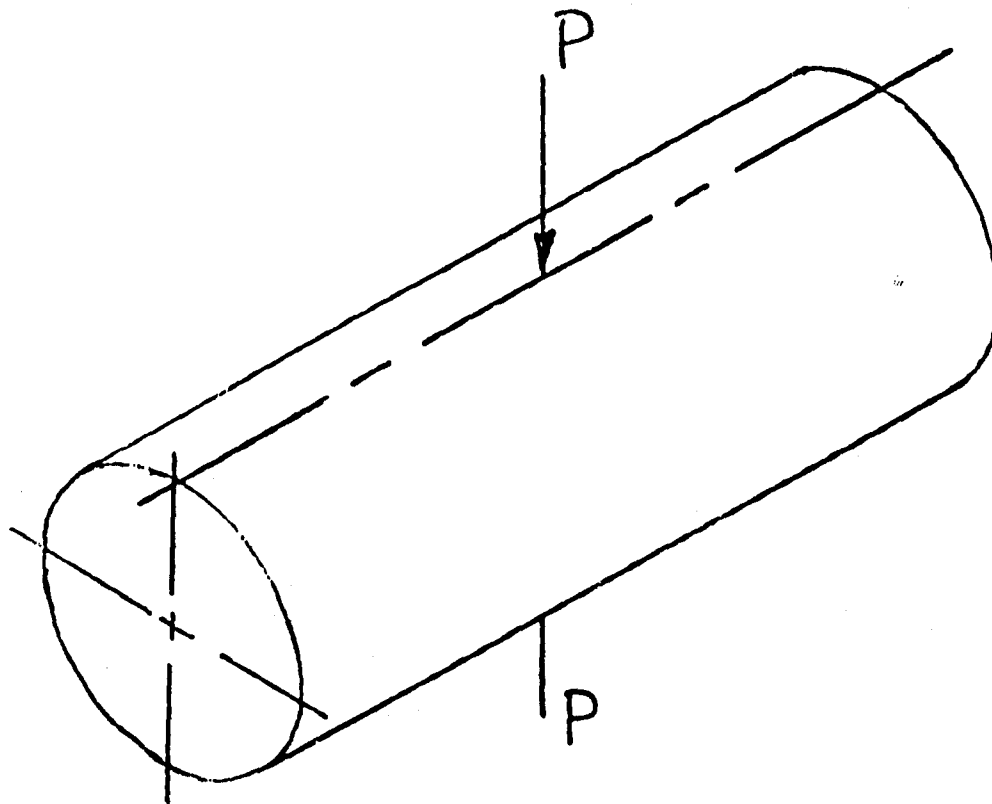
CROSS- SECTION

VARIATIONS

- Circumferential variation of Material Properties
- Material Behavior
- Wall Construction
- Thermal Loading

Figure 22 - Two Sample Problems used in LMSC Studies

5. Plinched Cylinder



Variations

- Dimensions
- Loading
- Boundary Conditions

Figure 23 - Sample Problem used in IMSC Studies

TYPE OF LOADING AND RESPONSE	SAMPLE PROBLEM					
	1. 2. SHELL OF REVOLUTION	3. CIRCULAR CONICAL SHELL	4. 2. ELLIPTICAL CONICAL SHELL	5. CYLINDRICAL SHELL W/ CUTOUT	6. 4. SPHERICAL CAP	7. 5. CANTILEVER CYLINDER
STATIC						
1. Uniform axial end load			x	x		
2. Nonuniform shear end load			x	x		
3. Uniform lateral pressure	x		x		x	
4. Point load (lateral)					x	x
5. Half cosine lateral pressure	x					
BUCKLING AND/OR COLLAPSE						
a. Linearized Problem						
1. Uniform axial end load	x					
2. Nonuniform shear end load	x					
3. Uniform lateral pressure	x					
4. Imperfection sensitivity to above	x					
b. Nonlinear (Collapse) Problem						
1. Uniform axial end load			x	x		
2. Nonuniform Shear end load			x	x		
3. Uniform lateral pressure	x		x		x	
4. Lateral pressure over small area					x	
DYNAMIC						
a. Linear						
1. Modal behavior	x		x	x	x	x
2. Impulsive half cosine pressure load		x	x	x		
3. Pulsating axial load	x	x				
b. Nonlinear						
1. Impulsive half cosine pressure load		x		x		
2. Dynamic collapse due to lateral pressure over small area					x	

Figure 24 - Schedule of Loading and Response for IMSC Sample Problems